

Oil & Natural Gas Technology

DOE Award No.: DE-FC26-04NT15509

**Final Technical Report
11/1/04–10/30/08**

INTEGRATED SYNTHESIS OF THE PERMIAN BASIN: DATA AND MODELS FOR RECOVERING EXISTING AND UNDISCOVERED OIL RESOURCES FROM THE LARGEST OIL-BEARING BASIN IN THE U.S.

Submitted by:

Bureau of Economic Geology, John A. and Katherine G. Jackson School of Geosciences, The University
of Texas at Austin, Austin, TX 78713-8924

Prepared for:

United States Department of Energy
National Energy Technology Laboratory



Office of Fossil Energy

INTEGRATED SYNTHESIS OF THE PERMIAN BASIN:
DATA AND MODELS FOR RECOVERING EXISTING AND UNDISCOVERED OIL
RESOURCES FROM THE LARGEST OIL-BEARING BASIN IN THE U.S.

FINAL TECHNICAL REPORT

11/01/04 – 10/30/08

Stephen C. Ruppel, Principal Investigator

prepared for U.S. Department of Energy
under contract no. DE-FC26-04NT15509

Bureau of Economic Geology
Scott W. Tinker, Director
John A. and Katherine G. Jackson School of Geosciences
The University of Texas at Austin
Austin, TX 78713-8924

July 2009

Disclaimer

This report was prepared as an account of work sponsored by an agency of the United States Government. Neither the United States Government nor any agency thereof, nor any of their employees, makes any warranty, express or implied, or assumes any legal liability or responsibility for the accuracy, completeness, or usefulness of any information, apparatus, product, or process disclosed, or represents that its use would not infringe privately owned rights. Reference herein to any specific commercial product, process, or service by trade name, trademark, manufacturer, or otherwise does not necessarily constitute or imply its endorsement, recommendation, or favoring by the United States Government or any agency thereof. The views and opinions of authors expressed herein do not necessarily state or reflect those of the United States Government or any agency thereof.

CONTENTS

SUMMARY OF PROJECT ACCOMPLISHMENTS.....	1
Introduction.....	1
Written Play Summaries	4
Data	4
Data Distribution.....	10
Technology Transfer	12
Conclusions.....	12
Acknowledgments.....	13
Reference	13
GEOLOGIC PLAY SUMMARIES.....	14
Lower Ordovician Ellenburger Group	15
Middle-Upper Ordovician Simpson Group	107
Upper Ordovician Montoya Group	148
Ordovician-Lower Silurian Fusselman	207
Middle-Upper Silurian Wristen Group	237
Lower Devonian Thirtyone Formation	279
Mississippian System.....	340
Pennsylvanian Morrow Series	380
Pennsylvanian Atoka Series.....	459
Pennsylvanian Strawn Series	526
Pennsylvanian Canyon/Cisco Series.....	623
Permian Wolfcamp Series.....	740
Permian Delaware Mountain Group	767
Permian Artesia Group	847
APPENDIX.....	947

SUMMARY OF PROJECT ACCOMPLISHMENTS

INTRODUCTION

The Permian Basin is the richest hydrocarbon basin in the United States. To date, nearly 30 billion barrels of oil has been produced from an approximate original oil in place of 106 billion barrels (nearly one-fourth of the total discovered oil resource in the United States). However, current annual production rates have fallen drastically from the peak of 665 million barrels per year in the early 1970's to less than 300 million barrels per year—half the peak production. Despite the continuing fall in production, the Permian Basin still holds a significant volume of oil. Studies by the Bureau of Economic Geology (Tyler and Banta, 1989) calculate that as much as 30 billion barrels of mobile oil and 54 billion barrels of residual oil (accessible to tertiary oil recovery technologies) remain in existing reservoirs. Such studies suggest that an additional 3.5 billion barrels of oil and NGL resources remains to be discovered in the basin.

One of the critical barriers to generating new enthusiasm, interest, and commitment to recovering this remaining resource has long been the lack of up-to-date, fully integrated and synthesized, readily accessible data sets on the stratigraphic and depositional framework, facies architecture, reservoir properties and characteristics, play boundaries, and applicable reservoir models in the Permian Basin. The goal of this project was to fill this need by creating and distributing a synthesis of Permian Basin data in readily accessible and usable digital formats.

Project Goals and Methodology

The goals of the project were to produce a detailed, comprehensive analysis and history of Paleozoic depositional and reservoir systems in the Permian Basin and to create spatially integrated databases of depositional, stratigraphic, lithologic, and petrophysical properties.

These goals were approached in two ways. The first objective was to develop comprehensive syntheses of major hydrocarbon-bearing plays in the Permian Basin. These syntheses have taken the form of written, illustrated summary reports on each depositional episode in the Paleozoic section of the basin. Each report details the stratigraphy, facies, structural and depositional history, diagenesis, causes of reservoir formation, and reservoir distribution. Report text is supported by illustrations of important geological characteristics of each system, including (1) maps of facies, thickness, and structure; (2) regional and reservoir-specific cross sections; (3) illustrations of core facies and cyclicity; (4) reservoir and depositional models; (5) depictions of wireline-log character; (6) seismic models; (7) photographs of representative facies; and (8) representative outcrop data.

A second objective was to collect, interpret, synthesize, and distribute all available data on hydrocarbon-bearing systems in the basin. Data collected include regional structure maps, subcrop maps, thickness maps, paleogeographic maps, regional cross sections, reservoir cross sections, reservoir and outcrop geological models, core descriptions, core analysis data, lists of available cores, lists of publications, and copies of PowerPoint reports and posters.

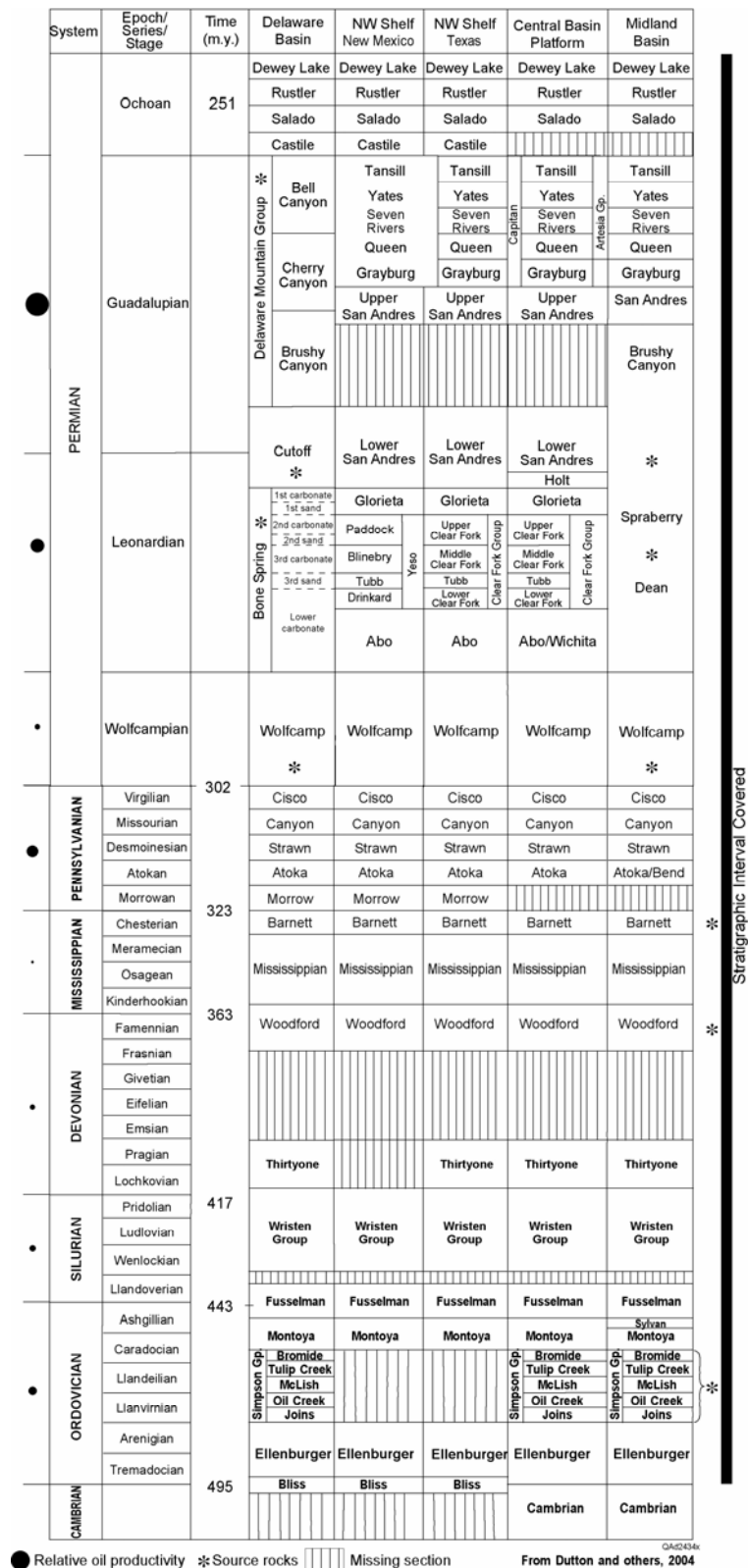


Figure 1. Stratigraphy of the Permian Basin showing scope of study.

Both data and reports have been prepared for easy digital access and use and are available digitally through the project website. Where possible, data have been integrated into a geospatial database using an ARC/GIS-based format.

One of the keys to project success was the involvement of a large, multidisciplinary group of geoscientists. The research team included 22 research professionals (17 affiliated with the Bureau of Economic Geology) and 9 students (from The University of Texas at Austin).

Geologic and Geographic Scope

The project scope included nearly all hydrocarbon-producing rocks in the Permian Basin, ranging from the Lower Ordovician Ellenburger Group to the Upper Permian Yates Formation, nearly the entire Paleozoic stratigraphic succession (fig. 1). The geographic scope was largely confined to the Permian Basin (fig. 2). However, interest and availability of data sets allowed expansion eastward to the Fort Worth Basin for the Pennsylvanian and Mississippian parts of the succession. We have also extended some mapping into Oklahoma.

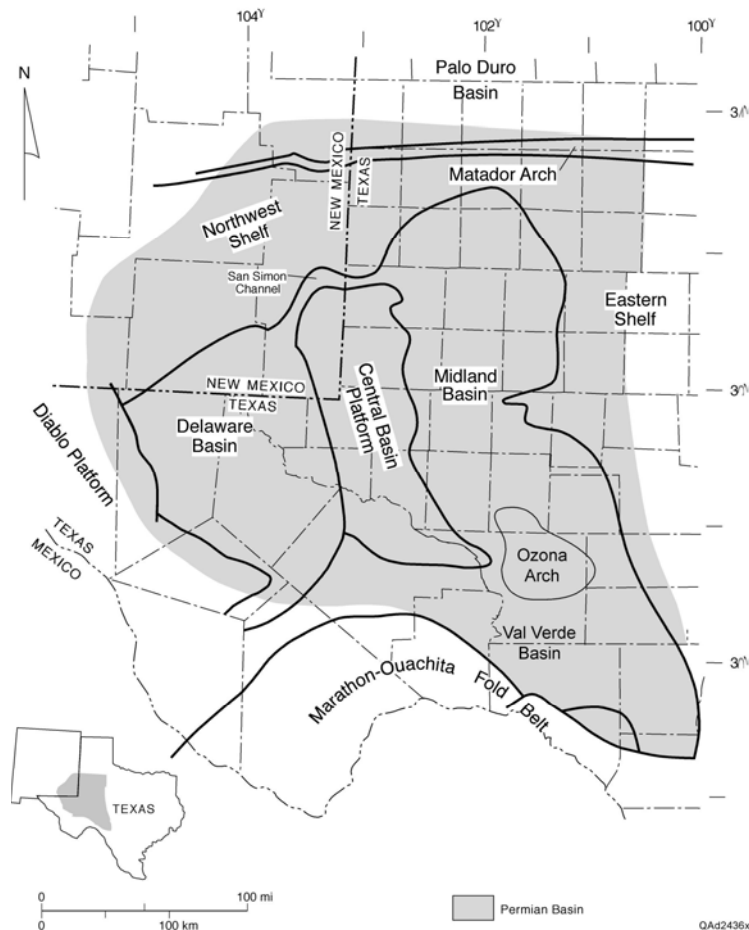


Figure 2. Map of west Texas and New Mexico showing primary study area.

WRITTEN GEOLOGIC PLAY SUMMARIES

Fourteen written play summaries have been completed and are currently available for distribution. These include the following geologic successions: Ellenburger, Simpson, Montoya, Fusselman, Wristen, Thirtyone, Mississippian, Morrow, Atoka, Strawn, Canyon/Cisco, Wolfcamp, Artesia Group, Delaware Mountain Group. All of these reports are included in the body of this final report.

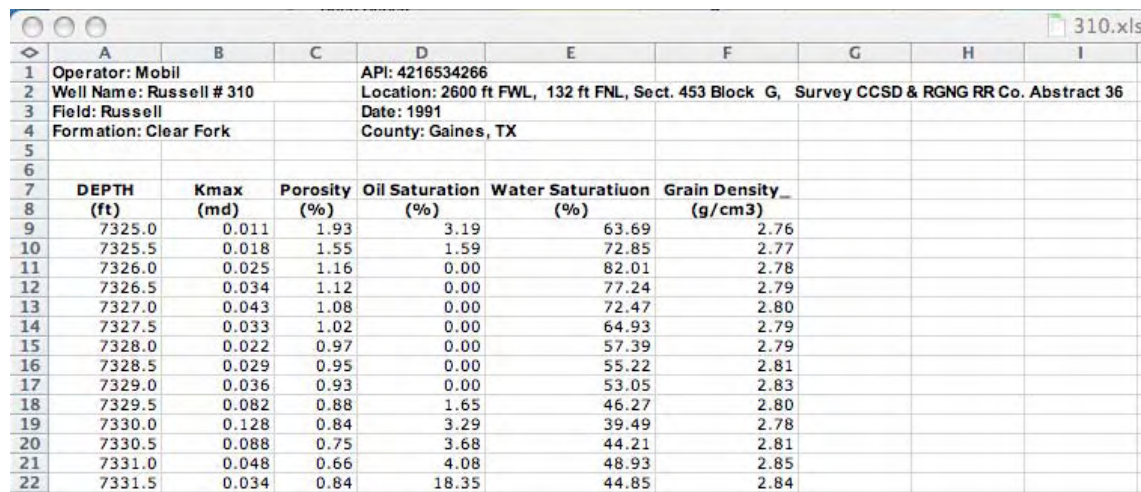
Six other summaries are nearly complete and will be made available later in 2009. These include the following successions: Woodford, Leonard (Clear Fork, Wichita, Abo, Glorieta), Wolfcamp, Spraberry/Dean, Bone Spring, and San Andres. We expect that two additional reports, one on the Yates and one on the Grayburg, will be completed and made available in 2010. When complete, these 22 reports will provide up-to-date and in-depth perspectives on all producing reservoir successions in the Permian Basin.

In addition to play reports, we have compiled and completed several reports on detailed studies of geological and engineering aspects of individual oil reservoirs. Finally, one report was completed on outcrop studies; this work forms a fundamental basis for understanding many subsurface reservoirs in the Permian Basin. These are not included in the Final Report (owing to space limitations) but, like all data, are available for download from the project website. Additional field studies will be made available through the website as they are completed.

In addition to these written reports, poster presentations and PowerPoints from oral presentations are also available for access and download from the project website.

DATA

A wide variety of data have been collected, digitized, and made available for distribution. These include the following: core analysis data (fig. 3), type logs (fig. 4), reservoir cross sections (fig.5), regional cross sections (fig.6), structure maps (fig.7), distribution maps (fig.8), paleogeographic maps (fig.9), and lists of available cores (fig.10). We also compiled comprehensive lists of published papers for each play. These and all other data are available for download from the project website. New data will be added to the website as they are obtained on a continuing basis.



	A	B	C	D	E	F	G	H	I
1	Operator: Mobil			API: 4216534266					
2	Well Name: Russell # 310			Location: 2600 ft FWL, 132 ft FNL, Sect. 453 Block G, Survey CCSD & RGNG RR Co. Abstract 36					
3	Field: Russell			Date: 1991					
4	Formation: Clear Fork			County: Gaines, TX					
5									
6									
7	DEPTH	Kmax	Porosity	Oil Saturation	Water Saturation	Grain Density			
8	(ft)	(md)	(%)	(%)	(%)	(g/cm3)			
9	7325.0	0.011	1.93	3.19	63.69	2.76			
10	7325.5	0.018	1.55	1.59	72.85	2.77			
11	7326.0	0.025	1.16	0.00	82.01	2.78			
12	7326.5	0.034	1.12	0.00	77.24	2.79			
13	7327.0	0.043	1.08	0.00	72.47	2.80			
14	7327.5	0.033	1.02	0.00	64.93	2.79			
15	7328.0	0.022	0.97	0.00	57.39	2.79			
16	7328.5	0.029	0.95	0.00	55.22	2.81			
17	7329.0	0.036	0.93	0.00	53.05	2.83			
18	7329.5	0.082	0.88	1.65	46.27	2.80			
19	7330.0	0.128	0.84	3.29	39.49	2.78			
20	7330.5	0.088	0.75	3.68	44.21	2.81			
21	7331.0	0.048	0.66	4.08	48.93	2.85			
22	7331.5	0.034	0.84	18.35	44.85	2.84			

Figure 3. Example of core analysis data collected during the project.



TYPE LOG Fullerton Clear Fork Field

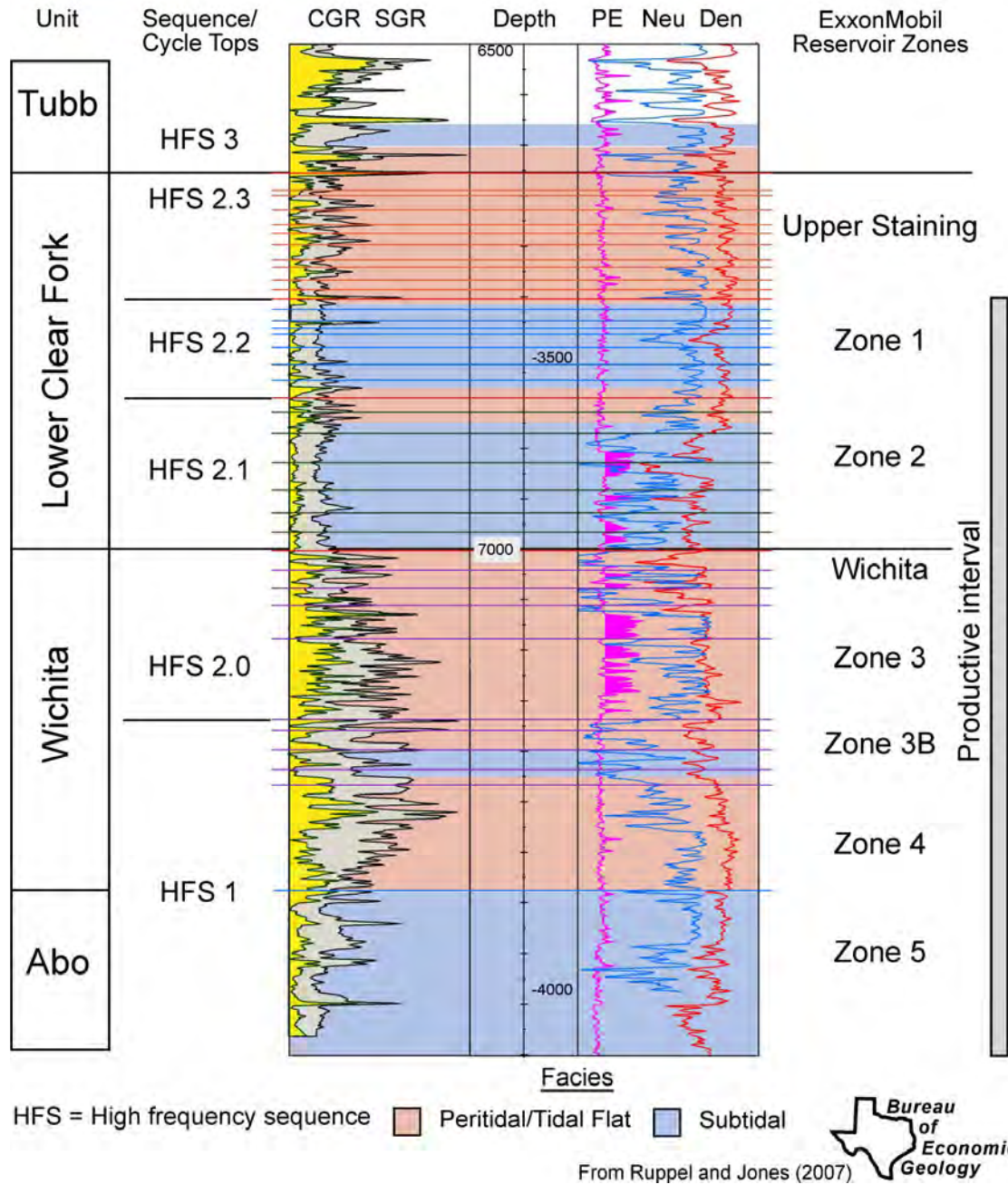
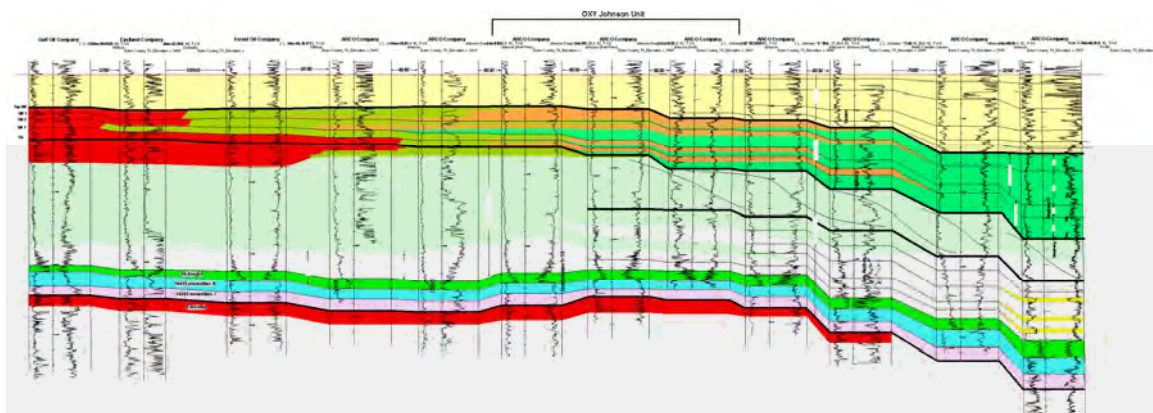
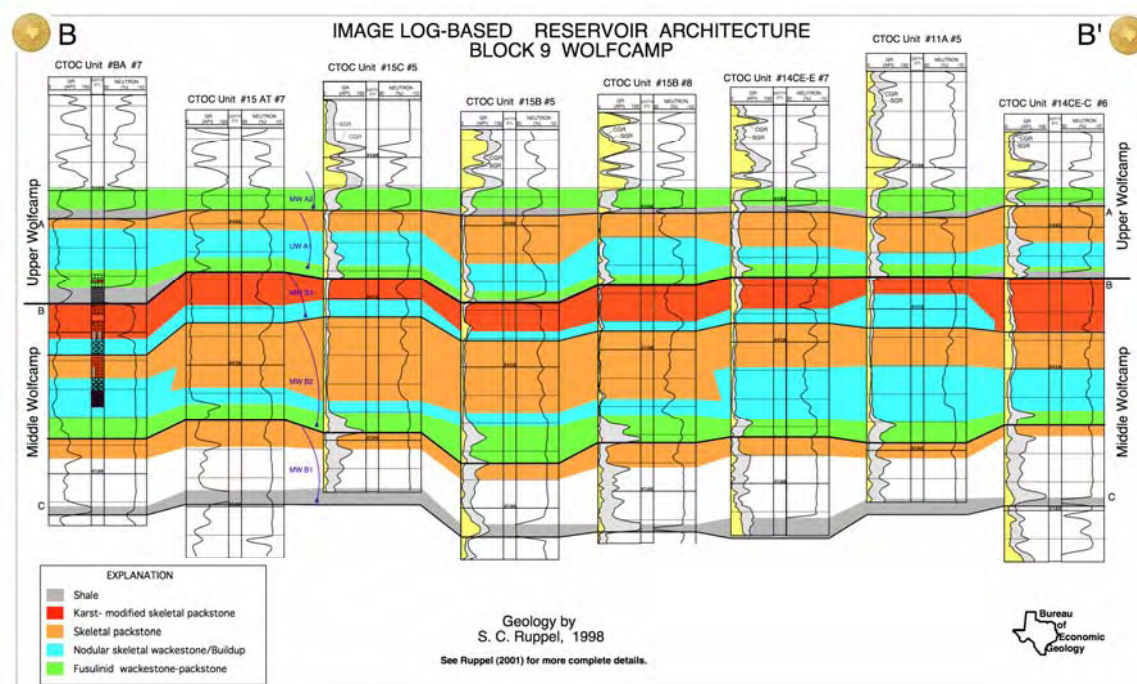


Figure 4. Example of type log produced during the project (Fullerton Clear Fork field).



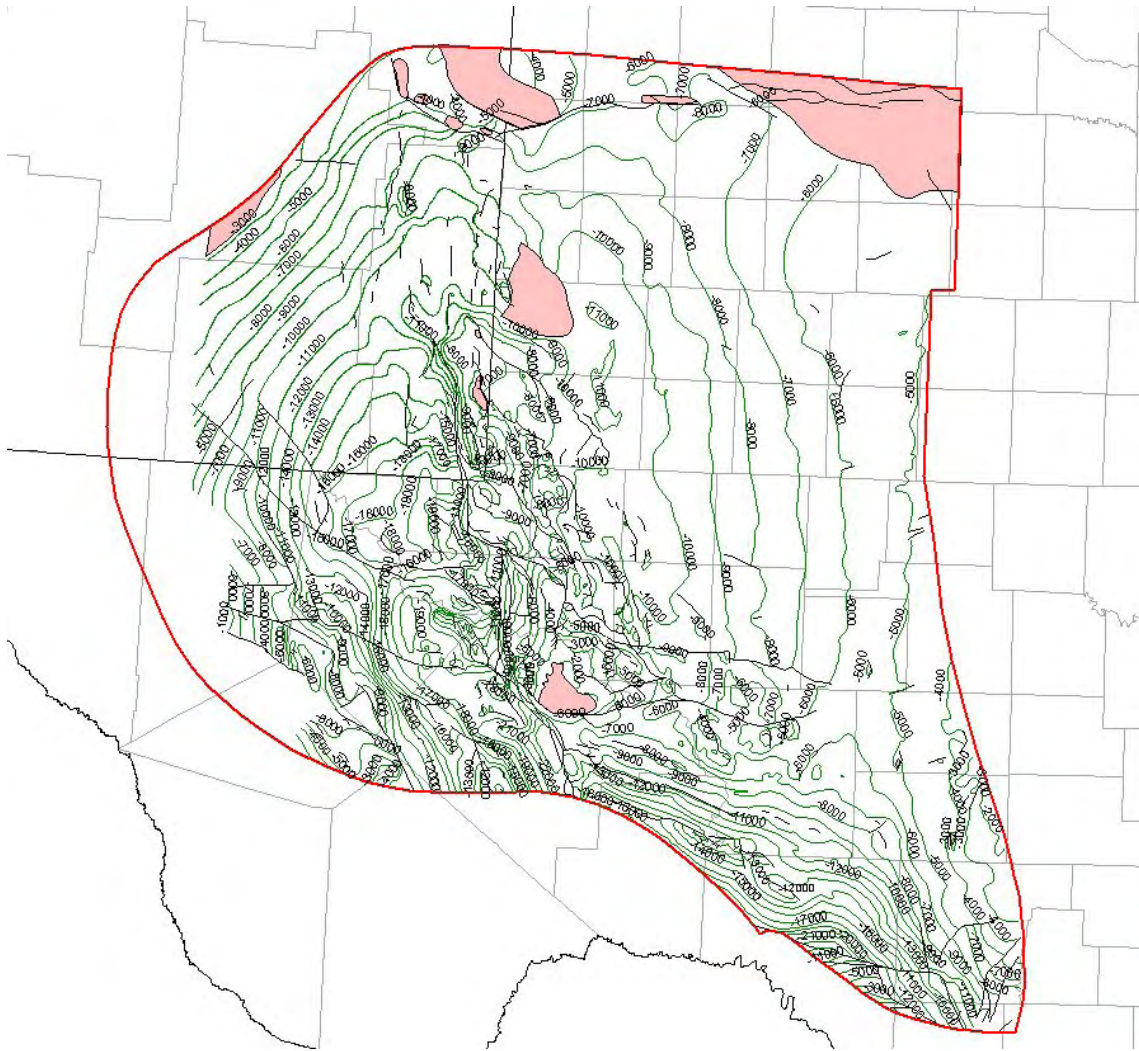


Figure 7. Example of structure map produced during the project (Ellenburger Group [Lower Ordovician]).

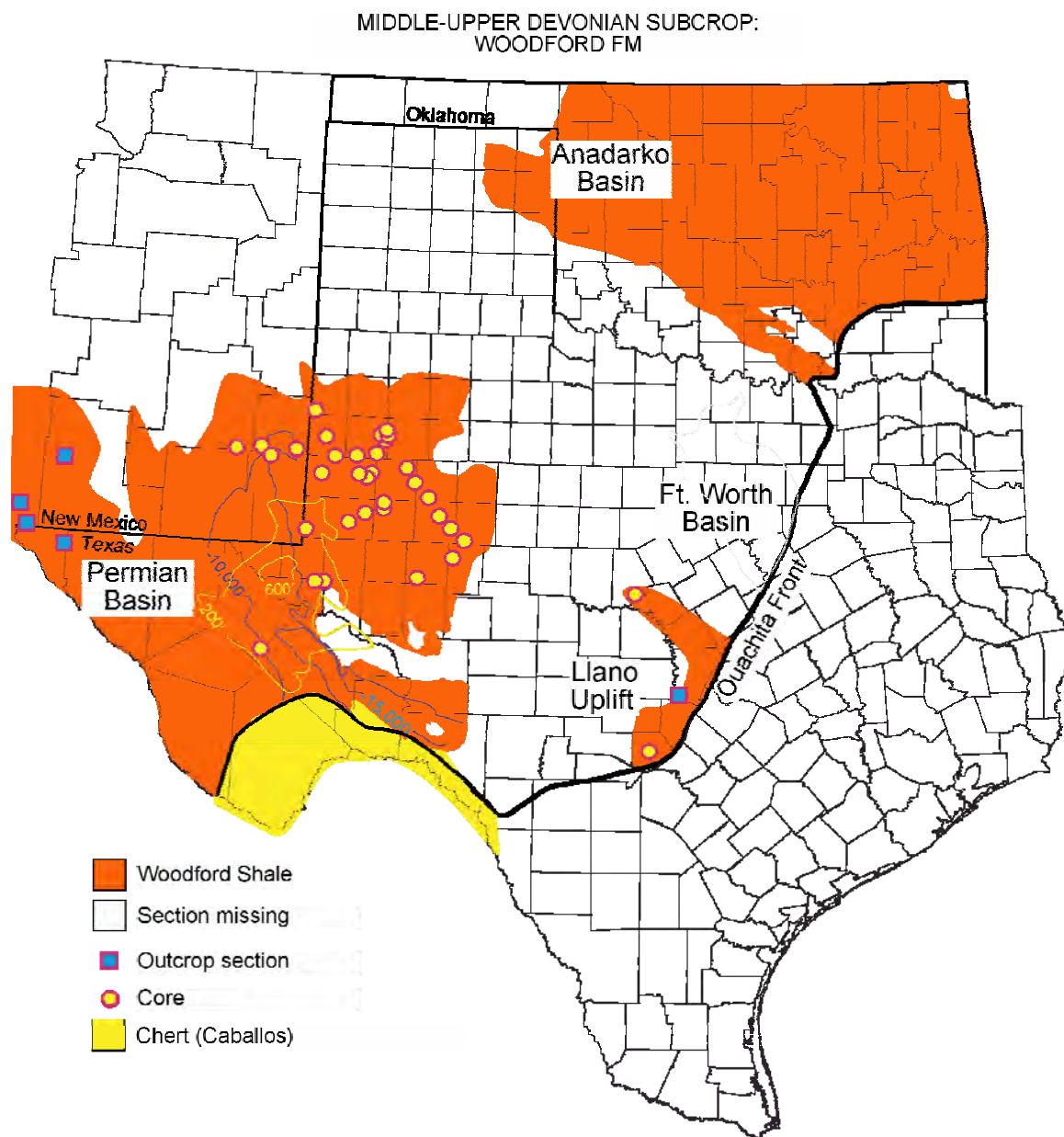


Figure 8. Example of distribution map (Woodford Formation).

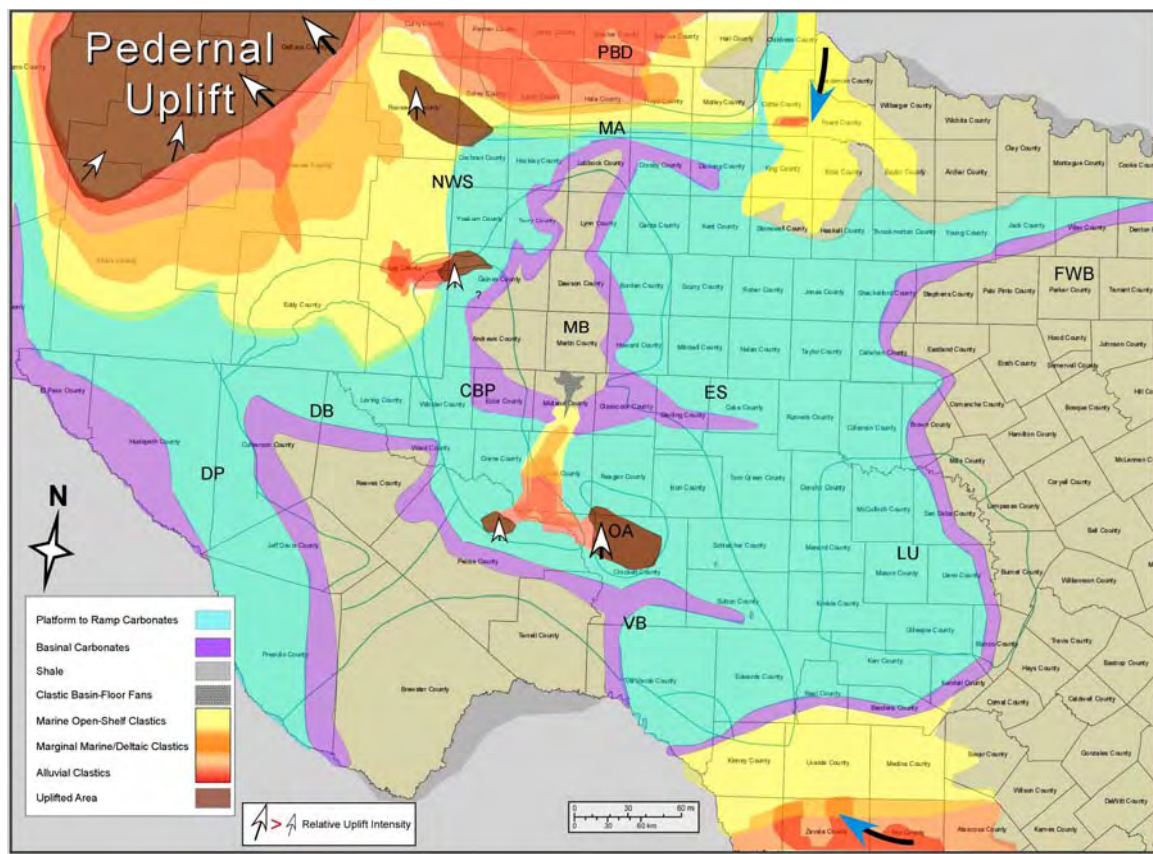


Figure 9. Example of paleogeographic maps produced during the project (Lower Pennsylvanian [Atokan]).

Artesia cores.xls									
Accession #	API #	County	Operator	Lease	Field	top	bottom	Formation	
1	001394	ANDREWS	TEXACO	STATE OF TEXAS CJ 6	MAGUTEX	4858	4936	QUEEN	
2	003002	ANDREWS	TEXACO	STATE OF TEXAS CN 4		4850	4925	QUEEN	
3	008810	ANDREWS	SUN OIL CO.	O.B. HOLT ACCOUNT 2 #28	NORTH COWDEN	4421	4792	GRAYBURG-ANDRES	
4	009828	ANDREWS	SUN OIL CO.	J.S. MEANS #A-3	MEANS QUEEN	4025	4087	QUEEN SAND	
5	S00701	ANDREWS	SCHOENIMAN	PERKINS #3		4270	4415	GRAYBURG	
6	S00306	ANDREWS	PAN AMERICAN PETROLEUM CORP.	FASKEN, DAVID #1-AO		4745	5253	GRAYBURG/SAN ANDRES	
7	S00870	ANDREWS	PAN AMERICAN PETROLEUM CORP.	FASKEN, DAVID #1-AR		4750	4950	GRAYBURG	
8	S00552	ANDREWS	LIVELY & REED	CREWS-MAST #1		2930	2973	YATES	
9	003747	ANDREWS	EXXON	WILSON, H.M. #B-21	FULLERTON	8134	8351	SILURIAN	
10	S00558	ANDREWS	COSDEN	PARMER CSL #1	WILDCAT	4700	4781	QUEEN	
11	S00152	ANDREWS	BARNES, J.C.	UNIVERSITY #QX-4	MCFARLAND	4776	4815	QUEEN	
12	S00153	ANDREWS	BARNES, J.C.	UNIVERSITY #1-S	MCFARLAND	4789	4809	QUEEN	
13	S00154	ANDREWS	BARNES, J.C.	UNIVERSITY #WX-4	MCFARLAND	4804	4841	QUEEN	
14	001964	CRANE	TEXACO (SEABOARD)	TXL D #1	CONCHO BLUFF	7737	13073	QUEEN	
15	003094	CRANE	TEXACO (SEABOARD)	TXL E 3	CONCHO BLUFF	4081	4181	QUEEN	
16	003093	CRANE	TEXACO (SEABOARD)	TXL E 2	CONCHO BLUFF	4125	4150	QUEEN	
17	003091	CRANE	TEXACO (SEABOARD)	TXL D 2	CONCHO BLUFF	4132	4204	QUEEN	
18	003092	CRANE	TEXACO (SEABOARD)	TXL E 1	CONCHO BLUFF	4120	4156	QUEEN	
19	003095	CRANE	TEXACO (SEABOARD)	TXL F 1	CONCHO BLUFF	4166	4211	QUEEN	
20	003081	CRANE	TEXACO	EVERITT & GLASS #10	CONCHO BLUFF	4164	4167	QUEEN	

Figure 10. Example of lists of available cores compiled during the project.

DATA DISTRIBUTION

Data and reports created during the project are available for access and download at the project website: [<http://www.beg.utexas.edu/resprog/permianbasin/integrsynthesis.htm>] (fig. 11).

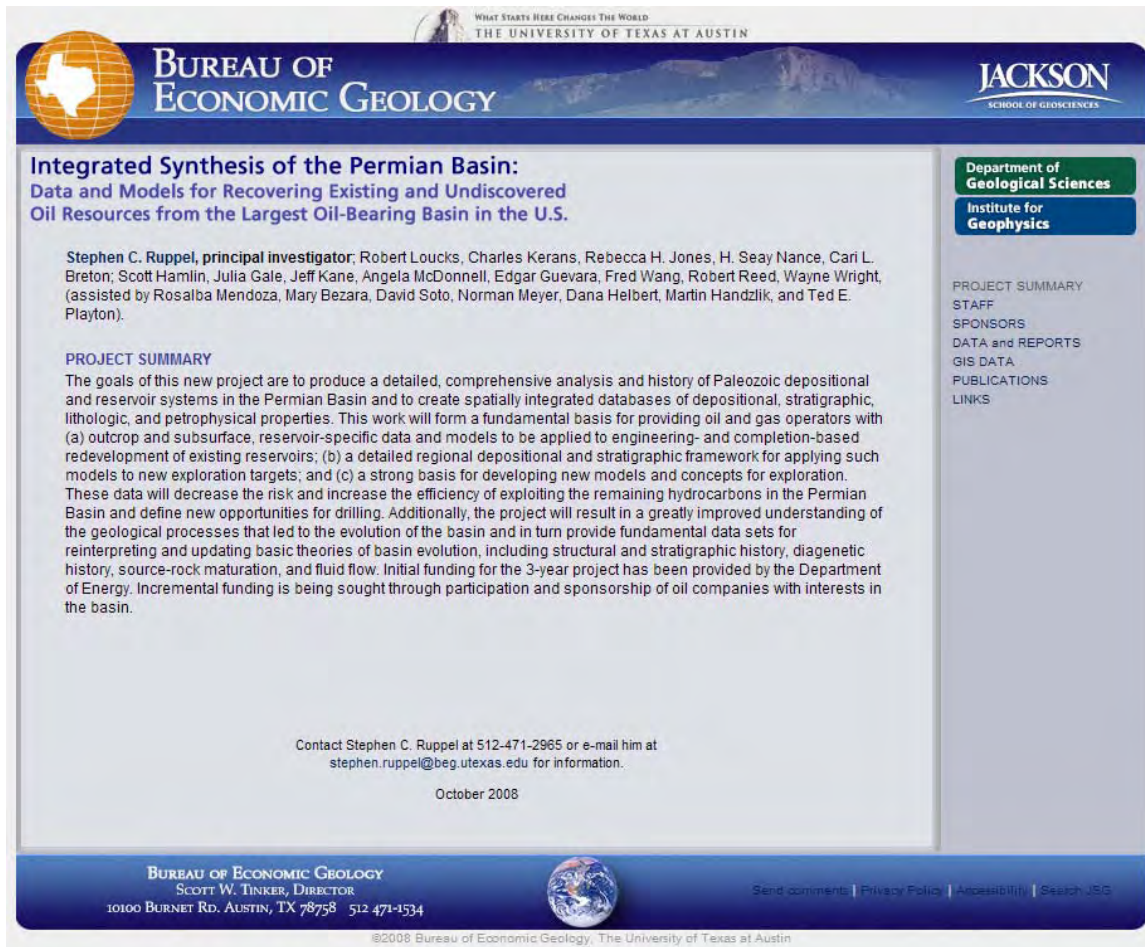


Figure 11. Front page, project website.

The project website provides access to project data in two formats: (1) as stand-alone files and (2) as data in geospatially registered shape files that can be loaded into Arc/GIS software. Most stand-alone data files are available in common file formats that can be read by readily available software such as Acrobat (pdf files), Excel (data files), and PowerPoint. These files are directly downloadable from the Data and Reports page (fig. 12).

Many data are also linked geospatially in ARC/GIS-based format. These files can be downloaded and inserted into suitable data-viewing software. Instructions for downloading files and obtaining access to a data viewer are given on the website (fig. 13).

 BUREAU OF ECONOMIC GEOLOGY  					
Integrated Synthesis of the Permian Basin: Data and Models for Recovering Existing and Undiscovered Oil Resources from the Largest Oil-Bearing Basin in the U.S.					
DATA and REPORTS					ISPB Home
	Written reports [PDF]	Core analysis data files [Excel]	Reference lists [Word]	Lists of BEG cores in Permian Basin [Excel]	Powerpoint presentations
Permian					
Artesia Group	Artesia		References	Core list	Nance Artesia, 2006
Dollarhide Field		Yates 15-7-C			
Delaware Mountain Group	Delaware Mountain Group		References	Core list	Nance DMG, 2006
Apollo Field		MU 21-36 No. 2			
Little Joe Field		PU 31-A No. 1			
Quito East Field		U 18-29 no. 6			
War-Wink Field		TU 1			
Grayburg					
Block 2 Field		110W			
Johnson Field					
N Foster Field					
S Foster Field					
North McElroy Field		NMU 2856			
Rhodes Cowden Field					
North Cowden Field					
South Cowden Field		Moss Unit 6-20			
San Andres					Kerans SA, 2006
Emma Field		Emma 9-7			
Penwell Field		Penwell 194			
Fuhrman Mascho Field		FMU 124			Ruppel FMU_2001
Taylor Link Field		WSA #84			
Clear Fork			References		Ruppel CF, 2006
Dollarhide Field					
N Dollarhide Field					
Empire Field					
Keystone S Field					
Russell Field		RCFU 129			
Drinkard Field		NEDU 514			
Fullerton Field	Fullerton Field Study	FM-1			
Monahans Field		SS 164			
North Robertson Field		NRU 207			
South Wasson Field	South Wasson Field Study				

Figure 12. Data and reports download page at the project website.

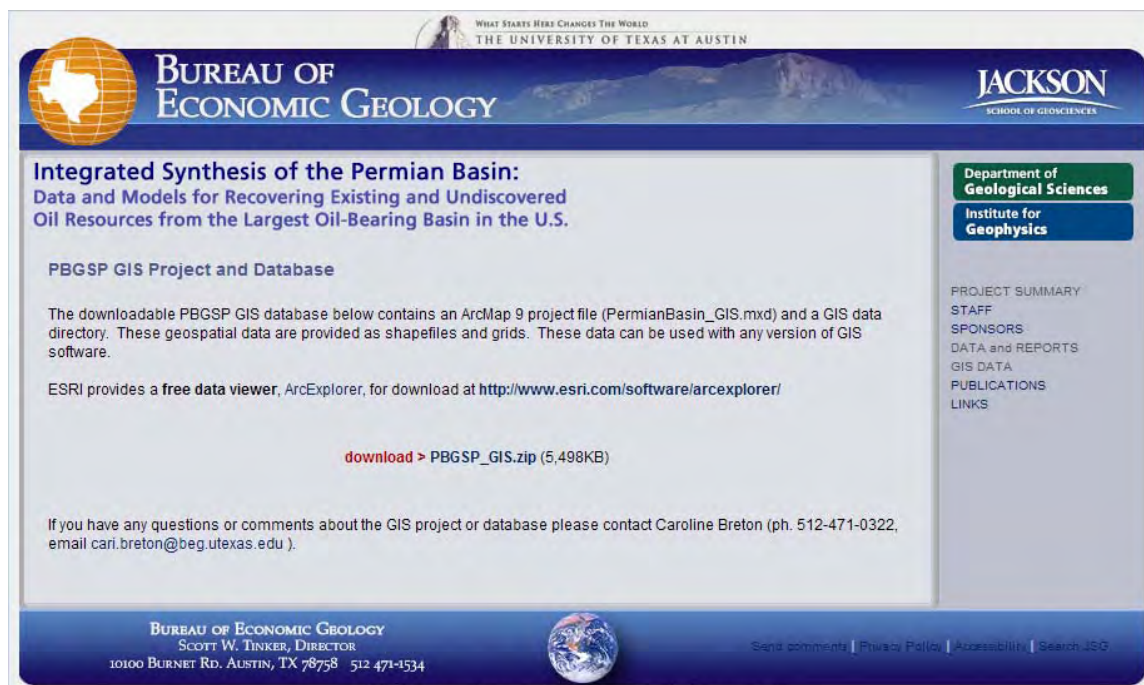


Figure 13. GIS data access page on the project website.

TECHNOLOGY TRANSFER

In addition to direct transfer of data by our website, we have delivered results of the research to professional audiences through published papers, oral and poster presentations, workshops, and direct interaction with oil and gas company scientists and engineers. These activities include 29 published papers dealing with aspects of Permian Basin and Fort Worth Basin Paleozoic geology, 35 oral and poster presentations given at professional society meetings, and 116 oral and poster presentations given at the 10 workshops and short courses conducted during the project. A complete list of these technology transfer activities is included in the Appendix to this report.

CONCLUSIONS

The project has been highly successful in obtaining, interpreting, synthesizing, and providing access to a large number of data on the geology of Paleozoic hydrocarbon-producing successions of the Permian Basin that previously were unavailable. The availability of these data and interpretations should greatly improve the existing knowledge base on Permian Basin hydrocarbon systems and form the basis for new concepts and approaches to exploiting the large volumes of oil and gas still remaining in this prolific basin.

ACKNOWLEDGMENTS

This research was funded by the U.S. Department of Energy under contract number DE-FC26-04NT15509. Additional funding was provided by industry sponsors including Alpine Energy, Anadarko, Apache, Brigham, BP, Chevron, Cimarex, ConocoPhillips, Forest, Lynx, Matador, Osborne Heirs, Oxy, Pioneer, Samson, St. Mary Trail Mountain, Whiting, and Yates Petroleum Corp. The support of these companies was crucial to accomplishing the objectives of the project and allowing activities to continue after termination of the Doe-funded research. Lana Dieterich edited the manuscripts. Support for graphics was provided by Joel Lardon and his staff. John Roberts of Geological Data Services kindly provided access to stratigraphic tops in the basin. Dan Ferguson and Virginia Weyland served as contract officers for DOE.

REFERENCE

Tyler, Noel, and Banta, N. J., 1989, Oil and gas resources remaining in the Permian Basin: targets for additional hydrocarbon recovery: The University of Texas at Austin, Bureau of Economic Geology Geological Circular 89-4, 20 p.

GEOLOGIC PLAY SUMMARIES

THE LOWER ORDOVICIAN ELLENBURGER GROUP, PERMIAN BASIN, WEST TEXAS

Robert Loucks

Bureau of Economic Geology
Jackson School of Geosciences
The University of Texas at Austin
Austin, TX

ABSTRACT

The Ellenburger Group of the West Texas Permian Basin is part of a Lower Ordovician carbonate platform sequence that covers a large area of the United States. During the Early Ordovician, the Permian Basin area was located on the southwest edge of the Laurentia plate between 20° and 30° latitude. The equator crossed northern Canada, situating Texas in a tropical to subtropical latitude. The area of Texas was a shallow-water shelf, with deeper water conditions to the south where it bordered the Iapetus Ocean.

Shallow-water carbonates were deposited on the shelf, and deep-water shales and carbonates were deposited on the slope and in the basin. The interior of the shelf produced restricted environments, whereas the outer shelf produced open-marine conditions. Diagenesis of the Ellenburger Group is complex, and the processes that produced the diagenesis spanned millions of years. Three major diagenetic processes strongly affected Ellenburger carbonates: (1) dolomitization, (2) karsting, and (3) tectonic fracturing. Pore networks in the Ellenburger are complex because of the amount of brecciation and fracturing associated with karsting. Networks can consist of any combination of the following pore types, depending on depth of burial: (1) matrix, (2) cavernous, (3) interclast, (4) crackle-/mosaic-breccia fractures, or (5) tectonic-related fractures.

The Ellenburger Group is an ongoing, important exploration target in West Texas. Carbonate depositional systems within the Ellenburger Group are relatively simple; however, the diagenetic overprint is complex, producing strong spatial heterogeneity within the reservoir systems.

INTRODUCTION

The Ellenburger Group of the Permian Basin is part of a Lower Ordovician carbonate platform sequence that covers a large area of the United States (Figures 1, 2) (Ross, 1976; Kerans, 1988, 1990). It is well known for being one of the largest shallow-water carbonate platforms in the geologic record (covering thousands of square miles and as much as 500 mi wide in West Texas), being extensively karsted at the Sauk unconformity, with its widespread hydrocarbon production. Hydrocarbon production ranges from as shallow as 856 ft in West Era field in Cooke County, Texas, to as deep as 25,735 ft in McComb field in Pecos County, Texas. A review of the Ellenburger Group will help explain the sedimentology and diagenesis that have resulted in this widespread producing unit.

The first inclusive studies of the Ellenburger Group were completed by Cloud et al. (1945), Cloud and Barnes (1948, 1957), and Barnes et al. (1959). These studies cover many aspects of the group, ranging from stratigraphy to diagenesis to chemistry. Much has been learned since then about carbonate sedimentology and diagenesis, and these new concepts were integrated into later studies by Kerans (1988, 1989), which cover regional geologic setting, depositional systems, facies analysis, depositional history, diagenesis, and paleokarsting. Many other papers have described the local geology of fields (e.g., Loucks and Anderson, 1980, 1985; Combs et al., 2003) and outcrop areas (e.g., Goldhammer et al., 1992; Lucia, 1995, 1996; Loucks et al., 2004) or have elaborated on paleokarsting (e.g., Lucia, 1971, 1995, 1996; Loucks and Anderson, 1985; Kerans, 1988, 1989, 1990; Candelaria and Reed, 1992; Loucks and Handford, 1992; Loucks, 1999; Loucks et al., 2004; Loucks, 2007; McDonnell et al., 2007).

Major objectives of this paper are to review (1) regional geological setting and general stratigraphy; (2) depositional systems, facies analysis, and depositional history; (3) general regional diagenesis; (4) reservoir characteristics; and (5) the petroleum

system. Many of the data are from published literature; however, new insights can be derived by integrating these data.

REGIONAL GEOLOGICAL SETTING

At global plate scale during the Early Ordovician, the West Texas Permian Basin area was located on the southwest edge of the Laurentia plate between 20° and 30° latitude (Figure 1) (Blakey, 2005a, b). The equator crossed northern Canada (Figure 1), situating Texas in a tropical to subtropical latitude (Lindsay and Koskelin, 1993). Much of the United States was covered by a shallow sea. Most of Texas was a shallow-water shelf with deeper water conditions to the south, where it bordered the Iapetus Ocean. The Texas Arch (Figures 2), a large land complex, existed in North Texas and New Mexico.

Ross (1976) and Kerans (1990) pointed out that the main depositional settings within the Permian Basin for the Ellenburger Group were the deeper water slope and the shallower water carbonate platform. Ross (1976) presented the broad Lower Ordovician carbonate platform as having an interior of dolomite and an outer area of limestone (Figure 2). Seaward of the limestone he postulated black shale. Kerans (1990) interpreted Ross's map in terms of depositional settings (Figure 3), the dolomite being a restricted shelf interior and the limestone being an outer rim of more open-shelf deposits. Seaward of the platform was a deeper water slope system (shales), which Kerans (1990) claimed to be represented by the Marathon Limestone. The Ellenburger Group in the south part of Texas, where the deeper water equivalent strata would have been, was strongly affected by the Ouachita Orogeny when the South American plate was thrust against the North American plate (Figure 2). Basinal and slope facies strata were destroyed or extensively structurally deformed. Ellenburger Group facies cannot be traced south of the slope setting in southwest Texas because of the Ouachita Orogeny.

Kerans (1990) recognized that several peripheral structural features affected deposition of Ellenburger sediments in the West Texas New Mexico area (Figure 4); however, most of the platform was relatively flat. Major structural features in the area that formed after Early Ordovician time include the Middle Ordovician Toboas Basin and the Pennsylvanian Central Basin Platform (Galley, 1958).

Structural maps of the top Ellenburger Group (Figure 5) and top Precambrian intervals (Figure 6) show the Ellenburger Group as a structural low in the area of the Permian Basin. In the Midland Basin area, the top of Ellenburger carbonate is as deep as 11,000 ft, shallower over the Central Basin Platform, and as deep as 25,000 ft in the Delaware Basin. Isopach maps (Figure 4) by the Texas Water Development Board (1972), Wilson (1993), and Lindsay and Koskelin (1993) show thickening of the Ellenburger Group into the area of the Permian Basin.

GENERAL STRATIGRAPHY

The Ellenburger Group is equivalent to the El Paso Group in the Franklin Mountains, the Arbuckle Group in northeast Texas and Midcontinent, the Knox Group in the eastern United States, and the Beekmantown Group of the northeastern United States. In West Texas the Ellenburger Group overlies the Cambrian Bliss subarkosic sandstone (Loucks and Anderson, 1980). In the Llano area, Barnes et al. (1959) divided the Ellenburger Group from bottom to top into the Tanyard, Gorman, and Honeycut Formations. Kerans (1990) compared the Llano stratigraphic section to the subsurface stratigraphy of West Texas (Figure 7). A worldwide hiatus appeared at the end of Early Ordovician deposition, creating an extensive second-order unconformity (Sauk-Tippecanoe Supersequence Boundary defined by Sloss [1963]; Figure 7). This unconformity produced extensive karsting throughout the United States and is discussed later in this paper. In West Texas, the upper Middle Ordovician Simpson Group was deposited above this unconformity (Figure 7).

A general second-order sequence stratigraphic framework was proposed by Kupecz (1992) for the Ellenburger Group in West Texas (Figure 8). The contact between the Precambrian and the Lower Ordovician intervals represents a lowstand of sea level of unknown duration; the Bliss Sandstone sediments are partly lowstand erosional deposits (Loucks and Anderson, 1985). The lower second-order transgressive systems tract includes the Bliss Sandstone and the lower Ellenburger alluvial fan to interbedded shallow-subtidal paracycles. The second-order highstand systems tracts include the upper

interbedded paracycles of peritidal deposits. The next second-order lowstand produced the Sauk-Tippecanoe sequence boundary.

A detailed sequence stratigraphy of the Lower Ordovician of West Texas (Figure 9) was worked out by Goldhammer et al. (1992), Goldhammer (1996), and Goldhammer and Lehmann (1996), who worked in the Franklin Mountains in far West Texas and who compared their work to that in other areas, including the Arbuckle Mountains in Oklahoma (Figure 9). They divided the general Lower Ordovician section, which they called the Sauk-C second-order supersequence, into nine third-order sequences (Figure 9) on the basis of higher order stacking patterns. Each third-order sequence had a duration of 1 to 10 million years. Goldhammer et al. (1992) stated that the origin and control of third-order sequences in the Lower Ordovician remain problematic because this period of time lacks evidence of major glaciation.

In the Franklin Mountains, Goldhammer et al. (1992), Goldhammer (1996), and Goldhammer and Lehmann (1996) recognized only the lower seven sequences (Figure 9), and they included the Bliss Sandstone as the lowest sequence. The sequences in this area range from 2 to 6 million years in duration. Within the third-order sequences, these researchers recognized numerous higher order sequences at the scale of fourth- and fifth-order parasequences, which are detailed depositional units that consist of meter-scale aggradational or progradational depositional cycles. This is the stratigraphic architectural scale that is used for flow-unit modeling in reservoir characterization (Kerans et al., 1994).

DEPOSITIONAL FACIES AND DEPOSITIONAL SYSTEMS

Ellenburger Platform Systems

Loucks and Anderson (1980, 1985) presented depositional models (Figures 10, 11) of the Ellenburger section in Puckett field, Pecos County, West Texas. Their data consist of two cores that provide ~1,700 ft of overlapping, continuous coverage of the section (Figure 12). They defined the lower Ellenburger section as being dominated by alluvial fan/coastal sabkha paracycles, the middle Ellenburger as subtidal paracycles, and the upper Ellenburger as supratidal/intertidal paracycles. Numerous fourth- and fifth-

order cycles occur within this Puckett Ellenburger section. These researchers recognized many solution-collapsed zones that they attributed to exposure surfaces of different duration (Figure 12).

Kerans (1990) completed the most detailed and complete regional Ellenburger depositional systems and facies analysis on the basis of wireline-log and core material. Much of the rest of this section is a summary of Kerans' work. (See Kerans [1990] for complete description and interpretation of facies.) He recognized six general lithofacies (Figure 7):

- (1) Litharenite: fan delta – marginal marine depositional system
- (2) Mixed siliciclastic-carbonate packstone/grainstone: lower tidal-flat depositional system
- (3) Ooid and peloid grainstone: high-energy restricted-shelf depositional system
- (4) Mottled mudstone: low-energy restricted-shelf depositional system
- (5) Laminated mudstone: upper tidal-flat depositional system
- (6) Gastropod-intraclast-peloid packstone/grainstone: open shallow-water-shelf depositional system

Fan Delta – Marginal Marine Depositional System

Description: Kerans (1990) noted that this system contains two prominent facies: cross-stratified litharenite and massive to cross-stratified pebbly sandstone to conglomerate. Sedimentary structures include thick trough and tabular crossbeds, parallel current lamination, and graded and massive beds. Clastic grains are composed of granite and quartzite rock fragments, feldspar, and quartz.

Interpretation: According to Kerans (1990) this unit was deposited as a fan delta – marginal marine depositional system. It is a basal retrogradational clastic deposit where the Ellenburger Group onlaps the Precambrian basement. Loucks and Anderson (1985) presented a similar interpretation of a fan-delta complex prograding into a shallow subtidal environment (Figure 11).

Lower Tidal-Flat Depositional System

Description: Kerans (1990) stated that the dominant facies are mixed siliciclastic-peloid packstone-grainstone, intraclastic breccia, stromatolitic boundstone containing silicified nodular anhydrite, ooid grainstone, and carbonate mudstone. These facies are mostly dolomitized. Kerans (1990) noted that the siliciclastic content is related to distribution of the sandstone below. Sedimentary structures include relict cross-stratification, scour channels, stromatolites, flat cryptalgal laminites, and silica-replaced evaporate nodules.

Interpretation: According to Kerans (1990) this unit was deposited in a lower tidal-flat depositional system in close association with the fan-delta depositional system (Figure 10). Upward in the section carbonate tidal flats override the fan deltas. Kerans (1990) presented the idealized cycle within this system as an upward-shoaling succession. Tidal-flat complexes prograded across subtidal shoals and intervening lagoonal muds (Figure 10). The relict evaporate nodules indicate an arid sabkha climate (Loucks and Anderson, 1985; Kerans, 1990). Kerans (1990) pointed out that thin siliciclastic sand laminae in tidal-flat laminites represent eolian deposits, whereas thicker sand units represent periodic sheetflood deposits from adjacent alluvial fans. Loucks and Anderson (1985) also recognized quartz sandstone units in the algal laminae.

High-Energy Restricted-Shelf Depositional System

Description: Kerans (1990) noted that this system is characterized by ooid grainstone; ooid-peloid packstone-grainstone; laminated, massive, and mottled mudstone; and minor cyanobacterial boundstone. It also contains coarse-crystalline white chert and rare gastropod molds. Coarse dolomite fabric is common. Depositional structures include cross-stratification, intraclastic breccias, small stromatolites, cryptalgal mats, and silicified relict nodular anhydrite.

Interpretation: According to Kerans (1990) this unit was deposited in a high-energy restricted-shelf depositional system. He stated that this system represents the period of maximum marine inundation during the Ellenburger transgression. He noted that extensive ooid shoals dominated the shelf and bioturbated mudstones formed in protected settings between shoals (Figure 11). Cryptalgal laminites and mudstones (tidal

flats) with relict evaporate nodules may mark local shoaling cycles or more extensive upward-shoaling events. Kerans (1990) noted that the lack of fauna suggests restricted circulation on the shelf produced by shoal-related restriction or by later destruction by dolomitization.

Low-Energy Restricted-Shelf Depositional System

Description: Kerans (1990) described this widespread system as a “remarkably homogeneous sequence of gray to dark-gray, fine- to medium-crystalline dolomite containing irregular mottling and lesser parallel-laminated mudstone and peloid wackestone.” He noted sparse fauna of a few gastropods and nautiloids. The facies is highly dolomitized.

Interpretation: According to Kerans (1990) this unit was deposited in a low-energy restricted-shelf depositional system (Figure 11). The mottling is considered to be the result of bioturbation. It is a restricted shelf deposit ranging from subtidal mudstones to shoaling areas with tidal flats. Kerans (1990) noted that seaward this system interfingers with the open-marine, shallow-water shelf depositional system, fitting the model of Ross (1976) (Figure 2).

Upper Tidal-Flat Depositional System

Description: Kerans (1990) noted that the dominant facies in this system is smooth and parallel or irregular and crinkled laminated dolomite. Other facies include mottled mudstone, current-laminated dolostone, and beds of intraclastic breccia. Sedimentary structures include desiccation cracks, current laminations, nodular chert (relict evaporates?), and stromatolites.

Interpretation: According to Kerans (1990) this unit was deposited in an upper tidal-flat depositional system. A common cycle is composed of a basal bioturbated mudstone passing through current-laminated mudstone and into cryptalgal laminated mudstone, with desiccation structures and intraclastic breccias (Figure 11). Kerans (1990) noted that the mottled and current-laminated mudstones intercalated with the laminites are low-energy shelf deposits and intercalated ooid-peloid grainstone beds are storm

deposits transported from high-energy shoals offshore (Figure 11). Kerans (1990) suggested that the upper tidal-flat depositional system consisted of a broad tidal-flat environment situated landward of the lagoon-mud shoal complex. This model is similar to that presented by Loucks and Anderson (1985) (Figure 11). The depositional system occurs near the top of the Ellenburger succession.

Open Shallow-Water-Shelf Depositional System

Description: Kerans (1990) noted that the rocks in this system are mainly limestone, which is in contrast to many of the other sections of the Ellenburger interval. Facies include peloid and ooid grainstones, mollusk-peloidal packstones, intraclastic breccias, cryptalgal laminated mudstones, digitate stromatolitic boundstones, bioturbated mudstones, and thin quartzarenite beds. Again, in general contrast to the other depositional systems, this system has abundant fossils, including sponges, trilobites, gastropods, bivalves, and cephalopods. Kerans (1990) described the grainstones and packstones as massive or displaying parallel current laminations. He noted abundant desiccation cracks in the laminites, as well as fenestral fabric.

Interpretation: According to Kerans (1990) this unit was deposited in an open, shallow-water-shelf depositional system. He described the depositional setting as a complex mosaic of tidal-flat subenvironments, shallow-water subtidal carbonate sand bars, and locally thin stromatolite bioherms and biostromes (Figure 11). He interpreted the greater diversity of fauna, lack of evaporate evidence, and presence of high-energy grainstones and packstones as suggesting a moderate-current energy environment with open-marine circulation. He speculated that this system may have occurred close to the shelf edge or slope break.

Marathon Limestone Deeper Water System

The Marathon Limestone is the time-equivalent, deeper water slope facies of the Ellenburger shallow-water-platform facies (Berry, 1960; Young, 1968; Ross, 1982; Kerans, 1990). In West Texas, it occurs in the Marathon Basin (Young, 1968) and on the west margin of the Diablo Platform (Lucia, 1968, 1969).

Description: Kerans (1990) described the unit as containing graptolite-bearing shale, siliciclastic siltstone, lime grainstone and lime mudstone, and debris-flow megabreccia. Sedimentary structures consist of graded beds, horizontal laminations, sole marks, flute casts, and soft-sediment deformation structures (slump folds).

Interpretation: According to Kerans (1990) this unit was deposited in a more basinal setting than the laterally equivalent Ellenburger depositional systems. He defined the setting as a distally steepened ramp. He recognized that the thin-bedded shale, siltstone, and lime grainstone-mudstone packages are Bouma turbidite sequences produced by turbidity currents on a deeper water slope. Both Young (1968) and Kerans (1990) interpreted the massively bedded megabreccias as deeper water debris-flow deposits.

General Depositional History of the Ellenburger Group

Kerans (1990) summarized the depositional history of the Ellenburger Group in four stages (Figure 13).

Stage 1: Marked by retrogradational deposition of fan delta – marginal marine depositional system continuous with Early Cambrian transgression (Kerans, 1990). Kerans (1990) described interfingering of the basal siliciclastics with overlying tidal-flat and shallow-water subtidal deposits of the lower tidal-flat depositional system. This transition represents initial transgression and associated retrogradational sedimentation. Kerans (1990) noted that this stage was followed by regional progradation and aggradation of peritidal carbonate facies. This stage of deposition filled in existing paleotopography resulting in a low-relief platform.

Stage 2: Kerans (1990) documented rapid transgression and widespread aggradational deposition of the high-energy, restricted-shelf depositional system across much of West and Central Texas during this stage. He noted that the transgression produced an extensive carbonate sand sheet over much of the platform. He interpreted a moderately hypersaline setting on the basis of rare macrofauna, evidence of evaporites, and abundance of ooids.

Stage 3: Kerans (1990) stated that upward transition from the high-energy, restricted-shelf depositional systems to the low-energy, restricted-shelf depositional

systems is evidence of a second regression across the Ellenburger shelf. Progradation during this stage is marked by transition of landward upper tidal flats to more seaward, low-energy, restricted subtidal to intertidal facies to farthest seaward, open-marine, shallow-water-shelf facies. Kerans (1990) recognized that laminated mudstones of the upper tidal-flat depositional system represent maximum regression across the Ellenburger inner shelf.

Stage 4: Near the end of the Early Ordovician there was a worldwide eustatic lowstand, the timing of which is reported to be Whiterockian in age (Sloss, 1963; Ham and Wilson, 1967), and whose length of exposure covered several million years. Throughout the United States, an extensive karst terrain formed on the Ellenburger platform carbonates (Kerans, 1988, 1989, 1990). During this long period of exposure, thick sections of cave developed, resulting in extensive paleocave collapse breccias within the Ellenburger section (Lucia, 1971; Loucks and Anderson, 1980, 1985; Kerans, 1988, 1989, 1990; Wilson et al., 1992; Loucks 1999). The time-equivalent, slope-deposited Marathon Limestone was not exposed during this sea-level drop (Kerans, 1990). The area appears to have had continuous deposition from the Early Ordovician through the Middle Ordovician.

GENERAL REGIONAL DIAGENESIS

Diagenesis of the Ellenburger Group is complex, and the processes that produced the diagenesis covered millions of years (e.g., Folk, 1959; Lucia, 1971; Loucks and Anderson, 1985; Lee and Friedman, 1987; Kerans, 1988, 1989, 1990; Kupecz and Land, 1991; Amthor and Friedman, 1991; Loucks, 1999, 2003). Several studies have presented detailed diagenetic analysis of the Ellenburger (Kerans, 1990; Kupecz and Land, 1991; Amthor and Friedman, 1991). A paragenetic chart is presented in Figures 14. Three major diagenetic processes are important to discuss: (1) dolomitization, (2) karsting, and (3) tectonic fracturing. Other diagenetic features are present but do not impact the appearance or reservoir quality of the Ellenburger as much as these three do. In the following discussion of these diagenetic processes, only an overview will be presented,

and the reader is referred to literature on Ellenburger diagenesis for a complete and detailed discussion.

Understanding Diagenesis in the Ellenburger Group

As stated earlier, diagenesis of the Ellenburger Group is complex. Detailed diagenesis can be worked out for any location, but trying to explain the complete diagenetic history for the entire Ellenburger carbonate section in West Texas may be beyond our reach because of relatively sparse subsurface data, length of time (± 20 million years), thick stratigraphic section (possibly as many as six third-order sequences), and the large area involved. Remember that carbonates generally undergo diagenesis early in their history, especially if they are subjected to meteoric water. With the number of third-order sequences in the section and the time represented by each sequence (2 to 5 million years), extensive early and shallow diagenesis probably occurred but was later masked by intense dolomitization.

At the end of Early Ordovician time, a several-million-year hiatus occurred, exposing the Ellenburger Group and subjecting it to meteoric karst processes. Several authors have demonstrated that the karst affected strata at least 300 to 1,000 ft beneath the unconformity (e.g., Kerans 1988, 1989; Lucia, 1995; Loucks, 1999). With the occurrence of Ouachita thrusting from the Mississippian through the Pennsylvanian, vast quantities of hydrothermal fluids moved through available permeable pathways within the Ellenburger, producing late-stage diagenesis (e.g., Kupecz and Land, 1991). Following lithification, different parts of the Ellenburger Group were subjected to tectonic stresses, producing fractures and more late-stage diagenesis, which probably affected local areas (e.g., Loucks and Anderson, 1985; Kearns, 1990; Loucks, 2003).

Loucks (2003) presented an overview of the origins of fractures in Ordovician strata and concluded that in order to explain the complex diagenesis in these strata, one must sort all events into a well-documented paragenetic sequence—the most reliable method of delineating timing of events and features. He demonstrated that karsting and paleocave collapse breccias and related fractures and some tectonic fractures had occurred before the hydrothermal events that had produced saddle dolomite. But first he had to establish well-documented paragenetic relationships.

Dolomitization

Of the several authors (Kerans, 1990; Kupecz and Land, 1991; Amthor and Friedman, 1991) that have attempted to understand the regional dolomite history, Kupecz and Land (1991) appear to have made the most progress. This section will mainly address findings of Kupecz and Land (1991) but will still include observations and conclusions from the other authors. Kupecz and Land's (1991) paragenetic sequence is presented in Figure 14. Their study covered a large area of West Texas, as well as the Llano Uplift area in Central Texas. They used both cores and outcrop as a data source and combined petrography with carbon, oxygen, and strontium isotopes.

Kupecz and Land (1991) recognized five general stages of dolomitization (Figure 14). Generations of dolomite were separated into early-stage dolomitization, which predated the Sauk unconformity, and late-stage dolomitization, which postdated the Sauk unconformity. They attributed 90% of the dolomite as early stage and 10% as late stage.

Kupecz and Land (1991) Dolomite Types:

- (1) Stage 1 prekarstification early-stage dolomite (Dolomite E1)
 - a. Description: Crystal size ranges from 5 to 700 m but varies by facies. In cryptalgal laminites crystal sizes range from 5 to 100 m. These euhedral crystals have planar interfaces. In millimeter-laminated facies crystal size ranges from 5 to 70 m and in the bioturbated mudstones crystal size ranges from 5 to 700 m. Kupecz and Land (1991) thought that some of the coarser crystals were a product of later recrystallization.
 - b. Interpretation: Kupecz and Land (1991) documented that this dolomite replaced lime mud or mudstone and that the dolomite predated karstification because it is found in nonkarsted rock as well as in clasts created by karsting. Therefore, it must have formed before karsting for it to have been brecciated. Probable source of Mg for dolomitization is seawater (Kupecz and Land, 1991).
- (2) Stage 2 postkarstification late-stage dolomite (Dolomite L1)

- a. Description: This replacement dolomite consists of coarse-crystalline euhedral rhombs with crystal size ranging from 200 to 2,000 m. Its homogeneous cathodoluminescence and homogeneous backscattered imaging suggest that this dolomite type has undergone recrystallization (Kupecz and Land, 1991). This stage of dolomitization is a regional event and is related to hydrothermal fluids.
 - b. Interpretation: Late-stage origin is based on coarse-crystal size (Kupecz and Land, 1991).
- (3) Stage 3 postkarstification late-stage dolomite (Dolomite L2)
- a. Description: Crystals have planar interfaces, sizes range from 100 to 3,500 m and crystals have subhedral to anhedral shapes. Extinction ranges from straight to undulose.
 - b. Interpretation: This stage is a replacement type of dolomite (Kupecz and Land, 1991). Late origin is based on relationship to a later stage chert and its replacement of early-stage dolomite E1. Much of the grainstone facies is replaced by this stage of dolomitization, which is related to hydrothermal fluids. Probable source of Mg for dolomitization is dissolution of previously precipitated dolomite (Kupecz and Land, 1991).
- (4) Stage 4 postkarstification late-stage dolomite (Dolomite C1)
- a. Description: Crystals are subhedral with undulose extinction (saddle/baroque dolomite), and sizes range from 100 to 5,000 m.
 - b. Interpretation: Pore-filling cement (Kupecz and Land, 1991). Paragenetic sequence is established by the fact that Dolomite C1 postdates Dolomite L2 and was corroded before Dolomite C 2 was precipitated. Probable source of Mg for dolomitization is dissolution of previously precipitated dolomite (Kupecz and Land, 1991). This stage of dolomitization is a regional event and is related to hydrothermal fluids.
- (5) Stage 5 postkarstification late-stage dolomite (Dolomite C2)
- a. Description: Subhedral white crystals with moderate to strong undulose extinction (saddle/baroque dolomite), and crystal sizes range from 100 to 7,500 m. Contain abundant fluid inclusions.

- b. Interpretation: Pore-filling cement (Kupecz and Land, 1991). Occurred after corrosion of Dolomite C1. Probable source of Mg for dolomitization is dissolution of previously precipitated dolomite (Kupecz and Land, 1991). This stage of dolomitization is related to hydrothermal fluids.

Kupecz and Land (1991) provided the only integrated analysis of fluid-flow pathways and sources of Mg for the different dolomitizing events. Early-stage prekarstification dolomite is associated with muddier rocks, and the source of Mg was probably seawater. Kerans (1990) similarly attributed these finer crystalline dolomites to penecontemporaneous replacement of mud in tidal flats and to regionally extensive reflux processes during deposition.

Late-stage postkarstification dolomites are attributed by Kupecz and Land (1991) to warm, reactive fluids, which were expelled from basal shales during the Ouachita Orogeny. The fluids are thought to have been corrosive, as evidenced by corroded dolomite rhombs (Kupecz and Land, 1991). This corrosion provided the Mg necessary for dolomitization. The warm, overpressured fluids were episodically released and migrated hundreds of miles from the foldbelt toward New Mexico (Figure 15). These fluids migrated through high-permeability aquifers of the Bliss Sandstone, basal subarkose facies of the Ellenburger, as well as grainstone facies and paleocave breccia zones. Figure 15 from Kupecz and Land (1991) shows the regional isotopic composition of late-stage Dolomite L2. The pattern of lighter to heavier $\delta\text{-O}^{18}$ away from the foldbelt to the south suggests movement and cooling of fluids to the northwest. Kupecz and Land's (1991) regional dolomitization model is displayed in Figure 15. Figure 16 shows the tectonic setting that produced the hydrothermal fluids.

Kerans (1990) defined three major styles of dolomitization:

- (1) Very fine crystalline dolomite that he considered as a replacement product penecontemporaneous with deposition in a tidal-flat setting.
- (2) Fine- to medium-crystalline dolomite appearing in all facies and that contributed to regionally extensive reflux processes during Ellenburger deposition.
- (3) Coarse-crystalline replacement mosaic dolomite and saddle (baroque) dolomite associated with burial.

Kerans' first two types of dolomite are probably equivalent to Kupecz and Land's (1991) early-stage Dolomite E1. His coarse-crystalline replacement mosaic dolomite and saddle dolomite are equivalent to Kupecz and Land's (1991) late-stage dolomites.

Amthor and Friedman (1991) also recognized early- to late-stage dolomitization of the Ellenburger Group (Figures 17, 18). Similar to Kerans (1990) and Kupecz and Land (1991), Amthor and Friedman (1991) described early-stage, low-temperature, fine-crystalline dolomites associated with lime muds, where the Mg was supplied by diffusion from overlying seawater. Amthor and Friedman (1991) also described medium- to coarse-crystalline dolomite that replaced grains and matrix in the depth range of 1,500 to 6,000 ft. These dolomites are postkarstification and are probably replacement Dolomite L1 and L2 of Kupecz and Land (1991). Amthor and Friedman's (1991) last stage of dolomite is assigned a deep-burial origin (>6,000 ft) and consists of coarse-crystalline saddle dolomite. Its occurrence is both pore filling and replacive, and it is Dolomite L2, C1, and C2 of Kupecz and Land (1991). Amthor and Friedman (1991) also noticed extensive corrosion of previously precipitated dolomite, and they invoked a fluid-flow model similar to that of Kupecz and Land (1991), in which fluids were associated with the Ouachita Orogeny.

Overall, much of the Ellenburger is dolomitized. Dolomitization favors preserving open fractures and pores because it is mechanically and chemically more stable than limestone. Pores within dolomites are commonly preserved to deeper burial depths and higher temperatures than those of pores in limestone. Also, limestone breccia clasts tend to undergo extensive pressure solution at their boundaries and lose all interclast pores (Loucks and Handford, 1992), whereas dolomite breccia clasts are more chemically and mechanically stable with burial.

Karsting

Karsting is a complex, large-scale diagenetic event that strongly affected the Ellenburger Group. The process may affect only the surface of a carbonate terrain, forming *terra rosa*, or extensively dissolve the carbonate surface, creating karst towers (Figure 19). It can also produce extensive subsurface dissolution in the form of dolines,

caves, etc. (Figure 19). The next several paragraphs are meant to provide a background on karst systems that are seen in the Ellenburger Group.

Review of Caves and Paleocaves

Loucks (1999) provided a review of paleocave carbonate reservoirs. He stressed that to understand the features of paleocave systems, an understanding of how paleocave systems form is necessary. The best approach to such an understanding is to review how modern cave systems form at the surface and evolve into coalesced, collapsed-paleocave systems in the subsurface. Loucks (1999) described this evolutionary process, and the review presented here is mainly from that investigation.

To describe the features or elements of both modern and ancient cave systems, Loucks (1999) proposed a ternary classification of breccias and clastic deposits in cave systems based on relationships between crackle breccia, chaotic breccia, and cave-sediment fill (Figure 20). Crackle breccias have thin fractures separating breccia clasts. Individual clasts can be fitted back together. Mosaic breccias are similar to crackle breccias, but displacement between clasts is greater and some clast rotation is evident. Chaotic breccias are characterized by extensive rotation and displacement of clasts. The clasts can be derived from multiple horizons, producing polymictic breccias. Chaotic breccias grade from matrix-free, clast-supported breccias to matrix-supported breccias.

Loucks (1999) also showed that paleocave systems have complex histories of formation (Figure 21). They are products of near-surface cave development, including dissolutional excavation of passages, breakdown of passages, and sedimentation in cave passages. These are followed by later-burial cave collapse, compaction, and coalescence.

Phreatic or vadose-zone dissolution creates cave passages (Figures 19, 21). Passages are excavated where surface recharge is concentrated by preexisting pore systems, such as bedding planes or fractures (Palmer, 1991), that extend continuously between groundwater input, such as sinkholes, and groundwater output, such as springs (Ford, 1988).

Cave ceilings and walls are under stress from the weight of overlying strata. A tension dome—a zone of maximum shear stress—is induced by the presence of a cavity (White, 1988), and stress is relieved by collapse of the rock mass within the stress zone,

which commonly starts in the vadose zone. In the phreatic zone, water supplies 40% of the ceiling support through buoyancy (White and White, 1968). Removal of this support in the vadose zone weakens the ceiling and can result in its collapse. Major products of collapsed ceiling and walls are chaotic breakdown breccia on the floor of the cave passage (Figures 19, 21). In addition, stress release around cave passages produces crackle breccias in cave-ceiling and cave-wall host rocks (Figures 19, 21).

Near-surface dissolutional excavation and cave sedimentation terminate as cave-bearing strata are buried into the subsurface. Extensive mechanical compacting begins, resulting in collapse of remaining passages and further brecciation of blocks and slabs (Figure 21). Multiple stages of collapse occur over a broad depth range, and foot-scale bit drops (cavernous pores) are not uncommon at depths of 6,000 to 7,000 ft (Loucks, 1999). The areal cross-sectional extent of brecciation and fracturing after burial and collapse is greater than that of the original passage (Figure 21). Collapsed, but relatively intact, strata over the collapsed chamber are fractured and form burial cave-roof crackle and mosaic breccias with loosely to tightly fitted clasts (Figure 21). Sag feature and faults (suprastratal deformation) can occur over collapsed passages (Figure 21) (Lucia, 1971, 1995, 1996; Kerans, 1988, 1989, 1990; Hardage et al., 1996; Loucks, 1999, 2003, 2007; McDonnell et al., 2007).

Development of a large collapsed paleocave reservoir is the result of several stages of development (Figure 22). The more extensive coalesced, collapsed-paleocave system originated at composite unconformities, where several cave systems may overprint themselves during several million years of exposure to karst processes (Figure 22) (Esteban 1991; Lucia, 1995; Loucks, 1999). As the multiple-episode cave system subsides into the deeper subsurface, wall and ceiling rock adjoining open passages collapses and forms breccias that radiate from the passage and may intersect with fractures from other collapsed passages and older breccias within the system. This process forms coalesced, collapsed-paleocave systems and associated reservoirs that are hundreds to thousands of feet across, thousands of feet long, and tens to hundreds of feet thick. Internal spatial complexity is high, resulting from the collapse and coalescing of numerous passages and cave-wall and cave-ceiling strata. These breccias and fractures are commonly major reservoirs in the Ellenburger Group. The reader is referred to

Kerans (1988, 1989, 1990), Loucks and Handford (1992), Hammes et al. (1996), and Loucks (1999, 2001, 2003) for discussions about paleocave systems in the Ellenburger Group.

Loucks and Mescher (2001) developed a classification of paleocave facies (Figure 23, Table 1). Six basic cave facies are recognized in a paleocave system and are classified by rock textures, fabrics, and structures: (1) undisturbed strata (undisturbed host rock), (2) disturbed strata (disturbed host rock), (3) highly disturbed strata (collapsed roof and wall rock), (4) coarse chaotic breccia (collapsed-breccia cavern fill), (5) fine chaotic breccia (transported-breccia cavern fill), and (6) sediment fill (cave-sediment cavern fill). Each paleocave facies can be distinct and adjoin sharply with adjacent facies, or they may show gradation into adjacent facies within the coalesced, collapsed-paleocave system. Pore networks associated with paleocave reservoirs can consist of cavernous pores, interclast pores, crackle- and mosaic-breccia fractures, tectonic fractures, and, less commonly, matrix pores. The paleocave facies classification, in conjunction with burial-history data, can be used to describe the complex geology expressed in coalesced, collapsed-paleocave systems and can be used to explain and predict pore-type distribution and magnitude of reservoir quality.

Table 1. Summary of general paleocave facies. From Loucks and Mescher (2001).

Cave Facies	Interpretation	Description	Pore System/ Reservoir Quality
Undisturbed strata	Undisturbed host rock	Excellent bedding continuity for hundreds to thousands of feet.	Minor matrix and fracture pores. $\phi < 3\%$ to 5% $K < \text{few millidarcys}$
Disturbed strata	Disturbed host rock	Bedding continuity is high but folded and offset by small faults. Commonly overprinted with crackle and mosaic brecciation.	Minor matrix pores and crackle to mosaic fracture pores. $\phi < 5\%$ K is as much as tens of millidarcys
Highly disturbed Strata	Collapsed host rock (cave-roof and cave-wall rock) over passages	Highly disturbed, very discontinuously bedded strata with pockets and layers of chaotic breccia. Small-scale folding and faulting are common. Commonly overprinted with crackle and mosaic brecciation.	Localized pockets or layers of breccia might have porosities in the range of 5% to 15% and permeabilities in the tens to hundreds of millidarcys.
Coarse chaotic breccia	Collapsed-breccia cavern fill	Mass of very poorly sorted, granule- to boulder-sized chaotic breccia clasts 1 to 10 ft long. Commonly clast supported but can contain matrix material. Ribbon- to tabular-shaped body as much as 45 ft across and hundreds of meters long.	Abundant interclast pores. Porosity can exceed 20% , and permeability can be in the darcys.
Fine chaotic breccia	Transported-breccia cavern fill	Mass of clast-supported, moderately sorted, granule- to cobble-sized clasts with varying amounts of matrix. Clasts can be imbricated or graded. Ribbon- to tabular-shaped body as much as 45 ft across and hundreds of feet long.	Abundant interclast pores. Porosity can exceed 20% , and permeability can be in the darcys.
Sediment fill	Cave-sediment cavern fill	Carbonate and/or siliciclastic debris commonly with sedimentary structures.	Siliciclastic fill is commonly tight. Carbonate fill might be permeable.

Ellenburger Karsting

In the Ellenburger Group, extensive cave systems formed at a composite unconformity (Sauk unconformity) that lasted several million years to several tens of million years. Many authors have recognized this karsting and associated features in the Ellenburger Group. Barnes et al. (1959) recognized solution collapse in the Ellenburger

Group, stating that "... a matrix composed of material foreign to the formation indicates breccia formed by solution and collapse probably related to an erosional unconformity." Lucia (1971) was the first to promote that the extensive brecciation seen in the El Paso Group (equivalent to the Ellenburger Group) was associated with karst dissolution and was not the result of tectonic brecciation. Loucks and Anderson (1980, 1985) in Puckett field in Pecos County also realized that many of the breccias in the Ellenburger Group were related to solution collapse (Figure 11). They associated them with exposed diagenetic terrains. Kerans (1988, 1989, 1990) strongly established karsting and cave development in the Ellenburger Group. He proposed paleocave models (Figure 24) that were immediately accepted and applied.

Lucia's (1971, 1995, 1996) work in the El Paso Group in the Franklin Mountains of far West Texas presents an excellent outcrop analog for coalesced, collapsed-paleocave systems. He mapped a large paleocave system that was developed in the upper 1,000 ft of the El Paso Group during a 33-m.y. time gap (Figures 25, 26). Large fracture systems and collapse-breccia zones 1,000 ft thick, 1,500 ft wide, and >1 mi long mark the collapsed-paleocave system. Lucia (1995) noted that the cavernous porosity could have been as high as 30% before infilling with cave-sediment fill and cement.

Within the southern Franklin Mountains, Lucia (1995) described the Great McKelligon Sag in McKelligon Canyon along the eastern face (Figure 27). The sag, ~1,500 ft wide and ~150 ft deep, formed by collapse of paleocaves in the El Paso section after the Montoya and Fusselman units were deposited, buried, and lithified. It is an important feature that paints a complete picture of a coalesced, collapsed-paleocave system (Loucks, 1999). Hardage et al. (1996), Loucks (2003), and McDonnell et al. (2007) all stressed that collapse of a coalesced-paleocave system not only affects the karsted unit, but also strongly affects the units above (Figure 22). Loucks (2003) called the deformation of younger lithified units "suprastratal deformation." Besides the example of suprastratal deformation shown in the Great McKelligon Sag, examples of suprastratal deformation from seismic in the Ellenburger Group can be seen in Hardage et al. (1996), Loucks (1999, 2003), and McDonnell et al. (2007) and from wireline-log cross sections by Kerans (1989) (his Figure 25).

Kerans (1988, 1989, 1990) presented an excellent overview of paleokarst in the Ellenburger Group. His paleocave models (Figure 24) were the first to define paleocave floor, paleocave sediment fill, and paleocave roof. Figures 28 through 32 present several cores and associated core slabs from collapsed-paleocave systems, which emphasize Kerans' paleocave model. Paleocave terrigenous-bearing sediment fill is strikingly apparent from gamma-ray, spontaneous potential, and resistivity logs (Kerans, 1988, 1989, 1990). Paleocave fabrics can also be recognized on electrical imaging tools (Hammes, 1997). Kerans (1988, 1989) discussed several breccia types, including (1) a laterally persistent breccia association formed in the upper phreatic zone (water table) karst and (2) a laterally restricted breccia association formed by deep phreatic dissolution and collapse.

Kerans (1990), in his sequence of diagenetic events (his Figure 37), noted that the Ellenburger section had been subjected to karsting during several periods of time. The main karst event was at the Early Ordovician Sauk-Tippecanoe Supersequence boundary. In local areas it was karsted several more times. In the Llano area of Texas, Kupecz and Land (1991) showed that the Ellenburger stayed near the surface until deep burial during Later Pennsylvanian subsidence (Figure 33A). Loucks et al. (2000) recognized conodonts in cave-sediment fill from paleocaves in the Llano that would indicate exposure during the Middle to Late Ordovician, Late Devonian, and Earliest Mississippian times. Also, they established other strong periods of karsting during Pennsylvanian, Cretaceous, and Tertiary times. Combs et al. (2003) noted a second period of karsting in the Ellenburger interval in Barnhart field in Reagan County, where the Wolfcamp clastic overlies the Ellenburger Group. Their burial-history diagram (Figure 33B) displays the two periods of karsting.

Tectonic Fracturing

In the past there has been controversy on the origin of many of the breccias and fractures in the Ellenburger Group. Some workers (e.g., Ijirighoi and Schreiber, 1986) wanted to assign most, if not all, fractures and breccias to a tectonic origin. They thought that faulting could produce these widespread breccias. The extensive size and shape of

most Ellenburger breccias and the inclusion of cave-sediment fill, speleothems, and younger conodonts preclude a simple tectonic origin (Loucks, 2003).

However, several authors have noted tectonic fractures in the Ellenburger section (e.g., Loucks and Anderson, 1985; Kerans, 1989; Holtz and Kerans, 1992; Combs et al., 2003). Each of these authors recognized that tectonic fractures cut across lithified breccias. Kerans (1989) noted the fractures cutting late saddle dolomite and suggested that the Pennsylvanian foreland deformation that affected much of West and Central Texas, as described by Budnik (1987), probably produced many tectonic-related fractures. However, as pointed out by many authors, paleocave collapse can also produce fractures that are not associated with tectonic events. Kerans (1990), Lucia (1996), and Loucks (1999, 2003) showed that suprastratal deformation above collapsing paleocave systems can create sags, faults, and numerous fractures (Figure 22).

Kerans (1989) pointed out several distinct ways to separate karst-related fractures from tectonic-related fractures:

- (1) Tectonic fractures are commonly the youngest fractures in the core and generally crosscut karst-related fractures.
- (2) Tectonic fractures postdate saddle dolomite. In the Llano area, however, saddle dolomite fills in a well-developed Pennsylvanian fracture set (Loucks, 2003).
- (3) Karst-related fractures are generally near the top of the Ellenburger section, whereas tectonic-related fractures can occur throughout the Ellenburger section.

Loucks and Mescher (1998) presented additional criteria for separating karst-related fractures from tectonic-related fractures:

- (1) Tectonic fractures generally show a strong relationship to regional stress patterns and have well-defined, oriented sets of fractures, whereas karst-related fractures respond to near-field stresses and fracture orientation is more random than tectonic fractures.
- (2) Regional tectonic fractures are generally spaced at >1-inch scale and commonly at 1-ft or larger scale. Karst-related fractures (crackle-breccia fractures) can be closely spaced—only a fraction of an inch apart.
- (3) Breccias associated with tectonic-derived faults commonly form a narrow band around the fault only a few feet wide but may be tens of feet wide. Karst-related

breccias can be thousands of feet wide and hundreds of feet thick, contain a large range of clast sizes, and show hydrodynamic sedimentary structures in the sediment fill.

- (4) Tectonic faults are linear or curved in map view. Karst-related faults are linear, curved, or cylindrical (Hardage et al., 1996; Loucks, 1999, McDonnell et al., 2007) in map view.

Tectonic- and karst-related fractures are both present in the Ellenburger section. Detailed analysis of the fractures can commonly define their origin.

RESERVOIR CHARACTERISTICS

Pore Types

Pore networks in the Ellenburger are complex because of the amount of dolomitization, brecciation, and fracturing associated with karsting and regional tectonic deformation. Pore networks can consist of any combination of the following pore types, depending on depth of burial (Loucks, 1999): (1) matrix, (2) cavernous, (3) interclast, (4) crackle-/mosaic-breccia fractures, or (5) tectonic-related fractures.

Loucks (1999) presented an idealized plot of how karst-related Ellenburger pore networks probably change with depth (Figure 34). Relative abundance of pore types and relative depth of burial are estimates based on review of near-surface modern cave systems and buried paleocave systems (see Table 2 in Loucks, 1999). Large voids may be preserved down to 8,000 to 9,000 ft of burial, but they eventually collapse, forming smaller interclast pores and fractures associated with crackle and mosaic breccias. Coarse-interclast pores between large clasts are reduced by rotation of clasts to more stable positions and by rebrecciation of clasts to smaller fragments (Figure 21). As passages and large interclast pores in the cave system collapse, fine-interclast pores first increase and then decrease, whereas fracture pore types become more abundant. Cave-sediment fill is commonly cemented tight during burial diagenesis in the Ellenburger carbonates, especially if it is terrigenous sediment or it has a terrigenous sediment component. In the Ellenburger carbonates, matrix porosity is generally low (<5%), consisting of common matrix pore types such as interparticle, moldic, intercrystalline, or

micropores. See Table 1 (Loucks and Mescher, 2001) for a general estimate of reservoir quality by paleocave facies types.

Three-Dimensional Architecture of an Ellenburger Coalesced, Collapsed-Paleocave System

The three-dimensional, interwell-scale architecture of a Lower Ordovician Ellenburger coalesced, collapsed-paleocave system was constructed through integration of 7.8 mi of ground-penetrating radar (GPR), 29 shallow cores (~50 ft long), and outcrop data within a large quarry (McMechan et al., 1998, 2002; Loucks et al., 2000; Loucks et al., 2004). Data were collected near Marble Falls in Central Texas over an area (~2,600 × ~3,300 ft) that could cover several oil-well locations (~160 ac) typical of a region such as West Texas (Figure 35). Integration of core-based facies descriptions with GPR-reflection response identified several paleocave facies that could be deciphered and mapped using GPR data alone (Figure 36): (1) continuous reflections image the undisturbed strata, (2) relatively continuous reflections (more than tens of feet) characterized by faults and folds image the disturbed strata, and (3) chaotic reflections having little to no perceptible continuity image heterogeneous cave-related facies recognized in core that cannot be individually resolved with GPR data. These latter facies include highly disturbed strata, coarse-clast chaotic breccia, fine-clast chaotic breccia, and cave-sediment fill.

The three-dimensional architecture of the coalesced, collapsed-paleocave system based on core and GPR data indicates that trends of brecciated bodies are as much as 1,100 ft wide, >3300 ft long, and tens of feet high (Figures 37, 38). These brecciated bodies are coalesced, collapsed paleocaves. Between the brecciated bodies are areas of disturbed and undisturbed host rock that are jointly as much as 660 ft wide. Representative cores from the study are presented in Figure 39.

As a cave system is buried, many structural features form by mechanical compaction, and these features, including folds, sags, and faults, were documented in the study by McMechan et al. (1998, 2002) and Loucks et al. (2004). Folds and sags measure from ~10 ft to several hundred feet wide. Collapse-related faults are numerous and can have several feet of throw. Most are normal faults, but some reverse faults also occur. See

Figures 40 to 43 for examples of collapsed-paleocave features from GPR and outcrop data.

Megascale Architecture

Coalesced, collapsed-paleocave systems are megascale geologic features that can have dimensions of hundreds to thousands of square miles laterally and several thousand feet vertically (Loucks, 1999, 2003). Strata above and below the unconformity are affected by late collapse in the subsurface (Figure 22).

A coalesced, collapsed-paleocave system can be divided into two parts (Loucks, 2007): (1) a lower section of karsted strata that contains collapsed paleocaves and (2) an upper section of strata that is deformed to various degrees (suprastratal deformation) by the collapse and compaction of the lower section of paleocave-bearing strata (Figure 22). The collapse and compaction of cave systems provide the potential for development of large-scale fracture/fault systems that can extend from the collapsed interval upward several thousand feet. These fracture/fault systems are not related to regional tectonic stresses.

Both Kerans (1990) and Loucks (1999, 2007) speculated that the regional pattern of karsted Ellenburger reservoirs probably follows a rectilinear pattern as a result of regional fractures controlling cave development. Loucks (1999) presented data from subsurface seismic and from mining areas that express the rectilinear pattern of paleocave systems (Figure 44). Lucia (1995) presented a map of the paleocave system in the El Paso Group that also displays a rectilinear pattern (Figure 26). The coalesced brecciated bodies mapped by Loucks et al. (2004) in the Marble Falls area are rectilinear (Figure 37). At a larger scale, Canter et al. (1993) showed a regional isopach map of Ellenburger paleocave sediments over tens of square miles (Figure 45) having a strong rectilinear pattern. Also, a modified map of Hardage et al. (1996) of rectilinear suprastratal deformation trends, associated with Ellenburger subsurface paleocave collapse, in Wise County, Texas, lines up in a rectilinear pattern (Figure 46). A later study of this area by McDonnell et al. (2007) presents this pattern as well, but in more detail. Strong evidence therefore suggests that coalesced, collapsed-paleocave systems have rectilinear patterns that may be associated with regional fracture systems. However, at present no definitive study has

shown an actual regional paleofracture system that has controlled these rectilinear patterns.

HYDROCARBON PRODUCTION

Holtz and Kerans (1992) estimated that the original in-place oil in the Lower Ordovician strata had been ~11 million barrels of oil equivalent (MMboe), 3.8 MMboe of which had been produced at the time of their article. Production from the Ellenburger since 1970 from Railroad Commission of Texas files has been 488.5 million barrels (MMbbl) of oil and 13.5 trillion cubic feet (Tcf) of gas (personal communication from Romulo Briceno, Bureau of Economic Geology). Total hydrocarbons produced are 2, 249 billion barrels of oil equivalent (Bboe).

Holtz and Kerans (1992) tabulated 149 oil and/or gas reservoirs that each has produced >1 MMbbl of oil equivalent. According to Railroad Commission of Texas files, there are approximately 700 fields of various sizes within the Ellenburger Group in Texas (personal communication from Romulo Briceno, Bureau of Economic Geology).

Holtz and Kerans (1992) divided Ellenburger reservoirs into three groups (Figure 47):

- (1) Karst-modified reservoirs: Reservoirs formed in the inner-ramp depositional setting and affected by extensive dolomitization and karsting. Karst-related fractures and interclast pores are the main pore types, with tectonic fractures secondary. These reservoirs are characterized by moderately thick net pay, low porosity, moderate permeability, low initial water saturation, and moderate residual oil saturation.
- (2) Ramp carbonates: Reservoirs formed in middle- to outer-ramp depositional settings and dolomitized to various degrees. Predominant pores types are intercrystalline and interparticle, with tectonic and karst fractures being secondary. These reservoirs are characterized by thinnest net pay, highest porosity, moderate permeability, highest initial water saturation, and highest residual oil saturation.
- (3) Tectonically fractured dolomites: Reservoirs formed in the inner-ramp depositional environment, subsequently extensively dolomitized, karsted, and,

lastly, extensively tectonically fractured. Tectonic-related fractures are the dominant pore type, and the other pore types are commonly fractures. These reservoirs are characterized by the thickest net pay, lowest porosity, lowest permeability, and lowest initial water saturation.

Tables 2 and 3 from Holtz and Kerans (1992) summarize geologic and reservoir traits of each group. Note that Ellenburger reservoirs generally have low porosities (a few percent) and fair permeabilities (one to a few hundred millidarcys). The low porosities and fair permeabilities are the result of permeability being related to fracture-type pores. Figure 48 shows field averages of porosity and permeability for a number of Ellenburger fields. Average porosities are low, whereas permeabilities are fair. This relationship is the result of karst-related fracture pores. Figure 49 is a histogram of productive (past and present) wells drilled into the Ellenburger Group. Producing wells show a range from 856 ft (Originala Petroleum #1 Gensler well in Archer County, Texas) to 25,735 ft (Exxon Mobil McComb Gas Unit B well in Pecos County, Texas). A recent review of Texas oil fields by Dutton et al. (2005) states that the Karst-Modified Reservoir play had produced ~1.5 Bbbl of oil and the Ellenburger Ramp Carbonate play had produced ~164 MMbbl of oil as of 2005.

Figure 50 by Katz et al. (1994) is an event chart for the Simpson-Ellenburger petroleum system, showing the temporal relationships of essential elements and processes. Even though the source of the petroleum system is problematic, these workers thought that the source rocks are shales within the Simpson Group. However, where the Simpson is absent, Ellenburger oil appears to be sourced from the Woodford Shale or younger strata (Pennsylvanian or Permian) (Kvenvolden and Squires, 1967). Katz et al. (1994) mentioned that the level of organics within the Ellenburger section is too lean (<0.5% total organic carbon [TOC]) to be capable of generating commercial quantities of hydrocarbons. The Simpson has >1% TOC. These workers' ideas about reservoir rock type in Ellenburger carbonates come from articles cited earlier in this paper, and these reservoir rocks within this petroleum system are buried between 8,530 and 13,240 ft (Central Basin Platform area). Katz et al. (1994) stated that trap development was associated with the collisional event that subdivided the Permian Basin into its major

structural units ~290 m.y.a. Traps are predominately faulted anticlines (Figure 51). Seal rocks are Simpson shales in the Central Basin Platform area. Traps formed about 50 m.y. before peak generation at ~245 m.y.a. (Figure 50). Katz et al. (1994) mentioned that API oil gravity ranges from 35° to 50°, thus allowing a recovery factor of 40%.

Table 2. Geologic characteristics of the three Ellenburger reservoir groups. From Holtz and Kerans (1992).

	Karst Modified	Ramp Carbonate	Tectonically Fractured Dolostone
Lithology	Dolostone	Dolostone	Dolostone
Depositional setting	Inner ramp	Mid- to outer ramp	Inner ramp
Karst facies	Extensive sub-Middle Ordovician	Sub-Middle Ordovician, sub-Silurian/Devonian, sub-Mississippian, sub-Permian/ Pennsylvanian	Variable intra-Ellenburger, sub-Middle Ordovician
Fault-related fracturing	Subsidiary	Subsidiary	Locally extensive
Dominant pore type	Karst-related fractures and interbreccia	Intercrystalline in dolomite	Fault-related fractures
Dolomitization	Pervasive	Partial, stratigraphic and fracture-controlled	Pervasive

Table 3. Petrophysical parameter of the three Ellenburger reservoir groups. From Holtz and Kerans (1992).

Parameter	Karst Modified	Ramp Carbonate	Tectonically Fractured Dolostone
Net pay (ft)	Avg. = 181, Range = 20 - 410	Avg. = 43 Range = 4 - 223	Avg. = 293, Range = 7 - 790

Porosity (%)	Avg. = 3 Range = 1.6 - 7	Avg. = 14 Range = 2 - 14	Avg. = 4 Range = 1 - 8
Permeability (md)	Avg. = 32 Range = 2 - 750	Avg. = 12 Range = 0.8 - 44	Avg. = 4 Range = 1 - 100
Initial water saturation (%)	Avg. = 21 Range = 4 - 54	Avg. = 32 Range = 20 - 60	Avg. = 22, Range = 10 - 35
Residual oil saturation (%)	Avg. = 31 Range = 20 - 44	Avg. = 36 Range = 25 - 62	NA

APPROACHES TO EXPLORATION AND FIELD DEVELOPMENT

Exploration

The vast majority of Ellenburger fields are trapped in anticlinal or faulted anticlinal structures (Figure 51). Because Ellenburger reservoirs are mainly structural plays, seismic is needed to define these structural prospects. Complexities of the structure must be delineated to focus on correct trapping geometry. Stratigraphic trapping in the highly karsted and fractured Ellenburger carbonate is probably not common because some level of communication is generally within the carbonate, although poor. After a structure is defined, fault compartmentalization of the structure must be mapped. If 3-D seismic analysis is able to display the sag features produced by collapse of the cave system (Loucks, 1999), these collapsed zones may contain the highest reservoir quality (Purves et al., 1992).

Many wells testing the Ellenburger section penetrate only the top of the interval to prevent water from being encountered when drilling too deep (Kerans, 1990). Caution must be taken to ensure that the full prospective section is tested and that any vertical permeability barriers are penetrated (Loucks and Anderson, 1985; Kerans, 1990). Kerans (1990) provided an excellent example from University Block 13 field in Andrews County, Texas, where a series of wells drilled into the very top of the Ellenburger section were produced and then later deepened (Figure 52). The deepened wells encountered new hydrocarbons that had been separated from the upper unit by paleocave fill and tight carbonate. The cave-fill-prone intervals are distinctive on wireline logs. Note that a cave

fill by itself cannot be a laterally continuous permeability barrier because its limited lateral extent is controlled by the size of the original cave itself (Loucks, 1999, 2001).

Kerans (1990), Loucks and Handford (1992), Hammes et al. (1996), and Loucks (1999) all stressed that karsted reservoirs can have stacked porous brecciated zones (Figure 29). These stacked reservoir zones are results of multiple cave passages forming during base-level drop while a cave system is developing (Figure 19). Commonly each of the paleocave passage levels will be in contact with one another because of cave collapse and associated fracturing. However, as Kerans (1990) showed for University Block 13 field, this is not always the case.

In any test of the Ellenburger section, a core or image log is necessary to evaluate the section properly. Commonly porosity will be low (<5%) as calculated from wireline logs; however, permeability from karst-related fracturing may be in the hundreds of millidarcys. Core will provide a proper reservoir quality analysis, and image logs will provide a description of the fractured pore network in the rock (Hammes, 1997).

Field Development

Field development of paleocave reservoirs should be based on integrated studies that include data from 3-D seismic surveys, cores, borehole image logs, conventional wireline logs, and engineering data (Loucks, 1999). In some cases it might be possible to identify cavernous or intraclast porosity from 3-D seismic data (Bouvier et al., 1990). Cores and borehole image logs are necessary to recognize and describe paleocave reservoir facies (Hammes, 1997). Whole-core data are recommended over core-plug data because of the scale and complexity of pore systems in paleocave reservoirs. Sags associated with cave collapse should be mapped because they may indicate location of the best coalesced reservoirs (Purves et al., 1992; Lucia, 1996; Loucks, 1999). Different cave passage levels of the paleocave system need to be identified and analyzed to determine whether they are separate reservoirs or in vertical communication with one another (Kerans, 1988, 1990). Because of the significant spatial complexity within coalesced paleocave systems, horizontal wells may be an option for improving recovery. Kerans (1988) stated that in the Mobil Block 36 lease of the Emma Ellenburger reservoir, “Adjacent wells in this 40-acre-spaced reservoir have varied in production, one to the

other, anywhere from 0 to 900,000 barrels of oil from the lower collapse zone.” He noted that this variability is probably related to changes in paleocave facies. The detailed paleocave system maps provided by Loucks et al. (2004) would support this conclusion. Kerans (1988) listed other fields, such as Shafter Lake and Big Lake fields, as showing strong lateral reservoir heterogeneity. Other workers that addressed different aspects of exploration and development are Kerans (1990), Wright et al. (1991), Mazzullo and Mazzullo (1992), Hammes et al. (1996), Lucia (1996), Mazzullo and Chilingarian (1996), and Loucks (1999).

CONCLUSIONS

The Ellenburger Group of the Permian Basin is part of a Lower Ordovician carbonate platform succession that covered large areas of the United States. During the Early Ordovician, the West Texas Permian Basin area was located on the southwest edge of the Laurentia plate between 20° and 30° latitude. The equator crossed northern Canada, situating Texas in a tropical to subtropical latitude. Texas was a shallow-water shelf with deeper water conditions to the south where it bordered the Iapetus Ocean. The Ellenburger Group in the south part of the Permian Basin, where the deeper water equivalent strata would have been, was strongly affected by the Ouachita Orogeny. The basinal and slope facies strata were destroyed or extensively structurally deformed. A worldwide hiatus appeared at the end of Early Ordovician deposition, creating an extensive second-order unconformity (Sauk-Tippecanoe Supersequence Boundary). This unconformity produced extensive karsting throughout the United States, including Texas.

The general depositional history of the Ellenburger was defined by Kerans (1990) as (1) Marked by retrogradational deposition of a fan delta – marginal marine depositional system continuous with the Early Cambrian transgression. This stage was followed by regional progradation and aggradation of peritidal carbonate facies. (2) Rapid transgression and widespread aggradational deposition of the high-energy restricted-shelf depositional system across much of West and Central Texas during this stage. It has been interpreted as a moderately hypersaline setting, given the rare macrofauna, evidence of evaporites, and abundance of ooids. (3) Upward transition from the high-energy restricted shelf depositional system to the low-energy restricted-shelf

depositional systems as evidenced by a second regression across the Ellenburger shelf. Progradation during this stage is marked by transition of landward upper tidal flats to more seaward, low-energy restricted subtidal to intertidal facies to farthest seaward open-marine, shallow-water shelf facies. (4) Near the end of the Early Ordovician there was a worldwide eustatic lowstand—the exposure spanned several million years and exposed the Ellenburger Platform in West Texas, producing an extensive karst terrain.

Diagenesis of the Ellenburger Group is complex, and the processes that produced it spanned millions of years. Three major diagenetic processes are important to recognize: (1) dolomitization, (2) karsting, and (3) tectonic fracturing. Five general stages of dolomitization were recognized by Kupecz and Land (1991). Generations of dolomite were separated into early-stage dolomitization, which predated the Sauk unconformity, and late-stage dolomitization, which postdated the Sauk unconformity. They attributed 90% of the dolomite to prekarstification, early-stage dolomite, and 10% of the dolomite to postkarstification, late-stage dolomite. Early-stage prekarstification dolomite is associated with muddier rocks, and the source of Mg was probably seawater. Late-stage postkarstification dolomites are attributed to warm, reactive fluids, which were expelled from basinal shales during the Ouachita Orogeny. Fluids are thought to have been corrosive, as evidenced by corroded dolomite rhombs. This corrosion provided the Mg necessary for dolomitization. The fluids migrated through high-permeability aquifers of the Bliss Sandstone, basal subarkose facies of the Ellenburger, as well as grainstone facies and paleocave breccia zones. In the Ellenburger Group, extensive cave systems formed at a composite unconformity (Sauk unconformity) that lasted several million years to several tens of million years. These cave systems collapsed with burial, creating widespread brecciated and fractured carbonate bodies that form many of the Ellenburger reservoirs. As much as 1,000 ft of section can be affected, but more commonly only the top 300 ft is affected. Lithified strata above the karsted Ellenburger are also affected by suprastratal deformation. The West Texas area has been periodically tectonically active following Ellenburger deposition, producing faults and fractures associated with these tectonic periods.

Pore networks in the Ellenburger are complex because of the amount of brecciation and fracturing associated with karsting. Pore networks can consist of any

combination of the following pore types, depending on depth of burial (Loucks, 1999): (1) matrix, (2) cavernous, (3) interclast, (4) crackle-/mosaic-breccia fractures, or (5) tectonic-related fractures. The pore network evolved with burial and diagenesis.

Coalesced, collapsed-paleocave systems are megascale geologic features that can have dimensions of hundreds to thousands of square miles laterally and several thousand feet vertically. Strata above and below the unconformity are affected by late collapse in the subsurface. A coalesced, collapsed-paleocave system can be divided into (1) a lower section of karsted strata that contains collapsed paleocaves and (2) an upper section of strata that is deformed to various degrees (suprastratal deformation) by the collapse and compaction of the lower section of paleocave-bearing strata. The regional pattern of karsted Ellenburger reservoirs probably follows a rectilinear pattern as a result of regional fractures controlling original cave-system development.

The Ellenburger Group is an ongoing important exploration target in West Texas. The structural play covers a depth interval of >25,000 ft. Carbonate depositional systems within the Ellenburger Group are relatively simple; however, the diagenetic overprint is complex and it is this complex diagenetic overprint that produces strong spatial heterogeneity within the reservoir systems.

ACKNOWLEDGMENT

Publication authorized by the Director, Bureau of Economic Geology. Special thanks are given to Lana Dieterich for editing the manuscript. Funding for this study came from the State of Texas Advanced Resource Recovery Program.

REFERENCES

- Amthor, J. E., and Friedman, G. M., 1991, Dolomite-rock textures and secondary porosity development in Ellenburger Group carbonates (Lower Ordovician), West Texas and southeastern New Mexico: *Sedimentology*, v. 38, p. 343–362.
- Barnes, V. E., Cloud, P. E., Jr., Dixon, L. P., Folk, R. L., Jonas, E. C., Palmer, A. R., and Tynan, E. J., 1959, Stratigraphy of the pre-Simpson Paleozoic subsurface rocks of Texas and southeast New Mexico: University of Texas, Austin, Bureau of Economic Geology Publication 5924, 294 p.

- Berry, W. B. N., 1960, Graptolite faunas of the Marathon region, West Texas: University of Texas, Austin, Bureau of Economic Geology Publication 6005, 179 p.
- Blakey, R., 2005a, Regional paleogeographic views of earth history; paleogeographic globes: <http://jan.ucc.nau.edu/~rcb7/RCB.html>.
- Blakey, R., 2005b, Paleogeography and geologic evolution of North America; Images that track the ancient landscapes of North America:
<http://jan.ucc.nau.edu/~rcb7/RCB.html>.
- Bouvier, J. D., Gevers, E. C.A., and Wigley, P. L., 1990, #-D seismic interpretation and lateral prediction of the Amposta Marino field (Spanish Mediterranean Sea): *Geologie en Mijnbouw*, v. 69, p. 105–120.
- Budnik, T. T., 1987, Left-lateral intraplate deformation along the Ancestral Rocky Mountains: implications for late Paleozoic plate motions: *Tectonophysics*, v. 132, p. 195–214.
- Candelaria, M. P., and Reed, eds., C. L., 1992, Paleokarst, karst related diagenesis and reservoir development: Examples from Ordovician-Devonian age strata of West Texas and the Mid-Continent: Permian Basin Section, Society of Economic Paleontologists and Mineralogists Publication No. 92-33, 202 p.
- Canter, K. L., Stearns, D. B., Geesaman, R. C., and Wilson, J. L., 1993, Paleostructural and related paleokarst controls on reservoir development in the Lower Ordovician Ellenburger Group, Val Verde Basin, *in* Fritz, R. D., Wilson, J. L., and D. A. Yurewicz, D. A., eds., Paleokarst related hydrocarbon reservoirs: SEPM Core Workshop No. 18, New Orleans, April 25, p. 61–101.
- Cloud, P. E., and Barnes, V. E., 1948, The Ellenburger Group of Central Texas: University of Texas, Austin, Bureau of Economic Geology Publication 4621, 473 p.
- Cloud, P. E., and Barnes, V. E., 1957, Early Ordovician sea in Central Texas: *Geological Society of American Memoir* 67, p. 163–214.
- Cloud, P. E., Barnes, V. E., and Bridge, J. 1945, Stratigraphy of the Ellenburger Group in Central Texas—a progress report: University of Texas, Austin, Bureau of Economic Geology Publication 4301, p. 133–161.

- Combs, D. M., Loucks, R. G., and Ruppel, S. C., 2003, Lower Ordovician Ellenburger Group collapsed paleocave facies and associated pore network in the Barnhart field, Texas, *in* Hunt, T. J., and Lufholm, P. H., The Permian Basin: back to basics: West Texas Geological Society Fall Symposium: West Texas Geological Society Publication #03-112, p. 397–418.
- Custer, M. A., 1957, Polar field, Kent County, Texas, *in* Heard, F. A., ed., Occurrence of oil and gas in West Texas: University of Texas, Austin, Bureau of Economic Geology Publication No. 5716, p. 200–282.
- Dutton, S. P., Kim, E. M., Broadhead, R. F., Breton, C. L., Raatz, W. D., Ruppel, S. C., and Kerans, Charles, 2005, Play analysis and digital portfolio of major oil reservoirs in the Permian Basin: The University of Texas at Austin, Bureau of Economic Geology Report of Investigations No. 271, 287 p., CD-ROM.
- Entzminger, D. J., 1994, Shafter Lake (Ellenburger), *in* Oil & gas fields in West Texas: West Texas Geological Society Publication 94-96, v. 4, p. 247–250.
- Folk, R. L., 1959, Thin-section examination of Pre-Simpson Paleozoic rocks, *in* Barnes, V. E., Cloud, P. E., Jr., Dixon, L. P., Folk, R. L., Jonas, E. C., Palmer, A. R., and Tynan, E. J., Stratigraphy of the pre-Simpson Paleozoic subsurface rocks of Texas and southeast New Mexico: University of Texas, Austin, Bureau of Economic Geology Publication. 5924, p. 95–130.
- Ford, D. C., 1988, Characteristics of dissolutional cave systems in carbonate rocks, *in* James, N. P., and Choquette, P. W., eds., Paleokarst: Springer-Verlag, p. 25–57.
- Esteban, M., 1991, Palaeokarst: practical applications, *in* Wright, V. P., Esteban, M., and Smart, P. L., eds., Palaeokarst and palaeokarstic reservoirs: Postgraduate Research for Sedimentology, University of Reading, PRIS Contribution No. 152, p. 89–119.
- Galley, J. E., 1958, Oil and geology in the Permian Basin of Texas and New Mexico, *in* Weeks, W. L., ed., Habitat of oil: American Association of Petroleum Geologists Special Publication, p. 395–446.
- Goldhammer, R. K., 1996, Facies architecture, cyclic and sequence stratigraphy: the Lower Ordovician El Paso Group, West Texas, *in* Stoudt, E. L., ed., Precambrian-Devonian geology of the Franklin Mountains, West Texas—Analog for

- exploration and production in Ordovician and Silurian karsted reservoirs in the Permian basin: West Texas Geological Society Annual Field Trip Guidebook, WTGS Publication No. 96-100, p. 71–98.
- Goldhammer, R. K., and Lehmann, P. J., 1996, Chaos in El Paso, *in* Stoudt, E. L., ed., Precambrian-Devonian geology of the Franklin Mountains, West Texas—Analogues for exploration and production in Ordovician and Silurian karsted reservoirs in the Permian basin: West Texas Geological Society 1996 Annual Field Trip Guidebook: WTGS Publication No. 96-100, p. 125–140.
- Goldhammer, R. K., Lehmann, P. J., and Dunn, P. A., 1992, Third-order sequence boundaries and high frequency cycle stacking pattern in Lower Ordovician platform carbonates, El Paso Group (Texas): Implications for carbonate sequence stratigraphy, *in* Candelaria, M. P., and Reed, C. L., eds., Paleokarst, karst related diagenesis and reservoir development: examples from Ordovician-Devonian age strata of West Texas and the Mid-Continent: Permian Basin Section, SEPM (Society for Sedimentary Geology), Publication No. 92-33, p. 59–92.
- Ham, W. E., and Wilson, J. L., 1967, Paleozoic epeirogeny and orogeny in the central United States: American Journal of Science, v. 265, no. 5, p. 332–407.
- Hammes, U., 1997, Electrical imaging catalog: microresistivity images and core photos from fractured, karsted, and brecciated carbonate rocks: The University of Texas at Austin, Bureau of Economic Geology Geological Circular 97-2, 40 p.
- Hammes, Ursula, Lucia, F. J., and Kerans, Charles, 1996, Reservoir heterogeneity in karst-related reservoirs: Lower Ordovician Ellenburger Group, West Texas, *in* Stoudt, E. L., ed., Precambrian–Devonian geology of the Franklin Mountains, West Texas—analogs for exploration and production in Ordovician and Silurian karsted reservoirs in the Permian Basin: West Texas Geological Society, Publication No. 96-100, p. 99–117.
- Hardage, B. A., Carr, D. L., Lancaster, D. E., Simmons, J. L., Jr., Elphick, R. Y., Pendleton, V. M., and Johns, R. A., 1996, 3-D seismic evidence of the effects of carbonate karst collapse on overlying clastic stratigraphy and reservoir compartmentalization: Geophysics, v. 61, p. 1336–1350.

- Hardwick, J. V., 1957, Block 32 field, Crane County, Texas, *in* Heard, F. A., ed., Occurrence of oil and gas in West Texas: The University of Texas at Austin, Bureau of Economic Geology Publication No. 5716, p. 40–46.
- Holland, R. R., 1966, Puckett, Ellenburger, Pecos County, Texas, *in* Oil and gas fields in West Texas—A symposium: West Texas Geological Society Publication 66-52, p. 291–295.
- Holtz, M. H., and Kerans, C., 1992, Characterization and categorization of West Texas Ellenburger reservoirs, *in* Candelaria, M. P., and Reed, C. L., eds., Paleokarst, karst related diagenesis and reservoir development: examples from Ordovician-Devonian age strata of West Texas and the Mid-Continent: Permian Basin Section SEPM Publication No. 92-33, p. 31–44.
- Ijirighoi, B. T., and Schreiber, J. F., Jr., 1986, Origin and classification of fractures and related breccia in the Lower Ordovician Ellenburger Group, West Texas: West Texas Geological Society Bulletin, v. 26, p. 9–15.
- Katz, B. J., Dawson, W. C., Robison, V. D., and Elrod, L. W., 1994, Simpson—Ellenburger(.) petroleum system of the Central Basin Platform, West Texas, U.S.A., *in* Magoon, L. B. and Dow, W. G., eds., The petroleum system—from source to trap: AAPG Memoir 60, p. 453–461.
- Kerans, Charles, 1988, Karst-controlled reservoir heterogeneity in Ellenburger Group carbonates of West Texas: reply: AAPG Bulletin, v. 72, p. 1160–1183.
- Kerans, Charles, 1989, Karst-controlled reservoir heterogeneity and an example from the Ellenburger Group (Lower Ordovician) of West Texas: The University of Texas at Austin, Bureau of Economic Geology Report of Investigations No. 186, 40 p.
- Kerans, Charles, 1990, Depositional systems and karst geology of the Ellenburger Group (Lower Ordovician), subsurface West Texas: The University of Texas at Austin, Bureau of Economic Geology Report of Investigations No. 193, 63 p., 6 pl.
- Kerans, Charles, Lucia, F. J., and Senger, R. K., 1994, integrated characterization of carbonate ramp reservoirs using Permian San Andres outcrop analogs: AAPG Bulletin, v. 78, p. 181–216.

- Kvenvolden, K. A., and Squires, R. M., 1967, Carbon isotopic composition of crude oils from Ellenburger Group (Lower Ordovician), Permian basin, West Texas and eastern New Mexico: AAPG Bulletin, v. 51, p. 1293–1303.
- Kupecz, J. A., 1992, Sequence boundary control on hydrocarbon reservoir development, Ellenburger Group, Texas, *in* Candelaria, M. P., and Reed, C. L., eds., Paleokarst, karst related diagenesis and reservoir development: examples from Ordovician-Devonian age strata of West Texas and the Mid-Continent: Permian Basin Section, (Society for Sedimentary Geology), Publication No. 92–33, p. 55–58.
- Kupecz, J. A., and L. S. Land, 1991, Late-stage dolomitization of the Lower Ordovician Ellenburger Group, West Texas: Journal of Sedimentary Petrology, v. 61, p. 551–574.
- Lee, I. Y., and Friedman, G. M., 1987, Deep-burial dolomitization in the Ordovician Ellenburger Group carbonates, West Texas and southeastern New Mexico—Reply: Journal of Sedimentary Petrology, v. 58, p. 910–913.
- Lindsay, R. F., and Koskelin, K. M., 1993, Arbuckle Group (Late Cambrian-early Ordovician) shallowing-upward parasequences and sequences, southern Oklahoma, *in* Keller, D. R., and Reed, C. L., eds., Paleokarst, karst related diagenesis and reservoir development: examples from Ordovician-Devonian age strata of West Texas and the Mid-Continent: Permian Basin Section SEPM Publication No. 92-33, p. 45–65.
- Loucks, R. G., 1999, Paleocave carbonate reservoirs: origins, burial-depth modifications, spatial complexity, and reservoir implications: AAPG Bulletin, v. 83, p. 1795–1834.
- Loucks, R. G., 2001, Modern analogs for paleocave-sediment fills and their importance in identifying paleocave reservoirs: Gulf Coast Association of Geological Societies Transactions, v. 46, p. 195–206.
- Loucks, R. G., 2003, Understanding the development of breccias and fractures in Ordovician carbonate reservoirs, *in* Hunt, T. J., and Lufholm, P. H., The Permian Basin: back to basics: West Texas Geological Society Fall Symposium: West Texas Geological Society Publication No. 03-112, p. 231–252.

- Loucks, R. G., 2007, A review of coalesced, collapsed-paleocave systems and associated suprastratal deformation: *Acta Carsologica*, v. 36, no. 1, p. 121–132.
- Loucks, R. G., and Anderson, J. H., 1980, Depositional facies and porosity development in Lower Ordovician Ellenburger dolomite, Puckett Field, Pecos County, Texas, *in* Halley, R. B. and Loucks, R. G., eds., *Carbonate reservoir rocks: SEPM Core Workshop No. 1*, p. 1–31.
- Loucks, R. G., and Anderson, J. H., 1985, Depositional facies, diagenetic terrains, and porosity development in Lower Ordovician Ellenburger Dolomite, Puckett Field, West Texas, *in* Roehl, P. O., and Choquette, P. W., eds., *Carbonate petroleum reservoirs*: Springer-Verlag, p. 19–38.
- Loucks, R. G., and Handford, R. H., 1992, Origin and recognition of fractures, breccias, and sediment fills in paleocave-reservoir networks, *in* Candelaria, M. P., and Reed, C. L., eds., *Paleokarst, karst related diagenesis and reservoir development: examples from Ordovician-Devonian age strata of West Texas and the Mid-Continent: Permian Basin Section, SEPM (Society for Sedimentary Geology)*, Publication No. 92–33, p. 31–44.
- Loucks, R. G., and Mescher, P. A., 1998, Origin of fractures and breccias associated with coalesced collapsed paleocave systems (abs.), *in* Rocky Mountain Association Symposium on Fractured Reservoirs: Practical Exploration and Development Strategies, unpaginated.
- Loucks, R. G., and Mescher, P., 2001, Paleocave facies classification and associated pore types, *in* American Association of Petroleum Geologists, Southwest Section, Annual Meeting, Dallas, Texas, March 11–13, CD-ROM, 18 p.
- Loucks, R. G., Mescher, P., and McMechan, G. A., 2000, Architecture of a coalesced, collapsed-paleocave system in the Lower Ordovician Ellenburger Group, Dean Word Quarry, Marble Falls, Texas: Final report prepared for the Gas Research Institute, GRI-00/0122, CD-ROM.
- Loucks, R. G., Mescher, P. K., and McMechan, G. A., 2004, Three-dimensional architecture of a coalesced, collapsed-paleocave system in the Lower Ordovician Ellenburger Group, Central Texas: *AAPG Bulletin*, v. 88, no. 5, p. 545–564.

- Lucia, F. J., 1971, Lower Paleozoic history of the western Diablo Platform, West Texas and south-central New Mexico, *in* Cys, J. M., ed., Robledo Mountains and Franklin Mountains—1971 Field Conference Guidebook: Permian Basin Section, SEPM, p. 174–214.
- Lucia, F. J., 1968, Sedimentation and paleogeography of the El Paso Group, *in* Stewart, W. J., ed., Delaware basin exploration: West Texas Geological Society Guidebook No. 68-55, p. 61–75.
- Lucia, F. J., 1969, Lower Paleozoic history of the western Diablo Platform of West Texas and south-central New Mexico, *in* Seewald, K., and Sundeen, D., eds., The geologic framework of the Chihuahua tectonic belt: West Texas Geological Society, p. 39–56.
- Lucia, F. J., 1995, Lower Paleozoic cavern development, collapse, and dolomitization, Franklin Mountains, El Paso, Texas, *in* Budd, D. A., Saller, A. H., and Harris, P. M., eds., Unconformities and porosity in carbonate strata: AAPG Memoir 63, p. 279–300.
- Lucia, F. J., 1996, Structural and fracture implications of Franklin Mountains collapse brecciation, *in* Stoudt, E. L., ed., Precambrian-Devonian geology of the Franklin Mountains, West Texas—Analogues for exploration and production in Ordovician and Silurian karsted reservoirs in the Permian basin: West Texas Geological Society 196 Annual Field Trip Guidebook, WTGS Publication No. 96-100, p. 117–123.
- Mazzullo, S. J., and G. V. Chilingarian, 1996, Hydrocarbon reservoirs in karsted carbonate rocks, *in* Chilingarian, G. V., Mazzullo, S. J., and Rieke, H. H., eds., Carbonate reservoir characterization: a geologic-engineering analysis, Part II: Elsevier, p. 797–685.
- Mazzullo, S. J., and Mazzullo, L. J., 1992, Paleokarst and karst-associated hydrocarbon reservoirs in the Fusselman Formation, West Texas, Permian basin, *in* Candelaria, M. P., and Reed, C. L., eds., Paleokarst, karst related diagenesis and reservoir development: examples from Ordovician-Devonian age strata of West Texas and the Mid-Continent: Permian Basin Section, SEPM (Society for Sedimentary Geology), Publication No. 92-33, p. 110–120.

- McDonnell, Angela, Loucks, R. G., and Dooley, Tim, 2007, Quantifying the origin and geometry of circular sag structures in northern Fort Worth Basin, Texas: paleocave collapse, pull-apart fault systems, or hydrothermal alteration? AAPG Bulletin, v. 91, no. 9, p. 1295–1318.
- McMechan, G. A., Loucks, R. G., Mescher, P. A., and Zeng, Xiaoxian, 2002, Characterization of a coalesced, collapsed paleocave reservoir analog using GPR and well-core data: Geophysics, v. 67, no. 4, p. 1148–1158.
- McMechan, G. A., Loucks, R. G., Zeng, X., and Mescher, P. A., 1998, Ground penetrating radar imaging of a collapsed paleocave system in the Ellenburger dolomite, Central Texas: Journal of Applied Geophysics, v. 39, p. 1–10.
- Palmer, A. N., 1991, Origin and morphology of limestone caves: Geological Society of America Bulletin, v. 103, p. 1–21.
- Purves, W. J., E. B. Burnitt, L. R. Weathers, and L. K. Wipperman, 1992, Cave/pillar definition in the Ordovician Ellenburger reservoir by 3-D seismic, Pegasus field, Midland and Upton counties, Texas (abs.): AAPG Annual Meeting Program and Abstracts, p. 108.
- Ross, R. J., Jr., 1976, Ordovician sedimentation in the western United States, *in* Bassett, M. G., ed., The Ordovician System: Proceedings of a Paleontological Association Symposium: Birmingham, p. 73–105.
- Ross, R. J., Jr., 1982, The Ordovician System in the United States—correlation chart and explanatory note: International Union of Geological Sciences Publication 12, 73 p.
- Ruppel, S. C., Jones, R. H., Breton, C. L., and Kane, J. A., 2005, Preparation of maps depicting geothermal gradient and Precambrian structure in the Permian Basin: The University of Texas at Austin, Bureau of Economic Geology, contract report prepared for the U.S. Geological Survey under order no. 04CRSA0834 and requisition no. 04CRPR01474, 23 p. + CD-ROM.
- Sloss, L. L., 1963, Sequences in the cratonic interior of North America: Geological Society of America Bulletin, v. 74, p. 93–114.
- Texas Water Development Board, 1972, A survey of the subsurface saline water of Texas: Austin, TWDB, v. 1, 113 p.

- White, W. B., 1988, *Geomorphology and hydrology of karst terrains*: New York, Oxford University Press, 464 p.
- White, E. L., and White, W. B., 1968, Dynamics of sediment transport in limestone caves: *National Speleothem Society Bulletin*, v. 30, 115–129.
- Wilson, J. L., Medlock, R. L., Fritz, R. D., Canter, K. L., and Geesaman, R. G., 1992, A review of Cambro-Ordovician breccias in North America, *in* Keller, D. R., and Reed, C. L, eds., *Paleokarst, karst related diagenesis and reservoir development: examples from Ordovician-Devonian age strata of West Texas and the Mid-Continent*: *Permian Basin Section SEPM Publication No. 92-33*, p. 19–29.
- Wright, V. P., Esteban, M., and Smart, P. L., eds., 1991, *Palaeokarst and palaeokarstic reservoirs*: *Postgraduate Research for Sedimentology, University, PRIS Contribution No. 152*, 158 p.
- Young, L. M., 1968, *Sedimentary petrology of the Marathon Formation, (Lower Ordovician), Trans-Pecos Texas*: The University of Texas at Austin at Austin, Ph.D. dissertation, 234 p.

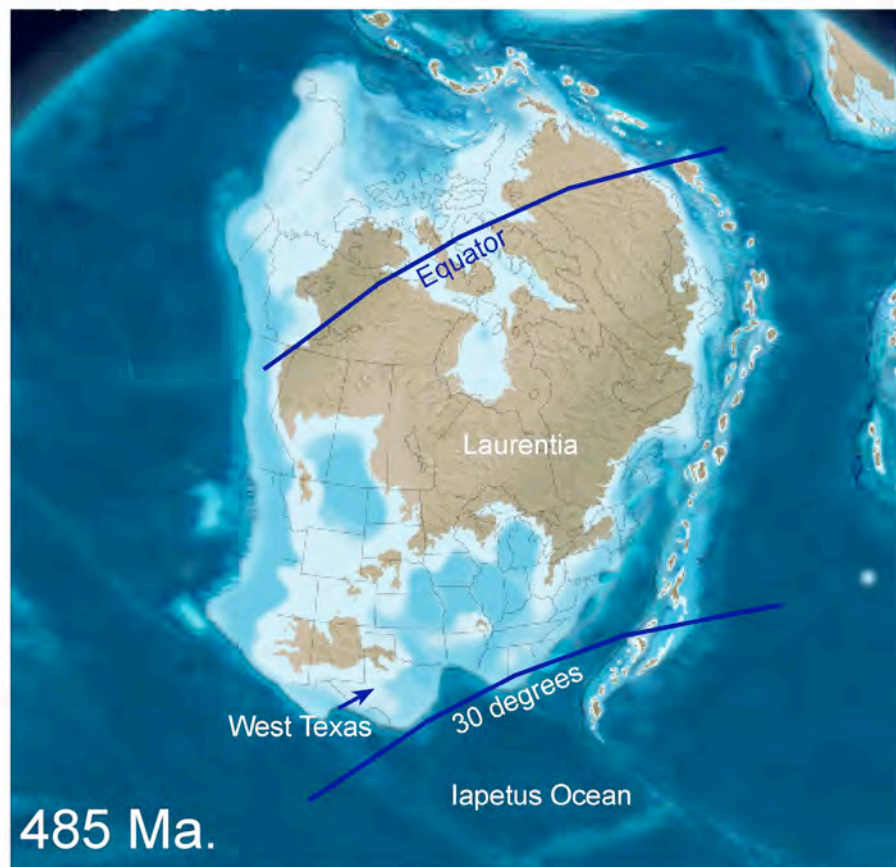
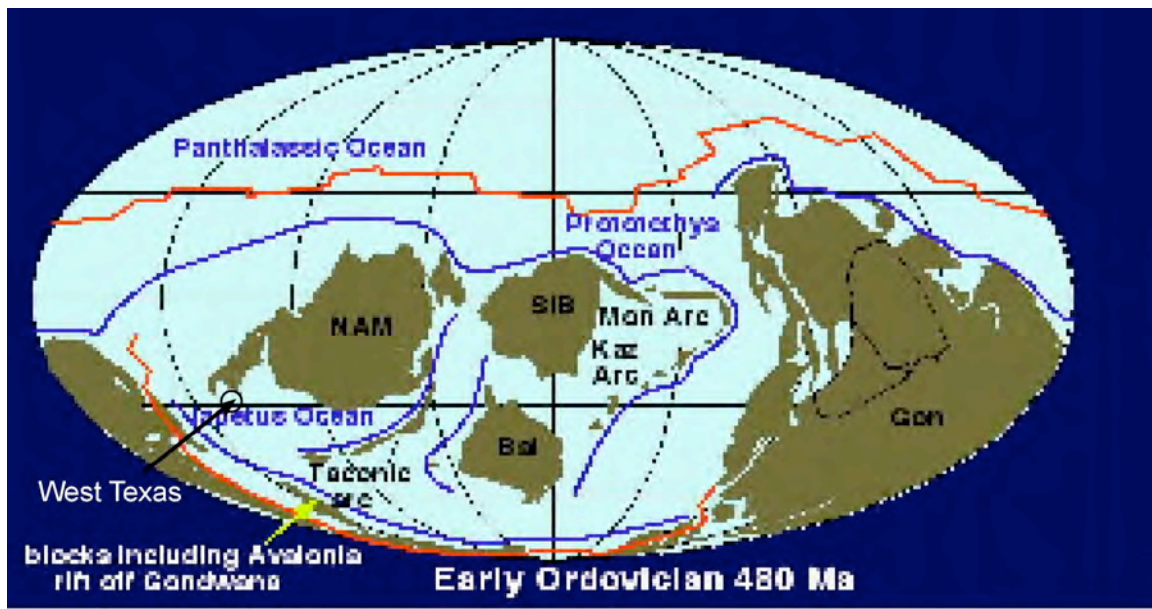


Figure 1. Reconstruction of Laurentia Plate for the Lower Ordovician (480 Ma at top and 485 Ma at bottom). West Texas was located at the southwest edge of the continent bordering the deep Iapetus Ocean. Upper map is from Blakey (2005a) and lower map is from Blakey (2005b). The lower map is slightly modified by present author. The location of the equator and 30 degrees latitude are estimated from the upper global diagram.

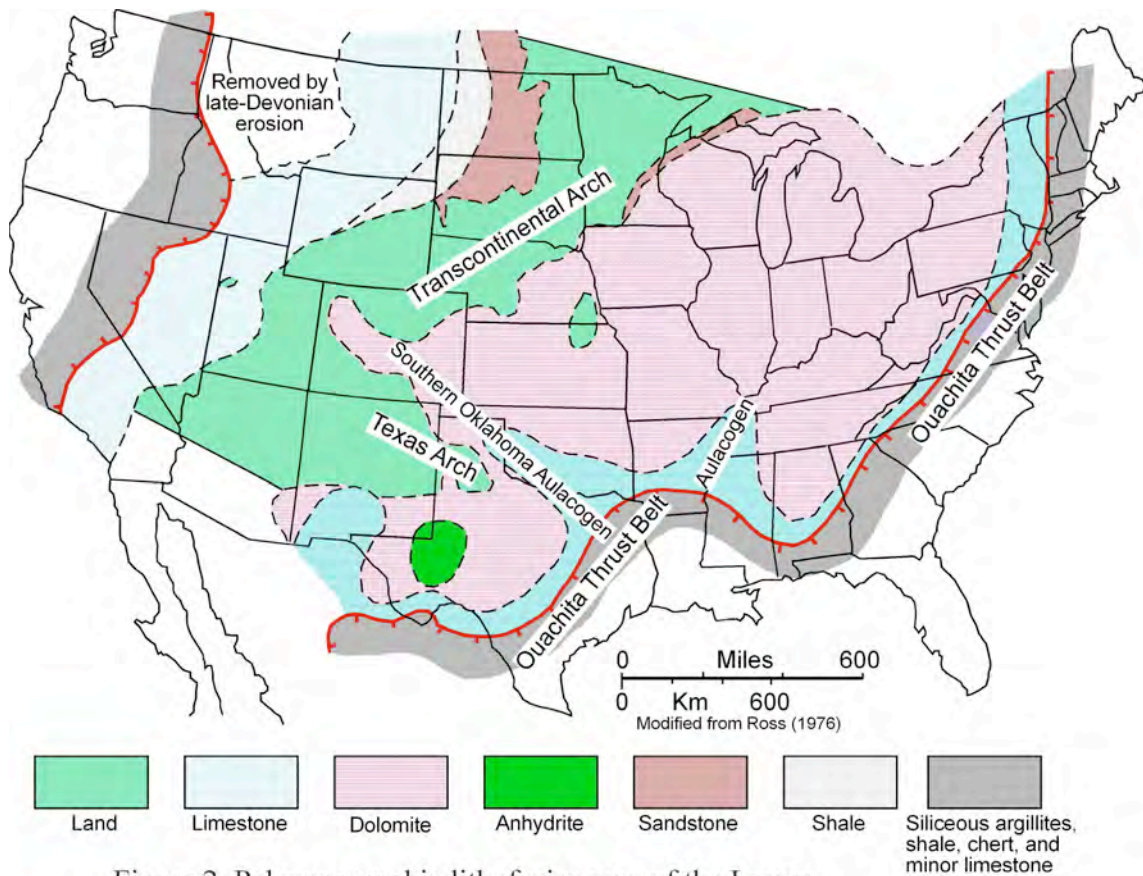


Figure 2. Paleogeographic lithofacies map of the Lower Ordovician section in the United States. From Ross (1976).

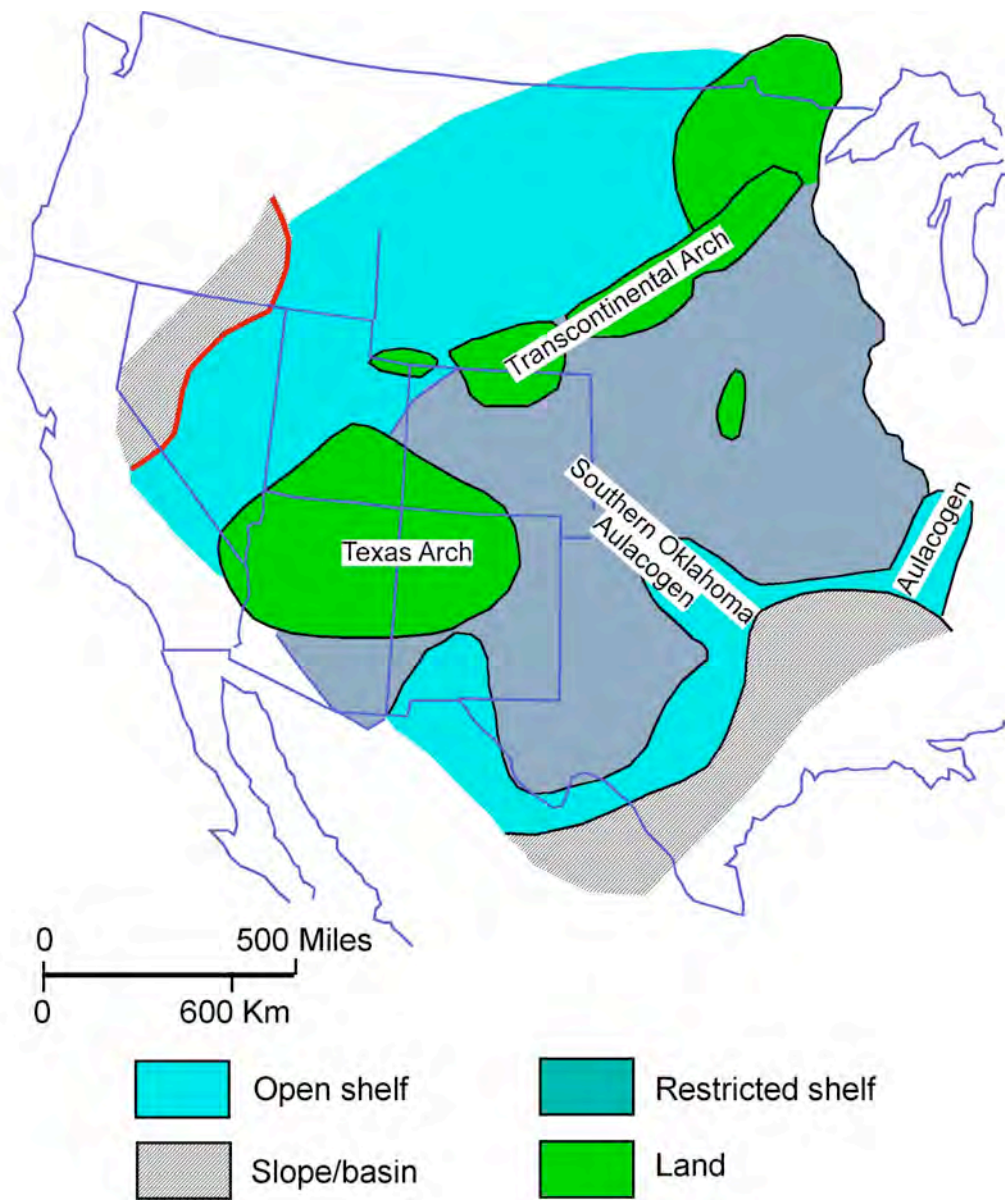


Figure 3. Interpreted regional depositional setting during Early Ordovician time. After Ross (1976) and Kerans (1990).

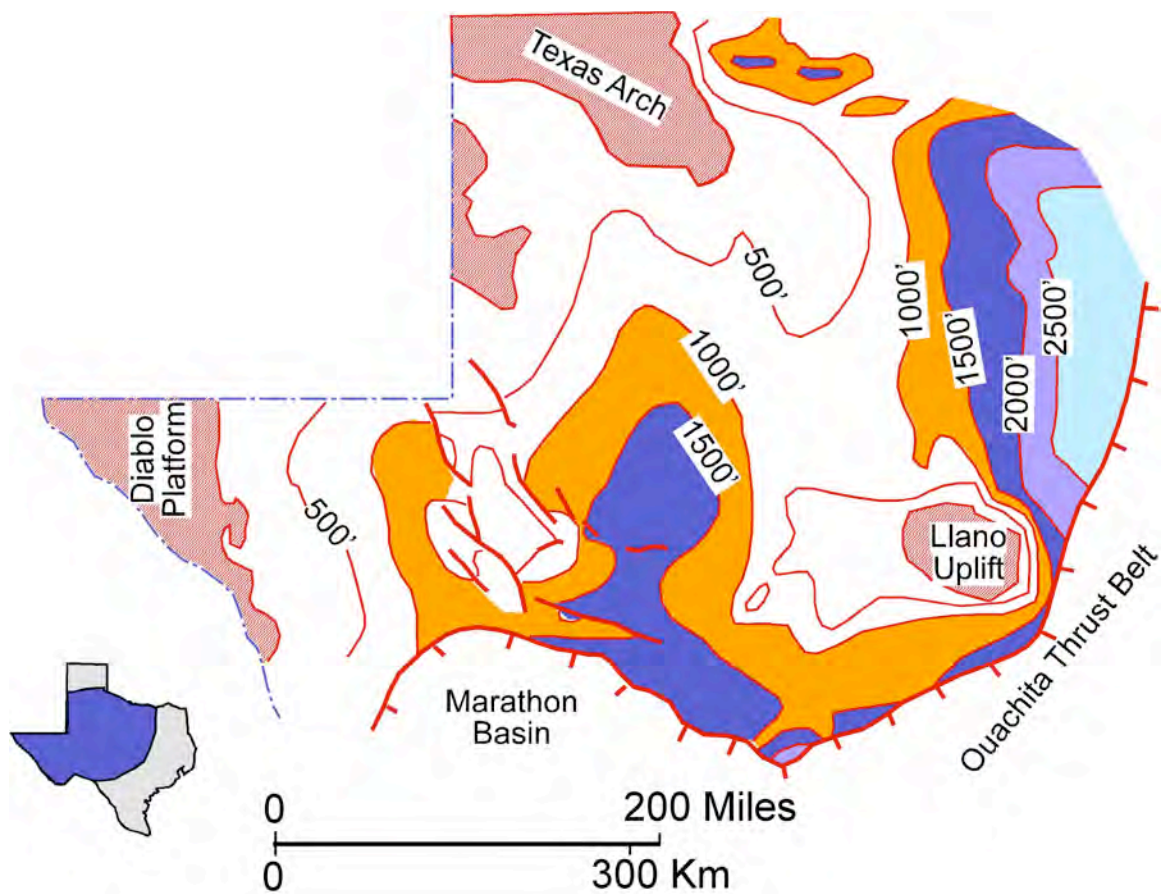


Figure 4. Generalized isopach map of the Ellenburger Group in West Texas. Thickest areas are colored. After Kerans (1989) who modified Texas Water Development Board (1972) figure.

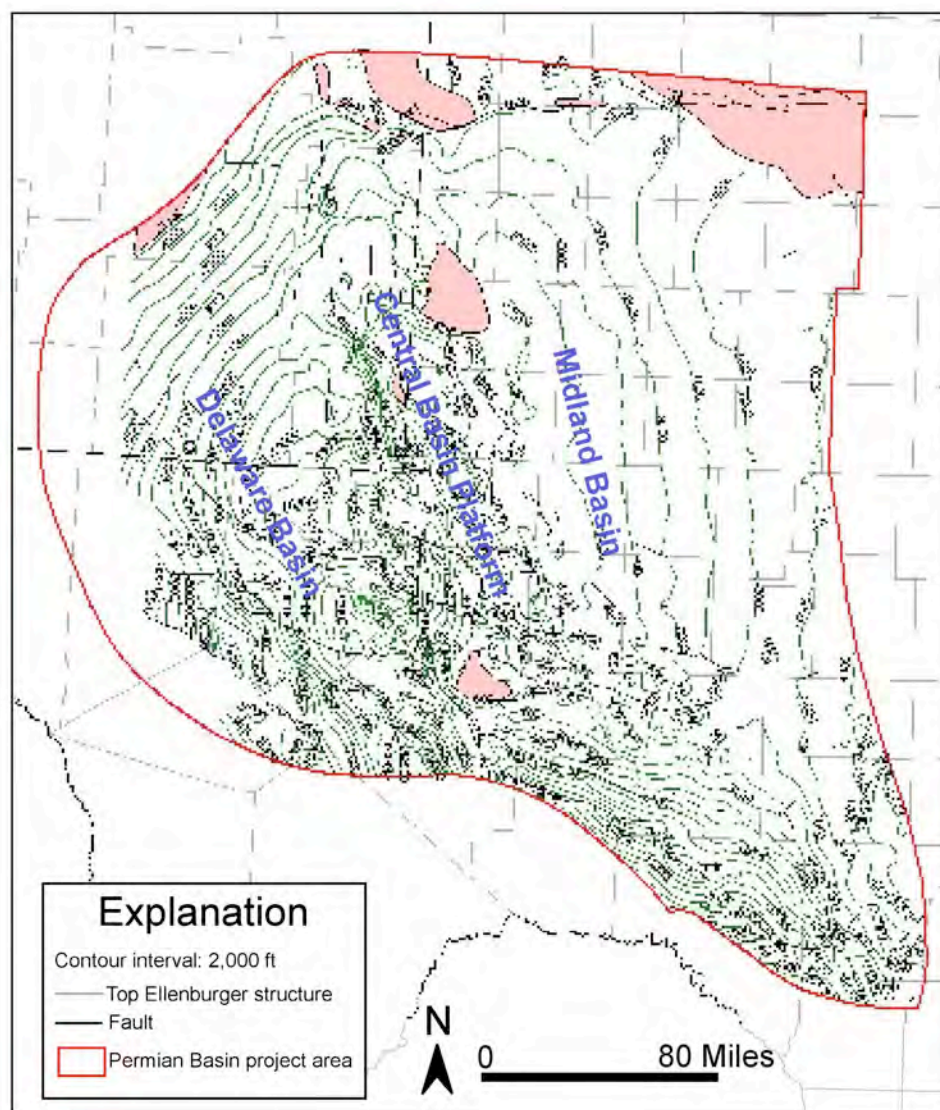


Figure 5. Structure map on top of Ellenburger Group from Ruppel et al. (2005). Contours are subsea depths.

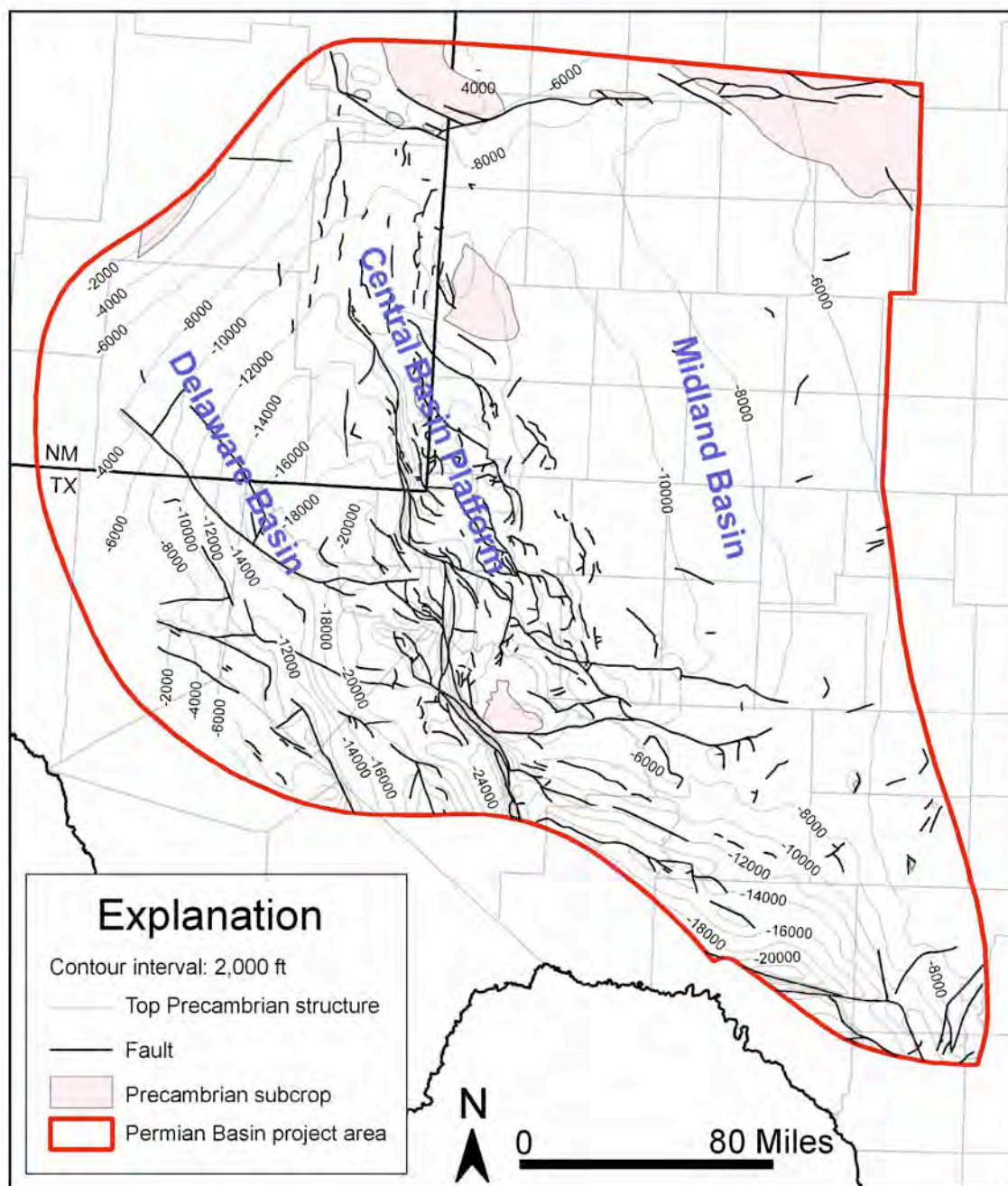


Figure 6. Structure map on top of Precambrian strata from Ruppel et al. (2005). Contours are subsea depths.

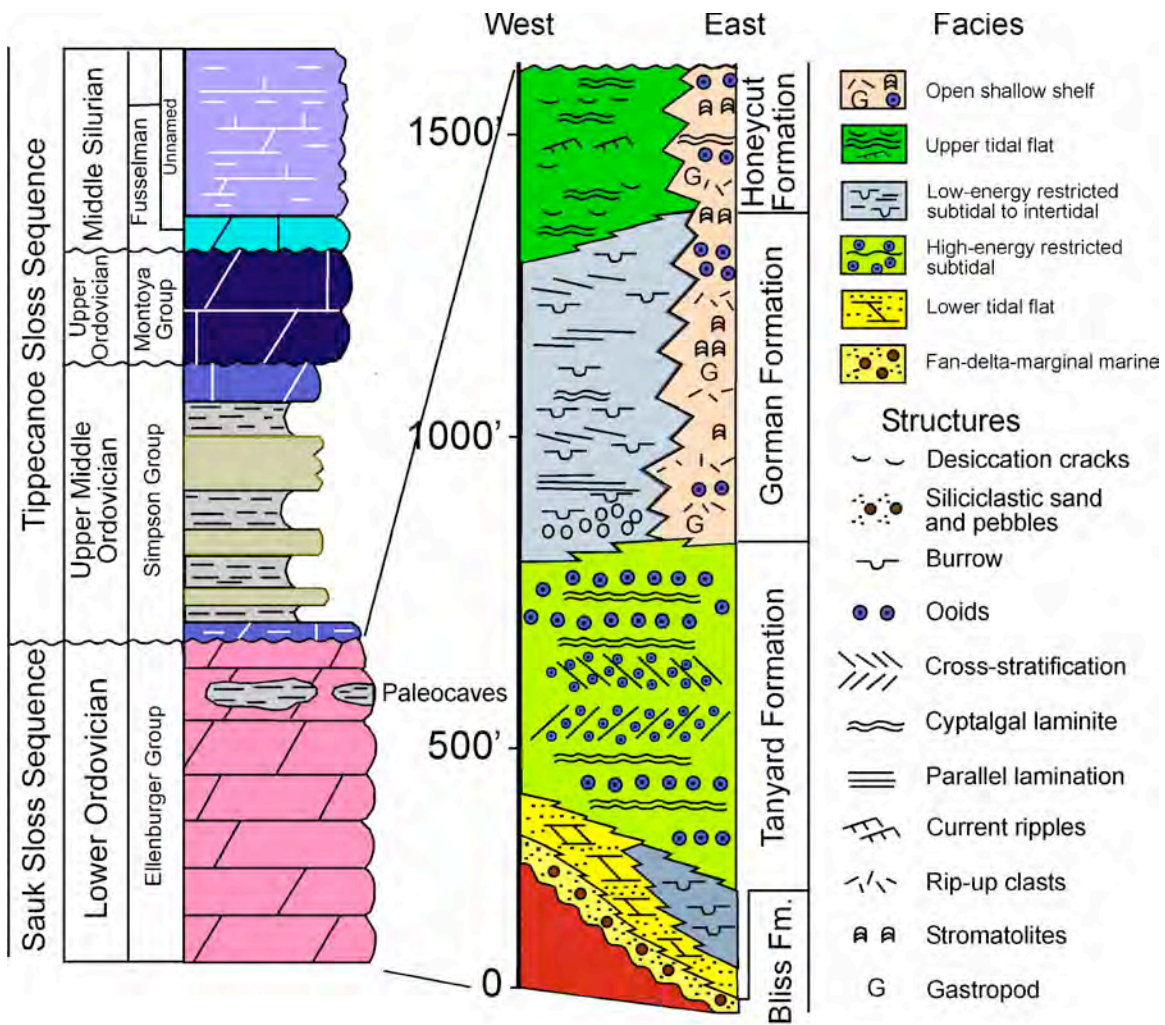


Figure 7. Schematic representation of Ellenburger depositional systems in West Texas compared with formalized Ellenburger stratigraphic units in the Llano area. Thickness of descriptive Ellenburger section is approximate. From Kerans (1990) with minor additions.

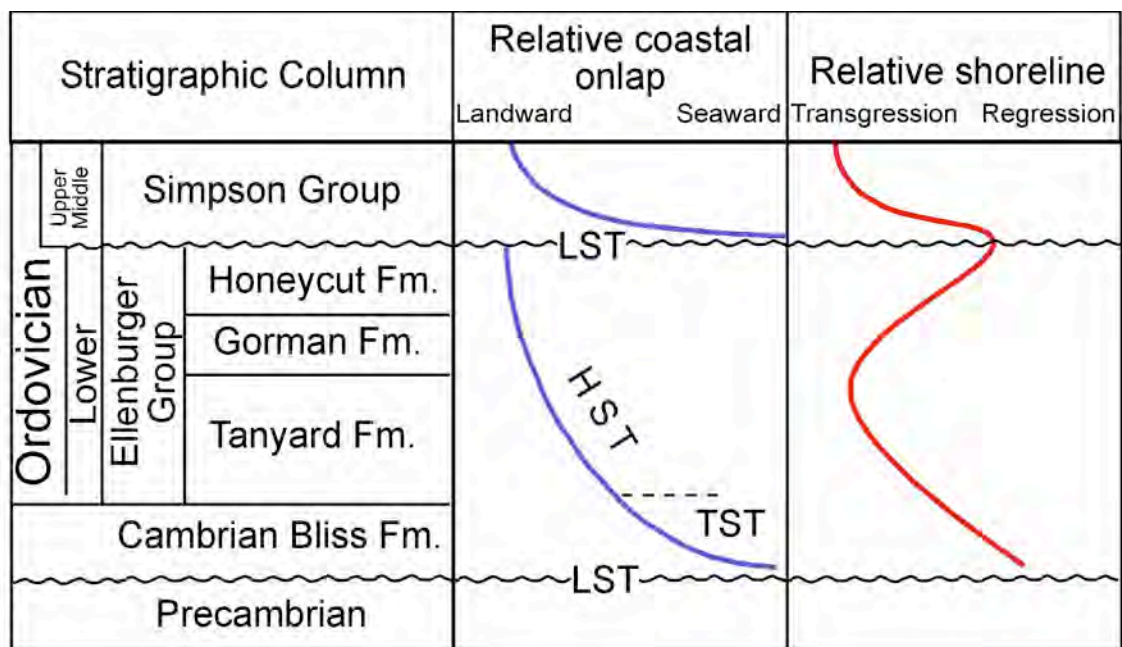


Figure 8. Interpretation of the second-order relative coastal and relative shoreline curves for the Ellenburger Group. Modified from Kupecz (1992).

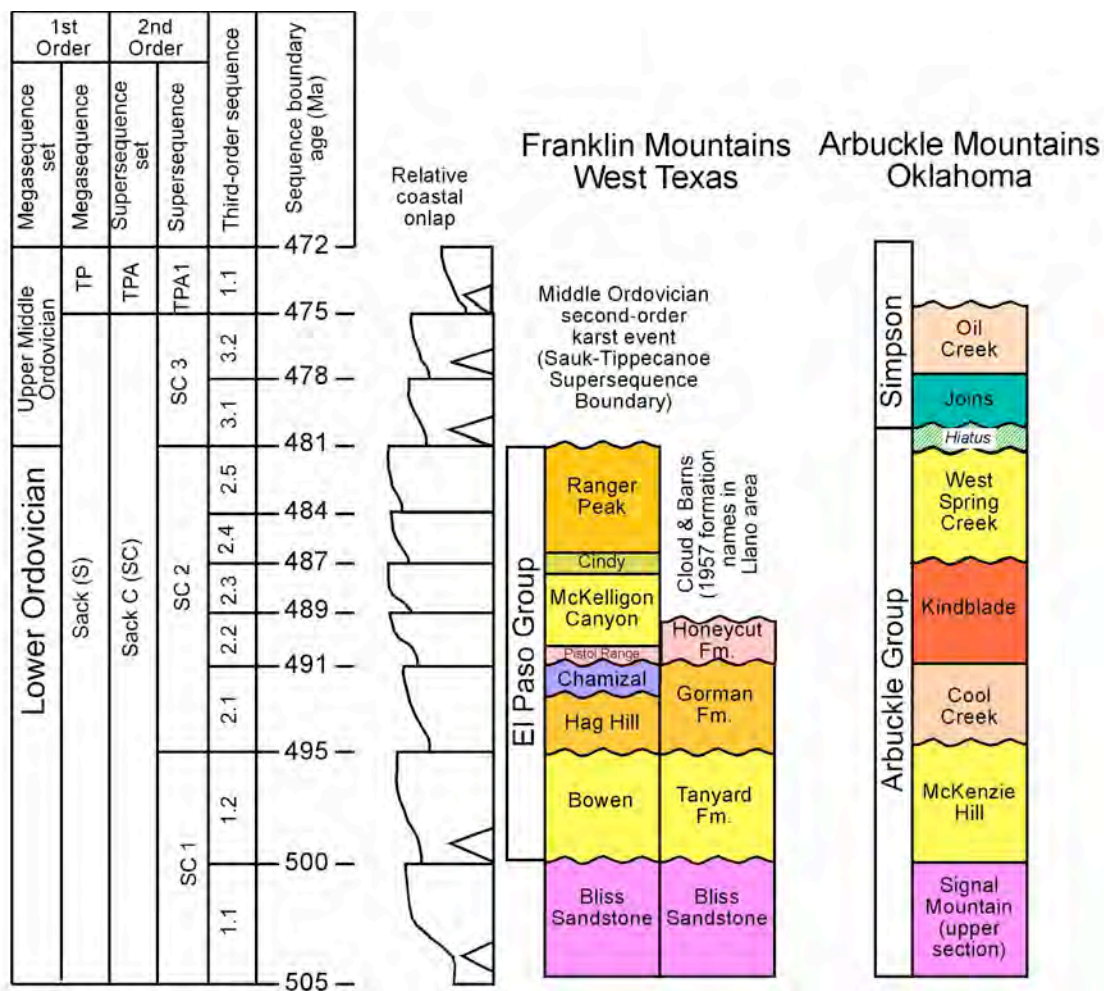


Figure 9. Chronostratigraphic summary of third-order depositional sequences in the Franklin Mountains of West Texas. Modified from Goldhammer et al. (1992).

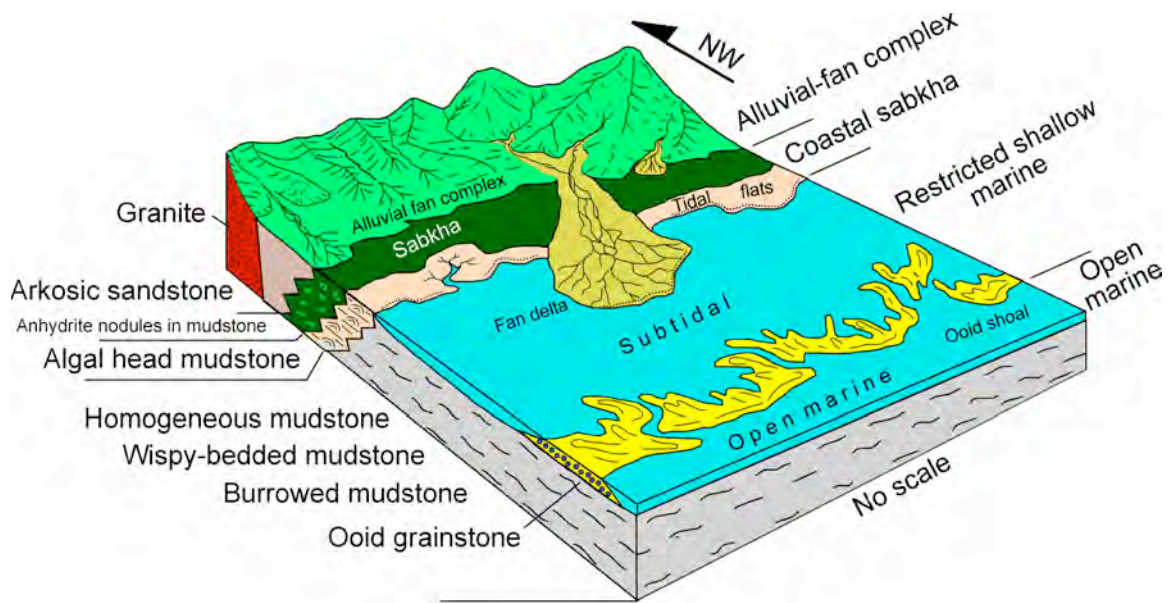


Figure 10. Depositional model for the Bliss and lower Ellenburger sections. Modified slightly from Loucks and Anderson (1985).

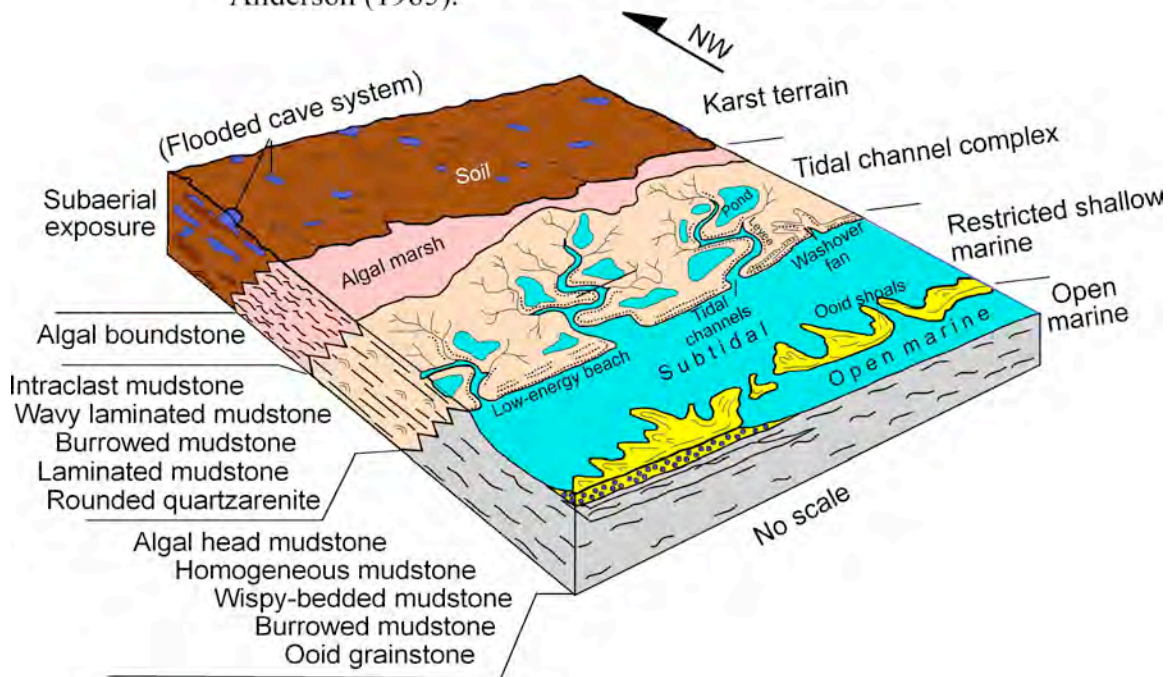


Figure 11. Depositional model for the middle and upper Ellenburger sections. Modified slightly from Loucks and Anderson (1985).

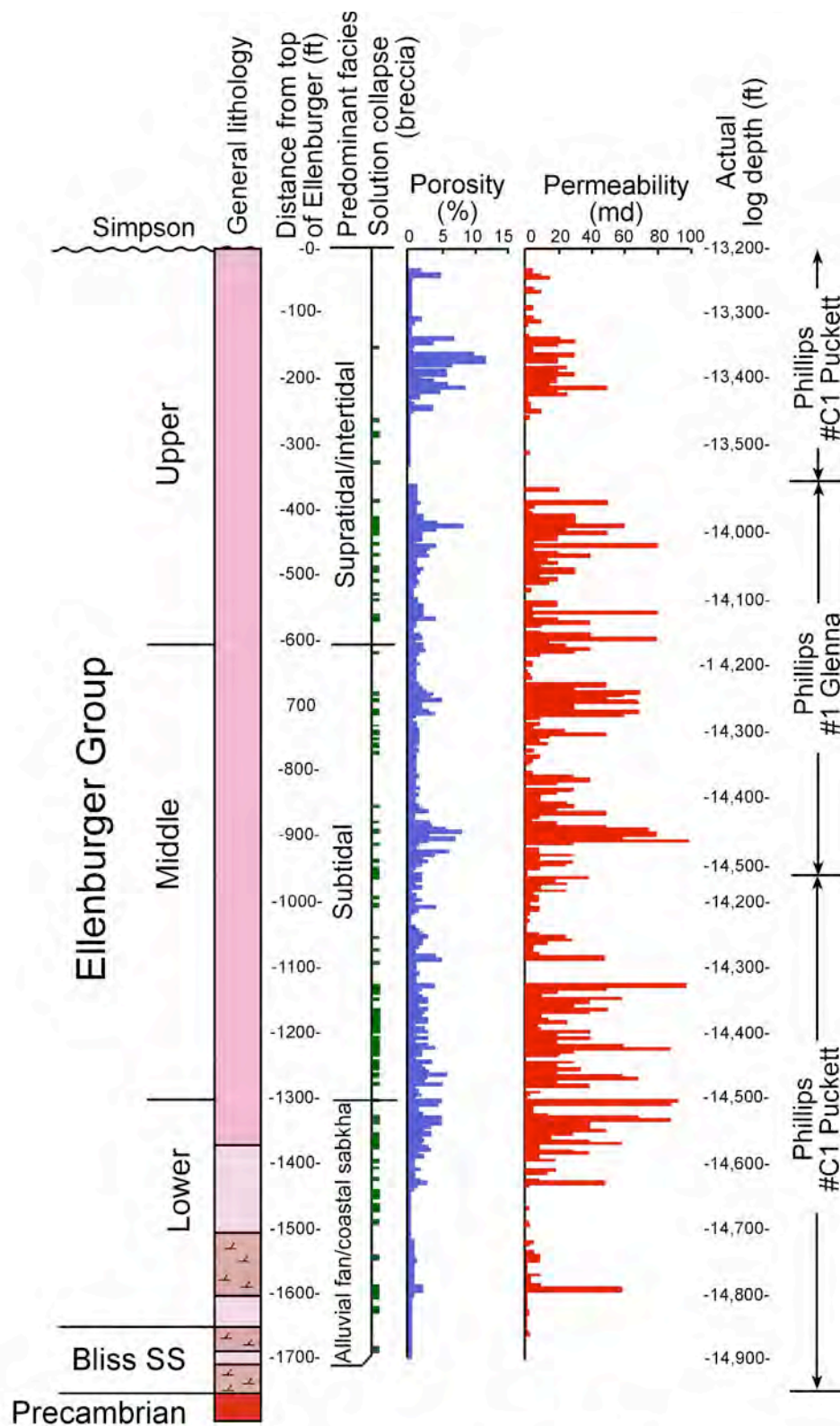


Figure 12. Profiles of porosity and permeability versus depth in the Phillips #C1 Puckett and #1 Glenna wells. Both well-log depths and depth below top of Ellenburger section are shown. "Predominant facies" refers to the facies comprising largest proportions of individual cycles. From Loucks and Anderson (1980, 1985).

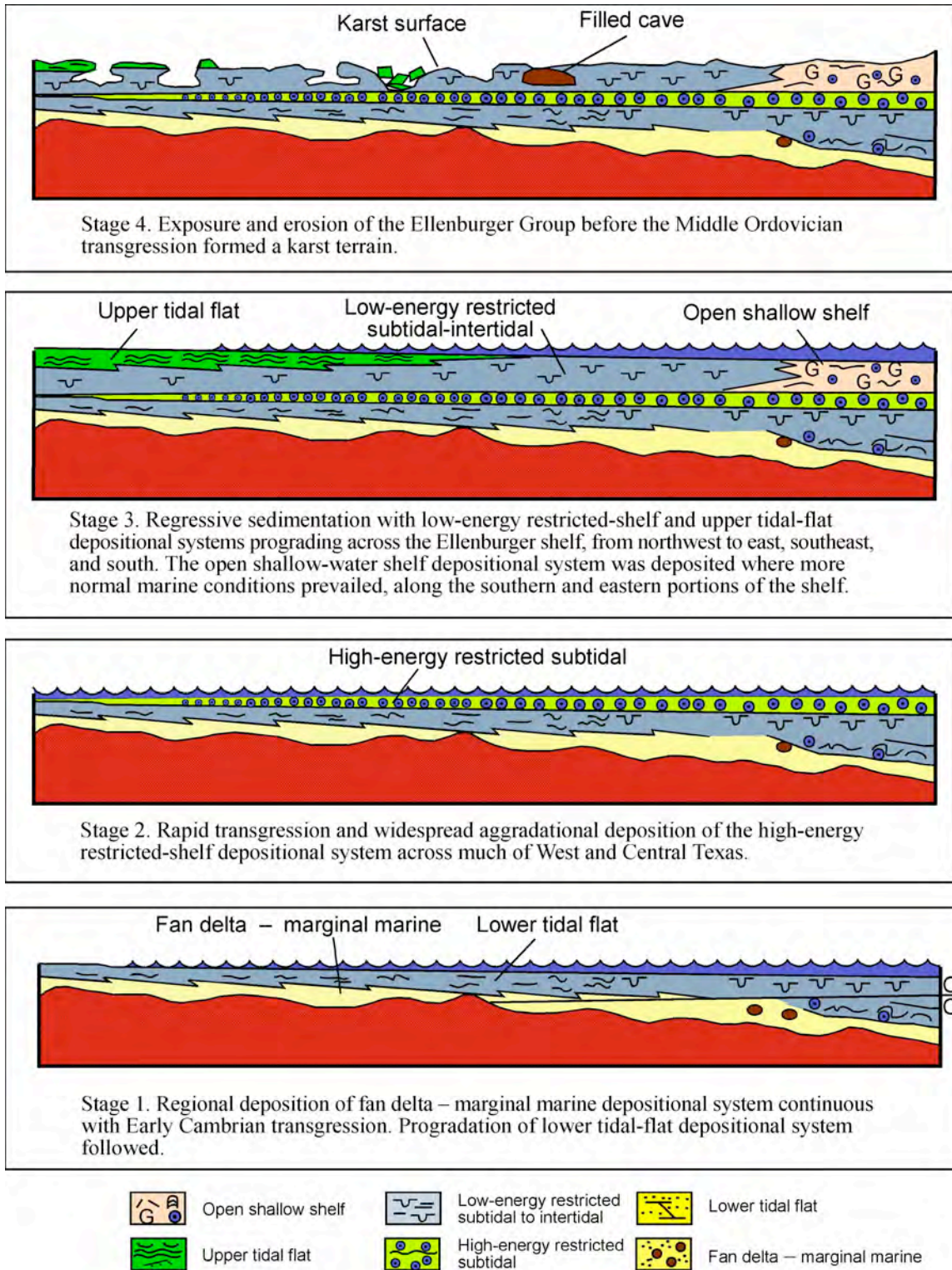


Figure 13. General depositional history of Ellenburger Group by stages. From Kerans (1990). Description of stages is taken directly from Kerans original figure caption.

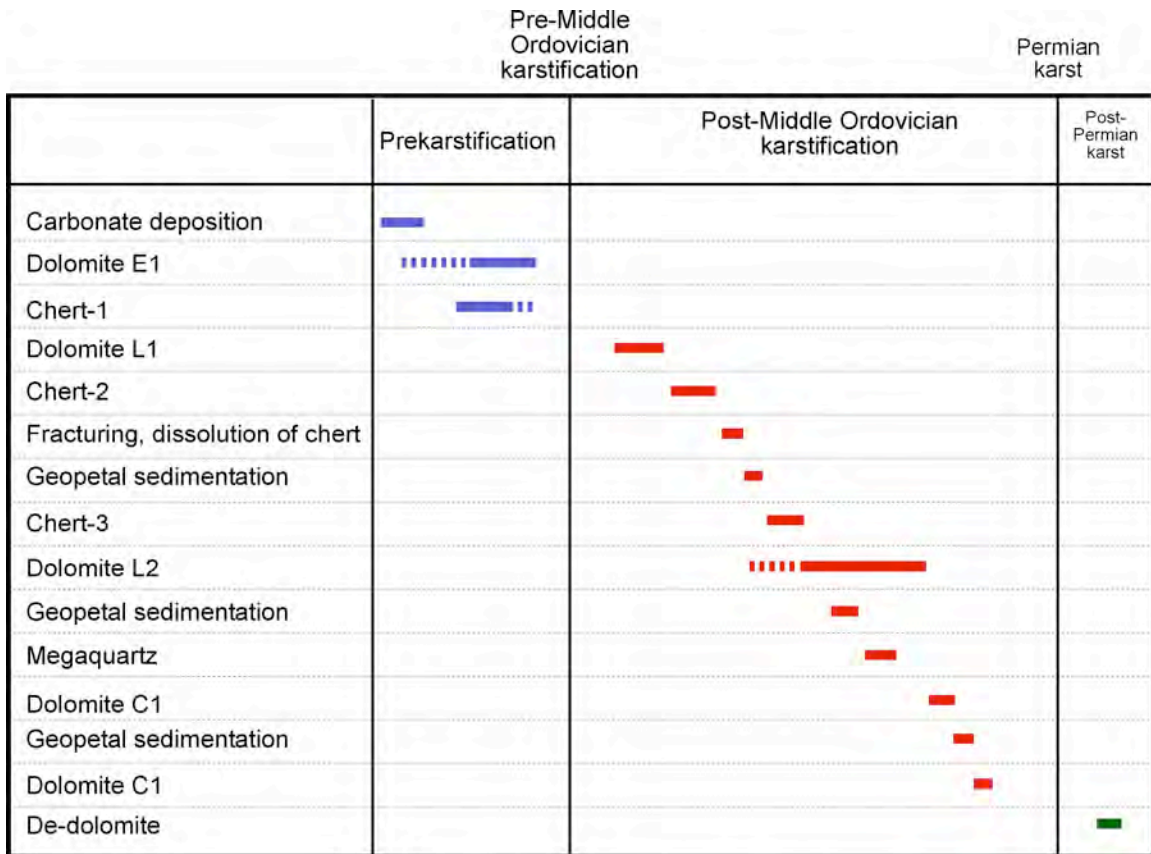


Figure 14. Paragenetic sequence of regional Ellenburger diagenesis by Kupecz and Land (1991). Figure from Kupecz and Land (1991).

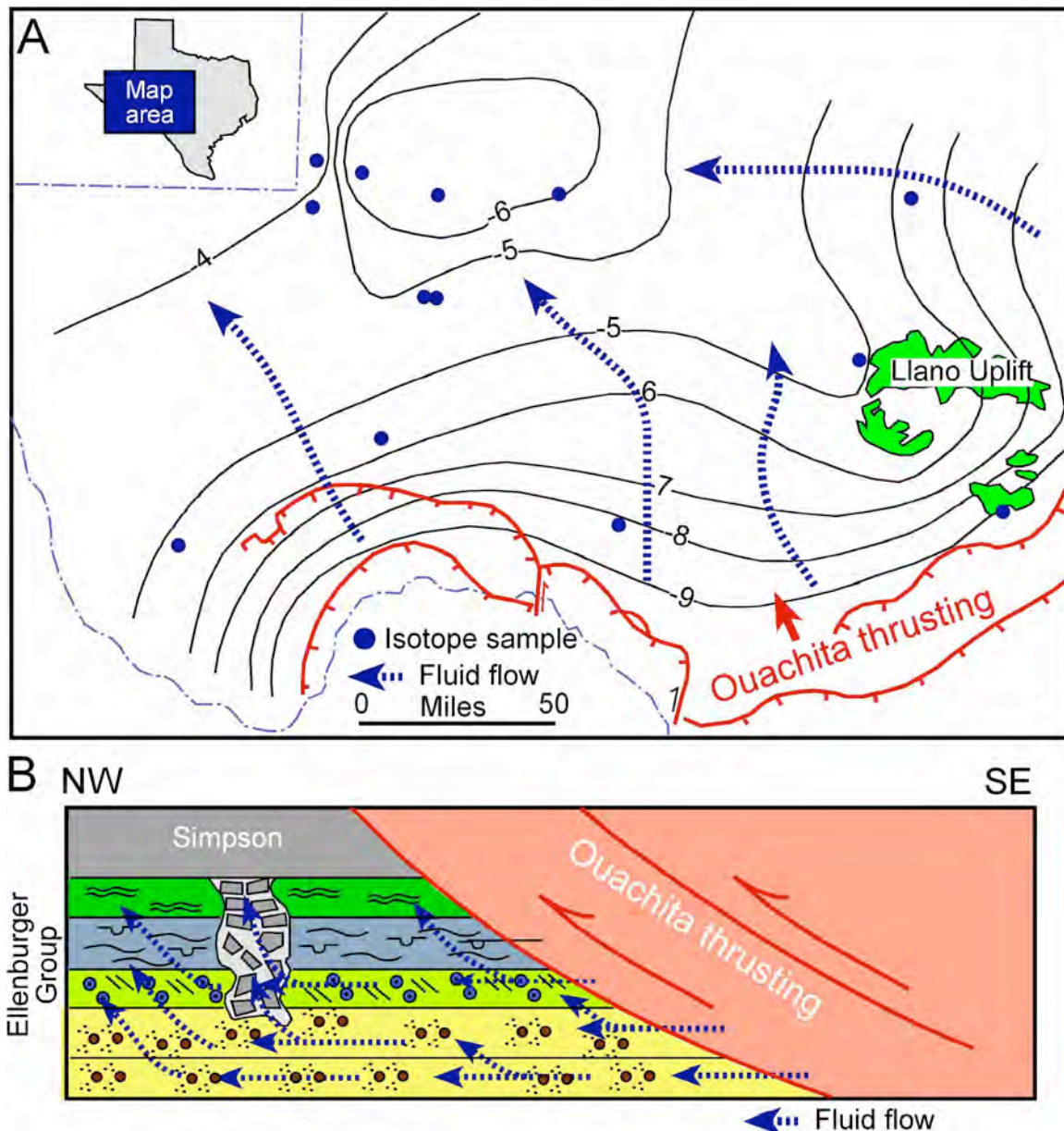


Figure 15. Fluid-flow model of Kupecz and Land (1991) for late-stage replacement Dolomite-L2. Figures from Kupecz and Land (1991). (A) Contour map of δO^{18} isotopes of the late-stage replacement Dolomite-L2. Hypothetical fluid pathway-flow lines added by present author. The map indicates that hydrothermal fluids moved from the Ouachita Orogeny front in the southeast toward New Mexico to the northwest. (B) Schematic diagram showing the pathways for the hydrothermal fluids expelled by thrusting during the Ouachita Orogeny. The fluids moved along permeable faults, fractures, karst-breccia zones, and matrix pore-rich units.

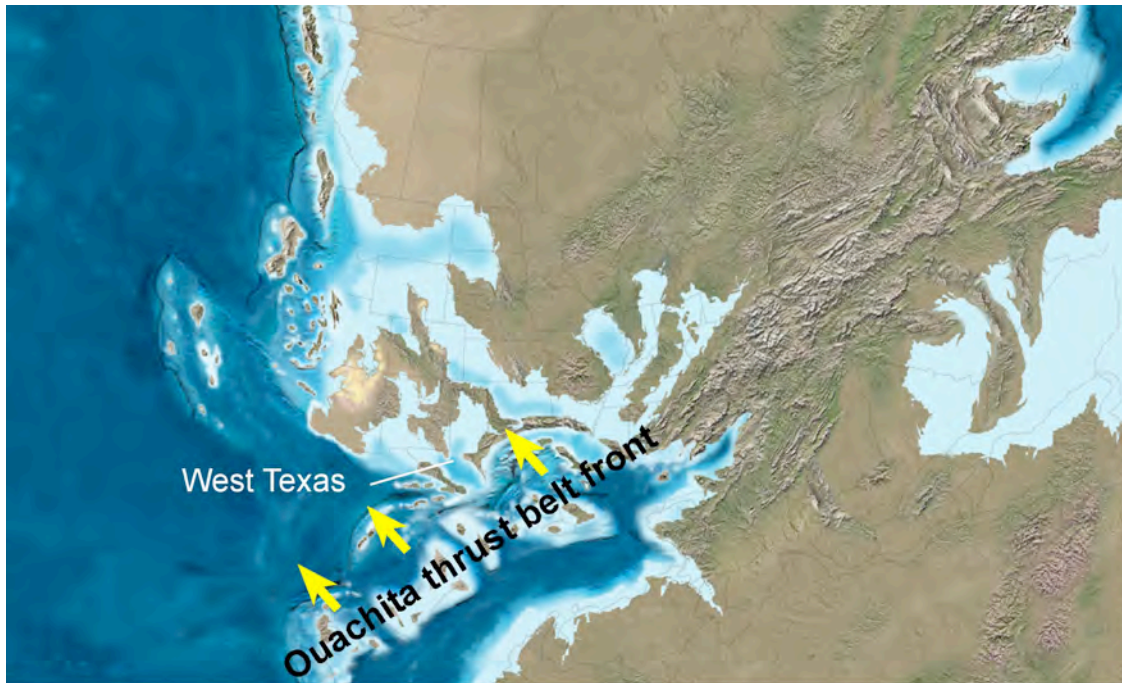


Figure 16. Plate reconstruction map of Early Pennsylvanian (315 Ma) by Blakey (2005b). The Ouachita thrusting injected dolomitizing fluids into the Ellenburger Group in the Central and West Texas areas. The yellow arrows indicate direction of thrust-fault movement.

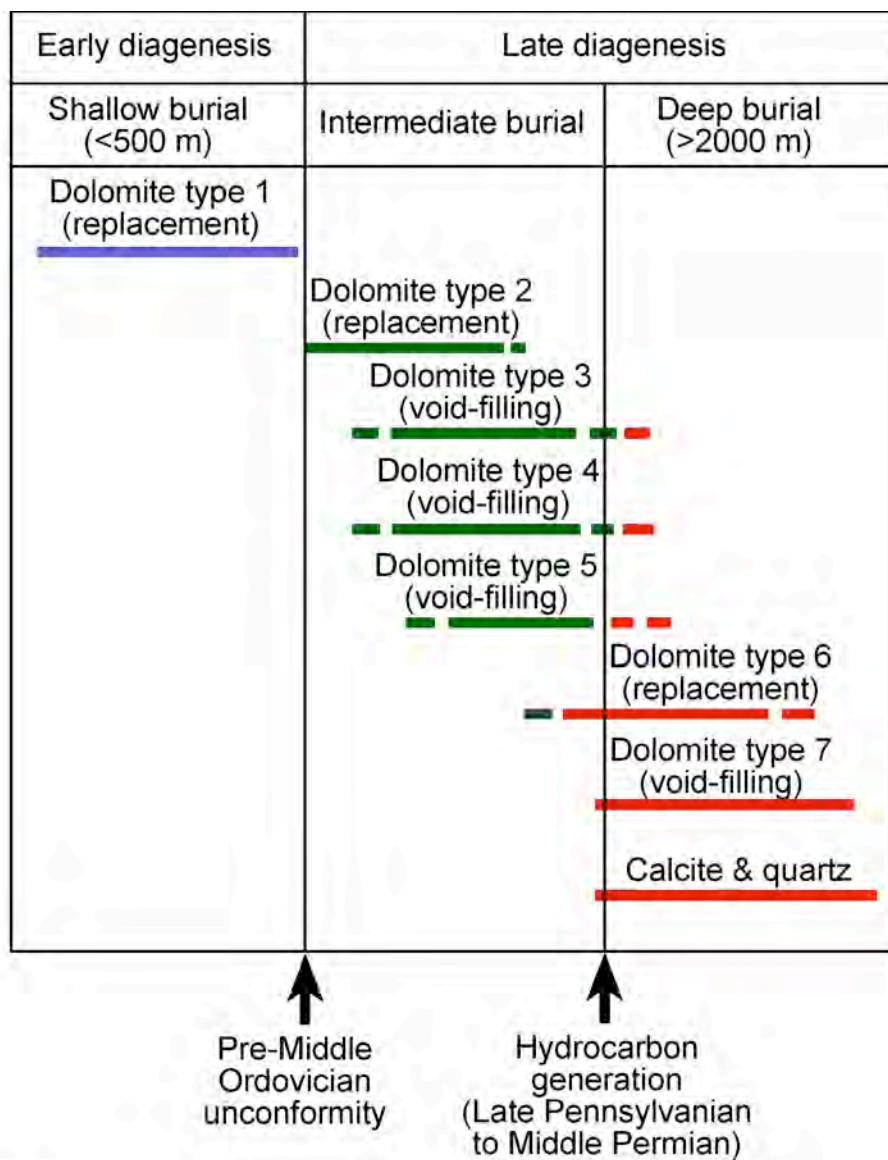
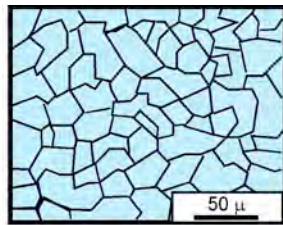
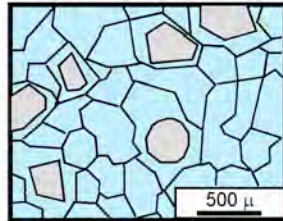


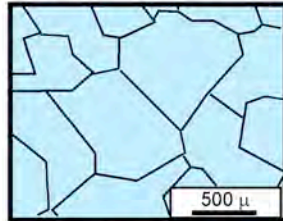
Figure 17. Paragenetic sequence of Amthor and Friedman (1991) for Ellenburger regional diagenetic study. Figure from Amthor and Friedman (1991).



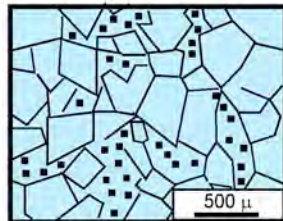
Dolomite type 1: Unimodal, very fine to fine-crystalline planar-s mosaic dolomite; dense, dark mosaics, replacing lime mud, preserving sedimentary structures.



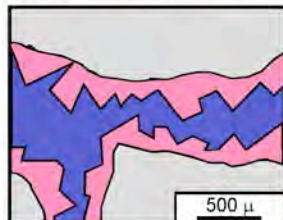
Dolomite type 2: Unimodal, medium- to coarse-crystalline planar-s mosaic dolomite; milky white to clear or cloudy core, clear rim texture, nonmimic replacement of grains.



Dolomite type 3: Coarse- to very coarse crystalline planar-s dolomite; milky to clear crystals; no replacement features; fills void space and fractures.



Dolomite type 4: Medium- to coarse-crystalline planar-e mosaic dolomite; clear or cloudy core, clear rim texture; not replacement features; occurs in mottles or breccias or near stylolites.



Dolomite type 5: Medium- to coarse-crystalline planar-e dolomite; clear crystals lining void space and fractures filled by late dolomite and/or calcite.



Dolomite type 6: Coarse- to very coarse crystalline nonplanar-a dolomite; dark, inclusion-rich crystals, with serrated, irregular, curved, or otherwise distinct boundaries; undulose extinction; vague nonmimic replacement of grains.



Dolomite type 7: Coarse- to very coarse crystalline nonplanar-c dolomite milky white to clear crystals with undulose extinction and curved crystal faces (saddle dolomite); void filling; associated with authigenic quartz and late calcite.

Figure 18. Dolomite textures described by Amthor and Friedman (1991). Figure from Amthor and Friedman (1991).

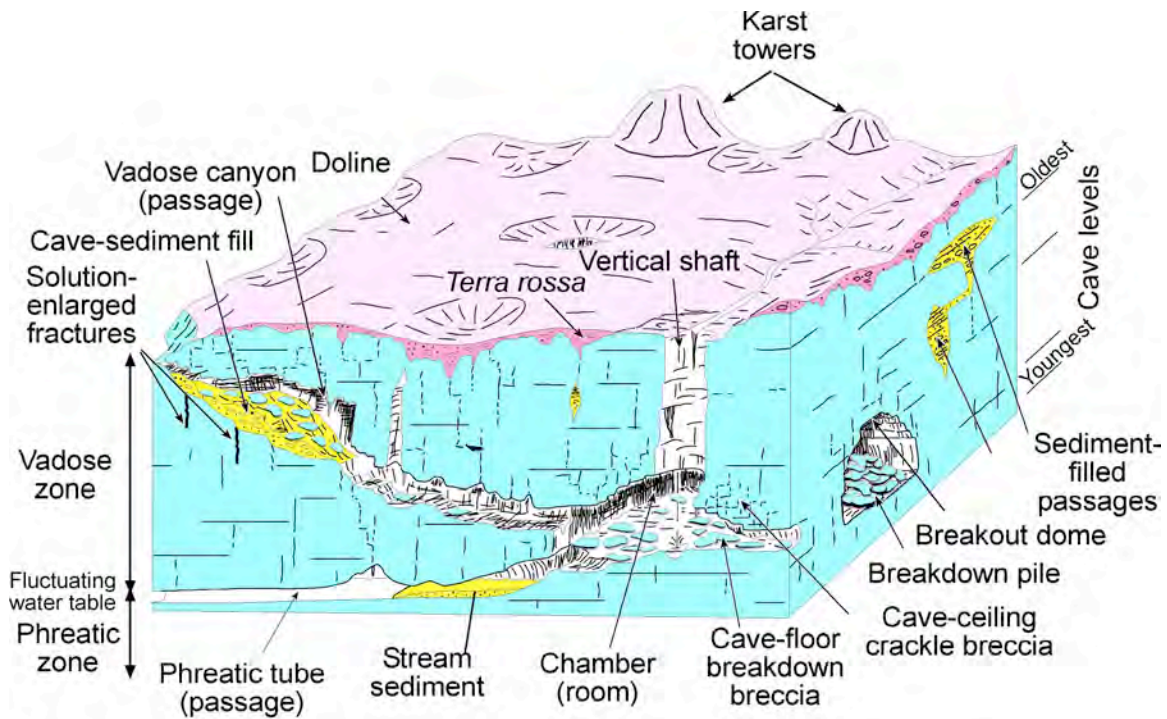


Figure 19. Block diagram of a near-surface modern karst system. The diagram depicts four levels of cave development (upper right corner of block model), with some older passages (shallowest) having sediment fill and chaotic breakdown breccias. Breccia and fracture development begin in a cave system while it is at the surface. As the water table drops, increased stress develops around caverns promoting brecciation and fracturing. Modified from Loucks (1999).

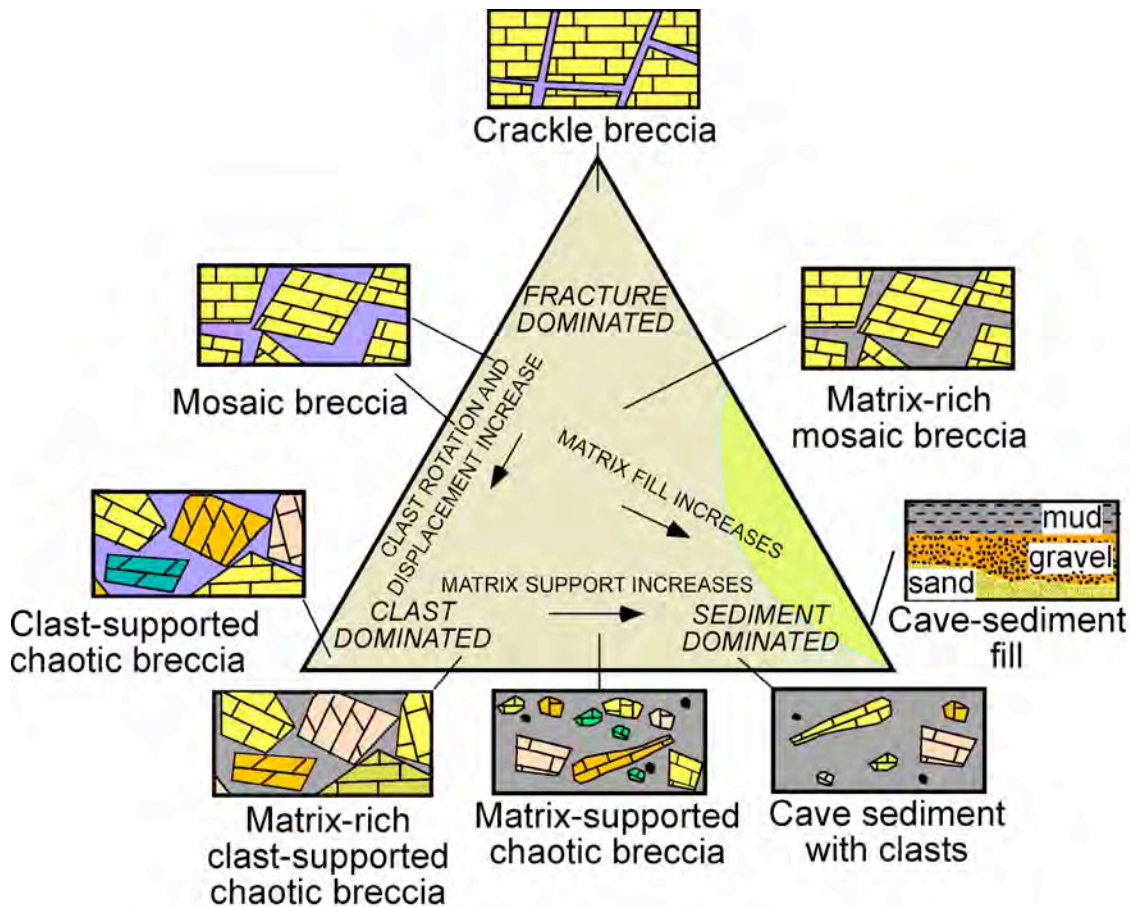


Figure 20. Classification of breccias and cave-sediment fills. Shaded area in the lower right of the diagram indicates that no cave features plot in this area. Cave-sediment fills and breccias can be separated into three end members: crackle breccia, chaotic breccia, and cave-sediment fill. Crackle breccias show slight separation and displacement. Mosaic breccias display some displacement, but they can be fitted back together. Chaotic breccias are composed of displaced clasts that cannot be fitted back together, and they can be composed of clasts of different origins (polymictic). Cave-sediment fill can form a matrix within the breccia, as well as support individual clasts. The best reservoir quality is in the matrix-free breccias. From Loucks (1999).

BURIAL EVOLUTION **NEAR-SURFACE EVOLUTION**

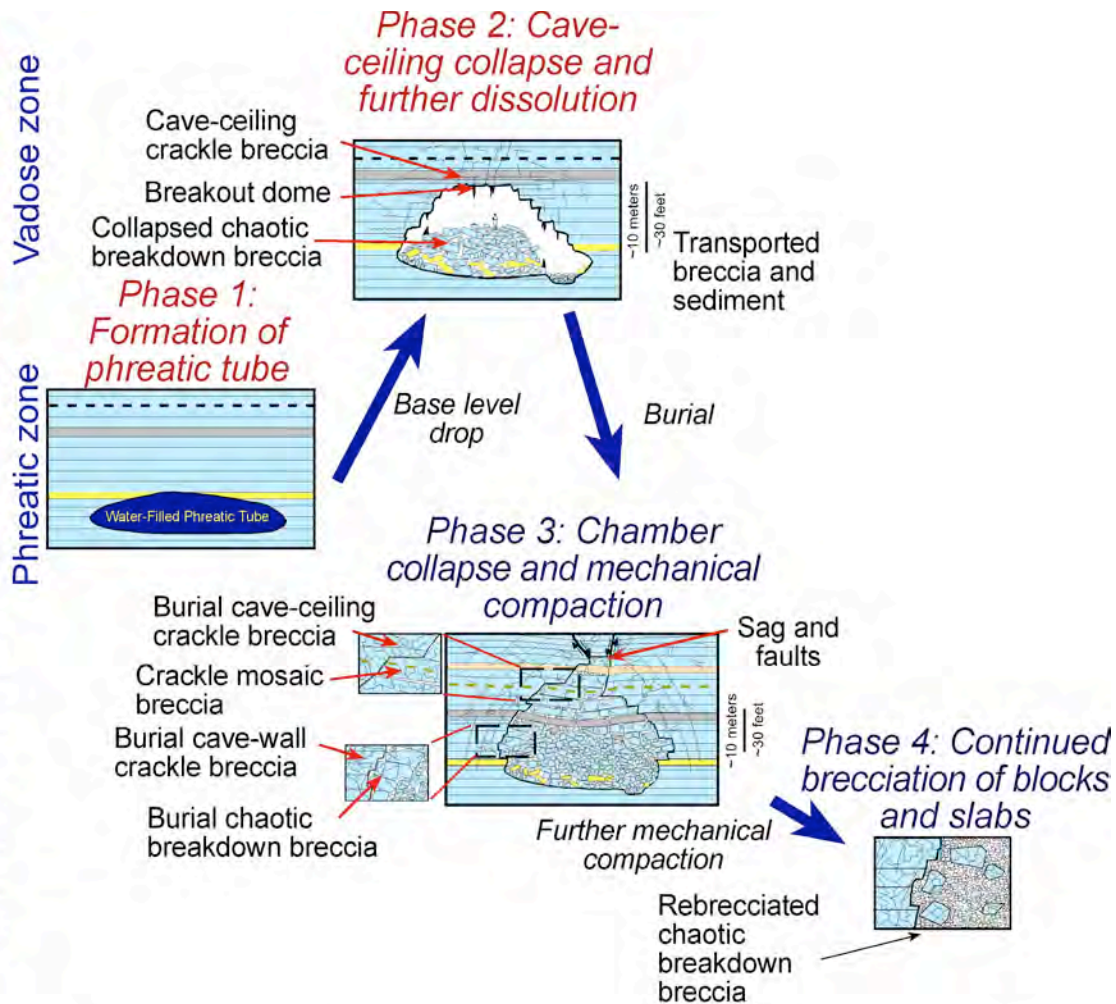


Figure 21. Schematic diagram showing evolution of a single cave passage from its formation in the phreatic zone of a near-surface karst environment to burial in the deeper subsurface. In the near-surface, excavation and associated breakdown are major processes. Many near-surface cave passages contain abundant breccias and cave-sediment fill. Crackle breccia fracturing affects the wall and ceiling rock early in the history of the cave. Excavation solution and cave sedimentation terminate as the cave-bearing strata subside into the subsurface. Mechanical compaction increases and restructures the existing breccias and remaining cavities. Most large voids collapse after several thousand feet of burial, forming more chaotic breakdown breccia. Some large interclast pores may be preserved. Differentially compacted but relatively intact strata over the collapsed chamber are fractured and form burial cave-roof crackle and mosaic breccias with loosely to tightly fitted clasts. Continued burial leads to more extensive mechanical compaction of the previously formed breakdown, thus causing blocks with large void spaces between them to fracture and pack more closely together. The resulting product is a rebrecciated chaotic breakdown breccia composed of smaller clasts. Many of the clasts are overprinted by crackle fracture brecciation.

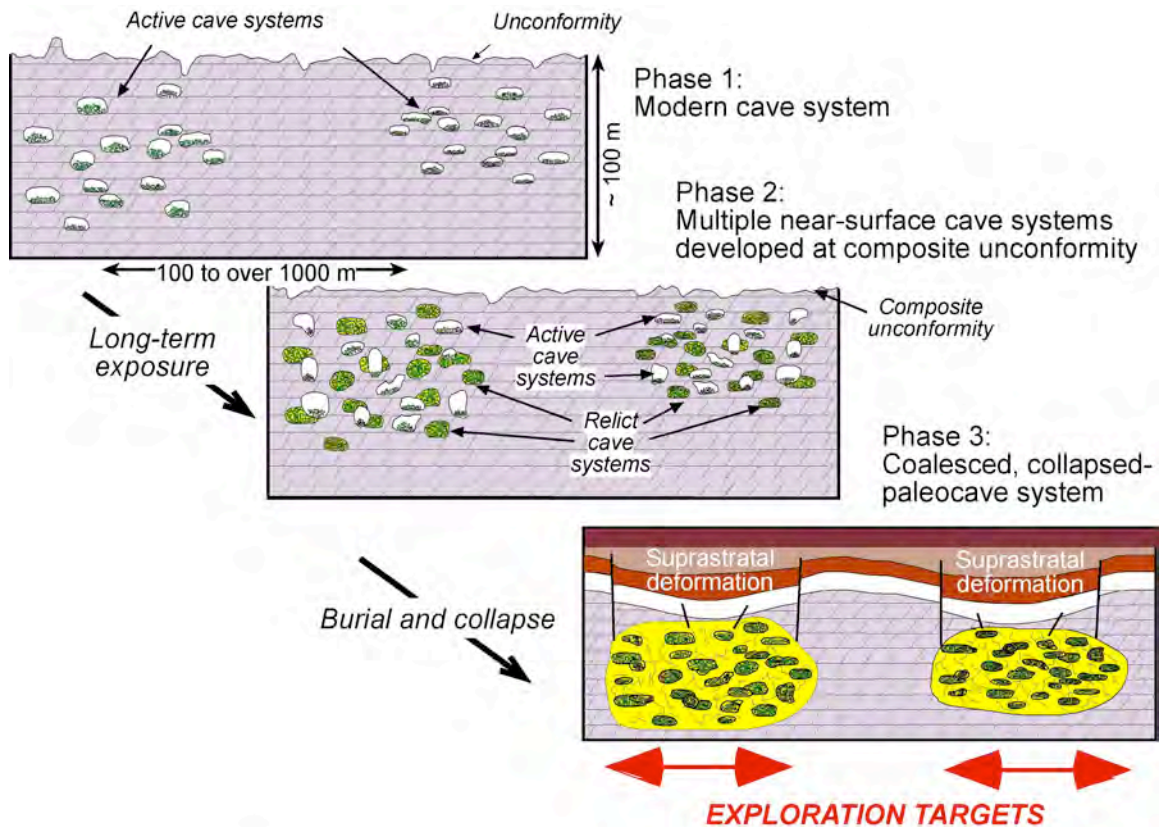


Figure 22. Schematic diagram showing the stages of development of a coalesced, collapsed-paleocave system. The development of a large collapsed-paleocave reservoir is the result of several stages of development. Multiple cave-system development at a composite unconformity may be necessary in order to produce a high density of passages. As the multiple-episode cave system subsides into the deeper subsurface, wall and ceiling rocks adjoining open passages collapse and form breccias that radiate out from the passage, and may intersect with fractures from other collapsed passages and older breccias within the system. The result is the coalescing of the cave system into a spatially complex reservoir system. The resulting coalesced breccia/fractured bodies can be thousands of feet of across, thousands of feet long, and hundreds of feet thick. Strata above the collapsed cave system are deformed by brecciation, faulting, and sagging (suprastratal deformation) Modified from Loucks (1999).

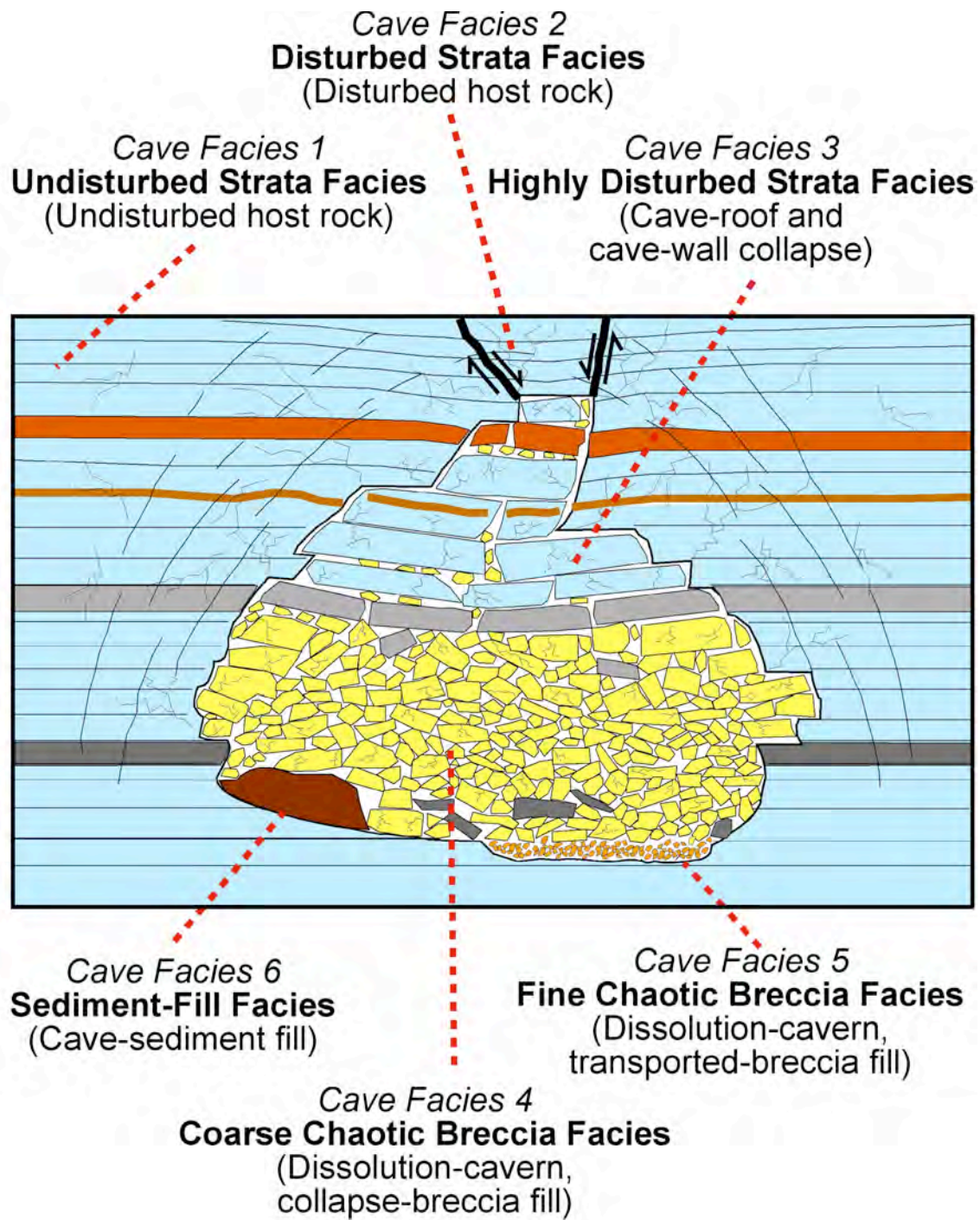


Figure 23. Paleocave facies classification by Loucks and Mescher (2001). See Table 1 for details.

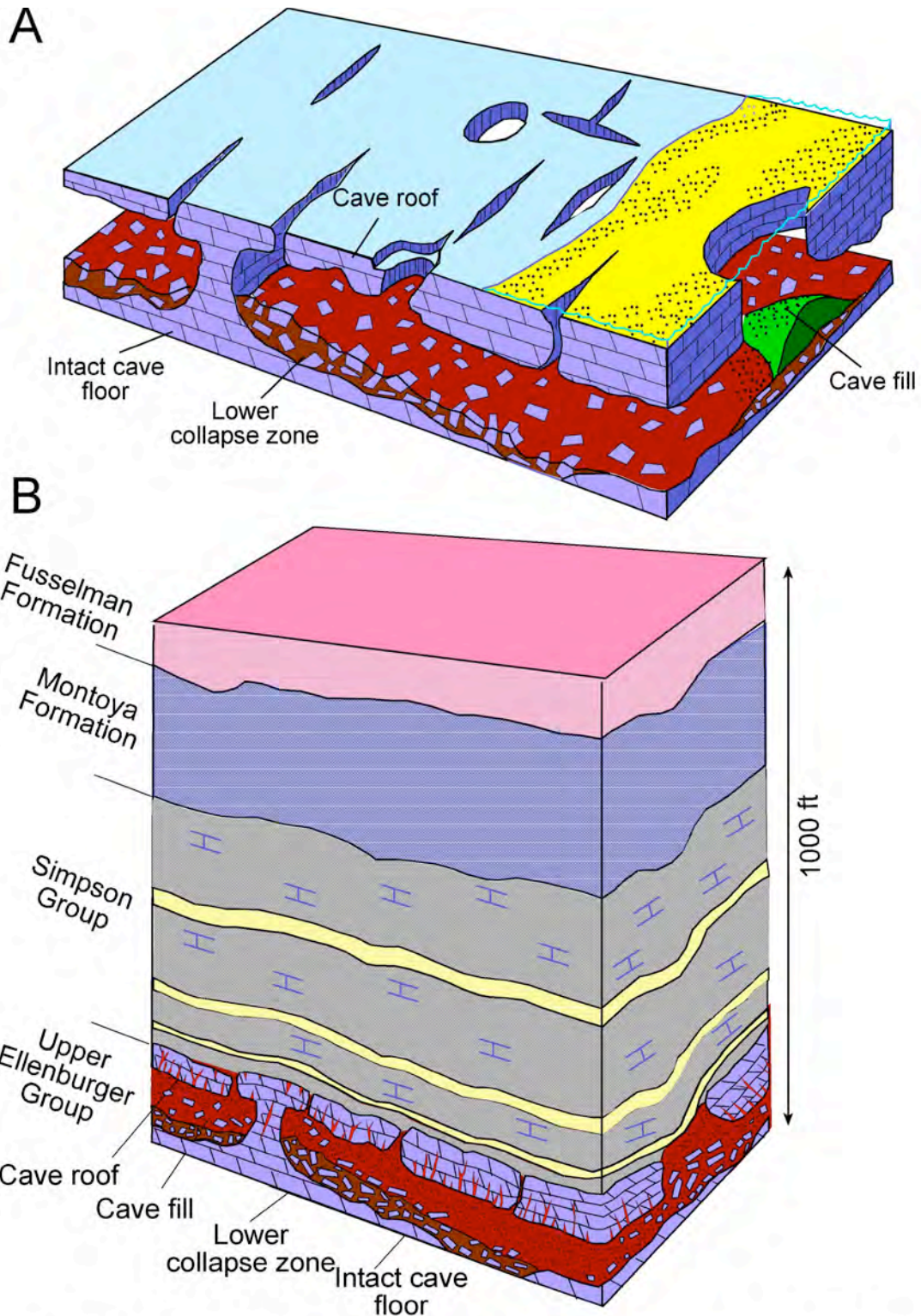


Figure 24. Paleocave models of Kerans (1988, 1989). (A) Schematic block diagram of a cave in the Lower Ordovician of West Texas showing cave floor, cave roof, cave-sediment fill, and collapsed breccia. Simpson siliciclastic material is filling cave during later transgression. (B) Schematic block model showing the collapsed Ellenburger paleocave system buried by successive Ordovician and Silurian deposits. Burial resulted in fracture brecciation of the roof and sagging of later units.

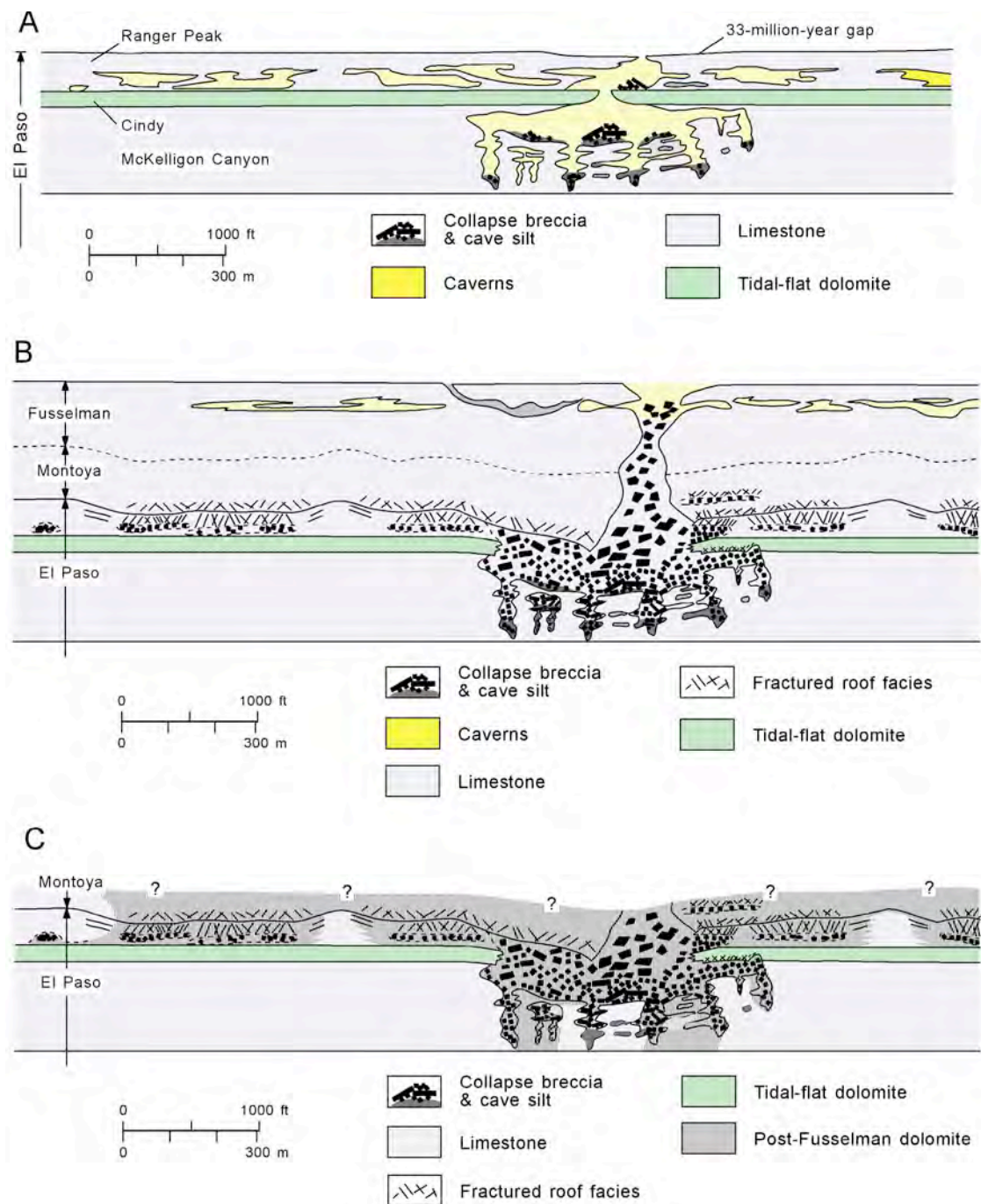


Figure 25. Reconstruction of El Paso paleocave system by Lucia (1995). Figure caption is directly from Lucia (1995). (A) Penecontemporaneous dolomitization of the Cindy Formation and development of tabular, laterally continuous caverns in the Ranger Peak Formation and vertical, laterally discontinuous caverns in the McKelligon Canyon Formation. (B) Collapse of the El Paso caverns showing collapse of the Montoya, development of breccia pipes up into the Fusselman Formation, and development of caverns in the Fusselman Formation. (C) Late-stage dolomitization of the El Paso and Montoya groups controlled by fluid flow through collapse breccia, fractures, and into adjacent carbonates.

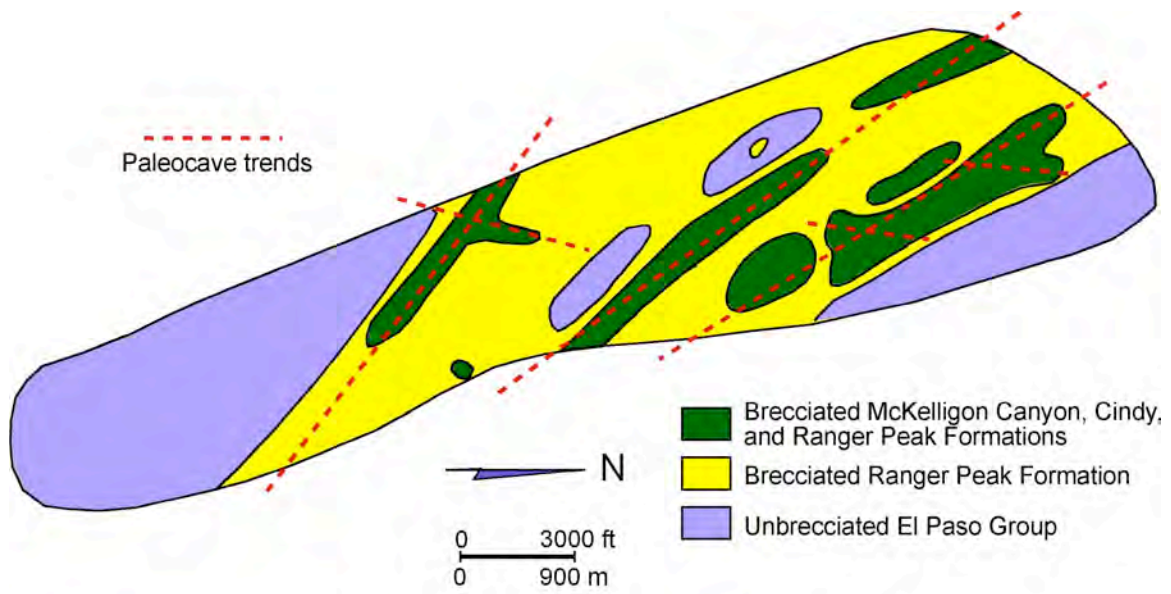


Figure 26. Reconstruction by Lucia (1995) of the different collapsed breccia in the Franklin Mountains, Texas. Paleocave trend lines are by present author.

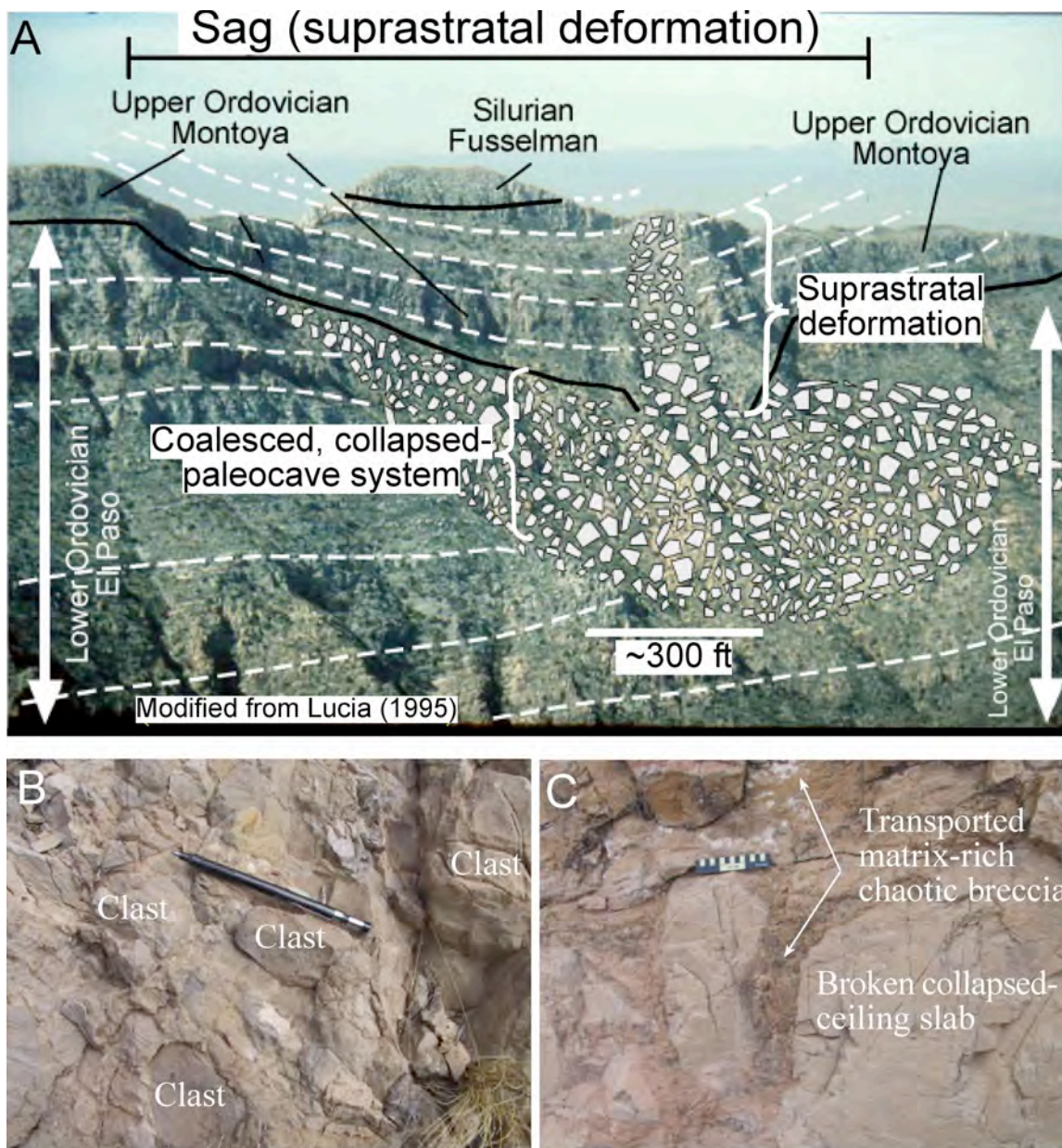


Figure 27. (A) Photograph of the Great McKelligon Sag in the Franklin Mountains of far West Texas. Photograph and general interpretation are from Lucia 1995 but modified by present author. This is an outstanding outcrop example of a coalesced, collapsed paleocave system with associated overlying suprastratal deformation. (B) Transported matrix-rich chaotic breccia. (C) Broken collapsed ceiling slab embedded in transported matrix-rich chaotic breccia.

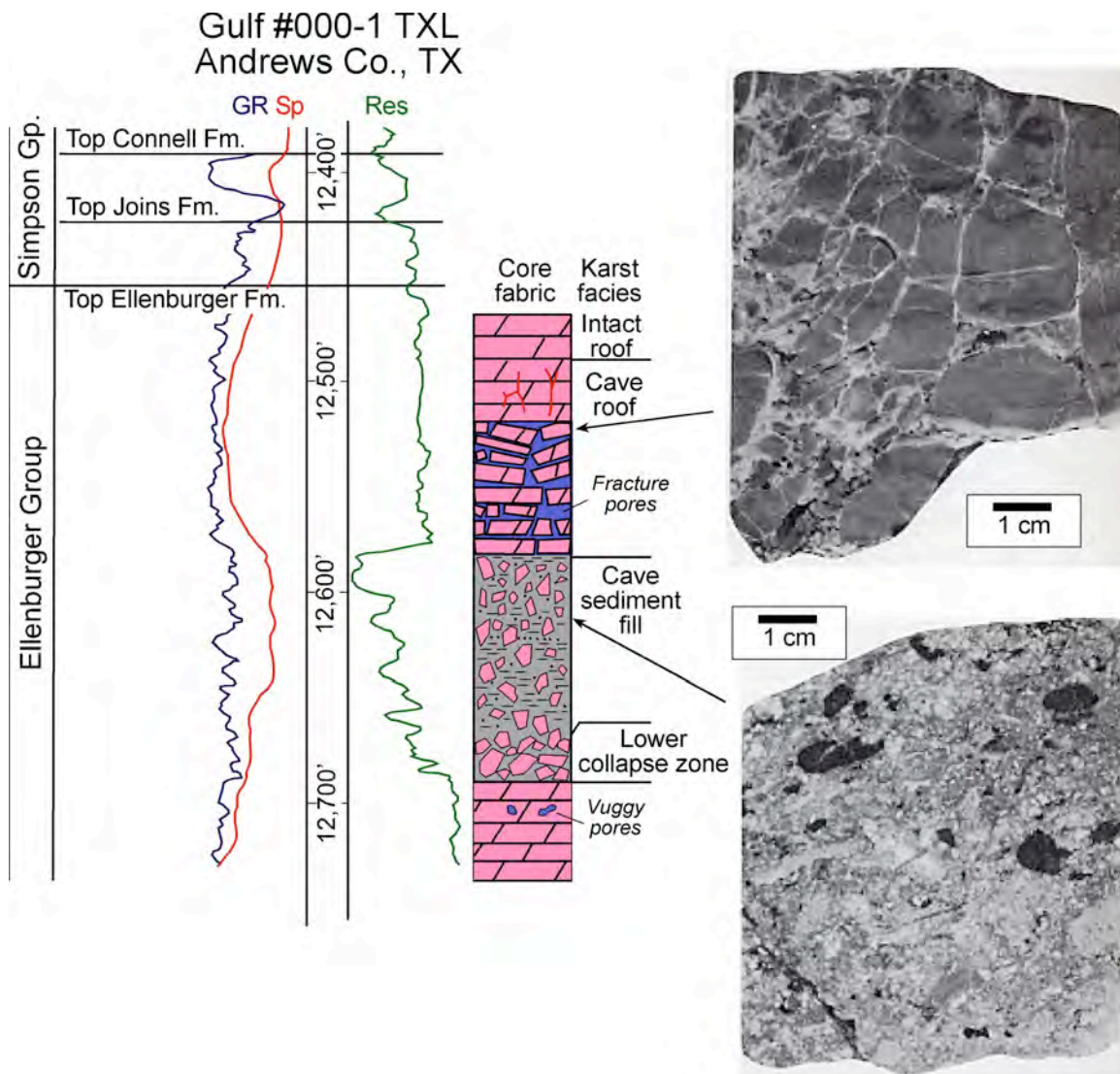


Figure 28. Core and wireline logs from the Gulf #000-1 TXL, Emma reservoir (Andrews County, Texas). Upper photograph from 12,526 ft shows crackle-fracture pores in collapse cave roof. Lower photograph from 12,610 ft shows cave-sediment fill (debris flow) with clasts floating in matrix of chloritic shale and quartz sand. From Kerans (1989).

ARCO Block 31
Crane Co., TX

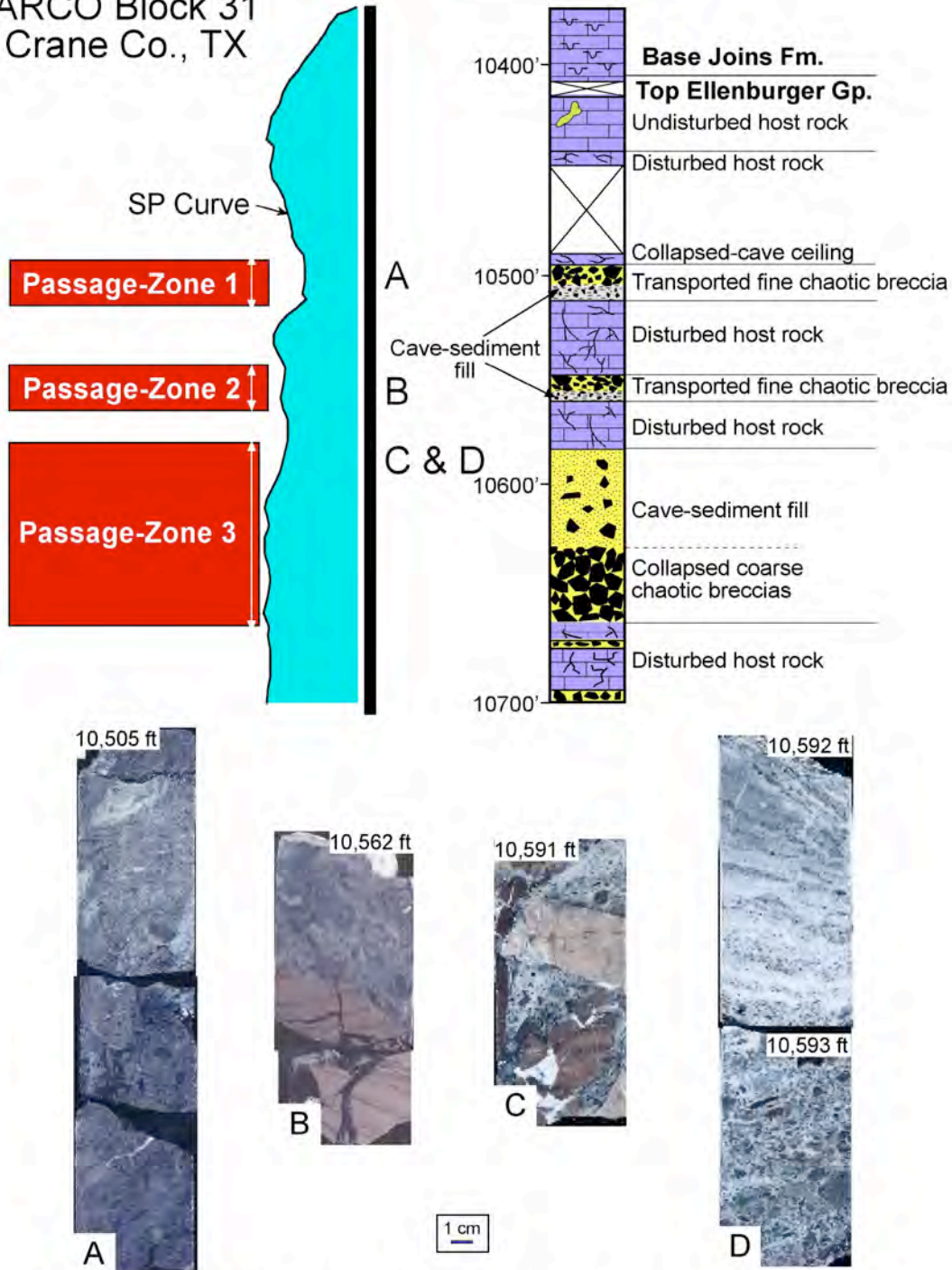


Figure 29. Core description and associated SP log for the Arco Block 31 core in Crane County, Texas. Photograph A is from a debris flow of transported fine chaotic breccia (cave-sediment fill in a passage). Photograph B from a debris flow of transported fine chaotic breccia (cave-sediment fill in a passage). Photograph C is siliciclastic-rich sand and carbonate clast cave-sediment fill (cave-sediment fill in a passage). Photograph D is a debris flow at the base overlain by siliciclastic cross-bedded sandstone (cave-sediment fill in a passage). Modified from Loucks and Handford (1992) and Loucks (2001)

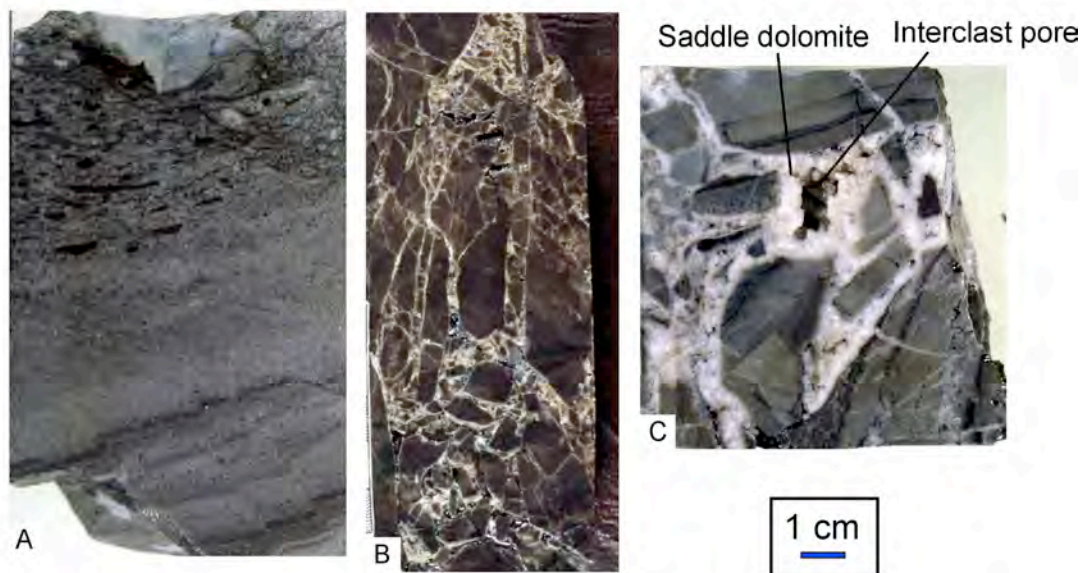
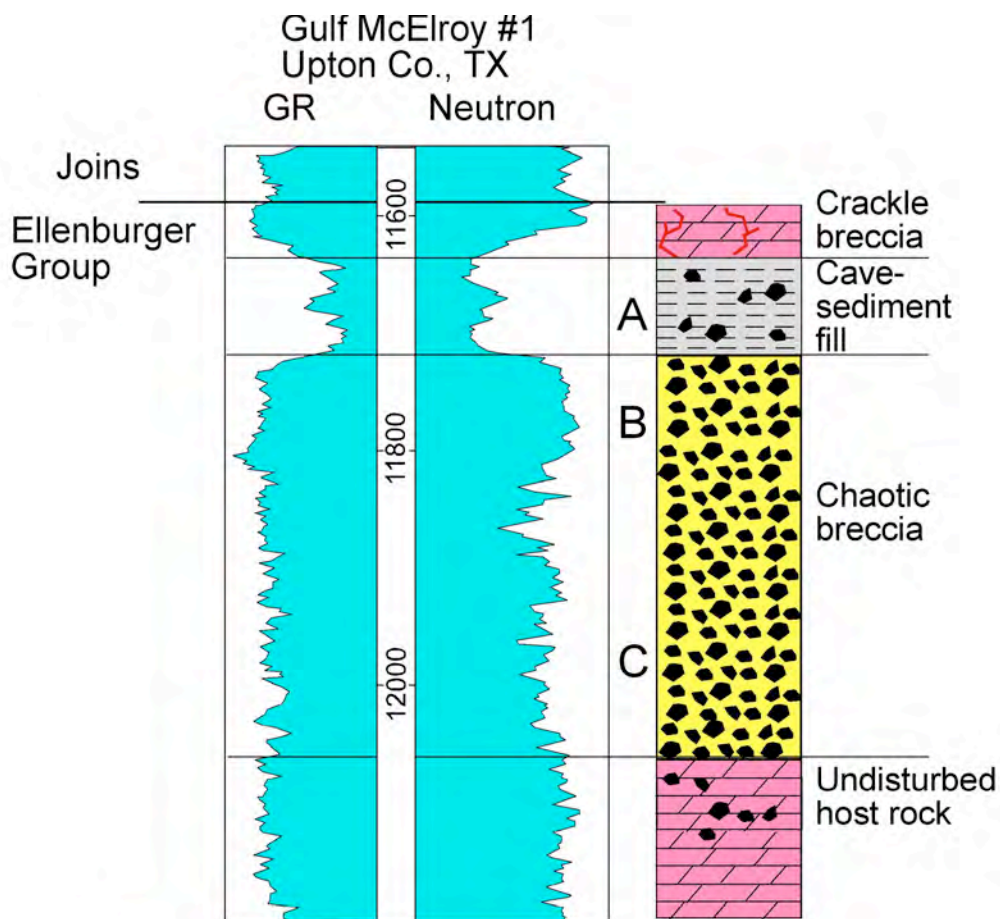


Figure 30. Core description and associated gamma-ray log for the Gulf #1 McElroy core in Upton County., Texas. Photograph A is from the cave-sediment fill in a passage. Photograph B from a chaotic breccia pile in a passage. The clasts show late crackle brecciation. Photograph C from a chaotic breccia pile in a passage. Because of the lack of matrix between the clasts and incomplete filling by saddle dolomite, there are interclast pores present. From Kerans (1989).

Goldrus Producing Company Unit #3 Reagan County, Texas

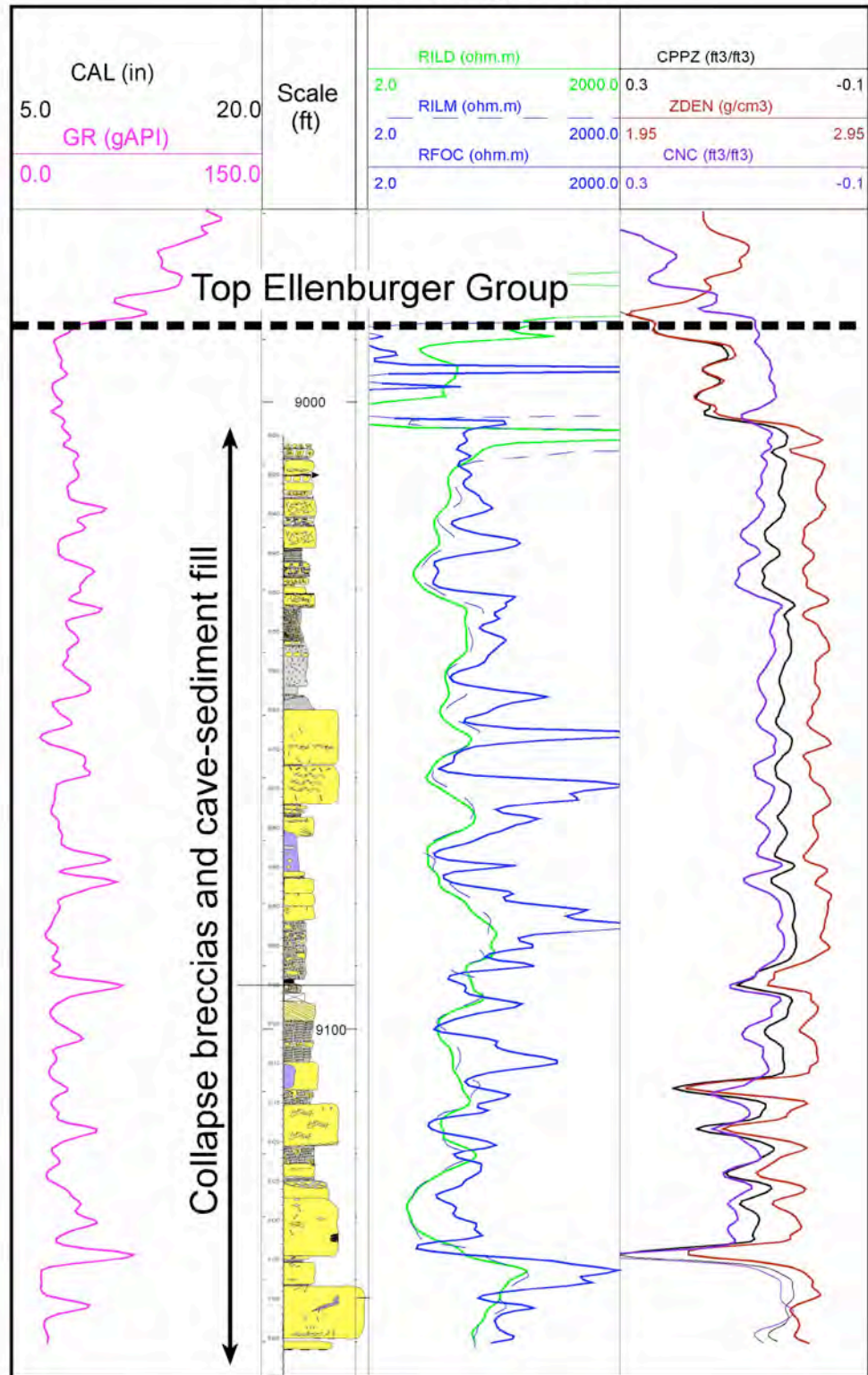
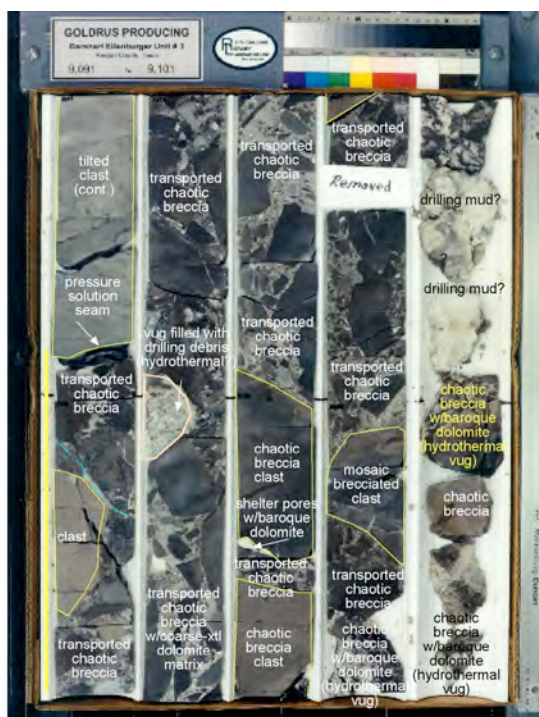


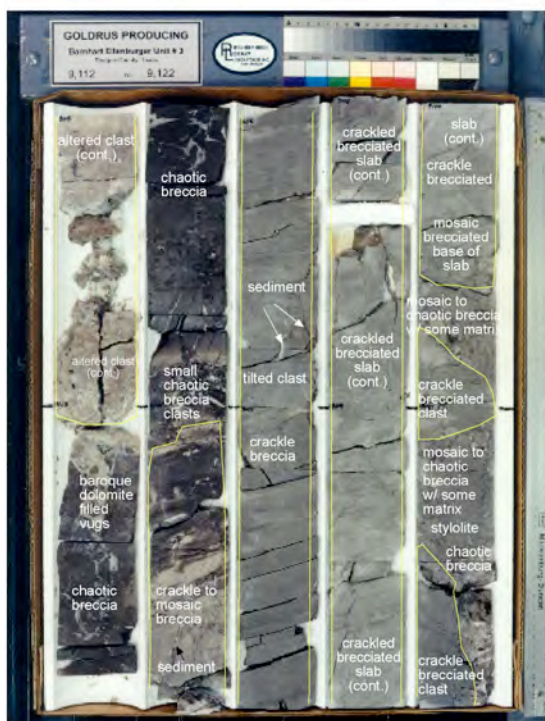
Figure 31. Goldrus Producing Company Unit #3 core and associated wireline logs in Barnhart field (Reagan County, Texas) is extensively karsted. See Figure 32 for examples of rock types. From Combs et al. (2003).



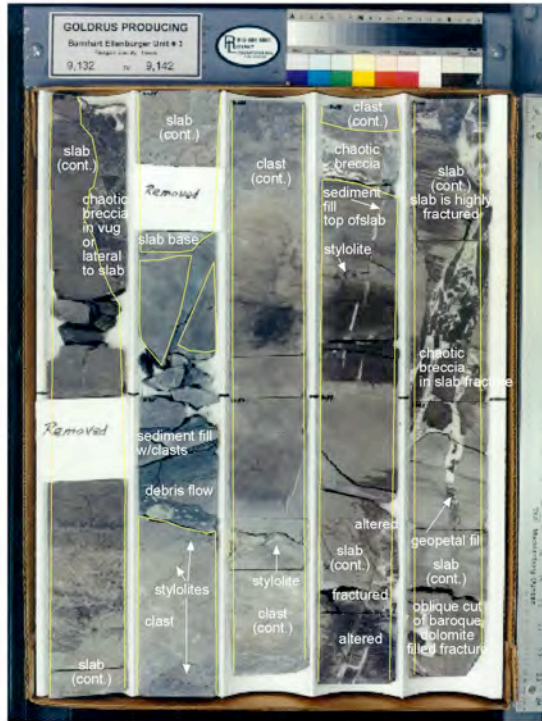
Debris-flow breccia in a paleocave passage. Some of the clasts show crackle brecciation.



Large deformed blocks with crackle-breccia overprint interbedded with cave-sediment fill.



Large deformed blocks with crackle-breccia overprint.



Large deformed blocks with crackle-breccia overprint.

Figure 32. Example of several Ellenburger paleocave facies from the Goldrus Unit #3 Barnhart core in Regan County, Texas. From Combs et al. (2003).

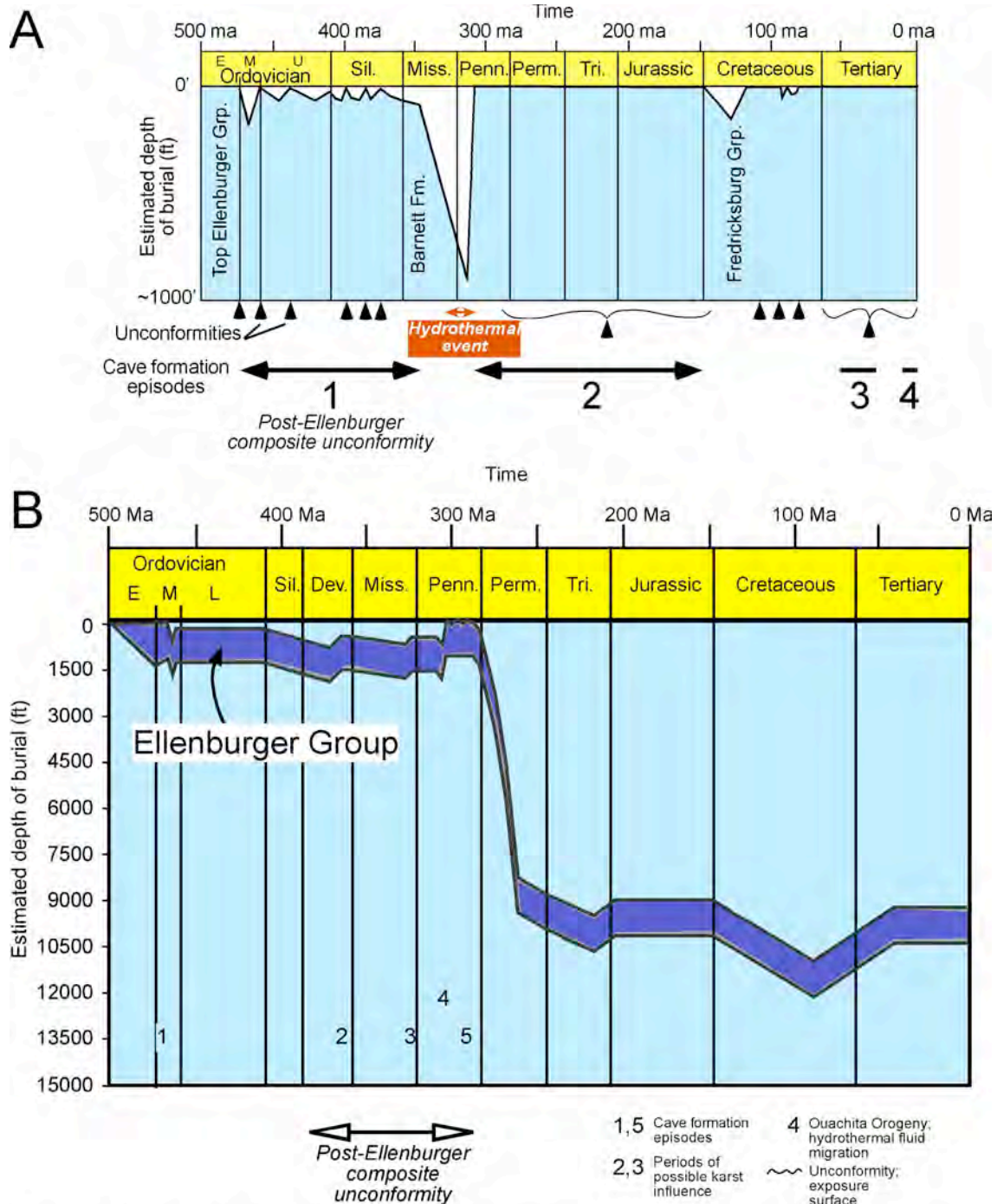


Figure 33. (A) Schematic burial history plot for the Lower Ordovician Ellenburger Group in the Llano Uplift area of Central Texas. From Kupecz and Land (1991). (B) Generalized burial history of the Ellenburger Group within Barnhart field in Regan Co., Texas. Barnhart field underwent several episodes of uplift. At least two of these episodes exposed the Ellenburger Group to karstification and cave formation: (1) Early-Middle Ordovician and, (2) Pennsylvanian times. The Ellenburger Group was also brought close to the surface during the Devonian and Mississippian, and may have experienced some karst influence here. During the Early Pennsylvanian time the Ellenburger Group experienced hydrothermal processes and tectonic uplift related to the Ouachita Orogeny. From Combs et al. (2003).

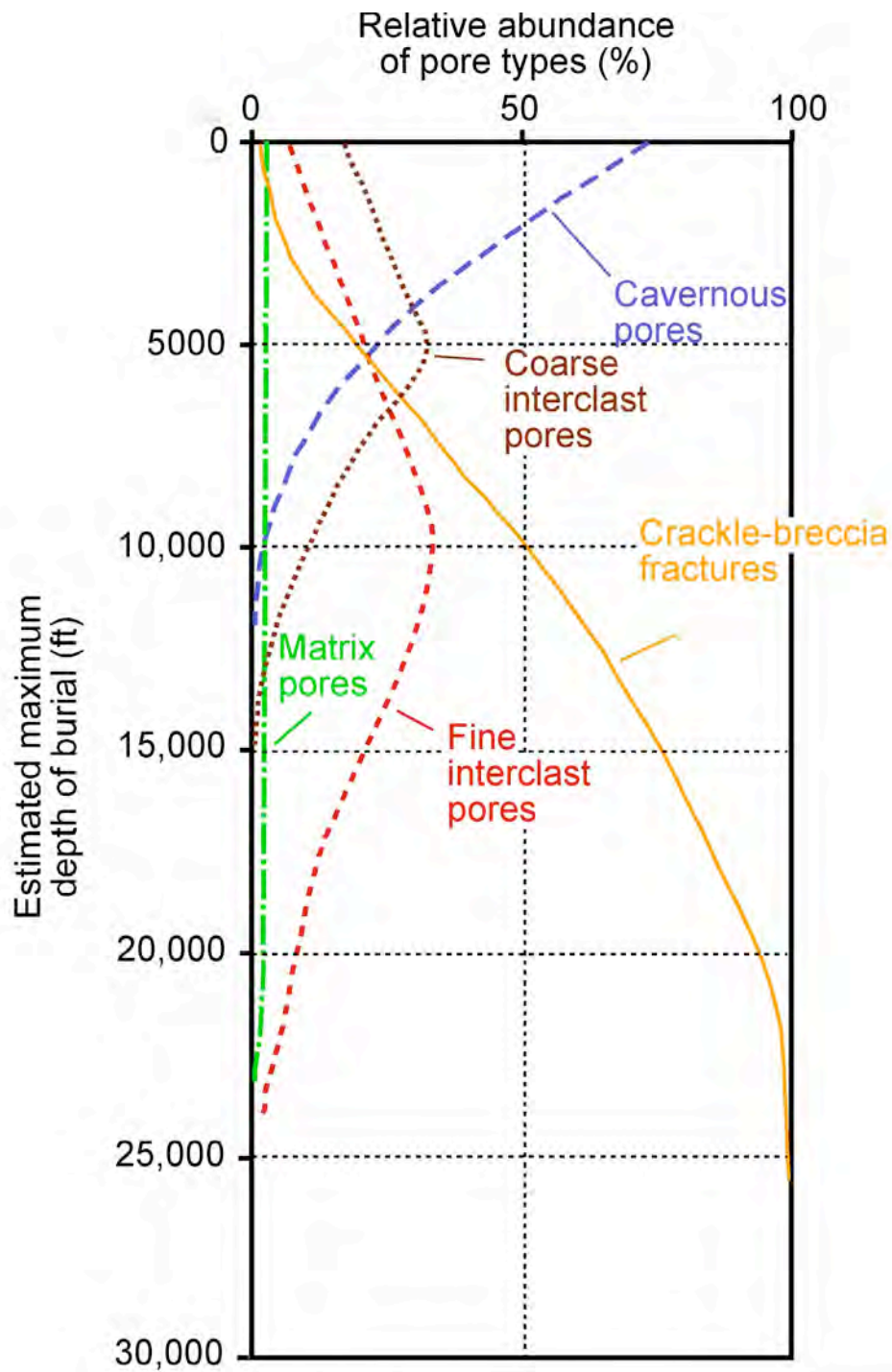


Figure 34. Generalized burial evolution of a cave-system pore network with relative proportions of pore types. The dividing line between fine clast and coarse clasts is 6 cm. The relative abundance of pore types and estimated burial depth are estimates based on review of near-surface and buried paleocave systems presented in Tables 1 and 2 of Loucks (1999). After 20,000 ft of burial, the graph is very speculative. Figure modified from Loucks (1999).

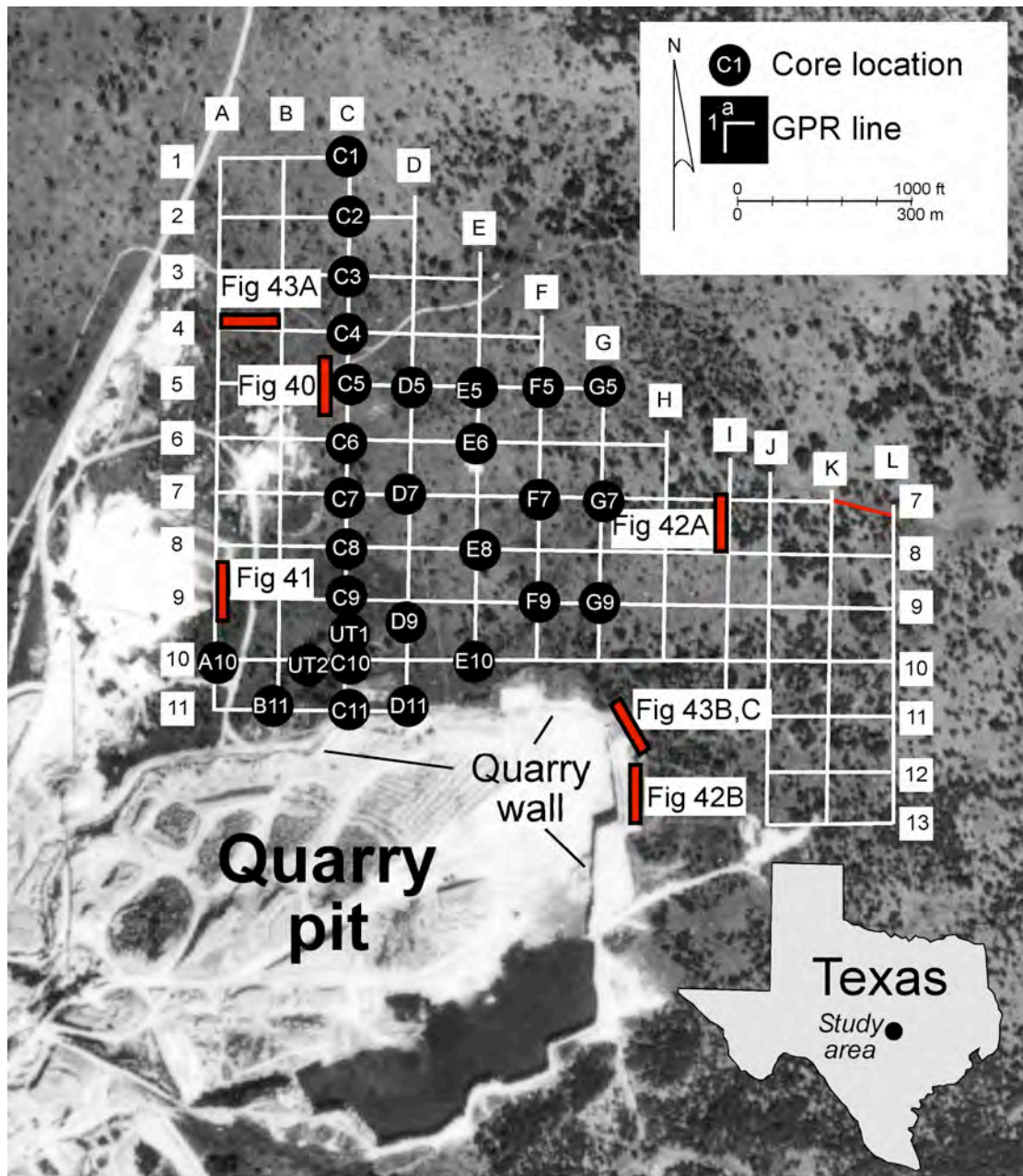


Figure 35. Aerial photograph of Dean Word Quarry showing location of grid of ground-penetrating radar (GPR) lines and cores. Locations of GPR lines illustrated later in the paper are labeled. From Loucks et al. (2004).

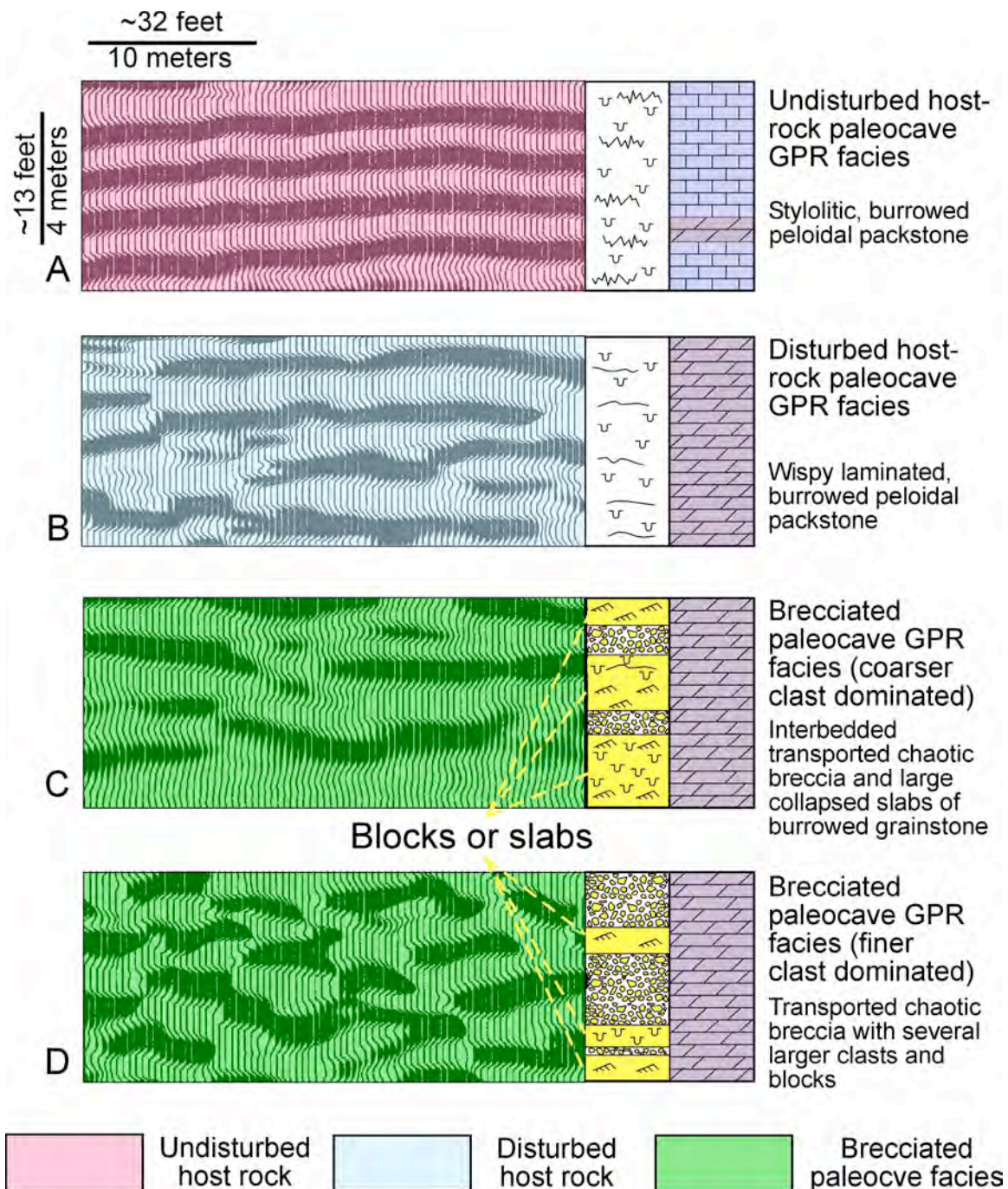


Figure 36. Type ground-penetrating radar reflection patterns for different paleocave facies. Each reflection pattern is matched to core. From Loucks et al. (2004).

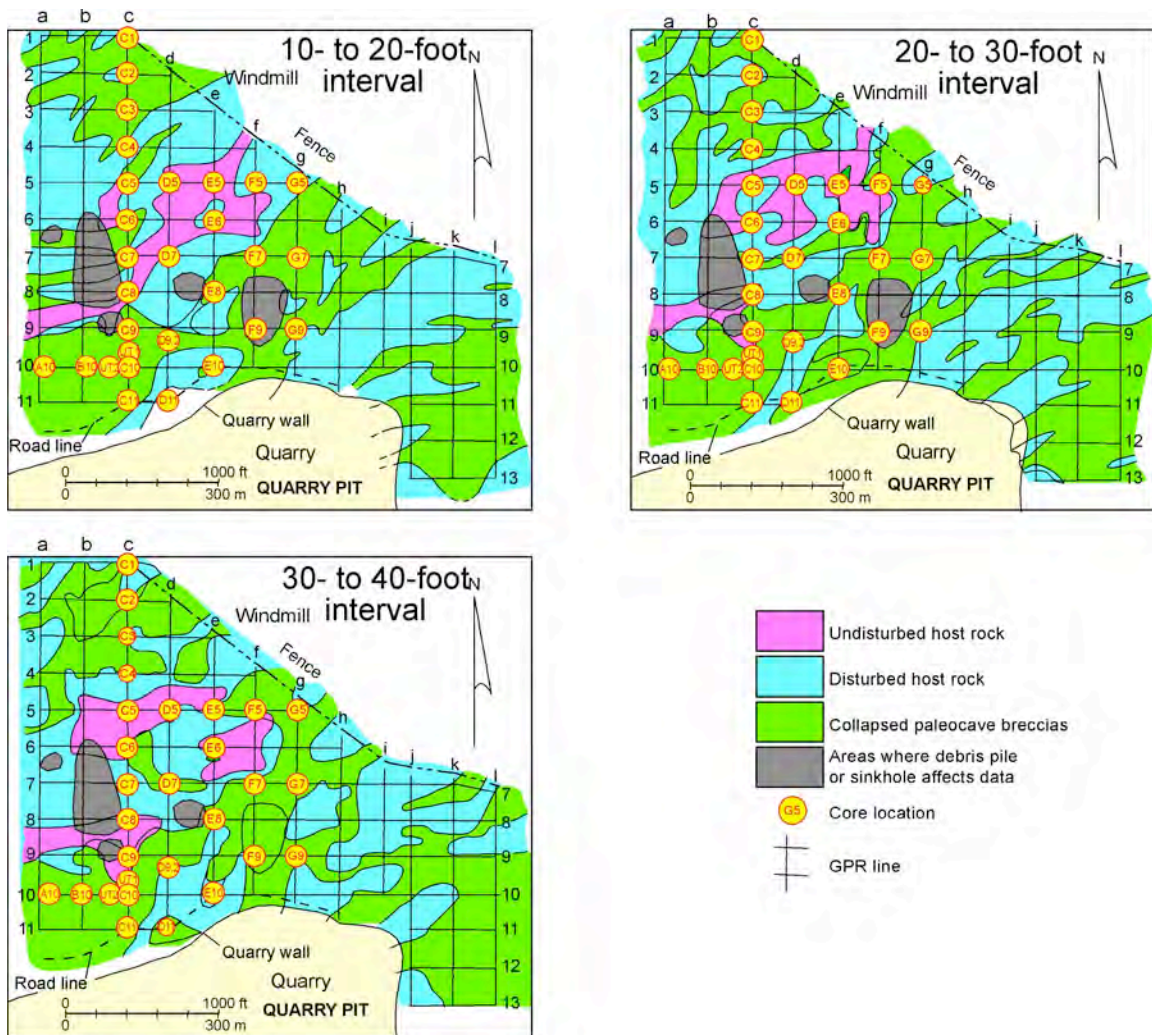


Figure 37. Integration of core and GPR data allows a three-dimensional interpretation of the paleocave system. The mapped volume is divided into three depth zones to display the distribution of paleocave facies. The brecciated bodies, which outline the trends of former passages, are as much as 1100 ft wide. The intervening areas between the breccias are as much as 660 ft wide. From Loucks et al. (2004).

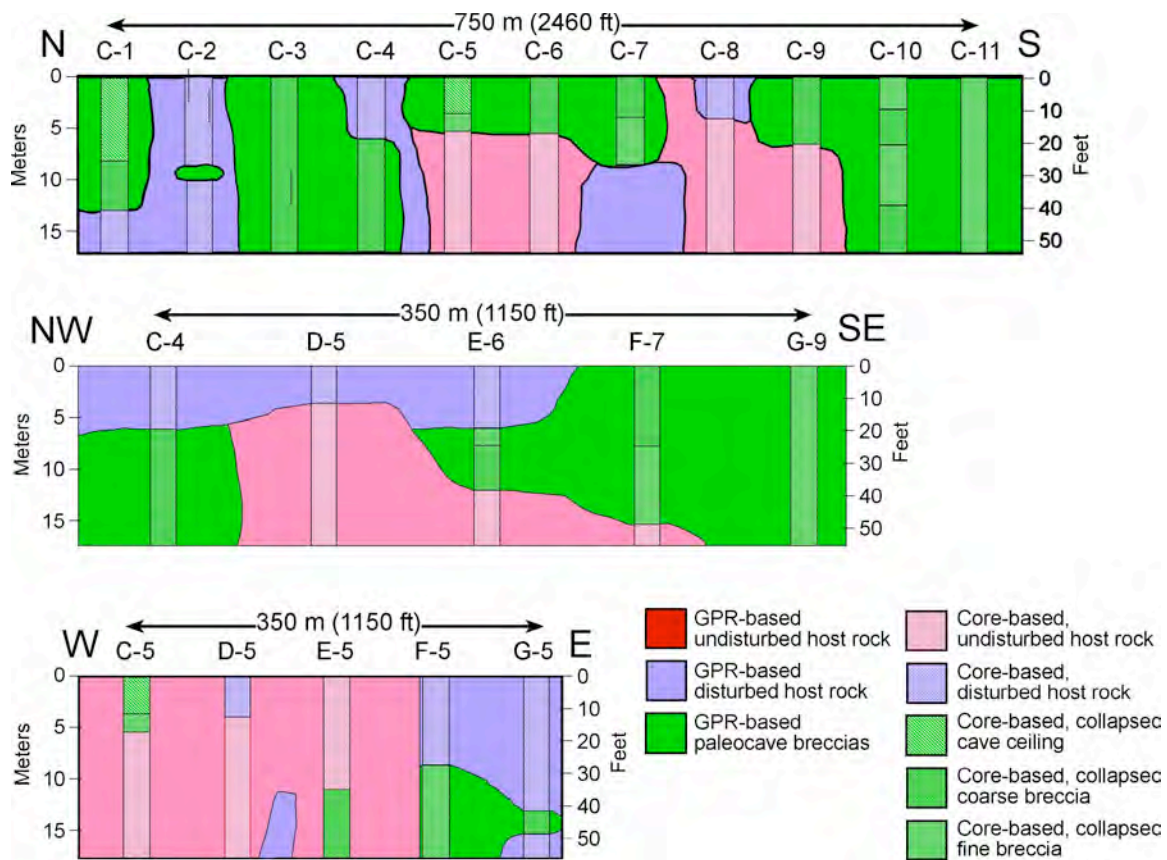


Figure 38. Simplified facies cross sections using core and GPR data. See Figure 35 for location of wells used on lines of sections. From Loucks et al. (2004).

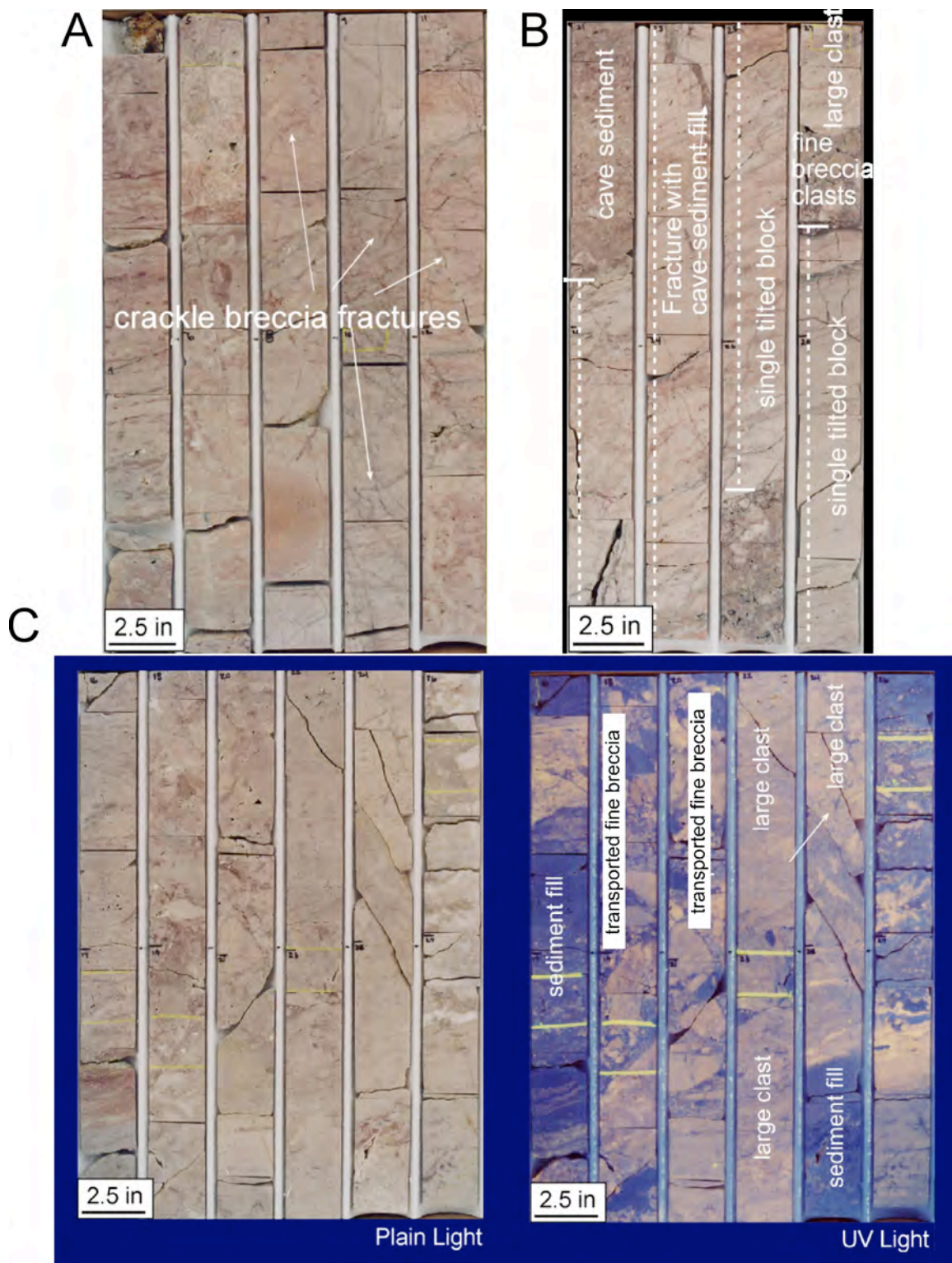


Figure 39. Core examples paleocave facies. (A) Cave roof showing extensive crackle breccia fractures. (B) Cave-passage fill composed of large blocks of chaotic breccia blocks and interbedded cave-sediment fill. (C) Cave-passage fill composed of large blocks of chaotic breccia blocks and interbedded cave-sediment fill. From Loucks et al. (2004).

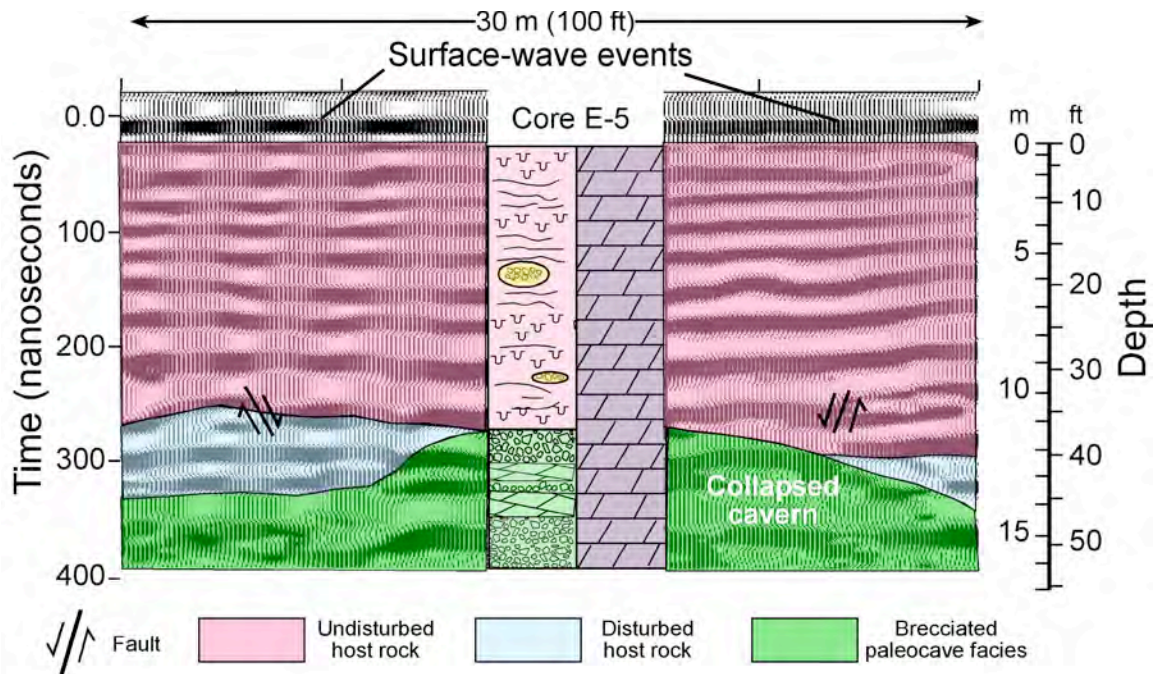


Figure 40. GPR section and core description showing a sequence of cave-fill breccias overlain by undisturbed host rock. A few small faults occur in the host rock above the collapsed cavern. See Figure 35 for location of GPR line and core. From Loucks et al. (2004).

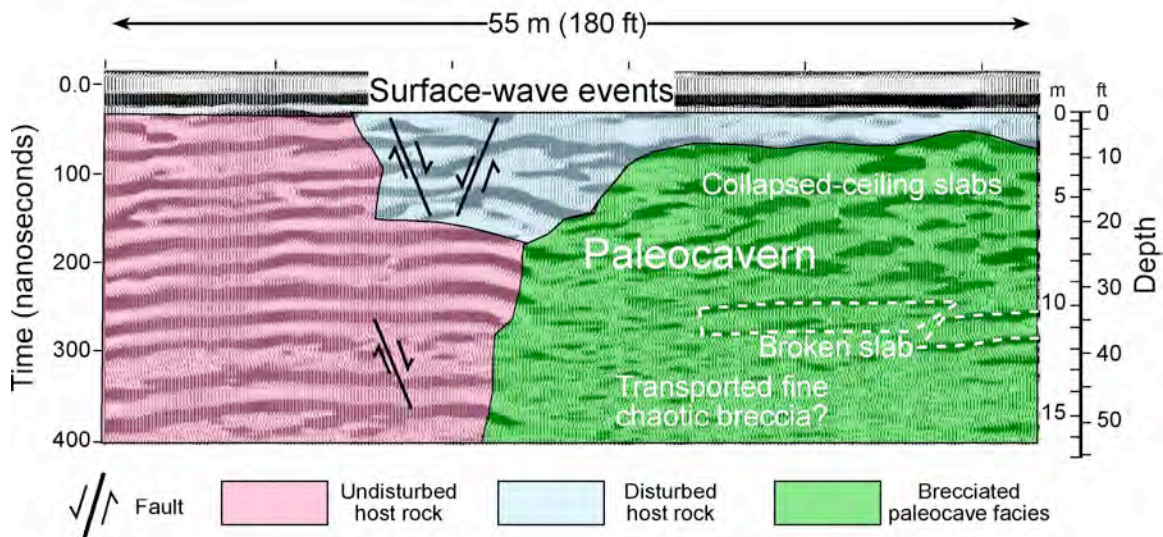


Figure 41. Collapsed paleocavern in contact with undisturbed and disturbed host rock. Several faults occur in the disturbed host rock. Reflection patterns in the collapsed cavern show probable fine breccia in the lower part of the chamber (no reflections) and coarser breccia (slabs) near the top (higher amplitude events). A large broken cave-ceiling slab may also be imaged. See Figure 35 for location of GPR line. From Loucks et al. (2004).

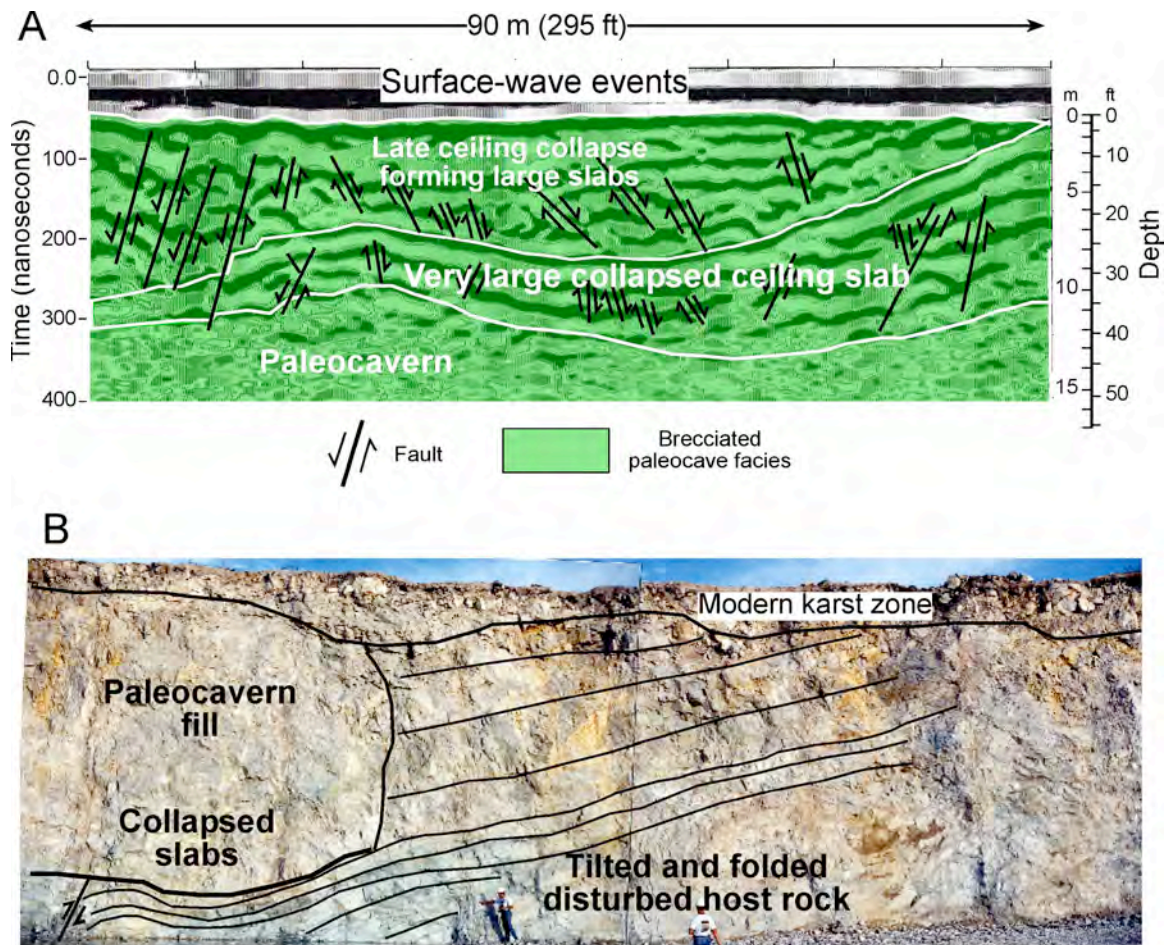


Figure 42. (A) Very large, folded, cave-ceiling slab overlying a paleocavern filled with chaotic breccia. The upper section of the cave ceiling appears to have collapsed after the large slab below on the basis of the onlapping reflection pattern between the two sections. See Figure 35 for location of GPR line. (B) Complex sag and fold feature along east wall in Dean Word Quarry showing features similar to GPR line presented in Figure 42A above. The lower part of the quarry face shows continuous tilted but folded bedding that is interpreted to have sagged or collapsed into a lower paleocavern. The upper part of the tilted block dips into a paleocavern filled with chaotic breccias and slabs. See Figure 35 for location of photograph. From Loucks et al. (2004).

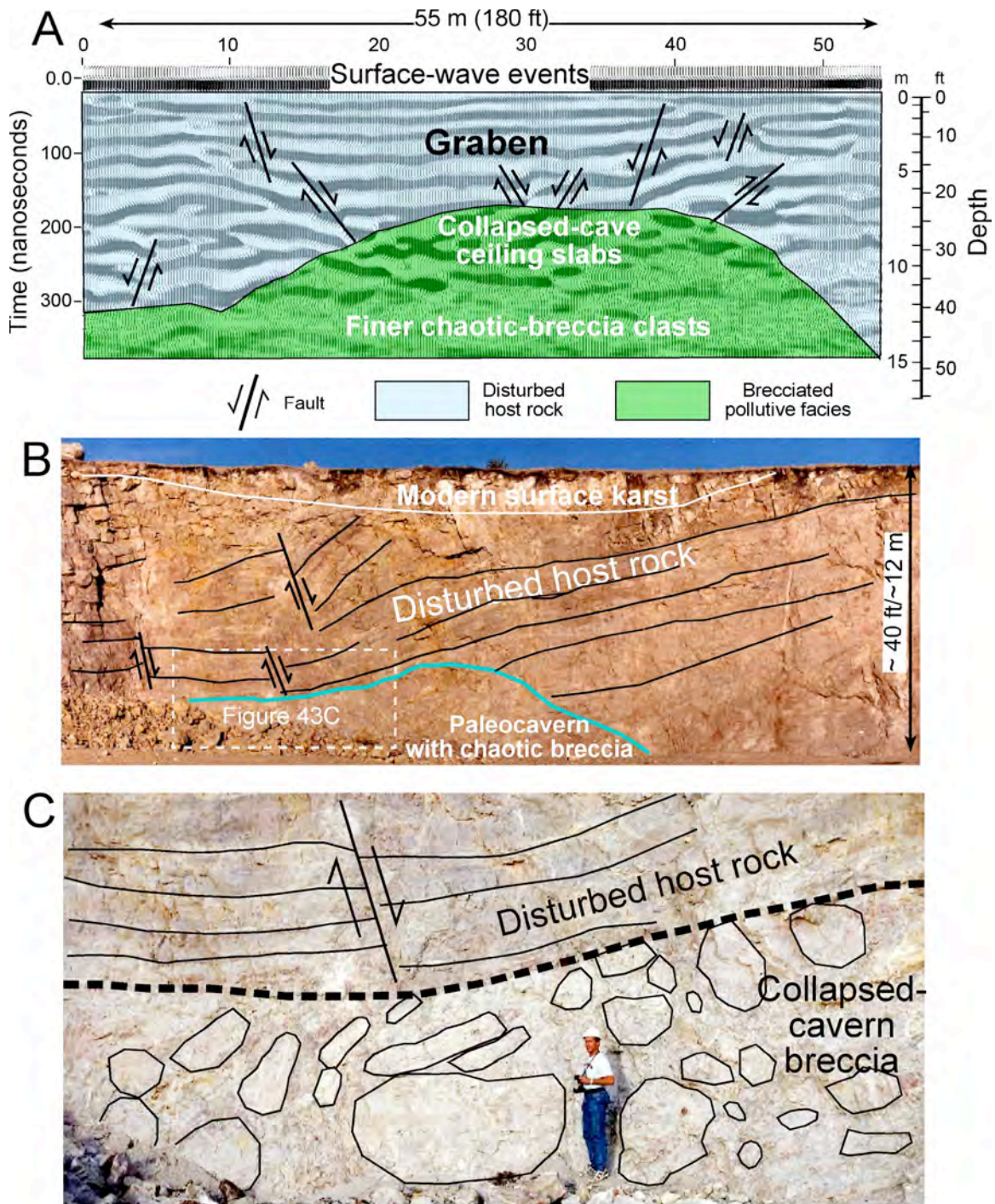


Figure 43. Faults over collapsed paleocaverns. (A) Graben and associated fault system in disturbed host rock overlying a collapsed paleocavern. Within the paleocavern, coarser slabs appear to be at the top and finer breccia at the bottom on the basis of the change in reflection pattern continuity. See Figure 35 for location of GPR line. (B) Example of faulted, disturbed host rock over a collapsed paleocavern similar to GPR line in Figure 43A. Detail of the collapsed paleocavern outlined in dashed box is shown in Figure 43C. (C) Close up of collapsed cavern shown in Figure 43B. Large collapse blocks, up to several meters across, are within the paleocavern (several prominent blocks are outlined). See Figure 35 for location of photographs. From Loucks et al. (2004)

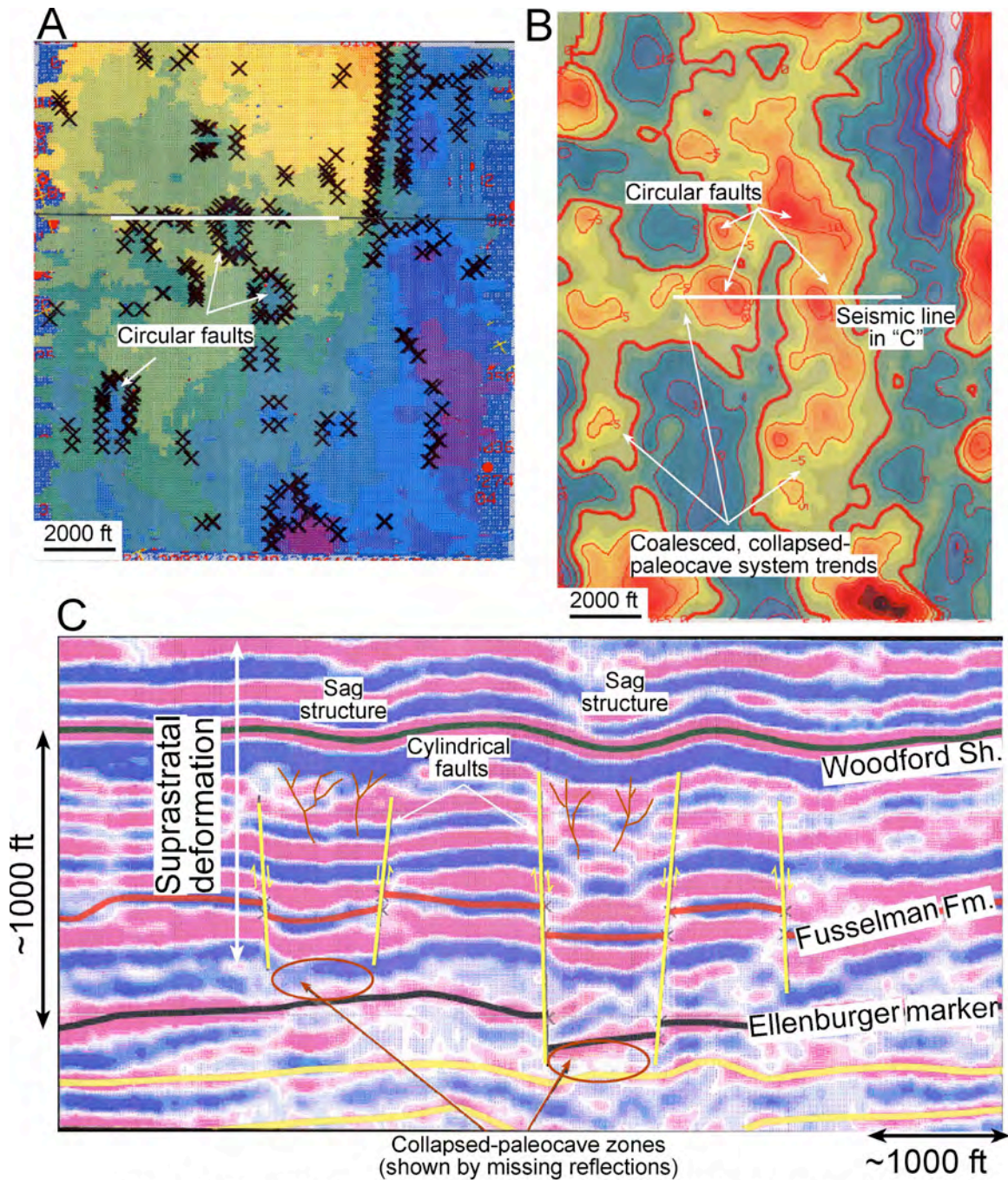


Figure 44. 3-D seismic example over an Ellenburger paleocave system from the Benedune field in West Texas. (A) Structure map on Fusselman Formation showing cylindrical faults produced by burial collapse of the Ellenburger cave system. (B) Second-order derivative map displaying sag zones produced by collapse in the Ellenburger interval. (C) Seismic line showing missing sections (collapse in Ellenburger section), cylindrical faults, and sag structures. Suprastratal deformation is over a thousand feet thick in this section. Modified from Loucks (1999).

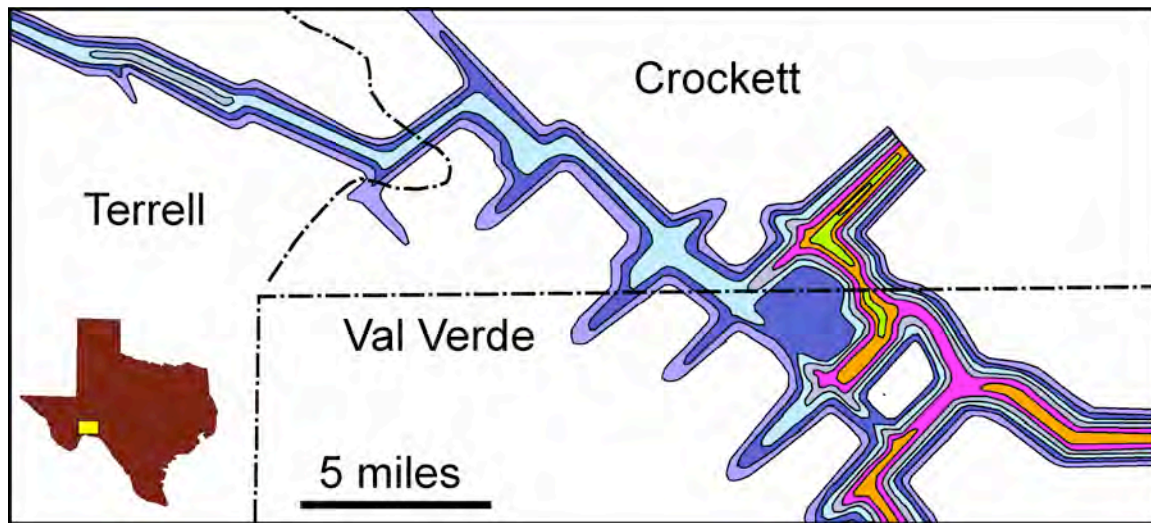


Figure 45. Isopach map of cave-sediment-fill prone interval in Ellenburger Group from wireline logs. The map shows a strong rectilinear pattern that is probably controlled by preSauk unconformity paleofractures. Hot colors are the thicker sections of cave-sediment fill. Figure from Canter et al. (1993).

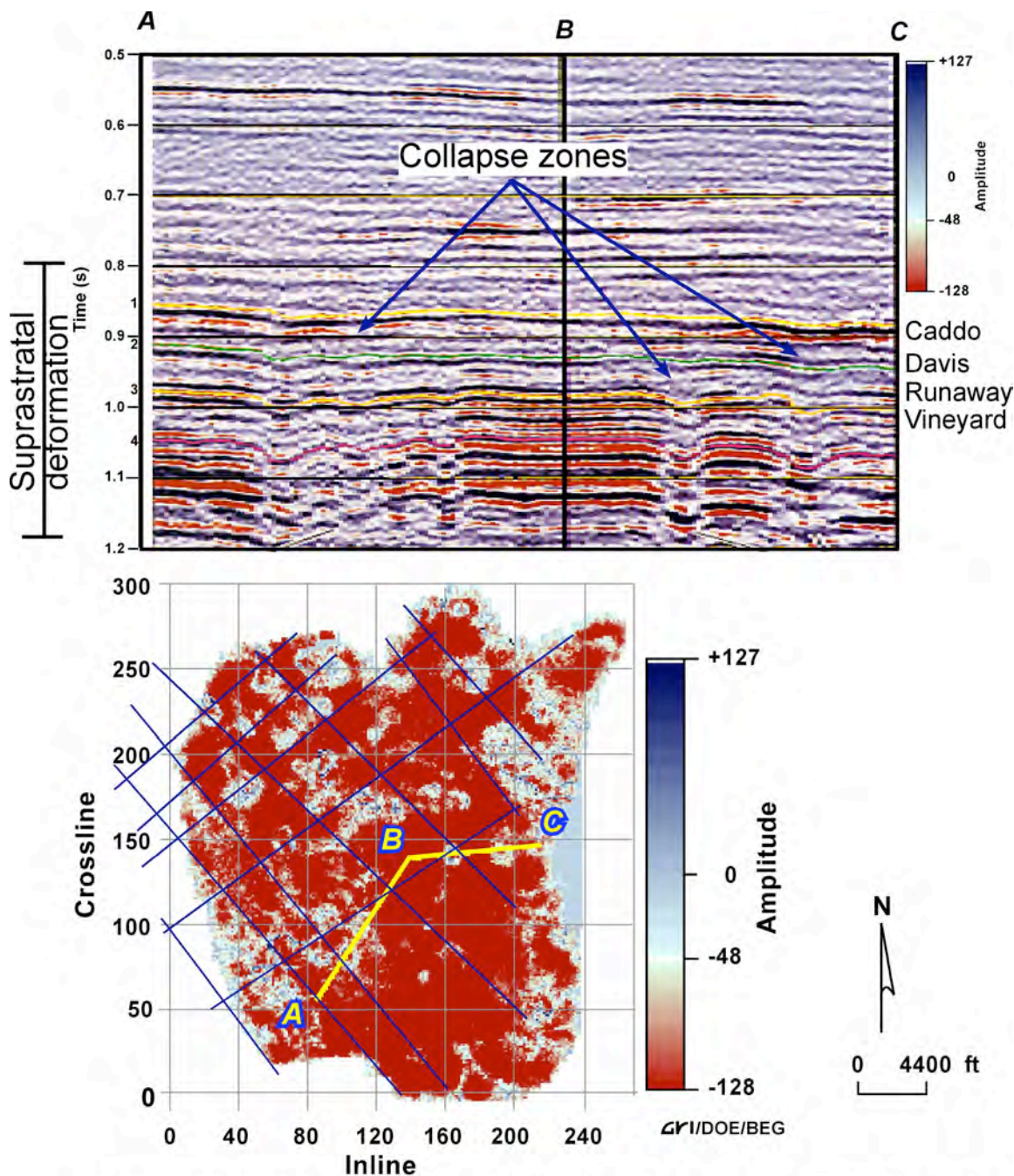


Figure 46. Seismic example of buried collapsed karst features from Boonsville on the line of Jack and Wise Counties in north Texas by Hardage et al. (1996). (A) Seismic profile along line ABC (see figure below), which traverses these collapse zones. Figure was stretched laterally by present author. Zones are up to 2000 ft thick. (B) Seismic reflection amplitude response on the Vineyard surface. The red areas show continuity, whereas the semicircular white areas show disruption of continuity. The white areas are late burial collapse related to karsting of the Ellenburger Group. The blue lines drawn by present author are meant to emphasize the northwest and northeast alignment of the collapse features.

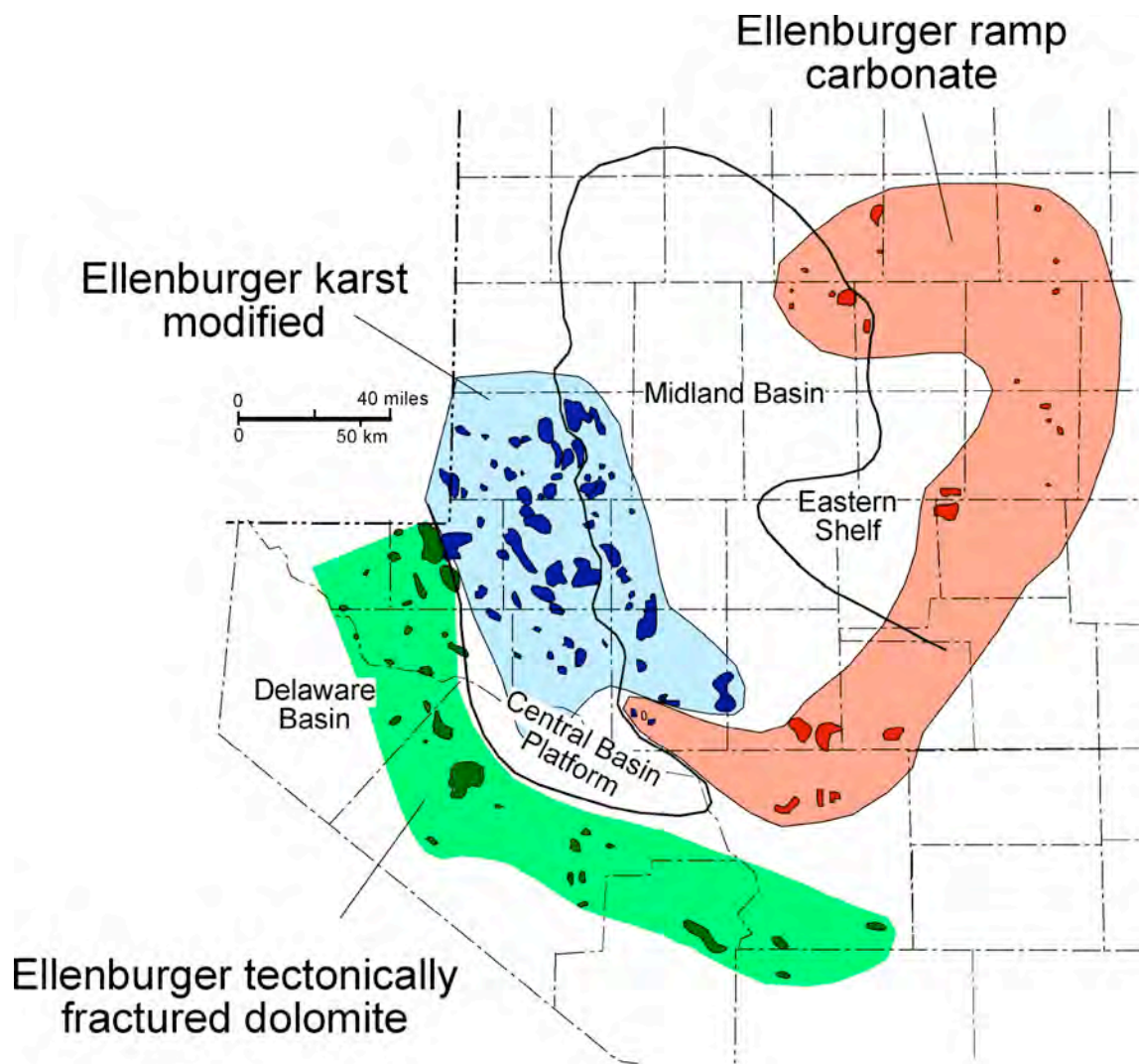


Figure 47. Distribution of Ellenburger Group reservoir types by Holtz and Kerans (1992).
Figure modified from Holtz and Kerans (1992).

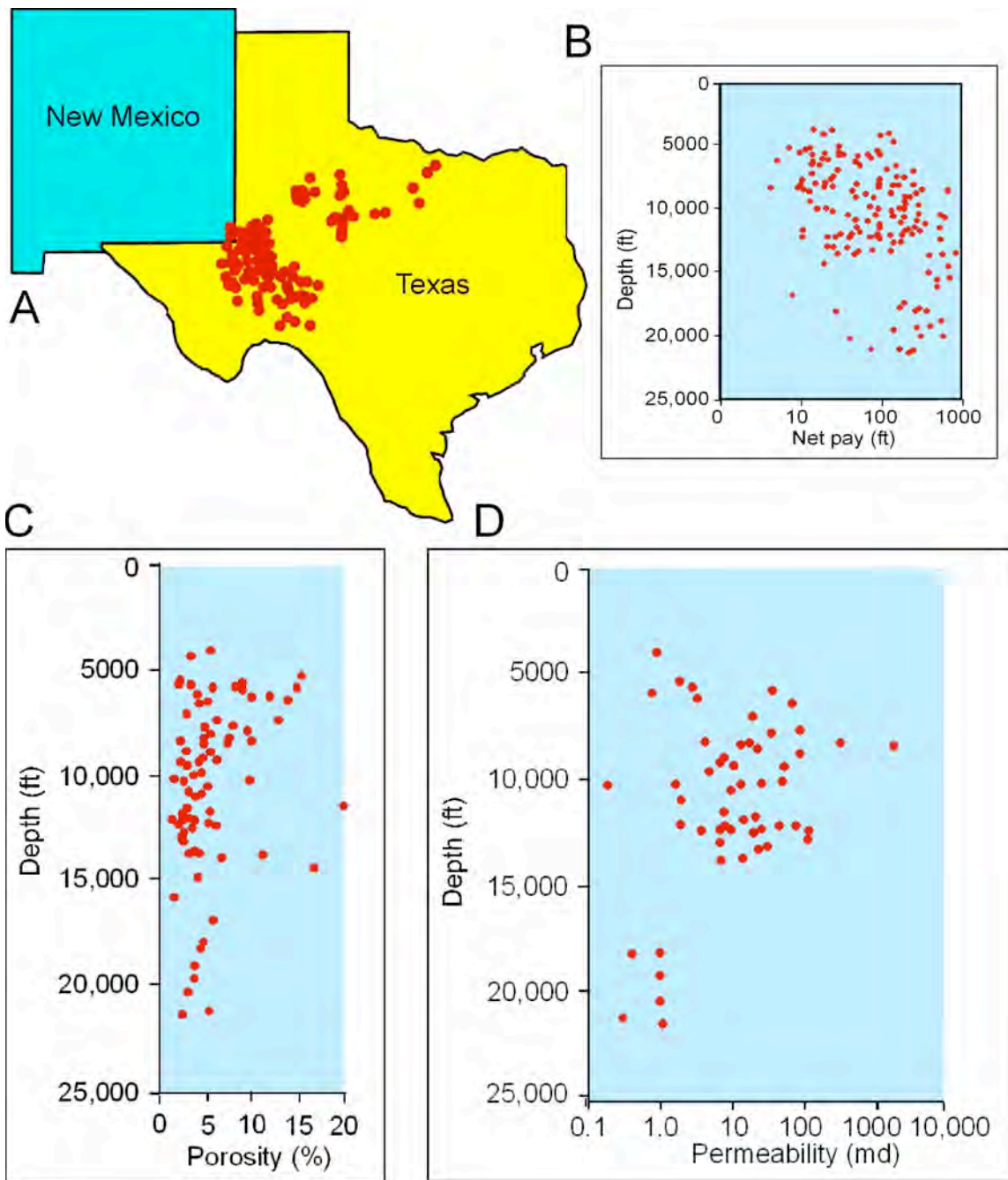


Figure 48. Field data from a 1985 Nerhing database (exact reference not available). (A) Map showing field locations. (B) Thickness of net pay. (C) Average reservoir porosity versus depth. Note most porosity values are 5% or less. (D) Average reservoir permeability versus net pay. Note good permeabilities despite low porosity values.

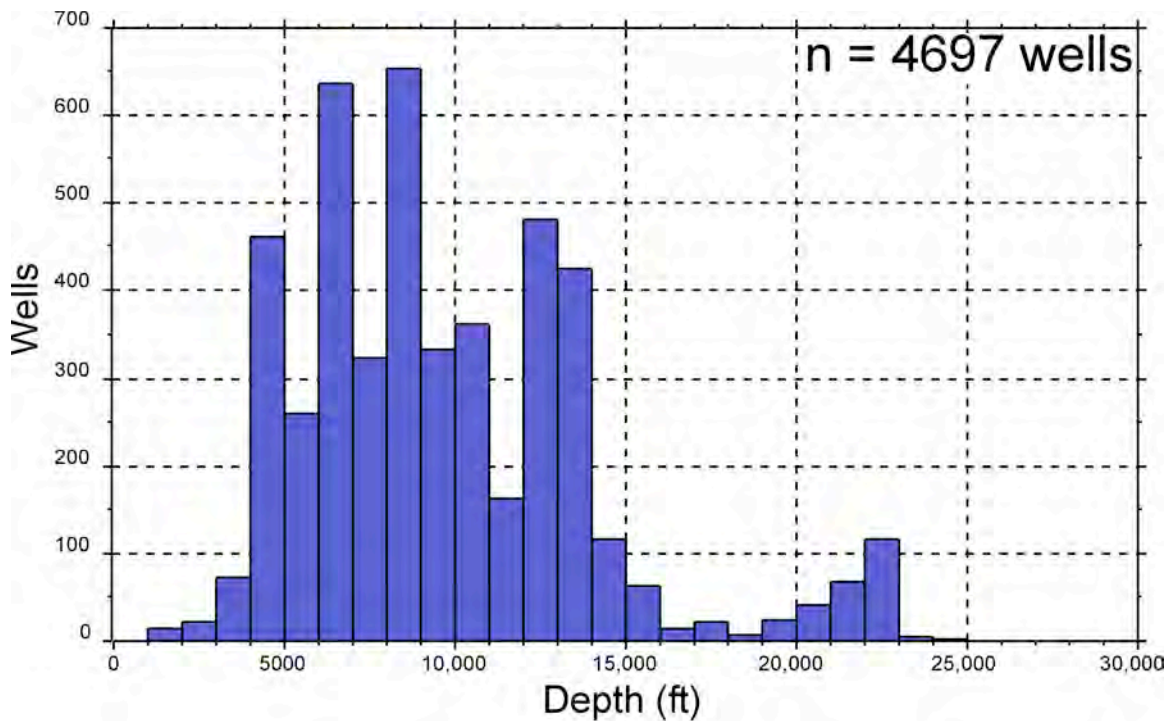


Figure 49. Histogram of productive (past and present) wells drilled into the Ellenburger Group. Producing wells show a range from 856 ft (Originala Petroleum #1 Gensler well in Archer County, Texas) to 25,735 ft (Exxon Mobil McComb Gas Unit B well in Pecos County, Texas).

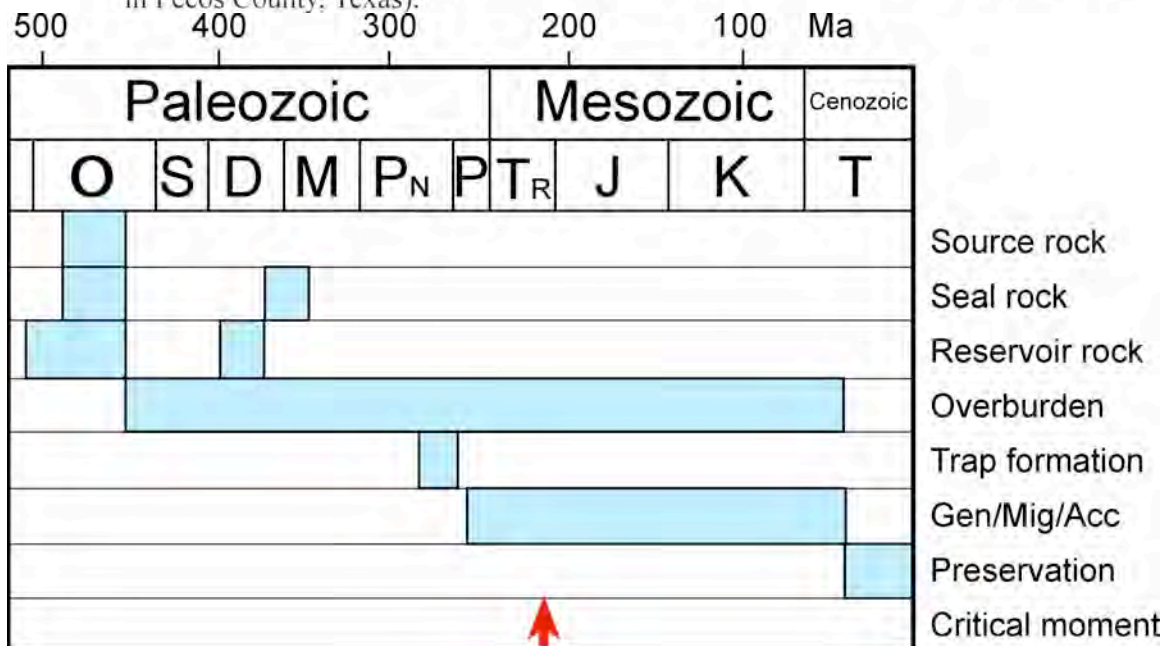


Figure 50. Event chart for the Simpson-Ellenburger petroleum system in the area of the Central Basin Platform showing the temporal relationships of the essential elements and processes. From Katz et al. (1994).

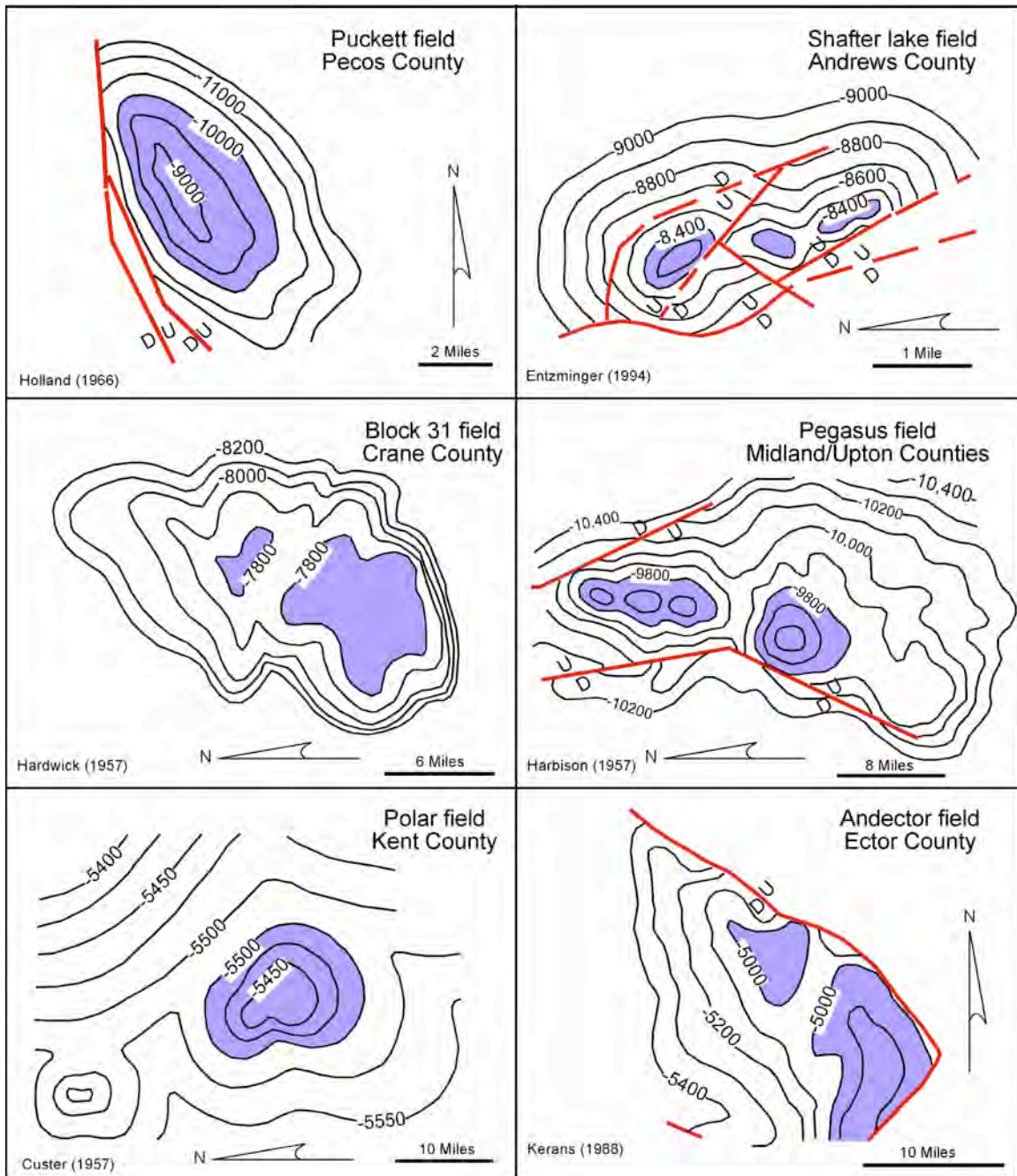


Figure 51. Examples of structural trapping geometries of Ellenburger reservoirs. Structures are relatively simple anticlines or faulted anticlines.

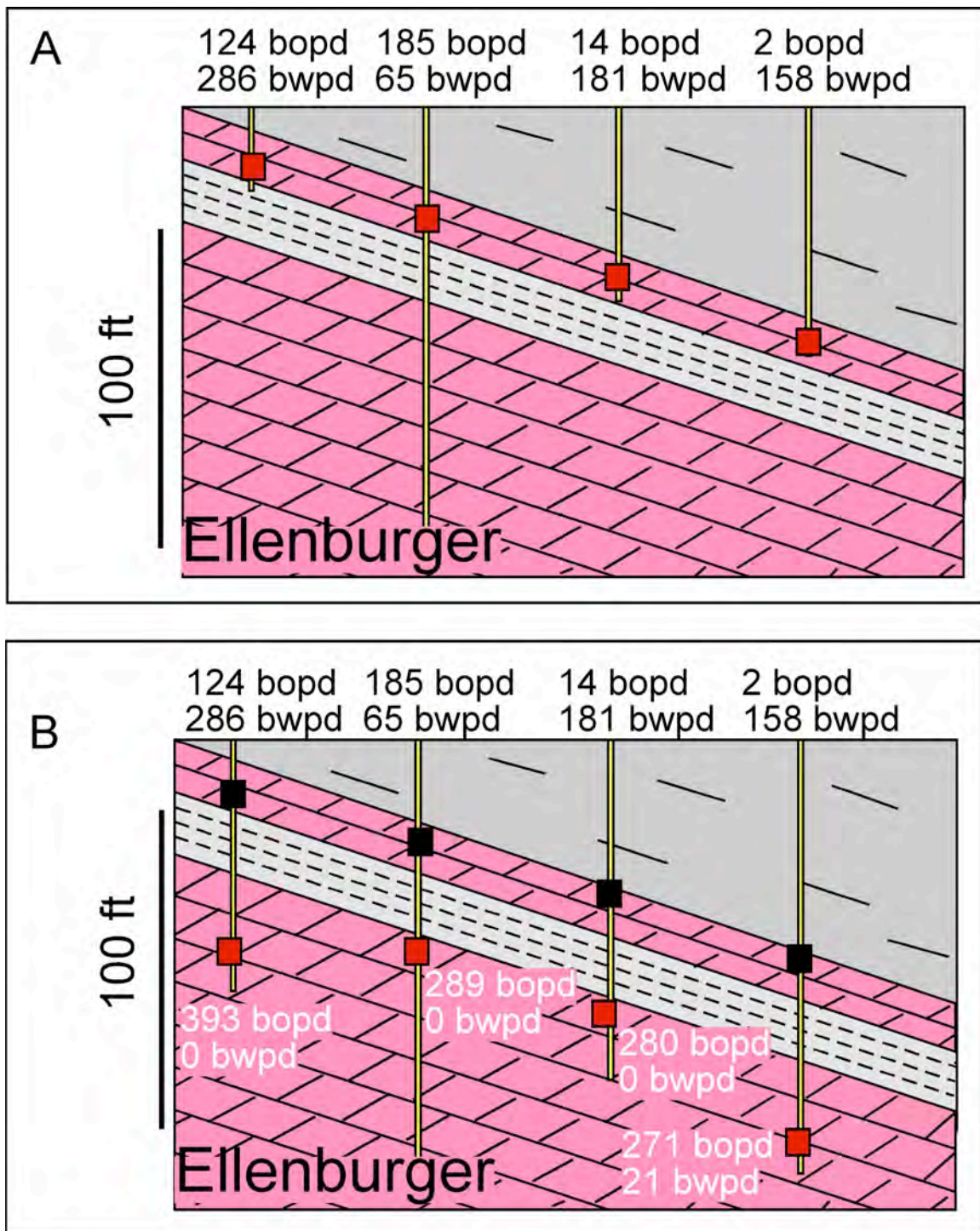


Figure 52. University Block 31 field example from Kerans (1988) that shows permeability barrier within the upper part of the Ellenburger. (A) Initial completions (pre-1977) were above the cave-sediment-prone zone. (B) The wells were deepened after 1977 and new hydrocarbon intervals were encountered.

THE MIDDLE-UPPER ORDOVICIAN SIMPSON GROUP OF THE PERMIAN BASIN: DEPOSITION, DIAGENESIS, AND RESERVOIR DEVELOPMENT

Rebecca H. Jones

Bureau of Economic Geology
Jackson School of Geosciences
The University of Texas at Austin
Austin, Texas

ABSTRACT

Middle Ordovician Simpson Group rocks were deposited in greenhouse conditions during a period of overall sea-level rise and marine transgression following an extensive hiatus and development of an irregular karst topography on the underlying Lower Ordovician Ellenburger carbonates. Simpson Group production is from three sandstone units in the middle of the group, each sourced from eroding highs to the north and east and transported to the cratonic margins by eolian and fluvial processes. These sandstones represent lowstand and/or early transgressive deposits of three third-order sequences; nonreservoir shales and clay-rich carbonates deposited during maximum flooding, and normal marine and restricted carbonates deposited during highstand comprise the balance of the sequences. Carbonate sequences are present above and below these three reservoir-bearing sequences, for a total of five third-order Simpson Group sequences within Sloss's second-order Tippecanoe I sequence.

The three sandstone members of the Simpson Group—the Connell, Waddell, and McKee—occur at the base of the Oil Creek, McLish, and Tulip Creek Formations, respectively, from oldest to youngest. The Simpson Group also includes the underlying Joins and overlying Bromide carbonate formations. Simpson rocks were deposited during the Rangerian to middle Turinian stages of the Whiterockian and early Mohawkian series (North American) of the Middle to Upper Ordovician.

Productive sandstones are quartz rich and typically 20 to 50 ft thick. Pore-filling carbonate cements and pore-lining clays commonly reduce porosity. The Simpson play has limited production in the Permian Basin of Texas and New Mexico compared with that in

Oklahoma. In both areas, production is primarily from structural traps; despite favorable depositional conditions, stratigraphic traps have not been widely explored. The Simpson has an important nonreservoir role in Permian Basin production because its organic-carbon-rich shales are the likely source of the Ordovician oil found in many Central Basin Platform area reservoirs, including the Lower Ordovician Ellenburger. The Simpson is thickest in Pecos and Reeves Counties in Texas and thins to the north and east, being absent over all but the southeasternmost part of New Mexico and at the eastern edge of the Permian Basin region.

INTRODUCTION

The Simpson Group is a thick Middle to Upper Ordovician carbonate and clastic succession present in two distinct depocenters in the southwestern U.S.: (1) West Texas and southeastern New Mexico and (2) southern Oklahoma. This study focuses on the Texas/New Mexico depocenter but employs observations and models from Oklahoma as analogs. Simpson Group thickness reaches a maximum of more than 2,000 ft in Pecos County and more than 2,500 ft in Reeves County in West Texas. It thins to the west, north, and east, becoming absent in Roosevelt County, New Mexico, and Cochran, Terry, Dawson, Howard, Glasscock, and Reagan Counties, Texas.

Simpson Group production is relatively low, given its thickness. As a reservoir play in Texas and New Mexico, the Simpson Group comprises 19 reservoirs having individual cumulative production greater than 1 MMbbl of oil through 2000. Cumulative production from these reservoirs totaled only 103.2 MMbbl (Dutton and others, 2005; fig. 1). Production comes from three sandstone intervals that are quartz rich and typically 20 to 50 ft thick. These sandstones are separated by nonreservoir intervals composed of mostly green shales (Galley, 1958). However, these organic-carbon-rich Simpson shales are significant because they are the likely source of the Ordovician oil found in many Central Basin Platform area reservoirs, including the Lower Ordovician Ellenburger. The Simpson Group is also significant because it overlies a major hiatus in the Lower Ordovician and records a unique Middle Ordovician depositional environment in which both clastics and carbonates were deposited during a period of overall sea-level rise.

This report presents a synthesis of previous work and data from a new core study. Additional core descriptions and new regional and local wireline-log correlations will be needed

to fully establish a comprehensive sequence stratigraphic framework for the Middle to Upper Ordovician Simpson Group in Texas and New Mexico. Such a framework will not only provide a basis for new strategies in tapping this underexplored play, particularly through stratigraphic traps, but will also improve our understanding of a relatively unknown unique depositional setting and time.

PREVIOUS WORK

Decker and Merritt (1931) defined five formations within the Simpson Group in Oklahoma. These formation names were later applied to Texas and the productive sandstones named as members by Cole and others (1942). From oldest to youngest, the formations are the Joins, Oil Creek, McLish, Tulip Creek, and Bromide (fig. 2). Sandstones are present at the base of the Oil Creek, McLish, and Tulip Creek Formations in both Texas/New Mexico and Oklahoma but only defined formally in Texas (as the Connell, Waddell, and McKee sandstone members, respectively [fig. 2]; Wright, 1965). Simpson formation names are used consistently in Oklahoma, Texas, and New Mexico in outcrop and the subsurface, with one exception: in the Marathon Uplift region of Texas, the Woods Hollow Formation is equivalent to the Simpson Group.

A wealth of state survey and regional geologic association reports and field-trip guides on the Texas and New Mexico Simpson Group depocenter in the region known as the Permian Basin were published from 1950 to 1965. These reports typically describe known outcrops and subsurface penetrations in the context of lithostratigraphy and the developing nomenclature for early exploration and production. Descriptions of the Simpson Group are contained within early regional summaries by Jones (1953), Herald (1957), Galley (1958), Barnes and others (1959), and Gibson (1965). More recent compilations, for example Wright (1979) and Frenzel and others (1988), are mostly restatements of earlier interpretations with minor updates. Newer data and interpretations have been brief (abstracts and short transactions) and narrow in scope.

In contrast to those of Texas and New Mexico, Simpson Group reservoirs are significant contributors to total production in the southern Oklahoma depocenter. Accordingly, this succession has been the subject of numerous reservoir-specific early investigations reported in special volumes, such as the 1965 *Tulsa Geological Society Symposium on the Simpson*, as well as more modern reports—for example, Candelaria and others (1997), O'Brien and Derby (1997),

and Bosco and Mazzullo (2000). Simpson and Viola (Montoya-equivalent) Group reservoirs account for much of Oklahoma's production, and three Simpson Group fields have more than 500 MMbbl oil or 3.5 Tcf gas in place (Northcutt and Johnson, 1997). Most studies of the Simpson Group in Oklahoma invoke parallelism with the equivalent sandstones of West Texas (subsurface Permian Basin and Sierra Diablo region outcrops) but fail to cite specific examples. Candelaria and others (1997) published one of very few reports that established a sequence stratigraphic context for the formations and members in either depocenter. These authors noted the importance of establishing such a framework to provide a better understanding of stratigraphic traps for future exploration.

REGIONAL SETTING

Globally, the Ordovician was a time of one supercontinent, Gondwana, and three major terranes; present-day North America was the Laurentian terrane (Cocks and Torsvik, 2004). Laurentia was stable during this time—staying in a transequatorial position throughout the Ordovician with little rotation or movement (Cocks and Torsvik, 2004).

Global plate reconstructions by Blakey (2004) indicate that present-day West Texas and southeastern New Mexico were located near 30°S during the Middle Ordovician (fig. 3). Regional highs were the Canadian Shield in northeastern North America and the Pedernal Massif in the present-day southwestern U.S. (Blakey, 2004). Mountain building was occurring along the northeastern coast of the present day U.S. and Canada as part of the Taconic Orogeny, resulting in narrowing of the Iapetus Ocean to the east of Laurentia (Blakey, 2004).

The Middle and Upper Ordovician are included as part of the Tippecanoe I second-order supersequence set (Sloss, 1988) of the Tippecanoe first-order megasequence (Sloss, 1963), which spans the Middle Ordovician to the Lower Devonian (fig. 2). This was a time of greenhouse climate conditions, when glaciation was relatively minor and sea-level changes were relatively low amplitude and frequent (Read and others, 1995). The boundary with the earlier Sauk megasequence is characterized by a major unconformity in the North American cratonic interior and lacuna at the cratonic margins (Sloss, 1988). The boundary between the Upper Ordovician and the Lower Silurian (Tippecanoe II supersequence set) is an indistinct disconformity, likely related to Gondwana continental glaciation (Sloss, 1988).

Expression of the Sauk–Tippecanoe unconformity ranges from a completely removed underlying Sauk megasequence on higher parts of the craton, such as central Idaho, to a nearly fully preserved underlying section in marginal basins, such as the Appalachian Basin (Sloss, 1963). Other areas with significant pre-Tippecanoe erosion include the Sweetgrass Arch (in northwestern Montana and southern Alberta, Canada), Wyoming Shelf, Wisconsin Arch, Kankakee Arch (in Indiana and Illinois), and Ozark Dome (in Arkansas and Oklahoma) (Sloss, 1963).

Exceptionally clean quartz sandstone is typical of the early transgressive leg of the Tippecanoe megasequence and provides a sharp contrast to the underlying Sauk carbonates, readily identifying the Sauk-Tippecanoe sequence boundary. In some areas, carbonates were deposited prior to the clastics, such as in the subsiding basins of the south-central U.S.—in Oklahoma and north Texas, West Texas, the Mississippi Valley, and the Illinois Basin (Sloss, 1988). Regularly interbedded quartz sand, marine shale, and minor carbonate followed deposition of carbonates in Oklahoma (Sloss, 1988) and West Texas (Frenzel and others, 1988) depocenters.

Marine transgression most likely occurred across the entire western craton, including the Transcontinental Arch, and onlapping sandstones were deposited during continued overall sea-level rise, punctuated by minor sea-level fall. Sandstones were subsequently eroded on cratonic highs and preserved in lows. Evidence of this scenario is the absence of shorelines or depositional limits in preserved strata (Sloss, 1988) and, in a New Mexico example, lack of a known shoreline or nearshore deposits (Kottlowksi, 1970). As a result, later Middle Ordovician carbonates rest unconformably on the underlying Sauk in some areas without a basal clastic zone (Sloss, 1963). A similar situation is present along the Appalachian cratonic margin. Early Tippecanoe sandstone is not present along the margin; instead, Tippecanoe limestones rest unconformably on Sauk dolostones (Sloss, 1963). By contrast, both clean quartz sandstones and carbonate were deposited along the passive Cordilleran margin, but shale content greatly increases to the west, indicating a shelf-to-slope transition (Sloss, 1988).

The Transcontinental Arch was a significant regional topographic high during the Middle Ordovician and it, along with the Canadian Shield, has been invoked as the source of the clean quartz sandstone of the Simpson in West Texas and Oklahoma (Sloss, 1988). The Pedernal

Massif in central and north-central New Mexico was also a regional high and supplied sediment for Simpson sandstones and siltstones in southeastern New Mexico (Kottlowksi, 1970).

A local extension of the Transcontinental Arch, called the Texas Arch (fig. 4), was present during the Middle to Late Ordovician (Wright, 1979) and acted as a boundary between the two primary Simpson Group depocenters. These depocenters in Oklahoma and West Texas have been described as having similar depositional patterns (Suhm and Ethington, 1975), despite being at least partly separated by this broad (600 × 250 mi), low-relief feature (Wright, 1979). The Texas Arch was the dominant positive topographic feature in the Permian Basin region during Simpson time. There is no evidence that the Central Basin Platform was a positive feature during deposition of the Simpson (Frenzel and others, 1988); it formed later during the late Mississippian (Tai and Dorobek, 2000).

This Simpson Group depocenter has historically been referred to as the Tobosa Basin (Wright, 1965). However, the mechanism for development of this basin has not been fully explained, leaving open the possibility of alternate interpretations. The idea of a “basin” may have originated from thickness maps showing thickening toward a central point. Perhaps the most widely available Simpson Group isopach map was originally drafted by Galley (1958) and then republished with some updates by Frenzel and others (1988). This map shows a central thick of more than 2,000 ft in Ward, Reeves, and Pecos Counties and gradual, even thinning to a zero line in north-central Texas and all but southeastern New Mexico. In contrast, a map with documented well control and faults published by the Texas Water Development Board (1972) and presented in simplified format (recontoured without faults) in figure 4, portrays irregular thickness variations. Some of these variations occur across faults, indicating structurally thickened strata, whereas others may be due to deposition on an irregular surface or postdepositional erosion.

Because the Simpson Group was deposited when sea level rose in the Middle Ordovician and marine transgression ended the period of exposure and karstification of the underlying Ellenburger (Kerans, 1988), local thickening may be explained by the irregular accommodation provided by the karsted surface. Thinning is also apparent over preexisting structures (for example, at Midland Farms field in Andrews County), where much of the basal Joins Formation thins on structure (Mears and Dufurrena, 1984).

A significant unconformity also exists between the Simpson Group and the overlying Montoya Group (fig. 2), suggesting that postdepositional erosion may have occurred. Outcrop studies in the Beach and Baylor Mountains indicate that the Montoya directly overlies the Oil Creek Formation, and a distinct unconformity exists between the two (Suhm and Ethington, 1975). This unconformity suggests that the McLish, Tulip Creek, and Bromide Formations were either removed through erosion or never deposited in this area. This truncation occurs progressively from SSW to NNE in a correlation section of subsurface wells in West Texas (fig. 5; Wright, 1965). Postdepositional erosion also took place along the eastern and western extents of the Simpson Group (Gibson, 1965). Whereas many published cross sections (fig. 5) show all Simpson Group formations and members thinning equally, it is more likely that thinning was accomplished through irregular accommodation, erosion, and/or nondeposition. The apparent uniform thinning shown in figure 5 is in the direction of the Texas Arch (fig. 4), a local arm of a regional high during the Tippecanoe sequence. Evidence of subaerial erosion of the uppermost Simpson (Bromide Formation) has been documented at Midland Farms field in Andrews County (Mears and Dufurrena, 1984). These local thinning trends are consistent with widespread erosion of the Simpson Group and equivalent rocks on major arches at the first-order sequence boundary between the Sauk and Kaskaskia sequences (Sloss, 1988).

Finally, structural complexity may be responsible for localized thickening shown on isopach maps in Ward, Reeves, and Pecos Counties (fig. 4). At Waha field in this area, overturned and therefore apparently thickened and repeated Simpson sections were encountered in a vertical well bore and verified by 3-D seismic (Hardage and others, 1999). Fault-thickened Simpson Group strata were also observed at Midland Farms field in Andrews County (Mears and Dufurrena, 1984).

FACIES AND SEDIMENTOLOGY OF THE SIMPSON GROUP

Biostratigraphy and Age

Recent conodont biostratigraphy indicates that Simpson Group rocks were deposited during the Rangerian to middle Turinian stages of the Whiterockian and early Mohawkian series (North American) of the Middle to Late Ordovician (fig. 2). This level of precision has not always been possible: Early Simpson Group biostratigraphy was based on graptolites in the Marathon region outcrops in southwestern Texas, and the succession was dated simply as Middle

Ordovician (Jones, 1953). More precise modern biostratigraphic correlations (using graptolites, trilobites, and conodonts) are now typically possible at the third-order sequence scale (Ross and Ross, 1992) in localized areas. Because the Simpson Group consists of dominantly nonmarine or marginally marine rocks with rare or poorly preserved diagnostic fossils, however, biostratigraphic correlation across North America remains difficult (Ross and Ross, 1992) despite extensive faunal studies (Sweet and others, 1971).

Derby and others (1991) presented what is perhaps the most comprehensive report of conodont work in the Simpson. These authors synthesized more than 20 years of work on Simpson outcrops in southern Oklahoma to define specific conodont zones for the lithostratigraphic formations. Comparison of this synthesis with that of Webby and others (2004) provides a basis for placing the Simpson in a global chronostratigraphic framework (fig. 2). The species-based conodont zonation developed by Webby and others (2004) (fig. 2) now appears to be the standard, rather than the previously proposed numbered zones established by Sweet and others (1971). It is reasonable to assume that these zones are also applicable to West Texas/New Mexico, given the facies similarity between the two depocenters and absence of any published modern studies stating otherwise. The Marathon Uplift succession has also been recently reevaluated using graptolite biostratigraphy. Biostratigraphy in this area has been especially challenging because seemingly noncorrelative graptolite faunas in this area are a function of deeper water depths and different water mass vs. graptolite faunas elsewhere in North America and the world (Goldman and others, 1995). In addition, a significant hiatus occurred between deposition of the Simpson-equivalent Woods Hollow Formation and the overlying Montoya-equivalent Maravillas Formation. These findings were used to define the position of Marathon equivalents in figure 2.

General Facies and Thickness

Rocks of the Simpson Group are composed of interbedded shale, limestone, and sandstone. The Joins and Bromide Formations are sandy carbonates; intervening formations are clay-rich carbonates and shales, each with a basal sandstone member. Sandstones make up only approximately 5 percent of the total thickness of the Simpson Group in West Texas and southeastern New Mexico. This sandstone volume increases toward the apparent source of the

siliciclastics to the northwest: a Precambrian granitic and metamorphic outcrop in New Mexico and the Pedernal Massif in southern Colorado (Wright, 1965).

Simpson Group outcrops in West Texas analogous to the subsurface Permian Basin have been described in the Baylor, Beach, and Sierra Diablo Mountains in Culberson County and in the Marathon Uplift and Solitario regions in Brewster and Presidio Counties in southwest Texas (Jones, 1953; Wilson, 1954; Wright, 1965, 1979; Suhm and Ethington, 1975). This work is primarily lithostratigraphic and biostratigraphic. Early workers described the Baylor and northeastern Sierra Diablo outcrops as consisting of sandstone, dolomite, and green and dark shale with a maximum total Simpson Group thickness of 137 ft in the Baylor Mountains (Jones, 1953; Wright, 1965). Several descriptions of the facies making up Simpson Group formations and members in the subsurface have also been published. These include a summary of various core descriptions from subsurface wells by Wright (1965) and a focused study of the McKee sandstone in several cores from Crane, Andrews, and Lea (New Mexico) Counties by Bosco and Mazzullo (2000).

Simpson Group thickness is highly variable throughout West Texas and New Mexico. A summation of the maximum ranges (from Wright, 1965) for each formation yields a maximum Simpson Group thickness of 1,650 ft. However, the total thickness of 400 to 320 ft reported in a study of cuttings from Midland Farms field wells in Andrews County (Mears and Dufurrena, 1984) is probably more typical of fields outside the thickest part of the depocenter.

Joins Formation

Distribution and Age

The Joins Formation is Middle Ordovician (Whiterockian North American Stage), according to age and conodont relationships in Pope (2004) and Webby and others (2004) (fig. 2). Distribution is likely irregular, given that it was deposited on the karst topography of the underlying Ellenburger; partial infilling relationships between the Joins and the underlying El Paso/Ellenburger Groups support this hypothesis (Suhm and Ethington, 1975). The Joins appears to be present in both Oklahoma and West Texas/New Mexico, given conodont biostratigraphic correlations (Suhm and Ethington, 1975).

Facies

The Joins is composed of slightly shaly limestone that grades into dolostone (Wright, 1965). The fine crystalline dolostone facies is argillaceous (silty to sandy), pale-orange, and thin to medium bedded, and it contains trilobites and brachiopods (Suhm and Ethington, 1975). Both lithofacies contain frosted quartz grains and clasts of the Ellenburger (cherty dolostone) below. In addition, the basal Joins Formation is glauconitic and contains thin beds of shale and sandstone in some areas (Wright, 1965).

Depositional Setting

Given the similarity in facies between the Texas/New Mexico and Oklahoma depocenters, a depositional model proposed for Arbuckle Mountain outcrops in Oklahoma should also be applicable to the Simpson Group in Texas and New Mexico. Denison (1997) interpreted the Joins to have been deposited during relatively low sea level, with early shallow marine conditions and subaerial exposure in some areas, followed by a transition to terrigenous conditions.

Subsurface Recognition and Correlation

The Joins exhibits a high gamma-ray response and reverse or positive spontaneous potential typical of shales and other clay-rich facies (figs. 6, 7). These log characteristics are markedly different from those of the underlying Ellenburger carbonate. Because it was deposited on the irregular Ellenburger topography, regional correlation is often not possible, although widely published Simpson Group cross sections show it to be regionally present and correlative (fig. 5).

Formations with a Basal Sandstone Member: Oil Creek, McLish, and Tulip Creek

The middle three Simpson Group formations each contain a basal sandstone member overlain by mud-rich carbonate and shale strata. From oldest to youngest (with basal sandstone member) these are the Oil Creek Formation (Connell Sandstone Member), the McLish Formation (Waddell Sandstone Member), and the Tulip Creek Formation (McKee Sandstone Member) (fig. 2).

Distribution and Age

Classic lithostratigraphic correlation sections depict all three formations areas present over much of the subsurface (fig. 5, cross-section locations in fig. 4); however, it is likely that the section is incomplete in many areas owing to erosion or nondeposition. For example, only the Oil Creek Formation is present in the Beach and Baylor Mountain outcrops, where a distinct unconformity separates the Oil Creek from the overlying Montoya carbonate (Suhm and Ethington, 1975). This observation implies that the rest of the Simpson Group (McLish, Tulip Creek, and Bromide) was removed by erosion or not deposited in this area. All three formations are Middle Ordovician (Whiterockian North American Stage) according to age and conodont relationships (Pope, 2004; Webby and others, 2004) (fig. 2).

Facies

The Oil Creek Formation is composed primarily of green, and locally red, shale with thin limestone interbeds; the Connell Sandstone Member consists of medium to coarse, well-rounded, calcareous sandstone in the subsurface and is locally iron rich and interbedded with red and gray shale (Wright, 1965). In Beach and Baylor Mountain outcrops, this sandstone is fine to coarse grained and contains frosted rounded quartz grains with variable amounts of dolomite cement and quartz overgrowths (Suhm and Ethington, 1975) and, locally, thin beds of light-colored dolostone. These authors noted that the Connell resembles equivalent Midcontinent sandstones in containing 95 percent or more quartz and well-sorted, rounded, frosted grains. Overlying the Connell, the Oil Creek Formation comprises a series of brownish-gray dolostone and argillaceous dolostone intervals that range from 20 to 45 ft in thickness, exhibit very fine crystal size, and contain local stromatolites, chert, and vugs (Suhm and Ethington, 1975).

The McLish Formation consists of gray-green shale interbedded with sandy limestone and fine-grained sandstone; medium-coarse grained calcareous sandstones make up the Waddell Member at the base of the McLish Formation in the subsurface (Wright, 1965). Shale dominates the section north of Ward and Crane Counties, and shaly limestone dominates the subsurface elsewhere outside of the main producing area.

Rocks of the Tulip Creek Formation are primarily thinly bedded, green shale thinly interbedded with limestone in the subsurface. Two sandstone layers separated by green shale and sandy limestone characterize the McKee; the sandstones are medium to coarse, white, green, or

red in color, and they contain phosphate, as well as abundant frosted quartz (Wright, 1965). The basal McKee Member comprises sandstone, muddy sandstone, and sandy mudstone lithologies in cores from Andrews and Crane (Texas) and Lea (New Mexico) Counties (Bosco and Mazullo, 2000). The sandstones are subquartzose to quartzose (50–100 percent quartz) quartz arenites (<2 percent feldspar) that are fine to fine grained and moderately well sorted. Deformed rounded mudstone lithoclasts of varying sizes are present locally. Four distinct McKee facies were observed in conventional cores in Andrews and Crane Counties, Texas, and Lea County, New Mexico: (1) green-yellow laminated very fine to fine-grained muddy quartzose sandstones with bioturbation and abundant clay and occasional phosphate grains; (2) sandstones similar to those in 1 but containing common carbonate, phosphate, clay and lithoclasts, as well as scattered fossils; (3) dark-colored, laminated, very fine to medium-grained muddy sandstone and sandy mudstone with abundant fossils and common phosphate grains; and (4) laminated, very fine grained, quartzose, yellow-brown sandstones with rare green-brown mudstone interlaminae, bioturbation, and common fossils (Bosco and Mazzullo, 2000).

A new core description conducted during this study provides additional insight into the McKee sandstone member of the Tulip Creek Formation (fig. 8). Four distinct facies and a range of grain sizes and structures were observed, including (1) massive crossbedded, tan, locally bioturbated sandstone (fig. 9a); (2) mixed carbonate and shale with carbonate lenses (fig. 9b) (3) finely laminated gray carbonate and green-gray shale with bioturbation, roots, and limited sand (fig. 10a); and (4) green-black carbonaceous shale (fig. 10b). All four facies occur over a relatively short section of core (core in fig. 11 and corresponding log and core description in fig. 8).

Depositional Setting

A depositional model proposed for the Simpson Group in the Arbuckle Mountain outcrops in Oklahoma (Denison, 1997) appears applicable to the Simpson Group in West Texas. This model proposes that basal Oil Creek, McLish, Tulip Creek, and Bromide Formation sandstones were formed by the reworking of clean eolian sands from terrigenous sources during marine transgression. During sea-level highstand, a peritidal carbonate platform developed, accounting for the deposition of the carbonate units in the upper parts of each formation. This model is consistent with outcrop observations in West Texas: the Connell sandstone was

interpreted to have been deposited in high-energy shoreface and nearshore environments on the basis of observations from Beach Mountain outcrops (Suhm and Ethington, 1975).

Diagenesis

Simpson Group sandstones are exceptionally clean. However, carbonate cementation is locally common and can reduce porosity and permeability. Cementation ranges from absent to pervasive in all three sandstone intervals (Wright, 1965). Detrital clays (dominantly illite) and authigenic cements—carbonate, clay, and quartz—are also present in McKee sandstone cores from Andrews and Crane (Texas) and Lea (New Mexico) Counties (Bosco and Mazullo, 2000). The clays are grain lining, and the carbonate cements are pore filling in these cores. These authors demonstrated that bioturbation and mineralogy are systematically related to color in these sandstones. Brown and yellow sandstones are typically clay free and contain authigenic quartz cement. Gray sandstones contain large amounts of micritic mud and carbonate cement. Green sandstones contain glauconite and illite (lighter variations contain less clay and are friable). Red sandstones owe their color to hematite-rich clay. In addition to detrital clays, white and black phosphatic grains are also present in the McKee sandstone (Wright, 1965).

Subsurface Correlation

Published literature on modern subsurface wireline correlations and seismic interpretation in the Simpson is sparse. Given the mixed lithology of the Simpson—including carbonate, sandstone, and shale—both types of correlation present challenges.

Most published wireline correlations date to the discovery of the major Simpson Group fields (1965 or earlier) and as such are based on spontaneous-potential–resistivity wireline logs (fig. 7). Modern gamma-ray–neutron–porosity wireline logs are available from fields with production above and below the Simpson, such as at Dollarhide field (fig. 6), but the Simpson is typically not correlated on these logs in published cross sections.

Not only does the mixed lithology present challenges in seismic interpretation, but the complexity of structures involving the Simpson Group can also further distort imaging of this succession. Seismic data at Waha field in Reeves and Pecos Counties show that complex faulting and overturned strata can be misleading when Simpson Group horizons are picked. Hardage and

others (1999) observed that Simpson beds were overturned, highly faulted, and folded, resulting in apparent thickening and repeat sections in vertical well bores.

Published gamma-ray–neutron type logs characterize the sandstone members as having a low gamma response and high neutron response (fig. 6), and the mixed carbonate and shale parts of the formations as having a mixed gamma response and low neutron response. Early electric logs show upward-coarsening relationships (normal or negative spontaneous potential) in Connell, Waddell, and Oil Creek type logs at productive fields (fig. 7) but lack truly diagnostic log character in correlation sections (fig. 5).

Bromide Formation

Distribution and Age

Like the McLish and Tulip Creek Formations, the Bromide Formation is absent owing to erosion or nondeposition in the Beach and Baylor Mountain outcrops, where a distinct unconformity separates the Oil Creek from the overlying Montoya carbonate (Suhm and Ethington, 1975), but it is present in much of the subsurface (Wright, 1965). The Bromide is Middle to Late Ordovician (Whiterockian to Mohawkian North American Series) in age, according to conodont relationships portrayed by Pope (2004) and Webby and others (2004) (fig. 2).

Facies and Depositional Setting

The Bromide Formation comprises massive fossil-rich limestone that is thinly interbedded with green shale and sandstone in the subsurface; the limestone is increasingly sandy and shaly away from the Central Basin Platform, to the south, southeast, and west (Wright, 1979). During Bromide time, marine transgression was more extensive than during earlier Simpson deposition (Oil Creek, McLish, and Tulip Creek), resulting in shallow subtidal to supratidal marine conditions and less deposition of eolian sand (Denison, 1997).

Subsurface Recognition and Correlation

Because of similarities between lithologies of the Bromide and those of the underlying upper Tulip Creek, the base of the Bromide is difficult to characterize on wireline logs. In contrast, the top of the Bromide is readily defined on wireline logs; the clean, low-gamma-ray

wireline response of the overlying Montoya Formation is distinct from the higher gamma-ray response of the Bromide. A type log from Block 31 field in Crane County (fig. 7a) shows that the Bromide has resistivity higher than that of the underlying Tulip Creek. However, this difference is less distinct in many wells (figs. 5, 7b). On gamma-ray–neutron logs from Dollarhide field (fig. 6), the Bromide shows the expected response for a primarily carbonate section with low radioactivity and high apparent neutron porosity. Interbedded shale and sandstone are also distinct (high radioactivity, low neutron) on these logs.

Woods Hollow Formation

The Woods Hollow Formation consists of Simpson Group-age outcrops in the Marathon Uplift and Solitario regions of southwestern Texas (Jones, 1953) (fig. 2). In the Marathon region, these rocks are green-black shale with thinly interbedded siltstone and limestone, and they contain scattered conglomerate boulders; in the Solitario region, these rocks are green-black shale and thin-bedded sandstone (Wright, 1965, 1979; Wilson, 1954). The Woods Hollow Formation was deposited in deeper water than the Simpson Group. Graptolite-brachiopod-pelagic trilobite assemblages characteristic of deep-water conditions typify Marathon-area outcrops as compared with the shallow-water corals, bryozoans, sponges, calcareous brachiopods and nektonic-benthic trilobites reported in West Texas and Oklahoma outcrops (Wilson, 1954). Information from these outcrops is useful in understanding regional paleogeography but not as relevant to Simpson Group production in the subsurface Permian Basin owing to marked differences in facies.

Sequence Stratigraphy of the Simpson Group

It is important to keep in mind that Simpson Group formations and members are lithostratigraphic units defined in outcrop, not chronostratigraphic units. Several authors have recognized the time-transgressive nature of Simpson formations and members in Oklahoma, where subsurface data and interpretations are more abundant owing to the greater economic significance of Simpson reservoirs there. Statler (1965) published an early sequence stratigraphic interpretation (fig. 12) that was then incorporated into the model proposed by Candelaria and others (1997) (fig. 13). Candelaria and others (1997) presented perhaps the most complete description of Simpson formations and members in terms of third-order sequences. This

sequence stratigraphic framework developed for Oklahoma is likely applicable to the West Texas subsurface, given the similarities in depositional setting.

The five Simpson Group lithostratigraphic formations have been interpreted to represent four (fig. 13) or five third-order sequences suggested by sea-level curve (fig. 2). These sequences represent the early parts of the second-order Tippecanoe I sequence (Middle and Upper Ordovician) and the first-order Tippecanoe megasequence (Middle Ordovician to Lower Devonian) (Sloss, 1988).

The Simpson Group was deposited on the Lower Ordovician Ellenburger, following a hiatus during the Rangerian stage of the Middle Ordovician, and it was typically overlain by the Upper Ordovician Montoya Group, following a hiatus during the Chatfieldian stage (fig. 2). The basal Simpson unconformity is both a first- and second-order sequence boundary, and the upper unconformity is a third-order sequence boundary (fig. 2). Locally, both the base and top of the Simpson Group are composite unconformities. In southern New Mexico, for example, the Simpson Group was deposited on Precambrian basement (Lower Ordovician Ellenburger absent), and in the Central Basin Platform and Reagan uplift areas the Simpson Group is overlain by Pennsylvanian and Lower Permian strata (Upper Ordovician-Mississippian absent and Simpson somewhat eroded) (Wright, 1965).

Sea-level fluctuations defining third-order sequences in the Ordovician were given for North America and Europe by Ross and Ross (1992) (sea-level curve in fig. 2). These cycles, lasting 1 to 8 million years, were associated with sea-level changes typically of 66 to 328 ft (Ross and Ross, 1992). An idealized Ordovician cratonic sequence consists of a transgressive sandstone base followed by a maximum flooding condensed section, early highstand normal marine limestones, and late highstand restricted carbonate and evaporate (Schutter, 1992). Sandstones represent sequence bases in this area, consisting of quartz arenite (arkosic where filling irregular lows) deposited by eolian to coastal processes. Green marine shales or evaporites are locally present with these sandstones. Organic-rich green, pyritic, or brown shales were commonly deposited next. Normal marine conditions followed during maximum flooding, with deposition of bioturbated subtidal wackestones and packstones. High-energy grainstone shoal facies were locally deposited next, followed by peritidal laminated and fenestral lime mudstones, dolostones, and evaporites during later highstand, with evidence of subaerial exposure and possible karst.

Candelaria and others (1997) subdivided the Simpson Group into four third-order sequences on the basis of Oklahoma subsurface data (fig. 13). In their mode, the Joins represents the first of these third-order sequences (fig. 2, O5) and differs in style from the successive sequences in that carbonate was deposited throughout the sequence (with some minor basal clastics). These authors documented many 3- to 10-ft-thick fourth- or fifth-order sequences in the Joins, each consisting of sandy siltstone overlain by coarse calcarenite and generally becoming increasingly sand dominated up section in Arbuckle Mountain outcrops.

By contrast, the overlying three Simpson Group sequences contain basal sandstones overlain by shale and much less carbonate. Simpson strandline fluvial and eolian sandstones were deposited initially during sea-level lowstands and were then reworked into a series of widespread, back-stepping, shoreface complexes representing the transgressive systems tract during sea-level rise (Candelaria and others, 1997). Alternatively, the sandstones may represent only the transgressive systems tract without initial fluvial or eolian deposits (Schutter, 1992). In either case, increased clastic input from eroding regional highs was essential to the carbonate to clastic facies change from the underlying Joins and restricted Ellenburger carbonate.

The Oil Creek Formation comprises the first sandstone-based Simpson sequence (Candelaria and others, 1997); the basal Oil Creek sandstone (equivalent to the Connell member in the Permian Basin) represents both a lowstand wedge and a transgressive shoreface complex in this area (fig. 13). The top of O6 (*polonicus* zone, fig. 2) is represented by a hiatus across New Mexico, Texas, and Oklahoma. The next sequence is composed of the McLish Formation (Candelaria and others, 1997); basal McLish sandstones (equivalent to the Waddell member in Texas/New Mexico) comprise transgressive shoreface complexes (without prior lowstand deposition) (fig. 13), suggesting an overall decrease in accommodation in this area (fig. 2, O7).

Both the Tulip Creek Formation and its basal sandstone (McKee member in the Permian Basin) (fig. 2, O8) and the Bromide Formation (fig. 2, O9) comprise the third sandstone-based sequence (Candelaria and others, 1997). The basal sandstone is again interpreted to represent the transgressive systems tract only. This grouping of both the Tulip Creek and Bromide into one sequence is consistent with the interpretation of Statler (1965), but not the sea-level curve given by Ross and Ross (1992) (fig. 2), which suggests two sea-level rise-and-fall events during this time.

Insights into the Tulip Creek cyclicity are provided by core from the McKee member in Pecos County. Cycles within the McKee section here are upward fining (fig. 8). Cycle bases are typically bioturbated, followed by high-energy planar, crossbedded, massive sandstone (facies 1, fig. 9a). Cycles fine into mixed carbonate and shale (facies 2, fig. 9b), finely laminated carbonate and shale (facies 3, fig. 10a) and, in some cases, green carbonaceous shale (facies 4, fig. 10b). These cycles shallow consistently upward, as shown by an upward decrease in high-energy planar crossbeds and an increase in bioturbation. Unfortunately, core coverage is too limited for interpretations to be made about larger scale sequence stratigraphic patterns.

However, sequence stratigraphic interpretations of the Simpson Group have been established in Oklahoma, and the similarity of facies stacking patterns between the Texas and Oklahoma depocenters suggests that it is reasonable to extrapolate the sequence stratigraphic model established by Candelaria and others (1997) to the Texas succession. This approach implies that the Connell sandstone of sequence O6 represents both lowstand and stranded transgressive shoreface deposits. The Waddell and McKee members represent transgressive shoreface deposits of sequences O7 and O8, respectively (fig. 2). Whereas the general ideas presented by Candelaria and others (1997) describe the facies observed in the Texas/New Mexico depocenter, as well as that of Oklahoma, several variations are apparent from wireline-log patterns and cores from Permian Basin successions.

Log patterns in the Texas/New Mexico depocenter depict a single, thin, upward-coarsening sandstone typical of transgressive deposits picked as the Connell member and representing the base of sequence O6 (fig. 2). In Crane and Pecos Counties at Abell, Block 31, and McKee fields (fig. 7a), there is no evidence of the blocky, sharp-based pattern typical of lowstand deposits, such as those described by Candelaria and others (1997). The Connell sandstone is not definable in the logs from fields farther north (Keystone field in Winkler County, TXL field in Ector County, or Martin field in Andrews County). Log patterns do show, however, thin, upward-coarsening sandstone at Keystone and Martin (fig. 7b). The section at TXL field, a bit farther to the east, appears shaly throughout the interval and may have been deposited in a more distal shelf setting.

Similarly, in the next sequence (O7), logs from wells in the Texas/New Mexico depocenter indicate a thin, upward-coarsening sandstone at the base of the sequence. This sandstone is called the Waddell member and is present at both Bell and McKee fields in Pecos

and Crane Counties and at Martin field in Andrews County (fig. 7b). Two thicker, upward-coarsening sandstones also called the Waddell member are present at Block 31 (fig. 7a), Keystone, and TXL fields. These patterns are consistent with the Candelaria and others (1997) interpretation of transgressive deposits at the base of this sequence in the depocenter.

Log patterns and core descriptions in the Texas/New Mexico depocenter suggest that not one but two (Candelaria and others, 1997) successive Simpson Group sequences were then deposited. The first, sequence O8, mimics the previous sequence, containing two upward-coarsening to serrate sandstones at the base of the sequence. These sandstones are assigned to the McKee sandstone and are present in most Texas/New Mexico fields (fig. 7). These log-defined facies patterns can also be interpreted as transgressive deposits, an interpretation that is compatible with the Candelaria and others (1997) model. The next younger sequence, O9, shows even greater marine transgression, with a decrease in clastic input and better development of marine carbonates. It is difficult to ascertain the presence of a sequence boundary without cores, but sea-level curves suggest a marked decrease, followed by increase, in sea-level change at this boundary (fig. 2).

Reservoir Development

Simpson Group reservoirs are developed in the three sandstone members: the Connell, Waddell, and McKee. Each succession has highly variable thickness and continuity. Increasing thickness trends from north to south (eastern Lea County, NM, to eastern Ward County are 20 to 70 ft for the Connell, 20 to 120 ft for the Waddell, and 100 to 175 ft (central Winkler County) for the McKee (Wright, 1979). The maximum thickness of the McKee sandstone in the Permian Basin has been recently reported as approximately 230 ft (Bosco and Mazzullo, 2000). These data suggest that a total of 420 ft of gross sandstone could be encountered in the Simpson Group if the maximum thickness of each sandstone member occurred in the same location in the Permian Basin. Conversely, a minimum Simpson gross sandstone thickness could be as little as 140 ft in the Permian Basin and even less where the Simpson has been eroded. The Simpson Group as a whole is more sandstone dominated in Oklahoma and Arkansas: gross sandstone thickness is more than 400 ft in south-central Oklahoma and more than 300 ft thick in western Arkansas (Holden, 1965).

Reported maximum thicknesses for the entire reservoir-bearing formations (sandstone members and overlying shale) in the subsurface Permian Basin are 280 ft (Oil Creek), 475 ft (McLish), and 400 ft (Tulip Creek) (Wright, 1979). The nonreservoir Bromide and Joins Formations reach a maximum thickness of 375 and 120 ft in the subsurface Permian Basin, respectively (Wright, 1965). The Woods Hollow Formation is 180 to 500 ft thick in the Marathon region and 340 to 400 ft thick in the Solitario region (Wilson, 1954; Wright, 1965, 1979).

Reservoir Distribution

Simpson Group production in West Texas and southeastern New Mexico was developed in the Waddell sandstone in Sand Hills field in Crane County in 1936. This field (fig. 1) remains one of the top three producers in terms of cumulative production (Dutton and others, 2005). The first McKee sandstone production occurred soon after, in 1938, in Pecos County, and Connell sandstone production began in 1948 in Crane County (Wright, 1965). Production is developed in the Waddell sandstone in Crane, Ector, and Pecos Counties; in McKee sandstones in Andrews, Crane, Ector, Lea (New Mexico), Pecos, and Winkler Counties; and in Connell sandstones in Andrews, Crane, Ector, Lea (New Mexico), Pecos, and Terrell Counties (Wright, 1979).

As a reservoir play in Texas and New Mexico, the Simpson Group comprises 19 reservoirs with individual cumulative production greater than 1 MMbbl of oil through 2000 that totaled only 103.2 MMbbl of cumulative production (Dutton and others, 2005). The top three fields accounting for most of this production include, in descending order, Running W field in Crane County (25.3 MMbbl), Hare field in Lea County (New Mexico) (17.2 MMbbl); and Sand Hills field in Crane County (13.1 MMbbl) (fig. 1). All other Simpson fields have produced less than 10 MMbbl of cumulative production, and only two have produced more than 50 MMbbl. All of these fields were discovered prior to 1965. Note that the Simpson Group is present west, east, and south of the production-based play area and especially thick to the west (play area defined by Dutton and others, 2005, and shown in fig. 1; Simpson thickness shown in fig. 4).

Porosity Development

Simpson Group clastic reservoirs are composed of extremely mature quartz sandstones with primary porosity (Schutter, 1992). Porosity varies from 7 percent at Connell Block 31 to

16 percent at Martin McKee (Tyler and others, 1991). Permeability averages 45 md in Crawar Waddell (Wojcik, 1990) and 164 md in Running W Waddell field (Galloway and others, 1983).

Reservoir quality is controlled by grain size, thickness, degree of carbonate cementation, and interbedded silts or shales. The McKee member has the best reservoir quality of the three Simpson Group sandstones. It is the coarsest, thickest, and cleanest in the Central Basin Platform area (Wright, 1965). Porosity in the Connell sandstone is generally high, but permeability decreases locally where sandstone grades into sandy shale (Wright, 1965). Permeability reduction in the Waddell sandstone has also been observed locally where silt is present (Wright, 1965). Pore-filling carbonate cements and pore-lining clays can commonly reduce porosity (Galley, 1958). No regional or stratigraphic patterns of cementation or clay presence have been reported.

Traps, Seals, and Sources

Oil was trapped in the producing sandstones of the Simpson Group along the postdepositionally folded and faulted structures of the Central Basin Platform, with Simpson shales providing the seal (Dutton and others, 2005). High-angle faults on the flanks of the anticlines also contributed to trap formation, as observed at Teague McKee field. Anticlinal structural traps are responsible for reservoir accumulation in the following fields (and formations): Block 31 (Connell) in Crane County, TXL (Waddell) in Ector County, and Warren (McKee) in Lea County, New Mexico (Wright, 1965).

Other reservoirs produce where Simpson Group sandstones are truncated by erosion along the flanks of anticlines underneath a major regional unconformity. The seal is provided by overlying post-Simpson rocks, mainly Pennsylvanian and Permian shales and carbonates (Gibson, 1965; Wright, 1979; Galloway and others, 1983). The unconformity was formed during major late Paleozoic uplift that formed the Central Basin Platform and the smaller structures associated with Simpson traps. The top-producing Running W field in Crane County (fig. 1) produces where the Waddell sandstone has been erosionally truncated and overlain by Permian rocks (Galloway and others, 1983). Permian strata similarly seal both Connell and McKee sandstones at Hare field in Lea County, New Mexico (Wright, 1965)—another top producer (fig. 1). Crawar Waddell field produces from a north-south-trending anticline that is bound on the east by a northwest-southeast-trending reverse fault (Wojcik, 1990).

The only documented purely stratigraphic traps in the Simpson Group are at Abell field (Crane and Pecos Counties), owing to an updip decrease in porosity in tilted Waddell reservoir sandstones, and at Tucker field (Crane County), where Waddell sandstones become increasingly shaly and therefore less permeable updip.

Each producing sandstone interval in the Simpson Group has its own oil-water contact, suggesting sealing and in situ generation of hydrocarbons by intervening shales (Williams, 1977). Where both Ellenburger and Simpson reservoirs are productive along the postdepositionally folded and faulted structures of the Central Basin Platform region, similarities in oil character also suggest a common source (Wright, 1965, 1979).

Simpson Group shales are considered primary pre-Permian source rocks (Williams, 1977). The source capabilities of the Simpson Group are supported by the presence of Ordovician oil in Ellenburger reservoirs where overlain by Simpson shales and the lack thereof in Ellenburger reservoirs where the Simpson Group is absent. The area of productive Ellenburger reservoirs, in the Central Basin Platform and southwestern Midland Basin regions, coincides with the thickest deposition of the Simpson Group, suggesting that the superjacent Simpson Group shales provided the hydrocarbon source (Gibson, 1965). The oil-prone relationship between total organic carbon (TOC) and total hydrocarbons in Simpson Group shales in both west Texas and Oklahoma, compared with the lack of such a relationship in Ellenburger samples, lends additional support to the idea that Simpson Group shale sourced Ordovician reservoirs (Katz and others, 1994). Simpson Group shales reached the oil window of hydrocarbon generation in the Late Permian and may have generated and expelled 180 to 540 Bbbl of oil for migration into Central Basin Platform reservoirs (Katz and others, 1994).

Opportunities for Additional Resource Recovery

Simpson Group exploration strategies have focused almost exclusively on structural traps. However, extensive stratigraphic traps are likely in this depositional setting. Thus, the Simpson Group may contain a distributed but potentially significant remaining resource. Simpson Group stratigraphic traps may have been created in three systems tracts: (1) lowstand sandstones, (2) transgressive shoreface sandstones, and (3) aggradational carbonate shoal facies and progradational carbonate banks (Candelaria and others, 1997).

Stratigraphic traps are underexplored relative to structural Simpson Group traps (Candelaria and others, 1997) and have potential for future exploration. To accomplish such exploration, new regional and detailed wireline correlations using gamma-ray–neutron logs in a sequence stratigraphic framework will be necessary. Whereas wireline logs are widely available because of extensive underlying Ellenburger production, cores and core data are sparse and discontinuous. Once stratigraphic traps are identified, Simpson Group production could be accomplished through low-cost recompletion of existing Ellenburger wells.

SUMMARY AND CONCLUSIONS

The Middle Ordovician Simpson Group contains a highly varied mixture of both reservoir and nonreservoir rocks that have been poorly examined owing to its relatively low contribution to Permian Basin production. Simpson rocks were deposited in greenhouse conditions during the early transgressive leg of the Tippecanoe megasequence, following an extensive hiatus and development of a karst topography on the underlying Lower Ordovician Ellenburger carbonates of the Sauk megasequence. Simpson production is from three sandstone units in the middle of the group, each sourced from eroding highs to the north and east and transported to the cratonic margins by eolian and fluvial processes. These sandstones represent lowstand and/or early transgressive deposits of three third-order sequences; nonreservoir shales and clay-rich carbonates deposited during maximum flooding and normal marine and restricted carbonates deposited during highstand compose the balance of the sequences. Most published interpretations for West Texas and New Mexico are based on lithostratigraphic analysis and therefore do not depict the true reservoir geometry of these irregularly distributed reservoir sandstones. Modern sequence stratigraphic interpretations are sparse and are generally based on Simpson Group rocks in Oklahoma, where production is more significant. New regional and detailed wireline correlations using gamma-ray–neutron logs and development of a sequence stratigraphic framework are necessary for a better understanding of the remaining potential of Simpson Group sandstones. Not all sandstones are likely present in all areas owing to their depositional setting facies changes up- and downdip, and many of the remaining traps are likely stratigraphic and therefore subtle. However, there are several reasons to reconsider the Simpson Group: reservoir quality is generally adequate; the sandstones, although thin, can be stacked; source rock is present within the group; and reservoir sandstones are well sealed. Extensive

production of the underlying Ellenburger also means that wireline-log data are abundant, and Simpson production could be accomplished through low-cost recompletions of existing Ellenburger wells.

REFERENCES

- Barnes, V. E., Cloud, P. E., Jr., Dixon, L. P., Folk, R. L., Jonas, E. C., Palmer, A. R., and Tynan, E. J., 1959, Stratigraphy of the pre-Simpson Paleozoic subsurface rocks of Texas and southeast New Mexico: University of Texas, Austin, Bureau of Economic Geology Publication 5924, v. I–II, 836 p.
- Blakey, R. C., 2004, Regional paleogeographic views of earth history, sedimentation, tectonics, and paleogeography of the North Atlantic region, Mid-Ordovician: Northern Arizona University, <http://jan.ucc.nau.edu/~rcb7/470NAt.jpg>.
- Bosco, M. J. and Mazzullo, J., 2000, Lithology and cyclicity in Middle Ordovician McKee Sandstone Member (Tulip Creek Formation, Simpson Group) in the Tobosa Basin, Southeast New Mexico and West Texas, *in* Johnson, K. S., ed., Marine clastics in the southern Midcontinent, 1997 Symposium, Oklahoma Geological Survey Circular 103, p. 53–64.
- Candelaria, M. P., Handford, C. R., and Reed, C. L., 1997, Sequence model for the Simpson Group of the southern mid-continent: key to a new stratigraphic play, *in* Johnson, K. S., ed., Simpson and Viola groups in the southern Midcontinent, 1994 Symposium, Oklahoma Geological Survey Circular 99, p. 218–223.
- Cocks, L. R., and Torsvik, T. H., 2004, Major terranes in the Ordovician, *in* Webby, B. D., Paris, F., Droser, M. L., and Percival, I. G., eds., The great Ordovician biodiversification event: Columbia University Press, p. 61–67.
- Cole, C. T., Cordry, C. D., and Hemphill, H. A., 1942, McKee and Waddell sands, Simpson Group, West Texas: American Association of Petroleum Geologists Bulletin, v. 26, no. 2, p. 279–282.
- Decker, C. E. and Merritt, C. A., 1931, The stratigraphy and physical characteristics of the Simpson Group: Oklahoma Geological Survey Bulletin 55, p. 5-49.

- Denison, R. E., 1997, Contrasting sedimentation inside and outside the southern Oklahoma aulacogen during the middle and late Ordovician, *in* Johnson, K. S., ed., Simpson and Viola groups in the southern Midcontinent, 1994 Symposium, Oklahoma Geological Survey Circular 99, p.39–47.
- Derby, J. R., Bauer, J. A., Miller, M. A., Creath, W. B., Repetski, J. E., Dresbach, R. I., Ethington, R. L., Loch, J. D., Stitt, J. H., Sweet, W. C., McHargue, T. R., Taylor, J. F., Miller, J. F., and Williams, M., 1991, Biostratigraphy of the Timbered Hills, Arbuckle, and Simpson Groups, Cambrian and Ordovician, Oklahoma: a review of the correlation tools and techniques available to the explorationists: Oklahoma Geological Survey Circular 92, p. 15–41.
- Dutton, S. P., Kim, E. M., Broadhead, R. F., Breton, C. L., Raatz, W. D., Ruppel, S. C., and Kerans, C., 2005, Play analysis and digital portfolio of major oil reservoirs in the Permian Basin: The University of Texas at Austin, Bureau of Economic Geology Report of Investigations No. 271, 287 p., CD-ROM.
- Frenzel, H. N., Bloomer, R. R., Cline, R. B., Cys, J. M., Galley, J. E., Gibson, W. R., Hills, J. M., King, W. E., Seager, W. R., Kottlowski, F. E., Thompson, S., III, Luff, G. C., Pearson, B. T., and Van Siclen, D. C., 1988, The Permian Basin region, *in* Sloss, L. L., ed., Sedimentary cover—North American Craton, U.S.: Boulder, Colorado, Geological Society of America, The Geology of North America, v. D-2, p. 261–306.
- Galley, J. D., 1958, Oil and gas geology in the Permian Basin in Texas and New Mexico, *in* Weeks, L. G., ed., Habitat of oil—a symposium, Tulsa, Oklahoma: American Association of Petroleum Geologists, p. 395–446.
- Galloway, W. E., Ewing, T. E., Garrett, C. M., Jr., Tyler, N., and Bebout, D. G., 1983, Atlas of major Texas oil reservoirs: The University of Texas at Austin, Bureau of Economic Geology, 139 p.
- Gibson, G. R., 1965, Oil and gas in southwestern region—geologic framework, *in* Young, A., and Galley, J. E., eds., Fluids in the subsurface environment: American Association of Petroleum Geologists Memoir 4, p. 66–100.

- Goldman, D., Bergström, S. M., and Mitchell, C.E., 1995, Revision of the Zone 13 graptolite biostratigraphy in the Marathon, Texas, standard succession and its bearing on Upper Ordovician graptolite biogeography: *Lethaia*, v. 28, no. 2, p. 115–128.
- Hardage, B. A., Pendleton, V. M., and Asquith, G. B., 1999, 3-D seismic interpretation of deep, complex structures in the Delaware Basin, West Texas: The University of Texas at Austin, Bureau of Economic Geology Geologic Circular 99-1, 42 p.
- Herald, F. A., 1957, Occurrence of oil and gas in West Texas: University of Texas, Austin, Bureau of Economic Geology Publication 5716, 442 p.
- Holden, F. T., 1965, The Simpson Group of the Arkoma Basin, Oklahoma and Arkansas, *in* Herndon, T. and Schramm Jr., M. W., eds., Symposium on the Simpson: Tulsa Geological Society Digest, v. 33, p. 134–143.
- Jones, T. S., 1953, Stratigraphy of the Permian Basin of West Texas: West Texas Geological Society Publication 53-29, 63 p.
- Katz, B. J., Robison, V. D., Dawson, W. C., and Elrod, L. W., 1994, Simpson-Ellenburger petroleum system of the Central Basin Platform, West Texas, U.S.A., *in* Magoon, L. B., and Dow, W. G., eds., The petroleum system; from source to trap: American Association of Petroleum Geologists Memoir, v. 60, p. 453–461.
- Kerans, C., 1988, Karst-controlled reservoir heterogeneity in Ellenburger Group carbonates of West Texas: American Association of Petroleum Geologists Bulletin, v. 72, p. 1160–1183.
- Kottlowski, F. E., 1970, Influence of the Pedernal uplift on sedimentation, *in* Basins of the Southwest, v. 1, Symposium of the 10th Annual Meeting Southwest Section of American Association of Petroleum Geologists, February 7–9, 1968, Wichita Falls, Texas: West Texas Geological Society Publication 70-68, p. 21–40.
- Mears, C. E. and Dufurrena, C. K., 1984, Pre-Leonardian geology of Midland Farms field area, Andrews County, Texas, *in* Transactions, Southwest Section AAPG, 1984 Convention, Midland, Texas: West Texas Geological Society Publication 84-78, p. 111–123.

- Northcutt, R. A. and Johnson, K. S., 1997, Major Simpson and Viola oil and gas reservoirs in Oklahoma, *in* Johnson, K. S., ed., Simpson and Viola Groups in the southern Midcontinent, 1994 Symposium: Oklahoma Geological Survey Circular 99, p. 48–57.
- O'Brien, J. E., and Derby, J. R., 1997, Progress report on Simpson and Viola correlations from the Arbuckles to the Ozarks, *in* Johnson, K. S., ed., Simpson and Viola Groups in the southern Midcontinent, 1994 Symposium: Oklahoma Geological Survey Circular 99, p. 260–266.
- Pope, M. C., 2004, Cherty carbonate facies of the Montoya Group, southern New Mexico and western Texas and its regional correlatives: a record of Late Ordovician paleoceanography on southern Laurentia: *Palaeogeography, Palaeoclimatology, Palaeoecology* 210, p. 367–384.
- Read, J. F., 1995, Part 1. Overview of carbonate platform sequences, cycle stratigraphy and reservoirs in greenhouse and ice-house worlds, *in* Read, J. F., Kerans, C., and Weber, L. J., eds., Milankovitch sea level changes, cycles and reservoirs on carbonate platforms in greenhouse and ice-house worlds: SEPM Short Course Notes 35, p. 1–102.
- Ross, J. R., and Ross, C. A., 1992, Ordovician sea-level fluctuations, *in* Webby, B.D., and Laurie, J. R., eds., Global perspectives on Ordovician geology: Proceedings of the Sixth Annual International Symposium on the Ordovician: University of Sydney, Australia, July 15–19, 1991, p. 327–335.
- Schutter, S. R., 1992, Ordovician hydrocarbon distribution in North America and its relationship to eustatic cycles, *in* Webby, B. D. and Laurie, J. R., eds., Global perspectives on Ordovician geology: Proceedings of the Sixth Annual International Symposium on the Ordovician, University of Sydney, Australia, July 15–19, 1991, p. 421–432.
- Sloss, L. L., 1963, Sequences in the cratonic interior of North America: *Geological Society of America Bulletin*, v.74, no. 2, p. 93–113.
- Sloss, L. L., 1988, Tectonic evolution of the craton in Phanerozoic time, *in* Sloss, L. L., ed., Sedimentary cover—North American Craton, U.S.: Boulder, Colorado, Geological Society of America, The Geology of North America, v. D-2, p. 25–51.

- Statler, A.T., 1965, Stratigraphy of the Simpson Group in Oklahoma, *in* Herndon, T., and Schramm, M. W., Jr., eds., Symposium on the Simpson: Tulsa Geological Society Digest, v. 33, p. 162–210.
- Suhm, R. W., and Ethington, R. L., 1975, Stratigraphy and conodonts of Simpson Group (Middle Ordovician), Beach and Baylor Mountains, West Texas: American Association of Petroleum Geologists Bulletin, v. 59, p. 1126–1135.
- Sweet, W. C., Ethington, R. L., and Barnes, C. R., 1971, North American Middle and Upper Ordovician conodont faunas: Geological Society of America Memoir 127, p. 163–193.
- Tai, P. C. and Dorobek, S. L., 2000, Tectonic model for late Paleozoic deformation of the Central Basin Platform, Permian Basin region, West Texas, *in* DeMis, W. D., Nelis, M. K., and Trentham, R. C., eds., The Permian Basin: proving ground for tomorrow's technologies: West Texas Geological Society Publication 00-109, p. 157–176.
- Texas Water Development Board, 1972, A survey of the subsurface saline water of Texas, v. 1, 113 p.
- Tyler, N., Bebout, D. G., Garrett, C. M., Jr., Guevara, E. H., Hocott, C. R., Holtz, M. H., Hovorka, S. D., Kerans, C., Lucia, F. J., Major, R. P., Ruppel, S. C., and Vander Stoep, G. W., 1991, Integrated characterization of Permian Basin reservoirs, University Lands, West Texas: targeting the remaining resource for advanced oil recovery: The University of Texas at Austin, Bureau of Economic Geology Report of Investigations No. 203, 42 p.
- Webby, B. D., Cooper, R. A., Bergstrom, S. M., and Paris, F. 2004, Stratigraphic framework and time slices, *in* Webby, B. D., Paris, F., Droser, M. L., and Percival, I. G., eds., The great Ordovician biodiversification event: Columbia University Press, p. 41–47.
- Williams, J. A., 1977, Characterization of oil types in the Permian Basin: text of talk presented to Southwest Section, American Association of Petroleum Geologists, Abilene, Texas, March 7, 1977.
- Wilson, J. L., 1954, Ordovician stratigraphy in the Marathon folded belt, West Texas: American Association of Petroleum Geologists Bulletin, v. 38, no. 12, p. 2455–2475.

- Wojcik, R., 1990, Crawar (Waddell), *in* Grace, R. M., ed., Oil and Gas Fields in West Texas Symposium, v. 5: West Texas Geological Society Publication 90-86, p. 71–72.
- Wright, W. F., 1965, Petroleum geology of the Simpson Group, West Texas and Southeast New Mexico, *in* Herndon, T. and Schramm, M. W., Jr., eds., Symposium on the Simpson: Tulsa Geological Society Digest, v. 33, p. 62–73.
- Wright, W. F., 1979, Petroleum geology of the Permian Basin: West Texas Geological Society Publication 79-71, 98 p.
- Young, S. A., Saltzman, M. R., and Bergström, S. M., 2005, Upper Ordovician (Mohawkian) carbon isotope ($\delta^{13}\text{C}$) stratigraphy in eastern and central North America: regional expression of a perturbation of the global carbon cycle: *Palaeogeography, Palaeoclimatology, Palaeoecology*, v. 222, p. 53–76.

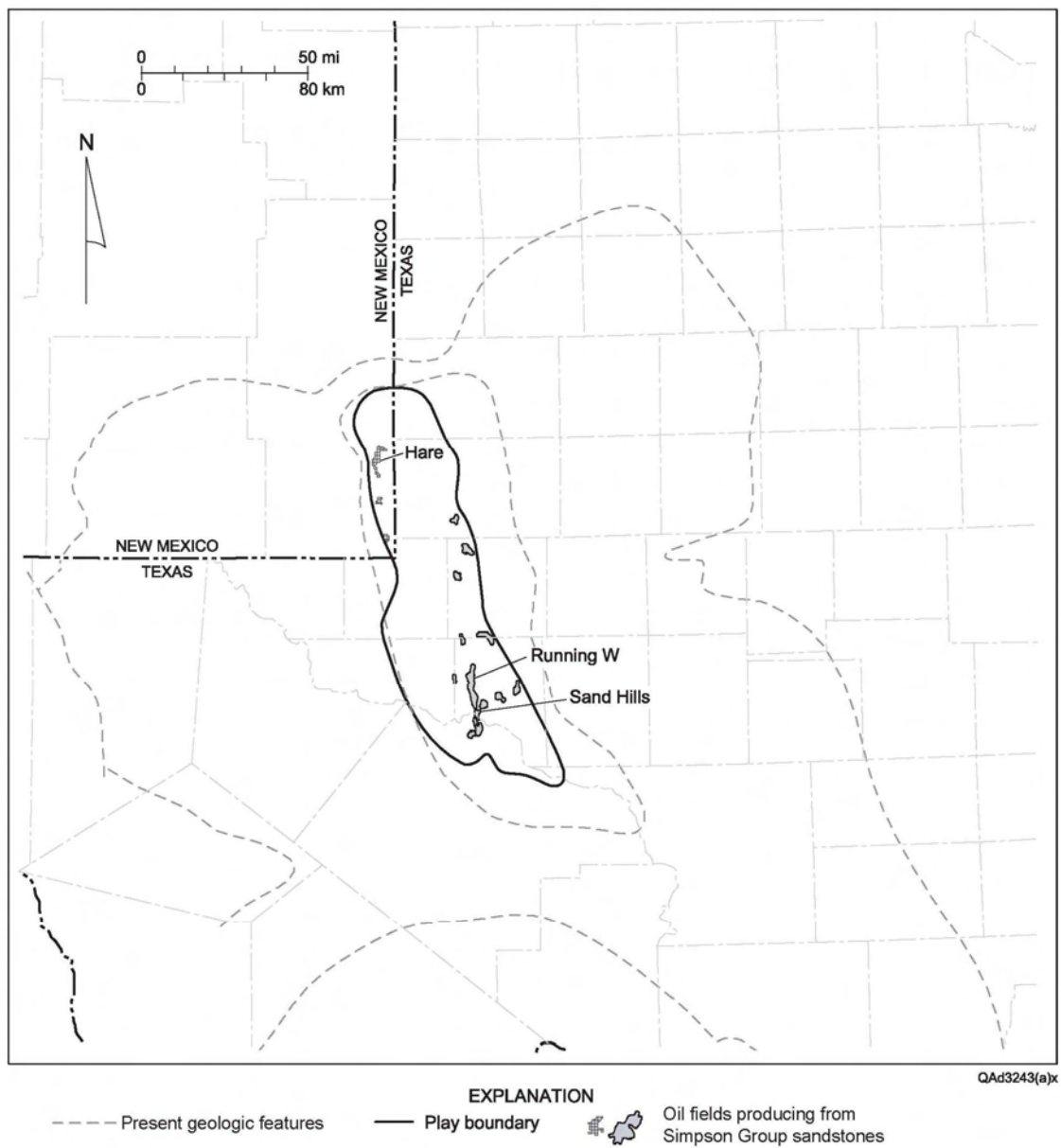
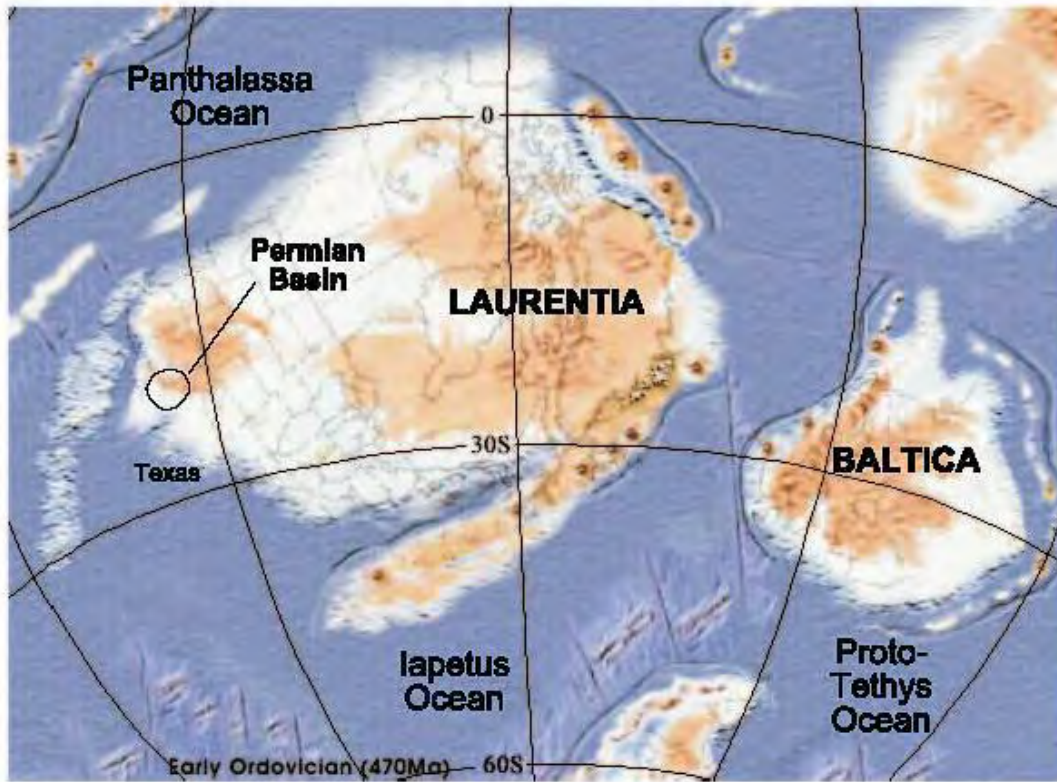


Figure 1. Location map showing Simpson fields with production greater than 1 MMbbl, top three cumulative producing fields, and present geological features. Modified from Dutton and others (2005).

ORDOVICIAN										Global sea level change	
System	UPPER				Age Ma	Oklahoma outcrop	Marathon Uplift outcrop	Permian Basin subsurface	Sequence Stratigraphy		
	British Ser.	N. Am. Ser.	North American Stage	North American conodonts							
SIL	Lland.	Ashgillian	Cincinnatian	Rhuddanian			Caballos Novaculite	Fusselman (upper)	Tipp. II	S1	High
				Himantian/Garnachian	<i>shatzeri</i>	443	Keel	Fusselman (lower)		O14	
				Richmondian	<i>divergens</i>						
					<i>grandis</i>		Sylvan	Maravillas	Montoya Gp.	Cutter	O13
				Maysvillian	<i>robustus</i>	450				Aleman	O12
				Edenian	<i>velicuspis</i>					Upham	O11
				Chatfieldian	<i>confuens</i>		Viola Gp.			Cable Canyon	O10
					<i>tenuis</i>		Viola Springs				
					<i>undatus</i>						
				Turinian	<i>compressa</i>						
					<i>quadridentatus</i>						
					<i>aculeata</i>						
					<i>sweeti</i>	460					
					<i>friendshillensis</i>	460.5					
					<i>polonicus</i>		Simpson Gp.			Tulip Creek	O8
					<i>holodentata</i>					McKee	O7
					<i>sinuosa</i>					McLean	O6
					<i>altifrons</i>					Oil Creek	O5
										Connell	O4
				Rangerian	<i>flabellum/laevis</i>	470		Fort Peña			
				Blackhillian			Arbuckle Gp.	El Paso Gp.	Ellenburger	Sauk III	O3

Figure 2. Stratigraphic column. Data sources include Webby and others (2004) (North American stages, conodonts, and time scale); Young and others (2005) and Derby and others (1991); Goldman and others (1995); Pope (2004); Sloss (1988, 1963); and Ross and Ross (1992).



from Blakey (2004): <http://jan.ucc.nau.edu/~rcb7/340Nat.jpg>

Figure 3. Global plate reconstruction for Ordovician (Blakey, 2004).

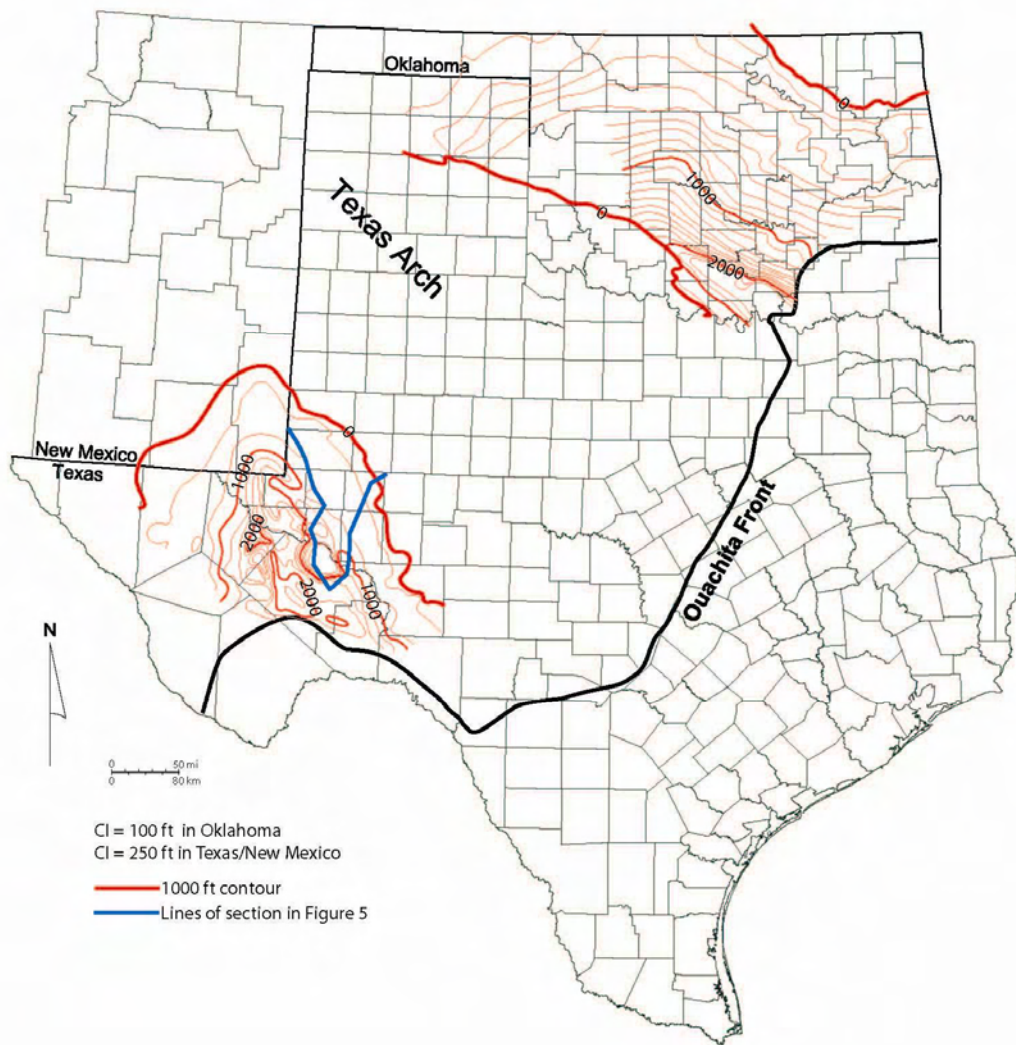


Figure 4. Thickness map of Simpson Group modified from Texas Water Development Board (1972), Frenzel and others (1988), and Northcutt and Johnson (1997). Thousand-foot contour lines and locations of figure 5 cross sections shown in heavy red and blue lines, respectively. Note that contour interval is 100 ft for Oklahoma and 250 ft for Texas and New Mexico.

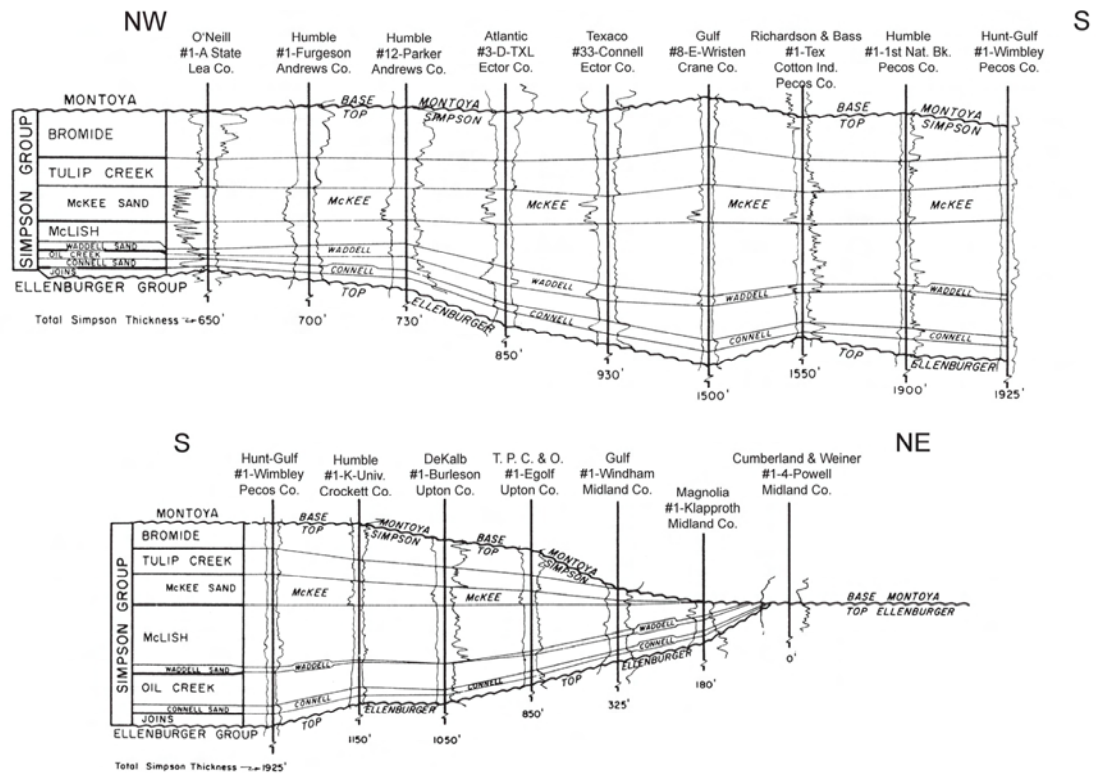
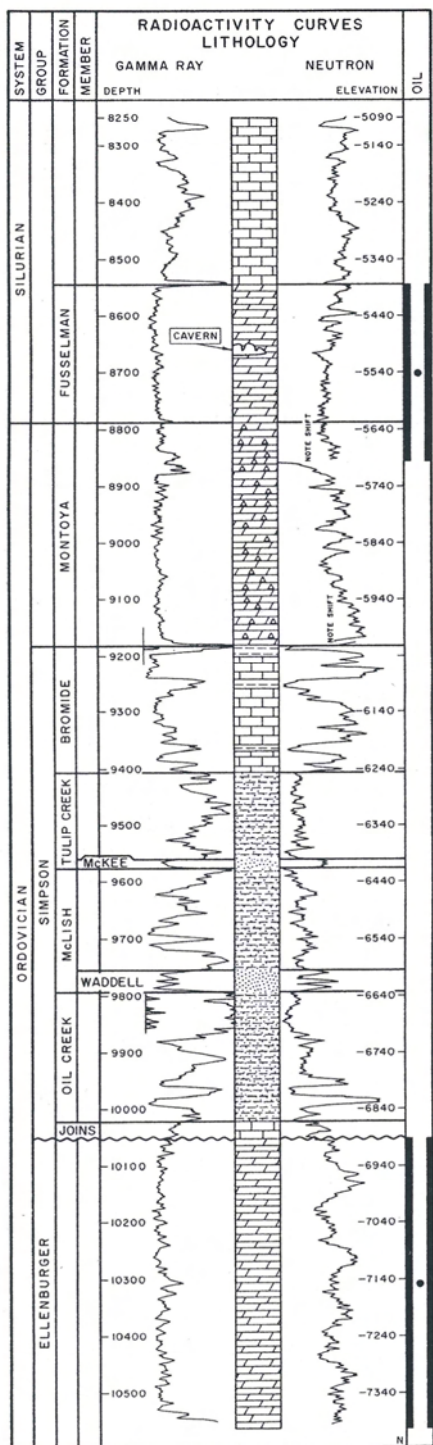


Figure 5. Cross sections showing thickness trends of Simpson Group (Wright, 1965). Cross-section locations shown in figure 4.



EXPLANATION

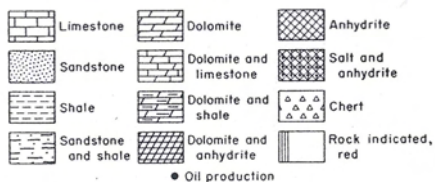


Figure 6. Type wireline log with gamma-ray neutron logs and lithology, Dollarhide field, Andrews County, Texas, and Lea County, New Mexico (Herald, 1957).

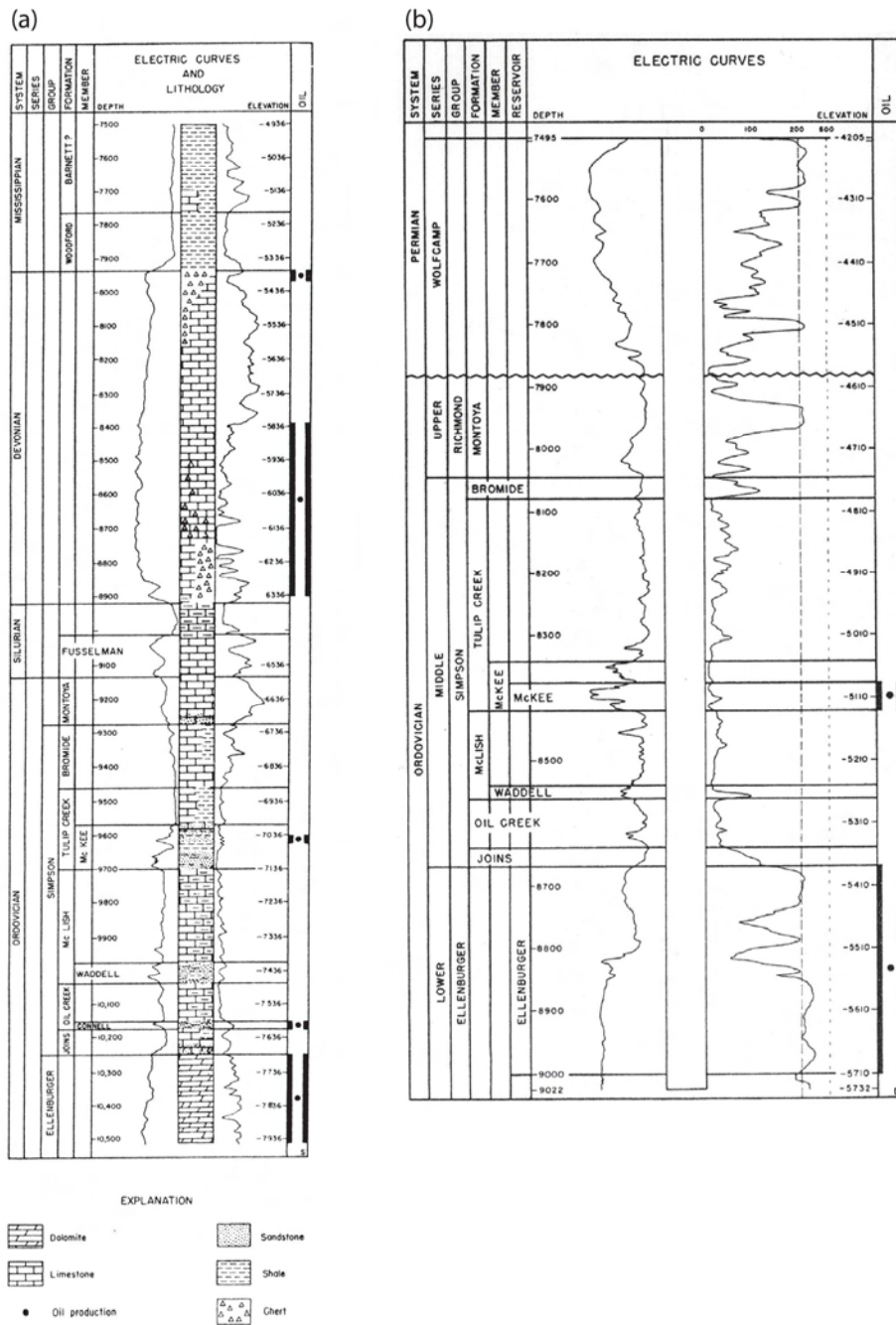


Figure 7. Type wireline logs with electric logs: (a) Block 31 field, Crane County, Texas, and (b) Martin field, Andrews County, Texas (Herald, 1957).

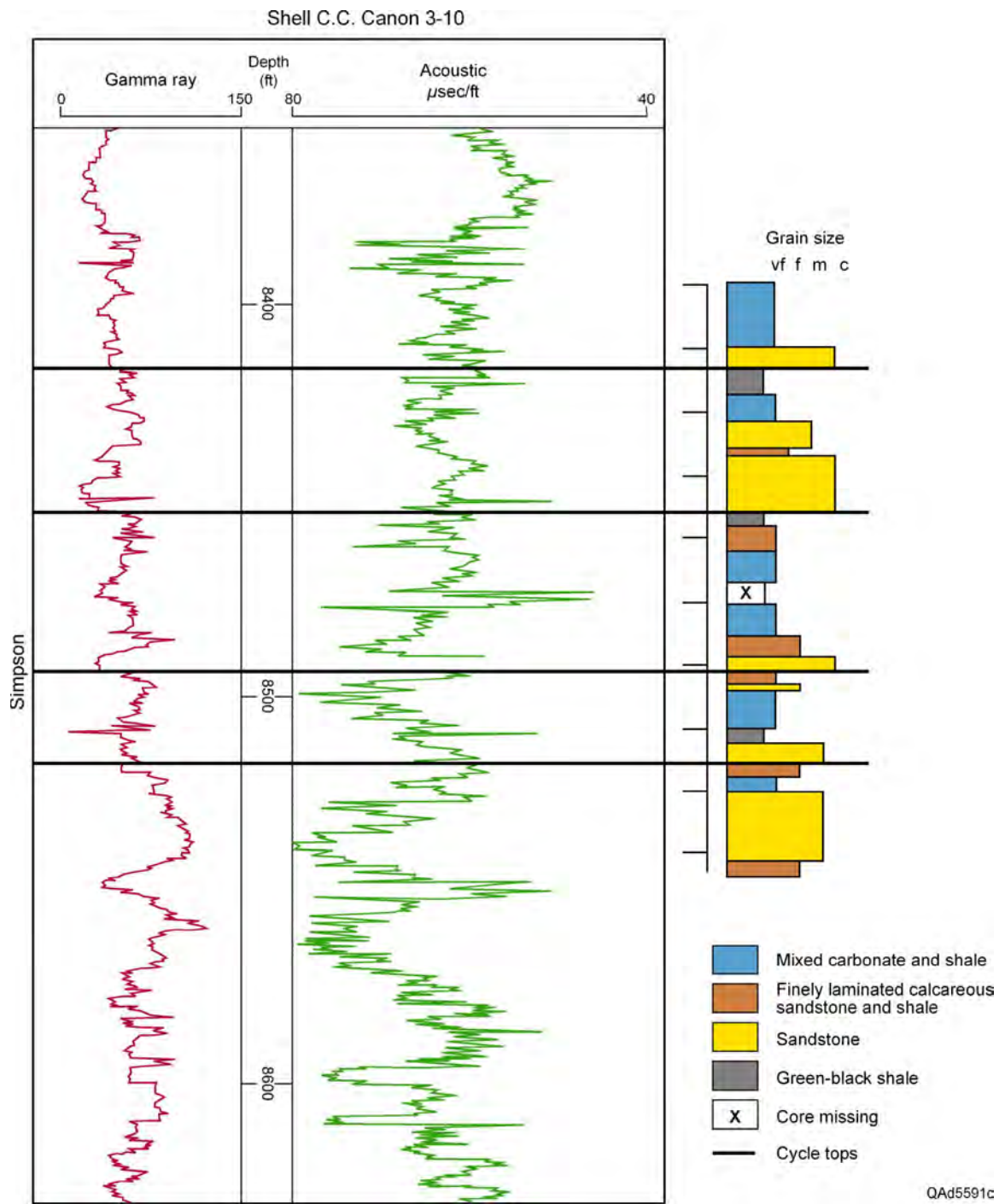


Figure 8. Core description and interpreted cycles from section assigned to McKee Member, Tulip Creek Formation, Shell C.C. Canon 3-10 well, Pecos County, Texas.

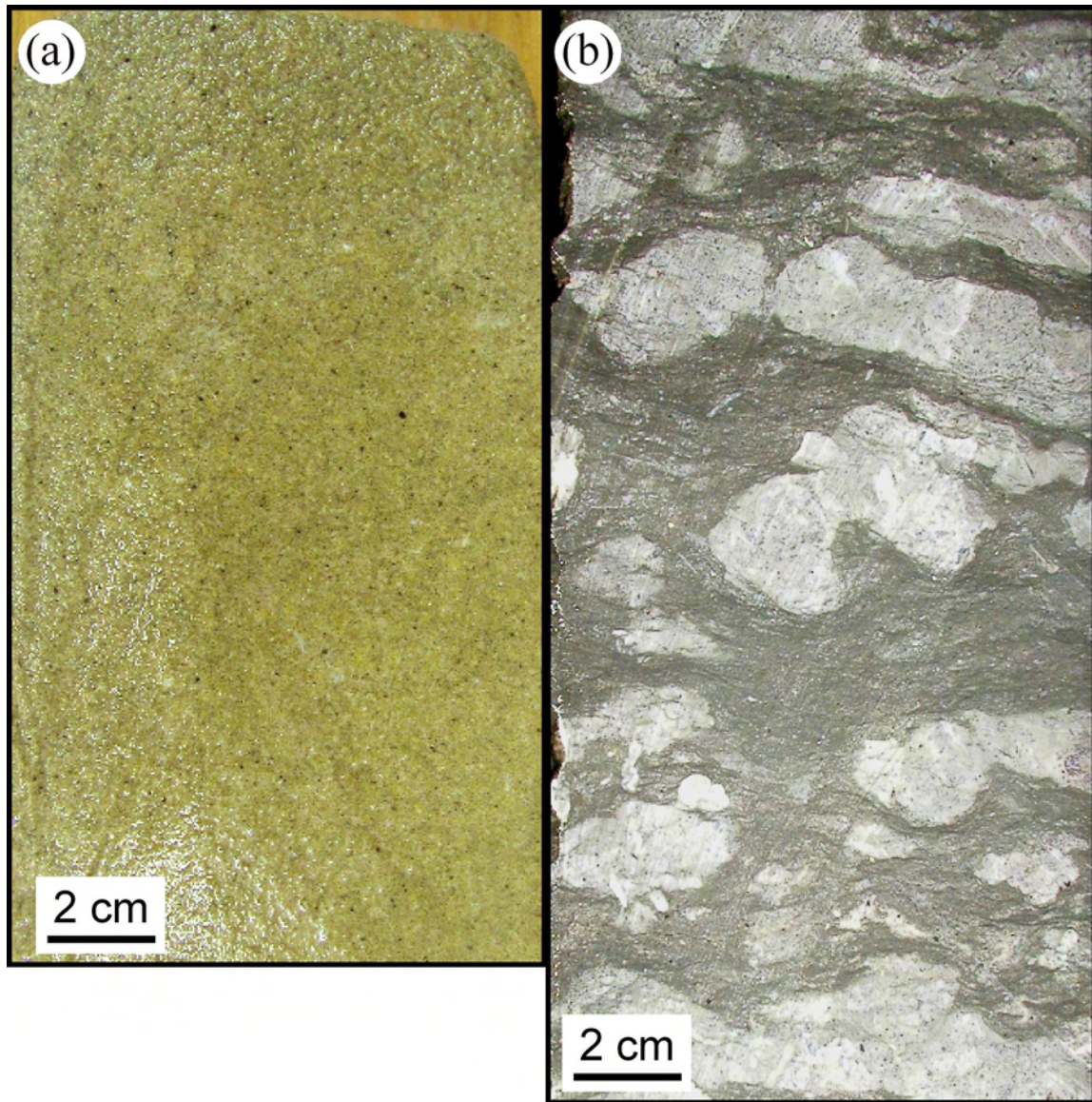


Figure 9. Core photos of McKee Member, Tulip Creek Formation, Shell C.C. Cannon 3-10 well, Pecos County, Texas. Slab width is approximately 4 inches. (a) Facies 1: massive crossbedded tan sandstone with some bioturbation. Depth: 8,483 ft. (b) Facies 2: mixed carbonate and shale with carbonate lenses. Depth: 8,464 ft.

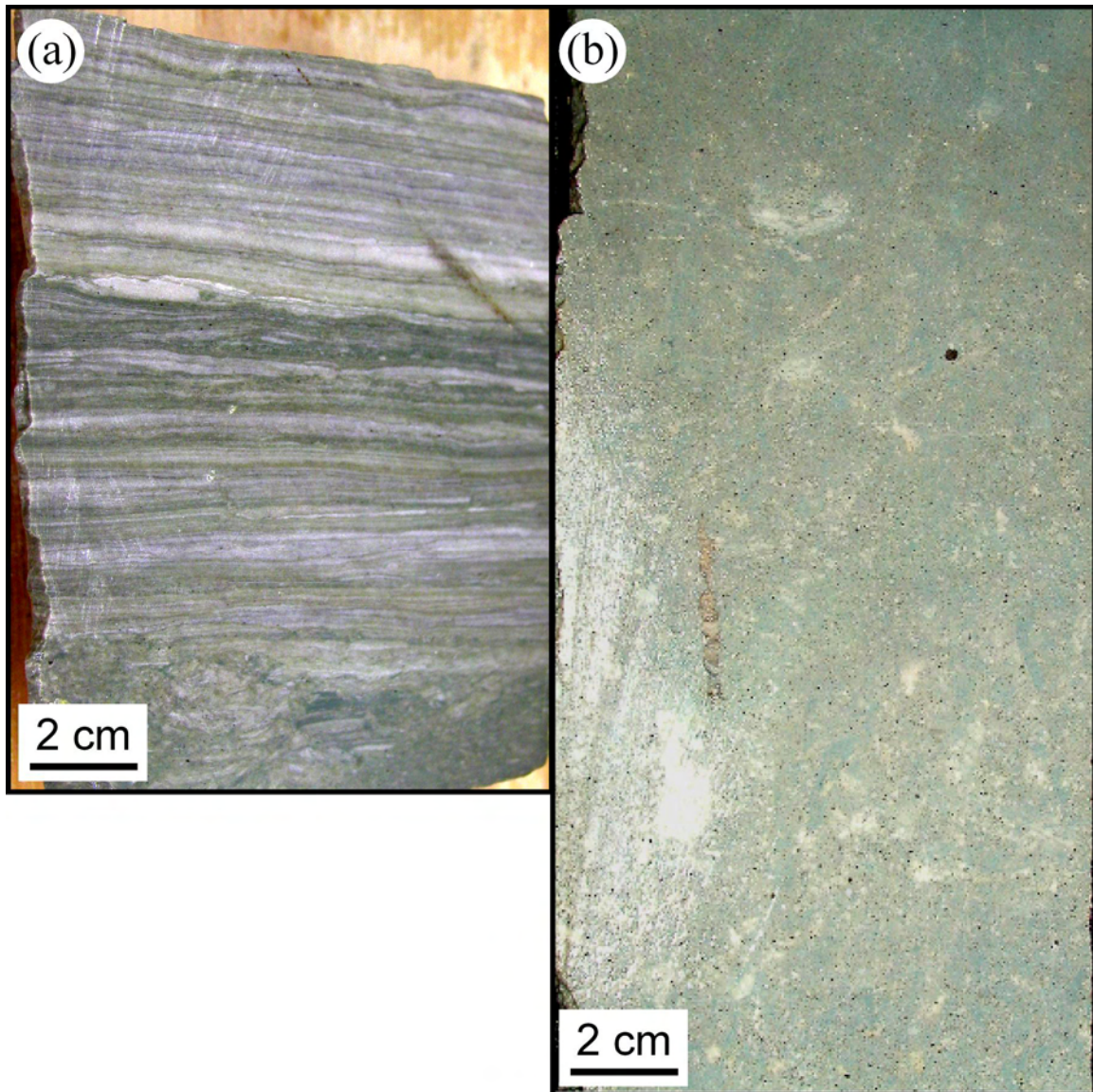


Figure 10. Core photos of McKee Member, Tulip Creek Formation, Shell C.C. Cannon 3-10 well, Pecos County, Texas. Slab width is approximately 4 inches. (a) Facies 3: finely laminated gray carbonate and green-gray shale with bioturbation, roots, and minor sandstone. Depth: 8,501 ft. (b) Facies 4: green-black carbonaceous shale. Depth: 8,479 ft.

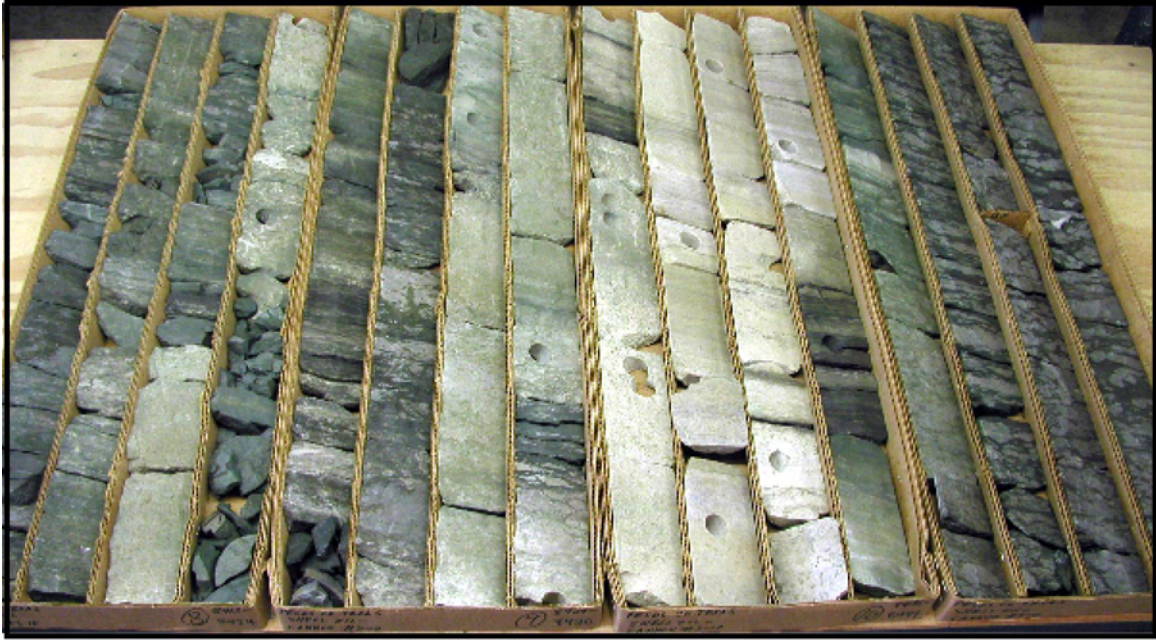


Figure 11. Photo of core from 8,412 to 8,464 ft (described in fig. 8), Shell C.C. Cannon 3-10 well, Pecos County, Texas. Slab width is approximately 4 inches. Core depth increases from left to right.

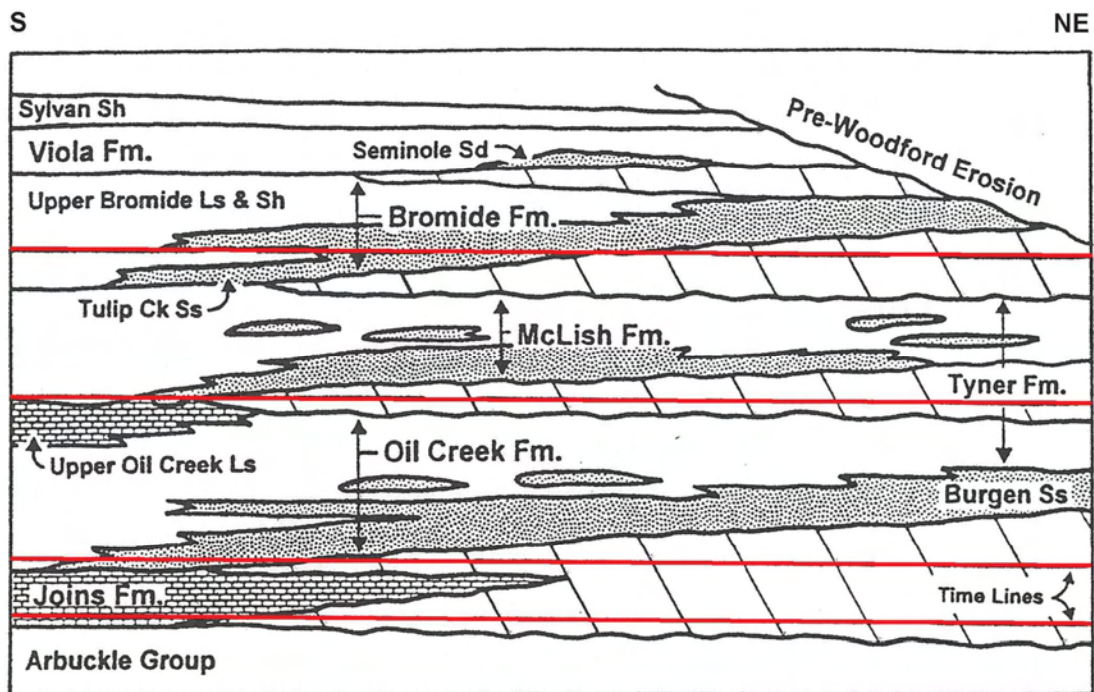


Figure 12. Simpson Group sequence stratigraphic model for Oklahoma constructed by Statler (1965). Figure as modified by Candelaria and others (1997). Red lines highlight timelines.

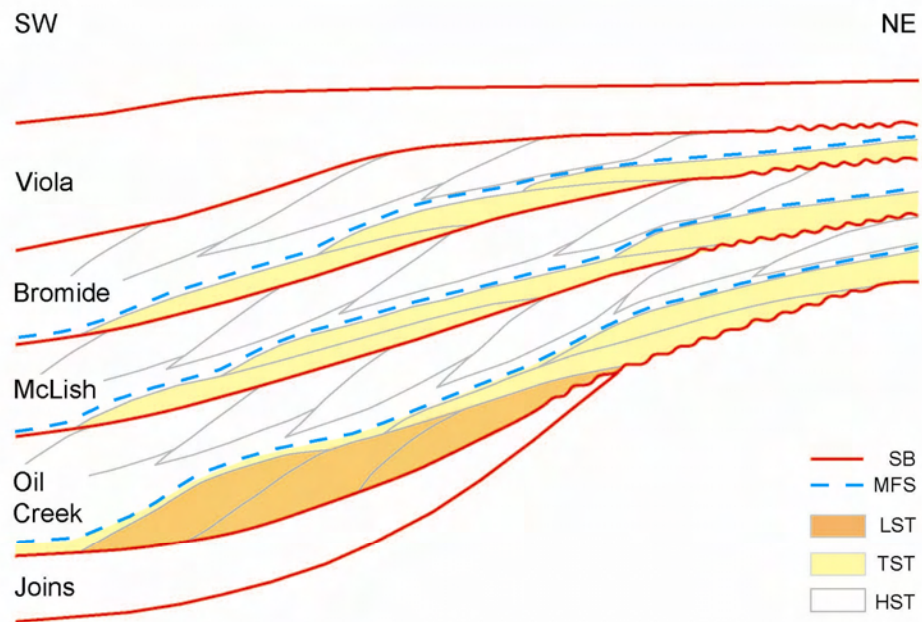


Figure 13. Simpson Group sequence stratigraphic model for Oklahoma production redrafted from Candelaria and others (1997). Note that this model focuses only on the productive area and does not show up- or downdip facies changes.

PATTERNS OF MONTOYA GROUP DEPOSITION, DIAGENESIS, AND RESERVOIR DEVELOPMENT IN THE PERMIAN BASIN

Rebecca H. Jones

ABSTRACT

Rocks composing both the Montoya (Upper Ordovician) and Fusselman (Lower Silurian) Formations were deposited during the global climate transition from greenhouse conditions to unusually short-lived icehouse conditions on a broad, shallow-water platform. The Montoya and the Fusselman also share many reservoir characteristics and have historically been grouped together in terms of production and plays. Recently, however, the Montoya has garnered attention on its own, with new gas production in the Permian Basin and increased interest in global Ordovician climate. Recent outcrop work has yielded new lithologic and biostratigraphic constraints and an interpretation of four third-order Montoya sequences within Sloss's second-order Tippecanoe I sequence.

The Montoya Group comprises the Upham, Aleman, and Cutter Formations, from oldest to youngest. The Upham contains a basal, irregularly present sandstone member called the Cable Canyon. The boundary between the Montoya and the Fusselman is readily definable where a thin shale called the Sylvan is present but can be difficult to discern where the Sylvan is absent. Montoya rocks were deposited from the latest Chatfieldian to the end of the Richmondian stage of the late Mohawkian and Cincinnati series (North American) of the Upper Ordovician.

Montoya reservoir quality is generally better in the northern part of the Permian Basin where it is primarily dolomite compared to limestone Montoya reservoirs in the south. Reservoir quality is also better in the lower part of the unit compared to the upper, owing to a predominance of porous and permeable subtidal ooid grainstones and skeletal packstones in the former and peritidal facies in the latter.

INTRODUCTION

The Montoya Group comprises a moderately thick (100 to 600 ft) Upper Ordovician carbonate ramp succession present in both outcrop and the subsurface of

West Texas and southeastern New Mexico. The four Montoya Group formations, the Upham (and Cable Canyon Member sandstone), Aleman, and Cutter have been defined and well-studied in outcrop but are generally not correlated to the subsurface. Montoya Group thickness reaches a maximum of 590 ft thick in outcrop (Pope, 2004a) and 600 ft thick in the subsurface in Loving, Pecos, Ward, and Winkler Counties and as the Montoya-equivalent Maravillas Formation in Brewster County (Texas Water Development Board, 1972). The subsurface distribution limit is reached in Garza, Borden, Howard, Glasscock, and Reagan counties to the east, Culberson and Jeff Davis counties to the west and Hockley and Lynn Counties to the north (Figure 1) (Texas Water Development Board, 1972). In southeastern New Mexico, the Montoya's presence extends to Chaves and Roosevelt Counties in the north and Dona Ana County in the west (Wright, 1979). The Montoya Group was largely deposited on the Middle-Upper Ordovician Simpson Group but locally overlies on the Lower Ordovician Ellenburger or equivalent. The Sylvan Shale, where present, and the Fusselman Formation generally overlie the Montoya.

Montoya reservoirs are better known for their recent gas production than their relatively low cumulative oil production. From 1993- 2007, 497 BCF of gas and 16.6 MMbbl of oil were produced from Montoya reservoirs (Drilling Info, 2007). Notable gas fields include Block 16 (109.9 BCF) and R.O.C. (27.8 BCF) in Ward County and Waha (40.0 BCF) in Pecos/Reeves Counties (all amounts produced from 1993-2007), and Beall (31.3 BCF produced from 1999-2007) in Ward County (Texas Railroad Commission, 2008). Top producing oil fields with production clearly attributed to reservoirs developed in Montoya rocks (and cumulative production as of the year 2000) include Abell field in Pecos and Crane Counties, Texas (12.6 MMbbl), Tex-Hamon in Dawson County, Texas (4.8 MMbbl), Halley (3.0 MMbbl) and Monahans North (1.0 MMbbl) fields in Winkler County, Texas, and Justis field in Lea County, New Mexico (11.0 MMbbl) (Dutton and others, 2005) (Figure 2).

Other Texas fields (and counties) with Montoya production include Martin (Andrews); East Tank (Borden); Abell Northeast (Crane); Tippet North and Tippet West (Crockett); Effort (Dawson); TXL (Ector); Azalea East (Midland); Abell West, GMW, Heiner, Lehn-Apco, Lehn-Apco North, Mesa Vista, Oates Southwest, Pecos

Valley, Pecos Valley East, Pecos Valley South, and Pikes Peak (Pecos); Worsham-Bayer (Reeves); McEntire, WAM, WAM South, and Westbrook (Sterling); Tokio (Terry); Beall East, and Halley South, and Wink South (Ward).

Distinguishing oil production from rocks in the Montoya Group vs. that from rocks in the Fusselman Formation in the Permian Basin is difficult due to the practice of reporting Montoya and Fusselman production together, the lack of seal between the Montoya and Fusselman, and potential commingling with production from the Ellenberger Formation in places where there is an unconformable contact between Montoya and Ellenburger rocks.

Outcrops studies from the mountains of West Texas and New Mexico and in the Marathon Region in southwestern Texas describe the Montoya Group as a series of subtidal carbonate facies deposited in inner- to outer-ramp settings during waning greenhouse conditions. Very little has been published on the subsurface. This report synthesizes previous work and describes new core and outcrop data with the aim of improving the understanding of Montoya reservoirs and their relationship to outcrops in West Texas and southeastern New Mexico.

PREVIOUS WORK

General accounts of the Montoya reservoir were included in early publications by Jones (1953), Herald (1957), Galley (1958), Howe (1959), and Pratt and Jones (1961). Outcrop descriptions were also published early, by Pray (1958) and Pratt and Jones (1961), and have continued with publications by McBride (1970), Measures (1984, 1985a, and 1985b), and Brimberry (1991). Pope and Steffen (2003) and Pope (2002a, 2002b, 2004a, 2004b, and 2004c) recently developed a sequence stratigraphic model based on outcrop observations and related Montoya facies to regional climatic events. Several authors have described cores taken during recent Montoya exploration: Ball (2002 and 2003) and Behnken (2003) described a core from Dollarhide field and Thomas and Liu (2003) presented observations from cores in a study area including Ward, Pecos, and Reeves Counties.

REGIONAL SETTING

Paleogeography and Climate

In the Late Ordovician, the relatively stable conditions that had prevailed for most of the Ordovician began to change. Landmasses were assembled into a supercontinent, Gondwana, and three major terranes; North America was the Laurentian terrane (Cocks and Torsvik, 2004). Within Laurentia, present-day West Texas and southeastern New Mexico were located near 30°S (Blakey, 2004) (Figure 3). Gondwana began to migrate across the South Pole in the Late Ordovician — a move that likely caused a unique, short-lived episode of glaciation during this waning period of greenhouse conditions (Crowley and Baum, 1995, Pope, 2004b).

Based on Webby (2004), the Montoya Group was deposited from about 452-448 Ma in a mature passive margin setting characterized by fluctuating climatic conditions. The nearest highlands were located in northern New Mexico (Figure 3). The subtidal, gently dipping ramp carbonates making up the Montoya formed during the transitional period to an unusual, short-lived Gondwana glaciation within a longer period of overall greenhouse conditions characterized by high CO₂ concentrations (Pope, 2004b). Global sea-level was at or near the Paleozoic maximum and an extensive oceanic upwelling zone along the southern margin of Laurentia, in what now is New Mexico, Texas, and Oklahoma, resulted in deposition of subtidal ramp carbonates continuing up to 70% spiculitic chert by volume and 1 to 5 weight percent phosphate (Pope and Steffen, 2003). Faunal assemblages suggest that a deep marine basin occupied the area basinward of the Ouachita-Marathon overthrust (Figure 4). Glaciation of the region reached a maximum during the Hirnantian Stage (Figure 5), following deposition of the Montoya (Saltzman and Young, 2005; Young and others, 2005). Greenhouse conditions would again prevail by the end of the Silurian.

Isotopic Evidence for Climate Change

Carbon isotope stratigraphy of K-bentonite-bound horizons, biostratigraphy, and facies analysis has been used to identify the onset of oceanic upwelling that was

associated with cooling and glaciation. Upwelling of cooler nutrient-rich waters (Si and PO_4), increased primary productivity and resulted in preferential sequestration of isotopically light (^{12}C) carbon during the Hirnantian.. (Young and others, 2005). Following a period of upwelling and carbon sequestration, disproportionately more heavy carbon (^{13}C) was sequestered in the seawater causing fewer nutrients to be available for carbonate production. Seawater with higher $\delta^{13}\text{C}$ ratios circulated onto the carbonate platform and became incorporated into skeletal packstones and grainstones, resulting in a distinct isotopic enrichment in these skeletal-rich strata compared to the mud- and chert-rich strata below.

Two isotope excursions have been documented in the Late Ordovician: the first occurred at during the early Chatfieldian stage and has been referred to as the Guttenberg carbon isotope excursion (GICE); the second occurred in the Hirnantian. Both events have been associated with glaciation of Gondwana and tied to changes in ocean circulation. During the GICE, $\delta^{13}\text{C}$ ratios were enriched by $\sim 3\text{‰}$ in Upper Ordovician strata from numerous locations throughout North America, including the Viola Group in the Arbuckle Mountains of Oklahoma, equivalent intervals in Kentucky, Virginia, and West Virginia (Young and others, 2005), and the Nashville Dome area in Tennessee (Holland and Patzkowsky, 1997). The GICE marks a fundamental change in the style of carbonate deposition, the cause of which has been interpreted as a minor episode of Gondwana glaciation. These locations also have similar ϵ_{Nd} ratios, indicating that they are from the same continuous body of water (Holmden and others, 1998), eliminating the possibility that the $\delta^{13}\text{C}$ excursions are due to geochemically-distinct epicontinental masses of water, rather than climatic changes. The Hirnantian isotope excursion included enrichment of both $\delta^{13}\text{C}$ and $\delta^{18}\text{O}$ by $\sim 2\text{‰}$ in brachiopod samples from around the world, suggesting a short-lived period of global glaciation lasting approximately 0.5-1 million years (Brenchley and others, 1994).

Thus, the Montoya Group was deposited between two short-lived episodes of continental glaciation during an overall greenhouse climate. Most Montoya facies reflect the upwelling and sea-level rise associated with the transitional conditions preceding Hirnantian glaciation; however, the siliciclastic basal Cable Canyon Member was likely deposited during lowstand conditions that prevailed immediately following the first,

minor glaciation event. Evidence for this conclusion comes from recent work on the Eureka Quartzite in Nevada, which is approximately time equivalent to the Cable Canyon in West Texas and southeastern New Mexico outcrops (Pope and Steffen, 2003). Eureka Quartzite workers concluded that the GICE was followed by a significant fall in sea level with deposition of lowstand clastics as a result of continental glaciation (Saltzman and Young, 2005).

Structure

A cratonic origin has been invoked by both historical and contemporary authors for Cambrian – Ordovician clastics, including the Middle-Late Ordovician Simpson Group. Exposed Precambrian basement and Cambrian granitic plutons formed paleotopographic highs (Pedernal Uplift, Diablo Arch) that sourced the Cambrian Bliss Sandstone (Goldhammer and others, 1993). The Pedernal Massif in central and north-central New Mexico was also a regional high and supplied sediment for Simpson sandstones and silts in southeastern New Mexico (Kottlowski, 1970) and likely the southeastern extension of these deposits into West Texas. By ca. 450 Ma, the cratonic sediment supply no longer reached the area south of Ouachita-Marathon fold belt, according to neodymium isotope analysis of Maravillas Formation sediments from this area (Gleason and others, 1995). Prior to this time, siliciclastics were transported from eroding highs in the northwest and deposited as the Cable Canyon Member sandstone. The lack of local highs in this shallow marine platform setting eliminates the possibility of a local provenance for these siliciclastics (Figure 4). An isopach map of the Cable Canyon sandstone in southeastern New Mexico (Figure 6) lends further support to this idea by depicting a northwest-southeast-striking locus of deposition and thickening towards the northwest.

Post-depositional structural thickening of both Montoya and Simpson Group rocks in front of the Ouachita-Marathon overthrust (Reeves, Pecos, and Ward Counties) was observed in 3-D seismic (Hardage, 1999), reprocessed 2-D seismic (Swift and others, 1994), and well data from this area, with repeated section created through both high-angle reverse faults (Figure 7) and overturned structures (Figure 8). Not only are these observations relevant to wireline correlations, but they also may explain the discrepancy

between modern and historical interpretations of depositional environment; without seismic data, the structurally thickened strata may have misled previous workers into interpreting a basin setting for the Montoya Group, e.g., figure 11 in Galley, 1958. Deeper water conditions were likely present basinward of the Ouachita-Marathon overthrust (Figure 3) where the Maravillas Formation is present, but not landward, where the Montoya facies are characteristic of a shallow carbonate platform setting.

FACIES AND SEDIMENTOLOGY OF THE MONTOYA GROUP

The Montoya Group was initially described as a formation with two members, the Second Value and the Par Value, before being renamed as a group with four subdivisions: the Cable Canyon Sandstone, the Upham Dolomite, the Aleman Formation, and the Cutter Formation (Kottlowski et al., 1956). The Cable Canyon is now referred to as a member of the Upham Formation in both outcrop and the subsurface, (Pope 2004a and Thomas and Lui, 2003) (Figure 5). Montoya Group equivalents include the Maravillas Formation in the Marathon region of Texas and the Viola Group in Oklahoma and northern Texas (Anadarko Basin).

Unconformities are present both above and below the Montoya Group. Conodont data (Sweet, 1979) indicate major breaks in sedimentation at both boundaries; however, the basal unconformity has not been observed in Oklahoma (Dennison, 1997). The Montoya Group was deposited on Simpson Group carbonates and sandstones in the center of the Montoya subcrop area in West Texas and southeastern New Mexico (Figure 1). Where the Simpson is absent, i.e., in the eastern and the very northern Midland Basin, western Delaware Basin, and far western Texas and New Mexico outcrops (Figure 1), the Montoya overlies the Ellenburger or the equivalent El Paso Group. The upper unconformity marks a significant period of erosion related to post-depositional uplift (Mears and Dufurrena, 1984); in some cases large portions of the upper Montoya Group were removed. Montoya rocks reach a maximum of 590 ft of thickness in outcrop (Pope, 2004a) and over 600 ft in subcrop (Wright, 1979). Outcrops are present in the Beach, Hueco, and Franklin Ranges of West Texas and the Sacramento, San Andres, Franklin, and Caballo Ranges of southeastern New Mexico (Pope, 2004a). Montoya outcrops have also been reported in the Baylor and Sierra Diablo Ranges in Texas (Jones, 1953).

The Montoya is Cincinnati series in age, having been deposited during the Edenian and Richmondian stages of the Upper Ordovician, based on conodont biostratigraphy (Sweet, 1979) and ages assigned to conodont species zones (Webby, 2004) (Figure 5). The Viola Group in Oklahoma has been often discussed as equivalent; however, conodont data from outcrops in this region (Derby and others, 1991) indicate that only the Upper Viola Springs Formation, the Welling Member, and the Sylvan Formation are truly age-equivalent (Figure 5). Even more problematic are correlations with the Maravillas Formation in the Marathon Uplift region of West Texas. Graptolite biostratigraphy (Goldman and others, 1995) and graptolite-conodont age equivalents (Webby, 2004) indicate that these strata are Richmondian and therefore only overlap with the latter half of Montoya deposition (part of the Aleman through Cutter deposits) in Texas/New Mexico and latest Sylvan deposits in Oklahoma.

The Montoya Group was largely deposited in a shallow-water platform setting characterized by normal marine conditions. Cool water currents from both the north and south were present along the western coast of Laurentia (Figure 3) related to the pending Hirnantian glaciation. The southerly ocean currents resulted in upwelling of cool waters in present day West Texas and New Mexico with deposition of cherty carbonate updip and cherty shale downdip as observed in outcrop (Pope, 2004a). These chert trends are also interpreted to be present in the subsurface of the northwestern and southwestern Permian Basin, respectively (Figure 4).

Upham Formation and Cable Canyon Member

The Upham Formation, including the Cable Canyon Member sandstone where present, rests unconformably on the karsted surface of the Lower Ordovician El Paso Group in most outcrops and on the Simpson or Ellenburger in subcrop and in outcrops east of the Hueco Range. The Cable Canyon member is thin (10 cm or less) and irregularly present in the Franklin Mountains, ranges from less than 0.5 m to over 2 m in the Sacramento Mountains (Brimberry, 1991), and is greater than 15 m thick in the Cooks Range (Pope, 2002) (outcrop locations shown in Figure 1). It is poorly documented in the subsurface, but similarly thin (2 to 20 ft) (Thomas and Liu, 2003). The Cable Canyon Member and Upham Formation are both exposed at the Scenic Drive and McKelligon

Canyon outcrops in the Franklin Mountains on the northern edge of El Paso, Texas (Figure 9).

The Cable Canyon and Upham are interpreted to have been deposited from 452-451 Ma during the Edenian stage, a period of time corresponding to the late *confluens* and *velicuspis* conodont zones. These units comprise one third-order sequence and document the start of marine transgression following a significant hiatus in deposition (Figures 5 and 10). Cable Canyon siliciclastics were likely deposited during lowstand and then reworked during transgression.

Facies

Cable Canyon lithofacies include gravel conglomerate and carbonate-cemented (primarily dolomite) quartz sandstone (Pope, 2004a; Bruno and Chafetz, 1988) that are poorly sorted with grains ranging from 0.1 mm to >2.0 mm in outcrop (Brimberry, 1991). This unit is dominantly medium-grained but coarsens where more thickly deposited, with a grain-size profile that increases from the base to middle and then decreases from the middle to top of the unit in New Mexico outcrops (Bruno and Chafetz, 1988). This carbonate-rich siliclastic unit was originally deposited by traction transport, i.e. fluvial or aeolian, processes (Bruno and Chafetz, 1988), but most of the original cross-bedding has been masked by extensive burrows, which can include 1.5 m deep vertical *Skolithos* burrows that are filled with quartz sandstone (Pope, 2002b). Quartz grains are well-rounded; the plentiful fossil fragments include crinoids, gastropods, brachiopods, and bryozoans (Pope, 2002b). At Scenic Drive outcrops in the Franklin Mountains, the Cable Canyon/Upham contact is gradational, with sand incorporated into the lowermost Upham (Figure 11a). This contact is much sharper at McKelligon Canyon, where the Cable Canyon comprises sandstone with thin lenses of carbonate, which appear to have been reworked from the underlying El Paso Group (Figure 11b). In subsurface Permian Basin cores, the Cable Canyon consists of poorly sorted, well-rounded, variable coarseness sandstone and sandy packstone with skeletal fragments (Thomas and Liu, 2003).

The Upham comprises coarse-grained skeletal wackestones-packstones and grainstones that are variably colored, massive, and can be highly bioturbated in outcrop (Pope, 2004a; Pope and Steffen, 2003). This basal Upham can contain up to 30% quartz

at the very base in places where a distinct Cable Canyon unit is absent. Faunal assemblages include corals, crinoids, brachiopods, bryozoans, gastropods, receptaculitid algae, and nautiloids. The dominant skeletal wackestones-packstones are punctuated and capped by coarse-grained crinoidal grainstone beds and a massive unit with rare cross-bedding, respectively. Phosphate (pellets and replacement of bryozoans) and hardgrounds were also observed in outcrop (Pope, 2002b).

Bioturbated skeletal wackestones containing large coral (Figure 12) were observed at the Scenic Drive outcrop and color variation was observed at the McKelligon Canyon outcrop (Figure 13), both in the Franklin Mountains. These dolostones and locally present limestones contain phosphate (pellets, encrusted hard grounds, and replaced skeletal grains) and chert (irregular nodules, diagenetic replacement) (Pope and Steffen, 2003). The fauna at Scenic Drive include a distinct species of solitary rugose coral, *neotryplasma floweri*, that are known only to exist in this area and the Ural region of Russia (Elias, 1986). In subsurface cores from the Permian Basin, the lower Upham comprises dark-colored chert bearing skeletal packstones, wackestones, and mudstones and the upper Upham comprises light-colored packstones and grainstones with a coarser texture and more diverse fauna (Thomas and Liu, 2003).

Depositional Setting

The Cable Canyon Member, Upham Formation, and the lower part of the Aleman Formation represent inner-, mid-, and outer-ramp facies within a second-order transgressive systems tract (Figure 14a). The Cable Canyon was deposited in waters 5-15 m deep as a sand-wave complex deposited by asymmetrical tidal currents (Bruno and Chafetz, 1988) during initial sea-level rise and may represent reworked siliciclastics from earlier traction deposits (Bruno and Chafetz, 1988) or sand dune deposits (Pope, 2002b) deposited during lowstand following a very brief, pre-Montoya episode of glaciation described earlier. The source of siliciclastics was likely eroding Precambrian basement highs to the northwest, a source also invoked for the Middle Ordovician Simpson Group. The Cable Canyon isopach map over southern New Mexico (Figure 6) lends support to this idea, in that the locus of deposition trends northwest-southeast with thickening towards the interpreted sediment source in the northwest. This thickness variation is

interpreted to be purely depositional, rather than evidence for erosion because the contact between the Cable Canyon and the overlying Upham Formation is gradational (Bruno and Chafetz, 1988). Contacts observed in the Franklin Mountains were also gradational and characterized by high sand content in the lower Upham (Figure 11). The Upham burrowed skeletal wackestones-packstones were deposited in the shallow subtidal mid-ramp with warm waters, that developed during continued sea-level rise within the same 3rd-order sequence (Pope, 2004c, Figure 10). Energy levels increased and shoals likely developed, in which the crinoid-rich grainstones were deposited. The hardgrounds and phosphate and iron coatings were likely created subaqueously under anoxic conditions, when frequent sea-level rises and upwelling currents brought phosphate-rich waters into this dominantly shallow ramp (Pope, 2002b).

Aleman Formation

The Aleman Formation overlies the Upham Formation in West Texas and New Mexico outcrops (outcrop locations shown in Figure 1) and is exposed at the McKelligon Canyon outcrops in the Franklin Mountains on the northern edge of El Paso, Texas (Figure 9). Several described cores have been assigned to the Aleman formation, including cores from the southern Delaware Basin (Thomas and Liu, 2003) and a recent core from Dollarhide field in Andrews County (Ball, 2002 and Behnken, 2003), which was also examined in this study and will be discussed in the Reservoir Geology section. The Aleman Formation is Maysvillian to Richmondian in stage, corresponds to the *robustus* and early *grandis* conodont zones, and was deposited from 451-449.5 Ma. Portions of the Aleman are contained within two 3rd-order sequences (Figures 5 and 10)

Facies

The Aleman Formation comprises interbedded carbonate and chert. The carbonate has been extensively dolomitized with the exception of a locally present basal limestone. In outcrop, chert is abundant (30-40%) and phosphate content is similar to that of the Upham Formation (Pope and Steffen, 2003).

A thin-bedded chert interval (Figure 15), overlain by a middle grain-rich interval (Figure 16), and an upper nodular chert interval (Figure 17) were observed at outcrops in

McKelligon Canyon in the Franklin Mountains (Figure 9). These patterns have been observed in other West Texas and New Mexico outcrops, e.g., Pope 2002a, 2002b, 2004a, 2004b, 2004c, and Pope and Steffen, 2003. These workers describe three facies in the Aleman: 1) even-bedded laminated calcisiltite or mudstone and spiculitic chert, 2) skeletal wackestones to packstones with discontinuous bedded to nodular chert, and 3) skeletal packstone to grainstone with abundant crinoids, bryozoans and brachiopods interbedded with thin coral bafflestones. The lower Aleman is dominantly facies 1 with some overlying facies 2, the middle Aleman is facies 3, and the upper Aleman is facies 2.

Three types of chert have been interpreted from these outcrops by Pope (2004a): primary, early diagenetic and late diagenetic. Primary chert was deposited as thin beds or lenses of sponge spicules, between layers of mudstone and calcisiltite. The lack of sedimentary structure suggests that the spicules were deposited below storm wave base. Most chert nodules observed in outcrop were surrounded by bent laminations, suggesting that they formed on the seafloor before complete lithification and therefore represent an early stage of diagenesis. Relict sponge spicules were also observed within chert nodules in Aleman Formation outcrops in the Silver City Range in southwestern New Mexico (Geeslin and Chafetz, 1982). Late diagenetic chert formed through three mechanisms: 1) as replacement of evaporate nodules in tidal flat facies, 2) replacement of evaporates in subtidal facies, which were likely formed by burial brines during reexposure of platform, or 3) veins or tabular beds.

Depositional Setting

The lower bedded chert facies in Aleman Formation were deposited in a deep ramp setting characterized by cool waters and rare storm waves. Sponge spicules were likely transported into this setting from up ramp and interbedded with the *in situ* calcisiltite and mudstone (Pope, 2002b). The middle Aleman skeletal packstone to grainstone facies was deposited in a warm-water high-energy shoal, as evidenced by cross-bedding (Pope, 2002b). Both the lower and upper Aleman contain skeletal wackestones to packstones with bedded and nodular chert, which are representative of a slightly shallower setting between the deep ramp calcisiltite and grainstone shoals. The

chert breccia facies rarely encountered in the Aleman represents slumping of early-formed chert (Pope, 2002b).

Cutter Formation

The Cutter Formation overlies the Aleman Formation in West Texas and New Mexico outcrops (outcrop locations shown in Figure 1) and is exposed at the McKelligon Canyon outcrops in the Franklin Mountains on the northern edge of El Paso, Texas (Figure 9). It is eroded in some places in the subsurface, at least partially owing to post-depositional structural uplift (Mears and Dufurrena, 1984). The Cutter Formation is Richmondian stage, corresponds to the *grandis* conodont zone, and was deposited from 450-448 Ma. It comprises one full and one partial third-order sequence (Figures 5 and 10).

Facies

Bioturbated skeletal wackestones and laminated mudstones, evaporates, and rare secondary silica nodules (evaporate replacement) comprise the Cutter Formation (Pope and Steffen, 2003). Distinct facies include skeletal packstones (bryozoans, brachiopods, and crinoids abundant), burrowed mudstone with locally interbedded green-brown shale, and laminated and fenestral mudstone (Pope, 2002). This overall light-colored fine-grained interval consists of dolomite with minor chert (Pope, 2004a). Brachiopod wackestone with lenses of crinoidal packstone (Figure 18), overlain by wackestone to laminated mudstone (Figure 19) were observed at outcrops in McKelligon Canyon in the Franklin Mountains (Figure 9). In core from the subsurface Permian Basin, dark-colored chert-bearing wackestones and mudstones of the Lower Cutter are overlain by packstones and grainstones with decreasing chert content (Thomas and Liu, 2003).

Depositional Setting

These facies are interpreted to represent shallow subtidal to peritidal deposition. Skeletal packstones were deposited during a relatively brief period of open marine conditions; burrowed mudstones were deposited in a restricted subtidal setting (lagoon);

and laminated and fenestral mudstones were deposited in a tidal flat setting, with semi-arid and humid climates, respectively (Pope, 2002b).

The Viola Group and Sylvan Formation in Oklahoma

The Viola Group and Sylvan Shale are approximate Montoya Group equivalents in eastern Texas, Oklahoma, and Arkansas. Age-equivalency based on the latest conodont biostratigraphy and age data (Figure 5) show that the lower part of this group, the Lower Viola Springs Formation, does not have age-equivalent Montoya formations, and that the upper part of the group, the Upper Viola Springs Formation, including the Welling Formation, is equivalent to the Cable Canyon Member and Upham and lower Aleman Formations in the Montoya Group. The Sylvan Shale was deposited at the same time as the upper Aleman and Cutter Formations. Duration of deposition of the Sylvan has been estimated at 3 million years and there is no evidence of an unconformity at its base (Dennison, 1997), but age relationships suggest that a significant hiatus occurred between deposition of the Sylvan and the overlying Keel Formation (Figure 5).

Facies

The lower Viola Springs Formation comprises interbedded laminated calcisiltite or carbonate mudstone and bedded and nodular chert in the Arbuckle Mountains (Mitchell, 2003). This is overlain by bioturbated thinly-bedded calcisiltite and mudstone with nodular chert. Skeletal wackestone-packstone with chert nodules and medium to thick bedding characterize the upper Viola Springs Formation and skeletal packstones and grainstones with thick bedding characterize the Welling Formation (Mitchell, 2003). Primary porosity is present in the grainstones and closely spaced post-depositional (Pennsylvanian) fractures are present in the mud-rich rocks of the Viola Springs (Dennison, 1997). The consistent thickness (100-300 ft) and clay-richness of the Sylvan create an effective seal for the highly productive Viola Group (Dennison, 1997).

Depositional Setting

The depositional setting of the Viola Group has been interpreted to be similar to that of the Montoya (Mitchell, 2003). The group comprises an overall shallowing-upward

succession with deeper water mudstones grading into shallow water grainstones (Dennison, 1997). Contourite and turbidite sedimentary structures suggest that the carbonate ramp was steep (Pope, 2002b). The Sylvan shale was deposited in a shallow subtidal marine setting with low energy (Sternbach, 1984) when a new sediment source of clay abruptly ended carbonate deposition (Dennison, 1997).

Sylvan Formation in Texas

The Sylvan Formation in Texas is not age equivalent to that in Oklahoma (Figure 5) and therefore may represent entirely different shale. The Sylvan nomenclature has been applied to an irregularly present thin shale has been used as a high gamma-ray wireline log pick to separate the Montoya Group from the overlying Fusselman in the subsurface. There can be numerous high gamma-ray responses in the upper portions of the Montoya (Figure 20) that do not represent shales, as we discovered when logging the upper part of the Montoya in a core from Dollarhide field in Andrews County, Texas. Distinct Montoya and Fusselman facies were recognizable in core, but the portion of core that would have contained the formation boundary was missing, so any shale/gamma ray relationships could not be confirmed by this core. Nonetheless, the lack of correlation between shale and high gamma ray wireline response in the upper Montoya suggest that caution should be used in picking the Montoya/Fusselman boundary on the basis of high gamma-ray wireline log responses alone.

The Maravillas Formation

The Maravillas outcrops in the Marathon Uplift area of southwestern Texas are considered equivalent to the Montoya (McBride, 1970) although biostratigraphy indicates both a significant hiatus during the early period of Montoya deposition and an overall deeper depositional environment setting for a distinct biofacies when compared to the Montoya Group and equivalents in the rest of North America (Goldman and others, 1995). This formation describes facies deposited in the area in West Texas labeled “deep marine basin” in Figure 4. Neodymium isotope analysis of sediments from this area suggests that sediments in this area were not derived from the Laurentian craton; rather, passive margin shales with strongly negative ϵ_{Nd} values gave way to less negative ϵ_{Nd}

orogenic turbidites from the emerging Appalachian orogen at this time (Gleason and others, 1995).

The Maravillas is a 60-500 ft thick chert-rich formation with three informal members based on variations in lithology (McBride, 1970). The lowermost member contains dominantly limestone with chert, the middle member contains dominantly chert with limestone, and the thin upper member contains chert and shale. The upper member has been previously called the Solitario and the Persimmon Gap Members. The upper shale is likely correlative with the Sylvan in West Texas and New Mexico where present and in southeastern Oklahoma (Wilson, 1954).

The Maravillas comprises 40% black chert, 30% limestone (calcarenite, micrite, and marlstone), 14% shale, 10% non-black chert, 5% limestone pebble conglomerate, and 1% dolomite (McBride, 1970). Bedding is regular with thickness varying from three to 12 inches. Whereas some earlier authors invoke a shallow-marine setting invoked on the basis of bryozoans and primary chert, McBride (1970) suggests that the depositional setting of these rocks was deep-water slope to basin floor and concludes that the bryozoans were transported and the chert was secondary. Additional evidence for a deep-water depositional environment include the lack of typical shallow water structures, such as wave formed ripples and bedding, coupled with the presence of characteristic deep water features, including slump structures, coarse conglomerates, and anoxic conditions indicated by high organic matter and lack of bioturbation (McBride, 1970).

Sequence Stratigraphy of the Montoya Group

The Upper Ordovician is part of the Tippecanoe I second-order supersequence set (Sloss, 1988) of the Tippecanoe first-order megasequence (Sloss, 1963) (Figure 5). As described early, the Montoya Group was deposited between two short-lived episodes of Gondwana glaciation and therefore most facies were strongly influenced by the transitional greenhouse-icehouse climate. Sea level changes were therefore higher amplitude (20-50 m) and more frequent than would be expected during normal greenhouse conditions (Read and others, 1995). Montoya deposition following a significant mid-Tippecanoe I hiatus after deposition of the Middle-Upper Ordovician Simpson Group and was fully deposited before the beginning of the Tippecanoe II

second-order sequence in the Silurian (Figure 5). This depositional hiatus occurred throughout the study area and is interpreted to have had a particularly long duration in the Marathon Uplift area (Goldman and others, 1995). Montoya facies are interpreted to have been deposited during a 2nd-order highstand systems tract (HST) and transgressive systems tract (TST) (Figure 14). The Montoya Group comprises four complete 3rd-order sequences and portions of two others (Figure 10).

First and Second-Order Sequences

The Montoya Group was deposited during the transgressive leg of the Tippecanoe first-order megasequence (Sloss, 1963), called the Tippecanoe I second-order supersequence set (Sloss, 1988). Within this second-order sequence, skeletal sandstone and granule conglomerate were deposited in an inner ramp setting (likely reworked lowstand deposits) followed by mid-ramp transgressive systems tract packstones and grainstones, and then deep ramp calcisiltite and spiculitic chert (Figure 14a). Continued deep ramp deposition continued followed by chert-bearing wackestones and packstones as conditions shallowed to mid-ramp. Then, packstones and grainstones were deposited followed by burrowed skeletal wackestones and laminated and fenestral mudstones during the highstand systems tract (Figure 14b). A simple link can be made between second-order systems tracts and formation names: the Upham was deposited during initial transgression across the ramp, the Aleman during major deepening (late TST/early HST), and the Cutter during widespread highstand peritidal conditions (Pope and Steffen, 2003).

Third-Order Sequences

The four Montoya Group lithostratigraphic formations can be fit into four widespread, plus two irregularly present, third-order sequences (1 to 3 m.y.) (Figure 10). Workers in the subsurface Permian Basin have defined four third-order sequences in the Montoya Group: the first sequence comprises the Cable Canyon member (lowstand deposits) and the Upham (transgressive and highstand systems); the second sequence comprises the lower part of the Aleman shallowing-upward succession; the third sequence comprises the upper part of the Aleman shallowing-upward succession; and the

fourth sequence comprises the Cutter Formation (Thomas and Liu, 2003). The north-south outcrop section scheme developed by Pope (2004a) (Figures 1 and 10) places the Cable Canyon and Upham facies in the initial transgressive sequence, the lower Aleman cherty facies and the lower part of the medial subtidal grain-rich Aleman facies in the second sequence, the upper part of the medial subtidal grain-rich Aleman facies, the upper Aleman cherty facies, and part of the Cutter peritidal facies in the third sequence, and the Cutter peritidal facies in the fourth sequence. An additional sequence of Cable Canyon and Upham facies is present locally at the base and an additional sequence of shallow subtidal mid-ramp carbonates with open marine fauna is present locally at the top.

Reservoir Geology

In cores from a study area including Ward, Pecos, and Reeves Counties, facies consists of dark-colored chert-bearing wackestones and mudstones overlain by chert-free packstones with a grainstone cap, overlain by numerous coarsening-upward cycles of chert-bearing packstone to grainstone (Thomas and Liu, 2003). These facies were interpreted to correspond to the lower, middle, and upper Aleman, respectively.

A core at Dollarhide field in Andrews County (from the Dollarhide 25 2-S well) has also been assigned to the Aleman Formation by Ball (2002 and 2003) and Behnken (2003). This core was also examined by this study, but correlation to the outcrop formations not made. Incomplete coring of the Montoya interval (including no coverage of the Montoya/Fusselman boundary) and known unconformities at both the base and top of the Montoya were factors in deciding not to attempt these correlations without additional data.

Facies observed in the Dollarhide core (Figure 20 and 21) include chert mudstone (Figure 22), mudstone, dolowackestone (Figure 23), and dolopackstone – grain-dominated dolopackstone (Figures 24 and 25). A section of chert-bearing mudstone is present from 8457-8479 ft; chert is also present in wackestones at the base of the core. Chert nodules contain relict sponge spicules and fracturing and microporosity are developed around their rims (Figure 26). Interpretation of depositional environments from this core has been difficult. The lack of diagnostic exposure surfaces coupled with

abundant chert and numerous thin grain-rich intervals make definitive assignment of facies to a peritidal vs. subtidal environment challenging. This base of the core is clearly subtidal, with upward-shallowing cycles comprised of peloidal packstone or wackestone (Figures 24 and 23) at cycle bases and grain-dominated dolopackstones (Figure 25) at cycle tops; however, the upper part of the core has been interpreted as both peritidal ((Ball, 2002 and Behnken, 2003) and restricted subtidal to transitional (this study). We were not convinced that there were sufficient exposure surfaces or diagnostic peritidal features, such as development of fenestral porosity, to definitively place this core in a peritidal setting. We also were not convinced that an interpretation of karst (Behnken, 2003) could be supported by this core. The limited areas of intensely fractured strata could represent local deformational features, similar to those observed in outcrop. Additional studies of nearby cores to provide context will be necessary to resolve the ambiguity about the depositional environment of this core.

Further compounding the problem of subsurface-outcrop correlations is the lack of distinct wireline log characteristics. Wireline log correlations are generally problematic in the Montoya, particularly in differentiating the Montoya from the overlying Fusselman. Both units have low gamma ray responses and wireline porosity is often related to dolomitization, rather than facies. Examination of picks from a database provided by Geological Data Services and published wireline correlations suggests that the combined thickness of the Fusselman and Montoya is often simply halved to make a top Montoya pick where the Sylvan shale is absent. The wireline data give little if any indication of facies, so it is difficult to get away from this approach; however, it is far from ideal. Isopach maps constructed from such picks show neither the true deposition thickness nor the magnitude of unconformities.

Whole core porosity and permeability data from the Dollarhide core show that the best reservoir facies are grain-dominated dolopackstones, located in the lower third of the core (Figures 20 and 25). Porosity ranges from 7-13.2% and permeability from 1.5-183 md in these fabrics. Porosity ranges from 0.3-16.1% and permeability ranges from 0.01-183 md permeability (k90) throughout the cored interval. Porosity and permeability are highest in dolomitized rocks, making mineralogy prediction important; however, predicting mineralogy with grain density data alone can be misleading in this core. Thin

sections demonstrate that many intervals contain a mix of dolomite and chert with grain densities ranging from 2.71- 2.79 g/cc. This range reflects a mix of dolomite grain density of 2.85 g/cc and chert (quartz) grain density of 2.65 g/cc (Klein, 1993). Limestones composed of calcite with a grain density of 2.71 g/cc (Klein, 1993) and a small amount of dolomite could also fall into this range.

Reservoir Development

Many Montoya reservoirs have been recently developed for gas production, which has now far surpassed production from the limited number of oil reservoirs. As of 2007, 497 BCF of gas and 16.6 MMbbl of oil have been cumulatively produced from Montoya reservoirs (Drilling Info, 2007). Notable gas fields include Block 16 (109.9 BCF) and R.O.C. (27.8 BCF) in Ward County and Waha (40.0 BCF) in Pecos/Reeves Counties (all amounts produced from 1993-2007), and Beall (31.3 BCF produced from 1999-2007) in Ward County (Texas Railroad Commission, 2008). Top producing oil fields with production clearly attributed to reservoirs developed in Montoya rocks (and cumulative production as of the year 2000) include Abell field in Pecos and Crane Counties, Texas (12.6 MMbbl), Tex-Hamon in Dawson County, Texas (4.8 MMbbl), Halley (3.0 MMbbl) and Monahans North (1.0 MMbbl) fields in Winkler County, Texas, and Justis field in Lea County, New Mexico (11.0 MMbbl) (Dutton and others, 2005) (Figure 2).

Reservoir Distribution

The Montoya is thickest in Pecos, Reeves, and Ward Counties, as shown by an isopach generated from a database of picks supplied by Geological Data Services (Figure 27). This is a structurally complex area, as mentioned earlier, and thicknesses are probably not representative of deposition, but rather may reflect repeat section through high angle reverse faulting and overturned structures (see Figures 7 and 8). Representative maximum depositional thicknesses are present in part of Ward, Loving, Winkler, and Culberson counties. The group thins quickly to the east (becoming absent in Borden Howard, Glasscock, and Reagan Counties) but oversteps the underlying Simpson group to the west (extending as far as Otero County, New Mexico) (Galley,

1958). Post-depositional erosion due to structural uplift is at least in part responsible for this thinning; up to 17% of the original section has been removed in some areas (Mears and Dufurrena, 1984).

Oil reservoirs are developed predominantly in the dolomitized subtidal facies (skeletal grain-dominated packstones and packstones) located in the northern part of the Permian Basin; gas reservoirs are developed in areas with sufficiently hydrocarbon maturity to yield gas. In both cases, traps are structural. Commingling with the overlying Fusselman is common, but the Sylvan shale, where present, and tight peritidal facies of Cutter Formation can sufficiently seal the reservoir interval, as exemplified by Dollarhide field, where the Fusselman reservoir has watered out but the Montoya produces (Ball, 2003).

Porosity Development

Porosity development in the Montoya Group is controlled by both facies and diagenesis. The highest porosity has been developed in dolostones, which are more abundant in the northern part of the Permian Basin, whereas limestones are dominant in the Marathon region outcrops and southern Permian Basin. The transition from limestone to dolostone occurs in Hudspeth, Culberson, Reeves, Andrews, Martin, and Howard Counties and in the Franklin Mountain outcrops (Jones, 1953). Porosity is also better developed in subtidal ramp facies of the lower Montoya (average 6.2%) than in the dominantly peritidal facies of the upper Montoya (average 2.5%) at Dollarhide field in Andrews County (Behnken, 2003). The highest reservoir quality occurs in the lower part of the reservoir where dolomitized ooid grainstones and skeletal packstones have both moldic and intercrystalline porosity; however, lower quality chert-bearing dolomudstones with intercrystalline and fenestral porosity in the upper part of the reservoir are also productive (Behnken, 2003). Chert intervals are also productive at Waha field (Reeves County), where moldic spicules, small pores (< 0.05 mm pore throats), microporosity in fine-grained skeletal grainstone with chert, and slightly dolomitized skeletal packstone with chert constitute part of the Aleman pay zone (Thomas and Liu, 2003).

Coarse dolomite with intercrystalline porosity was observed in thin sections taken from dolopackstones and grain-dominated dolopackstones in the Dollarhide core

described in this study (Figures 24 and 25). These samples are likely represent of the highest unfractured reservoir properties, with whole core porosity of 8.1 and 8.4% and permeability of 40.9 and 6.33 md, respectively. Higher porosity and permeability values were observed in chert mudstones but likely represent fracture, not matrix properties. Some microporosity was observed around chert nodule rims (Figure 26), but its contribution to reservoir porosity is relatively minor.

Pore lining and poikilotopic dolomite and tabular to acicular anhydrite have reduced reservoir porosity, as has late calcite, which is present in oomolds and fractures at Dollarhide field (Behnken, 2003). By contrast, caverns and fractures have enhanced porosity and permeability in some Montoya reservoirs (Gibson, 1965). Natural fractures are a key component of porosity and permeability development in horizontal wells producing from the Viola Group in southern Oklahoma (Candelaria and Roux, 1997).

Traps, Seals, and Sources

Most Montoya trap include structural and/or fault closure. The trap at Dollarhide field is a fault-bounded anticline structural trap (Figure 21); however, stratigraphic trapping may occur through changes from subtidal to peritidal facies upsection and dolomitization and several karsting events (Ball, 2002). A lack of effective barrier (shale or porosity change) between the Montoya and the overlying Fusselman in many areas (for example, where the Sylvan is absent) has allowed hydrocarbons to migrate upwards into the Fusselman (Wright, 1979) and in some cases the Montoya reservoir is connected to the underlying Ellenburger (Gibson, 1965). Given the continuous Montoya/Fusselman oil column observed in many fields, it seems likely that Montoya would share the Fusselman oil source, which has been clearly identified as the Upper Devonian Woodford shale (Williams, 1977).

Opportunities for Additional Resource Recovery

The location of currently producing gas fields overlaps with the area of greatest thickness and deepest burial, as well as greatest structural complexity. Additional gas resources may be recoverable from the southern Delaware Basin with detailed 3-D

seismic interpretation. This will be necessary to understand the complex structural traps and repeat section characteristic of the area (Figures 7 and 8).

Careful mapping of facies and mineralogy may also lead to identification of bypassed pay. As shown in the model developed from outcrop (Figure 10), the mid-ramp subtidal facies (skeletal grain-dominated packstones with the highest reservoir quality) are thickest in medial positions on a landward-basinward transect. Placing subsurface data in terms of this model would allow for identification of the mid-ramp facies fairway and thereby the best locations for recompletions or new drilling. The outer ramp chert mudstones and wackestones are lower reservoir quality, but may also hold bypassed resources in areas where the grain-dominated packstones have been produced or waterflooded with the appropriate reservoir management strategies.

SUMMARY AND CONCLUSIONS

The Montoya Group of the Permian Basin reflects a unique transitional climate, during which greenhouse conditions were changing to reflect the pending glaciation of Gondwana, which would occur immediately following deposition. This changing climate had a profound effect on sea-level fluctuations and facies, including 1) high-amplitude, frequent sea-level changes (four complete and two partial third-order sequences), 2) carbonate depositional environments ranging from peritidal to outer ramp, and 3) an abundance of chert and phosphate from upwelling waters. Montoya oil reservoirs are dominantly developed in mid-ramp skeletal grain-dominated packstones, particularly in the northern part of the Permian Basin, where porosity has been enhanced through dolomitization. Gas production has superseded oil, in terms of both quantity and recent interest, and is focused in the southern part of the Delaware Basin, where reservoir quality is likely lower due to more distal facies, but hydrocarbon maturity obviously more advanced. A deep marine equivalent, the Maravillas Formation, is present in the Marathon Uplift area but not known to be productive. The Viola Group of Oklahoma is also considered an equivalent, although facies/age relationships do not exactly match.

Extensive work in Montoya Group outcrops in West Texas and New Mexico has resulted in a sequence stratigraphic context for the formations. The limited core examined in this report suggests that outcrop models can be applied to the subsurface; however,

additional core work is needed to fully establish this relationship and utilize these models for reservoir development. Further rock-based will also be necessary to establish the reservoir architecture, facies patterns, and porosity/permeability relationships required for recovery of the remaining oil and gas resources in Montoya reservoirs.

REFERENCES

- Adler, F.L., 1971, Future petroleum provinces of the Mid-Continent: Tulsa Geological Society Digest, v. 38, p. 985-1042.
- Ball, B.C., 2003, Identifying bypassed pay in the Fusselman and Montoya reservoirs of the Dollarhide field, Andrews County, Texas, *in* Hunt, T.J., and Lufholm, P.H. (eds.), The Permian Basin: Back to Basics: West Texas Geological Society Publication 03-112, p. 1–12.
- Ball, B.C., 2002, A Fusselman and Montoya core from the Dollarhide field, Andrews County, Texas, *in* Hunt, T.J., and Lufholm, P.H. (eds.), Permian Basin: Preserving our Past—Securing our Future: West Texas Geological Society Publication 02-111, p. 207–208.
- Behnken, F.H., 2003, Montoya conventional core description, depositional lithofacies, diagenesis and thin section petrography from the Pure Resources, Inc., Dollarhide Unit 25-2-S, Andrews County, Texas, *in* Hunt, T.J., and Lufholm, P.H. (eds.), The Permian Basin: Back to Basics, West Texas Geological Society Publication 03-112, p. 13–35.
- Bergström, S.M. and Mitchell, C.E., 1986, The graptolite correlation of the North American Upper Ordovician Standard: *Lethaia*, v. 19, no. 3, p. 247-266.
- Blakey, R.C., 2004, Regional Paleogeographic Views of Earth History, Sedimentation, Tectonics, and Paleogeography of the North Atlantic Region, Late Ordovician: <http://jan.ucc.nau.edu/~rcb7/450NAt.jpg>.
- Brenchley, P.J., Marshall, J.D., Carden, G.A.F., Robertson, D.B.R., Meidla, T., Hints, L., and Anderson, T.F., 1994, Bathymetric and isotopic evidence for a short-lived Late Ordovician glaciation in a greenhouse period: *Geology*, v. 22, p. 295-298.

- Brimberry, D.L., 1991, Depositional and diagenetic history of the Late Ordovician Montoya Group, Sacramento Mountains, south-central New Mexico, *in* Johnson, K.S. (ed.), Late Cambrian-Ordovician geology of the southern Midcontinent, 1989 symposium: Circular - Oklahoma Geological Survey, 1991, v. 92, p. 154-170.
- Bruno, L. And Chafetz, H.S., 1988, Depositional environment of the Cable Canyon Sandstone: A Mid-Ordovician sandwave complex from southern New Mexico: New Mexico Geological Society Guidebook, 39th Field Conference, Southwestern New Mexico, p. 127-134.
- Candelaria, M.P., and Roux, B.P., 1997, Reservoir analysis of a horizontal-well completion in the Viola Limestone “chocolate brown zone,” Marietta Basin, Oklahoma, *in* Johnson, K.S. (ed.), Simpson and Viola Groups in the southern Midcontinent, 1994 Symposium: Oklahoma Geological Survey Circular 99, p. 183–193.
- Chenoweth, P.A., 1966, Viola oil and gas fields of the Mid-Continent: Tulsa Geological Society Digest, v. 34, p. 110-118.
- Cocks, L.R. and Torsvik, T.H., 2004, Major terranes in the Ordovician, *in* Webby, B.D., Paris, F., Droser, M.L., and Percival, I.G. (eds.), The Great Ordovician Biodiversification Event, Columbia University Press, p. 61-67.
- Collins, E.W., and Raney, J.A., 2000, Geologic Map of West Hueco Bolson, El Paso Region, Texas: Bureau of Economic Geology Miscellaneous Map 40, The University of Texas at Austin, Austin, Texas.
- Crowley, T.J. and Baum, S.K., 1995, Reconciling Late Ordovician (440 Ma) glaciation with very high (14X) CO₂ levels: *Journal of Geophysical Research*, v. 100, no. D1, p. 1093-1101.
- Derby, J.R., Bauer, J.A., Miller, M.A., Creath, W.B., Repetski, J.E., Dresbach, R.I., Ethington, R.L., Loch, J.D., Stitt, J.H., Sweet, W.C., McHargue, T.R., Taylor, J.F., Miller, J.F., and Williams, M., 1991, Biostratigraphy of the Timbered Hills, Arbuckle, and Simpson Groups, Cambrian and Ordovician, Oklahoma: A review

- of the correlation tools and techniques available to the explorationist: Oklahoma Geological Survey Circular 92, p. 15-41.
- Denison, R.E., 1997, Contrasting sedimentation inside and outside the southern Oklahoma aulacogen during the middle and late Ordovician, *in* Johnson, K.S. (ed.), Simpson and Viola groups in the southern Midcontinent, 1994 Symposium: Oklahoma Geological Survey Circular 99, p.39-47.
- DrillingInfo, 2007, Montoya production data accessed from <http://www.drillinginfo.com> on July 10, 2007.
- Dutton, S. P., Kim, E. M., Broadhead, R. F., Breton, C. L., Raatz, W. D., Ruppel, S. C., and Kerans, Charles, 2005, Play analysis and digital portfolio of major oil reservoirs in the Permian Basin: The University of Texas at Austin, Bureau of Economic Geology Report of Investigations No. 271, 287 p., CD-ROM.
- Elias, R.J., 1986, New Late Ordovician solitary rugose coral with perforate septa: *Journal of Paleontology*, v. 60, no. 1, p. 14-25.
- Flower, R.H., 1969, Early Paleozoic of New Mexico and the El Paso region: Guidebook - El Paso Geological Society, Annual Field Trip, Issue 3, Ordovician symposium, p. 31-101.
- Frenzel, H.N., Bloomer, R.R., Cline, R.B., Cys, J.M., Galley, J.E., Gibson, W.R., Hills, J.M., King, W.E., Seager, W.R., Kottlowski, F.E., Thompson, S., III, Luff, G.C., Pearson, B.T., and Van Siclen, D.C., 1988, The Permian Basin region, *in* Sloss, L.L. (ed.), *Sedimentary cover—North American Craton.: The Geology of North America*, Geological Society of America, Boulder, Colorado, v. D-2, p. 261–306.
- Galley, J.D., 1958, Oil and gas geology in the Permian Basin in Texas and New Mexico, *in* Weeks, L. G. (ed.), *Habitat of oil—a symposium*, Tulsa, Oklahoma: American Association of Petroleum Geologists, p. 395–446.
- Geeslin, J.H. and Chafetz, H.S., 1982, Ordovician Aleman ribbon cherts: An example of silicification prior to carbonate lithification: *Journal of Sedimentary Petrology*, v. 52, no. 4, p. 1283-1293.

- Gibson, G.R., 1965, Oil and gas in southwestern region—geologic framework, *in* Young, A., and Galley, J.E. (eds.), *Fluids in the subsurface environment: American Association of Petroleum Geologists Memoir 4*, p. 66–100.
- Gleason, J.D., Patchett, P.J., Dickinson, W.R., and Ruiz, J., 1995, Nd isotopic constraints on sediments sources of the Ouchita-Marathon fold belt: *Geological Society of America Bulletin*, v. 107, no. 10, p. 1192-1210.
- Goldhammer, R.K., Lehman, P.J., and Dunn, P.A., 1993, The origin of high-frequency platform carbonate cycles and third-order sequences (Lower Ordovician El Paso GP, West Texas): Constraints from outcrop data and stratigraphic modeling: *Journal of Sedimentary Petrology*, v. 63, no. 3, p. 318-359.
- Goldman, D., Bergström, S.M., and Mitchell, C.E., 1995, Revision of the Zone 13 graptolite biostratigraphy in the Marathon, Texas, standard succession and its bearing on Upper Ordovician biogeography: *Lethaia*, v. 28, p. 115-128.
- Hardage, B.A., Pendleton, V.M., and Asquith, G.B., 1999, 3-D Seismic Interpretation of Deep, Complex Structures in the Delaware Basin, West Texas: Bureau of Economic Geology Geologic Circular 99-1, 42 p.
- Herald, F.A., ed., 1957, Occurrence of oil and gas in West Texas: The University of Texas at Austin, Bureau of Economic Geology Publication 5716, 442 p.
- Howe, H.J., 1959, Montoya group stratigraphy (Ordovician) of Trans-Pecos Texas: *American Association of Petroleum Geologists Bulletin*, v. 43, no. 10, p. 2285-2332.
- Holland, S.M. and Patzkowsky, M. E., 1997, Distal orogenic effects on peripheral bulge sedimentation: Middle and Upper Ordovician of the Nashville Dome: *Journal of Sedimentary Research*, v. 67, no. 2, p. 250-263.
- Holmden, C., Creaser, R.A., Muehlenbachs, K., Leslie, S., and Bergstrom, S.M., 1998, Isotopic evidence for geochemical decoupling between ancient epeiric seas and bordering oceans: Implications for secular curves: *Geology*, v. 26, no. 6, p. 567-570.

- Huffman, G.G., 1959, Pre-Desmonian isopachous and paleogeographic studies in central mid-continent region: American Association of Petroleum Geologists Bulletin, v. 43, no. 11, p. 2541-2574.
- Jones, T.S., 1953, Stratigraphy of the Permian Basin of West Texas: West Texas Geological Society Publication 53-29, 63 p.
- Klein, C., 1993, Manual of Mineralogy (after James D. Dana), 21st Edition: Wiley, New York, 681 p.
- Kottlowski, F.E., 1970, Influence of the Pedernal uplift on sedimentation, *in* Basins of the Southwest, v.1, Symposium of the 10th Annual Meeting Southwest Section of American Association of Petroleum Geologists, February 7-9, 1968, Wichita Falls, Texas: West Texas Geological Society Publication 70-68, p.21-40.
- Kottlowski, F.E., Flower, R.H., Thompson, M.L., and Foster, R.W., 1956, Stratigraphic studies of the San Andres Mountains, New Mexico: New Mexico Bureau of Mines and Mineral Resources Memoir 1, p. 7-27.
- Measures, E.A., 1985, Carbonate facies of the Montoya Group – Description of a shoaling-upward ramp, Part I: West Texas Geological Society Bulletin, v. 25, no. 2, p. 4-8.
- Measures, E.A. 1985, Carbonate facies of the Montoya Group – Description of a shoaling-upward ramp, Part II: West Texas Geological Society Bulletin, v. 25, no. 3, p. 4-8.
- Measures, E.A., 1984, Petrography, depositional environments, and dolomitization of the Ordovician Montoya Group, New Mexico and Texas [Master's thesis]: Sul Ross State University, Alpine, Texas, 198 p.
- Mears, C.E. and Dufurrena, C.K., 1984, Pre-Leonardian geology of Midland Farms field area, Andrews County, Texas, Transactions Southwest Section American Association of Petroleum Geologists, 1984 Convention, Midland, Texas: West Texas Geological Society Publication 84-78, p. 111-123.

- McBride, E.F., 1970, Stratigraphy and origin of Maravillas Formation (Upper Ordovician), West Texas: American Association of Petroleum Geologists Bulletin, v. 54, no. 9, p. 1719-1745.
- Mitchell, J.S., 2003, Facies analysis and chert geochemistry of Late Ordovician cherty carbonates on the southern margin of Laurentia [M.S. thesis]: Washington State University, 71 p.
- Nielsen, A.T., 2004, Ordovician Sea level Changes: A Baltoscandian Perspective, in Webby, B.D., Paris, F., Droser, M.L., and Percival, I.G. (eds.), The Great Ordovician Biodiversification Event: Columbia University Press, p. 84-93.
- Northcutt, R.A. and Johnson, K.S., 1997, Major Simpson and Viola oil and gas reservoirs in Oklahoma, *in* Johnson, K.S. (ed.), Simpson and Viola Groups in the southern Midcontinent, 1994 Symposium: Oklahoma Geological Survey Circular 99, p. 48-57.
- Pope, M.C., 2004a, Cherty carbonate facies of the Montoya Group, southern New Mexico and western Texas and its regional correlatives: A record of Late Ordovician paleoceanography on southern Laurentia: *Palaeogeography, Palaeoclimatology, Palaeoecology* 210, p. 367– 384.
- Pope, M.C., 2004b, Upper Ordovician and Lower to Middle Silurian Miogeoclinal Rocks, *in* Mack, G.H. and Giles, K.A. (eds.), The Geology of New Mexico, A Geologic History: New Mexico Geological Society Special Publication 11, p. 45-58.
- Pope, M.C., 2004c, Upper Ordovician Montoya Group outcrops in the Cooks Range of New Mexico and Southern Franklin Mountains of Texas: Permian Basin Section-SEPM Fieldtrip to accompany 2004 Southwest Section American Association of Petroleum Geologist Annual Meeting in El Paso, Texas, 22 p.
- Pope, M.C. and Steffen, J.B., 2003, Widespread, prolonged late Middle to Late Ordovician upwelling in North America: A proxy record of glaciation?: *Geology*, v. 31; no. 1; p. 63–66.

- Pope, M.C., 2002a, Early Ordovician El Paso Formation and Late Ordovician Montoya Formation, Rhodes Canyon, *in* Lueth, V.; Giles, K.A.; Lucas, S.G.; Kues, B.S.; Myers, R.G.; Ulmer-Scholle, D. (eds.), *Geology of White Sands: New Mexico Geological Society Guidebook 53*, p. 35-39.
- Pope, M.C., 2002b, Cherty facies of the Late Ordovician Montoya Group, southern New Mexico and western Texas: Implication of Laurentia oceanography and duration of Gondwana glaciation, *in* Lueth, V.; Giles, K.A.; Lucas, S.G.; Kues, B.S.; Myers, R.G.; Ulmer-Scholle, D. (eds.), *Geology of White Sands: New Mexico Geological Society Guidebook 53*, p. 159-165.
- Pray, L.C., 1958, Stratigraphic section, Montoya Group and Fusselman Formation, Franklin Mountains, Texas: *West Texas Geological Society Guidebook*, p. 30-42.
- Pratt, W.P. and Jones, W.R., 1961, Montoya dolomite and Fusselman dolomite in Silver City region, New Mexico: *American Association of Petroleum Geologists Bulletin*, v. 45, no. 4, p. 484-500.
- Read, J.F., 1995, Part 1. Overview of carbonate platform sequences, cycle stratigraphy and reservoirs in greenhouse and ice-house worlds, *in* Read, J.F., Kerans, C., and Weber, L.J. (eds.), *Milankovitch sea level changes, cycles and reservoirs on carbonate platforms in greenhouse and ice-house worlds: SEPM Short Course Notes 35*, p. 1-102.
- Ross, R.J. and Ross, C.A., 1992, Ordovician sea-level fluctuations, *in* Webby, B.D. and Laurie, J.R. (eds.), *Global Perspectives on Ordovician Geology, Proceedings of the Sixth Annual International Symposium on the Ordovician*, University of Sydney, Australia, July 15-19, 1991, p. 327-335.
- Ross, R.J., 1976, Ordovician sedimentation in the western United States, *in* Bassett, M.G. (ed.), *The Ordovician System: Proceedings of a Palaeontological Association Symposium*, University of Wales Press and National Museum of Wales, p. 73-105.

- Saltzman, M.R. and Young, S.A., 2005, Long-lived glaciation in the Late Ordovician? Isotopic and sequence-stratigraphic evidence from western Laurentia: *Geology*, v. 33, no. 2, p. 109-112.
- Sloss, L.L., 1988, Tectonic evolution of the craton in Phanerozoic time, *in* Sloss, L. L. (ed.), *Sedimentary cover—North American Craton: The Geology of North America*, Geological Society of America, Boulder, Colorado, v. D-2, p. 25–51.
- Sloss, L.L., 1963, Sequences in the cratonic interior of North America: *Geological Society of America Bulletin*, v.74, no. 2, p. 93-113.
- Sternbach, C.A., 1984, Deep-burial diagenesis and Dolomitization in the Hunton Group carbonate rocks (Upper Ordovician to Lower Devonian) in the Anadarko Basin of Oklahoma and Texas [Ph.D. dissertation]: Rensselaer Polytechnic Institute, 144 p.
- Sweet, W.C., 1979, Late Ordovician conodonts and biostratigraphy of the western mid-continent province: *Geology Studies*, v. 26, Brigham Young University, p. 45-85.
- Swift, D.B., Reeves, J.J., Erdlac, R.J., Jr., Barrow, K.T., and Schoellhopf, A.P., 1994, Exploration potential of the Diablo Platform-Delaware Basin margin, Trans-Pecos Texas, *in* Ahlen, J., Peterson, J., and Bowsher, A.L. (eds.), *Geologic activities in the 90s*, Southwest Section of AAPG 1994, Ruidoso, New Mexico: New Mexico Bureau of Mines and Mineral Resources Bulletin, no. 150, p. 53-69.
- Texas Railroad Commission, 2008, Field production data accessed from online database at <http://webapps.rrc.state.tx.us/PDQ/home.do> on February 26, 2008.
- Texas Water Development Board, 1972, A survey of the subsurface saline water of Texas, v. 1, 113 p.
- Thomas, D.M. and Liu, H., 2003, Upper Ordovician Montoya sequence stratigraphy and chert porosity in southeastern Delaware basin, *in* Hunt, T. J., and Lufholm, P. H. (eds.), *The Permian Basin: Back to Basics*: West Texas Geological Society Publication 03-112, p. 37–43.
- Webby, B.D., Cooper, R.A., Bergstrom, S.M., and Paris, F. 2004, Stratigraphic framework and time slices, *in* Webby, B.D., Paris, F., Droser, M.L., and Percival,

- I.G. (eds.), The Great Ordovician Biodiversification Event, Columbia University Press, p. 41-47.
- Williams, J.A., 1977, Characterization of oil types in the Permian Basin: text of talk presented to Southwest Section, American Association of Petroleum Geologists, Abilene, Texas, March 7, 1977.
- Wright, W.F., 1979, Petroleum geology of the Permian Basin: West Texas Geological Society Publication 79-71, 98 p.
- Young, S.A., Saltzman, M.R., and Bergström, S.M., 2005, Upper Ordovician (Mohawkian) carbon isotope ($\delta^{13}\text{C}$) stratigraphy in eastern and central North America: Regional expression of a perturbation of the global carbon cycle: *Palaeogeography, Palaeoclimatology, Palaeoecology*, v. 222, p. 53-76.

FIGURES

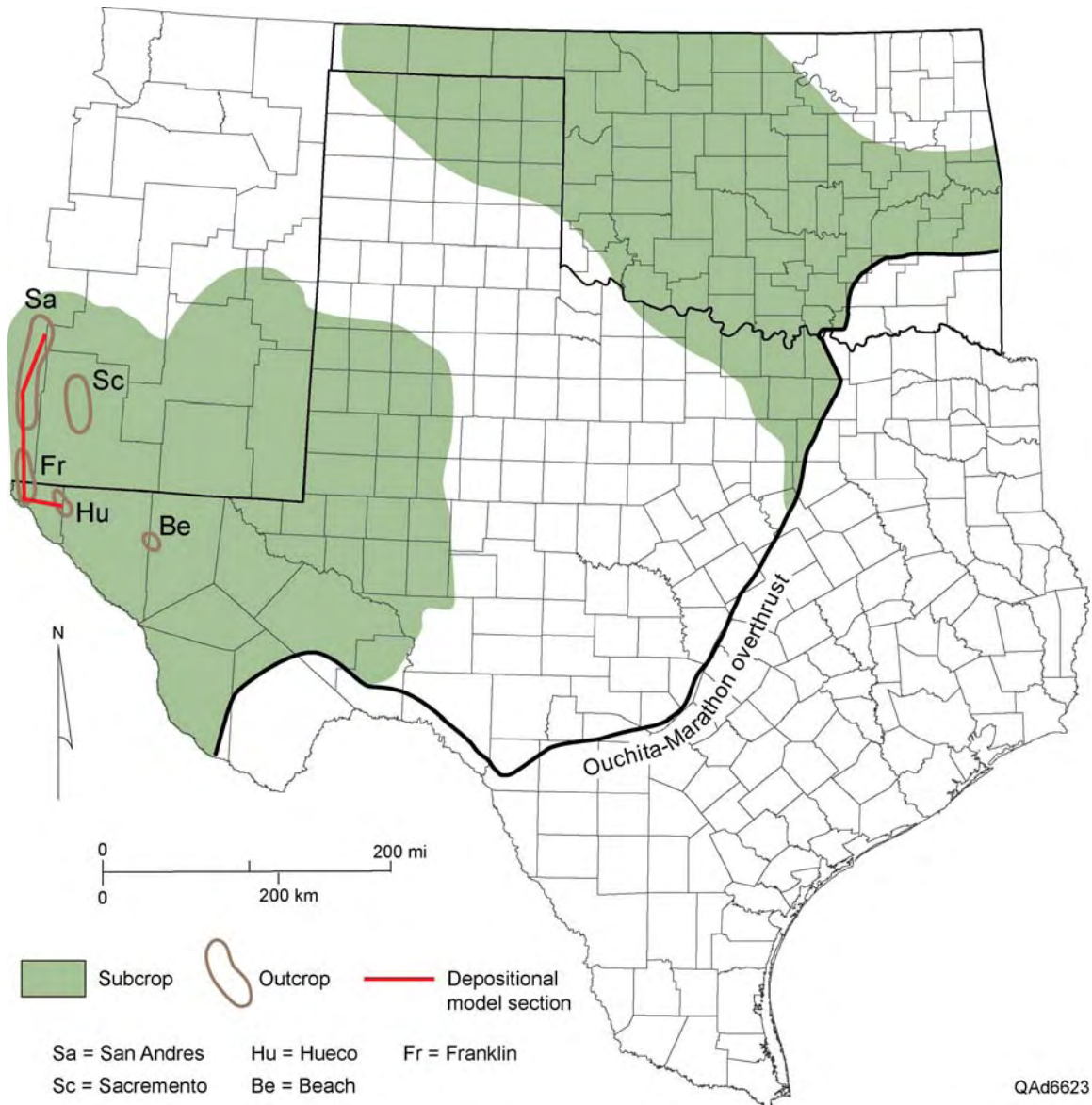
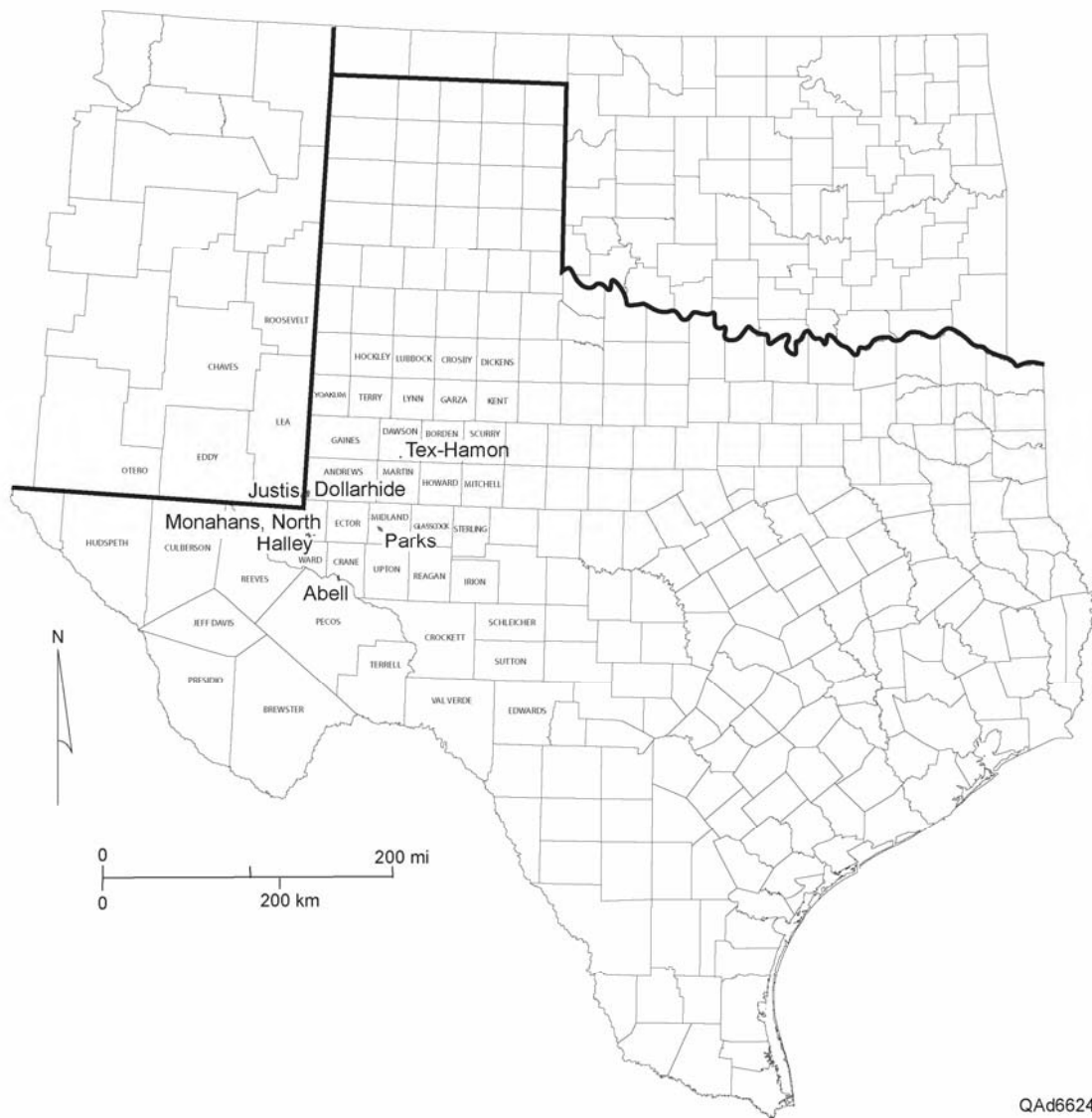


Figure 1. Montoya Group outcrop/subcrop map Outcrop locations after Pope, 2004; subcrop data from published maps in the following regions: Marathon area (Texas Water Development Board, 1972); New Mexico (Frenzel and others, 1988); and Oklahoma (Huffman, 1959, Chenoweth, 1966, and Adler and others, 1971). Line of section shows outcrop transect used to develop the model in Figure 5.



QAd6624

Figure 2. Map showing Montoya fields with production greater than 1 MMbbl.

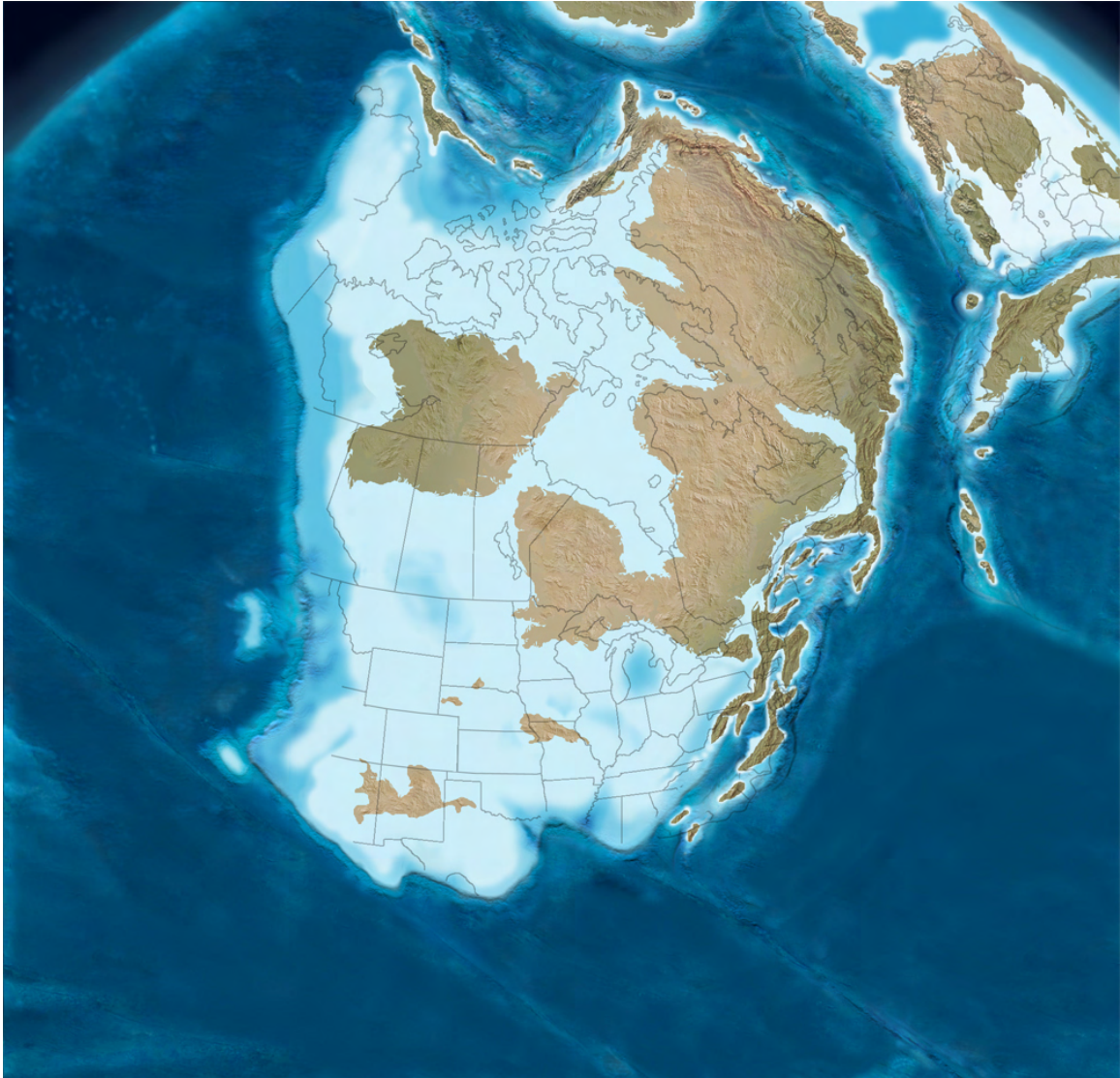
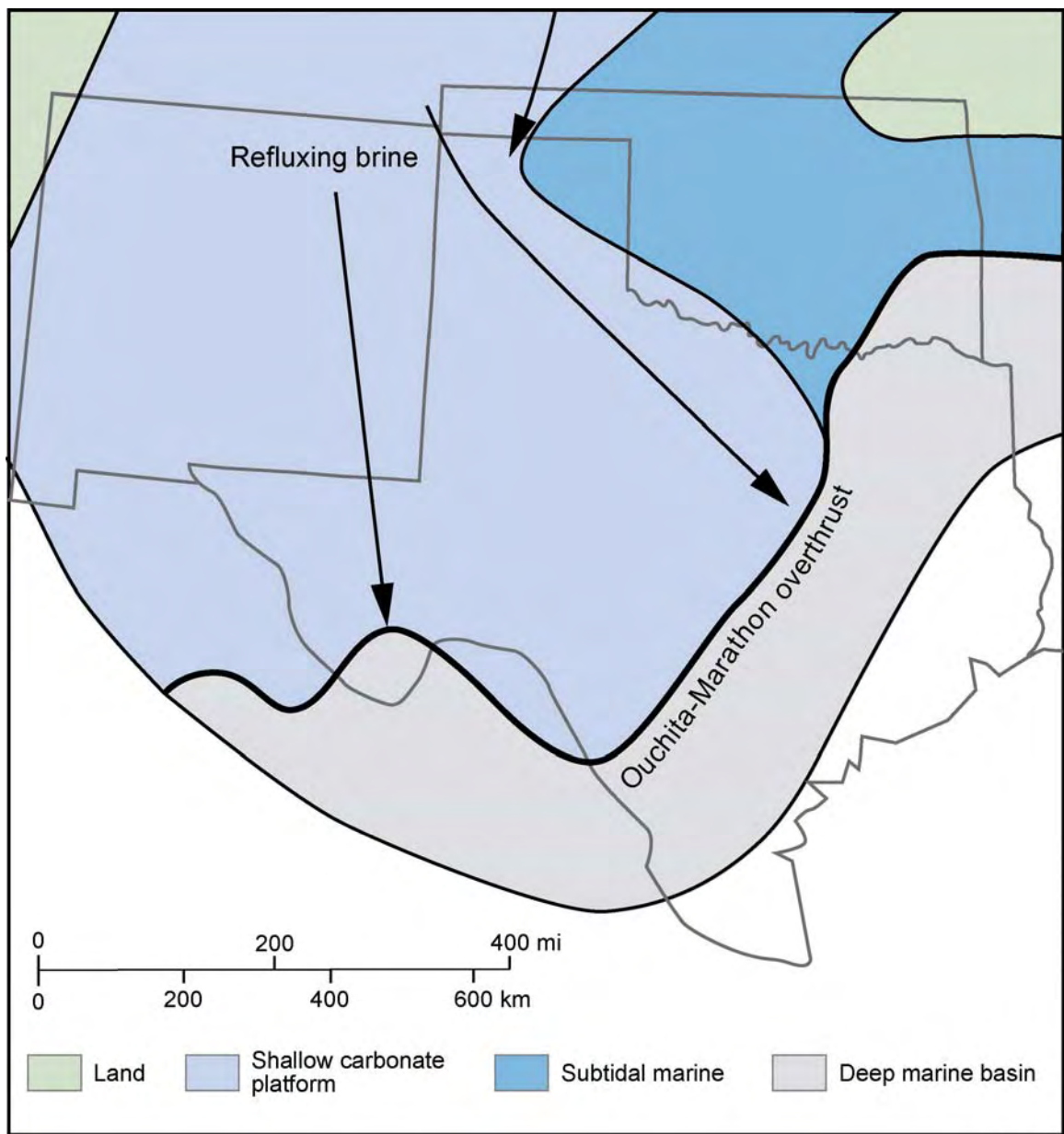
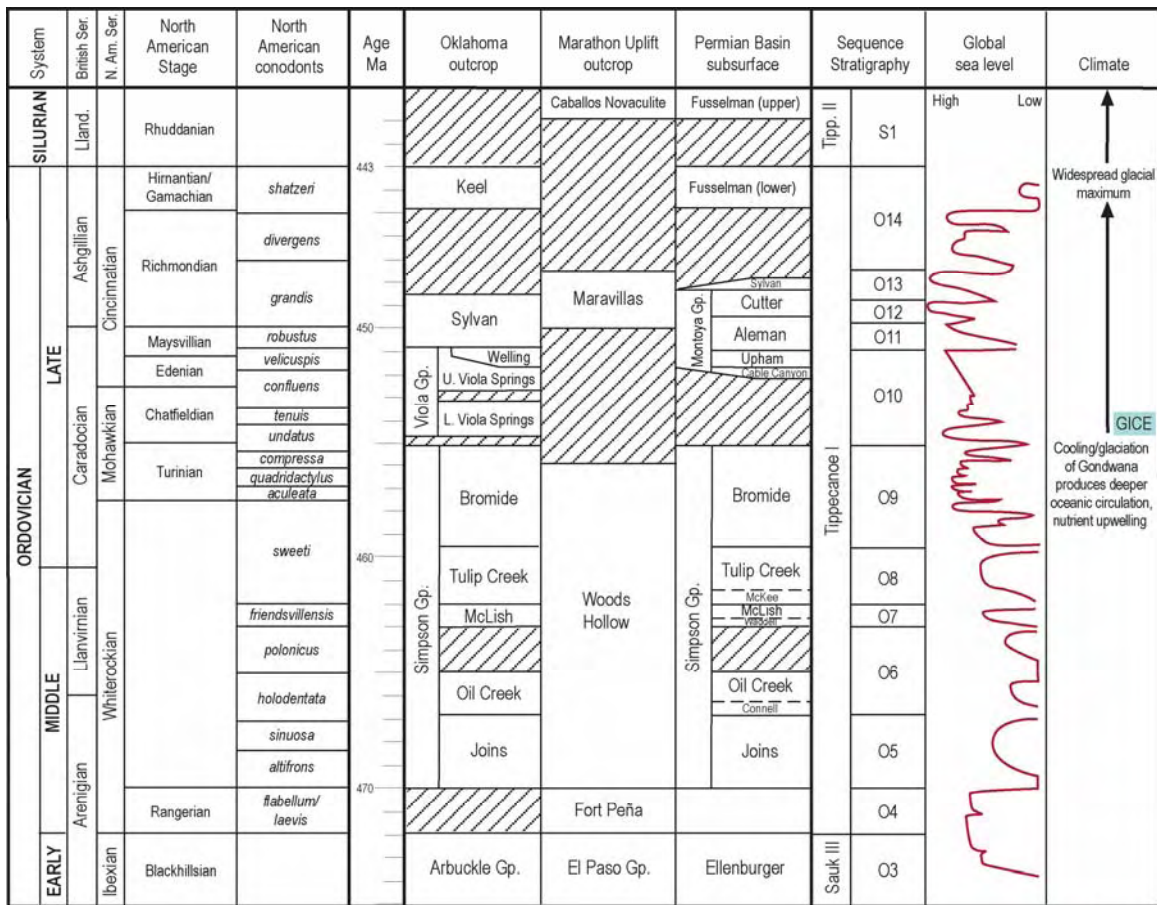


Figure 3. Global plate reconstruction/paleogeography for the Late Ordovician (Blakey, 2004).



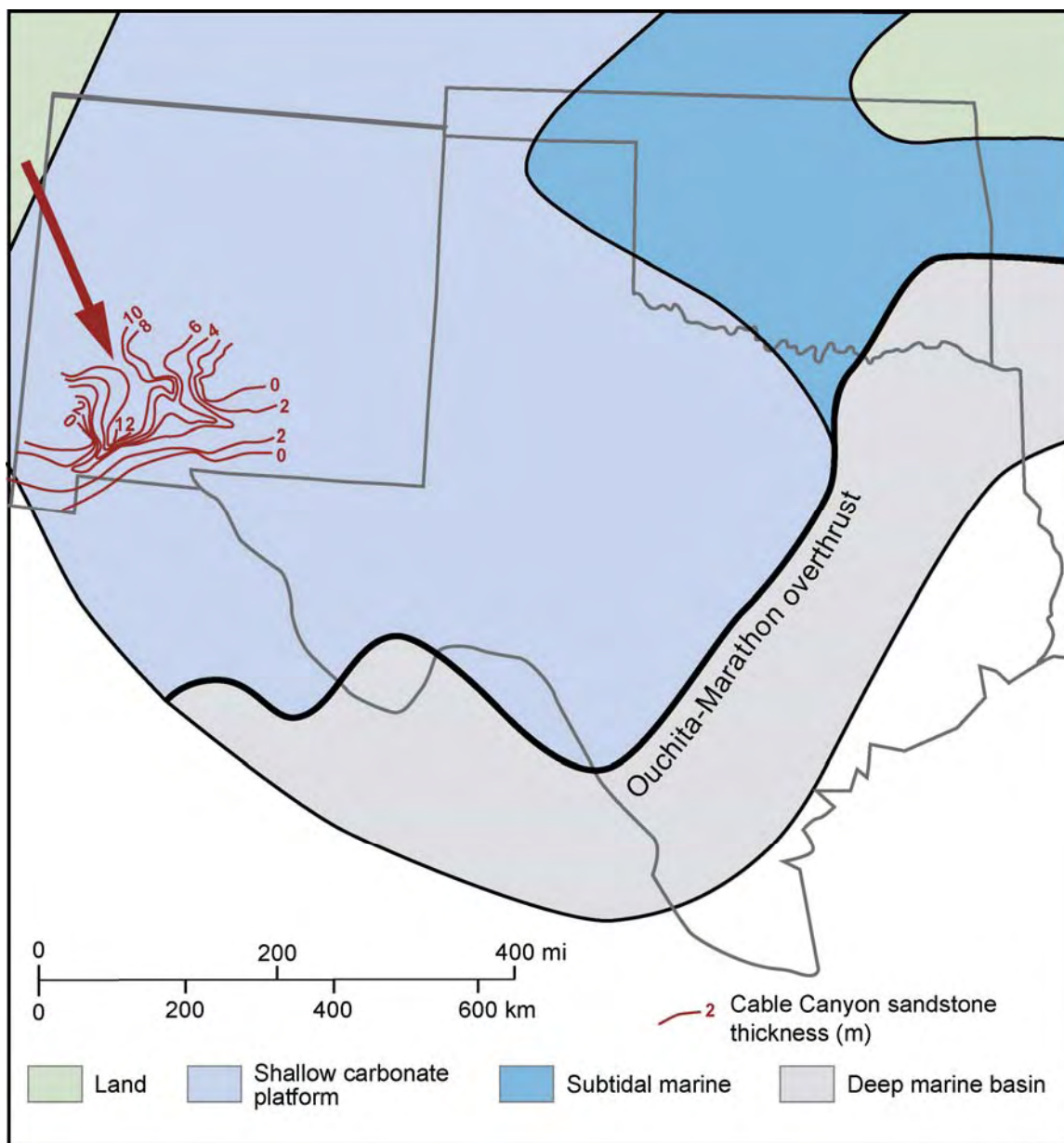
QAd6626

Figure 4. Paleogeography of Texas, New Mexico, and Oklahoma during the Middle to Late Ordovician. After Ross, 1976.



QAd6627

Figure 5. Stratigraphic column. In addition to our own interpretations, sources of information include: Webby and others, 2004 (North American stages, conodonts and time scale); Young and others, 2005 and Derby and others, 1991 (Oklahoma outcrop); Goldman and others, 1995; Bergstrom and others, 1986 (Marathon Uplift outcrop); Pope, 2004 and Sweet, 1979 (Permian Basin subsurface); Sloss, 1988 and 1963 (sequence stratigraphic megasequences); and Ross and Ross, 1992 (global sea level change, note time rescaled to fit biostratigraphy).



QAd6628

Figure 6. Thickness contours of the Cable Canyon Member in southern New Mexico (after Bruno and Chafetz, 1988) superimposed on paleogeography of the Late Ordovician (after Ross, 1976). Arrows denote interpreted transport direction of sediment eroding from Precambrian basement exposed in the NW to deposition in the SE.

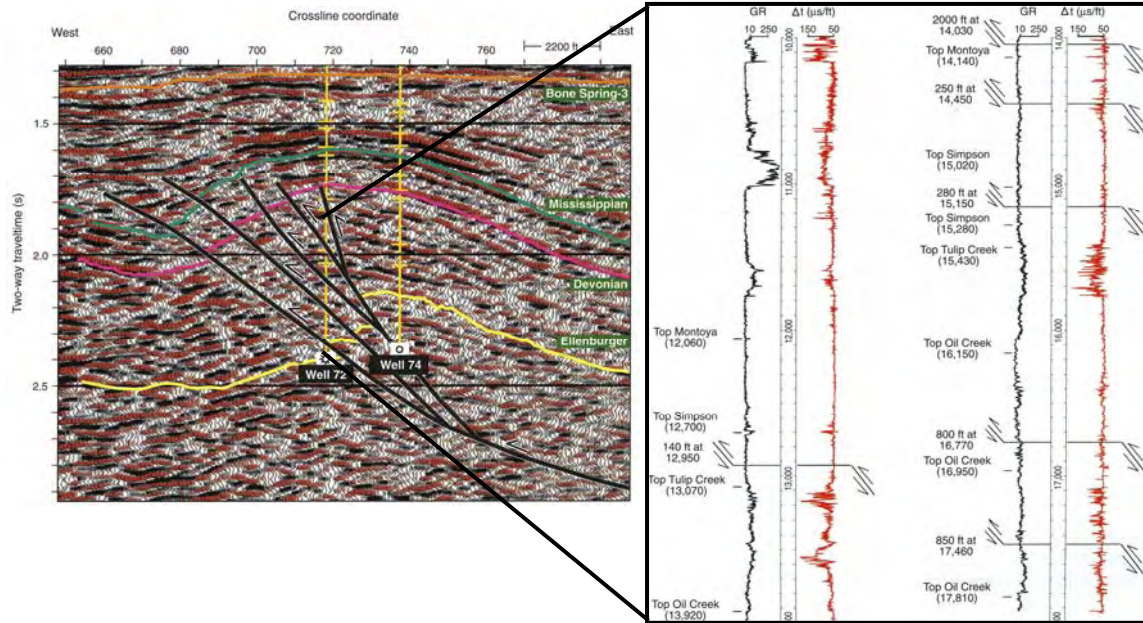


Figure 7. Example of repeated section created through high-angle reverse faulting at Waha Field, Pecos County, Texas (Hardage and others, 1999).

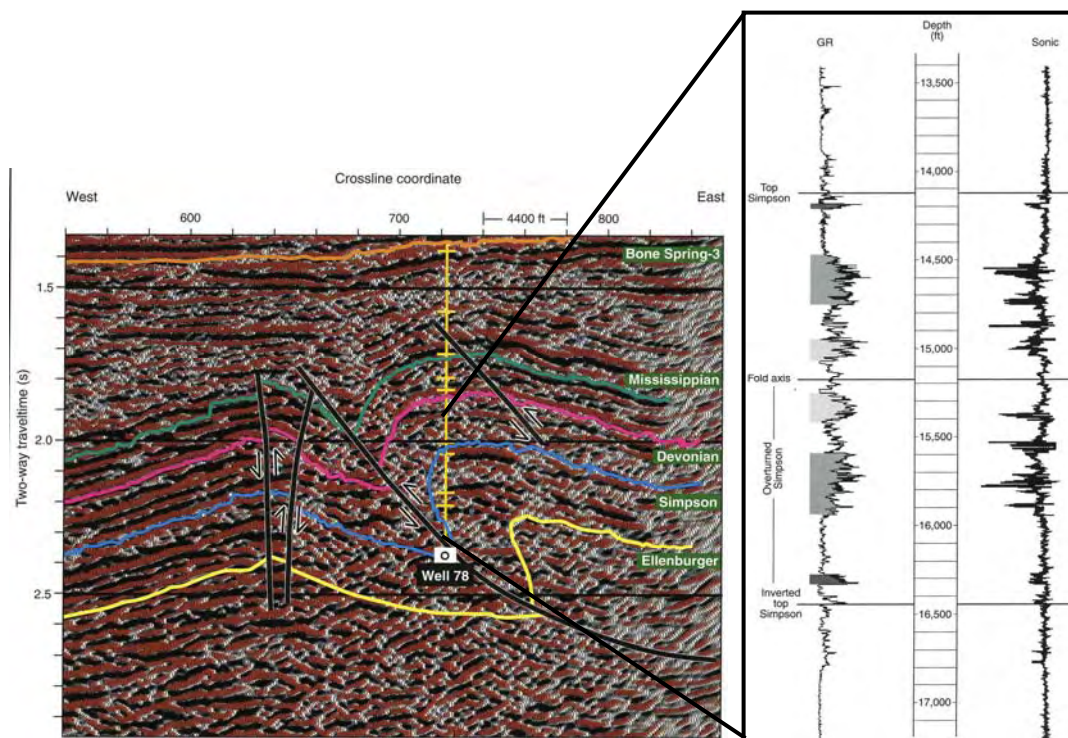


Figure 8. Example of repeated section created through overturned structure at Waha Field, Pecos County, Texas (Hardage and others, 1999).

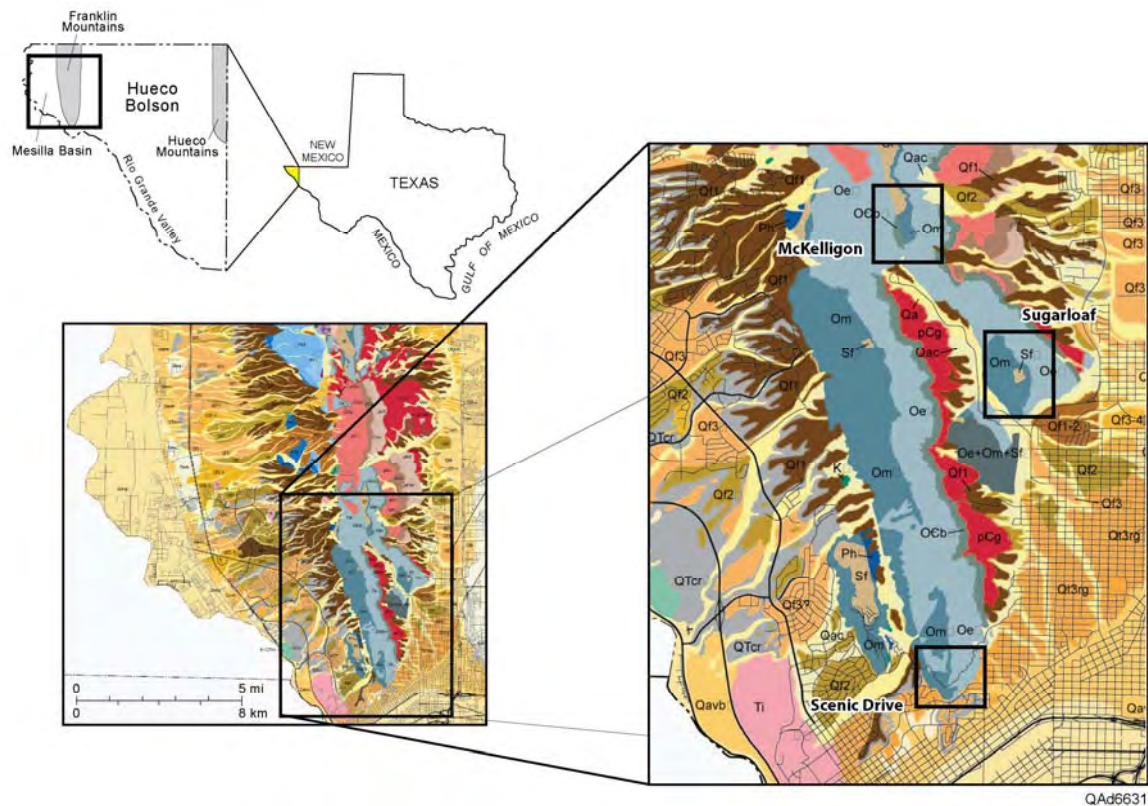


Figure 9. Geologic map of the Franklin Mountains showing Montoya distribution (Om) and field locations (geology from Collins and Raney, 2000).

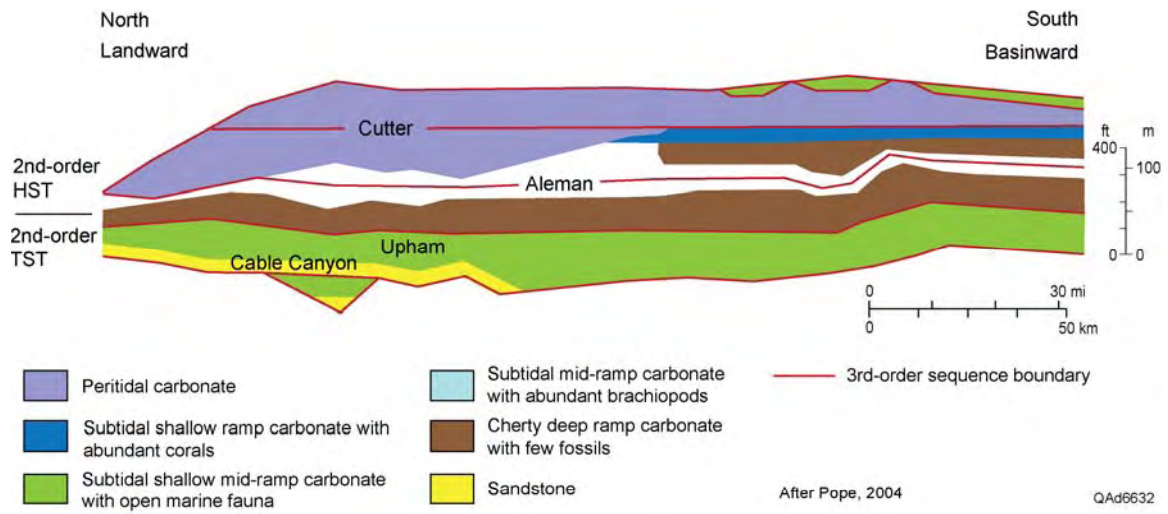


Figure 10. Third-order sequence stratigraphic model based on Montoya Group outcrops (after Pope, 2004a). Outcrop line of section shown in Figure 1.



Figure 11. Outcrop photo of contact between the more resistant Upham Formation of the Montoya Group overlies the more recessive sandstones of the thin Cable Canyon Member, Franklin Mountains, McKelligon Canyon, El Paso, Texas.



QAd6634

Figure 12. Outcrop photos of large coral in the Upham Formation, Murchison Park stop along Scenic Drive, Franklin Mountains, El Paso, Texas.

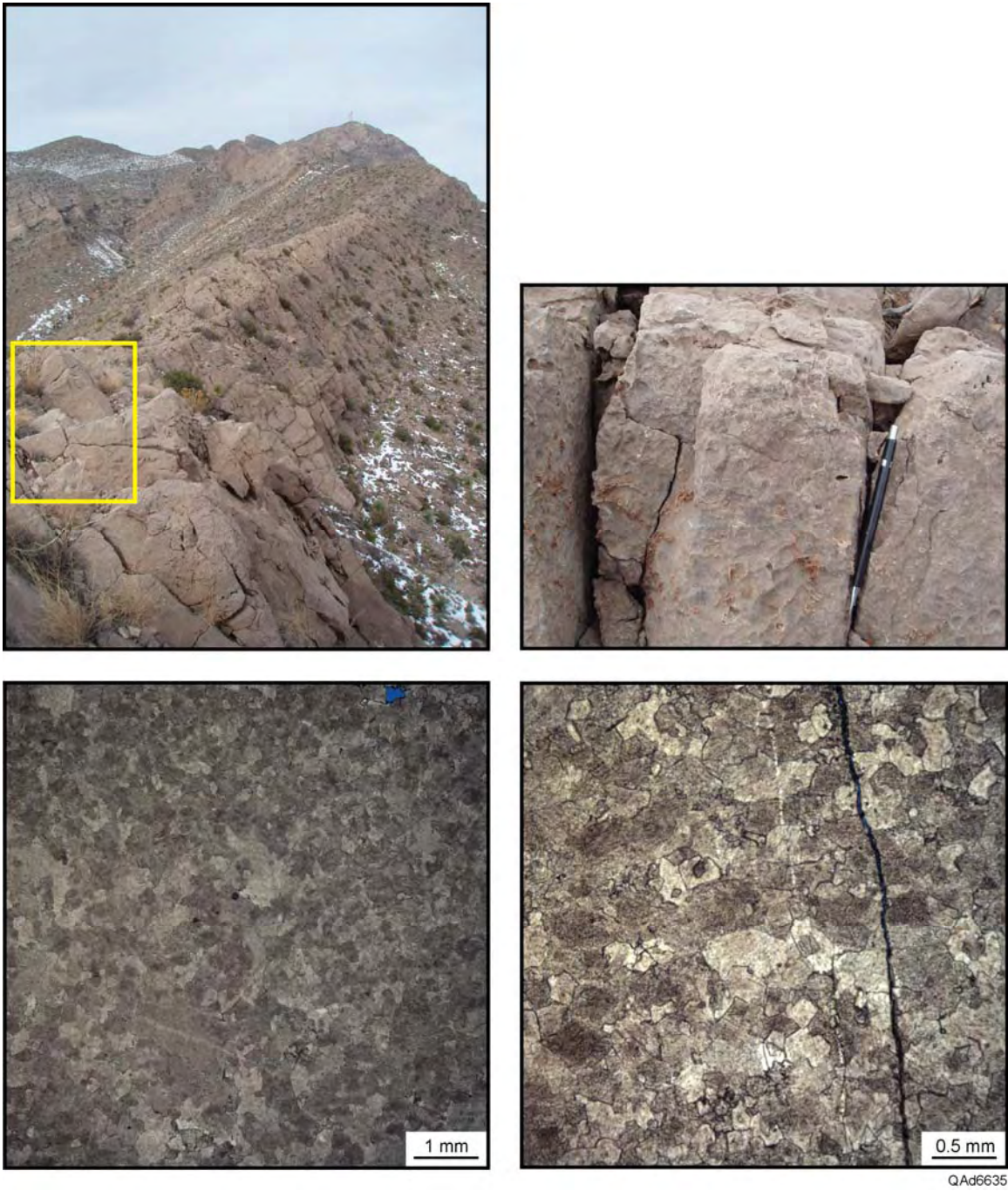


Figure 13. Outcrop photos and corresponding photomicrographs of thin sections in the lower Upham Formation, McKelligon Canyon, Franklin Mountains, El Paso, Texas. Black box in ridge pan denotes area of close-up and thin sections.

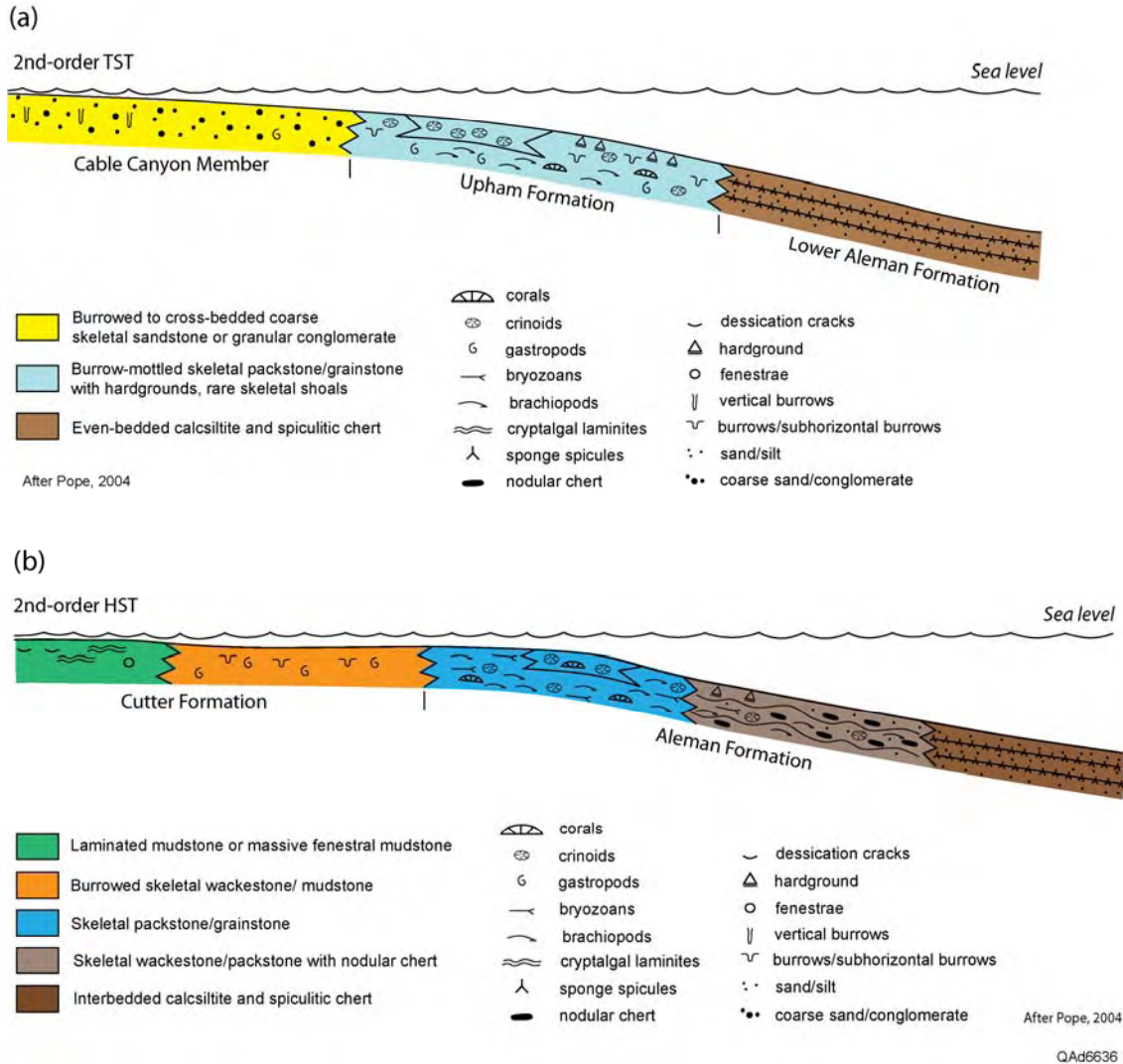


Figure 14. (a) Second-order transgressive systems tract facies related to Montoya Group Formations (after Pope, 2004a). (b) Second-order highstand systems tract facies related to Montoya Group Formations (after Pope, 2004a).

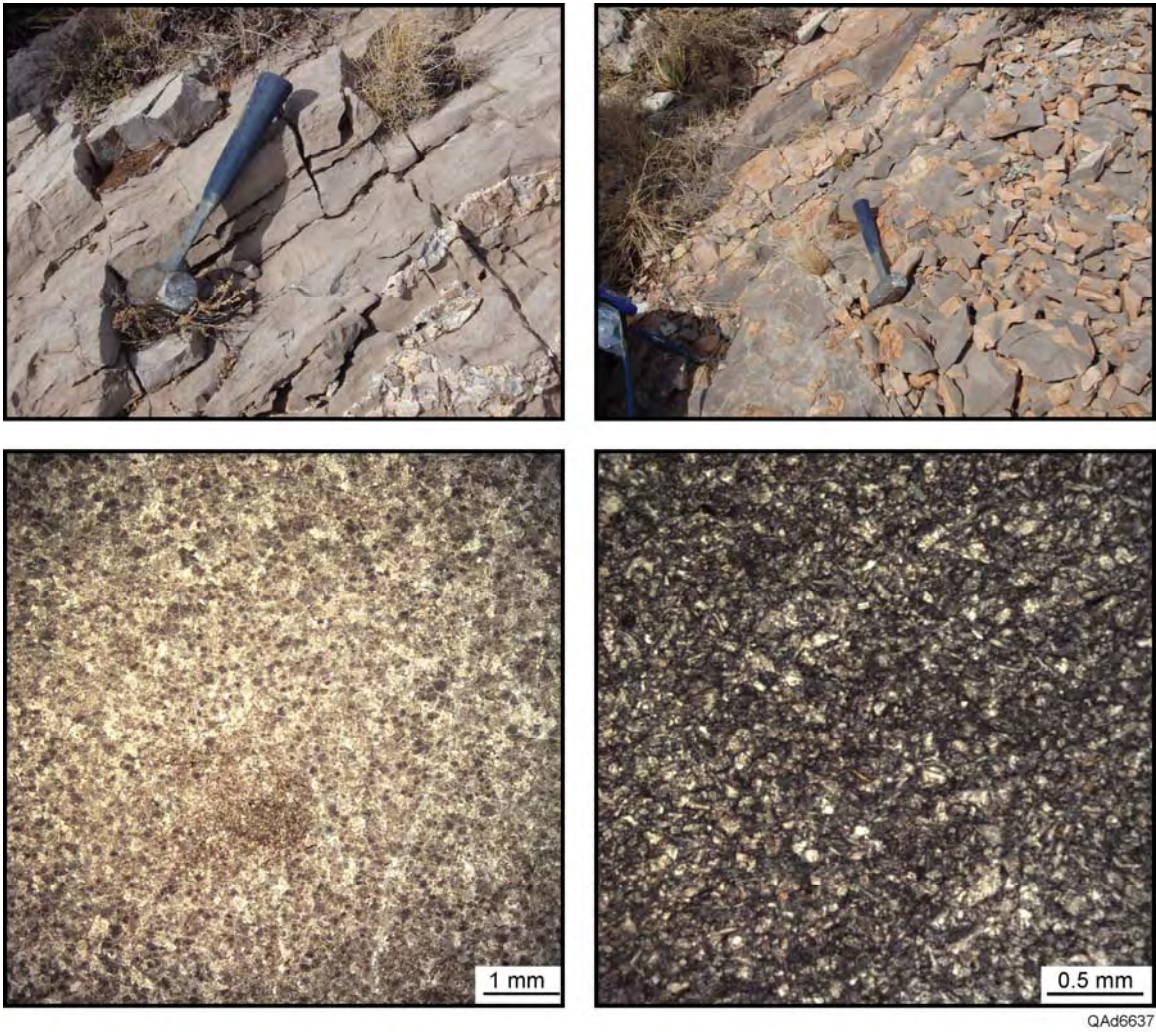
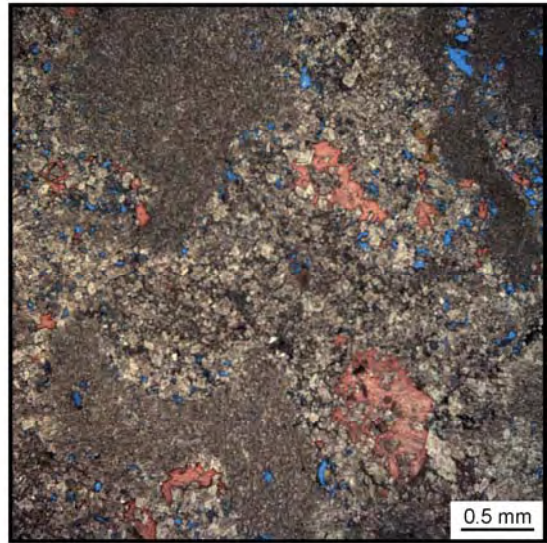
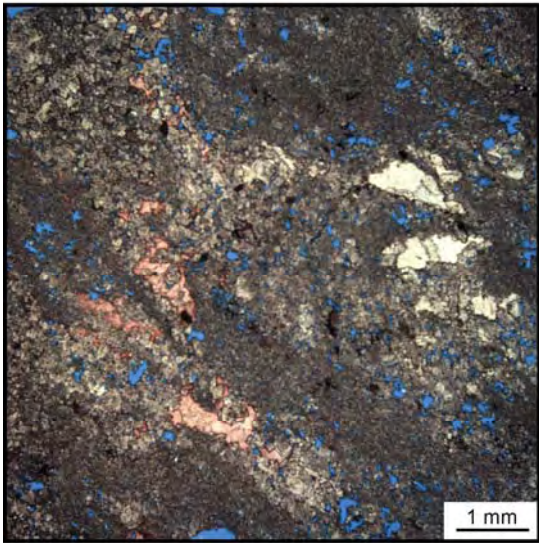
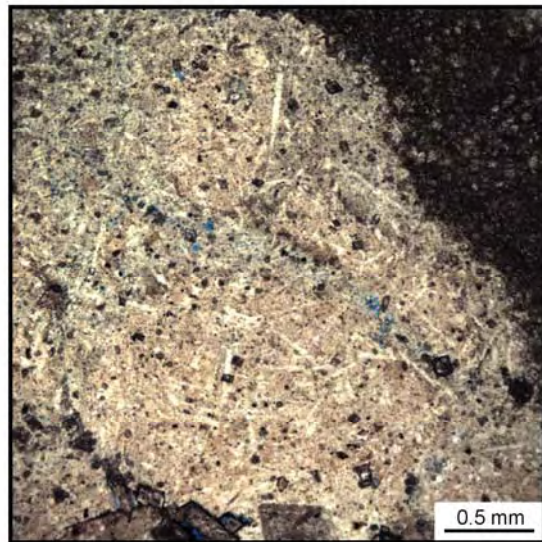
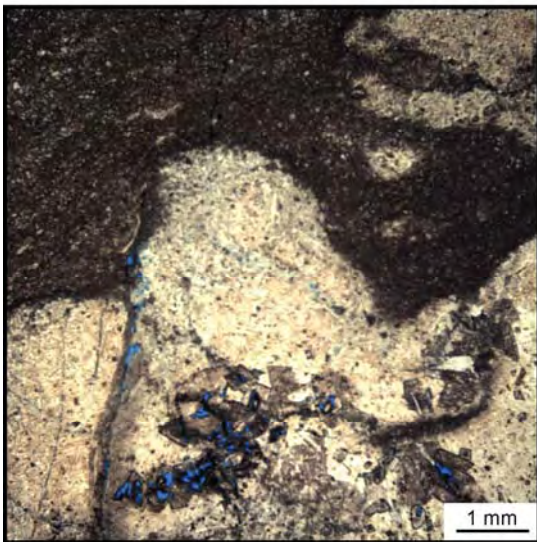


Figure 15. Outcrop photos and corresponding photomicrographs of thin sections of the lower Aleman Formation thin-bedded chert, McKelligon Canyon, Franklin Mountains, El Paso, Texas. Thin section photomicrographs show complete dolomitization with no preservation of porosity.



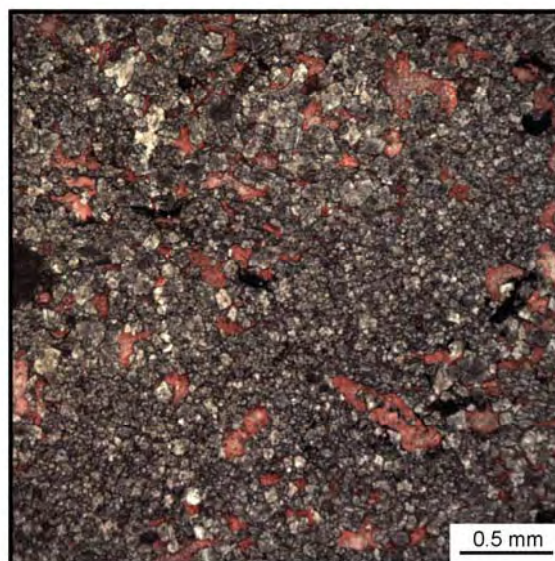
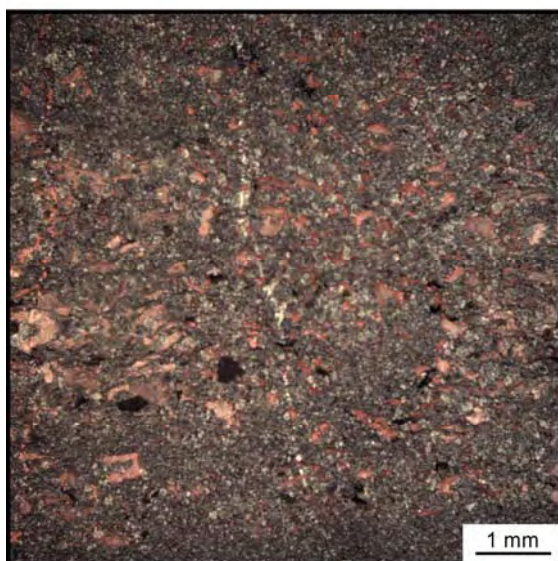
QAd6638

Figure 16. Outcrop photo and corresponding thin section photomicrographs of the Aleman Formation medial bryozoan-rich skeletal packstone, McKelligon Canyon, Franklin Mountains, El Paso, Texas. Note presence of bryozoans both on surface of outcrop and in thin section. Late calcite (stained pink with Alizarin red) partially fills bryozoan molds, but some porosity has been preserved.



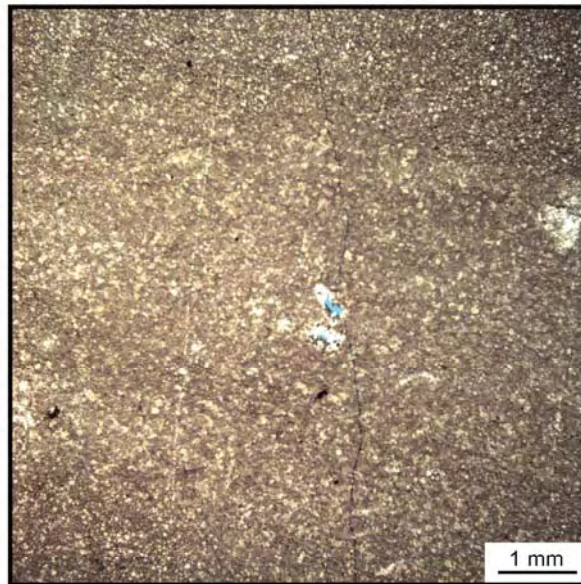
QAd6639

Figure 17. Outcrop photo and corresponding thin section photomicrographs of the upper Aleman Formation chert (chaotic, nodular), McKelligon Canyon, Franklin Mountains, El Paso, Texas. Note sponge spicules, minor microporosity, and dolomite rhombs within chert nodules in photomicrographs.



QAd6640

Figure 18. Outcrop photo and corresponding thin section photomicrographs of the lower Cutter Formation, McKelligon Canyon, Franklin Mountains, El Paso, Texas. Photomicrographs show calcite (pink, stained with Alizarin red) filling molds and a fracture.



QAd6641

Figure 19. Outcrop photo and corresponding thin section photomicrograph of the lower Cutter Formation, McKelligon Canyon, Franklin Mountains, El Paso, Texas. This location is above Figure 26, but still in the lower Cutter Formation. The outcrop consists of finely laminated mudstone, with laminae more resistant to weathering. The thin section photomicrograph shows laminated fine crystalline dolomite with rare molds.

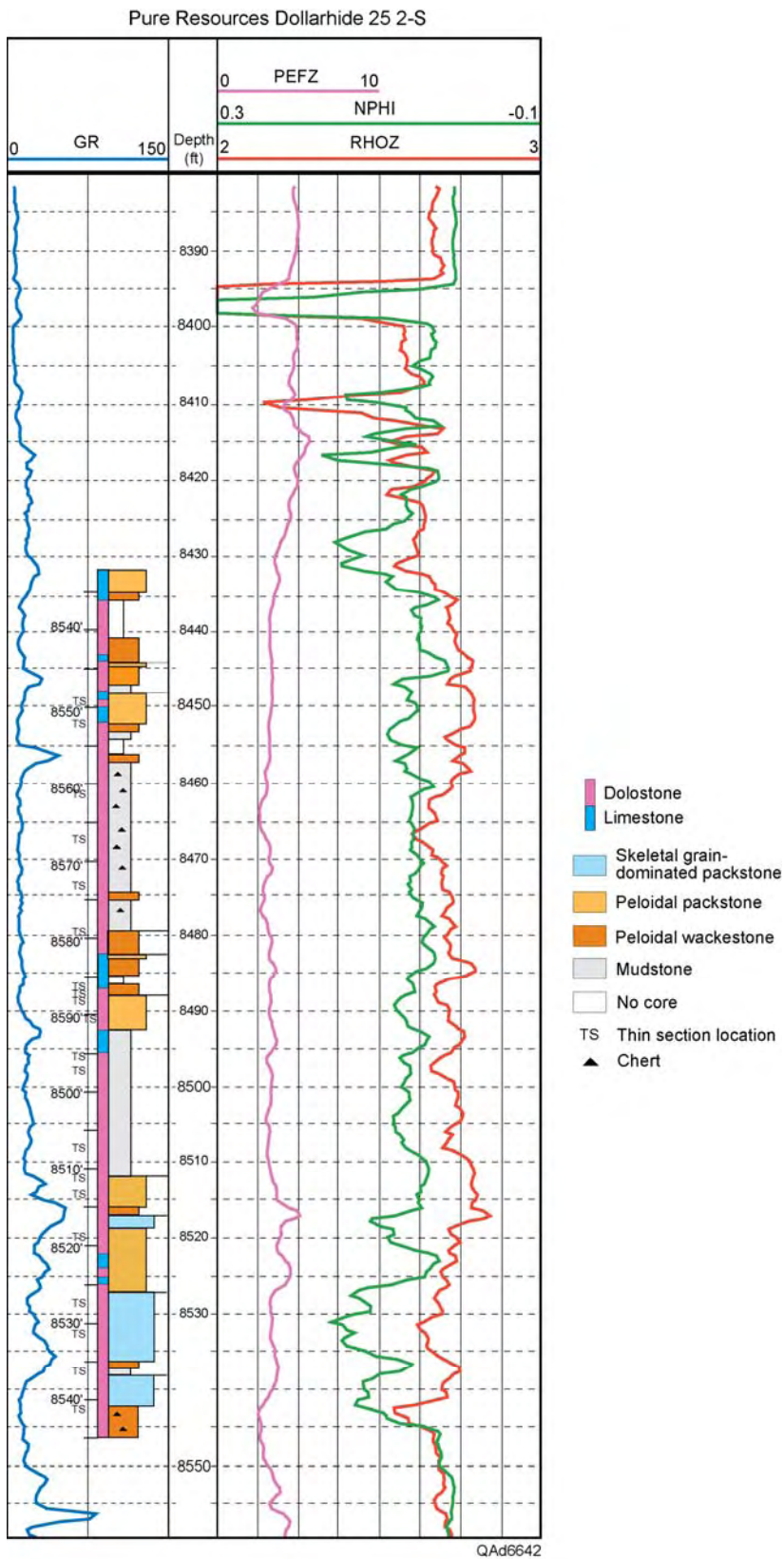


Figure 20. Description of the Montoya cored section in the Dollarhide 25-2-S well.

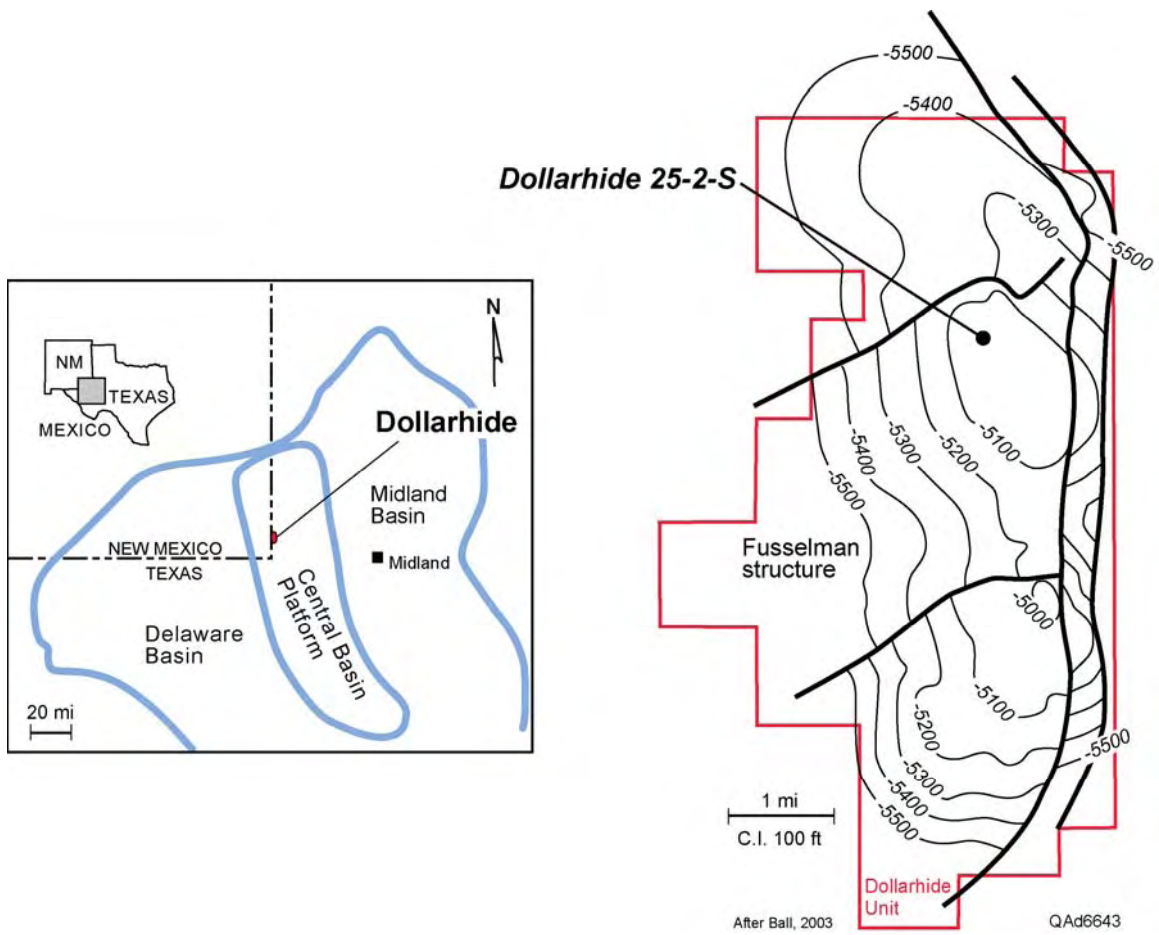
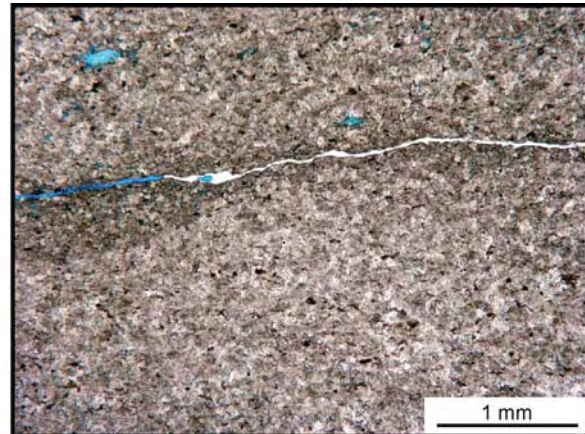
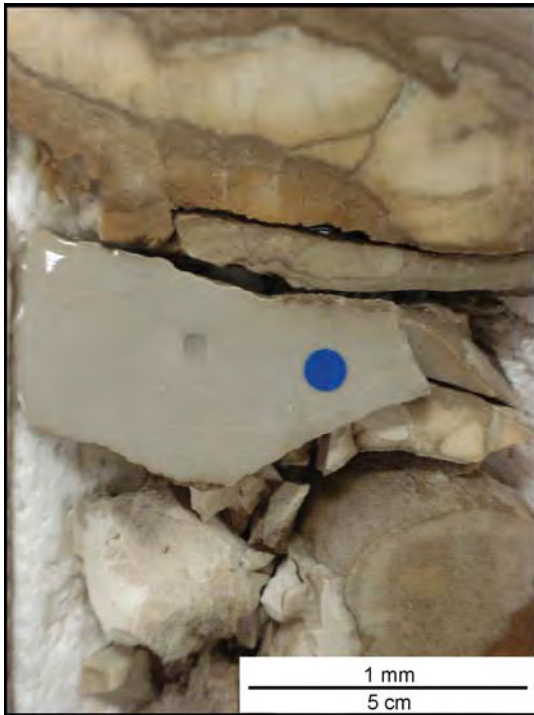


Figure 21. Map of Dollarhide field showing field location, structure (top Fusselman), and core location.



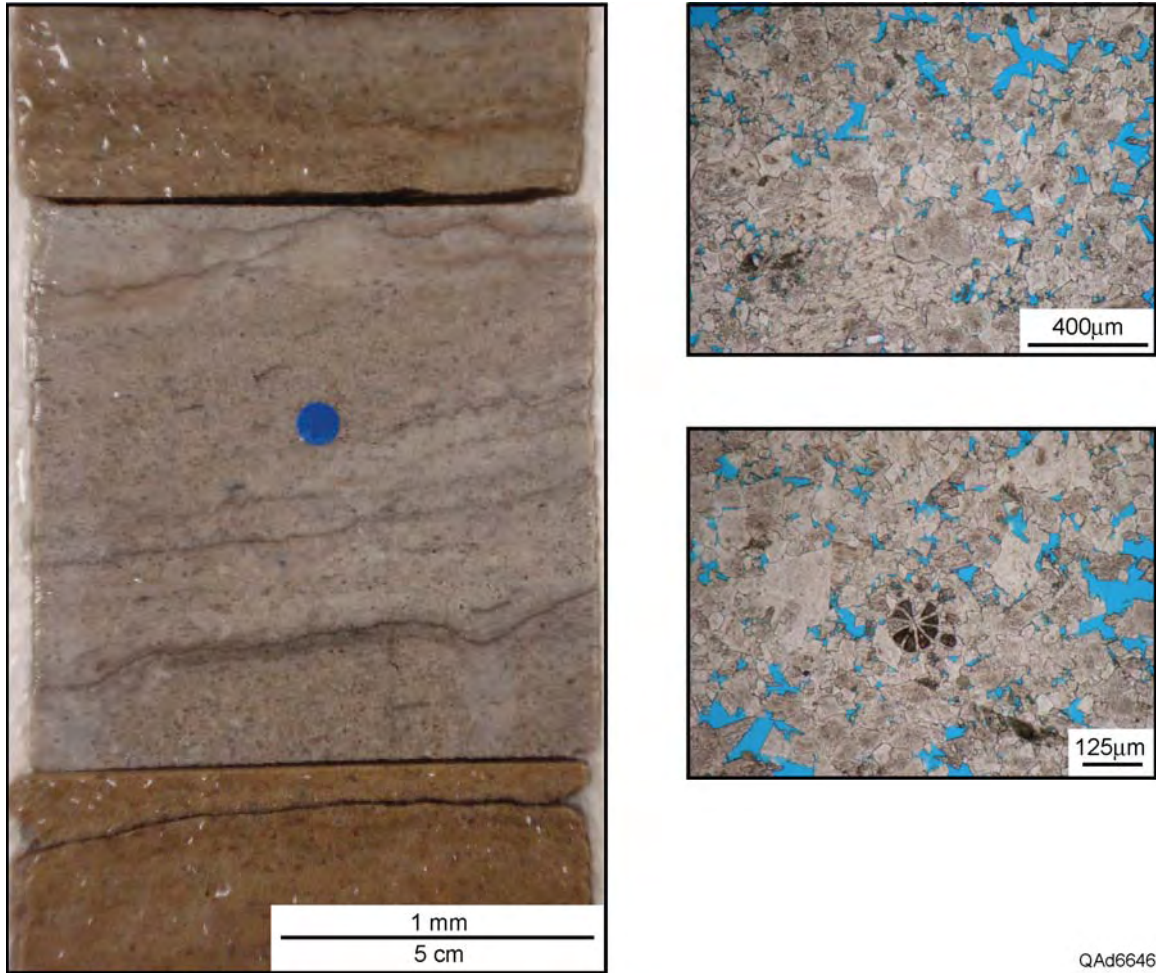
QAd6644

Figure 22. Core photo and thin section photomicrograph of cherty mudstone/chert, Dollarhide field 25-2-S, 8541 ft. Photomicrograph shows fine dolomite and fracture partially filled with chert.



QAd6645

Figure 23. Core photo and thin section photomicrograph of crinoid wackestone, Dollarhide field 25-2-S, 8452 ft. Note crinoid fragment (pleochroic in polarized light) and a lack of porosity.



QAd6646

Figure 24. Core photo and thin section photomicrographs of dolopackstone, Dollarhide field 25-2-S, 8487 ft. Coarse dolomite obscures most grains, but peloidal shapes and grain-supported structure are visible. Both photomicrographs show abundant intercrystalline porosity. Whole core porosity = 8.1%, permeability = 40.9 md.

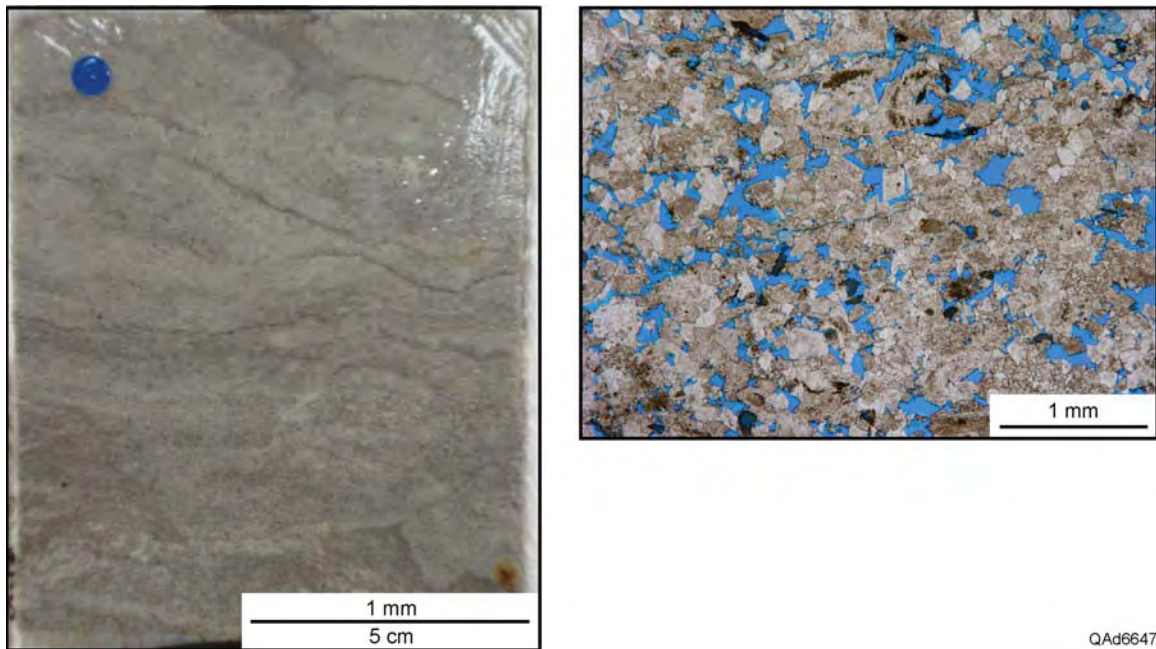


Figure 25. Core photo and thin section photomicrograph of grain-dominant dolopackstone, Dollarhide field 25-2 S, 8527 ft. Grain ghosts are apparent despite coarse crystalline dolomite and abundant intercrystalline porosity. Whole core porosity = 8.4%, permeability = 6.33 md.

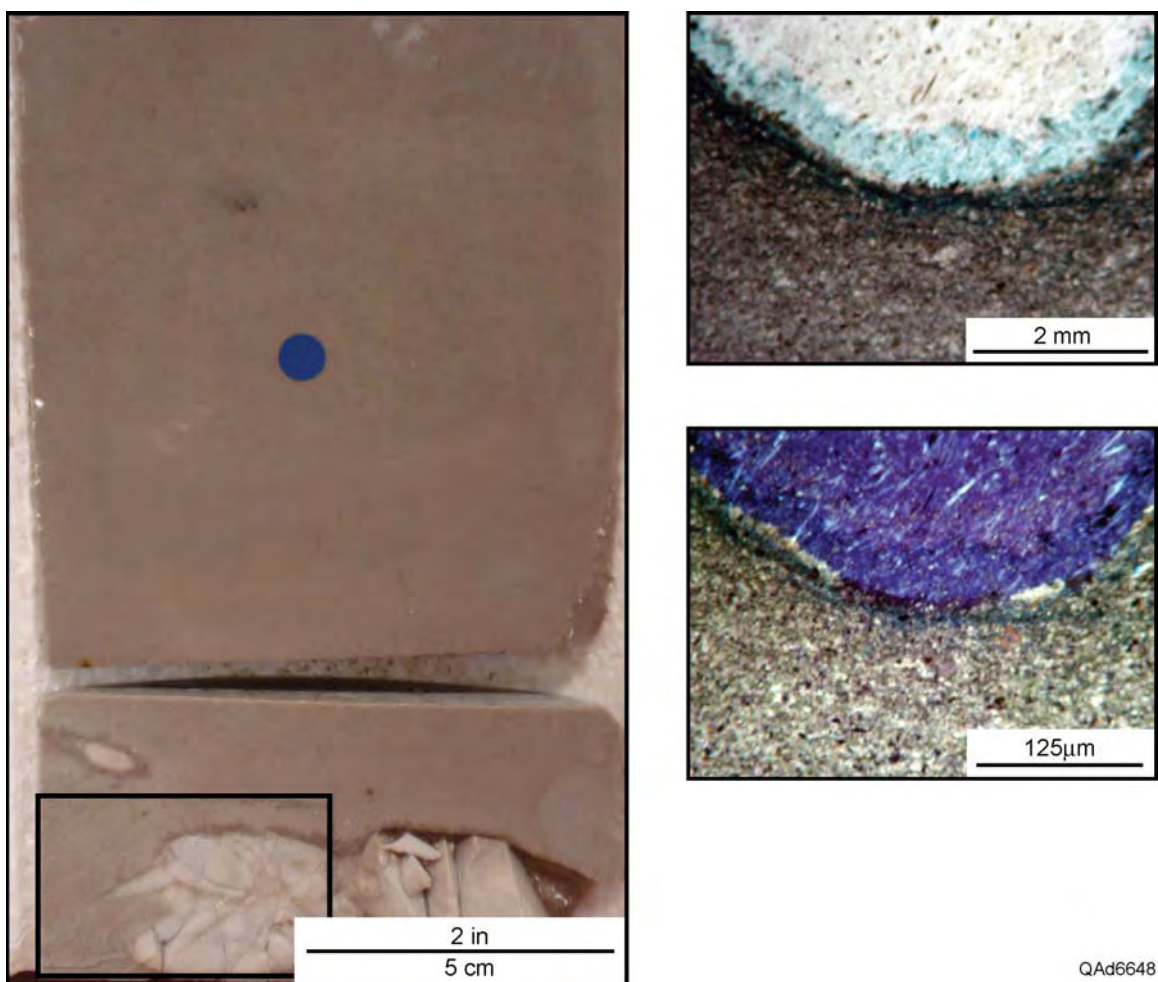


Figure 26. Core photo and thin section photomicrographs of chert mudstone, Dollarhide field 25-2, 8467 ft. Thin section was taken to image chert nodule rim (black box denotes location of section). Top photomicrograph is in plane light and shows microporosity (light blue) along the lower rim of the chert nodule and hints of sponge spicules within the chert nodule. Sponge spicules are more obvious in polarized light (bottom photomicrograph).

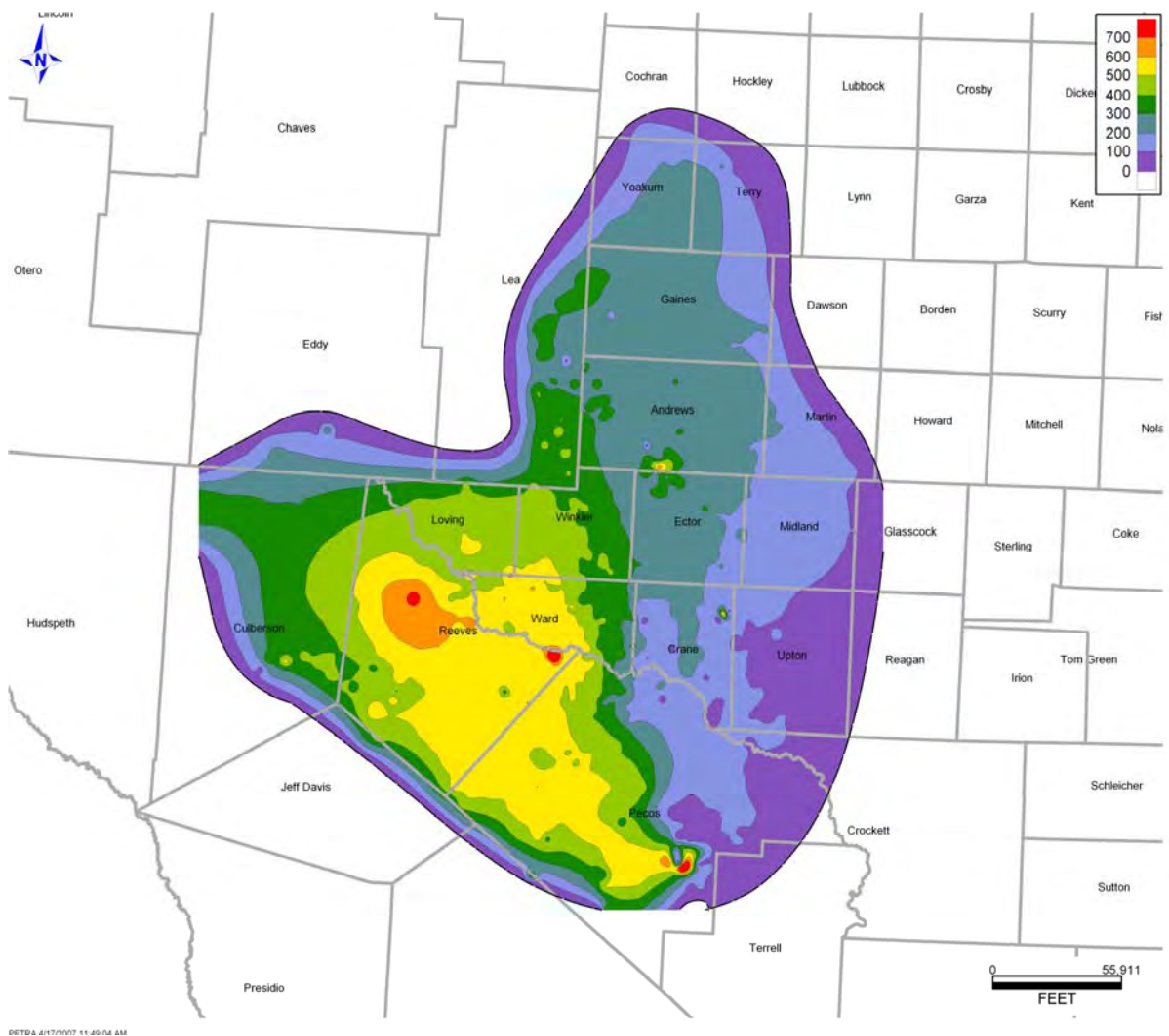


Figure 27. Regional thickness map of Montoya. Data based in part on tops provided by Geological Data Services, Inc.

THE FUSSELMAN OF THE PERMIAN BASIN: PATTERNS IN DEPOSITIONAL AND
DIAGENETIC FACIES DEVELOPMENT ON A STABLE PLATFORM DURING THE LATE
ORDOVICIAN—EARLY SILURIAN ICEHOUSE

Stephen C. Ruppel

Bureau of Economic Geology
Jackson School of Geosciences
The University of Texas at Austin
Austin, Texas

ABSTRACT

The Fusselman Formation of the Permian Basin consists of shallow-water carbonate sediments that were deposited on a regionally extensive, relatively stable platform along the southern margin of the Laurentian paleocontinent during the Late Ordovician to Early Silurian. Core studies show that the Fusselman is dominated by typical normal marine facies throughout most of its extent. Reservoirs are developed principally in basal ooid grainstones and overlying pelmatozoan packstones, both of which are areally extensive. Porosity development is largely associated with original interparticle porosity in ooid grainstones and leaching of carbonate mud fractions in pelmatozoan packstones. Evidence of karst processes, ranging from large, cave-fill successions to minor dissolution features, is locally apparent across the Permian Basin. Global studies indicate that the Fusselman was deposited during a period of icehouse climatic conditions, when high-amplitude sea-level rises and falls were common. Although there has been relatively little documentation of the sequence and cycle stratigraphy of these rocks, it seems certain that patterns of facies stacking and diagenesis within the Fusselman are tied to these icehouse eustatic fluctuations and that these patterns, although poorly known, are important keys to the reservoir heterogeneity.

INTRODUCTION

As of the year 2000, reservoirs developed in rocks assigned to the Fusselman Formation in the subsurface of the Permian Basin of West Texas and New Mexico had accounted for more than 356 million barrels of oil production (Dutton and others, 2005). Despite the economic significance of this geologic succession, relatively little detailed geological information is available about these rocks or the key aspects of reservoir development. Published data from subsurface regional and field-specific studies are generally limited in scope, and the thick outcrop succession of Fusselman rocks (in southern New Mexico) has been studied only superficially. Available global and regional data suggest that the Fusselman, which contains rocks deposited during the Late Ordovician to Early Silurian icehouse to waning icehouse climatic period, contains a depositionally and diagenetically complex succession of carbonate platform deposits. This report synthesizes existing global, regional, and reservoir specific data to describe the major controls on deposition, diagenesis, and reservoir development within this important carbonate succession in the Permian Basin.

PREVIOUS WORK

Early descriptions of the Fusselman were published by Jones (1953) and Galley (1958). McGlasson (1967), Wright (1979), and Canfield (1985) provided additional data on facies and stratigraphy. More recent studies by Geesaman and Scott (1989) and Garfield and Longman (1989) focus on local variations in facies and depositional setting in the Fusselman Formation in a small area in the Midland Basin. Canter and others (1992) proposed a model for sequence stratigraphic correlation of the subsurface Fusselman. Ruppel and Holtz (1994) described regional geological characteristics of the Fusselman and provided play-specific data on engineering attributes. Barrick (1995) demonstrated, on the basis of conodont biostratigraphy, that the Fusselman comprises a lower Upper Ordovician part and an upper Lower Silurian part (fig. 1). Lemone (1992), Lucia (1995), and Mazzullo (1993) described *karst* features in Fusselman *outcrops*. Several authors have concluded on the basis of wireline-log evidence that subsurface Fusselman rocks also display evidence of karsting (Mazzullo and others, 1989;

Mazzullo and Mazzullo, 1992). Mear (1989) and Garfield and Longman (1989) documented cave breccia deposits from cores.

REGIONAL SETTING

During deposition of the Fusselman Formation, the Permian Basin area lay in a tropical to low subtropical setting along the southern margin of the Laurentian continent (fig. 2). Although the eastern margin of Laurentia underwent tectonic deformation (the Taconic Orogeny) associated with the approaching continental landmass of Baltica at this time, the southern margin appears to have been an area of relative tectonic quiescence. This conclusion is consistent with the apparent widespread distribution and relatively uniform persistent facies character of the Fusselman throughout the region.

Deposition of rocks included in the Fusselman Formation of West Texas and New Mexico began during the Late Ordovician on an extensive shallow-water platform, whose development began with deposition of the Montoya Group during the Cincinnati. Fusselman Formation carbonate deposits reflect the continued growth and development of this shallow-water platform from the Late Ordovician into the Early Silurian. The similarity of depositional facies across the region indicates that conditions were relatively uniform over great distances. Equivalent rocks in Oklahoma, for example, are lithologically similar (fig. 1; Barrick, 1995). Johnson (1987) presented data suggesting that this Early Silurian platform extended across most of the North American continent. Depositional analyses and worldwide stratigraphic equivalents of the Fusselman demonstrate that accumulation of these rocks was punctuated by at least five major rise and fall cycles of relative sea level (McKerrow, 1979; Johnson, 1987, 1996) of about 2-m.y. duration. Globally these eustatic events are reflected in unconformities and associated diagenetic alteration of these shallow-water carbonate facies. Clearly these hiatuses were associated with considerable erosion and/or long periods of nondeposition. Biostratigraphic evidence indicates that the 100 to 300 ft of preserved Fusselman in the subsurface of the Permian Basin spans an interval of about 10 m.y. (fig. 1; Barrick and others, 2005).

Widespread, shallow-water platform conditions characteristic of Fusselman deposition were abruptly terminated by sea-level rise probably associated with tectonic downwarping and drowning of the platform, most likely during the early Wenlockian (Ruppel and Holtz, 1994). This event and its impact of sedimentation in the Permian Basin are discussed more fully in the chapter on the Middle and Upper Silurian Wristen Group. Downwarping of the Fusselman Platform in Texas, and equivalent successions in Oklahoma and the Illinois Basin, may have been a product of early foreland deformation along the southern margin of the North American plate, which was associated with plate convergence that preceded later Ouachita tectonism in the region. Walper (1977) suggested that convergence of the North American and South American/African plates began as early as the Late Ordovician.

Distribution and Age

The Fusselman Formation was named by Richardson (1909) for thick intervals of dolostone of presumed Middle Silurian age that outcrop in the vicinity of El Paso, Texas. As defined in the subsurface, the Fusselman is much thinner but relatively continuous across much of West Texas. The Fusselman is readily recognized and mapped where underlain by the Sylvan Formation (shale of Late Ordovician age) and overlain by the Wink Formation of the Wristen Group (figs. 3, 4). Where the Wink and Frame Formations are absent (north of central Andrews County), it is very difficult to distinguish the top of the Fusselman from overlying shallow-water carbonates of the overlying Fasken Formation (Wristen Group). Similarly, where the Sylvan shale is absent (in the western part of the region), the Fusselman is difficult to separate from the underlying Montoya Formation.

The Fusselman attains maximum thicknesses of more than 600 ft in southeasternmost New Mexico and far West Texas and thins eastward (fig. 5). Average thicknesses where the Sylvan is present range from 50 to 200 ft. The northwest-trending subcrop margin of the Fusselman (fig. 5) coincides with the western margin of what is widely referred to as the Concho Arch, an assumed axis of intermittent and frequent uplift during the Paleozoic. However, it is unclear whether

truncation of the Fusselman along this trend represents postdepositional truncation, penecontemporaneous thinning, or both.

On the basis of studies of faunas in outcrops at the type section in the Franklin Mountains, the Fusselman has long been considered of Early to Middle Silurian age (Wilson and Majewski, 1960; Harbour, 1972). More recent studies based on conodonts, however, reveal that the subsurface Fusselman is actually Late Ordovician (Hirnantian) to Early Silurian (Llandoveryan) in age (J. Barrick, personal communication, 1989). This interpretation is consistent with ages established for nearly identical lithological successions in Oklahoma (Amsden and Barrick, 1986) and further suggests that the nearly 1,000 ft of section assigned to the Fusselman at the type section is equivalent to the Fusselman *and* the overlying Wristen Group in the subsurface (Wilson and Majewski, 1960). Faunal studies in the Marathon Basin of southern West Texas show that the subsurface Fusselman is equivalent to the Lower Caballos Novaculite of the Ouachita overthrust belt and that the Wristen correlates with the middle chert and shale member (Noble, 1993, 1994; Barrick and Noble, 1995).

Facies

The Fusselman comprises a diverse succession of shallow-water carbonate facies. Throughout the central part of the study area (for example, Andrews, Midland, Ector, Upton, Crane Counties) the Fusselman is composed of a consistent series of lithofacies (fig. 3). The base of the Fusselman is typically formed by a thin (>10-ft-thick) interval of ooid grainstone (fig. 6a, b). These deposits, which are of Late Ordovician (Hirnantian) age (Barrick, 1995), are typically well sorted and in some instances crossbedded. Basal ooid grainstone is widely distributed across the region (Canfield, 1985; Ruppel and Holtz, 1994; Barrick 1995). The equivalent Keel Formation in the Texas Panhandle and Oklahoma is virtually identical in lithology, as are coeval deposits in Arkansas and Missouri (Amsden and Barrick, 1986; Barrick, 1995).

Overlying the lower Fusselman ooid grainstone facies is an interval of fenestral mudstone (fig. 3) that locally displays shale-filled solution/erosion pits at its upper surface. This unit is generally thin (>3 ft) and is locally absent.

The upper Fusselman is most characteristically composed of gray to pink pelmatozoan grainstone and packstone (fig. 6c). These rocks, which are generally well sorted and locally crossbedded, are composed of pelmatozoans and subordinate bryozoans; brachiopods, ostracodes, corals and mollusks are locally present (fig. 6c, d). These grain-rich packstones and grainstones, which in some areas grade laterally into skeletal wackestone containing pelmatozoans, brachiopods, and ostracodes, overlie fenestral mudstone facies or rest directly on a basal ooid grainstone-packstone unit. Typically these deposits are composed of well-sorted skeletal sands; however, in some areas (for example, Winkler County) they are represented by poorly sorted rudstones that contain corals. Locally the pelmatozoan facies contains sediment- and spar-filled geopetal structures, some of which resemble stromatactoid structures. Some of these structures may indicate local carbonate buildup in this part of the Fusselman section (fig. 8). Other sediment- and cement-filled geopetal voids are also locally common within this facies (fig. 6e). These voids appear to be vugs produced by secondary leaching and subsequent sediment infill and cementation. In some instances, multiple successions of these voids appear to exhibit crosscutting relationships.

The upper Fusselman pelmatozoan facies is present across most of the study area except near the Fusselman subcrop margin (for example, in Terry and Glasscock Counties). Geesaman and Scott (1989) also reported the local absence of this facies in the Glasscock County area, where the unit apparently thins onto paleohighs (fig. 7). Thickness of the pelmatozoan grainstone-packstone facies appears to increase in parallel with total Fusselman thickness trends (that is, toward far West Texas and New Mexico). Grain size also increases to the west.

The upper pelmatozoan, grainstone-packstone facies of the Fusselman grades upward into more mud-rich facies, including wispy-laminated to nodular-bedded, locally siliceous wackestone containing ostracodes and less common pelmatozoans (fig. 3). These deposits

resemble those typical of the overlying Wink Formation of the Wristen Group (Canfield, 1985; Mear, 1989; Ruppel and Holtz, 1994).

The contact of the Fusselman Formation with the overlying Wink Formation of the Wristen Group appears unconformable. This likelihood, suggested by thickness variations apparent on cross sections, is confirmed by core data. In central Andrews County (Austral Oil Co., University No. 1) for example, the uppermost Fusselman is a dolomitized and partly silicified breccia that is sharply overlain by burrowed siltstone (Ruppel and Holtz, 1994). Canfield (1985) described cores from Pecos and Midland County wells in which the upper Fusselman was sharply overlain by reported shales of the basal Wink. Small amounts of greenish-colored shale are locally common in the upper Fusselman, as are zones of multiple-stage, geopetal cavity fills (fig. 8b). Garfield and Longman (1989) also documented truncation of the Fusselman beneath the Wristen Group in the Martin/Midland/Glasscock County area. This hiatus, which has also been defined in temporally equivalent rocks in Oklahoma, corresponds to the Llandoveryan/Wenlockian boundary (fig. 1).

Depositional Setting

The Fusselman Formation documents deposition on an open-marine, shallow-water carbonate platform that probably formed during Late Ordovician time. Underlying Montoya Group deposits represent the earlier development of this platform that extended across much of West Texas and New Mexico. Basal Fusselman ooid grainstones represent deposition in relatively high-energy tidal-flat to shallow subtidal conditions. The extent of these deposits indicates that the platform was broad and flat and extended across much of West Texas. Capping fenestral mudstones indicate at least local exposure of these deposits, which is supported by the occurrence of meniscus and pendant cements that are indicative of vadose diagenesis (fig. 8a). Virtually identical facies and cements have been reported from modern ooid sand shoals that have developed on intermittently exposed shallow water in the Bahamas (Harris, 1979). Regional data indicate that basal Fusselman ooid deposits may have experienced much longer periods of

exposure. Biostratigraphic studies of coeval and overlying Silurian deposits in Oklahoma and elsewhere document a widespread late Llandoveryan hiatus between the Fusselman and overlying Wenlockian strata (Amsden and Barrick, 1986; fig. 1).

The Fusselman pelmatozoan grainstone/packstone facies is thicker and more widespread than the underlying ooid facies, indicating that these deposits occupied an even broader area of the Early Silurian platform. The paucity of carbonate mud and good sorting in these facies suggest that much of this facies was deposited in high-energy shoals or bars. Deposits exhibiting stromatactis and sediment- and cement-filled geopetal cavities suggest local development of carbonate buildups. Coarser-grained, more poorly sorted sections of pelmatozoan/coral packstone in the western part of the study area (for example, Emperor field in Winkler County, Texas) may reflect buildup development in somewhat deeper water conditions. Fusselman encrinites are very similar to correlative rocks in Oklahoma (Cochrane and Clarita Formations; see Amsden, 1980), indicating development of a continuous, broad, shallow platform.

The overall continuity of Fusselman facies across the region indicates development of widely continuous depositional environments. There is evidence, however, that locally these extensive, sheetlike environments were interrupted by more complex depositional regimes created around topographic highs. Such relationships were documented by Garfield and Longman (1989) over paleotopographic highs in the Midland/Glasscock County area and are also common along the eastern subcrop margin of the Fusselman. On the basis of regional core studies, Canter and others (1992) inferred the presence of a general east-west platform margin with gradually shallower water middle- and inner-shelf conditions prevailing progressively to the north (fig. 9).

Stratigraphic and diagenetic patterns in the Fusselman indicate that deposition was punctuated by episodic rise and fall of relative sea level. Johnson (1987) documented five major sea-level falls during the time represented by Fusselman deposition. These sea-level rise/fall cycles (sequences) are well chronicled in the biostratigraphically well constrained Fusselman-equivalent outcrops in Oklahoma (Amsden and Barrick, 1986, 1988). This interpretation implies

that (1) the lower ooid grainstone member of the Fusselman (which is equivalent to the Keel in Oklahoma) is separated from the upper pelmatozoan facies (equivalent to the Cochrane) by a long-duration hiatus (~4–5 m.y.) and (2) the upper pelmatozoan facies experienced at least four significant falls in relative sea level, including a hiatus of 1 to 2 m.y. at the end of Fusselman deposition (fig. 1). These conclusions are supported by diagenetic features recognized in Fusselman core successions (Ruppel and Holtz, 1994) and from correlative biostratigraphic and facies studies of Fusselman equivalents in Oklahoma outcrops (Barrick, 1995). The multiple generations of geopetally filled vugs in the pelmatozoan facies may be a record of both of these late Llandoveryian sea-level falls. There is good evidence that episodic eustatic fall during the Late Ordovician and Early Silurian, which may be related to continental glaciation in North Africa at that time (Amsden and Barrick, 1986), left a strong depositional and diagenetic imprint on Fusselman rocks in the Permian Basin.

Mineralogy and Diagenesis

Mapping of the Fusselman by several authors (McGlasson, 1967; Wright, 1979; Mear, 1989) illustrates that the section is largely dolostone in the northern part of its extent but is predominantly limestone in the south (fig. 10). Ruppel and Holtz (1994) pointed out that the distribution of dolostone in the Fusselman closely parallels the extent of largely dolomitized shallow-water platform facies (Fasken Formation) in the overlying Wristen Group. This relationship suggests that dolomitization may have been associated with the repeated sea-level falls that characterized Wristen shallow-water platform sedimentation.

It is likely that parts of the Fusselman had already been subjected to variable degrees of diagenesis or alteration prior to the Wristen and post-Wristen dolomitization events discussed earlier. Evidence of meteoric diagenesis in the basal ooid grainstone/packstone facies, combined with regional indications of a widespread hiatus, indicates that these basal deposits may have locally undergone significant diagenetic alteration. In many instances, the ooid grainstone facies is dolomitized, and overlying Fusselman facies are not. This alteration may be related to episodic

sea-level fall during Fusselman deposition. Successive generations of geopetally filled dissolution vugs in the upper Fusselman may record similar events. Such eustatic fluctuations are supported by studies of the Early Silurian worldwide (McKerrow, 1979; Johnson, 1987; 1996). Sharp contacts between Fusselman dolostones and basal Wristen limestones in some areas suggest that dolomitization may have also occurred during the last Fusselman sea-level fall event (before the onset of Wristen deposition).

There is good evidence that the Fusselman has undergone karst-related diagenesis. Sediment- and breccia- filled karst features are common in outcrops of the Fusselman in the Franklin Mountains (McGlasson, 1967; Lemone, 1992). (Note that outcrops assigned to the Fusselman almost certainly include Wristen rocks as well.) As previously discussed, dissolution features and breccias possibly related to karsting have been reported from several cores in the Fusselman (Mear, 1989; Mazzullo and Mazzullo, 1992; Troschinetz, 1989).

Sequence Stratigraphy

Global studies document one Ordovician and four Silurian sea level rise/fall cycles during the time represented by the subsurface Fusselman (fig. 1). The oldest of these cycles corresponds well with the lower Fusselman ooid-bearing succession of late Ordovician age. The upper Fusselman spans much of the Llandovery and thus may include as many as four sequences. Each of the sea-level drops that created these sequence boundaries was potentially associated with exposure-related diagenesis that may have enhanced or reduced reservoir quality. Thus, definition of the number and location of these events is important to accurate reservoir characterization in the upper Fusselman. Canter and others (1992) recognized two sequence boundaries within the upper Fusselman on the basis of apparent karst horizons. However, it is clear that further work based on well-dated cores will be necessary to accurately define both the number and placement of Fusselman depositional sequences.

Reservoir Development

Fusselman reservoirs in the Permian Basin have been assigned to the Fusselman Shallow Platform Carbonate Play (Ruppel and Holtz, 1994; Dutton and others, 2005). Ruppel and Holtz (1994) documented a total of 233 productive reservoirs in the Fusselman in 1989, only 47 of which had produced more than 1 MMbbl at that time. As of 2000, 63 Fusselman reservoirs had produced more than 1 MMbbl of oil (fig. 11); cumulative production from the play was 356.3 MMbbl (Dutton and others, 2005).

Reservoir Distribution

Fusselman rocks are productive in two major end-member settings (fig. 11): (1) on major, typically fault-bounded structures on the Central Basin Platform and adjacent Midland Basin and (2) along the Fusselman subcrop margin. Reservoirs developed along the subcrop margin can be considered a distinct subplay, in which production is developed primarily where the Wristen has been removed by erosion and the Woodford directly overlies the Fusselman (Ruppel and Holtz, 1994).

Porosity Development

Three general styles of pore development are observed in the Fusselman: (1) primary intergranular pores in basal ooid grainstones, (2) leached intergranular pores in pelmatozoan packstones, and (3) strongly leached, predominantly vuggy and intercrystalline pores at the top of the Fusselman (Ruppel and Holtz, 1994).

As discussed previously, primary intergranular porosity is developed locally in basal Fusselman ooid grainstones (figs. 3, 6a, b). Where these pores are preserved, these deposits make excellent reservoirs (for example, in Mound Lake, Emma, Warfield, and SW Midland fields).

Highest porosity is commonly developed in the upper Fusselman pelmatozoan packstone facies (Canfield, 1985). These rocks contain secondary porosity owing to leaching of skeletal packstone. Examples include Good SE, Lowe, Emma, Emperor, Pegasus, and SW Midland fields. This secondary porosity takes the form of intergranular pores, molds, and small vugs

formed by meteoric leaching during one or more of the falls in relative sea level during and following Fusselman deposition.

Both styles of pore development are probably mostly associated with very early diagenesis, either during deposition of the Fusselman or shortly thereafter. Accordingly, this type of reservoir development can be observed throughout the Fusselman subcrop (Ruppel and Holtz, 1994). Much more extensive diagenesis is encountered where the Fusselman has been unroofed by erosion or faulted and fractured. In these reservoirs, which are located primarily in the northern part of the Fusselman subcrop and along the eastern subcrop margin (fig. 11), the top of the Fusselman section commonly displays more extensively leached zones. Reservoirs developed in these areas are commonly dolomitized (fig. 10) by processes of matrix replacement and partial pore filling by dolomite cements. Leaching and associated fabric-destructive dolomitization is most common where removal of the Fasken has allowed meteoric fluids more frequent access during Silurian and Devonian exposure events. This leaching is less strongly controlled by depositional facies and more a function of paleotopography and paleohydrology. Porosity in these highly leached and altered rocks typically takes the form of intercrystalline pores and large vugs. Strongly leached and altered reservoir successions are also encountered on major structural highs, where faulting has provided fluid conduits for entrance of diagenetic fluids (for example, Dollarhide field).

Traps, Seals, and Sources

Fusselman reservoir traps are both structural and stratigraphic. Most larger fields on the Central Basin Platform and in the Midland Basin are dominantly structural (for example, Dollarhide and Keystone). Structures that form most traps were formed during late Carboniferous foreland basin deformation associated with the collision of Gondwana and Laurussia plates. However, Mazzullo and others (1989) showed that there is good evidence that the Fusselman and overlying Wristen Group (and Thirtyone Formation) underwent significant deformation during Middle Devonian (pre-Woodford) time. Fields developed in this setting are

actually compound structural traps (for example, Tex-Hamon and Wells). As Mazzullo and others (1989) pointed out, such structural traps are not reflected in the structure of the Woodford Formation and can thus be cryptic.

In most Fusselman fields, the top seal is provided by shales and mudstones of the Frame and Wink Formations of the Wristen Group (for example, Dollarhide and Keystone). In many fields along the eastern subcrop, the Fusselman is overlain and sealed by the Woodford (Mazzullo and others, 1989; Comer, 1991). Where the Woodford has been removed by erosion, Permian shales provide the seal (for example, Abell and Pecos Valley). On the basis of a comparison of produced Fusselman oil types and Permian Basin source rock character, Williams (1977) concluded that most of the oil charge in the Fusselman came from the Woodford Formation.

Opportunities for Additional Resource Recovery

Although basic Fusselman facies types and pore types are fairly well known, insufficient information is available regarding controls of cyclicity and diagenesis on reservoir development and architecture. A better understanding of these processes could elucidate new opportunities for focused field redevelopment. For example, facies stacking patterns, facies continuity, and the relative importance of depositional facies versus diagenesis on porosity are not well understood. Especially needed is a sequence stratigraphic framework, within which both depositional facies and diagenesis can be defined and modeled. Such a framework would lead to a better appreciation for the development and significance of Early Silurian global sea-level-fall events and their impact on reservoir architecture and porosity development. A detailed study of the excellently exposed Fusselman section in the Franklin Mountains would provide fundamental data and models needed for better interpretation of existing core and wireline-log data in the subsurface.

SUMMARY AND CONCLUSIONS

As conventionally defined in the subsurface of the Permian Basin, the Fusselman consists of shallow-water carbonate platform deposits of Late Ordovician and Early Silurian age. Lower Fusselman (Ordovician-age) rocks comprise ooid grainstones and interbedded mudstones. The upper Fusselman (Early Silurian age) commonly consists of deeper-water, more open marine facies, most typically crinoid grainstones and packstones. Evidence of exposure-related diagenesis is present at several horizons within the Fusselman and is consistent with multiple episodes of high-amplitude, sea-level oscillation documented in deposits of similar age around the world. Reservoir porosity is most commonly associated with primary interparticle pore space in lower Fusselman grainstones and with dissolution-related interparticle porosity in the upper Fusselman crinoid packstones. Internal reservoir architecture is poorly known because of the general scarcity of cores and absence of detailed outcrop study. Large-scale karst features are common in some Fusselman reservoirs, but the timing, origin, cause, and geometry of these features and their impact on reservoir performance is known.

REFERENCES

- Amsden, T. W., 1980, Hunton Group (Late Ordovician, Silurian, and Early Devonian) in the Arkoma Basin of Oklahoma: Oklahoma Geological Survey Bulletin 129, 136 p.
- Amsden, T. W., and Barrick, J. E., 1986, Late Ordovician–Early Silurian strata in the Central United States and the Hirnantian stage: Oklahoma Geological Survey Bulletin 139, 95 p.
- Amsden, T. W., and Barrick, J. E., 1988, Late Ordovician through Early Devonian annotated correlation chart and brachiopod range charts for the southern midcontinent region, U.S.A., with a discussion of Silurian and Devonian conodont faunas: Oklahoma Geological Survey Bulletin 143, 66 p.
- Barrick, J. E., 1995, Biostratigraphy of uppermost Ordovician through Devonian depositional sequences in the Permian basin, west Texas and Southeastern New Mexico, *in* Pausé, P. H., and Candelaria, M. P., eds., Carbonate facies and sequence stratigraphy: practical applications of carbonate models: Permian Basin Section-SEPM Publication 95-36, p. 207–216.
- Barrick, J. E., Klapper, G., and Amsden, T. W., 1990, Late Ordovician—Early Devonian conodont succession in the Hunton Group, Arbuckle Mountains and Anadarko Basin, Oklahoma, *in* Ritter, S. M., ed., Early to middle Paleozoic conodonts of the Arbuckle Mountains, southern Oklahoma: Oklahoma Geological Society Guidebook 27, p. 55–92.
- Barrick, J. E., Meyer, B. D., and Ruppel, S. C., 2005, The Silurian-Devonian boundary and the Klunk event in the Frame Formation, subsurface West Texas, *in* Barrick, J. E., and Lane, H. R., eds., A standing ovation: papers in honor of Gilbert Klapper: Bulletins of American Paleontology, No. 369, p. 105–122.
- Barrick, J. E., and Noble, P. J., 1995, Early Devonian conodonts from a limestone horizon in the Caballos Novaculite, Marathon Uplift, west Texas: Journal of Paleontology, v. 69, p. 1112-1122.
- Barton, J. M., 1945, Pre-Permian axes of maximum deposition in West Texas: American Association of Petroleum Geologists Bulletin v. 29, no. 9, p. 1336–1348.
- Canfield, B. A., 1985, Deposition, diagenesis, and porosity evolution of the Silurian carbonates in the Permian basin: Texas Tech University, M.S. thesis, 138 p.

- Canter, K. L., Wheeler, D. M., and Geesaman, R. C., 1992, Sequence stratigraphy and depositional facies of the Siluro-Devonian interval of the northern Permian Basin, *in* Candelaria, M. P., and Reed, C. L., eds., Paleokarst, karst-related diagenesis, and reservoir development: examples from Ordovician-Devonian age strata of West Texas and the Mid-Continent: Permian Basin Section-SEPM, Field Trip Guidebook, Publication No. 92-33, p. 93–109.
- Comer, J. B., 1991, Stratigraphic analysis of the Upper Devonian Woodford Formation, Permian Basin, West Texas and New Mexico: The University of Texas at Austin, Bureau of Economic Geology Report of Investigations No. 201, 63 p.
- Derby, J. R., Podpechan, F. J., Andrews, J., and Ramakrishna, S., 2002a, U.S. DOE-sponsored study of West Carney Hunton filed, Lincoln and Logan Counties, Oklahoma: a preliminary report (Part I, Conclusion): *Shale Shaker*, v. 53, p. 9-19.
- Derby, J. R., Podpechan, F. J., Andrews, J., and Ramakrishna, S., 2002b, U.S. DOE-sponsored study of West Carney Hunton filed, Lincoln and Logan Counties, Oklahoma: a preliminary report (Part II, Conclusion): *Shale Shaker*, v. 53, p. 39-48.
- Dutton, S. P., Kim, E. M., Broadhead, R. F., Breton, C. L., Raatz, W. D., Ruppel, S. C., and Kerans, Charles, 2005, Play analysis and digital portfolio of major oil reservoirs in the Permian Basin: The University of Texas at Austin, Bureau of Economic Geology Report of Investigations No. 271, 287 p., CD-ROM.
- Galley, J. E., 1958, Oil and gas geology of the Permian Basin of West Texas, *in* *Habit of oil—a symposium*: American Association of Petroleum Geologists, Special Publication, p. 395–446.
- Garfield, T. R., and Longman, M. W., 1989, Depositional variations in the Fusselman Formation, Central Midland Basin, West Texas, *in* Cunningham, B. K., and Cromwell, D. W., eds., *The Lower Paleozoic of West Texas and southern New Mexico—modern exploration concepts*: Permian Basin Section-SEPM, Publication No. 89-31, p. 187–202.
- Geesaman, R. C., and Scott, A. J., 1989, Stratigraphy, facies, and depositional models of the Fusselman Formation, Central Midland Basin, *in* Cunningham, B. K., and Cromwell, D. W., eds., *The Lower Paleozoic of West Texas and southern New Mexico—modern exploration concepts*: Permian Basin Section-SEPM, Publication No. 89-31, p. 175–186.

- Harbour, R. L., 1972, Geology of the Franklin Mountains, Texas and New Mexico: U.S. Geological Survey Bulletin 1298, 129 p.
- Harris, P. M., 1979, Facies anatomy and diagenesis of a Bahamian ooid shoal: *Sedimenta VII*: The University of Miami, The Comparative Sedimentology Laboratory, 163 p.
- Johnson, M. E., 1987, Extent and bathymetry of North American platform seas in the Early Silurian: *Paleoceanography*, v. 2, no. 2, p. 185–211.
- Johnson, M. E., 1996, Stable cratonic sequences and a standard for Silurian eustasy, *in* Witzke, B. J., Ludvigson, G. A., and Day, J., eds. *Paleozoic sequence stratigraphy: views from the North American Craton*: Geological Society of America, Special Paper 306, p. 203–211.
- Jones, T. S., 1953, Stratigraphy of the Permian Basin of West Texas: *West Texas Geological Society*, 57 p.
- Kaufmann, B., 2006, Calibrating the Devonian time scale: a synthesis of U-Pb ID-TIMS ages and conodont stratigraphy: *Earth Science Reviews*, v. 76, p. 175–190.
- Lemone, D. V., 1992, The Fusselman Formation (Early–Middle Silurian) Franklin Mountains, El Paso County, Texas and Dona Ana County, New Mexico, *in* Candelaria M. P., and Reed, C. L., eds., *Paleokarst, karst-related diagenesis, and reservoir development: examples from Ordovician-Devonian age strata of West Texas and the Mid-Continent: Permian Basin Section-SEPM, Field Trip Guidebook*, Publication No. 92-33, p. 121–125.
- Lucia, F. J., 1995, Lower Paleozoic cavern development, collapse, and dolomitization, Franklin Mountains, El Paso, Texas, *in* Budd, D. A., Saller, A. H. and Harris, P. M., eds., *Unconformities and porosity in carbonate strata: American Association of Petroleum Geologists Memoir*, v. 63, Chapter 14, p. 279–300.
- Mazzullo, L. J., Mazzullo, S. J., and Durham, T. E., 1989, Geologic controls on reservoir development in Silurian and ?Devonian carbonates, northern Midland Basin, Texas, *in* Cunningham, B. K., and Cromwell, D. W., eds., *The Lower Paleozoic of West Texas and southern New Mexico—modern exploration concepts: Permian Basin Section-SEPM, Publication No. 89-31*, p. 209–218.
- Mazzullo, S. J., 1993, Outcrop and subsurface evidence for karsted reservoirs in the Fusselman Formation (Silurian), Permian Basin, Texas, *in* Johnson, K. S., ed., *Hunton Group core workshop and field trip: Oklahoma Geological Survey, Special Publication*, p. 53–59.

- Mazzullo, S. J., and Mazzullo, L. J., 1992, Paleokarst and karst-associated hydrocarbon reservoirs in the Fusselman Formation, West Texas, Permian Basin, *in* Candelaria M. P., and Reed, C. L., eds., Paleokarst, karst-related diagenesis, and reservoir development: examples from Ordovician-Devonian age strata of West Texas and the Mid-Continent: Permian Basin Section-SEPM, Field Trip Guidebook, Publication No. 92-33, p. 110–120.
- McEvers, L. K., 1984, Stratigraphic and petrographic analysis of the Fusselman dolomite (lower to Middle Silurian), North Franklin Mountains, Dona Ana County, New Mexico: The University of Texas at El Paso Masters thesis, 139 p.
- McGlasson, E. H., 1967, The Siluro-Devonian of West Texas and southeast New Mexico, *in* Oswald, D. H., ed., International Symposium on the Devonian System, v. II: Calgary, Alberta, Alberta Society of Petroleum Geologists, p.937–948.
- McKerrow, W. S., 1979, Ordovician and Silurian changes in sea level: Journal of the Geological Society of London, v. 136, p. 137–145,
- Mear, C. E., 1989, Fusselman reservoir development at Flying W Field, Winkler County, Texas, *in* Cunningham, B. K., and Cromwell, D. W., eds., The Lower Paleozoic of West Texas and southern New Mexico—modern exploration concepts: Permian Basin Section-SEPM, Publication No. 89-31, p. 203-208.
- Noble, P. J., 1993, Biostratigraphy and depositional history of the Caballos Novaculite and Tesnus Formation, Marathon Uplift, West Texas: The University of Texas at Austin, Ph.D. dissertation, 275 p.
- Noble, P. J., 1994, Silurian radiolarian zonation for the Caballos Novaculite, Marathon Basin, West Texas: Bulletins of American Paleontology, v. 106, no. 345, 55 p.
- Richardson, G. B., 1909, Description of the El Paso Quadrangle: U.S. Geological Survey Geological Atlas Folio 166, 11 p.
- Ruppel, S. C., and Holtz, M. H., 1994, Depositional and diagenetic facies patterns and reservoir development in Silurian and Devonian rocks of the Permian Basin: The University of Texas at Austin, Bureau of Economic Geology Report of Investigations No. 216, 89 p.
- Troschinetz, John, 1989, An example of karsted Silurian reservoir: Buckwheat field, Howard County, Texas, *in* Candelaria, M. P., and Reed, C. L., eds., Paleokarst, karst-related

diagenesis, and reservoir development: examples from Ordovician-Devonian age strata of West Texas and the Mid-Continent: Permian Basin Section-SEPM, Field Trip Guidebook, Publication No. 92-33, p. 131–133.

Walper, J. L., 1977, Paleozoic tectonics of the southern margin of North America: Gulf Coast Association of Geological Societies Transactions, v. 27, p. 230–241.

Williams, J. A., 1977, Characterization of oil types in the Permian Basin: text of talk presented at Southwest Section Meeting, American Association of Petroleum Geologists, Abilene, Texas, March 7.

Wilson, J. L., and Majewski, O. P., 1960, Conjectured Middle Paleozoic history of Central and West Texas, *in* Aspects of the geology of Texas: a symposium: University of Texas, Austin, Bureau of Economic Geology, Publication No. 6017, p. 65–86.

Wright, W. F., 1979, Petroleum geology of the Permian Basin: West Texas Geological Society Publication No. 79-71, 98 p.

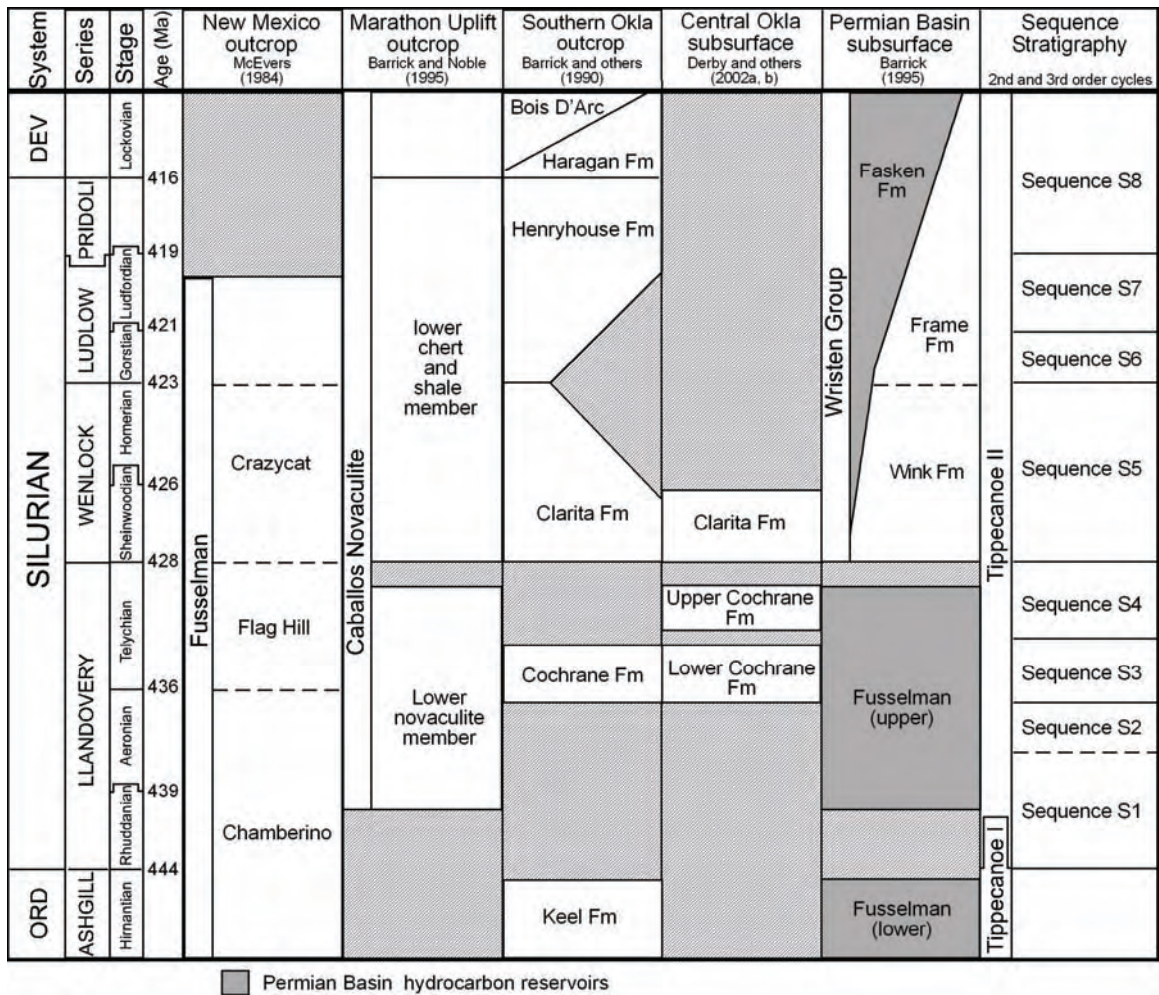
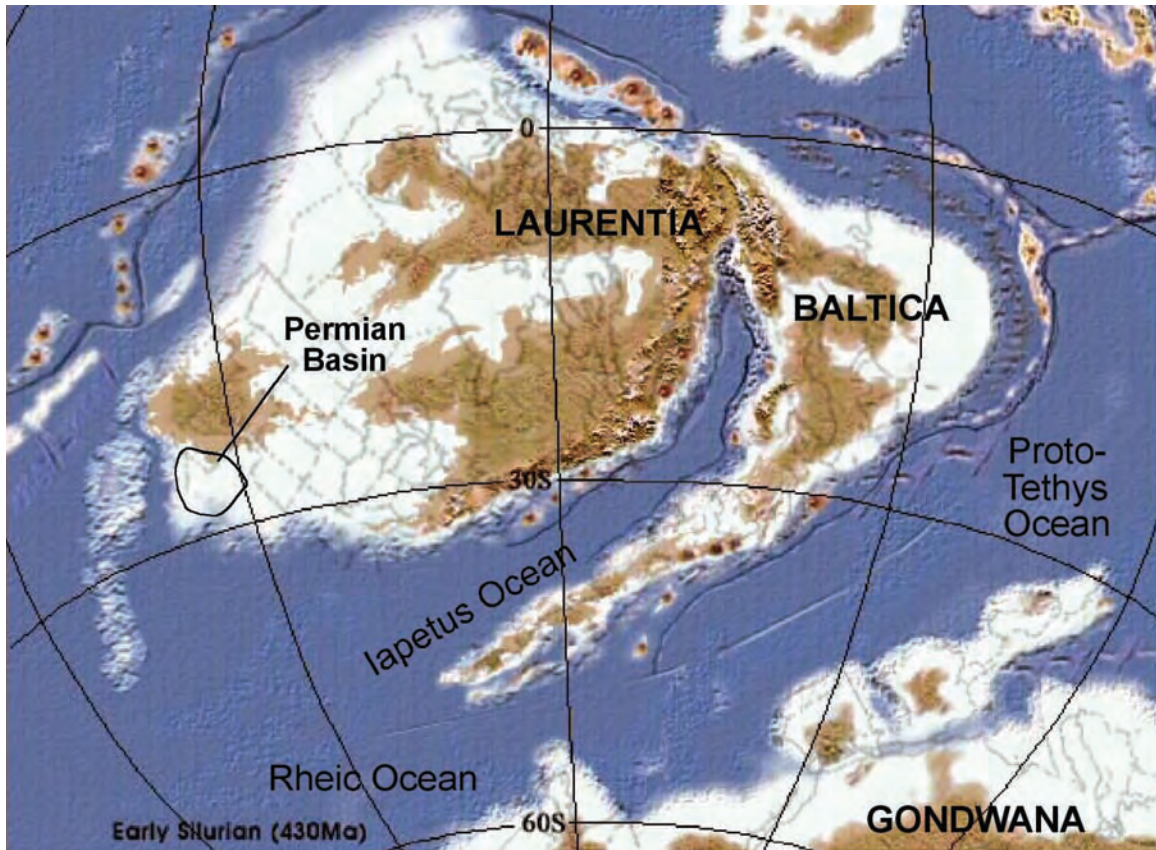


Figure 1. Correlation of Silurian Devonian strata in West Texas with successions in Oklahoma and the Illinois Basin (Indiana-Illinois). Age dates are from Kaufmann (2006).



From Blakey (2004): <http://jan.ucc.nau.edu/~rcb7/430NAt.jpg>

QAd4985x

Figure 2. Global reconstruction of the Laurentian continent for the Late Ordovician. Note that the Permian Basin area occupied the southern margin of the continent facing the open Iapetus Ocean. From Blakey (2004).

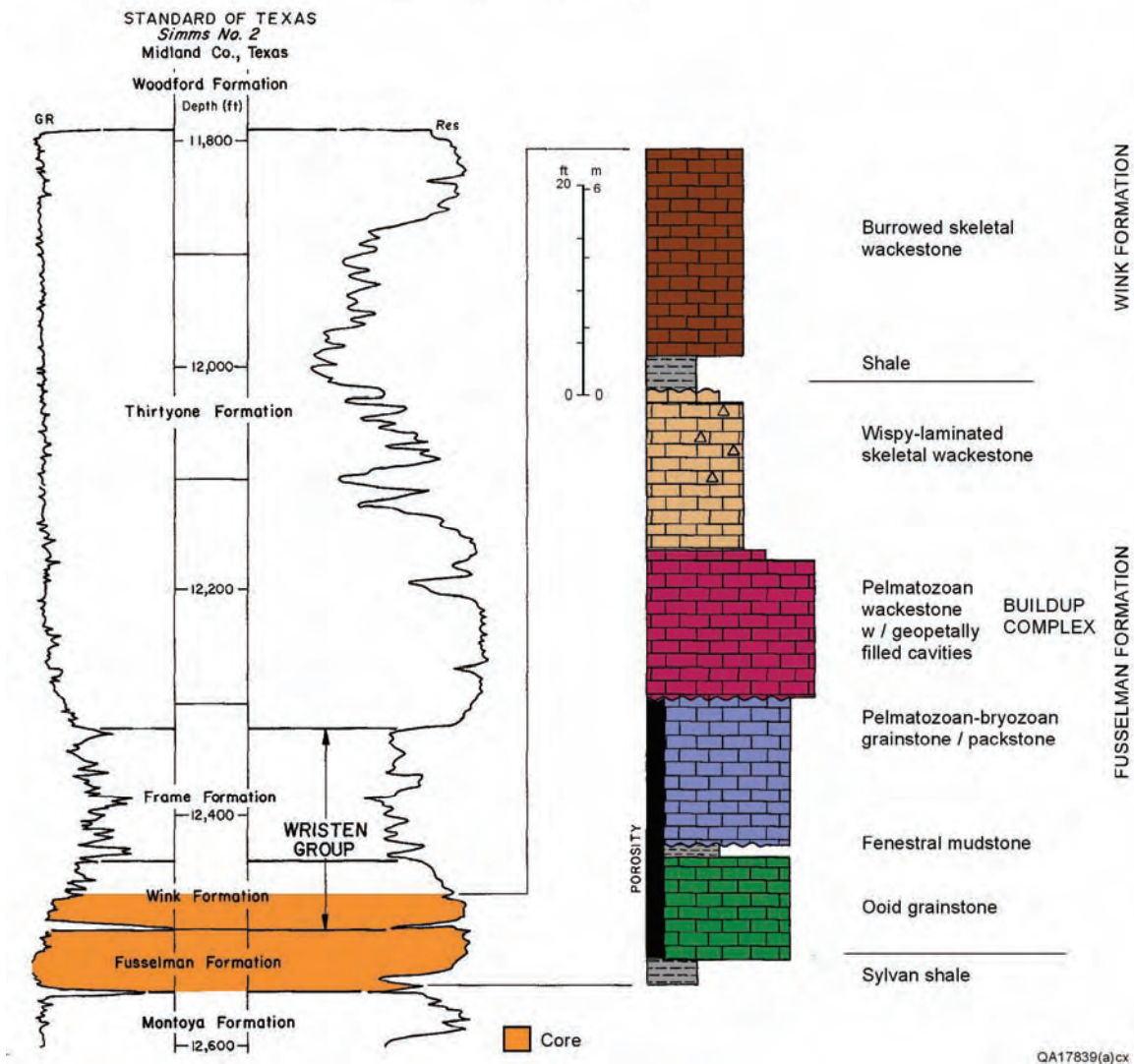


Figure 3. Typical log and facies succession for the Fusselman and adjacent deposits, Standard of Texas, Simms No. 2, Midland County, Texas. Facies are typical of the Fusselman throughout much of the area. Modified from Ruppel and Holtz (1994).

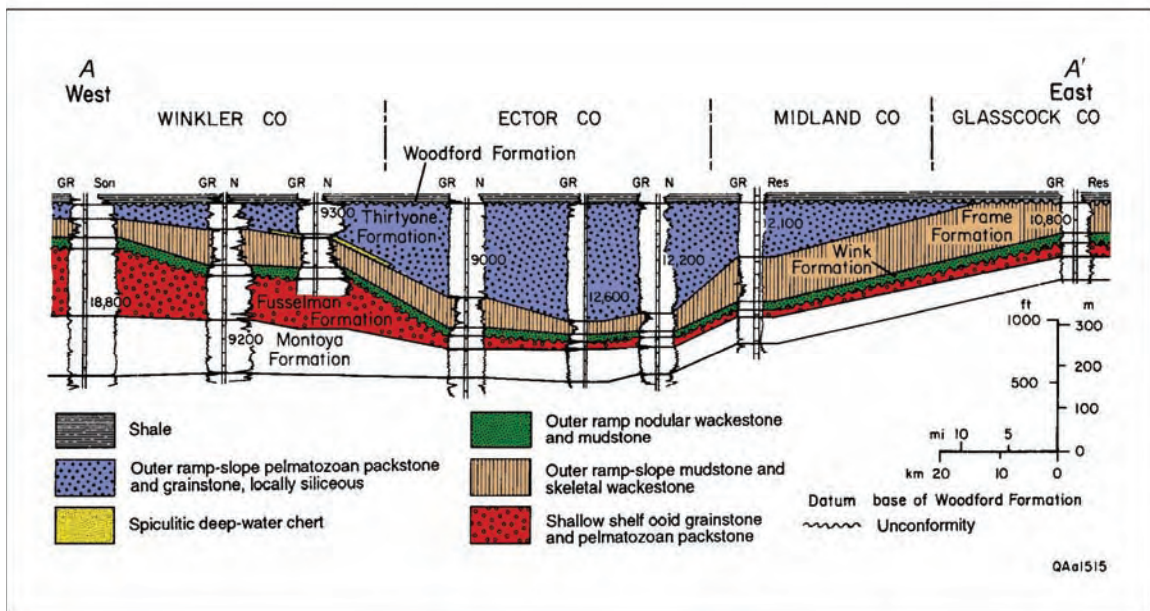
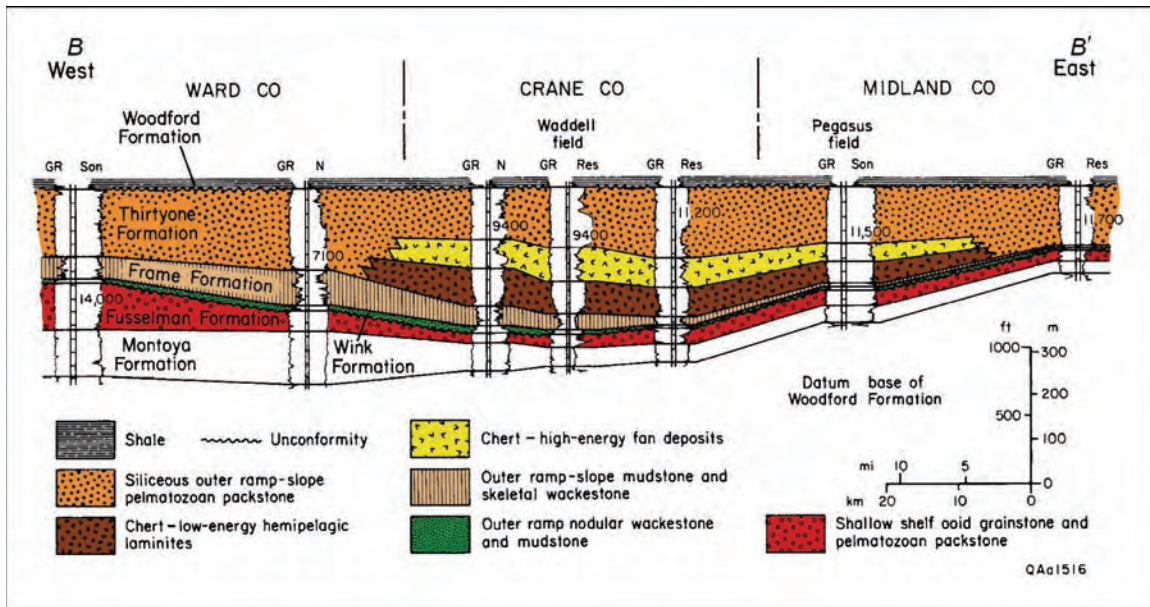


Figure 4. Cross sections showing thickness trends of Fusselman Formation and relationships to underlying and overlying Silurian and Devonian units. Both sections show the eastward thinning of the Fusselman. Lines of section shown on figure 5. Modified from Ruppel and Holtz (1994).

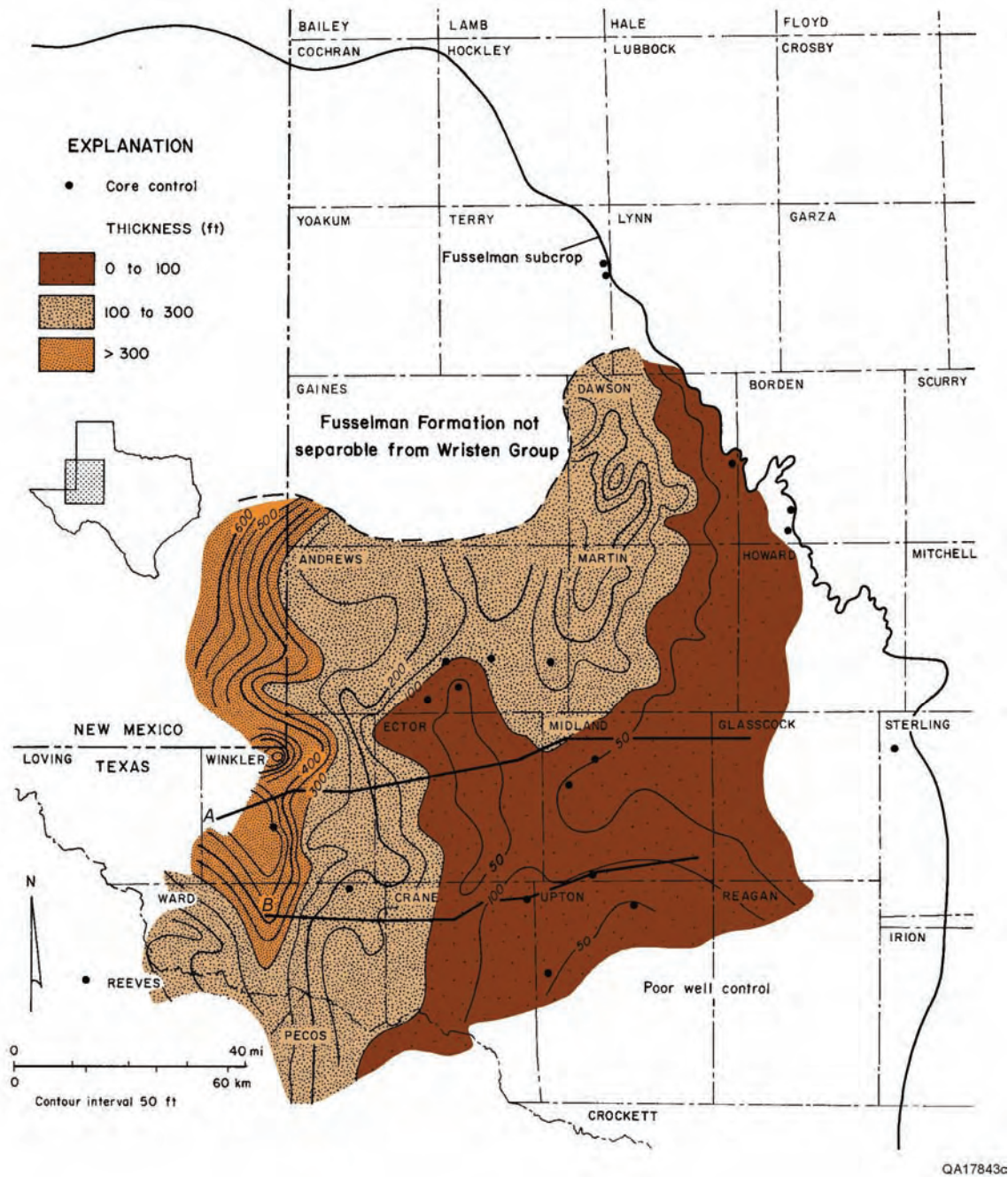


Figure 5. Thickness of Fusselman Formation in West Texas. Contours in the eastern part of the area are modified from Geesaman and Scott (1989).

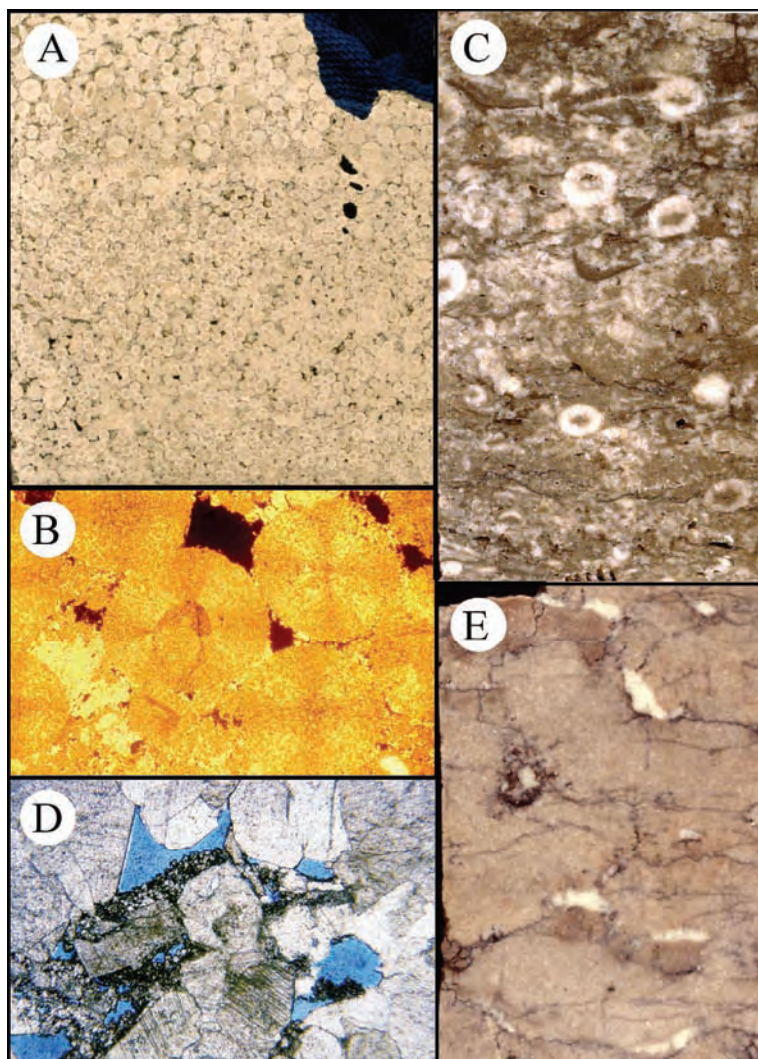
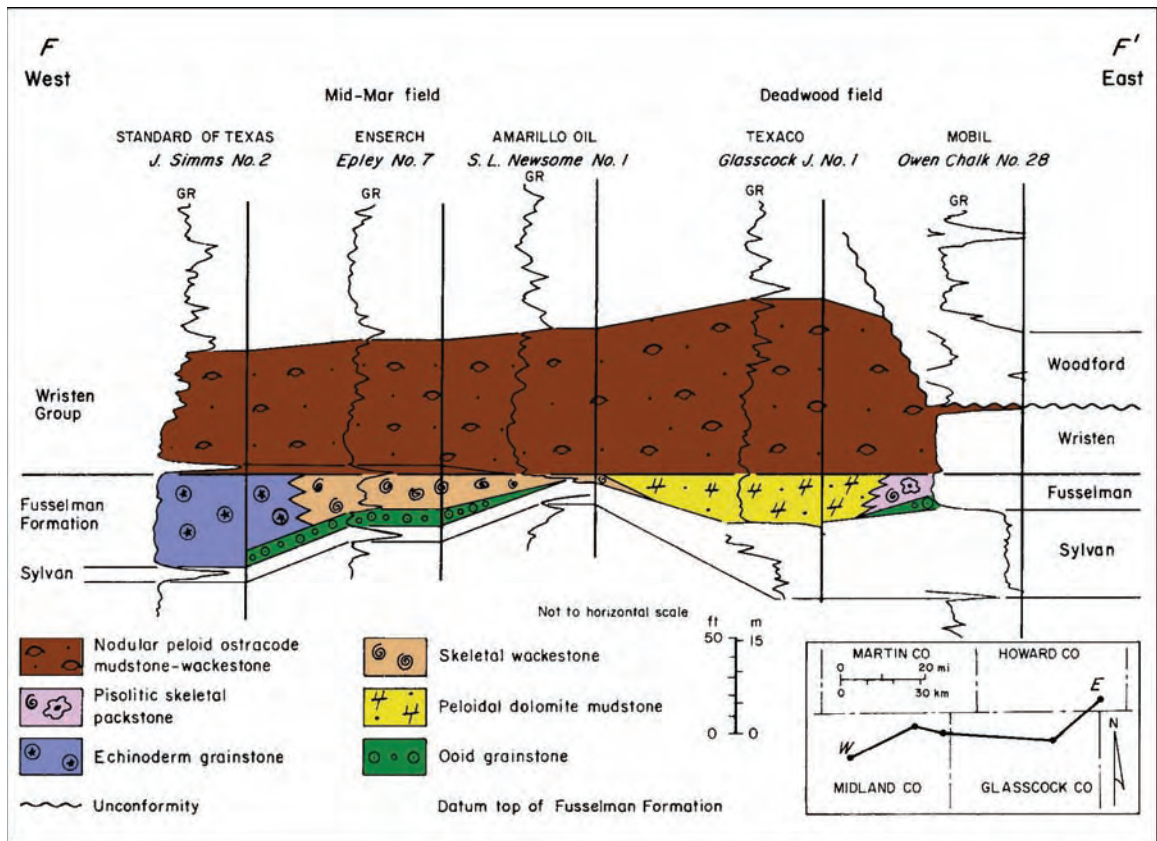


Figure 6. Typical facies of the Fusselman Formation. (A) Slab photograph of ooid grainstone facies showing large, well-sorted ooids with well-developed intergranular porosity. Depth: 12,536 ft. Slab is 6 cm wide. Standard of Texas, Simms No. 2, Midland County, Texas. (B) Cathodoluminescence photomicrograph of ooid grainstone facies. These rocks contain common interparticle porosity. Standard of Texas, Simms No. 2, Midland County, Texas. Depth: 12,536 ft. Field of view is 7 mm. (C) Slab of typical pelmatozoan grainstone-packstone facies. These light-colored encrinites are the most common lithology in the Fusselman throughout most of West Texas and constitute a major reservoir lithofacies. Large, geopetally filled vugs and smaller vugs containing dead oil are commonly developed below intrareservoir unconformities. Porosity is rare in grainstones but is developed as intergranular and intragranular pores in leached packstones. Slab is 8 cm wide. Seaboard, Meiners No. 1, Upton County, Texas. Depth: 12,693 ft. (D) Photomicrograph of pelmatozoan packstone facies. Standard of Texas, Simms No. 2, Midland County, Texas. Depth: 12,536 ft. Field of view is 3.5 mm. (E) Slab photograph of pelmatozoan packstone facies showing abundant geopetally-filled vugs. Many of these vugs are filled with sediment and cement, but some are open and contain hydrocarbons. Seaboard Meiners No. 1, Upton County, Texas. Depth: 12,690 ft. Slab is 8 cm wide.



QAa1487(a)ox

Figure 7. West-east cross section depicting facies changes associated with a paleotopographic high near the eastern subcrop margin of the Fusselman. Modified from Garfield and Longman (1989).

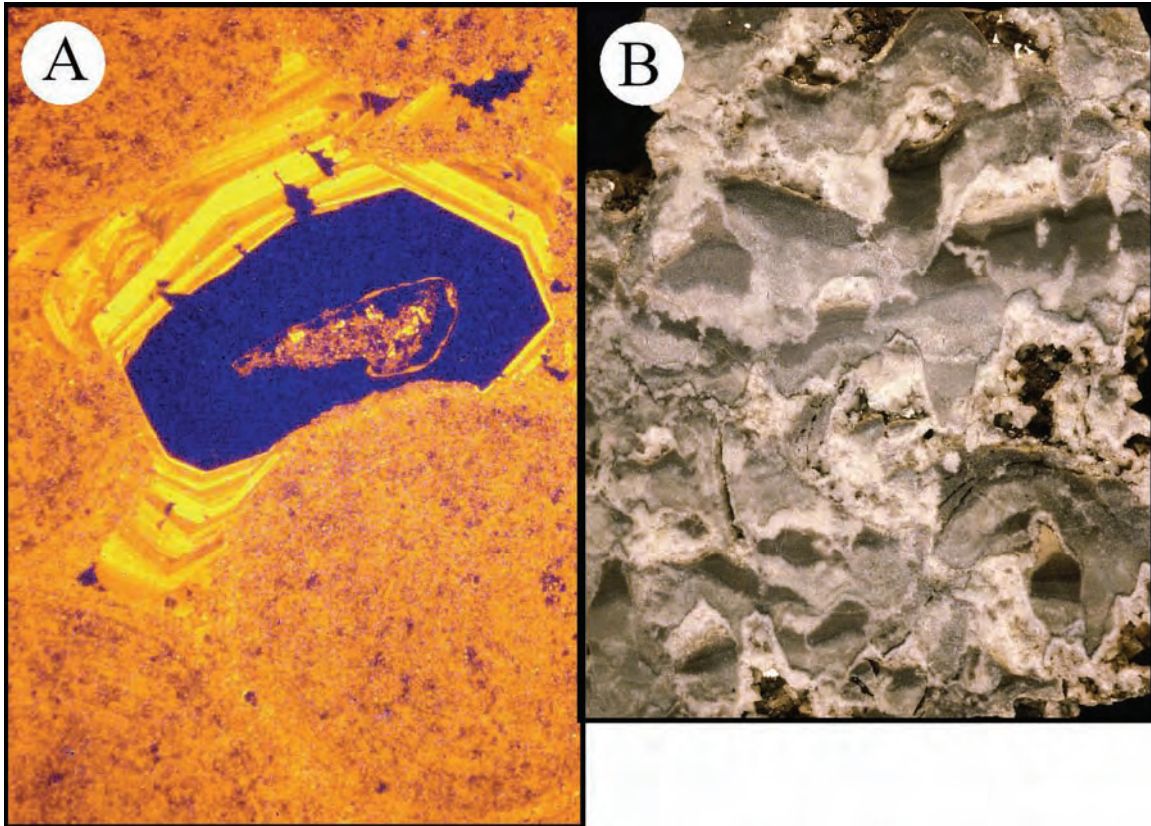
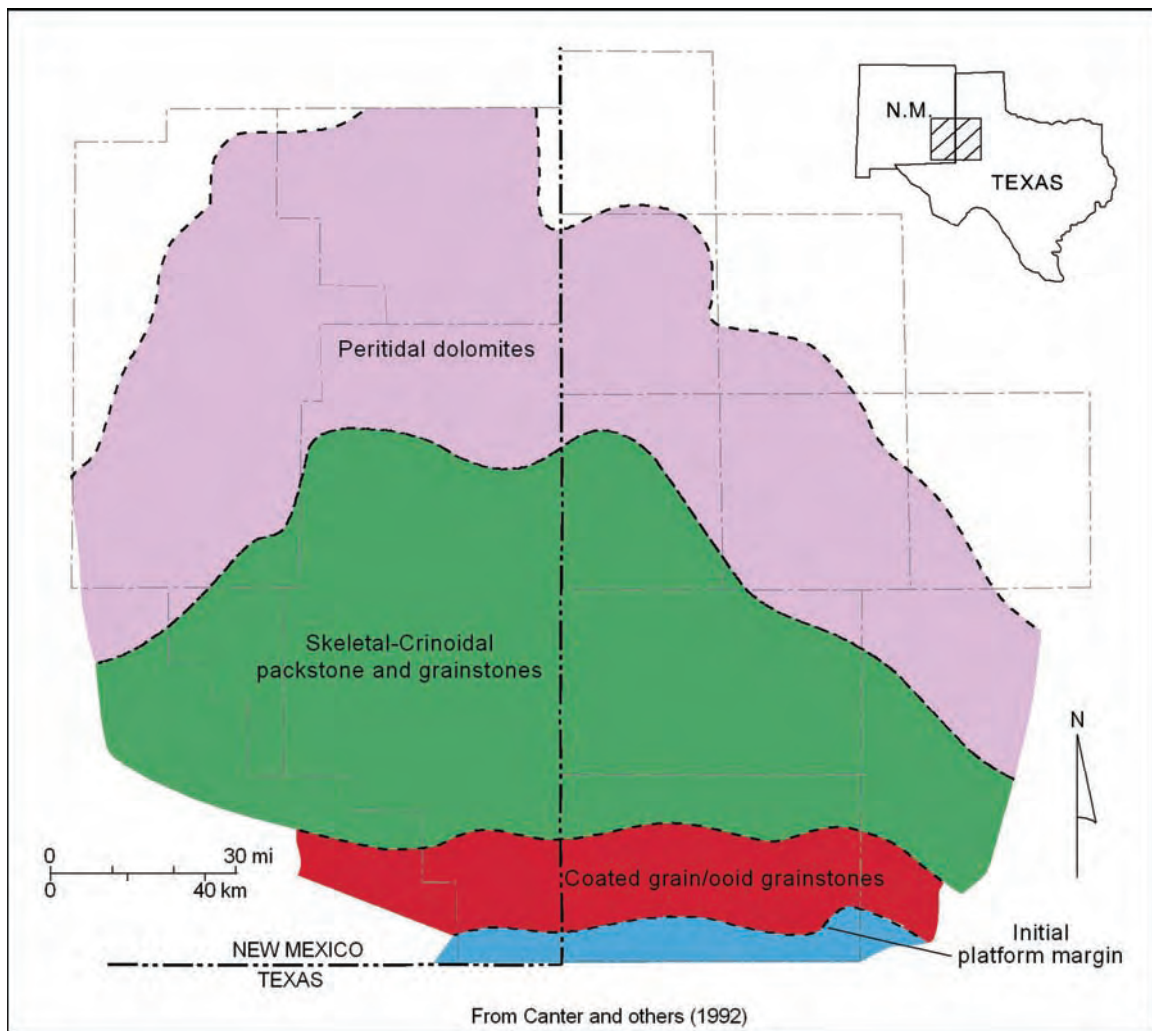


Figure 8. Styles of early and late diagenesis in the Fusselman. (A) Cathodoluminescence photomicrograph of Fusselman ooid grainstone showing well-developed intergranular pores and early fringing meniscus cement. Standard of Texas, Simms No. 2, Midland County, Texas. Depth: 12,536 ft. Width is 4 mm. (B) Slab photograph of upper Fusselman Formation showing multiple, late-stage dissolution and geopetal infilling sediment and cements. Rock is composed almost entirely of cavity fills that consist of greenish-gray silt/clay and drusy cements. Such fabrics are striking evidence of dissolution and karsting of the top of the Fusselman produced during sea-level fall prior to Wristen deposition. Austral Oil Co., University No. 1, Andrews County, Texas. Depth: 12,114 ft. Slab is 8 cm wide.



QAd4829x

Figure 9. Paleogeographic reconstruction of middle to late Fusselman time.

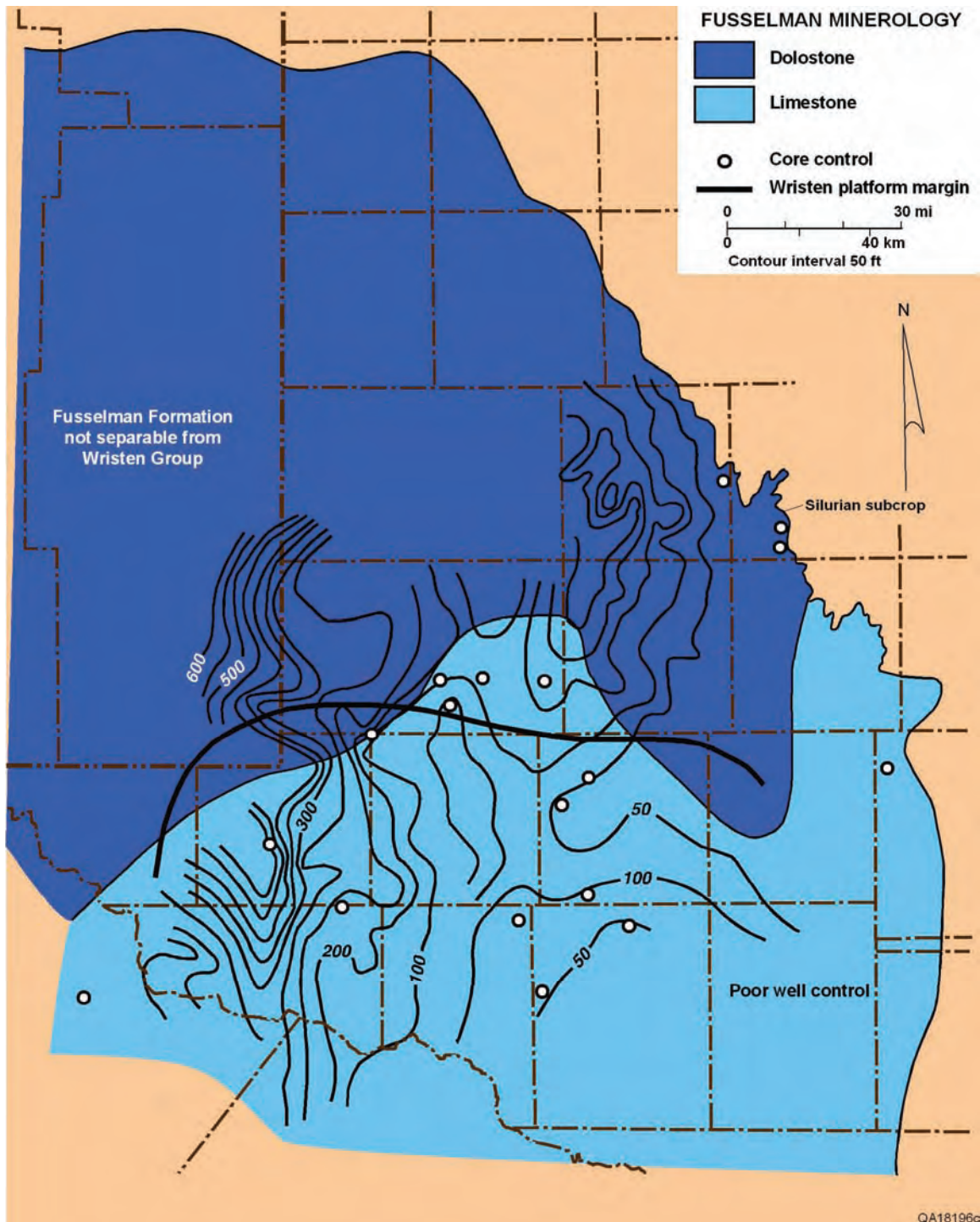


Figure 10. Distribution of dolostone and limestone in the Fusselman Formation. Although this map is highly generalized, the boundary between predominantly dolostone and limestone shown here follows the trend of the Wristen carbonate platform margin, suggesting that some diagenesis leading to dolomitization of the Fusselman was associated with sea-level fall prior to Wristen deposition and/or episodic fall during Wristen deposition (see text). Modified from McGlasson (1967) and Wright (1979).

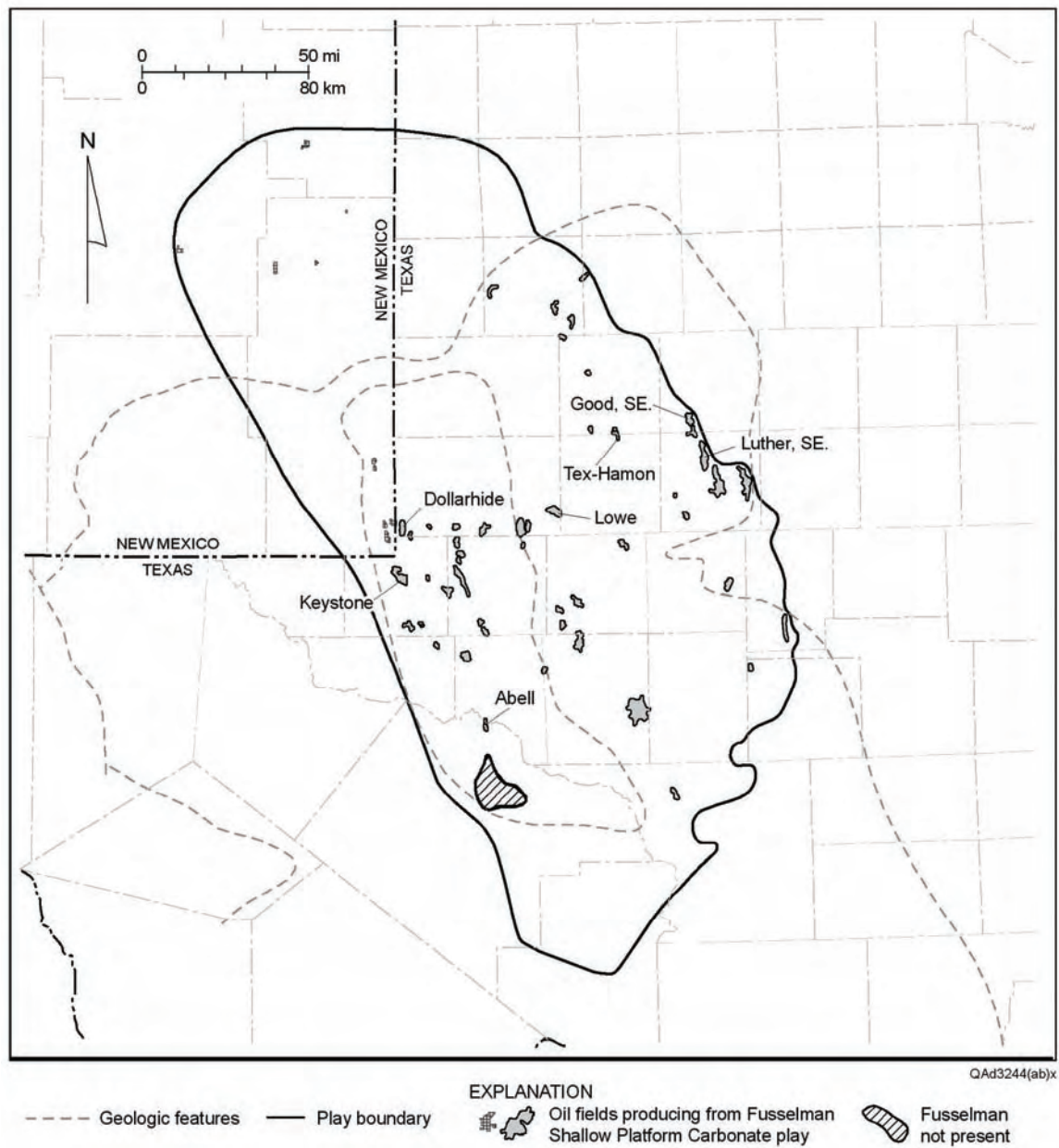


Figure 11. Map of West Texas and New Mexico showing location of Fusselman reservoirs, from which more than 1 MMbbl of oil has been produced (as of 1/1/2000). Cross sections are illustrated in figures 5 and 6. From Dutton and others (2005).

THE WRISTEN OF THE PERMIAN BASIN:
EFFECT OF TECTONICS ON PATTERNS OF DEPOSITION, DIAGENESIS, AND
RESERVOIR DEVELOPMENT IN THE LATE SILURIAN

Stephen C. Ruppel

Bureau of Economic Geology
Jackson School of Geosciences
The University of Texas at Austin
Austin, Texas

ABSTRACT

Rocks of the Upper Silurian Wristen Group display a range in facies and depositional style that contrasts markedly with the more homogeneous character of the underlying Middle to Lower Silurian Fusselman Formation. The Wristen contains distinct (1) shallow-water platform (Fasken Formation) and (2) deeper water, outer platform to slope carbonate facies (Frame and Wink Formations) that document crustal downwarping of the southern margin of the Laurentian paleocontinent during the Middle Silurian.

Deeper water facies of the Frame and Wink Formations dominate the more southerly areas of the Wristen subcrop in the Permian Basin and consist of nodular mudstones and wackestones (Wink) and carbonate debris flows and shales (Frame). Wristen platform facies are assigned to the Fasken Formation and include platform-margin carbonate buildup successions and a complex variety of middle to inner platform facies ranging from small carbonate buildup facies to skeletal wackestones and packstones to tidal-flat complexes.

Hydrocarbon reservoirs are restricted to the Fasken Formation; more than 1.2 billion barrels of oil has been produced. A large volume of oil (more than 1.8 billion barrels) remains as a target for improved characterization of reservoir facies and architecture. The models and data presented here provide an important basis for better understanding of this complex depositional system.

INTRODUCTION

The Silurian of the Permian Basin constitutes a thick section (as much as 2,000 ft) of carbonate platform, platform-margin, and slope rocks. Most of this section (locally as much as 1,800 ft) is assigned to the Upper Silurian Wristen Group (fig.1), from which more than 1.2 billion barrels of oil had been produced as of 2000 (Dutton and others, 2005). Despite the economic significance of this reservoir play, relatively little detailed information exists regarding its stratigraphy, lithology, and reservoir character. This report documents the depositional and diagenetic history of the Wristen on the basis of available data and describes the controls on reservoir development, distribution, and heterogeneity.

PREVIOUS WORK

Early stratigraphic studies of Silurian rocks in West Texas (Jones, 1953; Galley, 1958) generally subdivided the Silurian and Devonian section in the Permian Basin into three parts: a lower Fusselman Formation, an overlying, unnamed “Silurian/Devonian” (or “Siluro-Devonian”) carbonate section, and an uppermost Woodford Formation. Wilson and Majewske (1960) recognized some of the distinctive differences between Silurian and Devonian depositional units, and McGlasson (1967) published a very accurate characterization of the basic architecture and character of these units. Hills and Hoenig (1979) formally named the component depositional units within the Siluro-Devonian. They assigned the term “Wristen” for the post-Fusselman/pre-Devonian part of the section. They further subdivided the interval locally into an upper Frame Member and a lower Wink Member. Ruppel and Holtz (1994) elevated the Wristen to group rank and the Frame and Wink to formation status. They also defined the Fasken Formation to represent the extensive oil-bearing succession of platform carbonates in the Wristen Group (fig. 1). Canfield (1985) presented an excellent analysis of the Frame and Wink facies. Barrick (1995) demonstrated, on the basis of conodont biostratigraphy, that the Wristen Group is dominantly Wenlockian to Pridolian (Late Silurian) (fig. 1). Ruppel and Holtz (1994) also provided detailed documentation on the extent and geological character of the Wristen, along with information on the reservoir attributes of producing Wristen fields in the Permian Basin.

REGIONAL SETTING

The Late Silurian (Wenlockian to Pridolian) was a period of significant global variability in terms of climate, sea level, and ocean chemistry. During the Late Ordovician and Early Silurian, icehouse conditions, caused by episodic advance and retreat of glacial ice in Gondwana (what is now Africa and South America), prevailed. This setting is well documented by numerous globally correlative unconformities in Early Silurian platform deposits (Caputo, 1998). Glaciation diminished during the Middle Silurian, and by the end of the period a greenhouse climate appears to have prevailed. Global paleogeographic reconstructions indicate that during the Silurian the U.S. Midcontinent was part of a broad, subtropical platform that occupied much of the western part of the Laurentian paleocontinent (fig. 2). In the Early Silurian, the area of the Permian Basin was bordered on the south by the Iapetus Ocean. Continuing collision between the Baltic and Laurentian plates along this margin during the Late Silurian resulted in closure of the Iapetus by the beginning of the Devonian. Deposits of the Wristen Group reflect the interplay between climatic, eustatic, and global tectonic drivers in the Permian Basin area during the Middle and Late Silurian.

In contrast to the underlying Late Ordovician to Early Silurian Fusselman Formation, which displays relatively widespread facies continuity indicating deposition on a regionally extensive, more-or-less flat platform, Wristen Group rocks display regional systematic variations in facies that document major tectonic downwarping and drowning of the platform in the Permian Basin area (Ruppel and Holtz, 1994; Ruppel and Hovorka, 1995). This downwarping of the distal part of the platform appears to have begun during the early Wenlockian (fig. 3B). Drowning is indicated by the shift from extensive shallow-water platform deposition reflected in the underlying Fusselman. A tectonic mechanism is implicated by the absence of evidence of a major world-wide eustatic rise event at this time (McKerrow, 1979; Johnson and others, 1998). Differential subsidence is documented by the rapid shift to outer platform and slope deposition in the southern part of the Permian Basin area while shallow-water platform conditions were maintained in the north. Successions in Oklahoma and the Illinois Basin show similar facies and subsidence patterns (Becker and Droste, 1978; Amsden and Barrick, 1988; Droste and Shaver, 1987). Further support for a tectonic subsidence event comes from a subsidence analysis of the Illinois Basin succession by Heidlauff and others (1986). Downwarping of the Fusselman platform in Texas, and equivalent successions in Oklahoma and the Illinois Basin, may have

been a product of foreland deformation along the southern margin of the North American plate associated with plate convergence and the closing of the Iapetus Ocean. Walper (1977) suggested that convergence of the North American and South American/African plates began as early as the Late Ordovician.

Drowning of the southern part of the platform was associated with the deposition of deep-water ramp/outer platform sediments of the Wristen Group (Wink and Frame Formations). These rocks contrast with the shallow-water platform Wristen Group deposits (Fasken Formation) that accumulated in the northern part of the area (fig. 3C). Deeper water Wink and Frame deposits document a classic drowning succession with outer ramp nodular wackestones and mudstones of the Wink Formation being overlain by more distal, deeper water, carbonate mudstones and shales of the Frame Formation. The increasing abundance of skeletal debris, in many cases in the form of carbonate turbidites, upward and northward in the Frame section attests to the aggradation of the Fasken platform to the north and downslope transport of platform material southward into the basin. Despite the evidence of basinward transport of platform-derived carbonate detritus, however, facies geometries in the Fasken and Frame Formations indicate that relatively little progradation occurred during Middle to Late Silurian Wristen Group deposition. Platform-margin buildups in the Fasken, for example, exhibit predominantly aggradational geometries and are confined to a relatively narrow belt through central Andrews County (Ruppel and Holtz, 1994; Ruppel and Hovorka, 1995).

The Middle to Late Silurian was punctuated on the Wristen platform by episodic rise and fall of relative sea level similar to that which affected Fusselman deposition. This cyclicity is reflected in both repetitive, upward-shallowing facies stacking patterns, recording sea-level rise and selectively leached cycle tops, associated with sea-level fall. Although Middle to Late Silurian eustasy is presently poorly defined, evidence from the Wristen platform succession suggests a record similar to that observed in the Early Silurian (Ruppel and Holtz, 1994).

Sedimentologic and stratigraphic relationships between the Wristen Group and overlying Lower Devonian Thirtyone Formation suggest that a major rise in relative sea level or major change in ocean chemistry or circulation occurred in West Texas and New Mexico in Early Devonian time (Ruppel and Holtz, 1994). Relative rise is suggested by the distinctly deeper water character of basal Thirtyone Formation chert-rich deposits compared with immediately underlying Wristen Group carbonates rocks. This is especially apparent in central Andrews

County (Andrews South field, for example), where deeper water Thirtyone chert deposits overlie Fasken reef successions (F. J. Lucia, personal communication, 1992; Canter and others, 1992; D. Entzminger, personal communication, 2005). A similar relationship is observed farther basinward where basal Thirtyone shales, and carbonate-chert mudstones of pelagic origin, sharply overlie more proximal deep-water deposits of the Frame Formation. The causes of this relative rise in sea level are uncertain. Evidence of global sea-level rise at this time is equivocal (cf., Vail and others, 1977; McKerrow, 1979). It seems more likely that deepening at the Silurian-Devonian boundary in West Texas may be in part related to a second pulse of foreland deformation associated with the continued convergence of the Laurentian and Gondwanan plates and the closure of the Iapetus Ocean.

FACIES AND SEDIMENTOLOGY OF THE WRISTEN GROUP

The Wrysten Formation was designated by Hills and Hoenig (1979) for Silurian rocks overlying the Fusselman and underlying Devonian rocks assigned to the Thirtyone Formation (fig. 1). Hills and Hoenig (1979) divided the formation into a basal Wink Member, an overlying Frame Member, and an unnamed “carbonate facies” (which is laterally equivalent to the Wink and Frame). Because of the importance of the unnamed carbonate unit in terms of its thickness and importance as a major hydrocarbon-producing reservoir interval, Ruppel and Holtz (1994) assigned the name Fasken Formation to this unit. They also elevated the Wink and Frame Members to formation status and the Wrysten to group status (fig. 1).

Studies of the Fusselman Formation suggest that the contact between the Wrysten Group and the underlying Fusselman Formation is unconformable. Preliminary studies of the conodont faunas across this boundary (Barrick, 1995) indicate, however, that the unconformity does not represent a major hiatus. This conclusion is supported by regional data that suggest a short-duration exposure event (Amsden and Barrick, 1988).

The Wrysten is overlain by the Lower Devonian Thirtyone Formation, except where the latter has been removed by erosion. This contact is commonly sharp, but it is unclear whether it represents a hiatus. Recent biostratigraphic studies have in fact shown that the top of the Frame Formation is Early Devonian in age (Barrick, 1995). This age assignment implies that the Fasken (the apparent updip equivalent of the Frame) is also of Early Devonian age at its top. Although some authors have suggested a major sea-level fall the end of the Silurian from world-wide data

(for example, Vail and others, 1977; Johnson and others, 1998), data from the Frame appear to contradict this notion. There is abundant evidence of karsting within the Fasken, but these features are usually developed where the Thirtyone has been removed. So it seems more likely that karsting of the Fasken is a younger event (perhaps Middle Devonian).

The Wristen subcrop margins are controlled by postdepositional erosion on the west (Baldonado and Broadhead, 2002), north, and probably east. Wristen rocks are thickest in western Gaines and Andrews Counties, Texas, and southeastern Lea County, New Mexico. According to Canter and others (1992) the Wristen reaches a maximum thickness of more than 1,500 ft in southeastern Lea County, New Mexico (fig. 4).

Wink Formation

Distribution and Age

The Wink Formation overlies the Fusselman across most of the southern half of the Silurian subcrop area (fig. 5). The Wink is relatively easily definable using gamma-ray wireline logs in this area where it and the Frame Formation underlie the Thirtyone Formation (Hills and Hoenig, 1979). Northward in central Andrews County, the Wink is difficult to distinguish from the Fasken Formation (fig. 5). In the mapped area (fig. 6) the Wink ranges from less than 50 ft in the southeastern part of the area to about 300 ft in the north where it grades into the Fasken.

On the basis of conodonts, Barrick (1995) showed that the Wink is Early Upper Silurian (Wenlockian) in age and equivalent to the Clarita Formation in Oklahoma (Amsden, 1980).

Facies

Hills and Hoenig (1979) defined the Wink as a gray limestone. Examination of cores indicates that these rocks are characteristically nodular-bedded, gray, lime wackestones and mudstones (fig. 7; Ruppel and Holtz, 1994). Thin-walled brachiopods and ostracodes are locally common, but other skeletal allochems are rare. The Wink contains small volumes of terrigenous clay and silt, which, as is apparent on gamma-ray logs (fig. 8), generally increase upsection as it grades into the siltier and more argillaceous Frame Formation. Canfield (1985) divided the Wink into a lower limestone section composed of skeletal packstones and wackestones and an upper dolostone unit dominated by silt-bearing wackestones.

Depositional Setting

Nodular wackestones and mudstones of the Wink Formation (fig. 7) represent deposition in outer platform, probably below-wave-base, conditions. These deposits document the beginning of drowning of the extensive shallow-water Fusselman platform during the Middle Silurian. As discussed earlier, this drowning was associated with the formation of a well-developed, platform-to-basin topography whose geometry controlled deposition for much of the remainder of the Silurian and the Early Devonian (Ruppel and Holtz, 1994).

Subsurface Recognition and Correlation

In cores, the Wink is usually readily distinguishable from the underlying Fusselman by its darker colored, more mud-rich, commonly nodular character and its sparser faunal content. The lighter colored Fusselman typically contains abundant pelmatozoan ossicles and much more grain-rich texture. The contact between the Wink and the Fusselman is also relatively easily defined on wireline logs. In most areas, the base of the Wink consists of a shaly mudstone whose high gamma-ray character makes recognition and correlation of this contact straightforward (fig. 8). The upper contact of the formation is more problematic. The upward-deepening nature of the Wink is marked on logs by a gradual upward increase in gamma-ray log response, reflecting an increase in mud-dominated facies and shale. The base of the overlying Frame is typically placed at the first occurrence of high-gamma-ray shales and mudstones (fig. 8).

Frame Formation

Distribution and Age

The Frame Formation (in part, the “Silurian shale” of some earlier workers) overlies the Wink and exhibits essentially the same distribution pattern as the latter (fig. 9). The unit can be recognized as far north as central Andrews County, where it grades into the Fasken Formation (fig. 5). It reaches maximum thicknesses of about 700 to 800 ft in this area (fig. 9). Like the Wink, the Frame is thinnest in the southeast.

Graptolite data (Decker, 1952) suggest that the Frame is probably equivalent to the Henryhouse Formation (Hunton Group) in Oklahoma and the Texas Panhandle (Amsden, 1980).

As mentioned, new conodont data (Barrick, 1995) show that the Frame ranges in age from Late Silurian to Early Devonian (Ludlovian-Lochkovian) (fig. 1).

Facies

According to Hills and Hoenig (1979) the Frame is largely shale in the type area in Pecos County. In much of the subcrop area, however, the unit consists of greenish-brown, argillaceous lime mudstone and wackestone (fig. 10d); fragments of pelmatozoans and pentamerid brachiopods are locally common, along with ostracodes and trilobites (Ruppel and Holtz, 1994). Also common, are rocks containing interlaminated mudstone and skeletal packstone-grainstone; some grain-rich intervals display normal graded bedding (fig. 10a,b). Less common are breccias and conglomerates but locally present (fig. 10d).

Depositional Setting

The muddy texture and general scarcity of skeletal remains in Frame Formation rocks indicate that they were formed in deep water, below wave-base conditions, probably representative of a slope or basinal setting. Beds of graded and laminated skeletal debris represent gravity flows of shallow-water skeletal sands derived from the Fasken shallow-water carbonate platform to the north (Ruppel and Holtz, 1994). Mapping of shale/carbonate fractions in the Wristen (McGlasson, 1967; Hills and Hoenig, 1979) suggests that the deepest part of the basin during Frame deposition probably lay along a north-trending axis through Pecos County, where predominantly shales accumulated. Areas surrounding this central basin received sand- to silt-sized carbonate detritus derived from surrounding areas of carbonate platform development.

Subsurface Recognition and Correlation

The Frame is distinctly different from either the underlying Wink or the updip Fasken. Because of the presence of clay-rich mudstones and shales, the Frame exhibits a high but variable gamma-ray response in most distal settings (fig. 8). In more proximal areas near the Fasken platform, the Frame contains platform-derived debris and interbedded shallower water deposits. Even in these settings the Frame tends to be distinguished from the overlying Fasken or Devonian Thirtyone Formations by its relatively higher gamma-ray response (fig. 5).

Fasken Formation

In their original definition of the Wristen Formation, Hills and Hoenig (1979) referred to the thick, predominantly carbonate unit that constitutes the post-Fusselman Silurian in the northern part of West Texas and New Mexico as simply the “carbonate facies” of the Wristen Formation. Recognizing the importance of this unit, which contains all of the known hydrocarbon resources in the Wristen, Ruppel and Holtz (1994) named this unit the Fasken Formation. They designated three co-type sections for the Fasken in wells in Andrews County, Texas. All of these wells have long cored intervals and comprehensive suites of wireline logs that illustrate some of the significant lithologic diversity that characterizes this rock unit.

Distribution and Age

The Fasken, as defined by Ruppel and Holtz (1994), consists of most of what has historically been referred to as the Siluro-Devonian carbonate section in the Permian Basin. The Fasken is typically underlain by the Frame Formation but also represents the northern, updip, shallow-water platform facies equivalent of the Frame Formation (fig. 5). The gradational lateral contact between the two units runs generally east-west through central Andrews County, Texas (fig. 4). Ruppel and Holtz (1994) showed that the Wink undergoes similar facies change to the north and may also be best considered in part a deeper water facies equivalent of the Fasken (fig. 5).

Where separable from the underlying Fusselman, the Fasken exhibits an east-to-west thickening trend. The unit reaches thicknesses of more than 1,500 ft in extreme western Andrews County and eastern Lea County, New Mexico (Canter and others, 1992; Ruppel and Holtz, 1994) and thins to less than 200 ft in Dawson County. Thickening trends are clearly defined by the total Fasken isopach map (fig. 11). Throughout most of the region, the Fasken is overlain by the Woodford Formation. Locally, where the Woodford has been removed by late Paleozoic erosion, the Fasken is overlain by Pennsylvanian/Permian clastics and carbonates.

The age of the Fasken Formation is imprecisely known. Recent conodont studies have shown that the Wristen Group ranges from Middle Silurian (Wenlockian) to Early Devonian (Barrick, 1995). This is consistent with previous interpretations that the Fasken (“Siluro-Devonian” of many earlier workers) contains a Middle Silurian-age (Niagaran) fauna. Part of the shallow-water platform succession that is assigned to the Fasken in this report has

also yielded Lower and Middle Devonian fossils (Wilson and Majewske, 1960). These isolated occurrences apparently document outliers or remnants of the eroded Thirtyone Formation carbonate platform facies. The shallow-water platform Fasken succession is probably represented in part by the Henryhouse Formation in Oklahoma. Although much of the Henryhouse is interpreted as deeper water (Barrick, 1995), the shallower water *Kirkidium* facies of the Henryhouse contains facies very similar to those of the Fasken, as does the Bois D'Arc Formation (a facies of the overlying dominantly deep-water Haragan Formation). A strikingly similar succession of Late Silurian-age (Ludlovian to Pridolian) platform and platform-margin carbonates also exists in the Illinois Basin (Becker and Droste, 1978; Droste and Shaver, 1982, 1987).

Facies

The Fasken Formation comprises a highly diverse assemblage of carbonate lithofacies. The unit can be subdivided into two general facies complexes: (1) platform-margin skeletal wackestones to grainstones and boundstones and (2) interior platform mudstones to pellet and skeletal wackestones to grainstones (Ruppel and Holtz, 1994).

A typical outer platform and platform-margin succession is illustrated in the type section for the Fasken Formation near the Hutex field area in southeastern Andrews County (fig. 12). The base of the cored interval in this well contains dark-colored skeletal wackestones that contain poorly sorted skeletal debris including stromatoporoids, corals, and pelmatozoans (fig. 13). These rocks pass upward into a section of wackestones that contain more abundant and larger fragments of stromatoporoids and corals (including *Halysites*). Stromatoporoids comprise both broken hemispherical forms that display all orientations and thin, laminate stromatoporoids in growth position (fig. 13a,b,c). Overlying these rocks are pelmatozoan/stromatoporoid packstones (fig. 13d). Pelmatozoan debris is well sorted, but stromatoporoids are variable in size throughout the unit. Locally, these deposits are interbedded with beds and lenses of ooid grainstone. These rocks are succeeded by a thin interval of relatively well sorted coral/bryozoan rudstone that exhibits considerable interparticle porosity (fig. 14a). The Fasken is capped in this section by coral framestone composed of small stick corals, bryozoans, and relatively uncommon stromatoporoids. These deposits contain geopetal cavities filled with sediment and, less commonly, cement (fig. 14c,d). Locally, these buildups are capped by ooid grainstone. Fasken

platform-margin buildups in Texas and New Mexico are similar to well-described outcropping Silurian buildups in the Illinois Basin in terms of both facies patterns and fauna (Lowenstam, 1948, 1950; Ingels, 1963; Wilson, 1975).

Across most of the Wristen platform, especially in the northern part of the area (Gaines County and northward), major buildup successions are less common (Ruppel and Holtz, 1994). In these areas, Fasken facies comprise diverse assemblages of shallow-water platform carbonate facies. The upper Fasken is typically composed of upward-shallowing, shallow subtidal to tidal-flat cycles (fig. 15). The basal subtidal facies in these cycles, which average 15 to 20 ft in thickness, are composed of skeletal wackestones containing stromatoporoids, corals, mollusks, and brachiopods (fig. 16a). Tidal-flat caps are laminated and mud rich and locally contain fenestral pores (fig. 16b). The lower Fasken contains a series of boundstone-capped cycles composed generally of more mud-dominated rocks at the base and increasingly grain-dominated deposits upward (fig. 17). Capping boundstones in these 30- to 35-ft-thick cycles are thin and, in some instances, are overlain by silt/clay-filled karst solution pit deposits. In a second core succession, less than 1 mi away, the facies are strikingly different. Here the Fasken is composed of a cyclic succession of upward-shallowing, subtidal to tidal-flat carbonates (fig. 17). Cycles show evidence of early dolomitization and porosity retention much like those of the Permian Clear Fork, San Andres, and Grayburg platform successions. Some of these cycles, which are more variable in thickness than boundstone-capped cycles, exhibit karst/solution profiles in their upper parts that contain collapse breccia and infilling, green mudstone/siltstone. Porosity is typically highest below karsted tidal-flat caps and generally decreases downsection (Ruppel and Holtz, 1994).

Depositional Setting

Fasken facies successions are typical of those found on shallow-water carbonate platforms. The margins of the Middle to Late Silurian Wristen platform are well defined by the change from platform facies of the Fasken to outer platform to slope, clay-rich facies of the Frame and Wink (figs. 3, 18). North and west of this margin, the outer part of the platform is marked by the presence of organic reef complexes (fig. 12). Because of the limited availability of cores through these complexes, understanding of their paleoenvironmental setting and facies

geometries is greatly facilitated by comparisons with the well-exposed, outcropping Silurian reefs of the Illinois Basin of Indiana and Illinois (Lowenstam, 1948, 1950; Ingels, 1963).

Like their Illinois Basin counterparts, Fasken Formation buildup deposits (e.g., fig. 12) typically overlie basal mudstones and sparse wackestones (Ruppel and Holtz, 1994). These mud-rich rocks are gradational to proximal Frame Formation deposits in facies and depositional setting and accumulated in a below-wave-base setting on the outer ramp. Overlying silt-sized skeletal packstones and wackestones represent the first indication of reef-influenced sedimentation. Thin, delicate, laminar stromatoporoids also indicate accumulation below fair-weather wave base (fig. 13b,c). Blocks and clasts of hemispherical stromatoporoids and corals common in these rocks document erosion and downslope transport from adjacent, shallow-water portions of the buildup complex, presumably due to storm activity (fig. 13b,d). Such debris beds are relatively uncommon in Illinois Basin buildups (Wilson, 1975). Pelmatozoan grainstones and packstones in Fasken buildup complexes (fig. 13d) represent skeletal debris derived from reef-top dwelling organisms. Such flanking encrinites are ubiquitous in Silurian, as well as other Paleozoic, buildup successions (Wilson, 1975). These encrinites, which may account for more than half of each buildup, can accumulate either above or slightly below wave base. Coral/bryozoan rudstones encountered in the upper parts of many Fasken buildup successions (fig. 14a) represent reef rubble produced by active erosion of the upper proximal reaches of the reef complex and deposited in relatively shallow water. Similar rubble beds have been documented at the tops of other Silurian buildups (Lowenstam, 1948). Coral framestone, which forms the top of some successions (fig. 14c), represents growth of the reef into wave base and the development of extensive and diverse reef faunas. Subsequent vertical growth of these buildups produces shoaling and lateral and basinward progradation of the reef complex (Wilson, 1975). Ooid grainstones encountered at the tops of some sections document aggradation, shoaling, and the end of buildup growth. By analogy with well-studied structures in Indiana and Illinois, depositional relief on Fasken platform-margin buildups may have reached as much as 130 to 220 ft (Wilson, 1975). On the basis of data from Silurian outcrops in the Illinois Basin, Ingels (1963) developed a model of buildup architecture that may be representative of platform-margin buildups in the Fasken. As this model shows (fig. 19A), the buildup complex is dominated by flanking debris; core boundstones are volumetrically minor. These features and the

general dimensions of this model seem to fit well with the known data on Fasken platform-margin successions like those in the Magutex and Hutex field areas (fig. 12).

Buildups are also common in the Wristen inner platform. However, these features are smaller in terms of both vertical relief and lateral dimensions (Ruppel and Holtz, 1994). Like smaller, inner platform buildups in the Illinois Basin (fig. 19B), Fasken shallow-platform buildups rarely contain framestone but are more typically dominated by skeletal wackestone. These rocks reflect lower energy deposition on the inner platform and suggest that platform-margin buildups acted as a partial baffle to wave energy. It should be emphasized, however, that there is no indication that any continuous shelf-margin rim was developed along the platform margin. Tidal-flat successions are locally developed across the platform probably associated with local paleotopographic highs. Sedimentation in the inner platform was in part controlled by episodic rise and fall of relative sea level. This is apparent from patterns of facies stacking and diagenesis (see below) in both tidal-flat and shallow-water subtidal sequences and somewhat deeper water, more grain-rich, buildup-associated sequences developed on the outer parts of the platform (figs. 15 and 17).

Diagenesis

The most apparent products of diagenetic alteration of the Fasken Formation are (1) dolomite and (2) karst-related, solution features. Examination of these features in the Fasken suggests that these two products are process related.

Previously published maps displaying the distribution of limestone versus dolostone in the Fasken Formation suggest the section is entirely dolostone (McGlasson, 1967, his fig. 8; Wright, 1979, his fig. 10). This interpretation is misleading, for although dolostone is present throughout most of the Fasken, limestone is also present in many sections (for example, figs. 12, 15, and 17). Because virtually all of the hydrocarbon production from the Fasken comes from dolomitized intervals, an appreciation of the distribution and origins of dolomite in these rocks is critical. Both matrix-replacive dolomite and pore-filling dolomite cement are common. Much of the dolomite is associated with hiatuses caused by relative-sea-level lowstand. Dolostone is most abundant below cycle tops, especially those that display solution or karst features, and decreases downsection (fig. 15). Although the timing of dolomitization cannot be unequivocally demonstrated, much of the dolomite may have formed soon after leaching (that is,

penecontemporaneously). Additional dolomite may have been precipitated at subsequent successive, lowstand events, fluid access being gained by karst pipes and channels.

Dolostones at the top of the Fasken section retain little or no original structure or texture. These rocks, which are overlain by the Upper Devonian Woodford Formation, may have undergone multiple episodes of postdepositional leaching and diagenesis during the more than 20 million years represented by this regional Middle Devonian hiatus. These multiple episodes of overprinting diagenesis have resulted in a wide variability in pore development at the top of the Fasken; solution vugs and molds are especially common.

Throughout the remainder of the Fasken inner platform section where fabric-retentive dolomite is dominant, porosity is composed of skeletal molds (for example, fig. 16a) and less common interparticle (largely intercrystalline) pores. However, where multiple episodes of leaching and dolomitization have occurred and fabric has been destroyed, vuggy and intercrystalline pores similar to those observed at the top of the section are common.

Solution-collapse and karst breccia horizons are common in the Fasken (Ruppel and Holtz, 1994). Some of these features appear to have formed associated with exposure at individual intraformational Fasken lowstands. However, many may be related to longer duration, post-Fasken lowstand events. For example, at Emerald field (Gaines County, Texas), karst features are found immediately below the Wristen a few feet below the overlying Woodford. This succession of cave-roof and cave-fill features was most likely formed during the Middle Devonian (Entzminger and Loucks, 1992). Cave-fill breccias of this sort are typically composed of poorly sorted, polymict clasts in a matrix of silt, glauconite, and carbonate mud (fig. 16c). Breccia zones may be found as much as 100 ft below the top of the Fasken. These karst features are probably very similar in origin and age to those developed in the Fusselman in the Franklin Mountains of West Texas and New Mexico (McGlasson, 1967). (Note that outcrop Fusselman sections are equivalent to both Wristen and Fusselman subsurface units.)

Subsurface Recognition and Correlation

Fasken facies associations are distinctly different from those of the Wink or the Frame, so these units are easily distinguished in cores. Wireline log distinction is also usually obvious. The shallow-water carbonates of the Fasken usually display a low gamma-ray response that contrasts

with the typically much higher gamma-ray values in the laterally equivalent Frame and underlying Wink caused by the presence of clay-rich carbonate mud (fig. 5).

Distinction of the Fasken from the Devonian Thirtyone Formation is locally problematic, especially along the updip subcrop limit of the latter where chert is relatively minor. Gamma-ray signatures in both are generally low, making distinction problematic. An understanding of the areal extent of the two formations is perhaps the best guide to their separation. In actuality, the two only coexist along a narrow band in southern Andrews County.

Where the Wink and Frame are absent (north and west of the Fasken/Frame facies transition area), the Fusselman is difficult to distinguish from the overlying Fasken Formation (fig. 5).

Sequence Stratigraphy of the Wristen Group

Core studies demonstrate that the Wristen Group in the Permian Basin is at least locally cyclic. As discussed above, some Fasken core successions reveal patterns of cyclicity and facies stacking that resemble middle Permian carbonate platform successions, which were also formed in transitional icehouse-greenhouse conditions, in terms of cyclicity and facies stacking patterns. However, documentation of the cycle- and sequence-scale stratigraphy of the Wristen remains scanty.

Two efforts have been made to develop a subregional sequence-stratigraphic framework for the Wristen (Canter *et al.*, 1992; Baldonado and Broadhead, 2002). However, both of these studies relied on wireline log correlations, none of which was supported by rigorous log calibration to cores, seismic, outcrops, or other depositional models. Experience with the Wristen and other carbonate platform successions in the Permian Basin illustrates that wireline logs are not a reliable basis for correlation unless used in conjunction with and closely calibrated to cores and outcrop models. Further work is needed before a useable sequence stratigraphy of the Wristen can be developed. Global studies of Middle and Upper Silurian stratigraphy suggest that the Wristen Group may constitute as many as four depositional sequences (fig. 4). Considering the potential impact of sea-level rise/fall events on depositional facies architecture and diagenesis, an improved understanding of the sequence stratigraphy of the Fasken is crucial to developing improved models for reservoir development in the Permian Basin.

Reservoir Development

Wristen platform reservoirs are assigned to the Wristen Buildups and Platform Carbonate play (Dutton and others, 2005). All of these reservoirs are productive from carbonates of the Fasken Formation of the Wristen Group. According to Dutton and others (2005), 85 reservoirs have produced more than 1 million barrels from this play through 2002. Total production from the play, as of 2000, stands at 889 million barrels (Dutton and others, 2005).

Reservoir Distribution

Wristen Group reservoirs are restricted to the northern part of the area where the Fasken Formation subcrops (fig. 20); the deeper water equivalent Frame and Wink Formations of the Wristen are not productive. The Woodford forms the top seal and probable source for nearly all of these reservoirs. Reservoirs are developed in two settings: (1) in platform-margin buildup successions along the Wristen platform margin in central Andrews County (for example, Magutex, Hutex, and Fullerton fields) and (2) in highly diverse shallow-water facies in the interior of the Wristen platform. In both instances, the reservoirs are predominantly localized over structural traps and sealed by the Woodford Formation.

Porosity Development

Porosity in Fasken Formation reservoirs is a function of both original depositional setting and diagenesis. In platform-margin buildups (for example, at Magutex and Hutex fields), two main styles of porosity development exist. Primary, intergranular porosity is observed locally in buildup grainstones (both skeletal and ooid grainstones) on the outer platform (fig. 14a,b). In inner platform, nonbuildup successions, porosity is typically moldic and intercrystalline, associated with leaching of allochem-rich intervals. As is the case with the Fusselman, leaching seems to be due to multiple exposure events both during and after Fasken deposition. Porosity development in many reservoirs is clearly related to these exposure events (for example, Fullerton field), as probably is dolomitization. Porosity in such reservoirs is commonly composed of moldic and intercrystalline pores whose distribution is in most cases controlled by original depositional facies.

The Fasken is also productive from reservoirs that exhibit more fabric-destructive diagenesis similar to that which is common at the top of the Fusselman Formation. Like the

Fusselman, porosity in these reservoirs is typically composed of vugs and intercrystalline pores in dolomite. This type of reservoir development is usually restricted to the top of the Fasken section (e.g., Little Lucky Lake field, Chaves County, New Mexico). These leached zones are the result of exposure, and in most cases later dolomitization, following Fasken deposition and are locally developed in both platform-margin buildup successions and inner platform sequences. In some cases, dissolution associated with the post-Wristen unconformity affects the Fasken to depths of many tens to hundreds of feet (for example, Fullerton field). In many instances the result of this dissolution is the development of solution-cavity and cave successions similar to those documented in Lower Ordovician Ellenburger reservoirs (Kerans, 1988; 1989; Loucks, 1999, 2003). Reservoirs in which dissolution has penetrated deep in the section are commonly those situated on major structural highs.

Traps, Seals, and Sources

Most Wristen reservoirs are formed by simple or fault-modified anticlinal closure. Examples of this structure include essentially all of the larger fields—for example, Fullerton, Hutex, Magutex, and Breedlove. In nearly all documented cases, productive Fasken reservoirs are overlain by the Upper Devonian Woodford Shale. This finding suggests that where the Woodford has been removed by erosion, younger strata have proved ineffective top seals. Studies of source rocks and reservoir oil character suggest that Fasken reservoir oil was sourced from the overlying Woodford (Williams, 1977). This interpretation also implies that Fasken productivity is tied directly to the presence of the Woodford.

Opportunities for additional resource recovery

Ruppel and Holtz (1994) determined that Fasken (Wristen Group) reservoirs contain more than 750 million barrels of remaining mobile oil. This large remaining oil resource is a function of the low average recovery efficiency (28%) characteristic of the play and the fact that the Fasken is one of the most poorly known carbonate reservoir successions in the Permian Basin. The low recovery efficiency indicates that the Fasken possesses a great deal of geological heterogeneity. Unfortunately, the data needed to define this heterogeneity are severely limited. The relative scarcity of cores and the absence of detailed outcrop or reservoir studies make construction of effective models for the distribution, geometry, and character of reservoir facies

difficult. There is great potential for markedly increasing the hydrocarbon recovery from existing Fasken fields and defining areas of probable untapped accumulation once detailed geological studies become available. The Fasken succession represents perhaps the most ignored plays in the Permian Basin. As such, it offers possibly the highest potential return on characterization and investment of all the reservoir plays in the basin.

SUMMARY AND CONCLUSIONS

The Wristen Group of the Permian Basin comprises a diverse assemblage of dominantly carbonate facies that reflect (1) the reshaping of the southern margin of the Laurentian paleocontinent by forces associated with the closing of the Iapetus Ocean and (2) high-frequency sea-level rise and fall events associated with waning but still active glaciation in Gondwana. The Wristen consists of two broad paleotopographic realms: a southern region characterized by fine-grained, deeper water carbonate mudstones and shales (Wink and Frame Formations), and (2) a northern shallow-water platform carbonate (Fasken Formation). All of the known hydrocarbon production in the Permian Basin has come from shallow-water platform facies of the Fasken Formation. Fasken rocks display considerable diversity ranging from platform-margin carbonate-buildup successions to interior platform tidal flats. Porosity development is a function of depositional textures and overprinting diagenesis, including dolomitization and karsting. Although the basic elements of Fasken facies and rock-fabric diversity can be defined from existing core investigations, additional, more detailed, rock-based studies are needed to adequately characterize reservoir architecture and controls of porosity and permeability development if more effective methods for the recovery of the remaining oil in these reservoirs are to be developed.

REFERENCES

- Amsden, T. W., 1980, Hunton Group (Late Ordovician, Silurian, and Early Devonian) in the Arkoma Basin of Oklahoma: Oklahoma Geological Survey Bulletin 129, 136 p.
- Amsden, T. W., and Barrick, J. E., 1988, Late Ordovician through Early Devonian annotated correlation chart and brachiopod range charts for the southern Midcontinent region, U.S.A., with a discussion of Silurian and Devonian conodont faunas: Oklahoma Geological Survey Bulletin 143, 66 p.
- Baldonado, D., and Broadhead, R., 2002, Preliminary investigation of the regional stratigraphy of Siluro-Devonian carbonates, Tobosa Basin, New Mexico, *in* Hunt, T. J., and Lufholm, P. H., eds., The Permian Basin: Preserving our past—securing our future: West Texas Geological Society, Publication 02-111, p. 55–69.
- Barrick, J. E., 1995, Biostratigraphy of uppermost Ordovician through Devonian depositional sequences in the Permian Basin, West Texas and Southeastern New Mexico, *in* Pausé, P. H., and Candelaria, M. P., eds., Carbonate facies and sequence stratigraphy: practical applications of carbonate models: Permian Basin Section–SEPM Publication 95-36, p. 207–216.
- Barton, J. M., 1945, Pre-Permian axes of maximum deposition in West Texas: American Association of Petroleum Geologists Bulletin v. 29, no. 9, p. 1336–1348.
- Becker, L. E. and Droste, J. B., 1978, Late Silurian and Early Devonian sedimentological history of southwestern Indiana: Indiana Department of Natural Resources, Geological Survey Occasional Paper 24, 11 p.
- Blakey, R., 2004, Plate tectonics and continental drift: regional paleogeographic views of Earth history: <http://jan.ucc.nau.edu/~rcb7/450NAt.jpg> and <http://jan.ucc.nau.edu/~rcb7/430NAt.jpg>
- Canfield, B. A., 1985, Deposition, diagenesis, and porosity evolution of the Silurian carbonates in the Permian Basin: Texas Tech University, unpublished MS thesis, 138 p.
- Canter, K. L., Wheeler, D. M., and Geesaman, R. C., 1992, Sequence stratigraphy and depositional facies of the Siluro-Devonian interval of the northern Permian Basin, *in*

- Candelaria, M. P., and Reed, C. L., eds., Paleokarst, karst-related diagenesis, and reservoir development: examples from Ordovician-Devonian age strata of West Texas and the Mid-Continent: Permian Basin Section-SEPM, Field Trip Guidebook, Publication No. 92-19, p. 93–109.
- Caputo, M. V., 1998, Ordovician-Silurian glaciations and global sea-level changes, *in* Silurian cycles; linkages of dynamic stratigraphy with atmospheric, oceanic, and tectonic changes: New York State Museum Bulletin, v. 491, p. 15–25.
- Decker, C. E., 1952, Texas graptolites change supposed Devonian zone to Silurian: American Association of Petroleum Geologists Bulletin, v. 36, p. 1639–1641.
- Droste, J. B. and Shaver, R. H., 1982, The Salina Group (Middle and Upper Silurian) of Indiana: Indiana Department of Natural Resources, Geological Survey Special Report 24, 41 p.
- Droste, J. B. and Shaver, R. H., 1987, Upper Silurian and Lower Devonian stratigraphy of the Central Illinois Basin: Indiana Department of Natural Resources, Geological Survey Special Report 39, 23 p.
- Dutton, S. P., Kim, E. M., Broadhead, R. F., Breton, C. L., Raatz, W. D., Ruppel, S. C., and Kerans, Charles, 2005, Play analysis and digital portfolio of major oil reservoirs in the Permian Basin: The University of Texas at Austin, Bureau of Economic Geology Report of Investigations No. 271, 287 p., CD-ROM.
- Entzminger, D. J. and Loucks, R. G., 1992, Paleocave reservoirs in the Wristen Formation at Emerald Field, Gaines and Yoakum Counties, Texas, *in* Candelaria, M. C., and Reed, C. L., eds., Paleokarst, karst-related diagenesis and reservoir development: examples from Ordovician-Devonian age strata of West Texas and the Mid-Continent: Permian Basin Section of SEPM, Publication 92-33, p.126–130.
- Galley, J. E., 1958, Oil and geology in the Permian Basin of Texas and New Mexico, *in* Weeks, L. G., ed., Habit of oil—a symposium: American Association of Petroleum Geologists, Special Publication, p. 395–446.
- Heidlauff, D. T., Hsui, A. T., and Klein, G. de V., 1986, Tectonic subsidence analysis of the Illinois Basin: Journal of Geology, v. 94, p. 779–794.

- Hills, J. M., and Hoenig, M. A., 1979, Proposed type sections for Upper Silurian and Lower Devonian subsurface units in Permian Basin, West Texas: American Association of Petroleum Geologists Bulletin v. 63, no. 9, p. 1510–1521.
- Ingels, J. J. C., 1963, Geometry, paleontology, and petrography of Thornton Reef Complex, Silurian of northeastern Illinois: American Association of Petroleum Geologists Bulletin, v. 47, p. 405–440
- International Commission on Stratigraphy, 2004, International stratigraphic chart: <http://www.stratigraphy.org/>.
- Johnson, M. E., Jiayu, R., and Kershaw, S., 1998, Calibrating Silurian eustasy against the erosion and burial of coastal paleotopography, *in* Silurian cycles; linkages of dynamic stratigraphy with atmospheric, oceanic, and tectonic changes: New York State Museum Bulletin, v. 491, p. 3–13.
- Jones, T. S., 1953, Stratigraphy of the Permian Basin of West Texas: West Texas Geological Society, 57 p.
- Kerans, Charles, 1988, Karst-controlled reservoir heterogeneity in the Ellenburger Group carbonates of West Texas: Association of Petroleum Geologists Bulletin, v. 72, p. 1160–1183.
- Kerans, Charles, 1989, Karst-controlled reservoir heterogeneity and an example from the Ellenburger Group (Lower Ordovician) of West Texas: The University of Texas at Austin, Bureau of Economic Geology Report of Investigations No. 186, 40 p.
- Loucks, R. G., 1999, Paleocave carbonate reservoirs: origins, burial-depth modifications, spatial complexity, and reservoir implications: American Association of Petroleum Geologists Bulletin, v. 83, p. 1795–1834.
- Loucks, R. G., 2003, Understanding the development of breccias and fractures in Ordovician carbonate reservoirs, *in* Hunt, T. J., and Lufholm, P. H., The Permian Basin: back to basics: West Texas Geological Society Fall Symposium: West Texas Geological Society Publication #03-112, p. 231–252.
- Lowenstam, H. A., 1948, Marine pool, Madison County, Illinois, Silurian reef producer, *in* Howell, J. V., ed., Structure of typical American oil fields: p.153–188.

- Lowenstam, H. A., 1950, Niagaran reefs of the Great Lakes area: *Journal of Geology*, v. 58, p. 430–487
- McGlasson, E. H., 1967, The Siluro-Devonian of West Texas and southeast New Mexico, *in* Oswald, D., H., ed., *International Symposium on the Devonian System*, v. II: Alberta Society of Petroleum Geologists, Calgary, Alberta, p. 937–948.
- McKerrow, W. S., 1979, Ordovician and Silurian changes in sea level: *Journal of the Geological Society of London*, v. 136, p. 137–145,
- Ruppel, S. C., and Holtz, M. H., 1994, Depositional and diagenetic facies patterns and reservoir development in Silurian and Devonian rocks of the Permian Basin: The University of Texas at Austin, Bureau of Economic Geology Report of Investigations No. 216, 89 p.
- Ruppel, S. C. and Hovorka, S. D., 1995, Chert reservoir development in the Devonian chert: Permian Basin, Texas: *American Association of Petroleum Geologists Bulletin* v. 79, p. 1757–1785.
- Vail, P. R., Mitchum, R. M., and Thompson, S., III, 1977, Global cycles of relative changes of sea level, *in* Payton, C. E., ed., *Seismic stratigraphy—applications to hydrocarbon exploration*: American Association of Petroleum Geologists, Memoir 26, p. 83–98.
- Walper, J. L., 1977, Paleozoic tectonics of the southern margin of North America: *Gulf Coast Association of Geological Societies Transactions*, v. 27, p. 230–241.
- Williams, J. A., 1977, Characterization of oil types in the Permian Basin: Southwest Section American Association of Petroleum Geologists, Abilene, Texas, unpublished text from oral presentation, 38 p.
- Wilson, J. L., 1975, *Carbonate facies in geologic history*: New York, Springer-Verlag, 471 p.
- Wilson, J. L., and Majewske, O. P., 1960, Conjectured Middle Paleozoic history of Central and West Texas, *in* *Aspects of the geology of Texas: a symposium*: The University of Texas, Austin, Bureau of Economic Geology Publication 6017, p. 65–86.
- Wright, W. F., 1979, Petroleum geology of the Permian Basin: West Texas Geological Society Publication No. 79-71, 98 p.

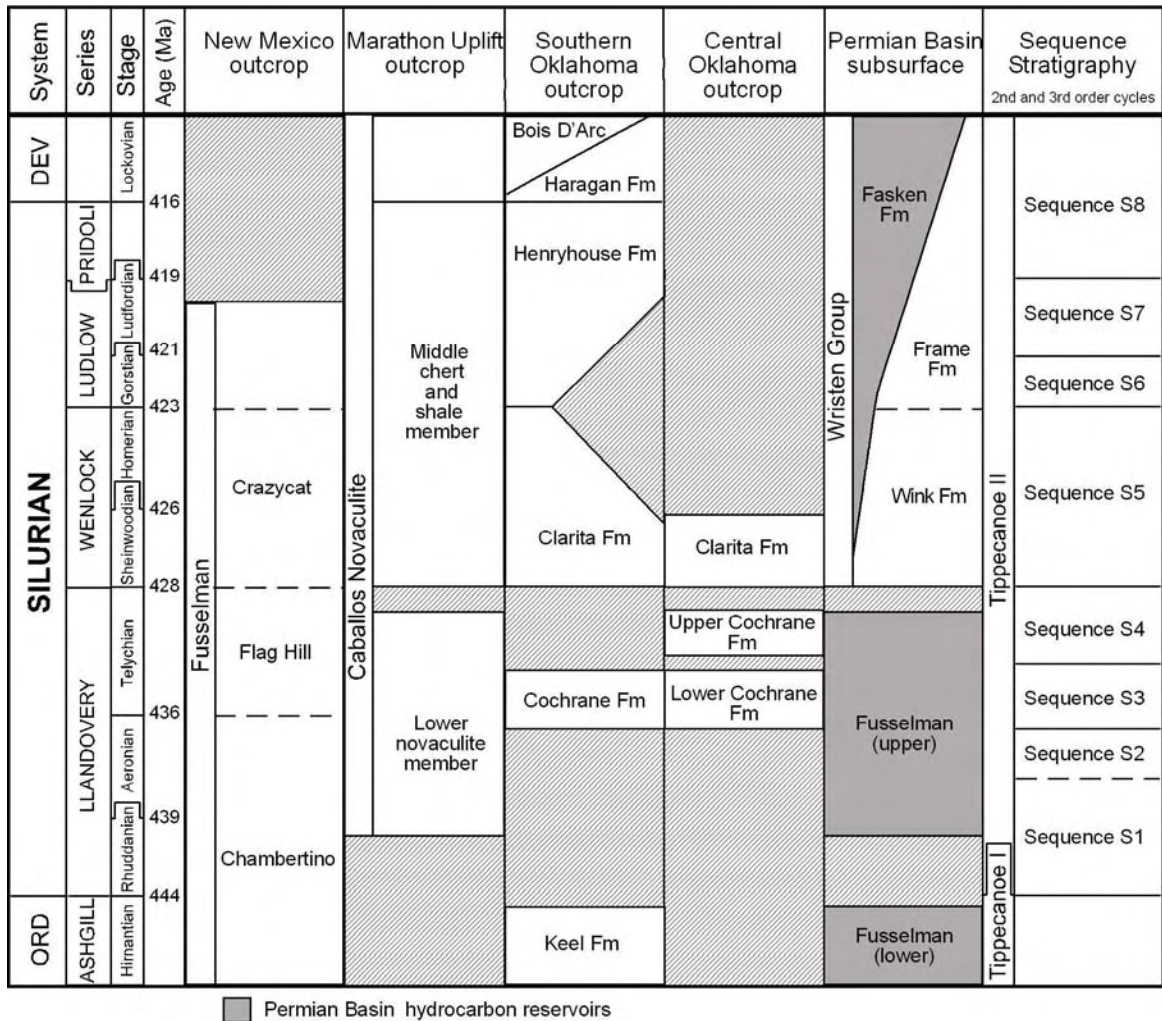
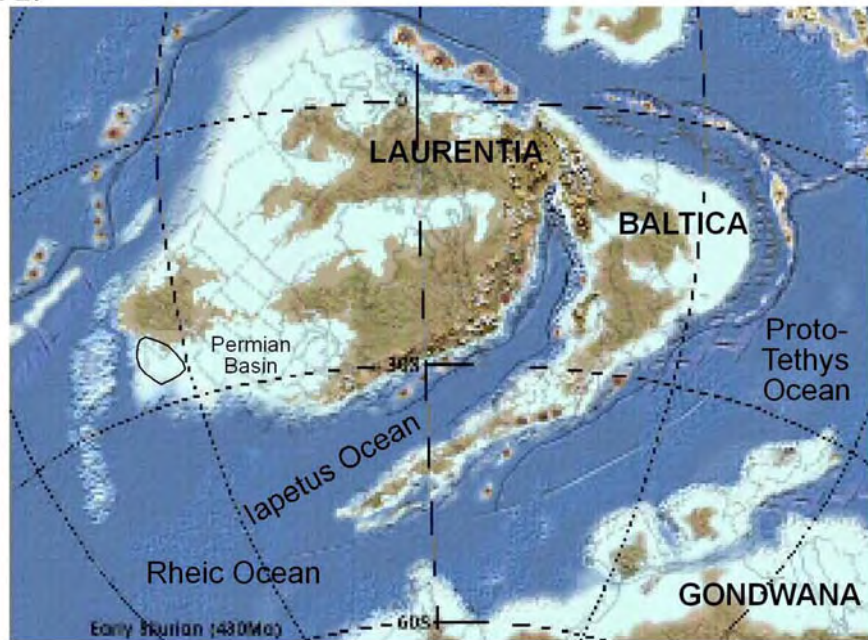


Figure 1. Correlation of Silurian Devonian strata in West Texas with successions in Oklahoma and New Mexico. Age dates are from International Stratigraphic Chart (2004).

A.



from Blakey (2004): <http://jan.ucc.nau.edu/~rcb7/430Nat.jpg>

B.



from Blakey (2004): <http://jan.ucc.nau.edu/~rcb7/400Nat.jpg>

Figure 2. Global reconstruction of the U.S. Midcontinent during the Silurian. The extensive carbonate platform that characterized the southern margin of Laurentia and (the Permian Basin area) during the Early Silurian (A) was downwarped to form a well-defined southfacing ramp during the Middle Silurian (B) associated with plate collision and the closing of the Iapetus Ocean. From Blakey (2004).

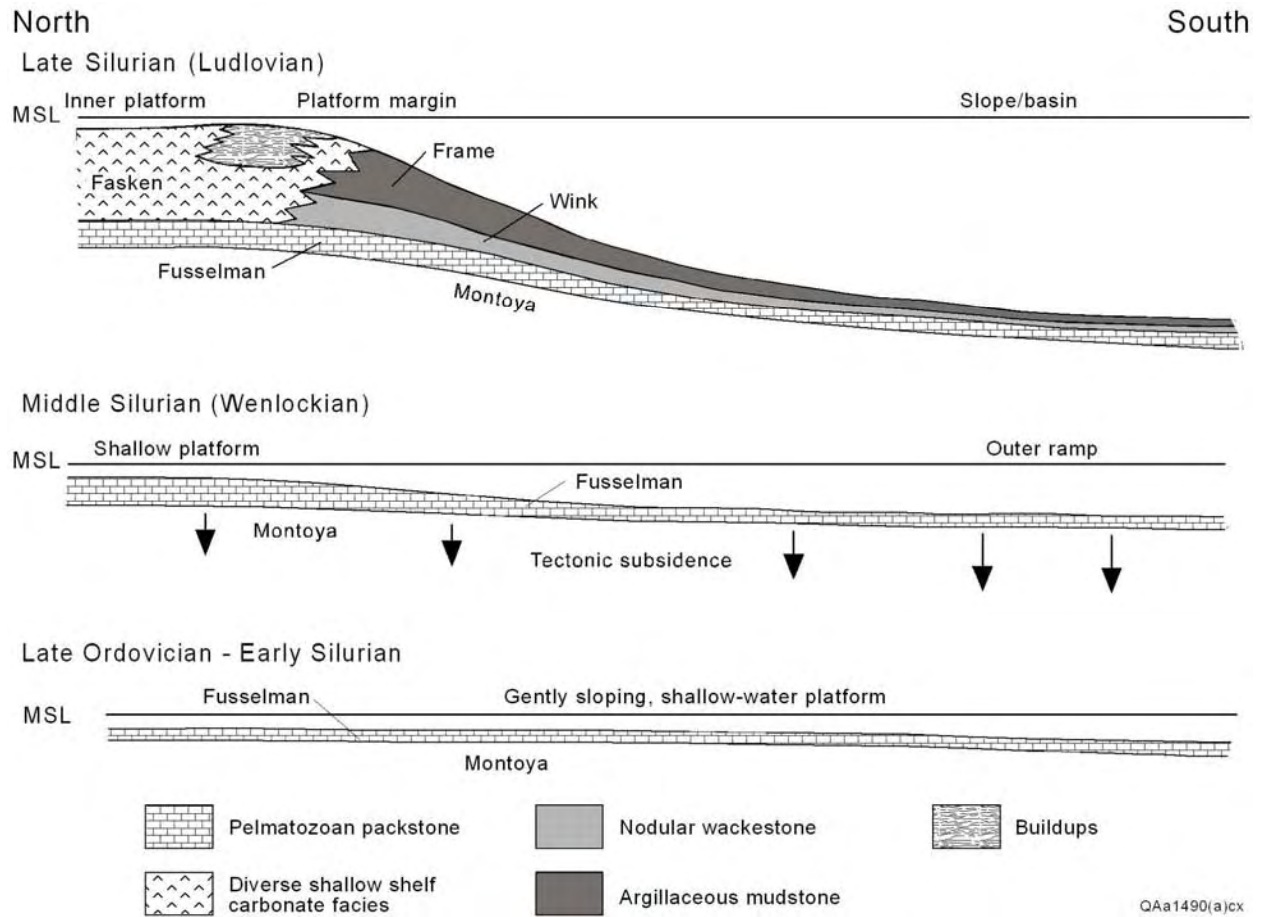
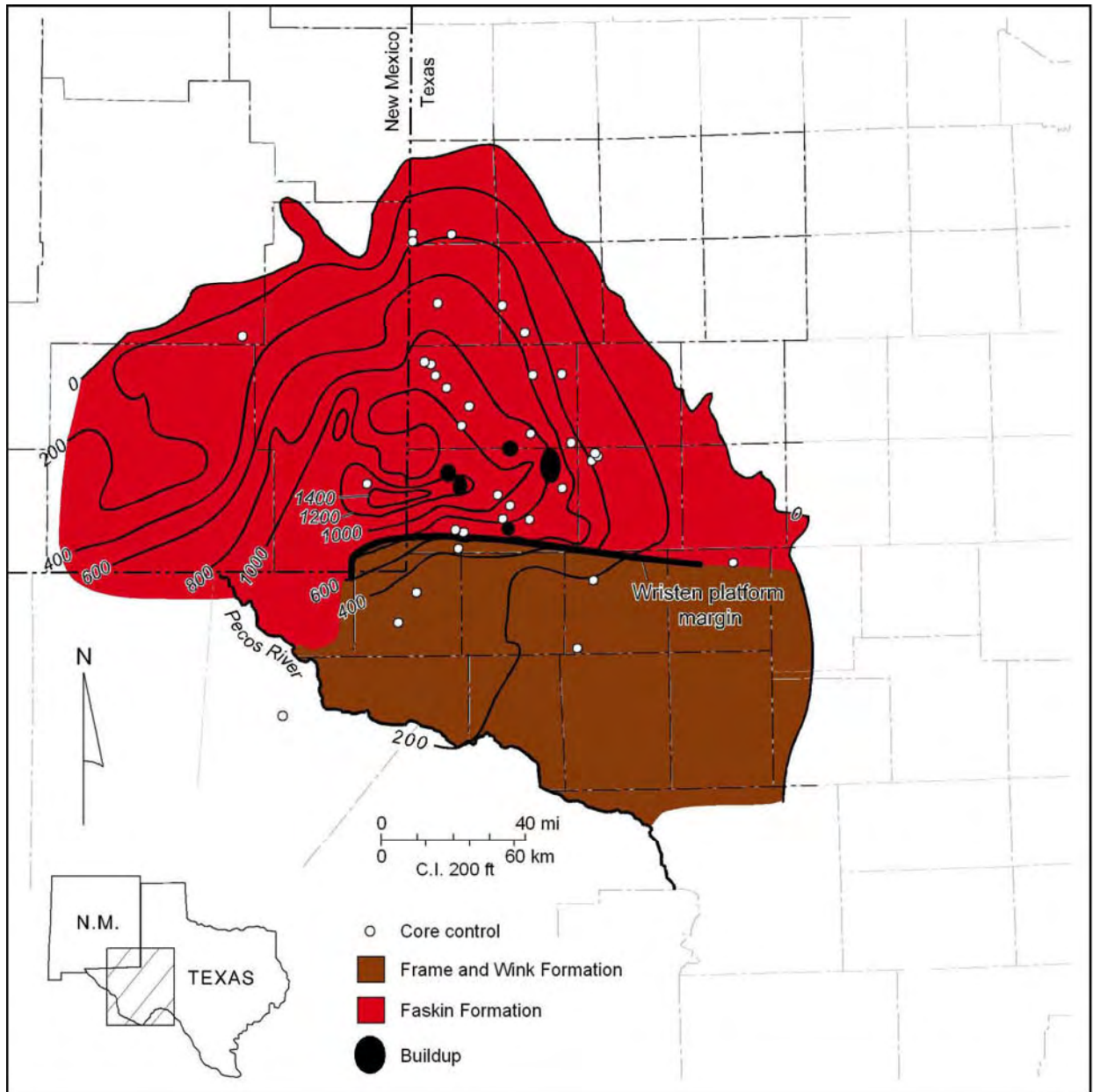


Figure 3. Diagrammatic dip cross section illustrating the depositional history and architecture of the Wristen Group in the Permian Basin.



QAd3351(a)x

Figure 4. Thickness and distribution of the Wristen Group. South of central Andrews County, the Wristen is composed of slope and basin mudstones and wackestones of the Frame and Wink Formations. North of this line, which defines the general position of the Wristen platform margin, the Wristen comprises a diverse assemblage of shallow-water platform carbonates herein assigned to the Faskin Formation. Note that carbonate buildups are common in the Faskin Formation in several areas, especially along and just landward of the platform margin in Andrews County. The Wristen Group is thickest along the Texas/New Mexico border in Andrews and Gaines Counties.

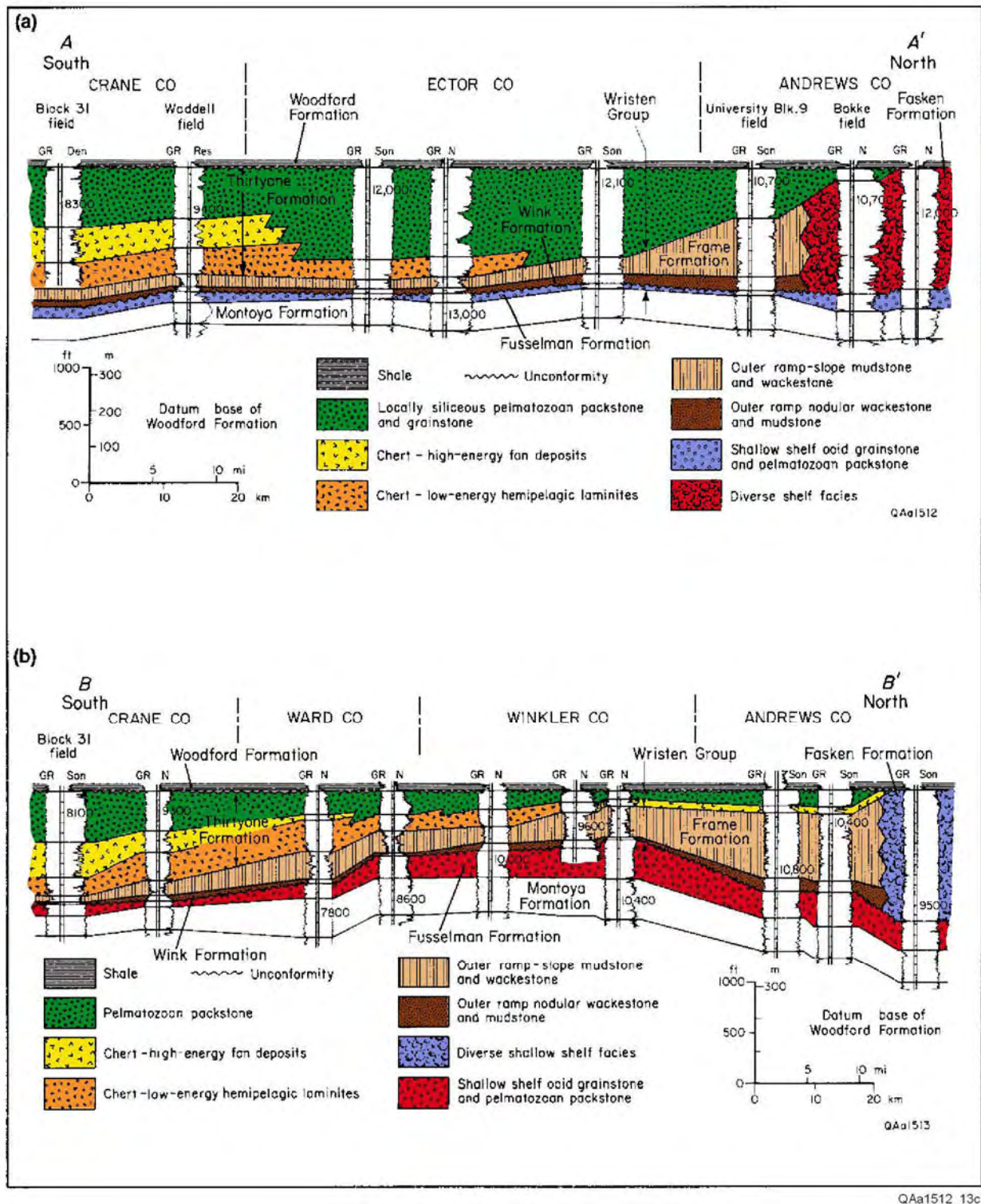
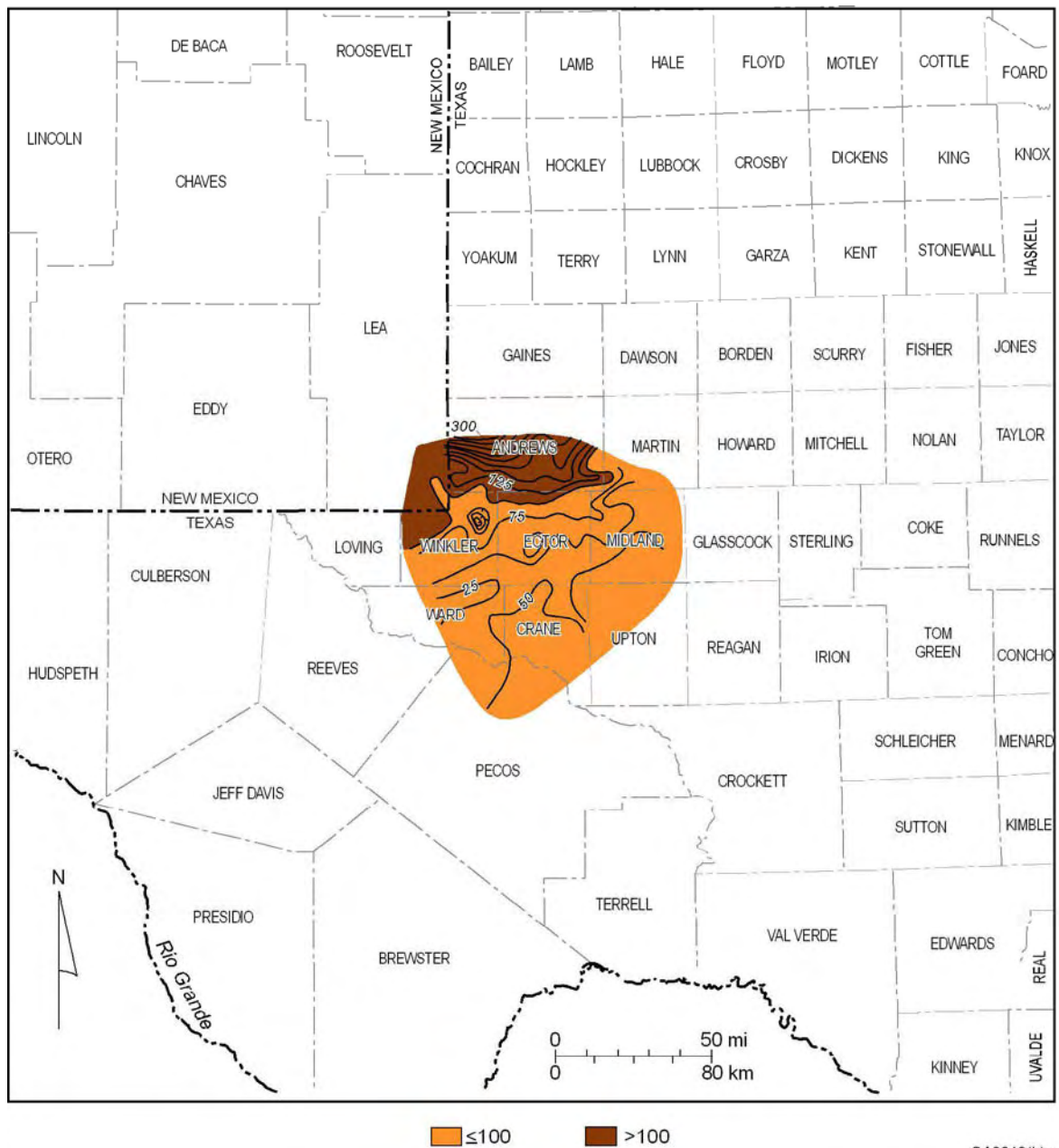


Figure 5. Dip cross sections showing general stratigraphy of the Wristen Group and overlying and underlying strata in West Texas. Lines of section shown in fig. 4.

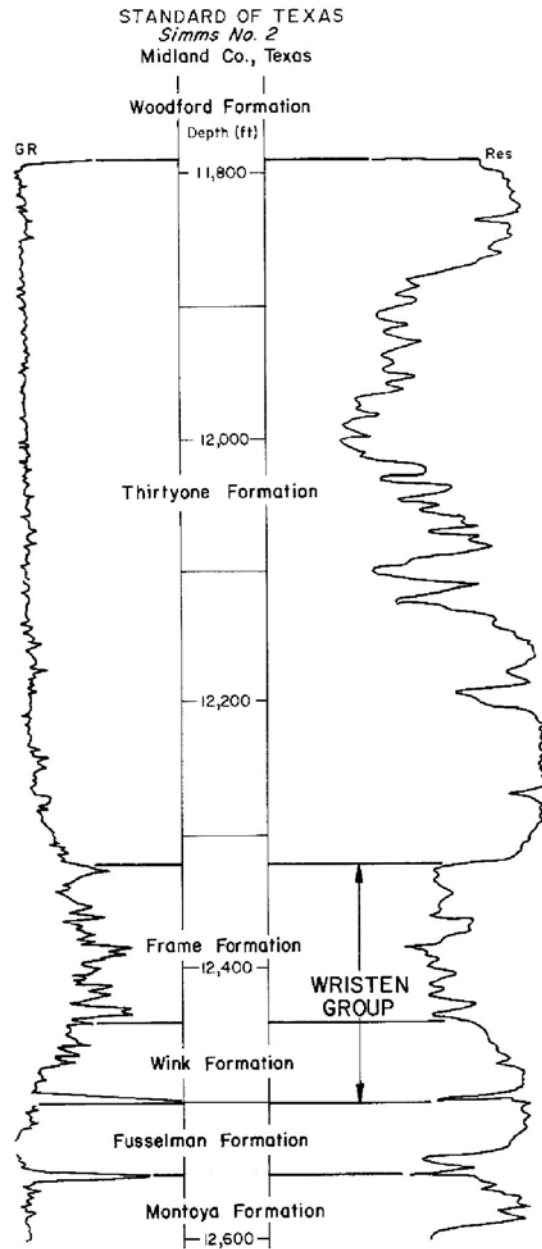


QA3319(b)x

Figure 6. Thickness of the Wink Formation. Neither the Wink nor the Frame Formation is readily separable from the Fasken Formation north of the Wristen platform margin in central Andrews County.



Figure 7. Slab photograph of nodular wackestone, Wink Formation. These wackestones contain scattered fragments of trilobites, thin-walled brachiopods, and ostracodes and locally grade into mudstone. Austral Oil Co., University No. 1, Andrews County, Texas. Depth: 12,030 ft. Slab is 8 cm wide.



QA17839(b)cx

Figure 8. Typical wireline signature of the Wristen Group in the southern, deeper water part of its subcrop area. Shallow-water platform Fasken Formation deposits are not present in this area; instead, the deeper water facies of the Wink and Frame Formations are typically overlain by the Thirtyone Formation.

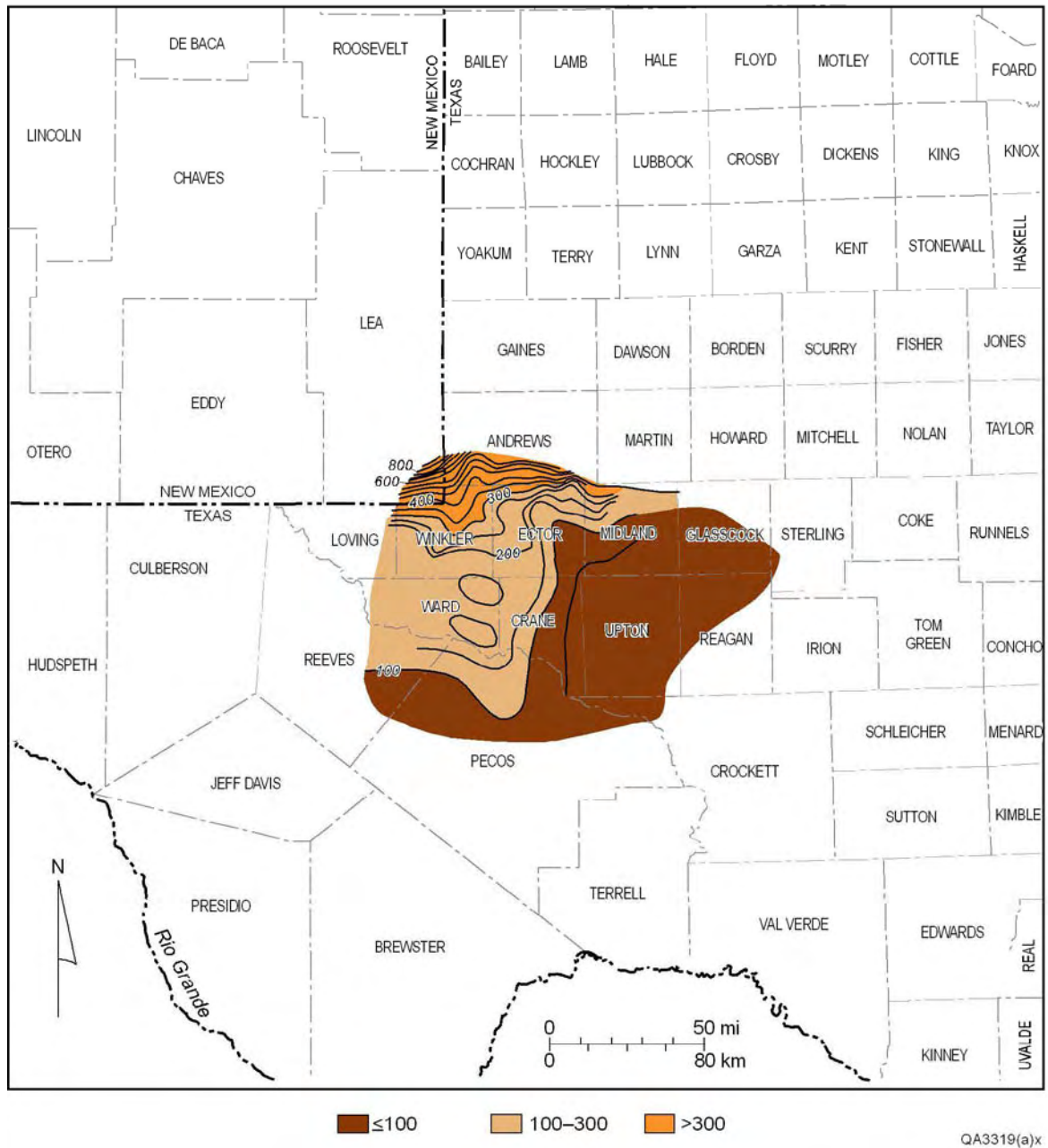


Figure 9. Thickness of the Frame Formation. Neither the Wink nor the Frame Formation is readily separable from the Fasken Formation north of the Wristen platform margin in central Andrews County.

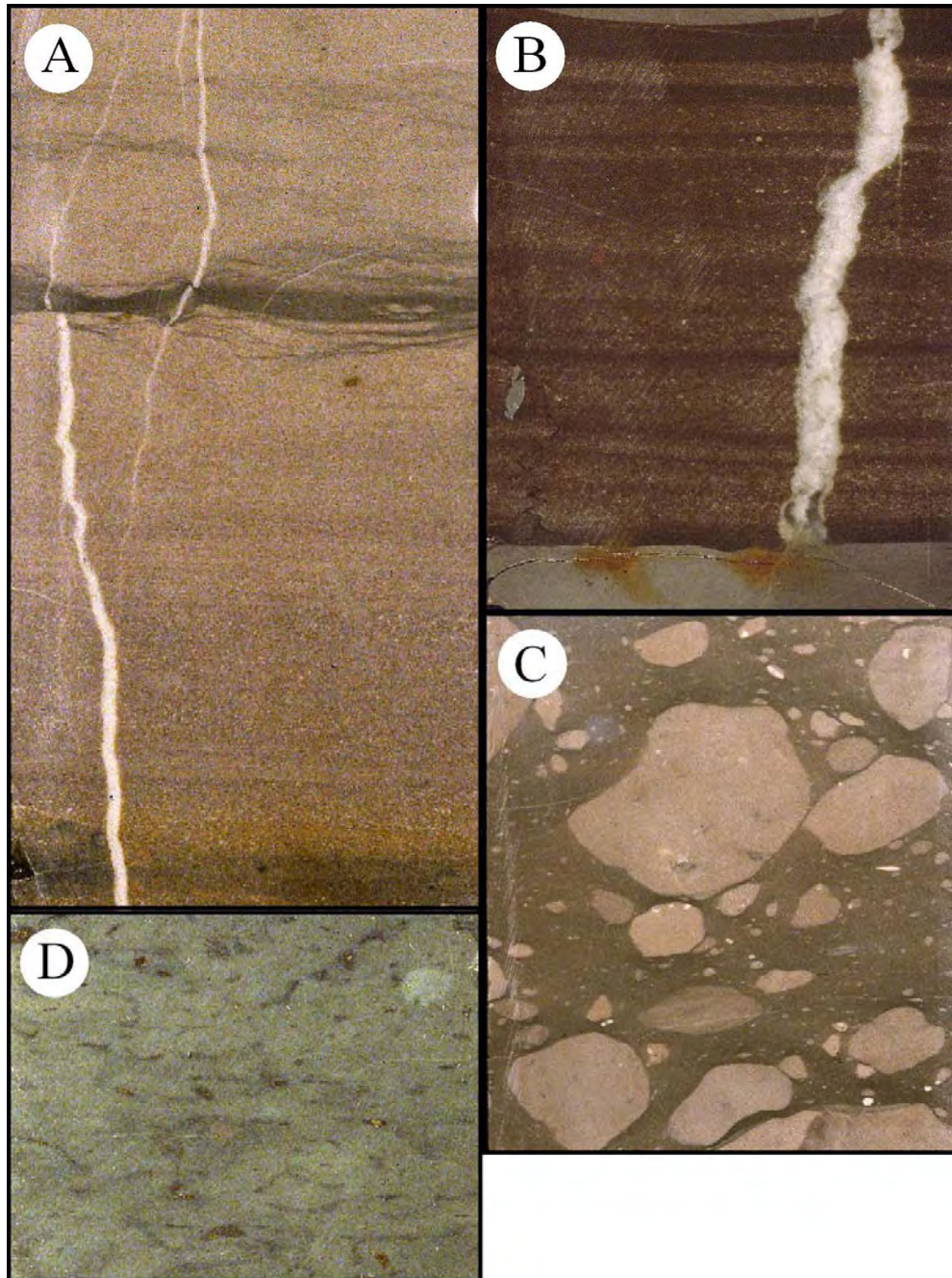
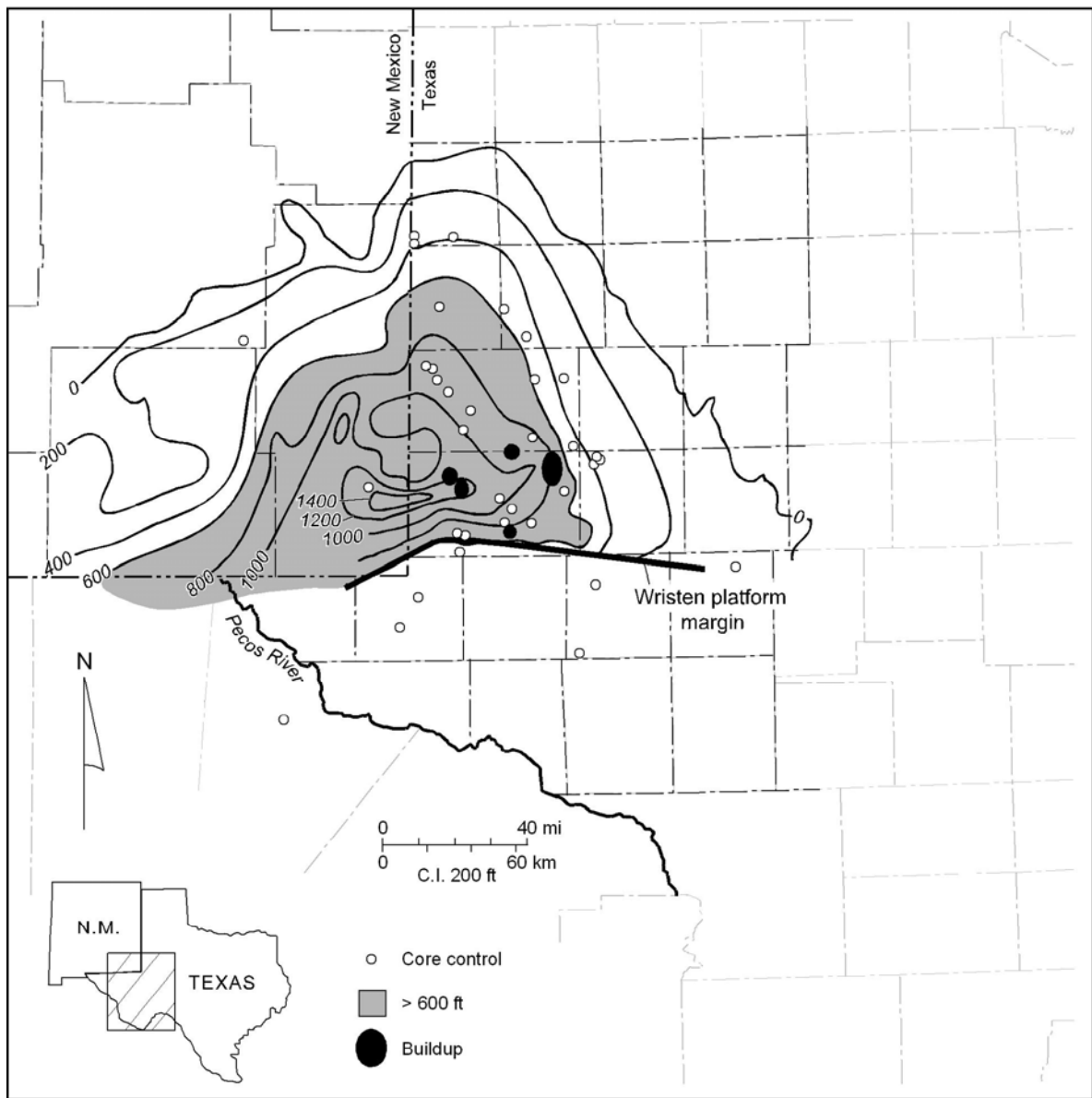


Figure 10. Typical outer ramp - slope facies of the Frame Formation (Wristen Group). A. Calcarenite displaying normal (upward-fining) graded bedding. Amoco Unit #74, Three Bar field, 8198 ft, Andrews County, Texas. B. Laminated skeletal calcarenite composed of grain-rich (packstone) and mud-rich (mudstone) layers. Shell McCabe #2, 9221 ft Emperor Field, Winkler County, Texas. C. Burrowed silty mudstone. Shell McCabe #2, 9221 ft Emperor Field, Winkler County, Texas. D. Mudstone containing clasts of skeletal packstone. Shell McCabe No. 2, Emperor Field, Winkler County, Texas. Slabs are 3 in (8 cm) wide.



QAd3351(b)x

Figure 11. Thickness and distribution of the Fasken Formation. The formation thickens to more than 1,500 ft in extreme western Gaines and Andrews Counties, Texas, and southeasternmost Lea County, New Mexico. Northeastward thinning in the northern part of the area is due to truncation of the Silurian section by Middle Devonian (pre-Woodford) erosion.

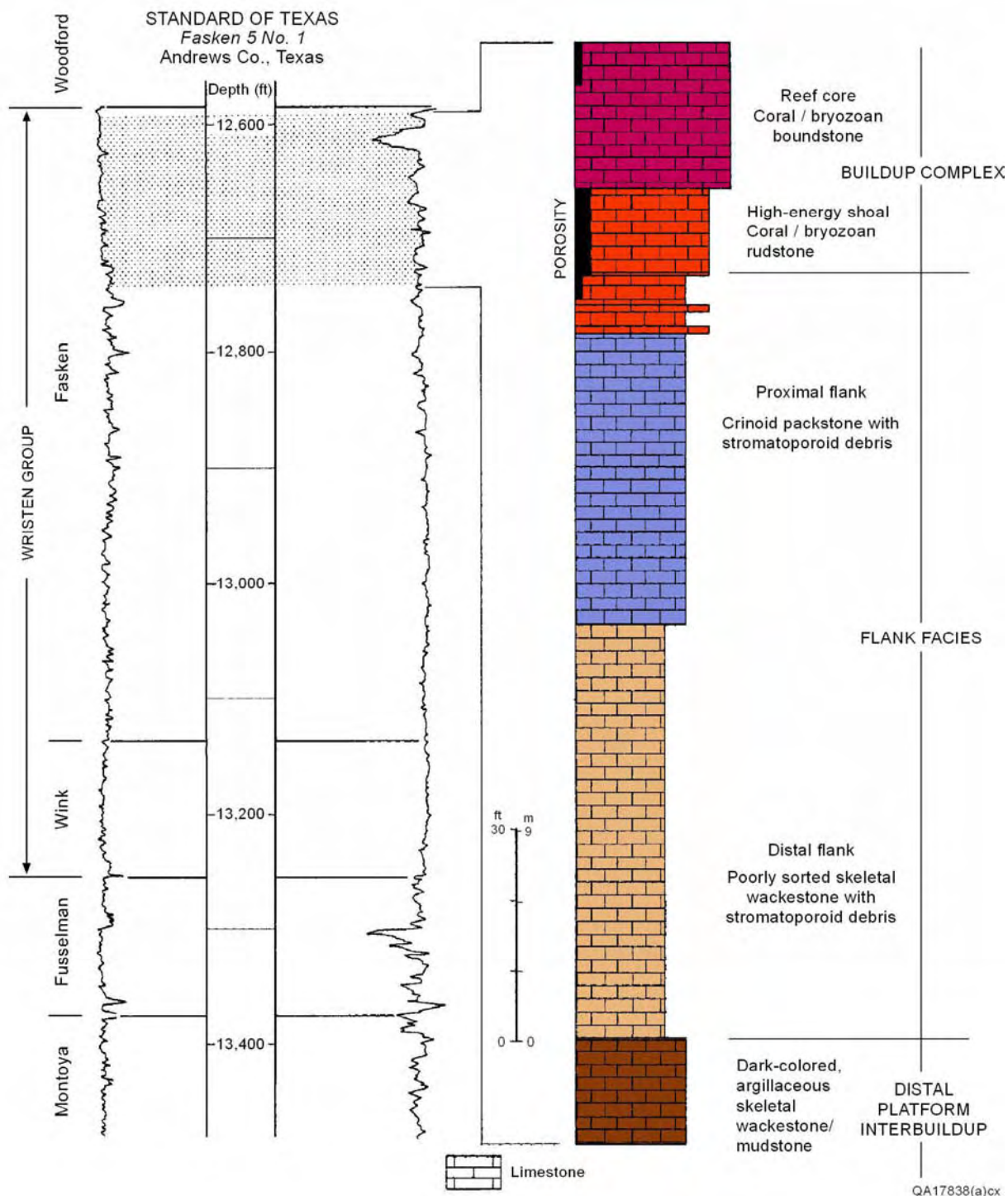


Figure 12. Fasken platform-margin buildup succession. Standard of Texas, Fasken 5 No. 1, Andrews County, Texas.

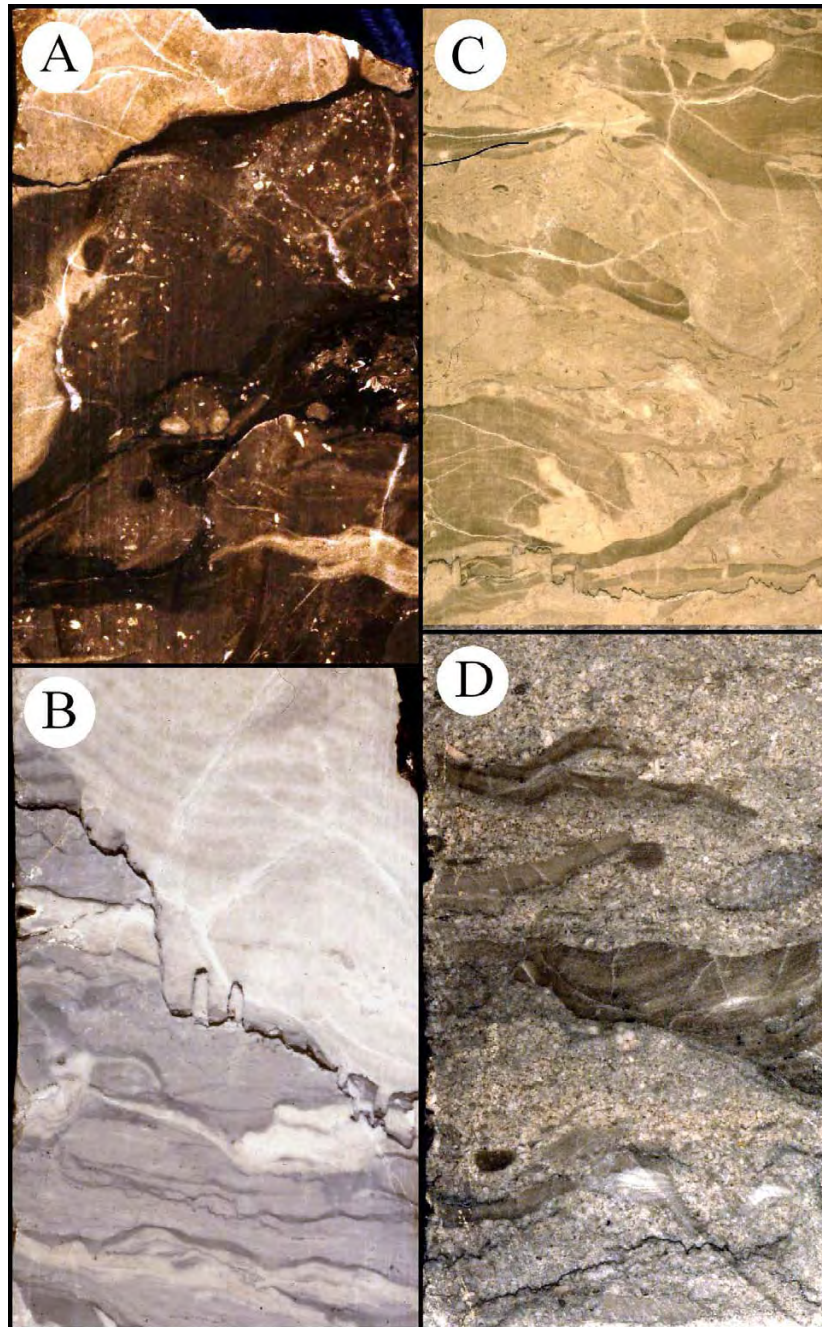


Figure 13. Distal facies of typical Fasken buildup successions. A. Skeletal wackestone containing rotated stromatoporoids typical of distal, outer-platform to slope deposits. Depth: 12740 ft. B, C. These mud supported rocks contain poorly sorted fragments of bryozoans, stromatoporoids, pelmatozoans, and corals (*Halysites*) transported downslope along buildup margins. Note some stromatoporoids are in growth position. Depth: 12632 (B) and 12731 (C). D. Pelmatozoan/stromatoporoid packstone containing a matrix of moderately well-sorted pelmatozoan debris and large clasts of hemispherical stromatoporoids. Depth: 12,629 ft. All slabs from Standard of Texas, Fasken 5 No. 1, Andrews County, Texas. Slabs 3 in (8 cm) wide.

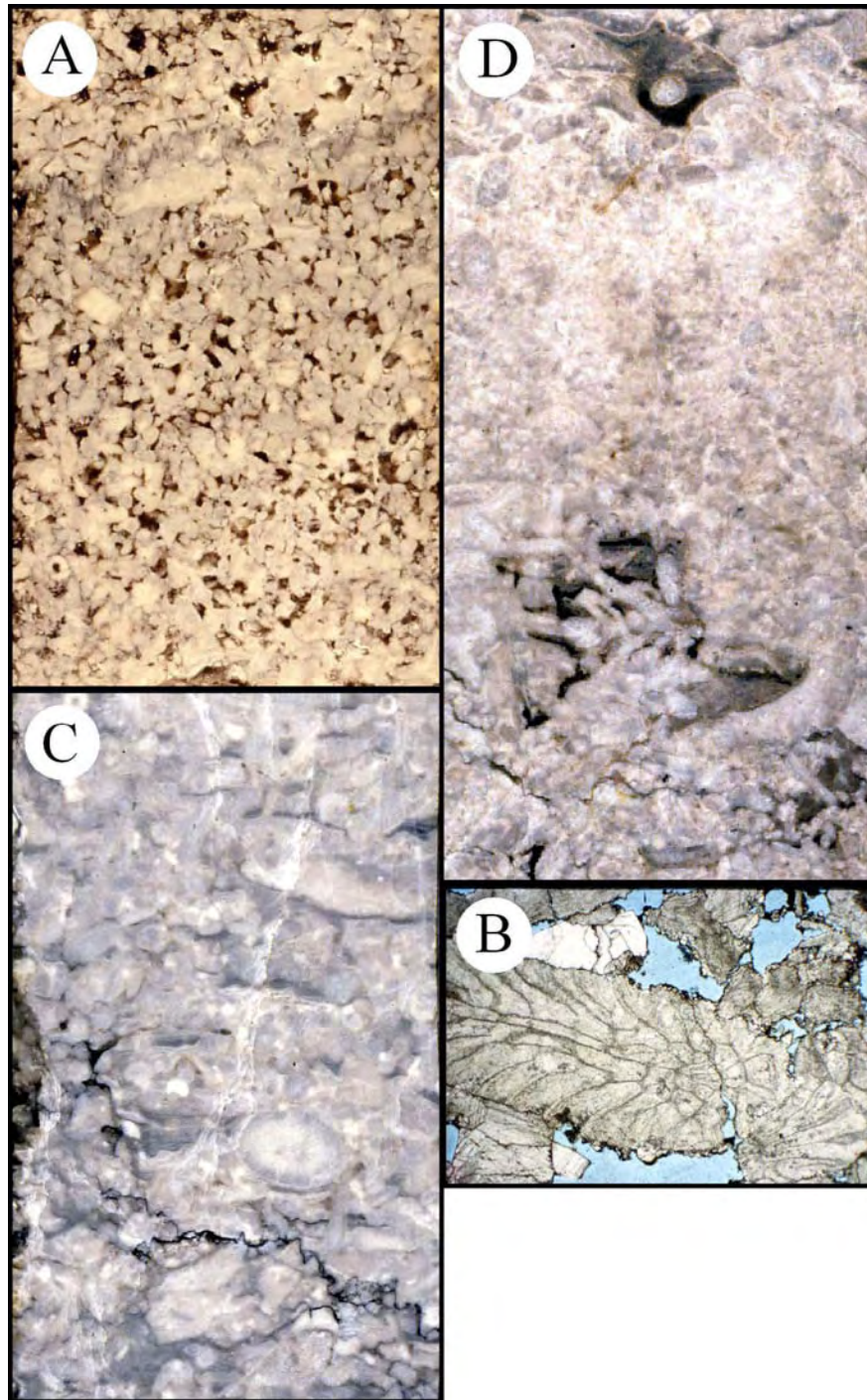


Figure 14. Proximal facies of typical Fasken buildup successions. A. Coral/bryozoan rudstone, Fasken Formation. These stick corals and ramose bryozoans were deposited as a coarse, high energy lag, at the tops of Fasken carbonate buildup successions. Depth: 12,620 ft. B. Thin section photomicrograph of A. Note the well-developed primary, intergranular porosity. C. Coral boundstone. Fauna is dominated by ramose corals and stromatoporoids. These deposits commonly exhibit numerous sediment-filled geopetals but are generally are non-porous. Depth: 12,597 ft. D. Bryozoan boundstone. Note local shelter porosity. Depth: 12 599. All slabs from Standard of Texas, Fasken 5 No. 1, Andrews County, Texas. Slabs 3 in (8 cm) wide.

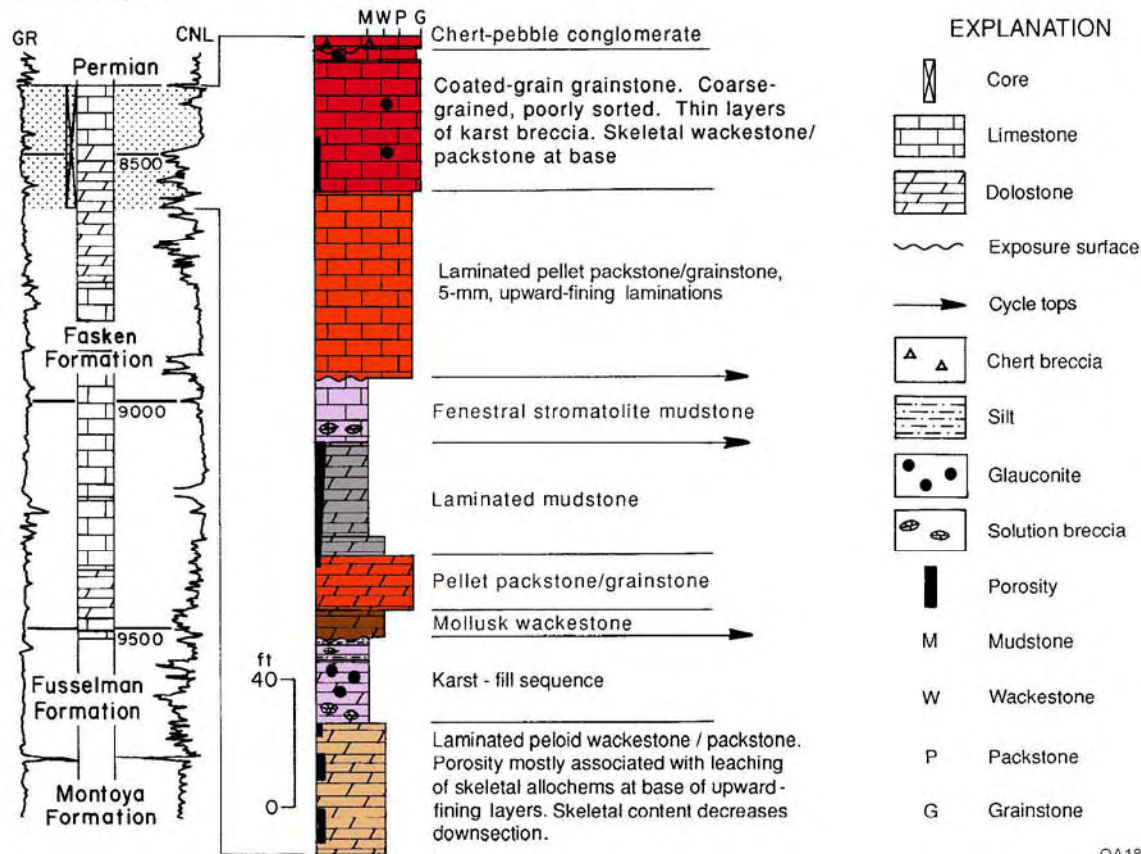


Figure 15. Upper Fasken Formation tidal flat succession, Fullerton field. In this well, the Fasken comprises a succession of tidal flat deposits punctuated by exposure and karsting. Note that porosity is most commonly developed beneath karst fills suggesting that porosity formation is controlled by leaching due to punctuated sea level fall. Amoco, University Consolidated, V, No. 12, Andrews County, Texas.

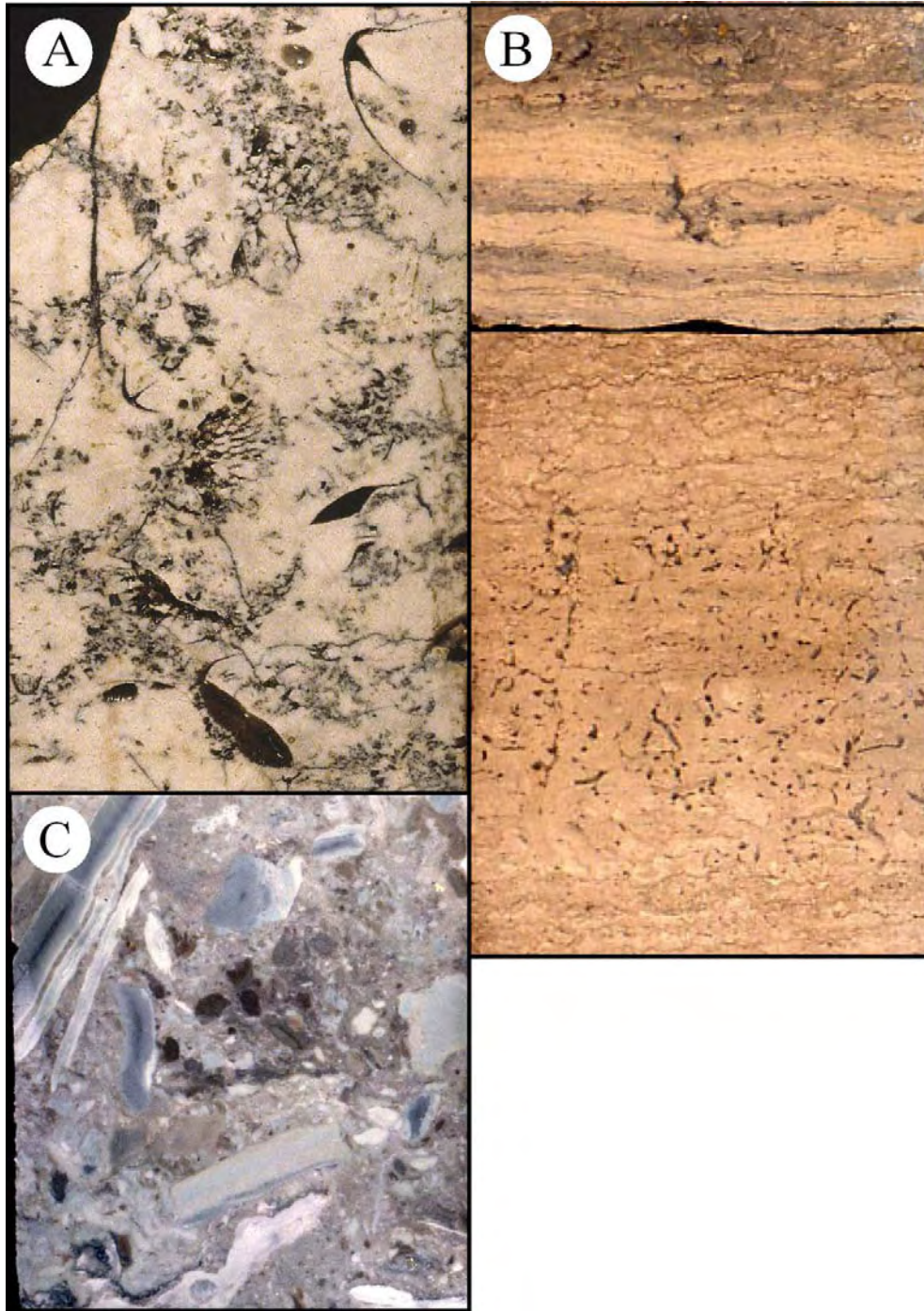
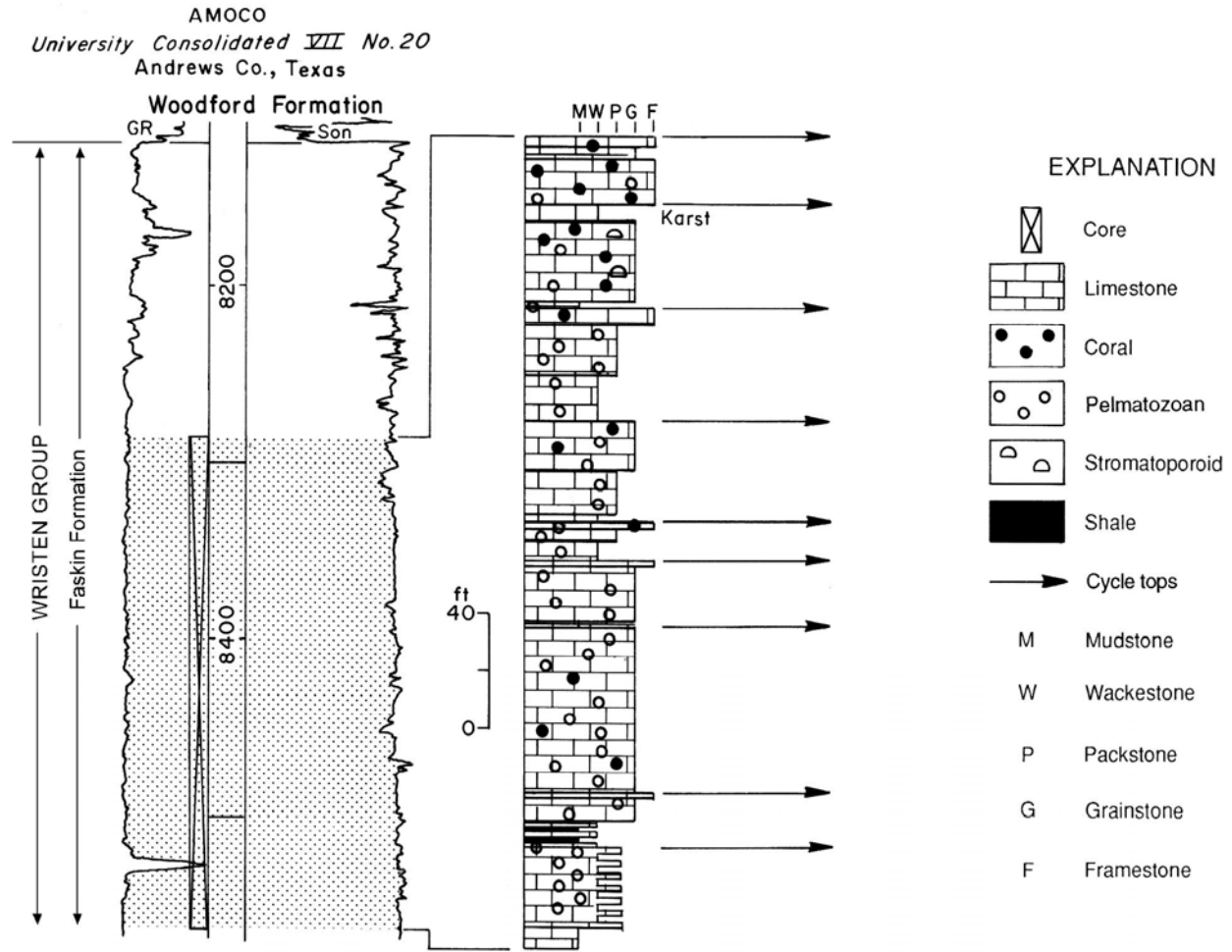


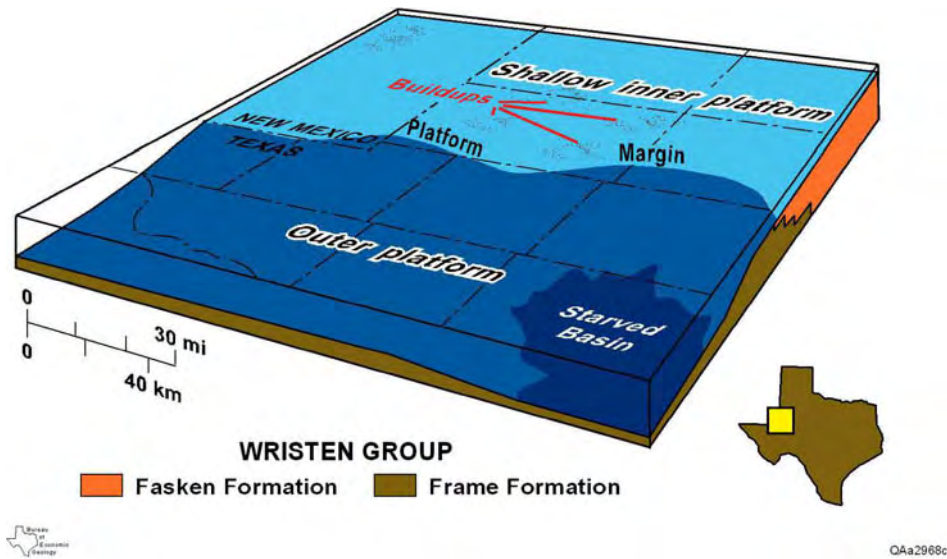
Figure 16. Facies of the Fasken inner platform. A. Subtidal skeletal wackestone. Skeletal debris consists principally of brachiopods, corals, and mollusks. Skeletal moldic pores like these typify the Fasken of the inner platform. Tex-Sin field, Texas. Texas Crude Oil Company, Chilton "B," No. 9-1, Gaines County, Texas. Slab is 8 cm wide. B. Laminated peritidal facies. These rocks define cycle tops and are typically dolomitized. Amoco University Consolidated V # 12, Fullerton field, Andrews County, Texas. Depth 8490 ft. C. Karst breccia. North Robertson field, Texas. Exxon Co., USA, Fee B-14, Gaines County, Texas. Depth: 9,748 ft. All slabs are 3 in (8 cm) wide.



QA18098c

Figure 17. Lower Fasken Formation, buildup-capped, middle platform successions, Fullerton field. In this well, the Fasken is composed of a succession of aggradational, upward-shallowing sequences capped by carbonate buildups. The tops of many cycles exhibit evidence of exposure and dissolution or karsting. Very little porosity is evident. Amoco, University Consolidated, VII, No. 20, Andrews County, Texas

A



B

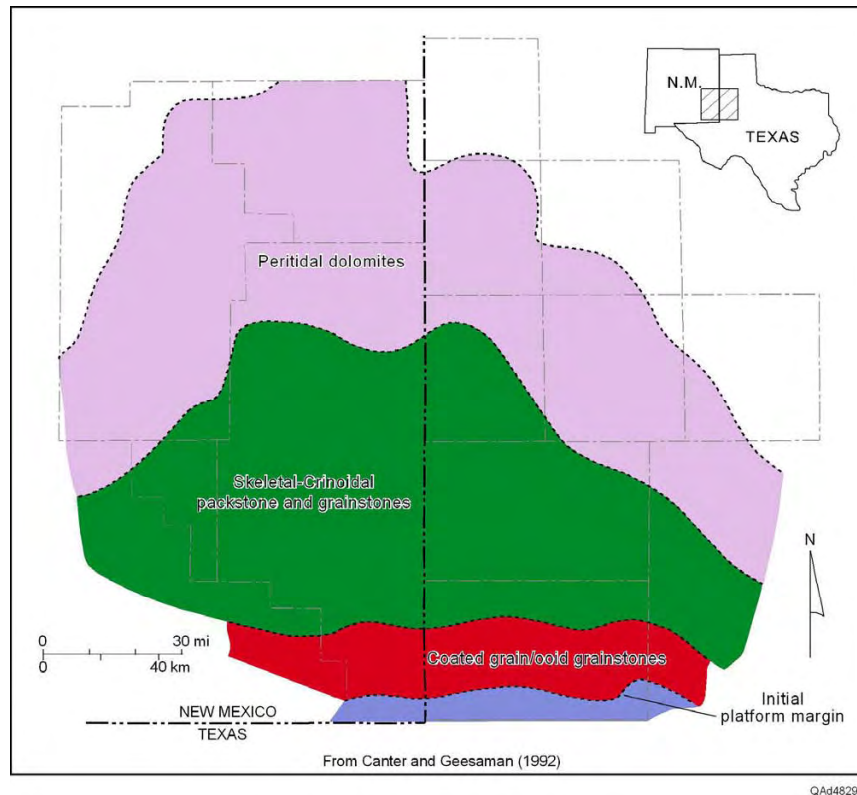


Figure 18. Paleogeographic reconstructions of Wrusten Group depositional environments during the middle Silurian. A. General regional model depicting northern platform and southern, outer platform – basin. Platform rocks comprise Fasken platform-margin buildup successions and inner platform shallow subtidal to tidal-flat sediments. Coeval, argillaceous mudstones of the Frame Formation and underlying Wink Formation were deposited south of the platform margin in a slope/outer platform setting. From Ruppel and Holtz, 1994. B. Reconstruction on northern platform area showing east-west striking facies belts and general northward shallowing of facies tracts. From Canter and others, 1992.

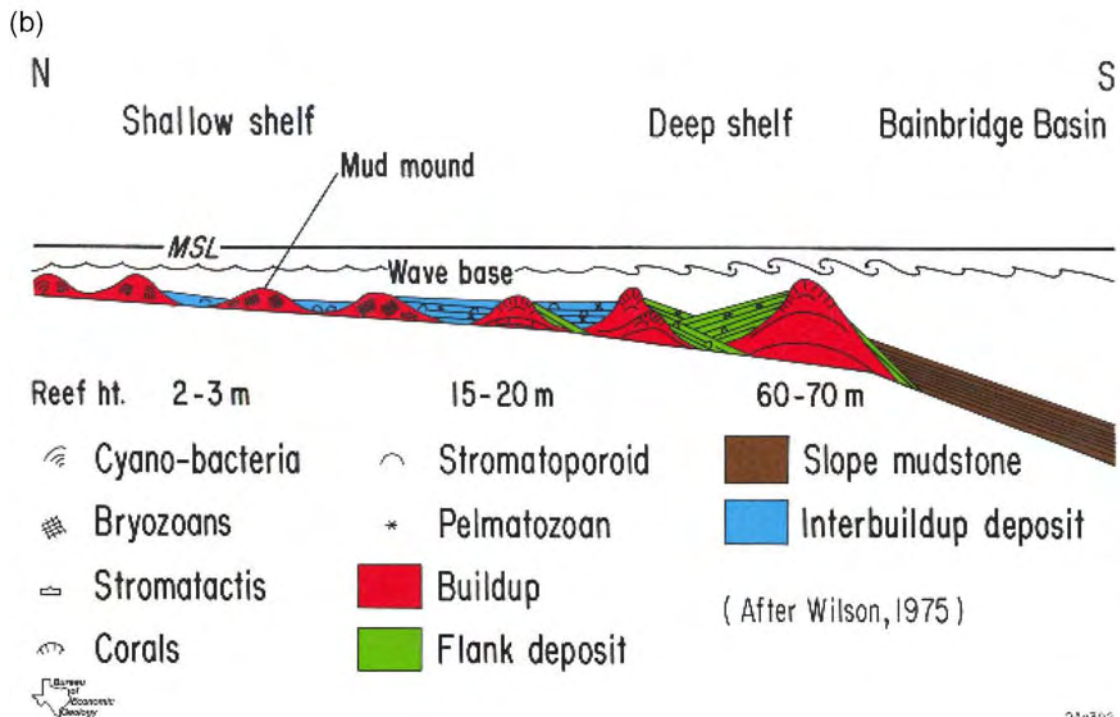
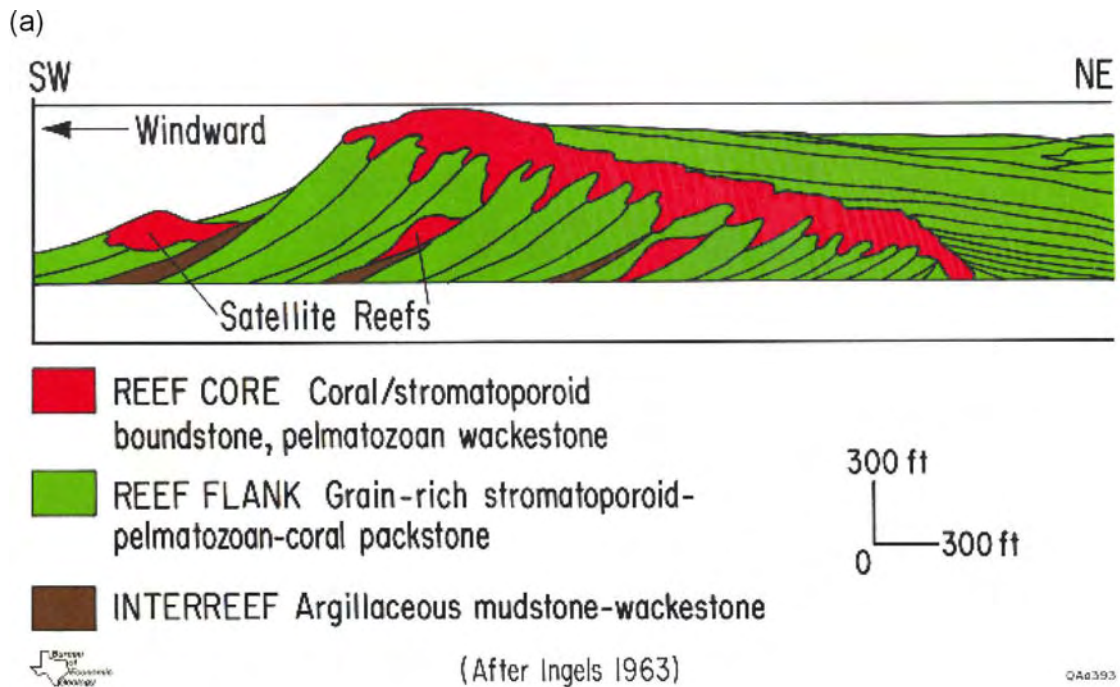


Figure 19. Models for Fasken buildup development. A. Model for platform margin buildup development based on Silurian outcrops in the Illinois Basin. From Ingels (1963). B. Platform interior buildups based on subsurface data from the Illinois Basin. From Wilson (1975).

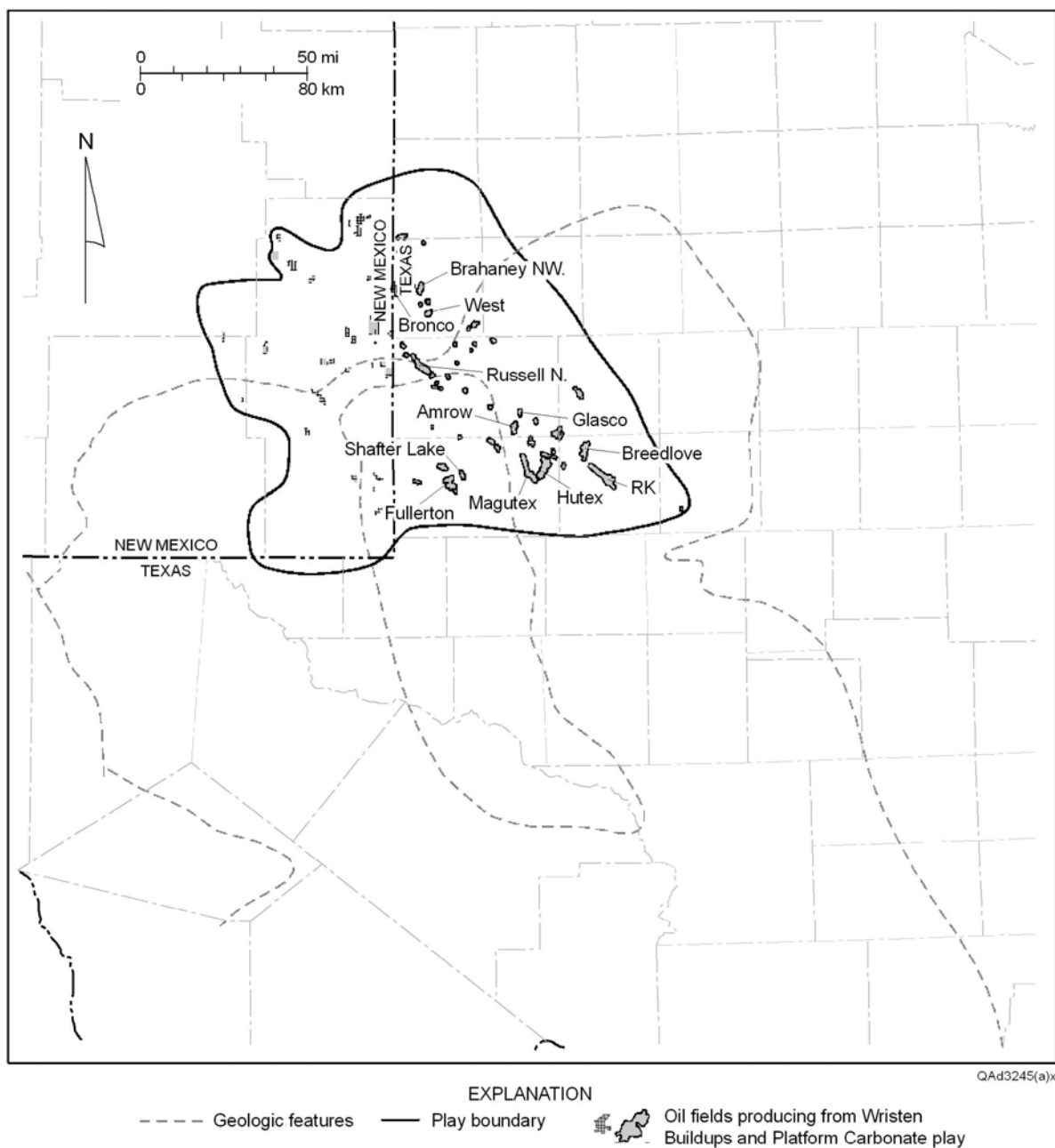


Figure 20. Map of the Permian Basin area showing distribution of reservoirs of the Wristen Buildups and Platform Carbonate play that have produced more than 1 million barrels of oil (from Dutton and others, 2005).

THE LOWER DEVONIAN THIRTYONE FORMATION OF THE PERMIAN BASIN: DOMINANCE OF DEEP-WATER, SILICEOUS SEDIMENTATION

Stephen C. Ruppel

Bureau of Economic Geology
Jackson School of Geosciences
The University of Texas at Austin
Austin, Texas

ABSTRACT

Devonian carbonate and chert rocks in the Permian Basin constitute an important hydrocarbon-bearing succession in West Texas and New Mexico; production from nearly 650 reservoirs developed in these rocks totals almost 2 billion barrels of oil. Patterns and styles of reservoir development and distribution in this nearly 2,000-ft-thick carbonate succession are a function of basin evolution. Three distinct stages of basin evolution can be recognized.

A major rise in sea level during the Early Devonian resulted in basin infilling, first by transgressive, slope/basin, spiculitic chert and then by progradational, highstand, skeletal carbonate. Reservoirs in these rocks (Thirtyone Formation) are developed in downdip cherts whose distribution is the result of cyclic sea-level rise and fall and processes of gravity mass transport, and in updip grain-rich carbonates that underwent leaching during regional Middle Devonian uplift.

Devonian rocks comprise three distinct hydrocarbon reservoir plays: Ramp Carbonates, Deep-Water Cherts, and Siliceous Shallow Water Carbonates. Analysis of play volumetrics illustrates that although these reservoirs contain relatively low current reserves compared with their cumulative production, a mobile oil resource of more than 900 million barrels, virtually equal to the amount already produced from these rocks, remains. In addition, recent discoveries have demonstrated that additional volumes of hydrocarbons exist in undiscovered traps.

INTRODUCTION

The Thirtyone Formation is a major hydrocarbon-bearing unit in the Permian Basin of West Texas. These rocks, which include deep-water cherts and shallow-water carbonates of Early Devonian age, have accounted for more than 800 million barrels of oil production as of January 1990. Most of the hydrocarbon resource in these rocks lies in the porous, deep-water chert facies. Ruppel and Holtz (1994) estimated that more than 700 million barrels has been produced from Thirtyone Formation chert reservoirs and that a similar amount of mobile oil remains. Carbonate and chert rocks of Devonian age constitute a thick (as much as 1,000 ft) hydrocarbon-bearing succession in the Permian Basin of West Texas and New Mexico. Nearly 1 billion stock-tank barrels (STB) of oil has been produced from reservoirs developed in these rocks, and current estimates suggest that another 900 million barrels of mobile oil remains.

PREVIOUS WORK

Although the Thirtyone Formation was not defined until 1979 (Hills and Hoenig, 1979), general aspects of the age and distribution of these rocks in West Texas were presented by Jones (1953), Wilson and Majewske (1960), and McGlasson (1967), who variously referred to them as the Siluro-Devonian, Lower Devonian, or Devonian cherty limestone. The Thirtyone Formation was named for a succession of light-colored chert and cherty carbonate rocks overlying Silurian carbonates and shales and underlying Upper Devonian shales (Woodford Formation) primarily based on analysis of well cuttings and wireline log character (Hills and Hoenig, 1979). Ruppel and Holtz (1994) presented a regional analysis of the Thirtyone as part of a study of the geology and reservoir development of the entire Silurian and Devonian section on the Permian Basin. Saller and others (1991, 2001) and Ruppel and Hovorka (1995b) presented detailed analyses of the Thirtyone Formation reservoirs in Dollarhide and Three Bar fields, respectively, in Andrews County, Texas. Montgomery (1998) summarized some of these published results and presented some previously unpublished reservoir data. Ruppel and Hovorka (1995a) analyzed the depositional and diagenetic controls on reservoir formation in the Thirtyone on the basis of regional and field-specific studies. Ruppel and Barnaby (2001) compared and contrasted facies architecture and reservoir development in updip and downdip parts of the Thirtyone.

REGIONAL SETTING

Recent conodont biostratigraphy indicates that the Thirtyone Formation is dominantly Pragian (Early Devonian) in age (Barrick, 1995) (fig. 1). Similar chert-bearing successions of Thirtyone age are extensive along the southern margins of the United States, including the Penters Formation of the Arkoma Basin of Arkansas (Medlock and Fritz, 1993), the New Harmony Group in the Illinois Basin (Collinson 1967; Droste and Shaver, 1987), and unnamed facies in the Black Warrior Basin of Alabama and Mississippi (Medlock and Fritz, 1993). These rocks were deposited in the Early Devonian in an extensive seaway developed along the southern margin of the Laurussian paleocontinent between the Transcontinental Arch and the developing Acadian mountains in the eastern United States (fig. 2). Reservoirs developed in the Hunton Group in the Anadarko Basin of the Texas Panhandle and Oklahoma are more proximal carbonate-dominated equivalents of the Thirtyone (Galloway and others, 1983; Kisters and others, 1989; Bebout and others, 1993).

The top of the Thirtyone Formation is a major unconformity that records subaerial exposure and erosion. Overlying rocks range from upper Devonian to Permian in age. The hiatus represented by this unconformity ranges from about 17 m.y. to as much as 127 m.y. (fig. 1). Across most of the Permian Basin, the Thirtyone Formation is overlain by black shales and mudstones of the Woodford Formation of Middle to Late Devonian age, which is both a top seal and a regional hydrocarbon source rock.

Underlying the Thirtyone is the Frame Formation, which consists of argillaceous lime mudstone and wackestone that accumulated in a slope to basinal setting (Ruppel and Holtz, 1994). This succession attains a maximum thickness of 800 ft in central Andrews County and thins basinward to the south to less than 100 ft (Ruppel and Holtz, 1994). Recent faunal data (Barrick, 1995) indicate a Middle Silurian to Early Devonian (Lochkovian) age for these rocks (fig. 1).

The Thirtyone Formation subcrops throughout most of the southern part of the Permian Basin, including Texas and small areas of New Mexico, and attains a maximum thickness of about 1,000 ft in southern Crane County, Texas (fig. 3). Thirtyone strata thin outward from this depocenter owing largely to pre-Woodford erosion and perhaps to some extent to decreased accommodation. To both the west and the north, the Thirtyone subcrop margin corresponds approximately to the position of the Silurian platform margin (Ruppel and Holtz, 1994). The eastern extent of the Thirtyone is poorly constrained because of the lack of core control, but

work by McGlasson (1967) suggests that the unit extends eastward to the Silurian/Devonian carbonate subcrop.

Throughout most of West Texas, Thirtyone Formation rocks comprise two distinct facies: (1) skeletal carbonates, primarily pelmatozoan packstones and grainstones, and (2) bedded, commonly spiculitic, chert (Saller and others, 1991; Ruppel and Holtz, 1994). Thirtyone carbonates are relatively more abundant in the upper part of the formation and up depositional dip to the north, whereas cherts are more abundant in the lower part of the formation and in the southern part of the subcrop area (fig. 4).

Chert is most abundant in the basin depocenter. In this region, the general stratigraphic succession consists of basal laminated dark cherts and lime mudstones that pass upward into laminated to massive spiculitic cherts overlain by skeletal lime packstones (Ruppel and Holtz, 1994; Ruppel and Barnaby, 2001). Skeletal packstones are overlain by an upper chert succession downdip, recording a renewed rise in relative sea level.

The Caballos Formation, which crops out in the Marathon Basin in the Ouachita overthrust belt, is a partial distal equivalent of the Thirtyone Formation (fig. 1). The “upper chert and shale” member of the Caballos, which is apparently of about the same age as the Thirtyone, averages about 250 ft in thickness (Folk and McBride, 1977), which is markedly thinner than the Thirtyone except where the latter has been truncated by erosion.

REGIONAL STRATIGRAPHY AND FACIES

Facies

Thirtyone chert facies are most abundant in the southern part of the region and downsection; carbonate facies are more abundant upsection and to the north (fig. 4). Chert intervals typically contain varying amounts of carbonate that is interbedded and intermixed at all scales. Vertical facies successions through the Thirtyone vary across the basin in part owing to differences in the proportions of these two end-member lithologies.

Cherty Thirtyone lithofacies are particularly well developed in the south-central part of the basin (Crane County), where thicknesses reach at least 1,000 ft (fig. 3). The stratigraphic section in this area displays a spectrum of lithofacies that encompasses most of the range seen in the Thirtyone across the basin. These facies are well represented in Block 31 and University Waddell fields (Ruppel and Holtz, 1994; Ruppel and Barnaby, 2001). The Thirtyone section in

this area constitutes an upward-shallowing succession that is chert rich at the base and carbonate rich at the top. Four facies, listed in order of generally decreasing water depth and chert/limestone ratio, can be defined from the base of the section up (fig. 5): (1) dark-colored, chert/carbonate laminite, (2) light-colored, thickly laminated to massive chert, (3) burrowed/laminated chert, and (4) skeletal packstone (Ruppel and Holtz, 1994; Ruppel and Barnaby, 2001) .

Dark-colored, abiotic, chert/carbonate laminites (fig. 6a) constitute basal Thirtyone deposits in the thickest parts of the basin, where they typically overlie carbonate mudstones and shales of the Silurian-Devonian Frame Formation (fig. 4). These deposits typically display centimeter-thick interbeds of structureless or finely laminated chert and carbonate mudstone. Carbonate beds are generally composed of dolomite but are locally calcitic. These characteristically nonporous, chert/carbonate laminites are thickest (nearly 300 ft) in the central area of the Thirtyone depocenter and thin toward the margins.

Thick-bedded, laminated to massive chert (figs. 6b), in striking contrast to the dark-colored chert and mudstone interval it typically overlies, is light colored, highly porous, and finely laminated to early massive in some instances. Dark-colored, organic-rich laminations are common at the tops of some successions of more massive chert, which can range to as much as 3 ft in thickness (fig. 6b). Fluid escape structures and vague wispy laminations are locally common ((fig. 6b). These rocks typically contain significant amounts of carbonate in the form of small, irregular patches of calcite and isolated dolomite rhombs. Rarely, patches are identifiable as corroded fragments of skeletal debris. Carbonate content is highly variable, ranging from less than 20 percent to more than 40 percent, and generally increases upsection. Thick-bedded, laminated chert constitutes the most important reservoir facies in the Thirtyone Formation. At many localities these deposits contain abundant sponge spicules. Spicules are well sorted and preserved both as open and quartz- or chalcedony-cemented molds. In the latter case, their recognition is difficult. Successions of thick-bedded, laminated chert reach thicknesses of as much as 150 ft (Ruppel and Holtz, 1994; Ruppel and Barnaby, 2001).

Burrowed/laminated chert includes both fine-laminated (2- to 3-mm laminations) chert and burrowed chert (fig. 6c). These two facies are interbedded on several scales. Like the thick-bedded, laminated chert facies, these rocks contain abundant carbonate “clasts,” although recognizable skeletal debris is rare. Laminated chert is more common in the lower parts of the Thirtyone, where it is interbedded with the thick-bedded, laminated chert facies. Burrowed chert

is increasingly abundant upsection, where it is commonly interbedded with carbonate packstone. The nodular chert and limestone facies, disrupted laminated chert facies, and burrowed chert facies of Ruppel and Barnaby (2001) are subfacies of this facies. Nodular chert and limestone facies are typified by alternating laminae to thin beds of gray chert and brown, organic, locally skeletal-rich lime mudstone to wackestone. These rocks are probably the result of differential compaction of alternating layers of carbonate and chert silica sediment. Burrowed facies display intensive bioturbation by *Zoophycos* and other burrowers that has locally obliterated much of the primary depositional stratification. Disrupted laminated facies are intergradational to both of the preceding facies. Stratification is locally disrupted by burrowing and soft-sediment deformation, resulting in convoluted, discontinuous, and wavy laminae.

Carbonate packstone dominates the upper part of the Thirtyone throughout all but the extreme southern parts of its distribution, where the upper part of the section has been removed by erosion that is, in the vicinity of the Fort Stockton Uplift). These deposits are primarily composed of fine-grained, well-sorted, grain-supported, skeletal packstones that contain abundant pelmatozoans and locally common bryozoans and ostracodes. Typically, these deposits are burrowed, although locally they are laminated and may display normal grading. As in cherty facies, *Zoophycos* burrows are common. Coarse-grained debris beds containing phosphatized clasts of shallow-water skeletal allochems including bryozoans, pelmatozoans, and calcareous algae are also locally common. Chert is present as patches of silicified carbonate and as thin laminations and beds up to several feet thick.

Thirtyone facies exhibit cyclic facies stacking patterns on at least two scales. The lower part of the section in the Thirtyone depocenter is characterized by cyclic alternations between chert/carbonate laminites and laminated, thick-bedded, calcareous chert (fig. 5). Farther upsection, cycles are composed of burrowed/laminated chert and thick-bedded chert. Yet farther upsection, cycles are composed of burrowed/laminated chert and skeletal wackestone-packstone. Laminated, thick-bedded, calcareous chert units are composed of thin, 10- to 50-cm-thick cycles characterized by grain-dominated bases and laminated, mud-dominated tops (fig. 6b).

In central Crane County (fig. 3), chert accounts for about 50 percent of the total section (although this varies widely). To the north, the percentage of carbonate increases dramatically. In Ector County, immediately north along the axis of the Thirtyone depocenter, the Thirtyone is almost entirely carbonate. Here, the section comprises an upward-shallowing succession of fine-grained, burrowed, skeletal packstones and wackestones that are overlain by progressively

coarser grained and higher energy, grain-dominated, skeletal grainstones and packstones. Chert is represented in this area primarily by a thin zone at the base of the section, although siliceous zones are locally present within the overlying carbonate section. Farther north, in southern central Andrews County, Thirtyone carbonates are composed of coarser grained, pelmatozoan and bryozoan packstone and grainstone. The distribution of coeval carbonate facies north of the Thirtyone chert subcrop in central Andrews County (fig. 4) is poorly constrained because of poor lithologic and biostratigraphic control. Potentially correlative rocks in this area are very similar to those that characterize the Fasken Formation. Isolated biostratigraphic data (conodonts and brachiopods), however, suggest at least isolated outliers of Thirtyone-equivalent carbonates are present (Wilson and Majewske, 1960; J. E. Barrick, personal communication, 1992).

Thirtyone chert facies also vary northward from the depocenter. Chert facies encountered in Winkler and southern Andrews Counties, Texas, for example, include about 100 ft of laminated, spicule grainstone and burrowed chert at the base of the Thirtyone section (fig. 4). Laminated spicule grainstone is similar to the laminated thick-bedded chert observed farther south but contains abundant spicules (fig. 6d). These spicule-rich rocks are found primarily along a northwest trend through eastern Winkler County and into southwestern Andrews County (Saller and others, 1991, 2001; Ruppel and Hovorka, 1995a, b).

Depositional Setting

Most authors (Saller and others, 1991; Ruppel and Holtz, 1994; Ruppel and Hovorka, 1995a; Montgomery, 1998; Ruppel and Barnaby, 2001) have interpreted the Thirtyone Formation to have been deposited in an outer platform to basin setting (fig. 7). These authors suggested chert sediments accumulated in a deep-water setting by processes of submarine gravity flow and hemipelagic sedimentation. Chert/carbonate laminites at the base of the section accumulated as hemipelagic muds on the basin floor in the southern part of the area. Alternations between silica mudstone and carbonate mudstone may reflect shifting sources of pelagic influx or variations in ocean chemistry, which in turn caused fluctuations in calcite or silica compensation depths. Thick-bedded, laminated cherts were deposited by turbidity or fluidized flow. The thick bedding and grading exhibited by many of these deposits are typical of sand- and silt-sized turbidites of both carbonate and siliciclastic composition (Howell and Normark, 1982; Cook, 1983; Walker, 1984; Piper, 1978). The presence of dewatering structures in some of these deposits indicates that these sediments were transported at least partially by fluidized flow

(Cook, 1983). Burrow-laminated cherts are typically cyclically interbedded with these thick-bedded cherts, suggesting that the former were deposited under lower energy conditions developed during cessations in flow or distal to active flow axes.

Ruppel and Hovorka (1995a) suggested that the distribution of thick-bedded, laminated chert deposits along a generally northwest-trending axis indicates that deposition was controlled by basin topography. The succession of alternating beds of higher energy, grain-dominated turbidites and lower energy, distal, more mud-rich deposits that characterizes lower Thirtyone deposition is typical of deposits recorded on submarine fans (Saller and others, 1991). Regional thickness trends indicate that siliceous sediment, like carbonate sediment, was sourced from Thirtyone platform areas to the north and/or west of the basin and accumulated along basin axes and depocenters.

The presence of carbonate in the upper part of the Thirtyone reflects a change in sedimentation style in the Early Devonian of the Permian Basin. Burrowed to laminated skeletal carbonate packstones mark the onset of rapid progradation of the Early Devonian carbonate platform from the north (fig. 7). The first appearance of significant carbonates in the section marks a change in depositional style from siliceous, submarine-fan deposition to carbonate-dominated deposition. Locally the first occurrences of carbonate in the section are associated with features suggestive of rapid downslope transport including poor sorting, lithoclasts, and a mixed faunal assemblage. These lowest carbonates in the section are typically interbedded with muddy burrowed/laminated chert that accumulated when episodic carbonate influx was low. Alternations between these two facies are thus a function of carbonate input and may reflect sea-level rise-fall patterns.

In several areas, primarily along the basin axis, thick-bedded, fan-deposited cherts are also encountered again in the upper part of the Thirtyone section above a thick carbonate section (fig. 4). Ruppel and Holtz (1994; see also Ruppel and Barnaby, 2001) interpreted these younger chert deposits to indicate relative sea-level rise creating additional accommodation and temporarily shutting off carbonate influx from the platform, thus facilitating renewed silica sediment deposition.

Current thickness patterns do not accurately reflect basin topography during Thirtyone deposition. Although the southern part of the Thirtyone depocenter in Crane County appears to have occupied a relatively deeper water position during the Early Devonian, patterns of chert distribution indicate that the axis of deeper water deposition extended to the northwest from

Crane County through Winkler County and into southwestern Andrews County, rather than trending north-south, as suggested by thickness patterns. The thick Thirtyone section in Ector County (fig. 3) is primarily composed of detrital carbonate deposited as a result of rapid progradation of the carbonate platform to the north. Progradation and upward shallowing in this area are demonstrated by grain-dominated carbonates that reflect increasingly higher energy conditions upsection.

The absence of basal chert deposits in central Andrews County, coupled with the presence of coarser grained, skeletal carbonates having more diverse faunal assemblages, suggests that Early Devonian paleotopography was controlled by the position of the Late Silurian (Wristen) platform margin. Sedimentation to the south was characterized by downslope transport and progradation of platform-derived carbonate and silica sediments. Sedimentation north of the hingeline was probably characterized by muddier, shallow-water deposits similar to those typical of the Wristen inner platform. Although pre-Woodford erosion has removed most of these shallow-water, Thirtyone-equivalent Devonian carbonates, isolated remnants have been identified biostratigraphically (Wilson and Majewske, 1960; J. E. Barrick, 1992, personal communication).

Diagenesis

Both the carbonates and the chert deposits of the Thirtyone Formation have undergone significant alteration since deposition. Chert facies have undergone both early and late episodes of diagenesis that have played important roles in reservoir development. Ruppel and Hovorka (1990, 1995a, b) and Saller and others (1991) addressed some aspects of this diagenesis in fields along the northern limit of the Thirtyone subcrop. It seems clear from these studies that chert diagenesis affected silica sediments very soon after deposition. On the basis of patterns of brecciation and chert porosity development, Ruppel and Hovorka (1995a,b) suggested that rates of silica diagenesis were closely associated with the distribution of carbonate-rich sediment layers. Williams and Crerar (1985) and Williams and others (1985) postulated that Mg^{++} released during carbonate diagenesis acts as a catalyst for chert diagenesis. This implies that opaline sediment adjacent to carbonate-rich sediment is more likely to undergo earlier and more complete diagenetic alteration from biogenic opal to more stable silica. Complete alteration to chert and quartz is likely to result in porosity loss, whereas slower rates favor retention of matrix microporosity. Ruppel and Hovorka (1995a,b) observed that nonporous chert is typically

associated with definable beds and patches of carbonate rock. The beds commonly also display more fracturing, suggesting earlier transformation to chert. Chert sediments distal to carbonate beds are typically porous, and fractures are uncommon, or more commonly indicative of more ductile deformation.

Ruppel and Hovorka (1995a, b) also concluded that the Thirtyone has been at least locally affected by late carbonate dissolution and cementation. Carbonate dissolution is apparent near the top of the Thirtyone section and along major fault zones. Areas of dissolution are commonly recognizable on wireline logs by high gamma-ray signatures caused by associated infiltrating clays. Although many of these karst zones are partly filled with calcite cement and clays, as shown by their log response, some are porous and large enough to have contributed to oil production in the field. Carbonate dissolution is important only locally in the Thirtyone. Along the northern extent of the Thirtyone subcrop, for example, where the Thirtyone was uplifted and partly truncated during the Pennsylvanian, dissolution of carbonate has locally formed vugs and enhanced matrix porosity.

Thirtyone carbonate facies have undergone diagenetic alteration much like that seen in similar facies in the Fasken and Fusselman Formations. Leaching of carbonate mud in skeletal packstone is the most important product of this alteration. Locally, these leached zones are dolomitized (for example, in Bakke and Andrews South fields, central Andrews County).

The present distribution of chert and carbonate in the Thirtyone Formation is probably a function of both depositional and diagenetic processes. Sedimentary structures and facies geometries indicate that chert-bearing rocks in the Thirtyone Formation were mostly deposited by deeper water processes (Ruppel and Hovorka, 1995a,b) It is apparent from the abundant spicules in many parts of the basin that these rocks had a high silica content during deposition. As McBride and Folk (1979) pointed out, however, it is difficult to accurately determine the original carbonate content of chert deposits. It is, therefore, possible that significant parts of Thirtyone cherty rocks may be the result of silica replacement of carbonate. This is certainly the case in parts of the mixed carbonate and chert successions in the upper Thirtyone, where silicified carbonate allochems are common, but it may also be true of the largely carbonate-free lower Thirtyone.

DEVONIAN BASIN EVOLUTION

Ruppel and Holtz (1994; Ruppel and Hovorka, 1995a,b) demonstrated that a major rise in relative sea level began in the region during the middle Silurian and continued into the Early Devonian. These authors also interpreted the depositional history of the Thirtyone on the basis of facies and stratigraphic relationships across the region (fig. 8). Basal Thirtyone sedimentation (fig. 8a) was marked initially by pelagic mud accumulation throughout the Thirtyone subcrop area. The distribution of these deposits is coincident with deeper water areas of the basin developed during the Silurian. Along the proximal, northwestern margin of the basin, accumulation of siliceous muds rapidly gave way to submarine-fan deposition of grain-rich, spiculitic sands (fig. 8b). These early chert deposits appear to have been derived from point sources on the platform in western Andrews County. At this time, siliceous muds (chert/carbonate laminite facies) continued to accumulate distal to these higher energy deposits and downdip (fig. 8c). Decreasing rates of sea-level rise and aggradation of the carbonate platform to the north resulted in basinward progradation along the northern platform margin. Progradation of the platform was most rapid in the Ector County area where skeletal carbonate deposits constitute the bulk of the rocks in the northern part of the Thirtyone depocenter.

Ruppel and Holtz (1994) and Ruppel and Hovorka (1995a,b) submarine-fan deposition of high-energy, grain-dominated cherts shifted southward in front of the advancing carbonate platform. They tied the geometries and textures of Thirtyone siliceous sediments to fan depositional processes with high-energy, grain-dominated sediments forming along fan/channel axes and more mud-dominated deposits accumulating in off-axis areas (fig. 9). With continued progradation, deposition of siliceous sediment was replaced by carbonate sediment consisting of debris derived from the platform to the north. Platform progradation produced progressive shallowing of the basin and terminated chert accumulation in all but extreme southern continental margin areas (that is, Caballos sediments of the Ouachita overthrust). The recurrence of similar chert deposits above these shallow-water, carbonate platform-derived, outer ramp/slope deposits suggests a later episode of relative sea-level rise and renewed chert sediment accumulation across the area (fig. 8d).

Truncation of the Thirtyone Formation, as well as underlying Wrusten Group and Fusselman Formation strata, probably occurred by the Middle Devonian. Regional studies suggest that uplift and truncation of much of the craton of the southwestern United States occurred at this time (Ham and Wilson, 1967). Work by Johnson and others (1985) also indicates

a global sea-level lowstand during the late Pragian. Many of the carbonate platform equivalents of the Thirtyone Formation were apparently removed by erosion at that time, although several erosional remnants still survive within the thick, predominantly Silurian, Wristen section of carbonate rocks present in the northern part of the area (Wilson and Majewske, 1960; J. E. Barrick, personal communication, 1992). Leaching of uppermost Thirtyone Formation rocks at several localities (for example, Bakke field) indicates that significant diagenetic alteration occurred during the Middle Devonian uplift.

SEQUENCE STRATIGRAPHY

Ruppel and Holtz (1994; Ruppel and Hovorka, 1995a,b) characterized several scales of cyclic sedimentation in the Thirtyone. Considering the deep-water setting of these deposits, however, most of these cycles relate to episodic flux of mass gravity flows (grain flows, turbidites) and perhaps the shifting of axes of deposition. These cycles are marked by changes in mud content (that is, grain size) and energy regime. Cyclic porosity development in these rocks (fig. 5) appears to reflect similar variations in energy of deposition and resultant facies. A connection between these depositional cycles and sea-level rise and fall is unclear.

The documented major shift from chert-dominated to carbonate-dominated deposition in the middle of the Thirtyone and the subsequent return to chert-dominated sedimentation may reflect sea-level-related control. Ruppel and Barnaby (2001) interpreted the presence of shallow-water carbonate sediments to reflect basinward progradation of the platform. They placed a sequence boundary at the top of these carbonate deposits, suggesting that the return to chert-dominated sediments above reflected sea-level rise and the landward backstep of the platform. However, no such sequence boundary was recognized by Johnson and others (1985), so further work will be necessary to document its existence.

RESERVOIR TYPES

Thirtyone Formation oil reservoirs in the Permian Basin can be grouped into two major depositional systems: (1) Deep-Water Cherts, and (2) Ramp Carbonates. Deep-water chert reservoirs dominate the central part of the Thirtyone subcrop. Ramp carbonate reservoirs are found along the northern margin, and siliceous ramp limestone reservoirs are found along the eastern part of the subcrop area (fig. 10). By far the greatest volumes of oil production have

come from chert-bearing and siliceous reservoirs (more than 88 percent of the total from the Thirtyone). Each of these plays has unique reservoir characteristics that must be considered in any detailed assessment of reservoir properties and resource potential.

Thirtyone Deep-Water Chert Reservoirs

Nearly all production from this play comes from Texas; the Thirtyone is absent from all but the extreme southeastern part of New Mexico (fig. 3). Two end-member styles of reservoir development are apparent. In the northern, or proximal, part of the Thirtyone depositional basin, reservoirs are developed at the base of the Thirtyone Formation (fig. 4) in a chert interval that is remarkably uniform, continuous, and tabular throughout an area of at least 250 mi² (fig. 10). Thirtyone cherts in this area are dominantly spiculitic and grain dominated but display subtle variations to more mud-rich facies that are probably the result of minor variations in topography or in delivery systems. These grain-rich, porous rocks grade laterally into more mud-dominated, low-porosity and low-permeability facies. The uniform architecture of these updip basal Thirtyone cherts in this part of the basin suggests that they accumulated in a low-relief, proximal platform to platform-margin setting. Three Bar field, Dollarhide, and Bedford fields are representative of this reservoir play (fig. 10). Downdip, into the Thirtyone depocenter, these basal cherts grade into nonporous, hemipelagic, laminated siliceous and calcareous mudstones (fig. 4).

Chert reservoirs in the southern or distal part of the Thirtyone basin are developed higher in the Thirtyone section overlying mud-dominated hemipelagic deposits (fig. 4). These cherts document basinward progradation of the Thirtyone and the southward shift of the locus of chert accumulation (fig. 4). While cherts were being deposited in the basin depocenter, shallower water skeletal carbonate sediments accumulated updip in more proximal areas (that is, at Three Bar field). Reservoir successions in more basinward chert deposits are thicker because of greater long-term accommodation caused by greater water depths and higher subsidence rates. Rapid progradation of northern and western carbonate platforms limited the accumulation of grain-rich siliceous deposits to a relatively small area in the basin center (Ruppel and Holtz, 1994). Reservoirs developed in this area are characterized by multiple, stacked successions of high-energy, grain-dominated chert grading upward into lower energy, more mud-dominated, burrowed cherts (fig. 4). These chert strata are much less continuous in their lateral extent than

are those to the north. Block 31 and University Waddell reservoirs are good examples of this reservoir type or subplay.

Proximal Thirtyone Chert Deposits

Proximal chert deposits are typified by those at Dollarhide, Bedford, and Three Bar fields in southern Andrews County near the northern limit of the Thirtyone Formation subcrop (fig. 10).

The Thirtyone Formation at Three Bar field typifies northern, more proximal chert reservoir successions (Ruppel and Hovorka, 1995). Other analogous reservoirs include Dollarhide (Saller and others, 1991, 2001) and Bedford, among others. At Three Bar, the Thirtyone is characterized by a rather stratiform basal succession of about 90 ft of chert and an overlying carbonate-dominated section of as much as 300 ft of largely nonporous limestone (fig. 11). Except where truncated, these units generally display sheetlike geometries with typically only subtle lateral variations in thickness. The chert-dominated interval contains mixtures of three facies: (1) translucent, nonporous chert, (2) porcelaneous, porous chert, and (3) skeletal carbonate. Chert intervals typically contain thin, discontinuous beds and irregular patches of skeletal lime wackestone to packstone composed of silt-sized allochems.

Chert Facies

Porous and nonporous chert differ primarily in allochem preservation and porosity. Both chert facies are massive to indistinctly laminated and pervasively burrowed (fig. 12A). Small *Planolites* and *Zoophycos* burrow traces are filled with carbonate or chert. Burrow-filling carbonate consists of skeletal packstone containing abundant ostracodes and is similar to that in carbonate interbeds within the chert section. Both cherts contains abundant sponge spicule molds as much as 300 μm long and 50 μm in diameter. These spicules, which make up 5 to 30 percent of the chert by volume, typically exhibit round and tubular cross sections of straight and curved monaxons (fig. 12B). Other allochems include peloids and carbonate skeletal debris, including primarily ostracodes and lesser amounts of fragmented pelmatozoans and brachiopods. This skeletal assemblage is identical to that found in carbonate interbeds within the lower, chert-dominated section but is notably different from that in the thick carbonate succession at the top of the Thirtyone Formation, which contains primarily pelmatozoan debris. Spicules are less well preserved in porous chert (fig. 12C) but are readily identified by their hollow round cross

sections and similarity of shape, size, and occurrence to the better preserved spicules in nonporous chert (fig. 12B).

Porous chert contains as much as 35 percent porosity comprising six pore types: (1) hollow axial channels of sponge spicules, (2) molds of dissolved spicules, (3) molds of dissolved calcitic and aragonitic bivalves, (4) molds of carbonate rhombs, (5) intercrystalline microporosity within the chert matrix, and (6) pores formed by solution enlargement of each pore type. Spicule molds, which measure 5 to 50 μm in diameter, and intercrystalline micropores in the interspicular matrix are dominant. Spicule molds are lined and partly filled with 2- to 10- μm euhedral, microquartz crystals and chalcedony cements (fig. 12D). Interspicular matrix areas contain loosely packed, 0.5- μm microquartz ellipsoids that are aggregated into irregular, 2- to 3- μm spheroidal masses (fig. 12E). Intergranular micropores between microquartz ellipsoids measure fractions of micrometers in diameter; larger pores are present between the spheroidal aggregates (fig. 12E). These microtextures have been observed in porous Thirtyone Formation cherts throughout West Texas, including Bedford, Cordona Lake, Block 31, and University Waddell fields.

Examination of depositional fabrics in porous and nonporous chert shows that both originated as thick beds of spicules in a finer siliceous matrix, with thin beds of carbonate admixed by pervasive burrowing. Preserved fabrics indicate no systematic contrast in original sediment composition between porous and nonporous chert. In hand sample, the two chert types are gradational, with local mottles of nonporous chert within porous chert (fig. 12A).

Carbonate Facies

The upper part of the Thirtyone Formation in Three Bar field is composed primarily of brownish-gray limestone that contains light-colored chert lenses and nodules. These rocks comprise predominantly skeletal packstone with well-sorted and abraded silt-sized pelmatozoan debris, less common brachiopods and mollusks, and relatively rare ostracodes. Although nearly massive in appearance, these rocks are burrowed and locally display normal grading, especially near the base of the carbonate interval. Sponge spicules are common, especially where larger masses of chert are developed (as nodules or lenses). Siliceous zones are associated with muddier carbonate textures but are very rarely developed in grain-rich pelmatozoan packstone and grainstone. Thirtyone carbonate rocks are largely nonporous; most intergranular pores are filled with syntaxial overgrowths around pelmatozoan grains.

Facies Architecture

Major Thirtyone Formation facies are remarkably uniform in thickness at Three Bar field. The lower chert-rich interval of the Thirtyone Formation is essentially constant in thickness throughout the field except where truncated along the updip margin (fig. 13). This architecture continues westward to New Mexico and southward into Ector and Winkler Counties (fig. 10).

Depositional Setting

The Thirtyone Formation succession at Three Bar field documents progressive upward shallowing. Basal chert is interbedded with fine-grained ostracode-bearing carbonate packstone suggestive of a distal quiet-water setting. Carbonates at the top of the section, however, contain predominantly pelmatozoan packstones. Regionally, these packstones grade into cross-laminated grainstones documenting high-energy, shallow-water conditions (Ruppel and Holtz, 1994). The presence of a relatively restricted marine fauna (ostracodes) in carbonates associated with the basal Thirtyone chert compared with a more diverse shallow-water fauna in the overlying carbonates supports the regional model that siliceous sediments accumulated in a distal, quieter water setting basinward of the prograding carbonate platform. Fine-scale interbedding observed in the chert section probably reflects minor fluctuations in delivery of siliceous and carbonate sediment. The basal Thirtyone chert section at Three Bar grades basinward into chert and carbonate mudstones suggestive of hemipelagic deposition (fig. 4; Ruppel and Holtz, 1994). Updip, cherts grade into proximal skeletal carbonates.

Fracturing and Faulting

Open and closed fractures are common in both chert and carbonate facies at Three Bar; however, cherts contain two to six times as many fractures as associated limestones. In addition, fractures detected in available cores are more abundant within or close to identified fault zones along the northern and southern edges of the field. The density of fractures is much less in the apparently less densely faulted middle and northern parts of the field (Ruppel and Hovorka, 1995b).

Styles of fracturing or brecciation also differ between porous and nonporous chert, reflecting the diagenetic history of these siliceous sediments. Nonporous cherts are characterized by angular to subangular, rotated clasts, open fractures, and incompletely detached blocks (fig. 12A). Porous cherts contain rounded and generally smaller clasts in a matrix that is virtually

identical in composition to that of the clasts. Brecciated porous chert commonly displays indistinct small-scale soft-sediment offsets that are completely healed, suggesting ductility at the time of deformation (Ruppel and Hovorka, 1995b). The contrast between chert brecciation styles indicates that nonporous chert sediments were better lithified than their porous counterparts at the time of brecciation.

Diagenesis

Both early and late episodes of diagenesis have played important roles in reservoir development. As previously discussed, Ruppel and Hovorka (1995a) showed that the distribution of porous and nonporous chert in the reservoir is a direct result of early chert diagenesis and the distribution of carbonate interbeds within the section. Their work showed that chert sediment distal to carbonate beds underwent slower chert lithification and porosity preservation. This scenario is consistent with the distribution of porous and nonporous chert in the Thirtyone at Three Bar—cherts adjacent to carbonate are invariably nonporous. Because most of the carbonate at Three Bar is stratiform and limited to two major intervals (fig. 13), porous chert is continuous throughout the field.

Late carbonate dissolution and cementation contributed to both development and reduction of porosity. Carbonate dissolution is apparent near the top of the Thirtyone section and along major fault zones. Areas of dissolution are commonly recognizable on wireline logs by high gamma-ray signatures caused by associated infiltrating clays. Although many of these karst zones are partly filled with calcite cement and clays, as shown by their log response, some are porous and large enough to have contributed to oil production in the field.

Porosity and Permeability

Core analyses indicate that porosity in Thirtyone cherts in Three Bar field ranges up to about 25 percent (fig. 14). Three types of pores are present: (1) molds, (2) intercrystalline to micro-intercrystalline pores within the chert matrix, and (3) fractures. Molds (fig. 12C) average 30 to 40 μm and typically constitute up to half of the pore space. Chert matrix porosity is composed of interparticle pores between quartz aggregates and micropores within aggregates (fig. 12D, 12E). Micropores average less than 5 μm in diameter. Capillary-pressure analysis of petrologically identical cherts in the nearby Bedford field (3 mi west) indicates that as much as half of the total chert porosity is composed of intercrystalline and micro-intercrystalline pores.

This result is consistent with the findings of Tinker (1963) and Saller and others (1991), who suggested that micropores account for at least 50 percent of the total porosity in Thirtyone Formation chert. A similar relationship is probable in the Three Bar reservoir; scanning electron microscope analysis and transmitted-light petrography of chert in Three Bar field confirm such pores are common. Although fractures are common throughout the chert section at Three Bar field, point-count data show they typically contribute less than 1 percent porosity.

Chert permeability at Three Bar field averages about 5 md (fig. 14). Core analyses suggest that permeability has both matrix and fracture components. Much of the scatter in these data is the result of fractures. True matrix porosity/permeability relationships in Thirtyone chert rocks were established by analyzing core plugs especially selected to have no fractures (fig. 14). These data suggest that maximum matrix permeability is generally about 10 to 20 md.

Reservoir Heterogeneity

Primary causes of heterogeneity and incomplete drainage and sweep of remaining mobile oil at Three Bar are (1) faulting and fracturing, (2) carbonate dissolution, and (3) small-scale facies architecture. Faults and fractures are abundant in the field and affect reservoir heterogeneity on several scales. In addition to promoting access to diagenetic fluids, faults and fractures may also facilitate or inhibit movement of hydrocarbons and injection waters. In the southern part of the field, zones of abundant faults and fractures are associated with areas of increased fracture permeability that are typically highly productive, suggesting that variations in fracture density may locally contribute to productivity by facilitating flow across facies-controlled permeability boundaries. Production and waterflood patterns reveal poor sweep efficiency and support the contention that fracture zones control fluid movement in parts of the reservoir.

Some faults may also be flow barriers. Bottom-hole-pressure data confirm that at least one fault separates distinct reservoir compartments. It is probable that other faults in the reservoir have produced complete or partial offset in major reservoir pay zones, thus creating reservoir compartmentalization. Correlation and mapping studies indicate that faulting is most common in the northeastern and southwestern parts of the Three Bar Unit, largely coincident with areas of interpreted karsting. More abundant faults and fractures in these areas have two consequences. First, some faults may act as flow barriers and thus create additional reservoir compartmentalization. Acquisition of modern high-resolution, 3-D seismic data is required to

accurately delineate fault distribution and fully evaluate the implications of potential compartmentalization due to faulting in the reservoir. Second, variations in fracture density across the reservoir may cause nonuniform water injection sweep. If this is the case, significant areas of matrix porosity are likely to have been bypassed by waterflood. These areas of the reservoir are possible sites of targeted infill drilling and selective completion and recompletion of existing wells. Borehole image logs may provide critical data for detecting the presence and distribution of fractures and faults within the reservoir.

Leaching and dissolution of carbonate intervals are also major causes of reservoir heterogeneity. Most carbonate porosity development is probably the result of leaching by diagenetic fluids that entered along the truncated and exposed updip margin of the field during the Pennsylvanian. Evidence of carbonate dissolution is apparent in cores, especially in areas of greater fault density, suggesting that faults have acted as flow pathways for diagenetic fluids. Porosity development in the carbonate interval that separates the two major chert intervals also appears to be more common on upthrown fault blocks and near the faults that offset them. Erosion on these high blocks and fluid movement along the bounding faults may have facilitated diagenesis. In areas in which carbonate interbeds are absent or have become porous because of subsequent leaching and diagenesis, for example, in the easternmost part of the field, vertical communication is enhanced and productivity is higher.

Distal Thirtyone Chert Deposits

University Waddell field (figs. 10, 15) contains a Thirtyone reservoir succession that is typical of those in a more distal depositional setting.

Geological Facies

Ruppel and Barnaby (2001) defined six major facies in the Thirtyone Formation at University Waddell field (fig. 16): (1) finely laminated chert and limestone; (2) nodular chert and limestone; (3) disrupted laminated chert; (4) burrowed chert; (5) thickly laminated to massive chert; and (6) skeletal packstone. All chert facies are intergradational and possess many common features, suggesting they were deposited under very similar conditions.

Finely Laminated Chert and Limestone

These rocks, which are confined to the base of the Thirtyone Formation and are generally nonporous and impermeable, comprise millimeter- to centimeter-thick parallel laminae of gray chert and brown, organic-rich lime mudstone (fig. 17A). Chert laminae display erosional bases and upward-fining grain-size trends of silt-sized indeterminate grains and siliceous sponge spicules (fig. 17B). Although burrowing is not extensive, *Zoophycos* burrows are locally present.

This facies, which accumulated in a low-energy, deep-water, basinal setting, represents the most distal of Thirtyone Formation deposits at University Waddell field. The silt-sized chert grains record distal turbidity sedimentation, whereas intercalated, organic-rich lime mudstones document hemipelagic sedimentation between episodic turbidity flow events. The well-developed lamination and the paucity of soft-sediment deformation and fluid escape structures imply relatively slow accumulation rates in a stable basinal setting (fig. 9). *Zoophycos* trace fossils are consistent with deposition in quiet, oxygen-deficient waters below storm wave base (Frey and Pemberton, 1984).

Nodular Chert and Limestone

Like the finely laminated chert and limestone facies to which they are closely related, these rocks consist of alternating laminae to thin beds of gray chert and brown, organic-rich lime mudstone. These rocks differ, however, in containing prominent nodular bedding, early fractures, fluid escape structures, and evidence of soft-sediment deformation, (fig. 17C). Chert consists of mud-dominated packstone composed of silt-sized abraded skeletal debris, peloids, and mud; siliceous sponge spicules, pelmatozoan fragments, and ostracodes are locally common. Lime mudstones contain scattered silt-sized peloids and abraded skeletal fragments. Burrowing by *Zoophycos* and other infauna is locally intense. Although these rocks typically display low porosity and permeability, they do contain minor intercrystalline porosity (fig. 17D).

The presence of peloid-skeletal debris in these rocks indicates deposition by influx of platform-derived sediment via turbidity currents rather than strictly by hemipelagic sedimentation. Soft-sediment deformation, early fractures, and fluid escape structures attest to episodic rapid deposition on an unstable slope. Locally intense bioturbation and in situ lithification imply intermittent periods of low sediment accumulation.

Disrupted Laminated Chert

These rocks display features of and gradational to both of the preceding facies. Stratification is locally disrupted by burrowing and soft-sediment deformation that result in convoluted, discontinuous, and wavy laminae (fig. 18A), although not to the degree seen in the nodular chert and limestone facies. Chert laminae, which display ripple laminations and normal grading, comprise packstones composed of fine-grained peloids, sponge spicules, abraded pelmatozoan, brachiopod, trilobite debris, and ostracodes (fig. 18B). Limestone laminae consist primarily of wackestone to mud-rich packstone, although lime mudstone is locally common as burrow fills. *Zoophycos* burrows are common, as are fluid escape structures. Intercrystalline and moldic grain dissolution pores are locally present, but these rocks are generally nonporous and impermeable.

The presence of ripple laminated peloid-skeletal debris in these rocks indicates they represent higher energy transport of platform-derived sediment than observed in preceding facies. This suggests a more proximal position relative to sediment delivery axes. Stratification is better preserved than in the nodular chert and limestone facies, suggesting dominance of sediment delivery over burrowing.

Burrowed Chert

Although burrowed cherts exhibit most of the features of the preceding facies in terms of sedimentary structures, grain size and grain composition, intensive bioturbation by *Zoophycos* and other burrowers has obliterated much of the primary depositional stratification (fig. 18C). Despite the extensive burrowing, however, ripple laminations, soft-sediment deformation, fluid escape structures, organic-rich laminations, and normal grading are locally apparent. Like other chert facies, these rocks contain silt- to fine sand-sized siliceous sponge spicules, abraded skeletal debris, peloids, and intraclasts (fig. 18D). Pelmatozoans, brachiopods, trilobites, and ostracodes dominate the fauna. Burrowed cherts are generally relatively nonporous and impermeable, although dissolution of siliceous sponge spicules has created minor local moldic porosity.

Graded bedding and ripple lamination suggest high-energy downslope transport of platform margin-derived sediment via turbidity flows. A slight increase in the grain size (up to fine-grained sand) suggests a more proximal, higher energy depositional setting. Individual chert laminae display ripple lamination with normal grading, indicating that this facies records higher

energy turbidite sedimentation. This facies is interpreted to have accumulated as distal submarine fans and overbank deposits on the margin of turbidite channels (fig. 9).

Thickly Laminated to Massive Chert

These rocks consist of thickly laminated to massive gray cherts (fig. 19A). Within individual thick laminae and thin beds, normal grading, ripple laminations, soft-sediment deformation, and fluid escape structures are locally present. Dark, organic-rich wispy laminations and stylolites are common at the tops of upward-fining successions. Bioturbation ranges from distinct burrows, including *Zoophycos*, to complete sediment homogenization. Burrowing, soft-sediment deformation, patchy silicification, and differential compaction have locally resulted in disrupted lamination and incipient nodular fabrics.

The chert in this facies consists of well-sorted, silt-sized to fine-grained, skeletal packstones/grainstones dominated by siliceous sponge spicules but also containing abraded pelmatozoans, ostracodes, and brachiopods (fig. 19B). Calcite generally represents 10 to 40 percent of the total mineralogy as corroded skeletal fragments, incompletely silicified matrix, laminae, nodules, and burrow fills.

This chert facies constitutes the dominant Thirtyone reservoir facies in University Waddell field. Much of the porosity, which locally exceeds 25 percent, takes the form of molds caused by dissolution of siliceous sponge spicules. Intercrystalline and primary interparticle pores are less significant contributors to total porosity. Core-log relationships indicate that nearly all porosity in the Waddell reservoir is associated with this facies (fig. 16). This relationship permits correlation and mapping of this facies within the Thirtyone succession using porosity logs and facilitates the definition of flow-unit architecture.

Thickly laminated to massive cherts record relatively high energy depositional conditions, as evidenced by good sorting, the slightly coarser grain size dominated by sponge spicules and shallow-water skeletal fragments, and the paucity of fine mud matrix. Normal grading and ripple laminations imply transportation via turbidity flows from the platform margin (fig. 9). Rapid deposition is indicated by the sedimentary structures and by the paucity of intense bioturbation relative to the burrowed chert facies. Individual depositional events, which are characterized by upward-fining successions with organic laminations at their tops, range up to the decimeter scale in thickness. Superposition and amalgamation of multiple depositional units along the axis of turbidite channel/proximal submarine fan fairways formed composite porosity

units ranging up to 20 ft thick with channel-form to lobate depositional geometries. These cherts pass laterally and vertically into relatively impermeable, more distal finely laminated to burrowed mud-rich cherts and limestones that record slower depositional rates dominated by overbank and hemipelagic sedimentation.

Skeletal Packstone

These gray, thin-bedded to massive limestones are composed of well-sorted skeletal packstones/grainstones that contain chiefly crinoids and minor siliceous sponge spicules, brachiopods, mollusks, ostracodes, bryozoans, and trilobites (figs. 19C, 19D). Chert is locally common as patchy silicification, as well as thin laminations and beds as much as several feet thick. As in cherty facies, *Zoophycos* burrows are common. The facies is relatively nonporous and impermeable because interparticle pore space is completely occluded by syntaxial and interparticle calcite cements and by lime mud.

A below-storm-wave-base depositional setting is indicated for these deposits by the absence of shallow-water sedimentary features including cross-stratification and upward-shoaling cycles. Skeletal grain-rich rock fabrics, with very coarse grained, shallow-water fossil assemblages, suggest basinward transport from the platform. This facies most likely records allochthonous transport of skeletal sands to a foreslope, slope, and toe-of-slope platform-margin setting. These rocks dominate the upper highstand portion of the Pragian 1 sequence (see below), recording more proximal deposition as the platform margin prograded basinward. Relatively minor thin limestone beds within the chert-dominated successions record episodic downslope transport of platform-derived carbonate silts and very fine sands to the basin. Limestones are essentially nonproductive facies; minor production attributed to these successions is from interbedded cherts and siliceous limestones.

Stratigraphy and Depositional Setting

Delineation of reservoir architecture in the Thirtyone Formation at Waddell field and surrounding areas has previously been inhibited by the difficulty of establishing intraformational correlations because of the low gamma-ray log response in these typically siliciclastic-poor cherts and limestones. We have identified three intraformational gamma-ray markers, however, that can be correlated to significant stratigraphic and lithologic surfaces (fig. 16). These markers

(fig. 20) are fundamental for defining the stratigraphic framework of the Thirtyone Formation at University Waddell field.

The lower Thirtyone Formation consists of approximately 500 ft of deep-water cherts and siliceous limestones, commonly referred to as the “lower chert.” Mud-rich, finely laminated chert and limestone facies and nodular cherts and limestones at the base of this succession (fig. 20) record a basinal environment dominated by hemipelagic sedimentation with episodic distal turbidite deposition (fig. 9). These facies pass upward into disrupted laminated and burrowed cherts that contain allochthonous shallow-water skeletal grains, indicating a more proximal setting with increased turbidite influx. Extensive burrowing suggests these rocks were deposited in areas of slower sediment accumulation on the margins of more active axes of sedimentation (fig. 9). Disrupted laminated and burrowed cherts are overlain by and grade laterally into well-sorted, skeletal grain-rich, thickly laminated to massive chert, that represent high-energy channel and fan deposition. These high-energy chert deposits compose the major reservoir succession in the field (figs. 16, 20).

The top of the “lower chert” is transitional from chert-dominated lithologies to overlying skeletal limestones. However, a gamma-ray marker (C; fig. 20) is well defined at this point in the section in University Waddell field and can be traced southward at least to Block 31 field. In the absence of known chronostratigraphic markers, this horizon is invaluable for correlating and subdividing the reservoir succession into mappable porosity units.

The lower chert is overlain by approximately 200 ft of skeletal-crinoidal packstones and siliceous limestones (fig. 20). The coarse grain size, moderate sorting, lack of shallow-water current stratification, and predominantly shallow water fossils in these rocks indicate limited downslope transport of skeletal sands to the slope during highstand progradation. Cherts are less abundant in this interval, because of rapid deposition of platform-derived carbonate debris (Ruppel and Barnaby, 2001).

The limestone section is overlain by another interval of chert and siliceous limestones termed the “upper chert” (fig. 20). These younger chert deposits document a return to deeper water deposition, suggesting renewed rise in relative sea level. Ruppel and Barnaby (2001) tentatively defined a sequence boundary at the base of this upper chert succession (fig. 20).

Upper chert facies consist of nodular chert and limestone, disrupted laminated and burrowed chert, thickly laminated to massive chert, and interbedded skeletal packstone. These strata are typical deeper water facies and thus define a transgressive facies tract offset, consistent

with interpretation of the A marker as a sequence boundary. The upper chert extends to the eroded top of the Thirtyone Formation (fig. 20).

The upper chert ranges from 230 to 300 ft in thickness. This variation in thickness reflects Middle Devonian, pre-Woodford erosion and truncation that resulted in a minimum topographic relief of 70 ft across University Waddell field. Isopach trends suggest a north-northeast trend, which may represent paleoridges and paleovalleys incised during Middle Devonian subaerial exposure. Because of erosional truncation at the unconformity, the thickness of Pragian 2 sequence is unknown.

Reservoir Development

Although reservoir porosity is developed in both the lower and upper chert intervals, reservoir quality is highest in the lower interval, which accounts for most of the oil production in the field. Lower chert reservoirs are composed of porous thickly laminated to massive cherts (fig. 16) dominated by well-sorted siliceous sponge spicules and carbonate skeletal debris. Depositional fabrics, sedimentary structures, and the dip-elongate channel-form to lobate geometry of individual porosity bodies suggest that these reservoir facies record a turbidite channel to fan depositional setting. Well-sorted, high-energy reservoir-grade facies pass vertically and laterally into relatively low permeability, mud-rich cherts and siliceous limestones that record hemipelagic, overbank, and distal turbidite sedimentation (fig. 9). Chert deposits appear to step progressively basinward (southward) upsection (fig. 4), perhaps reflecting decreasing accommodation associated with declining rates of sea-level rise. Renewed chert accumulation in the upper part of the Thirtyone (upper chert section) may indicate renewed sea-level rise and transgression.

Brecciation, Fracturing, and Diagenesis

According to Ruppel and Barnaby (2001), the fractured/brecciated cherts at Waddell resemble brecciated chert fabrics developed at the base of the chert section at Three Bar field, which have been interpreted to have formed by the entry of dissolution fluids along the contact between the Thirtyone and the underlying Frame Formation (Ruppel and Hovorka, 1995b). At Waddell, fractured/brecciated cherts are restricted to the top of the Thirtyone, below the pre-Woodford unconformity. This relationship suggests that such fabrics at Waddell were also created by diagenesis associated with entry of meteoric fluids during subaerial exposure, in this

case along the exposed top of the Thirtyone Formation. Irregular diagenetic overprinting of primary depositional fabrics in the upper chert interval may account for the poorly developed, highly discontinuous porosity zones in this interval that defy correlation and mapping efforts.

Petrophysics

Both neutron or density-neutron logs provide good resolution of porous facies; acoustic logs do a poorer job, because of the differing acoustic response to the highly variable admixtures of chert and carbonate in the reservoir facies. Log-derived porosity curves were used to refine correlations and were critical for reservoir mapping. Integration of core descriptions and core analyses with corresponding wireline logs indicates that nearly all of the significant porosity in the reservoir can be attributed to the thickly laminated to massive chert facies (fig. 16). Other facies exhibit little or no porosity, except in rare cases where extensive late fracturing has created minor porosity.

Reservoir Architecture

The well-defined relationship between porous chert facies and their wireline log response facilitates identification and correlation of these log facies throughout the study area. Detailed correlation and mapping of individual porosity units were limited to the major reservoir interval, the upper 150 ft of the “lower chert” succession, subjacent to the C log marker, where reservoir porosity is best developed.

Using core and wireline data, Ruppel and Barnaby (2001) correlated and mapped more than 30 porosity units in the area of detailed study in University Waddell field. Individual units range up to 20 ft in thickness and from less than 0.1 mi to several square miles in areal extent. Porosity zones are separated vertically from one another by nonporous chert facies (fig. 21). Isopach and ϕ^*h maps indicate that porosity units form lobate to elongate bodies that generally trend west-northwest to north, subparallel to the regional depositional axis. These maps show that porosity zones have distinctly different geometries and distribution across the field (fig. 22).

Core studies by Ruppel and Barnaby (2001) show that mapped porosity units consist of vertically stacked and amalgamated, centimeter- to decimeter-thick strata of thickly laminated to massive cherts. Facies data from cores combined with information on mapped geometries suggest that porosity units record multiple high-energy depositional events with sediment accumulation focused along channel/submarine-fan fairways (fig. 9). Porosity zones representing

higher energy grain-rich turbidite flows are separated from one another by more mud-rich rocks that reflect low-energy deposition. Areas distal from axes of active deposition were relatively sediment starved, receiving only mud-rich silt to very fine grained material from overbank and distal turbidite influx, in addition to hemipelagic sediment. Continued sedimentation along the channel/submarine-fan axes created depositional highs, ultimately resulting in their abandonment by channel avulsion, and sedimentation switched to adjacent, previously sediment-starved depositional lows. This pattern of deposition created a succession of vertically and laterally segregated chert reservoirs in University Waddell field and other fields near the Thirtyone Formation basin depocenter. This complex depositional architecture is a major contributing factor to reservoir heterogeneity and accompanying low recovery efficiency.

Fault and Fracture Induced Heterogeneity

In equivalent updip Thirtyone Formation reservoirs, including Dollarhide (Saller and others, 1991, 2001) and Three Bar (Ruppel and Hovorka, 1995a, b) fields, fault-induced reservoir compartmentalization has been documented (by 3-D seismic) or inferred. Ruppel and Barnaby (2001) documented several small-scale (<100 ft offset) reverse and normal faults at Waddell field that they inferred to be steeply dipping. They also found that open fractures, some partly infilled by quartz and/or calcite cement, are common. Although fracture patterns and their impact on reservoir permeability and anisotropy are not understood, production response suggested they play an important part in reservoir fluid flow. Producing wells immediately adjacent to water injection wells exhibited rapid breakthrough of injection water in the eastern parts of the field, whereas corresponding producers to the north and south did not. Such production trends indicate preferential permeability along an east-west direction, perhaps due to fractures and/or small-scale faults.

Summary of Heterogeneity in Distal Thirtyone Reservoirs

In contrast to proximal Thirtyone chert reservoirs like Three Bar field, where there is a single, continuous porous chert reservoir, Waddell field and related distal chert reservoirs contain numerous separate and discontinuous stacked porous chert units. In these reservoirs, lack of continuity is the primary contributing factor to heterogeneity and low recovery efficiency. The distribution of porous chert in distal settings is a function of sediment geometries associated with submarine-fan and turbidite deposition. Episodic downslope transport of siliceous spiculitic

sediment along the margins of the carbonate platform has resulted in vertical segregated and laterally discontinuous chert reservoir intervals. These deposits are interbedded with and grade laterally into lower energy mud-rich sediments that typically have low porosity and permeability. Although these muddy rocks are not flow barriers, they do act as baffles to flow and impact recovery efficiency. Detailed correlation and mapping of individual porous chert layers are critical for establishing a reservoir framework that can serve as a basis for defining recompletion and infill drilling targets. Such an approach has led to the identification of several drilling and recompletion prospects in Waddell field.

As in the case of Three Bar reservoir, the impact of faulting and fracturing on Waddell reservoir performance is not well known. Intrafield faults identified in the course of this study have sufficient displacement to offset porous flow units and may locally constitute lateral flow barriers. Waterflood breakthrough analysis suggests fracture contribution to permeability, but insufficient data are available to develop predictive models of fracture flow in the reservoir. Better resolution in the form of modern 3-D seismic would aid in developing a better model of the impact of faulting on reservoir compartmentalization and help define the distribution of chert reservoir intervals.

Thirtyone Formation Ramp Carbonate Reservoirs

The Thirtyone Ramp Carbonate play is the smaller of the two plays defined by Dutton and others (2005). Through 2001, production from reservoirs having produced at least 1 million barrels was 110 million barrels. Ruppel and Holtz (1994) showed that that these reservoirs typically exhibit low recovery efficiencies and thus contain the highest percentage of remaining oil among all Silurian and Devonian reservoirs.

Distribution

Nearly all of these reservoirs are located in Texas (fig. 23). They are located along the northern limit of the Thirtyone Formation subcrop and apparently represent the margin of the Thirtyone platform (fig. 10). In some fields, production also comes from underlying Thirtyone deep-water cherts (for example, Dollarhide and Bedford fields).

Depositional Facies and Paleoenvironments

Thirtyone ramp carbonate reservoirs are dominantly composed of skeletal grainstones and packstones (fig. 24a) Crinoids dominate the fauna, but bryozoans (both ramose and fenestrate) are locally abundant (fig. 24b,c). As described earlier, Thirtyone carbonate facies are dominantly grain rich. Downdip and downsection, carbonate facies are fine-grained, skeletal calcarenites that are locally graded. Upsection and updip these distal, transported carbonates grade into coarser grained, in situ, grain-rich, high-energy, platform-top shoal successions (fig. 25). Reservoirs assigned to the Thirtyone Ramp Carbonate play are developed in both of these end-member facies.

Diagenesis and Porosity Development

Four major types of diagenesis have affected Thirtyone carbonates of the Thirtyone Ramp Carbonate play: (1) early cementation and pore occlusion by syntaxial cement, (2) leaching of carbonate mud in packstones, (3) dolomitization, and (4) silicification. The first caused substantial porosity occlusion of original depositional pore space; the other three caused porosity retention or enhancement.

Because of the abundance of crinoids in virtually all of the succession, syntaxial cement is omnipresent in these rocks (figs. 24b,c). These cements (which grow as optically continuous rim cements around crinoids) apparently formed during early diagenesis in the marine realm. Crinoid grainstones are commonly composed of as much as 50 percent syntaxial cement and rarely contain significant porosity.

Evidence of postdepositional leaching or dissolution of selective grains is most common in packstones (fig. 24c). Leaching seems to have targeted carbonate mud and, to a lesser extent, bryozoans. Because of the leaching, carbonate packstones contain higher porosity than grainstones.

Dolomitized Thirtyone rocks contain the highest porosities observed in the play. Dolomite is most abundant at the top of the Thirtyone section, specifically in Andrews County (fig. 26). In these rocks, dolomite is locally pervasive and associated with extensive interparticle porosity (fig. 24d). Locally, porosity in these reservoirs reaches 10 to 15 percent. Dolomite is also present, although much less abundant, downsection. In these rocks (for example, at Bedford field, fig. 27), porosity and permeability are generally lower but still sufficient to facilitate oil production (fig. 28).

Thirtyone carbonates also locally display significant amounts of chert. Although this chert is present in small amounts throughout much of the carbonate section, it is most abundant in the eastern and southeastern parts of the play. This chert differs significantly from chert present in the lower and more distal parts of the formation (that is, deep-water chert facies) by being present only in carbonate packstones where it is entirely restricted to the matrix. As with dolomitized sections to the west, porosity is associated with the silicified matrix of packstones (fig. 24e); grainstones contain no mud, no silica, and no porosity. In some parts of the succession, packstones and grainstones form cycles of cycle-base porous rocks and cycle-top nonporous rocks (fig. 24f).

Reservoir Development

As a whole, the reservoirs of this play exhibit the lowest porosity values among Devonian plays. This is largely the result of the abundance of crinoid grainstones. Reservoir development is limited to areas that have undergone postdepositional diagenesis. In the western part of the play area this diagenesis is typically a combination of dolomitization and selective matrix leaching. Highest porosity is associated with rocks that been dolomitized. Dolomite is most common immediately below the unconformity that forms the top of the Thirtyone section (fig. 26). Several fields in central Andrews County are productive from reservoirs developed in these dolomites at the top of the Thirtyone (for example, Block 9 field, Bakke field). Some reservoirs are also developed in limestones that, although not extensively dolomitized, have undergone sufficient leaching and selective dissolution of matrix to develop and/or retain porosity. Such reservoirs (for example, at Dollarhide, Bedford, and Andrews South fields) typically display porosities less than 5 percent (fig. 28).

Production from the eastern part of the play area is commonly associated with successions that have been partially silicified. Pore space appears to be formed by silicification of carbonate mud matrix in skeletal packstones (Ruppel and Holtz, 1994). These reservoirs (including fields at Headlee, Parks, and Byant G) typically produce dominantly gas and condensate from these low-porosity/low-permeability rocks.

TRAPS, SEALS, AND SOURCES

Essentially all productive Thirtyone reservoirs are overlain by the shales of the Woodford Formation, which provides both a seal and a hydrocarbon source. Most of the large reservoirs are

formed over large anticlinal closures (for example, Block 31, University Waddell). However, in several reservoirs the Woodford has been partly (for example, Dollarhide, Three Bar) or completely (for example, Crossett, Cordona Lake) removed by Pennsylvanian erosion. These reservoirs are typically overlain and sealed by Permian carbonate mudstones. It should be noted that some production from some of these breached sections also comes from chert residuum and reworked chert conglomerates formed by weathering and erosion of the Thirtyone (for example, Tunis Creek, TXL).

OPPORTUNITIES FOR ADDITIONAL RESOURCE RECOVERY

Despite the large volume of oil already produced from the Thirtyone, significant oil remains in existing reservoirs. Distal deep-water chert reservoirs are especially good candidates for targeted infill drilling and recompletion programs based on modern, detailed geological characterization because their complex flow-unit geometries have not been well defined in many reservoirs. These reservoirs offer perhaps the best opportunity to delineate reservoir flow units through detailed geological mapping and modeling of depositional facies.

Many Thirtyone reservoirs are candidates for application of enhanced oil recovery technologies for increased production. Results of CO₂ injection in such reservoirs as Dollarhide (Saller and others, 1990, 1991) illustrates how better reservoir management and reservoir characterization and targeted infill drilling and recompletion coupled with gas injection can substantially increase production.

Recovery efficiency from the Thirtyone carbonate play is among the lowest of all carbonate reservoir plays in the Permian Basin and suggests that these reservoirs contain especially high potential for recovery of remaining mobile oil. Recent successes in fields like University Block 9 (Weiner and Heyer, 1999), Bryant G, and Headlee have demonstrated the value of horizontal wells in enhancing recovery from these rocks. There is also potential for the development of upper Thirtyone carbonate section in existing Thirtyone chert reservoirs because of the likelihood that these low-porosity carbonate reservoirs have been overlooked.

Finally, it is highly likely that significant potential exists for reservoir step-out and new field discovery if new and developing models are applied to reexploration of the Permian Basin. Occidental, for example, has had excellent success (more than 40 successful wells drilled) in greatly extending production from the Thirtyone in the TXL–Goldsmith field area of Ector

County, Texas, by applying models of upper Thirtyone chert development presented by Ruppel and Holtz (1994).

SUMMARY

The Thirtyone Formation documents the Early Devonian infilling of a significant platform-marginal slope/basin area developed during the Silurian on the southern margin of the Laurussian paleocontinent. Deposition was dominated by deep-water gravity transport and redistribution of platform-derived carbonate debris and siliceous fauna (sponge spicules and radiolarians). Depositional architecture in distal areas is a function of distributary pathways that evolved substantially in alignment and position through time. Facies vary from hemipelagic mudstones to relatively high energy, grain-rich, silica (chert) packstones, reflecting vastly differing energy regimes ranging from high-energy gravity flows to low-energy, below-wave-base conditions. Updip areas, in stark contrast, comprise high-energy, shallow-water carbonate shoal grainstones that reflect basinward progradation and accommodation filling.

Most reservoir development is associated with high-porosity/moderate-permeability chert facies whose character reflects a combination of depositional regime and early silica diagenesis. Best reservoir quality is associated with grain-rich chert facies that were deposited as debris flows. Lower energy burrowed facies are less porous and usually of poorer reservoir quality; however, variations in chert diagenesis locally overprint this trend. Updip carbonate facies are generally of much lower porosity but still locally quite productive. Reservoir quality in these rocks is controlled by diagenesis. Strongly dolomitized intervals provide the best porosity development, but partially dolomitized, leached, and/or silicified sections are also locally very productive.

Thirtyone chert and carbonate reservoirs contain a large remaining oil resource that is a target for more efficient exploitation techniques based on a better understanding of the geological controls on heterogeneity. Because these controls differ systematically between chert reservoirs developed in updip, proximal settings and downdip, distal settings, and among updip carbonate sections exposed to different styles of diagenesis, it is crucial that both regional and local geologic models of deposition and diagenesis be incorporated into modern reservoir characterization and exploitation efforts.

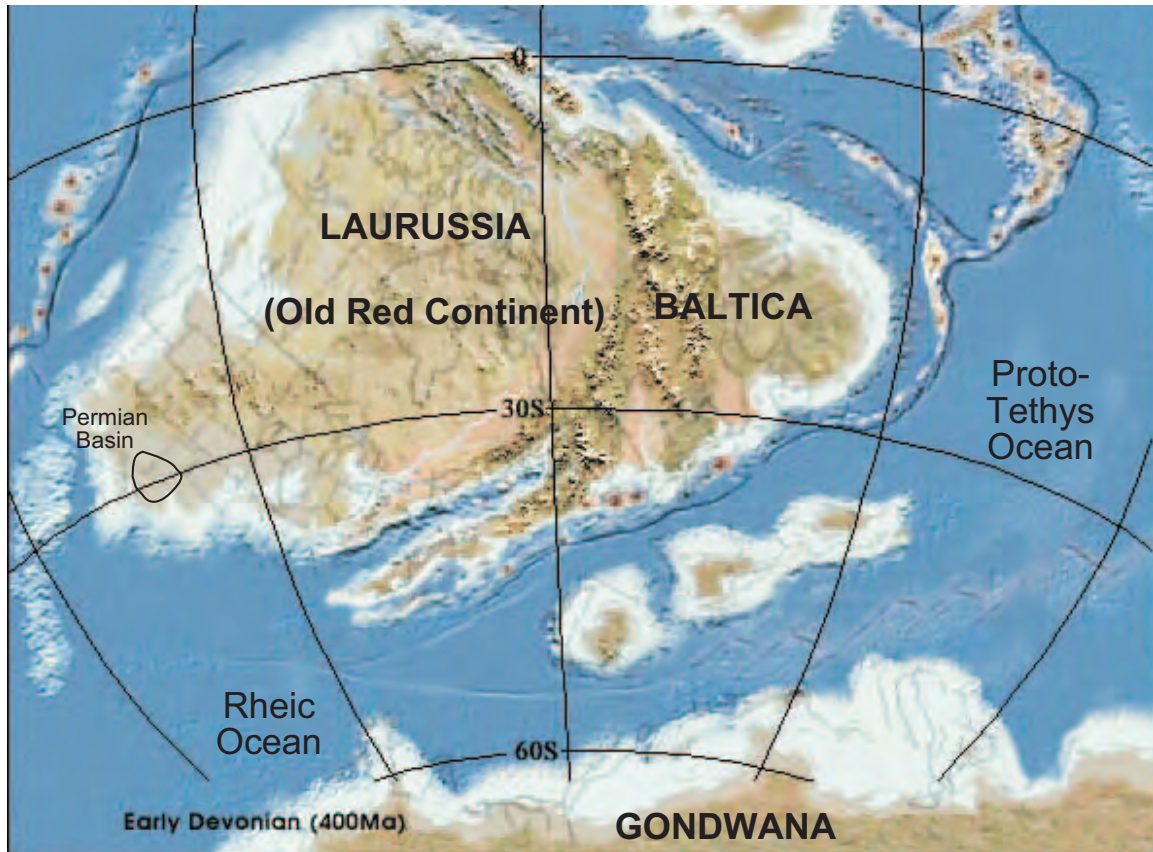
REFERENCES

- Barrick, J. E., 1995, Biostratigraphy of uppermost Ordovician through Devonian depositional sequences in the Permian Basin, West Texas and Southeastern New Mexico, *in* Pausé, P. H., and Candelaria, M. P., eds., Carbonate facies and sequence stratigraphy: practical applications of carbonate models: Permian Basin Section SEPM Publication 95-36, p. 207–216.
- Bebout, D. G., White, W. A., and Hentz, T. F., eds., 1993, Atlas of Midcontinent gas reservoirs: The University of Texas at Austin, Bureau of Economic Geology, 85 p.
- Blakey, R., 2004, Plate tectonics and continental drift: regional paleogeographic views of Earth history: <http://jan.ucc.nau.edu/~rcb7/400NAt.jpg>.
- Collinson, C. W., 1967, Devonian of the North-Central region, United States, *in* Oswald, D. H., ed., International Symposium on the Devonian System, v. II: Alberta Society of Petroleum Geologists, Calgary, Alberta, p. 933–971.
- Cook, H. E., 1983, Ancient carbonate platform margins, slopes, and basins, *in* Cook, H. E., Hine, A. C., and Mullins, H. T., Platform margin and deepwater carbonates: Society of Economic Paleontologists and Mineralogists Short Course No. 12, p. 5-1–5-189.
- Droste, J. B., and Shaver, R. H., 1987, Upper Silurian and Lower Devonian stratigraphy of the Central Illinois Basin: Indiana Department of Natural Resources, Geological Survey Special Report 39, 23 p.
- Dutton, S. P., Kim, E. M., Broadhead, R. F., Breton, C. L., Raatz, W. D., Ruppel, S. C., and Kerans, Charles, 2005, Play analysis and digital portfolio of major oil reservoirs in the Permian Basin: The University of Texas at Austin, Bureau of Economic Geology Report of Investigations No. 271, 287 p., CD-ROM.
- Folk, R. L., and McBride, E. F., 1977, The Caballos Novaculite revisited; Part I, Origin of novaculite members: *Journal of Sedimentary Research*, v. 46, p. 659–669.
- Frey, R. W., and Pemberton, S. G., 1984, Trace fossil facies models, *in*, Walker, R. G., ed., Facies models (2d ed.): Geoscience Canada, Reprint Series 1, p. 189–208.

- Galloway, W. E., Ewing, T. E., Garrett, C. M., Jr., Tyler, Noel, and Bebout, D. G., 1983, Atlas of major Texas oil reservoirs: The University of Texas at Austin, Bureau of Economic Geology Special Publication, 139 p.
- Ham, W. E., and Wilson, J. L., 1967, Paleozoic epeirogeny and orogeny in the central United States: *American Journal of Science* v. 265, p. 332–407.
- Hills, J. M., and Hoenig, M. A., 1979, Proposed type sections for Upper Silurian and Lower Devonian subsurface units in Permian Basin, West Texas: *American Association of Petroleum Geologists Bulletin* v. 63, no. 9, p. 1510–1521.
- Howell, D. G., and Normark, W. R., 1982, Sedimentology of submarine fans, *in* Scholle, P. A., and Spearing, Darwin, eds., *Sandstone depositional environments*: American Association of Petroleum Geologists, Memoir 31, p. 365–404.
- International Commission on Stratigraphy, 2004, International stratigraphic chart: <http://www.stratigraphy.org/>.
- Johnson, J. G., Klapper, G., and Sandberg, C. A., 1985, Devonian eustatic fluctuations in Euramerica: *Geological Society of America Bulletin*, v. 96, p. 567–587.
- Jones, T. S., 1953, Stratigraphy of the Permian Basin of West Texas: *West Texas Geological Society*, 57 p.
- Kosters, E. C., Bebout, D. G., Brown, L. F., Jr., Dutton, S. P., Finley, R. J., Garrett, C. M., Jr., Hamlin, H. S., Ruppel, S. C., Seni, S. J., and Tyler, Noel, 1989, Atlas of major Texas gas reservoirs: The University of Texas at Austin, Bureau of Economic Geology, Special Publication, 161 p.
- McBride, E. F., and Folk, R. L., 1979, Features and origin of Italian Jurassic radiolarites deposited on continental crust: *Journal of Sedimentary Petrology*, v. 49, p. 837–868.
- McGlasson, E. H., 1967, The Siluro-Devonian of West Texas and southeast New Mexico, *in* Oswald, D. H., ed., *International Symposium on the Devonian System*, v. II: Alberta Society of Petroleum Geologists, Calgary, Alberta, p. 937–948.
- Medlock, P. L., and Fritz, R. D., 1993, Penters Formation paleokarst in the Arkoma Basin and the Black Warrior Basin, *in* Johnson, K. S., ed., *Hunton Group core workshop and field trip*: Oklahoma Geological Survey, Special Publication 93-4, p. 149–159.

- Montgomery, S. L., 1998, Thirtyone Formation, Permian Basin, Texas: structural and lithologic heterogeneity in a Lower Devonian chert reservoir: American Association of Petroleum Geologists Bulletin, v. 82, p. 1–24.
- Piper, D. J. W., 1978, Turbidite muds and silts on deepsea fans and abyssal plains, *in* Stanley, D. J., and Kelling, G., eds., Sedimentation in submarine canyons, fans, and trenches: Stroudsburg, Pa., Dowden, Hutchinson & Ross, Inc., p. 163–176.
- Ruppel, S. C., and Barnaby, R. J., 2001, Contrasting styles of reservoir development in proximal and distal chert facies: Devonian Thirtyone Formation, Texas: American Association of Petroleum Geologists Bulletin, v. 85, no. 1, p. 7–33.
- Ruppel, S. C., and Holtz, M. H., 1994, Depositional and diagenetic facies patterns and reservoir development in Silurian and Devonian rocks of the Permian Basin: The University of Texas at Austin, Bureau of Economic Geology Report of Investigations No. 216, 89 p.
- Ruppel, S. C., and Hovorka, S. D., 1990, Controls on reservoir heterogeneity in the Three Bar Devonian chert reservoir, Andrews County, Texas, *in* Flis, J. E., and Price, R. C., eds., Permian Basin oil and gas fields: innovative ideas in exploration and development: West Texas Geological Society Publication 90-87, p. 57–74.
- Ruppel, S. C., and Hovorka, S. D., 1995a, Chert reservoir development in the Devonian Thirtyone Formation: Three Bar field, West Texas: The University of Texas at Austin, Bureau of Economic Geology Report of Investigations No. 230, 50 p.
- Ruppel, S. C., and Hovorka, S. D., 1995b, Controls on reservoir development in Devonian chert: Permian Basin, Texas: American Association of Petroleum Geologists Bulletin, v. 79, p. 1757–1785.
- Saller, A., Ball, B., Robertson, S., McPherson, B., Wene, C., Nims, R., and Gogas, J., 2001, Reservoir characteristics of Devonian cherts and their control on oil recovery: Dollarhide field, West Texas, USA: American Association of Petroleum Geologists Bulletin, v. 85, no. 1, p.35–50.
- Saller, A. H., Guy, B. T., and Whitacre, D. S., 1990, Reservoir geology of Devonian strata and their response to secondary and Tertiary recovery, Dollarhide field, Andrews County, Texas, *in* Flis, J. E., and Price, R. C., eds., Permian Basin oil and gas fields: innovative

- ideas in exploration and development: West Texas Geological Society, Publication No. 90-87.
- Saller, A. H., Van Horn, Donna, Miller, J. A., and Guy, B. T., 1991, Reservoir geology of Devonian carbonates and chert—implications for Tertiary recovery, Dollarhide field, Andrews County, Texas: American Association of Petroleum Geologists, Bulletin, v. 75, p. 86–102.
- Tinker, C. N., 1963, Pore space and silicification—their relationship and original lithologic controls exemplified by carbonate rocks from Crossett Devonian field, Texas: Shell Development Company, Houston, unpublished EPR Report no. 767, 34 p.
- Walker, R. G., 1984, Turbidites and associated coarse clastic deposits, *in* Walker, R. G., ed., Facies models (2d ed.): Geoscience Canada, Reprint Series 1, p. 171–188.
- Weiner, S. and Heyer, J., 1999, Geologic model of a highly compartmentalized reservoir; the Devonian Thirtyone Formation, University Block 9 Field, *in* Grace, D. T., and Hinterlong, G. D., eds., The Permian Basin; providing energy for America: West Texas Geological Society Publication 99-106, p. 1–8.
- Williams, L. A., and Crerar, D. A., 1985, Silica diagenesis, II: general mechanisms: Journal of Sedimentary Petrology, v. 55, no. 3, p. 312–321.
- Williams, L. A., Parks, G. A., and Crerar, D. A., 1985, Silica diagenesis, I: Solubility controls: Journal of Sedimentary Petrology, v. 55, no. 3, p. 301–311.
- Wilson, J. L. and Majewske, O. P., 1960, Conjectured Middle Paleozoic history of Central and West Texas, *in* Aspects of the geology of Texas: a symposium: The University of Texas, Bureau of Economic Geology Publication 6017, p. 65–86.



from Blakey (2004): <http://jan.ucc.nau.edu/~rcb7/400NAt.jpg>

Figure 2. Paleogeographic plate reconstruction of the Laurussian paleocontinent during the Early Devonian showing position of Permian Basin area on the southern continental margin. From Blakey (2004).

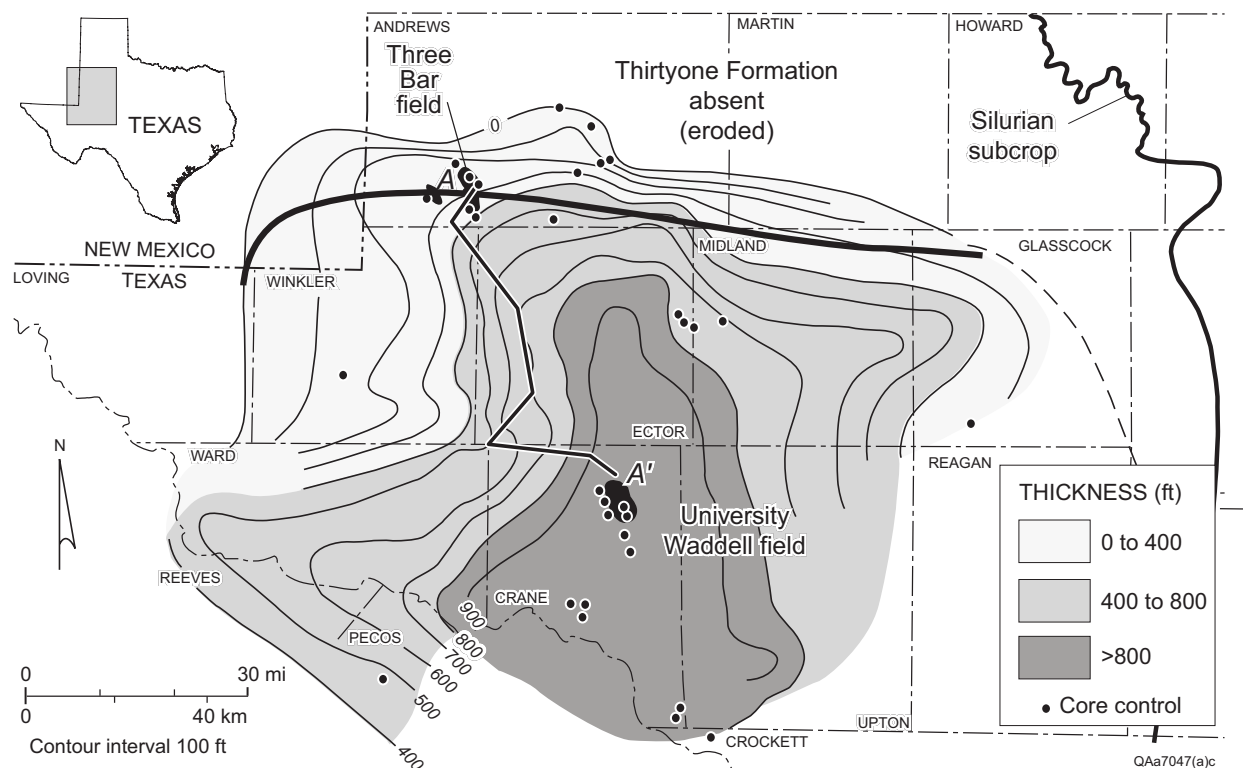


Figure 3. Thickness and distribution of the Devonian Thirtyone Formation in West Texas showing location of key fields. From Ruppel and Barnaby (2001).

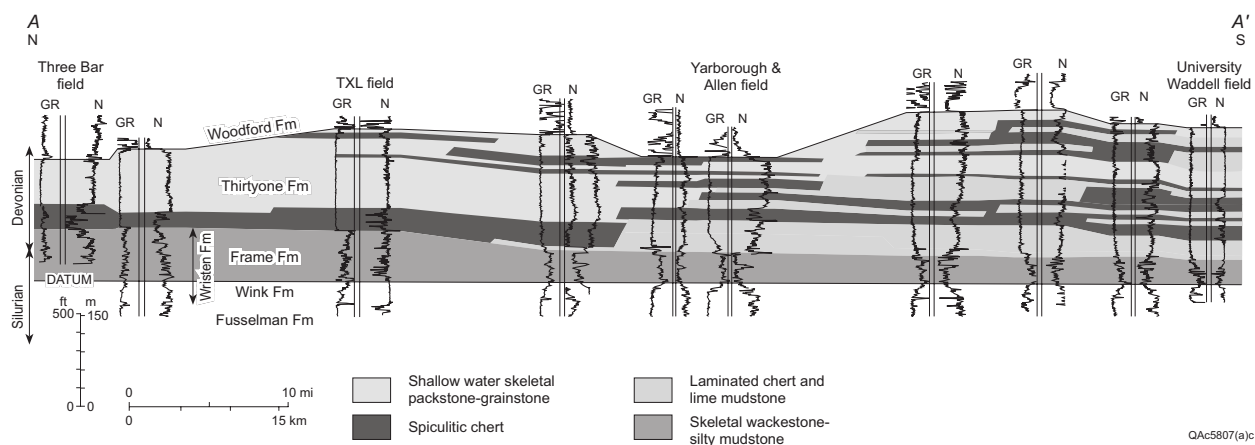
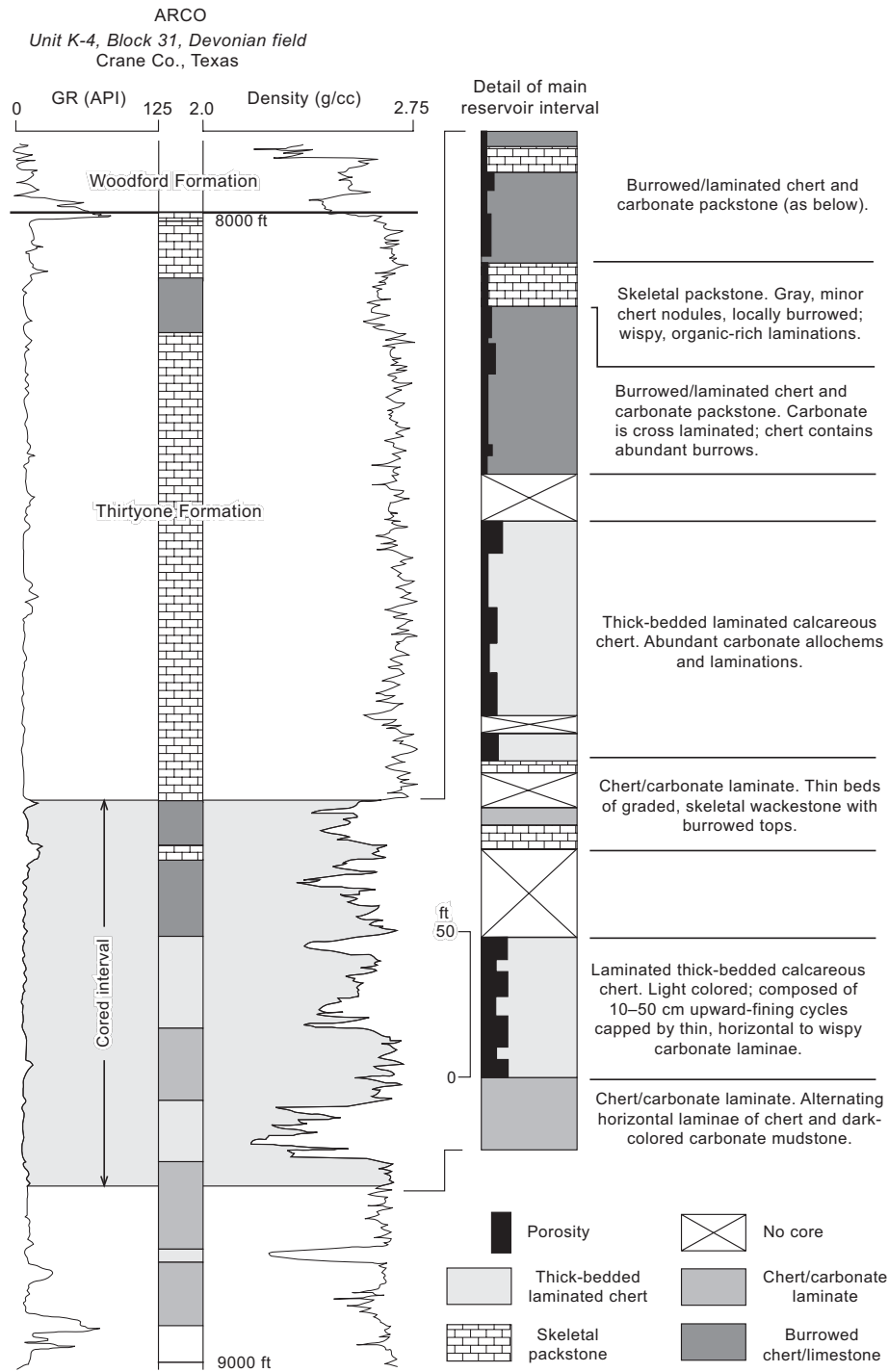


Figure 4. Cross section depicting Thirtyone Formation stratigraphy. Note contrast between high-continuity, tabular chert in northern (proximal) area and laterally and vertically discontinuous chert in southern (distal) area. Location of cross section shown in figure 3. From Ruppel and Barnaby (2001).



Ruppel & Hovorka figure 5

Figure 5. Stratigraphic section and log character of the Thirtyone in the southern, thickest part of the Thirtyone Formation depocenter. From Ruppel and Hovorka (1995b).

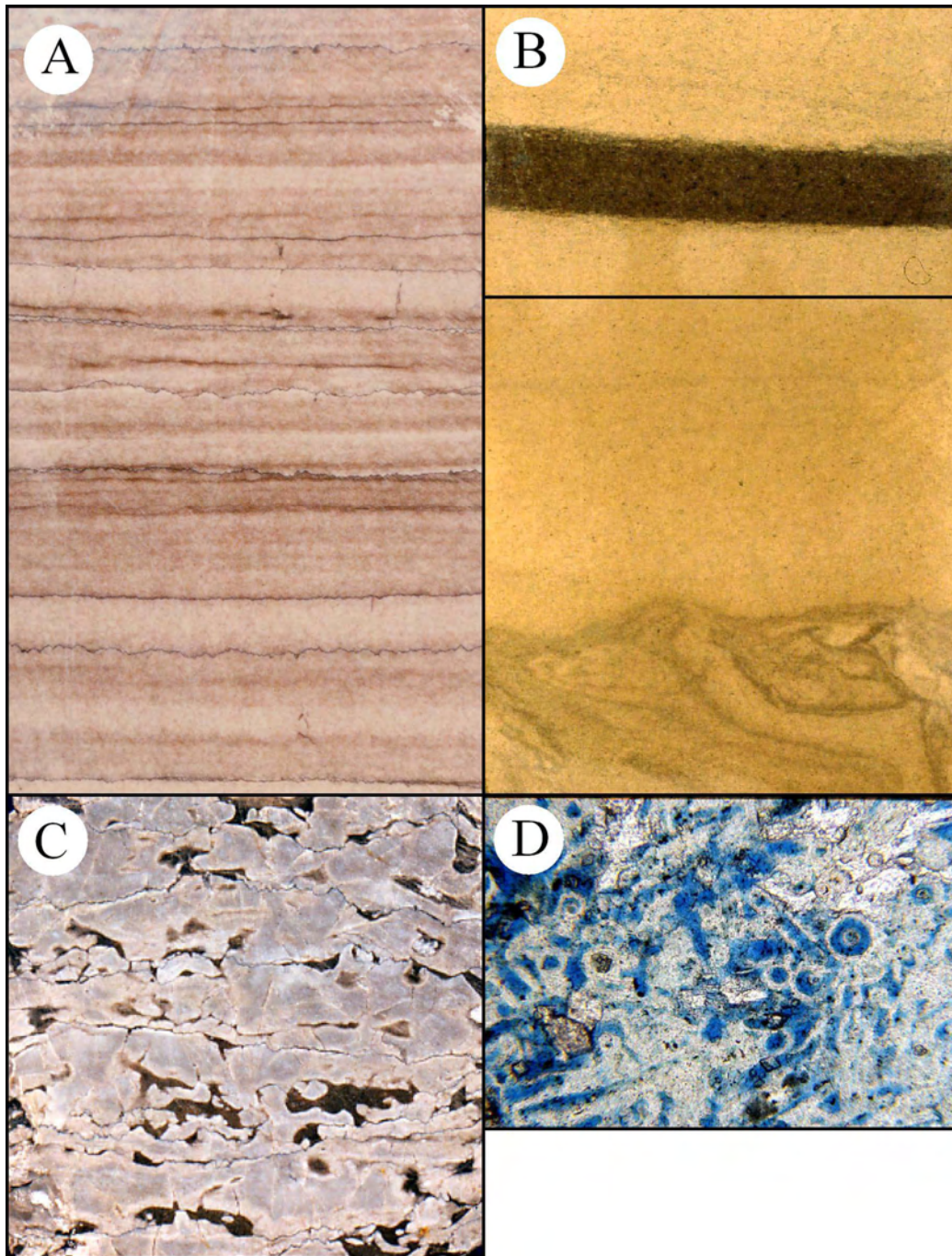
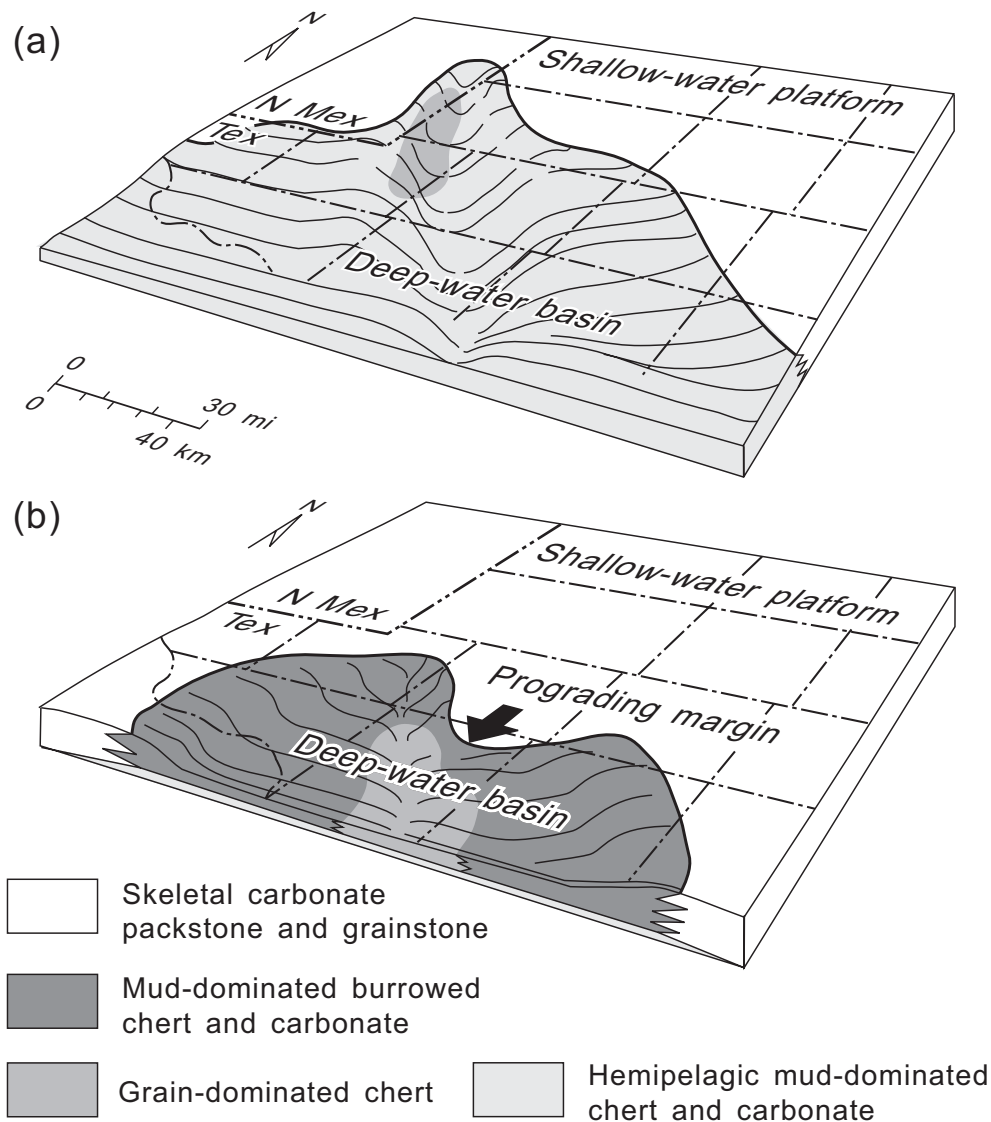


Figure 6. Thirtyone Formation facies. A. Chert/carbonate laminite facies representing hemipelagic deposition in a quiet-water, below-wave-base setting. Depth: 8,850 ft. B. Thick-bedded, laminated chert facies with organic-rich laminae at top. Depth: 8,800 ft. C. Burrowed chert facies. Dark patches, which are carbonate mudstone, are the result of burrowing and/or soft-sediment deformation. A, B, and C from ARCO Block 31 Unit No. K-4, Crane County, Texas. D. Photomicrograph of grain-supported, spiculitic chert of the thick-bedded, laminated chert facies, Thirtyone Formation. Porosity (31 percent) is developed as obvious, large (50–100 μm) molds and smaller (<5 μm), intercrystalline pores. Permeability is 27 md. Depth: 8,155 ft. Unocal, Dollarhide 46-5- D, Andrews County, Texas.



Ruppel & Hovorka figure 9

Figure 7. Paleogeographic evolution of the Permian Basin area during the Early Devonian. (A) Initial Early Devonian flooding of the Wristen (Silurian) platform was marked by hemipelagic chert-and-carbonate mud accumulation in the distal (southern) part of the region and grain-rich, spiculitic cherts in more northerly areas proximal to the carbonate platform. (B) Rapid southward progradation of the platform shifted the focus of high-energy, submarine-fan deposition southward. Chert reservoirs are, thus, developed in two spatially and temporally discrete stratigraphic successions. From Ruppel and Hovorka (1995a)

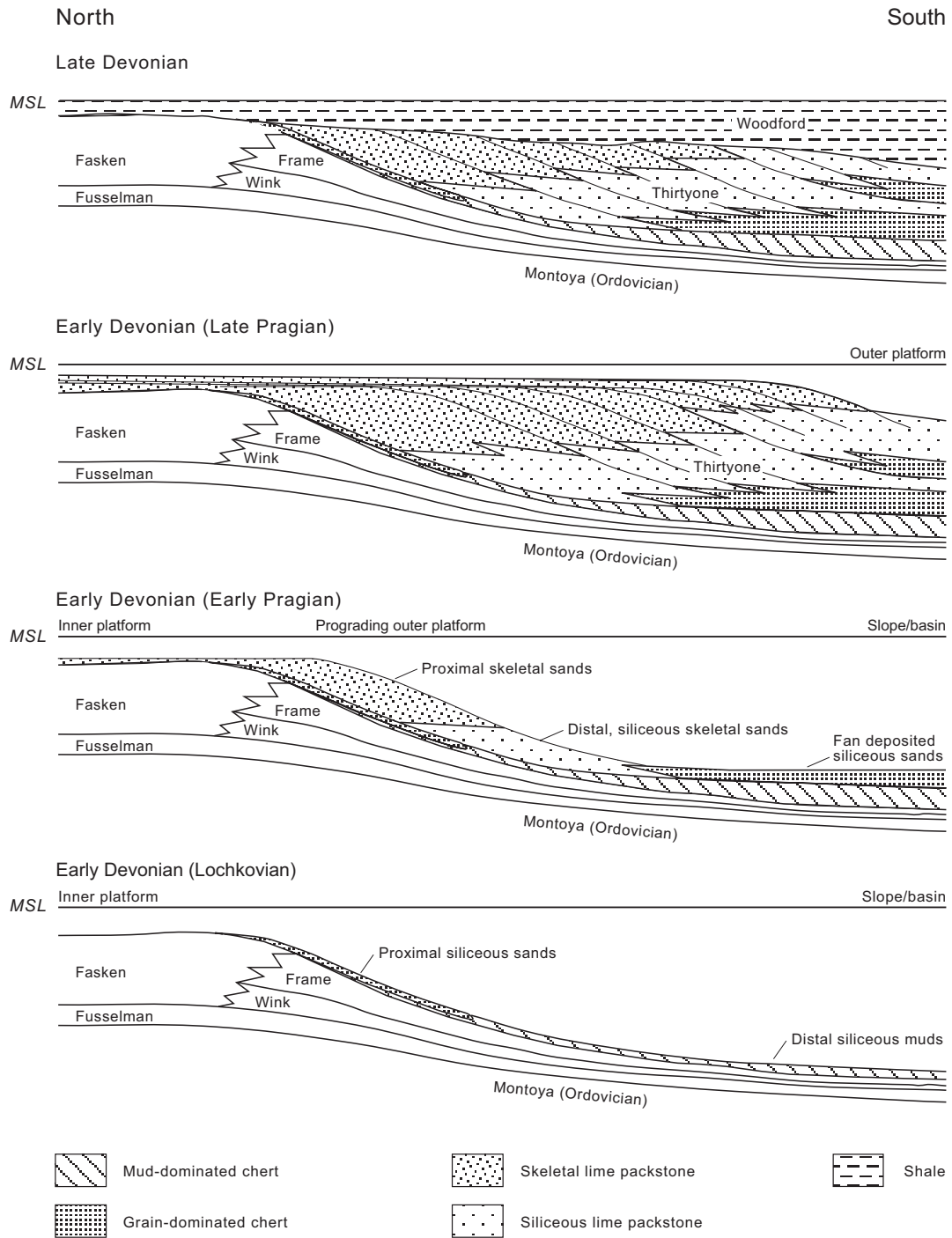


Figure 8. Diagrammatic north-south cross section depicting stratigraphic relationships and depositional history of Thirtystone Formation along approximate depositional dip. From Ruppel and Hovorka (1995a, b).

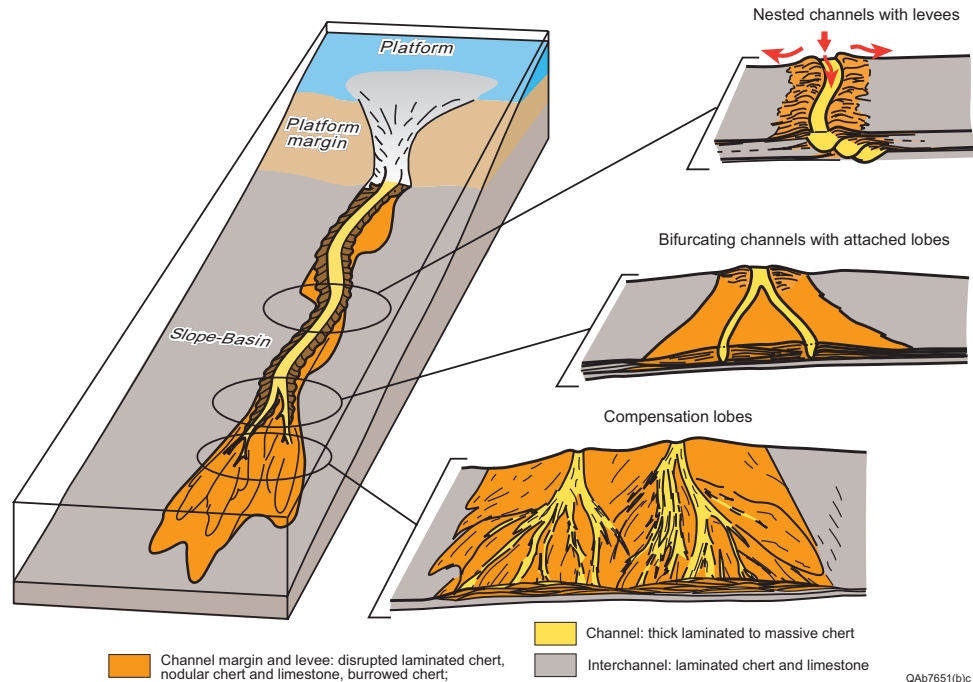


Figure 9. Model of deposition in distal Thirtyone chert reservoirs showing general morphology of turbidite channels and fans and proposed relationship to chert facies. From Ruppel and Barnaby (2001).

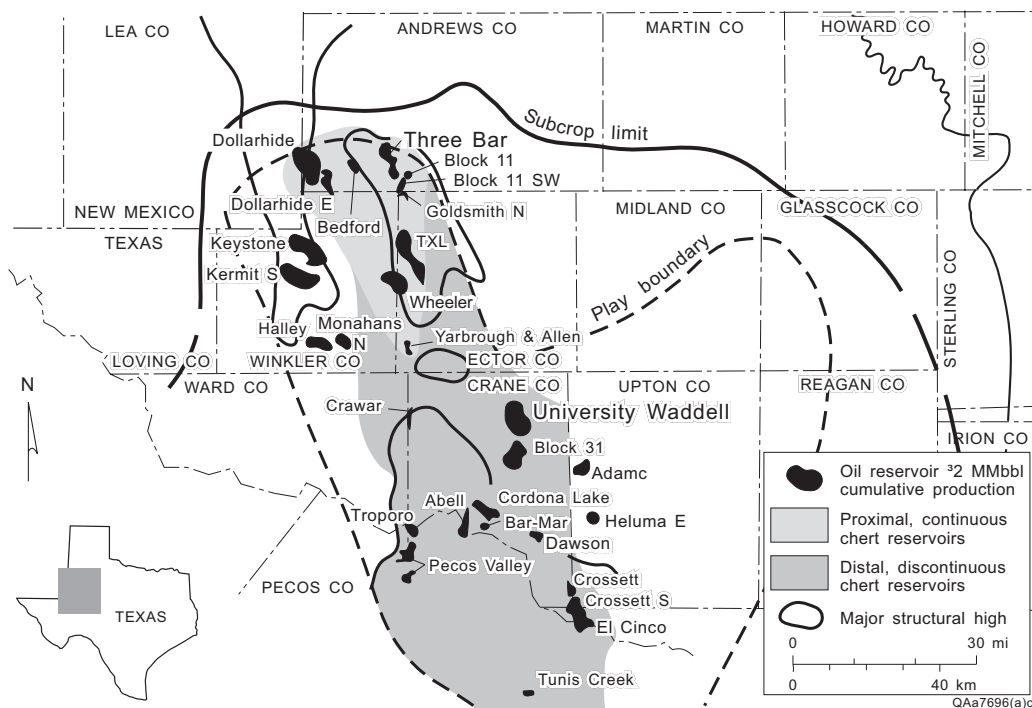
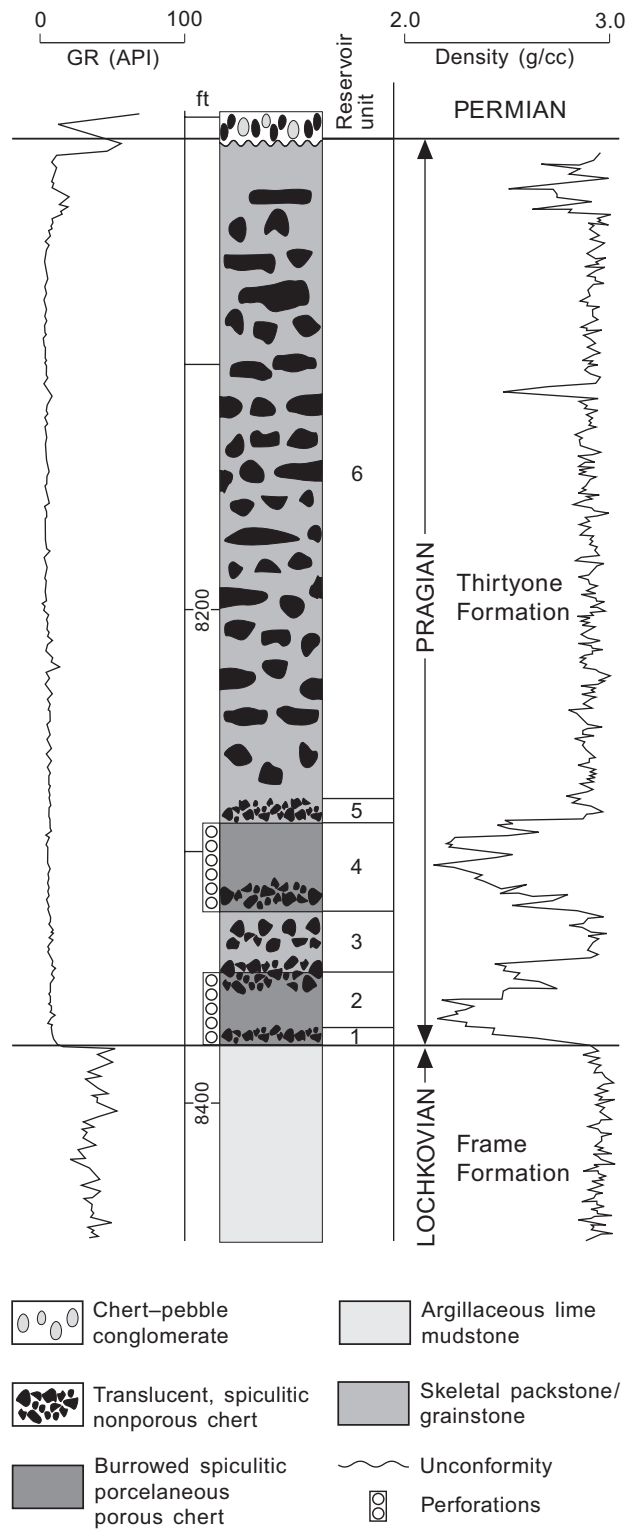


Figure 10. Distribution of proximal and distal reservoir styles. From Ruppel and Barnaby (2001).



QA18039c

Figure 11. Typical stratigraphic succession and wireline log signature of Thirtyone Formation in Three Bar field. Amoco Three Bar Unit No. 80. From Ruppel and Barnaby (2001).

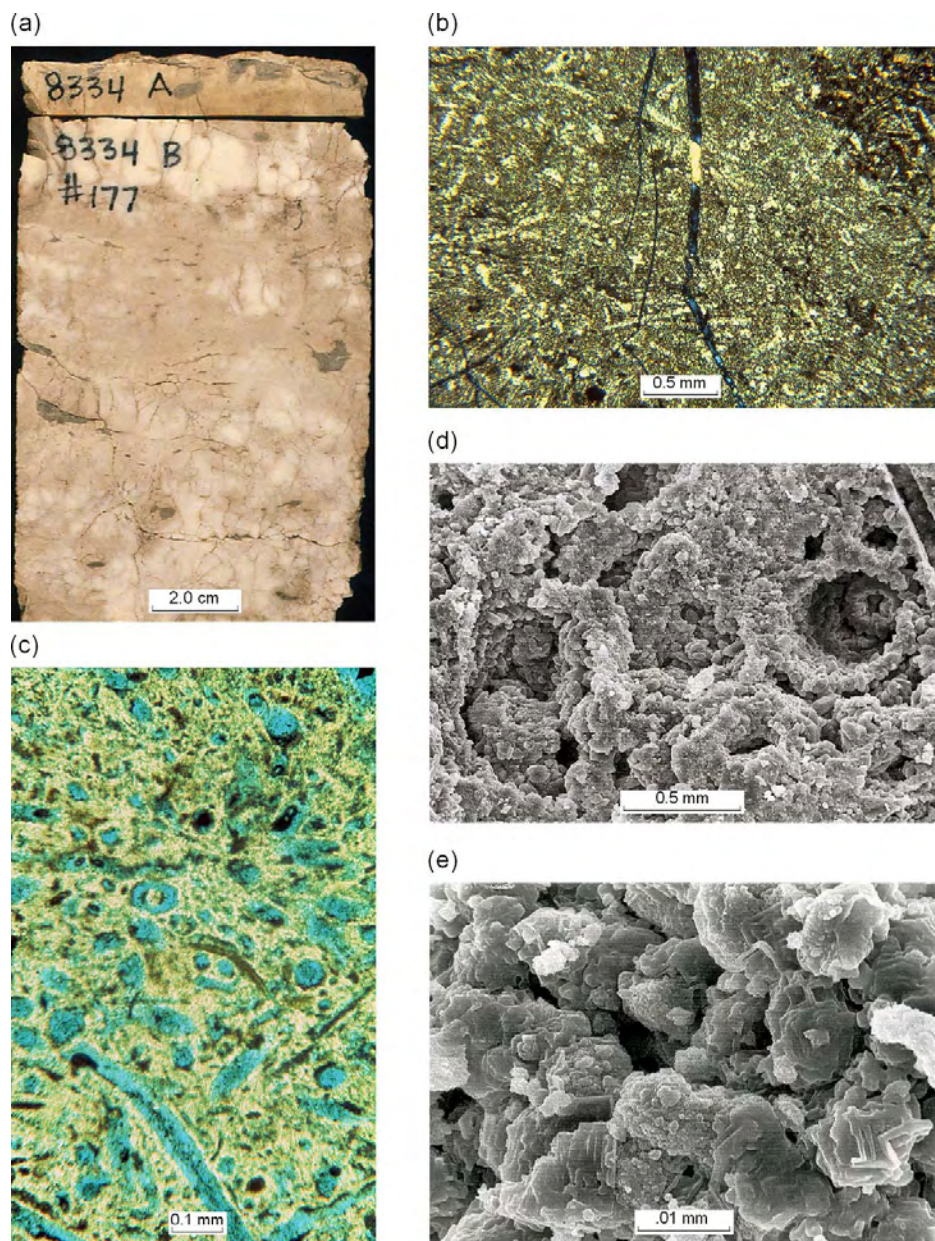


Figure 12. Textures of cherty rocks in the Thirtyone Formation at Three Bar field. (A) Core slab of white translucent chert with abundant vertical fractures containing dark chert and late calcite cements. Amoco Production Co., Three Bar Unit No. 80, 8,306 ft. (B) Photomicrograph of nonporous chert showing spicules replaced by chalcedony and microquartz. Matrix between spicules and in axial canals of spicules consists of finer grained chert. Crossed nicols. Three Bar Unit No. 80, 8,306 ft. (C) Photomicrograph of sponge spicule molds in porous chert. Plane light, Three Bar Unit No. 80, 8,305 ft. (D) Scanning electron microscope (SEM) photomicrograph of porous chert showing spicule molds and micropores in a matrix of aggregated chert ellipsoids. Three Bar Unit No. 55, 8,175 ft. (E) SEM photomicrograph of porous chert microstructure. Microporosity is developed between rounded 1- μ m ellipsoids and between larger aggregates of ellipsoids. Three Bar Unit No. 55, 8,137 ft. (F) Core slab showing styles of brecciation in Thirtyone chert. Contrasts between brittle and more ductile deformation are related to rates of silica diagenesis. From Ruppel and Barnaby (2001).

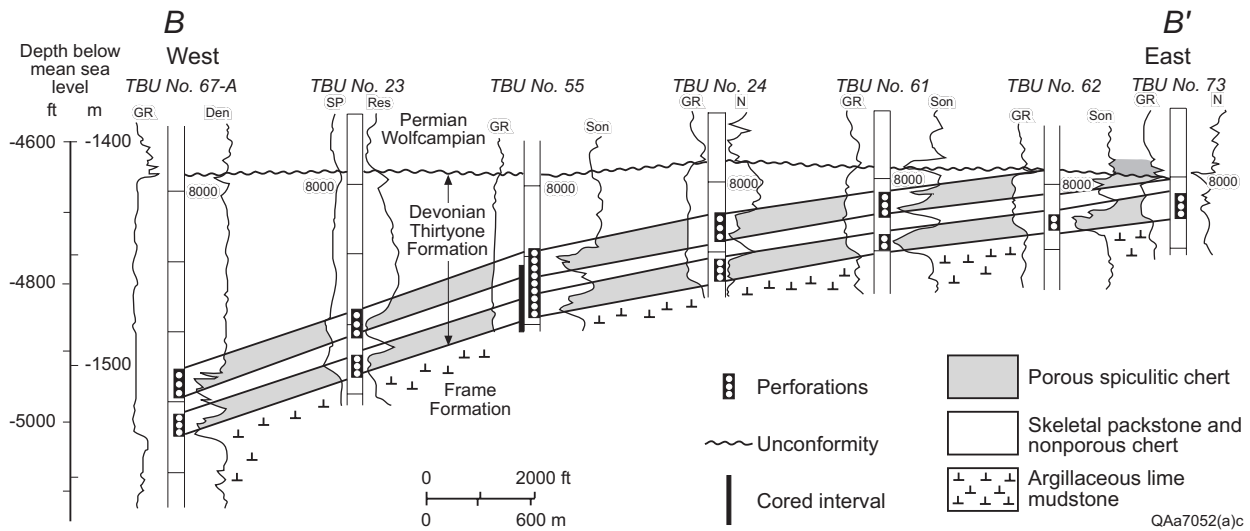


Figure 13. Structural cross section across Three Bar field, perpendicular to the structural axis, showing updip truncation of reservoir pay zone beneath the sub-Permian unconformity. Note continuity of chert pay zones. From Ruppel and Barnaby (2001).

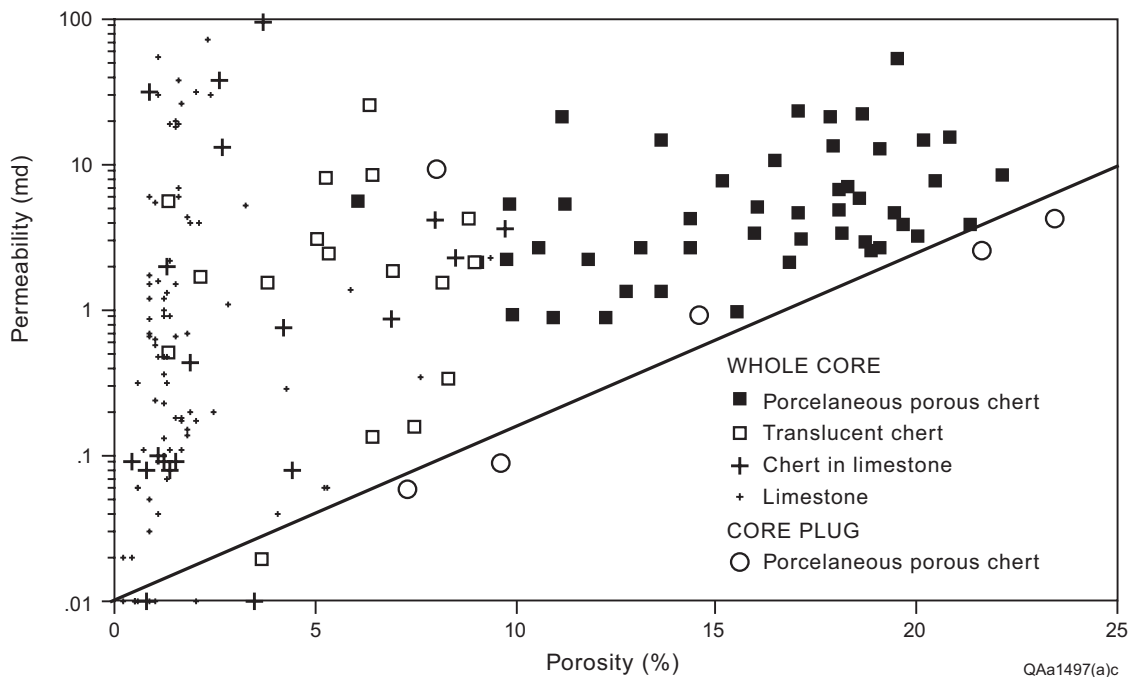


Figure 14. Porosity-permeability relationships in the Thirtyone Formation at Three Bar field. Because of abundant brecciation and fractures, most conventional core plug analysis displays fracture-enhanced permeability. True matrix porosity and permeability are best represented by specially selected, fracture-free plugs. From Ruppel and Barnaby (2001).

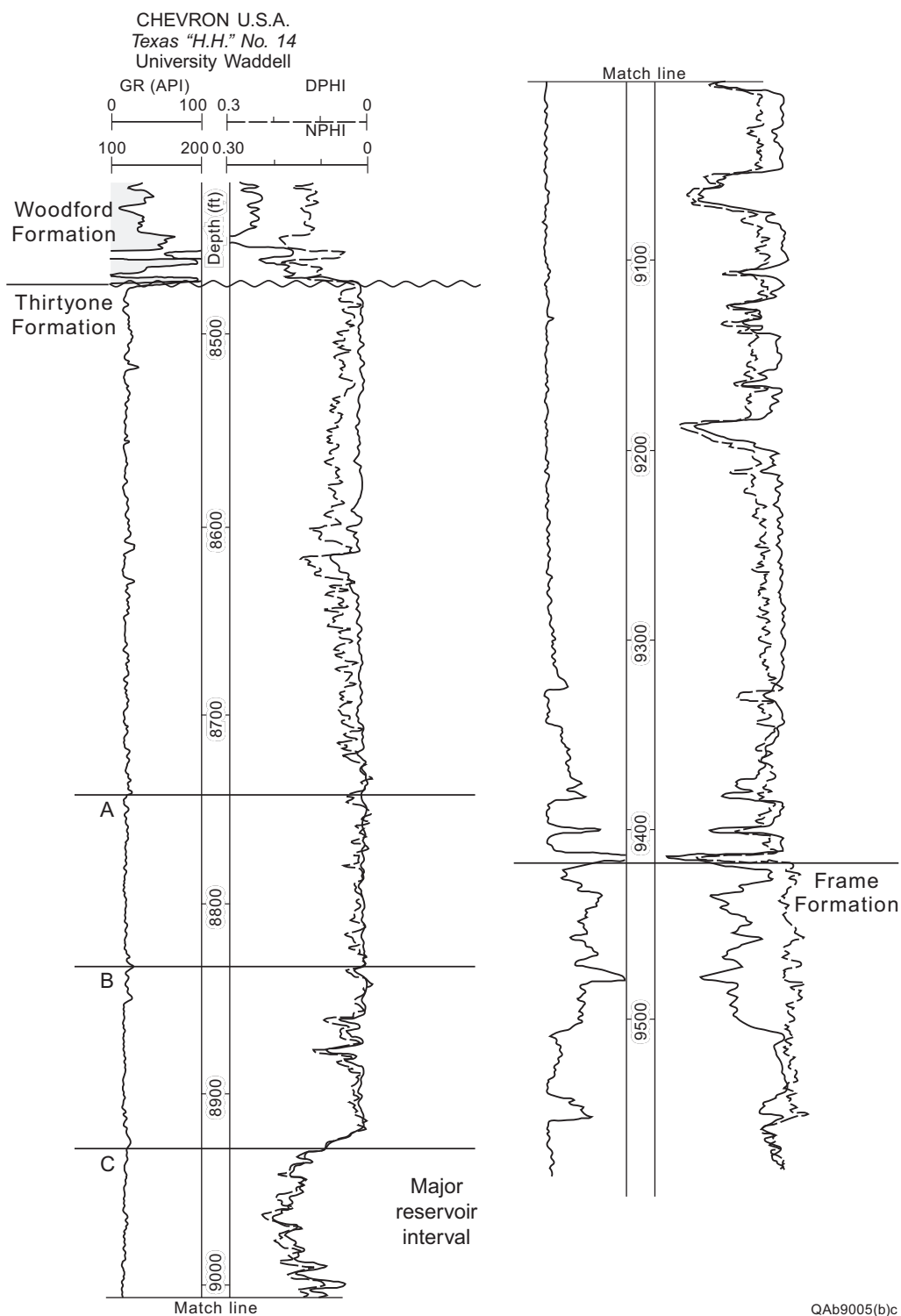


Figure 15. Type log for the Thirtyone Formation in University Waddell field. From Ruppel and Barnaby (2001).

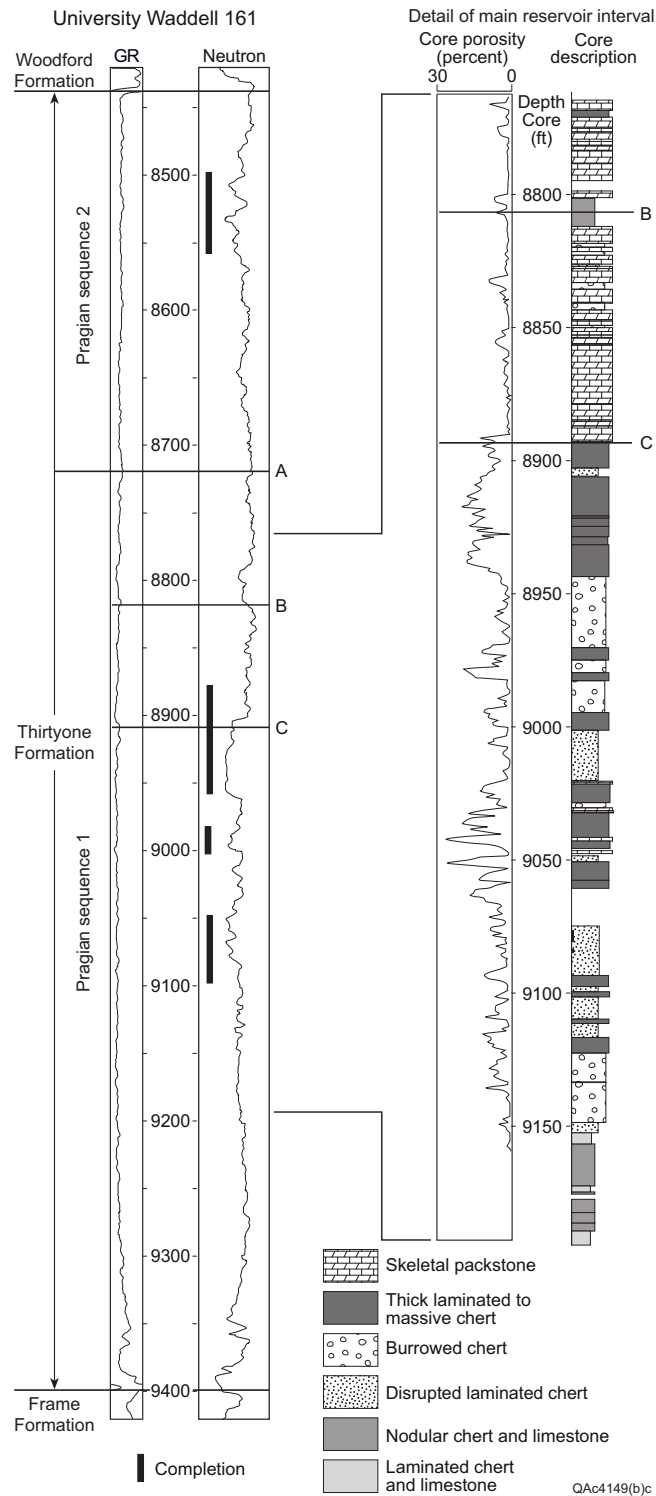
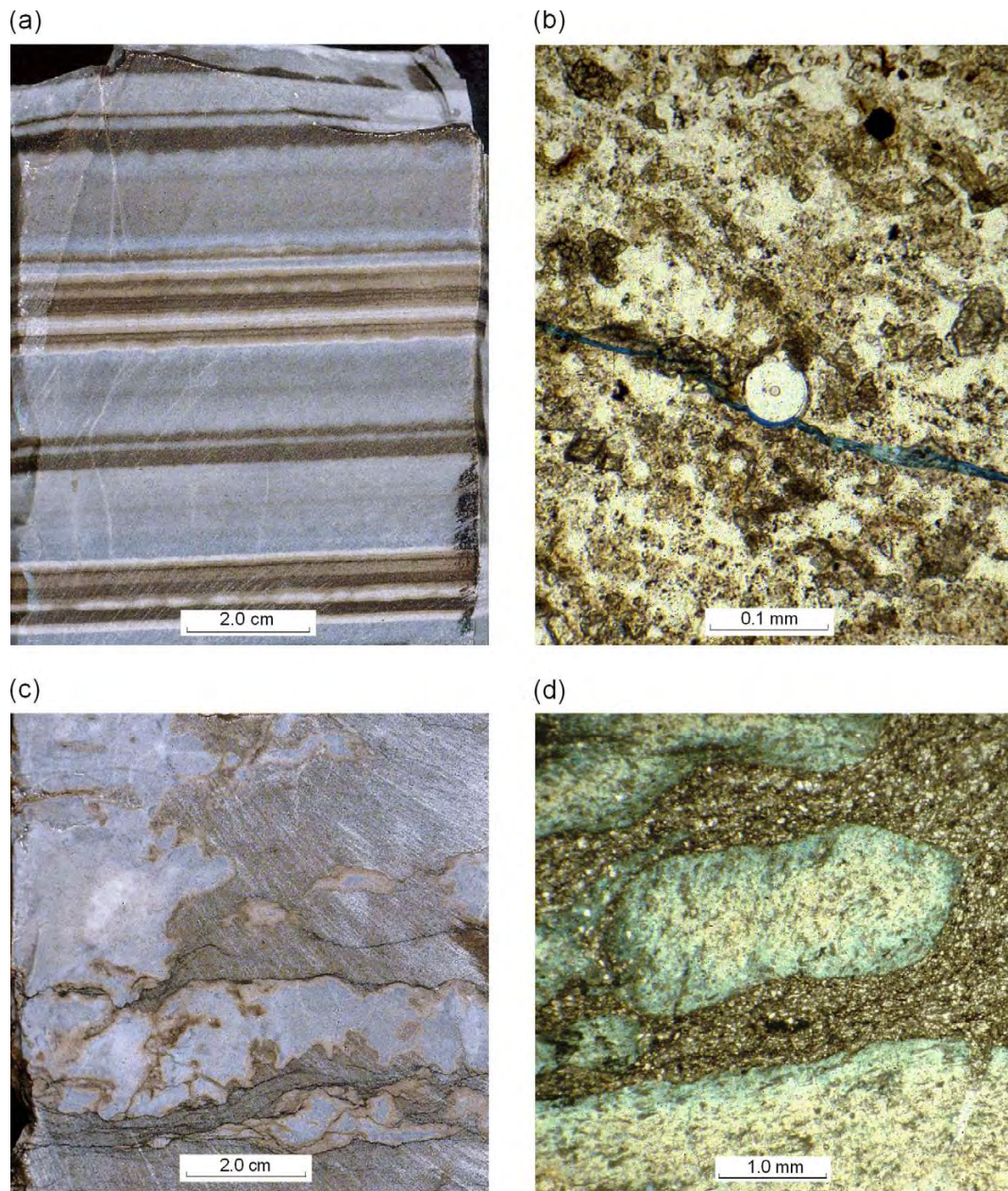


Figure 16. Reservoir facies at University Waddell field. From Ruppel and Barnaby (2001).



QA6078c

Figure 17. Textures of cherty rocks at University Waddell field. Finely laminated chert and limestone facies (A, B) and the disrupted laminated chert facies (C, D). (A) Core slab of alternating layers of gray chert, which display irregular bases and normal grading of silt-sized grains, and brown lime mudstone, University Waddell No. 161, 9,171 ft. (B) Thin section of chert laminae containing silica sponge spicules and indeterminate carbonate grains in siliceous matrix, University Waddell No. 161, 9,172 ft. (C) Core slab of highly convoluted laminated chert with abundant stylolitic dissolution seams, University Waddell No. 161, 8,577 ft. (D) Thin section of incompletely silicified chert packstone composed of silt-sized to very fine grained peloids and skeletal material, University Waddell No. 161, 9,128 ft. From Ruppel and Barnaby (2001).

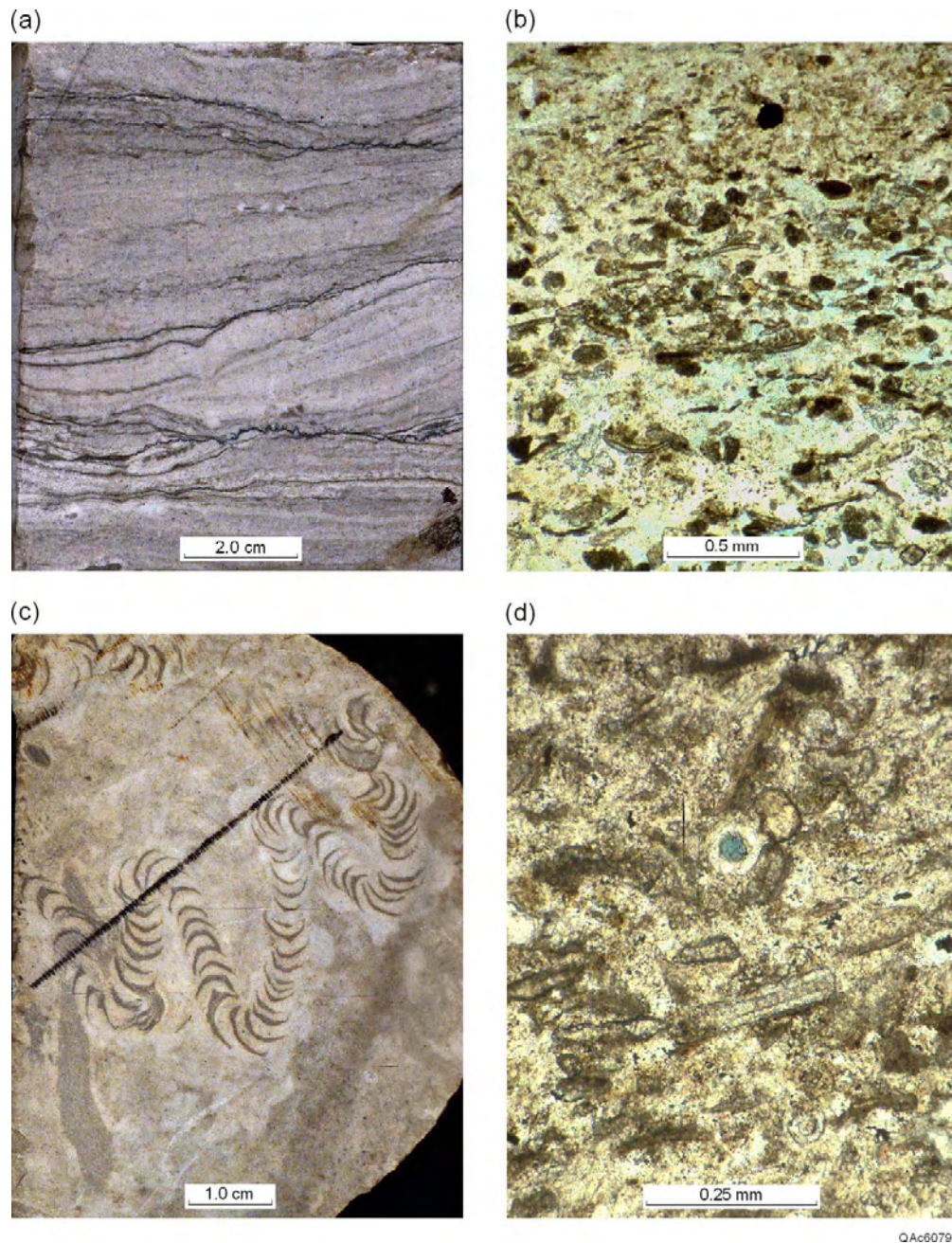


Figure 18. Textures of cherty rocks at University Waddell field. Nodular chert and limestone facies (A, B) and burrowed chert facies (C, D). (A) Core slab of irregular replacement chert nodules in lime mudstone matrix, University Waddell No. 161, 9,103 ft. (B) Thin section of chert nodules in organic-rich lime mudstone matrix showing minor intercrystalline porosity indicated by blue epoxy along periphery of silica nodules, University Waddell No. 161, 9,103 ft. (C) Core slab showing *Zoophycos* burrow parallel to bedding plane, University Waddell No. 161, 9,087 ft. (D) Thin section of incompletely silicified, poorly sorted, silt-sized to very fine grained skeletal packstones dominated by sponge spicules, University Waddell KK No. 10, 9,258 ft. From Ruppel and Barnaby (2001).

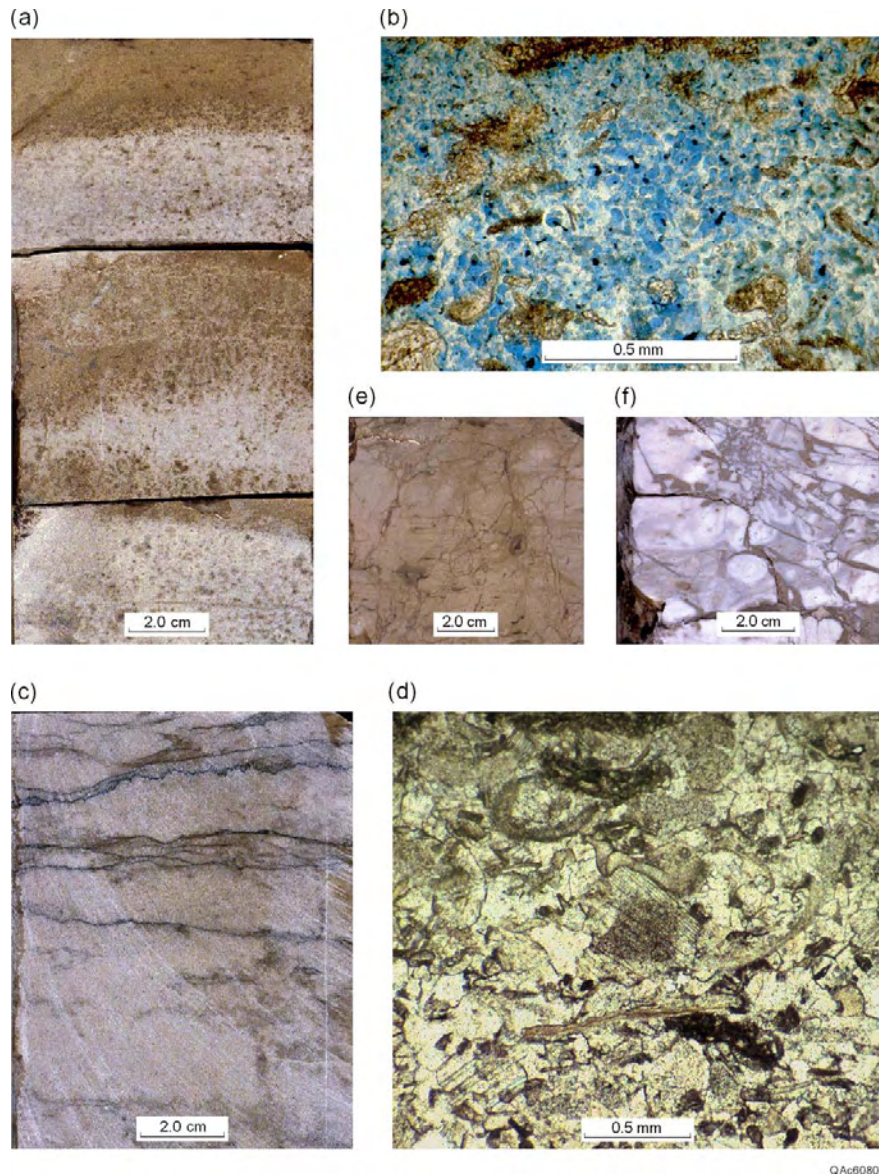


Figure 19. Textures of porous cherty rocks at University Waddell field. Highly porous, thickly laminated to massive chert facies (A, B), nonporous skeletal packstone facies (C, D), and brecciated porous and nonporous chert (E, F). (A) Core slabs showing highly porous hydrocarbon-stained intervals and lighter gray, more tightly cemented patches, University Waddell No. 161, 9,032 ft. (B) Thin section showing abundant sponge spicule molds and incompletely silicified carbonate skeletal debris in a well-sorted skeletal packstone. Moldic dissolution porosity is as much as 25 percent, University Waddell No. 161, 9,041 ft. (C) Core slab of light-colored thin-bedded to massive skeletal packstone with local burrows and stylolites, University Waddell No. 161, 8,828 ft. (D) Thin section of skeletal packstone with abundant coarse-grained crinoids, common brachiopods, and other skeletal grains. This facies is essentially nonporous owing to syntaxial calcite cements, University Waddell No. 161, 9,037 ft. (E) Core slab of oil-stained fractured/brecciated porous chert, University Waddell No. 161, 8,562 ft. (F) Core slab of brecciated, nonporous porcelaneous chert, University Waddell No. 161, 8,547 ft. From Ruppel and Barnaby (2001).

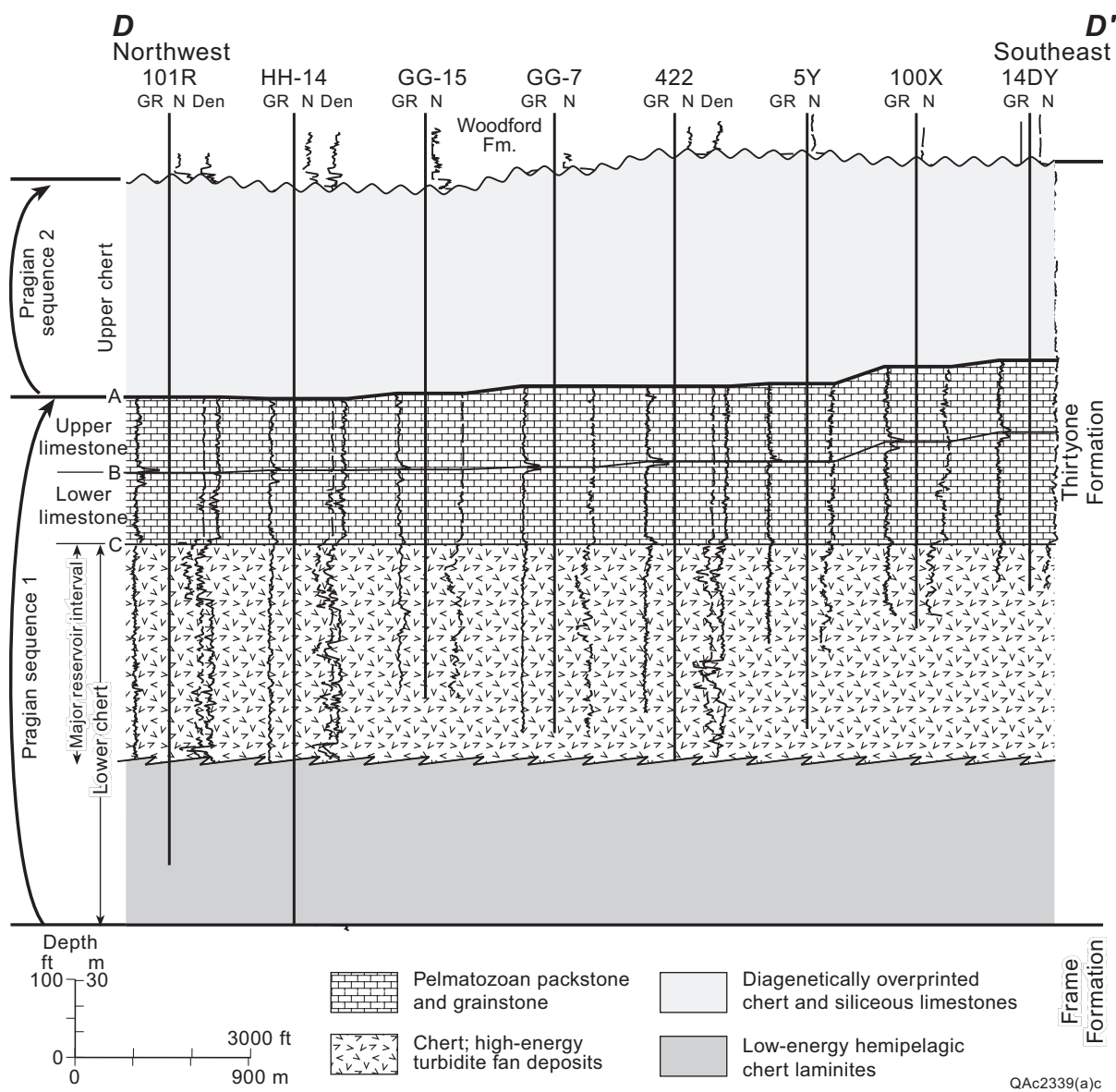


Figure 20. Stratigraphic cross section depicting reservoir architecture and sequence stratigraphy of the Thirtyone Formation. From Ruppel and Barnaby (2001).

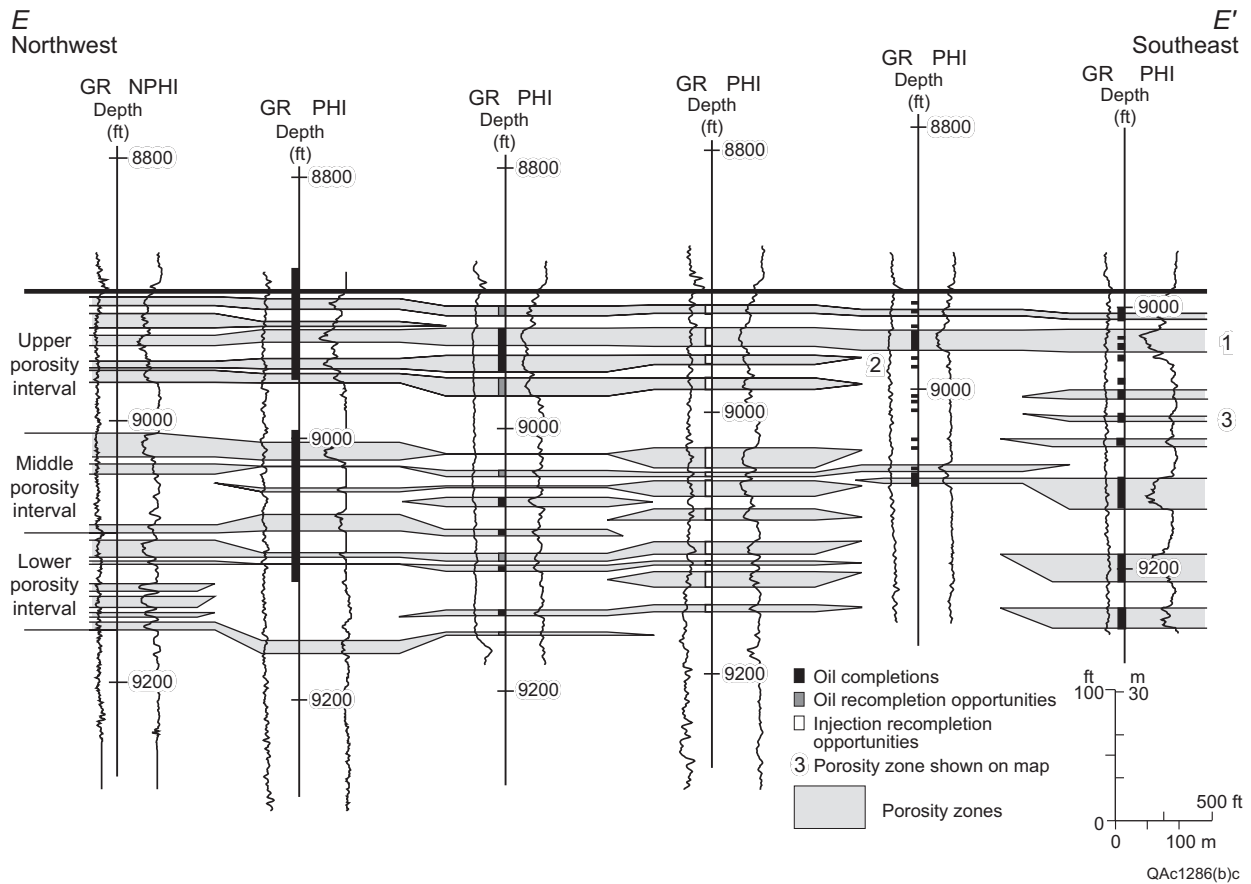


Figure 21. Dip-oriented stratigraphic cross section showing distribution and continuity of major porosity units. From Ruppel and Barnaby (2001).

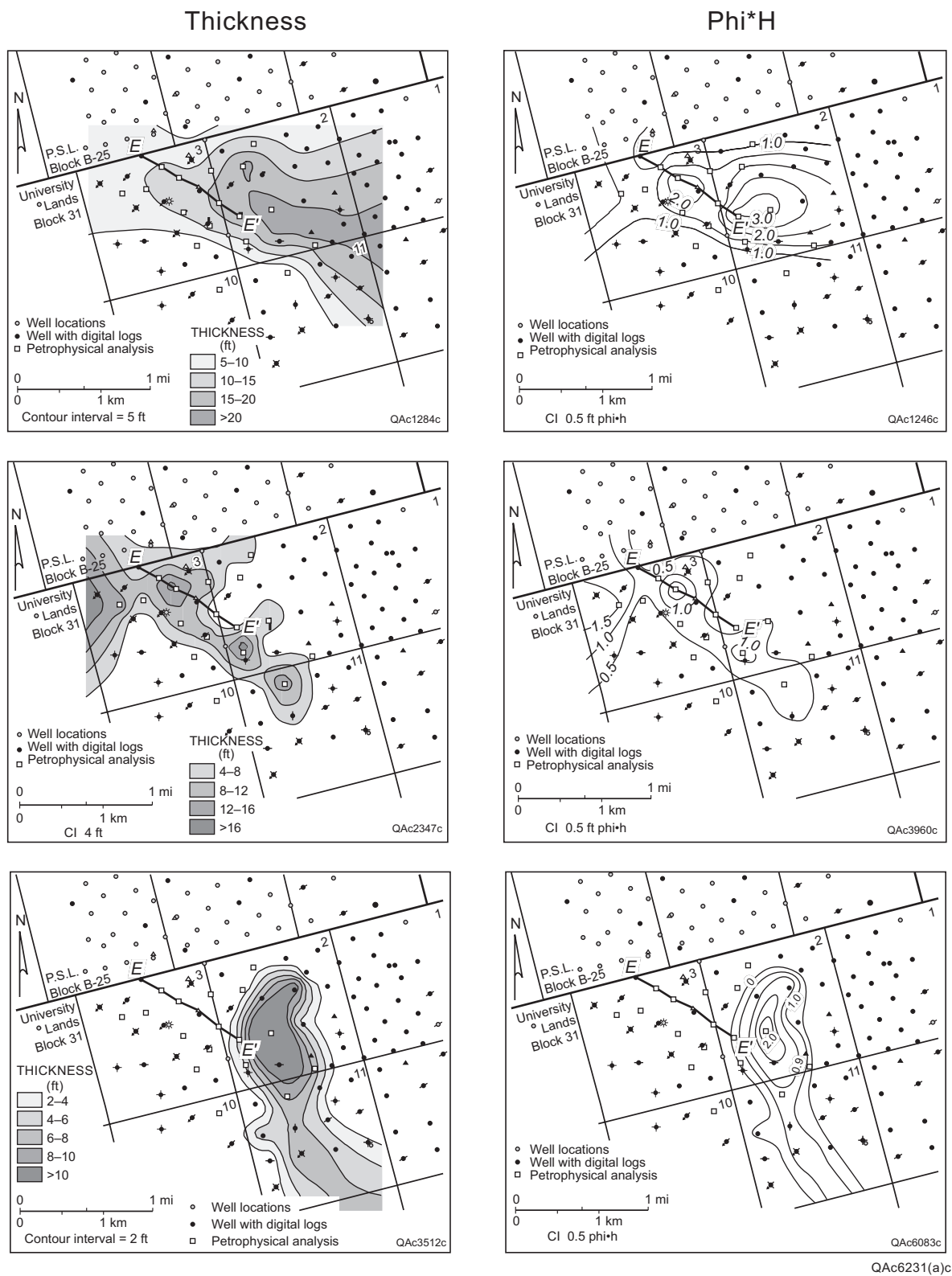


Figure 22. Paired maps of $\phi \cdot h$ and thickness for selected chert depositional units. Note the markedly dissimilar distribution of these potential flow units. Numbers correspond to units shown in figure 21. From Ruppel and Barnaby (2001)

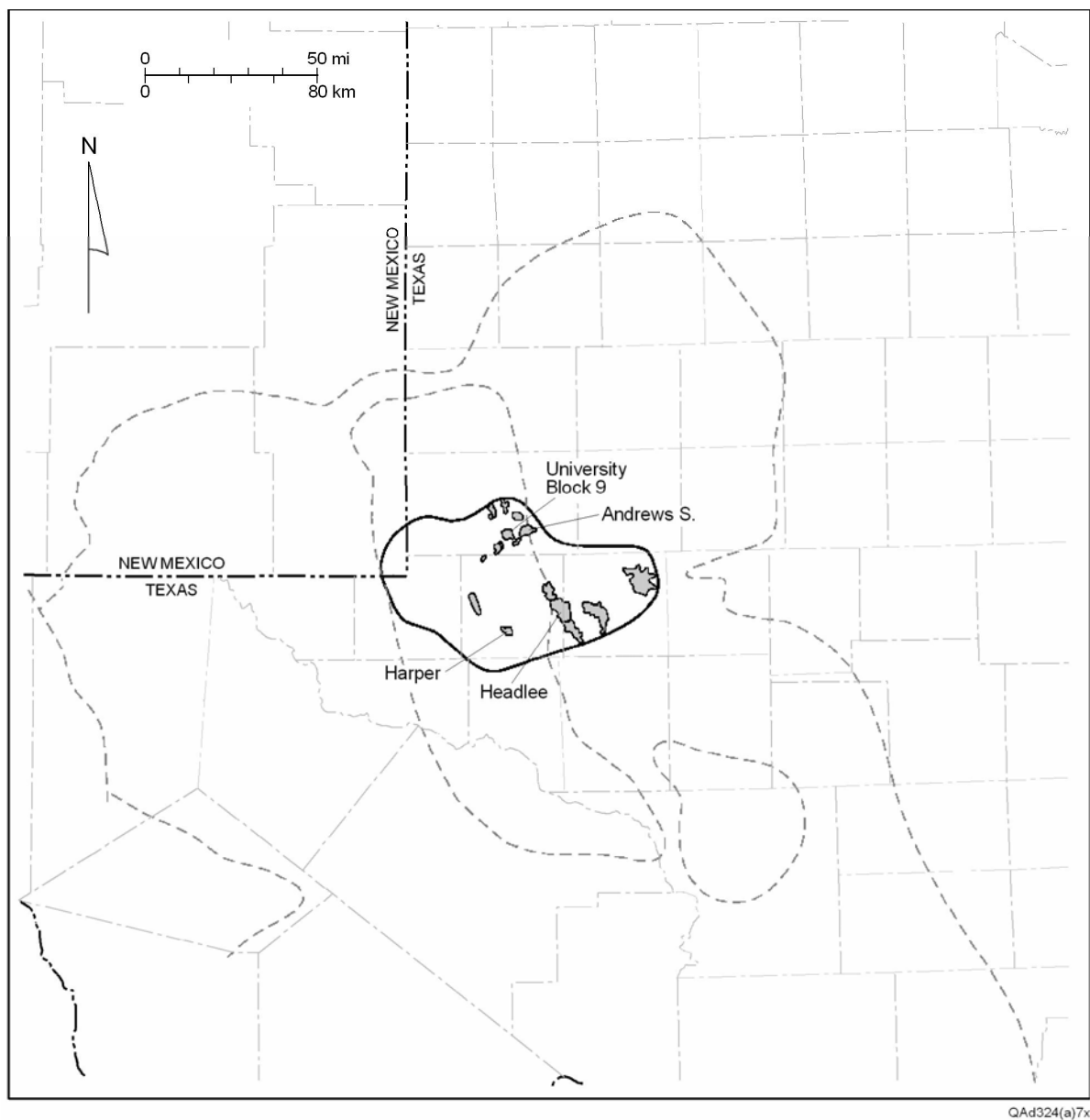


Figure 23. Map showing play boundary and the distribution of major reservoirs of the Thirtyone Carbonate Ramp play.

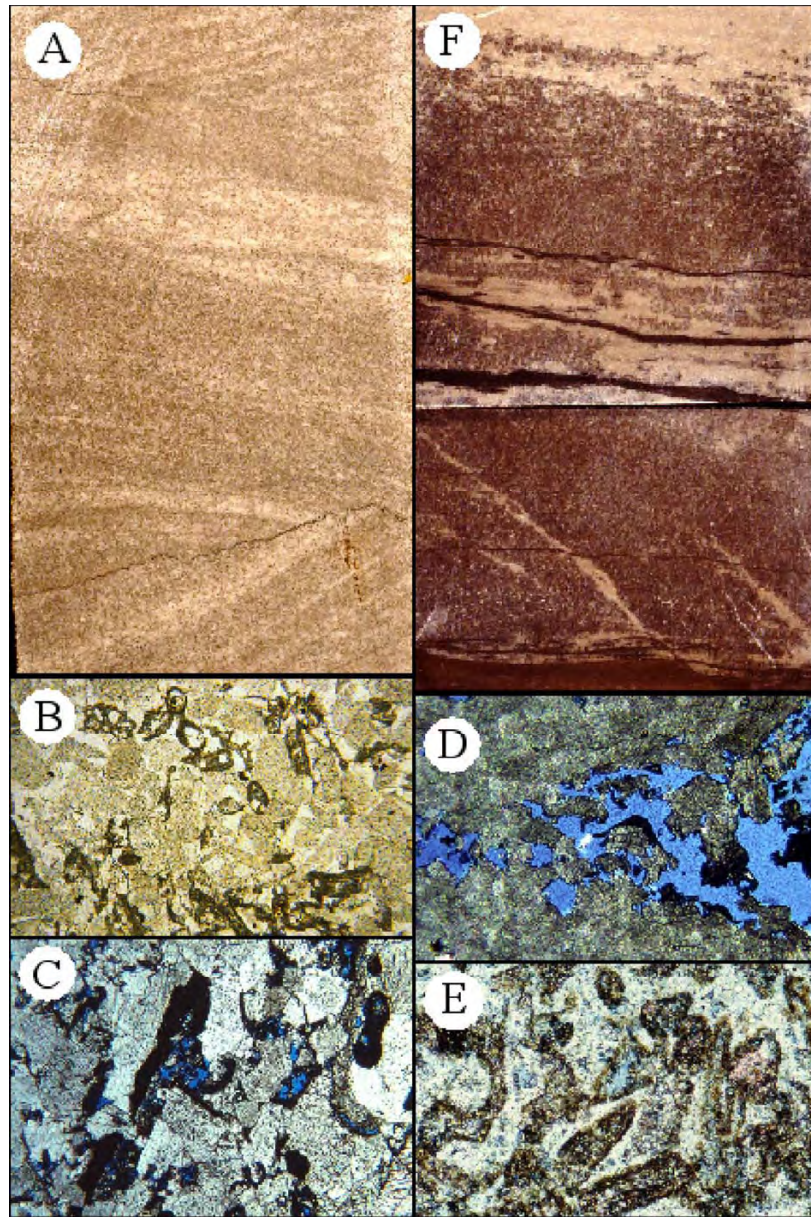
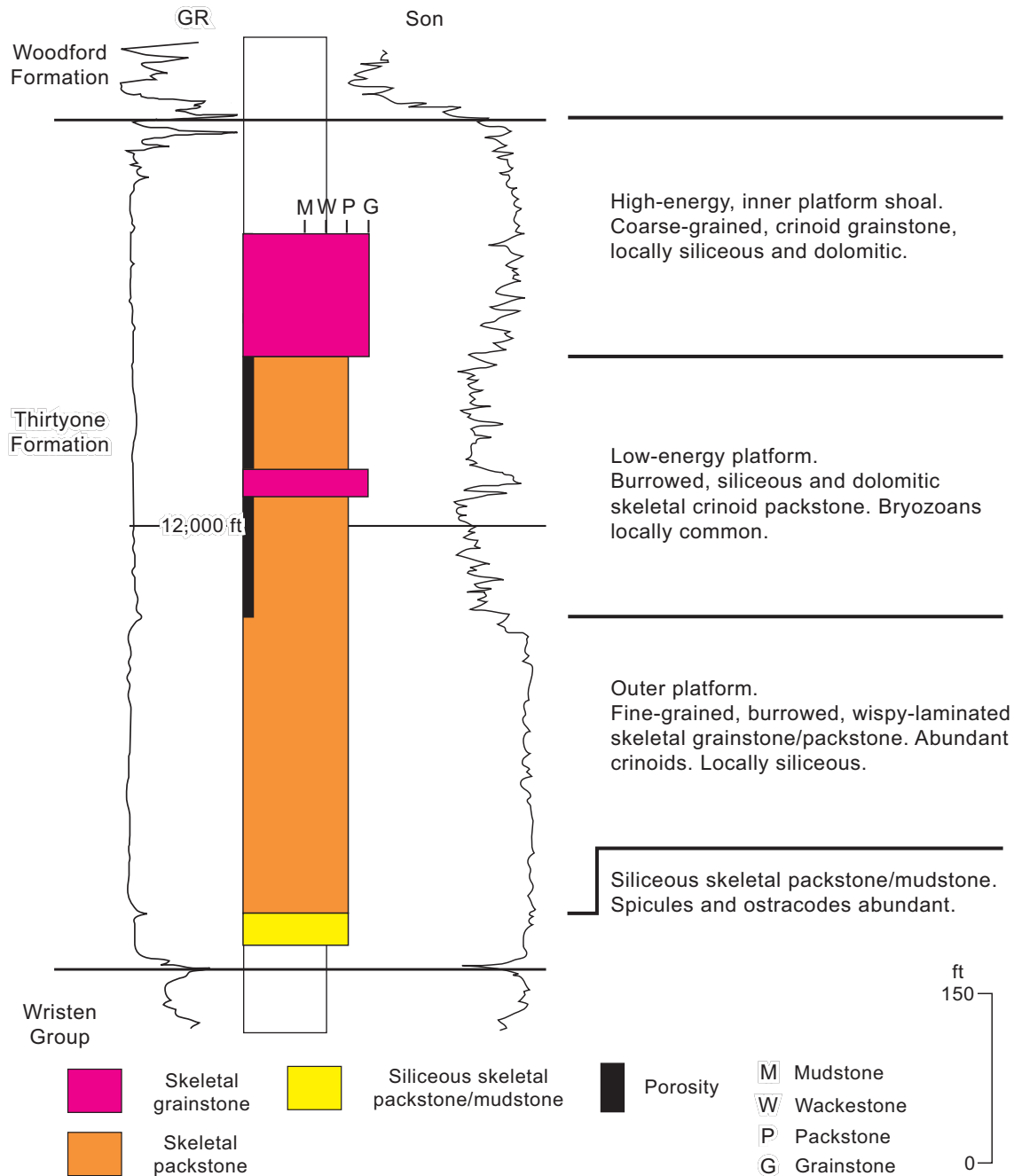


Figure. 24. Typical facies of the Thirtyone Ramp Carbonate play. A. Slab of crinoid grainstone facies showing cross laminations. Depth: 11,783 ft. Getty Headlee Unit No. 10-6, Midland County, Texas. B. Thin-section photomicrograph of crinoid/bryozoan grainstone. Note that pore space is entirely occluded by pore-filling syntaxial cements. Depth: 10,648 ft. Sinclair Emma Cowden No. 36, Andrews County, Texas. C. Thin-section photomicrograph of syntaxially cemented, crinoid/bryozoan grainstone. Note minor pore space associated with leached mud and within bryozoans. Depth: 10,519 ft. ARCO University No. 9 B-4, Andrews County, Texas. D. Thin-section photomicrograph of coarse crystalline dolostone. Note extensive interparticle pore space. Depth: 10,516 ft. ARCO University No. 9 B-4. E. Thin-section photomicrograph of siliceous skeletal packstone. Note interparticle porosity associated with siliceous matrix. Depth: 10,472 ft. ARCO University No. 9 B-4. F. Slab showing porous crinoid packstone overlain by nonporous grainstone. Depth: 11,798 ft. Getty Headlee Unit No. 10-6, Midland County, Texas.



From Ruppel and Hovorka (1995)

Figure 25. Composite log from Headlee field showing typical development of Thirtyone carbonate section in eastern and southeastern part of area. From Ruppel and Hovorka (1995a).

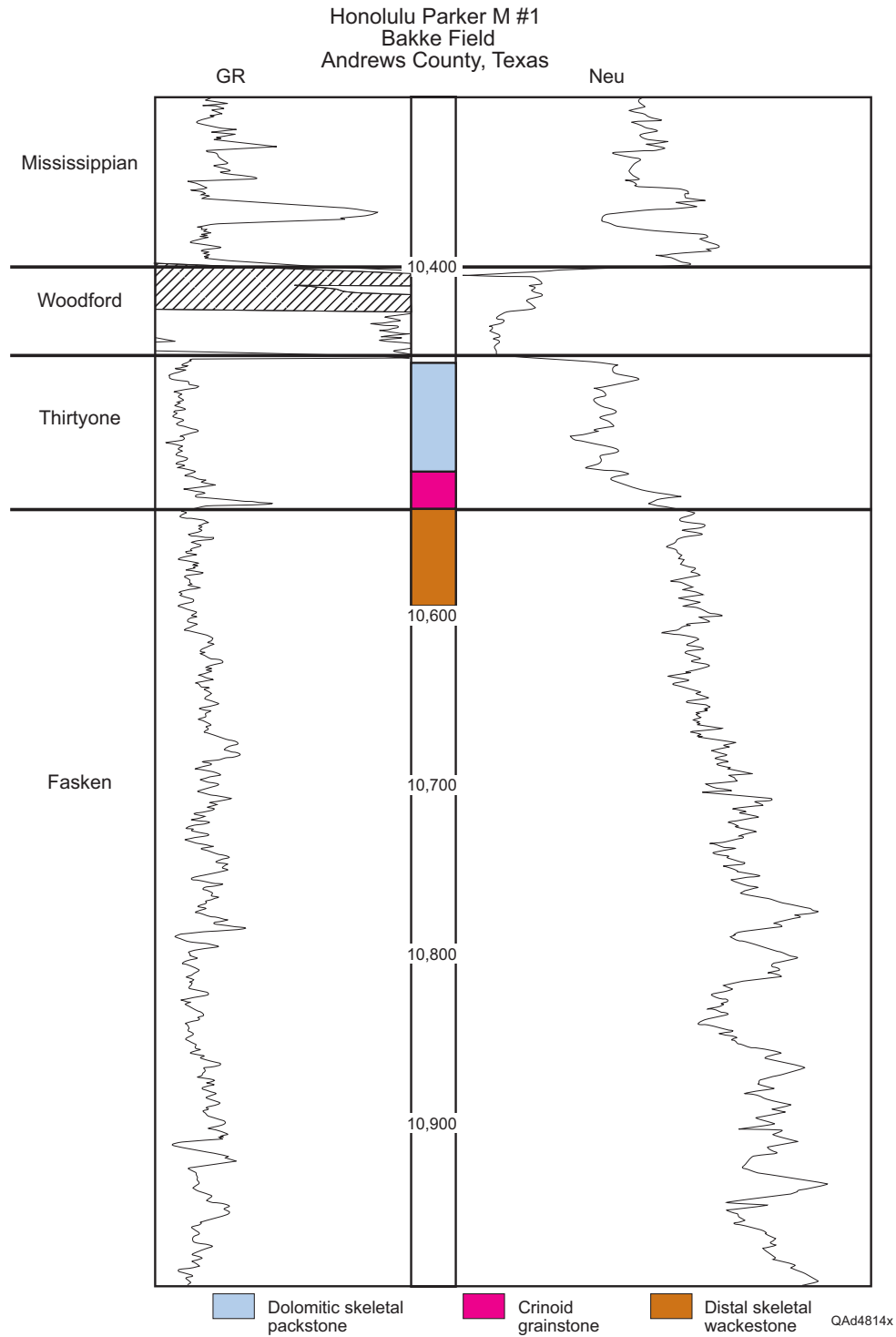


Figure 26. Typical development of facies and porosity in upper Thirtyone ramp carbonates. Note that essentially all reservoir porosity in the well is associated with dolomitized Thirtyone skeletal packstones. Bakke Field. Honolulu Parker M No. 1, Andrews County, Texas.

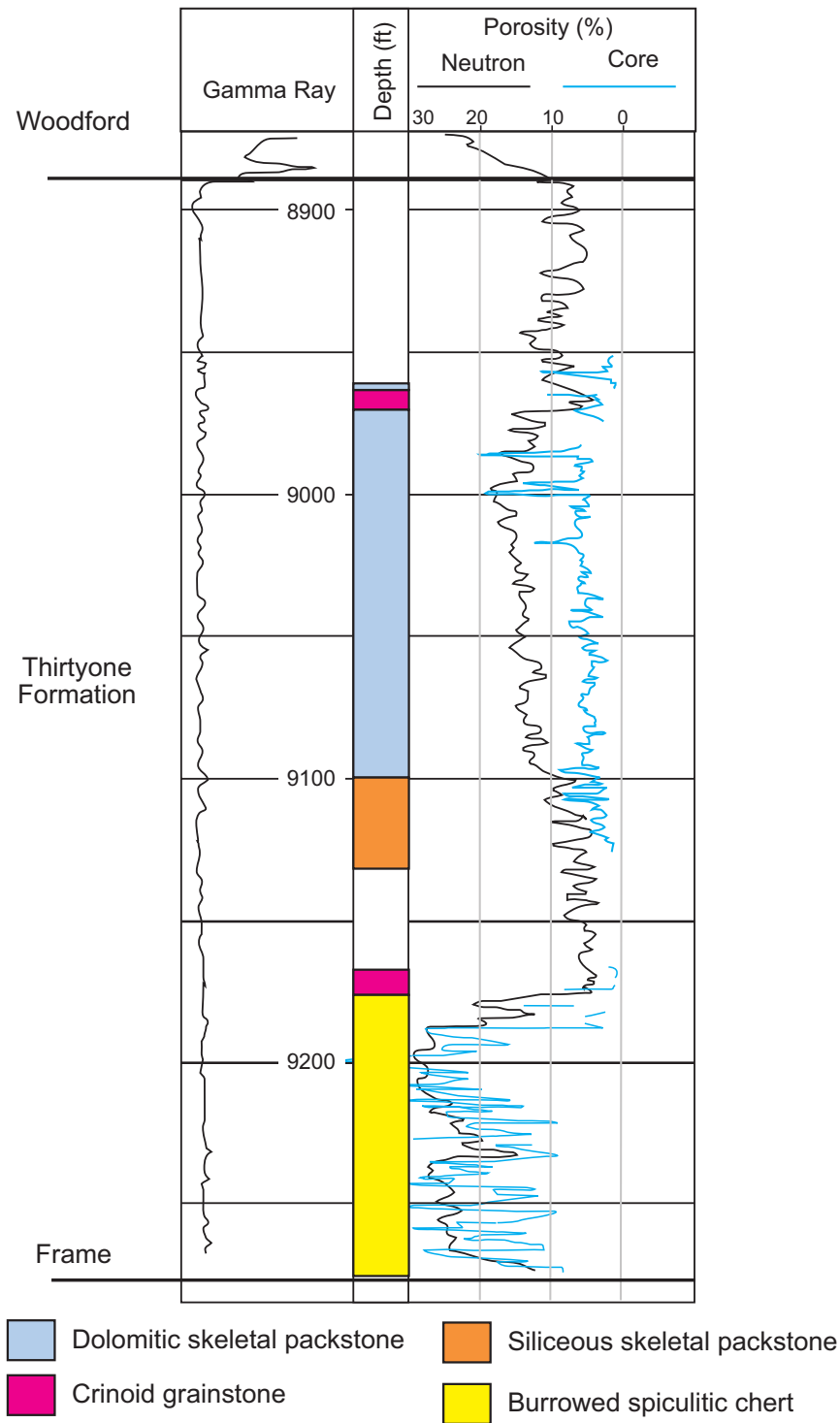


Figure 27. Facies development and porosity in upper Thirtyone ramp carbonates at Bedford field. Porosity in the upper Thirtyone is associated with dolomitized, graded, skeletal packstones. Note that much higher porosity is developed in Thirtyone deep-water cherts of the lower Thirtyone Formation. Bedford field, Shell Ratliff Bedford No. 20, Andrews County, Texas.

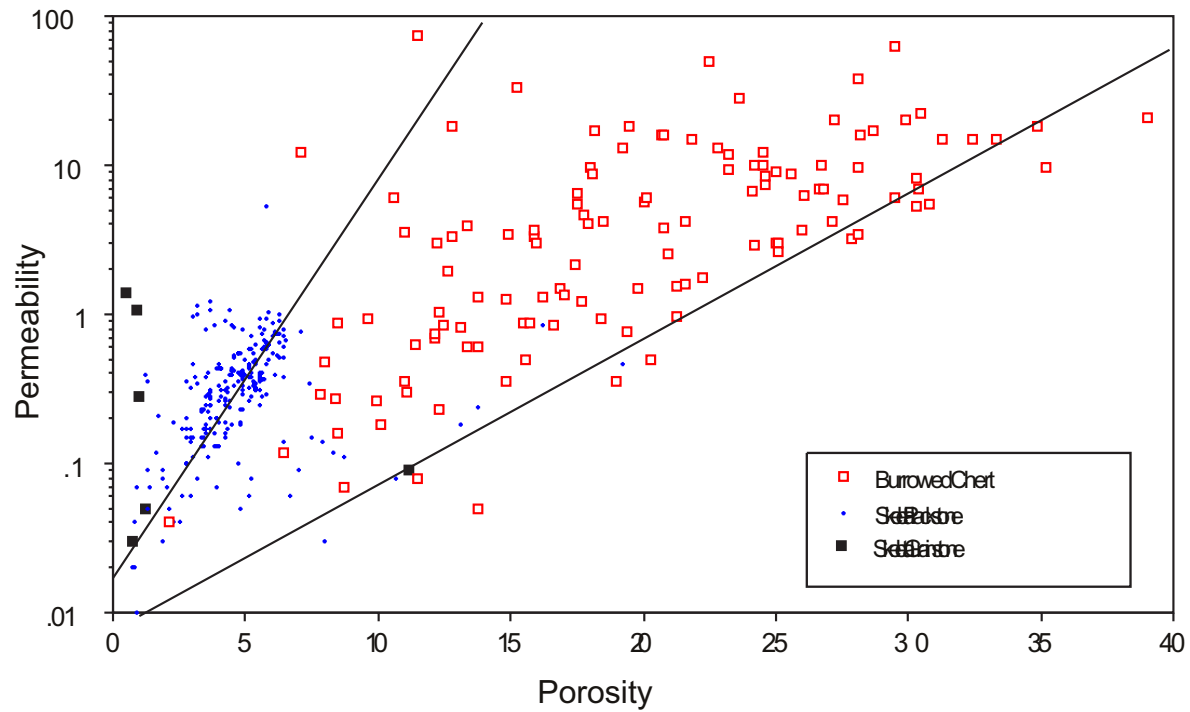


Figure 28. Porosity/permeability relationships in the Thirtyone section at Bedford field. Despite their low porosity and permeability, Thirtyone carbonates are productive at Bedford.

THE MISSISSIPPIAN BARNETT FORMATION:
A SOURCE-ROCK, SEAL, AND RESERVOIR PRODUCED BY EARLY
CARBONIFEROUS FLOODING OF THE TEXAS CRATON

Stephen C. Ruppel and Jeffery Kane

Bureau of Economic Geology
Jackson School of Geosciences
The University of Texas at Austin
Austin, Texas

ABSTRACT

The Early Carboniferous (Mississippian) was a time of crustal downwarping and flooding of southern Texas region. Mississippian facies documenting this flooding include a basal, updip, shallow to deep water carbonate succession and an overlying, downdip, deep water, fine grained siliciclastic mudrock succession. The basal carbonate succession, termed the Mississippian Limestone in the Permian Basin, includes the Chappel of the Llano Uplift and the Caballero-Lake Valley of southern New Mexico outcrops. These rocks document the margins of an extensive carbonate platform that occupied much of the western U.S. during the middle developed Mississippian. The overlying siliciclastic mudrock succession includes the Barnett formation of the Permian and Ft. Worth Basins and the Rancheria Formation of southern New Mexico outcrops. These rocks accumulated by autochthonous hemipelagic sedimentation and allochthonous mass gravity transport in low energy, below wave base, dysaerobic conditions in a platform marginal deep water basin formed on the southern margin of the Laurussian platform.

The carbonate section is poorly known and only of minor importance as a hydrocarbon reservoir in the Permian Basin. Key insights into the detailed character and architecture of these rocks are provided by analogous outcrops of the Lake Valley outcrop succession in New Mexico. The overlying Barnett mudrock succession, long recognized as a hydrocarbon source rock, is similarly poorly known but has recently attracted great attention as a target for gas exploration and development. Aspects of Barnett stratigraphy, sedimentology, mineralogy, and chemistry are inferred by comparisons to and extrapolations from better known data sets in the Ft. Worth Basin.

INTRODUCTION

The Mississippian is one of the most poorly known depositional successions in the Permian Basin. This is largely due to the fact that only small volumes of oil and gas have been produced from these rocks and there has thus been little interest in collecting data to interpret them. This has recently changed because of the successful development of the Barnett Formation in the nearby Ft. Worth Basin as a reservoir of natural gas (Montgomery, 2004; Montgomery and others, 2005). Now there is considerable interest in understanding the Barnett in the Permian Basin and its interrelationship with overlying and underlying rocks. However, because of the historical lack of interest in these rocks, very few reports on the Mississippian of the Permian Basin, in general, and no studies of the Barnett, more specifically, have been published. Basic aspects of the system are easily defined by the abundant wireline logs that penetrate the Mississippian across the basin. However, detailed rock data (e.g., cores) needed to calibrate geophysical data and to accurately characterize facies, petrophysics, diagenesis, and depositional history are lacking. Fortunately, such data are available in adjacent basins from both outcrops and the subsurface. This report integrates existing data and models from the Permian Basin – and surrounding areas – to develop interpretations and models for the Mississippian that constitute a fundamental basis for future exploration and development activities in the Basin.

PREVIOUS WORK

Because Mississippian rocks have not until recently been of great interest to oil and gas producers in the Permian Basin, relatively little published data exist for the section. By far the most comprehensive and useful report published is the USGS study of the Mississippian of the United States (Craig and Connor, 1979). Although regional in focus, this report contains discussions of formations, age relationships, thickness, depositional environments, and structural setting for the entire Mississippian System. Included in the report are thickness and structure maps, cross sections, that provide an good overview of sedimentologic and stratigraphic relationships in the Permian Basin. Gutschick and Sandberg (1983) published a valuable analysis of the middle Osagean (Lower Mississippian) section across the U.S.

primarily based on their work in western U.S. Their models are applicable over much of the U.S.

More focused studies of the Permian Basin region, however, are rare. One of the few is that by Bay (1954) who conducted a detailed stratigraphic analysis of the Mississippian section in Gaines and Andrews Counties, Texas based on wireline logs and well cuttings. Hamilton and Asquith (2000) described styles of deposition and diagenesis in the upper Mississippian Chester Group and documented the distribution of the Barnett in Lea County, New Mexico.

Considerably more information has been published on the adjacent Palo Duro and Ft. Worth basins. Ruppel (1985) described thickness and facies variations in the Mississippian section in the Palo Duro and Hardeman basins and also published a general stratigraphic model for the Hardeman – Ft. Worth Basin areas (Ruppel 1989). Henry (1982) provided a basic analysis of the Chappel and Barnett formations in the Ft. Worth Basin area. More recently, Montgomery (2004; see also Montgomery and others, 2005) contributed an extensive summary of the Barnett in the Ft. Worth Basin.

REGIONAL SETTING

During the Mississippian, the Permian Basin area straddled the outer margin of an extensive shallow water carbonate platform that covered much of southern and western Laurussia (in what is now the central and western U.S. (Figs. 1, 2)). Because of its setting in warm tropical waters and its isolation from sources of clastic sediment input, carbonate sedimentation dominated the interior of this platform (Figs. 1 and 2). Along the western and southern margins of the platform, isolated reefs and carbonate buildups were common. The southern margin of the platform was controlled by the position of the approaching Gondwana plate (Fig. 1). Regional sedimentological data (Craig and Connor, 1979) indicate that a deep trough (the Ouachita trough) formed ahead (north) of the Gondwana plate and that by at least middle Mississippian time the outer margins of this trough were uplifted and began to shed sediment northward into the trough. The Stanley Shale of the Ouachita overthrust belt in Oklahoma, a sandstone-bearing shale succession that is rich in coarse detrital sediments (Craig and Connor, 1979), reflects near-source, outer trough sedimentation. More proximal, inner trough sediments (which formed between the carbonate platform to the north and the trough

axis to the south) were characterized by siliceous muds formed by hemipelagic suspension and coarser grained carbonate detritus (transported from the carbonate platform to the north) and siliciclastic detritus (transported from the uplifted trough margin to the south) by mass gravity transport. [These sediments are represented by the Barnett Fm of the Permian and Ft. Worth Basins.] Based on studies of the western margin of the platform, Gutschick and Sandberg (1983) developed excellent models for platform margin to slope deposition that fit very well with existing evidence from the Permian and Ft., Worth Basin area (Fig. 3).

REGIONAL STRATIGRAPHY AND FACIES

As suggested above, Mississippian stratigraphy and facies development is very similar throughout most of the Permian Basin – Ft. Worth Basin region. However, there are key differences in styles and in data sets that make it worthwhile to discuss each area separately. The stratigraphic nomenclature and correlations of conventionally named Mississippian units in the Permian Basin and surrounding areas are depicted in figure 4.

Permian Basin

Stratigraphy

In general the Mississippian of the Permian Basin comprises two end-member lithologies: a carbonate dominated section updip and upsection, and a siliciclastic-rich (commonly termed “shale”) section in the southern part of the area. The basal carbonate section, which is defined and correlated by its relatively low gamma ray character is unnamed but is usually referred to as the Mississippian Lime or Limestone. The overlying high gamma ray section is commonly referred to as the Barnett Formation (Fig. 5). The basal Mississippian carbonate is underlain by the Woodford Shale in most parts of the Basin. The Barnett is generally overlain by carbonate-rich strata usually termed “Pennsylvanian Limestone” (or Lime).

Total Mississippian thickness varies widely across the Permian Basin area. A maximum thickness of more, than 2200 ft was reported by Craig and Connor (1979) in parts of Reeves and Ward counties, Texas. Most of the Mississippian section in this area is assigned to the Barnett. Figure 6 depicts the distribution and thickness of the Barnett across the region. Barnett

thickness decreases northward toward the updip carbonate platform. The position of the platform margin and the updip subcrop margin of the Barnett has been defined in Gaines and Andrews counties by Bay (1954) and in Lea County by Hamilton and Asquith (2000). This change from Barnett mudrock facies to carbonates is generally well imaged by gamma ray logs (Fig. 7). Using log data, outcrop descriptions, and new descriptions from cores from this study, it is possible to define the probable position of the margin of the Mississippian platform during the late Mississippian (Fig. 8). The line marking the platform margin also marks the approximate updip extent of the Barnett Formation.

Carbonate Facies

Very little has been published regarding the facies character of the Mississippian carbonate section in the Permian Basin area. Hamilton and Asquith (2000) showed that the upper Mississippian carbonate section in central Lea County, New Mexico was dominantly composed of ooid and crinoid grainstones. Although cores from the lower Mississippian carbonate section have not been previously reported, two cores examined during the course of this study demonstrate the wide variability in facies that exists across the region.

Core recovered from the lower Mississippian carbonate section in Gaines County (Fig. 9). illustrate marked facies diversity. The lower, low gamma ray part of the section consists of light gray to brown, coarse-grained crinoidal grainstone (Fig. 10 a,b). These rocks are well-sorted and contain extensive syntaxial cement typical of crinoid grainstones. These rocks probably represent carbonate shoal sediments deposited in a well-oxygenated, high energy setting. By contrast, the upper part of the Mississippian section in this well consists of very dark-colored, cherty mudstones and wackestones (Fig. 10 c, d) whose depositional textures suggest they were deposited in a dysaerobic low energy setting, probably below wave base.

The basal Mississippian carbonate section in the southern part of the basin differs greatly from that observed in Gaines County. Although they exhibit a similar low gamma ray signature (Fig. 11), these rocks are dark gray to black mudstones that are massive to locally laminated or burrowed (Fig. 12 a,b). The dark color of these rocks, absence of megafauna, and limited evidence of infauna indicates that they were deposited in a low energy, anoxic to dysoxic setting.

Llano Uplift

Type sections for both the basal Mississippian carbonate (Chappel Formation) and the upper Mississippian “shale” (Barnett Formation) succession are located in the Llano Uplift area of central Texas. Outcrops and newly described cores from subsurface wells in the Llano Uplift area provide key data for interpreting the Mississippian section in the subsurface elsewhere.

In outcrops, the Chappel Formation consists of light-colored, fine to coarse grained, skeletal packstone (Watson, 1980). Although ostracodes, corals, and other fossils are common, it is the abundance of crinoids, in many cases red, that distinguishes the Chappel. The thickness of the Chappel is typically only a few feet, but ranges from a few inches to more than 50 ft (in depressions in underlying Ellenburger Group (Lower Ordovician) carbonates. The Chappel is overlain by the Barnett formation which at the type section consists of 50 ft of thin bedded, black shale that contains carbonate concretions and lenses (Fig. 14a). The Barnett is typically highly petroliferous having yielded as much as 40 gallon of crude oil per ton from some outcrops in San Saba county, Texas. (Watson, 1980)

Cores of the Chappel-Barnett succession demonstrate key aspects of the two formations. In McCulloch County, Texas (Fig. 13), for example, the basal Chappel consists of 1 ft of red, skeletal packstone (Fig. 15a). Overlying rocks (which have been referred to as the Whites Crossing unit because of their facies and age (Hass, 1953) are typically coarse-grained crinoidal packstones that are locally interbedded with carbonate and siliciclastic mud (Fig. 15b,c,d,e). Although crinoidal debris dominated these rocks, other open marine fossil are locally common (Fig.15f). Whereas the basal Chappel appears to be largely indicative of in situ deposition, the Whites Crossing facies contain features (e.g., inclined bedding, slump features, poor sorting) that suggest downslope transport. The diverse fauna present in the Chappel demonstrate that these rocks were deposited in a well-oxygenated, normal marine setting typical of shallow water carbonate platforms.

The overlying Barnett in McCulloch County (Fig. 13) comprises dark gray to black siliciclastic mudstones that range from massive to thinly laminated and are locally very fossiliferous (Fig. 14b,d). The Barnett locally contains carbonate concretions (Fig. 14b) that can be seen in outcrop to have lens-like geometries (Fig. 14a). The fauna is dominated by two end-member types: thin walled brachiopods and crinoid debris (Fig. 14b,c,d). Crinoid debris (Fig. 14c) is most common at the base of the Barnett where it grades into the underlying Whites

Crossing (Fig. 13). Brachiopods, which are typical of deep water forms thought have been deposited at water depths greater than 200 ft (Thompson and Newton, 1987), appear to be in situ and are associated with dark-colored mudstones (Fig. 14d). The presence of these brachiopods coupled with the absence of burrows and in situ shallow water faunas suggest the Barnett formed in dysoxic conditions in deep water.

Conodont faunas from outcrop sections of the Chappel and Barnett indicate that the Chappel is Osagean in age whereas the Whites Crossing and Barnett are much younger Meramecian deposits (Hass, 1953, 1959). This suggests that the Chappel platform was emergent prior to flooding and deposition of the Barnett.

Ft. Worth Basin

The Mississippian section in the Ft. Worth Basin differs significantly from that in the Permian Basin by lying directly on much older (Ordovician) rocks and in containing no basal carbonate (i.e., Chappel or Mississippian Limestone) section. Mississippian rocks in the Ft. Worth Basin instead overlie Viola (Middle Ordovician) or Ellenburger (Lower Ordovician) carbonates and comprise the Barnett Formation and related rocks only. Because the Barnett exhibits a high gamma ray log response it is readily definable in the subsurface (Henry, 1980). Locally the Barnett is separated into upper and lower sections by a low gamma ray interval that has been termed the Forestburg (Fig. 16). Wireline logs and core analyses show that the low gamma ray character of the Forestburg is a function of the presence of calcite. The Barnett/Forestburg section generally increases in thickness to the east and northeast toward the Ouachita overthrust. The Forestburg, however, shows no systematic areal trends in thickness.

Facies

The textures, facies, mineralogies of the Barnett and Forestburg have recently been well documented and imaged by Papazis (2005). Both units are primarily dark gray to black, laminated mudstones (Fig. 17, 18). Some mudstones are very weakly laminated to nearly massive (Fig. 17c). Most, however, display laminae composed of silt-sized grains of quartz (Fig. 18b,c) or of phosphatic peloids or skeletal debris (Fig. 18a,c,e). Agglutinate foraminifera and thin walled brachiopods like those observed in the Barnett of the Llano uplift are also common (Papazis, 2005) (Fig. 18a,d,e). The Forestburg is generally somewhat lighter in color

than the Barnett reflecting its higher carbonate content (Fig. 17a). Forestburg mudstones are weakly laminated to nearly massive (Fig. 17c) but locally contain thin-walled brachiopods (Fig. 17c). Papazis (2005) reported that the Barnett is dominantly composed of quartz in the clay and silt size ranges and that clay minerals are relatively uncommon. This distinguishes Barnett mudrocks from typical shales which generally contain a high volume of clay minerals.

Synthesis of core and log data from the Ft. Worth Basin and nearby outcrops and cores from the Llano Uplift area indicates Barnett and Forestburg rocks were deposited in a restricted, low energy, deep water setting. The color and laminated character of the rocks indicates quiet water, hemipelagic sedimentation interrupted periodically by grain and/or turbid flows composed of clay to silt-size particles of quartz and/or carbonate. The limited autochthonous fauna of brachiopods and agglutinate foraminifera is characteristic of below wave base, dysaerobic conditions at depths probably greater than 200-300 meters (Thompson and Newton, 1987; Gutschick and Sandberg, 1982; Fig. 3). The Forestburg probably represents the distal tail of a platform derived, carbonate dominated, debris flow derived from the carbonate platform to the west of the Ft. Worth Basin.

MISSISSIPPIAN DEPOSITIONAL SETTING

Recent studies of cores and logs from the Permian and Ft. Worth Basins coupled with developing studies of outcrops in the Llano uplift region have provided new insights into depositional styles and facies development in the Mississippian section. It is apparent, for example, that the Barnett Formation documents an overall rise in relative sea level across the entire southern Laurussian paleocontinent during the Mississippian. In the Ft. Worth Basin area, this rise resulted in the flooding of a previously emergent carbonate platform of Ordovician rocks. It is probable that flooding was a response to downwarping of the southeastern margin of the platform associated with collisional flexure of the Laurussian plate caused by the approaching Gondwana plate (Fig. 1). In the Permian Basin area, where Mississippian deep water rocks overlie relatively deep water siliciclastics of the Woodford formation (Comer, 1991) this deepening event is less apparent.

Because of the characteristic log character of the Barnett, platform flooding is easily defined with wireline logs (i.e., these deep water mudrocks can be readily recognized by their

high gamma ray character). Although the carbonate-rich intervals can similarly be defined from gamma ray logs (by their low response) carbonate facies, and thus relative water depth and depositional environment cannot. The Forestburg interval is a good example of this. Many have assumed that this carbonate-rich interval is composed of shallow water platform carbonates but as we have stated, it is instead a deep water assemblage like the Barnett but with a higher carbonate content. The succession low gamma ray (Mississippian limestone) intervals in the Permian Basin present similar difficulties of interpretation. For example, low gamma ray carbonates in the lower Mississippian in Gaines County (Fig. 7, 9) consists of crinoidal grainstones and packstone that reflect shallow water platform deposition. By contrast, low gamma ray carbonates of the lower Mississippian in Reeves County (Fig. 11) are deep water (probably slope-basin) mudstones. Low gamma ray upper Mississippian rocks in Gaines County (Fig. 9) are also deeper water, platform margin to slope mudstones and wackestones. Thus, accurate definition of Mississippian carbonate facies is thus not possible with wireline logs alone. Cores and subsurface models are needed to accurately characterize the nature and distribution of the Mississippian carbonate succession in the Permian Basin.

Important insights to Mississippian facies character and architecture are provided by correlative, analogous outcrops in the Sacramento and San Andres Mountains of southern New Mexico (Fig. 4). The Caballero - Lake Valley Formations comprise a complex Osagean succession (Fig. 19) of carbonate grainstones, packstones, wackestones and mudstones that represent buildup, flank, interbuildup and deeper water outer ramp to slope environments (Meyers, 1975; Lane and Ormiston, 1982). The overlying Rancheria Formation (Fig. 4) consists of deeper water, laminated, locally spiculitic lime mudstones and mudstones that document major rise in relative sea level during the Meramecian (Yurewicz, 1977).

Bachtel and Dorobek (1998) reevaluated the facies distribution of the Caballero - Lake Valley - Rancheria succession and demonstrated that facies vary systematically in position and geometry when viewed in a sequence stratigraphic framework (Fig. 20). They recognized three sequences in the Caballero-Lake Valley succession each with a well defined transgressive systems tract (TST) assemblage of dark colored, low energy, deeper water mudstones and wackestones and a highstand systems tract (HST) dominated by shallow water, light-colored grainstones and packstones. Mud-rich buildups and flanking facies appear to have developed during TSTs but persisted into HSTs. The geometries of these three sequences define basinward

progradation and falling sealevel. The fourth and youngest sequence contains deep water mudstones and gravity flow deposits of the Rancheria Formation. These deposits onlap the Lake Valley succession and document sea level rise. Conodont biostratigraphy shows that the Lake Valley sequences are Kinderhookian to Osagean in age whereas the onlapping Rancheria is Meramecian (Lane, 1974; Lane and Ormiston, 1982). In updip platform areas the Rancheria succession (sequence 4 of Bachtel and Dorobek, 1998) overlies the Lake Valley succession (sequence 3) unconformably (Fig. 20) suggesting post sequence 3 lowstand exposure of the platform.

The Lake Valley succession provides a good model for understanding age and facies relationships within the Permian Basin succession. The facies succession in Gaines County area (Fig. 7. 9) represents a near platform-margin position on the shelf with the grainstones observed in core perhaps representing the HST of sequence M2 (point 1 on Fig. 20). The Mississippian succession observed in Reeves County (Fig. 11) reflects a more distal position perhaps at the downdip toe of sequence 3 (point 2 on Fig. 20). More accurate delineation of sequences, systems tracts, and facies will require more integrated core and log study of the succession.

WIRELINE LOG CHARACTER OF MISSISSIPPIAN FACIES

As has been discussed, basic separation of siliciclastic and carbonate facies is a relatively straightforward matter with gamma ray logs. The forgoing discussion has also demonstrated the complexity and difficulty of defining the details of age and facies interrelationships within the carbonate section even with good quality logs. However, new studies of log response in the Barnett suggest that there are systematic differences in mineralogy within the Barnett that can be defined with conventional wireline log suites. Spectral gamma logs, for example, show changes in the abundance of potassium, thorium and uranium that indicate stratigraphic differences in the sedimentology of the Barnett. Potassium, for example, exhibits a subtle and gradual decrease in abundance upward (Fig. 21). This suggests a slight reduction in the volume or increasing maturity of siliciclastics upsection and is reflected both by the potassium curve and the CGR curves (Fig. 21). Even more interesting is the clearly lower volume of thorium present in the basal 100 ft of the Barnett. This is reflected in the thorium concentration curve and the thorium/potassium ratio curves in figure 21.

Preliminary mineral modeling of these elemental changes suggests a systematic difference the clay mineral assemblage at the base of the section compared with the rest of the section (Fig. 22). The low thorium/potassium ratio suggests an assemblage of micas (or glauconite and feldspars) and illite in the lower 100 ft of the Barnett and a different assemblage of mixed layer clays in the remainder of the Barnett (upper part of the lower Barnett and the upper Barnett). These differences in sediment composition have implications for the depositional history of the Barnett and also may provide important insights into the geomechanical character of the rocks which is an important concern for reservoir development.

RESERVOIR DEVELOPMENT

Mississippian carbonate succession

According to Dutton and others (2005) the Mississippian Platform Carbonate play is the smallest oil-producing play in the Permian Basin, having cumulative production of little more than 15 MMbbl from the five reservoirs with cumulative production of greater than 1 million barrels as of 2001. The scarcity of productive Mississippian carbonate reservoirs may be tied to the abundance of crinoidal, grain-rich facies in platform successions; these rocks typically are associated with porosity occluding syntaxial cements. Most production from Mississippian reservoirs apparently comes from more porous upper Mississippian ooid grainstones (e.g., Austin field, in Lea County, New Mexico; Hamilton and Asquith, 2000). In at least some instances, production is also developed in dolomitized intervals (e.g., Brahaney field, Yoakum County, Texas; Wright, 1979). Grimes (1982) noted that the Mississippian production at Fluvanna field, Borden County, comes from weathered chert at the top of the Mississippian section. Reservoirs are limited to the northern part of the Permian Basin corresponding to the area of shallow water platform development (Fig. 23).

Barnett Formation

The Barnett of the Ft. Worth Basin has become a prolific producer of natural gas. As of 2006, more than 1.6 TCF of gas had been produced from the Ft. Worth Basin. The Barnett succession of the Permian Basin is depositionally analogous and may contain similar facies and mineralogies. Although parts of the Mississippian section have been removed by erosion, the Barnett is present across large areas of the Permian Basin (Fig. 23). Its extent is nearly as

great as in the Ft. Worth Basin and it locally attains much greater thicknesses (more than 2000 ft; Fig. 6).

Some key questions to consider in determining the potential for similar reservoir development in the Permian Basin are: (1) are Barnett facies as currently defined in the Permian Basin truly similar?, (2) what is the nature of overlying and underlying rocks and do variations play a role in completion strategies?, (3) what is the organic matter content and thermal maturity of Barnett facies?, and (4) are they fractured? No cores are currently available to answer facies or fractures questions. However, newly initiated wireline log –based studies of the Barnett are underway to develop initial models. We are also employing rock data from cores and outcrops in the Ft. Worth Basin and Llano areas to constrain wireline log models. Regional studies are providing improved resolution on the distribution, age, and facies character of both underlying carbonate successions and overlying units. We are also conducting detailed studies of fracture character based on core data. Organic matter data are not publicly available but recent vitrinite reflectance data from Pawlewicz and others (2005) provide initial key insights into the thermal maturity of the area. In summary, a great deal more study is needed to determine the depositional, mineralogical and structural character of the Barnett in the Permian Basin. These studies will be a fundamental basis for determining the potential of the Barnett as a viable economic resource.

SUMMARY AND CONCLUSIONS

Although information on the Mississippian succession in the Permian Basin is limited, data and models from outcrops and subsurface data from adjacent areas provides an initial basis for interpreting these rocks. Carbonates dominate the Mississippian section in the northern half of the area. These rocks are part of an extensive, shallow water carbonate platform that occupied much of the western U.S. during the middle Mississippian. In the southern part of the Basin, the section is composed primarily of siliciclastic mudrocks of the Barnett Formation. These rocks were deposited in below wave base conditions in a deep water platform to slope setting. The margin between shallow water carbonate deposition to the north and deeper water, hemipelagic and gravity transport deposition to the south ran east-west across most of the Permian Basin area. A peninsular extension of the platform margin appears to have extended

southward to the Llano Uplift. The platform carbonate succession (Mississippian Limestone) reaches thicknesses of about 500 ft in the north. South of the platform margin, the Mississippian Limestone thins rapidly and changes to deeper water, below wave base, carbonate mud facies. Barnett facies reach thicknesses of more than 2000 ft locally in the southern part of the Permian Basin but pinch out a short distance north of the platform margin.

Limited cores combined with data and models from outcrops in New Mexico provide constraints for interpretation of carbonate platform facies and stratigraphic architecture. However, more data are needed to accurately characterize these rocks. Core data for the Barnett are not yet available but cores and outcrops from the Ft. Worth Basin area provide keys for interpreting Barnett facies, mineralogy, and stratigraphy in the Permian Basin.. Integrated core and wireline log analysis shows great promise for providing more detailed information on the regional and local character of the Barnett in the Permian Basin as well as in the Ft. Worth Basin.

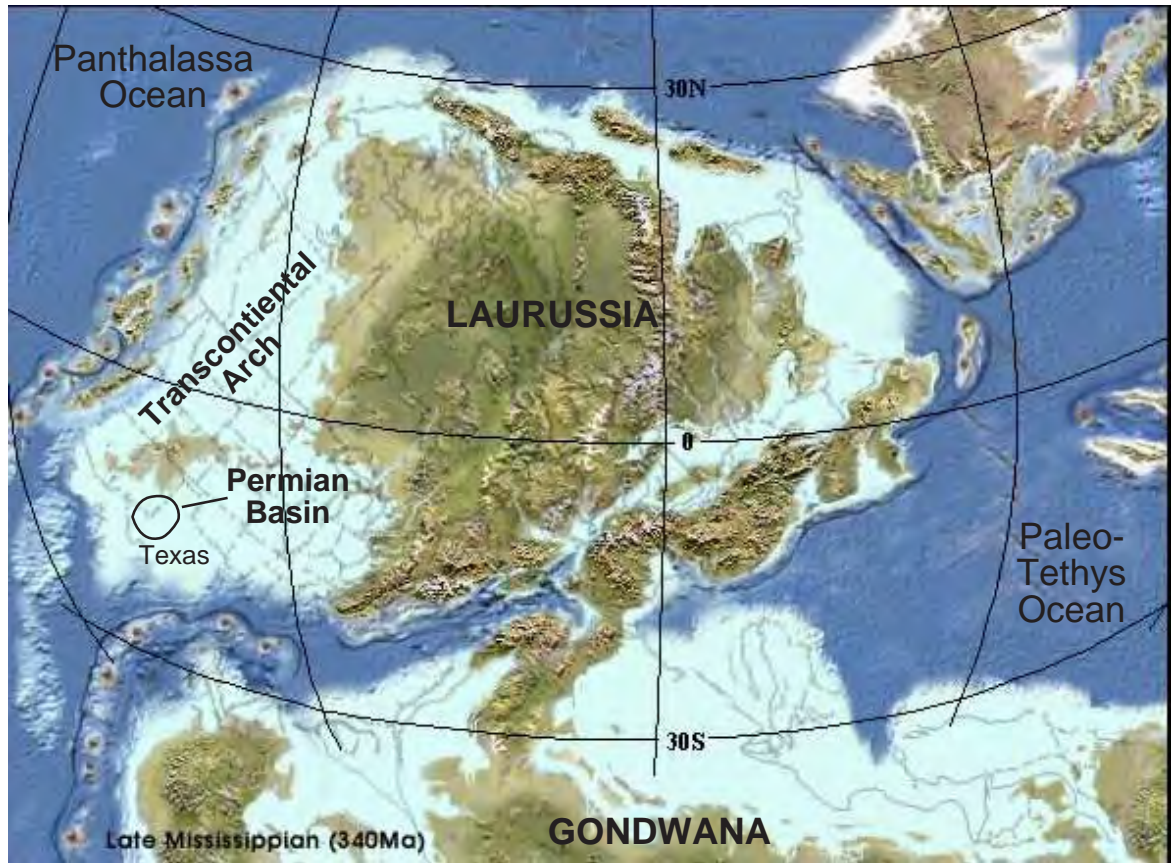
REFERENCES

- Bachtel, S., and Dorobek, S.L., 1998, Mississippian carbonate ramp-to-basin in south-central New Mexico: sequence stratigraphic response to progressively steepening Outer-Ramp Profiles, *Journal of Sedimentary Research*, v. 68, No 6, p. 1189-1200.
- Bay, T. A., Jr., 1954, Mississippian system of Andrews and Gaines counties, Texas: unpublished MS thesis, The University of Texas at Austin, 56 p.
- Comer, J. B., 1991, Stratigraphic analysis of the Upper Devonian Woodford Formation, Permian Basin, West Texas and New Mexico: The University of Texas at Austin. Bureau of Economic Geology, Report of Investigations 201, 63 p.
- Craig, L.C., and Connor, C. W., Coordinators, 1979, Paleotectonic Investigations of the Mississippian System in the United States, Geological Survey Professional Paper 1010, Part III..
- Dutton, S. P., Kim, E. M., Broadhead, R. F., Breton, C. L., Raatz, W. D., Ruppel, S. C., and Kerans, Charles, 2005, Play analysis and digital portfolio of major oil reservoirs in the

- Permian Basin: The University of Texas at Austin, Bureau of Economic Geology Report of Investigations No. 271, 287 p., CD-ROM.
- Grimes, D. N., 1982, Fluvanna field: selected oil & gas fields in West Texas: West Texas Geological Society Publication No. 82-75, p. 232–236.
- Gutschick, R., and Sandberg, C., 1983, Mississippian Continental Margins on the Conterminous United States, *in* Stanley, D.J. and Moore, G.T., The Shelf break: Critical Interface on Continental Margins: Soc. Econ. Paleontologist Mineralogists Special Publication 33, p.79-96
- Hamilton, D. C., and Asquith, G.B., 2000, Depositional, Diagenetic, and Production Histories of Chester Ooid Grainstones in the Austin (Upper Mississippian) Field: Lea County, New Mexico, *in* DeMis, W., Nelis, M., and Trentham R.C., eds., The Permian Basin : Proving Ground for Tomorrow's Technologies, West Texas Geological Society, Publication 00-109, p. 95-105
- Hass W. H., 1953, Conodonts of Barnett Formation of Texas, Geological Survey Professional Paper 243-F, p 69-94.
- Hass W. H., 1959, Conodonts from the Chappel Limestone of Texas, Geological Survey Professional Paper 294-J, 44 p.
- Henry, J. D., 1982, Stratigraphy of the Barnett Shale (Mississippian) and associated reefs in the northern Fort Worth Basin, *in* Martin, C. A., ed., Petroleum Geology of the Fort Worth Basin and Bend Arch Area: Dallas Geological Society, p. 157-178.
- Lane, H. R., 1974, Mississippian of Southeastern New Mexico and West Texas; A Wedge-on-Wedge Relation: American Association of Petroleum Geologists, Bulletin, vol. 58, no. 2, p. 269 - 282.
- Lane, H. R. and Ormiston, A. R., 1982, Waulsortian facies, Sacramento Mountains, New Mexico: Guide for an international field seminar, *in* Bolton, K. Lane, H. R., and Lemone, D. V. eds., Symposium on the Paleoenvironmental setting and distribution of the

- Waulsortian facies: El Paso Geological society and University of Texas at El Paso. P. 115-182.
- Montgomery, S. L., 2004, Barnett Shale: A New Gas Play in the Forth Worth Basin, *in* Petroleum Frontiers, HIS Energy, v.20, No.1, 74 p.
- Merrill, G. K., 1980, Preliminary Report on the Restudy of Conodonts from the Barnett Formation *in* Geology of the Llano Region, Central Texas, Guidebook to the Annual Field Trip of the West Geological Society, Publication 80-73, p 103-107.
- Meyers, W. J., 1975, Stratigraphy and diagenesis of the Lake Valley formation, Sacramento Mountains, in Pray, L. C. ,ed., A guidebook to the Mississippian shelf-edge and basin facies carbonates, Sacramento and southern New Mexico region: Dallas Geological society p. 45-65. Andres Mountains
- Montgomery, S. L., D. M. Jarvie, K. A. Bowker, and R. M. Pollastro, 2005, Mississippian Barnett Shale, Fort Worth basin, north-central Texas: Gas-shale play with multi-trillion cubic foot potential: American Association of Petroleum Geologists Bulletin, v. 89, p. 155-175.
- Papazis, P. K., 2005, Petrographic Characterization of the Barnett Shale, Fort Worth Basin, Texas: unpublished M.S. Thesis, The University of Texas at Austin, 142 p., Appendices.
- Ruppel, S. C., 1989, Summary of Mississippian stratigraphy in north and north-central Texas, *in* Mear, C. E., McNulty, C. L., and McNulty, M. E., eds., A symposium on the petroleum geology of Mississippian carbonates in north-central Texas: Fort Worth Geological Society and Texas Christian University, p. 49–55.
- Thompson, J. B., and Newton, C. R., 1987, Ecological reinterpretation of the dysaerobic Leiorhynchus fauna; Upper Devonian Genesee Black Shale, central New York: Palaios v. 2: 274-281
- Watson, W.G., 1980, Paleozoic Stratigraphy of the Llano Uplift Area: West Texas Geological Society Publication 80-73, p. 27-51.

Yurewicz, D. A., 1977, Sedimentology of Mississippian basin-facies carbonates, New Mexico and West Texas; the Rancheria Formation in Cook, H. E. and Enos, P. (eds.) Society of Economic Paleontologists and Mineralogists, Special Publication, no. 25, p. 203 - 219.



from Blakey (2004): <http://jan.ucc.nau.edu/~rcb7/340Nat.jpg>

Figure 1. Global reconstruction of North America region during the Late Mississippian. Note the proximity of the approaching Gondwana plate to the Permian Basin area.

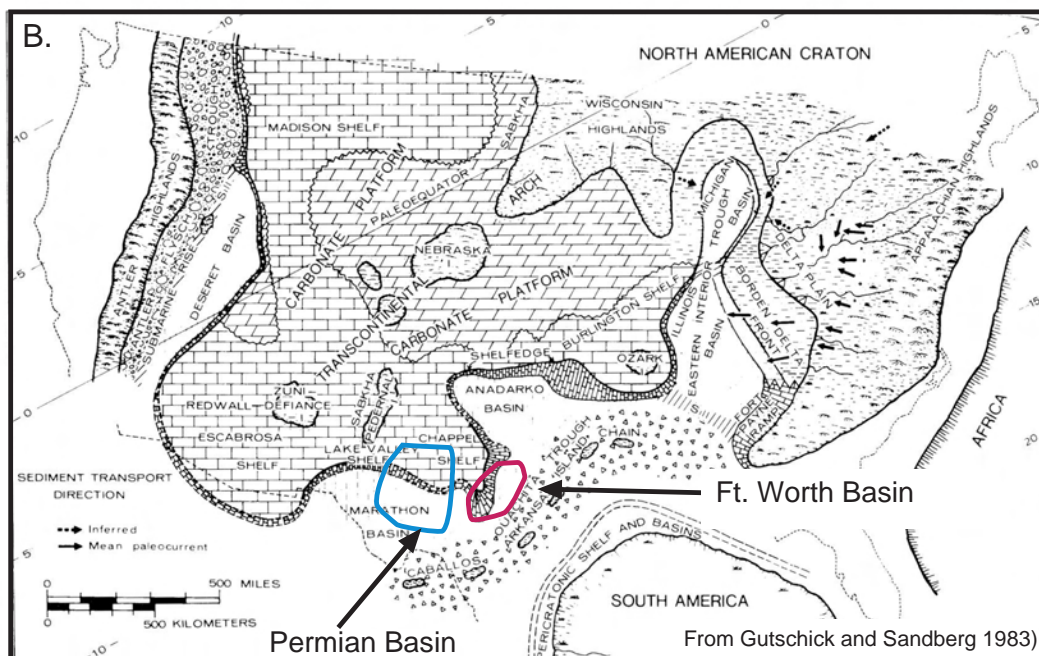
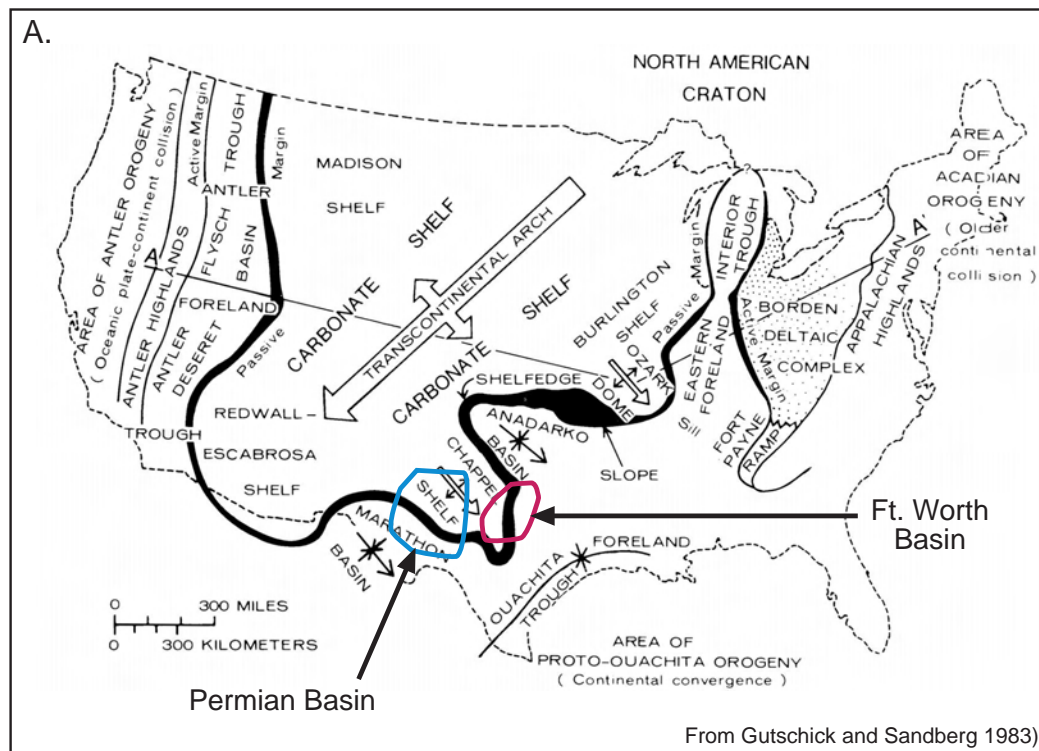
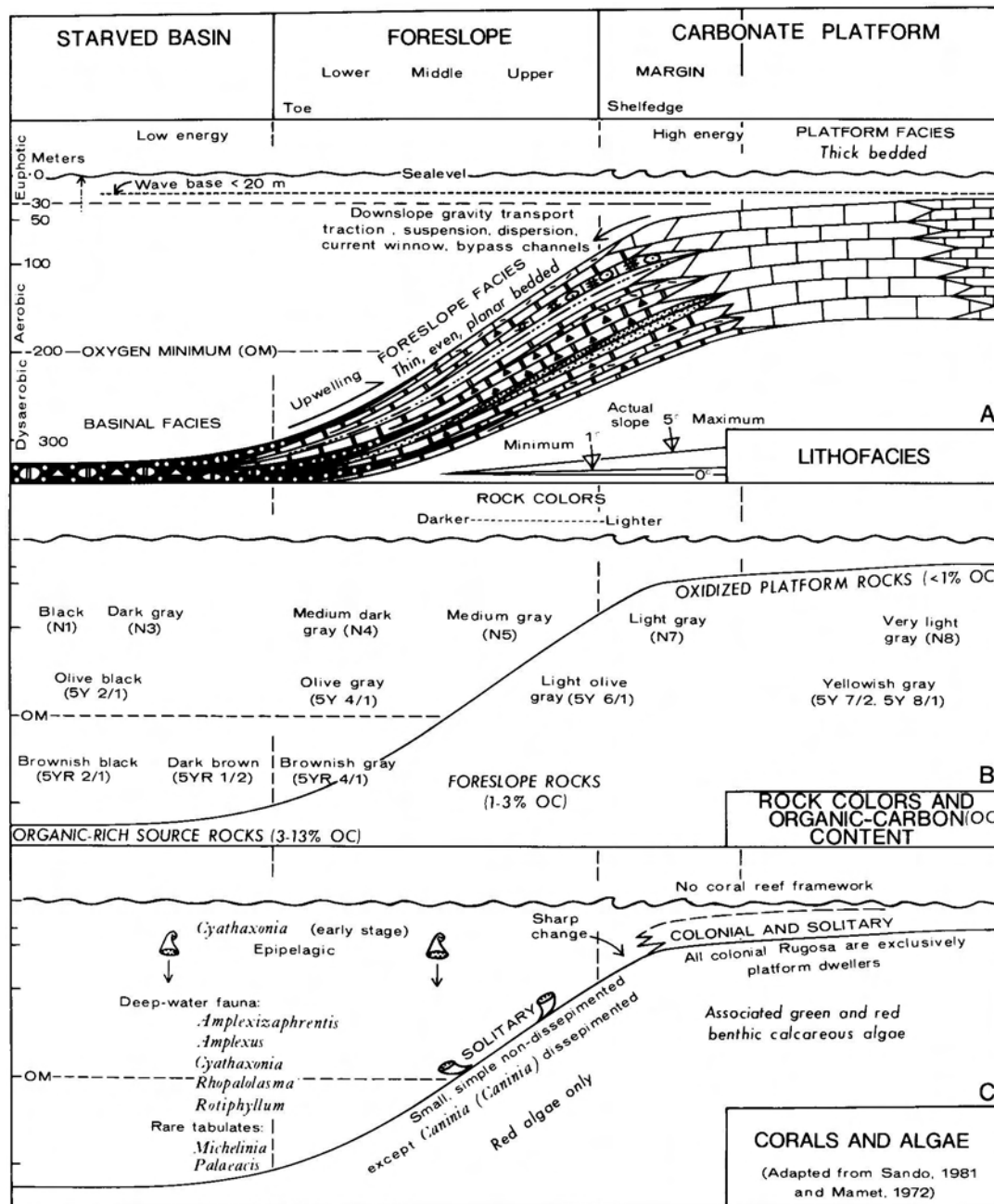
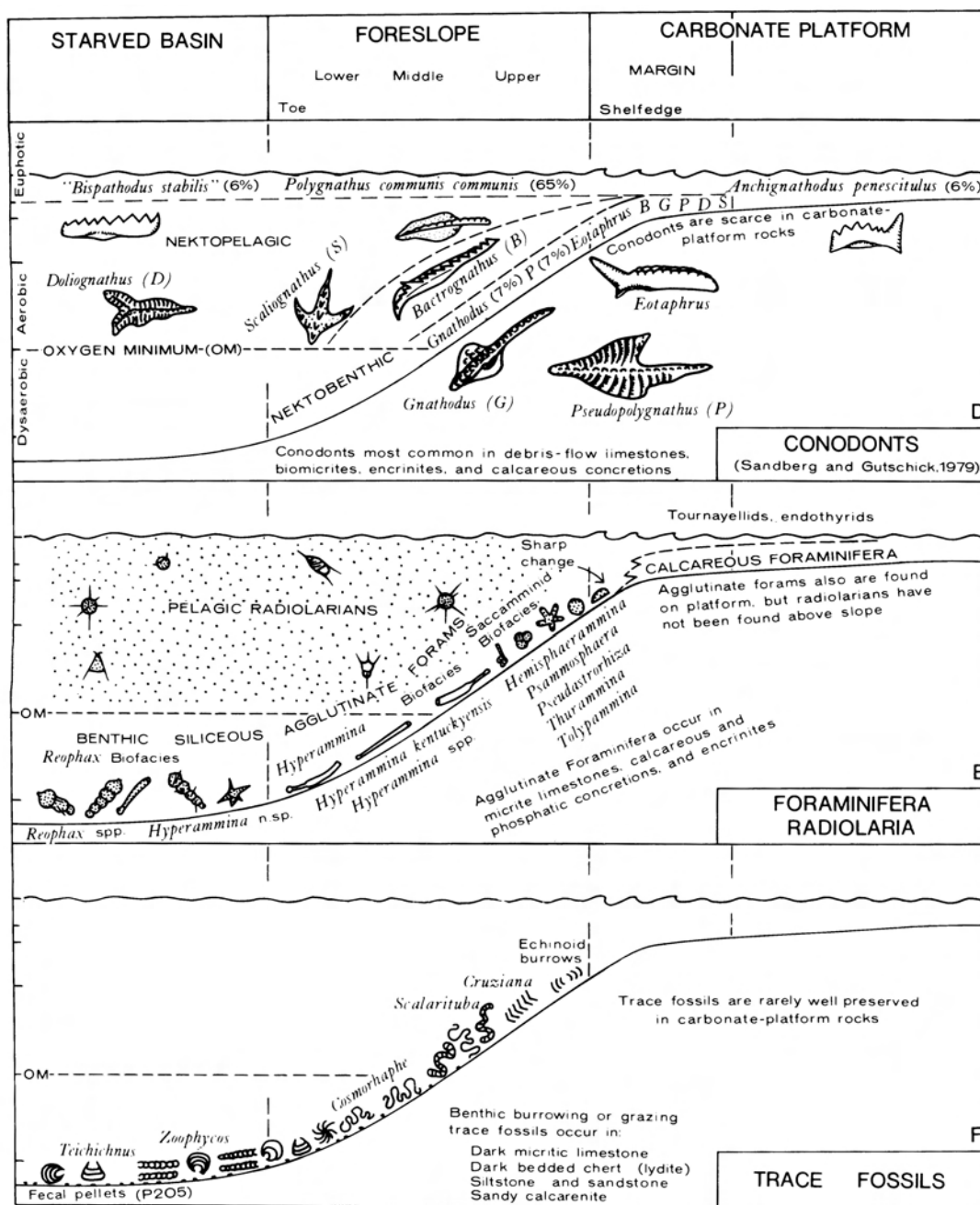


Figure 2. Paleogeography and structural features of the United States area during the Osagean (early middle) Mississippian).



From Gutschick and Sandberg 1983)

Figure 3. Models of facies and faunal development on Mississippian platforms and platform margins in western North America.



From Gutschick and Sandberg 1983)

Figure 3 (Continued). Models of facies and faunal development on Mississippian platforms and platform margins in western North America.

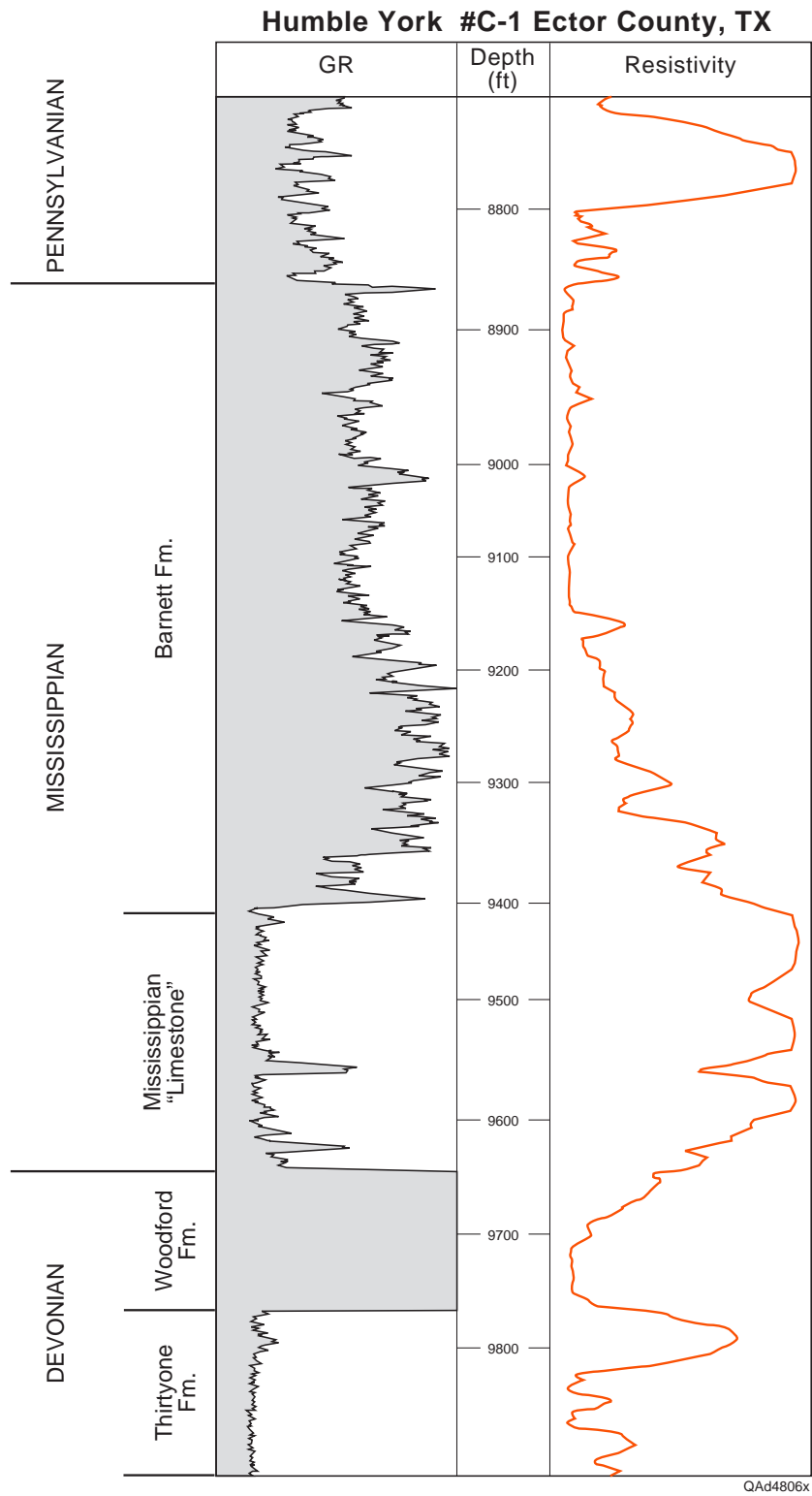


Figure 5. Typical log expression of the Mississippian section in the subsurface of the Permian Basin.

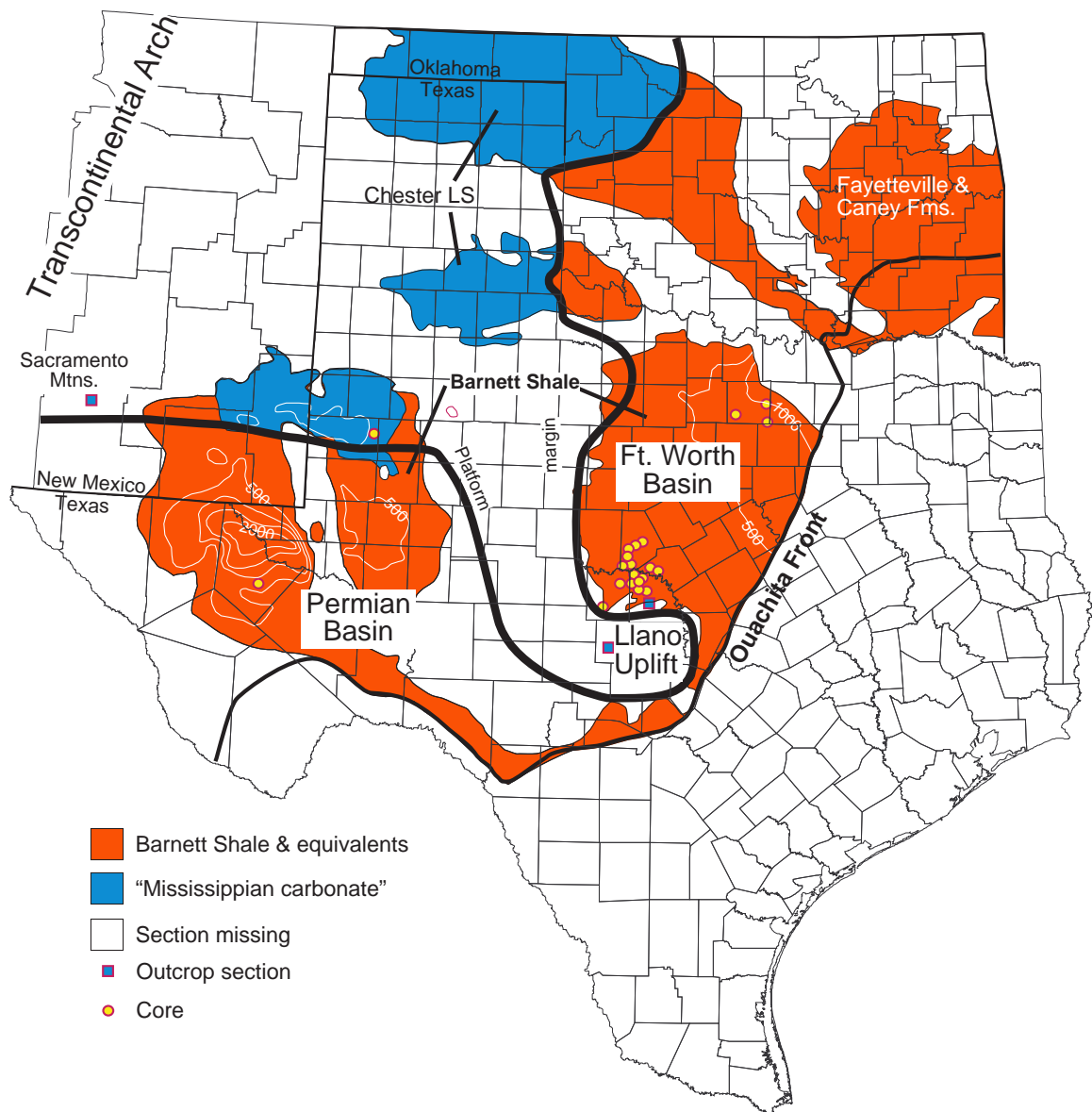


Figure 6. Distribution of Upper Mississippian rocks (outcrops and subcrops) in the southern midcontinent.

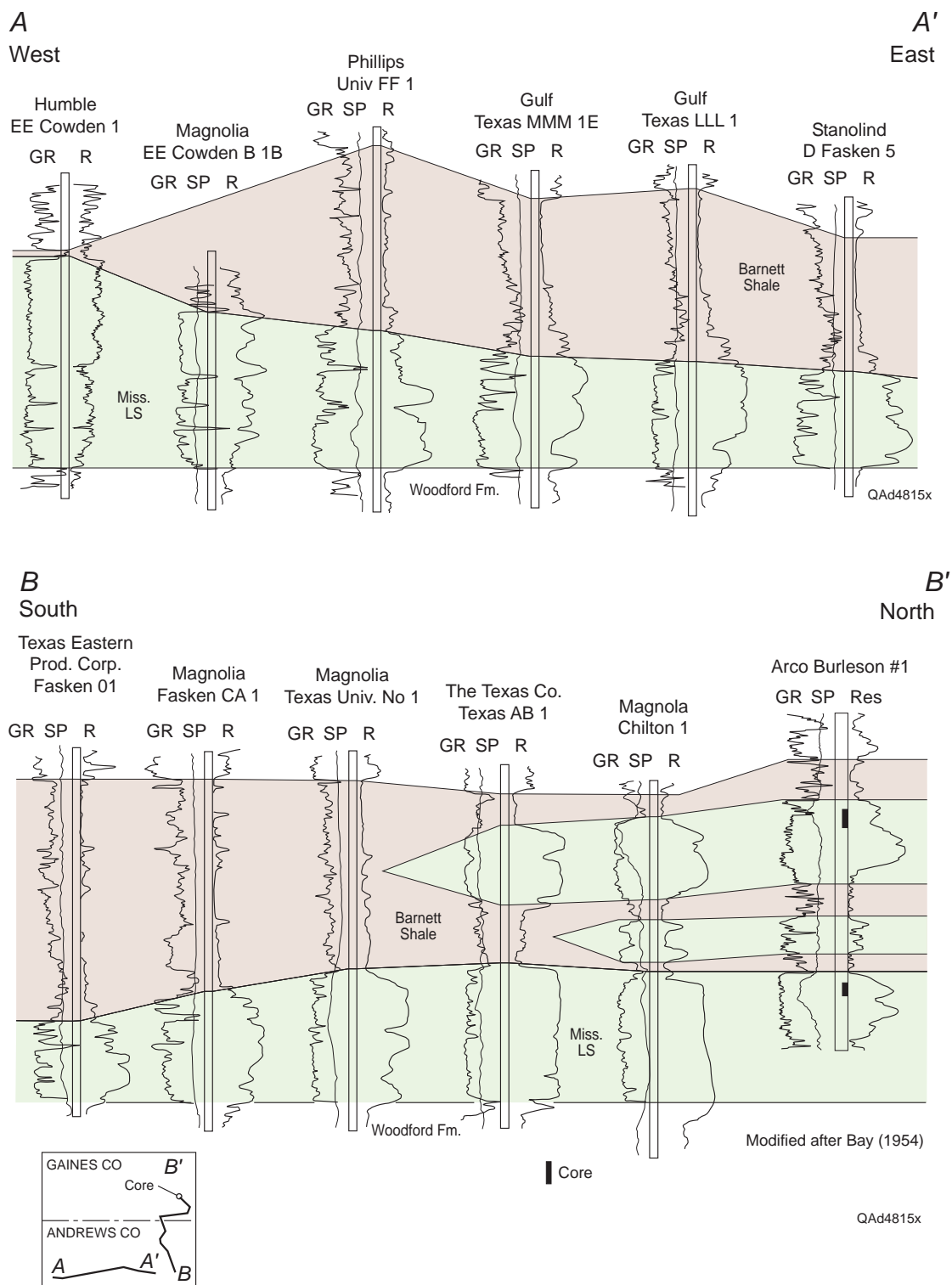


Figure 7. Cross sections showing wireline log signature and development of Barnett “shale” facies and Mississippian carbonate facies at the platform margin in the central part of the Permian basin.

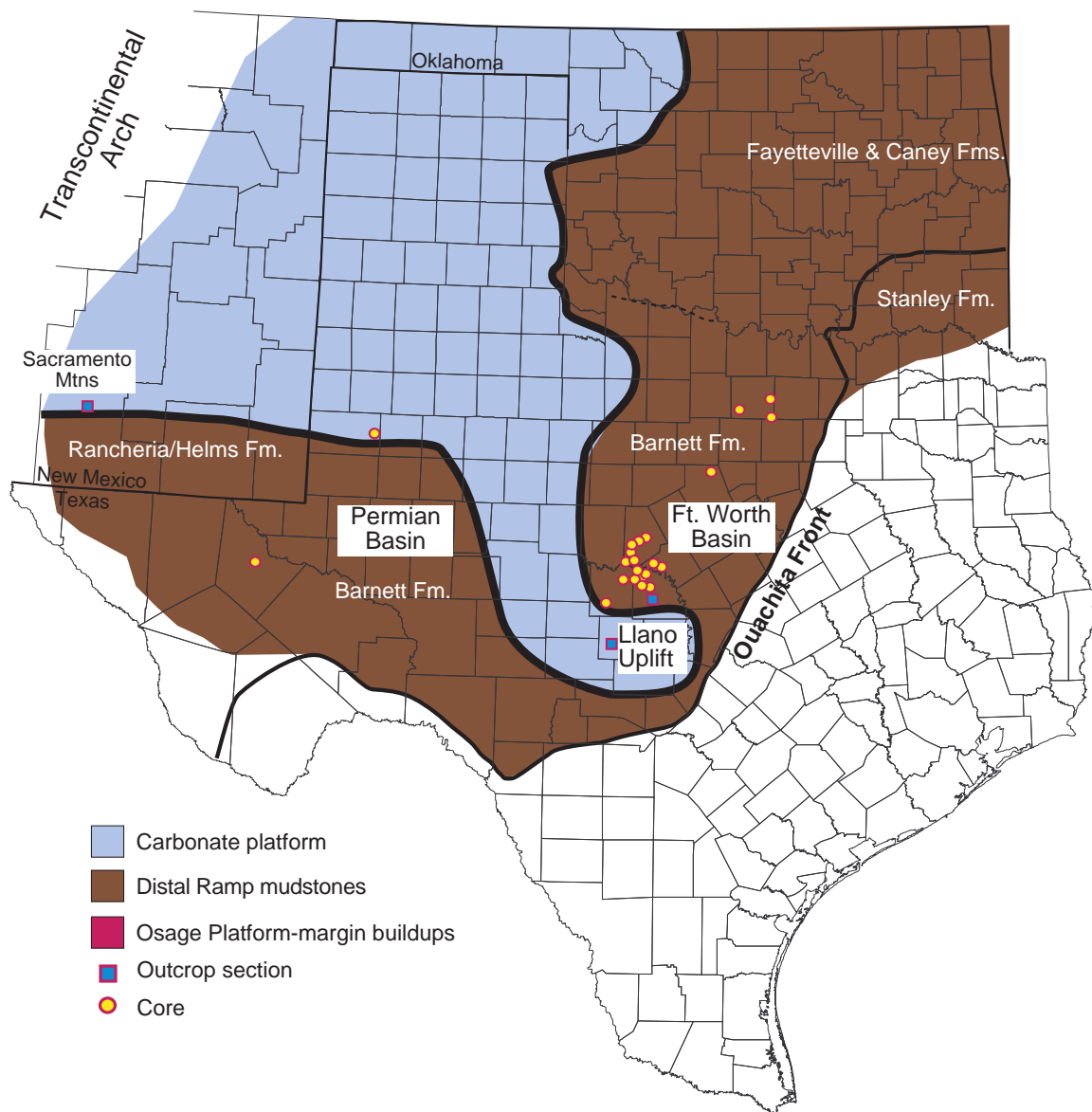


Figure 8. Paleogeography of Texas region during the Late Mississippian.

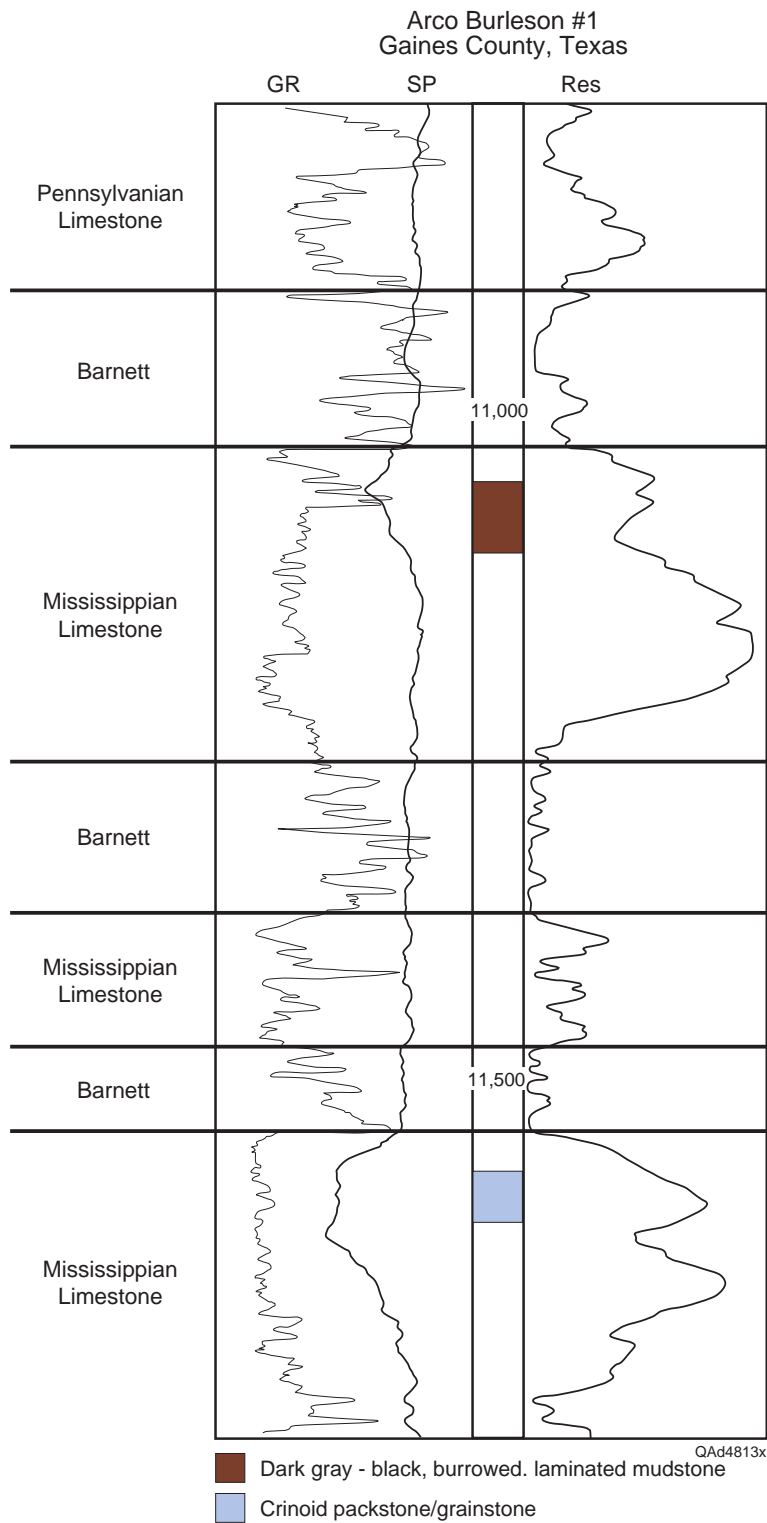


Figure 9. Typical wireline log signature from Mississippian cored well in the northern Permian Basin.

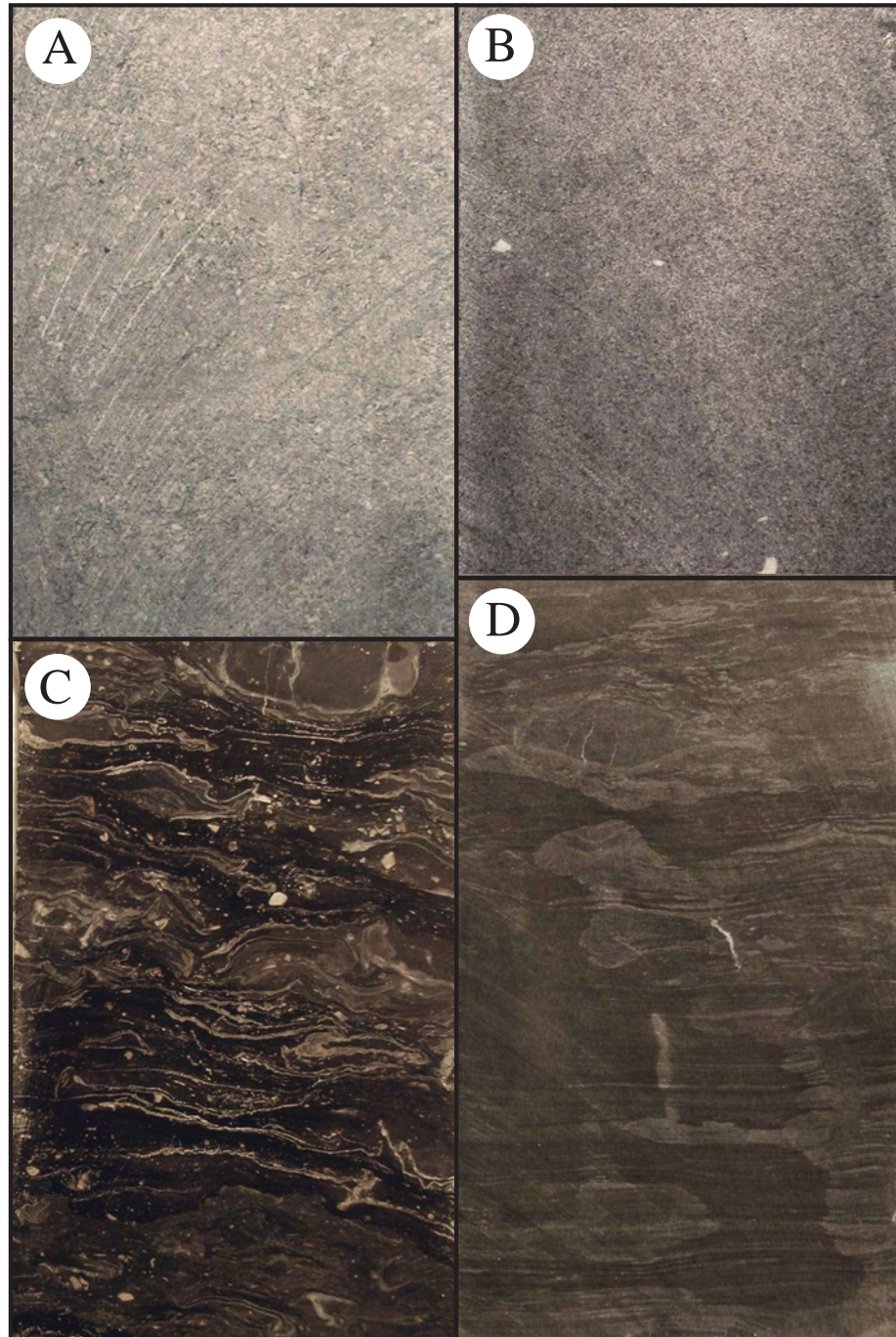


Figure 10. Slab photos of Mississippian carbonate facies succession in northern Permian Basin. Arco Burleson #1, Gaines County, Texas. A, B. Light gray-brown, coarse grained, well sorted, crinoid grainstones of the basal Mississippian. Depths: 11562 ft (A); 11598 ft (B). C. Black skeletal wackestone containing thin-walled brachiopods and crinoid debris. Depth: 11087 ft. D. Dark-gray to black, laminated, mudstone. Depth: 11106 ft. All slabs 4.5 in wide.

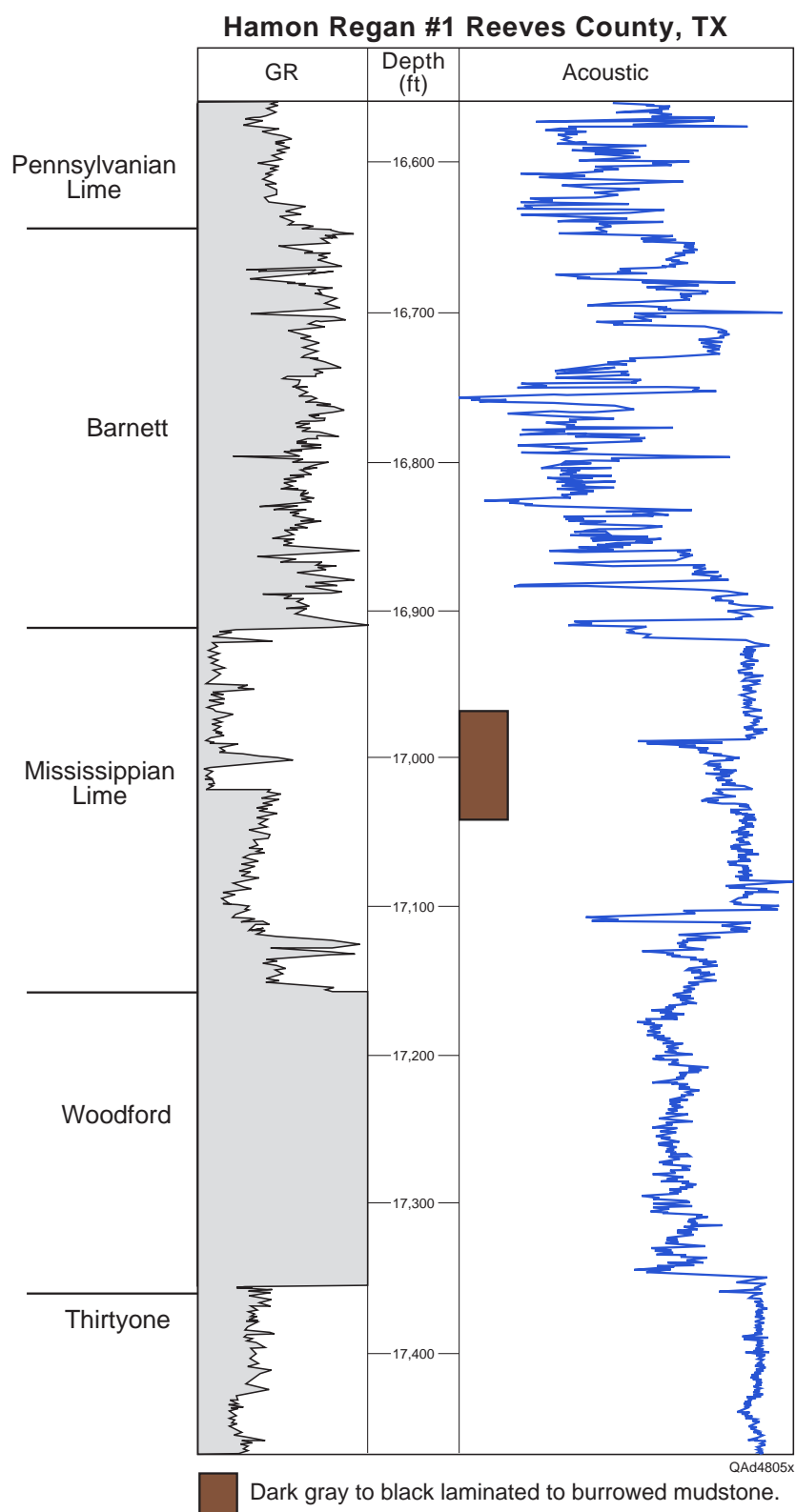


Figure 11. Typical wireline log signature from Mississippian cored well in the southern Permian Basin.

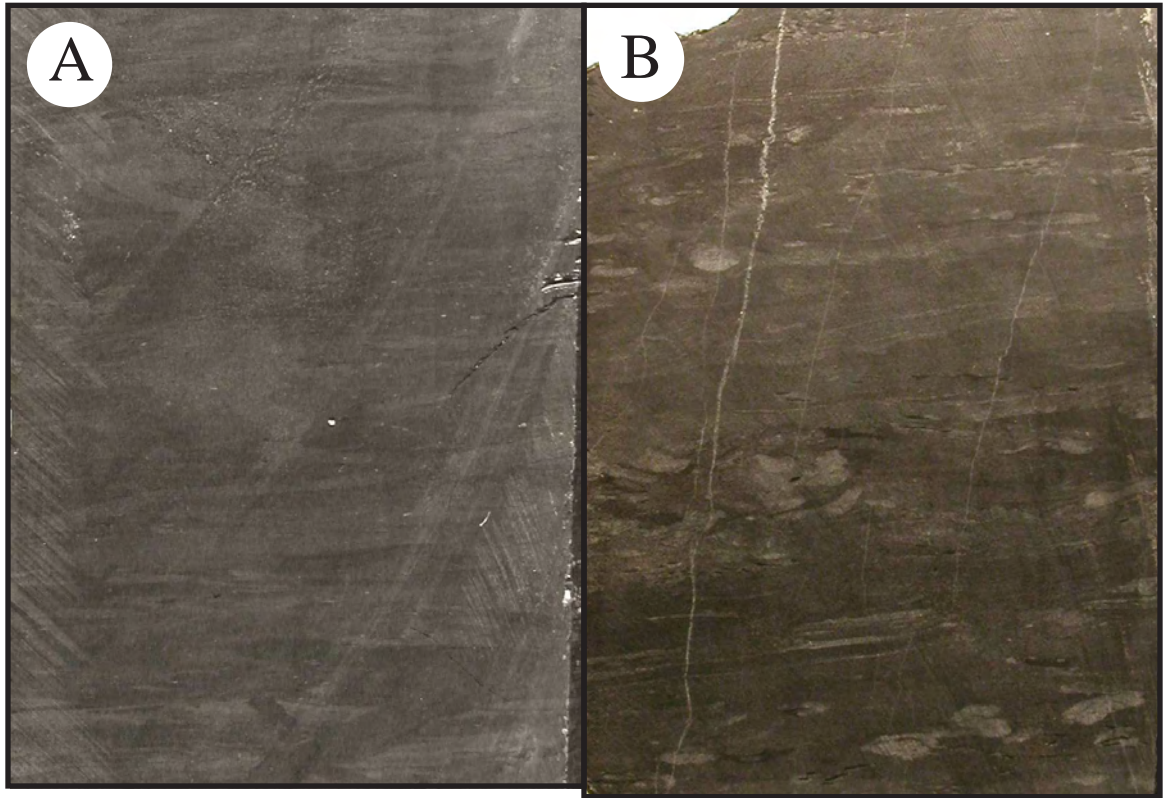


Figure 12. Slab photos of the basal Mississippian carbonate facies succession in the southern Permian Basin. Hamon Regan #1, Reeves County, Texas. A. Dark gray to black laminated to locally burrowed mudstone. Depth: 16982 ft. B. Dark gray to black burrowed mudstone. Depth: 17016 ft.

Houston Oil & Minerals Johansen MC-1
McCulloch, Co. TX

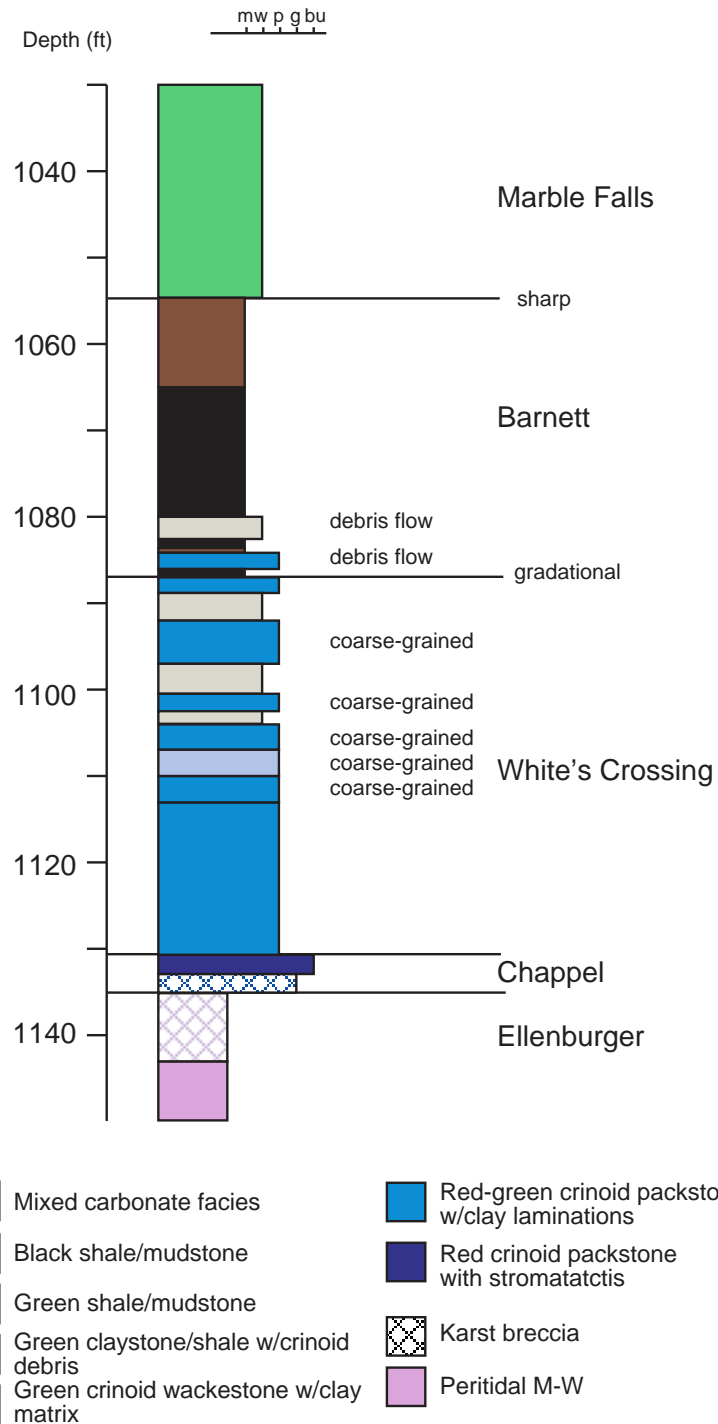


Figure 13. General facies character of Mississippian succession in the Llano Uplift area of central Texas.

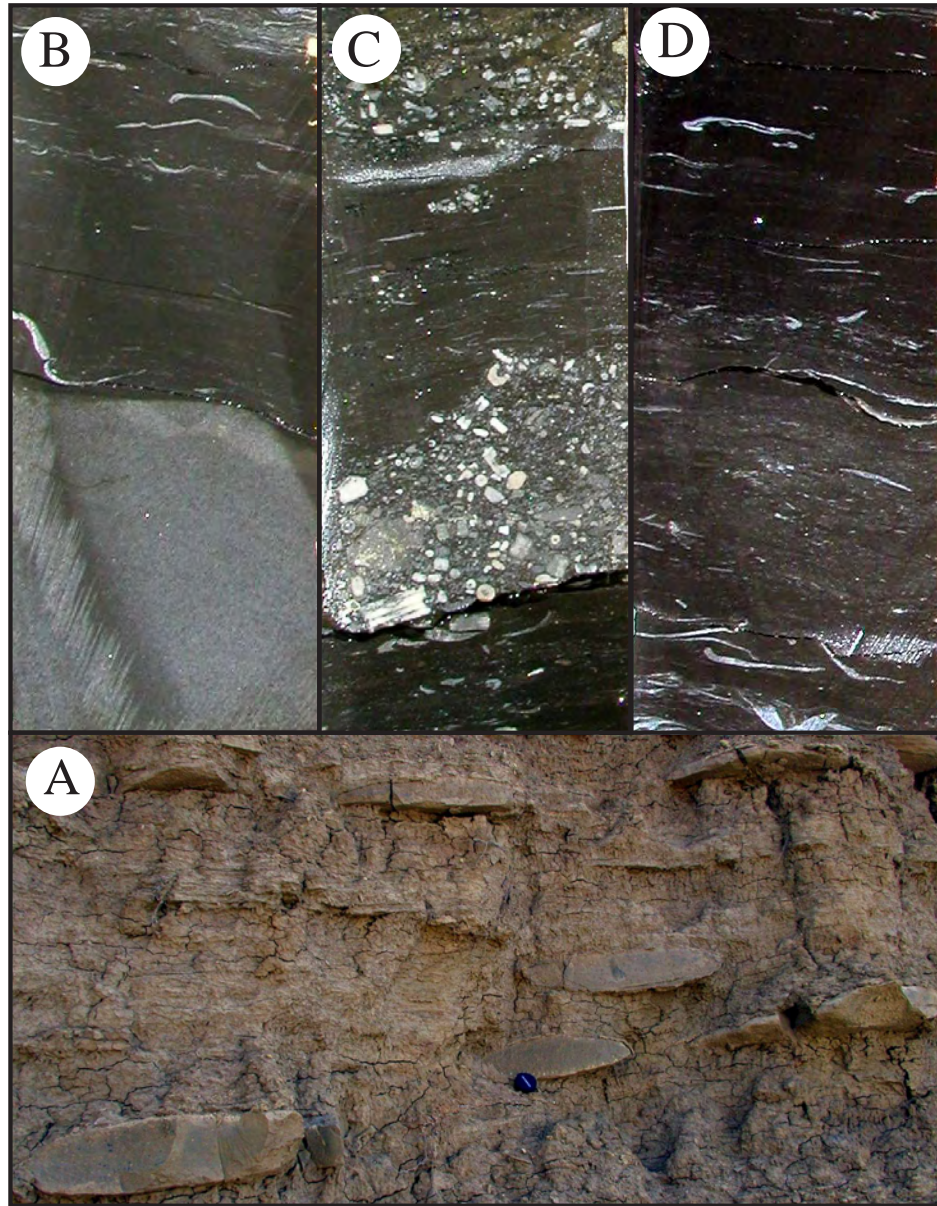


Figure 14. Slab photos of Mississippian Barnett facies succession in southwestern Ft. Worth Basin (Llano Uplift area). A. Outcrop photo showing carbonate concretion within the Barnett. Type section of Chappel Formation, San Saba County, Texas. Lens cap is 2 in diameter. B. Laminated mudstone with scattered thin-walled brachiopods overlying carbonate concretion. Depth: 1035 ft. C. Basal black mudstone with brachiopods documents in situ hemipelagic deposition, whereas overlying graded skeletal packstone to wackestone reflects debris flow. Depth: 1037 ft. D. Similar to C, showing hemipelagic sediments at bottom and top interrupted by debris flow bed. Depth: 1038 ft. B, C, and D from Houston Oil & Minerals Johanson MC-1, McCulloch County Texas.

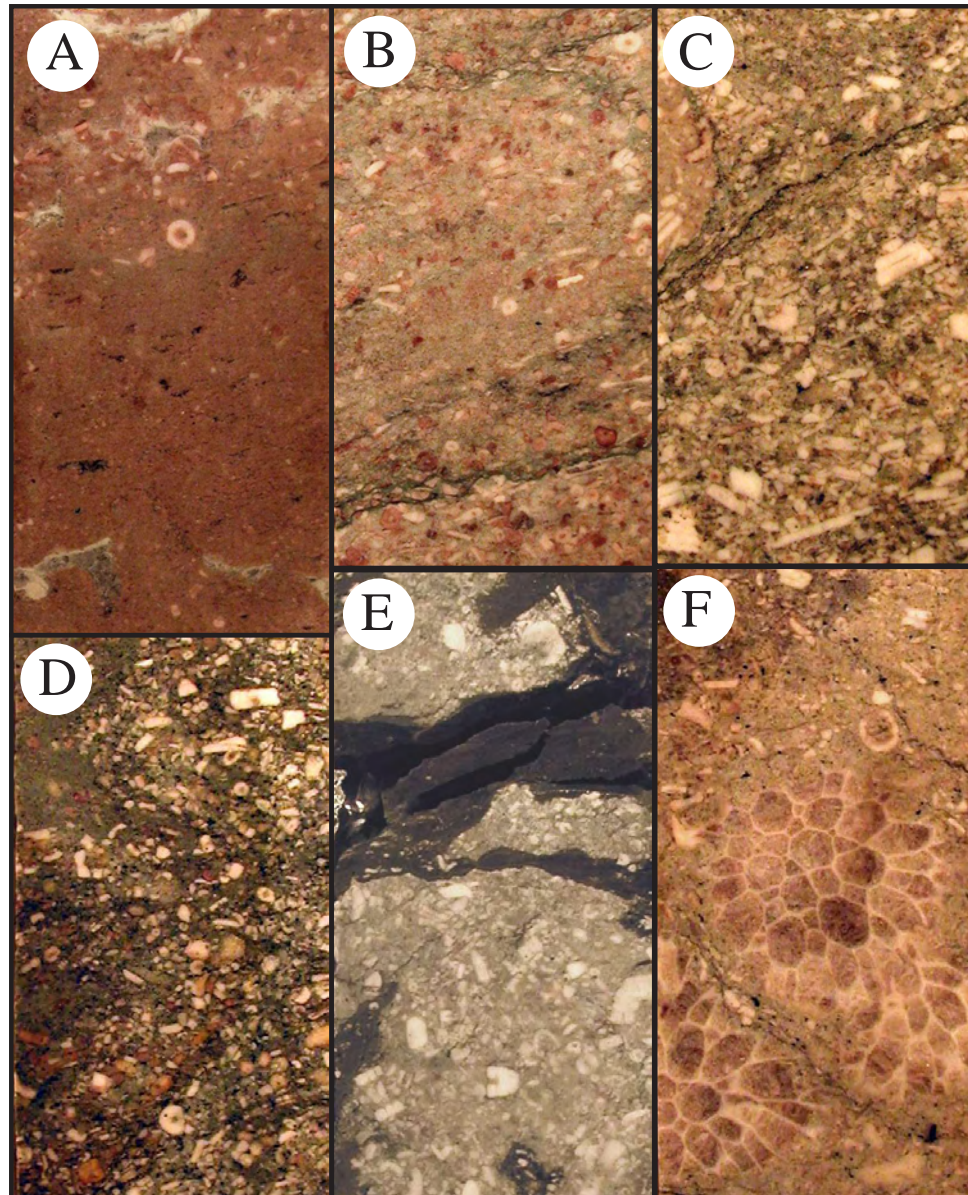


Figure 15. Slab photos of Mississippian Chappel facies succession in southwestern Ft. Worth Basin (Llano Uplift area) . Houston Oil & Minerals Johanson MC-1, McCulloch County Texas. A. Crinoidal packstone with stromatactis vugs. Basal Chappel. Depth: 1131 ft. B. Pink, poorly sorted crinoidal packstone. Depth: 1130 ft. C. Light brown, coarse-grained, poorly sorted crinoid packstone. Depth: 1110 ft. D. Brown, coarse-grained, poorly sorted crinoid packstone with green mud matrix. Depth: 1107 ft. E. Interbedded brown coarse-grained, poorly sorted crinoid packstone and black siliceous mudstone. Depth: 1098 ft. F. Coarse-grained, poorly sorted skeletal packstone. Note large corals. Depth: 1086 ft.

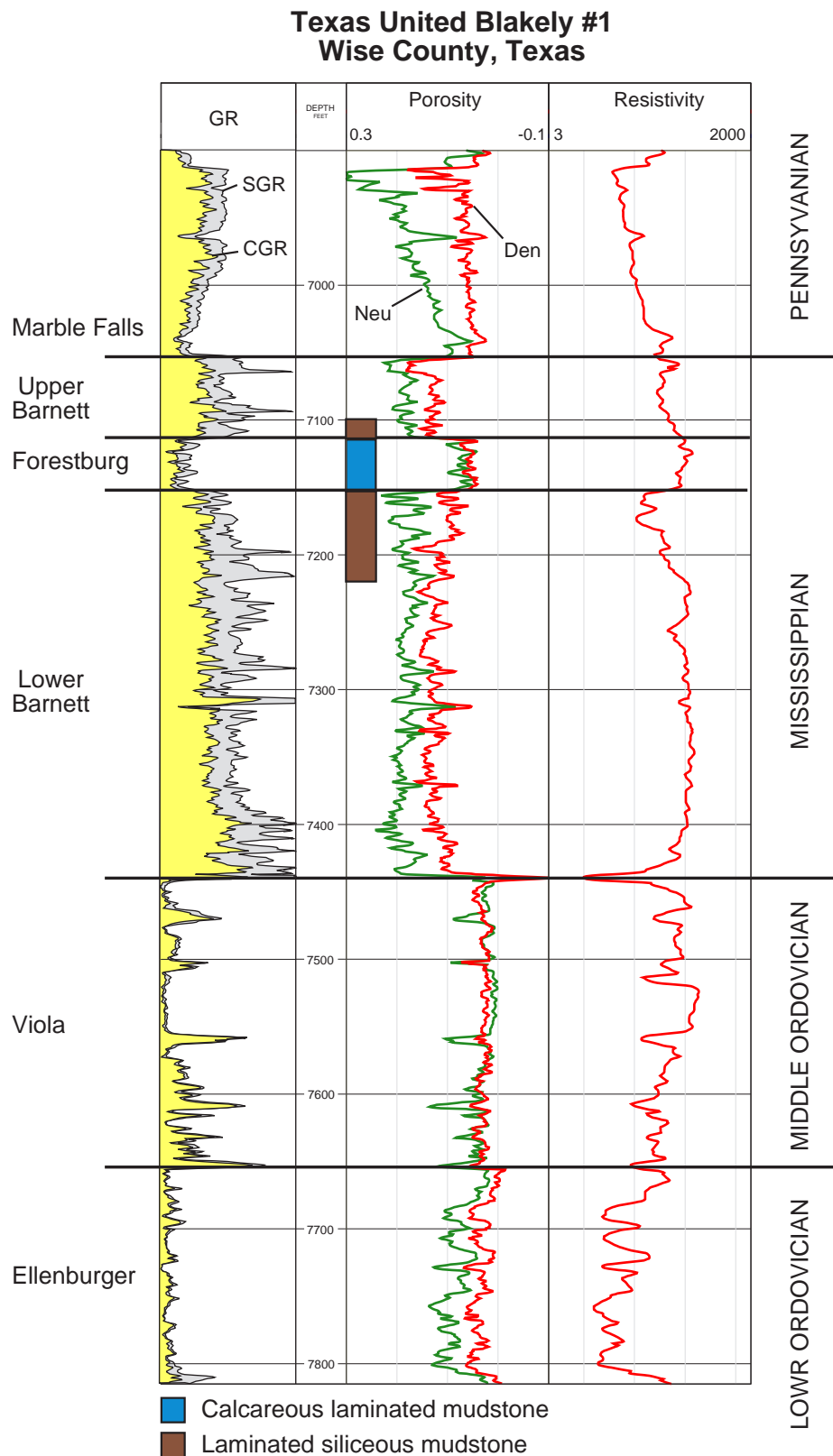


Figure 16. Typical wireline log signature of the Barnett Formation in the Ft. Worth Basin.

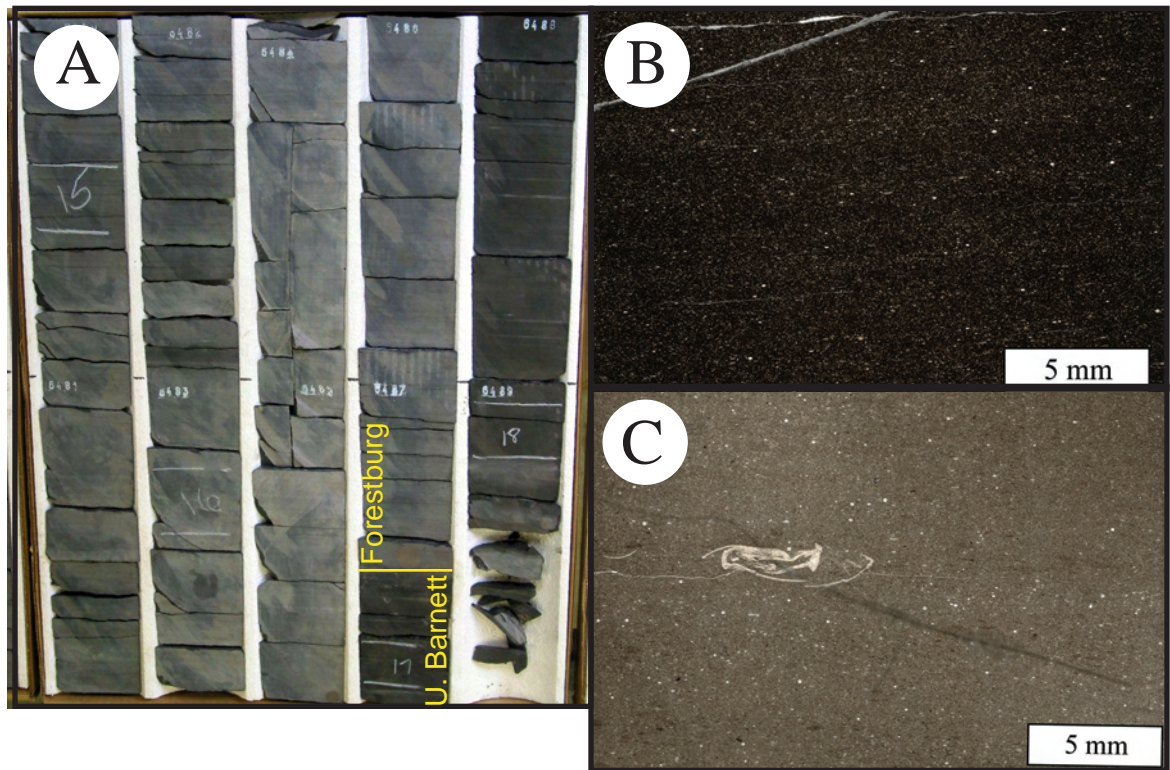


Figure 17. Photos of the Forestburg interval in central Ft. Worth Basin. A. Core slab section showing contrast in color between laminated mudstones of Forestburg and Barnett. Depth: 6480-90 ft. B. Photomicrograph of horizontally laminated mudstone with scattered silt grains. Depth: C. Photomicrograph showing graded bedding. Depth: Devon Adams SW # 7, Wise County, Texas. From Papazis (2005).

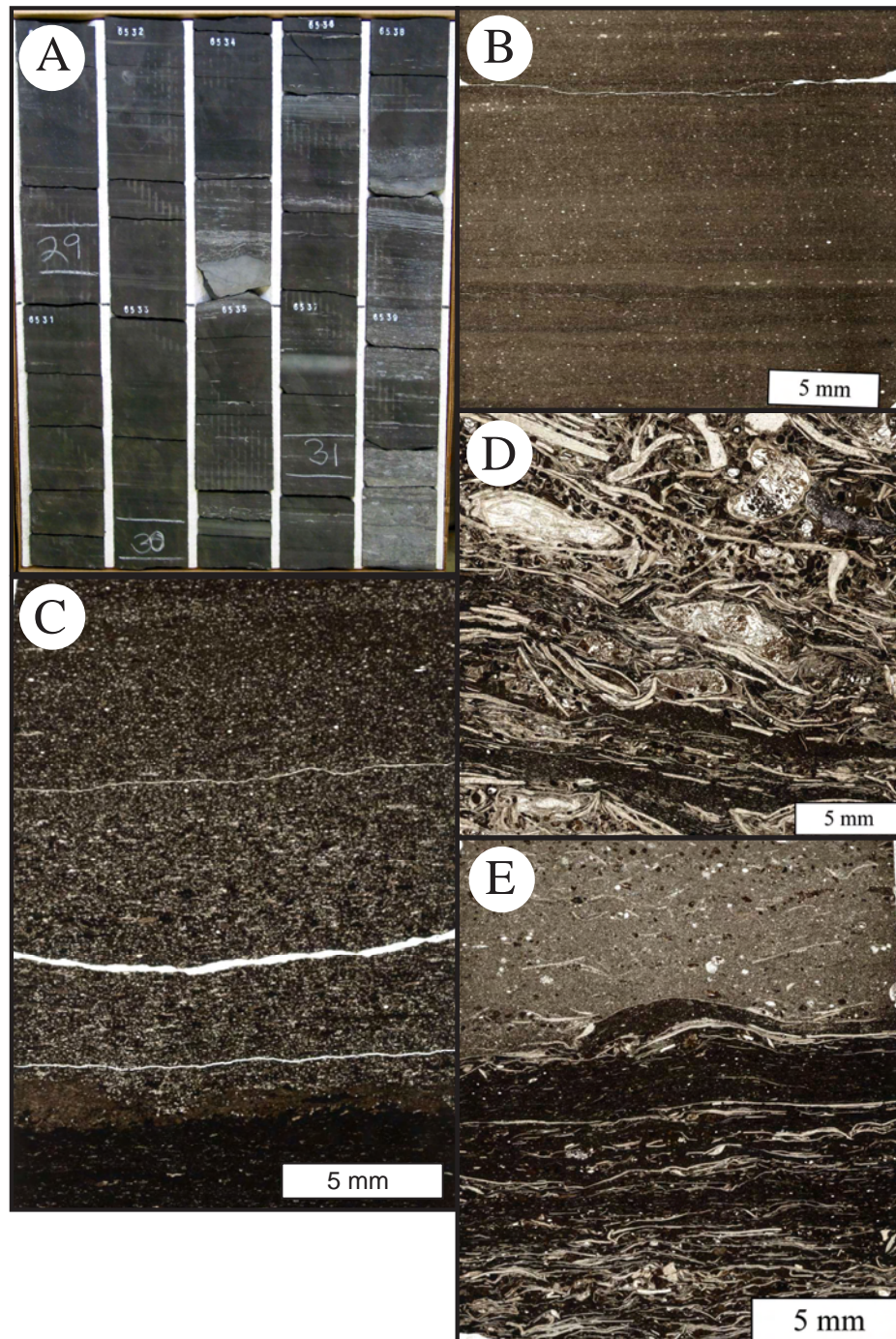


Figure 18. Photos of the Barnett Formation in central Ft. Worth Basin. A. Core slab section showing laminated mudstones and laminated skeletal wackestones of Barnett facies. Depth: 6530-40 ft. B. Photomicrograph of horizontally laminated mudstone with scattered silt grains. Depth: . C. Photomicrograph of graded bedding. Depth: . D. Photomicrograph of thin-walled deep water articulate brachiopods. Depth: . E. Skeletal wackestone (in situ deposit) overlain by skeletal calcisiltite (gravity flow deposit). Devon Adams SW # 7, Wise County, Texas. From Papazis (2005).

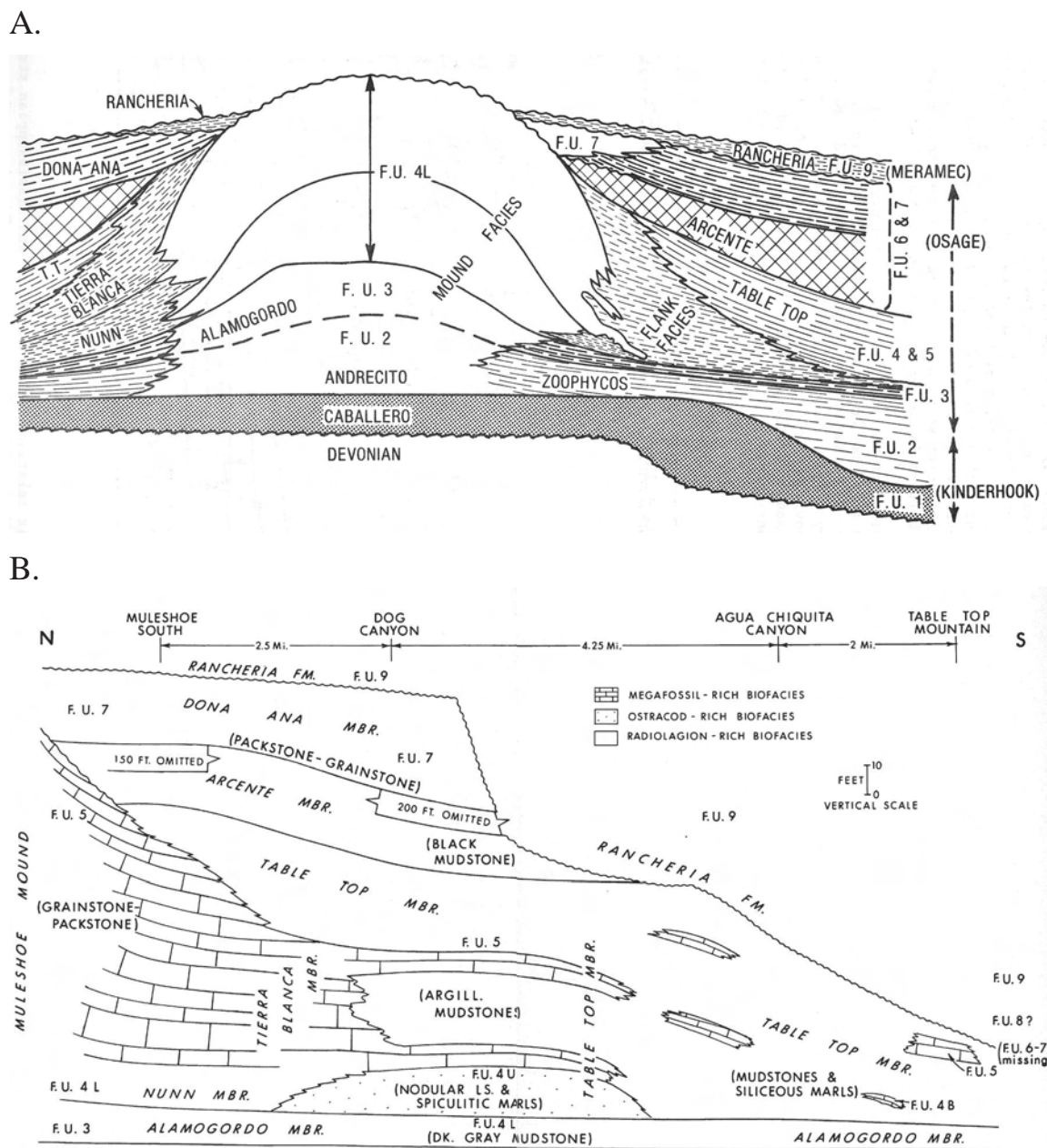
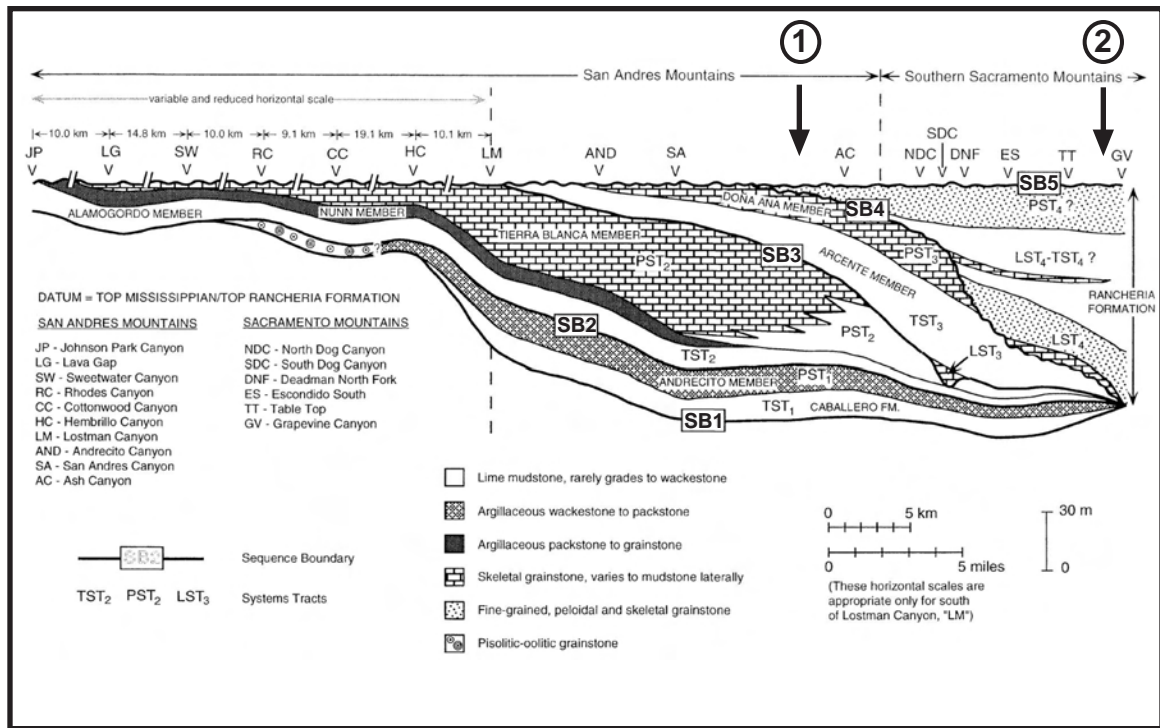


Figure 19. Stratigraphy of the Lake Valley Mississippian succession in southern New Mexico. A. Conceptual model of the architecture of the Lake Valley buildup outcrop succession. From Lane and Ormiston (1982). B. Stratigraphy and facies architecture showing downlapping Lake Valley and onlapping Rancheria. From Lane (1974).



From Bachtel and Dorobick (1998)

Figure 20. Sequence stratigraphy of the Mississippian outcrop succession in the San Andres and Sacramento Mountains of southern New Mexico. Circled numbers indicate probable depositional setting of key sections in the Permian and Ft. Worth Basins. 1. Gaines County, Texas. 2. Reeves County, Texas.

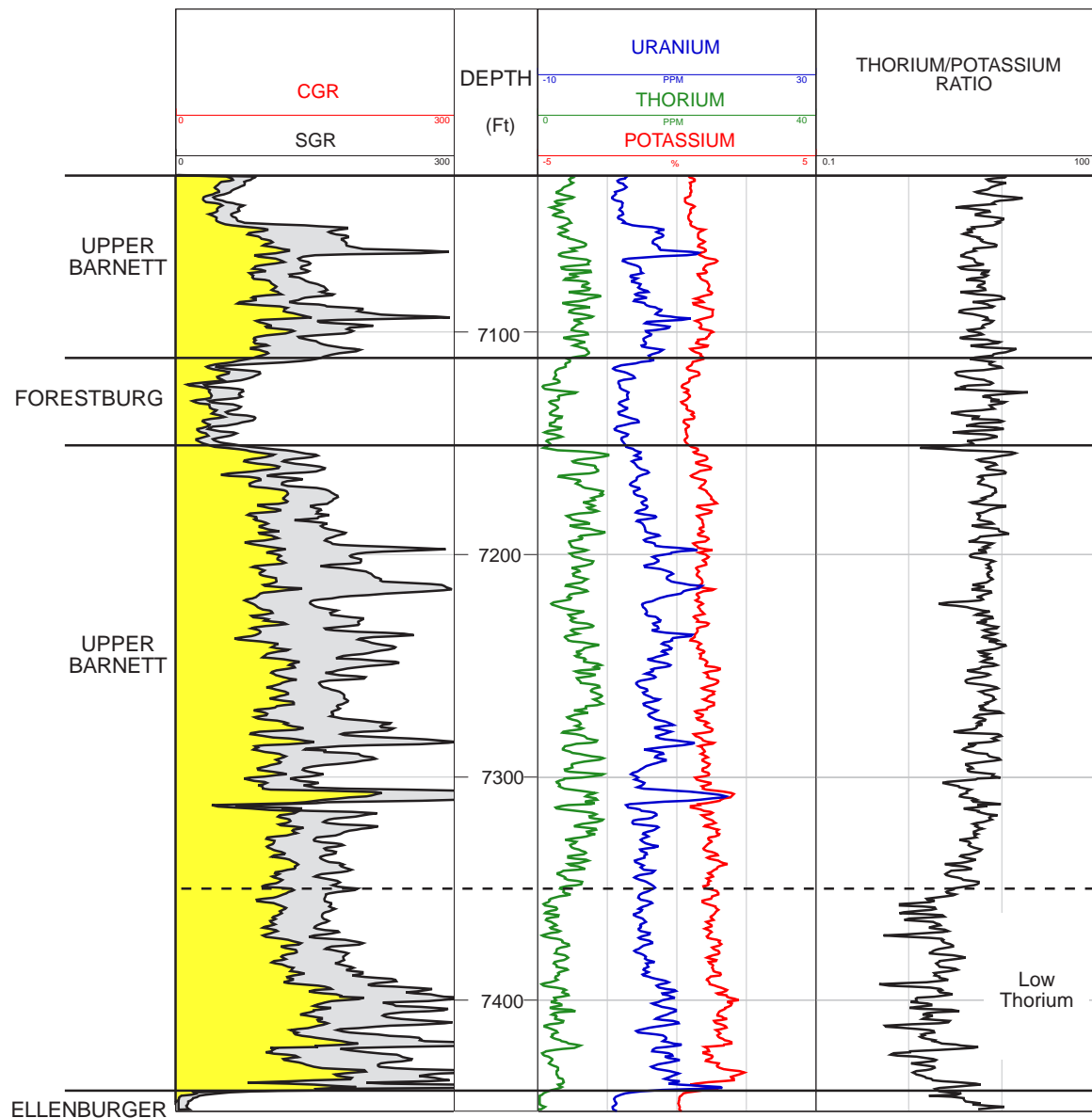


Figure 21. Spectral gamma ray log showing elemental composition of the Barnett Formation in the Texas United Blakely #1 well. Wise County, Texas. Note low thorium zone at base of lower Barnett section.

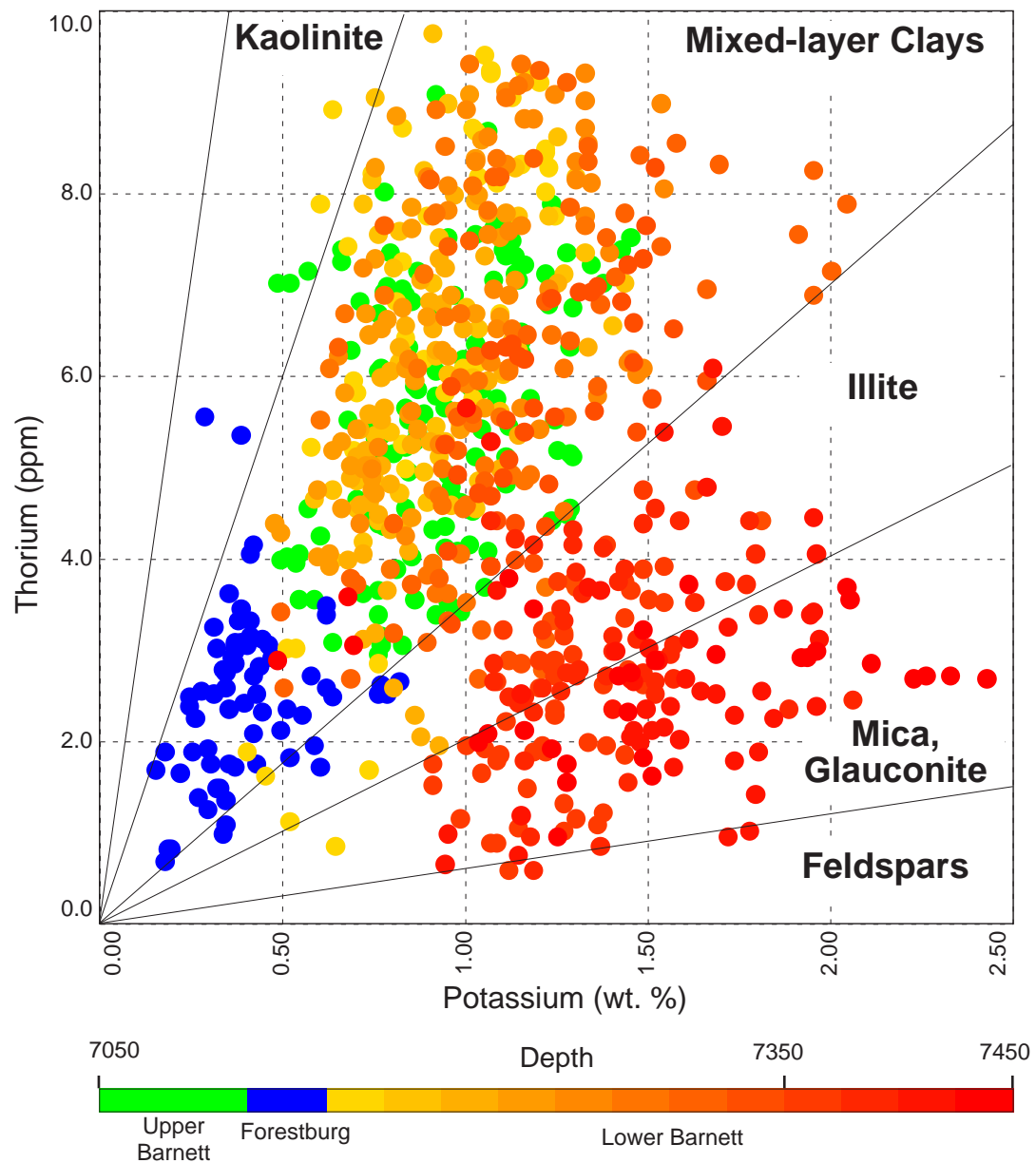


Figure 22. Crossplot of thorium and potassium content in showing systematic changes in apparent clay and feldspar composition with depth. Texas United Blakely #1, Wise County, Texas.

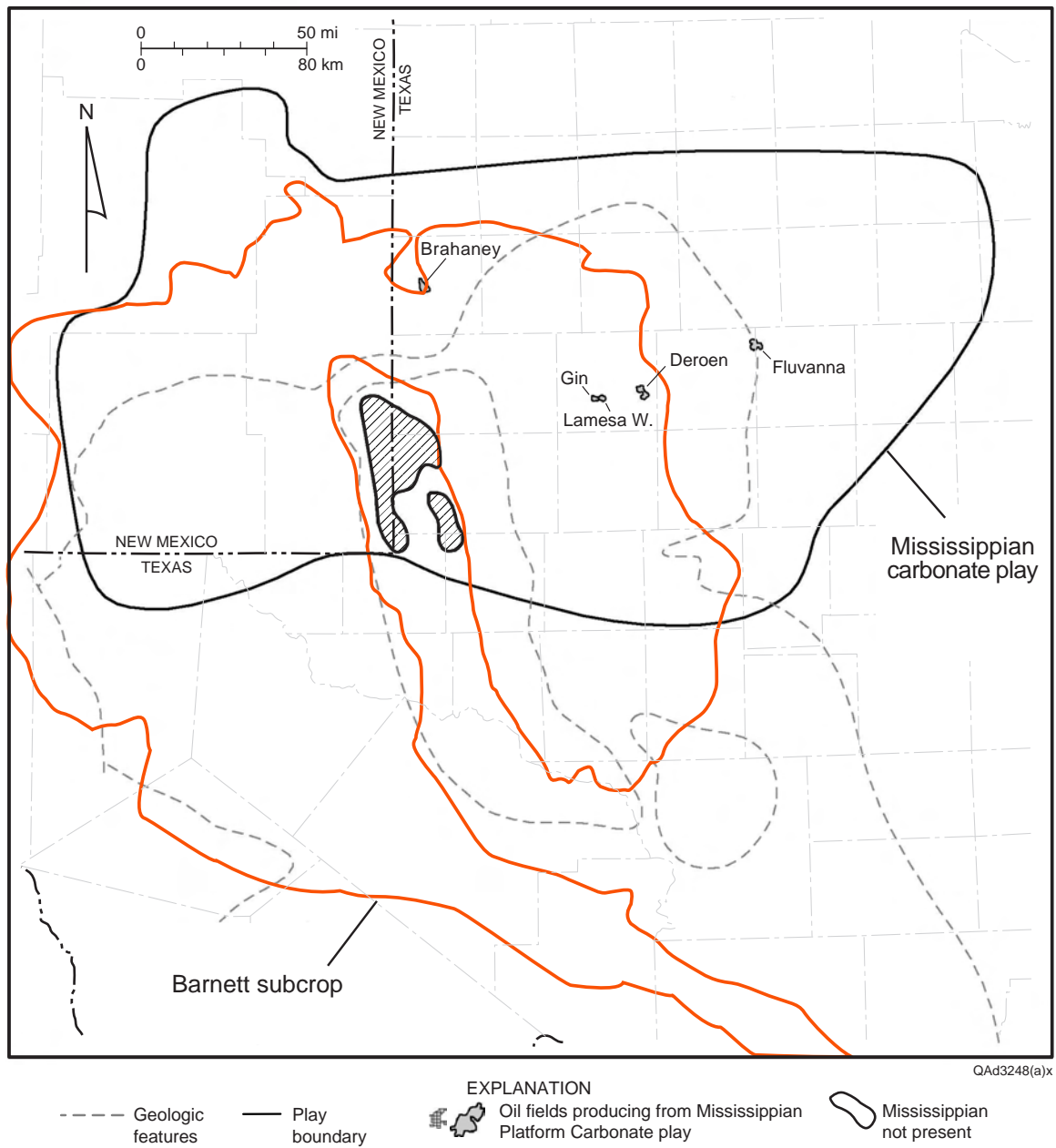


Figure 23. Map of Mississippian reservoir plays and major fields developed within the Mississippian carbonate play.

DEPOSITIONAL HISTORY OF THE MORROWAN SUCCESSION
(LOWER PENNSYLVANIAN) IN THE PERMIAN BASIN

Wayne R. Wright

Bureau of Economic Geology
Jackson School of Geosciences
The University of Texas at Austin
Austin, Texas

ABSTRACT

Morrowan-age units in the Permian Basin appear to show a “second-order” transgression from siliciclastic fluvial-deltaic to shallow-marine and subsequently to carbonate deposition. In general, Morrowan-age siliciclastics dominate deposition in the west of the Permian Basin, while carbonate deposition dominates in the east. The predominance of carbonate facies in the east is due to a lack of siliciclastic supply to that part of the basin.

Morrowan siliciclastic deposition is interpreted to have developed in a large incised-valley-fill system. An updip-to-downdip transition from fluvial and deltaic to estuarine and open-marine facies is interpreted. Excellent reservoir potential is noted in amalgamated, stacked channel systems and bayhead deltas. Significantly, these incising valleys may have served as conduits for shelf-margin bypass during periods of lowstand. It is proposed that such bypass channels may have fed sediment into the deeper basin, developing lowstand basin-floor-fan deposits. The Morrowan of the Permian Basin needs to be reassessed in terms of such a new play type, as basin-floor fans are known for their excellent reservoir potential.

This succession is overlain by Upper Morrowan carbonates. The deposition of the Upper Morrowan carbonate unit in the Permian Basin area probably indicates a switch from local tectonic to regional eustatic control as tectonism diminished in the hinterland and sediment supply from the north/northwest shut off. Overall, it appears that carbonate deposition occurred over a much larger area in the Permian Basin (Eastern Shelf and Delaware Basin) than previously documented. The presence of algal dominated bioherms and higher energy facies (ooid grainstones), augmented by fracture porosity, indicate potentially overlooked reservoir intervals. With the current explosion of interest in the shale gas systems (primarily the Barnett

but also the Smithwick), an overlying Marble Falls–type carbonate system may also hold potential as a fractured reservoir for expelled “Barnett” gas.

A new paleogeographic reconstruction for the Morrow of the Permian Basin is presented (fig. 1). In brief, from east to west, Morrowan-age carbonates are distributed over the Eastern Shelf and Llano Uplift. The depositional environment is interpreted to be a distally steepening east- and possibly southeast-facing ramp. A transition from the platform and/or ramp carbonates to more basinal carbonates and ultimately shales along the Eastern Shelf (ES), Midland Basin (MB), and Central Basin Platform (CBP) is speculated. A small number of Precambrian inliers appear to have been exposed and shed material into the basin. These and other minor topographically elevated regions are most likely rimmed by carbonates. Farther west, multiple amalgamated incised-valley systems are interpreted in the Delaware Basin, some of which may feed deeper water basin-floor fans. The Pedernal Uplift provides much of the sediment input and appears linked to the north with other channel systems feeding the Midcontinent. See the Paleogeographic Summary for a more detailed discussion of this paleogeography.

INTRODUCTION

This report discusses the styles of deposition and facies development of Morrowan-age sediments, concluding with a new paleogeography for the Morrowan Permian Basin (see Paleogeographic Summary). Morrowan deposition is discussed in two sections, one dealing with siliciclastic deposits and the other with deposits having a carbonate affinity. In each section a regional model for facies patterns and deposition is proposed. Data from areas adjacent to the Permian Basin are used as analogs for facies that are predicted to be present within the study area. More localized studies will be used to illustrate certain key aspects (for example, facies type, reservoir quality). However, an initial introduction to the area, placing it in a global perspective, will first be presented.

GLOBAL TECTONIC SETTING

Morrowan-age sediments in the Permian Basin are characterized as being deposited at a near-equatorial (10–15° south) position during the early stages of icehouse high-amplitude, high-frequency eustatic sea-level fluctuations, in an area undergoing initial tectonic activity of both uplift and subsidence related to the Ouachita-Marathon Orogeny and the birth of the greater

ancestral Rocky Mountains. Figures 2 and 3 illustrate two of many interpretations as to the position of Texas (in orange in fig. 2) relative to the major tectonic plates and the equator at the beginning of the Pennsylvanian (circa Morrowan age). The Pennsylvanian Epoch is characterized by increasing restriction caused by plate drift resulting in diminishing sea masses between Laurussia/Eurasia and Gondwana as the Pangean supercontinent was forming. This closure of a possible subequatorial seaway at the site of present-day Texas and the Permian Basin has profound implications on establishing and understanding the paleogeography and facies distribution of the region. However, currently too much controversy exists between Pennsylvanian paleogeographic plate reconstructions to be useful on the basin scale (Van der Voo and Torsvik, 2001; Saltzman, 2003; Torsvik and Cocks, 2004).

Figure 3 illustrates the potential dramatic changes in facies relationships and amount of marine influence in the area of the Permian Basin after closing of a proposed seaway by Morrowan time. Although detail is lacking from the Permian Basin area (red star in fig. 3), it is important to note that a global understanding of the region is required to make reasonable detailed geologic models of the area. However, the detailed data (core descriptions, facies interpretations, and log data) presented in this study must be incorporated into any paleogeographic and plate tectonic model for the Permian Basin and will probably result in substantial changes to current reconstructions.

REGIONAL TECTONIC SETTING AND FACIES DISTRIBUTION

Figure 4 illustrates the outline of the Permian Basin used in this study and the major geologic features commonly associated with the basin. Note, however, that not all the features developed simultaneously, and most were only incipient at Morrowan time. Figure 4 allows one to compare the Permian Basin with the regional paleogeography. Figures 5 and 6 depict previous facies distribution and uplift and subsidence patterns for Morrowan-age sediments in the Permian Basin and surrounding areas. The revised Permian Basin paleogeography presented in figure 1 is an attempt to incorporate previous interpretations where valid, in light of new and regionally synthesized data presented in this chapter.

Within the Permian Basin study area, facies appear largely restricted to depositional environments such as transitional zones (for example, lagoonal, deltaic), open-marine coastlines, clastic shelves, and minor carbonate platform to shelfal areas. An area denoted as a starved basin

is also prominent and is centered on the New Mexico–Texas border in Lea and Winkler Counties, respectively (fig. 5). However, seismic, well, and cross-sectional information indicates “thick” intervals of Morrowan-age sediments across the entire Delaware and Midland Basins (for example, Yang and Dorobek, 1995), although many authors would consider the basin centers to be largely starved of sediment. The most notable feature of the map by Ye and others (1996) is the lack of Morrowan-age sediments in most of the Permian Basin. In general, the Morrowan paleogeography is indicative of siliciclastic deposition in the northwest and north and carbonate deposition in the southeast.

The regional tectonic framework of Kluth (1986) for Mississippian to Morrowan time is generalized but indicates uplift (≤ 50 m/Ma) near or on the Central Basin Platform and the margins of the larger Permian Basin. Most data indicate no Morrowan-age units on the Central Basin Platform (fig. 6). The absence of sediments is commonly interpreted as a product of deep weathering over uplifted blocks; however, the data do not preclude the possibility of nondeposition in those regions.

It is quite obvious that the uplift and subsidence areas in figure 6 do not match the facies distribution outlined in figure 5 in the greater Permian Basin area. In many instances areas of net subsidence in figure 6 appear to correlate with areas of nondeposition (white) in figure 5. Correcting inconsistencies in the regional paleogeography of the Permian Basin and outlining more detailed depositional patterns were among the major goals of this chapter. The updated Permian Basin paleogeography previously presented is discussed within the Paleogeographic summary.

AGE RELATIONSHIPS

Correlation problems exist with establishing the true depositional nature of Morrowan-age units. Many studies are of local scale, lacking robust age control and regional perspective. Different interpretations and inconsistencies exist in defining what units and formations are actually Morrowan in age (fig. 7). In this study the upper Barnett Formation is considered laterally equivalent to lower Morrow sediments (fig. 7). This interpretation is based on paleontological data, regional correlations, and the transgressive nature of the Barnett Formation. Figure 7 illustrates the two contrasting interpretations of where the Mississippian/Pennsylvanian boundary can be placed noted by the large and small arrows. The interpretation in this study (large arrow) contrasts with many interpretations placing the base Morrowan-age units on top of

the Barnett Formation in an angularly unconformable relationship (figs. 8 and 9). Many authors contend that all Pennsylvanian sediments are in an unconformable relationship with Mississippian and/or older units (for example, Mazzullo, 1999; Roberts and Kohl, 1999), but conformable relationships have also been described (Harrell and Anonymous, 2003; Harrell and others, 2004).

SILICICLASTIC MORROWAN DEPOSITION

- **Broad Approach:** Observations from more regional studies are used as a reference framework for interpreting and integrating studies in the Permian Basin. Permian Basin data are presented and integrated into this overall depositional model.
- **General Depositional Setting:** Incised fluvial valley-fill system, grading from an updip fluvial system to downdip deltaic and estuarine conditions. The drainage system is largely sourced from the northwest. The adoption of a fluvial to estuarine facies distribution model over a standard open-marine layer-cake model will allow much more accurate prediction of compartmentalized reservoirs.
- **Reservoir Potential:** Updip fluvial amalgamated, stacked channels provide the best reservoir potential. In the transitional facies toward the downdip estuarine section, the fluvial channels are separated by lower quality reservoir estuarine sands, and reservoir quality, noticeably permeability, is decreased in these thinner, more marine facies. In the downdip facies tract (estuarine), reservoir facies are sparsely developed; the fluvial channels are narrow, disconnected, and thin, and they are separated by thick estuarine basin shales. However, bayfill deltas provide excellent local potential.
- **Diagenesis:** Dissolution of detrital grains and authigenic clays generating secondary porosity and permeability is very important to development of good reservoir quality, especially in the more estuarine to marine sands. The Middle Morrow sandstones are more compositionally variable and appear to have the best production.
- **Climate:** The Morrowan was a time of expansive ice-sheet development, and such times are typified by highly fluctuating sea level, which plays a role in controlling cyclicity and facies stacking patterns. Such highly fluctuating sea levels generally result in thinner, higher frequency cycles.

Before a discussion of the sediments and facies can be undertaken, the organization used for dividing the Morrowan-age siliciclastic units must be discussed. The convention within the petroleum industry is to deem Morrowan-age units as Morrow Formation siliciclastics with subsidiary carbonates. Within the Permian Basin (Delaware Basin, in particular) the Morrow Formation is generally separated into three units (figs. 8, 9). These units are termed the Lower, Middle, and Upper. Only the Lower and Middle Morrow “unit” facies are siliciclastic. Note that on the stratigraphic column in figures 8 and 9 the authors consider the Mississippian and Pennsylvanian contact as unconformable. The unconformable nature of the contact is not tenable throughout the entire Permian Basin and is largely a localized occurrence. The tripartite division of the Morrow in figure 8 is not universally accepted, and genetic divisions based on sequence stratigraphy have recently been proposed. The nomenclature used for dividing the Morrowan-age sediments and the Morrow Formation in the Delaware Basin and Northwest Shelf was proposed in isolation from other parts of the Permian Basin and the region.

Broadly, the Morrowan-age units in the Delaware Basin and Northwest Shelf of the Permian Basin appear to show a “second-order” transgression from siliciclastic fluvial-deltaic to shallow-marine and subsequently to carbonate deposition. Higher order cyclicity is evident, but regional correlation is not possible on the basis of the present dataset. The following section summarizes the depositional model for the Morrowan-age section in the Permian Basin area.

Regional Studies—Depositional Model

The proposed depositional model for the Morrowan-age section of the western Permian Basin is largely based on two regional studies outside the Permian Basin. In summary, siliciclastic deposition of the Morrowan-age units (Lower and Middle Morrow, figs. 8, 9) occurred in a large incised valley-fill system under icehouse conditions. Fluvial, deltaic, estuarine, and open-marine facies compose the valley-fill and intervalley sediments in updip, transitional, and downdip facies tracts.

Published literature on recent regional- and local-scale analysis of the depositional environments in a sequence-stratigraphic context for Morrowan-age sediments (generally Morrow Formation siliciclastics) has largely been restricted to occurrences outside of Texas. Bowen and Weimer (2003, 2004) established the regional sequence-stratigraphic framework and reservoir geology in western Kansas and eastern Colorado. As with studies in the Permian Basin,

the Morrow Formation is considered Early Pennsylvanian in age with an angular unconformity, the result of a Late Mississippian tectonic event, separating it from the underlying Mississippian carbonate strata. In contrast to New Mexico and Texas, the Morrowan strata in eastern Colorado and western Kansas are informally divided into a lower Morrow limestone interval and an upper Morrow siliciclastic-dominated interval (fig. 10).

The Morrow Formation in western Kansas and eastern Colorado is bounded at its base by a second-order sequence boundary (Sloss, 1963; Ross and Ross, 1988) and at its top by a third-order sequence boundary that separates Morrow siliciclastic strata from Atokan carbonate strata. The upper Morrow siliciclastic interval comprises at least five fourth-order depositional sequences. The thickness of the lower Morrow carbonate interval of Bowen and Weimer (2003, 2004) is decidedly thinner than the lower Morrow siliciclastic section in New Mexico (for example, 50 ft versus 200+ ft) (fig. 10).

In general, the upper Morrow interval is dominated by shallow-marine shales that were deposited on a low-gradient shelf northwest of the Anadarko Basin during relative highstands in sea level (Bowen and Weimer, 2003). Enclosed in the shale are valley-fill strata consisting of interbedded sandstones, siltstones, and shale. These valley fills (updip widths of 0.5–2.0 mi [0.8–3.2 km] and downdip of 1.0–4.0 mi [1.6–6.4 km]) developed when extensive river systems incised the subaerially exposed marine shelf during periods of relative lowstand. The simple and compound valleys incised to depths of as much as 100 ft (30.5m). The size of incisement is similar to that seen in the Buffalo Valley field in New Mexico within the Permian Basin.

Overall depositional environments *within* the valley fill vary from fluvial (braided to low-sinuosity to high-sinuosity river systems), estuarine, to marine. The medium- to coarse-grained fluvial sandstone valley-fill facies are the best reservoirs, with porosity values ranging from 18 to 28 percent and permeability ranging from 0.5 to 2.0 md. The overlying estuarine reservoirs commonly have lower porosity (8–18 percent) and lower permeability (10.0–500 md) than the fluvial reservoirs. A major flooding surface marks the top of the valley fill. Of key importance is that Bowen and Weimer (2003) note that within their study area individual valley-fill systems can be correlated, mapped, and put in a sequence-stratigraphic context over a large area (for example, single channel system mapped for 283 km). The other key observation in Bowen and Weimer (2003) is the overall extent of facies tract dislocation (~281 km/175 mi) between lowstand and highstand shoreline deposits. This extensive tract dislocation results in large

regions where identification of the overlying systems (for example, highstand) tract may not be possible and results in stacked lowstand or transgressive tracts within a valley-fill succession. The facies tract dislocation also requires a much greater areal distribution to be considered when exploring for new targets because the lowstand alluvial and fluvial sands of a sequence could be as much as 175 mi more basinward in relation to its underlying highstand shoreline deposits.

Observations from more regional studies provide a reference framework for interpreting and integrating studies in the Permian Basin. Figure 11 illustrates the key core descriptions and wireline log signatures for updip, transitional, and downdip facies tracts of valley-fill systems. These core and wireline signatures are similar to those from the Permian Basin, although historically interpreted differently. Figure 12 illustrates the overall upward change of succession from the lowstand systems tract incised valley upward into the overlying transgressive systems tract within a single well (Bowen and Weimer, 2003). The single-well succession illustrates a level of facies discrimination that is only possible using core data, as the wireline log signature for the lowstand and transgressive systems tract will be similar. The juxtaposition of the transgressive systems tract (shales at the base of the Bayhead Delta) on top of the lowstand coarse sands will result in localized and possibly regional compartmentalization of reservoir units when they are stacked in this manner. The well illustrated in figure 12 typifies the downdip facies tract of Bowen and Weimer (2003).

Bowen and Weimer (2003) illustrated the cross-sectional architecture of their informal facies tracts within a sequence-stratigraphic and reservoir-quality framework (figs. 13, 14). From an exploration and development perspective, recognizing which facies tract you are in is very important because the size, connectivity, and quality of the potential reservoirs all diminish downdip (fig. 13). In the updip position a well would penetrate amalgamated fluvial channels and have excellent reservoir potential through the entire interval, whereas in the transitional facies tract the fluvial channels are separated by lower quality reservoir estuarine sands (fig. 11B). In the downdip facies tract, a well may be likely to intersect no reservoir facies, as the fluvial channels are narrow, disconnected, thin, and separated by thick estuarine basin shales (fig. 13). From figure 14 and table 1 one can see that the updip amalgamated fluvial facies have the best reservoir quality.

Table 1. Morrowan and Atokan stratigraphic correlation chart (modified from Kier, 1980). The Morrow Formation is highlighted in blue, and the Atokan-age units are encompassed by the green highlighted area above the Morrowan to Atokan sequence boundary. Formations and members listed are of both carbonate and siliciclastic character.

Series			Group				Formation							Member		
Lampasas	Bend	Bend (Atokan Series)		Smithwick	Bend	Bend outcrop	Smithwick	Parks Caddo Pool Eastland Lake	Smithwick				Marble Falls Bend Subsurface	Smithwick	Siltstone facies Shale facies	Lower Caddo Ls. Lake Sandstone
			Marble Falls	Big Saline			Upper Marble Falls	Sipe Springs De Leon	Big Saline	Big Saline Upper Marble Falls	Big Saline	Lemons Bluff Big Saline		Brister Bluff/Soldiers Hole Lemons Bluff Aylor bluff/Brook Gibbons Cong.	Brister Lemons Bluff Gibbons Cong.	
Morrow	(Upper Morrow)		Marble Falls		Lower Marble Falls	Comyn	Sloan	Comyn (subsurf.) Lower Marble Falls	Sloan			Sloan Gibbons Cong.		Undivided	Aylor Sloan	

The transitional or downdip facies tracts, although poorer in overall reservoir quality than the updip facies tract, have intervals of excellent reservoir quality where reservoirs can be productive if they are understood. Bowen and Weimer (2004) expanded their discussion of the downdip “valley fill” to encompass estuarine systems in the upper Morrow Formation. Figure 15 is a comparison of the “updip incised valley system” (actually the transitional facies tract of Bowen and Weimer, 2003, fig. 13) with the downdip valley system. The change in scale of the environments is quite apparent with the distal estuarine system being much broader and having multiple input points. Multiple inputs into the less confined estuary allow for differentiation of the sediments into proximal and distal packages and are the key to having reservoir intervals.

After deposition of the minor fluvial fill, transgression flooded the area, and subsequently the estuary was partly filled by prograding bayfill deltas. In terms of reservoir quality in these distal, less confined estuaries, coarse-grained fluvial fill is still locally present at the base of the facies tract but is relegated to the minor role of linkage control in reservoir development and production. Distal areas of the deltas are nonreservoir owing to intense bioturbation resulting in mixing of the more abundant clays into the sands. However, the proximal areas of the deltas have excellent porosity and permeability resulting in good production. Overall, these bayfill deltas result in isolated reservoir compartments, unless linked at the base by fluvial “channel-fill” sands. Figures 16 and 17 illustrate some of the typical features found in core from these

environments, as well as the overall well log correlation illustrating facies variability. The surfaces and features noted in figure 16 are put in their vertical, lateral, and sedimentological context on the core logs in figure 17. Note the estuary central basin shale facies directly overlies the marine shale facies. Without detailed core data the ability to define these two facies and their associated boundaries would be nearly impossible using solely wireline logs (figs. 16, 17, J and L). The encasement of reservoir sands within estuary shale facies is potentially one of several analogs for the Permian Basin succession.

Climatic Conditions

A generalized conceptual sequence-stratigraphic model was put forward by Bowen and Weimer (2003) exhibiting decided differences in facies architecture between the idealized greenhouse model for incised-valley-fill systems (per Zaitlin and others, 1994) and their model in icehouse conditions of rapid and large sea-level fluctuation across a very wide low-angle muddy shelf (fig. 18). The applicability of the Bowen and Weimer (2003) model to the Permian Basin should be noted because most sequence-stratigraphic models are developed from units deposited under greenhouse conditions, whereas the Morrowan was a time of expansive ice-sheet development (see fig. 3), and such times are typified by highly fluctuating sea level. The sea-floor gradient in the Permian Basin (especially the Delaware Basin) is not well constrained and may be steeper than that used by Bowen and Weimer (2003). However, an icehouse sequence-stratigraphic model that reflects the thinner higher frequency cycles and greater dip length of facies groups must still be applied to the Permian Basin.

Ichnofacies

Another study performed outside the Permian Basin on the Morrow Formation provides insight into the significance of using ichnofacies to aid in correlating units and generating depositional models. In southwest Kansas, Buatois and others (2002) studied the lower Morrow sandstone. In contrast, Bowen and Weimer (2003, 2004) concentrated on the “upper” Morrow because the “lower” Morrow in their area was limestone. Before Buatois and others (2002) completed their study, the lower Morrow in Kansas was interpreted as regionally extensive offshore shales, and shoreface and offshore-bar sandstones. Buatois and others (2002) recognized and detailed extensive estuarine systems similar to those of Bowen and Weimer

(2004). The depositional models drew heavily on the use of ichnofacies as indicators of environment, as well as establishing facies architecture in a sequence-stratigraphic framework (for example, identification of a tidal-ravinement surface). Overall the Buatois and others (2002) model differs from that of Bowen and Weimer (2004) by having the discharge empty into an unconfined sea (fig. 19). A similar conceptual model was proposed by James (1984) for the Delaware Basin. The adoption of a fluvial to estuarine facies distribution model over a standard open-marine layer-cake model results in a much more accurate prediction of the compartmentalized reservoirs. Reservoir quality within the Buatois and others (2002) model is best within facies A, C, and I (up to 20 percent porosity), marginal in facies H, E, and J, and poor to nonexistent in facies B, D, F, G, K, L, M, N, and O (fig. 19). Figures 21 and 22 illustrate a lower Morrow correlation and core description showing indicator facies for the estuarine and shoreface environments. Figure 20 further illustrates the vertical stacking patterns of the facies highlighted in figure 19. As with the Bowen and Weimer (2004) study, the model by Buatois and others (2002) highlights the importance and difficulty of separating and defining the estuarine shale from those of more open marine affinity. This observation may not appear crucial to many because neither facies has any reservoir quality, but miscorrelation and identification of these units, in a sequence-stratigraphic context, will result in decreased exploration potential and misunderstandings in terms of reservoir lateral connectivity (fig. 20). Figure 20 also illustrates the composite nature of many of the sequence-stratigraphic boundaries (for example flooding surface [FS] and basal sequence boundary [SB] are picked at the same spot on well Fretz 16-1). Figure 23 illustrates the sequence-stratigraphic significance of the ichnofacies and guilds proposed by Buatois and others (2002). This type of data and classification system is very applicable to the Morrowan-age units in the Permian Basin and may aid in the identification of depositional environments and correlation. The depositional model for the lower Morrow by Buatois and others (2002) is subtly different from that proposed by Bowen and Weimer (2003, 2004), but all the models have similarities to facies patterns recognized in the Morrowan siliciclastic in the Permian Basin (for example, Rutan and others, 2002).

Permian Basin Data

The following section details a number of studies of the Morrowan-age section in the Permian Basin area. Most of these studies are at the field scale only and therefore reflect

different interpretations of the depositional environment. Broadly, the Morrowan-age units in the Permian Basin appear to show a second-order transgression from fluvial-deltaic to shallow-marine and subsequently to carbonate deposition. Higher order cyclicity is evident and is a key to understanding facies relationships; regional correlation, however, is difficult. The fields discussed below are illustrated in figure 24 and are centered on Eddy County, New Mexico, relative to the Permian Basin in figure 4. Regional thickness estimates for the Morrow Formation (including carbonates) range from essentially zero in the north and northwest parts of the Northwestern Shelf and Tatum Basin to 518 m in the southeast (northeast corner of the Delaware Basin) (fig. 4).

In the northern Delaware Basin (Logan Draw–Crow Flats field area), the historic Lower and Middle Morrowan interpretation for the area was deposition in low-accommodation fluvial, deltaic, and nearshore environments (fig. 24). Contrary to historical interpretations, Rutan and others (2002) suggested widespread transgressive valley-fill deposition after extensive incision into the underlying units, similar to the interpretation of Bowen and Weimer (2003). They further divided the lower part of the Morrow Formation into three genetic packages, the two lowermost packages representing valley fill and the uppermost youngest package representing transgressive deposition of thin marine shore-parallel sands. Retrogradational to progradational estuary fill overlain by marine shales represents the lowermost package, wherein estuary-mouth sands have the best reservoir quality, similar to the Bowen and Weimer (2004) and Buatois and others (2002) models. This package is overlain by marine sands and shales, which are in turn overlain by stacked sands thought to be of point-bar affinity (for example, Buatois and others, 2002). The stacked sands are excellent reservoirs in a multiply scoured succession of angular to coarse-grained upward-fining units. Downdip to the south of Logan Draw and Crow Flats, the stacked sands coalesce into a strike-oriented sand body about 75 m thick in a wave-dominated delta (for example, figs. 17, 18, Facies J). Overall, the thin strike-parallel marine sands of the uppermost unit are poor reservoirs unless transected by dip-oriented tidal channels (Rutan and others, 2002).

From the Cedar Lake area of the Delaware Basin, Carlile and Anonymous (1997) painted a slightly different picture for Morrow Formation deposition (fig. 24). He divided the Morrow sandstones into two facies tracts (the Lower and Middle Morrow), which are separated by marine Middle Morrow Shale. The Lower Morrow (*sensu* Carlile and Anonymous, 1997) is interpreted as a coarse-grained fluvial system. The paralic section of the Lower Morrow (*sensu* Carlile and

Anonymous, 1997) is characterized by backstepping, retrogradational parasequences bound by transgressive lags. This interval may be equivalent to the uppermost lower Morrow of Rutan and others (2002). Overlying these two facies tracts is the Middle Morrow, which is defined as a progradational (typical fine-grained sandstones in upward-coarsening cycles) delta system building toward the basin.

Differences between the Rutan and others (2002) and Carlile and Anonymous (1997) studies are related to different order cycle comparison (for example, fourth and fifth versus third and fourth order) and geography, both in potential source areas and in proximal and distal relationships to each other.

Farther to the southwest from the two previous studies Malon and others (2000) interpreted the Morrow in the White City field as possessing a lower half that consists of two southeast progradational fluvial-deltaic systems (fig. 24). This interpretation contrasts with previous findings of studies where a transgressive event is followed by a regressive event. In closer detail the packages are interleaved with short-duration higher order aggradational and retrogradational cycles. The overall progradational signal noted by Malon and others (2000) could be due to increased sediment load in their area. It was proposed that delta-lobe abandonment, possibly coupled with compaction or syndepositional faulting, or both, lead to marine incursion with abundant shale deposition (Malon and others, 2000). At the parasequence scale the upper portions of many of the sandstone packages contain thin reworked channel-mouth bars and beach barrier bar deposits. These “lowstand?” facies are commonly capped by transgressive marine shales and thin oolitic carbonates. Overall their interpretation could be put into the framework of the downdip facies tract of the estuarine model proposed by Bowen and Weimer (2004).

In the Osudo field area, the primary sediment source is the Pedernal Uplift, and a secondary source is a portion of the uplifting Central Basin Platform (James, 1984; Roberts and Kohles, 1999) (fig. 24). The Coker (2003) study of Osudo followed the tripartite division of the Morrow Formation from Mazzullo (1983) and Speer (1993) (figs. 8 and 9). Overall the lower Morrow Formation (*sensu* Coker, 2003) contains sediments reflecting four depositional environments ranging from (1) alluvial plain facies, (2) transitional marine, (3) shoreline to inner shelf, and (4) midshelf to basinal. The middle Morrow is separated from the lower Morrow by a transgressive radioactive marine shale, as noted by Malon and others (2000) and Carlile and

Anonymous (1997). The middle Morrow is part of a delta-front package and presents the same depositional environments as the lower Morrow with the addition of a proximal fluvial facies. Facies maps from Coker (2003) indicate a slight progradation (overall regression) of the middle Morrow environments relative to the lower Morrow, similar to that of James (1984) and Mallon and others (2000) (fig. 25). However, the regional layer-cake-style parallel facies bands illustrated by Coker (2003) do not appear realistic, given the scale, and don't reflect the perceived complicated juxtaposition of facies (for example, valley-fill channels vs. deltaic muds) that are present (fig. 25). Changes in the sediment-load conditions from the Lower to Middle Morrow were potentially influenced by Central Basin Platform uplift or quiescence. The Lower and Middle Morrowan facies patterns in eastern Lea County and western Winkler County may be quite different from those farther west and southwest, where other sediment sources or eustatic conditions dominated.

Within the lower and middle Morrow divisions multiple transgressive and regressive events can be documented, thereby making correlation of these cycles quite difficult (Coker, 2003). A shale is defined as the upper boundary of the Middle Morrow with carbonate deposition (Upper Morrow) above. This limestone is poorly defined and is discussed in the carbonate section of this chapter.

In terms of reservoir quality, the middle Morrow has the best production, yielding a cumulative production of 208 Bcf, largely from coarse-grained distributary channel sandstones. Coker (2003) suggested the possibility of syndepositional faulting controlling sedimentation patterns and resultant reservoir quality.

Mazzullo (1999) and Roberts and Kohles (1999) discussed the Morrow in a regional sense without major emphasis on field-scale heterogeneity. A subregional paleogeographic reconstruction for the entire Morrow Formation for southeastern New Mexico illustrates the complex facies interrelations possibly present over field-scale areas (fig. 24). On the basin-wide scale, Roberts and Kohles (1999) noted that the overall transgression in the Morrow is apparent; with the lower Morrow (A zone) being delta plain, the overlying younger middle Morrow (B zone) representing delta front, and the youngest upper Morrow (C zone) being carbonate shelf (fig. 9). Note, however, that in figure 24 the more basinal and marine sediments of the lower Morrow (A zone) are not illustrated and those displayed are actually younger zone B and zone C sediments. The correlation of Morrowan-age units in southeast New Mexico was expanded and

completed by Geological Data Services (GDS) (Roberts, personal communication, 2005) and further illustrates the difficulty and complexity of correlation within the aforementioned environments. Issues exist with picking the top of the Morrow (Upper Morrow Zone C) from the overlying Atoka “shaly” carbonates. The basal lower Morrow transgressive shale appears to be the most readily correlative over large areas, whereas the shale at the top of the middle Morrow is not as thick, distinct, or widespread and is more difficult to correlate, contrary to several other interpretations (fig. 26). Accurate identification of the base of the Morrow Formation relies heavily on the identification of Mississippian-age sandstones (informally Carlsbad Sand) within and equivalent to the Barnett Shale (fig. 26). The wireline log signature of the GDS type well is similar to the type log used by Bowen and Weimer (2003) (figs. 10 and 26).

Figure 27 illustrates a schematic regional cross section across Eddy County, New Mexico, employing about 1,000 wells. The model interpreted by Roberts and Kohles (1999) and Roberts (personal communication) relied heavily on the paleogeographic reconstruction put forth by James (1984) with prograding fluvial-deltaic channels and point bars sourced dominantly from the northwest during lower Morrow deposition. The Roberts and Kohles (1999) correlation in figure 27 appears the most realistic for publicly available Morrow Formation interpretations in New Mexico. However, an addition of deeply incised valleys is certainly required for the Lower Morrow section. Evidence of this incision is provided by the seismic data in the Van Dock and Gaiser (2001) study and the well log correlations by Lambert (1989).

James (1984) interpreted the shale (MMSH) dividing the lower Morrow from the middle as lagoonal in origin and not a transgressive open-marine shale (fig. 28). That interpretation may be supported by the inability of Roberts and Kohles (1999) to regionally correlate it. The middle Morrow succession in the Parkway area, is proposed to be transgressive beach and submarine bars that trend parallel to depositional strike, an interpretation supported by Lambert (1989) in the Empire field and Rutan and others (2002) in the Crow Flats field. Figures 28 and 29 illustrate the type log and characteristic facies relationships to petrophysical character used by James (1984). Note that in figure 28 there is no identification of a Mississippian sand by James (1984). However, a comparison of the log signatures from the two studies indicates a possible equivalent pick in the Parkway well to that in the Big Eddy well (figs. 26, 28). If either pick is correct, it changes the potential top Mississippian pick by more than 100 ft. The well log character in figure 29 is very similar to those illustrated by Bowen and Weimer (2003) and Buatois and others

(2002) and could reflect an incised valley fill overlain by an estuarine sequence, as opposed to the mouth-bar system proposed by James (1984). Only detailed core data could resolve this discrepancy.

Mazzullo (1999) illustrated the potential problems of regional wireline log correlation in these environments and proposed that tectonic effects may also control deposition of the units. Mazzullo (1999) noted that following a Late Mississippian tectonic event, the Central Basin Platform area probably had low relief and that regional large-scale tilting and erosion occurred after this event, thereby resulting in an irregular topography on which the Morrowan-age sediments were deposited. Uplifts during Morrowan-age sedimentation also resulted in possible areas of nondeposition and erosion (fig. 30). Further tectonic episodes with uplift and erosion during the Atokan through Wolfcampian stages further modified the continuity of Morrowan sediment patterns, resulting in the present-day mapped distribution.

From work on Empire field, Lambert (1989) suggested that the lower Morrow interval sandstones were deposited in a broad coastal plain environment dissected by channels (fig. 24). The upper delta-plain environment with its thick stacked sand bodies was gradually replaced by thinner sandstones and siltstones of the lower delta plain, eventually culminating in the probable maximum flooding surface noted as the highly radioactive Morrow shale. After a minor regressive event in the lower middle Morrow, a continued transgression influenced deposition of lower delta plain through to open-shelf marine sands in the middle Morrow. Lambert (1989) cited the presence of glauconite pellets as further evidence of the more open marine nature of the middle Morrow siliciclastics. Figure 31 is a strike-oriented well log cross section through the lower and middle Morrow Formation intervals in Empire field. The geometry of the facies illustrated in figure 31 is also consistent with a large-scale incised-valley system composed of both simple and compound valleys. Incision appears to go into the underlying Chester Formation, and channel thicknesses are on the order of 100 ft. In Empire field, the lower Morrow Formation sandstones display reservoir-quality linkage to depositional environment (multiple stacked fluvial channels). Middle Morrow sandstones, which appear more compositionally variable, possess the best reservoir quality after development of secondary porosity via dissolution of detrital grains and clays (Mazzullo and Mazzullo, 1984; Lambert, 1989). As in several other studies of the lower Morrow Formation, the best reservoir quality is present in multiple stacked fluvial channels (porosity of as much as 8 to 17 percent and permeabilities of as

much as 250 md). Reservoir quality, noticeably permeability, is decreased in the thinner, more marine facies. Dissolution of detrital grains and authigenic clays generating secondary porosity and permeability is very important to reservoir quality development, especially in the more estuarine to marine sands.

Seismic Data

Most of the publicly available data and interpretations on Morrowan-age sediments do not present or highlight the use of geophysical data. However, Van Dok and Gaiser (2001) noted that historically the Morrow Formation is an extremely difficult formation to resolve accurately using conventional compressional wave seismic data. In their study of Buffalo Valley, New Mexico, converted shear wave data was used for interpretation of the Morrow Formation (fig. 24). Improved shallow resolution appears to be provided by the shear wave data. Figure 32 illustrates a vertical shear wave data traverse through the field, highlighting the base of the incised valley in yellow overlain by lower and upper Morrow (green horizon) sediment. Interpretation of the image would indicate incision of the upper Morrow into the lower Morrow, as well as possible lower Morrow incision into the Barnett/Chester. The upper Morrow sand top pick in green would therefore be a composite sequence boundary for the Chester/Barnett to lower and upper Morrow, as well as the Atoka. The incisive nature of the facies and possible composite boundaries highlights the inadequacies of correlation in the Morrowan-age siliciclastics using only standard wireline logs. An isochron map compiled between the Atoka and Chester picks clearly outlines a large incised valley (fig. 33). The scale of the incised valley illustrated in figure 32 is similar to those illustrated by Bowen and Weimer (2003).

Good-quality seismic data and interpretations, coupled with extensive core logging and regional sequence-stratigraphic correlations, appear to be the only way to decipher the complexities of the Morrowan-age siliciclastics in the Permian Basin.

Equivocal Morrowan-Age Sediments

To add further to the complexities of the Morrowan-age siliciclastics in the Permian Basin, within Sutton and Schleicher Counties (technically Eastern Shelf) sediments of possible Morrowan age are informally termed the Penn “Detrital Zone.” These sediments have a variable lithologic character but appear dominated by red, green, or dark-gray shales having abundant

poorly sorted, poorly rounded chert pebbles and quartz grains. Thin sandstones and limestones are also present. The entire unit may rarely be composed entirely of chert pebbles. Overall, the unit averages 15 ft in thickness but can increase to a maximum of 150 ft (Rall and Rall, 1958). Recent interpretations of the “Penn Detrital” unit tend more toward an Atokan to Desmoinesian age (for example, Arenoso field, Winkler County, and Rojo Caballos, South, Pecos County) rather than Morrowan age; however, without excellent biostratigraphic and seismic control, the age of some of these units remains ambiguous (Van Der Loop, 1991; Hanson and Guinan, 1992). Other channel-fill sandstones of possible Morrowan-Atokan age have been documented in Baylor County on the “Texas Craton” south of the Palo Duro Basin (Staples, 1986). These siliciclastic sediments are included in the “Bend Group, Bend Clastic,” which is also present in the Palo Duro Basin (Dutton, 1980; Dutton and others, 1982). Bend clastics are also a substantial natural gas reservoir in Cottle and King Counties along the Matador Arch (Brister and others, 2002). In the Broken Bone graben the Bend Group (informally “Bend Conglomerate”) is considered to be of Atokan age, as it overlies a limestone thought to be of Morrowan age.

Summary of Morrowan Siliciclastic Deposition

Overall the Morrowan-age siliciclastics are best described as being deposited in a large-scale incised valley system. These valleys were back-filled by several different facies during transgression. Progradational and retrogradational geometries are linked to uplift and sediment input rates, as well as eustatic sea-level fluctuation. There are several key issues that can help to better understand the depositional geometries of the Morrowan-age siliciclastics. Many of these issues have a direct bearing on exploitation of, and exploration for, new reservoirs in the Permian Basin.

1. Scale and Stacking Patterns: Understanding and identifying higher order cyclicity in sediment packages is extremely important for establishing reservoir continuity for production and exploration. In icehouse time spans such as the Pennsylvanian, the higher order eustatic fluctuations can dominate over the lower order oscillations (for example, extensive progradation during transgression). Stacking patterns and facies tracts in icehouse systems may have substantially different geometries from those conventionally proposed for greenhouse situations. An example would be that the dip length of a fourth-

order fluvial system deposited during icehouse conditions is about three times longer than the equivalent third-order cycle in a greenhouse setting (per Bowen and Weimer, 2003).

2. **Unconformities:** Many of the stratigraphic relationships proposed for the Pennsylvanian rely heavily on the interpretation and identification of unconformities. Of particular importance is to understand the proposed end Mississippian unconformity and confirming whether it is truly a global event (type 1? sequence boundary) or is a type 2 sequence boundary. Understanding the nature, extensiveness, and duration of the unconformities and their correlative conformities in the Pennsylvanian section will have profound effects on how sequence-stratigraphic architectural models are applied. An example would be to conclude that the Barnett Formation is a transgressive systems tract and the overlying lower Morrow is part of the highstand systems tract. Alternatively, as illustrated in figure 27, the Barnett Formation could represent a lowstand prograding wedge with the Mississippian/Pennsylvanian boundary only equating to a transgressive surface and the overlying lower Morrow being the transgressive systems tract. These types of issues cannot be resolved in a review such as this; however, they are key to proper prediction of facies geometries and associations.
3. **Sediment Supply:** Sediment supply may be the largest controlling factor in Morrow siliciclastic sedimentation patterns. Extremely high or low sedimentation rates can produce sequence and facies stacking patterns that contradict those modeled for constant rates of sedimentation.

CARBONATE MORROWAN DEPOSITION

- **Broad Approach:** Carbonate rocks of Morrowan age in the Permian Basin have had little study historically. In this study it is thought that Morrowan-age carbonates present in the Permian Basin are laterally equivalent to extensive carbonates developed in adjacent areas such as the Marble Falls Formation. It is postulated that these adjacent areas act as excellent analogs for equivalent underexploited sections within the Permian Basin. Consequently, the approach that will be taken in this chapter is to discuss development of the Marble Falls Group, even though it is not geographically part of the

study area, so as to provide an analog to what is thought to be present in the Permian Basin.

- **General Depositional Setting:** Morrowan-age carbonates were deposited quite widely across the Permian Basin on a low-angle distally steepening east- and west-facing ramp. Isolated platforms or buildups are interpreted on or near the area of the Central Basin Platform.
- **Reservoir Potential:** Algal bioherms appear to be the most favorable reservoir facies. They may preserve excellent shelter porosity, and intergranular and vuggy porosity have also been locally retained in algal bioherms. Siliciclastic channels crosscutting these bioherms also provide excellent reservoir potential.
- **Diagenesis:** From analog study of the Marble Falls Formation very little primary porosity is retained in Morrowan carbonates. Fracture porosity appears critically important for production from Morrowan carbonate intervals. In units that possessed primary porosity, extensive calcite cementation and silicification have occurred, occluding the pore space. Although algal bioherms appear to provide the best primary (unfractured) reservoir potential, blocky calcite spar may occlude the pore space, resulting in a tight unit.

The only Morrowan carbonate unit near the Permian Basin is the Marble Falls Formation. The lower Marble Falls Morrowan carbonate unit has not been mapped in the Permian Basin but is located in the Llano Uplift area to the east (fig. 34). Although the Marble Falls limestone has been studied using outcrop and borehole data from areas outside the Permian Basin, little hard data are available for this section of Morrowan strata in the Permian Basin. In this study, it is thought that Morrowan-age carbonates are indeed present in the Permian Basin but have simply not been referred to as the Lower Marble Falls Formation, even though they are the most likely lateral equivalents. The extent of the Marble Falls is probably much greater than previously proposed, and the formation may extend into Runnels, Nolan, Coke, and Tom Green Counties within the Permian Basin. Kier (1980) further noted that the distribution of the Marble Falls included areas of the Concho Platform/Eastern Shelf, as well as near the Matador Arch, on the Northern Shelf of the Permian Basin. Figure 1 illustrates the proposed extent of the Lower Marble Falls limestone and its equivalents.

Marble Falls Group—Analog to Underexplored Permian Basin Equivalent Section

The focus of this section will be the Lower Marble Falls Formation of the Marble Falls Group as defined by Manger and Sutherland (1984), Groves (1991), and Erlich and Coleman (2005), which is wholly Morrowan in age. Figure 35 illustrates the lithostratigraphic relationships of the Morrowan-age units discussed in the Erlich and Coleman (2005) study. Some further detail regarding the age and stratigraphic relationship of the Marble Falls Formation can be found in the appendix.

Facies Associations and Depositional Environment

Overall the Morrowan-age carbonates were deposited quite widely across the Permian Basin on a low-angle distally steepening east- and west-facing ramp. Carbonates deposited on or near the area of the Central Basin Platform were isolated platforms or buildups. A wide variety of facies are present, with a shallow-water facies transition to deeper water carbonates and eventually shales that are Barnett Formation equivalents in the south part of the Permian Basin and the Fort Worth Basin.

The lower Marble Falls carbonate unit is characterized by several different facies types and associated depositional environments. In general, the formation comprises light to dark cherty limestones and thin shale beds (Kier, 1980). Algal biomicrites, biosparites, oosparite, spiculitic biomicrite, pelmicrite, micrite, mixed skeletal biosparite and micrite, coral and algal biolithite compose the limestone facies. The spiculitic biomicrite, micrite, and shale are considered off-platform, whereas the other facies are considered platform (fig. 36). Two depositional models have been proposed, first by Kier (1980) and secondly by Namy (1980) and Erlich and Coleman (2005), and will be discussed in that order.

As illustrated by fig. 36, Kier (1980) proposed that the platform margin was defined by an oolitic sand belt (oosparite facies) having minor seaward and landward spillover lobes. The platform interior comprises pelletal sand (pelletal biomicrite and biosparite), tubular, coralline and phylloid algae (for example, coral/algal biolithites) bands. Kier (1980) suggested that owing to better winnowing conditions near the margin of the platform the algal facies dominated with phylloidal and tubular algae occupying a slightly more landward position than the coralline algae. The platform and platform margin are dissected by channels filled with dominantly coarse crinoidal fill (for example, mixed skeletal biosparites and biomicrites). Although not illustrated

in figure 36, the algal biomicrite-biosparite and biolithites occur as platform interior buildups and overall are the most widely occurring rock types. These bioherms are thought to be *Cuneiphycus* (red algae) constructions and rarer *Donezella* boundstones and range in thickness from 1 to 10 m (Choh, 2004). In the off-platform and intermound (biohermal) areas spiculite-bearing facies dominate and are thought to be forming in quiet waters below wave base. This facies is associated with pure micrite and rarer shale.

In general Kier (1980) proposed that the lower Marble Falls member was deposited on a Bahamian-type platform on antecedent topography associated with the Llano Uplift. Namy (1980) and Erlich and Coleman (2005) contended that the Lower Marble Falls member (in the same area as Kier [1980]) was deposited on a southeast-facing distally steepening ramp. In this competing model, a thick (coalesced and stacked to ~120 ft [37 m]) algal bank complex forms at the shelf margin and rapidly grades to heavily bioturbated and eventually laminated spiculitic biomicrites seaward (Namy, 1980). Seaward of the algal banks minor channels (storm debris) filled with intraclasts of the algal banks, as well as crinoidal debris, occur punctuated by small coral reefs and algal mounds. Namy (1980) and Kier (1980) disagreed on the overall depositional environment for the lower Marble Falls Morrowan-age carbonates, but they did not place their studies in a sequence-stratigraphic context to aid comparison and interpretation. Lower Marble Falls facies stacking patterns documented by them indicate an overall regression during deposition, culminating in exposure and the formation of the sequence boundary separating the lower Marble Falls from the upper Marble Falls member. This overall regression is consistent with the sea-level curves of Ross and Ross (1987), at least at the second- and third-order scale (fig. 35). However, the third-order eustatic fluctuations are much higher amplitude than those of the second order and indicate a potentially sizable transgressive event prior to the final regression. Groves (1991) and Manger and Sutherland (1984) studied the Marble Falls Formation from a biostratigraphic point of view. They found algal-bearing and higher energy facies present in more proximal areas adjacent to the Llano Uplift, as well as punctuating the spiculitic dominated successions (fig. 39).

McCrary (2003) undertook a sequence-stratigraphic study of the Marble Falls limestone in the Pedernales Falls State Park area of Blanco County (fig. 34). Three outcrop sections (Archer Ranch, Maund Ranch, Maples Ranch/Pedernales Falls) over an area of approximately 5 mi were studied, and the Lower Marble Falls Member was found to be present at all localities.

Examples of facies and geometries observed in the Pedernales Falls area during recent field work are shown in figures 37 and 38.

McCrary (2003) divided the Lower Marble Falls into two parasequences. Parasequence 1 is characterized by a basal spiculitic packstone member approximately 70 ft (21 m) thick, which is overlain by medium- to thick-bedded mudstones and crinoidal packstones. In the Pedernales Falls section, several intercalations of crinoidal wackestone and spiculitic packstone are present above the thick-bedded mudstones. The uppermost facies present in the study area was an ooid grainstone. Overlying the ooid grainstone is either a fossiliferous and/or crinoidal packstone. Parasequence 2 was dominated by crinoidal packstones. The facies pattern of parasequence 1 is interpreted as a highstand systems tract capped by a sequence boundary. The sequence boundary is then overlain by a transgressive unit of fossiliferous packstone. The overall facies patterns above the sequence boundary suggest rising sea level (TST).

Reservoir Quality and Log Characteristics

On the basis of interpretation of the McCrary (2003) photomicrographs, very little primary porosity is retained in any of the facies of the lower and/or upper Marble Falls. In units that possessed primary porosity, extensive calcite cementation and silicification have occurred, thus occluding the pore space. Within the *Cuneiphyucus* algal bioherms, excellent shelter porosity was preserved underneath algal thalli (Choh, 2004). However, early blocky calcite spar largely occluded the pore space, resulting in a tight unit.

In terms of production, Jackson (1980) noted that within Brown County and eastern Coleman County at least six mappable units produce gas from the Marble Falls. Three main fields from shelf-edge buildups (Palo Davis and Lewis–Brown County and Santa Anna–Coleman County) dominated production but underwent rapid declines in production to 10 to 20 percent of their original potential. Oil was produced in the initial phases (API of 40–42) but largely gave way to high (~1,200) BTU gas. Overall, the reservoirs appear to be relatively tight but benefit from fracture porosity for production. Rothrock (1957), however, noted that intergranular (primary and secondary) and vuggy porosity are present in coarse-grained crinoidal/bioclastic calcarenites and limestones and that the reservoir is thought to be an algal bioherm. Within the Walton field, north of the Santa Anna and Pottsville, production occurred from siliciclastic channels crosscutting a bioherm, as well as within the bioherm itself (Harmon, 1957). The

bioherm is largely ovoid and approximately 200 ft (61 m) in thickness with a width of approximately 2000 ft (610 m). Figure 40 illustrates the typical wireline log character for the lower and upper Marble Falls within the Fort Worth Basin. The log character and thickness of the lower Marble Falls member changes quite rapidly between relatively closely spaced wells.

In summary, fracture porosity, vuggy porosity, and local intergranular porosity are necessary to produce from Morrowan-age carbonates. Calcite cementation and silicification can occlude pore space and result in tight units. Fracture porosity is considered of prime importance. The Morrowan carbonates from the Llano Uplift area just east of the Permian Basin should be considered an excellent analog for reservoir quality of Morrowan carbonates present within the Permian Basin.

Distribution

Distribution of the Morrowan-age carbonates is difficult to ascertain, as much of the analysis has been restricted to the Llano Uplift area. As mentioned previously, the extent of the Marble Falls is probably much greater than previously proposed and may extend into Runnels, Nolan, Coke, and Tom Green Counties within the Permian Basin. Kier (1980) also noted that the distribution of the Marble Falls included areas of the Concho Platform/Eastern Shelf, as well as areas near the Matador Arch on the Northern Shelf of the Permian Basin. Figure 1 illustrates the proposed extent of the Lower Marble Falls limestone and its equivalents.

The trend of the Lower Marble Falls bears little or no relation to the structural outline of the Llano Uplift (fig. 41). The extent of the Marble Falls is much greater than illustrated in that figure, as evidenced by fields producing from the Marble Falls in Brown and Coleman Counties (Jackson, 1980), neither of which is included in the outline of the Marble Falls Formation in figure 41. This and other evidence such as thinning of the Lower Marble Falls Formation by erosion over post-Morrowan-age uplifted localized areas points to the conclusion that the Marble Falls was of regional extent far beyond what has been previously considered and is interpreted to be present on the Eastern Shelf of the Permian Basin.

Erlich and Coleman (2005) illustrated in cross section, on the basis of well and outcrop data, the geometry of the lower Marble Falls member across the Llano Uplift from east to west (fig. 42). They indicated a major “thinning” south and west of the lower Marble Falls member from its maximum thickness of 230 ft (70 m) along the west margin of the Fort Worth Basin. An

estimated 33 to 66 ft (10 to 20 m) of the lower Marble Falls is thought to have been removed by erosion prior to deposition of the Upper Marble Falls (Erlich and Coleman, 2005). The extent of erosion of the Lower Marble Falls is poorly constrained and may have been much greater across the Bend Arch and Concho Platform and onto the Eastern Shelf. Consequently, thick sections of Lower Marble Falls-equivalent units may be preserved in the Permian Basin.

Permian Basin Data

Within the Permian Basin, Morrowan-age carbonates are present as a unit overlying two basal siliciclastic units on the Northern Shelf and the northern Delaware Basin within New Mexico and Texas (Malon and others, 2000). The carbonate unit is poorly described as a transgressive shallow-water, shelfal, gray limestone, dominantly oolitic with interbedded marine shales (James, 1984; Casavant, 1986; Malon and others, 2000). This unit is termed the “Upper Morrow” and is thought to be separated from the underlying Lower and Middle Morrow by a transgressive shale. Shallow shelfal carbonates were thought to be present in areas more basinward (that is, south into the Delaware Basin) from the Lower and Middle Morrowan alluvial, valley-fill, and deltaic successions (James, 1984). Morrowan-age oolitic limestones are also present in the McDonald field in Lea County, New Mexico, and Homman field, Gaines County, Texas.

Equivocal Carbonate Morrowan Deposition

Outside of the Permian Basin, to the north, a limestone of possible Morrowan age also exists below the “Bend”-age fan-delta siliciclastic succession in the Palo Duro and Dalhart Basins, whereas the Lower Morrow limestone in Kansas and Colorado is grainstone facies that occurs stratigraphically beneath the valley-fill succession described by Bowen and Weimer (2003).

Summary of Upper Morrow Carbonate Deposition

Because so little is known about the Permian Basin Morrowan-age carbonates, understanding and documenting the lower Marble Falls Formation helps to create possible outcrop and subsurface analogs. The Marble Falls-type carbonates have potential as both a primary (for example, leaching of bioclasts and primary porosity) and a secondary (fracture)

reservoir. Their possible equivalent units within the Permian Basin may be overlooked targets. With the current explosion of interest in the shale gas systems (primarily the Barnett but also the Smithwick) an overlying Marble Falls–type carbonate system may also hold potential as a fractured reservoir for expelled Barnett gas.

When comparing the carbonate succession regionally, one obvious factor that must be understood is the apparent differing response to eustasy and tectonics between the greater Llano Uplift area and the Northwest Shelf/Delaware Basin margin. Biostratigraphically the lower Marble Falls Formation (minus tens of meters removed by erosion) is time equivalent to the entire Morrowan siliciclastic and carbonate succession in New Mexico.

Broadly similar transgression and regression cycles are noted in the Permian Basin New Mexico study area and the Llano area, in that there is generally a regional transgression punctuated by a major regression. Local differences between the areas probably relate to the rate of sediment supply. Sediment input into the northwest Permian Basin is linked to rates of Pedernal area uplift. An increased sediment supply during uplift could outpace accommodation and result in progradation (apparent regression), whereas during times of quiescence or diminished uplift sediment supply diminishes or stops and results in apparent transgression (retrogradation). The deposition of the Upper Morrow carbonate unit in the Delaware Basin area probably indicates a switch from local tectonic to regional eustatic control as sediment supply shuts off and tectonism diminishes in the hinterland.

In summary, there are several key issues regarding the understanding of the Morrowan-age carbonates. Many of these issues have a direct bearing on exploitation of, and exploration for, new reservoirs in the Permian Basin.

1. Scale: Studies within and external to the Permian Basin need to be put into regional sequence-stratigraphic context.
2. Unconformities: Many of the stratigraphic relationships proposed for the Pennsylvanian rely heavily on the interpretation and identification of unconformities. However, many of the studies present conflicting or at best ambiguous stratigraphic interpretations. Understanding the nature, extensiveness, and duration of the unconformities and their correlative conformities in the Pennsylvanian section will strongly influence how sequence-stratigraphic architectural models are put forth. As illustrated in figure 35 the Barnett Formation probably represents a time-equivalent basinal facies to Mississippian

shallow-water carbonates, as well as Morrowan-age siliciclastics and ramp carbonates. Secondly, the presence of the unconformity between the Lower Marble Falls and Upper Marble Falls Formations should be confirmed and extended in the Permian Basin, if possible, for correlation purposes, and such an exposure surface could have strong bearing on the development of secondary porosity.

3. Nomenclature: A concerted effort must be made to unify the stratigraphic nomenclature applied to the Morrowan carbonates. It is proposed that the term “Lower Marble Falls Formation” be used for all platform to ramp carbonates in the greater Permian Basin area in outcrop and the subsurface.

OVERALL DISCUSSION AND SUMMARY

Within the Permian Basin, confirming the presence of Morrowan valley-fill systems and understanding their processes is important. An incised valley-fill depositional model appears most compatible with the Morrowan-age siliciclastics in the Permian Basin. The exploration strategy and approach for un-incised lowstand bypass systems versus those that are incised is different (Posamentier, 2001). In bypass systems excellent reservoir potential may be developed in the deeper basin, whereas in incised systems amalgamated stacked on-shelf channels provide excellent reservoirs. If shelf-edge bypass occurred, then previously unidentified plays may exist.

Incised valley-fill systems contain a much broader spectrum of facies and environments than standard un-incised lowstand alluvial systems (that is, range from alluvial to open marine). Overall, the areal extent of an un-incised alluvial system is greater than that of an incised valley fill. The more limited extent of valley-fill systems is a product of the duration of the period of sea-level fluctuation, erodibility of the substrate, and fluvial discharge (fig. 1).

The incision critical to valley-fill systems can be generated by sea-level fall, tectonic tilting/uplift, or discharge reduction. Given the amount and length of incision (that is, simultaneous incision over the entire length) in the Morrowan siliciclastics in New Mexico, Kansas, and Oklahoma, the ancestral Rocky Mountain tectonic uplift resulted in increased stream flow, thereby becoming a major controlling factor in incision. Within the Permian Basin, the uplift of the Pedernal Highland and possibly localized areas of the Central Basin Platform resulted in incision. Given the paleogeography of the Permian Basin, this system may have been linked to those drainage systems farther north and east in Colorado and Kansas (fig. 1).

Rapid and high-amplitude sea-level falls probably also contributed to incision of the Morrow Formation valley fills. Galloway (2001) illustrated a much larger but more confined (that is, single) depocenter that results in sediments bypassing the shelf edge during icehouse conditions, as compared with a greenhouse situation (fig. 43). The Delaware Basin was most likely a depocenter and had been for some time (for example, supporting data include thickness patterns of the Woodford Shale and gravity/magnetic data); therefore, the sea-floor gradient was potentially quite high, resulting in major incision during sea-level falls. Rapid and high-amplitude sea-level rises could allow rapid infilling and capping of the alluvial sediments within the valleys and result in facies-controlled traps and seals.

The potential for deepwater deposits in the Delaware was high, owing to shelf bypass. If the 125-mi-plus (200-km) estimates by Bowen and Weimer (2003) and Posamentier (2001) for valley incision and facies dislocation are applied to the Permian Basin, lowstand facies could be present much farther to the south within the Delaware and Midland Basins. In the deepest parts of the Delaware Basin, basin-floor fans might be present. Facies dislocations caused by eustasy and tectonic uplift require a reappraisal of the deeper Delaware Basin for lowstand deposits of Lower Morrow affinity as far south as Loving and possibly Reeves County.

Understanding Morrowan-age carbonate deposition in the Permian Basin is hampered by a lack of detailed data and regional interpretations. Overall, it appears that carbonate deposition occurred over a much larger area in the Permian Basin (Eastern Shelf and Delaware Basin) than previously documented. The presence of algally dominated bioherms and higher energy facies (ooid grainstones), augmented by fracture porosity, indicates potentially overlooked reservoir intervals. The Morrowan-age carbonate outcrop succession in the Llano Uplift area provides an analog for size, distribution, and reservoir character for “undiscovered” Permian Basin Morrowan carbonates.

PALEOGEOGRAPHIC SUMMARY

The proposed distribution of Morrowan-age (Middle Morrowan as per Delaware Basin siliciclastic succession) sediments across the Permian Basin and surrounding areas based on the above interpretations is illustrated in figure 1. The following discussion refers to interpretations represented in figure 1. Because much of the data is restricted to the Delaware Basin and the

Llano Uplift, facies interpretations across the Midland Basin (MB), Ozona Arch (OA), Val Verde Basin (VB), and the southern portion of the Delaware Basin (DB) are tentative.

Broadly, Morrowan-age siliciclastics dominate deposition in the west of the Permian Basin, whereas carbonate deposition dominates in the east. The predominance of carbonate facies in the east is due to the lack of siliciclastic supply to that part of the basin. The transition from the platform and/or ramp carbonates to more basinal carbonates and ultimately shales along the Eastern Shelf (ES), Midland Basin (MB), and Central Basin Platform (CBP) is suggested. This transition is supported by well log data in the Midland Basin, which indicate a westward change from carbonates to shalier lithologies. A small peninsula of platform to ramp carbonates is thought to have existed along the trend of the antecedent Central Basin Platform (CBP). Some Precambrian inliers on this trend appear to have been exposed and shedded material into the basin (for example, Eddy County, New Mexico), and it is assumed that along the margin of these inliers and other uplifting basement-cored highs carbonate deposition could also have occurred.

In the Delaware Basin (DB) the siliciclastic lowstand succession was dominated by extensive incised valleys. The valley systems were infilled by multiple facies types. The interpreted deepwater fan systems would be sourced through the incised valleys that bypass sediment to the deeper water. The size, geometry, and position of the deepwater siliciclastics depend largely on the gradient of the shelf-to-slope transition. The fan systems could be encased in deepwater carbonates or shales. If parts of the DB reflect a pre-Pennsylvanian depocenter, the transition zone from basinal carbonate to shale may not have existed and the region in Jeff Davis and Pecos Counties may have been an area of platform to ramp shallow-water carbonate deposition. The siliciclastic succession is shown to be dominantly receiving its sediment load from the east-southeast margin of the Pedernal Uplift. However, regionally the DB valley-fill system is linked to the north with other channel systems feeding the Midcontinent. To the west in Hudspeth and El Paso Counties siliciclastic influx appears to have been less, and a possible uplift of the Diablo Platform (DP) area resulted in carbonate deposition in a possibly double-sided ramp configuration.

KEY CONCLUSIONS

- Broadly, the Morrowan-age units in the Permian Basin appear to show a “second-order” transgression from siliciclastic fluvial deltaic to shallow marine and subsequently to carbonate deposition.
- Morrowan-age siliciclastics dominate deposition in the west of the Permian Basin, whereas carbonate deposition dominates in the east. The predominance of carbonate facies in the east is probably due to a lack of siliciclastic supply to that part of the basin. The deposition of the Upper Morrow carbonate unit probably indicates a switch from local tectonic to regional eustatic control as tectonism diminished in the hinterland and sediment supply from the north/northwest shut off
- Siliciclastic deposition of the Morrowan-age units occurred in a large incised valley-fill system. Fluvial, deltaic, estuarine, and open-marine facies are interpreted. Excellent reservoir potential is noted in amalgamated, stacked channel systems and bayhead deltas.
- These incising valleys may have served as conduits for shelf-margin bypass during periods of lowstand. It is proposed that such bypass channels may have fed sediment into the deeper basin, developing lowstand basin-floor-fan deposits. This represents an exciting new play type for the region.
- The Upper Morrowan carbonates were deposited over a much larger area in the Permian Basin (Eastern Shelf and Delaware Basin) than previously documented. The presence of algally dominated bioherms and higher energy facies (ooid grainstones), augmented by fracture porosity, indicates potentially overlooked reservoir intervals. These Morrowan carbonates hold potential as a fractured reservoir for expelled “Barnett” gas.
- The conclusions drawn herein should provide guidelines and ideas for interpretation of the Morrowan section within the Permian Basin.

APPENDIX. MARBLE FALLS

The term “Marble Falls” has been used as both a group and formation name (Cheney, 1940; Plummer, 1944; Cheney, 1947; Plummer, 1947, 1950; Cheney, 1951; Cheney and Goss, 1952). Table 2 illustrates the different classification systems and time equivalencies devised for this time unit. Formations within the Marble Falls Group are historically the Sloan, Comyn,

Lower Marble Falls, Upper Marble Falls, and Big Saline. If the Marble Falls is taken as a formation, it is commonly designated “lower” (including the Sloan and occasionally the Gibbons conglomerate members) and “upper” (with Gibbons Conglomerate, Big Saline, and Lemons Bluff Members). The term “Comyn Formation” is commonly used for the lower Marble Falls in the subsurface.

The Barnett and the Marble Falls Formations are thought to straddle the Mississippian/Pennsylvanian boundary, and within the northern Midcontinent this boundary is marked by a distinct paleosol (for example, Keir, 1980; Groves, 1991). A debate exists as to the placement and the conformability of the Mississippian/Pennsylvanian (basal Morrowan) boundary and the formation(s) within which it lies.

Biostratigraphic studies of the Barnett–Marble Falls succession in the Llano Uplift (Hoare and Merrill, 2004) indicate a conformable contact between the Barnett Formation and Marble Falls Group (fig. 7). Erlich and Coleman (2005) argued that the Barnett Formation–Marble Falls Formation contact is conformable in the westernmost Fort Worth Basin but unconformable, at least locally, on the Llano Uplift, where the upper Marble Falls overlies Mississippian Barnett Formation, Devonian, or Ordovician units.

Groves (1991) used fusulinid biostratigraphy to date the Lower Marble Falls “member” as Morrowan in age and the upper Marble Falls “member” as Atokan in age. Manger and Sutherland (1984) also proposed the same division on the basis of conodont biostratigraphy. They did note, however, that the entire lower Marble Falls member at the type section locality is biostratigraphically younger than the lithostratigraphically equivalent interval to the northeast.

An unconformity between the lower and upper Marble Falls members was noted by Groves (1991), Kier (1980), Watson (1980), Namy (1982), Manger and Sutherland (1984), and Erlich and Coleman (2005). Groves (1991), however, also noted that the Gibbons conglomerate overlies the lower/upper Marble Falls unconformity. Manger and Sutherland (1984) noted the presence of a limestone pebble conglomerate (termed “Sloan Conglomerate”) at the same unconformity.

REFERENCES

- Bell, W. C., 1957, Study of Lower Pennsylvanian and Mississippian rocks of the northeast Llano Uplift: paleozoic stratigraphy of the Fort Worth Basin: Abilene and Fort Worth Geological Societies joint field trip guidebook, 120 p.

- Bowen, D. W., and Weimer, P., 2003, Regional sequence stratigraphic setting and reservoir geology of Morrow incised-valley sandstones (lower Pennsylvanian), eastern Colorado and western Kansas: American Association of Petroleum Geologists Bulletin, v. 87, p. 781–815.
- Bowen, D. W., and Weimer, P., 2004, Reservoir geology of Nicholas and Liverpool Cemetery field (Lower Pennsylvanian), Stanton County, Kansas, and their significance to the regional interpretation of the Morrow Formation incised-valley-fill systems in eastern Colorado and western Kansas: American Association of Petroleum Geologists Bulletin, v. 88, p. 47–70.
- Brister, B. S., Stephens, W. C., and Norman, G. A., 2002, Structure, stratigraphy, and hydrocarbon system of a Pennsylvanian pull-apart basin in North-Central Texas: American Association of Petroleum Geologists Bulletin, v. 86, p. 1–20.
- Buatois, L. A., Mangano, M. G., Alissa, A., and Carr, T. R., 2002, Sequence stratigraphic and sedimentologic significance of biogenic structures from a late Paleozoic marginal- to open-marine reservoir, Morrow Sandstone, subsurface of Southwest Kansas, USA: Sedimentary Geology, v. 152, p. 99–132.
- Caran, S. C., Woodruff, C. M., and Thompson, E. J., 1981, Lineament analysis and inference of geologic structure: examples from the Balcones/Ouachita trend of Texas: Gulf Coast Association of Geological Societies Transactions, v. 31, p. 59–69.
- Carlile, K. Q., and Anonymous, 1997, Structural, depositional, and diagenetic analysis of the Pennsylvanian Morrow within the Cedar Lake area in the Delaware Basin of Southeast New Mexico: T. R. Southwest Section meeting v. 81, p. 866.
- Casavant, R. R., 1986, Paleoenvironmental reconstruction for infill drilling, White City Penn-South Carlsbad Field areas, Eddy County, New Mexico: American Association of Petroleum Geologists Southwest Section Convention, v. 70, p. 343.
- Cheney, M. G., 1940, Geology of north-central Texas, *in* Lloyd, D. A., ed., West Texas-New Mexico symposium: American Association of Petroleum Geologists Bulletin, v. 24, p. 65–118.
- Cheney, M. G., 1947, Pennsylvanian classification and correlation problems in north-central Texas, *in* Wanless, H. R., Symposium on Pennsylvanian Problems, v. 55, p. 202–219.
- Cheney, M. G., 1951, Guidebook, Pennsylvanian of Brazos River and Colorado River valleys, north-central Texas, June 1-2: West Texas Geological Society, 97 p.
- Cheney, M. G., and Goss, L. F., 1952, Tectonics of central Texas: American Association of Petroleum Geologists Bulletin, v. 36, p. 2237–2265.
- Choh, S.-J. S., 2004, Microfacies and depositional environments of selected Pennsylvanian calcareous algal deposits from southern U.S.A., and application of information technology for sedimentary petrology teaching and research: The University of Texas at Austin, Ph.D. dissertation, 185 p.
- Coker, A. D., 2003, Depositional environments of the Morrow Formation in the Osudo field, Lea County, New Mexico, *in* Hunt, T. J., and Lufholm, P. H., eds., The Permian basin: back to basics: West Texas Geological Society Publication 03-112, p. 327–334.
- Dalziel, I. W. D., Lawver, L. A., Gahagan, L. M., Campbell, D. A., and Watson, G., 2002, Texas Through Time, Plate's Plate Model, The University of Texas at Austin Institute for Geophysics, <http://www.ig.utexas.edu/research/projects/plates/movies>.

- Dutton, S. P., 1980, Depositional systems and hydrocarbon resource potential of the Pennsylvanian System, Palo Duro and Dalhart basins, Texas Panhandle: The University of Texas at Austin, Bureau of Economic Geology, Geological Circular 80-8, 49 p.
- Dutton, S. P., Goldstein, A. G., and Ruppel, S. C., 1982, Petroleum potential of the Palo Duro Basin, Texas Panhandle: The University of Texas at Austin, Bureau of Economic Geology Report of Investigations No. 123, 87 p.
- Erlich, R. N., and J. L. Coleman, 2005, Drowning of the Upper Marble Falls carbonate platform (Pennsylvanian), central Texas; a case of conflicting “signals?”, *in* *Sedimentology in the 21st Century: a tribute to Wolfgang Schlager*, v. 175, p. 479–499.
- Galloway, W. E., 2001, Cenozoic evolution of sediment accumulation in deltaic and shore-zone depositional systems, northern Gulf of Mexico Basin: *Marine and Petroleum Geology*, v. 18, p. 1031–1040.
- Groves, J. R., 1991, Fusulinacean biostratigraphy of the Marble Falls Limestone (Pennsylvanian), western Llano region, central Texas: *Journal of Foraminiferal Research*, v. 21, p. 67–95.
- Hanson, B. M., and Guinan, M. A., 1992, Rojo Caballos, South Field, U.S.A.: Delaware Basin, Texas, *in* *Stratigraphic traps: American Association of Petroleum Geologists*, III, v. 23, p. 83–112.
- Harmon, J. L., 1957, The Walton Field, Eastland County, Texas, *in* *Abilene & Fort Worth Geological Societies joint field trip guidebook*, p. 105–107.
- Harrell, J. E., and Anonymous, 2003, Sedimentology and depositional setting as physical evidence for a conformable Mississippian-Pennsylvanian boundary, Llano Uplift, Texas, *in* *Geological Society of America, Southeastern Section, 37th annual meeting*, v. 35, p. 18.
- Harrell, J. E., Lambert, L. L., and Anonymous, 2004, Sloan Formation: application and implications of a forgotten Carboniferous stratigraphic unit in the Llano Uplift, Texas, *Geological Society of America, South-Central Section, 38th annual meeting*, v. 36, p. 29.
- Hoare, R. D., and Merrill, G. K., 2004, A Pennsylvanian (Morrowan) Ostracode fauna from Texas: *Journal of Paleontology*, v. 78, p. 185–204.
- Jackson, T. C., 1980, Related oil and gas production north of the Llano Uplift, *in* Windle, D., ed., *Geology of the Llano region, central Texas: West Texas Geological Society*, p. 98–102.
- James, A. D., 1984, Lower Pennsylvanian reservoirs of the Parkway-Empire South Field area, Eddy County, New Mexico, *in* *American Association of Petroleum Geologists Annual Meeting Official Program*, p. 33–52.
- James, A. D., 1985, Producing characteristics and depositional environments of Lower Pennsylvanian reservoirs, Parkway-Empire South area, Eddy County, New Mexico: *American Association of Petroleum Geologists Bulletin*, v. 69, p. 1043–1063.
- Kier, R. S., 1980, Depositional history of the Marble Falls Formation of the Llano region, central Texas, *in* Windle, D., ed., *Geology of the Llano region, central Texas: West Texas Geological Society*, p. 59–75.
- Kluth, C. F., 1986, Plate tectonics of the ancestral Rocky Mountains, *in* Peterson, J. A., ed., *Paleotectonics and sedimentation in the Rocky Mountain region, United States: American Association of Petroleum Geologists*, v. 41, p. 353–369.
- Lambert, R. B., 1989, Environment of deposition and reservoir morphology of Lower Pennsylvanian Morrowan sandstones, South Empire Field, Eddy County, New Mexico, *in*

- Flis, J. E., Price, R. C., and Sarg, J. F., eds., Search for the subtle trap: hydrocarbon exploration in mature basins: West Texas Geological Society, v. 89-85, p. 235.
- Malon, K. M., Casavant, R. R., and Anonymous, 2000, Facies architecture of the Morrow sandstones, southeastern New Mexico: American Association of Petroleum Geologists Bulletin, v. 84, p. 1242.
- Manger, W. L., and Sutherland, P. K., 1984, Preliminary conodont biostratigraphy of the Morrowan-Atokan boundary (Pennsylvanian), eastern Llano Uplift, central Texas, *in* The Atokan Series (Pennsylvanian) and its boundaries: a symposium, v. 136, p. 115–121.
- Mazzullo, J. M., and Mazzullo, L. J., 1984, Detrital and authigenic clay minerals in the lower Morrow Sandstones of eastern New Mexico: American Association of Petroleum Geologists, Southwest Section, v. SWS-84-78, p. 53–60.
- Mazzullo, L. J., 1983, Stratigraphy and sedimentation of the lower and middle Morrow of southeastern New Mexico, Exploration in a mature area: American Association of Petroleum Geologists, Southwest Section, p. 168–189.
- Mazzullo, L. J., 1999, Significance of intraformational unconformities in the Morrow Formation of the Permian Basin, *in* Grace, D. T., and Hinterlong, G. D., eds., The Permian Basin: providing energy for America: West Texas Geological Society, v. 99-106, p. 55–61.
- McCrary, J. M., 2003, Sequence stratigraphy of the Marble Falls Limestone, Pedernales Falls State Park, Blanco County, central Texas: Nacogdoches, TX, Stephen F. Austin State University, Master's thesis, 130 p.
- Namy, J., 1980, Marble Falls algal bank complex, Marble Falls, Texas, *in* Windle, D., ed., Geology of the Llano region, central Texas: West Texas Geological Society, p. 172–174.
- Namy, J., 1982, Stratigraphy and hydrocarbon production of the Marble Falls Group, southern part of the Fort Worth Basin, *in* Martin, C. A., ed., Petroleum geology of the Fort Worth Basin and Bend Arch area Dallas, TX: Dallas Geological Society p. 213–222.
- Plummer, F. B., 1944, Stratigraphy of the Lower Pennsylvanian coral-bearing strata of Texas: University of Texas, Austin, Bureau of Economic Geology, Publication No. 4401, p. 63–76.
- Plummer, F. B., 1947, Lower Pennsylvanian strata of the Llano region, summary of classification: Journal of Paleontology, v. 21, p. 142–146.
- Plummer, F. B., 1950, The Carboniferous rocks of the Llano region of central Texas: University of Texas, Austin, Publication No. 4329, 170 p.
- Posamentier, H. W., 2001, Lowstand alluvial bypass systems: incised vs. unincised: American Association of Petroleum Geologists Bulletin, v. 85, p. 1771–1793.
- Rall, R. W., and Rall, E. P., 1958, Pennsylvanian subsurface geology of Sutton and Schleicher counties, Texas: American Association of Petroleum Geologists Bulletin, v. 42, p. 839–870.
- Roberts, J. E., and Kohles, K. M., 1999, Correlative subsurface database for the Atoka and Morrow formations and underlying Mississippian Barnett Shale of southeastern New Mexico, *in* Grace, D. T., and Hinterlong, G. D., The Permian Basin: providing energy for America: West Texas Geological Society, v. 99-106, p. 35–41.
- Ross, C. A., and Ross, J. R. P., 1987, Late Paleozoic sea levels and depositional sequences, *in* Ross, C. A., and Haman, D., eds., Timing and depositional history of eustatic sequences; constraints on seismic stratigraphy: Ithaca, NY, Cushman Foundation for Foraminiferal Research, v. 24, p. 137–149.

- Ross, C. A., and Ross, J. R. P., 1988, Late Paleozoic transgressive-regressive deposition, *in* Wilgus, C. K., Hastings, B. S., Ross, C. A., Posamentier, H., Van Wagoner, J., and Kendall, C. G. S. C., eds., *Sea-level changes: an integrated approach: SEPM (Society for Sedimentary Geology)*, v. 42, p. 227–247.
- Rothrock, H. E., 1957, The Santa Anna Field, Coleman and Brown counties, Texas: Abilene & Fort Worth Geological Societies joint field trip guidebook, p. 93–99.
- Rutan, D., Sullivan, E. C., and Anonymous, 2002, Morrow incised valley fill, Eddy County, New Mexico, *in* American Association of Petroleum Geologists SEPM Annual Convention Official Program, p. 153.
- Saltzman, M. R., 2003, Late Paleozoic ice age: Oceanic gateway or pCO₂? *Geology*, v. 31, p. 151–154.
- Scotese, C. R., 2004, A continental drift flipbook: paleoecology, paleogeography, and paleoclimatology: recent contributions honoring A. M. Ziegler, v. 112: Chicago, University of Chicago Press, p. 729–741.
- Sloss, L. L., 1963, Sequences in the cratonic interior of North America: *Geological Society of America Bulletin*, v. 74, p. 93–113.
- Speer, S. W., 1993, Permian Basin pre-Permian plays: overview, *in* Hjellming, C. A., ed., *Atlas of major Rocky Mountain gas reservoirs: New Mexico Bureau of Mines and Mineral Resources*, p. 153–164.
- Staples, M. E., 1986, Oil-productive basal Pennsylvanian channel-fill sandstones, southern Baylor County, Texas, *in* Ahlen, J. L., and Hanson, M. E., eds., *American Association of Petroleum Geologists, Southwest Section, transactions and guidebook of 1986 convention, Ruidoso, New Mexico, April 27–29, Socorro, NM: New Mexico Bureau of Mines and Mineral Resources*, p. 107–113.
- Torsvik, T. H., and Cocks, L. R. M., 2004, Earth geography from 400 to 250 Ma: a palaeomagnetic, faunal and facies review: *Journal of the Geological Society*, v. 161, p. 555–572.
- Van der Loop, M. L., 1991, Depositional environments in the Arenoso Field, Winkler County, Texas Permian Basin plays; tomorrow's technology today p. 73–91.
- Van der Voo, R., and Torsvik, T. H., 2001, Evidence for late Paleozoic and Mesozoic non-dipole fields provides an explanation for the Pangea reconstruction problems *Earth and Planetary Science Letters*, v. 187, p. 71–81.
- Van Dok, R., and Gaiser, J. 2001, Stratigraphic description of the Morrow Formation using mode-converted shear waves: interpretation tools and techniques for three land surveys: *The Leading Edge*, v. 20, p. 1042–1047.
- Watson, W. G., 1980, Paleozoic stratigraphy of the Llano Uplift area: a review, *in* Windle, D., ed., *Geology of the Llano region, central Texas: West Texas Geological Society*, p. 28–51.
- Yang, K.-M., and Dorobek, S. L., 1995, The Permian Basin of West Texas and New Mexico: tectonic history of a “composite” foreland basin and its effects on stratigraphic development, *in* Dorobek, S. L., and Ross, G. M., eds., *Stratigraphic evolution of foreland basins: SEPM (Society for Sedimentary Geology)*, v. 52, p. 149–174.
- Ye, H., Royden, L., Burchfiel, C., and Schuepbach, M., 1996, Late Paleozoic deformation of interior North America: the greater ancestral Rocky Mountains: *American Association of Petroleum Geologists Bulletin*, v. 80, p. 1397–1432.

Zaitlin, B. A., Dalrymple, R. W., and Boyd, R., 1994, The stratigraphic organization of incised-valley systems associated with relative sea-level change, *in* Dalrymple, R. W., Boyd, R., and Zaitlin, B. A., eds., *Incised-valley systems: origin and sedimentary sequences*: SEPM (Society for Sedimentary Geology), v. 51, p. 45–60.

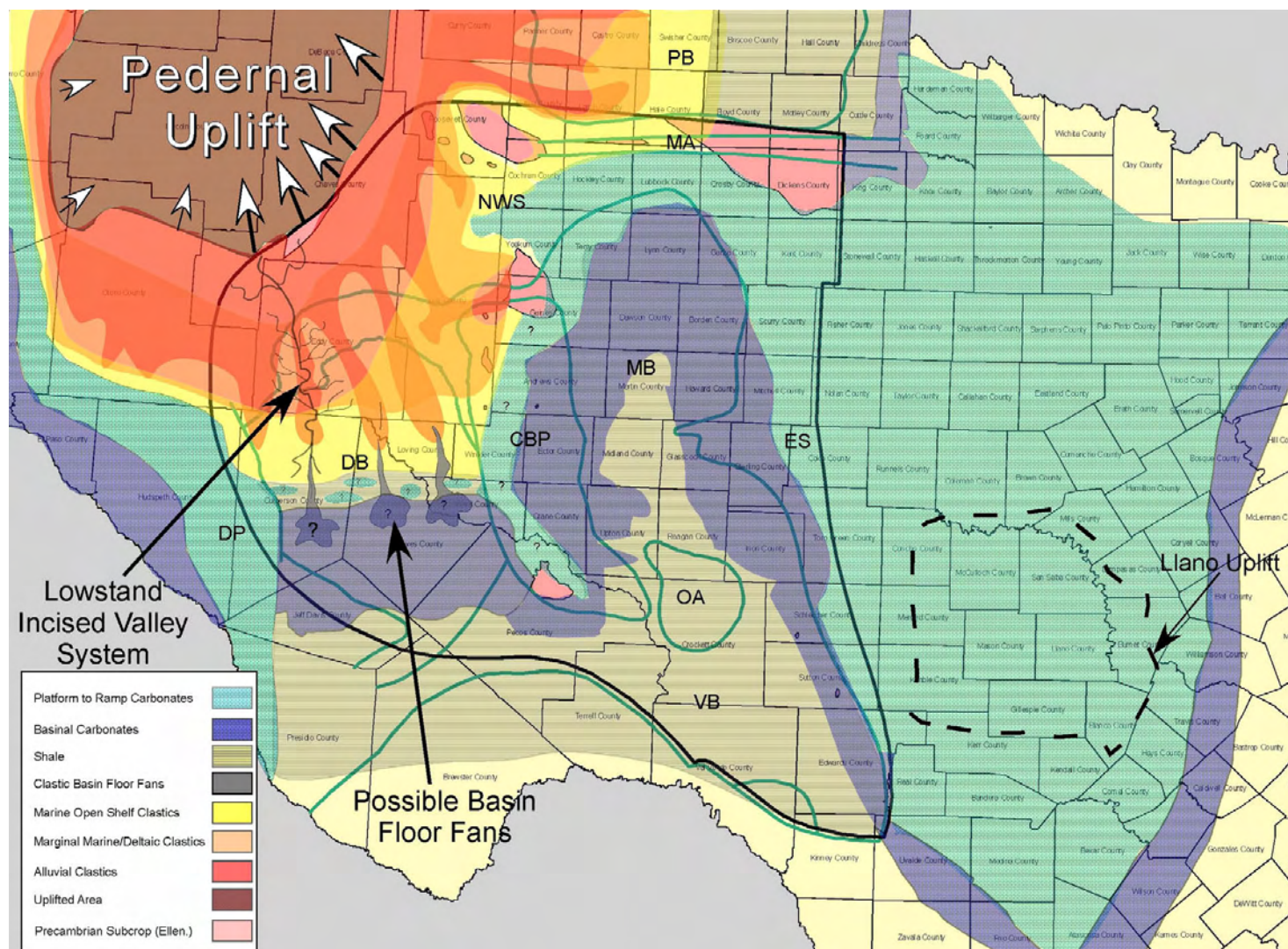


Figure 1. Regional paleogeographic reconstruction of Morrowan-age sediments. The illustration is based on a time slice possibly equivalent to the Middle Morrow Formation in the Delaware Basin during a lowstand event. Major subregions are labeled as follows and are outlined by dark-green lines: Central Basin Platform (CBP), Delaware Basin (DB), Diablo Platform (DP), Eastern Shelf (ES), Matador Arch (MA), Midland Basin (MB), Northwest Shelf (NWS), Ozona Arch (OA), Palo Duro Basin (PB), and Val Verde Basin (VB). Question marks indicate areas of inferred depositional environment and facies with limited data control. All geometries are schematic only and may not correspond to actual size and distribution. Llano Uplift area outlined by black dashed line. Sizes of arrows surrounding the Pedernal Uplift correspond to relative amount of uplift (that is, larger arrow equals greater relative uplift). Note that Pedernal Uplift is possibly linked to Sierra Grande Uplift to the north.

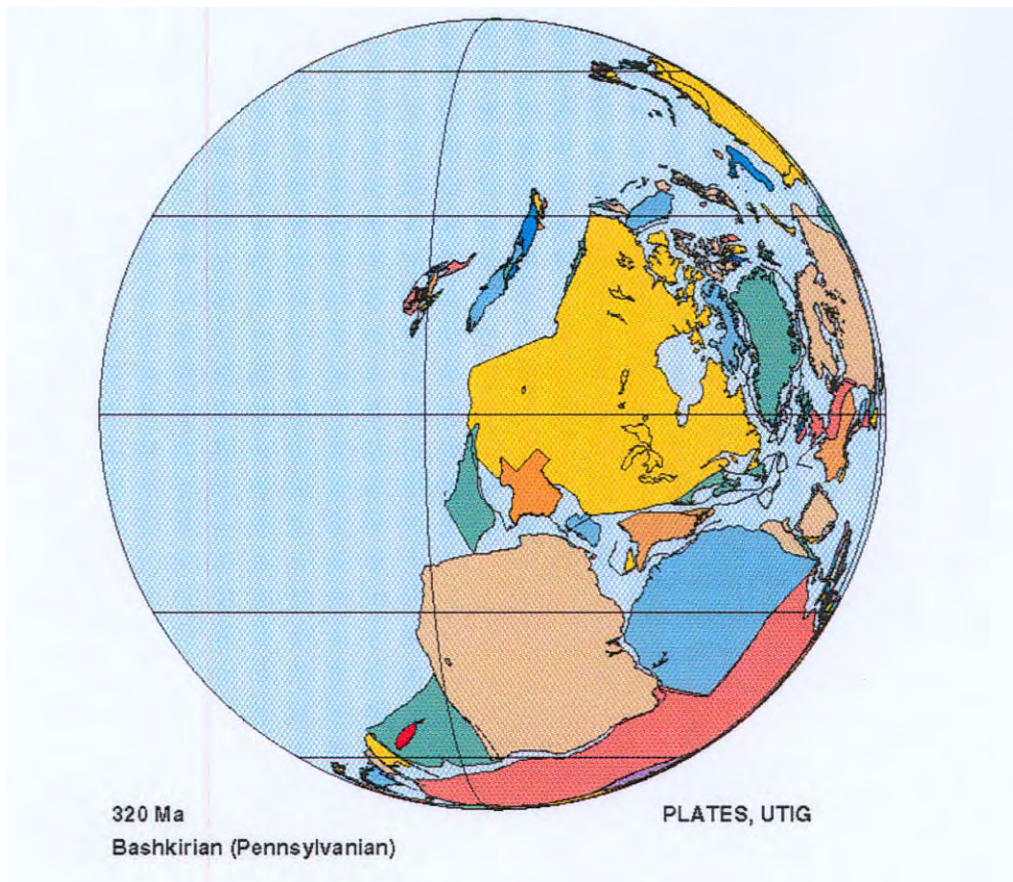


Figure 2. Morrowan-age Texas plate tectonic reconstruction. Note the marine (light-blue) to continental (light-orange) transition that occurs across Texas (dark-orange) in the area of the Permian Basin. Also note that suturing of the continents has resulted in a marine inland sea between the green, brown, dark-blue, and light-orange plates. Diagram modified from Dalziel and others (2002). Compare proposed extent of continental suturing in the Permian Basin area in figures 2 and 3.

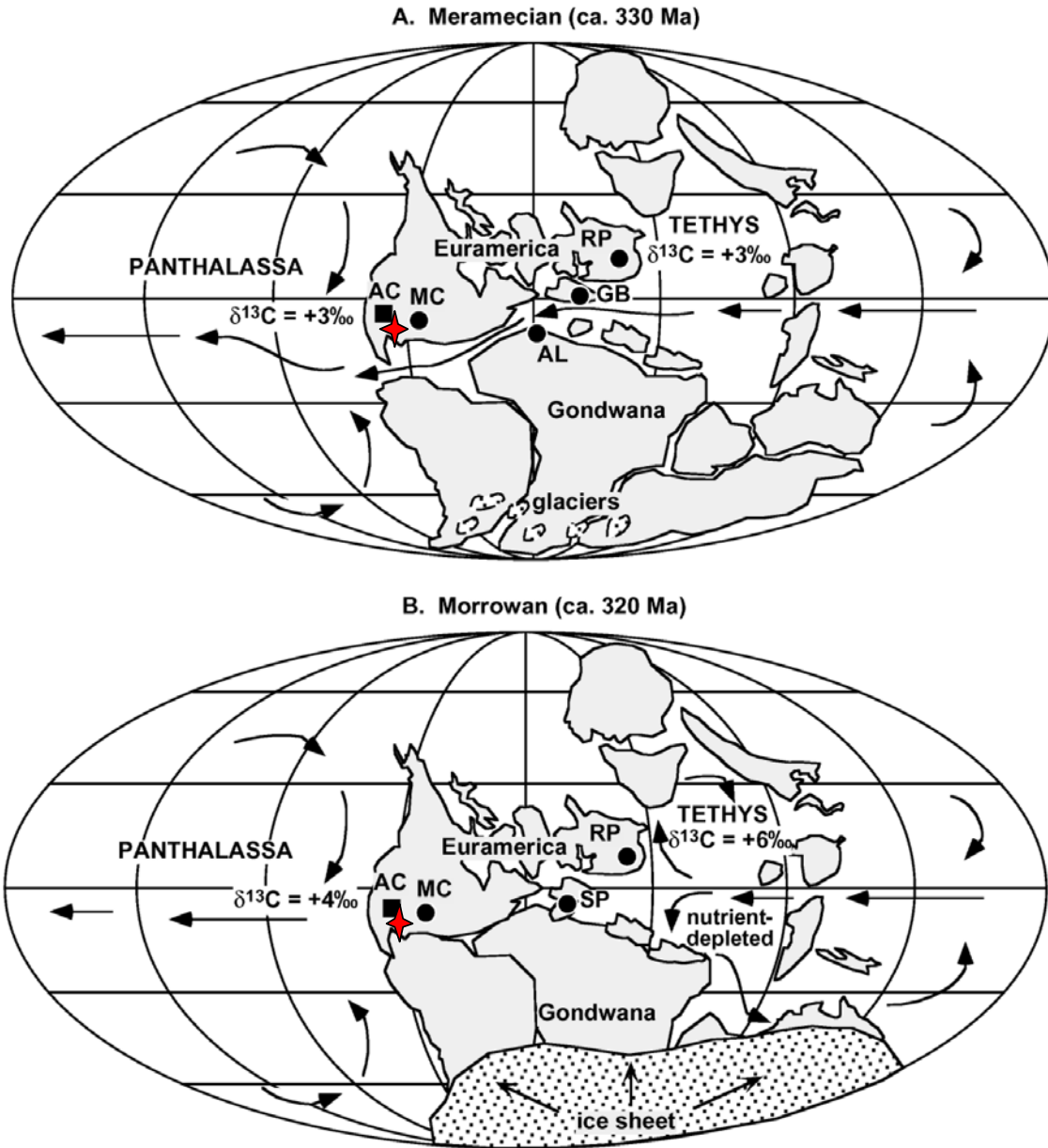


Figure 3. Paleogeographic global reconstructions illustrating simplified extent of glaciation, ocean-water circulation, and carbon isotope water mass values. Red star indicates approximate region of the Permian Basin. AC = Arrow Canyon, Nevada; MC = Midcontinent, USA. Note restructuring of oceanic currents from Meramecian to Morrowan times coincident with the closing of the seaway between Euramerica and Gondwana. Diagram modified from Saltzman (2003). Note that Morrowan plate geometries in figure 3 are similar to those presented by Scotese (2004).

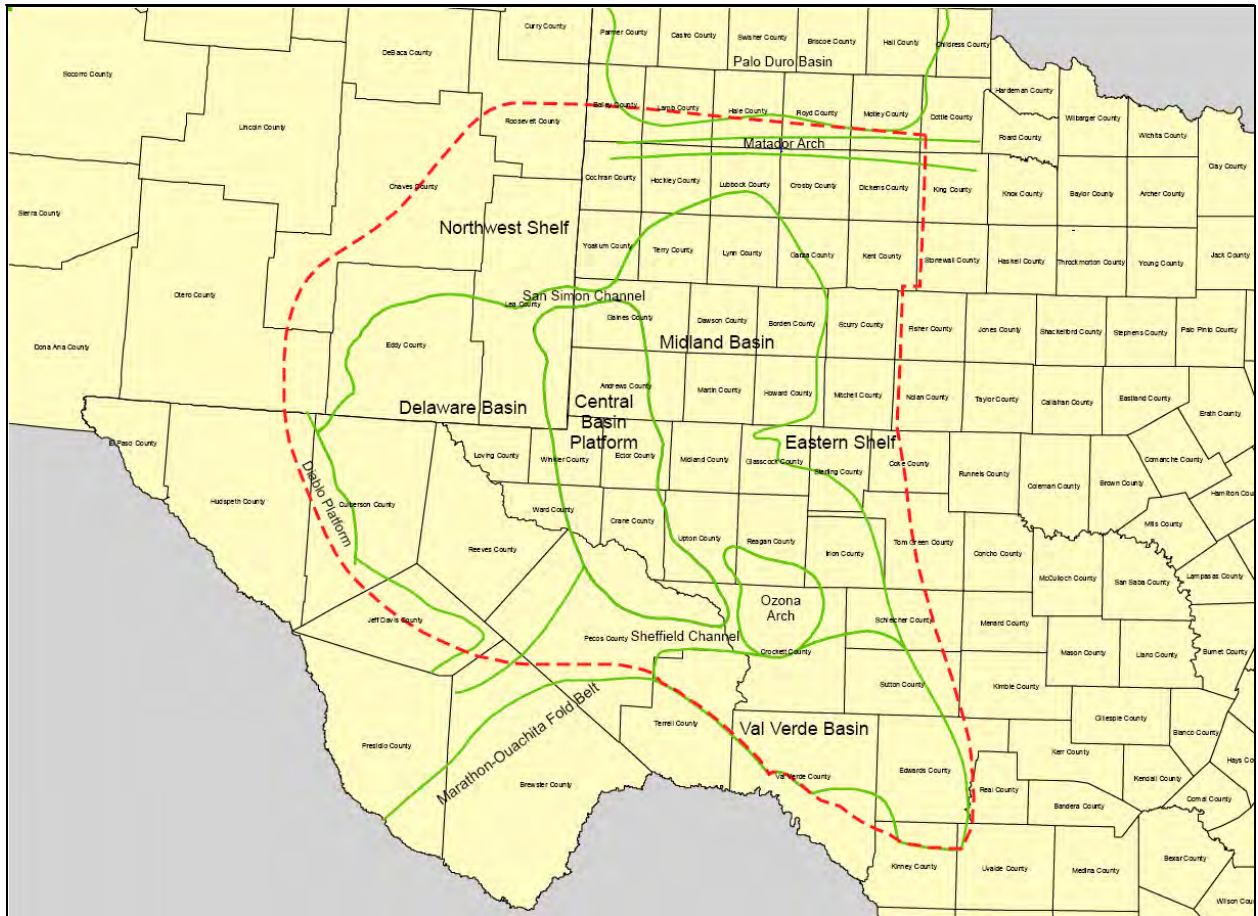


Figure 4. Permian Basin outline (dashed red) and major geologic features. Note that many features were not developed at Morrowan time. Also compare figure 4 with figures 5 and 6 for an idea of the distribution of facies relative to the basin outline.

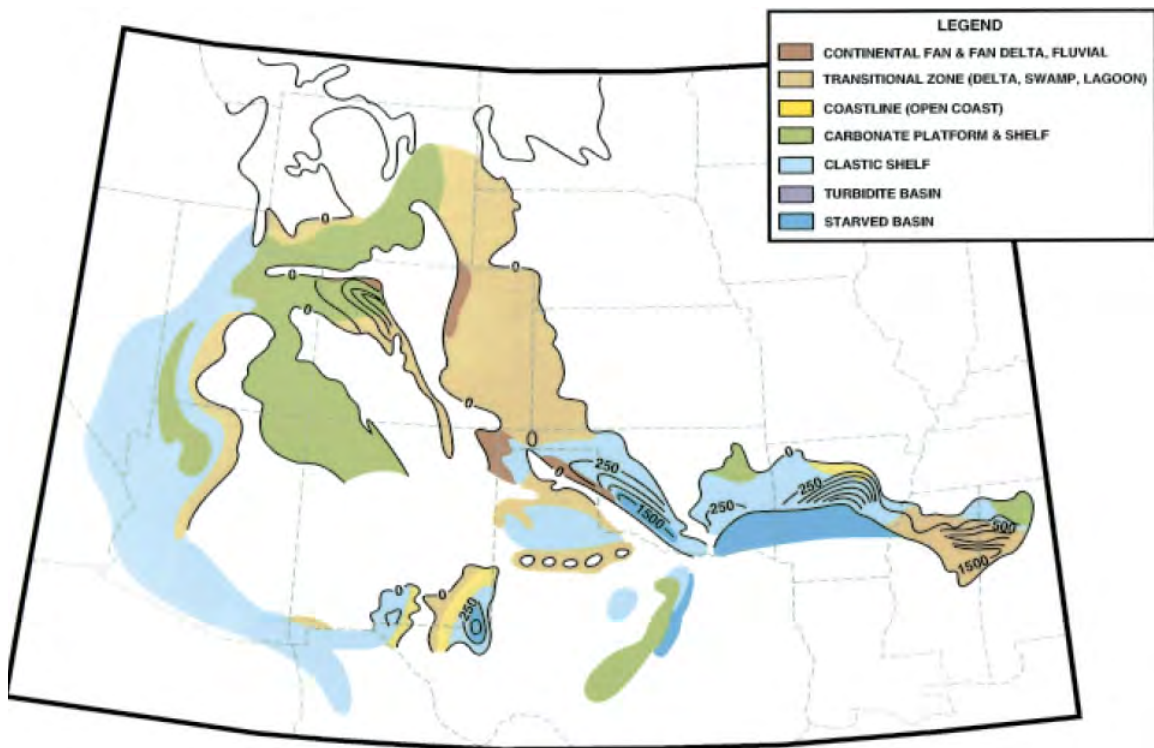


Figure 5. Generalized Rocky Mountain region and southern Midcontinent Morrowan paleogeography (modified from Ye and others, 1996). White areas indicate either nondeposition or erosion (not clarified in original text). Note that most of the Permian Basin was considered devoid of Morrowan sediments by Ye and others (1996).

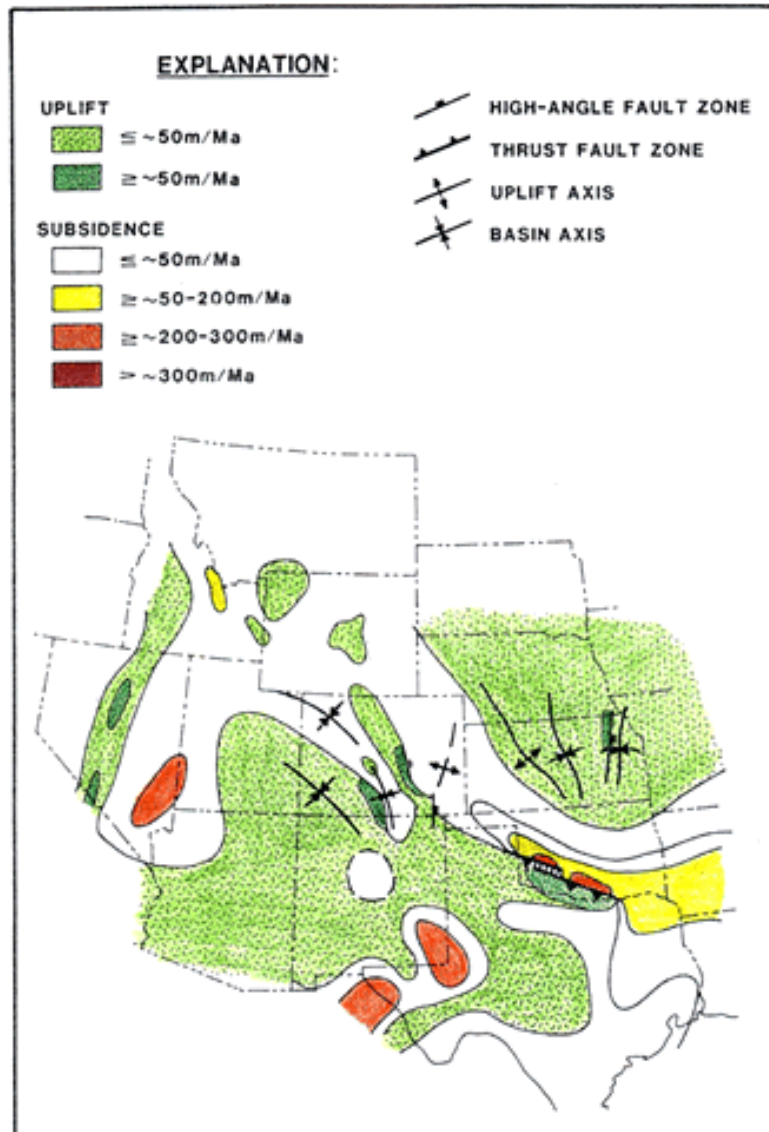


Figure 6. Morrowan net subsidence and uplift patterns for the Southern Rocky Mountain and Midcontinent regions (modified from Kluth, 1986). Green areas indicate net uplift, whereas white to red areas indicate net subsidence.

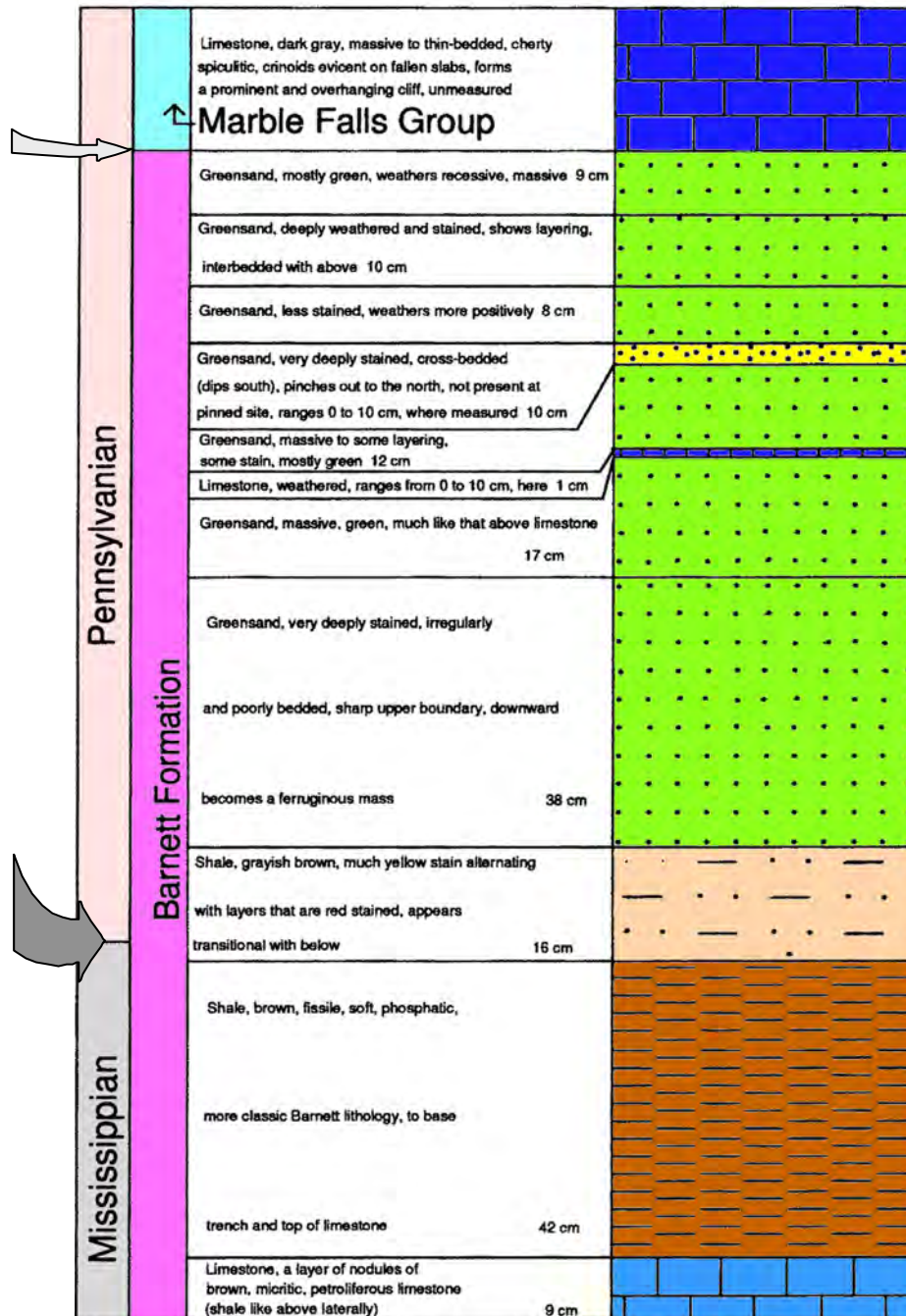


Figure 7. Llano Uplift stratigraphic column for a conformable Mississippian to Pennsylvanian transition (modified from Hoare and Merrill, 2004). Note that the Mississippian/Pennsylvanian boundary is placed within the Barnett Formation (large arrow), making the Upper Barnett (1.4 m [4.6 ft]) Pennsylvanian in age. Previous interpretations commonly place the Mississippian/Pennsylvanian boundary at the base of the Marble Falls Formation (small arrow).

Pennsylvanian	Atokan		
	Morrowan	“C” zone	Upper Morrow
		“B” zone	Middle Morrow
		“A” zone	Lower Morrow
Mississippian		Mississippian Limestone	Barnet Shale
Mississippian/Devonian		WOODFORD	

Figure 8. General stratigraphic column for Mississippian- and Pennsylvanian-age units in Northwest Delaware region of the Permian Basin (modified from Coker, 2003). Within Morrowan-age units the yellow fill in the Lower and Middle Morrow indicates a dominance of siliciclastic deposition in that area, whereas the blue fill of the Upper Morrow indicates carbonate deposition.

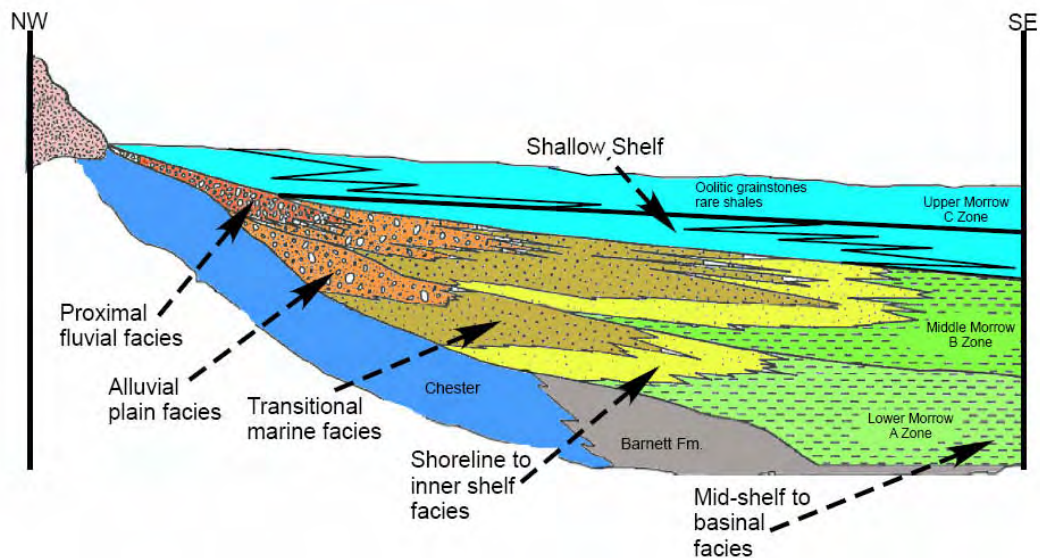


Figure 9. Schematic representation of Morrowan-age depositional environments, geometries, and the relationship to underlying units in New Mexico (modified from Mazzullo, 1984). However, in this study the uppermost Barnett Formation is included in the Lower Morrow.

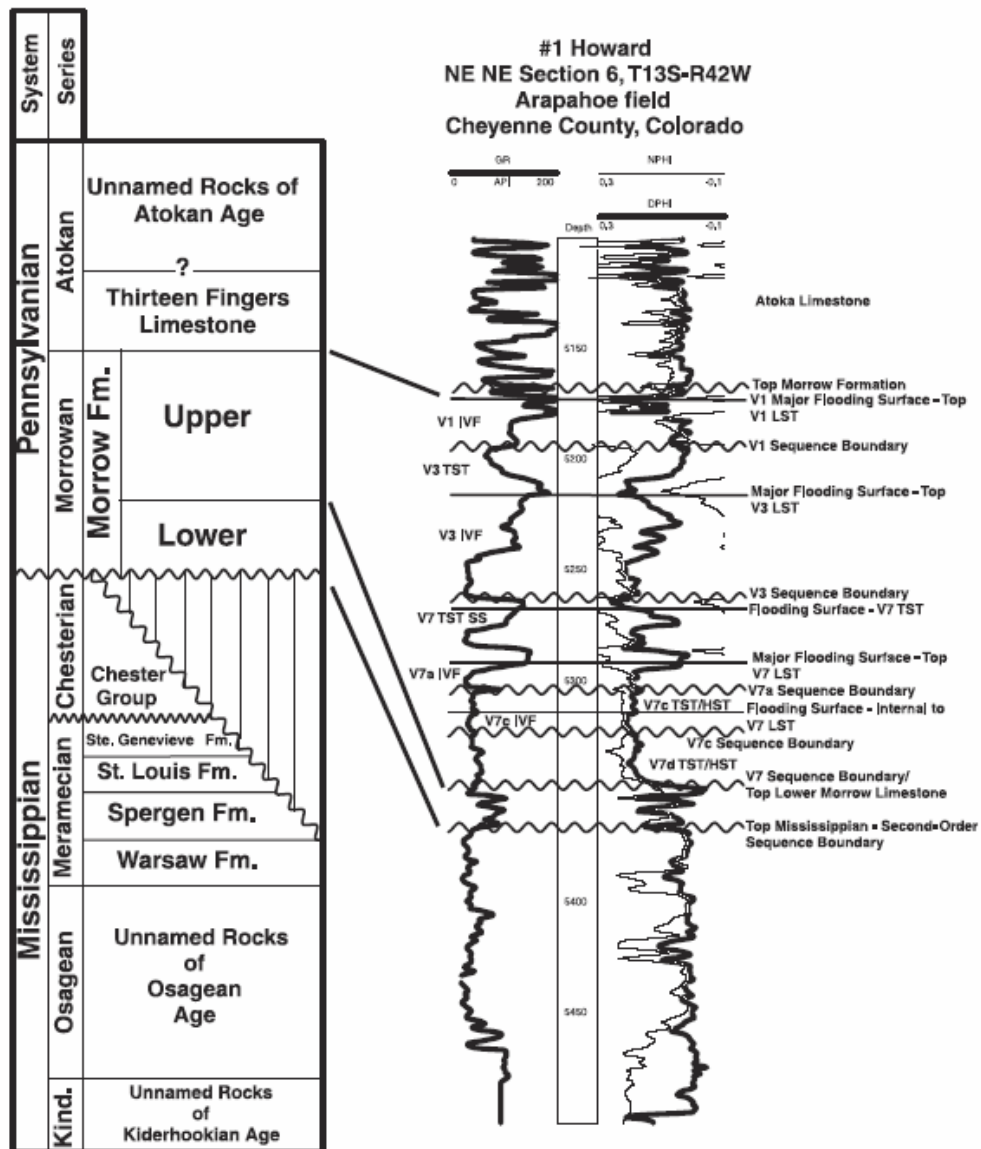


Figure 10. Type wireline-log section for Morrow Formation in western Kansas and eastern Colorado (modified from Bowen and Weimer, 2003). Note that Lower Morrow is carbonate, whereas Upper Morrow is siliciclastic. Also note V7 major flooding surface above the lowstand systems tract (LST). See figures 12 and 13 for relationship of flooding surface to facies descriptions and geometries.

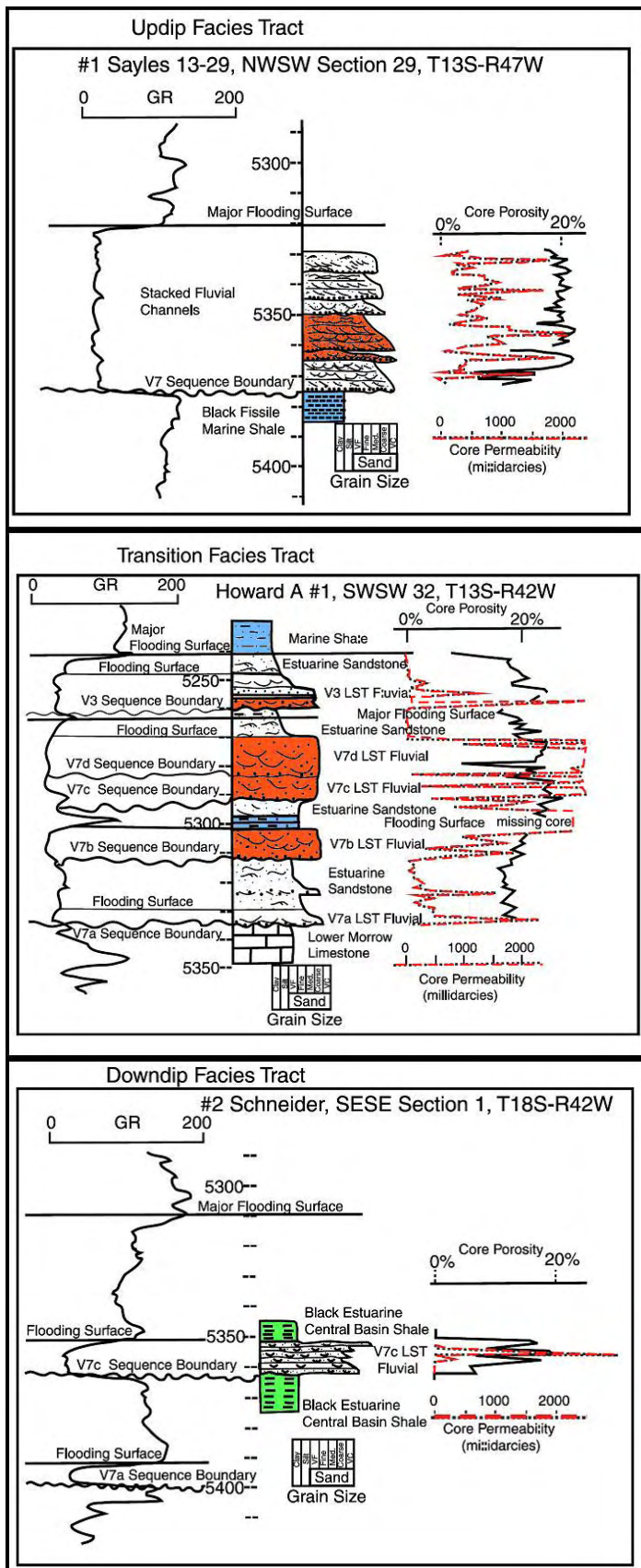


Figure 11. Core descriptions and wireline-log signatures for facies tracts defined by Bowen and Weimer (2003). Red dashed line indicates core permeability in millidarcys. Note different facies interpretation when compared with figure 29 by James (1984) for similar gamma patterns. Also note that within a given facies environment having consistent porosity, high permeability values are much more restricted (for example, updip facies tract of stacked fluvial channels highlighted in red). Modified from Bowen and Weimer (2003).

#3 Schneider 34-1
SWSE Section 1, T18S-R42W
Jace Field

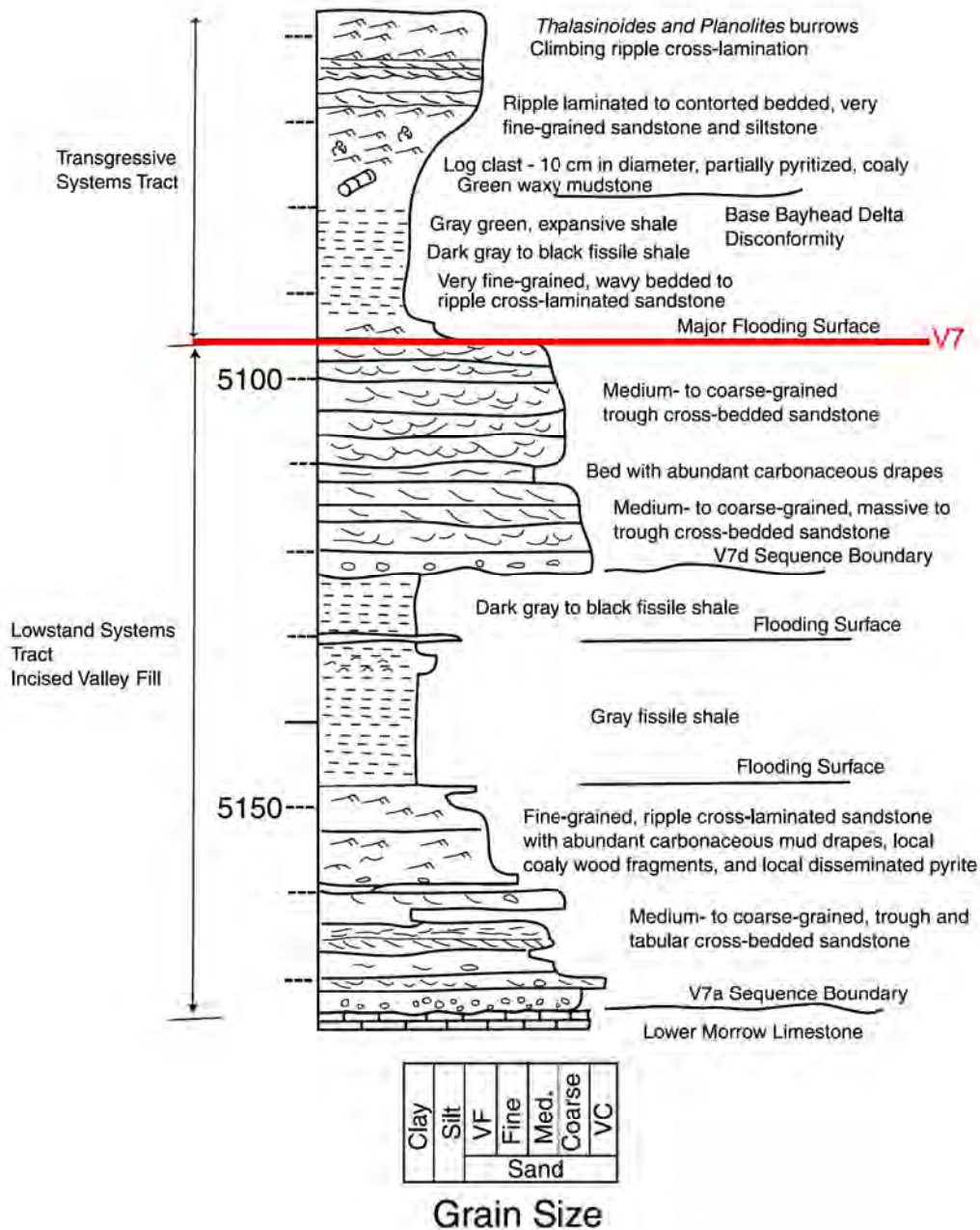


Figure 12. Sedimentological descriptive log for No. 3 Schneider 34-1 well illustrating facies stacking patterns for a “downdip facies tract.” See Bowen and Weimer’s (2003) figure 7a for accompanying core photos. Note V7 “regional” flooding surface highlighted in red. Note change from lowstand to transgressive systems tract that will not be overly apparent on wireline logs.

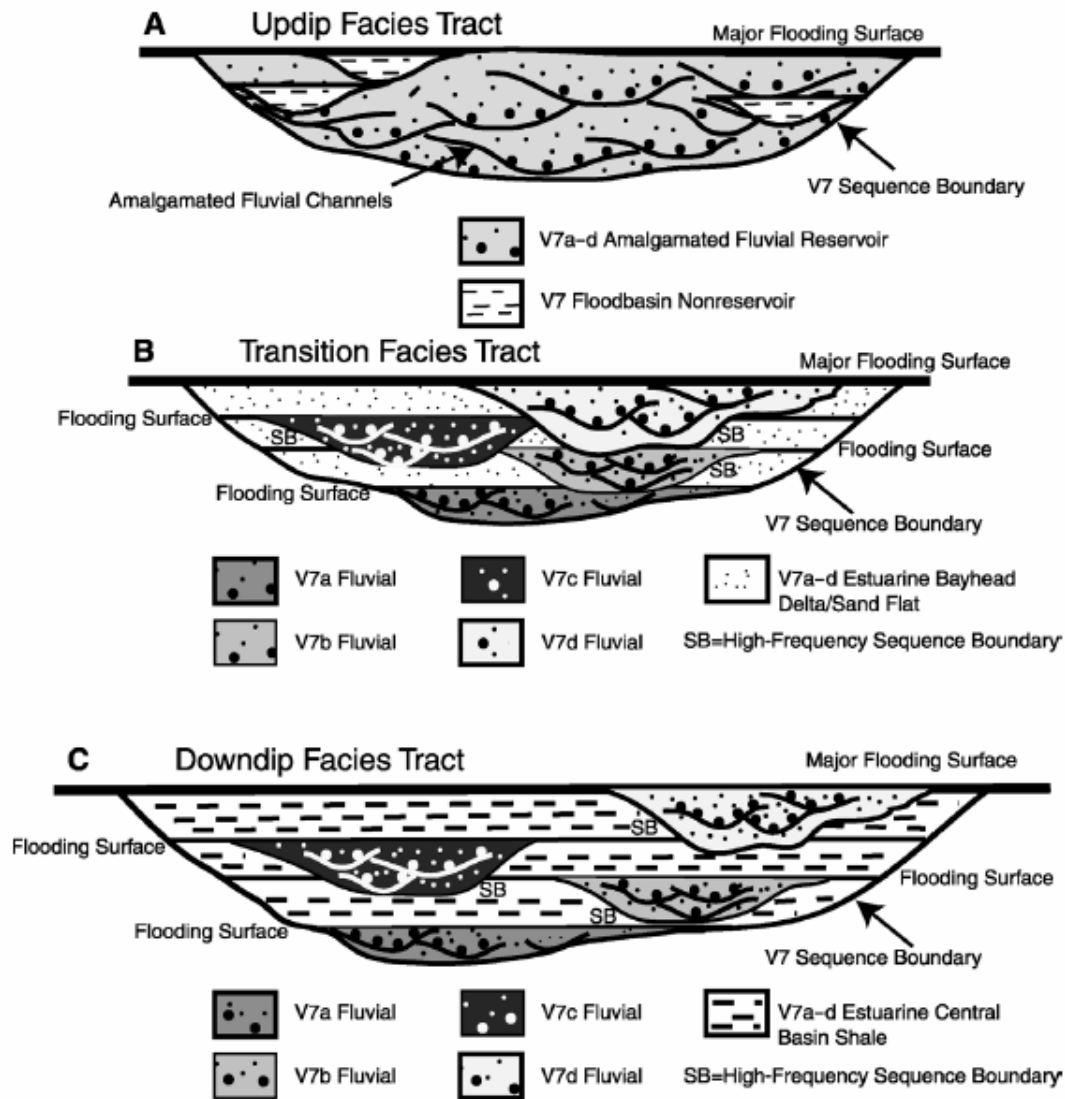


Figure 13. Illustration of the cross-sectional profiles and facies stacking patterns for updip, transitional, and downdip tracts (modified from Bowen and Weimer, 2003). Note that extent, quality, and connectivity of the reservoirs change between facies tracts. Note that major flooding surface (V7) at the top of each facies tract is equivalent.

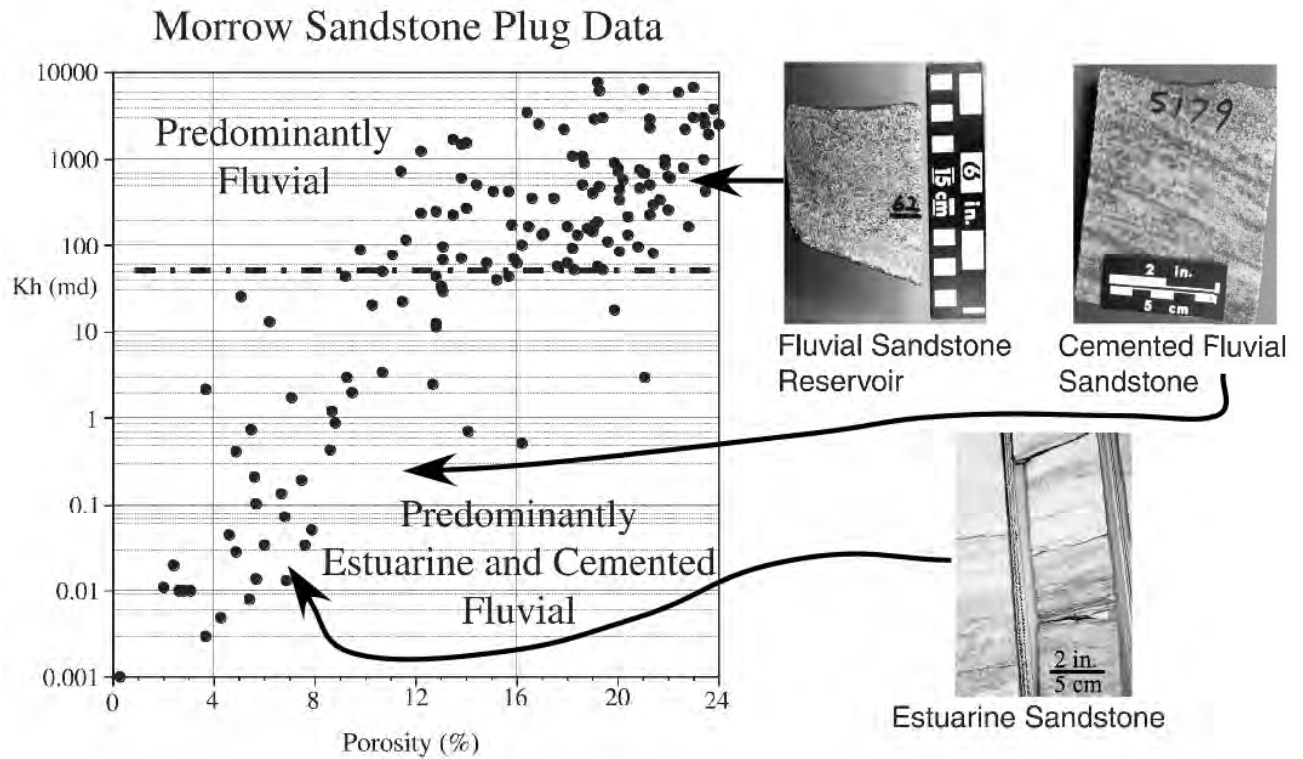


Figure 14. Porosity versus permeability cross plot with respective core photographs of associated facies. Note better reservoir quality in the fluvial sediments. Also note that the cemented fluvial facies with its decreased reservoir quality may be associated with the permeability trend noted in figure 11A (modified from Bowen and Weimer, 2003). In figures 11B and 10 the decreased reservoir quality of the estuarine sandstones is not apparent on wireline logs because porosity is relatively similar for fluvial and estuarine facies.

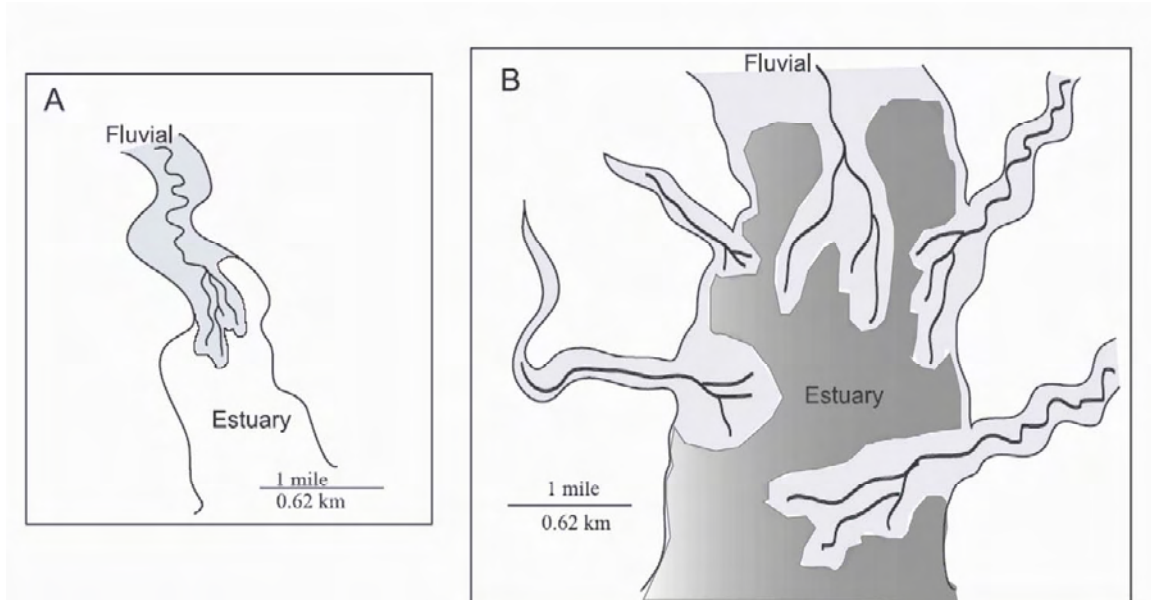


Figure 15. Aerial comparison of bayfill delta depositional area in (A) “updip” (transitional facies tract of Bowen and Weimer, 2003) confined valley-fill system versus (B) broader “down-dip” tributary estuary (modified from Bowen and Weimer, 2004). Note that a high proportion of shale is deposited in interdelta lobe areas (dark-gray) in the estuary. Bayhead delta (both proximal and distal) facies are in light-gray.

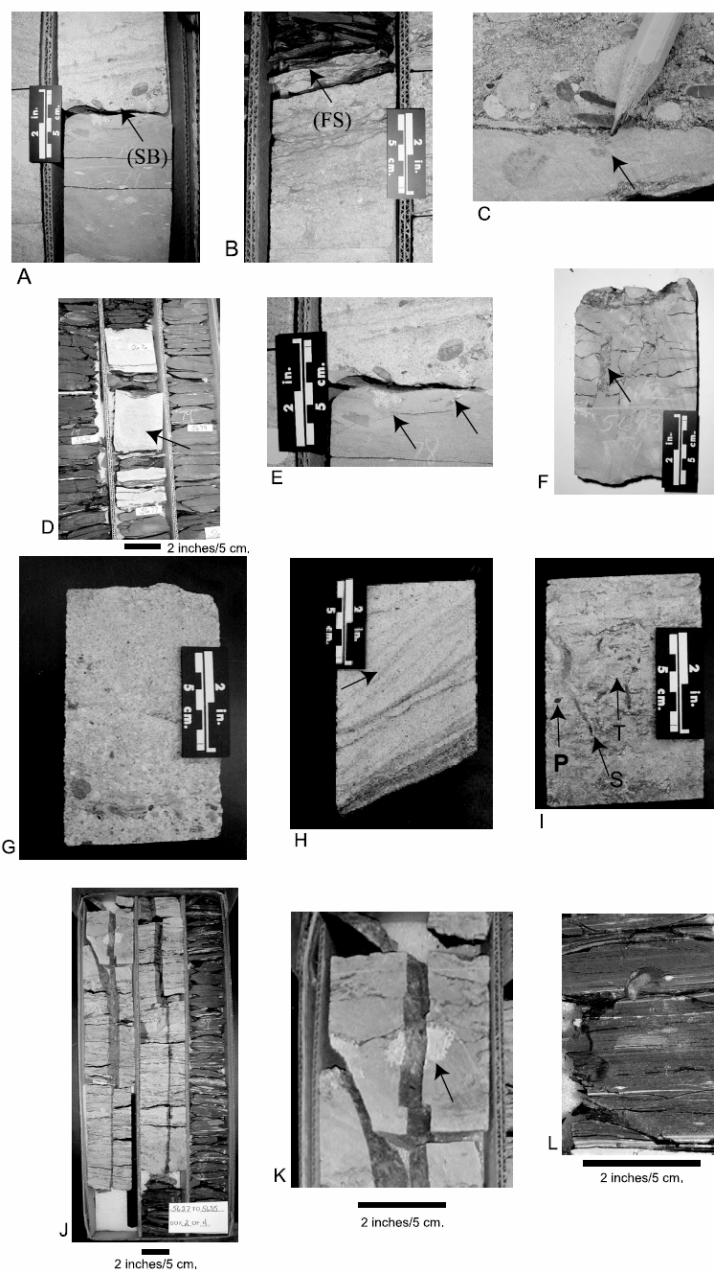


Figure 16. Key features identifiable in core (A) basal Morrow sequence boundary, (B) flooding surface at top of fluvial succession, (C) basal bayfill delta disconformity (*Glossifungites* surface), (D) transgressive lag at major flooding surface, (E) sand-filled burrows at base fluvial unconformity (*Glossifungites* surface), (F) pedogenic fractures in the Mississippian Chester Formation, (G) medium to coarse pebbly arkosic sand, (H) potential tidal influence (reactivation surface and double mud drapes), (I) bioturbated zone (includes *Skolithus*, *Planolites*, and *Teichicnus*), (J) laminated central “basin” estuary shale overlain by distal bayhead delta facies, (K) solitary coral from upper bayhead delta facies, and (L) marine shale above major flooding surface (modified from Bowen and Weimer, 2004). Note that all photos are related to core description and facies shown in figure 17.

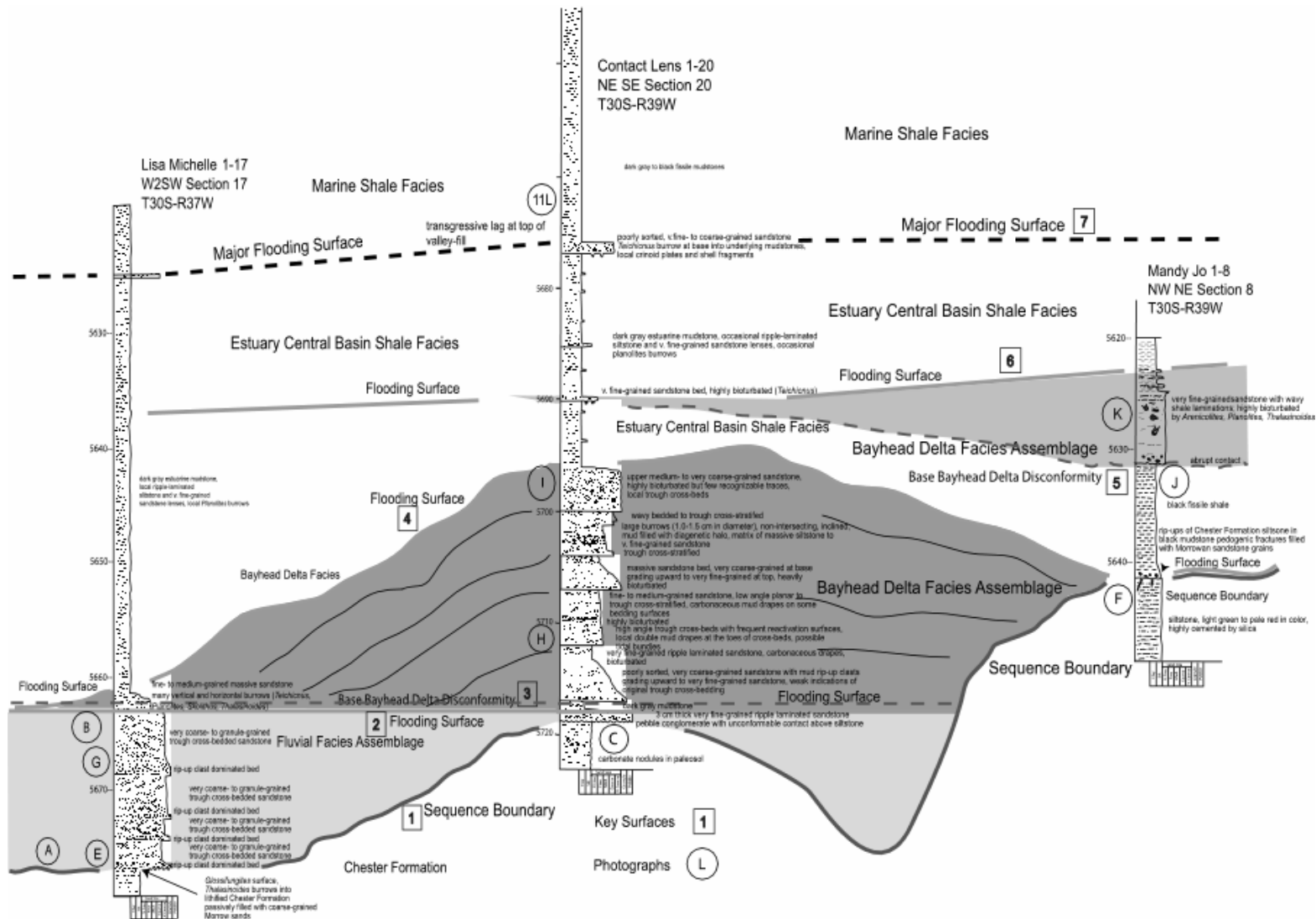


Figure 17. Descriptive log correlation illustrating facies interrelations between basal fluvial, bayhead delta, and estuarine shales within a large estuary complex (modified from Bowen and Weimer, 2004). Note stacked shale succession in Contact Lens 1-20 well.

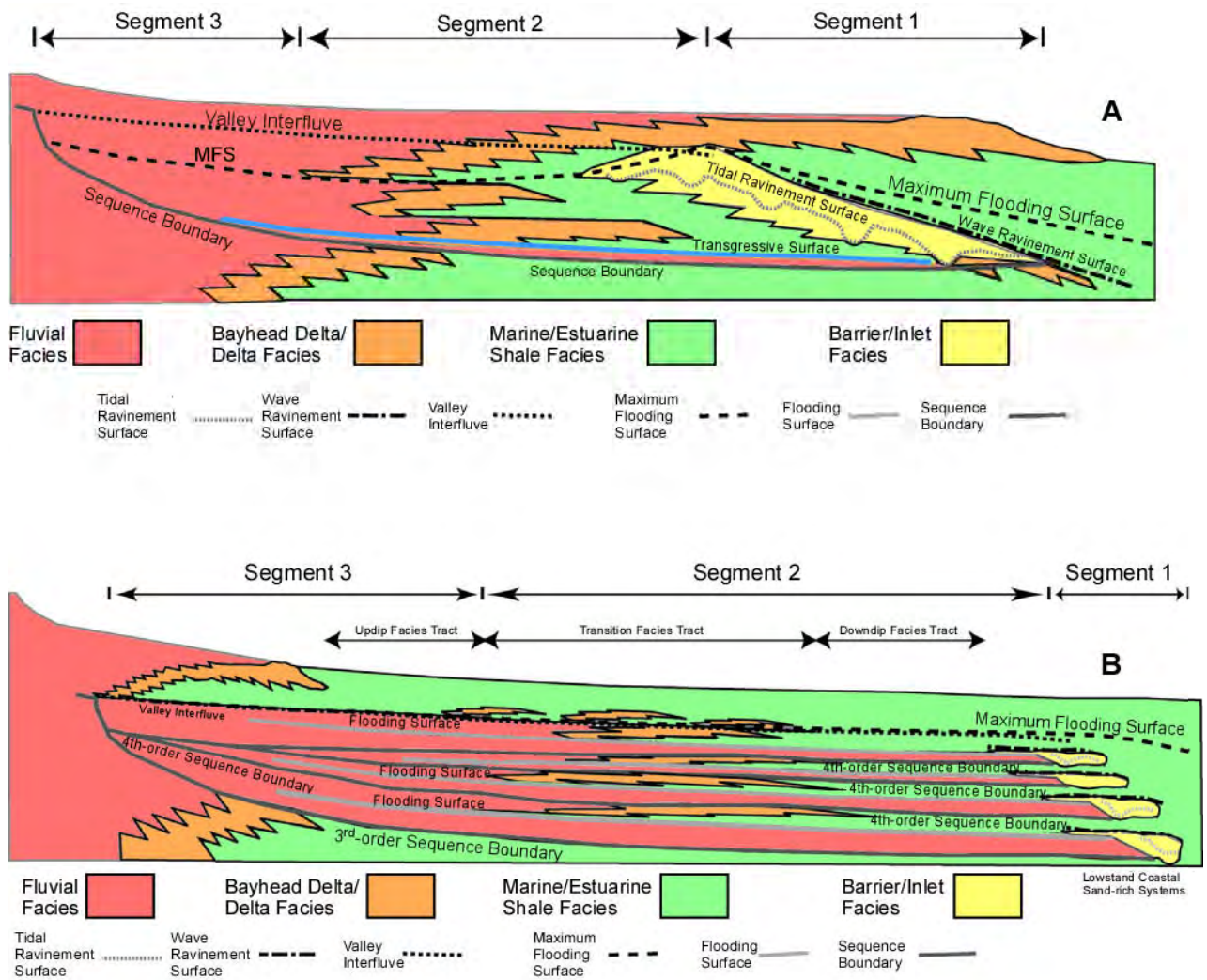


Figure 18. Sequence-stratigraphic architectural models for valley-fill-type sedimentation. (A) Greenhouse model devised by Zaitlin and others (1994), and (B) icehouse model designed by Bowen and Weimer (2003). Note differences in unit thicknesses, lengths, and segment area, as well as extent and position of wave and tidal ravinement surfaces.

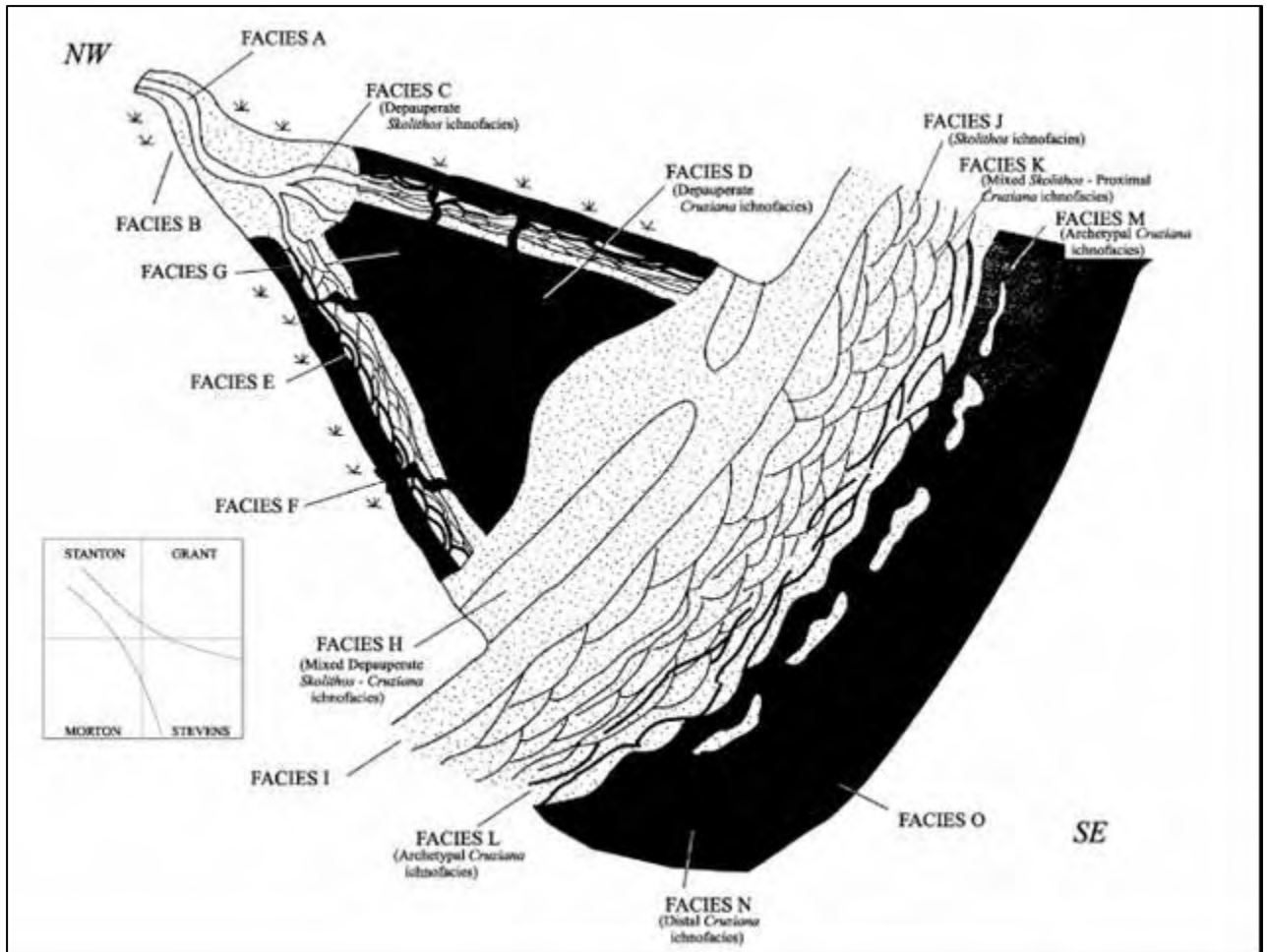


Figure 19. Depositional model for the Lower Morrow. Note similarity to regional model proposed by James 1985 (fig. 24). On the depositional model ichnofacies guilds and associations are also highlighted, resulting in better constraints for correlation (modified from Buatois and others, 2002). Best reservoir quality is in facies A.

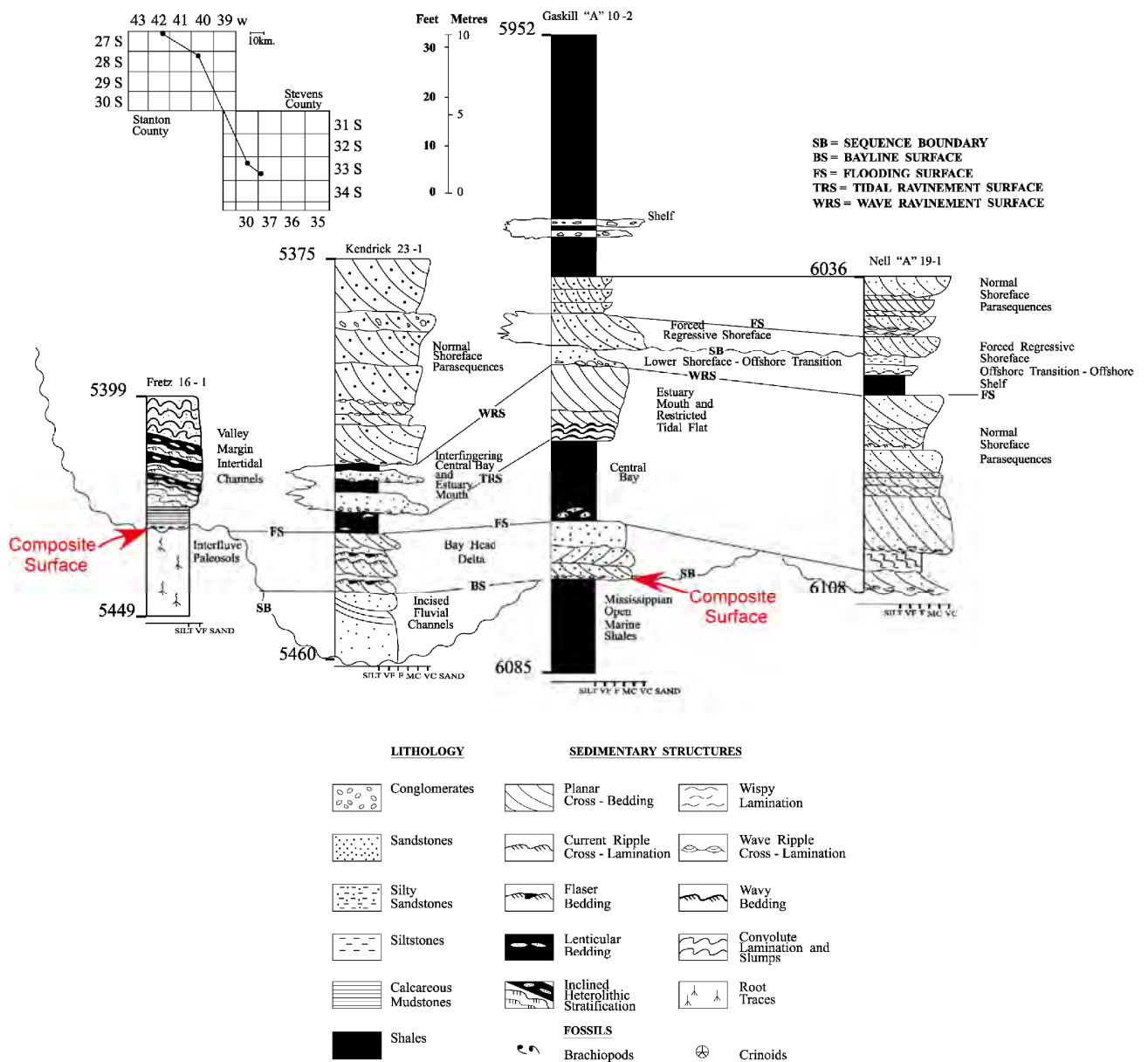


Figure 20. Log and core correlation of Lower Morrow in southwest Kansas. Note abrupt facies transitions between wells and upward replacement of estuarine shales by more marine shales Modified from Buatois and others (2002).

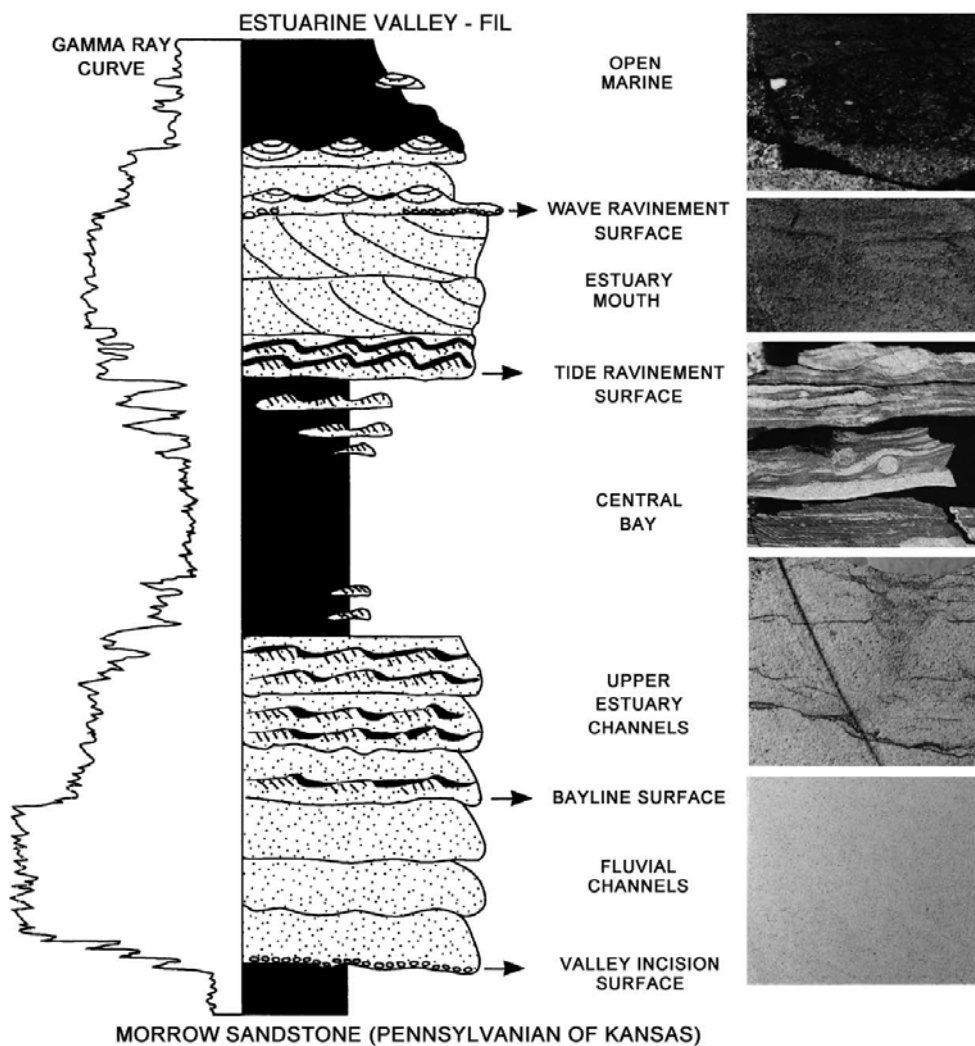


Figure 21. Core photographs, descriptive log, and gamma-ray correlation of estuarine valley-fill sediments. Note the gamma-ray values in upper estuary channel sands and equivalent gamma-ray values for open-marine and estuarine shales. Modified from Buatois and others (2002).

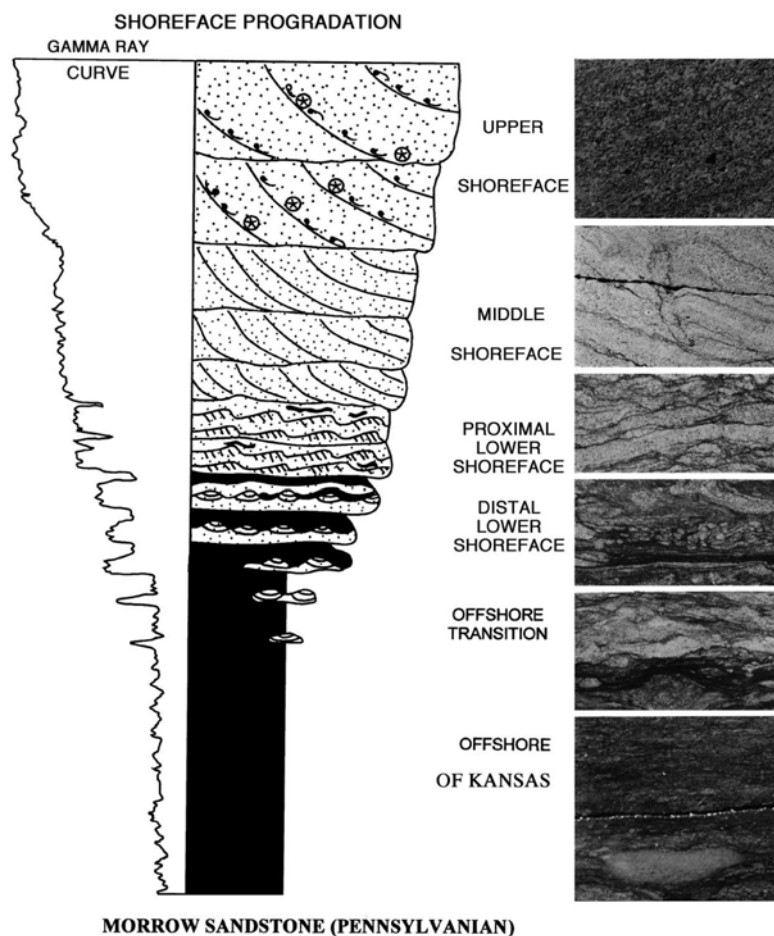


Figure 22. Core photographs, descriptive log, and gamma-ray correlation of the open-marine to shoreface cycles. Note similarity in gamma-ray values between estuary (fig. 21) and open-marine shales Modified from Buatois and others (2002).

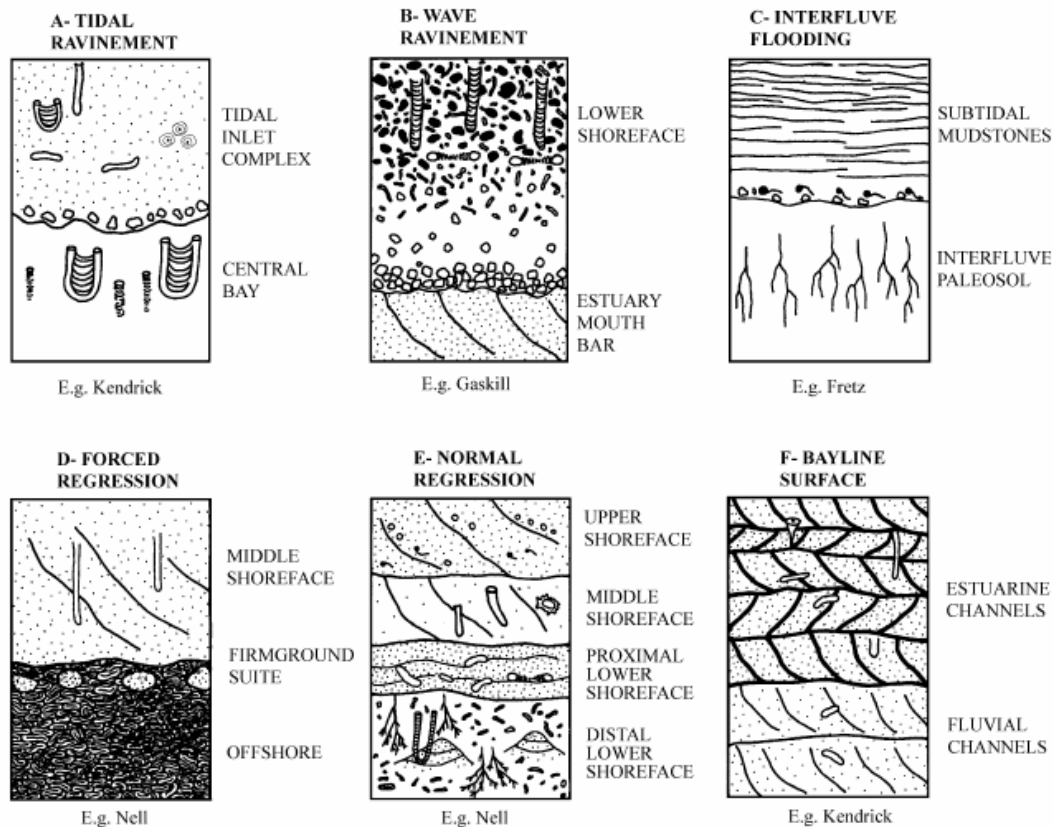


Figure 23. Schematic diagrams illustrating sequence-stratigraphic and sedimentologic significance of ichnofossils from the Lower Morrow in Kansas. (A) Tidal-ravinement surface with low-diversity suites of *Diplocraterion* and *Teichichnus* below surface being replaced by *Palaeophycus*, *Asterosoma*, *Diplocraterion*, and *Skolithos*; (B) wave-ravinement surface with passage from estuarine environment to intensely bioturbated shoreface deposits with tiered suites of open-marine *Cruziana* ichnofacies, including long *Diplocraterion*, *Rhizocorallium*, *Palaeophycus*, and *Planolites*; (C) paleosol interfluvial flooding with vertical replacement of paleosols (root traces) by subtidal mudstones; a transgressive lag occurs on top of paleosols; (D) forced regression illustrated by intense bioturbated offshore deposits having a distal *Cruziana* assemblage, including *Thalassinoides*, *Chondrites*, and *Phycosiphon* being abruptly replaced by erosive-based, middle-shoreface deposits with elements of the *Skolithos* ichnofacies; erosive contact further demarcated by a *Thalassinoides* firmground; (E) normal regression with a gradual change in softground trace fossil assemblages; archetypal *Cruziana* ichnofacies occurs in distal lower shoreface, whereas a combined *Skolithos*-proximal *Cruziana* ichnofacies characterizes the proximal lower shoreface; *Skolithos* ichnofacies present in the middle shoreface, whereas the upper shoreface is mostly unbioturbated; (F) bayline flooding surface with bayhead delta deposits of overlying lowstand fluvial deposits, as indicated by appearance of clay drapes of tidal origin and *Skolithos* and *Monocraterion*. Modified from Buatois and others (2002).

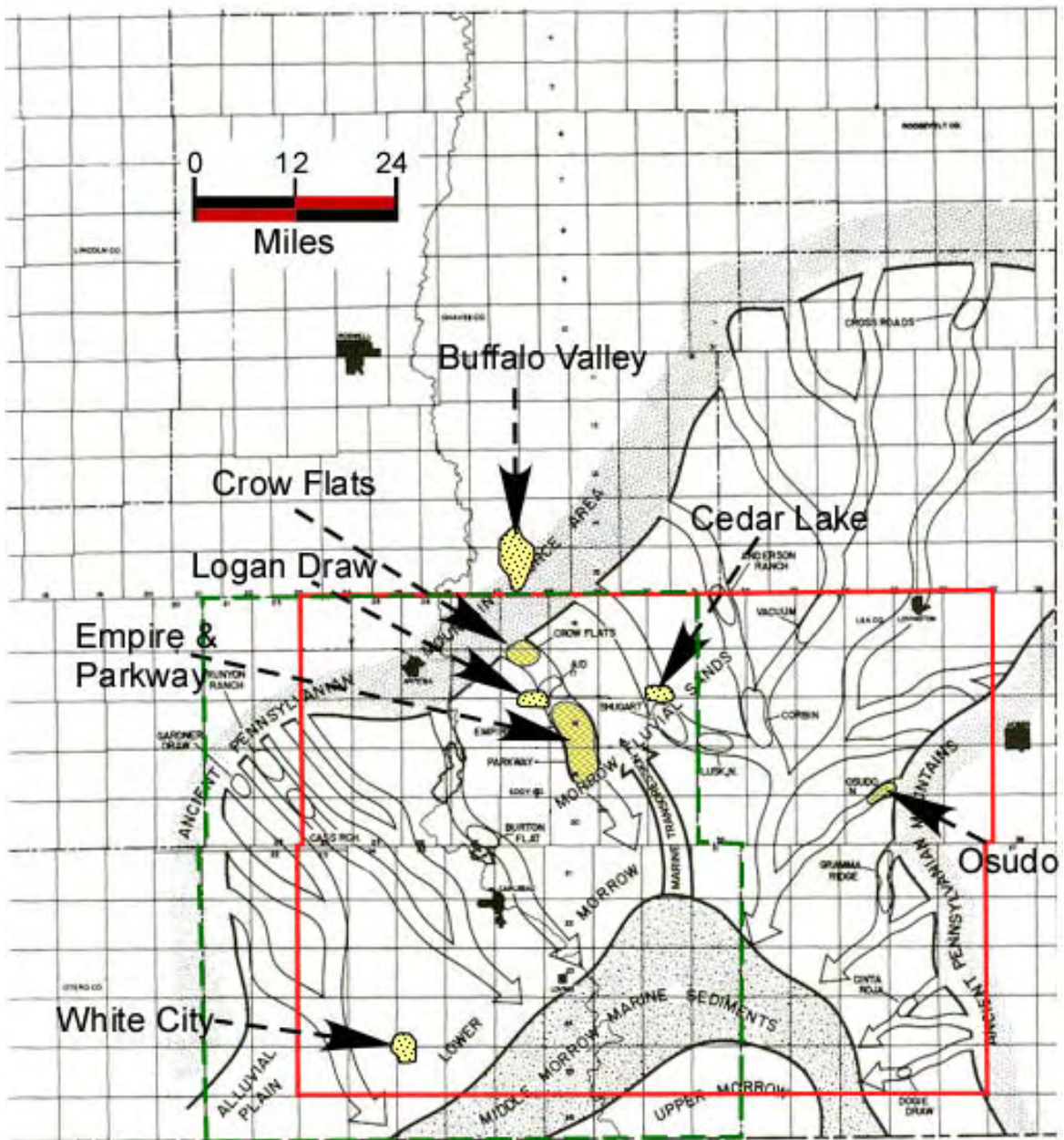


Figure 24. Regional distribution of Morrowan fields in New Mexico and generalized Morrowan paleogeography. Diagram modified from James (1984), with fields highlighted in yellow, Eddy County outlined in green. Facies tract area of Coker (2003) outlined in red corresponds to facies maps in figure 25.

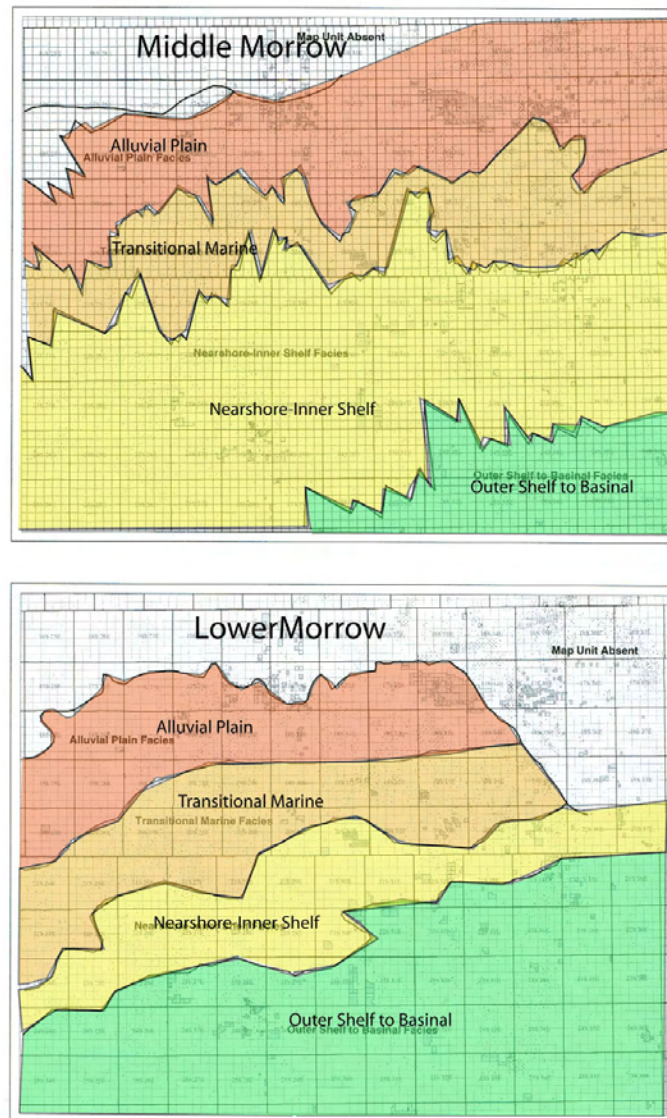


Figure 25. Facies progradation between Lower and Middle Morrow (modified from Coker, 2003). Note expansion and shift southeastward of the nearshore inner shelf facies belt. Overall, the siliciclastic succession is thought to thicken to the south. Note oversimplified layer-cake parallel facies distribution patterns and compare with figure 24. Note that area of the diagram corresponds to red outline in figure 24.

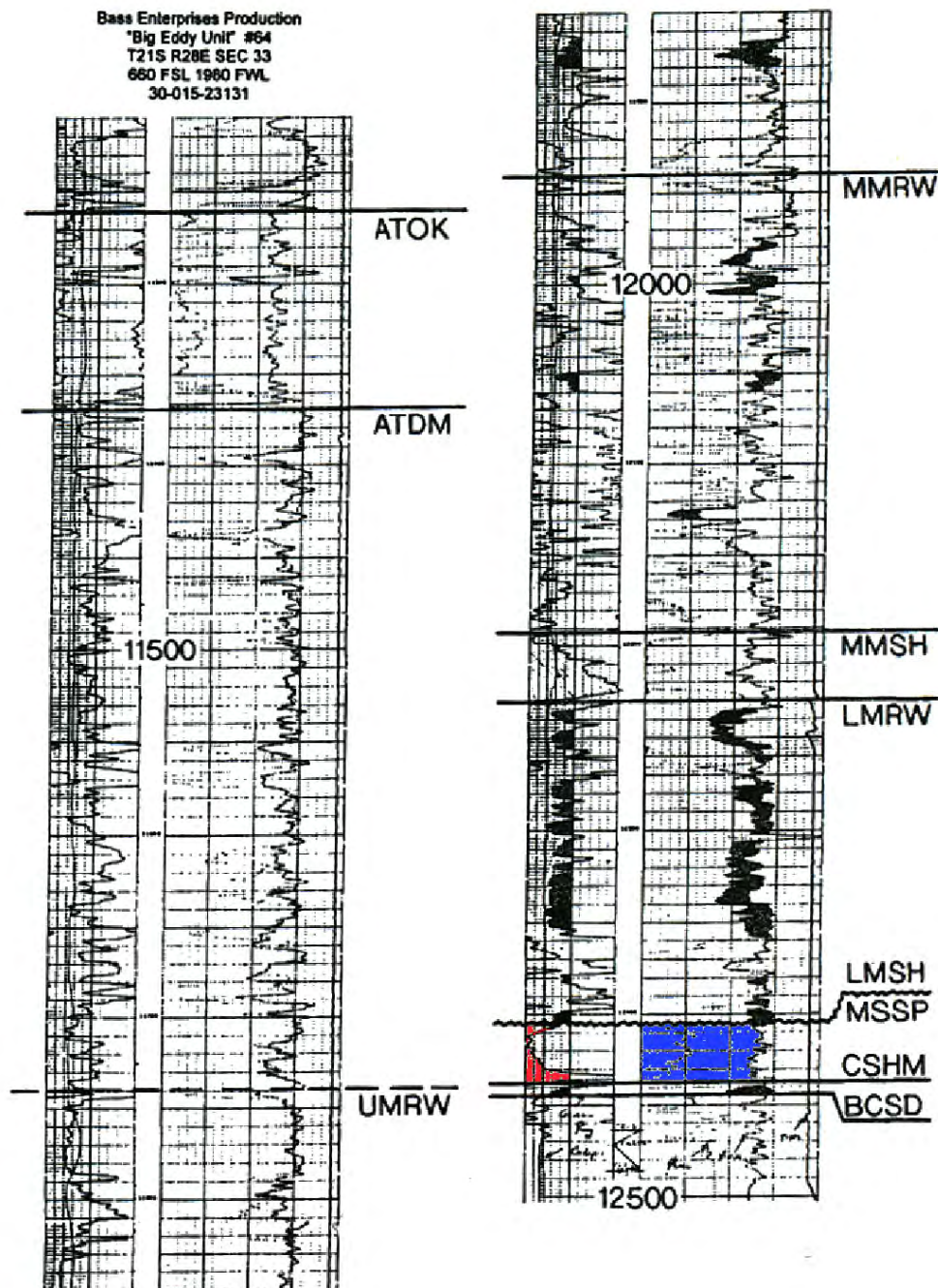


Figure 26. Type log for Morrowan-age sediments in New Mexico (modified from Roberts and Kohles, 1999). BCSD = base of Carlsbad sand, CSHM = Carlsbad shale marker, MSSP = top Mississippian (unconformity), LMSH = top of Lower Morrow marine shale, MMSH = top of Middle Morrow marine shale, ATOK = Atoka. Note that Middle Morrow shale is not considered correlative basinwide. Blue and red highlighted section of well log is proposed Mississippian-age Carlsbad sand.

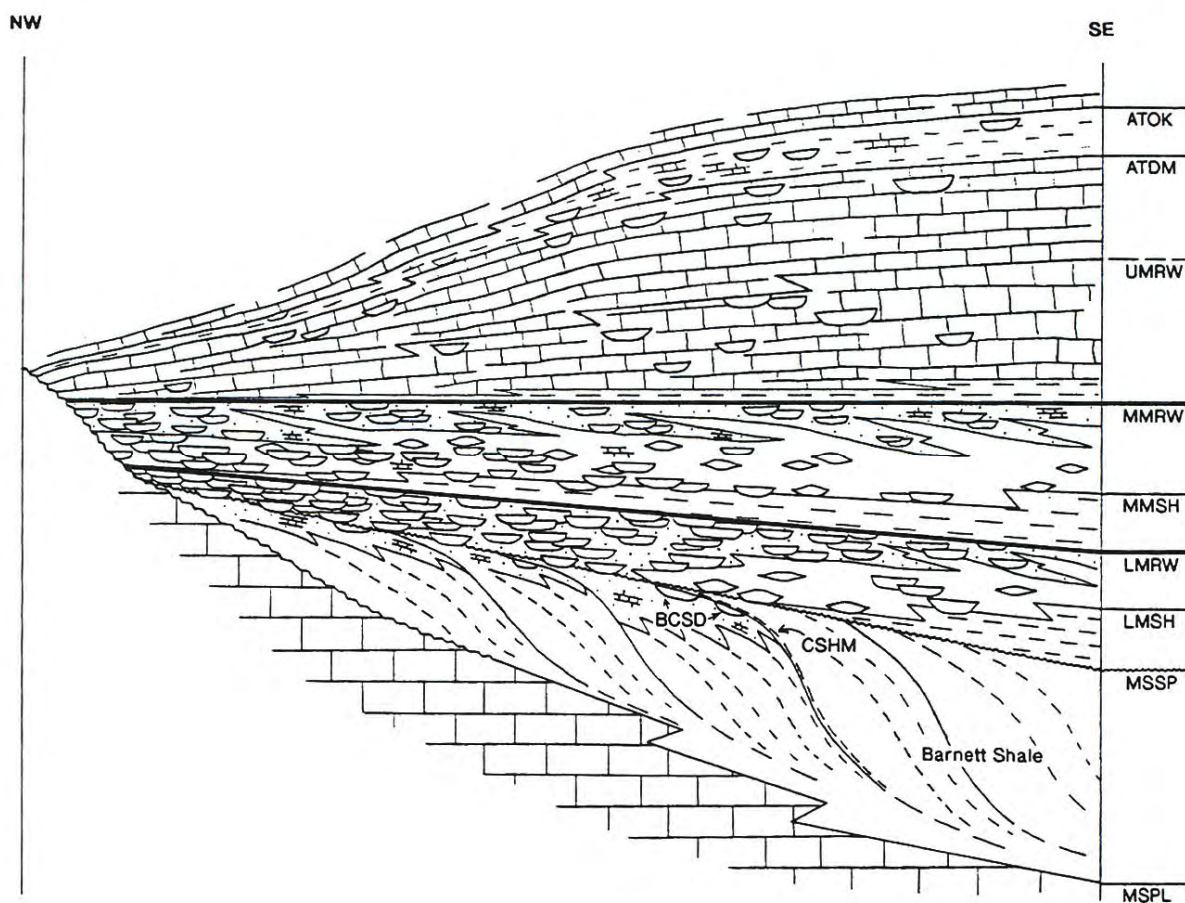


Figure 27. Schematic cross section of Morrowan and Atokan sediments in New Mexico (modified from Roberts and Kohles, 1999). Note apparent transgression in Lower Morrow (LMRW) and regression in Middle Morrow (MMRW).

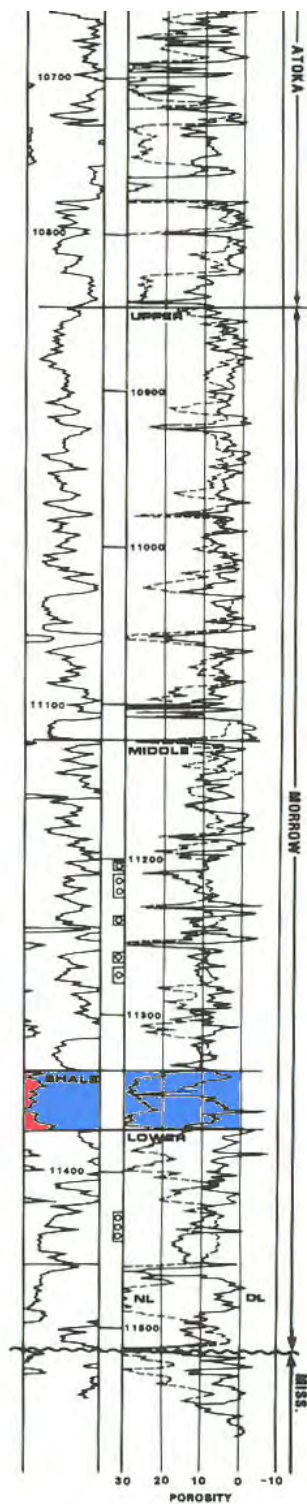


Figure 28. Southland Roy Parkway St. No.1 gamma-ray and compensated neutron-density log for Morrowan and Atokan sediments in New Mexico. Note lack of Mississippian-age siliciclastic unit (modified from James, 1984). Blue and red highlighted area is potential Carlsbad Sand used by Roberts and Kohles (1999).

AMOCO
EMPIRE, S. DEEP UT. No.16
7-18S-29E

LOGS SHOWING EXAMPLES OF ENVIRONMENTAL FACIES

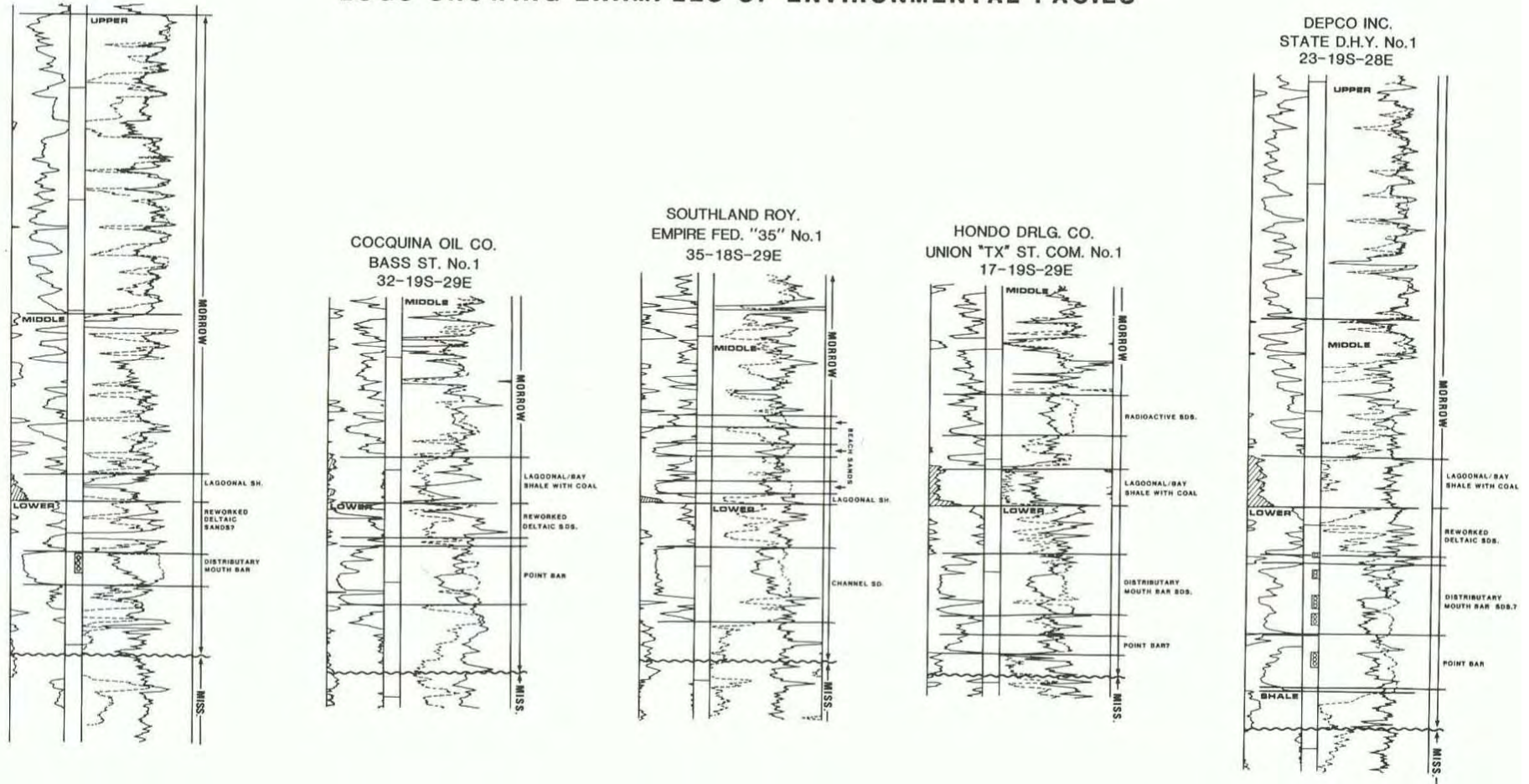


Figure 29. Petrophysical characteristics of Morrow Formation siliciclastic facies. Note environments ranging from mouth bar, lagoon, channel, to point bar, etc. (modified from James, 1984). An alternative depositional environment would be incised-valley fill overlain by estuarine to marine sediments. Note similarity in wireline-log character to that of figures 11, 12, 20, and 21.

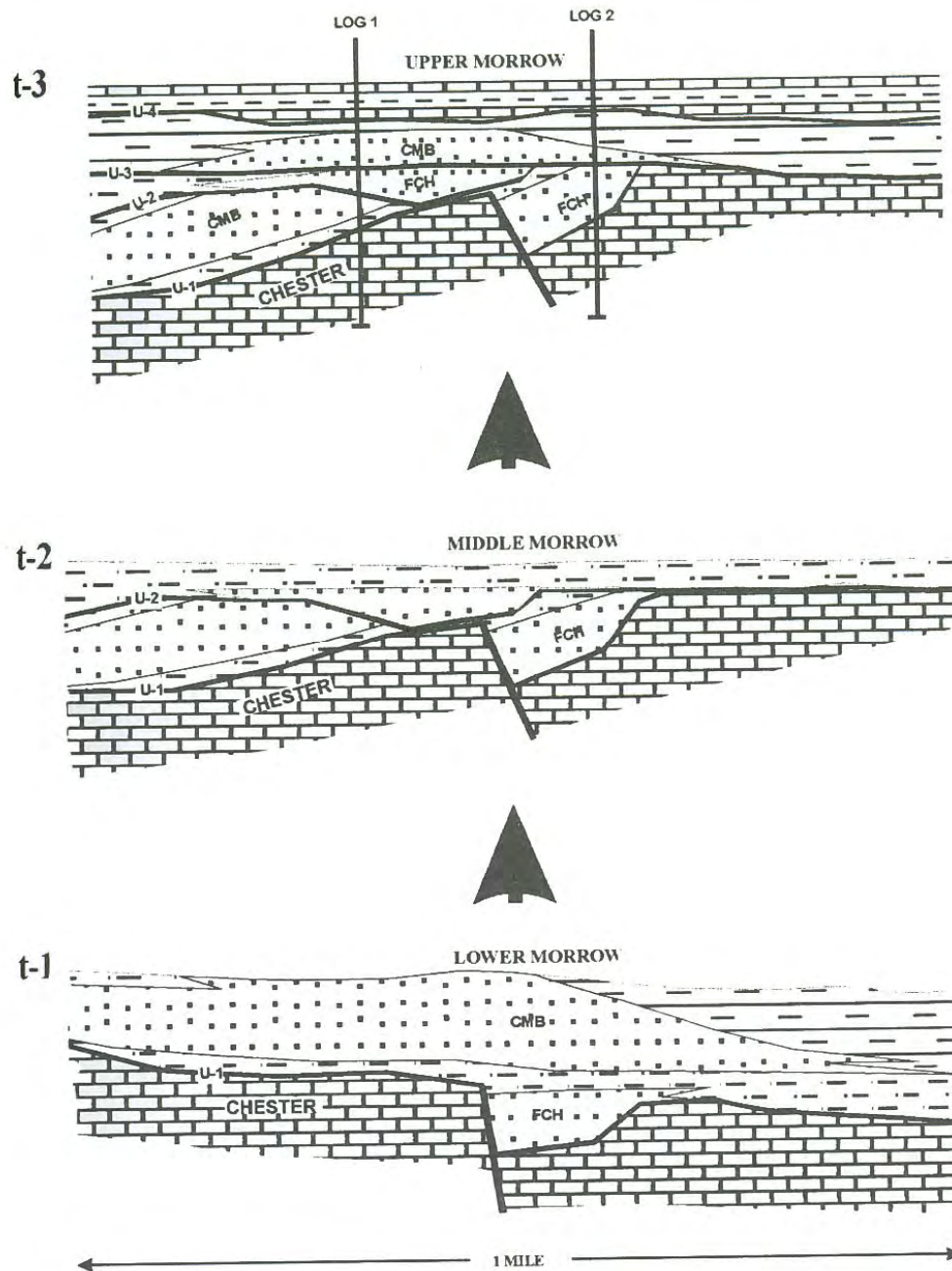


Figure 30. Predepositional and syndepositional controls on facies architecture in Morrow siliciclastics (modified from Mazzullo, 1999). Time = t, with t-1 being the oldest. U1-U4 = unconformity. FCH = fluvial channel, and CMB = channel-mouth bar.

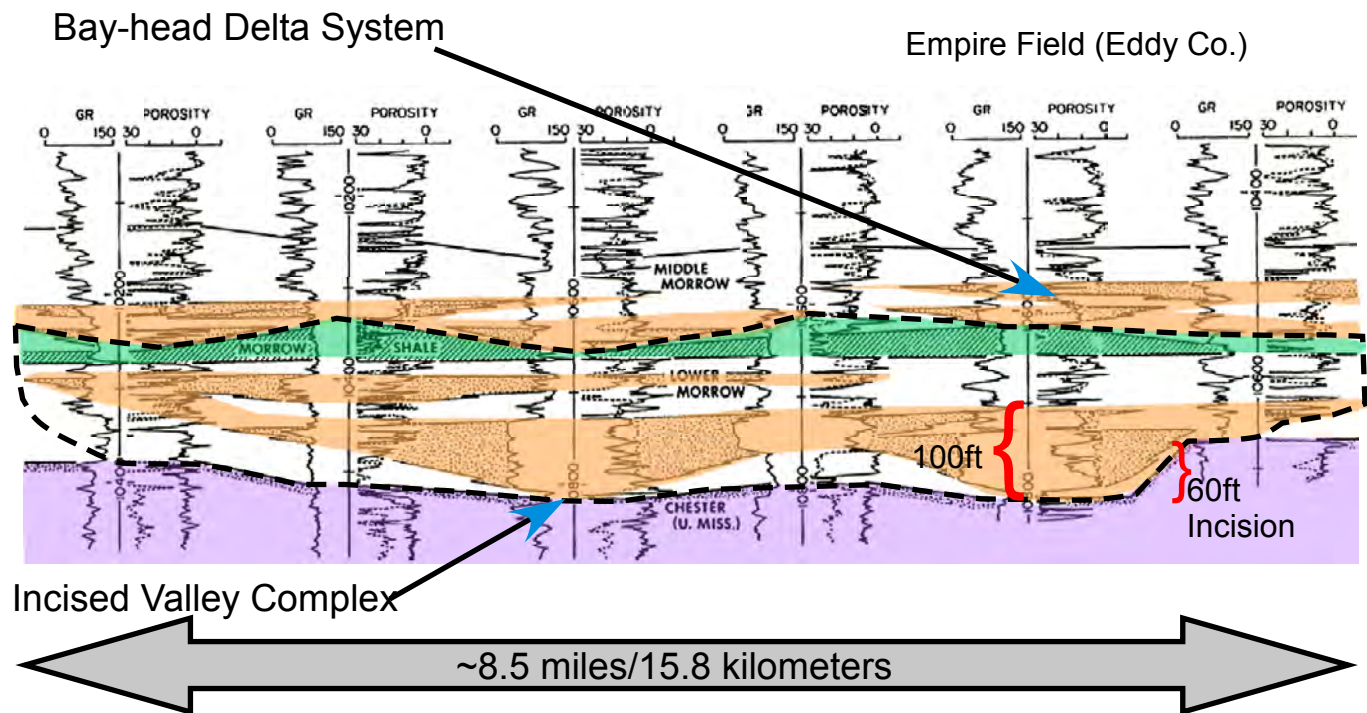


Figure 31. Strike-oriented stratigraphic cross section of Morrow Formation in Empire field, New Mexico (modified from Lambert, 1989). Note large incised valley-fill complex in Lower Morrow and smaller, more discontinuous bayhead delta sands in Middle Morrow.

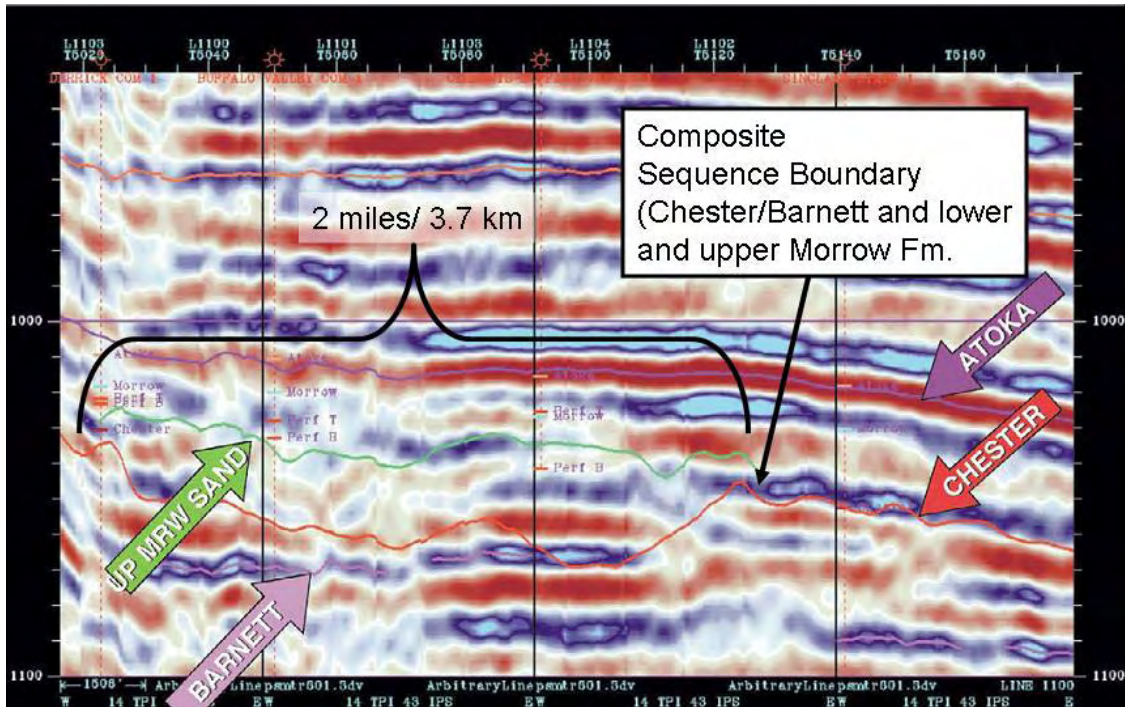
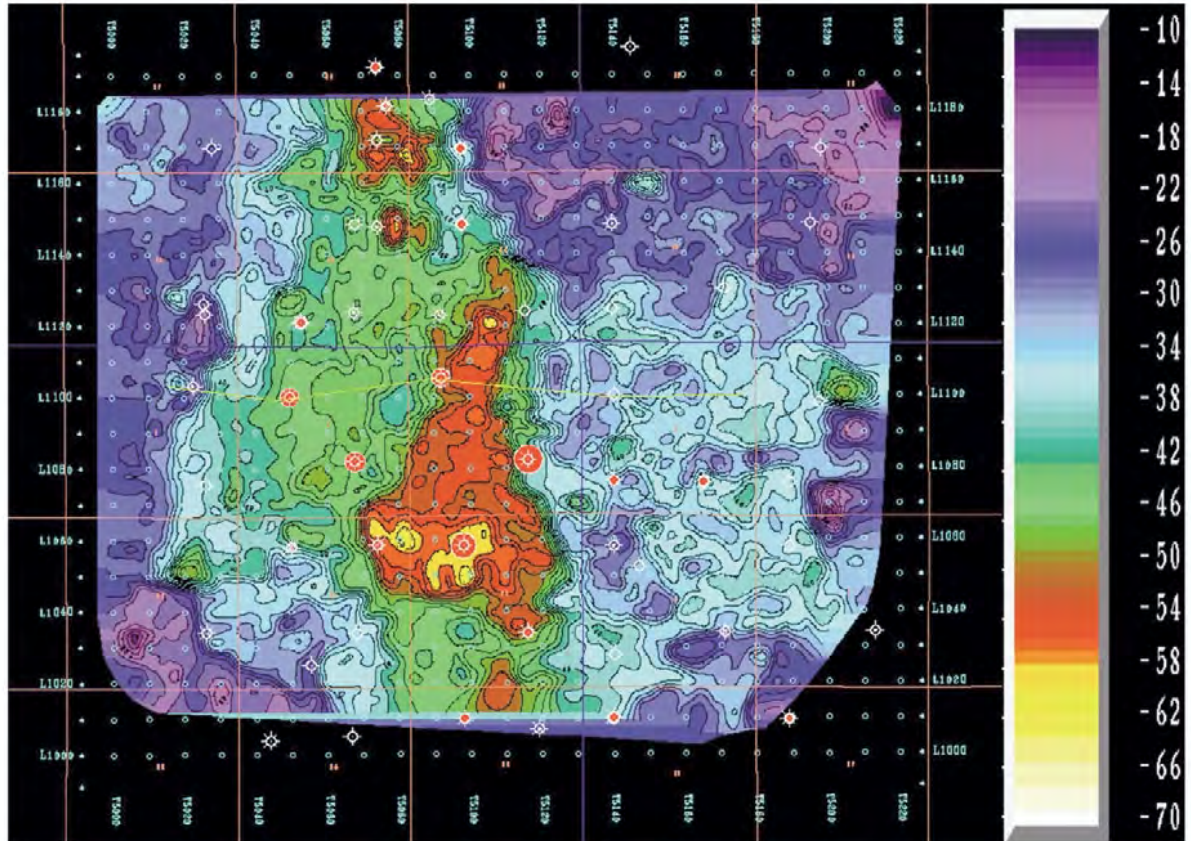


Figure 32. Vertical shear wave traversing through Buffalo Valley field, New Mexico. Note channel shape of Upper Morrow sand pick (top = green); Barnett top pick = lilac. Base of overlying Atoka Formation highlighted in purple. Modified from Van Dok and Gaiser (2001).



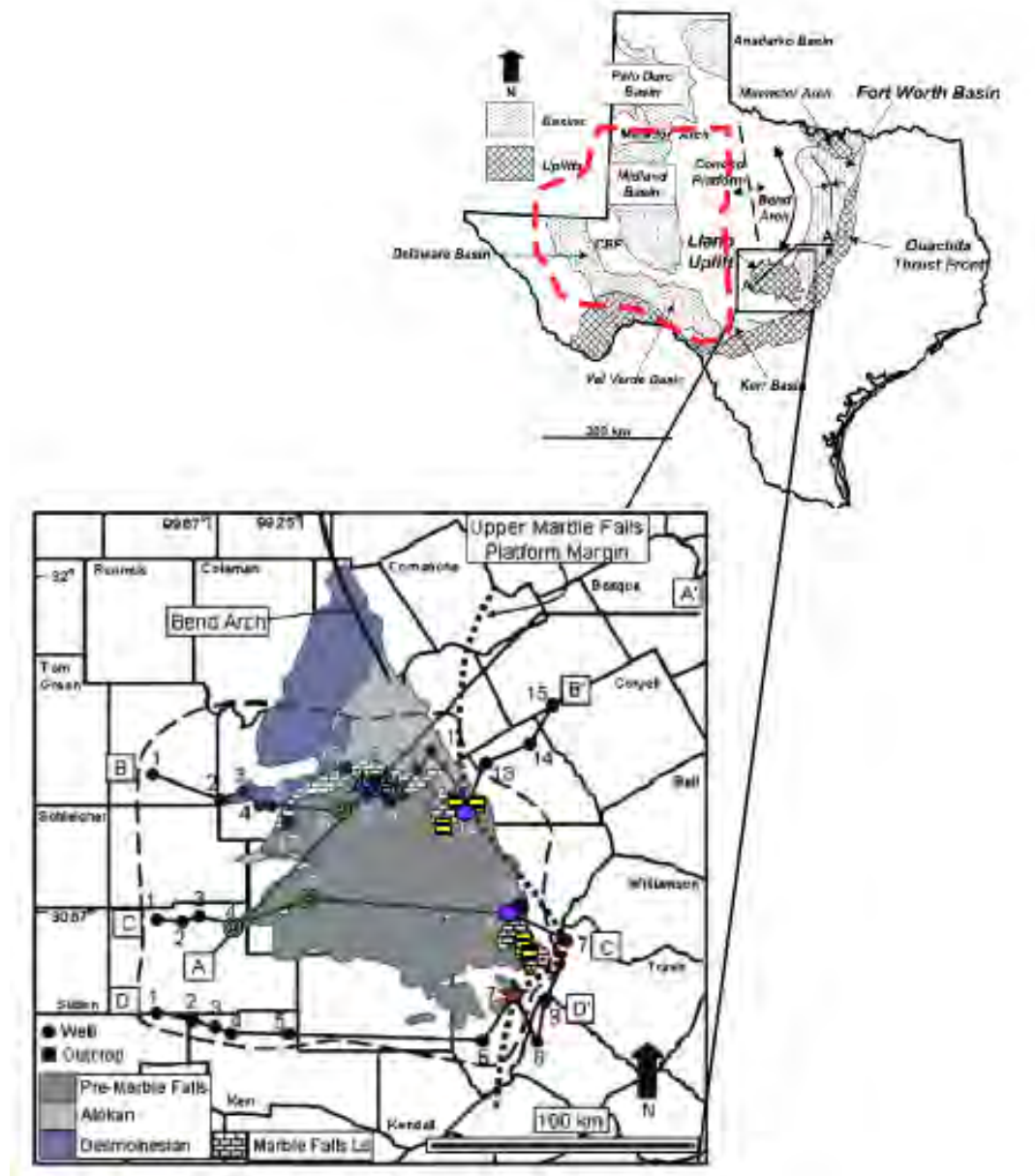


Figure 34. Field and regional area map of Marble Falls Formation. Note that the boundary of the Permian Basin as defined in this study is shown by the dashed red polygon on the regional-scale map (modified from Erlich and Coleman, 2005). Black dashed line is outline of Llano Uplift as proposed by Caran and others (1981). Study localities indicated by green bull's-eye Groves (1991), blue diamond (Bell, 1957), yellow dashed box (Manger and Sutherland, 1984), light-blue hexagon (Plummer, 1950), and red star (McCrary, 2003). Note that red star = Pedernales Falls State Park outcrop area. Kier (1980), Namy (1980), and Erlich and Coleman (2005) used most of the available outcrop data in their studies.

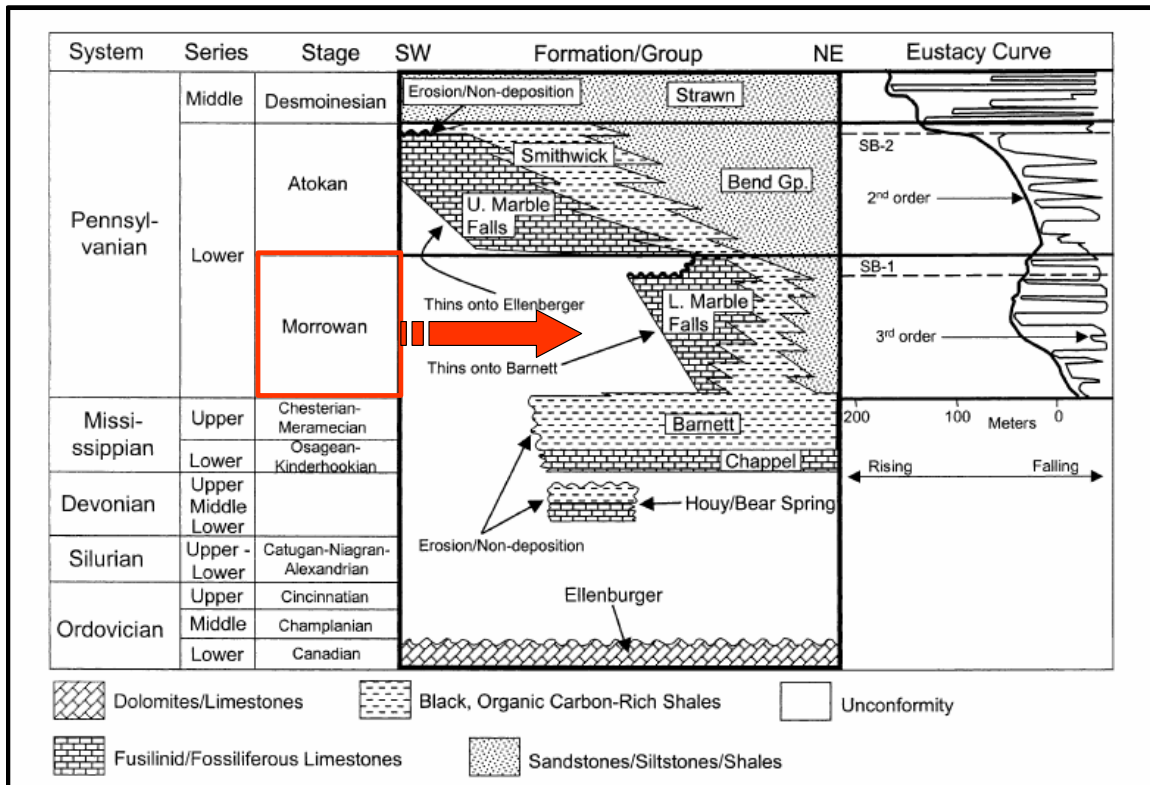


Figure 35. Lithostratigraphy and eustasy data for Llano Uplift region (from Erlich and Coleman, 2005). Eustasy data are from Ross and Ross (1987). Note lateral equivalence of Lower Marble Falls to Barnett and siliciclastics of the Bend Group.

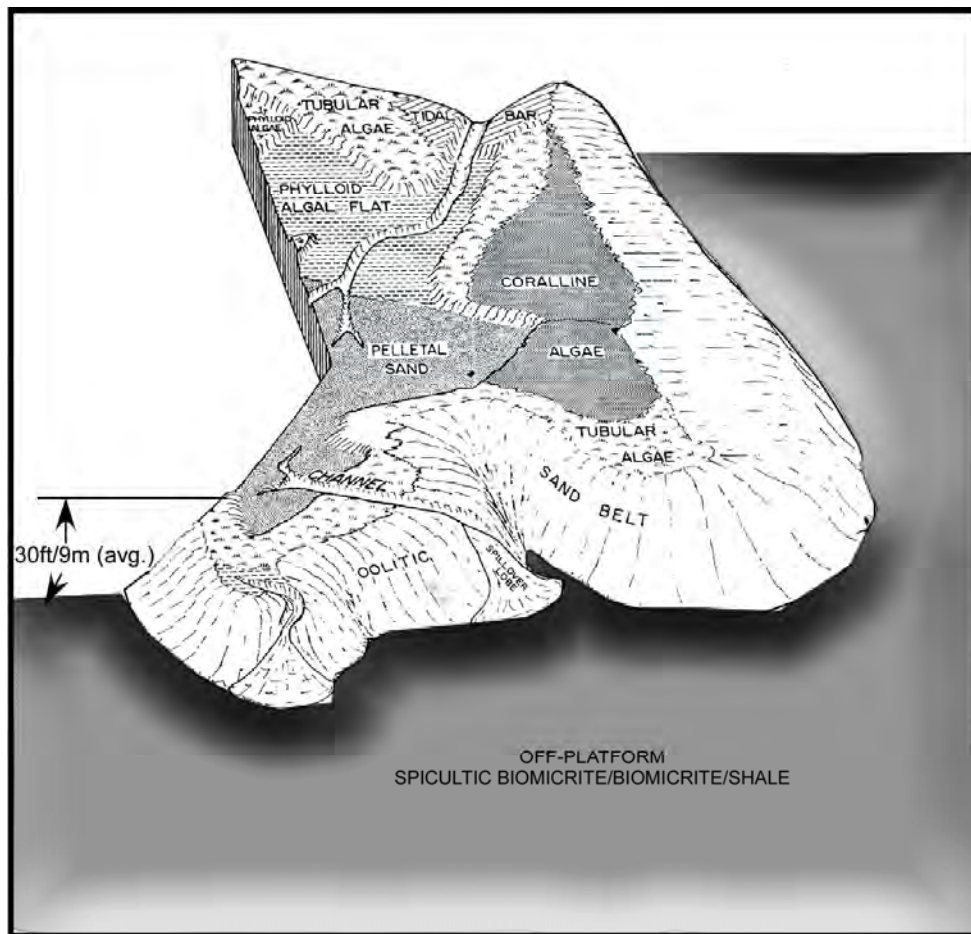


Figure 36. Generalized depositional model for Morrowan lower Marble Falls Formation (from Kier, 1980). General relief at platform margin thought to be 30 ft (9 m) on average. Average relief on platform interior thought to be as much as 16 ft (4.9 m).

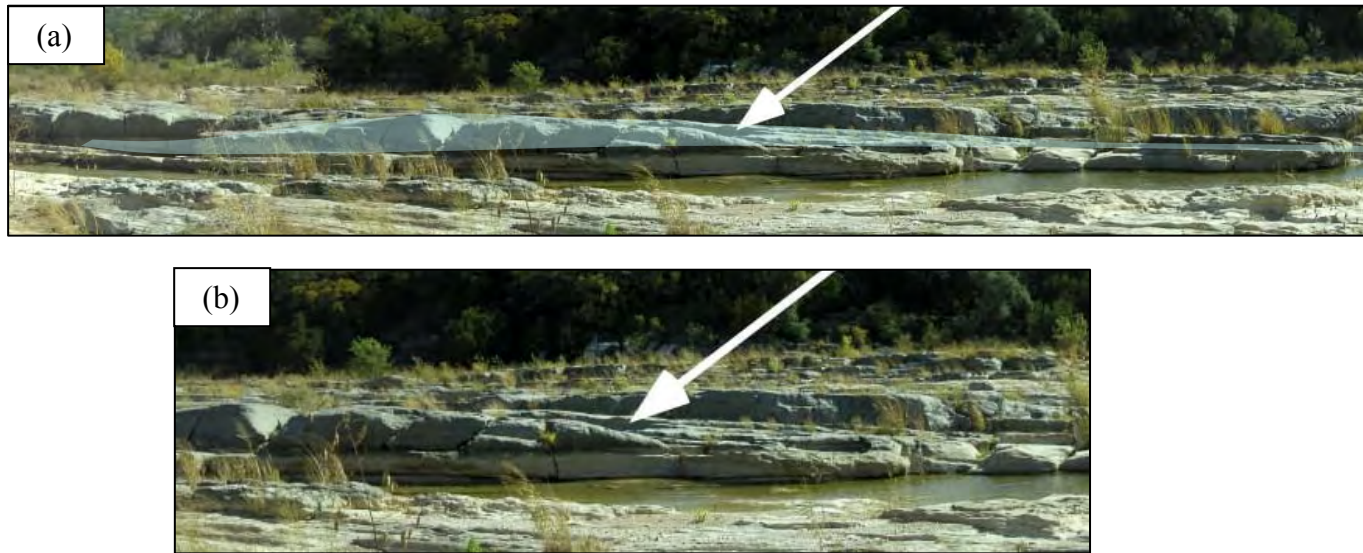


Figure 37. Mound facies (a) and flanking interbeds (b) in proposed Lower Marble Falls (Pedernales Falls State Park). Arrow denotes edge of small mound/bioherm and transition to flanking bed. Average thickness of mound is ~1.25 m.



Figure 38. Lower Marble Falls facies with high-energy bedforms in section. Previously thought to be dominated by spiculitic facies. Hammer is 12.5 inches (0.31 m) high.

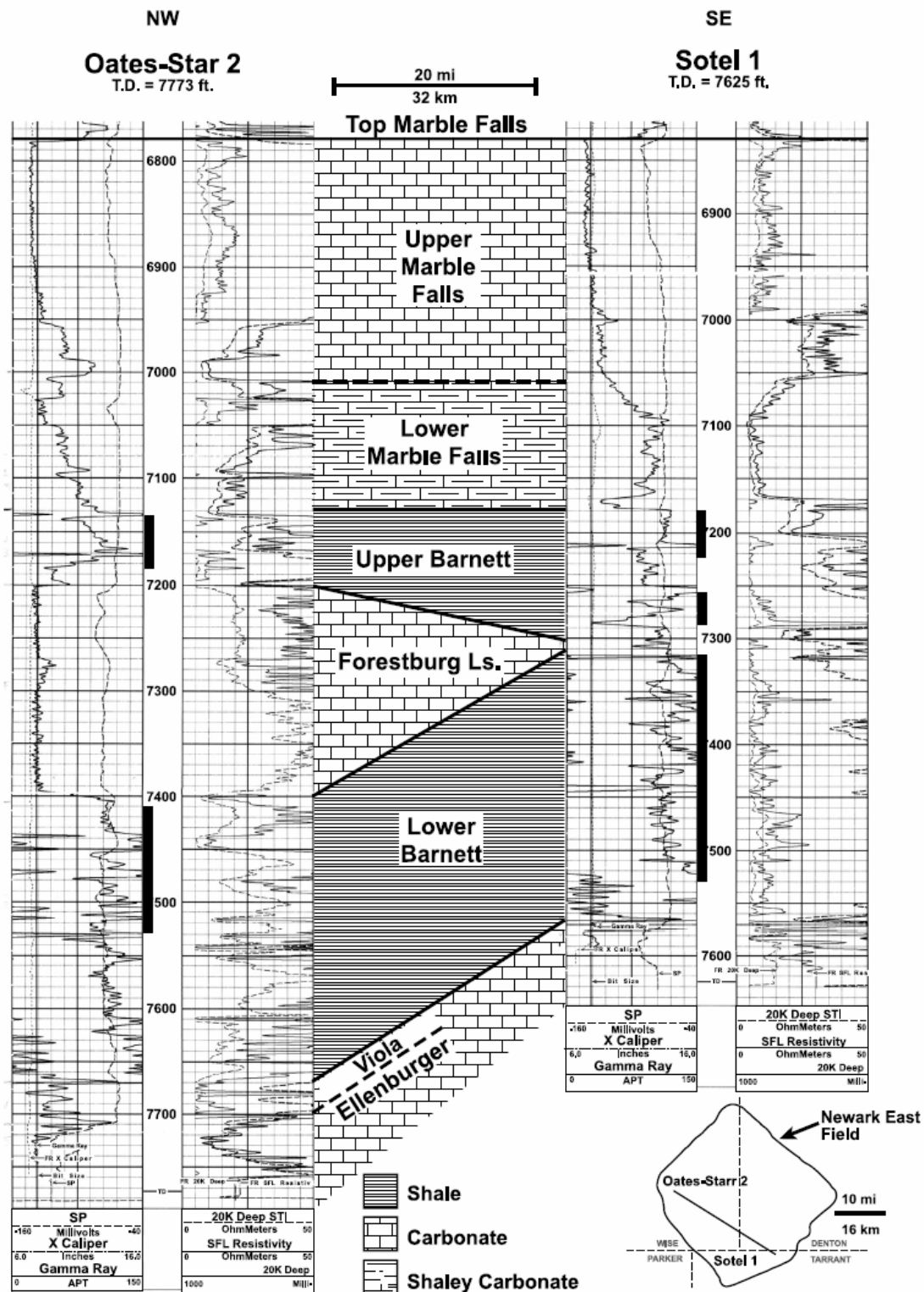


Figure 40. Sample logs to show typical wireline-log character of Barnett Formation through Upper Marble Falls Formation. Note log character differences between two wells at Lower Marble Falls interval.

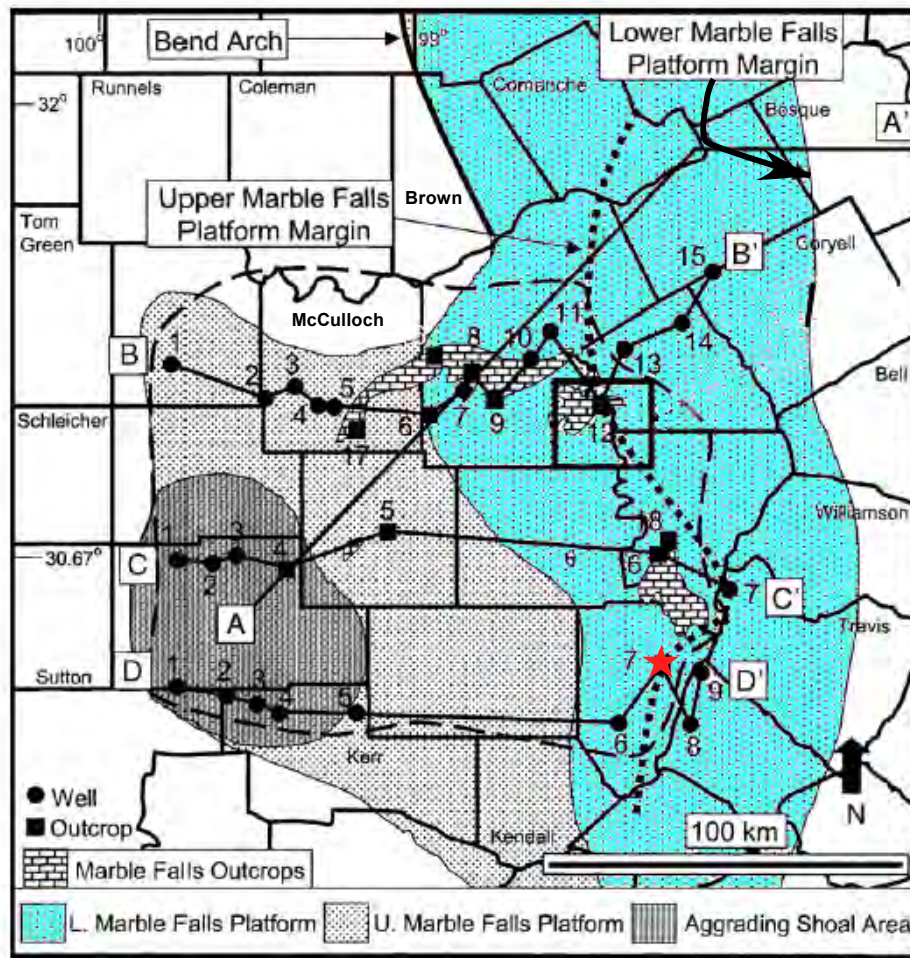


Figure 41. Regional distribution of Lower and Upper Marble Falls Platform (from Erlich and Coleman 2005). Note north-south orientation of Lower Marble Falls succession and lack of coincidence between platform and Llano Uplift boundary (long dashed line). Note position of platforms relative to Coleman and Brown Counties. Red star indicates Pedernales Falls State Park outcrop section studied by McCrary (2003).

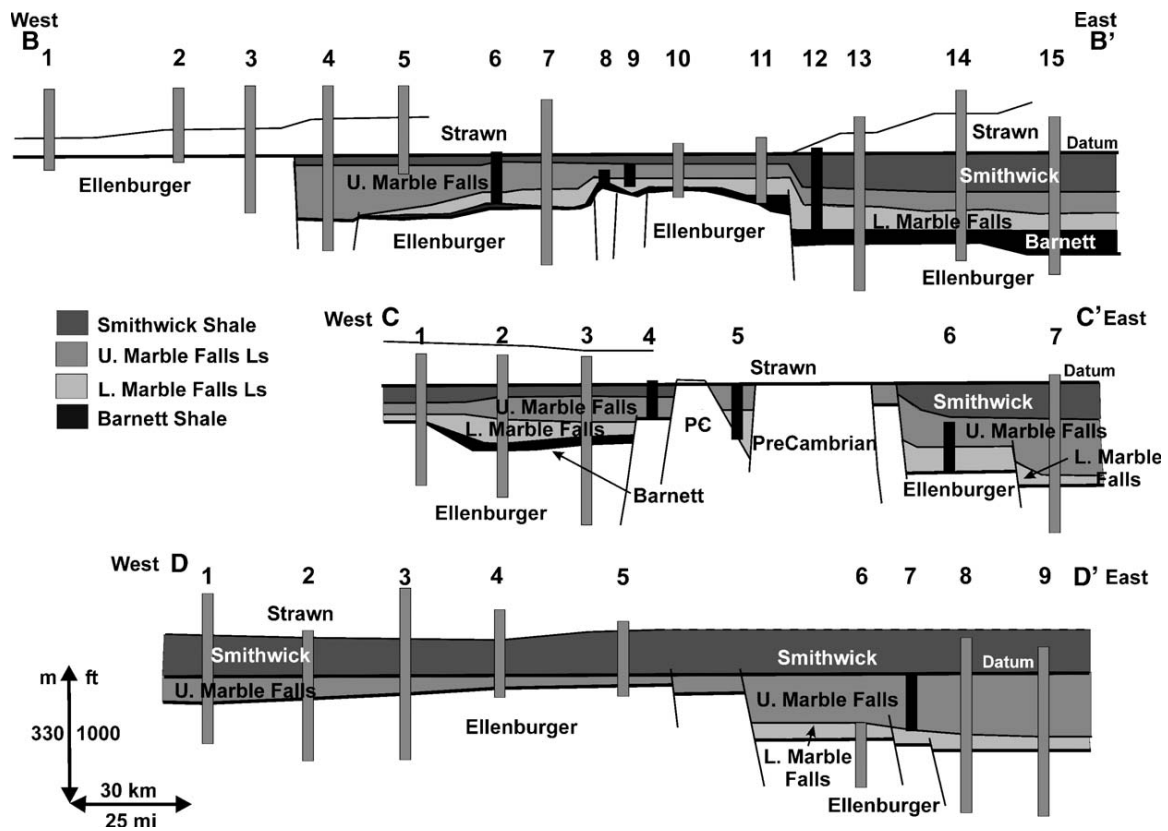


Figure 42. Stratigraphic cross sections of Llano Uplift. Well data are indicated by gray bars, whereas outcrop data are indicated by black bars (modified from Erlich and Coleman, 2005). Note that datum used in cross sections B-B' and C-C' is the top of the Smithwick Formation, whereas in section D-D' it is the top of the Marble Falls Formation. Location of section lines shown in figure 41. Note that location 7 on section D-D' is Pedernales Falls State Park and was considered wholly Upper Marble Falls by Erlich and Coleman (2005).

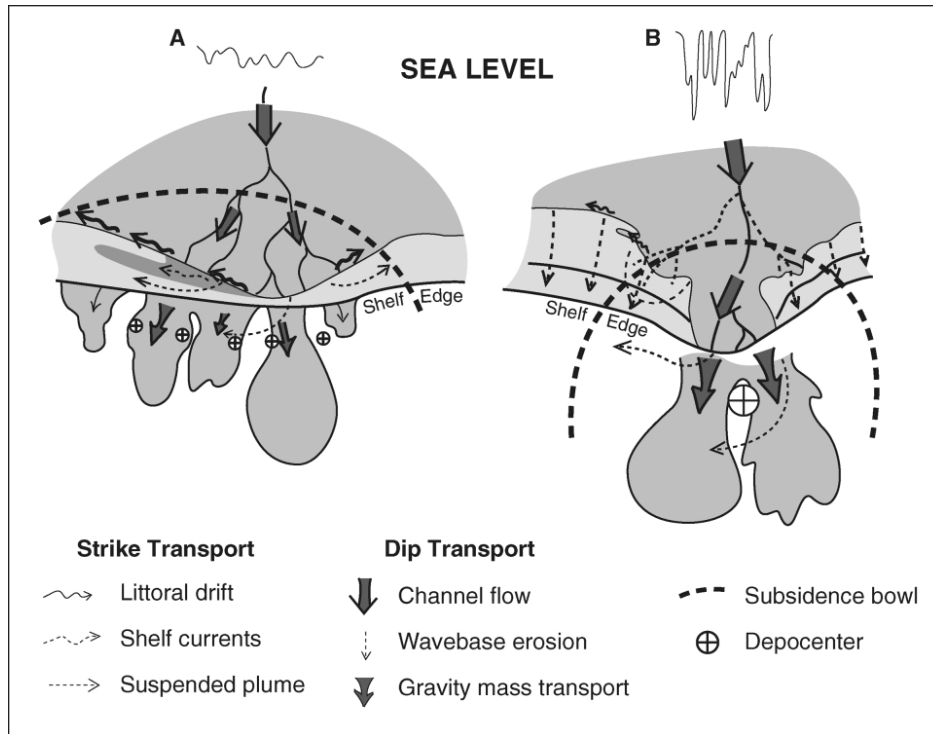


Figure 43. Differences in response of alluvial system transport past shelf edge during (A) greenhouse conditions versus (B) icehouse conditions. Note more confined but larger single depocenter during icehouse conditions (B). Modified from Galloway (2001).

DEPOSITIONAL HISTORY OF THE ATOKAN SUCCESSION (LOWER PENNSYLVANIAN) IN THE PERMIAN BASIN

Wayne R. Wright

Bureau of Economic Geology
Jackson School of Geosciences
The University of Texas at Austin
Austin, Texas

ABSTRACT

Atokan-age units in the Permian Basin record a 2nd-order transgression, with aerially restricted, lower Atokan fluvial to shallow-marine siliciclastics followed by pervasive carbonate deposition. In general, Atokan-age siliciclastics dominated deposition in the west of the Permian Basin while carbonate deposition dominated throughout the rest of the basin. Predominance of carbonate facies across most of the Permian Basin is due to (1) lack of siliciclastic supply, (2) overall 2nd-order rising sea level, and (3) progradation of the Upper Marble Falls Formation onto the Eastern Shelf. Progradation was due partly to lower accommodation to the west and backstepping/retreat from encroaching Atokan deltaics to the east.

The beginning of the Atokan is marked by a sea-level drop and subsequent lowstand conditions. A sequence boundary separates the Atokan from the underlying Morrowan carbonate section throughout the Permian Basin. Siliciclastic deposition in and around the Permian Basin is more aerially restricted than in the Morrowan. The earliest Atokan lowstand event is manifested in alluvial and fluvial incised-valley sediments in Lea County, New Mexico, and the Broken Bone Graben (Cottle County, Texas); fan-delta deposits in the Palo Duro Basin and Taylor Draw field (Upton County, Texas); and

post-Lower Marble Falls–pre-Upper Marble falls conglomerates (Gibbons Formation?) on the Llano Uplift. Following the lowstand event, a 2nd-order transgression appears to have dominated throughout the rest of the Atokan; however 3rd- and 4th-order, high-amplitude, sea-level fluctuations also occurred.

During the mid- to late Atokan, deltaic sediments and their deeper water prodelta shales prograded westward out of the Fort Worth Basin onto the Eastern Shelf. This progradation caused an abrupt west and southwestward backstepping of Atokan carbonate platforms and replacement of carbonate facies by deeper water (~100 m) shales (Smithwick Formation). Elongate shore-parallel transgressive sands on the northern Delaware Basin and Northwest Shelf of New Mexico represent either shelf ridges or transgressive barrier-bar systems. These transgressive, siliciclastic, marine-shelf ridge and/or barrier-bar systems are the dominant middle Atokan play type on the Northwest Shelf of New Mexico. Localized tectonic uplift and increased sediment load may have forced progradation in isolated areas of the northwest shelf.

Atokan carbonates were deposited over a larger area in the Permian Basin. A continuous carbonate platform to ramp existed between the Devils River Uplift (Val Verde and Edwards Counties) and the Eastern Shelf. Algally dominated bioherms and higher energy facies (ooid grainstones), affected by burial diagenesis and subsequently fractured, compose the best carbonate reservoirs. Subsidiary proximal-slope debris-flow plays are also likely present. Because producing carbonate reservoirs within the Delaware Basin are products of deep burial diagenesis, they are not readily linked to facies type. However, secondary porosity formed by calcite dissolution during exposure of carbonates should not be discounted as a primary reservoir-creation mechanism in other parts of the

Permian Basin. Atokan basinal and slope carbonates, interfingered with shale (for example, the Smithwick Formation), also hold potential as fractured reservoirs for expelled shale gas in the Delaware Basin (Reeves, Pecos, and Terrell Counties) and the northern proto-Midland Basin (Martin, Dawson, and Lynn Counties).

New paleogeographic reconstruction for the Atokan of the Permian Basin illustrates key depositional elements (fig. 1). From east to west, Atokan-age carbonates accumulated over the Llano Uplift, Eastern Shelf, parts of the Val Verde Basin, the Central Basin Platform (CBP), the northern Delaware Basin, and the Diablo Platform. The carbonate platform backstepped (east-facing margin) and prograded (west-facing margin) westward across the Eastern Shelf in response to lower accommodation rates and increased siliciclastic input from the east. Remaining carbonate-dominated areas (that is, Val Verde Basin, the CBP, the northern Delaware Basin, and the Diablo Platform) appear largely aggradational. That these platform carbonates grade to more basinal carbonates and, ultimately, shales in the northern Midland Basin and along the southwestern CBP is proposed. Extensive shales (Smithwick Formation) were also deposited to the east of the Llano Uplift. A small number of Precambrian inliers appear to have been exposed and shed material into the basin (for example, parts of the Ozona Arch and Fort Stockton High, Crockett and Pecos Counties). These and other minor topographically elevated regions were most likely rimmed by carbonates. The Pedernal Uplift provided limited sediment input for the northwest shelf but was disconnected from the other, more northerly channel systems feeding the Mid-continent. a later section of this paper gives a more detailed discussion of Atokan paleogeography.

INTRODUCTION

This paper discusses styles of deposition and facies development of Atokan-age sediments, concluding with a discussion of a revised paleogeography for the Atokan Permian Basin (fig. 1; p. 39). During the course of the paper, siliciclastic Atokan deposition and carbonate affinity are discussed as well. In each section, a regional model for facies patterns and deposition is proposed. Data from areas adjacent to the Permian Basin are used as analogs for facies that are predicted to be present within the study area. Localized studies are used to illustrate certain key aspects (for example, facies type and reservoir quality). However, an initial introduction to the area, placing it in a global perspective, is first presented.

GLOBAL TECTONIC SETTING

Atokan-age sediments (circa 310 Ma) in the Permian Basin were deposited at a near (8–12° south) equatorial position during icehouse conditions (high-amplitude, high-frequency, eustatic sea-level fluctuations). The greater Permian Basin area was undergoing initial tectonic activity of both uplift and subsidence related to the Ouachita-Marathon orogeny and birth of the greater ancestral Rocky Mountains. Figure 2 illustrates the position of Texas (in orange) relative to major tectonic plates and the equator at the beginning of the Pennsylvanian (circa Atokan-Desmoinesian age). During the Atokan, Texas occupied a more equatorial position than during the Morrowan. A less-restricted marine environment during the Atokan (compared with that of the Morrowan) is proposed, given the geometry of the microplates in the reconstruction (figs. 2, 3, “Depositional History of the Morrowan Succession (Lower Pennsylvanian) in the Permian Basin”).

REGIONAL TECTONIC SETTING AND FACIES DISTRIBUTION

The outline of the Permian Basin and major geologic features commonly associated with the basin are illustrated in figure 3. All features did not develop simultaneously, and most were only in the early stage of development during the Atokan. Figures 4 through 6 illustrate previous interpretations of facies distribution, uplift, and subsidence patterns for Atokan-age sediments in the Permian Basin and surrounding areas. The interpretations suggest that most of the Permian Basin was dominated by shallow to moderately deep water carbonate deposition. A revised Atokan Permian Basin paleogeography is presented here and discussed later.

Most of the Permian Basin was inferred to comprise carbonate-platform to carbonate-shelf environments by Ye and others (1996), with substantial uplifted area in the Diablo Platform, Ozona Arch, and Eastern Shelf areas (figs. 3, 4).

Areas of uplift, subsidence, and facies distribution in figures 4 through 6 do not all match. In many instances areas of net subsidence in figure 4 appear to correlate with areas of uplift in figure 6. On the basis of Kluth (1986), most of the Permian Basin area is illustrated as an area of net deposition, with subsidence rates ranging from less than or equal to 50 m/MA to approximately 200 to 300 m/Ma (fig. 5). One of the most important differences apparent between figures 4 through 6 is the extent of uplift on the CBP. Uplifted parts range from the south half in the interpretations by Ye and others (1996) and Kluth (1986), to a northeast part (Blakey, 2005), which is not coincident with the outline of the CBP (figs. 3–6). Correcting inconsistencies in the regional paleogeography of the Permian Basin and outlining more detailed depositional patterns are major goals of this paper (fig. 1).

GENERAL STRATIGRAPHY AND NOMENCLATURE

Atokan-age sediments within the Permian Basin include those termed Atokan (generally siliciclastic with rare carbonates), the Bend Group (generally siliciclastics), Bendian (mixed lithologies), the Upper Marble Falls Formation (carbonates), and the Smithwick Formation (shale with subsidiary sandstones). Significant correlation problems have been encountered in establishing the true depositional nature of Atokan-age units. Many studies are of local scale, lacking robust age control, and regional perspective. Different interpretations and inconsistencies exist in defining what units and formation are actually Atokan in age.

Nomenclature

As with the Morrowan interval, Atokan stratigraphic nomenclature is complex and confusing. A detailed correlation of named Atokan-age units is given in table 2 in Appendix 1 of “Depositional History of the Morrowan Succession (Lower Pennsylvanian) in the Permian Basin.” The Atokan, as defined in this study, contains all formations, groups, and members that are grouped within the Bend and Lampasas Series between the Morrow and Strawn (table 2, app. 1). In this study, Upper Marble Falls and Smithwick Formation names are applied to Atokan carbonate and shale lithologies, whereas the Bend is used for coarser siliciclastic facies (for example, conglomerates). Historically in the Midland Basin, CBP, and Delaware Basin regions, Atokan-age rocks have been referred to as either Atokan or Bend, regardless of lithology.

Siliciclastic Atokan Deposition

General Depositional Setting

Fan-delta, alluvial-channel, and basin-floor-fan depositional environments dominate in the earliest Atokan, with generally coarse grained, lowstand systems tract sediments. Incised-valley systems, much less widespread than in Morrowan time, are largely restricted to localized, small uplift areas. Uplift of the Ozona Arch area provided a local source for fan-delta and basin-floor-fan sediments in the Midland Basin. Fluvial and alluvial incised-channel systems also funneled sediments into the north margin of the Eastern Shelf, where it meets the Matador Arch. As mid-Atokan sea-level rose, tectonic uplift of the Pedernal area entered a stage of quiescence, and marginal-marine to open-marine deltaic to shelfal siliciclastic sedimentation began to dominate. Shoreline-parallel, barrier-bar to shelf-ridge sedimentation dominated in the Northwest Shelf area of New Mexico, with a sediment source still largely from the northwest. Extensive deposition of shale units (for example, Smithwick Formation) occurred during middle to upper Atokan time as the progradational front to Atokan siliciclastics migrating westward from the Fort Worth Basin. Shales of similar affinity to the Smithwick were deposited in the northern Midland and southern Delaware Basins (fig. 1).

Reservoir Potential

Updip fluvial, amalgamated, stacked channels and thick fan-delta units have the best reservoir potential and quality. Shoreline-parallel sand bodies in the northern Delaware Basin and Northwest Shelf have good reservoir potential owing to extensive lateral connectivity and a more predictable distribution pattern. Smithwick-type shales

have reservoir and source potential similar to that of the Barnett Formation shale-gas system.

Diagenesis

Dissolution of feldspar grains within fan-delta units enhanced porosity, whereas reprecipitation of dissolved bioclasts and calcite grains, as calcite cement within more distal fan-delta sediments, resulted in porosity occlusion. Quartz-overgrowth cementation is detrimental to reservoir quality in all coarse-grained facies.

Climate

As in Morrowan time, the Atokan was a time of expansive ice-sheet development, typified by highly fluctuating sea level. The fluctuation consequently plays a role in controlling cyclicity and facies stacking patterns. Such highly fluctuating sea levels generally result in thinner, higher frequency cycles.

PERMIAN BASIN

Eastern Shelf

Atokan siliciclastic units range from sandstones (Bend equivalent?) to shales (Smithwick equivalent?). In general, as elsewhere in the Permian Basin, Atokan units become more carbonate dominated upsection. Siliciclastics of the Bend series in Sutton and Schleicher Counties are Atokan, given the presence of *Fusulinella* fusulinids. However, in Sutton County, the Bend actually comprises a basal, dark shale interbedded with argillaceous limestone, some sandstone, and rare coals and ranges from 0 to 305 m (0–1,000 ft) in thickness. It is overlain by carbonate units. Bend deposits appear to be restricted to structural and topographic depressions, with limestone intervals in the middle massive unit thinning over positive structures and thickening into negative ones.

Presence of sand and glauconite in the Bend section in several of the wells in Sutton and Schleicher Counties led Rall and Rall (1958) to postulate that the Miers Horst (southern Sutton County) had been uplifted before Bend deposition and was supplying Cambrian-age siliciclastics into the area. Deposition of Atokan sediments was probably regionally continuous in the area but was subsequently removed by differential erosion (Conselman, 1954).

Midland Basin

In southern Upton County, Texas (Taylor Draw field), the Atokan comprises fan-delta systems (Troschinetz and Loucks, 1991), which contain low-permeability mud matrix conglomerates, or they are bioclastic. The low-permeability facies were deposited in the distal part of the complex, whereas high-permeability units are more proximal and were deposited as thick alluvial-channel sands (Troschinetz and Loucks, 1991). The most likely source area of these fan-delta sediments is the Ozona Arch (fig. 1). Yang and Dorobek's (1995) structural reconstructions suggest that pre-Desmoinesian tectonic movement was minor across the CBP. However, the semiregional pre-Desmoinesian unconformity indicates that the greatest amount of erosion and uplift occurred on the Ozona Arch. Localized uplift of the Fort Stockton Block southwest of Taylor Draw field may have also contributed sediment to the fan delta (Robert Loucks, Bureau of Economic Geology, personal communication); seismic and structural data do not, however, indicate major uplift of that area until after Atokan deposition.

The coarse-grained siliciclastics of Taylor Draw field appear quite different from typical "Atoka" detrital reservoirs in Andrews County to southeastern Midland County (Candelaria, 1990). The Atokan detrital plays and reservoirs in Andrews and Midland

Counties comprise a series of 15- to 20-ft, thick silty to bioclastic units encased in the Atoka shale. Exact ages of these reservoir intervals are uncertain, but they appear to range from Chesterian, to Morrowan, to Atokan. Producing Midland County fields such as Azalea, Bauman, Bradford Ranch, and Desperado, are considered Atokan in age. Candelaria (1990) proposed that the “Atoka Detrital” units were deposited as basin-margin siliciclastic wedges or submarine fans forming sheetlike units, generally up to 20 ft thick, during lowstand conditions. Midland County Atoka Detrital fields are likely the distal basin-floor-fan extension of the more proximal fan-delta and alluvial deposits of Upton County described by Troschinetz and Loucks (1991). The fauna present in the bioclastic members of the Atoka Detrital is diverse and composed largely of abraded, poorly sorted, shallow-water biota (crinoids and sponge spicules also present), which are sometimes associated with ooids. Detailed studies are unavailable to assess regional depositional environments for the carbonates. Poor sorting and lack of sorting indicate deposition as a debris flow.

Reservoir Quality

In Taylor Draw field, dissolution of bioclasts and calcite grains and reprecipitation of calcite resulted in occlusion of the pore space. The high-permeability facies are chert and quartz rich, with no mud matrix or calcite grains. Minor chalcedony cement is present in these facies (Troschinetz and Loucks, 1991).

Reservoir quality in the basin-floor-fan (Atoka Detrital) reservoirs is moderate, with 6 to 8 percent porosity and permeability at less than 0.1 md, over an average net thickness of 15 ft. Fracturing may, however, substantially elevate reservoir quality by linking reservoir intervals and fracturing encasing shales. Most traps appear stratigraphic

and are linked to facies pinch-out. Fractured encasing shales provide a secondary reservoir, as well as the source rock, which is siliceous and calcareous, with 1.1 to 4.7 percent total organic carbon (TOC) as Type II kerogen (Candelaria, 1990).

Delaware Basin

In Vacuum field, Lea County, New Mexico (fig. 7), Atokan-age siliciclastic rocks are divided into a lower fluvial succession and an upper deltaic to marine facies package. Within the lower Atokan, fluvial packages are stacked vertically, aggrading and fining upward, and are informally divided into lower and upper sand. The upper Atokan comprises upward-coarsening, deltaic, progradational sequences capped by flooding events that deposited black organic shale and limestones (Ota, 2001). Only the lower Atokan “lower sand” appears to have good reservoir characteristics. The depositional environment of this sandstone is similar to that of the underlying lower Morrowan, in that it comprises fluvial-channel sands in an incised channel/valley-fill environment. Small channel sand bodies are also present in McDonald field to the north of the Vacuum area (fig. 7). Upper Atokan sandstones are present in unconfined, meandering channels and delta-front to beach/bar-shoreface parallel (NE-SW) systems (James, 1985; Ota, 2001). Figure 7 illustrates the overall depositional environment for Atokan siliciclastics proposed by James (1985) for southwestern New Mexico. Sediment source of minor alluvial sandstones, such as at Buffalo Valley, and marine sandstones is from the northwest (James, 1985). Given the proximity to Morrowan-age uplifted areas on the ancestral CBP, a more eastern to northern source area is likely for Vacuum field. According to James (1985), the prograding shoreface-parallel beach sandstones depicted

in figure 7 are progressively younger toward the basin. The path of shoreline movement is numbered 1 through 5, oldest to youngest.

James (1985) proposed that increased sediment load provided by renewed uplift of the Pedernal area (fig. 7) provided the driving force for progradation (that is, forced regression) of siliciclastics into the Delaware Basin during an overall 2nd-order transgression. It seems equally likely that the elongate sand bodies are not beach deposits but sand shelf ridges or transgressive barrier-island bars (Reading and Collinson, 1996; Posamentier, 2002). Shelf ridges are formed by erosion of underlying shelfal sediments and redeposition during transgression. These shelf sand ridges are usually on the order of meters to kilometers wide, up to 20 km long, usually less than tens of meters thick, and encased in muddier to shaly sediments. These parameters match those described by James (1985) for siliciclastics on the north margin of the Delaware Basin. The shelf ridges described by Posamentier (2002) are not that dissimilar to the transgressive barrier-island-arc systems of Reading and Collinson (1996). In transgressive barrier-island sequences, landward migration of the barrier occurs either by shoreface retreat or in-place drowning. In transgressive deposits, shoreline sandstone ridges or barriers backstep rather than prograde (fig. 7). Large, 3rd-order sea-level drops have been documented for the Atokan (Ross and Ross, 1987). But except during the earliest Atokan lowstand, 2nd-order sea level was higher than at any time during the Morrowan. The shoreline therefore had to transgress and backstep relative to its position in the Morrowan and not prograde into the basin.

Reservoir Quality

Atokan production in Empire-Parkway fields (fig. 7) comes from two northeast-southwest-trending marine sand plays. Figure 8 illustrates the typical density neutron log for the Atokan sand interval, which is about 28 ft thick and ranges in porosity from 9 to 12 percent. Overall thin sands down to 5-ft thickness can be good producers because of their flow and drainage characteristics in these elongate, lenticular reservoirs.

REGIONAL STUDIES

Many data regarding depositional environments, facies types, and reservoir quality of Atokan succession have been collected in areas outside the Permian Basin (fig. 3). The greater Matador Arch area, specifically Cottle, King, Knox, and Stonewall Counties, is just at the margin of the Permian Basin, and facies described there are interpreted to continue into the Permian Basin (fig. 1). Units described for the greater Fort Worth, Palo Duro, and Dalhart Basins similarly provide analogs for depositional environments and reservoir attributes for the Upton County Midland Basin and Eddy and Lea Counties Delaware Basin Atokan reservoirs in New Mexico.

Greater Matador Arch Area

Within the Palo Duro and Dalhart Basins, Bend siliciclastics comprise alluvial-fan and proximal and distal fan-delta systems (Dutton, 1980). These units are localized in distribution to the two basins and reflect heightened tectonic activity associated with uplift of Amarillo-Wichita and Sierra Grande Uplifts and Bravo Dome. Isolated uplifted fault blocks along Matador Arch also provided material into the basins. Similar fan-delta systems have been identified in the southern Midland Basin (Upton County) and present a substantial play type if the structural history of the area can be clarified.

Figure 9 illustrates the typical wireline-log signature of Atokan fan-delta systems in the Palo Duro Basin. Figure 10 illustrates the rock character in core, and figure 11 is an overall correlation of the Pennsylvanian and Permian units within the basin. Overall porosity in the fan-delta units (often referred to as Granite Wash) averages 14 percent. Porosity is lessened by the extent of quartz overgrowth and carbonate cementation but enhanced by secondary leaching of feldspar grains. Less aurally significant deltaic sandstone units average about 12 percent porosity.

In King and Cottle Counties medium- to coarse-grained sandstones and conglomerates are present as offshore sand bars encased within calcareous shales (Edwards 1979). These units are analogous to mid- to upper Atokan Delaware Basin shore-parallel sandstone bodies (for example, Empire-Parkway fields, Eddy and Lea Counties, New Mexico). Within Baylor County, to the east of King County, Staples (1986) identified the presence of Atokan-age (Bend Group) fluvial-channel sandstones, which incise into the underlying Morrowan limestone. Ida and Stouffer fields (Baylor County) (1 km apart) produce from fluvial-channel sandstones and are interpreted to be a single reservoir. Overall reservoir quality is 15 to 19 percent porosity over a 28-ft-thick interval.

Broken Bone Graben

In southern Cottle County, the Broken Bone Graben appears to have been a large, fault-controlled depocenter that accumulated a thick succession of Atokan-age sediments (Bend) (see fig. 15 for graben location). The Bend Group reaches a maximum thickness of 5,000 ft, the lower two-thirds of the lower Bend Group being primarily nonmarine. The beginning of regional transgression is recorded in the upper one-third of the lower

Bend Group, which contains thin limestone units interbedded with nonmarine siliciclastic deposits (fig. 12). The Bend succession in Cottle County is analogous to Taylor Draw field in Upton County. Small (2 km long \times 7.5 km wide) isolated fault grabens similar to Broken Bone might also exist in Hale and Floyd Counties within the Permian Basin.

All units within the Broken Bone Graben appear to expand in thickness toward the structurally deep parts of the basin. The lower Bend interval in the Broken Bone Graben is probably equivalent to incised channel sands noted by Staples (1986) in Baylor County (fig. 13). Because the graben/basin was thought to have been constantly filled by sediment during its subsidence, only minor topographic relief was present on basin margins. Figure 12 illustrates the gamma-ray log signature and correlation of the entire Atokan interval (Bend and Smithwick Formations). Small red bars to the right of each well log indicate producing reservoir-quality sands, which appear largely unpredictable in distribution. High-resolution seismic over the graben illustrates thickening of units toward the basin center, as well as onlapping and infilling geometries of sediments upward (fig. 14). Attribute analysis of the seismic should provide better constraints on size, architecture, and distribution of incisive and unconfined alluvial channels in this depositional setting.

In a regional sense, continued marine transgression and eventual subsidence of the Palo Duro Basin north of the graben caused the regional depocenter to shift to a position nearer the Wichita-Amarillo mountain front, shutting off the coarse siliciclastic supply to the graben area (Brister and others, 2002). Figure 15 illustrates proposed regional distribution of lower Bend sandstones (Atokan), which are not restricted to the graben

area, and data suggest sandstone deposition in Kent and King Counties (Brister and others, 2002) (figs. 1, 15)

The upper Bend Group, which is entirely marine, is composed of calcareous shale and argillaceous basinal carbonate units that correlate to basin-rimming carbonate buildups. Discrete sandstone beds in the upper Bend in a few wells are interpreted to be offshore sandbars deposited locally along the basin rim and similar to those described by Edwards (1979) for the Fort Worth Basin area and James (1985) for the Northwest Shelf of the Permian Basin. The style of siliciclastic deposition in the Broken Bone Graben area is mimicked in the Northern Delaware/Northwest Shelf area, with a basal nonmarine alluvial system giving way to a more marine system. Transgression culminated in a maximum flooding event marked by the Smithwick Shale in the eastern Matador Arch area (fig. 12).

Cycles in the Broken Bone Graben basin fill are attributed to sedimentary response to local basin subsidence, not eustasy. Cyclically stacked sheets of poorly sorted muddy sandstone and mudstone units, alternating with winnowed sand-rich units, were deposited in alternating deltaic and braided-plain environments, depending on base level. Characteristic associated depositional environments are debris fans (pebbly mudstone), overbank sediments (coaly mudstone), and discrete, laterally limited distributary channels (sandstone). During tectonically quiescent periods and after reestablishment of a higher base level, throughgoing stream systems were reestablished, and fine materials were winnowed and carried southward toward the Knox-Baylor Trough, whereas coarser material dropped out of the system over the graben area. The final result was stratigraphically compartmentalized, braided channels that amalgamated laterally into

sheetlike deposits. Cross-axial, throughgoing streams are suggested by stratigraphically complex, vertically stacked, and laterally terraced sandbar development within channel systems incised into the pre-Bend strata in the region south of the graben (fig. 13).

Reservoir Quality

Within Rhombochasm field, reservoir quality in the lower Bend Atokan units is moderate, with an average of 12.6 percent porosity and 0.02 md permeability over a net interval of 75 ft encompassing approximately seven sandstone horizons. Figure 16 illustrates the detailed gamma-ray-log, porosity, and resistivity characteristics of the lower Bend stacked sandstone reservoirs over part of the productive interval. The wireline-log signature is similar to those interpreted to indicate fan-delta systems, as in figure 9. However, the Broken Bone succession provides an alternative analog to traditional models (for example, Palo Duro) because it is not governed by eustasy. Similar tectonically driven successions may exist in the northern Permian Basin, and the model may be directly applicable to Taylor Draw field in Upton County.

Greater Fort Worth Basin

Data from the Fort Worth Basin help to establish the amount of siliciclastic progradation into the Permian Basin and also provide depositional analogs. Within the Fort Worth Basin, Atokan siliciclastics are generally thought to have been deposited in a deltaic environment (Ng, 1979; Crowder, 2001). Atokan siliciclastic deposition in Jack, Palo Pinto, Parker, and Wise Counties is considered a product of the rising Ouachita Uplift area on the east and south of the Fort Worth Basin (Ng, 1979). In general, Atokan siliciclastics are considered part of a westward-prograding deltaic succession. The western limit of Atokan progradation was previously considered the Bend Arch, which

runs roughly northward through Mills and Comanche Counties. Timing and origin of the Bend Uplift are equivocal. But flexure (not uplift) may have initiated in late Morrowan time, although it was not a major feature until Atokan times. This supposition is supported by uniform thickness of the Lower Marble Falls Limestone across the entire area. Erosion of both Morrowan and Atokan sediments across the Bend and Concho Arch areas makes it difficult to define whether some Atokan sediments were deposited or eroded. However, identification of the Smithwick Shale overlying Bend siliciclastics in Cottle County and identification in core of Marble Falls and Smithwick Formations in McCulloch County indicate that progradation migrated much farther west than previously documented.

The Atokan siliciclastic succession in the Ng (1979) study area is actually dominated by shales with small discontinuous (vertically and laterally) sandstone bodies. Figure 17, a west-east cross section of Palo Pinto and Parker Counties, illustrates a westward-onlapping succession of shales and sands in lower and upper Atokan siliciclastics. The succession of transgressive sands and shales is similar to that described for the Northwest Shelf in New Mexico and Matador Arch areas for the middle to upper Atokan interval. Correlations within the units are subjective at best, given the quality and type of logs used for analysis (SP and resistivity). The upper shale-dominated Atokan of Ng (1979) is the Smithwick Formation and its lateral equivalents.

Smithwick Formation and Coeval Shales

The Smithwick Formation (informally called the Smithwick Shale), as formally defined, includes all shale between the underlying Marble Falls Limestone and the overlying Strawn Limestone. However, it has been recognized that the Smithwick

contained several facies and had abrupt and large thickness variation. Additionally, it has been noted that the formation was not only restricted in age to younger than the Upper Marble Falls; it was also its basinal equivalent (Plummer, 1950; Grayson and others, 1989; Groves, 1991; Erlich and Coleman, 2005). The Smithwick Shale, as defined, is not acknowledged in the Midland, Val Verde, or Kerr Basins to the west and south (Erlich and Coleman, 2005). However, the Bend succession in Schleicher and Sutton Counties is characterized by its abundance of shale through the defining interval (for example, Marble Falls to Strawn). Given the regional analysis, coeval shales are also probably present in the western Delaware Basin and within Gaines, Andrews, Dawson, and Lubbock Counties in the northern Midland Basin (fig. 1). In this study the Smithwick Formation is considered a deeper water, lateral equivalent to Atokan siliciclastics in the Fort Worth Basin, the Upper Marble Falls Formation on the Llano Uplift/Eastern Shelf, and the basal Atokan “Caddo” Formation on the Eastern Shelf. Understanding the depositional environment and establishing a regional correlation of the Smithwick Formation and its lateral equivalents are vital to the understanding of development of the Permian Basin. These shales potentially provide the only throughgoing (across platform and shelf and into the basin) lithologies and timelines that can be used to construct a sequence stratigraphic framework for the Atokan.

The Smithwick is a black, fissile, siliceous, phosphatic shale containing calcareous planktonic foraminifera and rare ammonoid and gastropod fauna. The upper section of the Smithwick, however, is coarser grained silt to sand, containing abundant bed forms in the Llano area. At the type locality, the Smithwick is 301 ft thick (Plummer, 1950). McBride and Kimberly (1963) performed a regional study of the Smithwick in the

Llano area and noted thicknesses of 400 ft in boreholes near the study area and over 5,600 ft of shale in the S. E. Purcell well No.1 in Williamson County. Figure 18 illustrates facies relationships between the Upper Marble Falls and the Smithwick north of the Llano area and the increased thickness of the Smithwick to the west. Proportions of sandstone increase upward in the Smithwick Formation and are generally thin (<2 ft), although containing abundant ripple cross-lamination, sole marks, flute casts, and other bedding-plane structures. Paleocurrent data indicate an average flow direction of S19°W; therefore, a northeastern source area is presumed. In general, McBride and Kimberly (1963) considered the entire Smithwick marine in origin and upper sandstone units as deep-water turbidites. Erlich and Coleman (2005) interpreted Smithwick shales in the Llano as being deposited in the outer-shelf to upper-slope environments. The shale also interbeds with platform-margin limestones, probably as a result of 3rd- and 4th-order flooding events.

Reservoir Quality

The importance of the Smithwick Formation lies not only in its helping us to understand overall sedimentology of the Permian Basin, but also its being an exploration target. On the Llano Uplift, high organic carbon contents (7.5 percent TOC) and a potential similarity in grain character to the Barnett Formation make the Smithwick Shale a potential self-sourcing shale-gas system similar to that of the Barnett Formation in the Fort Worth Basin. In the Broken Bone Graben, Atokan shales within siliciclastics of the Bend Group and the Smithwick Formation have source potential in this deep-basin setting (Brister and others, 2002). Mean TOC is 4.98 percent but ranges up to 20.01 percent and falls as low as 1.05 percent. The upper Bend group yields primarily

unstructured, lipid organic matter, with lower percentages of terrigenous vitrinite and inertinite, whereas the Lower Bend Group includes a high percentage of vitrinite (type III).

DISTRIBUTION OF ATOKAN SEDIMENTS

Interpretations of Atokan sedimentation patterns in the Midland Basin historically relied heavily on structural interpretation of the CBP. According to seismic and wireline-log correlations, it appears that only small, localized areas of the CBP were uplifted before the end of the Atokan. Regional reconstructions by Tai and Dorobek (1999; 2000) show no influence of the CBP on Atokan sedimentation patterns in the Midland Basin (figs. 19, 20). Distribution of Atokan-age sediments is relatively uniform in thickness and aerial distribution across Delaware and Midland Basins (Van der Loop, 1991; Yang and Dorobek, 1995). Yang and Dorobek (1995) illustrated numerous cross sections of Delaware and Midland Basins, illustrating only a slight thickening of Atokan-age units toward the proposed western boundary of the CBP. Most sedimentation appeared largely unaffected by uplift. A pre-Desmoinesian unconformity does exist, which results in the cutting out of variable amounts of the stratigraphic section. Post-Atokan differential uplift of blocks within the CBP resulted in erosion from Upper Pennsylvania units down to the Precambrian basement. Erosion and faulting make it difficult to decide confidently whether deposition of Atokan sediments occurred across the entire Permian Basin. However, it appears that Atokan sediments were pervasive across much of what would become the CBP during the Desmoinesian to Virgilian. Subtle thickness variations suggest that localized uplift of small blocks in the CBP area affected local deposition patterns and thickening of units. However, overall uplift appears to have been minor, and

areas without Atokan sediments are largely a product of later uplift and erosion.

Estimated time of major uplift of the CBP is Desmoinesian (Strawn) (Van der Loop, 1991; Yang and Dorobek, 1995; Ye and others, 1996). Earliest structural estimates for uplift of the CBP are Desmoinesian as well. However, given the regional distribution of the Desmoinesian Strawn Formation, it is more likely that uplift occurred during the Missourian to Virgilian.

Summary of Atokan Siliciclastic Deposition

Overall, siliciclastic deposition in and around the Permian Basin is more aerially restricted than in the Morrowan. Atokan siliciclastic deposition starts in the earliest Atokan with a lowstand event. This event is manifested in alluvial and fluvial incised-valley sediments in Lea County, New Mexico, and the Broken Bone Graben (Cottle County, Texas); fan-delta deposits in the Palo Duro Basin and Taylor Draw field (Upton County, Texas); and post-Lower Marble Falls–pre-Upper Marble Falls conglomerates (Gibbons Formation?) on the Llano Uplift. Following the lowstand event, a 2nd-order transgression appears to have dominated the rest of the Atokan, although 3rd- and 4th-order, high-amplitude, sea-level fluctuations also occurred.

Regional progradation of deltaic sediments and their deeper water counterpart shales migrated westward from the Fort Worth Basin onto the Eastern Shelf. This progradation caused an abrupt west-southwest backstepping of the lower Atokan carbonate platforms previously in that area and replacement of the carbonate facies by deeper water (~100-m) shales (Smithwick Formation). Elongate, shore-parallel, transgression sands on the northern Delaware Basin and Northwest Shelf of New Mexico are either shelf ridges or transgressive barrier-bar systems. Localized tectonic uplift and

increased sediment load forced progradation in isolated areas of the northwest shelf. High rates of subsidence within the Palo Duro Basin and the Broken Bone Graben funneled extensive amounts of localized siliciclastic sediments into each area. Subsidence in the Palo Duro Basin eventually outpaced that of the Broken Bone Graben/Matador Arch area, coinciding with uplifted areas migrating westward and toward the Permian Basin. A 2nd-order transgression became the driving force, and sedimentation rates decreased in the Broken Bone Graben, resulting in deposition of shales and argillaceous carbonates, which were eventually displaced by the Smithwick Shale from the east.

Fan-delta and basin-floor-fan assemblages in Upton, Midland, and Andrews Counties appear to have been sourced by the Ozona Arch area. Aerial distribution of the fan deltas and basin-floor fans is still poorly defined. Two areas of shale deposition occurring in Culberson, Gaines, and Andrews Counties are separate from the Smithwick Formation on the Eastern Shelf and eastern Midland Basin. The Smithwick Formation and its equivalent shales (average TOC 6.24 percent) throughout the Permian Basin have potential as an underexplored, untapped shale-gas system similar to that of the Barnett Formation.

Atokan Carbonate Deposition

Broad Approach

Carbonate rocks of Atokan age in the Permian Basin have been studied primarily in the Chapman Deep field area, Delaware Basin. In this study it is thought that Atokan-age carbonates present in the Permian Basin are laterally equivalent to extensive carbonates developed on the Eastern Shelf (that is, the Upper Marble Falls Formation). It is postulated that these adjacent areas act as excellent analogs for equivalent

underexploited sections within the Permian Basin. Consequently, the approach taken in this paper is to discuss development of the Upper Marble Falls Formation, along with Delaware Basin units. Although Upper Marble Falls field localities are not geographically part of the study area, extensions of that carbonate platform are present in the subsurface of the Permian Basin.

General Depositional Setting

Atokan-age carbonates were deposited widely across the Permian Basin on low-angle ramps that developed to more platformlike geometries through time.

Reservoir Potential

Shallow-water *Donezella* algal bioherms and oolitic-bioclastic grainstones are the most favorable reservoir facies because they may preserve excellent intergranular and intragranular porosity. Reservoir intervals are not confined to a particular facies or exposure surface, at least within the Delaware Basin. Off-platform, proximal, coarse-grained slope facies are a potentially overlooked reservoir target.

Diagenesis

Primary porosity appears largely occluded during early diagenesis. Extensive development of secondary dissolution porosity during burial, coupled with a microfracture network, results in good reservoir quality. In the Delaware Basin, dolomitization occurs during both early and late diagenesis, with positive and negative results in reservoir quality, respectively.

Detailed data on Atokan-age carbonate units in the greater Permian Basin are provided primarily by studies of the Atokan-age Chapman Deep field area of northern Reeves (Texas) and southern Eddy (New Mexico) Counties and the Upper Marble Falls

Formation of the Eastern Shelf/Llano Uplift area. Upper Marble Falls data and discussion are included in this paper because the Upper Marble Falls succession prograded from the Llano Uplift area onto the Eastern Shelf during the Atokan. These Eastern Shelf carbonates appear to be attached to the carbonate-platform to -ramp succession present in the Val Verde Basin. Upper Marble Falls studies provide detailed sedimentological and facies analogs for describing shallow- to deeper water carbonates present throughout the Permian Basin in middle to late Atokan times.

Delaware Basin

In the Delaware Basin, Reeves County carbonate facies age equivalent to the Upper Marble Falls Formation are present at Chapman Deep field, Reeves County (fig. 21). These consist of (1) shallow-water bank facies of *Donezella* algal bioherms, oolitic-bioclastic grainstones, and interbank to lagoonal lower energy facies; (2) slope facies that are spiculitic and crinoidal argillaceous limestones and interbedded shales; (3) basinal carbonate and siliciclastic turbidite facies (Mazzullo, 1981; Von Bergen, 1985). In the Chapman Deep field area, total thickness of the Atokan series ranges from 205 to 370 m (670–1,200 ft) and is divided into three major environments—basinal (<213-m [700-ft] water depth) (member A), proximal to distal slope (member B), and shallow-water ramp to platform (member C), with reservoirs being restricted to the latter. However, in Desmoinesian- to Virgilian-age carbonate units, proximal slope facies (member B), which are characterized by coarse debris, are also reservoir intervals and should not be overlooked from an exploration standpoint. A generalized sequence stratigraphic framework has been added to figure 21 to illustrate lateral facies packaging and the association of reservoir facies with highstand carbonate deposition.

Reservoir Quality

Within shallow-water carbonates (member C), the reservoir interval is not confined to a particular facies, and porosity and permeability are dominantly secondary in origin, occurring during deep-burial diagenesis. Figure 22 illustrates the abrupt vertical facies changes and lack of correspondence between facies type and/or subaerial exposure surfaces. Lateral facies changes are also pronounced. The lack of correspondence between facies and reservoir interval extends to the wireline-log signature, where gamma-ray and sonic logs do not show indicative profiles for any individual facies type (fig. 22). The pay zone in the Texaco Reeves “AZ” Fee #1 well is approximately 50 m (164 ft) thick (fig. 22).

Diagenesis of the carbonates is complicated but can be distilled into two categories (Mazzullo, 1981; Von Bergen, 1985; Eren, 2005). (1) Early diagenesis involved both vadose and phreatic dissolution and cementation but resulted in overall occlusion of primary and secondary pores, except for thin, volumetrically minor intervals below exposure surfaces. (2) Late diagenesis in the deep burial environment (3,962 m [13,000 ft]) resulted in establishment of a secondary pore and fracture network. This network is thought to be a result of moldic porosity forming from dissolution of ooids, inter- and intraparticle calcite cements, by undersaturated fluids expelled from organic compounds along stylolites. Later tectonic movement and erosional unloading produced a microfracture system that crosscuts grains and earlier cements. Eren (2005), however, contended that microfracture and stylolite development are synchronous in Atokan carbonates in southern Eddy County, New Mexico, and cannot be linked to regional stress fields. Regardless of the cause of fracturing, this system, coupled with the pore

dissolution system, resulted in the producing-reservoir interval. Stylolites contributing to enhanced reservoir quality are best developed within relatively clean, impurity-free limestones and are thereby related to lithology and facies type (Von Bergen, 1985).

Dolomitization also plays a key role in reservoir development. Dolomite is found as both an early diagenetic phase (dolo-silt) and a late replacive and cementing fracture-fill phase in Atokan carbonates of the Delaware Basin (Von Bergen and Mazzullo, 1981; Eren, 2005). Late fracture fill and replacive dolomite generally have negative effects on porosity via occlusion but may be indicators of high-temperature fluid flow related to petroleum migration. In Chapman Deep field, saddle dolomite (in a strict sense, nonplanar C [Sibley and Gregg, 1987]) partly to completely occludes fracture porosity. Within Eddy County, Eren (2005) used stable isotope data to argue that ferroan saddle dolomite precipitated from 52 to 55°C fluids. However, this temperature regime appears too low for saddle dolomite (nonplanar-C) formation (Wright, 2001). Understanding dolomitization temperature and fluid-flow regime is important for predicting enhanced or diminished reservoir quality because dolomite appears restricted to the Delaware Basin during the Pennsylvanian.

In the southern Delaware Basin, the Atokan section at Rojo Caballos field (northwest Pecos County) consists of shale interbedded with limestone, capped and based by dark-gray shale (Hanson and Guinan, 1992). Limestone is a siliceous biomicrite with foraminifera and crinoids. A deep-marine embayment is the proposed depositional environment for Atokan carbonates and shales (Hanson and Guinan, 1992). Presence of siliceous biomicrites and shales indicates that the Rojo Caballos section is analogous to off-platform facies in the Upper Marble Falls in the Eastern Shelf and Llano regions. The

Upper Marble Falls succession thus provides an excellent outcrop analog area in which to understand facies distribution patterns in Rojo Caballos. Gross average thickness of the Atokan-Morrowan interval at Rojo Caballos is 210 m (700 ft). Net thickness of the producing zone is 45 m (150 ft), with a maximum of 75 m (250 ft). Porosity is a mixture of vug and dissolution that averages 12 percent. Permeability averages 0.1 md. Cumulative gas production at Rojo Caballos is 38,789 Bcf.

Data on the Atokan from the Northwest Shelf within New Mexico are sparse. Overall, total Atokan thickness decreases to approximately 150 m northward, given the estimates of 200 to 370 m in the center of the Delaware Basin. On the Northwest Shelf the Atokan comprises basal quartz sandstone interbedded with gray shales grading upward into tan, cherty limestones (Kues and Giles, 2004). Atokan sediments are continuous over Matador Arch but are thought to thin (Kues and Giles, 2004).

Eastern Shelf and Llano Uplift

Comparison of Upper Marble Falls and Lower Marble Falls Formations indicates that Atokan carbonates tend to be finer grained overall, with more widespread interbedded spiculitic shales and limestones. Southeast of the Llano Uplift, the Upper Marble Falls reaches a thickness of 150 m (495 ft). To the west-southwest in Sutton and Schleicher Counties, Atokan-age limestones are interpreted to be Upper Marble Falls that prograded westward from the Llano area. These units, which overlie the siliciclastics previously described, compose a middle unit of light-colored massive limestone on the order of 46 to 76 m (150–250 ft) thick, overlain by an uppermost unit that is a variable mix of thin-bedded, light-colored limestone and shale (Smithwick Formation?) of varying description (Rall and Rall, 1958). To the northeast, within Wise County, in the Fort

Worth Basin, the Upper Marble Falls averages approximately 61 m (200 ft) in thickness (fig. 40, “Depositional History of the Morrowan Succession (Lower Pennsylvanian) in the Permian Basin”).

Erlich and Coleman (2005) defined seven lithofacies for the Upper Marble Falls Formation that range from low-energy fusulinid and spiculitic limestones to shallower water, subtidal algal and conglomeratic limestones and intertidal beach rock. Overall the depositional environment of the Upper Marble Falls Limestone is not dissimilar to that of the Lower Marble Falls and does not warrant a repetition of earlier discussion of the Lower Marble Falls.

However, the subtidal algal limestone identified in the Upper Marble Falls is distinctive enough from the underlying Lower Marble Falls facies that it requires discussion. This facies comprises skeletal sand shoals and mounds dominated and constructed by the green algae *Komia* spp., found in association with high-energy beach rock (fig. 23). Shape and size of the mound and shoal facies in the Upper Marble Falls are similar to those of the mound facies illustrated in the Lower Marble Falls (fig. 37, “Depositional History of the Morrowan Succession (Lower Pennsylvanian) in the Permian Basin”). Constituent grains and lithifying agents of the two mound types may be very different. This facies has reservoir potential because diagenetic modification (leaching) and primary porosity are greater than in the lower energy facies. This higher energy facies is also similar to mound and bioherm facies in the overlying Strawn succession, which are good reservoirs. Overall distribution and occurrence of these algal facies are important to regional exploration for Pennsylvanian carbonate plays, as illustrated by Mazzullo (1981) for Chapman Deep field in the Delaware Basin. Both

environment and, possibly, age are related to the type of organism creating bioherms/shoals. In the Lower Marble Falls, mounds are dominated by *Cuneiphyucus* and *Donezella*, whereas in the Upper Marble Falls they are dominated by *Komia* and *Chaetetes*. The energy of the environment may be responsible for change in the algal community because *Komia* and *Chaetetes* are much more robust, high-energy, tolerant forms than *Cuneiphyucus* and *Donezella*. In general, the aforementioned algae appear to give way in dominance to phylloid algae in younger units (Desmoinesian-Virgilian).

Reservoir Quality

The Upper Marble Falls higher energy mound/shoal facies have the best reservoir quality, with average porosity of 10 percent and 2 to 6 md permeability (Brown and Garrett, 1989) Llano Uplift/Eastern Shelf fields in Coleman, Brown, and Eastland Counties have produced approximately 127.1 Bcf of gas (circa 1989). Trapping style is generally stratigraphic (for example, facies pinch-out) with or without a structural overprint.

Facies Patterns and Sequence Stratigraphy

The relationship between the Smithwick Formation and carbonate units reflects a backstepping and drowning of the Upper Marble Falls platform/ramp. However, Upper Marble Falls sediments are characterized by an upward-shallowing sequence capped by a Type 1 unconformity and sequence boundary. It therefore appears that 3rd-order sea-level change dominated in controlling unconformities and sequences represented in the Upper Marble Falls, and overall lack of accommodation caused the final demise of the platform (Erlich and Coleman, 2005). The backstepping of the Upper Marble Falls relative to the Lower Marble Falls is illustrated in figures 41 and 42 of “Depositional History of the

Morrowan Succession (Lower Pennsylvanian) in the Permian Basin.” Note that in figure 41, the terminal position of the Upper Marble Falls platform is more than 100 km farther to the southwest and west than illustrated (Erlach and Coleman, 2005) (compare with fig. 1, “Depositional History of the Morrowan Succession (Lower Pennsylvanian) in the Permian Basin”). Final death of the carbonate factory occurred as Smithwick shales and Atokan siliciclastics prograded from the east over the greater Llano area.

It is apparent from current research that the distally steepened Lower Marble Falls ramp evolved into a steeper sided platform or rimmed shelf during transgression. The platform to rimmed-shelf area caught up and kept up with sea-level rise during transgression, resulting in units that display upward-shallowing trends. Mazzullo (1981) proposed a similar change from ramp to platform architecture for Atokan carbonates within Chapman Deep field, which was discussed in the previous section.

Understanding growth of the carbonate system (for example, platforms, ramps) and its response to high-frequency, high-amplitude, icehouse-condition, sea-level fluctuation and overall 2nd-order global sea-level rise of the Morrowan to mid-Virgilian is vitally important in creating a proper exploration model for the Permian Basin. In a standard abruptly backstepping and/or prograding carbonate platform, the overlying carbonate platform and potential reservoir are displaced relative to the underlying carbonate platform and reservoir (for example, Erlach and Coleman [2005] model). A change in architecture from ramp to platform and/or shelf in response to sea level will result in a greater likelihood of stacked carbonates and reservoir successions (for example, Read, 1985, type model). This observation becomes even more critical when trying to understand the nature of carbonates overlying Atokan-age units in the Permian

Basin. The Upper Marble Falls succession present in Eastern Shelf and Llano Uplift areas provides detailed data that are needed in understanding and mapping regional distribution of the subsurface Atokan carbonate facies in the Midland Basin, CBP, and the Delaware Basin.

DISTRIBUTION OF ATOKAN CARBONATES

Distribution of Atokan-age carbonates illustrated in figure 1 is the result of analysis of well logs, wireline logs, and detailed sedimentological data (for example, Llano Uplift and Delaware Basin areas). Overall, carbonate deposition is much more widespread in the Atokan than in the Morrowan. Westward progradation of the Upper Marble Falls Platform resulted in carbonate deposition across the Eastern Shelf. This carbonate platform appears to connect with a thick succession of carbonates nucleating on the Devils River Uplift in Val Verde and Edwards Counties. According to seismic and well log correlations, most of what later became the CBP was covered by a relatively uniformly thick succession of carbonates. This carbonate platform was linked eastward with the Eastern Shelf, southeastward with the Devils River Uplift, and westward with the northern Delaware Basin ramp to platform area. Given previous interpretations of the Diablo Platform and northern Northwest Shelf area, the Atokan was a time of more widespread carbonate deposition relative to the underlying Morrowan

SUMMARY OF ATOKAN CARBONATE SUCCESSION

Because relatively little is known about Permian Basin Atokan-age carbonates, understanding and documenting the Upper Marble Falls Formation from both outcrop and subsurface datasets are key to proper interpretation of the Permian Basin succession. Chapman Deep and Marble Falls type carbonates have potential as both a primary (for

example, leaching of bioclasts and primary porosity) and a secondary (fracture) reservoir. Atokan carbonates in the Permian Basin may be overlooked hydrocarbon targets, especially with respect to proximal slope facies targets. Interfingering of Smithwick Formation shales and equivalents with Atokan carbonates results in an interesting source/trap situation, where Upper Marble Falls Formation carbonates may also hold potential as fractured reservoirs for shale gas.

When comparing the carbonate succession regionally, one obvious factor that must be understood is apparent response to eustasy and tectonics between the greater Eastern Shelf/Llano uplift area, Northwest Shelf/Delaware Basin margin, and the CBP. At a 2nd-order eustasy level, all parts of the greater Permian Basin area appear to be reacting similarly (for example, lowstand followed by transgression). The 3rd- and 4th-order eustatic fluctuations are more important for overall reservoir organization and quality but are not defined well enough currently to help with exploration or production. Localized differences in rate of sediment supply also affected carbonate deposition by siliciclastic poisoning, such as in the areas of the Ozona Uplift and Gaines County Uplift.

In summary several key issues are crucial to an understanding of Atokan-age carbonates. Many of these issues have a direct bearing on exploitation of, and exploration for, new reservoirs in the Permian Basin.

1. Scale: Studies within and external to the Permian Basin must be put into regional sequence stratigraphic context.
2. Structure: Many stratigraphic relationships proposed for the Pennsylvanian rely heavily on interpretation and identification of structure (for example, the CBP). However, many of the studies present conflicting or, at best, ambiguous

structural/stratigraphic interpretations. Unraveling of the structural evolution of the Permian Basin requires intense, dedicated study and is discussed in its own paper.

3. Nomenclature: A concerted effort must be made to unify the stratigraphic nomenclature applied to Atokan carbonates. It is proposed that the term Upper Marble Falls Formation be used for all platform to ramp carbonates in the greater Permian Basin area in outcrop and subsurface.

DISCUSSION AND SUMMARY OF THE ATOKAN IN THE PERMIAN BASIN

Atokan coarse-grained, siliciclastic deposits are confined largely to the north and south margins of the Permian Basin (that is, the Northwest Shelf, Kent and Kinney Counties) and small areas in the center of the basin (that is, Upton and Midland Counties). These siliciclastics are coarse-grained, alluvial deposits at the base but are more marine upsection, in contrast to those of the Morrowan. Marine, shore-parallel sandstone bodies found in the Northwest Shelf and Matador Uplift areas provide a more geometrically and geographically definable play than do the underlying lower Atokan and Morrowan incised-valley-fill sediments. The presence of an extensive fan-delta to basin-floor-fan complex across Upton to Midland County, indicates that basin-floor-fan type plays might be present in other parts of the Permian Basin near uplifted areas (for example, Gaines, Dawson, Pecos, and Terrell Counties). Siliciclastics illustrated in figure 1 in Kinney and Uvalde Counties (that is, Kerr Basin) appear to have had an easterly source but did not migrate into the Val Verde owing to the carbonate platform associated with the paleohigh of the Devils River Uplift.

Carbonate deposition was widespread across much of the basin during most of the Atokan, varying from shallow-water, high-energy to basinal low-energy facies. The

effects of 3rd- and 4th-order sea-level falls are manifested in carbonates as subaerial exposure surfaces. Although these surfaces/events do not appear to control reservoir development within the Chapman Deep area, other reservoirs within the Permian Basin may nevertheless be largely controlled by diagenesis caused during exposure. The link of subaerial exposure to enhanced reservoir quality is extremely important in younger Desmoinesian- to Virgilian-age carbonate reservoirs in the Permian Basin.

Given the organic-carbon-content values of the Smithwick Shale and equivalents, more study is needed to further delineate distribution of these units because they have good potential as shale-gas reservoirs in the northern Midland Basin and southern Delaware Basin.

PALEOGEOGRAPHIC SUMMARY

Proposed distribution of Atokan-age sediments across the Permian Basin and surrounding areas, which is based on interpretations in this paper, is illustrated in figure 1. Exact age of the reconstruction is lower to middle Atokan. Areas of siliciclastic deposition illustrated in Upton, Midland, Kent, Stonewall, King, Knox, Cottle, Foard, and Hardeman Counties were transgressed by middle to late Atokan time and comprise carbonate and shale facies. In the late Atokan, carbonate lithologies dominated over the Ozona Arch area, whereas in the Matador Uplift area, the Smithwick Formation was present. In Eddy and Lea Counties, New Mexico, carbonate rocks with interbedded shales dominated by the late Atokan. The boundary between basinal carbonates and shales (Smithwick Formation) across the Llano Uplift and northward corresponds to latest Atokan time.

Early Atokan-age siliciclastics dominated deposition in the far west of the Permian Basin, northwest of the Ozona Arch, and east of the Matador Uplift, while carbonate deposition dominated elsewhere (fig. 1). The predominance of carbonate facies across most of the Permian Basin is a result of (1) lack of siliciclastic supply, (2) overall 2nd-order rising sea level, and (3) progradation of the west-facing margin of the Upper Marble Falls Formation westward owing to lower accommodation and backstepping of the east margin retreating from the encroaching Atokan deltaics from the east. A transition from platform and/or ramp carbonates to more basinal carbonates and, ultimately, shales in the center of the Midland Basin, CBP, and Delaware Basin is implied. This is supported by well data in the Midland Basin, indicating a westward shift from carbonates to shalier lithologies. A large area of platform to ramp carbonates is thought to have existed along the trend of the antecedent CBP and links with the northern Delaware Basin and Eastern Shelf.

A small number of Precambrian inliers on the CBP trend appear to have been exposed and to have been shedding material into the basin (for example, Lea County, New Mexico, and Pecos and Crockett Counties, Texas). One of these uplifted blocks is the Ozona Arch, which provided the source for alluvial channels of Upton County and basin-floor fans of Midland County, during the lowstand event at the beginning of the Atokan. At roughly the same time, a small uplifted area on or near the Fort Stockton High in Pecos County also emerged. According to seismic and facies data, a similar small, uplifted area also existed in Eddy and Gaines Counties. Another such positive feature is also apparent in Roosevelt County, New Mexico. This area corresponds roughly to the Bravo Dome area. The uplift of this area probably helped diminish the southward influx

of sediments from the Pedernal Uplift and also funneled them into the Palo Duro Basin. A shallow seaway probably still extended between the uplift (Bravo Dome) and the Pedernal highlands.

Siliciclastics in the Kerr Basin (for example, Kinney, Uvalde, and Zavala Counties) were sourced from the east by a sutured zone along the Ouachita Foldbelt. Although illustrated as marine to alluvial siliciclastics in figure 1, data are sparse, and sediments may instead reflect deposition from gravity-flow processes. In the Delaware Basin the siliciclastic lowstand succession was dominated by localized incised valleys. Valley systems were infilled by multiple transgressive facies types. Areas of shale deposition in the northern Midland and southern Delaware Basins reflect ensuing subsidence of these two basins, which becomes more prominent in younger successions.

KEY CONCLUSIONS

- Atokan-age units in the Permian Basin reflect an abrupt 2nd-order transgression from alluvial and shallow-marine siliciclastic deposition to carbonate deposition.
- Atokan-age siliciclastics dominated deposition in the northwest of the Permian Basin, while carbonate deposition dominated throughout the remainder of the basin.
- Early Atokan siliciclastic deposition took place in isolated incised-valley-fill systems. However, these systems were quickly replaced by shore-parallel, open-marine facies. The shore-parallel sands provide attractive exploration targets because they are geometrically and geographically constrained. Shore-parallel sandstone bodies are probably transgressive barrier bars or shelf ridges, not regressive deltaic and/or shoreline sands.

- In the southern Midland Basin, an incised valley sourced from the Ozona Arch and the CBP served as a conduit for fan-delta deposition and shelf-margin bypass, resulting in deposition of basin-floor-fan deposits in Midland County.
- The Smithwick Formation and shales of equivalent age within the Permian Basin have sedimentological characteristics and TOC similar to those of the Barnett Formation and ultimately may be good shale-gas targets.
- Atokan carbonates were deposited over a much larger area in the Permian Basin than previously documented. Especially important is the proposed link between carbonates on the Devils River Uplift (Val Verde and Edwards Counties.) and the Eastern Shelf. Algally dominated bioherms and higher energy facies (ooid grainstones), which were affected by burial diagenesis and subsequently fractured, comprise the best carbonate reservoirs. However, secondary porosity formed during exposure should not be discounted as a primary reservoir-creation mechanism. Proximal coarse-grain slope-carbonate facies are potentially another exploration target. Atokan basinal and slope carbonates interfingered with shale (for example, the Smithwick Formation) also hold potential as fractured reservoirs for expelled shale gas.
- The Smithwick Formation and its lateral shale equivalents have high enough TOC values to warrant studies to define their distribution and origin as potential shale-gas sources and reservoirs similar to those of the Barnett Formation.

Conclusions drawn herein should provide guidelines and ideas for interpretation of the Atokan section within the Permian Basin.

REFERENCES

- Blakey, R. C., 2005, Paleogeography and geologic evolution of ancestral Rocky Mountains: Geological Society of America Annual Meeting, Salt Lake City, p. 442. <http://jan.ucc.nau.edu/~rcb7/garmgeolhist.html>.
- Brister, B. S., Stephens, W. C., and Norman, G. A., 2002, Structure, stratigraphy, and hydrocarbon system of a Pennsylvanian pull-apart basin in North-Central Texas: American Association of Petroleum Geologists Bulletin, v. 86, p. 1–20.
- Brown, L. F., and Garrett, C. M., 1989, Upper Marble Falls Platform carbonate-bank limestone, *in* Kisters, E. C., Bebout, D. G., Seni, S. J., Garrett, C. M., Brown, L. F., Hamlin, H. S., Dutton, S. P., Ruppel, S. C., Finley, R. J., and Tyler, N., eds., Atlas of major Texas gas reservoirs: The University of Texas at Austin, Bureau of Economic Geology, p. 161 p.
- Candelaria, M. P., 1990, “Atoka” detrital a subtle stratigraphic trap in the Midland Basin, *in* Flis, J. E., and Price, R. C., eds., Permian Basin oil and gas fields; innovative ideas in exploration and development: West Texas Geological Society, v. 90-87, p. 104–106.
- Conselman, F. B., 1954, Preliminary report on the geology of the Cambrian trend of west central Texas: Abilene Geological Society Geological Contributions, p. 10–23.
- Crowder, W. T., 2001, “But, the logs looked great!”...commercial gas production in the lower Atoka (Grant) Sands, Parker County, Texas; does stratigraphic complexity

- induce this economic enigma?; *in* AAPG Southwest Section meeting; abstracts, p. 385.
- Dalziel, I. W. D., Lawver, L. A., Gahagan, L. M., Campbel, D. A., and Watson, G., 2002, Texas through time, Plate's plate model: The University of Texas at Austin Institute for Geophysics, http://www.ig.utexas.edu/research/projects/plates/movies/Texas_Through_Time_020312.ppt.
- Dutton, S. P., 1980, Depositional systems and hydrocarbon resource potential of the Pennsylvanian System, Palo Duro and Dalhart basins, Texas Panhandle: The University of Texas at Austin, Bureau of Economic Geology, Geological Circular 80-8, 49 p.
- Edwards, H. S., 1979, Atoka gas in southern Cottle and northern King counties, Texas: American Association of Petroleum Geologists Bulletin, v. 63, p. 1425–1426.
- Eren, M., 2005, Origin of stylolite related fractures in Atoka bank carbonates, Eddy County, New Mexico, U.S.A.: Carbonates and Evaporites, v. 20, 1, p. 42–49.
- Erlich, R. N., and Coleman, J. L., 2005, Drowning of the Upper Marble Falls carbonate platform (Pennsylvanian), central Texas; a case of conflicting “signals?” *in* Sedimentology in the 21st Century; a tribute to Wolfgang Schlager, v. 175, p. 479–499.
- Fort Worth Geological Society, 1957, Cross section Brown Co. to Hill Co., Texas: Fort Worth Basin Project Committee.
- Grayson, R. C., Merrill G. K., Trice E. L., and Westergaard E. H., 1989, Pennsylvanian strata of central Texas: stratigraphic and conodont biostratigraphic relationships:

- Carboniferous geology of the Northern Llano Uplift, Southern Fort Worth Basin and Concho Platform., *in* Southwestern Association of Student Geological Societies, Fieldtrip Guidebook, p. 1–14.
- Groves, J. R., 1991, Fusulinacean biostratigraphy of the Marble Falls Limestone (Pennsylvanian), western Llano region, central Texas: *Journal of Foraminiferal Research*, v. 21, p. 67–95.
- Hanson, B. M., and Guinan, M. A., 1992, Rojo Caballos, South Field, U.S.A.; Delaware Basin, Texas: stratigraphic traps III: *American Association of Petroleum Geologists*, v. 23, p. 83–112.
- James, A. D., 1985, Producing characteristics and depositional environments of Lower Pennsylvanian reservoirs, Parkway-Empire South area, Eddy County, New Mexico: *American Association of Petroleum Geologists Bulletin*, v. 69, p. 1043–1063.
- Kluth, C. F., 1986, Plate tectonics of the ancestral Rocky Mountains, *in* Peterson, J. A., ed., *Paleotectonics and sedimentation in the Rocky Mountain region, United States*: *American Association of Petroleum Geologists*, v. 41, p. 353–369.
- Kues, B. S., and Giles, K. A., 2004, The late Paleozoic Ancestral Rocky Mountains System in New Mexico, *in* Mack, G. H. and Giles, K. A., eds., *The geology of New Mexico*: *New Mexico Geological Society, Special Publication 11*, p. 137–152.
- Mazzullo, S. J., 1981, Facies and burial diagenesis of a carbonate reservoir; Chapman deep (Atoka) field, Delaware Basin, Texas: *American Association of Petroleum Geologists Bulletin*, v. 65, p. 850–865.

- McBride, E. F., and J. E. Kimberly, 1963, Sedimentology of Smithwick Shale (Pennsylvanian), eastern Llano region, Texas: American Association of Petroleum Geologists Bulletin, v. 47, p. 1840–1854.
- Ng, D. T. W., 1979, Subsurface study of Atoka (Lower Pennsylvanian) clastic rocks in parts of Jack, Palo Pinto, Parker, and Wise counties, North-central Texas: American Association of Petroleum Geologists Bulletin, v. 63, p. 50–66.
- Ota, S., 2001 Integrated 3-D seismic analysis of Atoka Formation sandstone reservoirs, Vacuum Field vicinity, Lea County, New Mexico: Socorro, NM, New Mexico Institute of Mining and Technology, Master's thesis, p. 89.
- Plummer, F. B., 1950, The Carboniferous rocks of the Llano region of central Texas: University of Texas, Austin, Bureau of Economic Geology, Publication No. 4329, 170 p.
- Posamentier, H. W., 2002, Ancient shelf ridges; a potentially significant component of the transgressive systems tract; case study from offshore Northwest Java: American Association of Petroleum Geologists Bulletin, v. 86, p. 75–106.
- Rall, R. W., and Rall, E. P., 1958, Pennsylvanian subsurface geology of Sutton and Schleicher counties, Texas: American Association of Petroleum Geologists Bulletin, v. 42, p. 839–870.
- Read, J. F., 1985, Carbonate platform facies models: American Association of Petroleum Geologists Bulletin, v. 69, p. 1–21.
- Reading, H. G., and Collinson, J. D., 1996, Clastic coasts, *in* Reading, H. G., ed., Sedimentary environments; processes, facies and stratigraphy: Oxford, Blackwell Science p. 154–231.

- Ross, C. A., and Ross, J. R. P., 1987, Late Paleozoic sea levels and depositional sequences, *in* Ross, C. A., and Haman, D., eds., Timing and depositional history of eustatic sequences; constraints on seismic stratigraphy: Ithaca, NY, Cushman Foundation for Foraminiferal Research, v. 24, p. 137–149.
- Sibley, D. F., and Gregg, J. M., 1987, Classification of dolomite rock textures: *Journal of Sedimentary Research*, v. 57, p. 967–975.
- Staples, M. E., 1986, Oil-productive basal Pennsylvanian channel-fill sandstones, southern Baylor County, Texas, *in* Ahlen, J. L., and Hanson, M. E., eds., Southwest Section American Association of Petroleum Geologists Convention, Ruidoso, New Mexico (April 27–29, field trips on April 26 and 27): New Mexico Bureau of Mines and Mineralogy Resources , p. 107–113.
- Tai, P.-C., and Dorobek, S. L., 1999, Preliminary study on the late Paleozoic tectonic and stratigraphic history at Wilshire Field, central Upton County, southwestern Midland Basin, West Texas: The Permian Basin; providing energy for America, v. 99-106, p. 19–29.
- Tai, P.-C., and Dorobek, S. L., 2000, Tectonic model for late Paleozoic deformation of the Central Basin Platform, Permian Basin region, West Texas: The Permian Basin; proving ground for tomorrow's technologies, v. 00-109, p. 157–176.
- Troschinetz, J., and Loucks, R. G., 1991, Reservoir quality distribution in the Pennsylvanian Bend Conglomerate fan-delta system off the southeastern Central Basin Platform, *in* Candelaria, M. P., ed., Permian Basin plays; tomorrow's technology today: West Texas Geological Society, p. 163.

- Van der Loop, M. L., 1991, Depositional environments in the Arenoso Field, Winkler County, Texas Permian Basin plays; tomorrow's technology today, p. 73-91.
- Von Bergen, D., 1985, Microfacies, depositional environments and diagenesis of Atokan carbonates, Delaware Basin, Reeves County, Texas, U.S.A.: University of Illinois at Urbana-Champaign, Master's thesis, 101 p.
- Wright, W. R., 2001, Dolomitization, fluid-flow and mineralization of the Lower Carboniferous rocks of the Irish Midlands and Dublin Basin regions: University College Dublin, National University of Ireland, Ph.D. thesis, 407 p.
- Yang, K.-M., and Dorobek, S. L. 1995, The Permian Basin of West Texas and New Mexico; tectonic history of a "composite" foreland basin and its effects on stratigraphic development, *in* Dorobek, S. L., and Ross, G. M., eds., Stratigraphic evolution of foreland basins: SEPM (Society for Sedimentary Geology), v. 52, p. 149–174.
- Ye, H., Royden, L., Burchfiel, C., and Schuepbach, M., 1996, Late Paleozoic deformation of interior North America; the greater ancestral Rocky Mountains: American Association of Petroleum Geologists Bulletin, v. 80, p. 1397–1432.

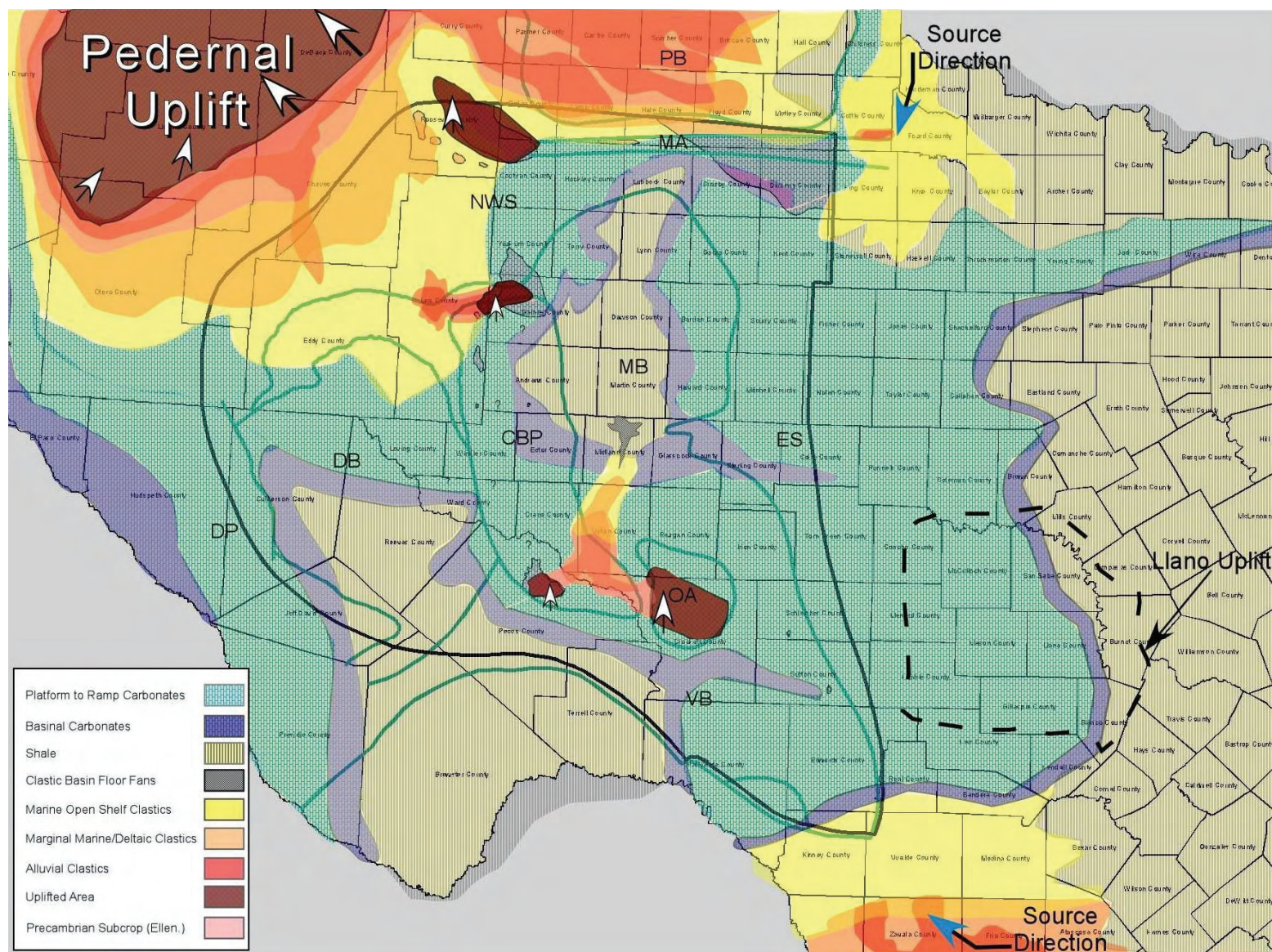


Figure 1. Atokan paleogeography and facies distribution map for the greater Permian Basin region during the early to middle Atokan. Siliciclastics illustrated in Upton, Midland, King, Cottle, Eddy and Lea Counties are largely transgressed by shales and carbonates by mid- to late Atokan times. Major subregions outlined by dark-green lines: Central Basin Platform (CBP), Delaware Basin (DB), Diablo Platform (DP), Eastern Shelf (ES), Matador Arch (MA), Midland Basin (MB), Northwest Shelf (NWS), Ozone Arch (OA), Palo Duro Basin (PB), Val Verde Basin (VB). Orange alluvial siliciclastic zone centered in Cottle County corresponds to Broken Bone Graben. Fort Worth Basin centered in Wise County. Llano Uplift area outlined by black dashed line. Sizes of arrows surrounding Pedernal and other uplifted areas correspond to relative amount of uplift (the larger the arrow, the greater the relative uplift).

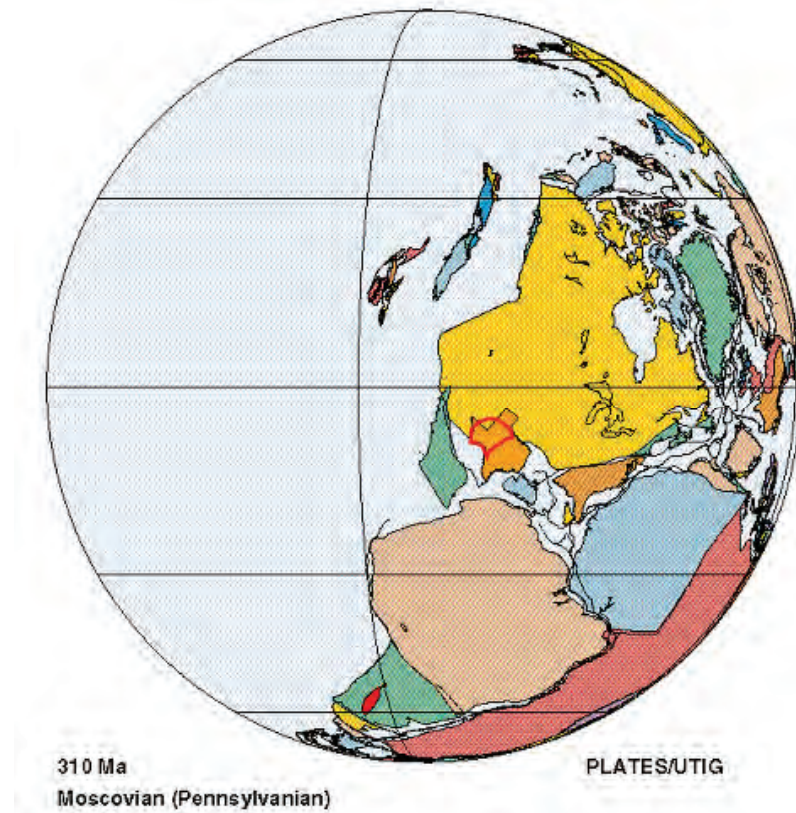


Figure 2. Atokan-age (circa 310 Ma) Texas plate tectonic reconstruction. Note marine (light-blue) to continental (light-orange) transition that occurs across Texas (dark-orange) in the area of the Permian Basin (red polygon). Suturing of continents has resulted in partly restricted marine subbasin between the plates. Diagram modified from Dalziel and others (2002). Permian Basin migrated north (that is, more equatorial) relative to its Morrowan position.

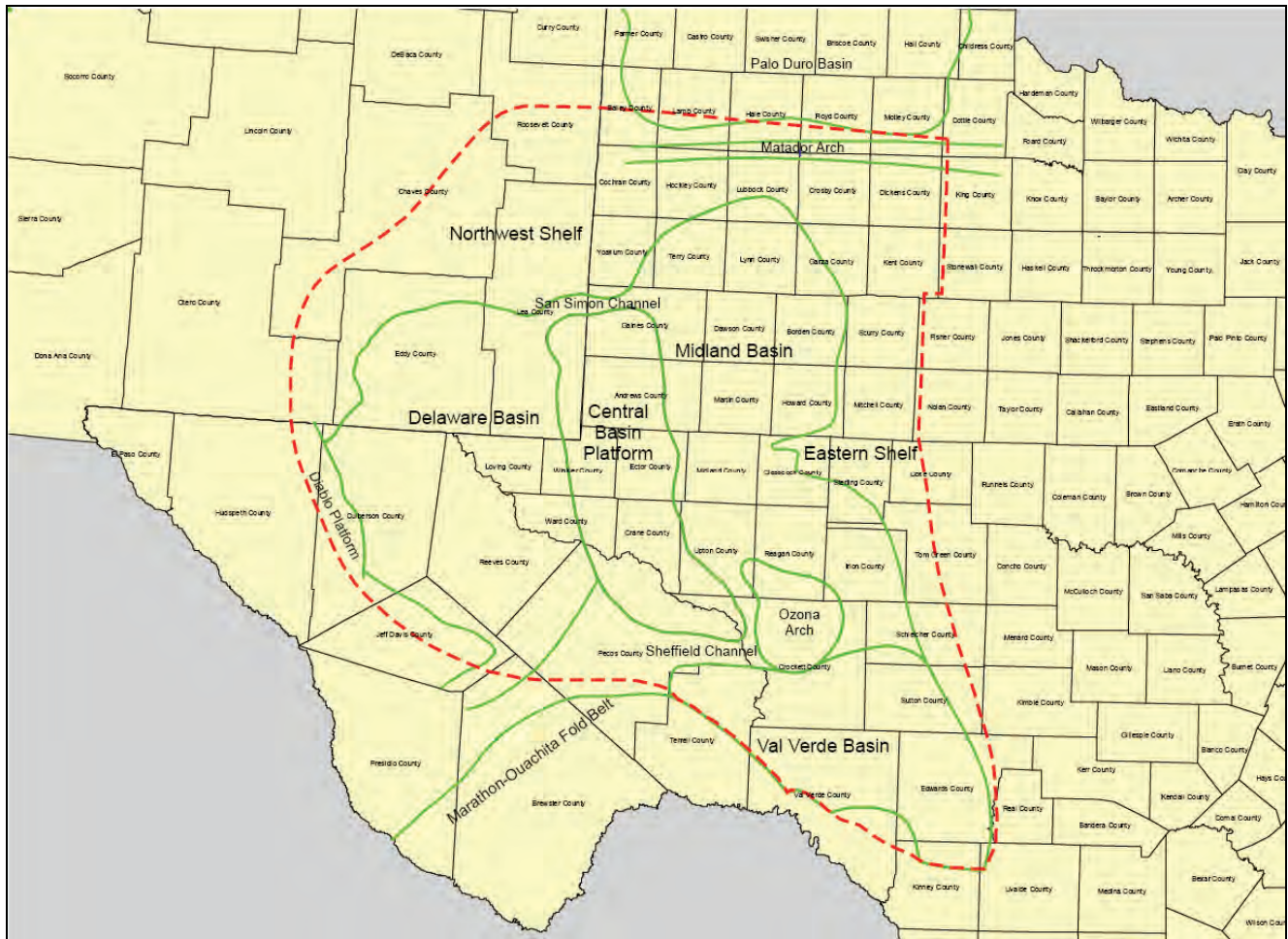


Figure 3. Permian Basin (dashed red line) and major geologic features. Many of the features were in the early stages of development during the Atokan. Compare figure 3 and figures 4 through 6 for previous models of facies distribution relative to the basin outline. Figure 1 illustrates the facies distribution for the greater Permian Basin area derived from this study. The west margin of the Fort Worth Basin runs north-south through Palo Pinto County.

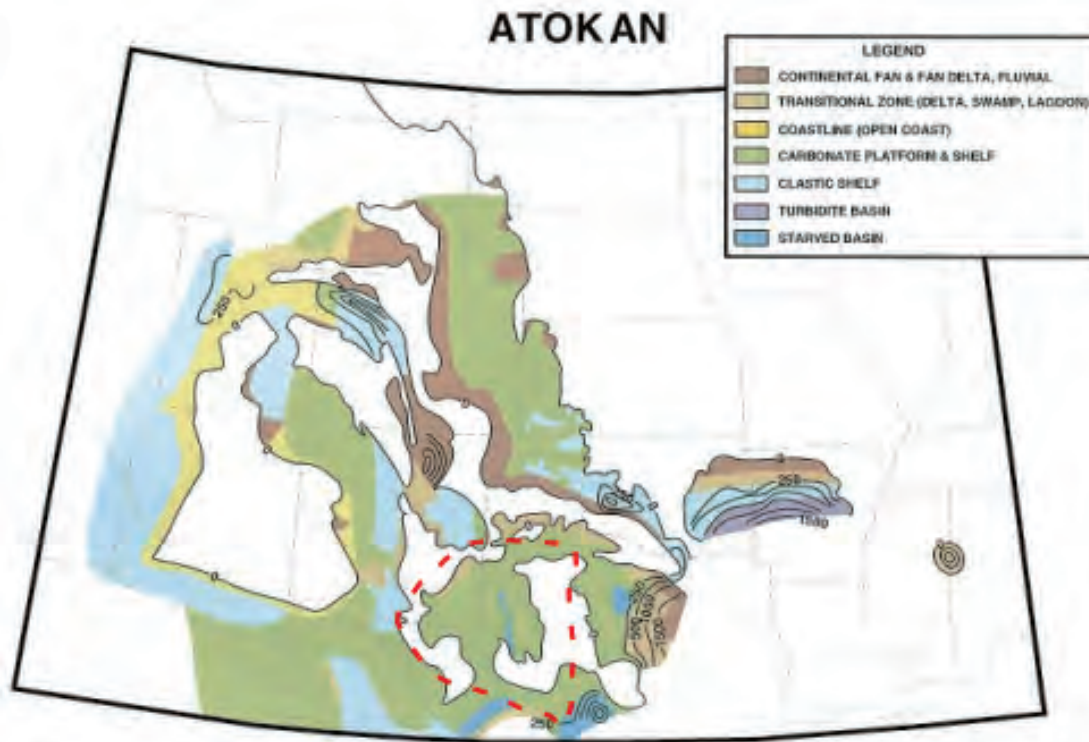


Figure 4. Generalized Rocky Mountain region and southern Midcontinent Atokan paleogeography (from Ye and others, 1996). White areas indicate either nondeposition or erosion (not clarified in the original text). Note that most of the Permian Basin (outlined by red dashed polygon) was considered a carbonate platform and/or shelf by Ye and others (1996). The Diablo Platform, Ozona Arch, and Eastern Shelf areas appear substantially uplifted in this model (fig. 3).



Figure 5. Areas of net subsidence (white <50 m/Ma to red >300 m/Ma) and net uplift (green <50 m/Ma) for the Atokan series (after Kluth, 1986). This interpretation shows that Llano and Ozona Arch areas were both uplifted and connected.

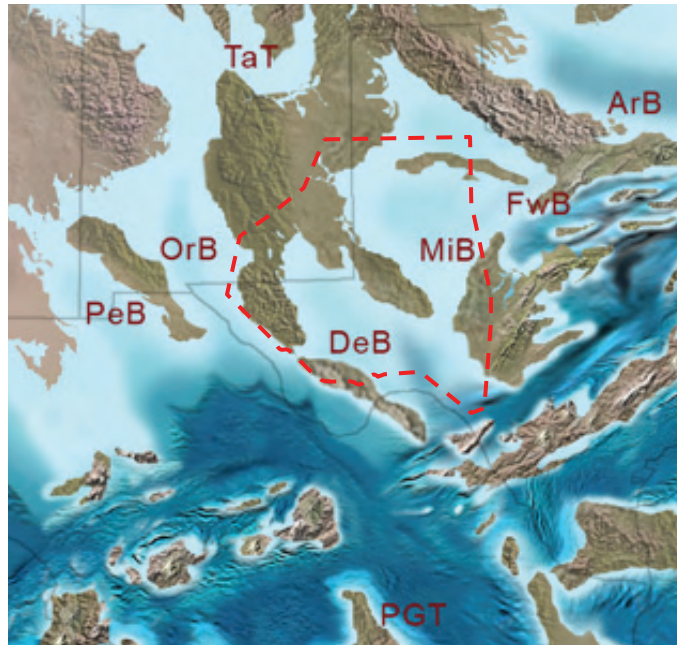


Figure 6. Regional paleogeography for the Atokan (circa 315 Ma). DeB and MiB refer to Delaware and Midland Basins, respectively. Permian Basin outlined by red dashed polygon. ArB—Anadarko Basin, FwB—Fort Worth Basin, OrB—Orogrande Basin, PeB—Pedregosa Basin, TaT—Taos Trough. Uplifted areas represented by browns, shallow marine by light- to medium-blues, and deep marine by dark-blue (from Blakey, 2005). Note prominent differences in uplifting and subsiding areas from those of figure 4, especially with respect to eastern and southeastern New Mexico and location of Pedernal Uplift, Central Basin Platform, and Eastern Shelf regions (figs. 1, 3).

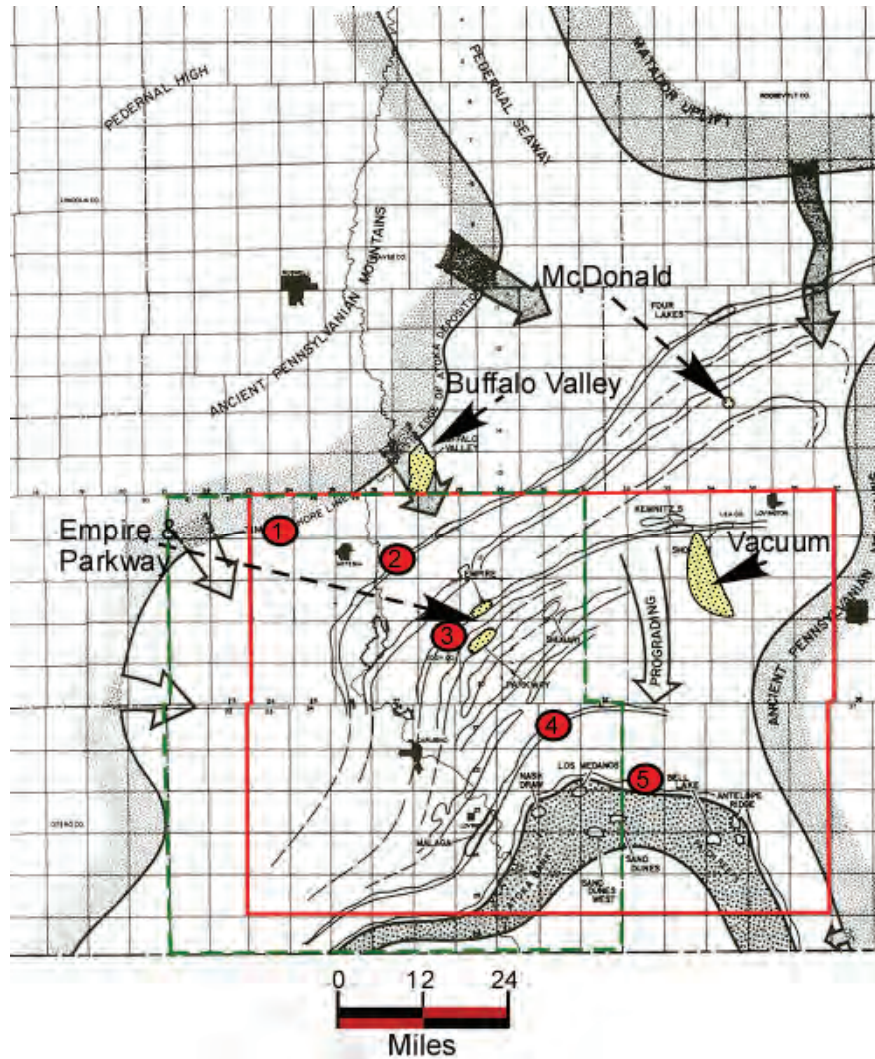


Figure 7. Atokan-age depositional paleogeography for the north Delaware Basin and Northwest Shelf (from James, 1985). James (1985) interpreted the shoreline position to step basinward through time (1 to 5 [oldest to youngest]). It is alternatively possible that shelf ridges or barrier bars formed during transgression and are younger updip (oldest at shoreline, 5 and youngest at 1). Note the need for an eastern source area for Vacuum field coarse valley-fill sediments because it is isolated from the Pedernal High to the northwest.

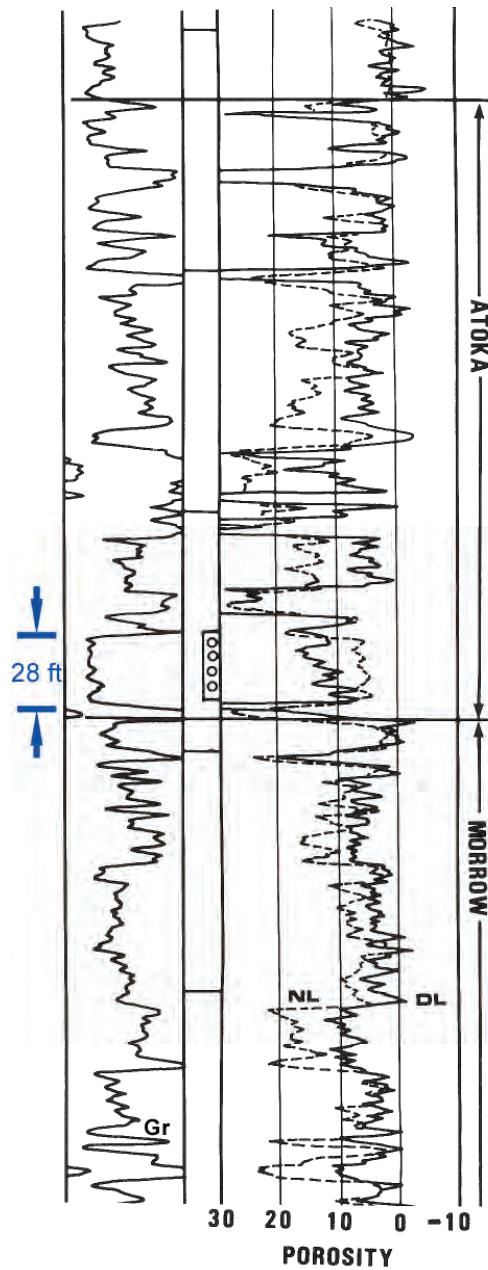


Figure 8. Typical log character of the Atokan section in the Southland Royalty “A” No.1 well in Empire field, Eddy County, New Mexico. Neutron-density crossover indicates gas effect on well log response.

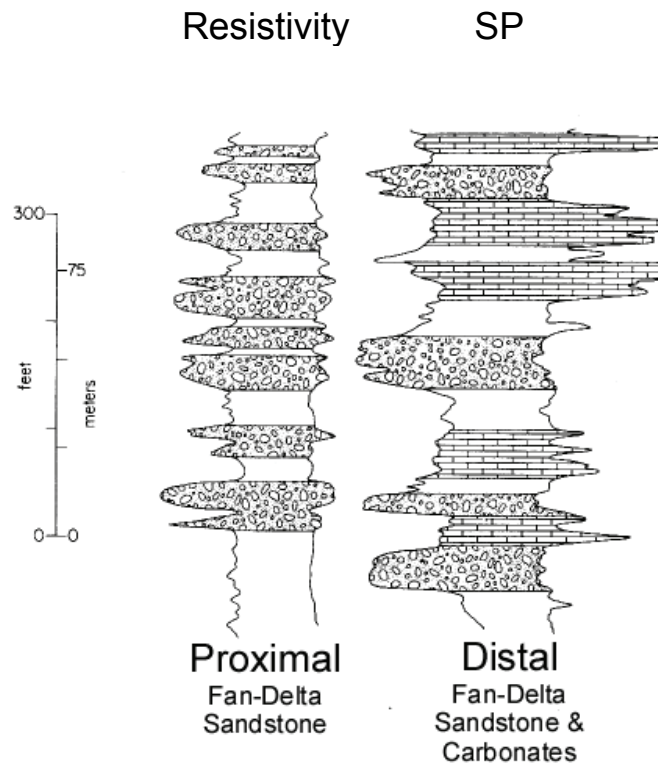
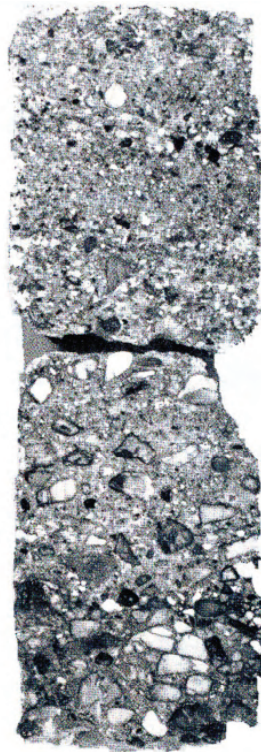
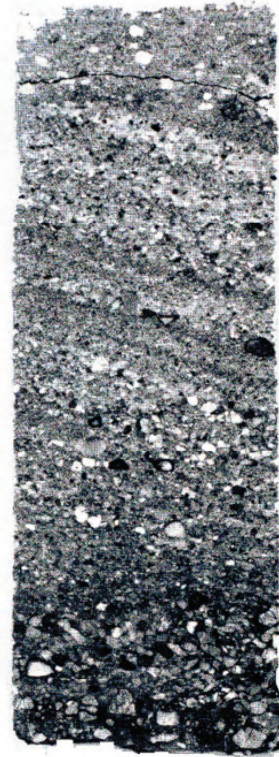


Figure 9. Schematic wireline-log signature for fan-delta facies (after Dutton, 1980).



2cm
Upward-fining sequence in
Atokan fan-delta from Standard
and Robinson #2 Tippen well, Cottle Co.



2cm
Crossbedding in Atokan fan-delta, from Standard
Oil #1 Barron well, Cottle Co.

Figure 10. Core-slab photographs of typical coarse-grained fan-delta facies (after Dutton, 1980).

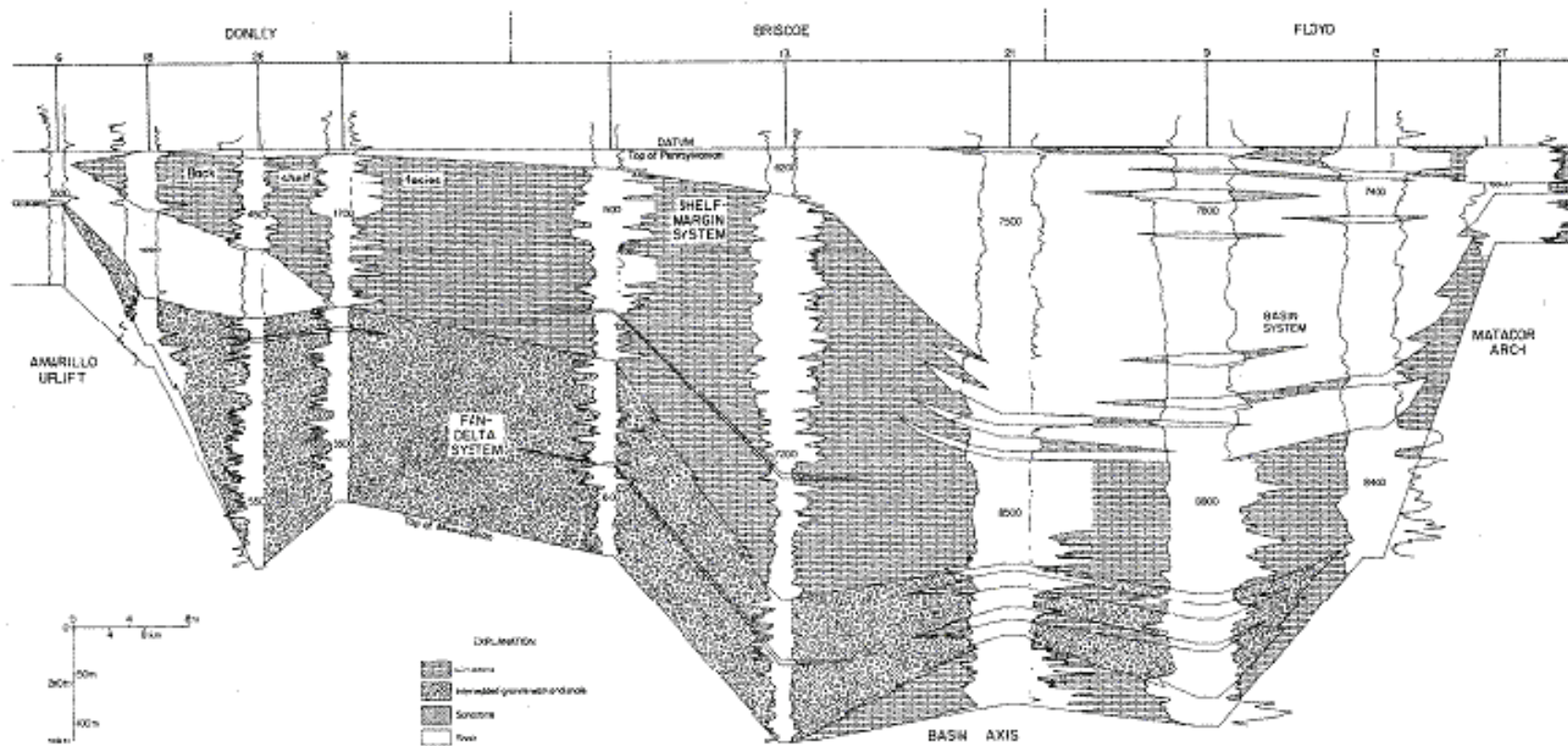


Figure 11. Regional correlation of Pennsylvanian units within the Palo Duro Basin (after Dutton, 1980). The fan-delta system is Atokan in age and is similar to fan deltas described for the Midland Basin (for example, Upton County).

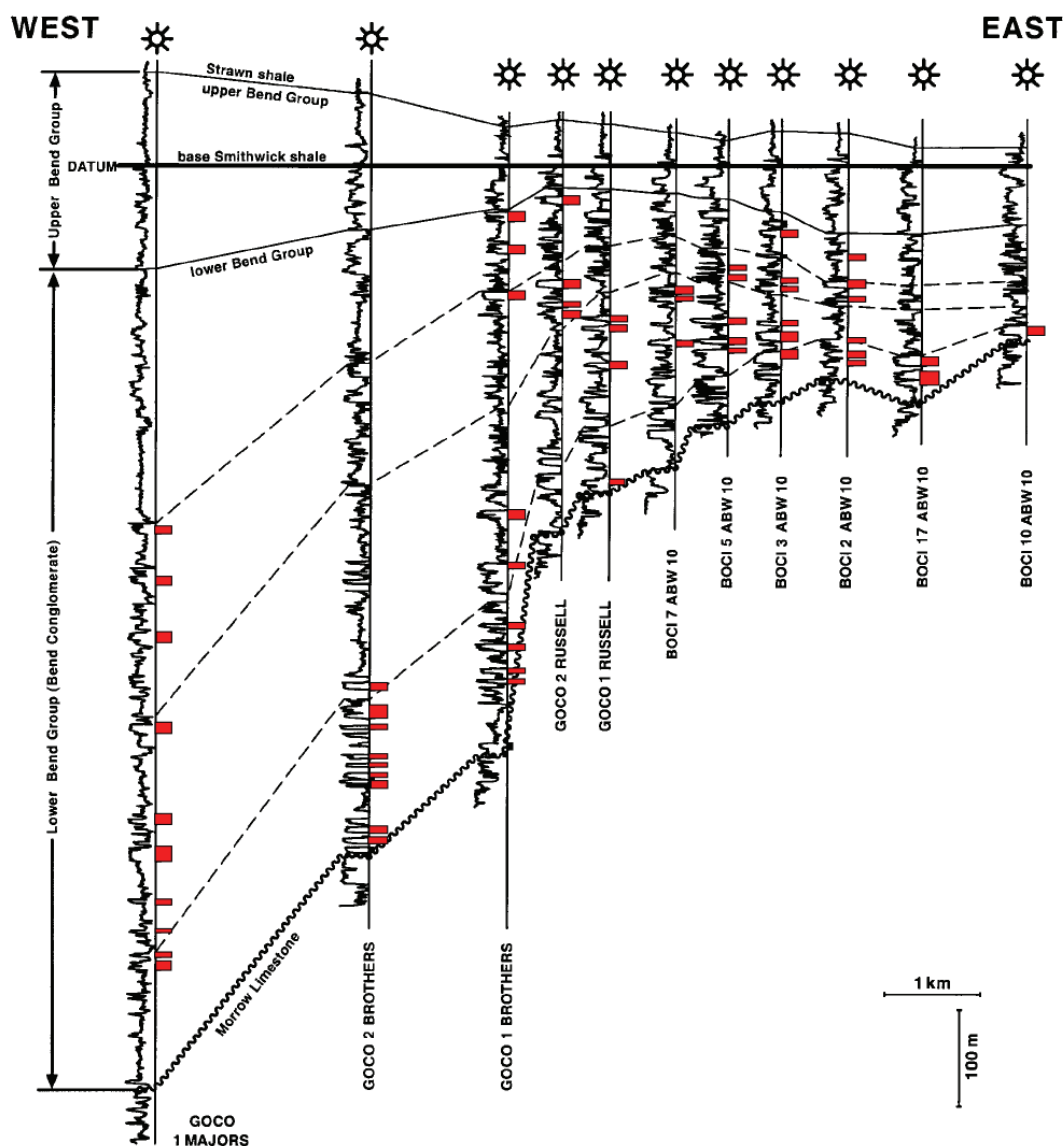


Figure 12. Gamma-ray log west-east correlation of entire Atokan interval (Bend and Smithwick Formations) within Broken Bone Graben. Small red bars on right-hand side of each well log indicate producing reservoir-quality sandstones. Note large number of reservoir-quality sandstones within lower unit that are disconnected from reservoir-grade intervals on upper flank of the structure (after Brister and others, 2002).

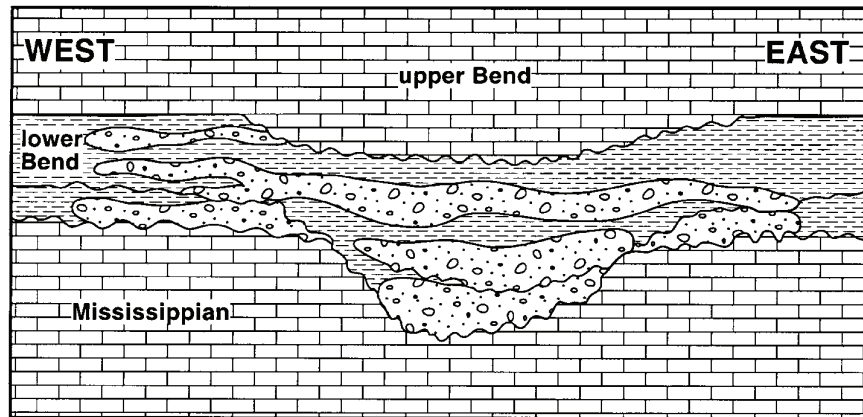


Figure 13. Illustration of incisive and unconfined alluvial channels encased in shale in lower Bend (Atokan age), overlain by dominantly carbonate upper Bend (modified from Brister and others, 2002). Architecture analogous to proximal alluvial facies in Taylor Draw field (Upton County), as well as “lower sand” interval in Vacuum field (Lea County, New Mexico).

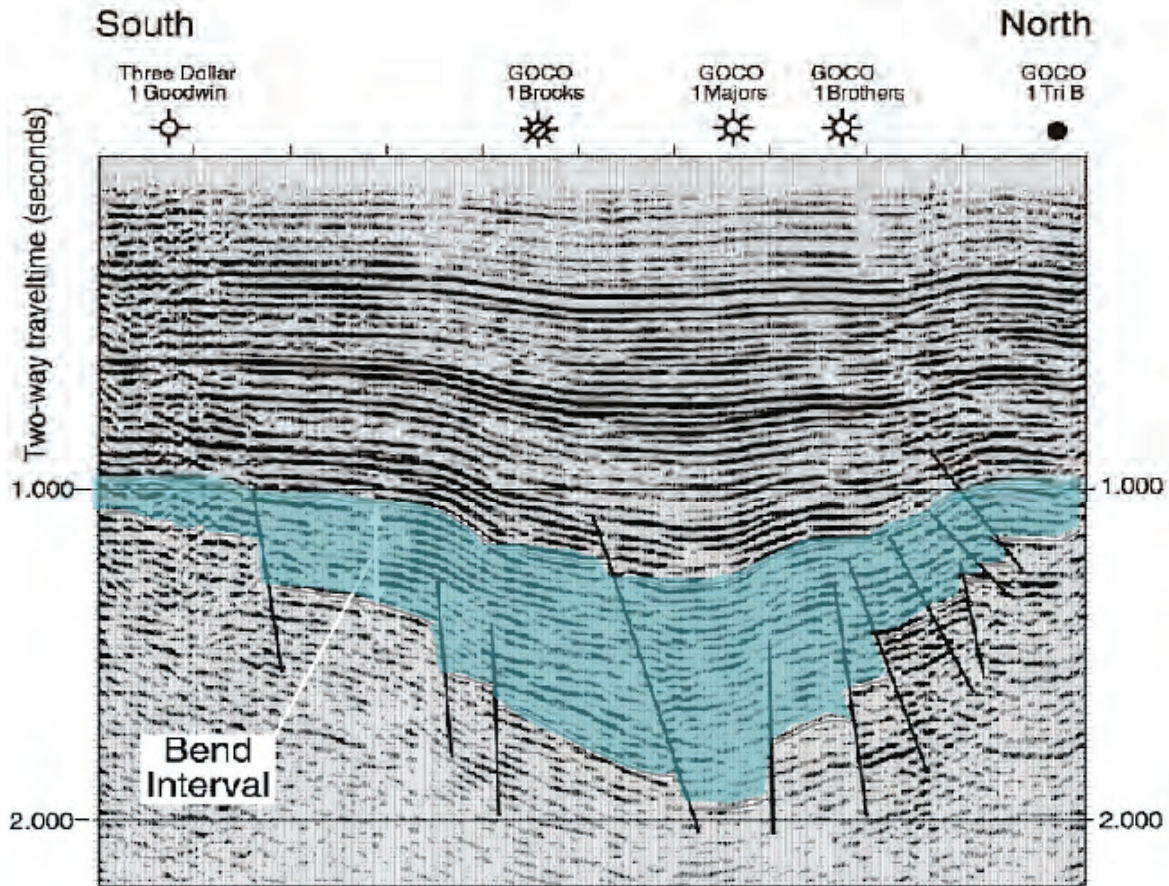


Figure 14. High-resolution seismic over Broken Bone Graben. Atokan-age Bend interval (upper and lower Bend and Smithwick) imaged and highlighted in blue. Note that orientation of seismic line is perpendicular to wireline cross section in figure 12. Onlapping geometries and changes in seismic character at approximately 1.7 and 1.5 s two-way traveltme potentially correspond to switch from nonmarine to marine sedimentation. Onlapping geometries also suggest pinch-out of facies and stratification of reservoir intervals in this type of setting, which might not be indicated by wireline-log correlation.

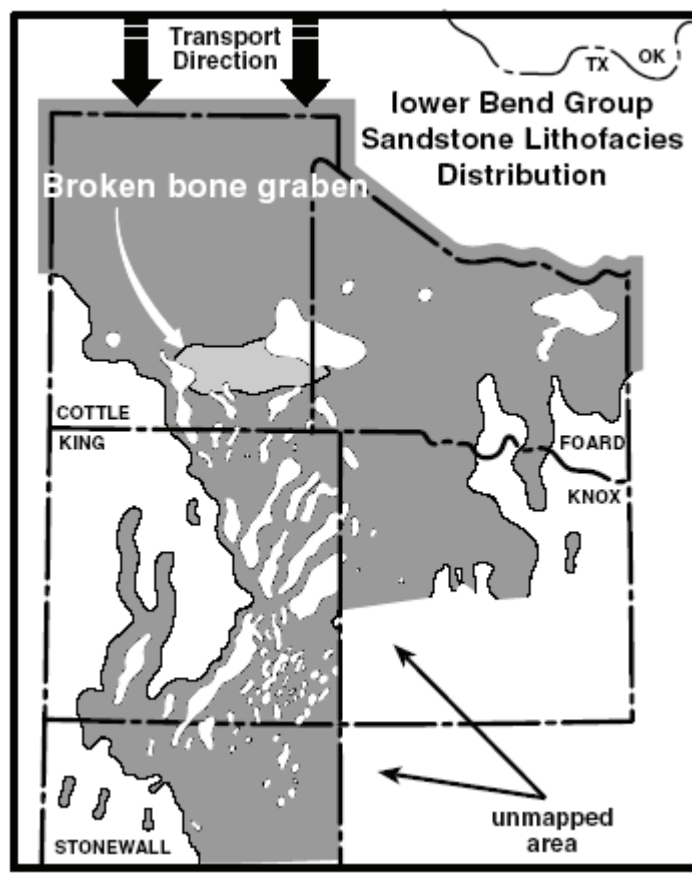


Figure 15. Distribution of lower Bend Group sandstones in gray. Light-gray area denotes Broken Bone Graben. White areas are either unmapped or they did not receive siliciclastic sediments. Note overall transport direction from the north toward the Permian Basin (after Brister and others, 2002). Note potential for encountering sandstones in southern Stonewall County and westward into Kent County. Alluvial-channel sands have already been identified in Baylor County, to the east of Knox County.

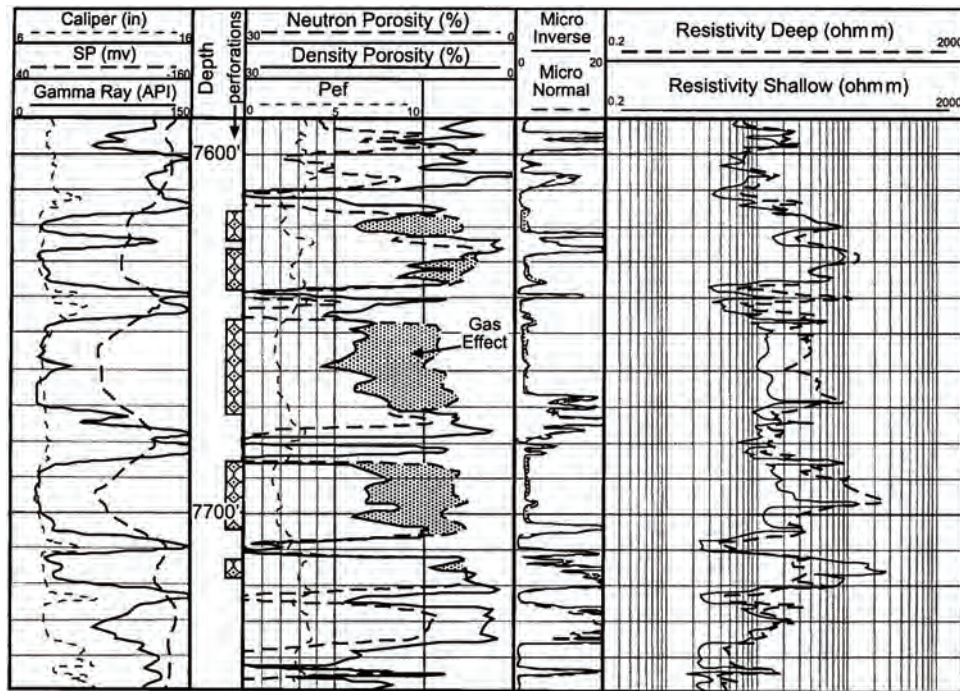


Figure 16. Detailed wireline-log-suite signature of lower Bend stacked sand pay horizons from Rhombochasm field. Productive sands are present in the interval, and low-resistivity high-gamma-ray mudstones/shales separate the sands. Figure modified from Brister and others (2002).

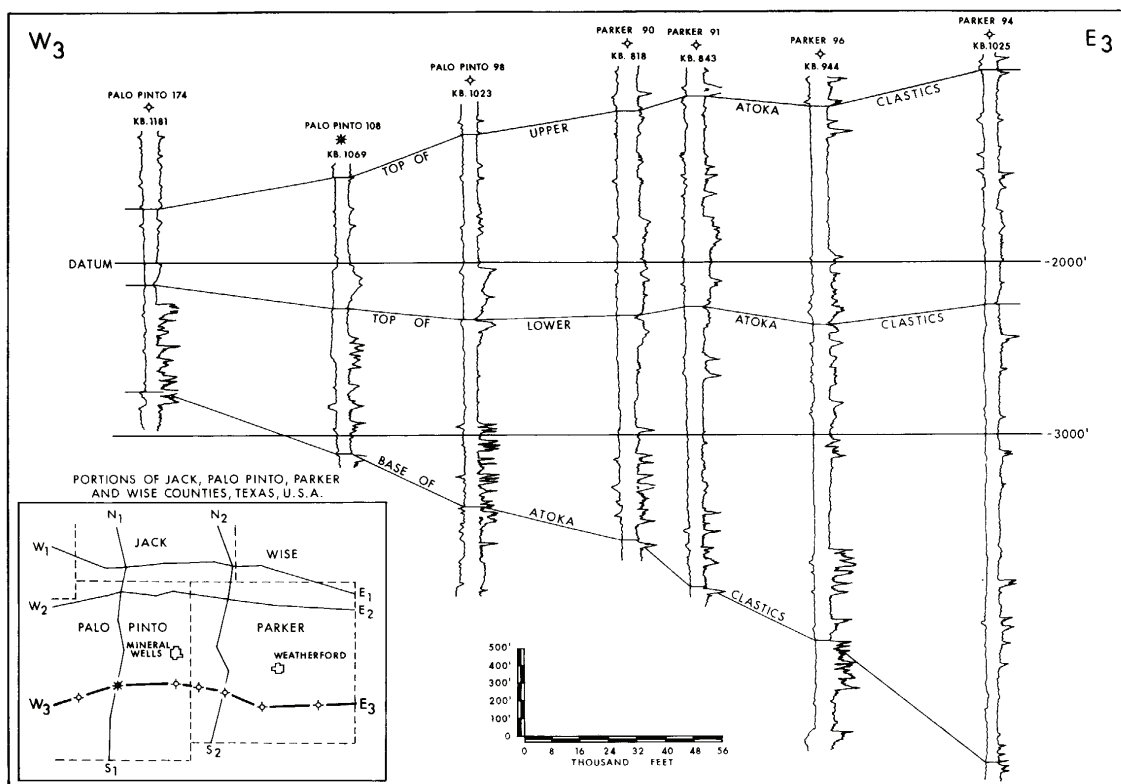


Figure 17. West-east SP- and resistivity-log correlation of Atokan-age units in Palo Pinto and Parker Counties (after Ng, 1979). According to upper and lower log picks of Ng (1979), lower Atokan siliciclastics appear to thin and onlap westward; however, the high-resistivity log interval is relatively uniform in thickness and does not indicate substantial thinning or onlap. The upper Atokan shale-dominated interval is equivalent to the Smithwick Formation.

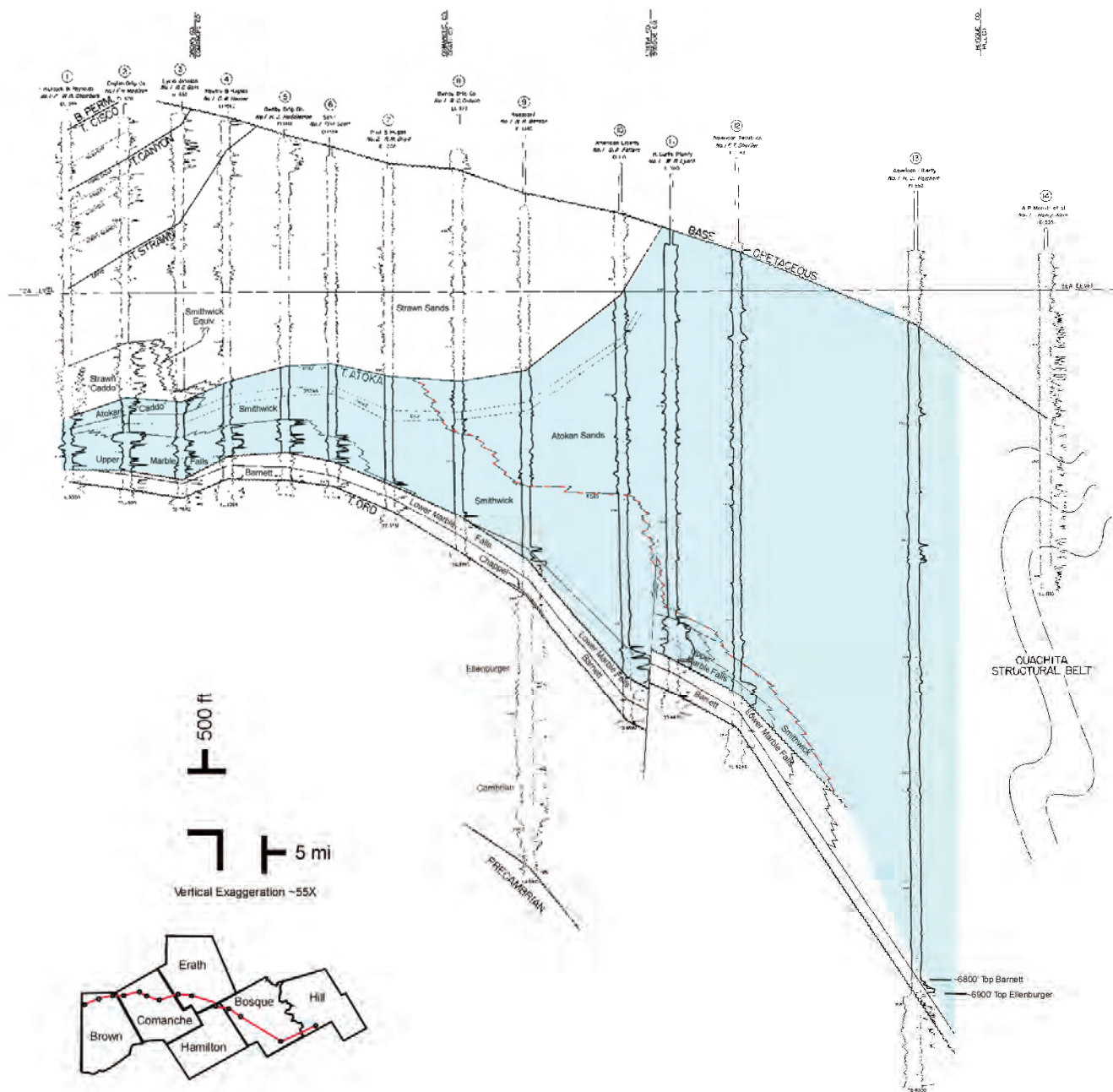


Figure 18. Regional west-east SP-resistivity well log correlation of Upper Mississippian and Pennsylvanian of Brown to Hill Counties north and northeast of the Llano Uplift. Atokan-age sediments highlighted in light-blue. Note east-west thickening of Upper Marble Falls limestone and thinning of coeval and younger Smithwick Formation in the same direction. All correlations are from original figure modified from Fort Worth Geological Society (1957). Presence of Smithwick between Upper Marble Falls and Strawn Formation may allow for regional correlation of this unit into the Permian Basin.

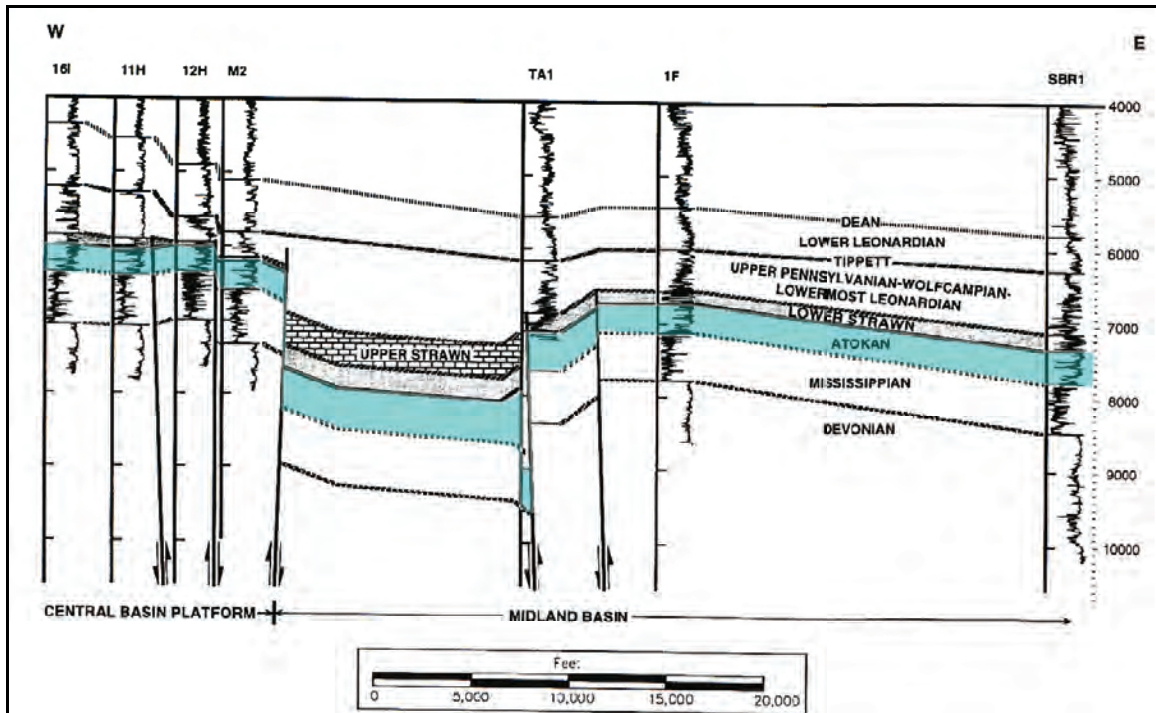


Figure 19. West-east structural cross section of 3D seismic grid over Wilshire field, central Upton County (cross section modified from Tai and Dorobek, 1999). Note Atokan, highlighted in blue, showing no thickness or wireline-log character changes from the Central Basin Platform into the Midland Basin.

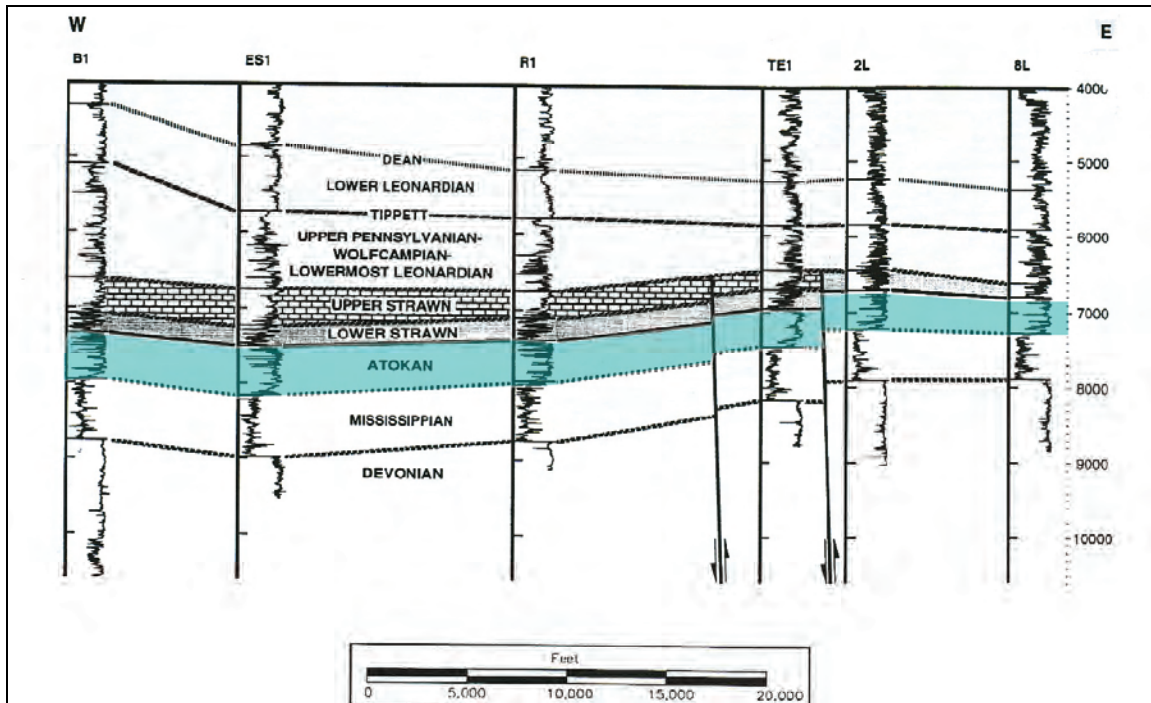


Figure 20. West-east structural cross section of 3D seismic grid over Wilshire field, central Upton County (cross section after Tai and Dorobek, 1999). Note Atokan, highlighted in blue, showing minor consistent thickness decrease to the east over the Wilshire structure. Wireline-log character does not change from west to east.

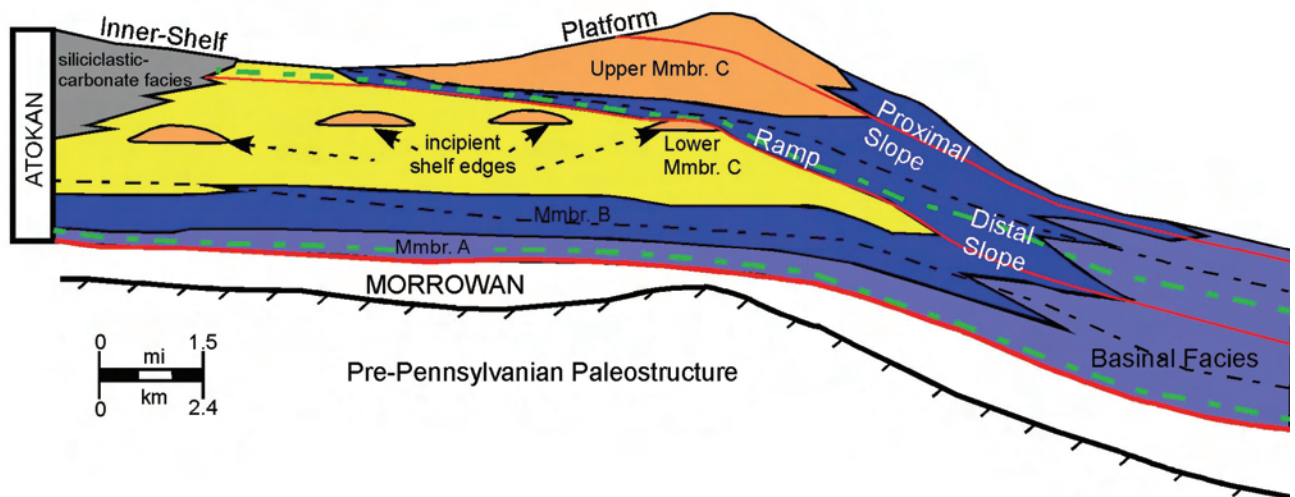


Figure 21. Schematic representation of facies architecture and sequence stratigraphic surfaces in the Chapman Deep Field area, Reeves County (modified from Mazzullo, 1981). Member A represents the basinal (<213-m [700-ft] water depth) environment, Member B represents the proximal to distal slope facies, and Member C comprises shallow-water ramp to platform facies. Sequence stratigraphic surfaces have been added to illustrate the lateral facies variations within each sequence tract. Transgressive surfaces are indicated by dashed green lines, flooding surfaces by black dotted and dashed lines, and sequence boundaries by solid red lines. Most of the reservoirs occur within highstand sequence tracts.

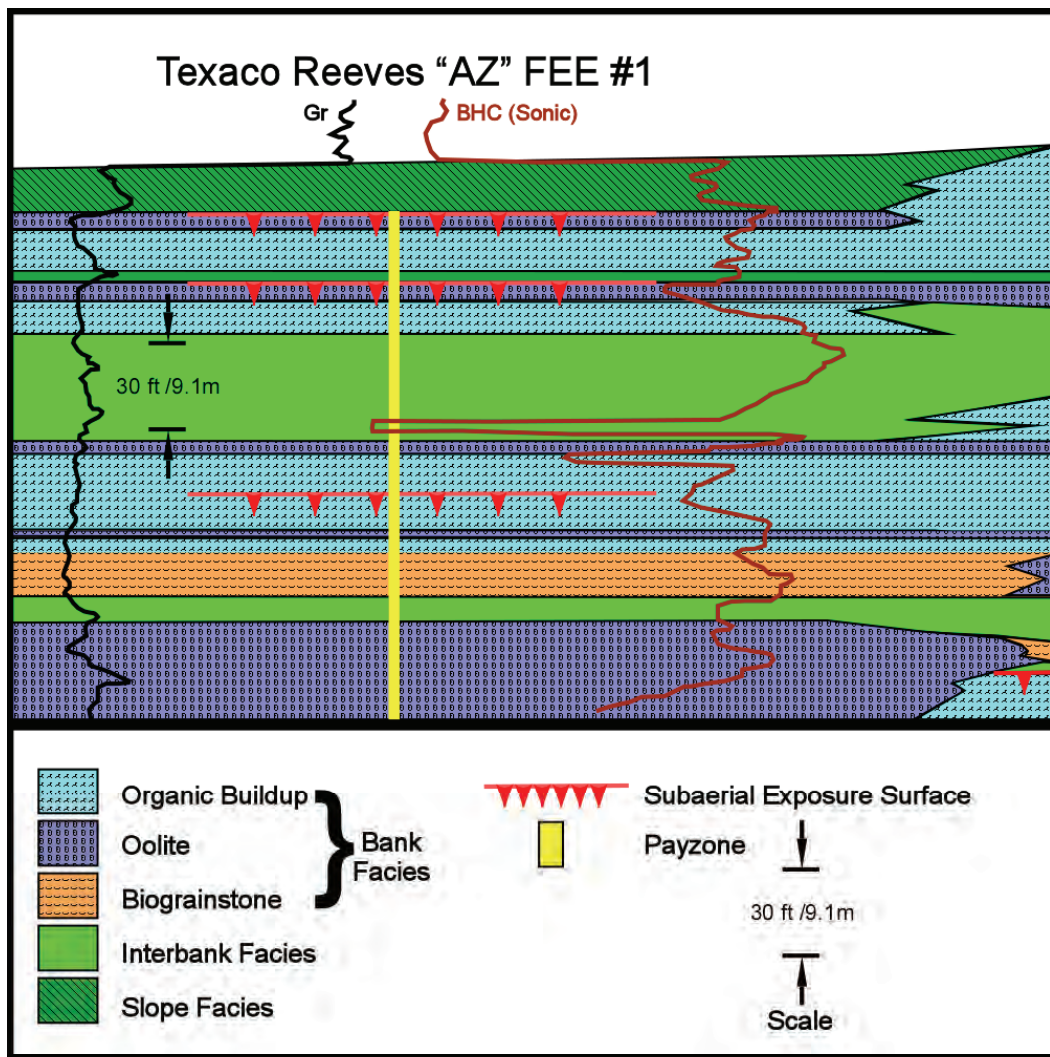


Figure 22. Type example of vertical and lateral facies variation in Atokan carbonate units of Delaware Basin (Chapman Deep field area) (modified from Mazzullo, 1981). Solid yellow vertical line indicates pay zone. Note lack of correlation between facies, pay zone, exposure surface, or wireline-log signature.

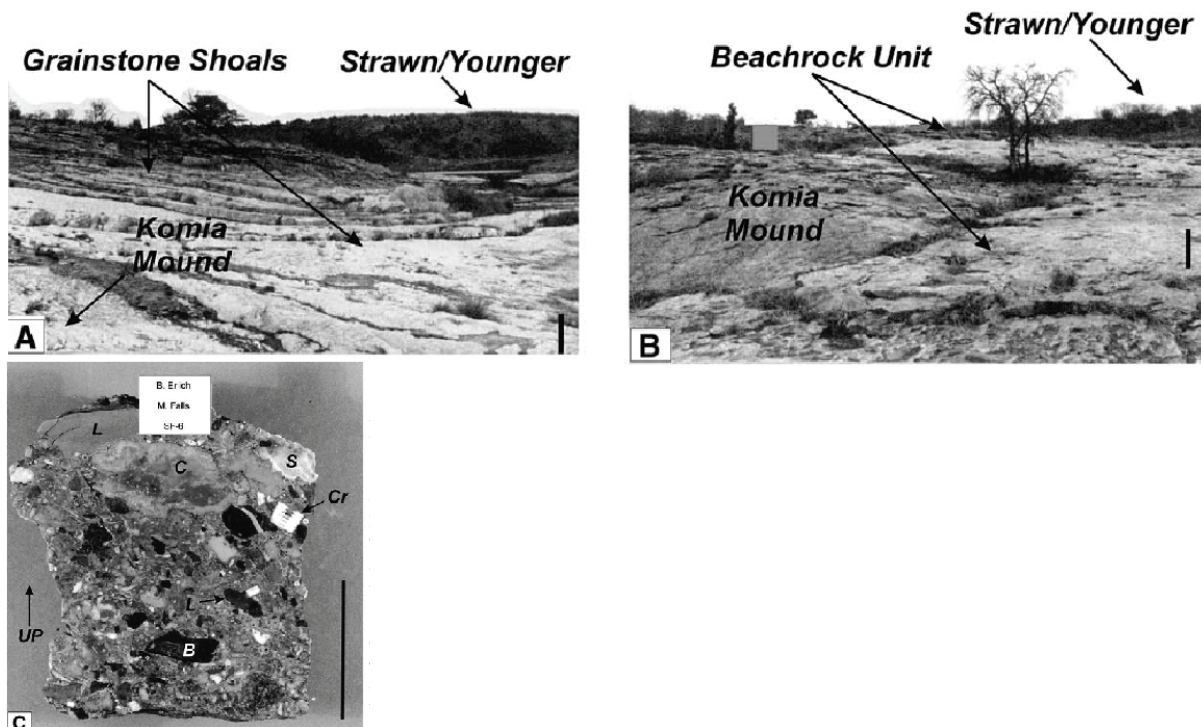


Figure 23. Upper Marble Falls Formation mound facies outcrop photographs and hand-specimen example of high-energy beach rock. (A) Crossbedded skeletal grainstone shoals. Paleobathymetric relief between *Komia* spp. algal mounds filled with migrating grainstone shoals. (B) *Komia* spp. algal mound overlapped by Upper Marble Falls beach-rock unit. Scale bar at right = 1 m. (C) Beach-rock unit from B; B = bryozoan, Cr = crinoid, S = stromatoporoid, C = coral, L = lithoclast. Scale bar at right = 5 cm. Size, geometry, and facies association of algal mounds and grainstones are similar to those encountered in Atokan Chapman Deep reservoirs and Morrowan Lower Marble Falls Formation (after Erlich and Coleman, 2005).

DEPOSITIONAL HISTORY OF THE DESMOINESIAN SUCCESSION (MIDDLE PENNSYLVANIAN) IN THE PERMIAN BASIN

Wayne Wright

Bureau of Economic Geology
Jackson School of Geosciences
The University of Texas at Austin
Austin, Texas

ABSTRACT

Distribution of the Desmoinesian reflects two large phases of deposition. Earliest Strawn Group deposition is reflected by widespread, generally uniformly thick carbonate deposition (that is, Odom Formation and equivalents). Carbonate deposition was followed by “downwarping” and subsidence of the Midland Basin, which resulted in a more geographically stable carbonate platform/shelf developing. This shelf edge strikes north-south and is generally coincident with the Fort Chadbourne Fault System (Fort Chadbourne High). Deposition of carbonates and siliciclastics is cyclic, although the shelf margin is largely stationary and reflects aggradation. The overall depositional environment detailed on the Eastern Shelf (for example, Odom and Goen, etc.) appears to be reflected in other parts of the Permian Basin. The ‘Lower’ Strawn is generally a relatively uniform thickness at approximately 225 to 275 ft, with a characteristic wireline-log signature. In localized areas of increased accommodation, the Strawn carbonate succession thickens dramatically (750 to 900 ft). Many of the historically termed Strawn siliciclastics have subsequently been reinterpreted using high-resolution 3D seismic and other means to actually be Permian (dominantly Wolfcampian) in age.

Desmoinesian-age units in the Permian Basin record a weak 2nd-order transgression. In general, calculations for rate of global sea-level rise are less steep in the Desmoinesian than in the underlying Atokan. The 2nd-order transgression is punctuated by high-amplitude 3rd-order regressive and transgressive events occurring at a very high frequency.

Desmoinesian carbonates were deposited over a much larger area in the Permian Basin than previously documented. Algally dominated bioherms and higher energy facies (ooid grainstones) affected by burial diagenesis and subsequently fractured compose the best carbonate reservoirs. Because producing carbonate reservoirs within the Midland Basin are products of both meteoric and deep-burial diagenesis, many zones can be linked to facies type and sequence stratigraphic surfaces.

Two new paleogeographic reconstructions of the Desmoinesian of the Permian Basin are presented (figs. 1, 2). Figure 1 is reconstructed at an early Desmoinesian time (Strawn Caddo to Lower Odom equivalent), whereas figure 2 is a late Desmoinesian reconstruction at approximately the Anson Bank depositional period.

In brief, early Desmoinesian-age alluvial, deltaic, and marine siliciclastics are distributed over the Llano Uplift, margins of the Eastern Shelf, parts of western Val Verde Basin (Kerr Basin), and the northern Delaware Basin. Siliciclastic shale deposition is volumetrically and physiographically isolated, with occurrences in the southern Delaware Basin and portions of the Midland Basin (southern Reagan County and parts of Martin, Howard, and Mitchell Counties). Widespread ramp to platform-carbonate deposition of a relatively uniform thickness dominates throughout the Permian Basin. Deeper basinal carbonates and shales are largely restricted to the Delaware Basin. The

small number of Precambrian inliers that were exposed during the Atokan are transgressed in early Desmoinesian time. The Pedernal Uplift provided limited sediment input for the northwest shelf, and the Bravo Dome area appears to have been exposed, although providing little in the way of material.

During the late Desmoinesian, structural downwarping of the Midland Basin appears to have initiated. This downwarping and subsidence led to an increased area of deeper water within the Midland Basin, and carbonates around the margins responded to the increased accommodation by aggrading substantially. This aggradation led to development of the first well-defined Pennsylvanian shelf margin of the Permian Basin. Initial development of the Val Verde Basin in Terrell County also occurred during the late Desmoinesian. The northern Eastern Shelf and north of the Llano Uplift comprise a series of cyclic carbonate and siliciclastic units. In figure 2 marginal marine and alluvial siliciclastics are feeding the Bowie and Perrin Deltas in the west (Jack, Young, and Clay Counties). To the west of the deltas, the Anson carbonate bank and shelf complex developed, which is part of the Eastern Shelf margin and shelf interior facies. To the west of the Anson Bank, across a shallow basin, are thick aggradational carbonates on the Red River Uplift (King County). A shallow trough possibly runs from the Knox and Baylor County area (Knox-Baylor Trough) and connects to the Midlands in Mitchell and Fisher Counties. A deepening of the basin also occurred in the Hockley-Lubbock County area. Subsidence in this area potentially led to development of a carbonate shelf margin in Hockley and Lubbock Counties, which would roughly correspond to the northern margin of the Horseshoe Atoll. The paleogeographic summary at the end of this chapter should be referred to for a more detailed discussion of Desmoinesian paleogeography.

INTRODUCTION

This chapter discusses styles of deposition and facies development of Desmoinesian-age sediments, concluding with a discussion of revised paleogeography for the Desmoinesian Permian Basin (figs. 1, 2; Summary). The chapter is divided into discussions of siliciclastic and carbonate Desmoinesian deposition. In each section a regional model for facies patterns and deposition is proposed. Data from areas adjacent to the Permian Basin are used as analogs for facies that are predicted to be present within the study area. More localized studies are used to illustrate certain key aspects (for example, facies type, reservoir quality). However, an initial introduction to the area, placing it in a global perspective, is first presented.

GLOBAL TECTONIC SETTING

Desmoinesian-age sediments in the Permian Basin are characterized by being deposited at a near (8 to 12° south) equatorial position during the middle stages of icehouse, high-amplitude, high-frequency eustatic sea-level fluctuations. It was an area undergoing increased tectonic activity of both uplift and subsidence related to Ouachita-Marathon orogeny and birth of the greater ancestral Rocky Mountains. Figure 3 illustrates the position of Texas (in orange) relative to major tectonic plates and the equator at the beginning of the Pennsylvanian (circa Atokan–Desmoinesian age). During Desmoinesian times, Texas continued its northward migration toward an equatorial position (fig. 3).

REGIONAL TECTONIC SETTING AND FACIES DISTRIBUTION

The outline of the Permian Basin and the major geologic features commonly associated with the basin are illustrated in figure 4. All features did not develop simultaneously but were in the early to middle stages of development during the Desmoinesian. Figures 5 through 7 illustrate previous interpretations of facies distribution, uplift, and subsidence patterns for Desmoinesian-age sediments in the Permian Basin and surrounding areas. Revised Desmoinesian Permian Basin paleogeography is presented and discussed in the summary. Interpretations suggest that most of the Permian Basin was an area of net subsidence during the Desmoinesian. The basin is inferred to be rimmed by carbonate-platform to shelfal environments, with substantial uplifted areas in the Diablo Platform and Central Basin Platform (CBP) (Ye and others (1996) (fig. 5).

The areas of uplift, subsidence, and facies distribution in figures 5 through 7 do not all match, although figures 5 and 7 are broadly similar. On the basis of Kluth (1986), most of the Permian Basin area is illustrated as an area of net subsidence, with rate ranges from $\leq 50\text{m/Ma}$ to $\sim 200\text{--}300\text{m/Ma}$ (fig. 6). One of the most important differences apparent between figures 5, 6, and 7 is the extent of uplift on the CBP. Uplifted parts range from the almost entire platform in interpretations of Ye and others (1996) and Blakey (2005) to the south region only in Kluth (1986) (figs. 4 through 7). Correcting inconsistencies in the regional paleogeography of the Permian Basin and outlining more detailed depositional patterns are the major goals of this chapter (figs. 1, 2).

GENERAL STRATIGRAPHY AND NOMENCLATURE

Desmoinesian-age sediments within the Permian Basin include those termed Strawn Formation (predominantly carbonates)—those of the Strawn Group and the underlying Caddo Limestone. Within the Permian Basin, most Desmoinesian-age sediments are referred to as Strawn Formation, and they are overwhelmingly carbonates. However, on the Eastern Shelf, the stratigraphy is more complicated, with multiple carbonate and siliciclastic units having been cyclically deposited during the Desmoinesian.

Nomenclature

As is true of the underlying Morrowan and Atokan intervals, stratigraphic nomenclature of the Desmoinesian interval on the Eastern Shelf is complicated (for example, Gunn, 1979; Cleaves, 1993). The reader is referred to figure 8 for detailed correlation of named units of Desmoinesian age on the Eastern Shelf. The Desmoinesian interval as defined in this study contains all formations, groups, and members that lie within the Strawn Group. Historically in the Midland Basin, CBP, and Delaware Basin regions, Desmoinesian-age rocks were referred to only as Strawn, regardless of lithology.

SILICICLASTIC DESMOINESIAN DEPOSITION

General Depositional Setting

Deltaic, fan delta, and incised-valley systems occur throughout the Desmoinesian. Incised-valley systems are largely restricted to north-central Texas, west of the Fort Worth Basin. Multiple deltaic depocenters were active during the Desmoinesian, funneling sediment onto the northeast and east margin of the Eastern Shelf. Delta-front

sediments are present in Coke, Runnels, and Coleman Counties along the Eastern Shelf. The Pedernal Uplift appears to have remained in a stage of quiescence that was established in the Atokan. Aerially restricted minor amounts of marginal marine to open marine deltaic to shelfal siliciclastic sedimentation may be present in the extreme northwest corner of the Permian Basin. The Bravo Dome in Roosevelt and Cochran Counties is thought to have been exposed during the Desmoinesian; however, no siliciclastic plays have been identified in this region yet. Overall, 2nd-order marine transgression during the Desmoinesian resulted largely in deposition of carbonates at the expense of siliciclastic lithologies.

Reservoir Potential

Updip fluvial, amalgamated, stacked channels and thick fan-delta units have the best reservoir potential and quality. However, it appears that most of the proximal facies occur to the east of the Permian Basin. Delta-front and channel-mouth bars along the Eastern Shelf have good reservoir quality (up to 15.2 percent porosity, mean 5.3 percent, and up to 387 md permeability). Trapping mechanisms range from structural to stratigraphic. In delta-front systems, bidirectional facies pinch-out of sand lenses to prodelta and delta-plain mudstones is a common trap style.

Diagenesis

Desmoinesian-age deltaic sediments reflect a long diagenetic history, with extensive cementation by quartz and calcite. Postcementation secondary dissolution and leaching of calcite cement and framework grains (for example, feldspar, rock fragments) produced/recovered current porosity in the facies.

Climate

The Desmoinesian was a time of expansive ice-sheet development typified by a highly fluctuating sea level. Amplitude and frequency of sea-level change are higher in the Desmoinesian than in underlying Atokan- and Morrowan-age units. Highly fluctuating sea levels generally result in thinner, higher frequency cycles and numerous periods of exposure.

PERMIAN BASIN

Eastern Shelf

Detailed studies were performed by Cleaves (1975, 1993, 2000) and Cleaves and Erxleben (1982, 1985) on the siliciclastic depositional patterns of the Desmoinesian northern Eastern Shelf. Figure 8 illustrates a schematic representation of Desmoinesian sedimentation patterns along the northern Eastern Shelf and farther eastward into the greater Fort Worth Basin area. During the Desmoinesian, siliciclastic sediments encroached fully only on the Eastern Shelf (that is, within the boundaries of the current Permian Basin, as defined in figure 4) (equivalent to Odom Bank Limestone) (fig. 8). In the northern Eastern Shelf, these two influx episodes are associated with Buck Creek and Dobbs Valley sandstones (fig. 8). In the Desmoinesian, because no highstand deltaics prograded across the entire shelf (Eastern Shelf), ramp and shelf-margin sediments are either carbonate or condensed marine shales. Highstand Desmoinesian deltaic lobes contain conglomeratic channel fill at the top of progradational parasequences, whereas lowstand deposits lack these deposits (Cleaves, 1993). Lowstand delta lobes appear to aggrade vertically at the delta front and delta plain, and coarser material is deposited

more proximally in the upper delta and coastal plain. An alternative explanation for the coarse fill at the top of the highstand systems tract is that the channel is actually part of overlying lowstand systems tracts in an incised-valley system. Figure 9 illustrates possible superimposition of highstand and lowstand deltaic systems tracts.

Within King County, delta facies interfinger with the carbonate ramp and platform in Bateman and Anne Tandy fields (Boring, 1993). Two large regressive and transgressive cycles are present in this area of the Knox-Baylor Trough. Tandy 5400 and Anne Tandy sandstones are in a basal cycle, and the Twin Peaks sandstone is in an upper cycle. Desmoinesian-age limestones interfinger with and transgress deltaic sediments; however, correlation is not sufficient to identify the carbonate sequences (for example, Odom, Goen, or Anson). The Tandy 5400 sandstone may be equivalent to the Hog Mountain sandstone to the east (fig. 8). The Tandy 5400 is interpreted as a distributary bar finger comprising crossbedded sandstones, whereas the Anne Tandy is a lobate delta. The Twin Peaks sandstone is thought to represent an offshore bar system (Boring, 1993). Most of this succession was previously interpreted as being deposited in deep-water conditions (Gunn, 1979). Given the regional geology gathered in this study, it appears that this succession is predominantly shallow water deltaic in origin.

Farther to the south of the area detailed in figure 8, within Taylor County, the “Gray Sandstone or Gray Interval” is time-equivalent to the Buck Creek Sandstone. The Gray Sandstone in West Tuscola field is the basal siliciclastic interval in a series that includes Gardner and Jennings intervals and is stratigraphically between the basal Caddo limestone and the upper Goen limestone (figs. 8, 10)

The facies present in the delta system at Tuscola field (Taylor County) comprise prodelta black shales; delta-front, bar-slope, burrowed, and intercalated carbonaceous sandstones with silty claystones; delta-front, bar-crest, laminated sandstones; delta-front, crossbedded coarse sandstones; delta-plain, carbonaceous shales; and shallow marine sandstones (fig. 11). Bar-crest, laminated sandstones are the main producing interval. Secondary production also comes from delta-front channels. The overall upward-shallowing succession from prodelta shales to highstand channels mimics the succession studied by Cleaves (1993) for the northern Eastern Shelf. Figure 12 illustrates core photographs of cross-laminated and rippled sandstones from the Desmoinesian deltaic facies.

Reservoir Quality

Reservoir quality in the Tuscola sandstones and siltstones ranges from 0 to 15.2 percent, with a mean of 5.3 percent. Permeability for the same units ranges from 0 to 387 md (Dutton, 1977). In deltaic sediments of the Tandy 5400 sandstone of King County, porosity averages 25 percent, and permeability ranges from 77 to 250 md. Within Tuscola field, precement porosity was approximately 22 percent; however, extensive cementation (up to 47 percent total volume of rock) substantially reduced reservoir quality. Cementation took place in several phases, starting with chlorite (minimal effect), followed by overgrowth quartz formation (major effect—50-percent porosity reduction), then calcite (major effect—40- to 50-percent further porosity reduction). After calcite cementation, the rocks were generally completely occluded. Secondary development of porosity was provided by dissolution of the calcite cement, thereby reestablishing a porosity of about 11 percent. Further dissolution of framework

grains (replaced by calcite and pristine), such as feldspar and clay clasts, appears to have augmented overall porosity by approximately 4 percent. Postdissolution cementation was limited to minor kaolinite (up to 5 percent), barite (1 percent), and, lastly, ferroan dolomite. Overall, precement porosity was similar in all coarser grained facies. Current porosity indicates that delta-front channel sandstones have the highest porosity, followed by delta-front, bar-crest facies. In general, highest porosities are found in high-energy, winnowed sandstones at the base of distributary channels and on mouth-bar crests. These facies have the largest mean grain size and the least amount of matrix and shale. Judging from isotopic and petrographic data, diagenesis of Tuscola deltaic sediments took place over a period of 300 Ma (Land and Dutton, 1978). Hydrocarbon maturation may have produced acidic fluids as a by-product of CO₂ degassing and H₂S generation, which have leached and dissolved calcite, feldspar, and rock fragments in the last 75 Ma.

MIDLAND AND DELAWARE BASINS

Siliciclastic deposition in Midland and Delaware Basins appears largely restricted to basin-center shales. No data are available about the sedimentology of these facies. In general, it appears that basin subsidence in both Midland and Delaware Basins was minimal during the early Desmoinesian (fig. 1) and increased dramatically in the late Desmoinesian (fig. 2). Therefore, regional distribution of the shales is greater in the late Desmoinesian relative to the early Desmoinesian.

DISTRIBUTION OF DESMOINESIAN SILICICLASTIC SEDIMENTS

Interpretation of Desmoinesian sedimentation patterns historically relied heavily on structural interpretation of the CBP. According to seismic and wireline-log correlations it appears that the entire CBP was transgressed and covered by carbonate sediments by the early Desmoinesian. Regional reconstructions by Tai and Dorobek (1999, 2000) show no influence by the CBP on Desmoinesian sedimentation patterns in the Midland, Delaware, or Val Verde Basin (figs. 13, 14). Desmoinesian-age sediments are relatively uniform in thickness and have a consistent aerial distribution across Delaware and Midland Basins (Van der Loop, 1990; Yang and Dorobek, 1995). Yang and Dorobek (1995) illustrated numerous cross sections of the Delaware and Midland Basins, illustrating only differential erosion of Desmoinesian sediments (lower and upper Strawn) (figs. 13, 14). Most sedimentation patterns appeared largely unaffected by uplift. A pre-Desmoinesian unconformity does exist, which results in the cutting out of variable amounts of the stratigraphic section in parts of the Val Verde Basin. Post-Desmoinesian differential uplift of blocks within the CBP resulted in erosion from Upper Pennsylvanian units down to the Precambrian basement. Desmoinesian sediments (dominantly carbonate lithologies) were pervasive across much of what would become the CBP during the Missourian to Virgilian. Major uplift of the CBP occurred during Missourian to Virgilian time.

SUMMARY OF DESMOINESIAN SILICICLASTIC SEDIMENTS

Desmoinesian siliciclastic deposition in and around the Permian Basin is even more aerially restricted than in the Atokan. Desmoinesian siliciclastic deposition is

reciprocal with carbonate sedimentation and is largely restricted to the northern Eastern Shelf. A 2nd-order transgression appears to have dominated throughout the rest of the Desmoinesian; however 3rd- and 4th-order, high-amplitude, sea-level fluctuations occurred at a high frequency. The result was an almost interlayered carbonate and siliciclastic stacking pattern on a 3rd-order scale.

Deltaic sediments continued their westward progradation from the Fort Worth Basin farther onto the Eastern Shelf. This progradation initiated in the Atokan and was governed largely by convergence of the Ouachita thrust foldbelt to the east of the Fort Worth Basin. During the early Desmoinesian, because subsidence in the Midland Basin, Fort Worth Basin, and Eastern Shelf was minimal, siliciclastic progradation advanced to its westwardmost point (that is, Buck Creek and Dobbs Valley sandstone sequences). During the mid- to late Desmoinesian, uplift and compression of the Ouachita diminished, and subsidence of the Midland Basin accelerated. These two factors, coupled with a 2nd-order rising sea level, resulted in eastward backstepping of the clastic to carbonate transition zone and a geographical fixing of the carbonate shelf. In the Permian Basin, distal parts of the deltaic systems are the most common. Coarser grained alluvial delta feeder systems are generally farther east.

DESMOINESIAN CARBONATE DEPOSITION

Approach

Carbonate rocks of Desmoinesian age in the Permian Basin have been studied extensively in the Midland and Delaware Basins and the Northwest and Eastern Shelves. The carbonate formations of the Eastern Shelf, including the Caddo (Desmoinesian

interval), Branson Bridge, Odom, Goen, Anson, Capps, and Village Bend, span the same time interval as the carbonate Strawn Formation in Midland, Delaware, and Val Verde Basins.

General Depositional Setting

The carbonate depositional environment during the Desmoinesian was varied in style (for example, ramps, patch reefs, shelf-margins, rimmed shelves) and geographic distribution. Early Desmoinesian-age carbonates were deposited almost ubiquitously across the Permian Basin in dominantly ramp settings. In the middle to late Desmoinesian, regional subsidence patterns changed, and the Midland, Delaware, and parts of the Val Verde Basins began to subside rapidly. Along the margin of these basins, carbonates aggraded almost vertically in response to increased accommodation. The carbonate margins became more steep sided in geometry, as opposed to ramplike, and in general a true shelf margin developed and became fixed geographically. Thick accumulations of shallow-water facies, including phylloid algal mounds and grainstones, developed through time (for example, south margin of the Horseshoe Atoll). Most of the thicker Desmoinesian sections underpin later Missourian and Virgilian carbonate growth. High-amplitude and high-frequency sea-level falls exposed the Desmoinesian carbonates on numerous occasions.

Reservoir Potential and Diagenesis

Shallow-water phylloid algal bioherms, *Chaetetes* reefs, and bioclastic packstone/grainstones are the most favorable reservoir facies. Overall, phylloid algae are common and tend to dominate the bioherm community during the Desmoinesian, which is a change from the Atokan and Morrowan, when *Komia*, *Donezella*, and *Cuneiphycus*

dominated the algal assemblage. Commonly, in the Desmoinesian, primary porosity was occluded largely during early diagenesis, and present reservoir quality is related to the extent of alteration during subaerial exposure. Within the Val Verde Basin, reservoir quality is also linked to late-stage fracturing and fluid flow. Reservoir intervals are not confined to a particular facies or exposure surface but commonly exist at the top of 10- to 30-ft-thick upward-shallowing cycles. Geometry of a potential reservoir interval varies radically between different carbonate depositional settings (for example, small and ovoid for patch reefs, narrow in width but long in strike length for shelf-margin buildup). The duration of exposure events during the Desmoinesian was less than in the Missourian or Virgilian. The resulting extent of diagenetic alteration during meteoric diagenesis is often only poorly developed. One exposure event appears to be correlative across a large area and may have regional sequence stratigraphic significance. The wireline-log expression of this event is confirmable only using spectral gamma-ray logs.

MIDLAND BASIN

In the Midland Basin, data relating to the depositional style of Desmoinesian carbonates (Strawn Formation) can be taken from regional cross sections and seismic data, originally gathered and interpreted for the younger Canyon and Cisco Formations in the Horseshoe Atoll. Figure 15 illustrates the general distribution of the Strawn Formation. The infrequently termed 'lower Strawn' appears to be a regionally consistent thickness of 225 to 275 ft. This part of the Strawn interval is represented in figure 15 as the thinnest interval underlying the gray Canyon deep-water shales. Thickness estimates for the Strawn increase on the Eastern Shelf and on the Horseshoe Atoll to a maximum of

around 750 ft. Increased thickness of the upper Strawn is a response to increased accommodation caused by accelerated rates of subsidence in the Midland Basin. Regional seismic data across the Horseshoe Atoll indicate a uniform Strawn, with possible small moundlike features (fig. 16) (Waite, 1993; Saller and others, 2004). Across the Horseshoe Atoll area (including fields of Diamond M, Kelly-Snyder, Cogdell, and Salt Creek), Waite (1993) defined the Strawn as a one- to three-reflector package comprising a single 3rd-order seismic sequence. However, in the areas of increased Strawn thickness, more seismic sequences may be present, although difficult to define (Waite, 1993). More recent vintage seismic and new processing techniques indicate that there is much more internal structure within the Strawn interval in the Midland Basin (figs. 17, 18). Major differences exist on the seismic pick for the top of the Strawn (for example, Waite, 1993; Saller and others, 2004). These differences result in very different interpretations of development of the Desmoinesian carbonate succession, as well as their relationship to the overlying Missourian (Canyon) and Virgilian (Cisco) and underlying Atokan and Mississippian. Figures 19 and 20 illustrate a regional correlation based on seismic indicating that the Strawn Formation was forming topographic highs (reefs/mounds?) in response to increased accommodation. These highs are the nucleation point for later Canyon and Cisco mounds. The Strawn section, according to biostratigraphic data, is approximately 500 ft thick, composing a major part of the entire Pennsylvanian reef complex, even in the off-mound position (figs. 19, 20). The alternative interpretation indicates that Desmoinesian carbonates had little effect on overlying depositional geometries of the Canyon and Cisco (fig. 18). Given the biostratigraphic control provided from the Waite (1993) study, it appears that a substantial part of the Missourian (Canyon)

section in figure 18 is actually Desmoinesian (Strawn). Previous interpretations rarely indicate the presence of an Atokan or Morrowan interval above the Mississippian in the Horseshoe Atoll area. This Mississippian section ranges from 100 to 290 ft in thickness and is largely unconstrained biostratigraphically. According to interpretations of previous chapters, Morrowan- and Atokan-age sediments are likely to be present under the Desmoinesian-age section.

In the Kelly-Snyder region, the Strawn comprises five cycles (parasequences) that are defined using wireline logs and biostratigraphy (fig. 20). Waite (1993) considered the contact between the underlying Mississippian and the Desmoinesian (Strawn Formation) a Type 1 sequence boundary evidenced by seismic onlap of the lowermost Strawn onto a top Mississippian erosional surface (Waite, 1993). However, as evidenced in figure 19, a conformable sequence of Atokan and Desmoinesian units is inferred for part of the Horseshoe Atoll near Vealmore and Oceanic fields. The exact nature of the contact between the Desmoinesian and their underlying units is still debatable. Most wells used for correlation across the Midland Basin do not penetrate to this level, and biostratigraphic dating of this interval is lacking. The uppermost contact between the Strawn and overlying Canyon/Cisco or Wolfcampian shales is equivocal. In the Mobil #1-380 McDonnell well, facies and associated seismic signature are interpreted to indicate depositional continuity, with subtidal facies overlying grainstones and packstones (Waite, 1993) (fig. 20). An alternative interpretation for the Mobil #1-380 McDonnell well is that the Canyon A interval is a transgressive flooding interval and the top of the Strawn is a sequence boundary, although not exposed in the Kelly-Snyder area. The Strawn-Canyon contact is considered a Type 1 sequence boundary marked by

subaerial exposure outside the Permian Basin (for example, Stafford, 1959; Boardman and Barrick, 1989; Reid and Reid, 1991). On the proto-CBP, it appears that the top of the Strawn is marked by a significant exposure event (for example, Saller and others, 1999a). The regional differences in exposure of the top of the Strawn may be related to accommodation and growth rates. In a high-angle (0.25°) ramp-type system, a large sea-level fall of 20 m would displace the lowstand and shoreface 4.6 km seaward, whereas in a more platform system with steeper sides (5 to 10°), the shoreline is displaced only 228 to 112 m basinward relative to the initial point. Differences in amount of carbonate exposed during a lowstand event and subject to exposure-related diagenesis are profound (5 km vs. 200 m).

The Desmoinesian (Strawn Formation) interval in the Mobil #1-380 McDonnell well is interpreted to comprise five 4th- to 5th-order cycles in an overall 3rd-order sequence (Waite, 1993). Judging solely from the Dunham character of the rocks, the entire Strawn sequence appears to shallow upward (for example, wackestones/packstones at the base, overlain by algal packstones, and overlain by grainstones) (fig. 20). This large-scale packaging with phylloid-rich algal packstones and wackestones above mudstones/wackestones and below grainstones is the same as that identified for the Strawn in the South Andrews area, University Block 9 field (Andrews County) and St. Lawrence field (Glasscock County). However, caution must be exercised in overinterpreting the significance of facies similarities. This type of cyclicity also occurs at 4th- and 5th-order scales, and biostratigraphic and wireline-log data are required to confirm whether equivalent sections of comparable duration are truly being compared. The Strawn succession in Seminole field (Gaines County) has a similar facies-stacking

pattern; however, the entire interval studied at Seminole equates only to the lower $\frac{1}{3}$ to $\frac{1}{2}$ of the Andrews or Block 9 intervals (Mazzullo, 1983).

Studies of the South Andrews area and Block 9 field provide detailed data on facies distribution and reservoir quality of the Strawn Formation. Figure 21 illustrates a three-well correlation of Pennsylvanian facies types within Andrews County. The Strawn is subdivided into four gross packages: (1) a lower package (wackestone and spiculitic mudstone dominated), (2) a *Komia*-rich package (calcareous algae) (wackestone and bioclastic grainstone dominated), (3) a phylloid-algae-rich package (phylloid wackestone and boundstone dominated), and (4) an upper package (basal spiculitic mudstone overlain by ooid-peloidal grainstones). The contact of the Strawn and lower Canyon is considered a sequence boundary. As interpreted for figure 20, the lower Canyon basal sequence indicates a transgression (deep-water spiculitic limestones overlying grainstones) over the sequence boundary. In detail, the lower part of the Strawn (8 to 15 m thick) contains fossiliferous wackestones and spiculitic mudstones, but cycles are hard to define, and no distinct upward shallowing or deepening trends or subaerial exposure surfaces are noted (Saller and others, 1999b). Deposition of the lower Strawn package (fig. 21) is interpreted to have occurred in deep water (30 to 100 m), with grainy intervals forming as products of debris flows. The *Komia*-rich second package is divided into three upward-shallowing cycles, capped by erosion surfaces (interpreted by Saller and others, 1999b, as subaerial exposure). The *Komia* package, approximately 20 m thick in the South Andrews field area, is characteristic of shallow shelf deposition. The phylloid-algal middle Strawn package, the thickest interval at about 50 m, comprises phylloid-rich wackestones, packstones, and boundstones with corals, as well as shaly and cherty intervals. The unit

was divided into nine cycles (seven bound by subaerial exposure; Saller and others, 1999a, b). The depositional environment is thought to be shallow shelf dotted by phylloid algal mounds and intermound areas. Both upward-deepening and -shallowing cycles are present in this interval, indicating an overall grouping of facies from separate systems tracts. Saller and others (1999a, b) interpreted the cycle trends (deepening or shallowing) as reflecting dramatic sea-level rises and falls. However, diagenesis associated with exposure still appears minimal, and many of the abrupt trends could be due to autocyclic switching between mound and intermound areas. The upper Strawn package (10 to 15 m thick) consists of two cycles each, with crossbedded ooid grainstones overlying cherty (spiculitic) mudstones. Both cycles, capped by exposure surfaces, have diagenetic alteration extending 1 to 2 m below the surface. Saller and others (1999b) suggested that at least a 20-m sea-level drop had occurred from the beginning to the end of each cycle.

Identification of sequence boundaries (both higher and lower orders) and exposure events is vital to understanding and predicting the reservoir quality and diagenesis of the Strawn Formation in Midland, Delaware, and Val Verde Basins. A hierarchy of exposure events is based on data from the Strawn Formation in the Southwest Andrews area (Saller and others, 1999a, b). Four stages of diagenetic alteration linked to subaerial exposure are postulated. Stage 1 is very brief to no exposure. Stage 2 is brief to moderate exposure. Stage 3 is moderate exposure, and Stage 4 is prolonged exposure. Each stage is characterized by its distinct (1) style of alteration below the exposure surface, (2) cycle thickness, (3) position on a Fisher plot, and (4) stable isotope composition. No Stage 3 or 4 exposure was identified by Saller and others (1999a) in the Southwest Andrews field study.

The lower and middle Strawn is characterized by Stage 1 diagenesis—that is, cycles with little petrologic evidence of subaerial exposure or meteoric diagenesis. Cycles are generally thick and about 4 m (although some are thin owing to low carbonate production in deep water), and $\delta^{18}\text{O}$ and $\delta^{13}\text{C}$ compositions are heavy (marine signature) (Saller and others, 1999a, b). Figure 22 illustrates the facies character, isotope profile, and wireline-log signature of a Strawn Stage 1 event. Figure 23 is the core photographs of this same interval, on which proposed Stage 1 exposure events are marked. From the core data, it is difficult if not impossible to infer evidence of exposure at proposed boundaries. Surfaces at the proposed exposure boundaries could alternatively be interpreted as transgressive surfaces. Note that the upper, high, total gamma-ray peak (with associated high thorium) is not in a shale, but in a fusulinid wackestone. Total gamma-ray signatures and their correlations can be misleading when compared with those of the actual rock. The lower proposed exposure surface in figure 23 is even more enigmatic and difficult to identify than that of the upper surface. Overall, exposure is taking place during deposition of the Strawn Formation; however, past studies appear to have overinterpreted the extent, value, and number of these surfaces. Saller and others (1999b) proposed a total of 16 cycles for the Strawn, most of which were interpreted to be capped by a subaerial exposure surface. In general, probably four to five cycles can and should be correlated in the field and possibly regionally.

The upper Strawn Formation is characterized by Stage 2 diagenesis, with minor to moderate alteration during subaerial exposure affecting most of the cycles. Caliche crusts, soil-related mottling, and rhizoliths occur in the upper 1 m of many of the cycles (Saller and others, 1999a, b). A few small vugs and fissures are present below the exposure surfaces. Cycles are

generally thick, 3 to 8 m. Light $\delta^{18}\text{O}$ occurs at the top of the cycles and extends deeply into them, suggesting alteration by meteoric water. Light $\delta^{13}\text{C}$ is confined to the uppermost meter of Stage 2 cycles, suggesting that exposure was not intense or prolonged. Figure 24 illustrates the Stage 2 diagenetic profile at the top of the Strawn in the Parker X-1 well. Five cycle tops (each with possible exposure) were interpreted by Saller and others (1999). The exposure event at 9,452 ft, 6 inches, has no visible manifestation on the spectral gamma-ray log. The interval above the top of the Strawn is characterized by a high thorium peak, indicating exposure. The total gamma spike at 9,480 ft appears to represent a small flooding or deepening event. In the absence of spectral gamma, the exposure surface at 9,440 ft (top of the Strawn) would probably be interpreted solely as a flooding event.

Figures 25 through 27 are core photographs of the entire interval described in figure 24 for well X-1. In figure 25, the upper dark crinoidal unit corresponds to the beginning of the Canyon Formation. Note that the high thorium values on the spectral gamma ray (fig. 24) correspond only to the basal 2 ft of this unit. Note that an intervening tight packstone facies is between the upper cycle boundary and the lower cycle boundary on top of the grainstone reservoir facies (figs. 24, 25). Even with core in good condition, these exposure events are difficult to identify and in some instances may indicate only a cycle top and not an exposure event. The lowermost unit in the figure marks the beginning of the upper Strawn reservoir interval (fig. 25).

Figure 26 illustrates finer scale cycles within the reservoir zone of the X-1 well. Several small cycles within the reservoir interval are proposed and are marked by blue sawtooth lines (fig. 26). On the original core description and wireline-log diagram, these facies are not highlighted; however, porosity type and overall reservoir quality are affected

by these facies changes. The surface at about 9,470 ft denotes the top of a laminated facies (peritidal muds?), which was identified in a neighboring well within the field at the same stratigraphic position and possesses similar wireline-log characteristics. This facies may indicate that the grainstone facies of figures 24 and 26 for well X-1 may be split into two cycles, which are separated by peritidal facies. This type of observation, only possible with core data, has a bearing on the lateral and vertical homogeneity of the reservoir interval. In a well about 2 mi away from X-1, the same interval has essentially no reservoir quality largely because the facies are different. The effects of exposure and diagenesis are therefore different. Figure 27 illustrates the lower facies and cycles from figure 24, from 9,475 to 9,495 ft. Yellow boxes outlining the facies from 9,480 to 9,482 ft correspond to the 2nd-highest total gamma-ray spike in the entire Strawn interval within well X-1. Note that the gamma-ray peak is composed almost entirely of uranium and the peak does not correspond to the darkest or most “organic-rich” facies. The use of this peak as a possible maximum flooding surface (MSF) is equivocal when viewed in association with the core and further highlights that spectral gamma ray should be used for correlation, not total gamma ray.

Reservoir Quality

Reservoir quality in the Desmoinesian carbonates of the Midland Basin is controlled by facies and grain type, as well as extent of diagenetic alteration occurring during subaerial exposure. Stage 1 diagenetic intervals, as defined by Saller and others (1999a, b) are dominated by wackestones and packstones with low present porosity. Average porosity in limestones is 1.6 percent (7.5 percent of the total limestone is reservoir grade [>4 percent]). Limestone affected by Stage 2 exposure has an average

porosity of 4.3 percent (35 percent of total limestone is reservoir grade). Grainstones at the top of the cycles tend to have calcite cement filling most intergranular pores; however, dissolution of aragonitic grains has resulted in moldic secondary porosity.

Figures 24 and 26 illustrate subtler changes in porosity and permeability related to facies type. Given the core porosity and permeability and wireline-log data, the entire reservoir interval is good quality, with a maximum of 20 percent porosity and permeabilities slightly above 10 md. Within the reservoir interval's upper facies, pore types are generally moldic and microintercrystalline. Fracture and interparticle porosity appear to increase in the underlying facies with a concomitant permeability increase. The lowest facies in the reservoir interval has dominantly moldic and fracture porosity (figs. 24, 26). Figure 28 illustrates the regional architecture of the reservoir interval on the basis of core porosity of the South Andrews field area. A similar pattern also exists for the University Block 9 area. The most porous zones are present directly below the sequence boundary and exposure surface marking the Strawn to lower Canyon transition. However, the same zone is clearly only weakly developed in well V#7. This situation is linked to the fact that facies present in well V7, at that depth, are dominantly wackestones and packstones, as opposed to grainstone shoals in the other two wells. The photomicrograph illustrates the high porosity (21.5 percent) but low permeability (0.99 md) commonly found in these moldic ooid grainstone reservoirs. Also on the diagram is a violet dashed line placed above the porous zone at approximately 2,940 ft in well X#1. This proposed surface corresponds to a second regional exposure surface that appears to be present across much of the Midland Basin. Below this surface lies a reservoir interval in areas such as Seminole field (Gaines County). The facies of this

lower Strawn interval in Seminole field are similar to those described for the Southwest Andrews field area. The uppermost unit (3.7 to 6 m thick) underlying this lower (second) exposure surface is composed of grainstones bearing fragments of *Chaetetes* and *Komia* and in situ bioherms of *Chaetetes* and *Komia*. Seminole field is interpreted as an isolated patch reef similar to the Goen patch reefs of the Eastern Shelf. Reservoir quality in the grainstone section averages 13 percent porosity and 29 md permeability (maximum permeability 94 md). Average reservoir thickness is 8.5 ft. Porosity and permeability in Seminole field are linked directly to diagenesis occurring as a consequence of exposure and influx of meteoric water. Fracturing does play a role in enhancing reservoir quality of the Strawn at Seminole field (Mazzullo, 1983). Fractures are dominantly vertical, open at the hairline, and larger scale. This fracturing is related to post-Strawn deformation in the area. Products of late-burial diagenesis are also present in the Strawn Formation, mainly in the form of coarsely crystalline to saddle dolomite. Dolomitization occurs as replacements and as cement. Reservoir quality reduction due to late diagenesis appears to be minimal.

In general, depositional facies determine limestone porosity and permeability in the subsurface. Phylloid boundstones are rare, but where present, they have moderate to high porosity (4 to 17 percent) and variable but commonly high permeability (1 to 300 md). Grainstones at the top of the cycles, below subaerial exposure surfaces, are good reservoirs, but grainstones in the transgressive part of the systems tract are usually not porous. Phylloid-rich wackestones to packstones in the Strawn can have good porosity and permeability. Matrix porosity is the main type that develops during subaerial exposure. Porosity is rare and widely scattered in the lower Strawn because of limited

exposure, whereas the more grainstone dominated upper Strawn has experienced brief but significant exposure. Porosity zones in the upper parts of the cycles may be less than a few hundred meters to several kilometers across.

Within the Midland Basin, the Strawn Formation, especially the lower interval, is not as predictable as the Canyon and Cisco (Missourian and Virgilian) units in terms of lateral connectivity of porous and permeable zones (Saller and others 1999a, b). The duration of exposure events may be linked directly to establishment of better reservoir intervals. The Strawn is thought to have experienced exposure events with durations several orders of magnitude less than expected for limestones in general and the overlying Desmoinesian and Virgilian (Yang, 2001). However, this assertion does not factor in differences in facies type (susceptibility to diagenetic alteration) or accommodation issues (that is, ramp vs. platform- to shelf-type margins).

NORTHWEST SHELF

Data regarding distribution and sedimentology of Desmoinesian (Strawn Formation) carbonates on the Northwest Shelf are restricted primarily to Parkway-Empire South fields (Eddy County, New Mexico). Strawn Formation carbonates are distributed in a broad arc trending southwest-northeast across Eddy and Lea Counties, New Mexico (figs. 1, 2, 29). Figure 29 illustrates the interpretation of James (1985) for distribution of Desmoinesian carbonates. In this interpretation, Strawn Formation limestones and reservoirs are thought to comprise elongate phylloid algal mounds trending northeast-southwest. In this study, with the addition of more regional data, the width and orientation of the “mound trend” in figure 29 are expanded eastward into the area James

(1985) considered uplifted (CBP Highlands). A large carbonate platform to ramp setting dominated across the CBP and Northwest Shelf during both the early and late Desmoinesian. The true shelf edge or slope transition into more basinal facies occurred much farther to the south, in what is currently Culberson and Reeves Counties. The mound trend noted by James (1985) probably relates to single or multiple phases of eustatic change during the Desmoinesian, where water depths on the ramp reached optimal conditions for phylloid algal growth. The eustatic influence on carbonates in these ramp settings can result in superimposition of both lowstand and highstand carbonates (including bioherms) or alternatively result in a mix of facies (and reservoirs) that geographically define a wide trend but were deposited at very different times and in very different conditions. The mound trend illustrated in figure 29 is probably a result of the latter.

Figure 30 is the wireline-log signature of the Strawn Formation interval from Parkway field (Eddy County, New Mexico), which is similar in its gamma-ray profile, porosity trends, and thickness to other Strawn successions (for example, Andrews, Gaines, Yoakum, Ector, and Scurry Counties) (for example, fig. 20). The gamma-ray spike (red box) with its underlying more-porous zone (orange box) is most likely related to exposure and may be correlative across much of the Permian Basin. In the Parkway Empire field area, Strawn thickness (“clean carbonate”) isopachs define mounded to oblong structures that have a maximum 100-ft vertical dimension (James, 1985). Effective porosity (4 to 10 percent) is often greatest over the apex of the mounds in a vertical zone of 10 to 40 ft, probably indicating more alteration during exposure. However, a direct correspondence of mound shape to porosity is not present, and areas

exist where no mound is defined and a porous interval is present, and vice versa. Because a “clean carbonate” well log cutoff was used in the derivation of the maps (not core data), facies variations were probably missed, resulting in a lack of correspondence between architecture and porosity. In Humble City and Knowles fields (Lea County near Lovington, S.E., field), porous Strawn intervals are found in both crinoidal and foraminiferal debris mounds, as well as phylloid algal-*Chaetetes* bioherms (Mazzullo, 1989). These bioherms and debris mounds are small ($<1.0 \times 1.0$ mi), generally equidimensional, with up to 75 ft of relief. Parkway Empire field, Strawn Formation, reservoirs most likely exhibit the same facies variations as those in Lea County.

Data on the Desmoinesian for the middle and southern Delaware Basin are extremely sparse. The Strawn succession in Block 16 field (Ward County) appears similar to successions in Upton and Andrews Counties.

EASTERN SHELF

The Eastern Shelf Desmoinesian succession comprises multiple carbonate units from differing depositional and geometric settings (fig. 8) (Cleaves, 2000). The following table illustrates depositional architecture, relative age, formation, and location of Desmoinesian carbonates on the Eastern Shelf.

Table 1. Relative age, formation, and location of different carbonate depositional architectures in the Eastern Shelf Desmoinesian succession.

Architecture	Relative Age	Group (Fm/Mbr)	Location
Ramp Shelf-interior banks Patch reefs	Early Desmoinesian	Lower Strawn (Caddo equivalent)	Western margin of ‘Concho platform’ facing the Midland Basin to the Eastern Shelf
	Middle Desmoinesian	Lower to middle Strawn (Odom) upper Strawn (Capps)	
	Middle Desmoinesian	Lower to middle Strawn (Goen) (for example, Fuzzy Creek and Pony Creek fields—Runnels and Concho Counties)	
	Late Desmoinesian	Upper Strawn (Capps)	
Shelf-margin /rimmed shelf	Late Desmoinesian	Upper Strawn (Anson Bank) (for example, Nena Lucia, Nolan County)	Eastern Shelf
Periplatform pinnacle reef (rare)	Middle-late Desmoinesian	Strawn	Parallel to Eastern Shelf and Ozona Arch area

Desmoinesian carbonate deposition on the Eastern Shelf evolved through several stages of development. Deposition started on a poorly defined carbonate ramp that graded westward from the Eastern Shelf into deeper water carbonates and areas of isolated shale deposition (Caddo and Odom Formations) (fig. 8). After deposition of Buck Creek and Dobbs Valley siliciclastic successions, the lower to middle Strawn Goen patch reefs established themselves in areas of low fluvial-deltaic input. Note that in figure 8 the extent of the Ada Sandstone is much smaller than either previous or subsequent siliciclastic depositional episodes. Rimmed-shelf and shelf-margin carbonate-bank growth started with development of the Anson Ramp (late Desmoinesian), which transformed into the true shelf-margin system of the Anson Bank. The Anson Bank

system was largely aggradational, with minor backstepping up section. The Capps limestone of the uppermost Desmoinesian appears to be a reestablishment of the Anson Bank aggradational shelf margin after a minor hiatus in carbonate deposition.

On the Eastern Shelf in Fisher, Nolan, and Coke Counties there is a series of Desmoinesian-age carbonate reservoirs (for example, Millican, Jameson, and Nena Lucia fields). The Strawn succession in Coke County (Jameson field) was divided into three units: (1) a lower unit comprising cherty limestones and thought to cover the entire Midland Basin except for topographic highs, (2) a middle massive carbonate to dark limestone with shale breaks (not present in the Midland Basin; Hopkins and Ahr, 1985), and (3) an upper buildup succession composed of shelf, reef, and back-reef facies (Hopkins and Ahr, 1985). The upper buildup succession is the producing interval at Jameson Reef field.

The tripartite system used for Strawn division on the Eastern Shelf clearly does not equate to the system used in the southwest Andrews field area (Midland Basin) (Saller and others, 1999a) or the Horseshoe Atoll (Waite, 1993). To further confuse matters, to the east of Jameson Reef field, in Concho and Runnels Counties, the proximity to siliciclastic input results in cyclic deposition of carbonates and siliciclastics throughout the Desmoinesian (fig. 8) (Marquis and Laury, 1989). In general, the Strawn interval in Jameson Reef field appears to be relatively low energy (dominated by wackestones and packstones). Grainstone cycle caps are present but very limited in distribution. Hopkins and Ahr (1985) interpreted the Jameson Reef to have formed on preexisting mud-mound accumulations, which were then colonized by *Chaetetes* and

Komia. These more-framework-type mounds coalesced into large, thicker (up to 300 m) ‘reef’ intervals.

The Strawn interval in St. Lawrence field (Glasscock County) has similarities to both the southwest Andrews field area and Seminole field of the Midland Basin (fig. 31). Two main producing zones are present in the St. Lawrence interval (one below the uppermost exposure surface, and one below the lower exposure surface, fig. 31). The lower surface is in a similar position relative to the wireline-log signature of both Seminole and Kelly-Snyder field examples. The sequence stratigraphic framework of the Glasscock “X” Fee #4 Strawn interval is interpreted to reflect a transgressive systems tract above the Atokan contact, with a possible maximum flooding surface at 9,910 ft. The highstand systems tract culminated in a 10-ft-thick crossbedded grainstone (which is the thickest producing interval in the well). A sequence boundary is inferred at the top of the grainstone, above which more open-marine, deeper water facies are noted and the overall gamma-ray signature increases. A thin lowstand systems tract may exist; however, data are equivocal. In the uppermost transgressive systems tract, sedimentation appears to have taken place largely in the open marine environment (dominated by sponge spicules, brachiopods, bryozoans, corals and echinoderms. From 9,845 to 9855 ft, dolomitization is common, as well as silicification (dissolution of sponge spicules). The dolomitized interval does not appear to have better reservoir quality than the limestones. Given the spatial proximity of the dolomitized interval to Canyon sediments, the dolomite may be associated with an undocumented sequence boundary/surface separating the underlying Strawn Formation from overlying Canyon sediments. The three major cycles below the proposed mid-upper Strawn sequence boundary are capped by higher energy facies.

These grain-rich (ooids, peloids, bioclasts) are the primary reservoir facies of the Strawn. Extensive development of exposure surfaces was indicated by Sivils (2002). However, some of these surfaces, when compared with other studies of the Strawn (for example, Saller and others, 1999a, b), are enigmatic and difficult to identify in core. The Glasscock “X” Fee #4 well in this study is interpreted to have four major cycles within the Strawn. Overall, many of the small-scale cycles noted by Sivils (2002) may not indicate upward shallowing but autocyclic switching from phylloid mound to intermound. These extremely fine scale cycles are usually only definable in a localized area. Defining the proper scale for a Strawn Formation sequence stratigraphic framework will result in better prediction of reservoir facies in other areas.

Farther eastward on the Eastern Shelf, in Runnels and Concho Counties, sedimentology and reservoir characteristics of the Desmoinesian Goen Limestone were discussed by Marquis and Laury (1989). Underlying the Goen limestone are four other Desmoinesian carbonate intervals, the Jennings, Gardner, Odom, and Caddo. Biostratigraphically the entire Eastern Shelf Desmoinesian succession (including younger Capps limestones) equates to the succession present in the Horseshoe Atoll, as well as in Andrews and Gaines Counties. The Eastern Shelf Desmoinesian succession is approximately 800 ft thick in Concho County. The Goen interval within it is approximately 70 ft thick.

The Goen limestone is considered a patch reef situated on the interior of a carbonate ramp (Marquis and Laury, 1989; Cleaves, 2000). Figure 32 is a schematic illustration of a Goen patch reef (Marquis and Laury, 1989), which comprises five facies: (1) a lower-ramp, outer subtidal zone dominated by clayey, spiculitic wackestone and

shales (>50 m water depth) and (2) a middle ramp (which also contains the foremount area) with mound-associated facies dominated by foraminiferal wackestones and packstones. Within the (3) mound community there are phylloid algal wackestones, packstones, and boundstones, with associated localized *Chaetetes* colonies. The (4) shallow-water upper-ramp facies is dominated by bryozoan-coral-green algae wackestones. (5) This facies is a very fine grained sandstone present in the middle ramp. The generalized model proposed for the Goen limestone is three upward-shallowing cycles all capped by transgressive marine mudstones and shales (Marquis and Laury, 1989). Nena Lucia field (Nolan County) represents an Eastern Shelf example of a middle to late Desmoinesian carbonate-rimmed shelf (fig. 33). The close proximity of the carbonate shelf to Desmoinesian siliciclastics (prodelta succession) results in interleaving of carbonate and siliciclastic facies. In the rimmed-shelf environment there is decided depositional relief between the shelf-margin interior and the outer shelf (fig. 33). Total carbonate thickness (Caddo+Odom+Anson Bank) ranges from about 600 ft at the shelf margin (reef) and interior (back reef) to about 300 ft on the outer shelf. The siliciclastic sequence capping the Anson Bank Formation is probably equivalent to the Brazos River Sandstone succession (fig. 8). Nena Lucia field parallels the shelf-margin crest for approximately 10 mi along depositional strike.

Reservoir Quality

Strawn reservoir quality in Jameson Reef field is different from that of Andrews, Block 9, or Seminole fields. In general, the process for causing secondary porosity is subaerial exposure, as in the other areas. However, the depositional mounded topography

resulted in uniform diagenesis across multiple facies. The coarser grained, higher energy facies (grainstones and packstones) appear to have been cemented early. The mound core facies, which are dominantly bioclastic wackestones, were subjected to more numerous and intense leaching episodes during exposure and meteoric water influx. Therefore, in more isolated reef mounds, like at Jameson, the reservoir is the structurally high, low-energy facies. These low-energy facies average 10 percent porosity but have small layers with up to 25 percent porosity.

As with the Midland Basin examples, two of the producing intervals in St. Lawrence field (Glasscock County) are associated with grain-rich facies below multiple exposure surfaces. The secondary dissolution of grains during exposure resulted in moldic and vuggy porosity. Maximum core porosity in the Strawn is 10 percent (fig. 31).

Atypically in Concho County (fig. 32), middle-ramp, shallow subtidal, foraminiferal wackestones (facies 2) and bryozoan, coral, algal wackestones (facies 4) are the reservoir intervals, whereas in other Goen patch reefs phylloid algal and *Chaetetes* boundstones and wackestones of the mound facies (facies 3) are the dominant reservoir (fig. 32). In the Concho County Goen patch reef, facies 2 reservoir quality ranges from 0.4 to 13 percent porosity (mean 2.9 percent) and 0.02 to 25 md permeability. Facies 4 reservoir quality averages 4.2 percent porosity (0.3 to 12.7 percent) and has a permeability range of 0.03 to 325 md. Facies 2 and 4 average 7.0 percent porosity in as many as six different zones (4.0 ft average thickness). Primary porosity is largely occluded by cementation. Secondary dissolution pores after phylloid algae and calcispheres are the dominant macropores. Vug and channel porosity is also important in

the reservoir and is generally the result of solution enlargement after algae dissolution. This porosity is common in the back reef (facies 4), not in the main algal mounds. Figure 34 illustrates the porosity-permeability relationship defined by Marquis and Laury (1989) for the Goen limestone, and four regions are defined on the poro/perm plot. Type IV is characterized by algal, moldic, vug channel, and fracture pores that have been significantly occluded by cementation; however, the micropores remain open. Type III is characterized by open fracture and/or stylolitic pores. Types I and II contain solution-enlarged algal moldic, vug, and channel pores. Type II differs from Type I only by having a slight occlusion of the pores, whereas in Type I, pore space is entirely open. As is obvious from figure 34, samples with Type I characteristics have the best reservoir quality.

Porosity in shelf-margin-style carbonate successions (for example, Nena Lucia field, Nolan County) is linked to dissolution of phylloid algae during subaerial exposure (fig. 33). Shelf-margin plays are better overall targets than many other Desmoinesian carbonate plays (for example, patch reefs or shelf-interior banks). The shelf-margin carbonate successions (especially on the Eastern Shelf) are generally thicker, have large lateral continuity along strike, and are easier to locate on seismic data. Also, Desmoinesian and subsequent Missourian shelf margins became largely fixed geographically by the middle Desmoinesian, resulting in a series of stacked reservoir intervals ranging from the Anson Ramp through the Missourian Palo Pinto Bank (fig. 8).

VAL VERDE BASIN

In the Val Verde Basin, identification of a productive Desmoinesian interval occurred in 1993 after drilling of the Tom Brown Inc. 49-1 ACU well. Following completion of that well, major advances in seismic acquisition and numerous 3D and 2D swath surveys resulted in development of the thrustured Strawn play (figs. 35, 36). The bulk of the data relating to the structure, sedimentology, and reservoir quality of the Strawn in the Val Verde Basin come from Terrell County and the area encompassing South Park, Deer Canyon, South Branch, ACU, and Pakenham fields (figs. 35, 36). Figure 35 illustrates a schematic representation of the thrustured Strawn reservoir style in the South Park field area. Along with the northward-thrustured Strawn interval, an underlying, unthrustured Strawn interval has been identified. This interval has not been developed yet, largely because of the drilling depths required (>15,000 ft in the Pakenham field area) and its dry-gas-only potential (Montgomery, 1996).

The area is structurally complex, and multiple interpretations have been put forward for the geometry of the thrusting. According to data from Pakenham field, the thrusting appears to have resulted in northward-verging, piggy-back thrust sheets crosscut and divided by numerous back thrusts (figs. 37, 38) (Montgomery, 1996; Newell and others, 2003). Khan and others (2002) proposed an alternative structural model based on seismic interpretation, proposing that the Strawn Formation (as well as Mississippian and Permian sections) is deformed by a single thrust sheet broken up by back thrusts and overlying possibly more deeply buried wrench-faulted pop-up structures (figs. 39, 40). The structural interpretation of this area is vitally important because the first interpretation results in multiple stacked reservoir intervals within the Strawn Formation,

whereas the later model (for example, Khan and others, 2002) results in a single Strawn target interval. A review of uninterpreted seismic from Pakenham field (fig. 41) and the wireline-log signature of the Riata Mitchell 11-1 well reveal that multiple thrust sheets of the Strawn Formation are present. However, given the size of individual thrusts (2.5 mi/4.0 km), it is likely that in other regions of the frontal thrust belt that only a single thrust package could be present and/or dominate. Structural interpretation data from Pakenham field can be compared directly with the log signature from the Riata Mitchell 11-1 well. The piggy-back nature of Strawn Formation thrust sheets resulted in two producing intervals within the Riata Mitchell 11-1 well (figs. 37, 42). The structural complexity of the thrust sheets appears to increase downward, resulting in multiple closures (fig. 43). The third Strawn interval is interpreted to back thrust in the well path of the Riata Mitchell 11-1 well, which may have resulted in migration of the hydrocarbons out of this interval (figs. 37, 42, 43). Thickness of the Strawn interval appears to increase with depth (figs. 37, 42). This increase is thought to be primarily depositional because the wireline-log character of the bottom sections of all three Strawn intervals is very similar. Juxtaposition of sediments from different facies environments would be expected in this type of structural setting. The depositional thickness changes are probably related to changes from a more outer shelf/outer ramp (for example, thin) to a more reef crest/inner ramp (for example, thick), as illustrated for Nena Lucia field in figure 33.

Sedimentological and reservoir-quality data for the Strawn succession in the Val Verde Basin comes from the South Park-Deer Canyon-South Branch complex of fields (Terrell County) (Newell and others, 2003) (fig. 36). Strawn lithofacies comprise graded

packstone to mudstone facies (lower third of the Creek Ranch #10-1 core), a very fine grained packstone to laminated wackestone facies (upper two-thirds of the Creek Ranch #10-1 core and lowest 10 ft of the Anna McClung #3-1 core), a structureless wackestone facies (lowest 10 ft of the Alex Mitchell #2-1R core), phylloid algal wackestone and packstone facies (most of the Anna McClung #3-1 and Alex Mitchell #2-1R cores), and a phylloid algal boundstone facies (top of the Anna McClung #3-1) (Newell and others, 2003) (fig. 44). These facies are arranged in multiple repetitive, shallowing, and upward-coarsening packages from 10 to 30 ft thick. The predominance of phylloid algae and other bioclasts also increases upward in each package. The boundary between the packages (cycles) is represented by a dark, laminated, poorly fossiliferous wackestone (base of next cycle) abruptly overlying the coarse phylloid algal packstone/wackestones (fig. 44). In general, cycle thickness appears to be decreasing toward the upper contact of the Strawn Formation (figs. 44 through 46).

Along with the standard facies, three breccia types were identified in the South Park-Deer Canyon-South Branch complex cores. The first breccia type is a polymict angular breccia, which is restricted to the Creek Ranch core. The second breccia is interpreted as a diagenetic pseudobreccia (fig. 45). The third breccia type is an autoclastic fitted breccia (fig. 46). Newell and others (2003) concluded that the intensity of brecciation does not have a strong correspondence to cycle boundaries. The breccias may have formed via early faulting, collapse of burrow pores, or karstic collapse (Newell and others, 2003). Atypically, cycle boundary tops show no evidence of subaerial exposure (paleosols, bird's-eye fabrics, root casts, etc.) according to Newell and others (2003). However, isotopic and textural data suggest that exposure did occur at several of the

cycle boundaries. In the Anna McClung #1-3 core, a pronounced 4-per-mil negative isotopic shift in both carbon and oxygen occurs at and below the cycle boundary at 11,062 ft (fig. 45). This isotopic excursion was interpreted by Newell and others (2003) as not indicative of exposure; however, this surface meets the geochemical criterion devised by Saller and others (1999) for at least a Stage 3 exposure surface. The texture of the “pseudobreccia” in figure 45 also appears to be diagenetic at the top of the sample, whereas the lower brecciation appears sedimentary. Overall, it does appear that the Strawn-age carbonate succession in the Val Verde Basin was subjected to subaerial exposure on several occasions. The depositional model for the Strawn Formation in the South Park-Deer Canyon-South Branch complex is a simple ramp setting, with the McClung and Mitchell cores representing shallow-water, ramp-crest, phylloid-algal buildups and debris, whereas the Creek Ranch core represents deeper water, distal-ramp facies, possibly of turbiditic origin (Newell and others, 2003).

Reservoir Quality

The diagenetic history of the Strawn succession in the Val Verde Basin is long lived and complicated (Newell and others, 2003). Intergranular and intragranular porosity (moldic) developed diagenetically early, via leaching of predominantly phylloid algae. Much of this early porosity was occluded by early and late calcite cements. The bulk of the present porosity is related to late burial diagenesis. The primary events important for the current reservoir porosity are (1) continued development of stylolites that crosscut all early diagenetic features; (2) fracturing; (3) dissolution to create moldic, vug, and enlarged fracture porosity; and (4) porosity reduction by late saddle dolomite and calcite cements (Newell and others, 2003). Fracturing and dissolution in the reservoir intervals

are linked. Moldic and vuggy pores correspond to zones of increased open and cemented fractures, and solution enlargement of pores occurred after stylolitization. The best porosity zone (up to 12 percent log values) is present in packstones and wackestones (for example, McClung core). The Creek Ranch core has virtually no porosity, which indicates that facies type played a crucial role in defining the location of the porous zones. This indication is contradictory to the assertion by Newell and others (2003) that porosity development is dominantly a secondary, late event. Porosity is slightly reduced by late calcite spar and saddle dolomite (found in 10 percent of the samples). Oil migration into the system was contemporaneous with the late-stage calcite and dolomite cementation (primary oil-filled (40+ API) fluid inclusions). Because the Strawn Formation in the Val Verde Basin is primarily a gas and condensate reservoir, the oil either migrated out of the succession or was flushed out by gas (Newell and others, 2003). This 'early' migration/flushing indicates that updip of the Strawn system, probably along thrust-fault paths, oil may have accumulated. Fluid-inclusion analysis of the saddle dolomite indicates maximum trapping temperatures of 136°C/277°F, which is approximately 45°C/113°F above the current formation temperature. Isotopic and fluid-inclusion data from dolomite and late calcite cements support a fluid origin of evolved connate, basinal, high-temperature brine. Newell and others, (2003) contended that the migration of high-temperature basinal fluids into a 'cooler' host rock (Strawn Formation) resulted in cooling-induced undersaturation of the fluid, which then leached the limestones. Overall, reservoir quality in the Val Verde Strawn succession is tied to facies-type extent of subaerial exposure and is overprinted by compression-induced fracturing followed by migration of connate, high-temperature, oil-bearing fluids.

DISTRIBUTION OF DESMOINESIAN-AGE CARBONATES

Desmoinesian-age carbonates were widespread in distribution in several different geologic settings (for example, ramps, shelf margins, patch reefs, etc.). Basin subsidence played a particularly important role in defining and changing the architecture of the carbonate depositional system in the Midland Basin. The east margin of the Midland Basin has been historically defined as the zone to the west of the Concho Arch (Galley, 1958). The Concho Arch is interpreted to trend northwest from the Llano Uplift through Concho, Runnels, Nolan, Fisher, Stonewall, and King Counties (fig. 47). In this study, given the regional data, the site for the east margin of flexure in the Midland Basin is the Fort Chadbourne Fault Zone (also referred to as the Fort Chadbourne High), which trends north-south from Schleicher to King Counties (fig. 47). There is a direct correspondence between the location of the mid- to upper Desmoinesian shelf margin and the Fort Chadbourne Fault Zone. It is proposed that downward, to-the-west flexure along this fault zone resulted in establishment of the topographic gradient that became the nucleation point for shelf-margin accretion during the mid- to late Desmoinesian and the Missourian. Continued downwarping along this flexure zone possibly impacted the distribution of facies during the Missourian.

SUMMARY OF DESMOINESIAN CARBONATE SUCCESSION

In summary several key issues come to bear on understanding Desmoinesian-age carbonates. Many of these issues have a direct bearing on exploitation of, and exploration for, new reservoirs in the Permian Basin.

1. Scale: Studies within and external to the Permian Basin need to be put into a regional sequence stratigraphic context. Several surfaces relating to 3rd-order sequences appear to be correlative within the Desmoinesian succession. The Eastern Shelf carbonate succession needs to be fully integrated and correlated into the Midland Basin. Unraveling the juxtaposed carbonate depositional motifs is required to get a true sense of facies distribution and establish relevant play trends. The use of spectral gamma-ray logs should be adopted to better correlate carbonate successions and help identify exposure surfaces.
2. Diagenesis: Reservoir development is linked to extent of subaerial exposure and to facies type. Multiple facies types can have good reservoir quality. However, shallow-water, phylloid algal bioherms generally are the best reservoirs. Structural interpretation in the Val Verde Basin appears crucial for identifying fluid-flow pathways, which controlled secondary reservoir development.
3. Structure: The currently supported structural model indicates that uplift of the Central Basin Platform was very limited during the Desmoinesian. Carbonate deposition was widespread across that area. Down-to-the west flexure along the Fort Chadbourne Fault Zone occurred during the mid- to late Desmoinesian, establishing a north-south-trending shelf margin for the remainder of the Desmoinesian and the Missourian.
4. Nomenclature: A concerted effort must be made to unify the stratigraphic nomenclature applied to Desmoinesian carbonates. The Eastern Shelf succession of Desmoinesian carbonates must be fully integrated and correlated into the Midland Basin.

DISCUSSION AND SUMMARY OF THE DESMOINESIAN IN THE PERMIAN BASIN

Within the Permian Basin, Desmoinesian siliciclastic deposition is confined to the Eastern Shelf. These siliciclastics are generally fine grained and associated with distal parts of deltaic lobes. The siliciclastics illustrated in figures 1 and 2 in Kinney and Uvalde Counties (that is, Kerr Basin) appear to have had an easterly source, but they did not migrate into the Val Verde Basin area because of a buttress provided by the carbonate platform on the paleohigh of the Devils River Uplift.

Carbonate deposition dominated the Desmoinesian and varied from shallow-water, high-energy to basinal, low-energy facies. Myriad carbonate depositional settings were present during the Desmoinesian, and a general transition from ramplike to steep-shelf margin occurred in the second half of the Desmoinesian within the Midland Basin. Defining water depths for the Desmoinesian facies is difficult. Off-platform and lower-ramp spiculitic facies can occur in water depths that range from as little as ten to hundreds of meters. This range makes defining ramp and shelf margins difficult without the use of 3D seismic. The effects of 3rd- and 4th-order sea-level falls are manifested in carbonates as subaerial exposure surfaces. These surfaces/events often control development of reservoir intervals within the Desmoinesian carbonates throughout the Permian Basin.

PALEOGEOGRAPHIC SUMMARY

Proposed distribution of early and late Desmoinesian-age sediments across the Permian Basin and surrounding areas based on interpretations that were mentioned earlier

is illustrated in figures 1 and 2. The following discussion refers to interpretations represented in those figures.

Early Desmoinesian-age siliciclastics dominated deposition only at the very periphery of the Permian Basin (primarily in the east). A thin band of marine open-shelf siliciclastics are thought to have existed in the extreme northwest corner of the Permian Basin. A tongue of marginal marine to deltaic sediments encroached on the eastern Permian Basin in Fisher County (Knox-Baylor Trough). In general, siliciclastics reached their farthest westward extent during the early Desmoinesian. The predominance of carbonate facies across most of the Permian Basin is due to (1) lack of siliciclastic supply and (2) continued overall 2nd-order rising sea level. Deep-water carbonates and carbonate and siliciclastic shales are only minor in distribution. These facies are centered in Howard, Reagan, and Reeves Counties. The early Desmoinesian carbonate succession is uniform in distribution and thickness across most of the Permian Basin. The CBP, not uplifted at this time, also possesses a blanket of carbonate sediments.

Precambrian inliers along the Matador Arch were uplifted during the Desmoinesian (for example, Bravo Dome, Roosevelt County). Carbonates appear to have dominated sedimentation around these uplifts. Siliciclastics in the Kerr Basin (for example, Kinney, Uvalde, and Zavala Counties) were sourced from the east Ouachita foldbelt. Although illustrated as alluvial to marine in figures 1 and 2, these siliciclastics are largely sedimentologically undefined. Areas of shale deposition in the northern Midland and Delaware Basin reflect ensuing subsidence of these two basins, which becomes more prominent in the late Desmoinesian.

The late Desmoinesian reflects a sedimentation pattern similar to that of the early Desmoinesian, with two notable exceptions. Basin subsidence begins in earnest during the middle to late Desmoinesian. Westward downwarping along the Fort Chadbourne Fault Zone defined the first true Permian Basin carbonate shelf margin during the Pennsylvanian. And the proto-Midland Basin was born. Concurrently the Delaware Basin continued to subside and expand, and the Val Verde Basin began to develop. The Eastern Shelf succession is represented by carbonates of the Anson Ramp to Bank succession. Carbonate development was punctuated by major siliciclastic deltaic progradation, which covered largely the same area but in general did not extend past the shelf edge of the previous cycle. Increased accommodation in areas surrounding the Permian Basin promoted aggradation of the Desmoinesian carbonates (Strawn, Anson Bank Formations). The Palo Duro Basin was characterized by shallow- and deep-water carbonate deposition. Juxtaposition of the deeper water carbonate facies of the Palo Duro and Midland Basins starts to define what is referred to as the Horseshoe Atoll. Overall, carbonate deposition dominated throughout the middle to late Desmoinesian. However, deposition was being affected by tectonic forces, which resulted in myriad carbonate environments being preserved across the Permian Basin.

KEY CONCLUSIONS

- Desmoinesian-age units in the Permian Basin reflect a continuation of 2nd-order transgression being established during the Atokan; 3rd- and 4th-order sea-level falls are crucial to development of reservoir-grade porosity in the carbonate succession.

- Desmoinesian-age siliciclastics occur primarily on the Eastern Shelf to the east of the Permian Basin. Shales within this succession can provide the regional correlation surfaces needed to integrate the Eastern Shelf mixed carbonate and siliciclastic succession into the rest of the Permian Basin.
- Siliciclastic deposition on the Eastern Shelf of the Permian Basin is dominated by distal delta-front and channel-mouth-bar facies. Coarser grained siliciclastic facies occur primarily to the east of the Permian Basin.
- Desmoinesian shallow-water carbonates were deposited over most of the Permian Basin. Carbonate deposition in the early Desmoinesian was uniform in distribution and thickness throughout the Permian Basin (including the CBP, Eastern Shelf, Val Verde Basin, and the Ozona Arch). The early Desmoinesian is characterized by ramplike depositional settings. The middle to late Desmoinesian is characterized by a variety of carbonate depositional environments (for example, ramps, shelf/reef margins, and patch reefs). Regional analysis of Desmoinesian carbonates indicates multiple exposure surfaces and sequence boundaries, some of which appear to be correlative on a regional scale. Phylloid-algal-dominated bioherms affected by subaerial exposure and burial diagenesis compose the best carbonate reservoirs. Desmoinesian *Chaetete* reefs are also good reservoirs, being more common than in the older Atokan or younger Missourian rocks. Fracturing and late diagenesis appear crucial in reservoir development in the Desmoinesian carbonate succession of the Val Verde Basin.

REFERENCES

- Blakey, R. C., 2005, Paleogeography and geologic evolution of ancestral Rocky Mountains, *in* Geological Society of America Annual Meeting, Salt Lake City , v. 37, p. 442
- Boardman, D. R., and Barrick, J. E., 1989, Glacial-eustatic control of faunal distribution in Late Pennsylvanian strata of the Midcontinent—implications for biostratigraphy and chronostratigraphy, *in* Franseen, E. K., and Watney, W. L., eds., *Sedimentary modeling: computer simulation of depositional systems*: Kansas Geological Survey, Subsurface Geology Series, p. 79–81.
- Boring, T. H., 1993, Upper Strawn (Desmoinesian) carbonate and clastic depositional environments, Southeast King County, Texas, *in* Johnson, K. S., and Campbell, J. A., eds., *Petroleum-reservoir geology in the southern Midcontinent*, 1991 symposium: University of Oklahoma, p. 195–198.
- Cleaves, A., 1993, Sequence stratigraphy, systems tracts, and mapping strategies for the subsurface Middle and Upper Pennsylvanian of the eastern shelf, *in* Crick, R. E., ed., *American Association of Petroleum Geologists Southwest Section, Regional Meeting, Transactions*: Fort Worth Geological Society, p. 26-42.
- Cleaves, A.W., 1975, Upper Desmoinesian-lower Missourian depositional systems (Pennsylvanian), North-Central Texas: The University of Texas Austin, Ph.D. dissertation.
- Cleaves, A. W., 2000, Sequence stratigraphy and reciprocal sedimentation in Middle and Late Pennsylvanian carbonate-bank systems, eastern shelf of the Midland Basin, north-central Texas, *in* Johnson, K. S., ed., *Platform carbonates in the southern Midcontinent*, 1996 symposium: University of Oklahoma, v. 101, p. 227–257.
- Cleaves, A.W., and Erxleben, A.W., 1982, Upper Strawn and Canyon (Pennsylvanian) depositional systems, surface and subsurface, North-central Texas, *in* Cromwell, D. W., ed., *Middle and Upper Pennsylvanian System of North-Central and West Texas (outcrop to subsurface): symposia and field conference guidebook*: West Texas Geological Society, v. 82-21, p. 49–85.
- Cleaves, A. W., and Erxleben, A. W., 1985, Upper Strawn and Canyon cratonic depositional systems of Bend Arch, north-central Texas, *in* McNulty, C. I., and McPherson, J. C., eds., *Transactions of the American Association of Petroleum Geologists Southwest Section Regional Meeting*: Fort Worth Geological Society, p. 27–46.
- Dalziel, I. W. D., Lawver, L. A., Gahagan, L. M., Campbel, D. A., and Watson, G., 2002, Texas through time Plate Model, The University of Texas at Austin, Institute for Geophysics, http://www.ig.utexas.edu/research/projects/plates/movies/Texas_Through_Time_020312.ppt.
- Dutton, S. P., 1977, Diagenesis and porosity distribution in deltaic sandstone, Strawn series (Pennsylvanian), North-Central Texas: Gulf Coast Association of Geological Societies Transactions, v. 27, p. 272–277.
- Ewing, T. E., 1990, Tectonic map of Texas: The University of Texas at Austin, Bureau of Economic Geology.

- Galley, J. E., 1958, Oil and geology in the Permian Basin of Texas and New Mexico, *in* Weeks, L. G., ed., *Habitat of oil: American Association of Petroleum Geologists Special Publication*, p. 395–446.
- Gunn, R. D., 1979, Desmoinesian depositional systems in the Knox-Baylor Trough, *in* Hyne, N. J., ed., *Pennsylvanian sandstones of the Mid-continent: Tulsa Geological Society*, p. 221–234.
- Hopkins, K. W., and Ahr, W. M., 1985, Reconstruction of the paleoenvironments of Jameson (Strawn) Reef Field, Coke County, Texas, *in* Transactions of the 35th annual meeting of the Gulf Coast Association of Geological Societies AAPG regional meeting and the 32nd annual meeting of the Gulf Coast Section of the Society of Economic Paleontologists and Mineralogists, v. 35, p. 117–124.
- James, A. D., 1985, Producing characteristics and depositional environments of Lower Pennsylvanian reservoirs, Parkway-Empire South area, Eddy County, New Mexico: *American Association of Petroleum Geologists Bulletin*, v. 69, p. 1043–1063.
- Khan, A., Ferris, C., Burdick, C., and Grant, N., 2002, A look into the Val Verde Basin, Texas: *The Leading Edge*, v. 21, p. 872–874.
- Kluth, C. F., 1986, Plate tectonics of the ancestral Rocky Mountains, *in* Peterson, J. A., ed., *Paleotectonics and sedimentation in the Rocky Mountain region, United States: American Association of Petroleum Geologists*, v. 41, p. 353–369.
- Land, L. S., and Dutton, S. P., 1978, Cementation of a Pennsylvanian deltaic sandstone: isotopic data: *Journal of Sedimentary Research*, v. 48, p. 1167–1176.
- Marquis, S. A., and Laury, R. L., 1989, Glacio-eustasy, depositional environments, diagenesis, and reservoir character of Goen Limestone cyclothem (Desmoinesian), Concho Platform, central Texas: *American Association of Petroleum Geologists Bulletin*, v. 73, p. 166–181.
- Mazzullo, S. J., 1983, Lower Strawn reservoir, Seminole S.E. Field, Midland Basin, Texas, *in* Shaw, R. L., and Pollan, B. J., eds., *Permian Basin Cores—a workshop: Permian Basin Section, SEPM*, v. 2, p. 69–93.
- Mazzullo, S. J., 1989, Subtle traps in Ordovician to Permian carbonate petroleum reservoirs, Permian Basin: an overview, *in* Search for the subtle trap: hydrocarbon exploration in mature basins: *West Texas Geological Society*, v. 89-85, p. 155–180.
- Montgomery, S. L., 1996, Val Verde Basin; thrust Strawn (Pennsylvanian) carbonate reservoirs, Pakenham Field area: *American Association of Petroleum Geologists Bulletin*, v. 80, p. 987–998.
- Newell, K. D., Goldstein, R. H., and Burdick, C. J., 2003, Diagenesis and late-stage porosity development in the Pennsylvanian Strawn Formation, Val Verde Basin, Texas, U.S.A., *in* Ahr, W. M., Harris, P. M., Morgan, W. A., and Somerville, I. D., eds., *Permo-Carboniferous carbonate platforms and reefs: Society for Sedimentary Geology (SEPM)*, v. 78, p. 333–350.
- Reid, A. M., and Reid, S. T., 1991, A postmortem of the Cogdell Field, Horseshoe Atoll, Midland Basin, Texas, *in* Candelaria, M. P., ed., *Permian Basin plays: tomorrow's technology today: West Texas Geological Society*, p. 39–66.
- Saller, A. H., Dickson, J. A. D., and Matsuda, F., 1999a, Evolution and distribution of porosity associated with subaerial exposure in upper Paleozoic platform

- limestones, West Texas: American Association of Petroleum Geologists Bulletin, v. 83, p. 1835–1854.
- Saller, A. H., Dickson, J. A. D., Rasbury, E. T., and Ebato, T., 1999b, Effects of long-term accommodation change on short-term cycles, upper Paleozoic platform limestones, West Texas, *in* Harris, P. M., Saller, A. H., and Simo, J. A., eds., Advances in carbonate sequence stratigraphy; application to reservoirs, outcrops and models: Society for Sedimentary Geology (SEPM), v. 63, p. 227–246.
- Saller, A. H., Walden, S., Robertson, S., Nims, R., Schwab, J., Hagiwara, H., and Mizohata, S., 2004, Three-dimensional seismic imaging and reservoir modeling of an upper Paleozoic “reefal” buildup, Reinecke Field, West Texas, United States, *in* Eberli, G. P., Masafarro, J. L., and Sarg, J. F. R., eds., Seismic imaging of carbonate reservoirs and systems: American Association of Petroleum Geologists, v. 81, p. 107–122.
- Shannon, J. P., and Dahl, A. R., 1971, Deltaic stratigraphic traps in West Tuscola field, Taylor County, Texas: American Association of Petroleum Geologists Bulletin, v. 55, p. 1194–1205.
- Sivils, D. J., 2002, Reservoir characterization of the Strawn Formation (Desmoinesian) for the St. Lawrence Field, Glasscock county, Texas, *in* American Association of Petroleum Geologists Southwest Section Meeting Transactions: Ruidoso, New Mexico, p. 193–197.
- Stafford, P. T., 1959, Geology of part of the Horseshoe atoll in Scurry and Kent counties, Texas: U.S. Geological Survey Professional Paper P 0315-A.
- Tai, P. -C., and Dorobek, S. L., 1999, Preliminary study on the late Paleozoic tectonic and stratigraphic history at Wilshire Field, central Upton County, southwestern Midland Basin, West Texas, *in* Grace, D. T., and Hinterlong, G. D., eds., The Permian Basin: providing energy for America: West Texas Geological Society, v. 99-106, p. 19–29.
- Tai, P. -C., and Dorobek, S. L., 2000, Tectonic model for late Paleozoic deformation of the Central Basin Platform, Permian Basin region, West Texas, *in* DeMis, W. D., Nelis, M. K., and Trentham, R. C., eds., The Permian Basin: proving ground for tomorrow’s technologies: West Texas Geological Society, v. 00-109, p. 157–176.
- Van der Loop, M., 1990, Amacker-Tippett Wolfcamp Field, Upton County, Texas, *in* Flis, J. E., and Price, R. C., eds., Permian Basin oil and gas fields: innovative ideas in exploration and development: West Texas Geological Society, v. 90-87, p. 133–151.
- Waite, L. E., 1993, Upper Pennsylvanian seismic sequences and facies of the eastern and southern Horseshoe Atoll, Midland Basin, West Texas, *in* Loucks, R. G., and Sarg, J. F., eds., Carbonate sequence stratigraphy; recent developments and applications: American Association of Petroleum Geologists, v. 57, p. 213–240.
- Yang, K. -M., and Dorobek, S. L., 1995, The Permian Basin of West Texas and New Mexico: tectonic history of a “composite” foreland basin and its effects on stratigraphic development, *in* Dorobek, S. L., and Ross, G. M., eds., Stratigraphic evolution of foreland basins: SEPM (Society for Sedimentary Geology), v. 52, p. 149–174.

- Yang, W., 2001, Estimation of duration of subaerial exposure in shallow-marine limestones: an isotopic approach: *Journal of Sedimentary Research*, v. 71, p. 778–789.
- Ye, H., Royden, L., Burchfiel, C., and Schuepbach, M., 1996, Late Paleozoic deformation of interior North America; the greater ancestral Rocky Mountains: *American Association of Petroleum Geologists Bulletin*, v. 80, p. 1397–1432.

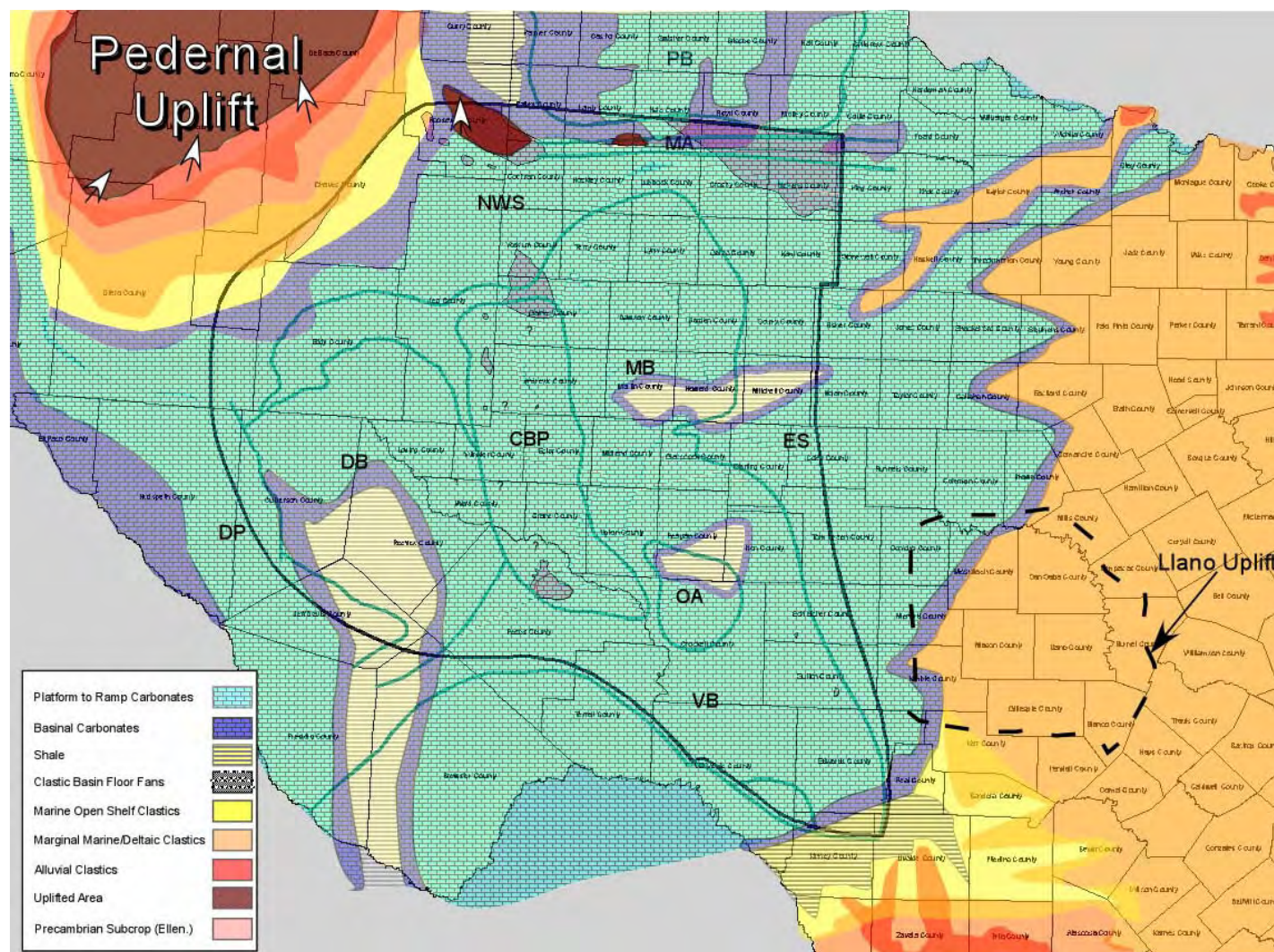


Figure 1. Early Desmoinesian paleogeography and facies distribution map of the greater Permian Basin region. The illustration is based on a time-slice equivalent of the lower Desmoinesian Caddo and early Odom limestone depositional event. Major subregions (outlined in dark green): CBP = Central Basin Platform, DB = Delaware Basin, DP = Diablo Platform, ES = Eastern Shelf, MA = Matador Arch, MB = Midland Basin, NS = Northwest Shelf, OA = Ozona Arch, PB = Palo Duro Basin, VB = Val Verde Basin. The orange siliciclastic zone centered on Knox and Baylor Counties corresponds to the Knox-Baylor Trough. The Fort Worth Basin is centered on Wise County. All geometries are schematic only and may not correspond to actual size or distribution. Llano Uplift area outlined by black dashed line. Sizes of arrows surrounding the Pedernal and other uplifted areas correspond to relative amount of uplift (that is, larger arrow, greater relative uplift).

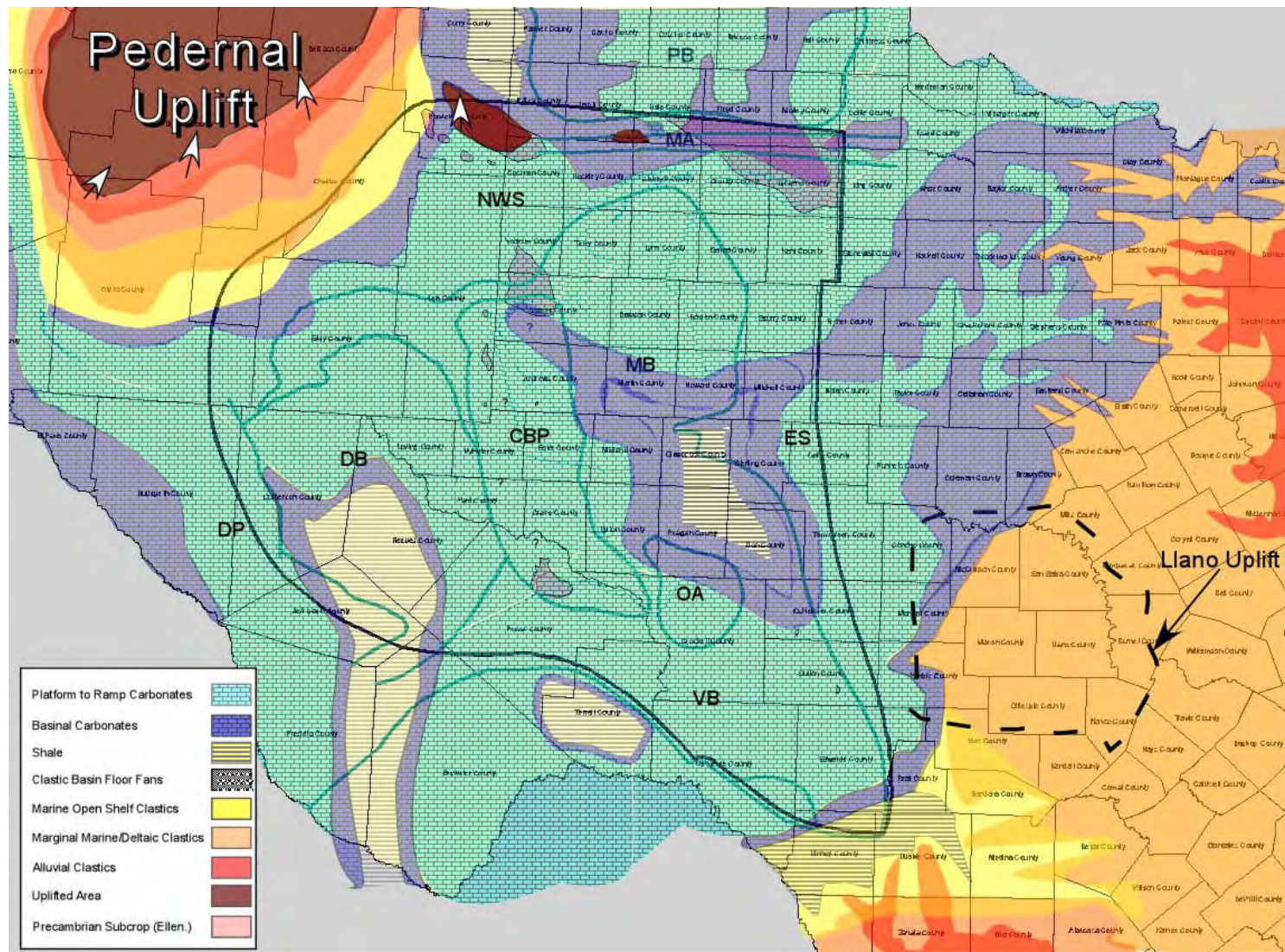


Figure 2. Late Desmoinesian paleogeography and facies distribution map of the greater Permian Basin region. The illustration is based on a time-slice equivalent of the upper Desmoinesian Anson Bank limestone depositional event. Major subregions (outlined in dark green): CBP = Central Basin Platform, DB = Delaware Basin, DP = Diablo Platform, ES = Eastern Shelf, MA = Matador Arch, MB = Midland Basin, NS = Northwest Shelf, OA = Ozona Arch, PB = Palo Duro Basin, VB = Val Verde Basin. The orange siliciclastic zone centered on Knox and Baylor Counties corresponds to the Knox-Baylor Trough. The Fort Worth Basin is centered on Wise County. All geometries are schematic only and may not correspond to actual size or distribution. Llano Uplift area outlined by black dashed line. Sizes of arrows surrounding the Pedernal and other uplifted areas correspond to relative amount of uplift (that is, larger arrow, greater relative uplift).

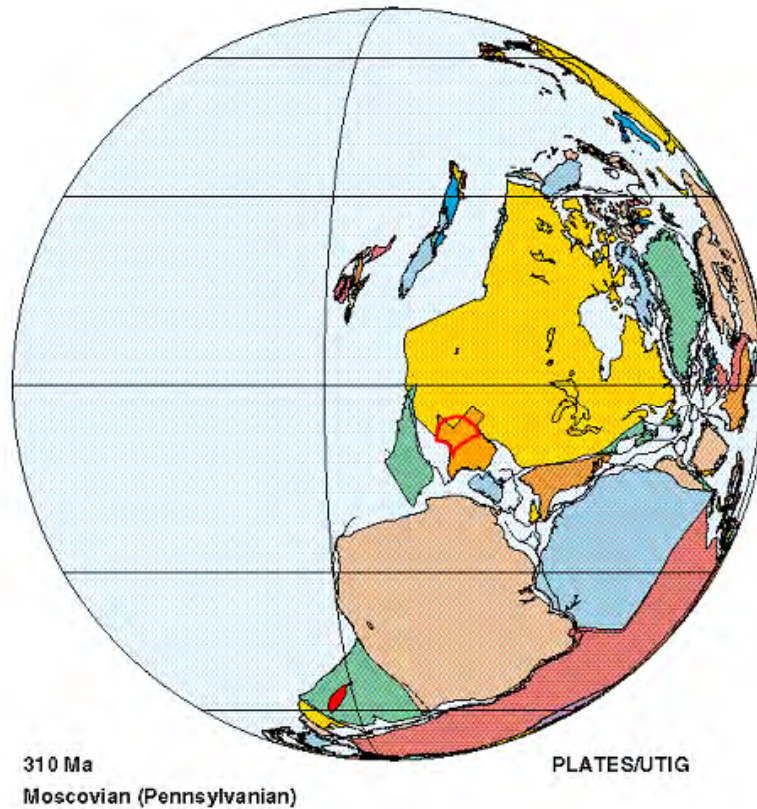


Figure 3. Atokan- to Desmoinesian-age (circa 310 Ma) Texas plate tectonic reconstruction. Note the marine (light-blue) to continental (light-orange) transition, which occurs across Texas (dark-orange) in the area of the Permian Basin. Suturing of the continents has resulted in partly restricted marine subbasin between the plates. Diagram modified from Dalziel and others (2002). The Permian Basin has migrated north (that is, more equatorial) relative to its Morrowan/Atokan position.

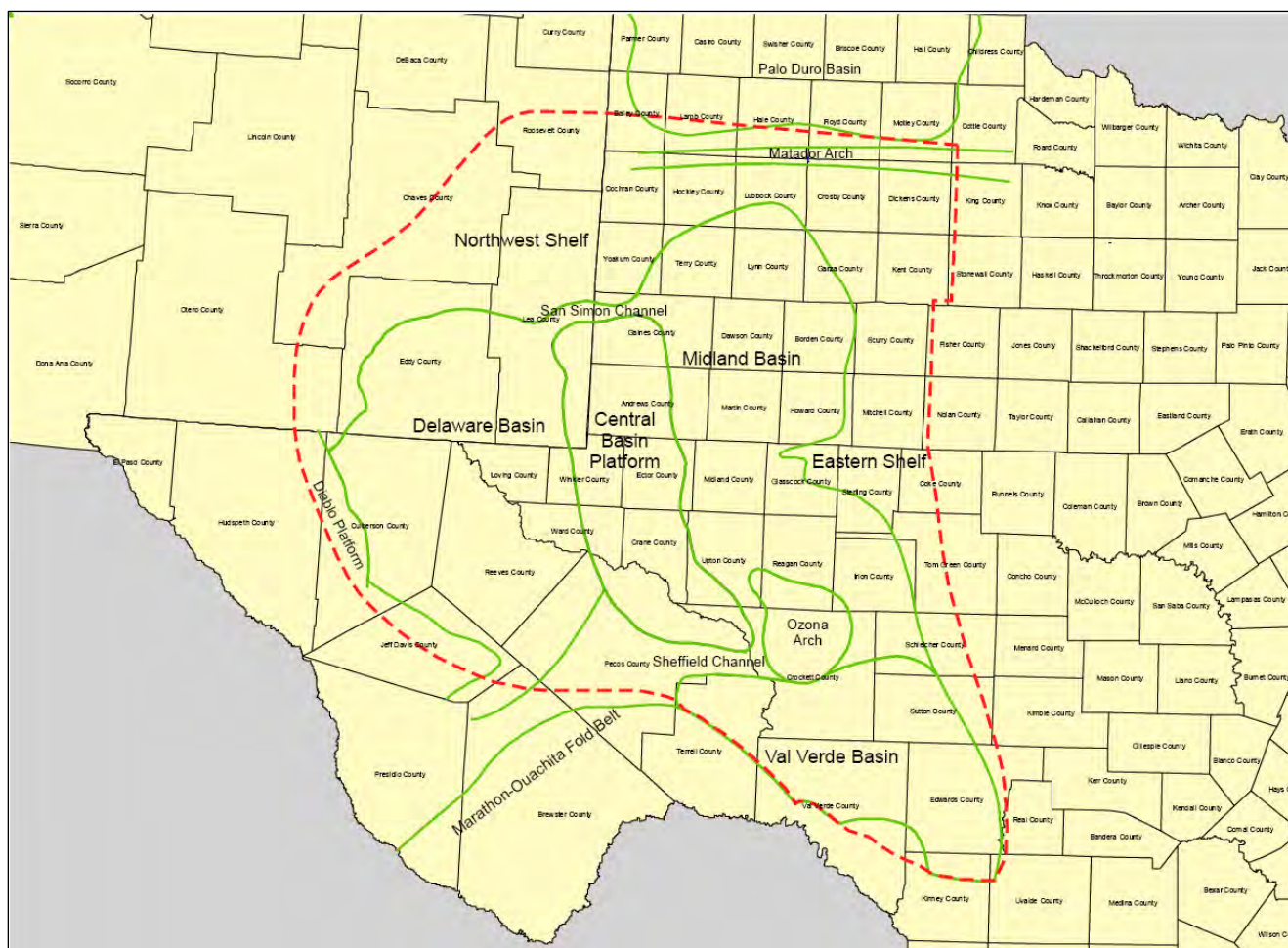


Figure 4. Permian Basin outline (dashed red) and major geologic features. Many of the features were developing during the late Desmoinesian. Compare figure 4 with figures.5 through 7 for previous models of facies distribution relative to the basin outline. Figure 1 illustrates facies distribution in the greater Permian Basin area derived from this study. The west margin of the Forth Worth Basin runs north-south through Palo Pinto County.

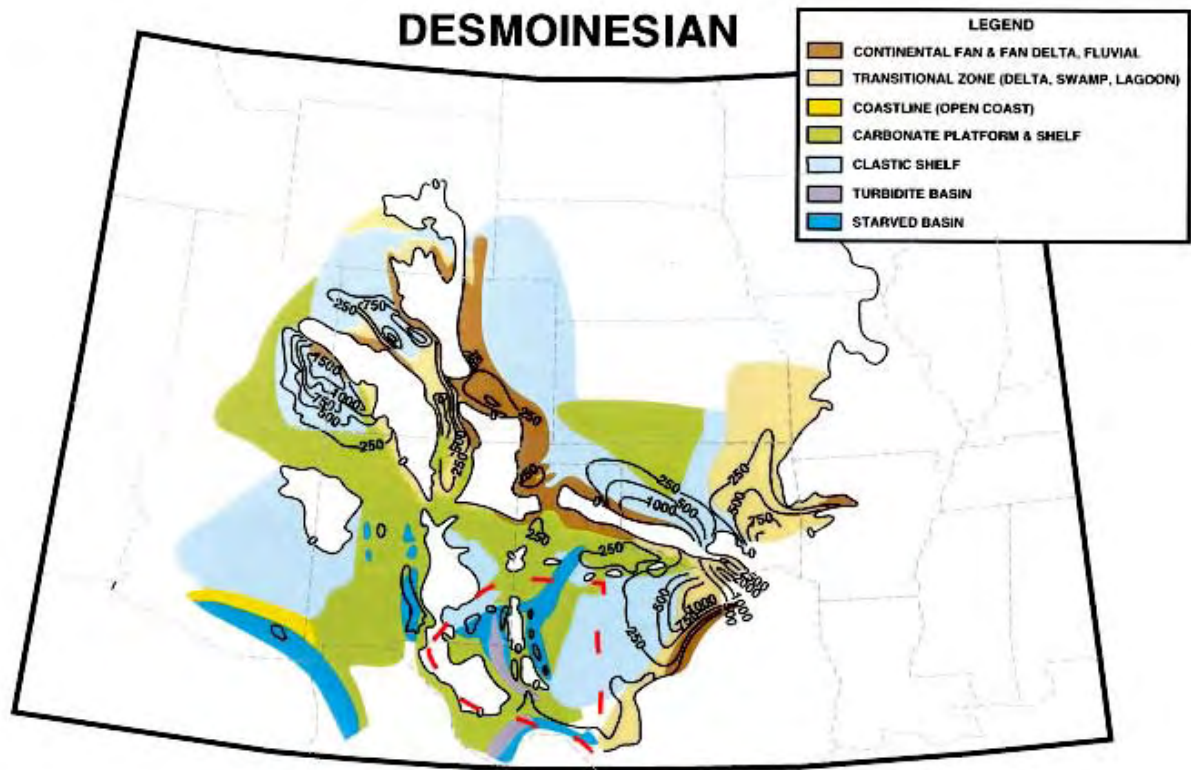


Figure 5. Generalized Rocky Mountain Region and Southern Midcontinent Desmoinesian Paleogeography (from Ye and others, 1996). White areas indicate either nondeposition or erosion (not clarified in original text). The Permian Basin is outlined by the dashed red polygon. Note that the Permian Basin is split into the Delaware and Midland Basins in this representation. The centers of both Midland and Delaware Basins are thought to be starved of sediment or to contain deep-water turbidite facies. Each of the basins is largely rimmed by carbonate-platform to shelfal sediments. A small siliciclastic shelf is represented near the Pedernal Uplift area, and a large siliciclastic shelf dominates most of the Eastern Shelf and Llano Uplift area. One major difference between figures 5 and 6 is the large uplifted areas spanning most of the Diablo Platform and western Delaware Basin. Refer to figure 4 for localities of major geologic features in the greater Permian Basin.

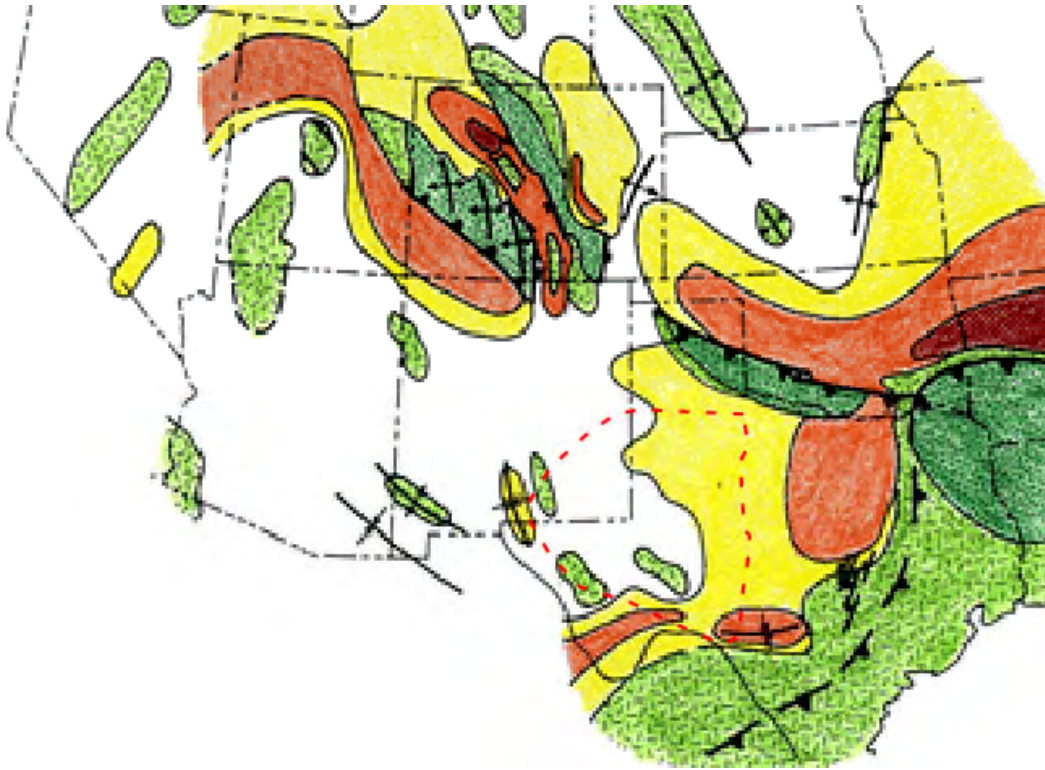


Figure 6. Areas of net subsidence (white <50m/Ma to red >300m/Ma) and net uplift (light-green <50m/Ma) for the Atokan Series (after Kluth, 1986). Permian Basin outlined by red dashed polygon. Kluth (1986) indicated that the south part of the Central Basin Platform area is uplifting along with the Diablo Platform area. All other areas, along with the Permian Basin, are undergoing net subsidence ranging from less than 50m/Ma in the Delaware Basin to more than 300m/Ma in the Val Verde and Fort Worth Basins.



Figure 7. Regional paleogeography of the Desmoinesian (circa 310 Ma). DeB and MiB = Delaware and Midland Basins, respectively. Permian Basin outlined by red dashed polygon. ArB = Anadarko Basin, FwB = Fort Worth Basin, OrB = Oriskany Basin, PeB = Pedregosa Basin, TaT = Taos Trough. Uplifted areas represented by browns, shallow marine by light- to medium-blues, and deep marine by dark-blue (from Blakey, 2005). Prominent differences in uplifting and subsiding areas when compared with those of figure 6, especially with respect to eastern and southeastern New Mexico and location of Pedernal Uplift and Central Basin Platform.

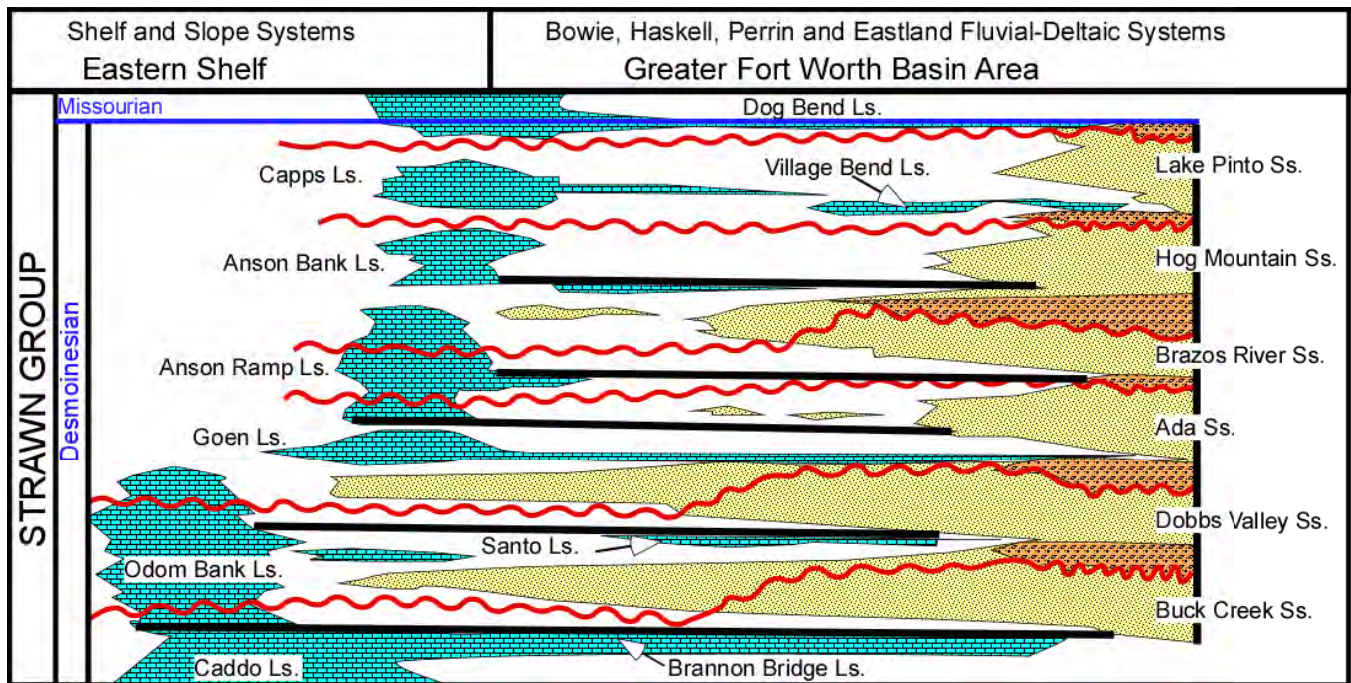


Figure 8. Regional schematic representation of the Desmoinesian-age Strawn group on the Eastern Shelf and the greater Fort Worth Basin area (modified from Cleaves, 1993, 2000). Red irregular lines are major sequence boundaries, and solid straight black lines are regional maximum flooding surfaces. Siliciclastic and carbonate sediments are represented by a series of at least six cyclic packages. The basal two packages, which include the Caddo and Brannon Bridge limestone to Buck Creek sandstone and the Odom Bank limestone and Dobbs Valley sandstone, extend the farthest west into the Permian Basin.

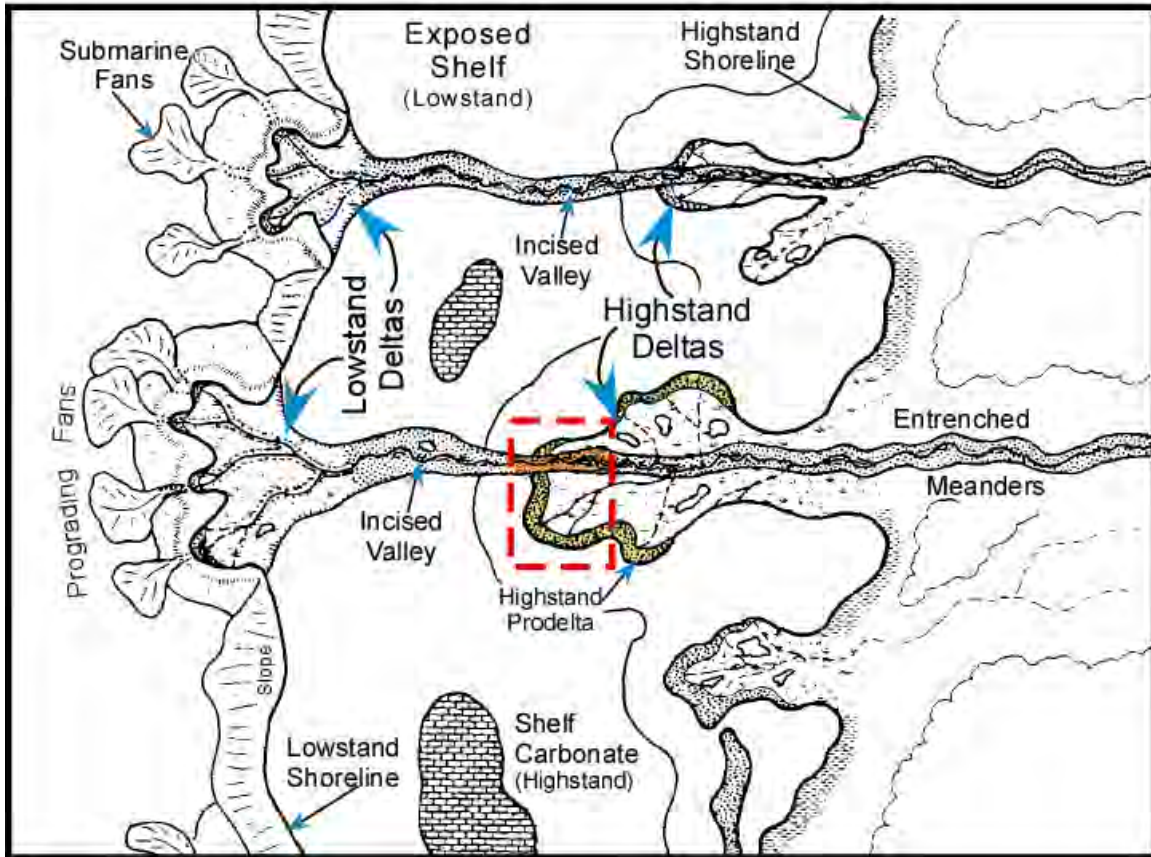


Figure 9. Schematic diagram illustrating possible superimposition of facies when a lowstand deltaic system progrades and downcuts across a highstand delta (after Cleaves, 1993). Red dashed box highlights an area of lowstand channel deposits incising into underlying delta-front bar crest and slope. This area may be analogous to Tuscola field (Taylor County) in figure 10.

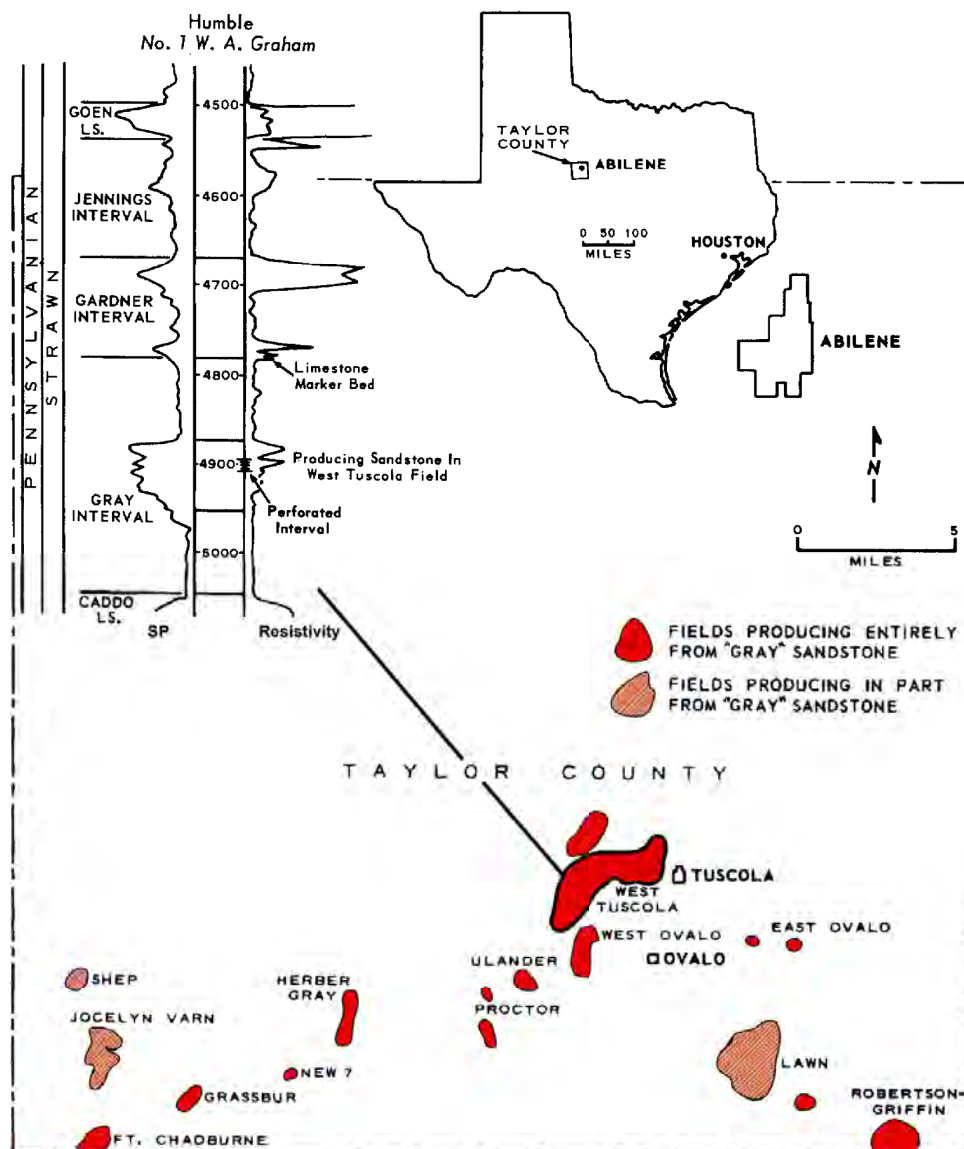


Figure 10. SP- and resistivity-log signature of southern Eastern Shelf siliciclastic interval (after Shannon and Dahl, 1971). 'Gray' producing zone comprises delta-front sediments. West Tuscola field is part of an elongate depositional trend that strikes toward Nolan and Coke Counties in the Permian Basin.

W

E

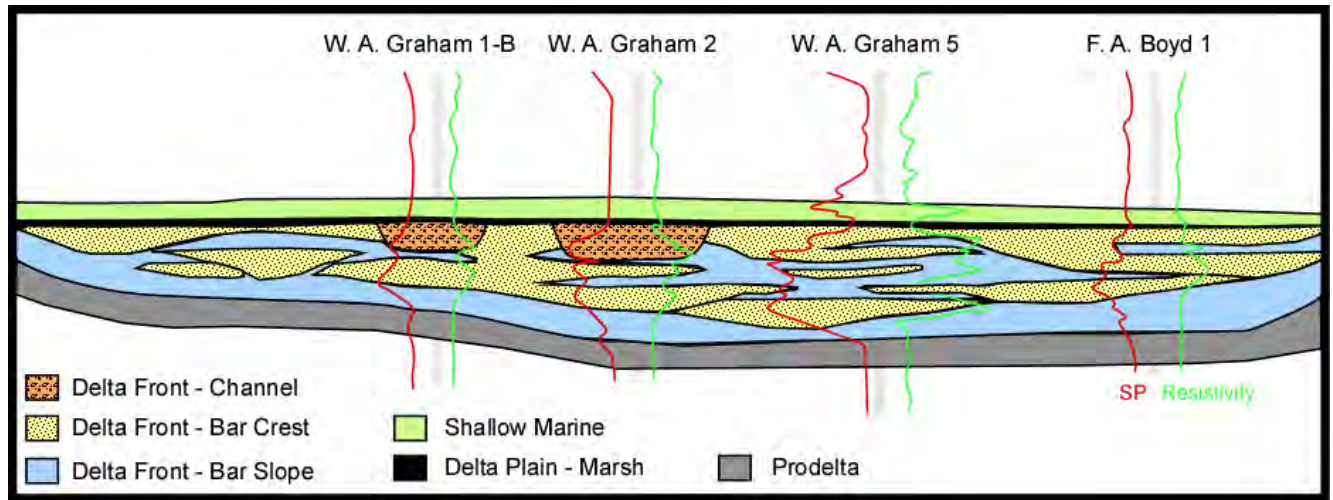


Figure 11. West-east, strike-oriented cross section of the 'Gray Interval,' West Tuscola field, Taylor County (after Shannon and Dahl, 1971). Entire thickness represented by wireline logs approximately 195 ft. The schematic representation of superimposed lowstand channels on a highstand delta in figure 9 may be representative of this field.

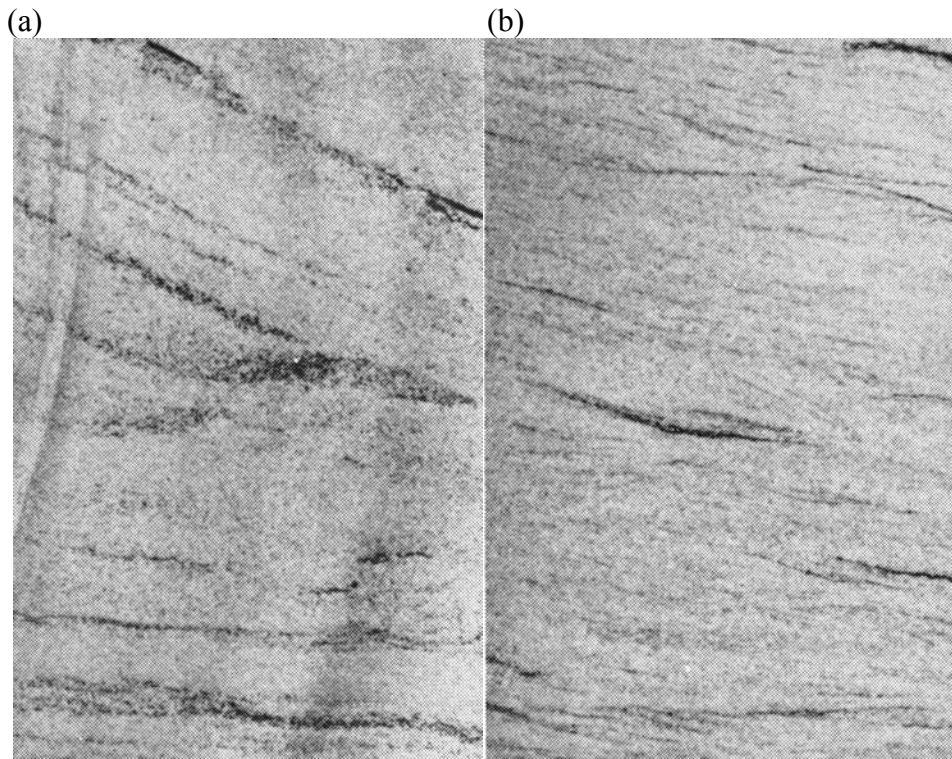


Figure 12. Core photographs of crossbedded and ripple-laminated deltaic facies of the 5,400-ft Anne Tandy Sandstone (Y-22-A, Anne Tandy field, King County). Modified from Gunn (1978). (A) Crossbedded sandstone 5,396 ft. (B) Ripple-laminated sandstone 5,405 ft. Core width is 2.25 inches. Porosity of these facies averages 25 percent, and permeability ranges from 77 to 250 md.

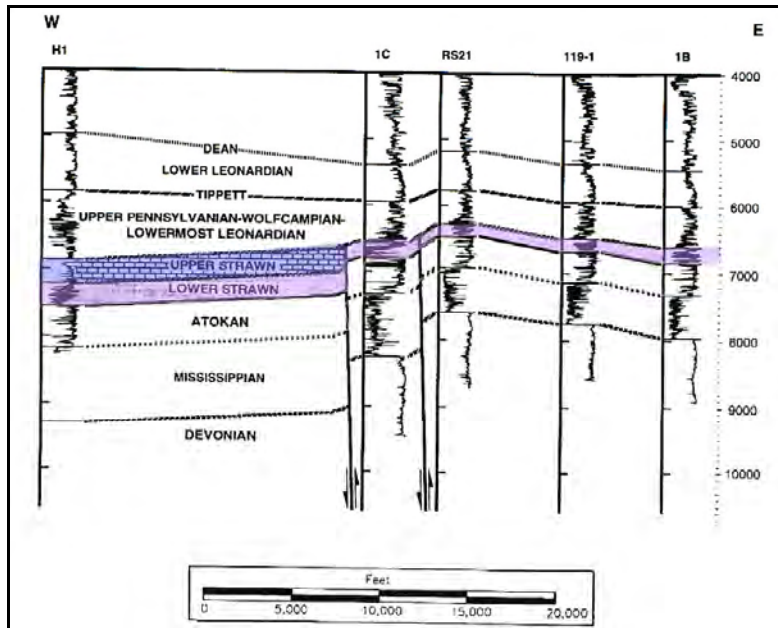


Figure 13. West-east structural cross section of 3D seismic grid over Wilshire field (Upton County). W2 cross section modified from Tai and Dorobek (1999). Note the Desmoinesian Strawn Formation highlighted in purple and blue, which shows thickness changes related to later differential erosion.

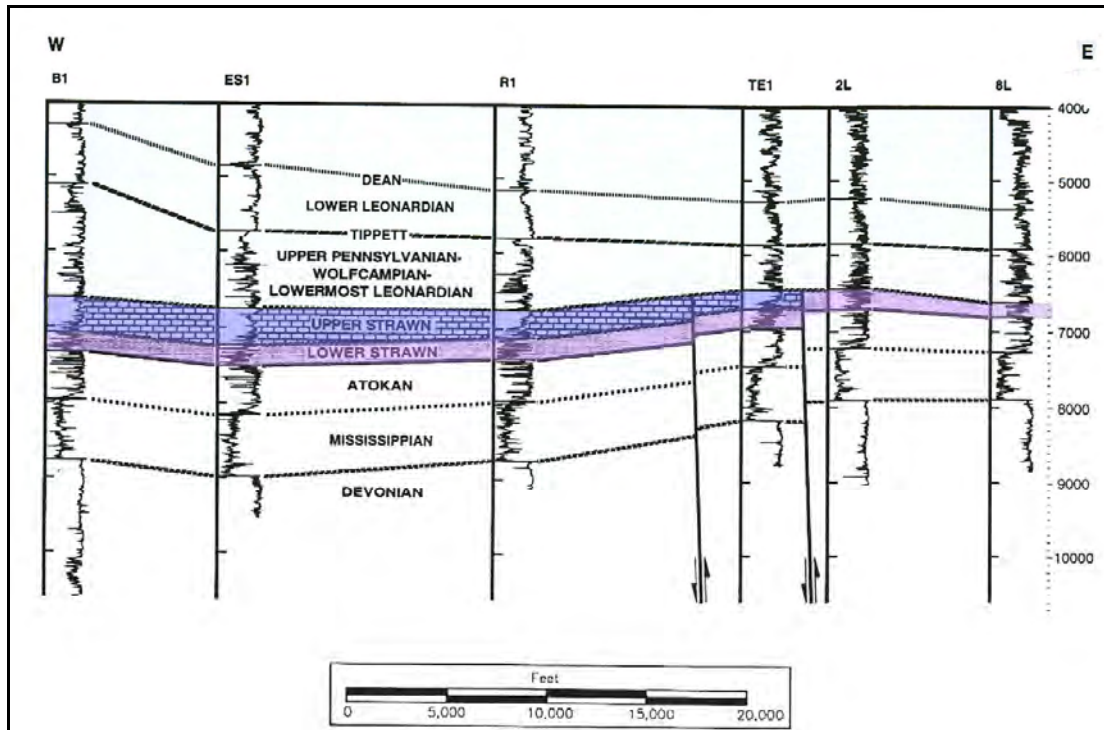


Figure 14. West-east structural cross section of 3D seismic grid over Wilshire field (Upton County). W3 cross section after Tai and Dorobek (1999). Note the Desmoinesian (Strawn Formation) highlighted in purple and blue, which shows differential erosion, not thickness changes, related to deposition.

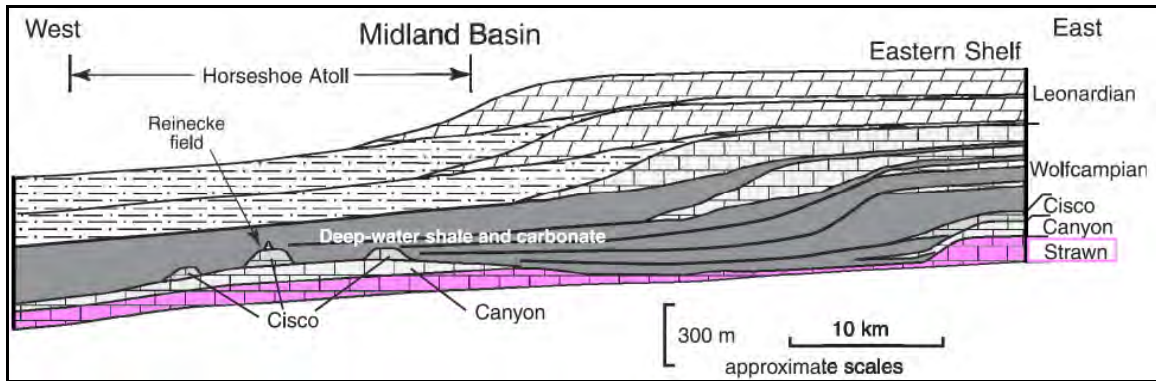


Figure 15. Regional conceptual diagram of Pennsylvanian and Permian facies distribution from the Midland Basin in the west eastward to the Eastern Shelf. After Saller (2004). Strawn interval highlighted in purple. Note that the thinnest part of the Strawn is still approximately 225 ft thick. The thinnest interval of the Strawn is the 'lower' Strawn of Waite (1993).

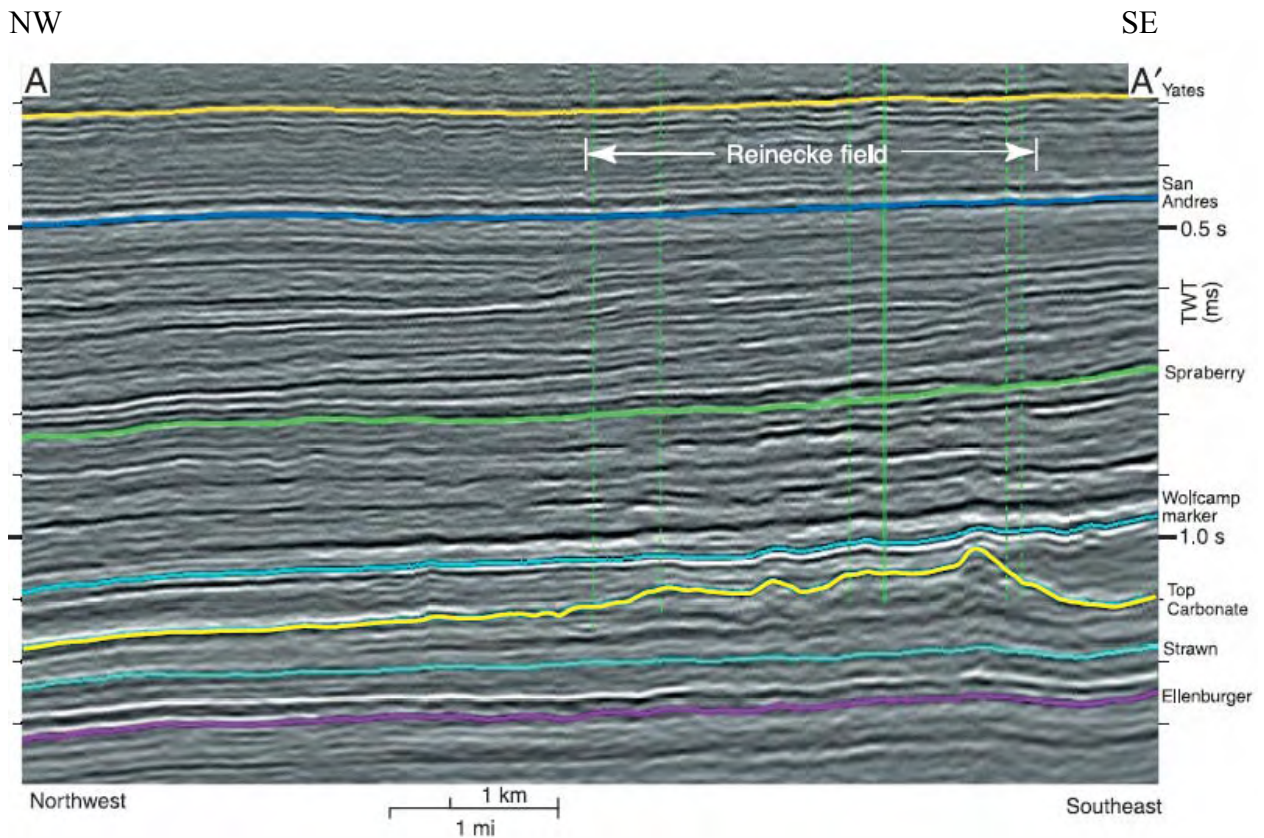


Figure 16. Regional NW-SE seismic cross section of Pennsylvanian and Permian facies distribution from Reinecke field area (Borden County) in the Midland Basin. After Saller (2004). Top of Strawn interval highlighted in cyan. Seismically the Strawn Formation is uniform in thickness. The high-amplitude reflection in the base of the Strawn to Ellenburger interval is either the Atokan Shales or the Mississippian Barnett Formation. The thinnest part of the Strawn is still approximately 225 ft thick. Orientation of line A-A' illustrated in figure 17.

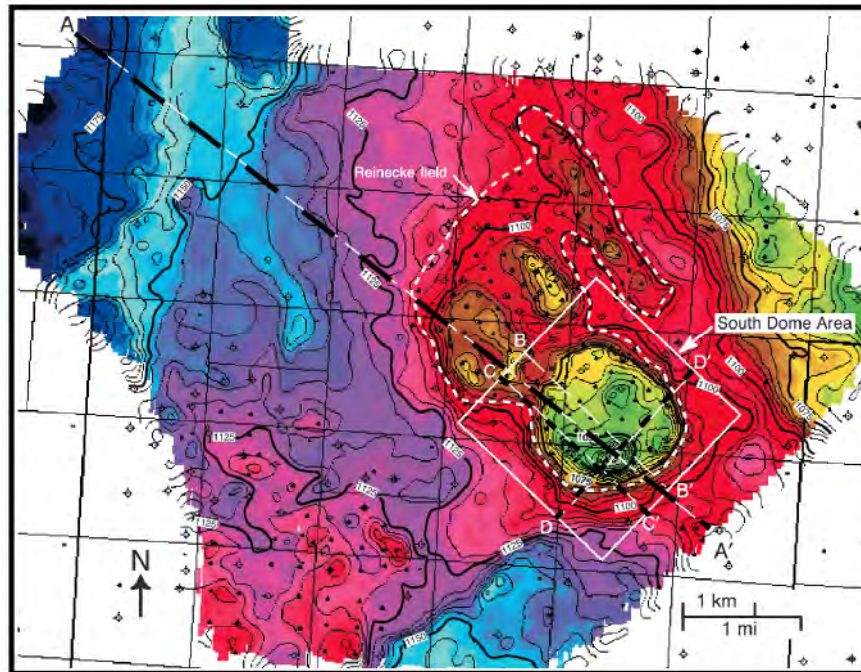


Figure 17. Seismic structure map of the Upper Pennsylvanian-lowest Permian carbonate across Reinecke field at 5-ms contours. Seismic lines A-A' (Figure 16), C-C' and D-D' (figure 18) illustrated by thick dashed black line. All three seismic cross sections go through main mound area and have data down to the Ordovician (Ellenburger).

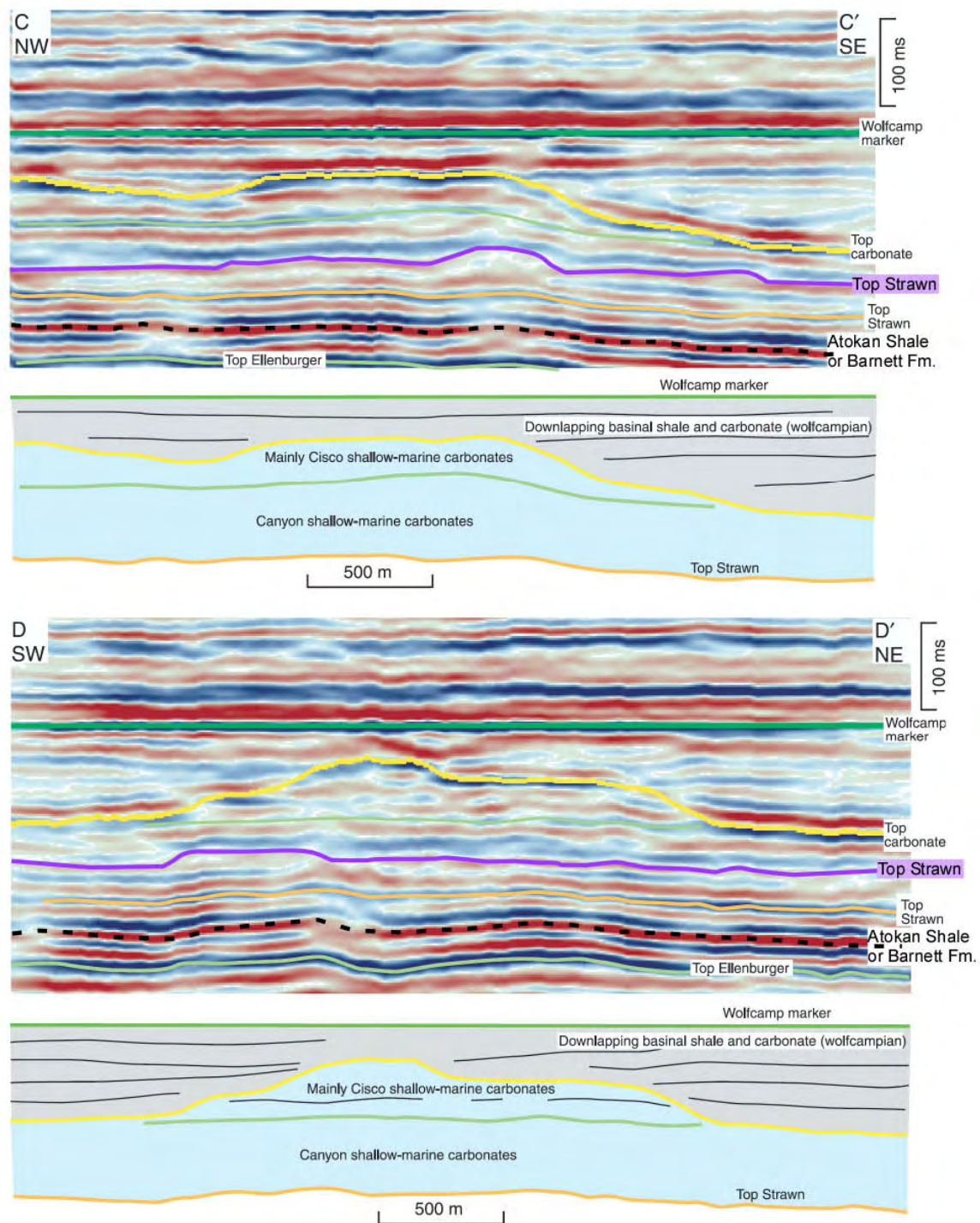


Figure 18. NW-SE (C-C') and SW-NE (D-D') seismic sections of Reinecke field After Saller (2004). For section orientation, see figure 17. On each seismic line, original interpretations of Saller and others (2004) are present, as well as new interpretations from this study. Revised top of Strawn indicated by purple line and proposed Atokan shale or Barnett Formation indicated by dashed black line. Interpreted shale underlying the Strawn Formation equivalent to high-amplitude reflector between Ellenburger and Strawn picks on figure 16.

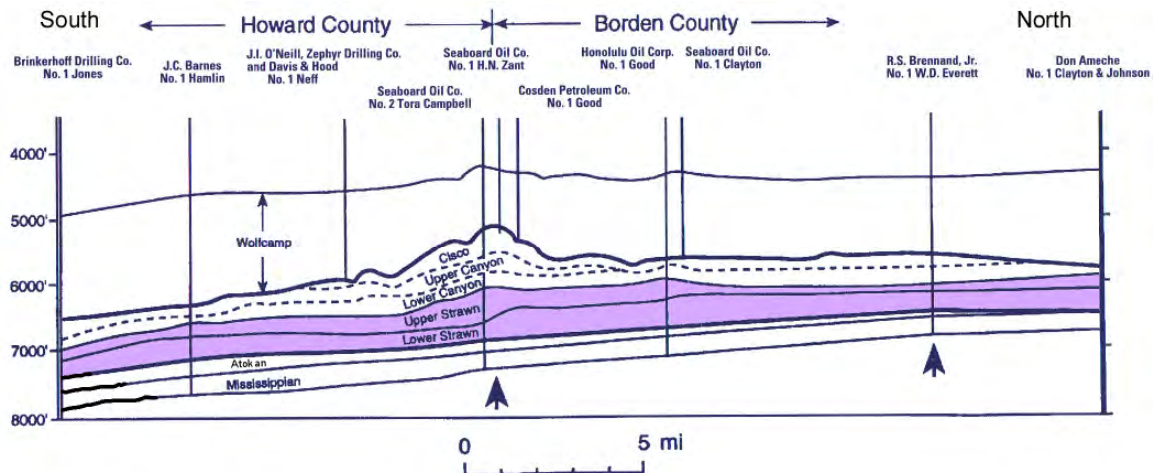


Figure 19. Regional south-north schematic, seismic-based cross section of Vealmoore and Oceanic fields After Waite (1993). Desmoinesian (Strawn Formation) highlighted in purple. Note addition of Atokan (previously referred to as Bend) interval, which was interpreted previously to thin northward. The Strawn Formation as illustrated above has dramatic thickness changes and appears to profoundly control subsequent growth and architectures of Missourian and Virgilian carbonates (Canyon and Cisco).

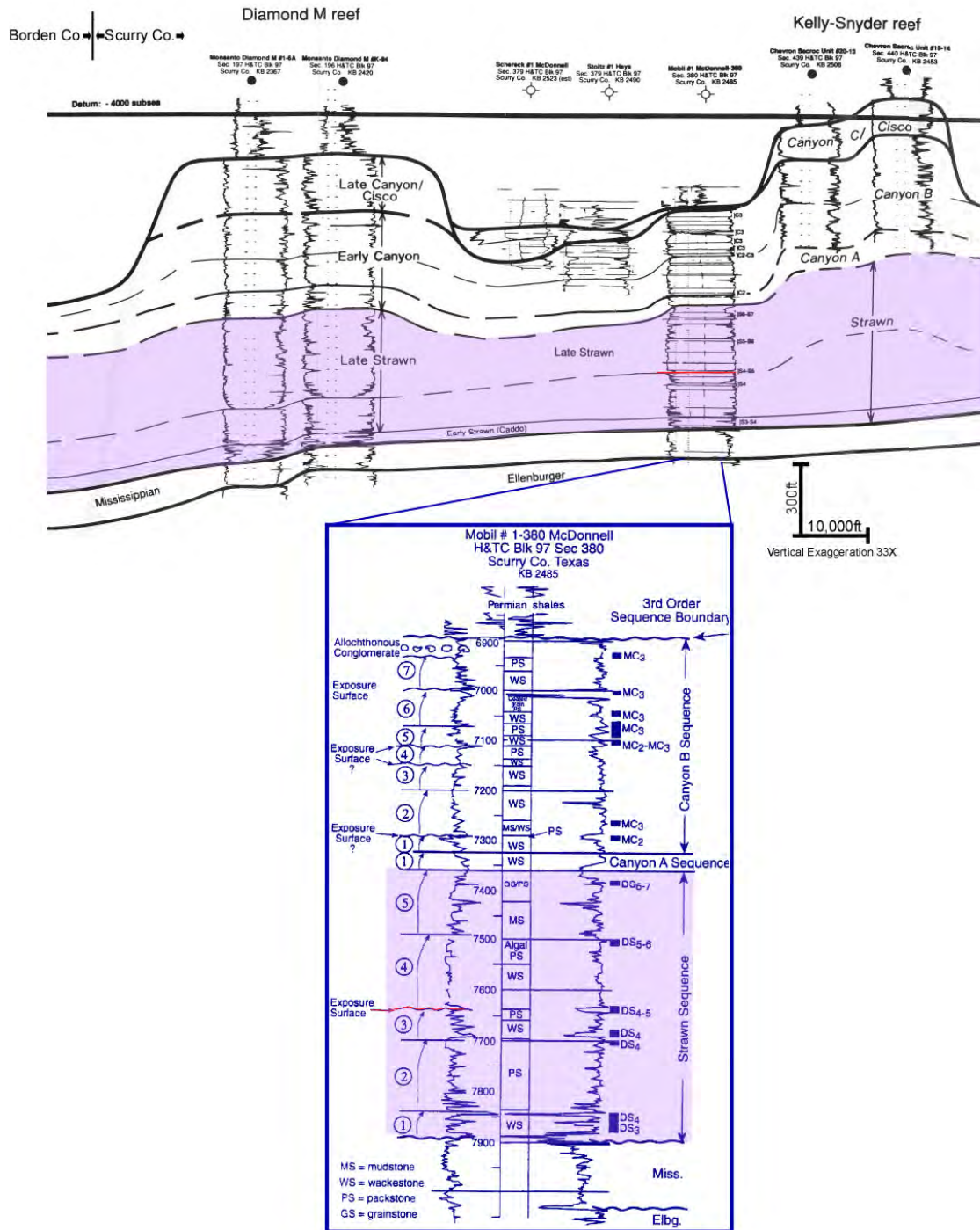


Figure 20. Regional schematic W-E, seismic-based cross section of Diamond M and Kelly Snyder Fields After Waite (1993). Desmoinesian (Strawn Formation) highlighted in purple. Mobil #1-390 well used in correlation illustrated at expanded scale. Circled numbers indicate 4th- to 5th-order cycles proposed by Waite (1993). Fusulinid biostratigraphic zone data provided on right side of log (for example, DS3-DS-7). Note that earliest Desmoinesian zones DS1 and DS2 are not represented in this well. Note exposure surface at top of cycle 3 within the Strawn (Waite, 1993). This surface may hold regional correlation potential. Overall facies stacking pattern indicates upward-shallowing succession. Note cycles stacking with wackestones and packstones underlying phylloid algal packstones, which are overlain by grainstones. This stacking pattern is typical of the Strawn.

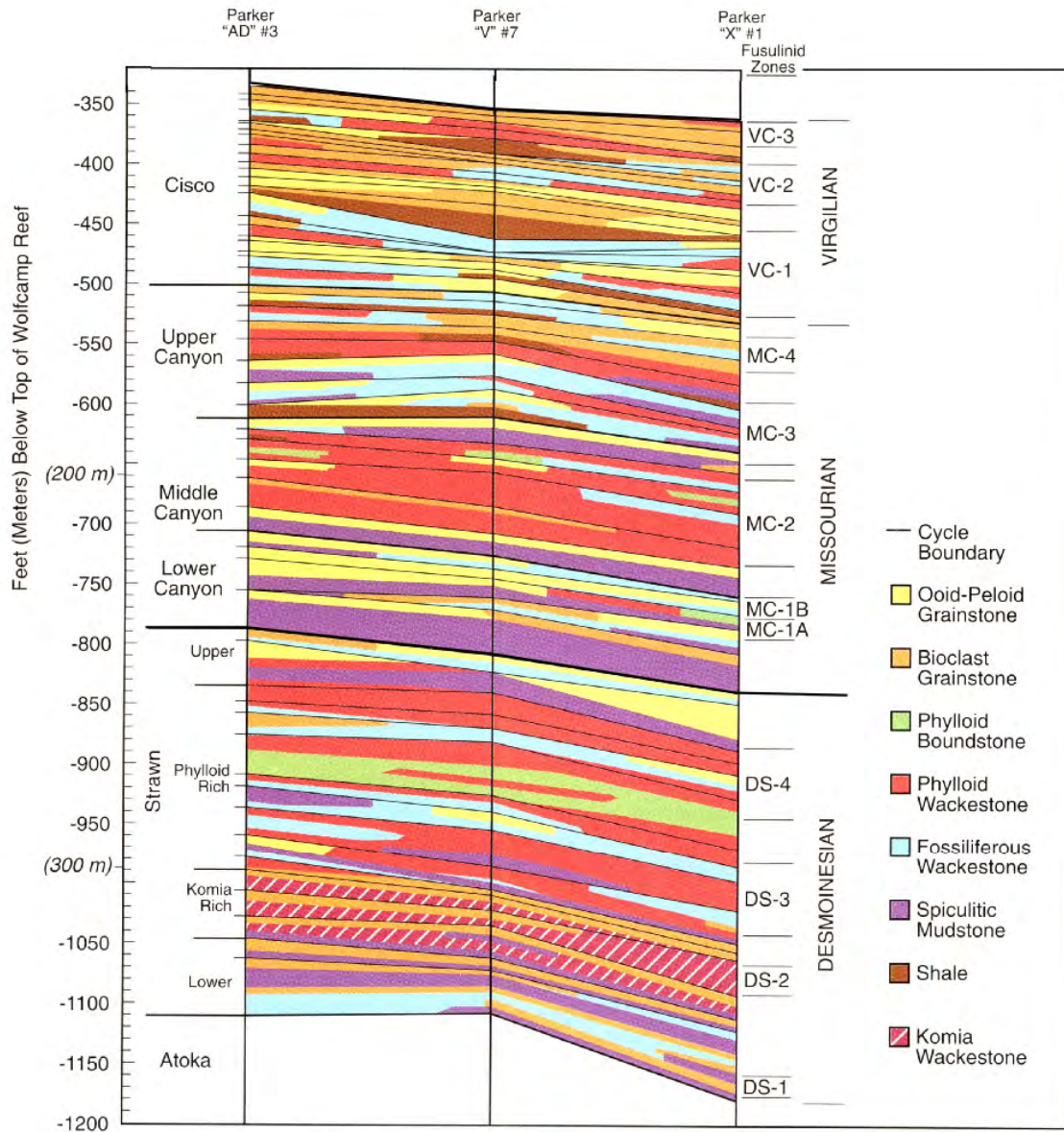


Figure 21. Three well facies and cycle boundary correlation of Pennsylvanian units in Southwest Andrews field Area (Parker, Andrews, and Deep Rock fields) (Andrews County). After Saller and others (1999). The Strawn is subdivided into four gross packages: (1) a lower wackestone and spiculitic mudstone-dominated unit; (2) a *Komia*-rich unit (wackestone and bioclastic grainstone dominates); (3) a phylloid-algal rich unit (phylloid wackestone and boundstone dominate); (4) upper unit (basal spiculitic mudstone overlain by ooid-peloidal grainstones). Contact of Strawn and lower Canyon considered a sequence boundary. As discussed in figure 20, the lower Canyon basal sequence indicates a transgression (deepwater spiculitic limestones overlying grainstones).

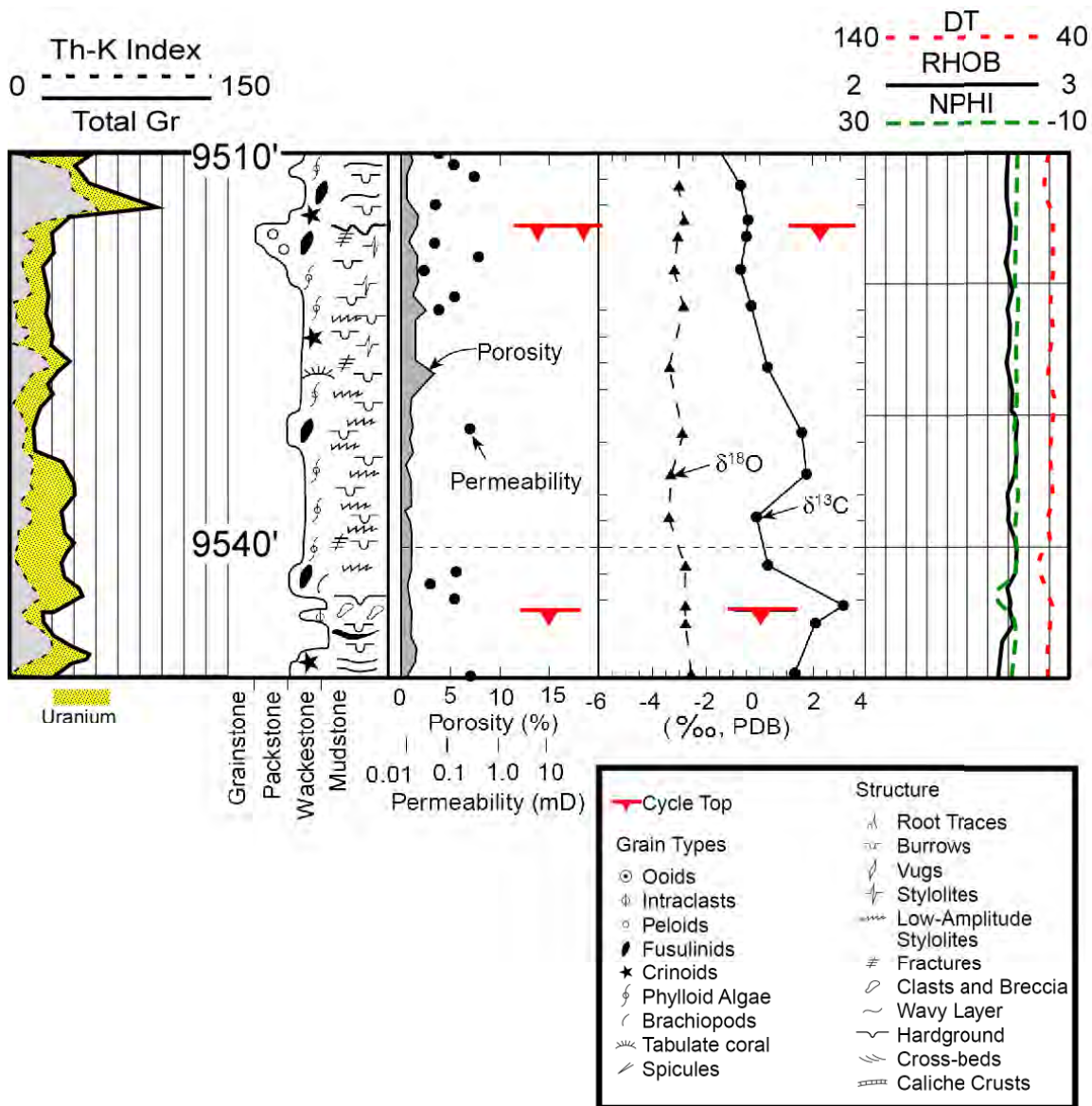


Figure 22. Core description, isotope data, and wireline-log signature of proposed Stage 1 diagenesis event in middle Strawn Formation (Well V#7). Modified from Saller and others (1999a, b). Different Stage 1 surfaces have different spectral gamma responses. Lower total gamma-ray peak centered on 9,540 ft composed primarily of uranium, whereas upper peak at ~9,514 ft has a decided thorium/potassium peak. Note that core and wireline-log porosity are low in entire interval. Permeability (black circles) variable but low <0.5 md. Also note that carbon and oxygen isotopes display marine values. Figure 23 illustrates core-slab photographs of this interval.

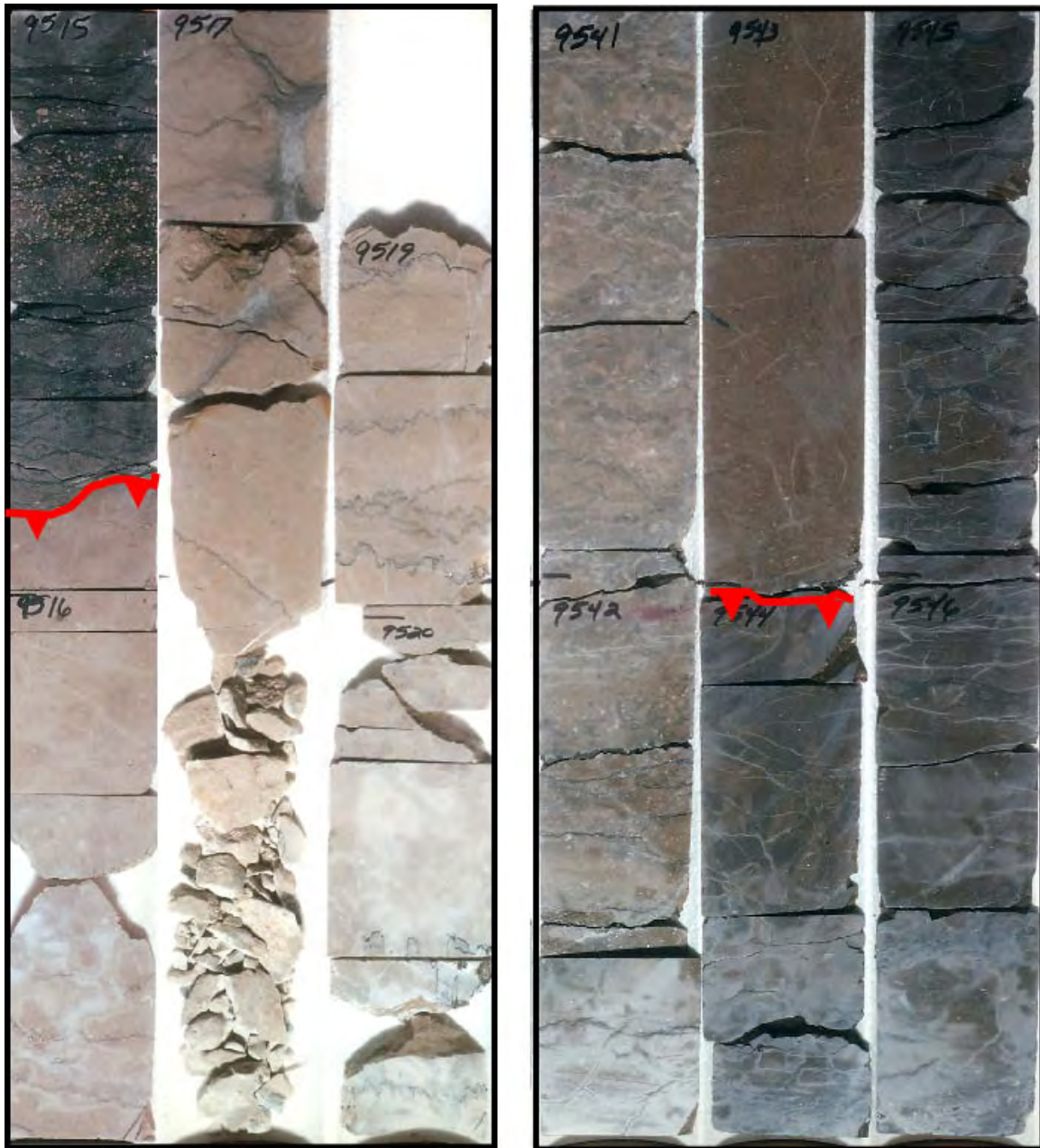


Figure 23. Core photos of Stage 1 Strawn interval in figure 22. Red lines with diamonds are exposure surfaces proposed by Saller and others (1999a, b). In both instances, above the surface can be interpreted as a purely transgressive surface without evidence of exposure. Note that dark fusulinid limestone at about 9,515 ft corresponds to high thorium peak in spectral gamma-ray log.

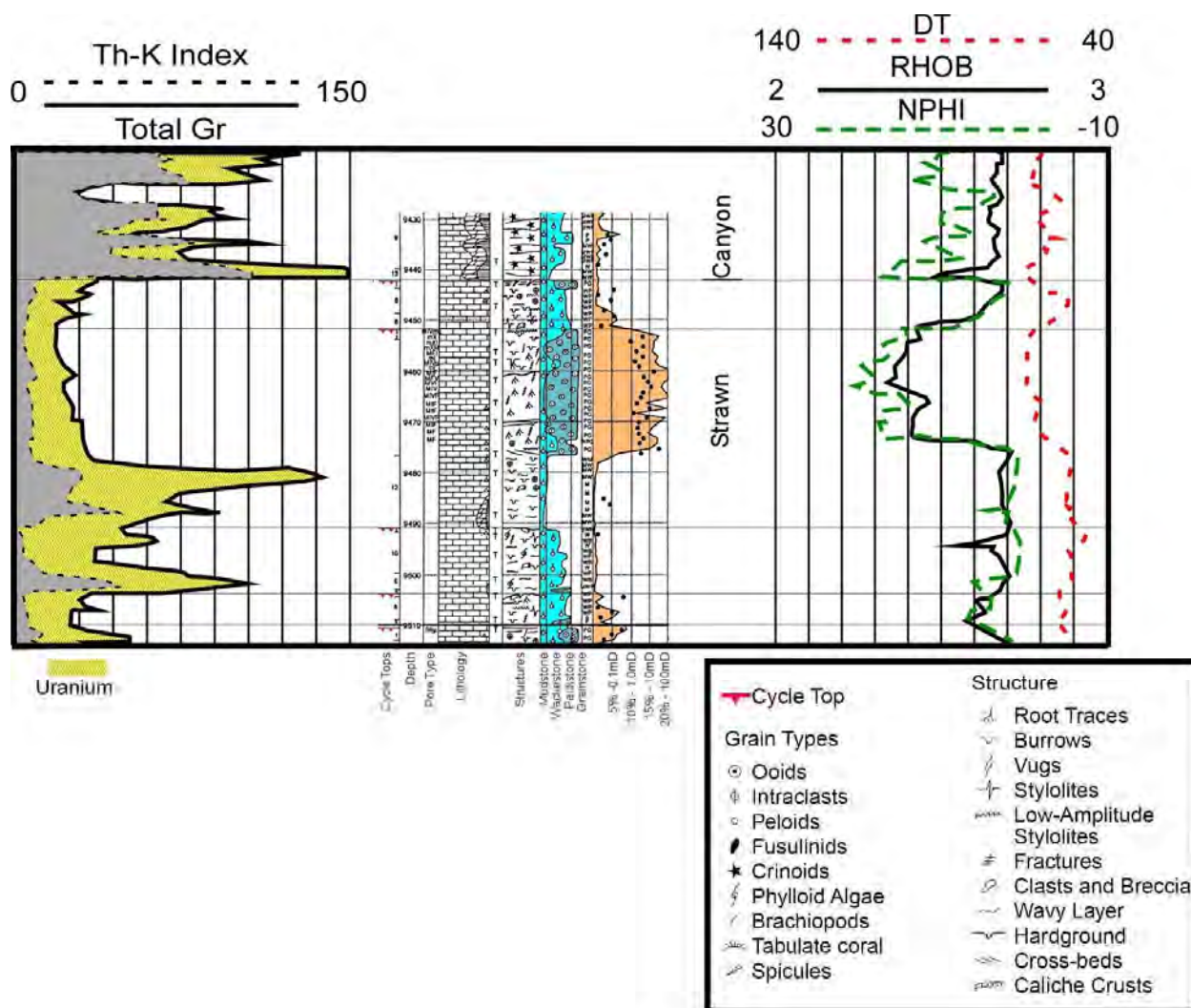


Figure 24. Core description, wireline-log signature, and core-analysis data for a Stage 2 alteration episode. This interval is at the top of the Strawn Formation in Parker X#1 well. Note that there are five cycle tops (each with possible exposure) interpreted by Saller and others, 1999. Exposure event at 9,452 ft 6 inches has no visible manifestation on spectral gamma-ray log. Interval above top of Strawn characterized by high thorium peak, indicating exposure. Total gamma spike at 9,480 ft appears to represent a small flooding or deepening event. In the absence of spectral gamma, exposure surface at 9,440 ft (top of Strawn) would probably be interpreted solely as a flooding event.

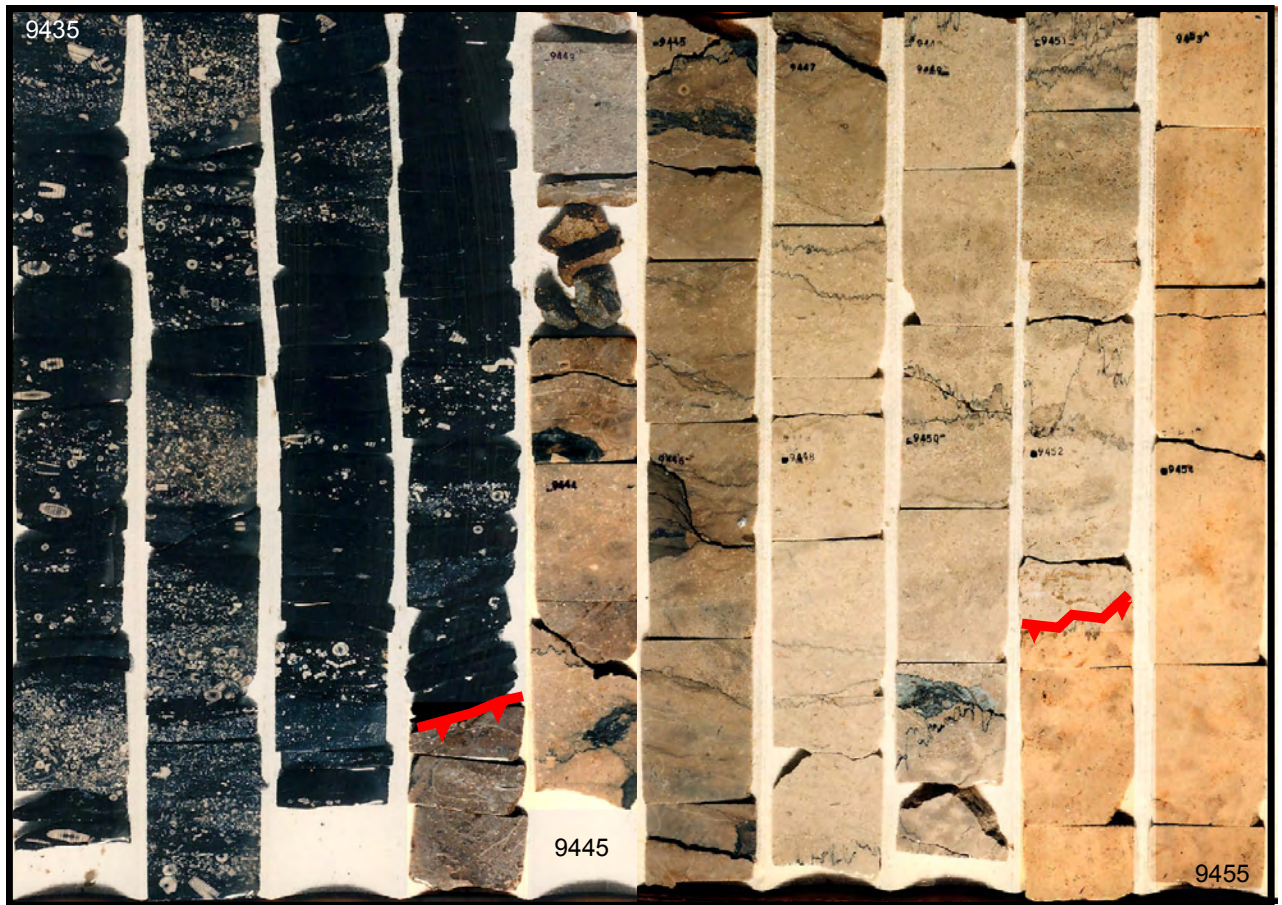


Figure 25. Core photos depicting cycle-top surfaces and facies picked by Saller and others (1999a, b) in the X1 well. Upper dark crinoidal unit corresponds to beginning of the Canyon Formation. Note that high thorium values on spectral gamma ray (fig. 24) correspond only to basal 2 ft of this unit. Interval considered a Stage 2 diagenetic event by Saller and others (1999a, b). Lowermost unit in figure marks beginning of upper Strawn reservoir interval. Judging from core porosity and permeability and wireline-log data, reservoir quality of this interval is good, with a maximum of 20 percent porosity and permeabilities slightly above 10 md. The porosity type found in the reservoir appears to be controlled by facies and grain type, as well as diagenetic alteration during exposure.

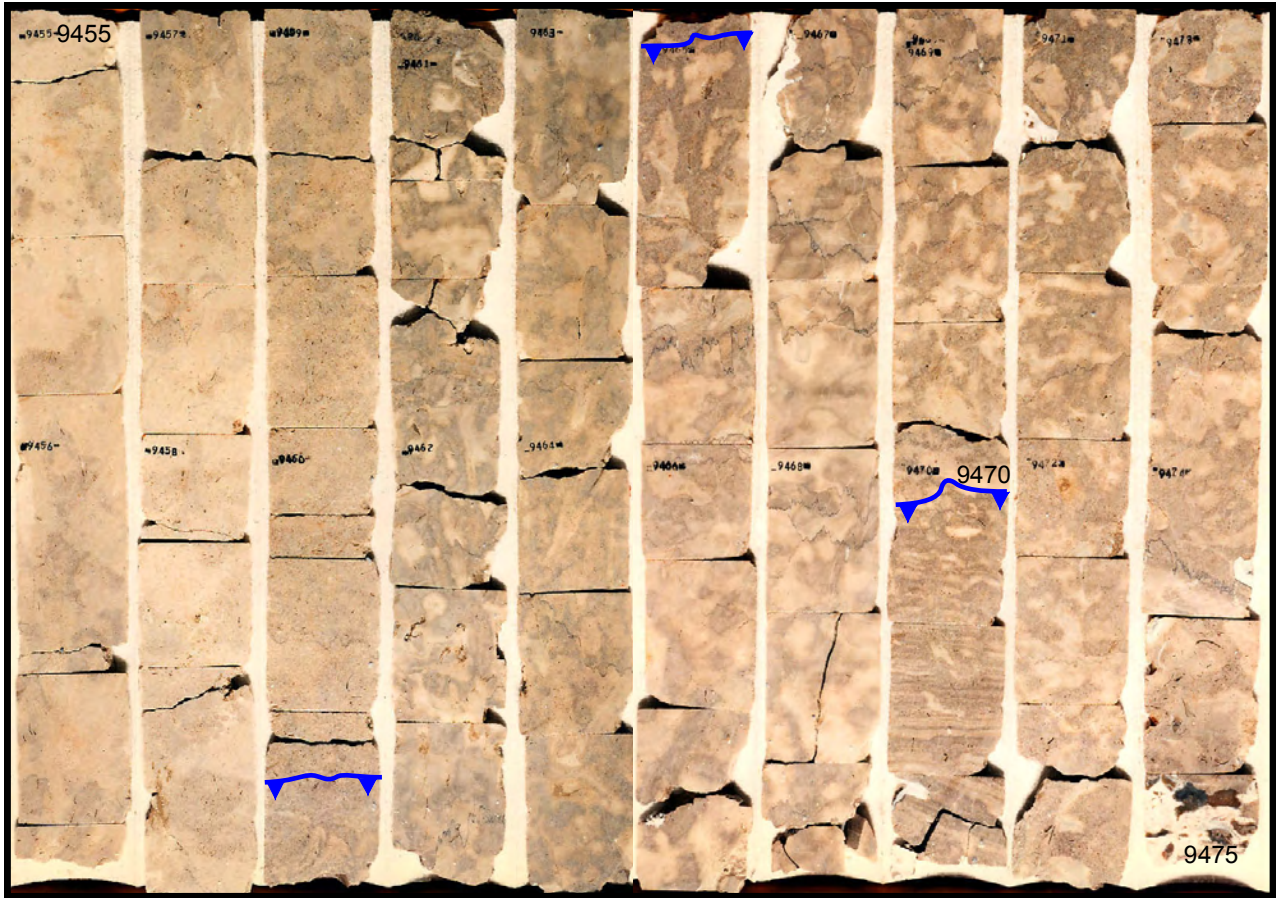


Figure 26. Core-slab photographs of X-1 well illustrating finer scale cycles within reservoir zone and Stage 2 exposure. Note that on the core description and wireline log diagram these facies are not highlighted; however porosity type and overall reservoir quality are affected by these changes. The surface in blue at about 9,470 ft denotes top of laminated facies (peritidal muds?). This facies was identified in another well within the field at the same stratigraphic position and similar wireline-log characteristics. This facies may indicate that the grainstone facies of figure 24 for well X-1 may be spilt into two cycles, which are separated by a peritidal facies. This type of observation, only possible using core data, has a bearing on lateral and vertical homogeneity of the reservoir interval.

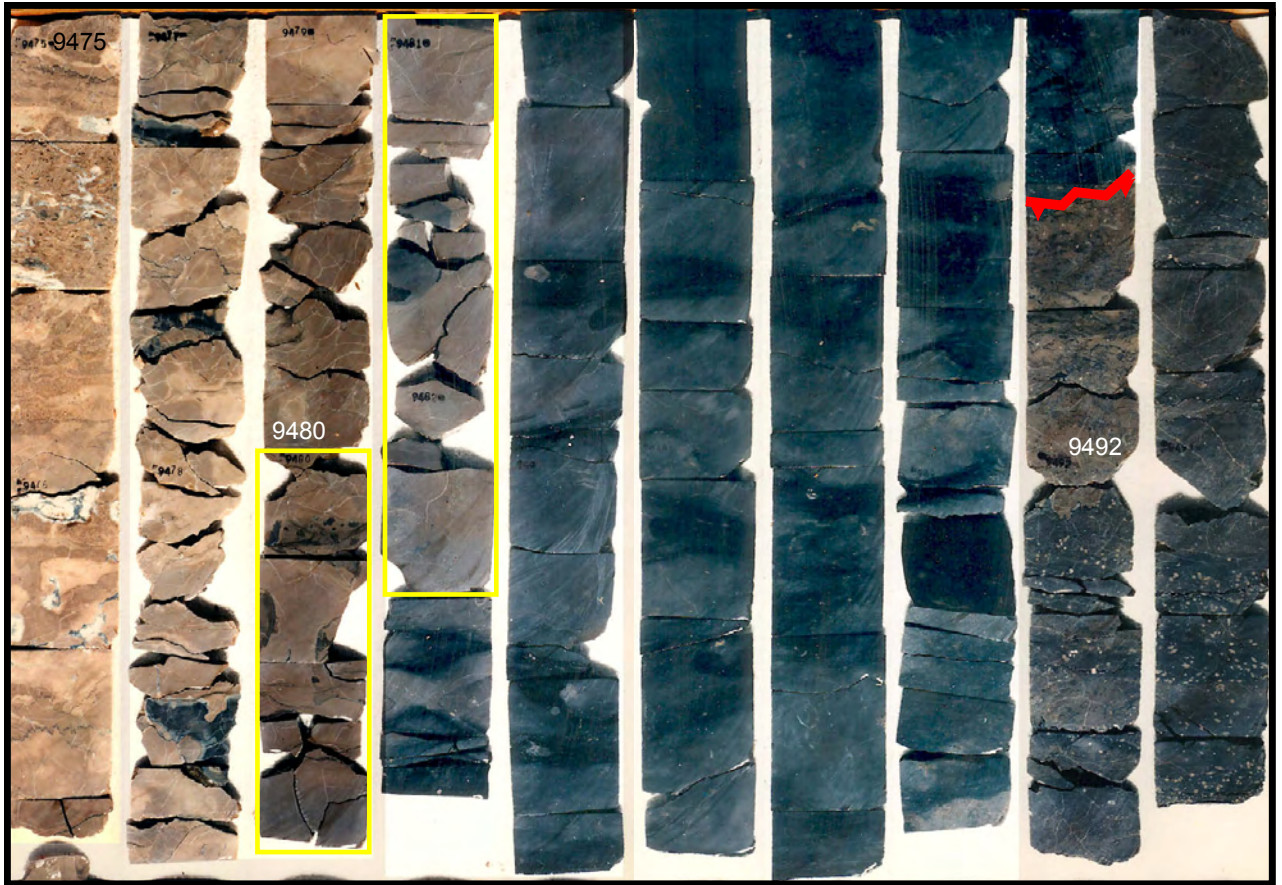
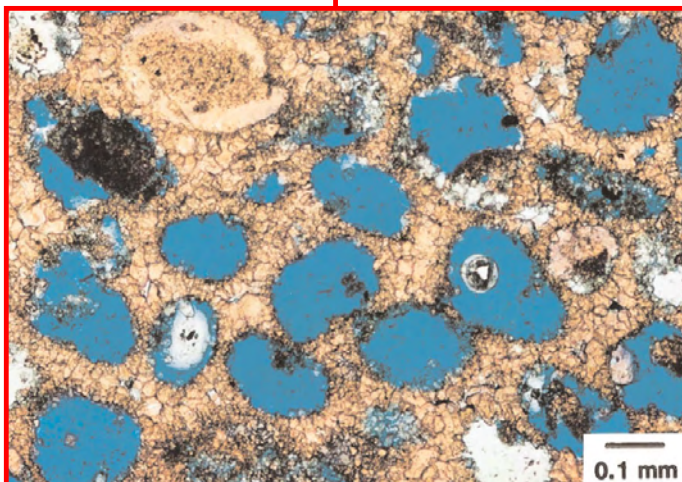
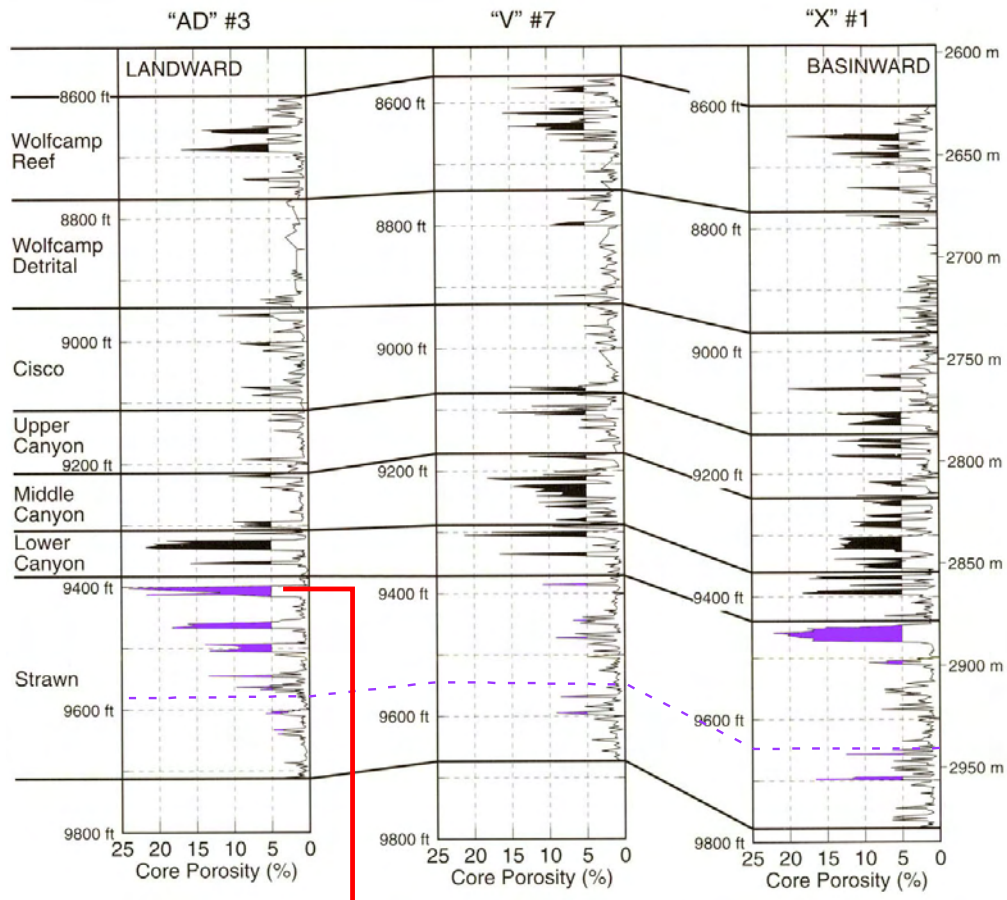


Figure 27. Illustration of lower facies and cycles in figure 24 from 9,475 to 9,495 ft. Yellow boxes outlining facies from 9,480 to 9,482 ft correspond to 2nd-highest total gamma-ray spike in the entire Strawn interval within well X-1. Note that the gamma-ray peak is almost entirely composed of uranium, and the peak does not correspond to the darkest or most “organic-rich” facies. The use of this peak as a possible MSF is highly suspect when viewed in association with core and further highlights that spectral gamma ray should be used for correlation, not total gamma ray.



Porosity= 21.5%
Permeability= 0.99mD

Calcite Cement

Figure 28. Subregional core-porosity correlation in southwest Andrews field area. Porous zones (above 4 percent) in Desmoinesian Strawn highlighted in purple. Thickest reservoir zone underlies sequence boundary and exposure event at top of Strawn. Dashed purple indicates lower, possibly regional, exposure surface under which reservoir intervals in other areas are located (for example, Seminole field, Gaines County, and Kelly-Snyder field, figure 20). Photomicrograph illustrates porosity and permeability associated with Stage 2 diagenesis of upper ooid grainstone package in Strawn (Saller and others, 1999a, b).

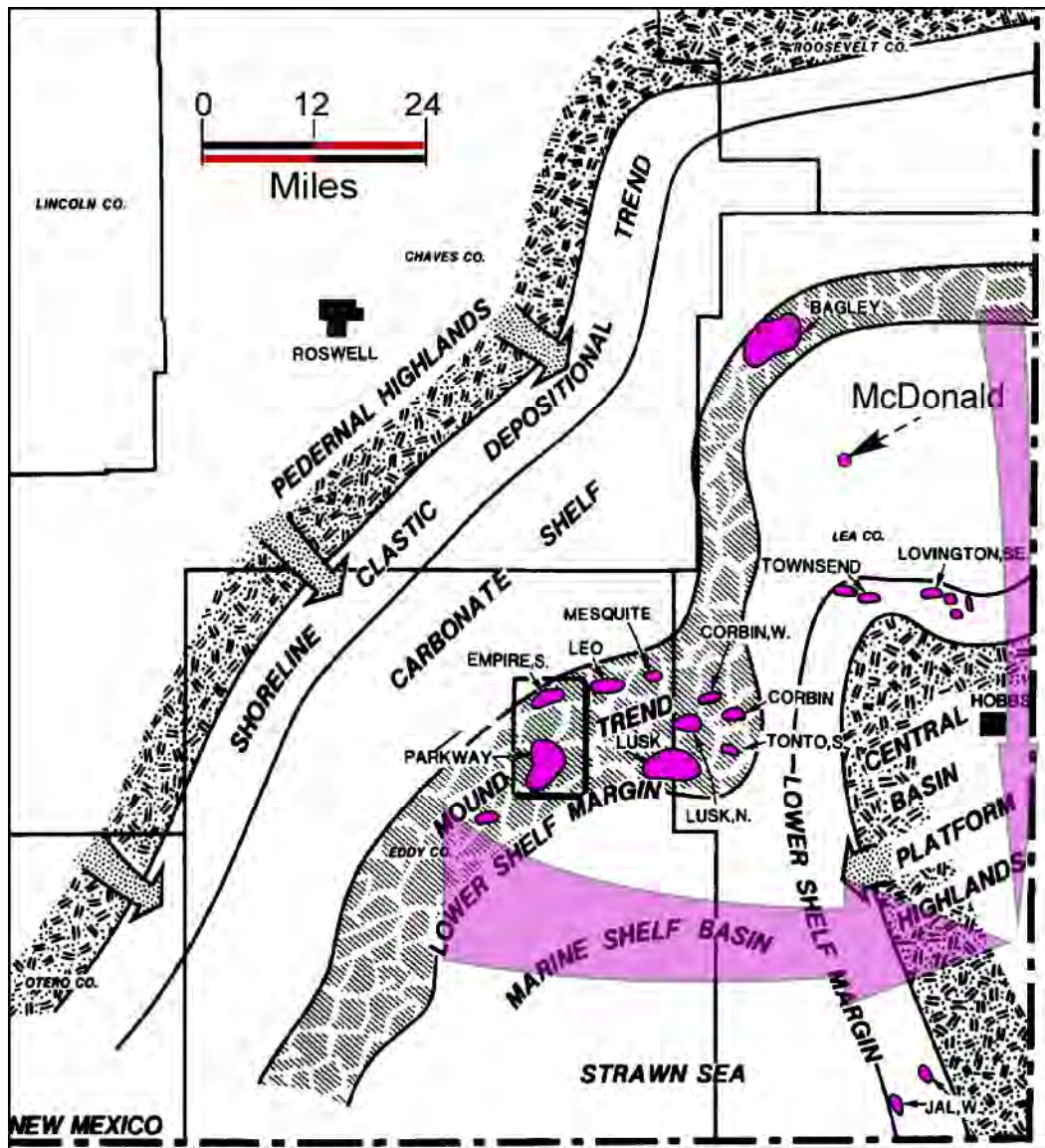


Figure 29. Regional interpretation by James (1985) of mound trend and lower-shelf margin of Strawn Formation during Desmoinesian. Trend likely composed of multiple carbonate bioherms and other facies that were deposited during several lowstand, transgressive, and highstand events. Resultant collage of targets extends much farther eastward onto the Central Basin Platform area, which was not emergent during the Desmoinesian (although it is depicted by James (1985) to be emergent).

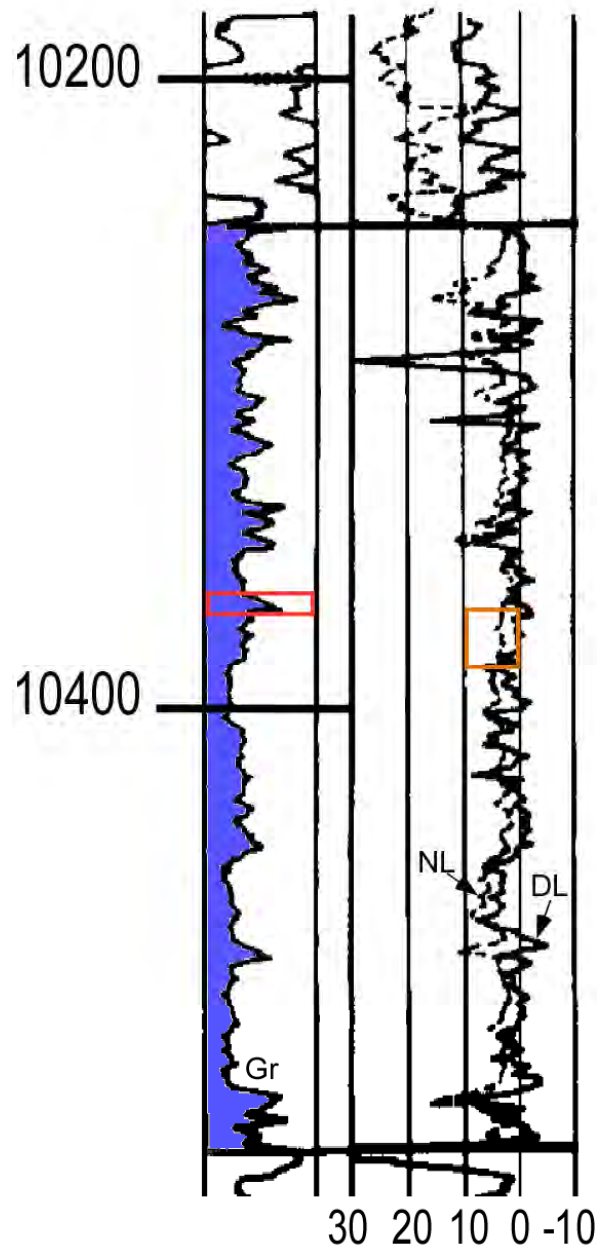


Figure 30. Characteristic gamma-ray and density-neutron log of Desmoinesian-age (Strawn Fm.) carbonates on Northwest Shelf. Southland Royalty Company 1 Parkway State well from Lea County, New Mexico. Strawn Formation Interval, indicated by blue, rests on Atokan sediments and is overlain by Missourian-age Canyon Formation. Gamma-ray spike outlined in red may be of regionally correlative significance. Overall wireline-log profile very similar throughout Permian Basin, with the exception of areas with expanded sections of the 'Upper Strawn.' Within fields such as Block 9 and Southwest Andrews, the highlighted gamma-ray peak contains a high thorium to uranium ratio interpreted as reflecting a possible exposure event below the peak. Area on porosity logs outlined in orange is interval of increased porosity, usually associated with alteration zone below exposure.

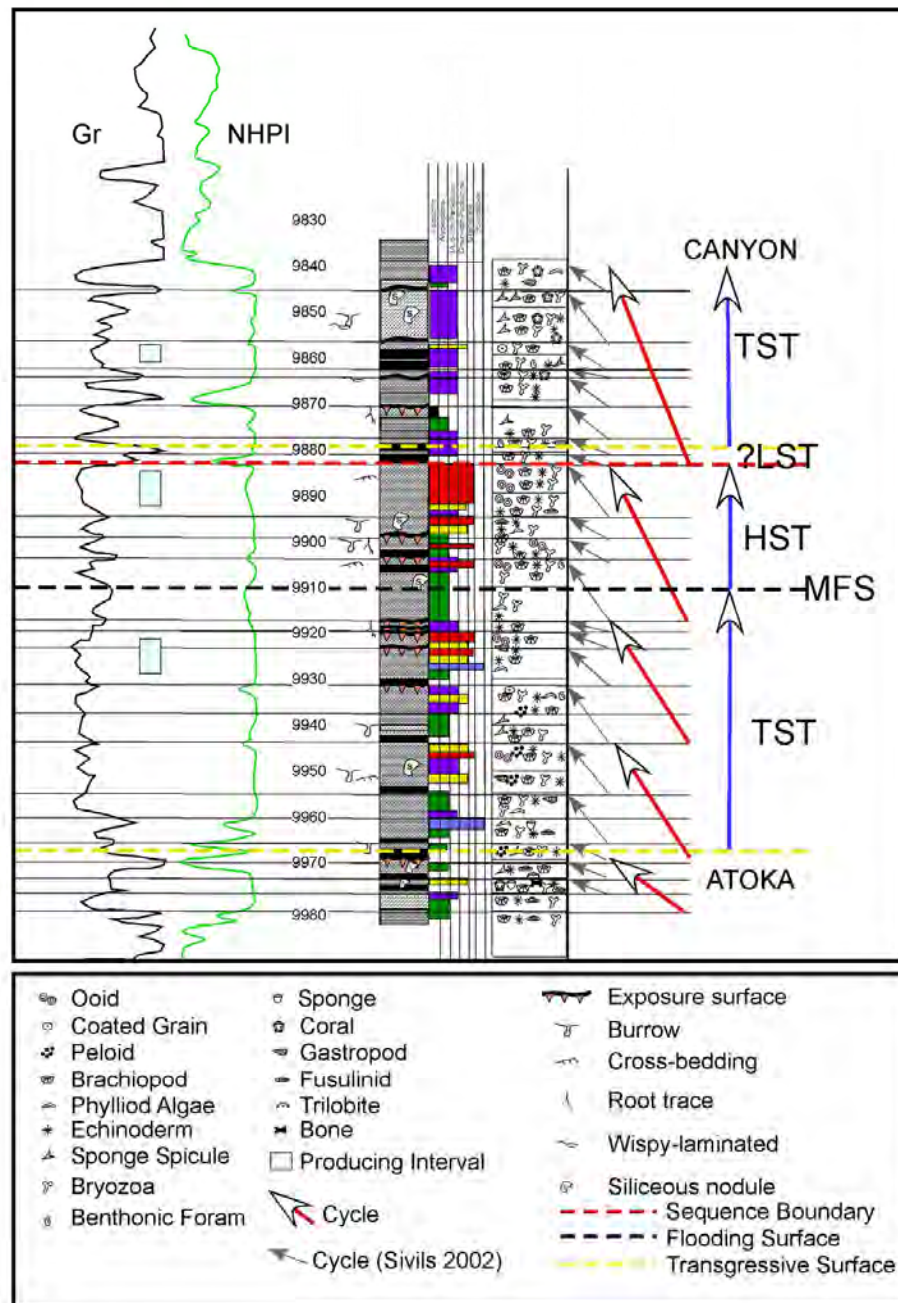


Figure 31. Detailed wireline and sedimentological log Texaco Glasscock "X" Fee #4, St. Lawrence field, Glasscock County. Modified from Sivils (2002). Red arrows on diagram indicate cycles/packages that are thought to be of possible regional scale. Gray arrows indicate 22 upward-shallowing cycles documented by Sivils (2002) for this interval. Sequence stratigraphic framework has been added to original diagram.

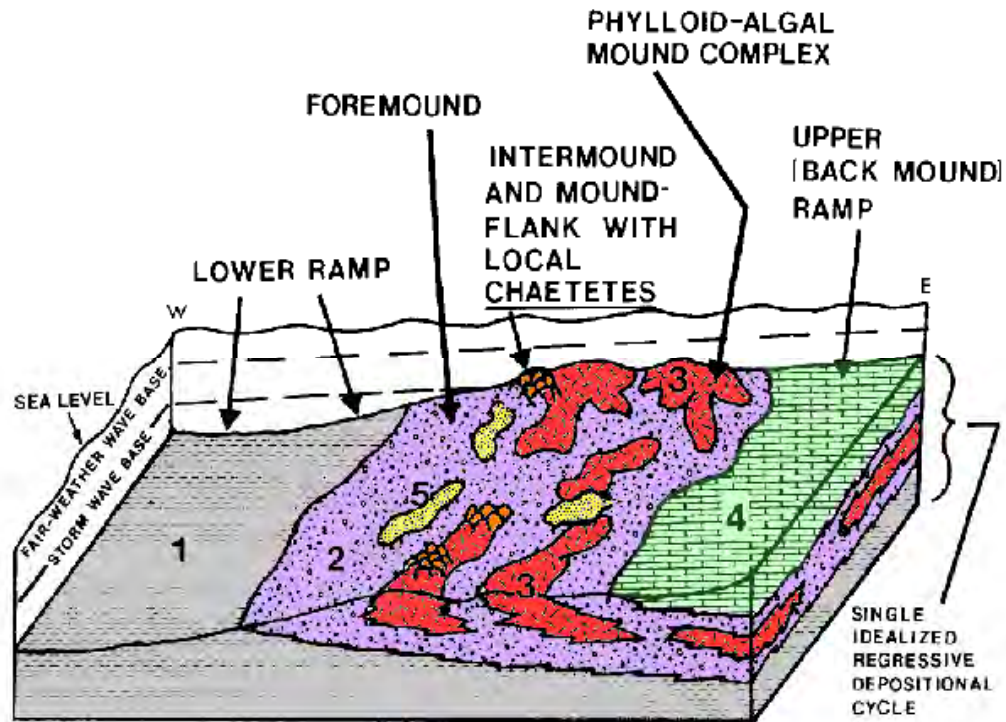


Figure 32. Idealized schematic representation of Goen limestone (patch reef) of Concho County, Eastern Shelf. After Marquis and Laury (1989). Facies tracts labeled 1 through 5 comprise (1) lower ramp (spiculitic mudstones and shales), (2) ramp center, foraminiferal wackestones with (3) localized phylloid-algal and Chaetetes bioherms, (4) upper ramp, bryozoan-coral wackestones, and (5) very fine calcareous sandstone assemblages. Overall Marquis and Laury (1989) thought that deposition represented regression. However, a more regional interpretation indicates that deposition occurred largely during transgression, with minor highstand development.

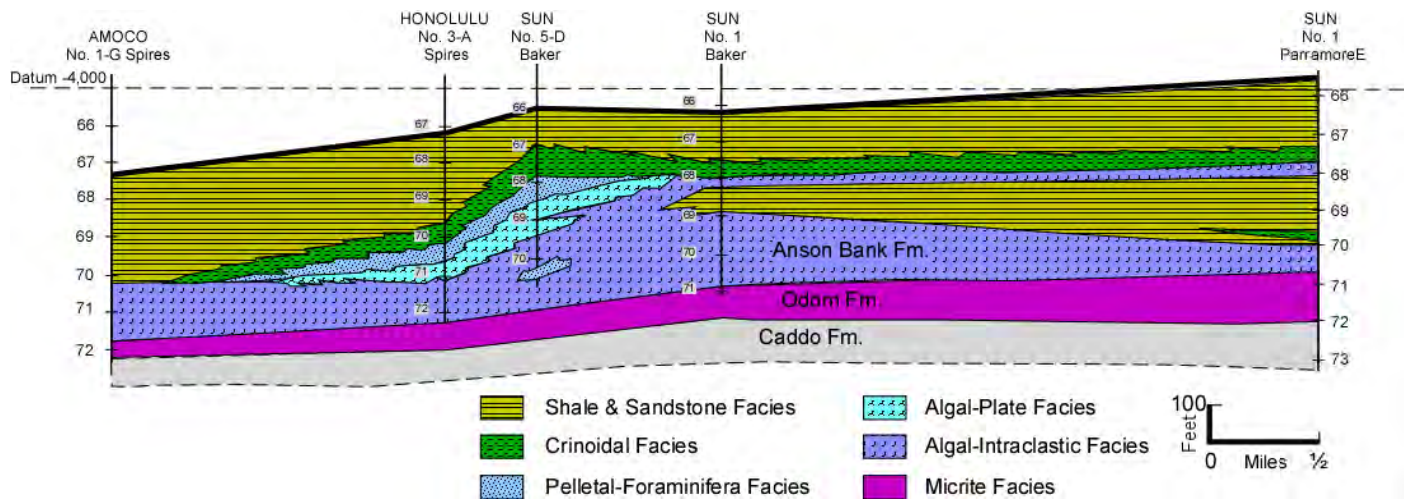


Figure 33. Depositional architecture and facies cross section of Desmoinesian Nena Lucia field, Nolan County. After Mazzullo, 1989). This shelf-margin to rimmed-shelf architecture is prominent on Eastern Shelf from mid-Desmoinesian onward. On diagram, total thickness of the Caddo Formation unknown.

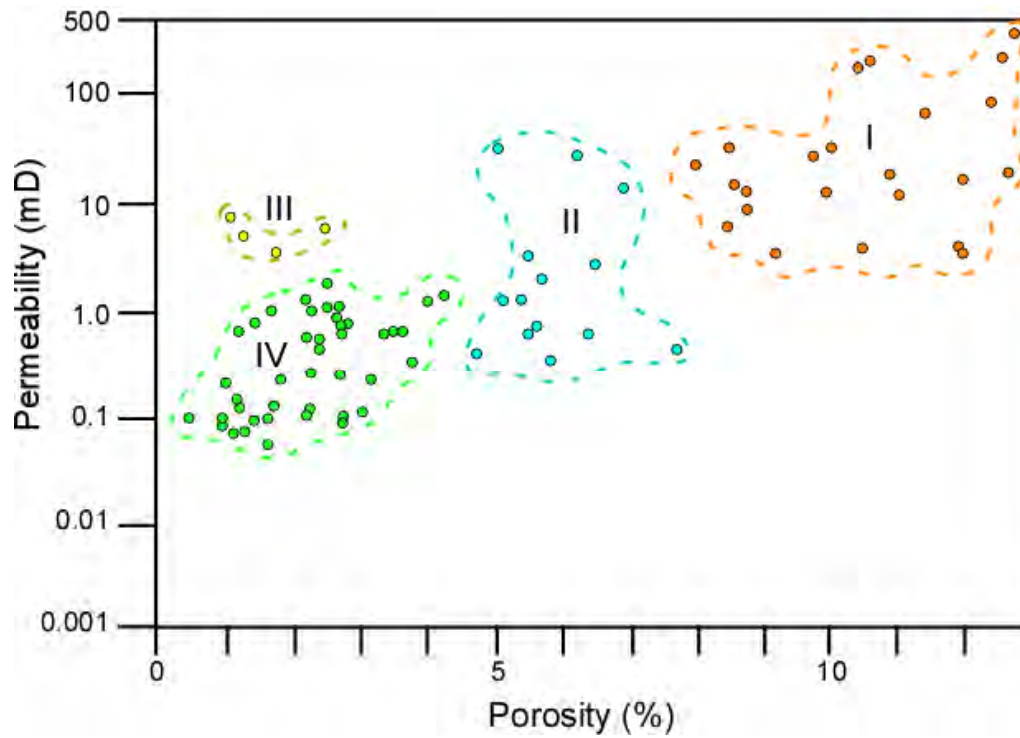


Figure 34. Porosity permeability cross plot for Goen Limestone reservoir. After Marquis and Laury (1989). Type I equals solution-enlarged, algal, moldic, vug, and channel open pores. Type II contains same pore population as Type I but is slightly occluded by later cement. Type III comprises open fracture and channel pores. Type IV contains Type I population of pore types but is dominated by open microporosity.

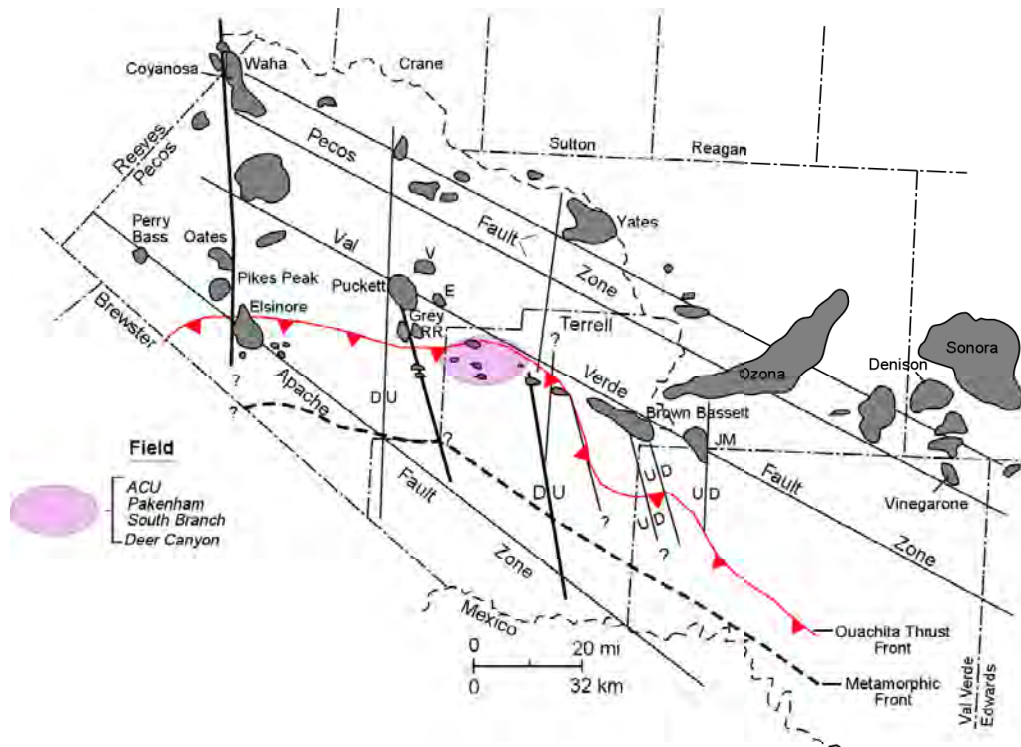


Figure 35. Regional map of the north edge of Val Verde Basin. After Montgomery (1996). Fields highlighted in gray. Most studied region containing Des Moinesian Strawn Formation reservoirs outlined in purple. Region contains ACU, Pakenham, South Branch, and Deer Canyon fields. North edge of Val Verde Basin indicated in red by Ouachita Thrust Front (alternatively called Foreland Thrust).

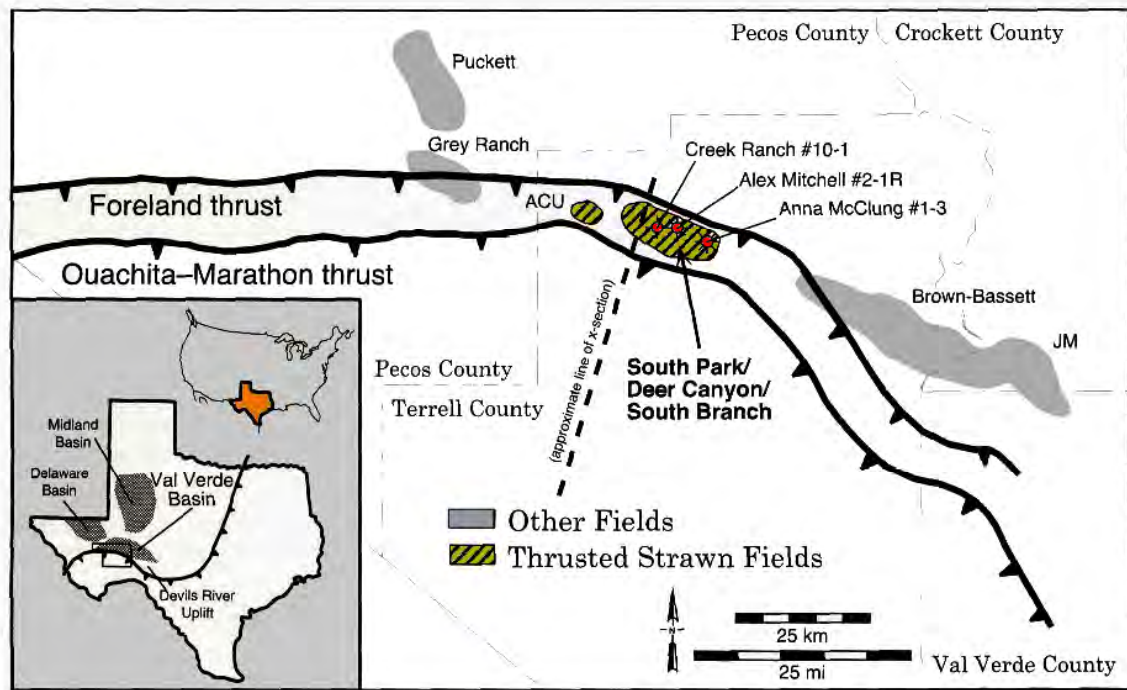


Figure 36. Subregional map illustrating position of thrust Strawn reservoirs in Val Verde Basin (Terrell County) After Newell and others (2003). Foreland thrust equates to Ouachita Thrust Front in figure 35.

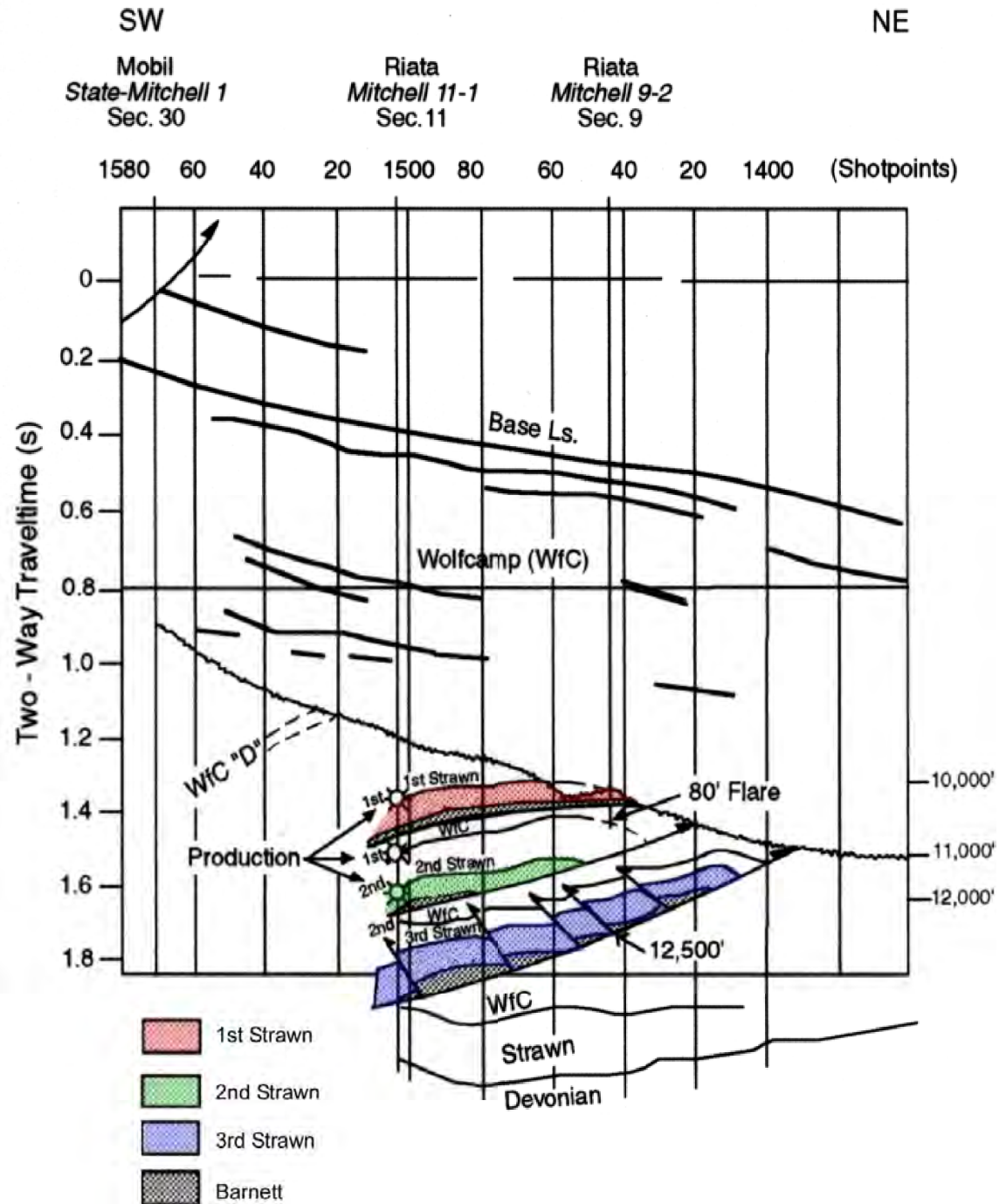


Figure 37. Geologic interpretation of SW-NE seismic line through Pakenham field. After Montgomery (1996). See figure 41 for comparison with uninterpreted seismic line from the same area. Multiple thrust Strawn Formation intervals (for example, 1st-3rd Strawn), as well as a thick allochthonous Strawn interval, are below the basal thrust. Structural complexity within thrust Strawn interval increases downward (fig. 43).

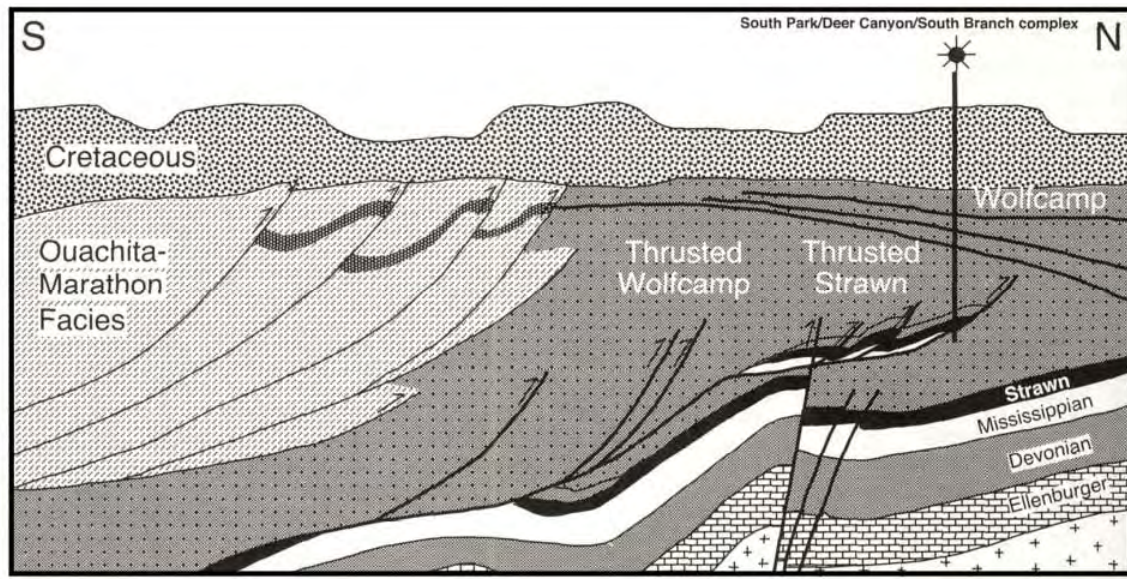


Figure 38. Schematic south-north diagram of Val Verde Basin thrust succession. After Newell and others (2003). There are two main thrust belts. The first contains thrust Mississippian, Strawn Formation, and Wolfcampian sediments and is termed the Foreland Thrust (fig. 36). The second is younger and contains Ouachita-Marathon siliciclastic facies and is termed the Ouachita Marathon Thrust.

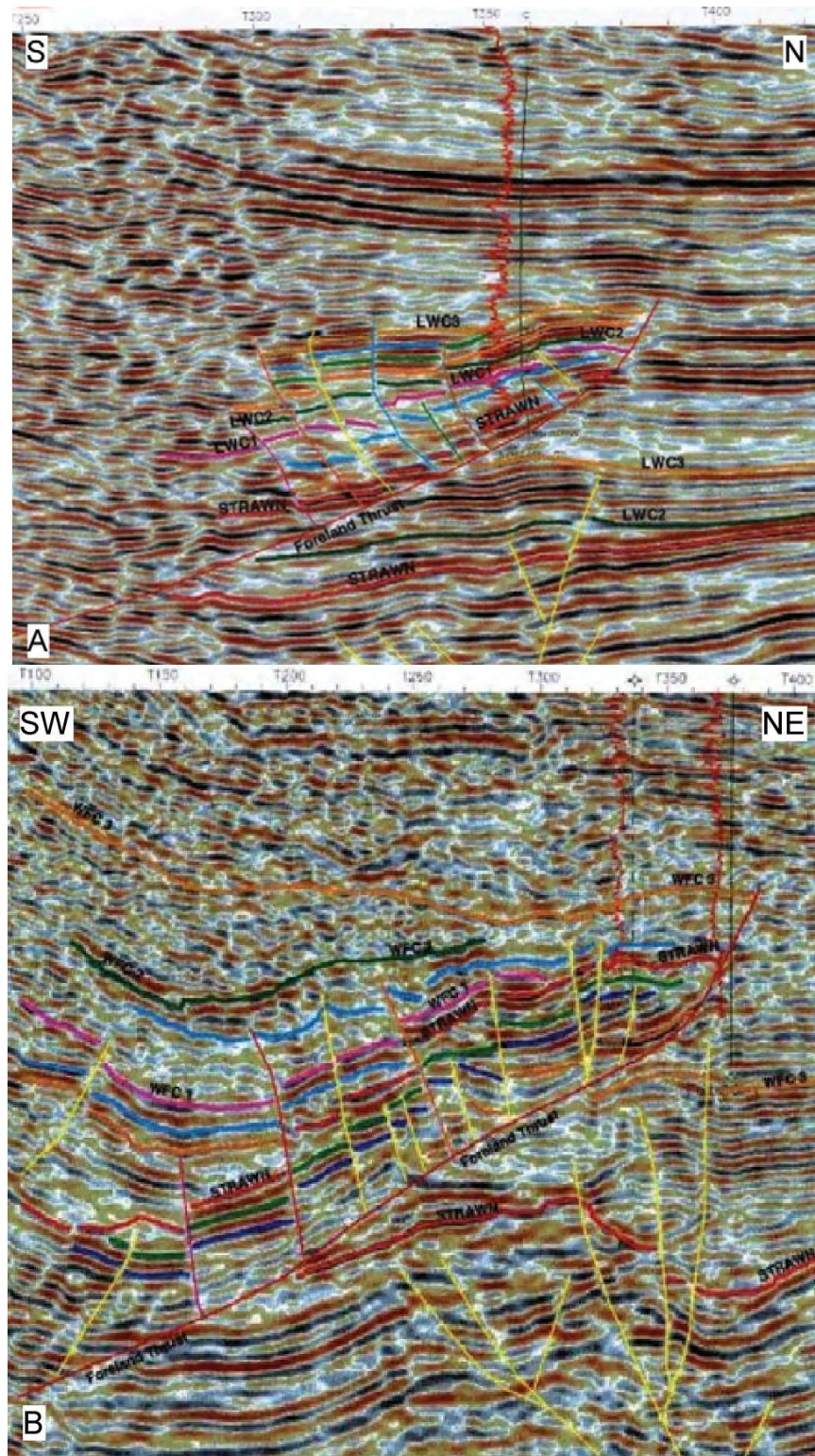


Figure 39. Interpreted (A) N-S and (B) NE-SW seismic lines through South Park area. After Khan and others (2002). Note structural variability between the two seismic lines. The uninterpreted seismic line in figure 41 would lie along strike between lines A and B above. Interpretations above indicate a single thrust interval of Strawn Formation.

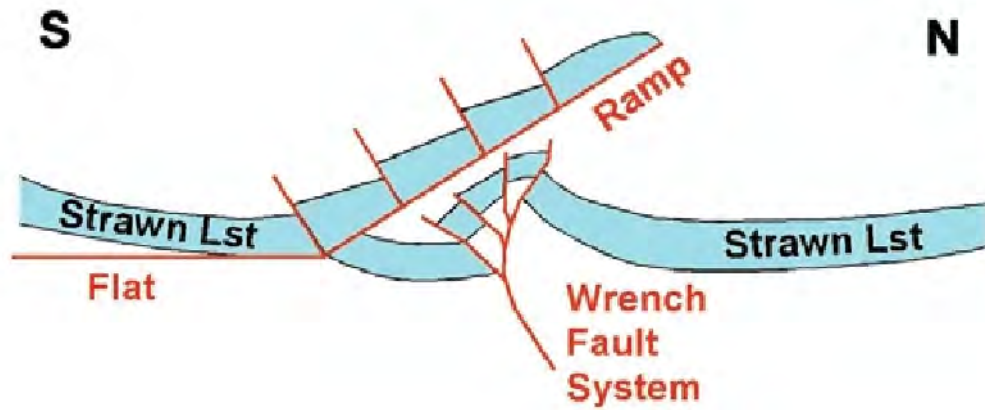


Figure 40. Structural interpretation of Strawn thrust reservoirs in Val Verde Basin. After Khan and others (2002). Model interprets that Strawn interval comprises single overthrust ramp, divided by back thrusts overlying wrench faulted pop-up structures. Model contrasts with those presented by Montgomery (1996) and Newell and others (2003) (figs. 37 and 38).

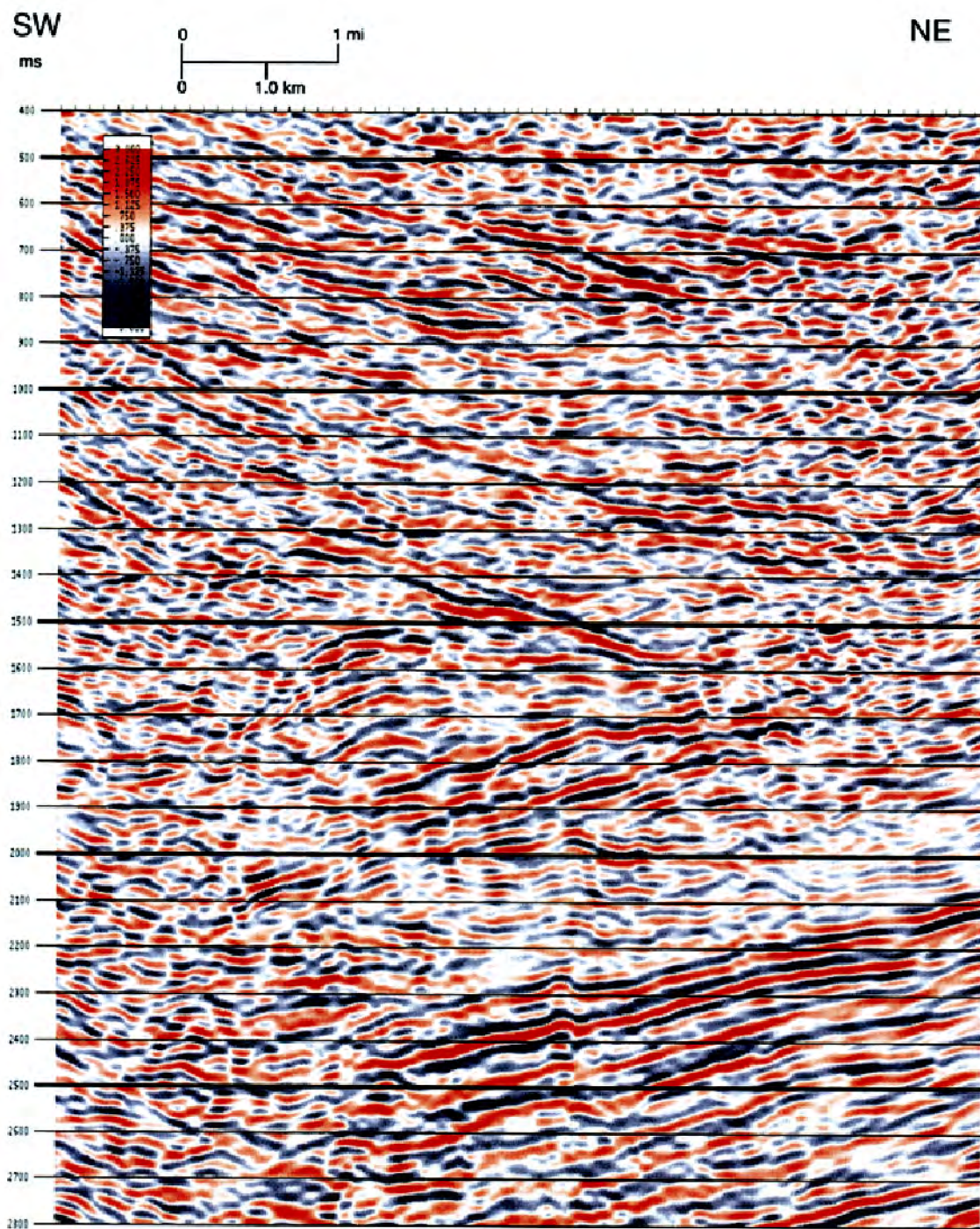


Figure 41. Uninterpreted seismic line trending SW-NE through Pakenham field (Terrell County). Seismic line illustrates structural complexity present in this part of Val Verde Basin. Figure should be compared with figure 37 for geologic and structural interpretation of this area. Figures 39 and 40 illustrate alternative, seismic-based, geologic and structural interpretations of the area.

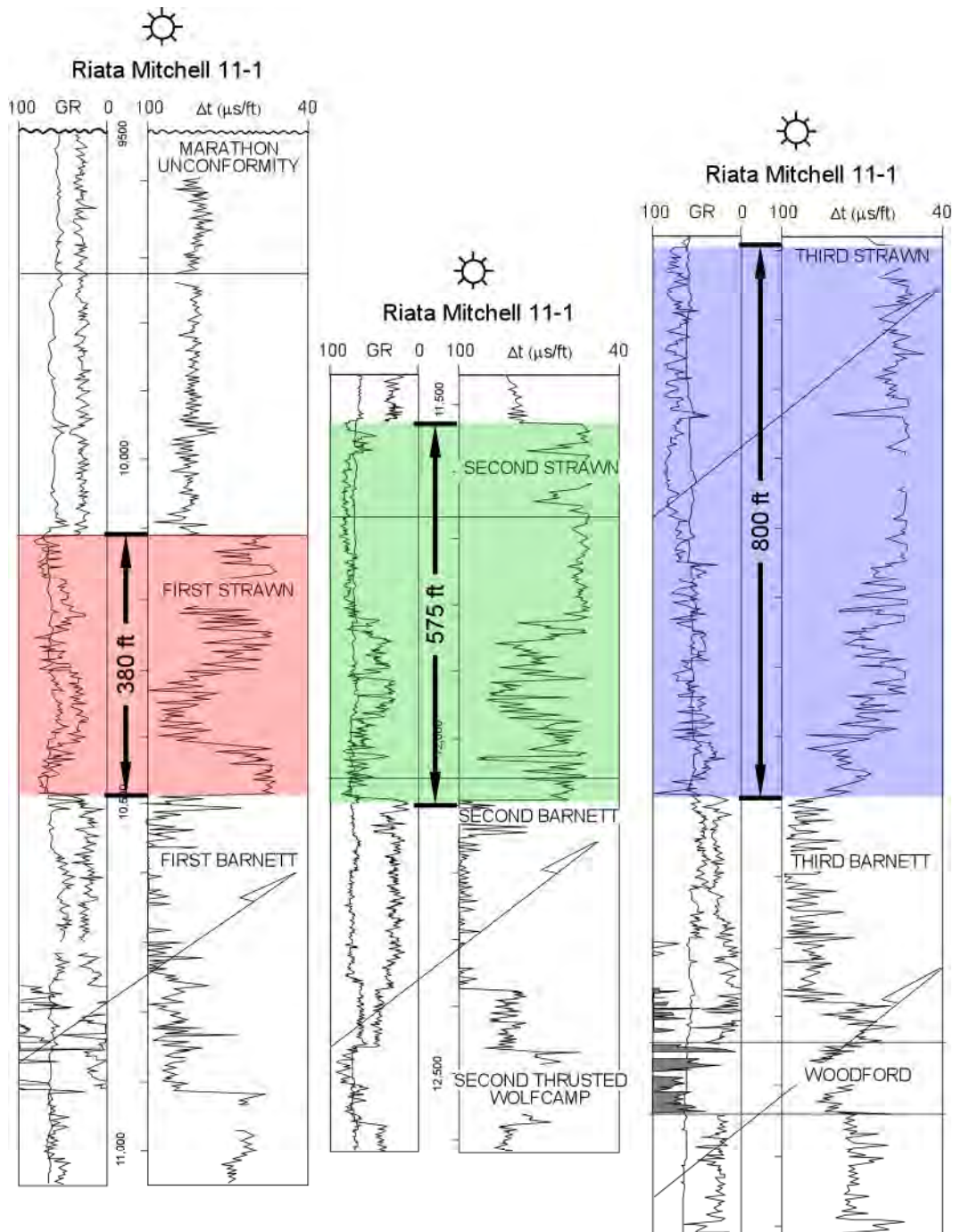


Figure 42. Wireline-log character of Woodford, Barnett, and Strawn Formations in Riata Mitchell 11-1 well (Pakenham field-Tyrell County). Each Strawn interval highlighted by different color (red, green, or blue). Structurally highest Strawn interval the First Strawn. Note that thickness of Strawn increases between first, second, and third Strawn intervals, indicating change in facies type (for example, possible outer-ramp position for First Strawn and inner ramp to mound core in second and third Strawn intervals). Judging from wireline-log character, lower part of all three Strawn intervals similar. Color coding of intervals corresponds to structural interpretations presented in figure 43.

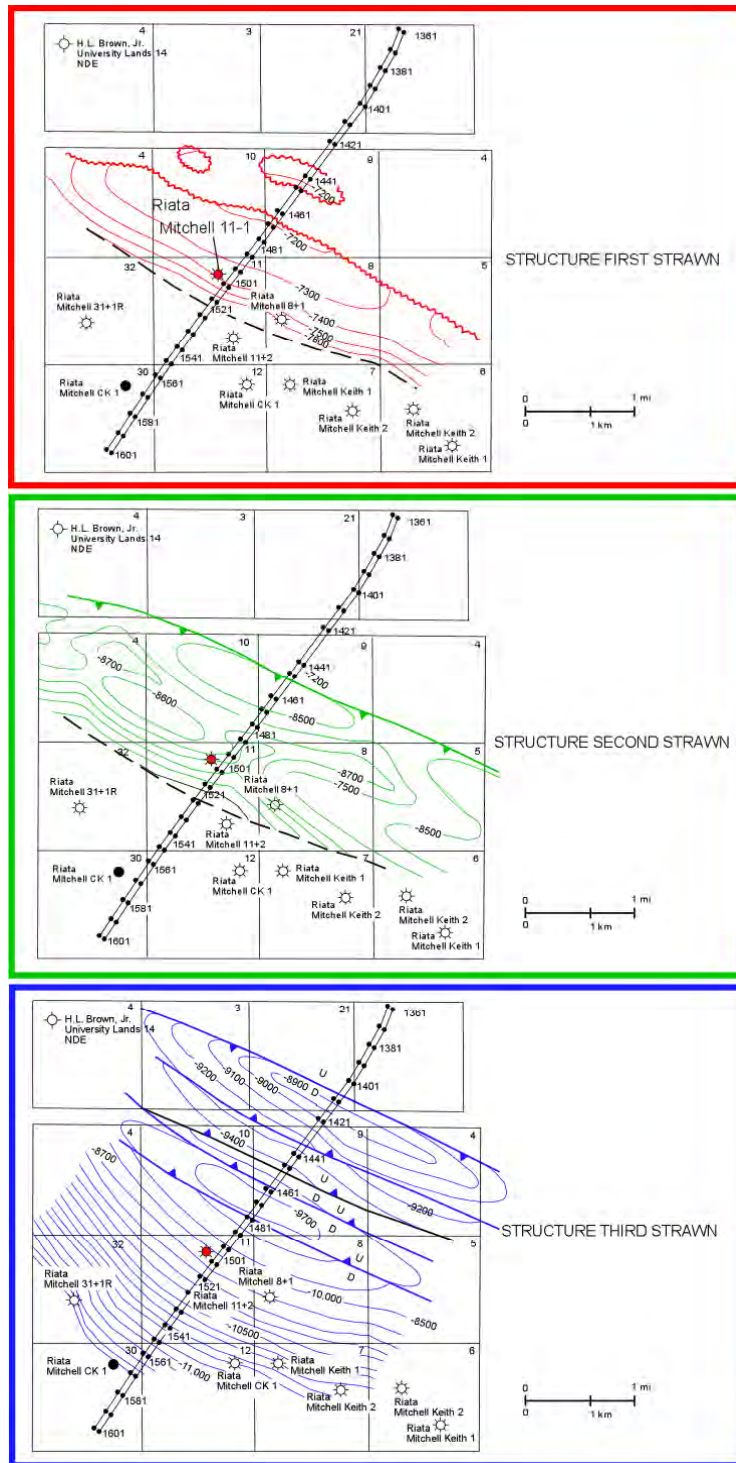


Figure 43. Structural interpretations of Pakenham field (Terrell County) at three Strawn intervals identified in Riata Mitchell 11-1 well (in red). Structural complexity increases with depth (“Third Strawn” most complex). Mounding and structural grain in Second Strawn may be partly depositional in origin. Uppermost Strawn interval has relatively simple closure, whereas lowermost interval has multiple closures in at least five back-thrust structures.

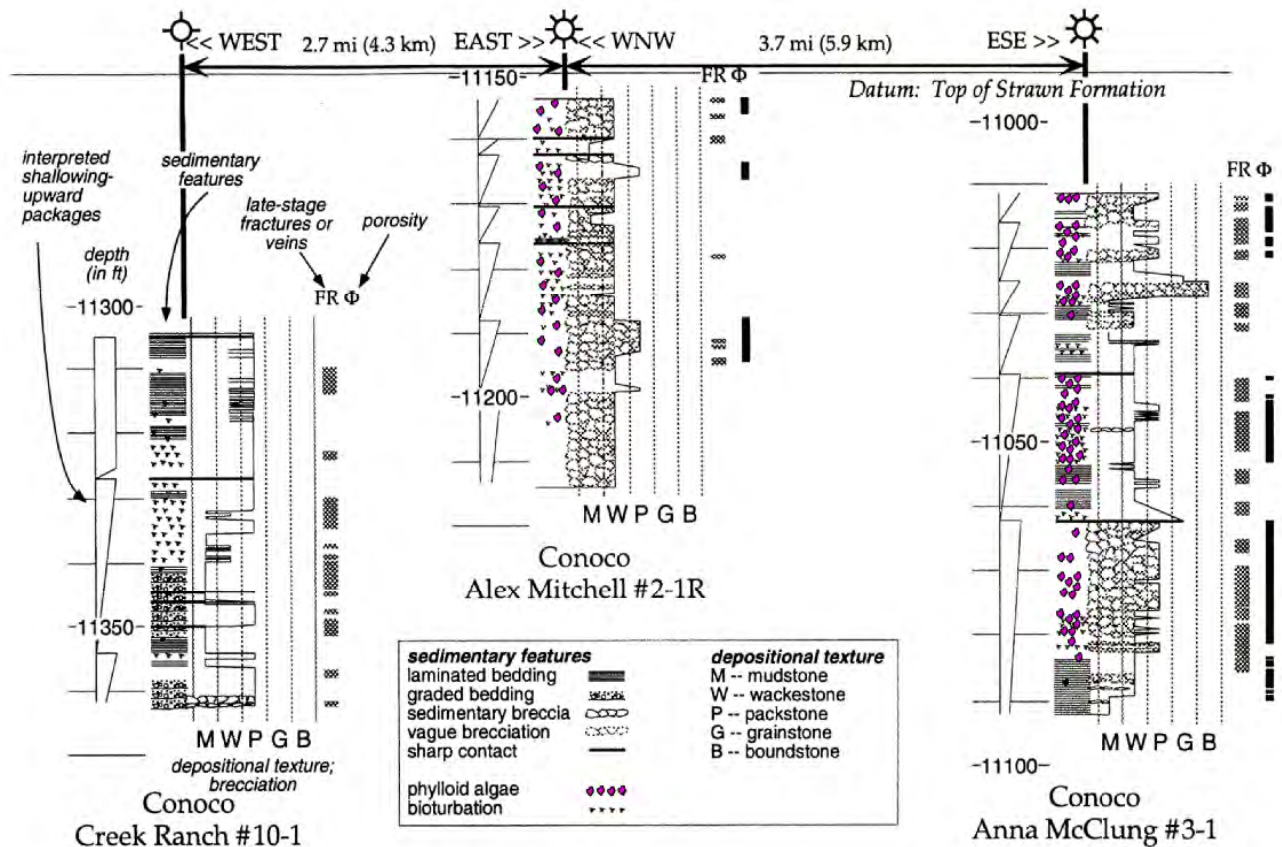


Figure 44. Lithologic description of three wells from South Park-Deer Canyon-South Branch complex of fields (Terrell County) (fig. 36). Creek Ranch #10-1 core dominated by graded packstone to mudstone and very fine grained, laminated packstone to wackestone facies. Both Alex Mitchell #2-1R and Anna McClung #3-1 intervals have coarser sediments containing large proportions of phylloid algae.

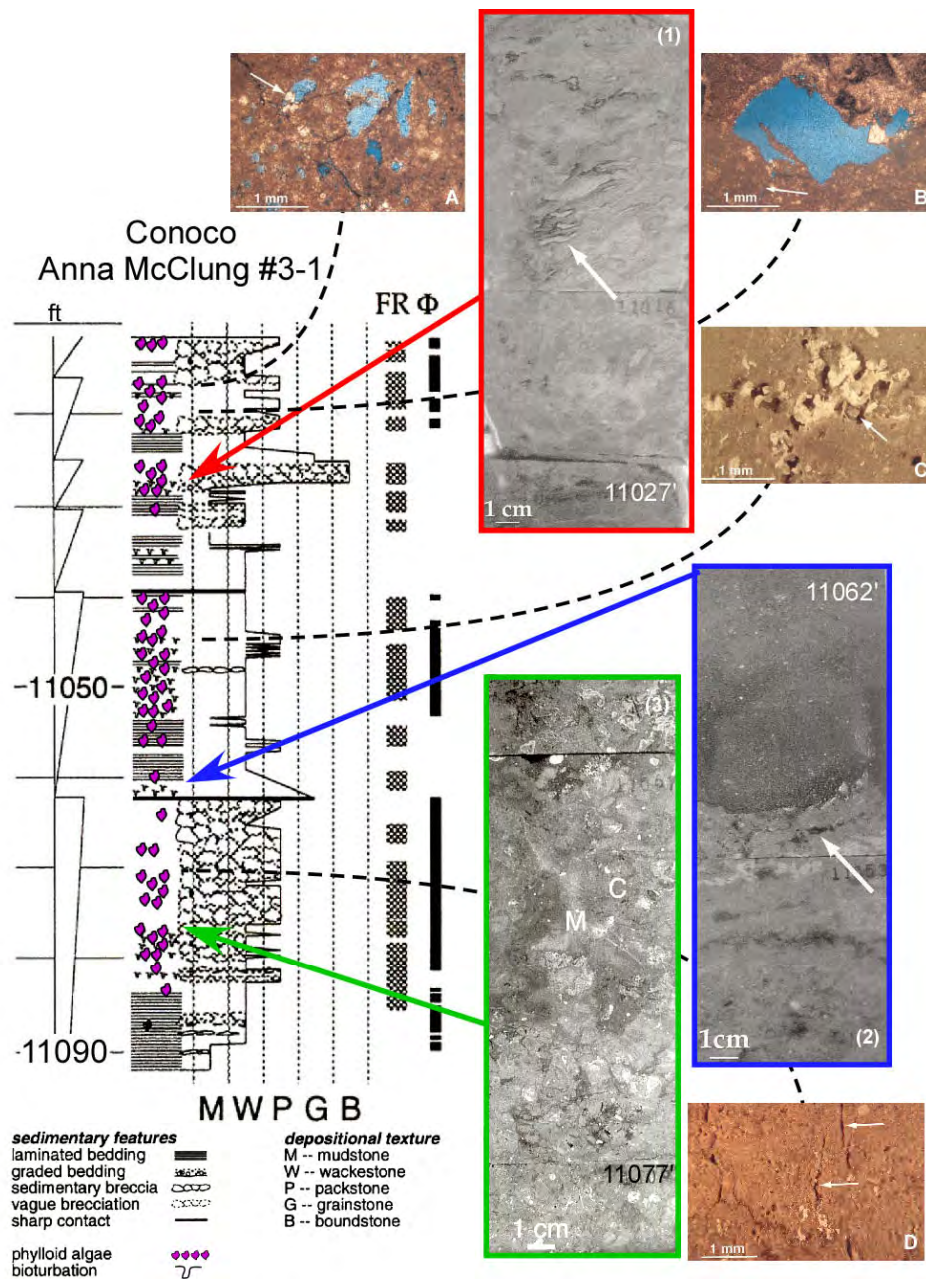


Figure 45. Detailed lithologic description of Anna McClung #3-1 core, with accompanying core photographs and photomicrographs. (1) Core photo of phylloid-algal boundstone (isopachous cement rim on algal plate denoted by arrow). (2) Core photo of cycle contact between underlying packstone facies and overlying very fine grainstone of next cycle (arrow denotes erosion and infilling into packstone). (3) Core photo of “pseudo-breccia” C-clast, M-matrix. (A) Photomicrograph of moldic porosity with dolomite crystal (white arrow) partly filling mold. (B) Photomicrograph of vug porosity with arrow denoting small dissolution-enlarged fracture extending away from vug. (C) Photomicrograph of interconnected solution-enlarged molds occluded by saddle dolomite (arrow). (D) Core photo illustrating solution-enlarged tension gashes (arrow) extending upward from a stylolite. Note that depth on core description is wireline-log depth, and photos of core slabs have been shifted accordingly.

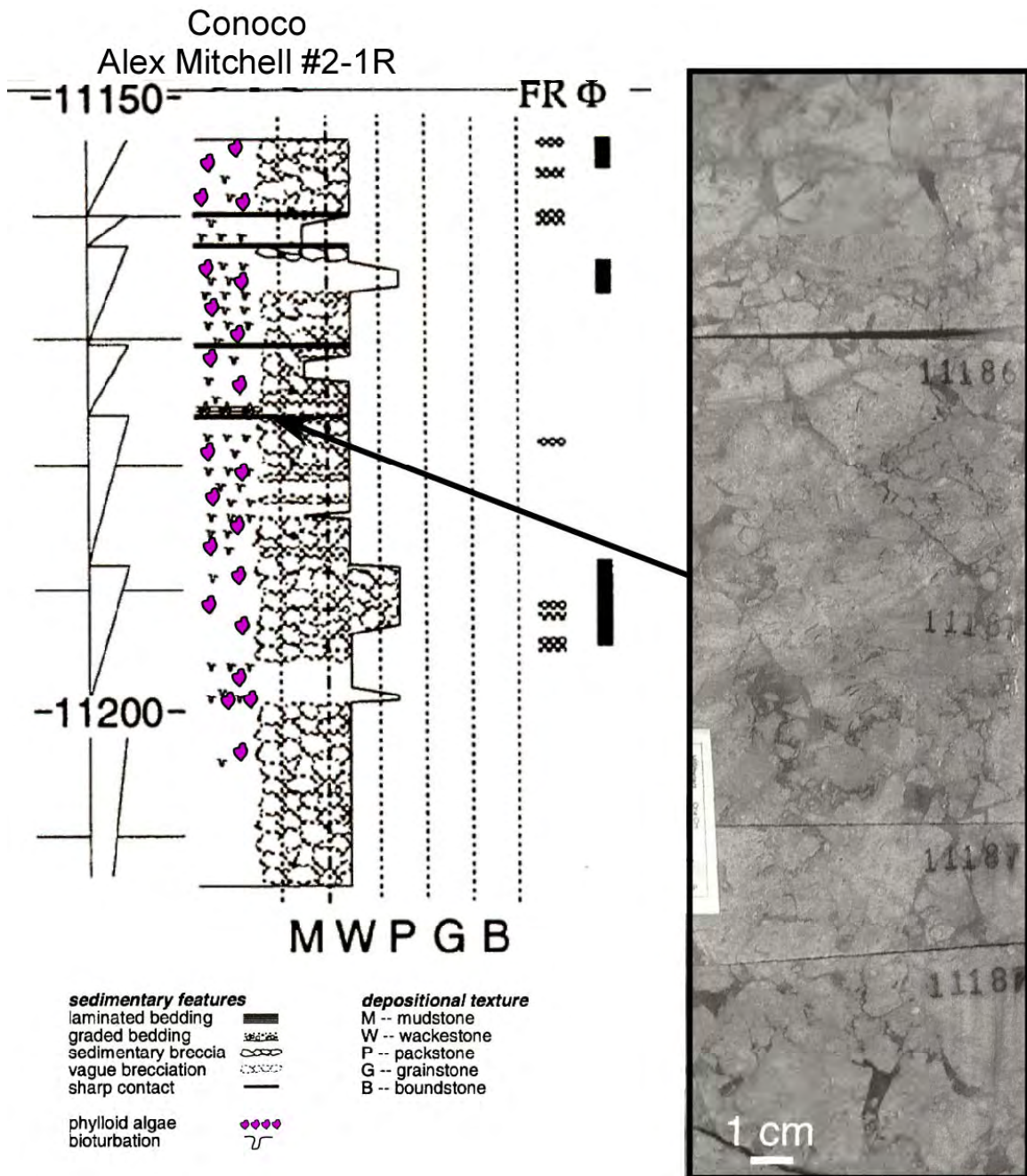
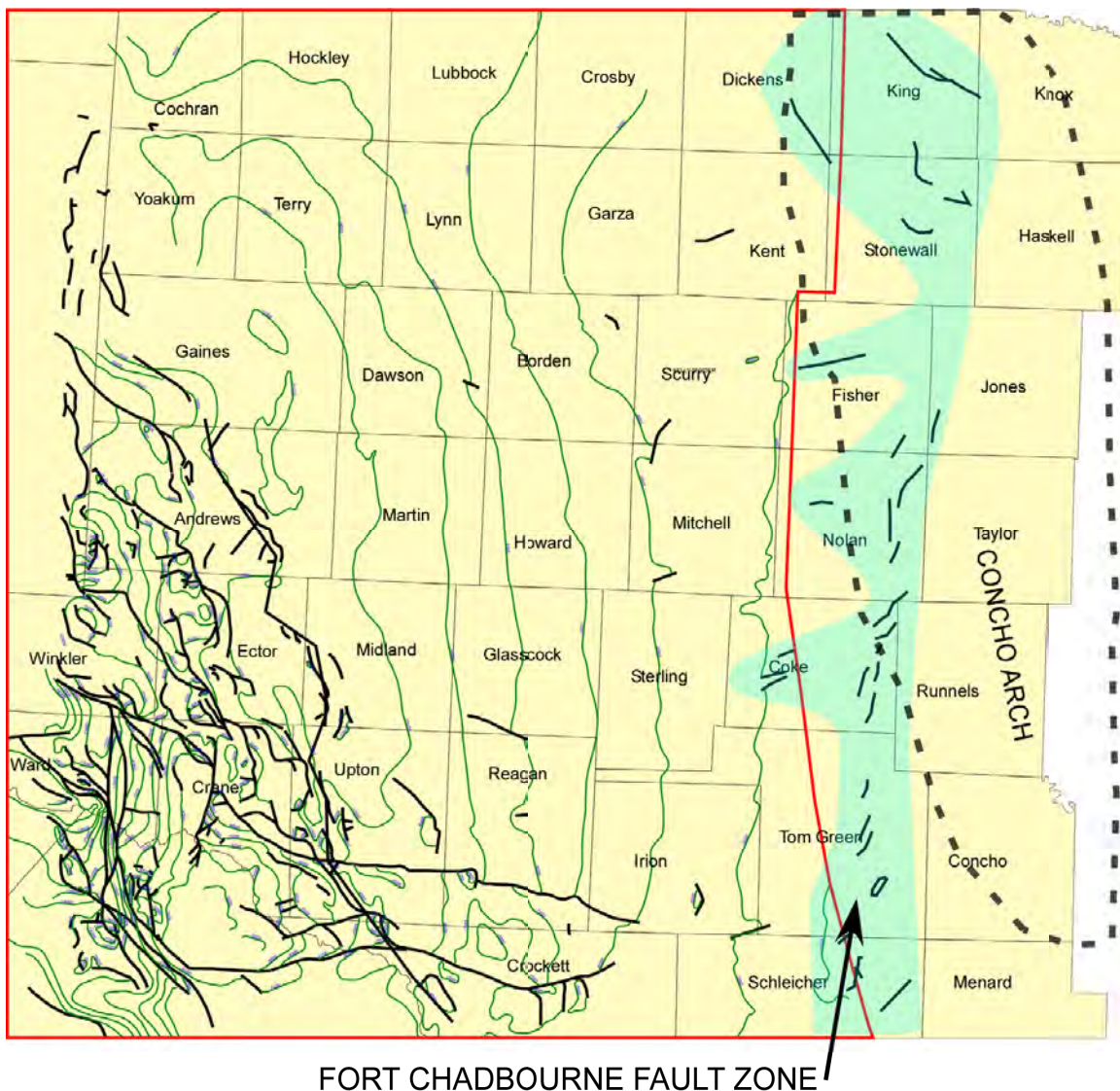


Figure 46. Detailed lithologic description of Alex Mitchell #2-1R core, with accompanying core-slab photograph illustrating brecciated wackestone composed of fitted clasts. Note that depth on core description is wireline-log depth and core-slab photo has been shifted accordingly.



FORT CHADBOURNE FAULT ZONE

Figure 47. Regional structure map of Midland Basin. Green contour lines from top Ellenburger structure. Faults in black derived from Ewing (1983). Fort Chadbourne Fault Zone outlined in blue. Trend of Concho Arch indicated by dashed polygon. Strong correspondence between mid- to late Desmoinesian shelf margin and fault zone.

DEPOSITIONAL HISTORY OF THE MISSOURIAN AND VIRGILIAN SUCCESSION (UPPER PENNSYLVANIAN) IN THE PERMIAN BASIN

Wayne Wright

Bureau of Economic Geology
Jackson School of Geosciences
The University of Texas at Austin
Austin, Texas

ABSTRACT

Missourian and Virgilian sediment distribution reflects a transgressive phase, followed by a more regressive phase of deposition. Because of increased subsidence in the Midland and Delaware Basins, the Canyon and Cisco depositional environments were generally fixed in geographic position. The 2nd-order transgression culminated in latest Missourian to early Virgilian, and mid- to late Virgilian sediments were deposited early in the succeeding 2nd-order regression.

Earliest Missourian deposition is reflected in continued aggradational carbonate growth on the Northeast Shelf, Central Basin Platform (CBP), Horseshoe Platform, and Eastern Shelf. Pronounced aggradational carbonate growth on the margins of the Midland Basin was a result of continued downwarping and subsidence of the basin, which began in the Desmoinesian. In general, deposition of coarse, siliciclastic sediments during the Missourian was restricted to areas east of the Fort Chadbourne high. Fine-grained siliciclastics were deposited in the Delaware, Val Verde, and Midland Basins. Owing to increased subsidence in all basins and an overall transgressive eustatic environment, most basin centers received only small volumes of sediment during the Missourian (starved

basins). High-amplitude, high-frequency, eustatic 3rd- and higher order fluctuations strongly influenced carbonate and siliciclastic facies distribution, composition, and deposition during the Missourian. Early Virgilian sedimentation mimicked patterns established during the Missourian, whereas the late Virgilian was a time of low sediment accumulation and drowning of previous areas of net sedimentation. Most late Virgilian sediments are shales.

Missourian carbonates, which compose the Canyon Group, were deposited over preexisting highs, shelf margins, and platforms around basin margins (for example, Delaware, Midland, and Val Verde) and on the CBP. Phylloid-algal-dominated bioherms and higher-energy facies (ooid grainstones) affected by exposure-related meteoric diagenesis compose the best carbonate reservoirs.

Early to middle Virgilian carbonates (composing the Cisco Group) were generally deposited in the same areas as those of Missourian age; however, the aerial extent of carbonate deposition was less, indicating an overall flooding of areas suitable for carbonate deposition. The late Virgilian (including the Bursam stage) was a time of sea-level fall at the 2nd- and 3rd- order scale, with progradation of carbonates occurring in isolated areas. Decreased accommodation during the mid- to late Virgilian within the Midland Basin resulted in thinner facies stacking patterns and greater proportions of shales thought to be fluvial or deltaic.

New paleographic reconstructions of the Missourian and Virgilian of the Permian Basin are presented (figs. 1, 2). Figure 1 is a reconstruction of a mid- to late Missourian time (mid- to late Canyon/Palo Pinto to Home Creek), whereas figure 2 is a mid- to late

Virgilian reconstruction during approximately the mid- to late Cisco/Breckenridge depositional episode.

Missourian alluvial and deltaic siliciclastics are restricted to the periphery of the Permian Basin (for example, east of the Eastern Shelf margin and within the eastern periphery of the Val Verde Basin). Marine siliciclastic shales are prevalent in the centers of the Midland and Delaware Basins; however, their ages are poorly defined. Widespread platform-carbonate deposition on the CBP, Midland and Delaware Basin margins, and Eastern Shelf occurred during the Missourian. Rapid downwarping and subsidence led to an increased area of deeper water within Midland and Delaware Basins, and carbonates around the margins responded to the increased accommodation by aggrading and backstepping.

Structural development of the Val Verde Basin in Terrell County intensified during the Missourian and Virgilian, and sediments contained in the basin are dominantly sandstones and shales deposited in channelized submarine-fan complexes within the emerging foreland basin. In the extreme southeast part of the Permian Basin, within the Kerr subbasin, coals of Virgilian age have been documented, indicating a depositional environment much shallower than along strike to the west of the Val Verde Basin. The northern Eastern Shelf, north of the Llano Uplift, comprises a series of cyclic carbonate and siliciclastic units similar to the underlying Desmoinesian succession. During the Missourian, marginal marine and alluvial siliciclastics (Devils Hollow, Turkey Creek, and Fambro sandstones) fed the Bowie, Perrin, Eastland, Oran, and Fambro delta systems in Callahan, Eastland, Shackelford, Stephens, Palo Pinto, Young, Archer, Clay, and Jack Counties) (fig. 1). To the west of the deltas, the Palo Pinto carbonate bank and shelf

systems (synonymous with the Canyon Platform) and the younger Home Creek carbonate shelf margin complex developed (fig.1). Because of continued subsidence of the Midland Basin, a shallow trough possibly ran from the Knox and Baylor County area (Knox-Baylor Trough) and connected to the Midlands in Mitchell and Fisher Counties. A deepening of the basin also occurred in the Hockley-Lubbock County area. Subsidence in this area potentially led to development of a carbonate shelf margin in Hockley and Lubbock Counties, which would correspond roughly to the north margin of the Horseshoe Atoll. The paleogeographic summary at the end of this chapter should be referred to for a more detailed discussion of the Missourian and Virgilian paleodepositional geography.

On the northern Eastern Shelf, eastern-sourced siliciclastics dominated the highstand and lowstand systems tracts but did not extend past the Home Creek shelf edge during the Missourian (Brown and others, 1990). This situation resulted in a predominance of hemipelagic sedimentation in a starved-basin scenario for the eastern Midland Basin. During the Virgilian, siliciclastic sedimentation was cyclic, with several episodes of greater retrogradation and progradation toward the Permian Basin. Ultimately, basin-plain and -floor submarine fans and prograding slopes were deposited in the eastern Midland Basin (Mitchell, Nolan, and Fisher Counties) during the mid- to late Virgilian in three episodes—Gunsight to Ivan, Blach Ranch to Breckenridge, and Crystal Falls to Flippen. The youngest episode of Pennsylvanian siliciclastic deposition on the Eastern Shelf resulted in a major lowstand leveed-slope and submarine-fan complex covering western Fisher and Nolan Counties, as well as eastern Scurry and Mitchell Counties. These submarine-fan complexes onlap against the base of the

aggradational and transgressive carbonate platform of Scurry, Kent, and Howard Counties (Horseshoe Atoll). On the southern Eastern Shelf, volumetrically minor but depositionally significant coarse siliciclastics were deposited in Schleicher County, within the Permian Basin. These sandstones appear to represent distal sheet sands.

CBP was a site of aggradational (Missourian) and progradational (Virgilian) carbonate growth on its east margin. The west margin probably began uplifting to the point of possible erosion during the Missourian in several disconnected segments. During the Virgilian the west margin continued to uplift and generally coalesced into one feature.

The bulk of the Delaware Basin appears to have been largely an area of shale deposition during both the Missourian and Virgilian but lack of age estimates for the shale succession means that the entire package could be of Permian age, and the basin may have been largely sediment starved during the Late Pennsylvanian. On the Northwest Shelf margin of the basin, carbonates were depositing on ramp setting and now compose aggradational, retrogradational, and progradational asymmetric clinoformal composite sequences. Producing fields on the Northwest Shelf appear dominantly in the mid- to outer-ramp position in moderately deep water. Extensive dolomitization is also prominent in this area. The poorly defined west margin of the Delaware Basin consists largely of outcrop exposure, with limited access. This area of the Diablo Platform/Uplift contains a relatively continuous succession of shallow- and deeper-water carbonate and siliciclastic sediments spanning the Pennsylvanian, including Missourian and Virgilian shelfal carbonates. The southern Diablo Platform/Uplift in Culberson, Jeff Davis, and Hudspeth Counties is poorly defined, with an unconformity present that juxtaposes basement and middle-Wolfcampian units. Therefore, either a model of pre-Missourian-

age uplift and nondeposition or early Wolfcampian uplift or erosion can be postulated for this region.

INTRODUCTION

This chapter discusses styles of deposition and facies development of Missourian- and Virgilian-age sediments, concluding with a discussion of revised paleodepositional maps for both stages in the Permian Basin (figs. 1, 2; Summary). Siliciclastic deposition and carbonate deposition are discussed separately, with a regional model for facies patterns and deposition proposed for each section. Data from areas adjacent to the Permian Basin are used as analogs for facies that are predicted to be present within the study area. More localized studies are used to illustrate certain key aspects (for example, facies type and reservoir quality). First, an initial introduction to the area, placing it in a global perspective, is presented.

GLOBAL TECTONIC SETTING

Recent plate models suggest that the Permian Basin was still in the southern latitudes during the Missourian and Virgilian (4–8° south) (Dalziel and others, 2002) or in the northern latitudes (0–4° north) (Walker and others, 1995) (fig. 3). In either case, Missourian- and Virgilian-age sediments in the Permian Basin are characterized as having been deposited at a near-equatorial position during the late stages of icehouse, high-amplitude, high-frequency, relative-sea-level fluctuations. Also during this time, the Permian Basin was undergoing heightened tectonic activity of both uplift and subsidence related to the Ouachita–Marathon Orogeny. Figure 3 illustrates the position of Texas (in

orange) relative to major tectonic plates and the equator during Missourian and late Virgilian times.

REGIONAL TECTONIC SETTING AND FACIES DISTRIBUTION

The outline of the Permian Basin and major geologic features commonly associated with the basin are illustrated in figure 4. The main features had developed by the mid-Missourian and stayed largely in a similar configuration through the Middle Permian. Figures 5 through 7 illustrate previous interpretations of facies distribution, uplift, and subsidence patterns for Missourian- to Virgilian-age sediments in the Permian Basin and surrounding areas. Previous interpretations suggest that the Delaware and Midland Basins of the Permian Basin were areas of net subsidence rimmed by carbonate-platform to shelfal environments, with substantial uplift in areas of the Diablo Platform, Central Basin Platform (CBP), and the Marathon–Ouachita foldbelt margin (Kluth, 1986; Ye and others, 1996; Blakey, 2005) (figs. 4–7).

Areas of uplift, subsidence, and facies distribution in figures 5 through 7 are roughly consistent between one another. According to Kluth (1986), most of the Permian Basin area is an area of net subsidence, with rate ranging from less than or equal to 50 m/Ma to approximately 200 m/Ma (fig. 6). Development of the foreland-thrust-bound Val Verde Basin is prominent on all Virgilian-age paleogeographic reconstructions. Continued uplift of the CBP and deepening of the foreland trough in the Val Verde Basin appear to be dominant areas of active tectonism in the Permian Basin during the Virgilian (Kluth, 1986; Ye and others, 1996; Blakey, 2005) (figs. 5–7). With the exception of the Blakey (2005) reconstructions, previous regional models neglect the west part of the

Delaware Basin and issues regarding development of the Diablo Platform/Uplift. Current facies distribution models of the Missourian and Virgilian series in the greater Permian Basin are discussed in the paleogeographic summary and differ substantially from those previously generated (figs. 1, 2). Details regarding structural configuration and development of the Permian Basin are reserved for a separate chapter.

GENERAL STRATIGRAPHY AND NOMENCLATURE

Missourian-age sediments within the Permian Basin include those termed *Canyon Formation* (predominantly carbonates) and those of the Canyon Group. Within the Permian Basin, most Missourian-age sediments are referred to as the Canyon Formation, and they are overwhelmingly carbonates. Virgilian-age sediments within the Permian Basin include those termed *Cisco Formation* (predominantly carbonates and shales) and those of the Cisco Group. However, on the Eastern Shelf, Missourian and Virgilian stratigraphy is divided into multiple carbonate and siliciclastic units.

Nomenclature

As is true of the underlying intervals, stratigraphic nomenclature for the Missourian and Virgilian interval on the Eastern Shelf is highly subdivided, stemming largely from extensive outcrop study in central Texas (figs. 8, 9). One point crucial to those readers unfamiliar with the Permian Basin succession is that the Cisco Group (*sensu stricto*) is not wholly Pennsylvanian and contains almost the entire Permian Wolfcampian succession at formal type localities.

SILICICLASTIC MISSOURIAN DEPOSITION

General Depositional Setting

Deltaic, fan-delta, and incised-valley systems occur throughout the Missourian, the latter of which are restricted largely to North-Central Texas, west of the Fort Worth Basin. Multiple deltaic depocenters were active during the Missourian, funneling sediment onto the northeast and east margin of the Eastern Shelf. Slope-fan and slope-wedge sediments appear to be locally present in Kent, Mitchell, Nolan, Sterling, Tom Green, Schleicher, and Sutton Counties along the Eastern Shelf (fig. 4). Coarse-grained siliciclastic sediments were restricted to the extreme east margin of the Permian Basin (as defined in this study). Locally the Llano Uplift appears to be the likely source area of a minor siliciclastic depositional episode on the southern Eastern Shelf. Historically, many of the siliciclastic reservoir intervals along the Eastern Shelf are termed Canyon sands. However, reinterpretation of these plays via seismic and wireline-log correlations indicates that most are Permian in age (Wolfcampian to Leonardian), and only a few are Pennsylvanian. These reservoirs will therefore not be discussed in this chapter.

Although the Pedernal Uplift appears to have entered a renewed stage of uplift, it contributed little in the way of siliciclastic sediments to the Delaware Basin. The San Simon Channel manifested itself between the northernmost part of the CBP and the Northwest Shelf. In the Permian Basin, 2nd-order transgression during the Missourian resulted largely in deposition of carbonates at the expense of coarse siliciclastic lithologies. During the Missourian, centers of the Midland and Delaware Basins seem to have received minimal sediment input, resulting in a starved-basin succession.

The role of the Diablo Uplift/Platform as a potential sediment source of the Delaware Basin is largely undefined. Fine siliciclastics may have been sourced from the southern Diablo Platform during a possible uplift and erosion event during the Virgilian.

The Val Verde Basin was generally starved of sediment, with rare channelized turbidite systems present, whereas in the Kerr subbasin to the east of the Val Verde Basin, Virgilian-age coals are present, indicating a dramatic decrease in accommodation between the two contiguous areas.

Reservoir Potential

Updip fluvial, amalgamated, stacked channels and thick fan-delta units have the best reservoir potential and quality. However, most, if not all, of the proximal facies occur to the east of the Permian Basin. Few data exist to confirm the presence of Missourian-age, deeper-water siliciclastic facies within the Midland or Delaware Basin. In general, only along the north part of the Eastern Shelf do shelf to basinal gradients appear steep enough to result in deposition of Missourian or Virgilian slope or basin-floor deposits.

Diagenesis

Clay diagenesis is likely the most important factor in determining productive Missourian- or Virgilian-age siliciclastic reservoirs in the Permian Basin. In the slope and basin-floor setting, amount of detrital clay and its subsequent diagenesis (growth and or dissolution) will largely control porosity and permeability.

Climate

The Missourian and Virgilian were times of expansive ice-sheet development typified by a highly fluctuating relative sea level. Amplitude and frequency of sea-level change are greater than at any other time during the Pennsylvanian. Highly fluctuating sea levels generally resulted in thinner, higher-frequency cycles and numerous periods of exposure. Given the relative changes of coastal onlap, the end of the Missourian stage marks the 2nd-order transgressive Pennsylvanian climax.

PERMIAN BASIN DATA

Eastern Shelf

Detailed studies were performed by Cleaves (1975, 1993, 2000) and Cleaves and Erxleben (1982, 1985) on the siliciclastic depositional patterns of the northern Missourian Eastern Shelf. Figure 8 illustrates a schematic representation of Missourian (Canyon Group) sedimentation patterns along the northern Eastern Shelf and farther eastward into the greater Fort Worth Basin. During the Missourian, siliciclastic sediments encroached upon the Eastern Shelf but never breached the carbonate-shelf margin-bank system (Palo Pinto Bank). In the northern Eastern Shelf, influx episodes are associated with Devils Hollow, Turkey Creek, and Fambro Sandstones (fig. 8). During the Virgilian, sedimentation is skewed 2:1 toward siliciclastics over carbonates, with the southern Eastern Shelf generally having more frequent transgressive carbonate deposition (fig. 9). During the Missourian, no highstand deltaics prograded across the entire shelf (Eastern Shelf), and ramp and shelf-margin sediments are either carbonate or condensed marine shales. A proposed slope system exists in Knox and Baylor Counties (fig. 10). This succession, termed the *Knox Slope System* or, alternatively, the *Canyon Slope System*

contains thin sandstones encased in shale. The origin of this slope system is equivocal and may be linked updip to the east across the carbonate-bank system (fig. 10) or alternatively linked northward. A northern/northeastern source appears more likely because no stratigraphic data support a siliciclastic depositional episode breaching the carbonate-shelf margin during this time. The Knox Slope System is coincident with a depositional low that trends northeastward from Mitchell to Baylor County that was established during the late Desmoinesian (fig. 2—Depositional architecture of the Desmoinesian in the Permian Basin). This trough became more pronounced during the Missourian as a result of high rates of aggradation in the carbonates and localized increased subsidence. Downslope and along strike, processes may have distributed thin sands toward the Permian Basin into Stonewall, Fisher, and Scurry Counties. Given the shelf-edge positions during the Missourian, the Knox Slope deposits would have been deposited at a time between Palo Pinto and Home Creek Formations (figs. 8, 9).

On the southern Eastern Shelf in Schleicher County, thin, discontinuous sandstones are present between Strawn carbonates and overlying Palo Pinto and Adams Branch limestones. These sandstones have various names in the subsurface, including Camar (possibly upper Missourian), Tillery, Harkey, and Crosscut. Because these sandstone bodies can be constrained to occurring below Missourian limestones (Palo Pinto and Adams Branch) and above true Desmoinesian carbonate (Strawn), they are truly Canyon sands (Missourian), as opposed to the “Canyon” sand of Sutton and Val Verde Counties, which are Permian in age. Examples of this play type are Camar and Tillery fields in eastern Schleicher County (figs. 11, 12). Missourian-age sandstones are historically interpreted to have been deposited in fluvial-deltaic channels (Hoffacker,

1990; McGookey, 1990). Apparent along-strike continuity of the sandstone bodies and their thickness (<100 ft) may indicate a more sheetlike geometry inconsistent with a channel origin (fig. 12). Dove Creek field, which straddles Irion, Schleicher, and Tom Green Counties, was proposed by Becker (1990) to contain numerous Missourian-age sandstones (Canyon D-A). However, well logs from that field do not indicate limestones, which are needed to put the reservoir into its proper stratigraphic position. Because of this lack of correlation, the field at Dove Creek and many others that extend across Irion and Sterling Counties are potentially Virgilian or younger.

To the south, in Sutton and Crockett Counties (technically Val Verde to Kerr subbasins), the entire Missourian and Virgilian succession is represented by a 0- to 200-m-thick condensed zone of hemipelagic drape sediments (Hamlin, 1999). This observation is important because it requires any Missourian-age siliciclastic unit on the southern Eastern Shelf (Coke, Tom Green, Irion, Schleicher, and Menard Counties) to have a source area to the east or east-northeast, in the area of the Llano Uplift. Reservoir quality of the Tillery sandstone (Tillery field, Schleicher County) ranges from 15- to 20-percent porosity (average 16 percent) over 50 gross ft (McGookey, 1990). Camar sandstones average 15-percent porosity and have permeability that ranges from 70 to 100 md.

MIDLAND AND DELAWARE BASINS

Siliciclastic deposition within the Midland and Delaware Basins appears to be largely restricted to basin-center shales. No data are available about the sedimentology of these facies. In general, basin subsidence in both Midland and Delaware Basins seems to have been high during the Missourian (fig. 1) and continued to increase dramatically in the Virgilian (fig. 2). However, regional structural interpretations indicate that subsidence rates between the Delaware, Midland, and Val Verde Basins were not equal (Tai, 2001). Further, subsidence rates within the Midland Basin appear much greater on the east side, along the Eastern Shelf, than along the west margin, which is the edge of the CBP (Tai, 2001).

DISTRIBUTION OF MISSOURIAN SILICICLASTIC SEDIMENTS

Given seismic and wireline-log correlations, it appears that the entire CBP was transgressed and covered by carbonate sediments by the early Desmoinesian. Regional reconstructions by Tai and Dorobek (1999; 2000) and Tai (2001) suggest an onlapping wedge-shaped geometry for the Missourian- to Wolfcampian-age sediments on the southern CBP in the Midland and Delaware Basins. Defining the geometry of Missourian- and Virgilian-age sediments is problematic because well logs and seismic do not indicate a definable break in lithology (that is, all high-gamma-ray shales) or geometry of this interval. The interval, commonly referred to as the *Late Pennsylvanian-Wolfcampian* (Tai, 2001), is characterized by abrupt and dramatic thickness changes across the southern CBP. Numerous cross sections of the Delaware, Midland, and Val Verde Basins illustrate differential thicknesses of Missourian and Virgilian sediments (termed *Canyon* and *Cisco*) (Tai and Dorobek, 1999) (fig. 13). Many sedimentation

patterns appear to have been affected by uplift events. However, uplift and subsidence patterns are not uniform within or between the Delaware, Midland, and Val Verde Basins. In general, areas of greatest uplift along the south and west margins of the CBP were sites of carbonate deposition. These areas grade rapidly “basinward” into siliciclastic and carbonate-rich shales, which compose most of the basin center fill across the Permian Basin. One of the more problematic issues regarding siliciclastic shales in the southern Permian Basin is defining a source area. Noncarbonate lithologies are rare on the CBP in the Pennsylvanian succession, and areas to the north of Fort Stockton had extensive carbonate deposition during the Missourian and Virgilian. Therefore, siliciclastics either came from the west (Diablo Uplift area) or from the south. Southern sources are unlikely, given the detailed studies of the Val Verde Basin (Hamlin, 1999), which describe the Missourian and Virgilian succession there as a thin, condensed, hemipelagic interval. In the absence of biostratigraphic and seismic data, it is possible that many of the Missourian and Virgilian shales of the southern Permian Basin are actually Permian in age.

VIRGILIAN SILICICLASTIC SEDIMENTS

Brown and others (1990) defined nine cyclic carbonate-siliciclastic depositional sequences on the northern Eastern Shelf for the Virgilian. Virgilian siliciclastic sediments do not consistently reach the Midland Basin and are largely stranded to the east in Stonewall, Fisher, and Nolan Counties. Siliciclastics that might reach the Midland Basin would largely be basin-plain to rare, prograding-slope, and basin-floor-fan sediments. The level of detail provided by Brown and others (1990) on Virgilian sedimentation on

the Eastern Shelf will not be attempted here, but three summary figures based on that work will help explain temporal and along-strike variability of the position of the shelf margin during the Virgilian, as well as the Missourian (figs. 14–16). At the end of the Virgilian, the northern Eastern Shelf margin (Flippen Limestone) was located as close to the Permian Basin boundary (as defined in this study) as it had been during the entire Virgilian (figs. 14–16). Virgilian carbonate margins acted as barriers to siliciclastic input into the Midland Basin (figs. 14–16), although north-south variability in the amount of aggradation and progradation was extensive. As during the Missourian, the Midland Basin appears largely starved of siliciclastic sediment, with the exception of basin-centered shales. True westward progradation and encasement of Virgilian carbonates in the Midland Basin did not occur until the Permian.

SUMMARY OF MISSOURIAN AND VIRGILIAN SILICICLASTIC SEDIMENTS

Missourian and Virgilian siliciclastic deposition in and around the Permian Basin has a distribution pattern similar to that of the Desmoinesian, with siliciclastic and carbonate reciprocal sedimentation. Given the placement of Missourian and Virgilian shelf edges on the Eastern Shelf, the maximum 2nd-order transgression seems to have culminated at the end of the Missourian, and a 2nd-order regression initiated during the Virgilian. However, as in the Desmoinesian, 3rd- and 4th-order, high-amplitude, sea-level fluctuations occurred at a high frequency. The result was an interlayered carbonate and siliciclastic stacking pattern on a 3rd-order scale. In general, siliciclastic highstand progradational platform-fan, fan-delta, and deltaic sediments dominate deposition on the Eastern Shelf but did not contribute volumetrically to Permian Basin succession. Deltaic

sediments continued their westward progradation from the Fort Worth Basin farther onto the Eastern Shelf, which initiated in the Atokan and was governed largely by convergence of the Ouachita thrust foldbelt to the east of the Fort Worth Basin. During the Missourian and Virgilian, subsidence in the Midland Basin increased, siliciclastic progradation advanced farther westward (that is, the Flippen Limestone equivalent). Aerially restricted Missourian-age siliciclastics on the southern Eastern Shelf (within the Permian Basin) probably had a source area in the Llano Uplift to the east and may not have been connected to the large deltaic systems to the north.

In the Delaware and Midland Basins, thick shales appear to have been deposited during the Missourian and Virgilian. However, because of sparse biostratigraphic control and a lack of lithologic variation, the shale succession could be predominantly Permian.

MISSOURIAN AND VIRGILIAN CARBONATE DEPOSITION

Approach

Carbonate rocks of Missourian and Virgilian age in the Permian Basin have been studied extensively in the Midland and Delaware Basins and Northwest and Eastern Shelves. Carbonate formations of the Eastern Shelf include the Palo Pinto, Winchell, Ranger, and Home Creek Limestones, which are within the Missourian Canyon Group, and the Virgilian-age Gonzales, North Leon, Bunker, Gunsight, Ivan, Blach Ranch, Breckenridge, Crystal Falls, and Flippen Limestones, which are part of the Cisco Group (Cleaves, 2000; Yang and Kominz, 2003) (figs. 8, 9, 14–16). Within the Permian Basin (Midland and Delaware), the equivalent carbonate succession is referred to only as the *Canyon and Cisco*.

General Depositional Setting

The carbonate depositional environment during the Missourian and Virgilian was dominated by shelf margins and isolated platforms that had developed their geographic distribution during the late Desmoinesian. However, owing to large variations in basin subsidence and a more distinct separation of subbasins, carbonate depositional architectures are quite varied around the Permian Basin. In the Eastern Shelf succession, the northern section was dominated by a stable aggradational platform during the Missourian, with a separate interior back system developing during the late Missourian transgression. During the earliest Virgilian, westward progradation of the shelf margin was substantial and was followed by middle to late Virgilian aggradation. Regionally, Virgilian carbonates generally compose the transgressive leg of the asymmetric systems tract on the Eastern Shelf. Aggradation, progradation, and retrogradation were **not** consistent along any single Eastern Shelf margin throughout the Missourian or Virgilian (figs. 14–16).

Along the west margin of the Midland Basin (east side of the CBP), carbonates are aggradational through the lower Missourian but have a decidedly eastward (basinward) progradation from the middle Missourian through the Virgilian (middle Canyon to Cisco). On the north margin of the Midland Basin, the stable carbonate platform displays an overall retrogradational, backstepping architecture and reduction in the shallow-water carbonate depositional area associated with the overall 2nd-order transgression. Lowstand carbonate complexes are present basinward of the main platform in the lower Missourian. These complexes may also be interpreted as flooded parts of the

earlier keep-up carbonate mounds/subplatforms or possibly as large-scale slope-failure products off the oversteepened platform. With the decrease in available shallow-water carbonate depositional area, the platform margin became steeper through the Virgilian, and downslope debris flows became common.

On the Northwest Shelf, the lower Missourian (Canyon 2 sequence [Tinker and others, 2004]) is characterized by aggradation followed by progradation (Canyon 1 sequence [Tinker and others, 2004]). Missourian sequences are separated from the overlying Virgilian progradational sequence by a major flooding surface equivalent to major transgression identified on the Eastern Shelf (similar to that on the CBP). Missourian and Virgilian carbonate architecture on the Northwest Shelf appears atypical of the Permian Basin, being represented by large-scale, asymmetric, sigmoidal clinoforms.

Reservoir Potential and Diagenesis

Throughout the greater Permian Basin, carbonate reservoir potential and associated diagenesis are more varied spatially and temporally in the Missourian–Virgilian succession than in underlying successions. Dolomitization of Missourian–Virgilian carbonates also played a role in both reservoir creation and destruction that were more substantial than in older parts of the Pennsylvanian succession.

Shallow-water, phylloid-algal banks and mounds dominate the biohermal succession recorded in the Missourian–Virgilian. These phylloid-algal accumulations appear to have diversified during the Late Pennsylvanian, commonly possessing both mound and bank geometries. Grain-dominated facies are also common reservoirs in the Missourian–Virgilian. More atypical reservoirs also present in the basin comprise deeper,

subtidal facies with biota more similar to those of the Early Pennsylvanian (for example, non-phylloid-algal boundstones, fusulinid packstones, and crinoidal wackestones).

Phylloid mounds tend to be massive to faintly bedded, with a flat base and distinctly convex upper surface, and were sited on shelf margins and on the top of topographically high carbonate shelves (Wahlman, 2002). The mounds, generally 10 to 20 m in thickness and 1 km or less in diameter, are best developed in normal marine settings at or near the shelf margin, as well as on the inner shelf. The mounds represent concentrated rapid vertical growth. In contrast, phylloid-algal banks are much larger (upward of 50 m in thickness and covering an area 50 km²), having a tabular to lens shape, and are internally well bedded (Wahlman, 2002). These large banks are thought to have grown on large, broad, topographic highs (for example, delta platforms with accentuated relief at the margins) but did not in themselves produce topography. They tend to have low-diversity fauna dominated by phylloid algae, suggesting a somewhat restricted environment, possibly with very shallow water depths. Concomitant elevated sea temperatures and salinities may have excluded many normal marine oceanic fauna.

Two of the hallmarks of phylloid-algal communities seem to be their resilience and recovery rates. The Late Pennsylvanian, from mid-Desmoinesian to the Permian, is typified by high-frequency and -magnitude eustatic sea-level fluctuations, which may have excluded less-resilient, robust, opportunistic biota, resulting in a *monospecific* bioherm community dominated by phylloid algae. Missourian and Virgilian shelf-margin phylloid-algal mounds have been described in several localities within and surrounding the Permian Basin (for example, Diamond M, Kelly-Snyder, Cogdell, Reineke, University Block 9, and Southwest Andrews fields and the Sacramento and Hueco

Mountains) (Schatzinger 1983, 1987, 1988; Saller and others 1992, 1994, 1999a, b, 2004; Kerans and Anonymous, 2001; Saller and Henderson, 2001; Wahlman, 2002). Codiaceans (for example, *Ivanovia*, *Eugonphyllum*), dasycladacean alga (*Epimastopora*), and red alga (*Archaeolithoporella*) are often associated with phylloid-algal bioherms (figs. 17, 18). Fusulinid foraminifera, bryozoans, *Tubiphytes*, brachiopods, and rugose corals also occur in minor abundances (fig. 19). Generally calcisponge-bryozoan mound communities, frequently microbially bound (laminar and encrusting forms), formed seaward of phylloid-algal mounds (fig. 20). During the Missourian and Virgilian, because phylloid- and calcisponge-dominated communities were probably still ecologically separate (Schatzinger, 1983; Wahlman, 2002), in the absence of seismic data, their identification can provide useful data regarding proximity to the shelf margin.

As in the Desmoinesian, primary porosity was largely occluded during early diagenesis, and present reservoir quality is related to the extent of alteration during subaerial exposure. Geometry of potential reservoir intervals varies radically between different carbonate depositional settings, and, coupled with a greater biotic diversity, results in a more complex mosaic of facies susceptible to diagenetic alteration. Duration of exposure events increased during the Missourian and peaked in the Virgilian. The increase in duration resulted in a negative feedback loop, in which too much exposure yielded cementation and occlusion of the secondary pore network.

MIDLAND BASIN

In the Midland Basin, data relating to the depositional style of Missourian and Virgilian carbonates (Canyon and Cisco Formations) come from regional cross sections,

seismic data, and field descriptions from the Northern Midland Basin—Horseshoe Atoll, CBP, and the Eastern Shelf. Although all areas are margins of the same basin, architectural style and depositional patterns for each area are distinct.

Figure 21a illustrates the general distribution of Missourian–Virgilian carbonates in the northern Midland Basin. Color change corresponding to overall thickness correlates roughly to age, with thickest intervals in geographically smallest areas containing Virgilian carbonates. According to biostratigraphic correlation, on the east side of the Horseshoe Atoll, isolated subplatforms tend to contain more Virgilian-age rock from south to north (Salt Creek>Cogdell>SACROC) (fig. 21b). Figure 21 illustrates that Missourian carbonates in general have a much larger aerial distribution and a greater and more consistent thickness than the overlying Virgilian carbonates. Studies based on individual subplatforms and fields have yielded a variety of depositional models for the Missourian–Virgilian carbonate succession. Studies at Reinecke field propose a generally stratiform distribution of facies throughout the Virgilian (Saller and others, 2004) (fig. 22a). At SACROC, a more variable distribution of facies comprising grain-dominated units admixed with deeper-water crinoidal wackestone is proposed for the Virgilian succession (Schatzinger, 1987; Kerans and Anonymous, 2001; Janson and Kerans, 2005, 2007) (fig. 22b). Figure 23 illustrates a comparison of wireline-log character of the Virgilian between Reinecke field and SACROC, both wells lying on the crestal part of each structure, and thickness of the Virgilian interval is comparable (~ 250 ft). Topography in the Virgilian succession at Reinecke field is thought to be a product of differential shallow-water carbonate growth, karstification, and postplatform, deep-marine erosion (fig. 23). On the other hand at SACROC, Kerans (2001) and Janson and

Kerans (2005, 2007) would contend, a large part of the irregular Virgilian topography is a depositional product of mud-mound and debris-apron formation in deeper water that was subsequently modified by erosion (fig. 22b).

In the northern Midland Basin, the Missourian interval (*Canyon* in the generic sense) is divided into four 4th-order sequences (Wilde 1990; Waite, 1993; Kerans, 2001), with a further biostratigraphic (fusulinid biozones) subdivision of seven units by Waite (1993). At Reineke field, Dickson and Saller (2006) contended that the entire Missourian to Wolfcampian succession is divisible into five units separated by exposure surfaces and indicated by carbon isotope excursions. However, other additional exposure surfaces within the succession do not correspond to isotopic excursions. Their geochemical model, when coupled with biostratigraphic data, indicates that the Virgilian succession is divisible into three units but is wholly middle-Virgilian. The underlying Missourian (*Canyon* in the generic sense) is late Missourian in age, and overlying Wolfcampian sediments are early Wolfcampian; therefore, the early and late Virgilian are missing from their studied succession. Generally for the Virgilian interval, three 4th-order sequences are proposed on the basis of biostratigraphic, seismic, and sequence stratigraphic analyses (Wilde, 1990; Saller and others 2004). However, Kerans (2001) expanded the number of sequences to five for the same interval. Thus, depending on the geographic position of the study area and the methodology employed to define cycles and sequences, the number of total sequences can vary widely.

The complexity and apparent differences between areas such as SACROC and Reinecke may not be entirely a product of individual interpretation (for example, placement and identification of sequence boundaries, seismic interpretation, and

depositional environment). Recent work by Kerans and Janson (2005) and Janson and Kerans (2007), indicates that the entire greater platform may be reacting predictably to overall accommodation and relative sea-level changes. Complexity of the facies identified in the Virgilian sediments of SACROC and Cogdell is characterized by mounded crinoidal wackestones with stromatactid cavities; steeply dipping, interbedded, crinoidal packstone; grainstone and grain-dominated packstones interpreted as turbidite flows; and more typical, flat-bedded, crinoidal-fusulinid, grain-dominated packstones (Schatzinger, 1987; Kerans and Janson, 2005; Janson and Kerans, 2007) (figs. 24, 25). Previous well log, core, and 3D seismic interpretation at SACROC also reveal large-scale lithoclastic debris beds and grain flow units flanking and almost encasing the entire platform (including Missourian-age sediments).

Within Virgilian-age sediments there is also high facies and architectural variability on the subplatform to field scale (fig. 22a). A structure-contour map of the top of SACROC field illustrates a flatter, wider profile on the south margin and increasing topography and irregularity to the north (fig. 26). This change is thought to indicate a higher proportion of unfilled to underfilled accommodation in the deeper, northern part of the platform (Kerans and Janson, 2005; Janson and Kerans, 2007). A series of seismic cross sections corresponding to C, B, and A on figure 26 further illustrate the architectural differences across the platform (fig. 27). An analogy has been made between Mississippian-age Lake Valley sequence 2 comprising Waulsortian-type mud mounds and flanking deposits and the Missourian-Virgilian succession in the northern Midland Basin (Kerans and Janson, 2005; Janson and Kerans, 2007). This comparison is one of the fundamental advances in understanding the distribution of facies and overall

architecture on the Horseshoe Atoll. Regional analysis illustrates that architectural control is governed by regional trends in accommodation on a northward-dipping ramp between SACROC and Cogdell (fig. 28a). Size, style, and internal architecture of the Missourian and Virgilian succession can be related directly to their relative positions along this ramp, with flatter, more stratiform architectures in the low-accommodation updip part, grading through more complex mounds with shingling and small, isolated mound tops at the flexural midpoints of the ramp and larger, more hemispherical-shaped architecture in the distal part of the ramp (fig. 28a). Additionally, outcrop studies of equivalent-aged Virgilian phylloid, mound-bearing carbonates of the Orogrande Basin have produced a similar updip-to-downdip architectural evolution model (Janson, 2007). The Virgilian succession studied by Janson (2007) is one of the few areas providing a viable outcrop analog to the Virgilian succession in the Midland Basin. Current knowledge of internal architecture of the Virgilian succession of the northern Midland Basin is limited by resolution of the seismic data, even when coupled with detailed core and wireline-log data; therefore, outcrop analogs are required to further understanding of reservoir heterogeneity in this succession.

Another complexity in the northern Midland Basin Missourian and Virgilian succession is proposed identification of Missourian-age lowstand carbonate subplatforms/buildups basinward of the main platform edge (fig. 29). These carbonate successions make up a basal phylloid-algal buildup capped by ooid grainstones and are subsequently capped by more phylloid-algal boundstones. The conceptual model put forward by Saller and others (1993) links deposition of these shallow-water carbonates

(ooid-rich grainstones and phylloid-algal boundstones) to lowstand events when sea level drops below the main platform margin and synchronous exposure and karsting are occurring on the main platform (fig. 29). BC field succession is thought to be a product of several of these lowstand episodes. Alternatively it is proposed that many of these lowstand carbonate buildups were largely keep-up mounds, with continued growth during both transgression and highstand, were large enough to withstand large fluctuations in sea level, and only met their demise and drowned out during the end of Missourian maximum transgression.

Alternatively, many proposed lowstand deposits may also be downslope debris shed from the main platform. These debris units are commonly composed of shallow-water grain types, such as ooids. As was illustrated in figure 28, phylloid-dominated mounds can form in a variety of water depths below storm-weather wave base (SWWB) and do not require extremely shallow water. Evidence of exposure in some cycles at BC does indicate limited shallow-water deposition, but this exposure could be regional, and recovery of the basinward carbonate factory could be synchronous with that of the main platform.

Lastly, when lowstand carbonate production is discussed, architecture of the main platform must be taken into account. In a high-angle (0.25°) ramp-type system, a large sea-level fall of 20 m would displace the lowstand and shoreface 4.6 km seaward, whereas in a nonramp platform system with steeper sides (5 to 10°), the shoreline is displaced only 228 to 112 m basinward of the initial point. Areal differences in amount of carbonate exposed during a lowstand event that are subject to exposure-related diagenesis are profound (5 km vs. 200 m). Regional depositional geometry (high vs. low angle) must

be accounted for when the presence of lowstand carbonate deposits is postulated. The main basinward, south-facing side of the northern Midland Basin isolated platform appears to have had a steep, relatively high relief margin, indicating that any lowstand carbonates would be formed near that platform margin. Only during extreme drops in relative sea level would the carbonate factory be displaced substantially basinward. Overall, genesis of Missourian-age carbonates basinward of the main carbonate platform succession needs to be reevaluated in light of newer seismic data and conceptual models.

The Eastern Shelf carbonate succession during the Missourian and Virgilian is sited largely to the east of the Permian and Midland Basins, as defined in this study (figs. 14–16). However, isolated platforms/buildups, such as Millican, Jameson, and IAB in Coke County, are present to the west of the main north-south-trending shelf margin (Zemkoski, 1985). These successions seem to have facies and stacking patterns similar to those in the northern Midland Basin and span a similar biostratigraphic interval (from early Missourian to late middle Virgilian–pre-Palo Pinto Formation to Blach Ranch). Although these isolated platforms appear to occupy a basinward position relative to the shelf margin (similar to that of BC field), their apparently continuous deposition does not make them viable candidates for punctuated deposition confined to lowstand events. They more likely represent areas of carbonate deposition of size sufficient to experience a keep-up scenario during the overall Missourian 2nd-order transgression.

The CBP side of the Midland Basin contrasts highly with the Missourian–Virgilian carbonate succession on the north Midland Basin margin. Many of the data concerning the Missourian–Virgilian carbonate development on the CBP come from studies of Southwest Andrews and University Block 9 fields. The main architectural

difference between the CBP and the northern Midland Basin is that the CBP is an attached system with increased accommodation eastward, toward the center of the Midland Basin. Regional seismic across the Block 9 and Southwest Andrews area indicates that the entire Pennsylvanian is largely stratiform, without any of the topography so dominant along the northern Midland Basin Platform. Facies intercalations and architectures on the CBP are largely below seismic resolution (fig. 30a).

Figure 30b illustrates a three-well correlation of Missourian and Virgilian facies within Andrews County, which are similar to those present in the northern Midland Basin. The Missourian (*Canyon* in the generic sense) is subdivided into three gross packages comprising four biostratigraphic zones: (1) a lower package (lower Canyon) that is spiculitic mudstone and ooid-peloidal grainstone dominated, (2) the middle Canyon that is dominated by phylloid-algal wackestones, and (3) the upper Canyon that has the most facies variability, containing shale, fossiliferous wackestone, phylloid wackestone, and bioclastic grainstones (fig. 30b) (Saller and others, 1999b).

The Virgilian (*Cisco* in the generic sense) was not subdivided by Saller and others (1999b). However, a change in sequence thickness and architecture is apparent between biostratigraphic zones VC-1 and VC-2. Below VC-2 the succession is variable but dominated by bioclastic and ooid-peloid grainstones with minor phylloid and fossiliferous wackestones. The transition to biozone VC-2 is marked by a shale, above which sequences are interpreted as thinner and largely dominated by bioclastic grainstones (fig. 30b). Figure 31 illustrates a fieldwide correlation of the Missourian and Virgilian succession in the University Block 9 area directly south of Southwest Andrews field. Very different facies types are present between the two areas. The equivalent

middle Canyon succession dominated by phylloid-algal wackestones in Southwest Andrews is dominated by skeletal-peloidal packstones in the University Block 9 area. The Canyon 3 interval is generally more similar between the two areas, both being dominated by lower energy wackestones. The Virgilian succession in both areas reflects a decrease in accommodation, yielding thinner cycles and abundant exposure; however, in the University Block 9 area there is a relative dearth of high-energy grainstones, and instead phylloid-algal mounds are present (figs. 30b, 31).

Subregionally, there are distinct differences in the abundance and distribution of porous zones in the same successions. Comparison of these two relatively closely spaced areas in an apparently flat lying succession indicates that even across small distances (<5 mi), intrasequence facies distribution will be different, and only by looking at more regional-scale data, including seismic, can we truly understand the architecture of this system. Both areas do highlight a major difference between the CBP and the northern Midland Basin—the Virgilian succession on the CBP appears to undergo basinward progradation while the same interval in the northern Midland Basin takes a decided backstep and decreases in carbonate depositional area.

As discussed for the Desmoinesian, identification of sequence boundaries (both higher and lower orders) and exposure events is vital to an understanding of reservoir architecture and prediction of reservoir quality in the Missourian and Virgilian succession of the Midland Basin. Figure 32 illustrates the proposed cycle stacking pattern and associated cycle thickness and accommodation trends of the Missourian and Virgilian succession in the Southwest Andrews field area. This figure illustrates the relatively dramatic change in cycle thickness between the Missourian and Virgilian succession that

appears to be represented basinwide. However, identification of exposure events and cycle boundaries in any succession can be, and often is, highly subjective. Also, Fischer-style plots, commonly used to illustrate cycle stacking and thickness trends, work on the premise that sedimentation rates are constant, which is rarely the case. The cycle thickness illustrated in figure 31 for the same succession as in figure 32 indicates a different architecture within the interval equivalent to the upper Canyon and possessing the thickest cycles relative to the rest of the Missourian succession. This difference in apparent accommodation must be related either to different local accommodation or sedimentation rates or to differences in the method of picking and identifying cycle boundaries because relative sea level should not vary dramatically between two geographically adjacent areas.

Figures 33 through 35 illustrate core photographs and their associated wireline-log and porosity/permeability signatures for the lower Missourian interval at Southwest Andrews field.

In figure 33, the dark crinoidal unit corresponds to the basal part of the Missourian succession (Canyon Formation). Note that high thorium values on the spectral gamma ray (fig. 33) correspond only to the basal 2 ft of this unit and not to the underlying exposure surface. Subtidal crinoidal facies dominate the lower Canyon interval at Southwest Andrews field (fig. 34). The grainstone facies present in the lower Canyon interval is thin (~8 ft) and encased by crinoidal grainstones above and below (figs. 34, 35). Although Saller and others (1999a) interpreted the top of the grainstones as an exposure surface, no corresponding excursion appears in the carbon isotope profile. The lower Missourian grainstones illustrated in figure 35 may not indicate the top of the upward-shallowing

cycle (as interpreted by Saller and others 1999a, b), but given their isolated nature, lack of an isotopic excursion, and their blocky wireline-log signature, they could be the result of platform-top shedding into the more shelfal subtidal region. Figures 36 and 37 illustrate the character of the upper Missourian (upper Canyon) interval at Southwest Andrews field. Although the cycle-top boundary between fusulinid wackestones in figure 37 is obvious, there is a high degree of alteration far below the thin grainstone interval (fig. 36). This interval appears to contain large subangular and subrounded clasts and appears more indicative of a debris flow or brecciated exposure horizon than the original description by Saller and others (1999a, b), indicating extensive bioturbation.

Figure 38 illustrates textural, well log, and facies characteristics of Virgilian rocks at Southwest Andrews field. The most obvious difference between this part of the succession and the underlying Missourian (figs. 36, 37) is extent of alteration. Numerous cycle-top exposure events were interpreted in this interval by Saller and others (1999a) (fig. 38). Facies appear to be generally higher energy, but they also contain a predominance of fusulinid and echinoid debris and a general lack of ooids (fig. 38). Overall, cycles and any potential reservoir interval are thinner than in the Missourian. Owing to negative feedback, the increased number and duration of exposure-related events in the Virgilian actually produce poorer reservoirs (that is, too much exposure yields a cemented, nonporous rock).

DELAWARE BASIN

The Missourian and Virgilian carbonate succession in the Delaware Basin is less well studied or understood than the corresponding Midland Basin succession. Missourian

and Virgilian shallow-water carbonates (that is, potential reservoirs) are restricted largely to the Northwest Shelf in an arc running across Eddy and Lee Counties, New Mexico (fig. 39). Farther west, across the proposed uplifted Diablo Platform/Uplift, an additional site of carbonate deposition rims the Orogrande Basin. The Orogrande succession has had extensive outcrop study but cannot be linked directly to the Permian Basin succession.

The bulk of data and interpretations of the Permian Basin come from studies of Dagger Draw and Indian Basin fields (fig. 39) (Brinton and others, 1998; Mazzullo, 1998; Tinker and others, 2004). Although the Missourian and Virgilian carbonate succession was conceptually drawn as a series of coalesced and stacked algal bioherms by Mazzullo (1998) (fig. 39, top) with substantial aggradation similar to that of the northern Midland Basin, this interpretation may be largely incorrect. In figure 39, lower generic facies and architectural diagrams more adequately describe the succession; however, facies partitioning types appear different at Dagger Draw field than in the conceptual model. Figure 40 is a dip-oriented seismic section of South Dagger Draw field. Seismic correctly illustrates the low-angle, shingled, sigmoidal, basinward-prograding-clinoform nature of the Missourian and Virgilian succession. This architecture is very different from that in the Midland Basin succession, especially compared to its north and east margins. Missourian to Virgilian progradation is more like that of the CBP succession, as opposed to the general retrogradation recorded in the northern Midland Basin (Horseshoe Atoll, Scurry Reef). The sigmoidal-clinoform architecture also implies a decidedly lower rate of accommodation generation than in the Midland Basin.

The depositional model for the high-frequency sequences at Dagger Draw illustrates early flooding of a low-angle ramp, with deposition of largely argillaceous mudstone-wackestone and shale giving way to more crinoid, brachiopod, and bryozoan-rich wackestone and fusulinid-to-crinoid wackestone and grainstone in the late transgressive systems tract (TST) (fig. 41a). The higher energy grainstone facies of the TST are aurally restricted to the middle ramp behind the true ramp crest (fig. 41a). During the associated early highstand (HST) the depositional area of the fusulinid-to-crinoid wackestones and grainstones expanded to occupy both middle ramp and crest (fig. 41b). The late HST is characterized by development of algal boundstones on the ramp-crest margin, with associated lower energy mudstones facies occupying the middle ramp area within the energy shadow of the crest (fig. 41b). Estimated water depths during the HST ranged from 1 to 2 m in the middle ramp to 10 m at the ramp crest, with the thin outer-ramp succession being deposited in at least 40 m of water (Tinker and others, 2004).

Figure 41 illustrates the conceptual architecture of a high-frequency sequence. High-frequency sequences (HFS's) are components of larger composite sequences (CS's) (fig. 42). Given the sigmoidal-clinoform nature of the Missourian and Virgilian succession, it is imperative that purely wireline-log correlations be avoided. In analyzing a dip section through a composite sequence, even sequence stratigraphic correlations are difficult. In the most proximal areas, the entire CS comprises stacked highstand sediments to the exclusion of other systems tracts (fig. 42—transect A). A well placed just behind the ramp crest would yield a facies package dominated by algal boundstones, creating a false sense of a mounded nature and aggradation (fig. 42—transect B). At the

ramp crest, facies and systems tracts are more symmetrical, containing LST-TST and HST sediments (fig. 42—transect C). In outer-ramp areas, the CS is dominated by thick LST-TST legs and thin to absent HST portions of the sequences (fig.42—transect-D).

Analysis of Missourian facies at South Dagger Draw illustrates some key differences when compared with the equivalent succession of the Midland Basin. Algal boundstones at South Dagger Draw, and presumably in many other places along the Northwest Shelf, are formed by encrusting and binding algae such as *Archaeolithophyllum* and *Tubiphytes* and not phylloid algae, which dominate in other areas (fig. 42—left photo; figs. 43a, b, 20). Unlike the Midland Basin, Missourian and Virgilian succession, no true high-energy wave-base-indicative grainstones or peritidal facies were identified in South Dagger Draw (Tinker and others, 2004). Algal boundstones are thought to be the shallowest water facies (<10 m water depth) (fig. 43a, b). The fusulinid packstone and packstone/wackestone facies that commonly occurs in the early HST of the high-frequency sequences is largely nonreservoir, having been deposited in moderate water depths (fig. 43c, d). Crinoidal, brachiopod, and bryozoan mudstone and wackestone represent deepest water, pure carbonate facies, generally occurring in the late TST (fig. 43e, f).

MISSOURIAN AND VIRGILIAN CARBONATE RESERVOIR QUALITY

Midland Basin

Reservoir quality in Missourian and Virgilian carbonates of the Midland Basin is controlled by facies and grain type, as well as extent of diagenetic alteration occurring during subaerial exposure. This situation is similar to that of the Desmoinesian

succession in many ways, but variability of facies type, thickness, and amount of exposure-related diagenesis are much greater in the Missourian and Virgilian succession. Following the diagenetic model proposed by Saller and others (1999b), the CBP succession underwent more of what is termed Stage 3 and Stage 4 alteration (figs. 36–38). The exposure-related diagenesis associated with Stage 3 is pervasive through each cycle and is evidenced by micritization, brecciation, and rhizolith formation. On average the cycles are 3 to 4 m thick, and the intergranular porosity of grainstone intervals is occluded largely by blocky calcite cements. Moldic porosity dominates the current open pore network, and minor secondary vuggy and fracture-enhanced porosity is present. Fine-grained wackestones and packstones are mostly tight. Average porosity and permeability in units affected by Stage 3 diagenesis are 3.1 percent and 1.89 md, respectively. Stage 3 diagenesis is most common in the middle to late Missourian and early Virgilian (upper middle and upper Canyon and lower Cisco) (Saller and others, 1999b) (figs. 36–37).

Stage 4 alteration, thought to be the most intense level of subaerial exposure-related diagenesis in the Missourian and Virgilian succession, is most abundant in the upper Virgilian (*upper Cisco* in the generic sense) (fig. 38). Features associated with this level of alteration are fractures, fissures, grikes, and brecciation extending as much as 1 m below the associated exposure surface. Average cycle thickness is less than 2 m. Both primary intergranular and secondary moldic pores are occluded by calcite cement. Vug, fracture, and fissure (grike) porosities are also largely occluded by burial cements. Average porosity and permeability in units affected by Stage 4 diagenesis are 2.2 percent and 0.18 md, respectively. In general, there is less of a correspondence between

permeability and porosity in the reservoir intervals of the Virgilian succession than in the underlying Missourian (figs. 36–38).

The Missourian succession (*lower Canyon* per Saller and others, 1999b) has much better reservoir quality than the younger units, as discussed earlier. Overall, cycles are thicker, facies more laterally persistent in architecture, phylloid-algal-dominated units more common, and rocks have experienced a lesser but optimal level of exposure-related diagenetic modification. Stage 2 alteration is most common for the interval, and associated reservoir quality is significantly better than in the overlying succession, with a higher average porosity of 4.27 percent and a much higher permeability of 10.77 md (Saller and others, 1999b).

Figure 44 illustrates a generic average-reservoir-quality plot of the Missourian and Virgilian intervals. These three-well-averaged (both per well and generic sequence) data indicate that the lower Missourian interval is generally the best in terms of overall (porosity and permeability) reservoir quality. However, core-porosity-based correlations from the same wells indicate that the middle Missourian (*middle Canyon* per Saller and others, 1999b) has the best and most extensive reservoir interval throughout the field on a dip section (fig. 45). For this apparent conflict to be addressed, porosity distribution is better viewed in a regional time-slice view. In general, the early Missourian succession (*lower Canyon* per Saller and others, 1999a) has the most aerially extensive high porosity, whereas the middle Missourian (*middle Canyon* per Saller and others, 1999b) has several thick, high-porosity intervals but a much smaller aerial distribution (fig. 46). The Virgilian succession (*Cisco* per Saller and others, 1999b) has the lowest overall porosity, and porous zones are largely laterally discontinuous (figs. 46, 47).

To the south, in University Block 9, we can examine porosity/permeability at a higher resolution (fig. 47). Two observations are readily apparent: (1) the best reservoir quality is also in the Missourian section and (2) it is roughly equivalent to the upper Canyon interval as defined by Saller and others (1999a, b). The reservoir interval is approximately 20 ft thick and averages 4.91 percent porosity and 3.91md permeability. Given the core data, the lower Missourian succession, as illustrated by the University 25 well, has good reservoir quality only in crossbedded ooid grainstones, which are approximately 3 ft thick (average 14.63 percent porosity and 2.125 md permeability) (fig. 31). The Penn #11 well was cored through the middle Canyon to near the top of the Cisco (fig. 31). Core analysis and wireline-log data indicate once again that the upper Canyon interval (F) has the best reservoir quality, with average porosity and permeability of 8.39 percent and 2.82 md, respectively. However, when this interval is examined in more detail it becomes apparent that porosity generally increases upward, even though permeability is highly variable and does not possess a linear correlation with porosity (fig. 48).

Figure 49 illustrates textural and component variability in the upper Canyon interval of the Penn # 11 well (fig. 31). Porosity is strongly controlled by biological constituents of the rock (that is, facies), and distribution of these components has a large bearing on resultant permeability (fig. 49). Slightly below the base of the reservoir interval is a thin grainstone unit, but primary porosity is largely occluded by calcite cement. Current porosity is intercrystalline, associated with coarse nonplanar-C/saddle dolomite, and therefore entirely unrelated to facies or subaerial exposure (fig. 49a, b). Samples from the lower part and center of the interval (depths 9,039, 9,041, and 9,050 ft)

illustrate one of the more common forms of porosity in Missourian and Virgilian carbonates of the Permian Basin. These samples illustrate that most pore space is related to molds formed after bioclasts, dominantly phylloid algae (fig. 49c–e). The main issue relating to permeability is the degree of contact between moldic grains. Isolated or clumps of bioclasts/phylloids yield an irregular permeability distribution (fig. 49c, d), whereas more parallel orientation of the grains yields higher permeability (fig. 49e).

As discussed earlier, Virgilian-age (Cisco) reservoir intervals are generally thinner than in the underlying Missourian and are predominantly high energy grainstones. In the case of University Block 9 field, in Penn #11 and 14CE #C6 wells, an algal wackestone to packstone is noted. In thin section these facies appear to be encrusting to laminated algae instead of typical phylloid algae (fig. 49e). Although apparently aurally restricted, this facies has good reservoir quality compared with that of the typical Virgilian tight limestone illustrated in figure 50, which possesses extensive cement both unrelated and related to exposure.

Exposure-related diagenetic events can be difficult to identify and range from subtle cracks and reddening of sediments to brecciation, rhizoliths, alveo-septal fabrics, soil crusts, desiccation cracks and glaebules (fig. 50a, b). In the absence of these identifying features, trace elements and isotopic data are required to confirm whether cements were of either meteoric (for example, exposure related) or marine affinity (fig. 50c, d).

Although reservoir quality on the CBP is variable, it is predictable in a gross sense, with Virgilian units generally of lesser quality and aerial extent. Exposure-related diagenesis is important, but in some instances it is overemphasized because original

facies and their architecture are equally important. Take, for example, the isolated platforms of the northern Midland Basin. At SACROC, Schatzinger (1987) performed a detailed core- and thin-section-based facies analysis and combined it with wireline-log data (fig. 51a, b). One key difference between the CBP and the northern Midland Basin is the latter's greater facies and architectural variability, even in the Missourian succession (fig. 51a, b). Figure 51 illustrates log-based porosity variability within a single well and between two wells and its link to facies type. In general, higher-energy oolitic to coated-grain grainstones have the highest porosity in the middle Canyon succession (fig. 51b), whereas the sponge-algal-bryozoan boundstone facies generally has lower porosity over a much thinner interval (fig. 51a). At Reineke field, Saller and others (2004) asserted that porosity and permeability are dominantly linked to exposure-related diagenesis and that reservoir-grade porosity ($>4\%$) and permeability (>1 md) are fairly continuous laterally and vertically in the Virgilian succession. However, core analysis data indicate that facies have moderate control over porosity distribution and strong control over permeability, especially vertically (fig. 52a). Dolomitization has occurred within the Virgilian succession at Reineke field, and dolomitized facies have generally lower average porosity and higher average permeability than their limestone counterparts (fig. 53). In a single type well for Reineke field, core and wireline-log porosity are relatively uniform and predominantly above 10 percent throughout the Virgilian succession (fig. 54). However, on close analysis, porosity and to some extent permeability are linked more to specific facies than to alteration zones beneath major sequence boundaries 300, 200, and 100, with which paleosol features have been identified (fig. 54). Therefore, true porosity

and permeability distribution seems to be controlled more by higher-order cycles and facies geometry than by long-duration exposure events.

As discussed previously, a layer-cake distribution of facies in the Virgilian succession does not reflect the intraplatform facies architecture. A much more complex geometry is envisaged, with progradational geometries, slope debris, and deep-water mounds commonly developed (figs. 25–28). In the northern Midland Basin, generating an accurate model of facies geometries and platform architecture appears to be of greater importance than identifying exposure-related diagenesis.

Figure 55 illustrates vertical facies variation in the SACROC area. Facies in the lower Canyon succession (*Canyon 1* per Charles Kerans, Jackson School, personal communication) and youngest Cisco sequences are dominated by crinoidal wackestones to packstones (fig. 55). The Canyon 2a sequence has a greater dominance of fusulinid-rich facies (for example, fusulinid-crinoidal-skeletal packstones, grain-dominated packstones and grainstones). Ooid grain-dominated packstones cap higher-order cycles (fig. 55). Canyon 2 and 3 sequences are similar to Canyon 2a in their stacking patterns and general facies composition but contain a greater proportion of higher-energy facies (for example, ooid grainstones and grain-dominated packstones, as well as skeletal rudstones) (fig. 55). The transition from Canyon 2a to Cisco 1 sequences indicates regional transgression, with the Cisco 1 being dominated by subtidal, fusulinid-rich facies.

Reservoir quality in the entire Missourian and Virgilian succession is variable, and both intergranular porosity (largely primary) and moldic pores are present in the grain-rich facies (fig. 55). In general, primary facies type (that is, grain rich or not) is

associated with highest porosities both in neutron log and petrographically. Presence of primary pores in many cycle-top facies indicates that not all current porosity is related directly to exposure-related diagenesis. The core photo from the uppermost Cisco 2 sequence illustrates texture of an exposure event; however, because the facies affected was a crinoidal wackestone to packstone little porosity was generated.

The Northwest Shelf Missourian to Virgilian succession is different in architecture and dominant facies type from the Midland Basin successions, as discussed earlier. Current models of porosity generation and preservation stem largely from studies at Dagger Draw and Indian Basin.

Dolomitization appears to play a crucial role in reservoir quality in this area. At Dagger Draw the entire succession is largely dolomitized. The dolomitization model for this area does not invoke early diagenetic fluids for dolomitization. Faults served as conduits for acidic brines, which then promoted dissolution and served as pathways for later pore-occluding hydrothermal (90–170°C) dolomitization, possibly during the Eocene–Oligocene (fig. 56) (Hiemstra and Goldstein, 2004; Tinker and others, 2004). A solution-enhanced fracture and vuggy pore system developed at the crestal position of sigmoidal clinoforms, where the faults, dolomitization, and shallowest water facies (still >10 m below wave base) intersected (fig. 56). This zone forms the reservoir interval when it is capped by transgressive shales, which provide a seal.

No evidence of subaerial exposure-related diagenesis was identified or documented in any of the facies or high-frequency cycles at Dagger Draw field. Macropore geometries vary widely, although all pores are technically intercrystalline (that is, between dolomite crystals)

(fig. 57). Depending on the dolomitized facies, pores can range from those reflecting an intergranular, primary origin to moldic pores after leached bioclasts, and even to fenestral or shelter pores associated with algae. Porosity/permeability relationships in dolomitized facies are even more difficult to predict than in their limestone counterparts. Reservoir quality, especially permeability, can often be linked to dolomite crystal size, which is a function of both the size of the replaced precursor as well as saturation of the fluid. Pores are irregularly distributed and moldic and vuggy in nature, and their associated permeability ranges from 0.1 to 1,000 md, being generally confined to four flow units (fig. 57) (Brinton and others, 1998; Tinker and others, 2004).

Regionally the Northwest Shelf Missourian and Virgilian succession is much more dolomitized than the equivalent succession in the rest of the Permian Basin. Such extensive dolomitization events typically require large fluid fluxes and are often associated with early diagenesis and modified seawater. The dolomitization model proposed by Hiemstra and Goldstein (2004) and Tinker and others (2004) is generally supported by data at Dagger Draw; however, this model may not be appropriate for the entire Northwest Shelf.

Across the Diablo Platform/Uplift (figs. 1, 4) within the Orogrande Basin, dolomite is relatively common in the Missourian and Virgilian succession. The general carbonate depositional model in this area is shelf-edge phylloid-algal buildups and associated flank deposits deposited as part of the reciprocal siliciclastic-rich sedimentation system, which is more like the Midland Basin (for example, Eastern Shelf) succession than the Delaware Basin/Northwest Shelf. Dolomitization in the eastern Orogrande Basin is thought to have formed via glacioeustatic transgressive reflux

(Soreghan and others, 2000). This model links eustatic sea-level fluctuation to dolomitization by concentrating the seawater's dolomitization potential during lowstands and flooding the platform with this fluid during early transgression. Although it is not proposed that Northwestern Shelf dolomites are a product of this process, this example illustrates that dolomitization can form via a variety of mechanisms. Each area requires a detailed diagenetic study before models of dolomitization can be inferred. It is the author's contention that several types of dolomite are potentially present within the Missourian to Virgilian succession on the Northwest Shelf. Multiple dolomitization events probably occurred, some diagenetically early, others late, and events could have been superimposed. Although the data from Dagger Draw indicate that subaerial, exposure-related diagenesis was minor to nonexistent in generating current reservoir quality, this assumption cannot be extended to the rest the shelf. Areas more proximal than Dagger Draw may have experienced extensive cycle-top diagenesis and have a reservoir quality distribution and evolution more similar to those of the CBP.

SUMMARY OF THE MISSOURIAN AND VIRGILIAN CARBONATE SUCCESSION

In summary, several key issues come to bear on an understanding of Missourian- and Virgilian-age carbonates. And many of these issues have a direct bearing on exploitation of, and exploration for, new reservoirs in the Permian Basin.

1. Scale: Studies within and external to the Permian Basin need to be put into a regional sequence stratigraphic context. In general, the regional transgression that occurs at the transition from the Missourian to the Virgilian is expressed throughout the Permian Basin, except for in the south (that is, Val Verde), where

the entire succession is expressed as a thin, condensed, pelagic, mudstone interval.

2. Diagenesis: Missourian reservoir development is linked to extent of subaerial exposure and to facies type. During the Virgilian increased frequency of exposure and much more diverse facies mosaic and architecture yielded poorer and less laterally and vertically extensive reservoir intervals. Multiple facies types can have good reservoir quality, and exposure-related diagenesis is often overemphasized. Generally, phylloid-algal bioherms are often the best reservoirs, but grain-dominated shoal successions become increasingly important in the Virgilian.
3. Architecture: The Missourian succession and, primarily, the Virgilian succession express themselves in different styles, depending on their location within the basin. The northern Midland Basin is distinct from the CBP and displays its own updip to downdip subregional variability that is crucial to an understanding of the succession. Accommodation was much greater in the Northern Midland Basin, with Virgilian-age facies often represented by deeper-water, crinoidal, mud-mound facies. This increased accommodation contrasts with the CBP, where the platform was narrower, with limited accommodation throughout its life and consequent progradation through the Virgilian. The Delaware Basin carbonate succession was deposited on a ramp and is dominated by subtidal facies. The regional end-Missourian 2nd-order transgression is identifiable on the Northwest Shelf, but it does not herald the distinct change in facies type, thickness, or

architecture within the overlying Virgilian, which is so prominent in the Midland Basin.

DISCUSSION AND SUMMARY OF THE MISSOURIAN AND VIRGILIAN IN THE PERMIAN BASIN

Globally and regionally a 2nd-order transgression peaked at the end of the Missourian. However, continued icehouse conditions with high-amplitude and -frequency asymmetric fluctuations in base level continued into the Virgilian. Virgilian sedimentation has the overprint of some of the highest amplitude (100 m+) and frequency-base-level falls recorded. These fluctuations help define stratal facies architectures, as well as their being a major driver behind both enhanced and diminished reservoir quality.

Although Missourian-age siliciclastics, present on the southern Eastern Shelf within the Permian Basin, have an eastern source, they are volumetrically minor. Localized development of a slope bypass system into the Midland Basin occurred in the north. Virgilian-age, coarse-grained siliciclastics are largely nonexistent within the basin. Significant siliciclastic deposition occurred to the east of the defined Permian Basin margin during the Virgilian, and the entire sequence is skewed 2:1 to highstand progradational platform-fan, fan-delta, and deltaic siliciclastics over carbonates. Apparent thick shale deposition occurred within the center of the Delaware and Midland Basins. In the Val Verde and Kerr Basins, the Missourian–Virgilian interval comprises a condensed hemipelagic mudstone (0.1–200 ft thick).

Carbonate deposition dominated the Missourian and Virgilian and varied from shallow-water, high-energy to basinal, low-energy facies. Myriad carbonate depositional

settings were present during the Missourian, but further diversification, including deep-water mounds, occurred during the Virgilian. Effects of 3rd- and 4th-order sea-level falls are often manifested in carbonates as subaerial exposure surfaces. These surfaces/events contributed to development of reservoir intervals within the Missourian carbonates throughout the Midland Basin. Architectural and facies geometries strongly controlled siting of the reservoir intervals, especially in the Virgilian. In platform areas more susceptible to cycle-top diagenesis, increased frequency and duration of exposure during the early Virgilian resulted in negative feedback, with dissolution being followed by extensive cementation and occlusion of secondary pore networks.

Carbonate successions display aggradational, progradational, and backstepping architectures intrabasinally and extrabasinally. In general, carbonate production was relatively “fixed” in its location and inherited gross geometries from underlying Desmoinesian carbonates. The Eastern Shelf succession displays variable magnitudes of progradation and retrogradation along strike within depositional episodes. Regionally, retrogradational and progradational cycles on the Eastern and Northwest Shelves and CBP are sequence stratigraphically out of phase relative to the northern Midland Basin. The major transgression at the end of the Missourian (*Canyon* in the generic sense) is identifiable throughout the Permian Basin.

On the Eastern Shelf, the northern section was dominated by a stable aggradational platform margin during the Missourian. An interior bank system developed in this area during late Missourian transgression. During the early Virgilian, progradation occurred on the outer-shelf margin, with aggradation occurring during the middle to late Virgilian. Virgilian carbonates compose the transgressive leg of the asymmetric systems

tract, which is actually dominated by siliciclastic sedimentation to the east of the Midland Basin.

Over the same time frame, the east-facing margin of the CBP had an apparently simpler evolution, with a general basinward (easterly) progradation from the middle Canyon through the Cisco, which was demarcated by high-energy ooid-grainstone facies. Porosity and permeability were diagenetically enhanced during subaerial exposure on the 3rd- and 4th-order scale. During the Virgilian (*Cisco* in the generic sense), more abundant, accommodation-limited, thinner, and grain-rich cycles were exposed more frequently and for longer intervals, resulting in increased cementation and yielding poorer reservoirs than the underlying Missourian (Canyon) carbonates. Throughout the Permian Basin, the best reservoir exists beneath exposure surfaces of moderate duration, usually confined to the lower to middle Missourian succession.

In the Delaware Basin along the Northwest Shelf, Missourian and Virgilian successions appear very different from those in the Midland Basin. Overall depositional geometry appears more ramplike than platform, and main producing fields are situated in the mid- to outer-ramp setting. Sequence tract architecture is asymmetric, with large-scale sigmoidal clinoformal geometries. This stacking pattern results in decreased to absent parts of the sequence tract (for example, no TST in the interior). The Missourian succession contains a lower aggradational composite sequence (CS 1) (Canyon-2—Tinker and others, 2004) and an overlying progradational composite sequence (CS 2) (Canyon 1—Tinker and others, 2004). CS2 is separated from the overlying progradational CS 3 Cisco (Virgilian) by the regional end-Missourian flooding surface. In general, there is a decided lack of diagenesis associated with exposure, and facies contain

a deeper subtidal fauna more similar to that of the Early Pennsylvanian (Morrowan and Atokan). High-energy, shallow-water facies are not prevalent, and main facies types are algal boundstones, fusulinid packstone/wackestones, and crinoidal wackestone. Although dolomite is much more pervasive on the Northwest Shelf than anywhere else in the basin and is crucial to reservoir generation, this diagenetic event is thought to have occurred substantially after deposition, making its prediction difficult.

The Missourian and Virgilian carbonate sedimentation pattern is complex, and many perceived fundamental observations are actually only local in occurrence. The retrogradational pattern (backstepping) from the Canyon–Cisco is really manifested only on isolated platforms of the northern Midland Basin. However, regional transgression at the end of the Missourian was basinwide. Diagenesis associated with exposure was often critical to adequate reservoir quality, but facies geometries and architecture are equally important. Phylloid algal buildups were common in the Missourian and diminished slightly in frequency during the Virgilian, but reservoirs are not restricted to this facies.

Within the Midland Basin, a series of associated lowstand complexes basinward of the main platform in the lower Canyon interval are present. It is difficult to assess whether all these basinward miniplatforms are tied to lowstand events or are better represented as keep-up platforms during the Missourian transgression. These basinward platforms are not identified outbound of the CBP or on the Northwest Shelf. In general, the Missourian succession is dominated by more subtidal facies than the Virgilian throughout the Midland Basin. However, this type of observation is highly subjective, depending on where along the platform the observation was made (for example, deeper-water phylloid-algal boundstones in the University Block 9 area laterally equivalent to

grainstones at Southwest Andrews). During the Virgilian on more isolated platforms, downslope debris flows became prevalent once platform-margin relief reached adequate heights. Associated with this debris are deeper-water crinoidal mud mounds. This facies association contradicts the generalization that the Virgilian (Cisco) succession is shallower, more grain rich, and higher energy than the underlying Missourian.

Although it is obvious and has been stated extensively that the Missourian and Virgilian succession is strongly controlled by eustatic variations, amount and local variation of subsidence are probably two of the key controls on facies distribution and architecture in the Permian Basin. The rate of subsidence in the northern Midland Basin was probably much higher than in the south and relative to the Delaware Basin. This differential subsidence is probably linked to differences in major structural and basement terrains of which the Permian Basin is composed.

PALEOGEOGRAPHIC SUMMARY

Based on the above interpretations, proposed distribution of Missourian and Virgilian sediments across the Permian Basin and surrounding areas is illustrated in figures 1 and 2. The following discussion refers to interpretations represented in those figures.

Missourian and Virgilian siliciclastic sedimentation dominated deposition to the east, south, and northwest of the Permian Basin (figs. 1, 2). A narrow zone of siliciclastic

sediment appears to have entered the eastern Midland Basin to the south of the carbonate shelfal sequences in Sutton, Schleicher, and Edwards Counties (figs. 1, 2), which was probably sourced by the Llano Uplift. A localized siliciclastic slope system also feeds into a troughlike area in Knox, Baylor, Stonewall, and King Counties along the Eastern Shelf east-southeast of the Matador Uplift. This depositional low initiated in the Desmoinesian, and its margins and configuration were modified numerous times during the Missourian and Virgilian by migration of carbonate shelf edges. Figures 1 and 2 illustrate times of carbonate- and shale-dominated deposition in that area. In the southern Permian Basin, including the Val Verde Basin, deposition of coarse siliciclastics was minimal. Occasional distal turbidites probably fed into the basin, but in general, sediment accumulation was low. On the northwest margin of the Permian Basin, the Pedernal Uplift became active again and expanded southward through the Missourian, potentially linking up with the Diablo Uplift (Diablo Platform) during the latest Virgilian to early Wolfcampian. Local areas along the Matador Arch also experienced renewed uplift, which peaked during the early Wolfcampian. Coarse and fine siliciclastics were shed from the Pedernal Uplift toward the Orogrande Basin to the west and east-southeast toward the Delaware Basin. A trough seems to have existed between the siliciclastics at the northwest margin of the Permian Basin and the midramp carbonates, forming an arc across Eddy County. In general, the siliciclastic input derived from the Pedernal Uplift had a much greater influence on sediments of the Orogrande Basin, where deposition was reciprocal with carbonates and volumetrically dominated by siliciclastics.

During the Missourian and Virgilian, carbonate deposition dominated in the Permian Basin, although volumetrically, shales and/or starved-basin conditions were

more regionally pervasive. For the Missourian, over the entire greater Permian Basin there was a general decrease in carbonate depositional area as compared with the Desmoinesian (figs. 1, 2—Depositional History of the Desmoinesian Succession [Middle Pennsylvanian] in the Permian Basin). This decrease in area suitable for carbonate factories continued through the Virgilian and was driven by two forces—a 2nd-order global transgression, which culminated in the late Missourian to early Virgilian, and highly variable differential basinal subsidence rates.

Missourian carbonate deposition on the Eastern Shelf occurred in a broad zone characterized by shelf-margin carbonates; inner-bank systems; and rare, more basinward, isolated buildups/platforms (fig.1). The area covered by carbonates diminished in the Virgilian and was generally restricted to shelf-margin systems (fig. 2). During both stages of evolution, shelf margins migrated only to the eastern periphery of the Midland Basin, consistent with the margin that developed during the Desmoinesian along the Fort Chadbourne fault system and the proto-Midland Basin (fig. 2). Note that the Eastern Shelf is depicted as carbonate dominated in both reconstructions, thus allowing the basin margin to be more accurately defined. In actuality, the Eastern Shelf system was one of reciprocal carbonate and siliciclastic sedimentation, with siliciclastics generally dominating except at the margin of the Midland Basin. Rates and extents of westward progradation of siliciclastics out of the Fort Worth Basin onto the Eastern Shelf controlled deposition in that area. This progradation was driven by continued uplift erosion and compression in the Fort Worth Basin area by the Ouachita Orogeny.

During the Missourian, the east margin of the CBP and the northern Midland Basin were sites of extensive carbonate deposition and appear to have been linked into a

single, large, isolated platform (fig. 1). On the west margin of the CBP, uplift was occurring on at least two isolated blocks separated by a central area of carbonate deposition. The northern Midland Basin part of the platform was isolated and separated from the Northwest Shelf by the San Simon Channel and an extension of the deeper-water part of the Palo Duro Basin (figs. 1, 4).

During the Virgilian, the CBP became distinct from the northern Midland Basin Platform probably because of increased subsidence in the northern Midland Basin around Gaines County (fig. 2). The northern Midland Basin Platform (Scurry Reef/Horseshoe) atoll exhibited a 2nd-order backstepping and reduction in carbonate depositional area, whereas the CBP prograded. Subregionally, the northern Midland Basin Platform succession had large-scale architectural updip-downdip variation (initiated in the Missourian) in its isolated subplatforms. In general, the platforms trend north-south from stratiform to shingled to mounded, consistent with increased accommodation in the greater Palo Duro Basin (figs. 1, 2).

On the Northwest Shelf, carbonates were being deposited at the shelf margin in a ramp environment as a series of basinward-prograding sigmoidal clinoformal composite sequences. The facies associated with these deposits are subtidal to deep subtidal and are extensively dolomitized. The Northwest Shelf carbonate depositional area appears to have been connected to the west margin of the Palo Duro Basin across the largely inactive Matador Arch (fig.1). Architecturally and facieswise, Virgilian carbonates are much the same as in the Missourian, but the depositional area covered by these units expanded basinward (fig. 2).

Missourian carbonates on the Diablo Platform/Uplift are less extensive in distribution than in the underlying Desmoinesian (fig.1), and shallow- and deeper-water facies are both present. Diablo Platform carbonates also form the south boundary of the incipient Orogrande Basin (fig.1). Phylloid-algal shelf-margin buildups are common along the east fault-bound margin of the Orogrande Basin. During the Virgilian, subsidence increased in the Orogrande Basin, and the Pedernal Uplift experienced heightened activity (fig.2). It is proposed that the southern section of the Diablo Platform was becoming uplifted to the point of erosion of the pre-Pennsylvanian succession and may have contributed siliciclastic sediment into the marginal areas of the Delaware Basin, but that carbonate factories still dominated deposition on the main platform (fig. 2).

KEY CONCLUSIONS

- Missourian and Virgilian sedimentation patterns and distribution reflect dismantling of the Permian Basin into its separate subbasins (Midland, Delaware, Val Verde), each with its own distinct evolutionary history.
- Varied and potentially extreme rates of differential subsidence between and within basins resulted in different architectures and stratigraphic stacking patterns for the same successions.
- Missourian-age units in the Permian Basin reflect a continuation of the 2nd-order transgression established during the Atokan. Virgilian-age sediments reflect deposition in the initial stage of a 2nd-order regression.
- Missourian- and Virgilian-age siliciclastic sedimentation was still relegated to the periphery of the smaller basins. Extensive, basin-centered shale deposition in the

Midland and Delaware Basins is problematic because source areas are limited and no concrete data exist as to the age of the sediments.

- Missourian and Virgilian dominantly shallow water carbonates were deposited around the north, west, and east margins of the Midland Basin, whereas deeper-water carbonates were deposited along the northwest margin of the Delaware Basin. Carbonate depositional environments and systems varied widely within the Midland Basin, as well as between it and the Delaware Basin. Identification of Virgilian deeper-water crinoidal mud mounds on the northern Midland Basin Platform is contrary to historical generalization that the succession is predominantly shallow-water carbonate facies.
- Reservoir quality within the Missourian Midland Basin carbonates is generally linked to extent and duration of exposure events, and 3rd- and 4th-order sea-level falls are crucial to development of reservoir-grade porosity in the carbonate succession. However, this assertion has been historically overemphasized; depositional geometries and facies distribution are equally important, especially in the younger Virgilian succession. In the Midland Basin, long-duration exposure episodes can lead to cementation of the secondary pore network that developed during initial exposure. Long-duration exposure episodes were especially common in the Virgilian succession, where cycle thicknesses are generally less than in the Missourian.
- The northern Midland Basin Missourian and Virgilian carbonate succession highlights the need for continued research into these systems because new models

indicate that this area has a multicomponent architecture of isolated platforms superimposed on a regional ramp system.

REFERENCES

- Becker, J. E., 1990, Dove Creek, South (6500), *in* Vanderhill, A. L., Godfrey, C., B. and Heard, F., eds., Oil and gas fields in West Texas; volume V: West Texas Geological Society Publication, v. 90-86, p. 79–84.
- Blakey, R. C., 2005, Paleogeography and geologic evolution of ancestral Rocky Mountains, *in* GSA Salt Lake City Annual Meeting, p. 442.
<http://jan.ucc.nau.edu/~rcb7/garmgeolhist.html>.
- Brinton, L., Cox, D. M., and Tinker, S. W., 1998, Cored reservoir examples from Upper Pennsylvanian and Lower Permian carbonate margins, slopes and basinal Sandstones, *in* West Texas Geological Society Fall Core Workshop.
- Brown, L. F., Jr., Goodson, J. L., and Harwood, P., 1972, Abilene sheet: The University of Texas at Austin, Bureau of Economic Geology, Geologic Atlas of Texas, scale 1:250,000.
- Brown, L. F., Jr., Solis-Iriarte, R. F., and Johns, D. A., 1990, Regional depositional systems tracts, paleogeography, and sequence stratigraphy, Upper Pennsylvanian and Lower Permian Strata, North- and West-Central Texas: The University of Texas at Austin, Bureau of Economic Geology Report of Investigations No. 197 , 116 p.
- Cleaves, A. W., 1975, Upper Desmoinesian-lower Missourian depositional systems (Pennsylvanian), North-central Texas: The University of Texas at Austin, Ph.D. dissertation, 466 p.
- Cleaves, A., 1993, Sequence stratigraphy, systems tracts, and mapping strategies for the subsurface Middle and Upper Pennsylvanian of the eastern shelf, *in* AAPG Southwest Section Regional Meeting: Fort Worth Geological Society, p. 26–42.
- Cleaves, A. W., 2000, Sequence stratigraphy and reciprocal sedimentation in Middle and Late Pennsylvanian carbonate-bank systems, eastern shelf of the Midland Basin, north-central Texas, *in* Johnson, K. S., ed., Platform carbonates in the southern Midcontinent, 1996 symposium: University of Oklahoma, v. 101, p. 227–257.
- Cleaves, A. W., and Erxleben, A. W., 1982, Upper Strawn and Canyon (Pennsylvanian) depositional systems, surface and subsurface, North-central Texas, *in* Cromwell,

- D. W., ed., Middle and Upper Pennsylvanian System of North-Central and West Texas (outcrop to subsurface): symposia and field conference guidebook: West Texas Geological Society, v. 82-21, p. 49–85.
- Cleaves, A. W., and Erxleben, A. W., 1985, Upper Strawn and Canyon cratonic depositional systems of Bend Arch, north-central Texas, in McNulty, C. I., and McPherson, J. C, eds., Transactions of the AAPG Southwest Section Regional Meeting: Fort Worth Geological Society. p. 27–46.
- Dalziel, I. W. D., Lawver, L. A., Gahagan, L. M., Campbell, D. A., and Watson, G., 2002, Texas through time, plate's plate model: The University of Texas at Austin, Institute for Geophysics,
http://www.ig.utexas.edu/research/projects/plates/movies/Texas_Through_Time_020312.ppt.
- Dickson, J. A. D., and Saller, A. H., 2006, Carbon isotope excursions and crinoid dissolution at exposure surfaces in carbonates, West Texas, U.S.A: Journal of Sedimentary Research, v. 76, no. 3, p. 404–410.
- Dorobek, S. L., and Bachtel, S. L., 2001, Supply of allochthonous sediment and its effects on development of carbonate mud mounds, Mississippian Lake Valley Formation, Sacramento Mountains, South-Central New Mexico, U.S.A.: Journal of Sedimentary Research, v. 71, p. 1003–1016.
- Dutton, S. P., Kim, E. M., Broadhead, R. F., Breton, C. L., Raatz, W. D., Ruppel, S. C., and Kerans, Charles, 2004, Play analysis and digital portfolio of major oil reservoirs in the Permian Basin: application and transfer of advanced geological and engineering technologies for incremental production opportunities: The University of Texas at Austin, Bureau of Economic Geology, and New Mexico Bureau of Geology and Mineral Resources, New Mexico Institute of Mining and Technology, annual report prepared for U.S. Department of Energy, under contract no. DE-FC26-02NT15131, 104.
- Hamlin, H. S., 1999, Syn-orogenic slope and basin depositional systems, Ozona Sandstone, Val Verde Basin, Southwest Texas: The University of Texas at Austin, Ph.D. dissertation, 134 p.
- Hoffacker, B. F. Jr., 1990, Camar, in Vanderhill, A. L., Godfrey, C., B. and Heard, F., eds., Oil and gas fields in West Texas; volume V: West Texas Geological Society Publication, v. 90-86, p. 45–51.
- Hiemstra, E. J., and Goldstein, R. H., 2004, The Indian Basin, New Mexico: a tectonically valved hydrothermal dolomite reservoir, in American Association of Petroleum Geologists Meeting Expanded Abstracts, v. 13, p. 62–63.

- Janson, Xavier, 2007, Day 3: Late Carboniferous (Virgilian) Ice-house cycle architecture and phylloid algae mound development, *in* Kerans, C., Janson, X., and Bellian, J., Linking depositional, diagenetic, facies, stratal geometries and cycle architecture: examples for Paleozoic carbonate systems of West Texas and southern New Mexico: The University of Texas at Austin, Bureau of Economic Geology, RCRL Spring Field Course Guide, p. 63–110.
- Janson, Xavier, and Kerans, Charles, 2007, Day 4: Deeper water mud mounds and crinoidal turbidites—Mississippian Lake Valley Formation, Sacramento Mountains—analogue for Cisco reservoir in SACROC and Cogdell, *in* Kerans, C., Janson, X., and Bellian, J., Linking depositional, diagenetic, facies, stratal geometries and cycle architecture: examples for Paleozoic carbonate systems of West Texas and southern New Mexico: The University of Texas at Austin, Bureau of Economic Geology, RCRL Spring Field Course Guide, p. 111–161.
- Kerans, C., and Anonymous, 2001, Stratigraphic and diagenetic controls on reservoir architecture of a non-reefal icehouse isolated platform: Sacroc Unit, Horseshoe Atoll, Texas, *in* American Association of Petroleum Geologists Southwest Section meeting abstracts, v. 85, no. 2, p. 386–387.
- Kerans, C., and Janson, X., 2005, Deeper water mud mounds and crinoidal turbidites—Mississippian Lake Valley Formation, Sacramento Mountains—analogue for Cisco reservoir in SACROC and Cogdell, *in* Carbonate slopes—the transition for ramps to steep-rimmed margins: examples for the Sacramento and Guadalupe Mountains: The University of Texas at Austin, Bureau of Economic Geology, Reservoir Characterization Research Laboratory Annual Field Trip Guide Book, p. 1–26.
- Kluth, C. F., 1986, Plate tectonics of the ancestral Rocky Mountains, *in* Peterson, J. A., ed., Paleotectonics and sedimentation in the Rocky Mountain region, United States: American Association of Petroleum Geologists, v. 41, p. 353–369.
- Kues, B. S., and Giles, K. A., 2004, The late Paleozoic Ancestral Rocky Mountains System in New Mexico, *in* Mack, G. H., and Giles, K. A., eds., The geology of New Mexico: New Mexico Geological Society, Special Publication 11, p. 137–152.
- Mazzullo, L. J., 1998, Past data goes back to the future: AAPG Explorer, Geophysical Corner, September, Search and Discovery Article # 40045.
- McGookey, D. P., 1990, Tillery (Canyon), *in* Vanderhill, A. L., Godfrey, C., B. and Heard, F., eds., Oil and gas fields in West Texas; volume V: West Texas Geological Society Publication, v. 90-86, p. 183–185.

- Saller, A. H., Dickson, J. A. D., and Boyd, S. A., 1994, Cycle stratigraphy and porosity in Pennsylvanian and Lower Permian shelf limestones, eastern Central Basin Platform, Texas: American Association of Petroleum Geology Bulletin, v. 78, no. 12, p. 1820–1842.
- Saller, A. H., Dickson, J. A. D., and Matsuda, F., 1999a, Evolution and distribution of porosity associated with subaerial exposure in upper Paleozoic platform limestones, West Texas: American Association of Petroleum Geology Bulletin, v. 83, no. 11, p. 1835–1854.
- Saller, A. H., Dickson, J. A. D., Rasbury, E. T., and Ebato, T., 1999b, Effects of long-term accommodation change on short-term cycles, upper Paleozoic platform limestones, West Texas, *in* Harris, P. M., Saller, A. H., and Simo, J. A., eds., Advances in carbonate sequence stratigraphy: application to reservoirs, outcrops and models: Society for Sedimentary Geology (SEPM), v. 63, p. 227–246.
- Saller, A. H., Frankforter, M. J., and Boyd, S. A., 1993, Depositional setting for lowstand carbonates in BC (Canyon) Field, Howard County: American Association of Petroleum Geology Bulletin, v. 77, no. 1, p. 81–89.
- Saller, A. H., Frankforter, M. J., Boyd, S. A., and Livesay, G. A., 1992, Depositional setting of lowstand carbonates in the Midland Basin; BC (Canyon) Field, W. Texas (abs.), *in* American Association of Petroleum Geologists Annual Convention, p. 113.
- Saller, A. H., and Henderson, N., 2001, Distribution of porosity and permeability in platform dolomites: insight from the Permian of West Texas: Reply: American Association of Petroleum Geologists Bulletin, v. 85, no. 3, p. 530–532.
- Saller, A. H., Walden, S., Robertson, S., Nims, R., Schwab, J., Hagiwara, H., and Mizohata, S., 2004, Three-dimensional seismic imaging and reservoir modeling of an upper Paleozoic “reefal” buildup, Reinecke Field, West Texas, United States, *in* Eberli, G. P., Masafarro J. L., and Sarg, J. F. R., eds., Seismic imaging of carbonate reservoirs and systems: American Association of Petroleum Geologists, Memoir 81, p. 107–122.
- Schatzinger, R. A., 1983, Phylloid algal and sponge-bryozoan mound-to-basin transition: a late Paleozoic facies tract from the Kelly-Snyder field, West Texas, *in* Harris, P. M., ed., Carbonate buildups; a core workshop: Society of Economic Paleontologists and Mineralogists, v. 4, p. 244–303.
- Schatzinger, R. A., 1987, Depositional environments and diagenesis of the eastern portion of the Horseshoe Atoll, West Texas: The University of Texas at Austin, Department of Geological Sciences, 340 p.

- Schatzinger, R. A., 1988, Changes in facies and depositional environments along and across the trend of the Horseshoe Atoll, Scurry and Kent counties, Texas, *in* Cunningham, B. K., ed., Permian and Pennsylvanian stratigraphy, Midland Basin, West Texas: studies to aid hydrocarbon exploration: West Texas Geological Society, Publication 88-28, p. 79–105.
- Soreghan, G. S., Engel, M. H., Furley, R. A., and Giles, K. A., 2000, Glacioeustatic transgressive reflux: stratiform dolomite in Pennsylvanian bioherms of the Western Orogrande Basin, New Mexico: *Journal of Sedimentary Research*, v. 70, no. 6, p. 1315–1332.
- Tai, P.-C., 2001, Late Paleozoic foreland deformation in the southwestern Midland Basin and adjacent areas: implications for tectonic evolution of the Permian Basin, west Texas: Texas A&M University, Ph.D. dissertation, 193 p.
- Tai, P.-C., and Dorobek, S. L., 1999, Preliminary study on the late Paleozoic tectonic and stratigraphic history at Wilshire Field, central Upton County, southwestern Midland Basin, West Texas, *in* Grace, D. T., and Hinterlong, G. D., eds., *The Permian Basin: providing energy for America*: West Texas Geological Society, Publication 99-106, p. 19–29.
- Tai, P.-C., and Dorobek, S. L., 2000, Tectonic model for late Paleozoic deformation of the Central Basin Platform, Permian Basin region, West Texas, *in* *The Permian Basin: proving ground for tomorrow's technologies*: West Texas Geological Society, Publication 00-109, p. 157–176.
- Tinker, S. W., Zahm, L. C., Caldwell, D. H., Brinton, L., and Cox, D. M., 2004, Integrated reservoir characterization of a carbonate ramp reservoir, South Dagger Draw Field, New Mexico: seismic data are only part of the story, *in* Eberli, G. P., Masaferrro, J. L., and Sarg, J. F. R., eds., *Seismic imaging of carbonate reservoir and systems*: American Association of Petroleum Geologists Memoir 81, p. 91–106.
- Waite, L. E., 1993, Upper Pennsylvanian seismic sequences and facies of the eastern and southern Horseshoe Atoll, Midland Basin, West Texas, *in* Loucks, R. G., and Sarg, J. F., eds., *Carbonate sequence stratigraphy: recent developments and applications*: American Association of Petroleum Geologists, v. 57, p. 213–240.
- Wahlman, G. P., 2002, Upper Carboniferous-Lower Permian (Bashkirian-Kungurian) mounds and reefs, *in* Kiessling, W., Fluegel, E., and Golonka, J., eds., *Phanerozoic reef patterns*: Society for Sedimentary Geology (SEPM), v. 72, p. 271–338.
- Walker, D. A., Golonka, J., Reid, A., and Reid, S., 1995, The effects of paleolatitude and paleogeography on carbonate sedimentation in the late Paleozoic, *in* Huc, A. -Y.,

- ed., Paleogeography, paleoclimate, and source rocks: American Association of Petroleum Geologists, v. 40, p. 133–155.
- Wilde, G. L., 1990, Practical fusulinid zonation: the species concept with Permian Basin emphasis: West Texas Geological Society Bulletin, v. 29, no. 7, p. 5–14
- Yang, K.-M., and Dorobek, S. L., 1995, The Permian Basin of West Texas and New Mexico: tectonic history of a “composite” foreland basin and its effects on stratigraphic development, *in* Dorobek, S. L., and Ross, G. M., eds., Stratigraphic evolution of foreland basins: SEPM (Society for Sedimentary Geology) v. 52, p. 149–174.
- Yang, W., and Kominz, M. A., 2003, Characteristics, stratigraphic architecture, and time framework of multi-order mixed siliciclastic and carbonate depositional sequences, outcropping Cisco Group (Late Pennsylvanian and Early Permian), Eastern Shelf, north-central Texas, USA: Sedimentary Geology, v. 154, no. 3-4, p. 53–87.
- Ye, H., Royden, L., Burchfiel, C., and Schuepbach, M., 1996, Late Paleozoic deformation of interior North America: the greater ancestral Rocky Mountains: American Association of Petroleum Geologists Bulletin, v. 80, p. 1397–1432.
- Zemkoski, S. S., 1985, Depositional environments and facies distribution of the Millican Carbonate Buildup, Coke County Texas: The University of Texas at Arlington, 162 p.

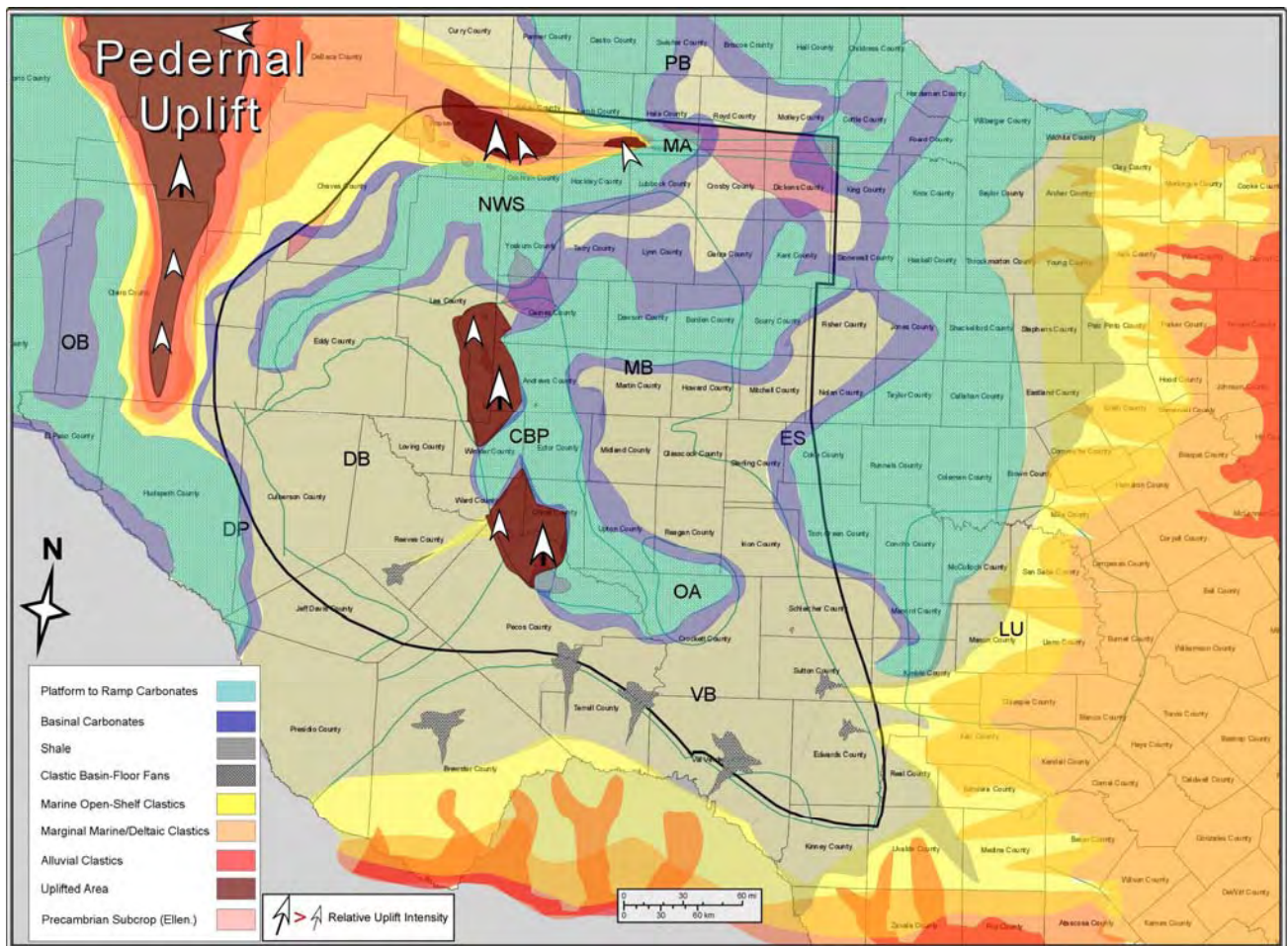


Figure 1. Missourian paleogeography and facies distribution map for the greater Permian Basin region during the early to middle Missourian. Major subregions are outlined by dark-green lines: Central Basin Platform (CBP), Delaware Basin (DB), Diablo Platform (DP), Eastern Shelf (ES), Matador Arch (MA), Midland Basin (MB), Northwest Shelf (NWS), Orogrande Basin (OB), Ozona Arch (OA), Palo Duro Basin (PB), Val Verde Basin (VB), LU (Llano Uplift). The Fort Worth Basin is centered on Wise County. The Llano Uplift area is outlined by the black dashed line. Sizes of arrows surrounding the Pedernal and other uplifted areas correspond to relative amount of uplift (that is, larger arrow, greater relative uplift).

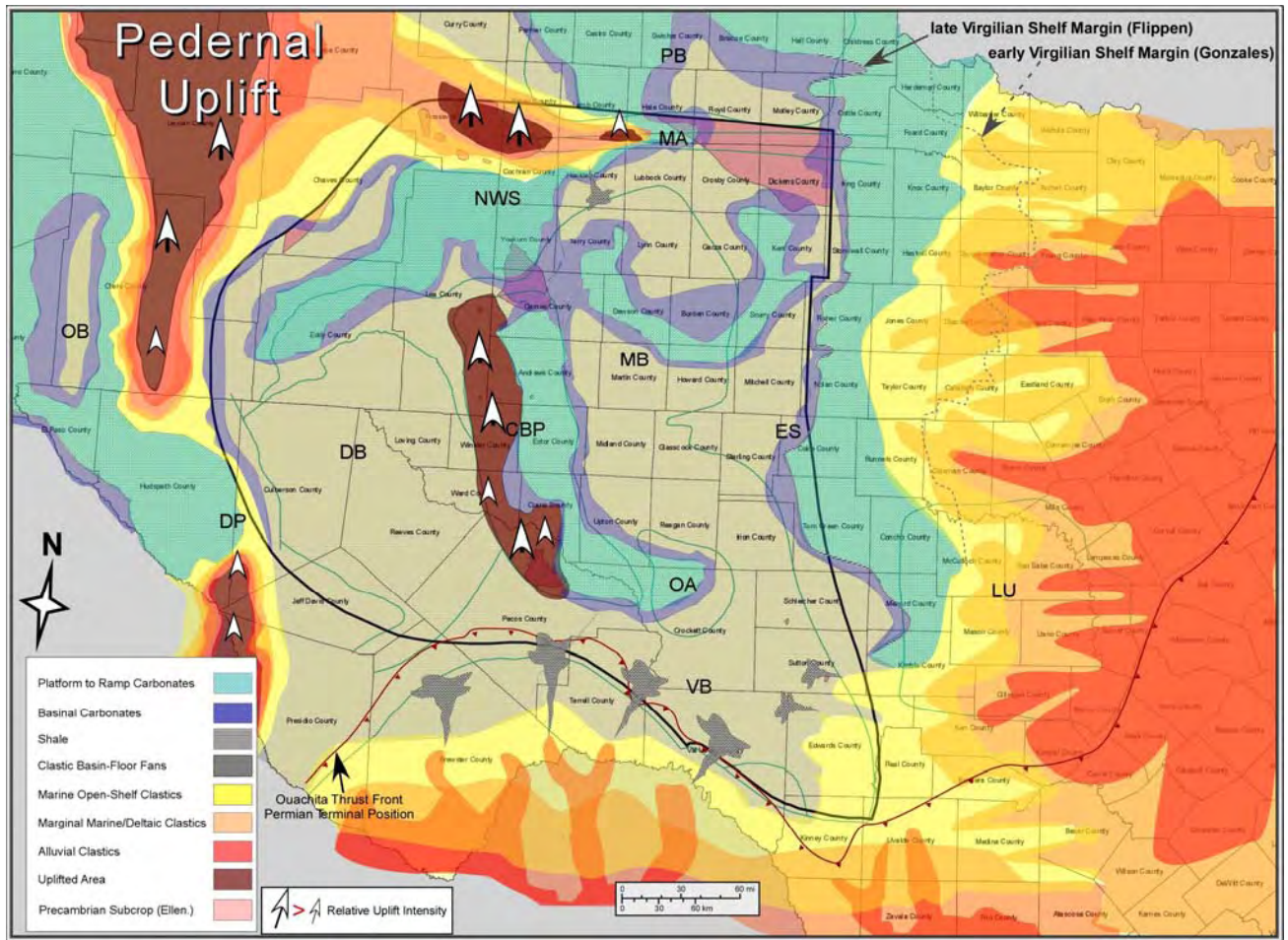


Figure 2. Virgilian paleogeography and facies distribution map for the greater Permian Basin region during the middle to late Virgilian. Major subregions are outlined by dark-green lines; Central Basin Platform (CBP), Delaware Basin (DB), Diablo Platform (DP), Eastern Shelf (ES), Matador Arch (MA), Midland Basin (MB), Northwest Shelf (NWS), Orogrande Basin (OB), Ozona Arch (OA), Palo Duro Basin (PB), Val Verde Basin (VB), and (LU) Llano Uplift. The Fort Worth Basin is centered on Wise County. Sizes of arrows surrounding the Pedernal and other uplifted areas correspond to relative amount of uplift (that is, larger arrow, greater relative uplift).

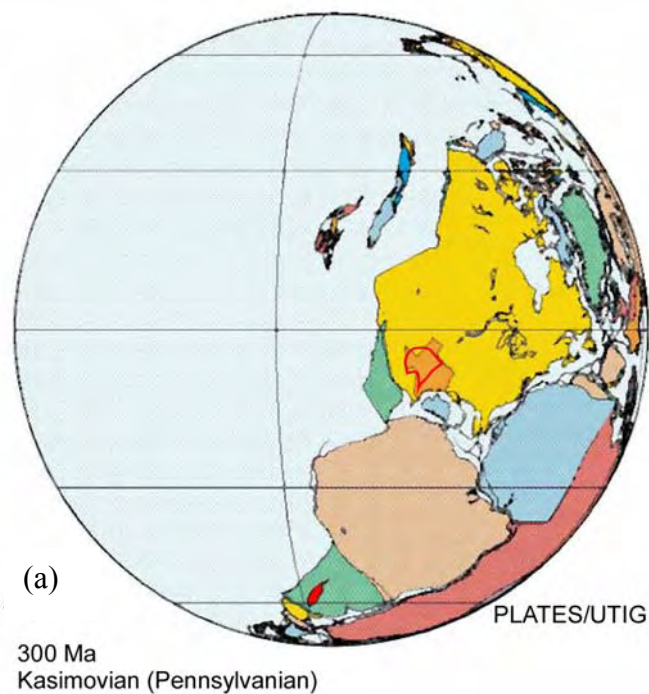
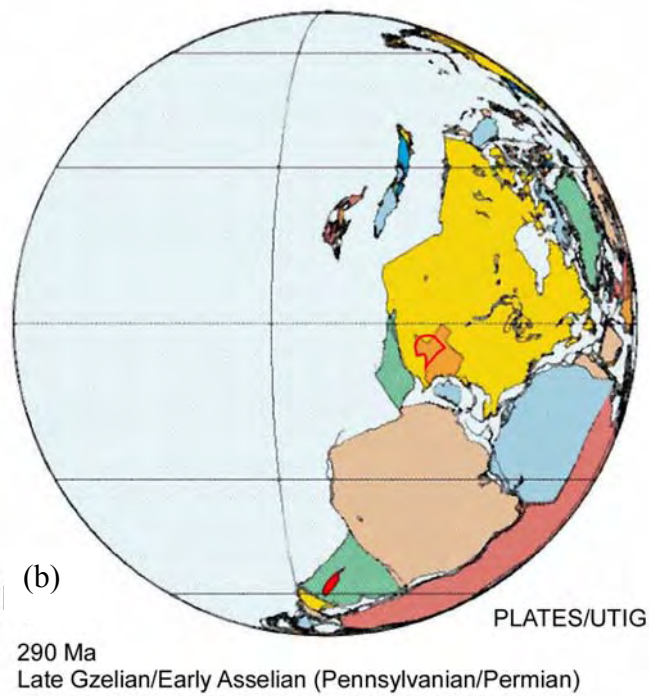


Figure 3. (a) Early Missourian-age (circa 300 Ma) Texas plate tectonic reconstruction. (b) Mid- to late Virgilian age (circa 290 Ma). In these reconstructions, the Permian Basin continues its northward migration (that is, more equatorial) relative to its Desmoinesian position. Diagram modified from Dalziel and others (2002).

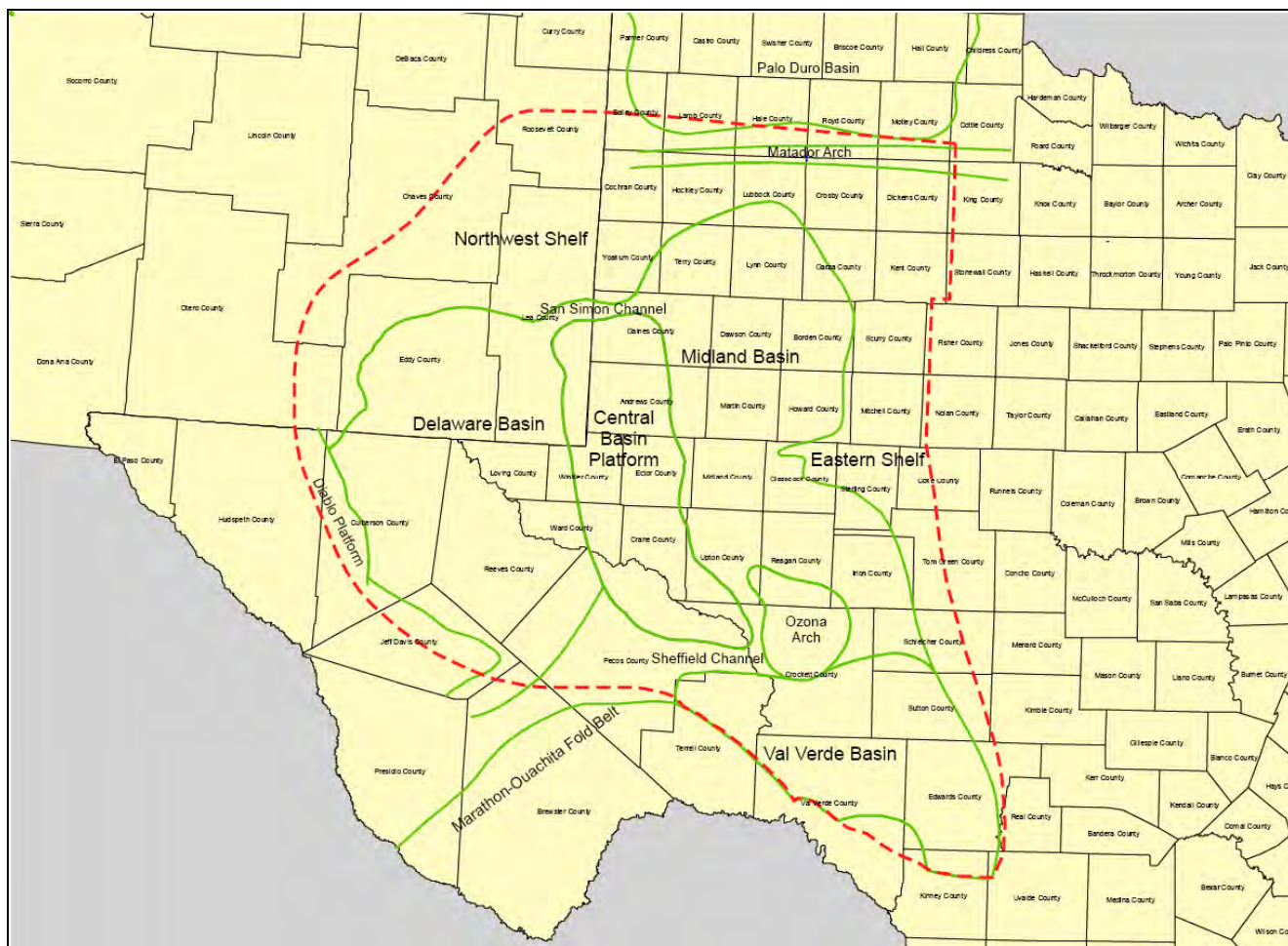
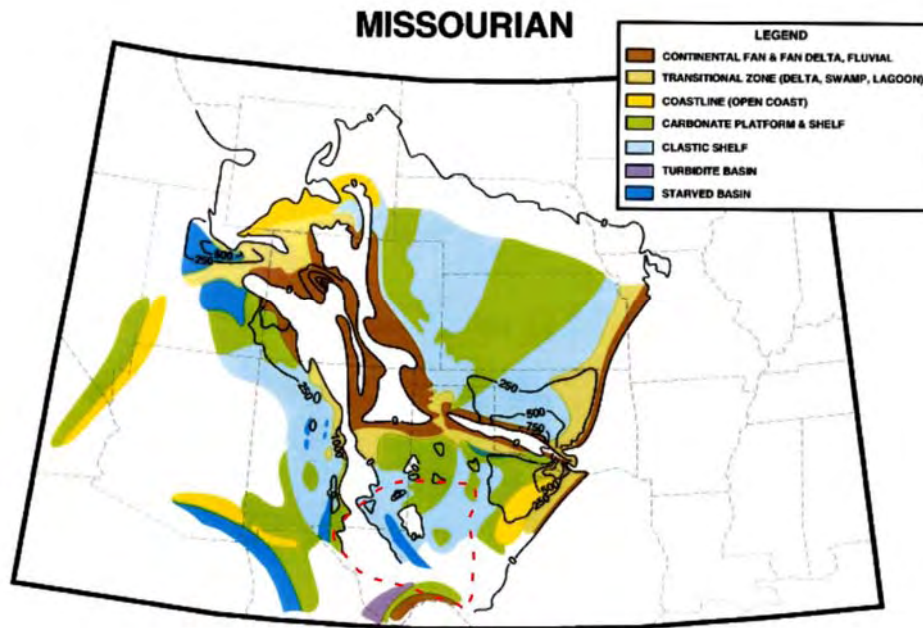


Figure 4. Permian Basin outline (dashed red) and major geologic features. Division of the Permian Basin into its physiomorphic component subbasins and platforms was completed largely by the end of the Missourian. Compare figure 4 with figures 5–7 for previous models of facies distribution relative to the basin outline. Figures 1 and 2 illustrate facies distribution for the greater Permian Basin area derived from this study. The west margin of the Forth Worth Basin runs north-south through Palo Pinto County.

(a)



(b)

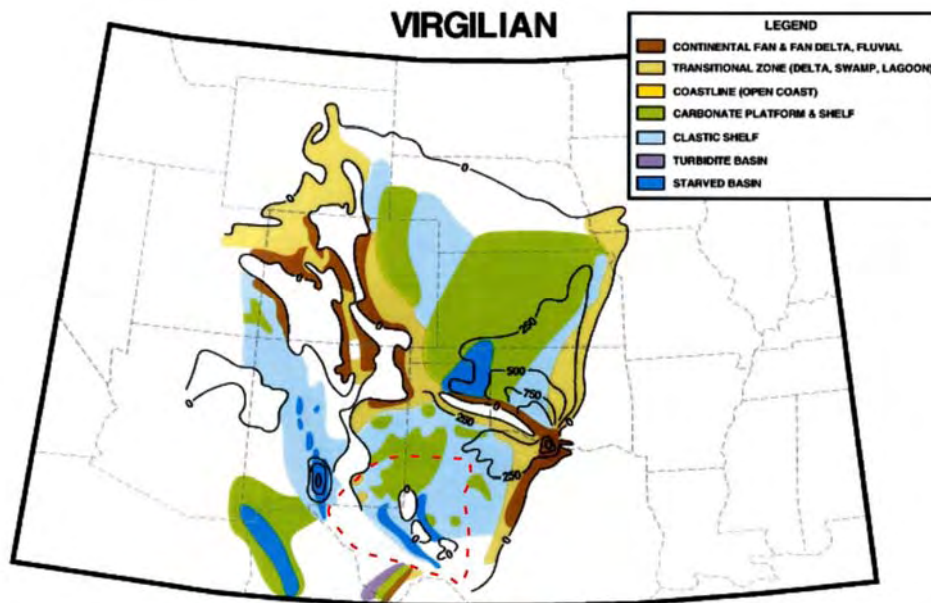
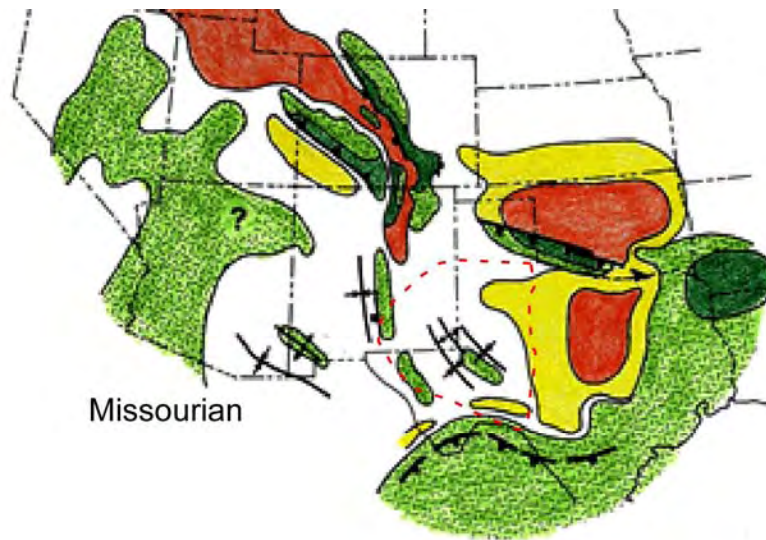
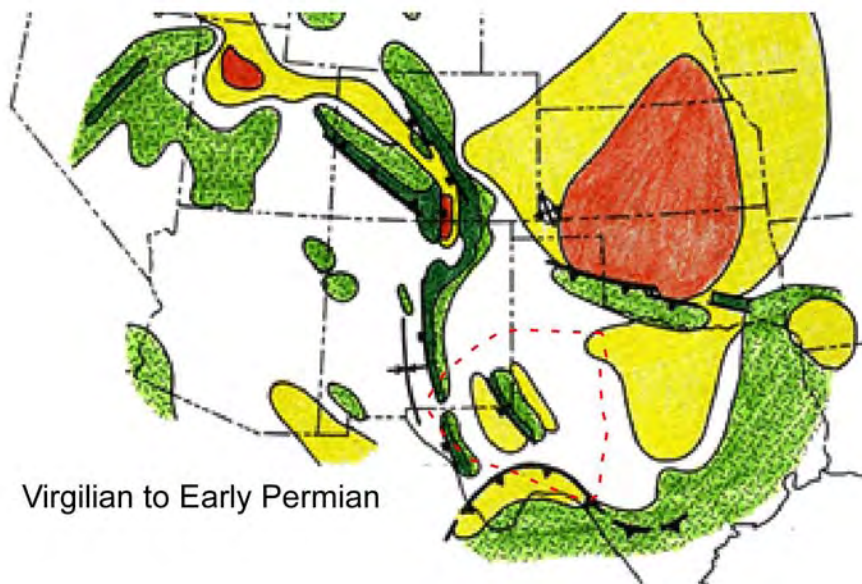


Figure 5. Generalized Rocky Mountain region and southern Midcontinent paleogeography for (a) Missourian and (b) Virgilian stages (from Ye and others, 1996). White areas indicate either nondeposition or erosion (not clarified in the original text). Note that Ye and others (1996) considered the lower half of the Permian Basin (outlined by red dashed polygon) to be either a siliciclastic shelf or an erosionally uplifted area during both the Missourian and Virgilian. Interpretations of the south-east half of the Permian are substantially revised in figures 1 and 2.



Missourian



Virgilian to Early Permian

Figure 6. Areas of net subsidence (white <50 m/Ma to red >300 m/Ma) and net uplift (green <50 m/Ma) for the Missourian and Virgilian (after Kluth, 1986). These interpretations show overall net subsidence for the Permian Basin except in the area of the Central Basin Platform, which appears to enlarge from the Missourian to the Early Permian.

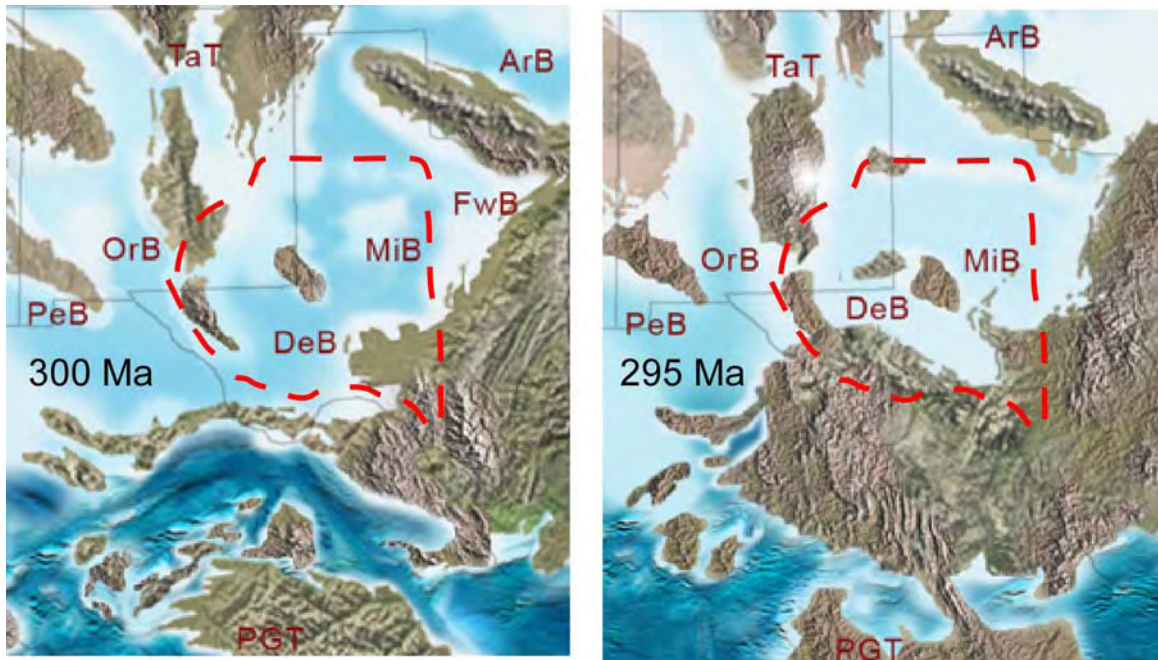


Figure 7. Regional paleogeography for the Missourian (circa 300 Ma) and Virgilian (circa 295 Ma). DeB and MiB refer to Delaware and Midland Basins, respectively. Permian Basin outlined by red dashed polygon. Anadarko Basin (ArB), Fort Worth Basin (FwB), Orogrande Basin (OrB), Pedregosa Basin (PeB), Taos Trough (TaT). Uplifted areas represented by browns, shallow marine by light- to medium-blues and deep marine by dark-blue (from Blakey, 2005). Note extensive increase in exposed landmass in the south part of the Permian Basin from the Missourian to the Virgilian (proposed time span of 5 Ma).

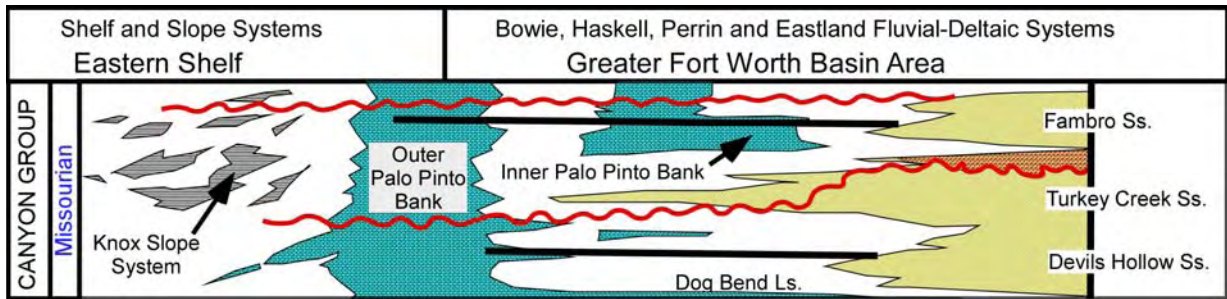


Figure 8. Chrono-, litho-, and sequence stratigraphy of the Canyon Group. In areas of more fixed and continuous carbonate deposition, a Canyon Platform interval is placed between the Palo Pinto bank system and the Home Creek limestone. Figure modified from Cleaves (1993, 2000).

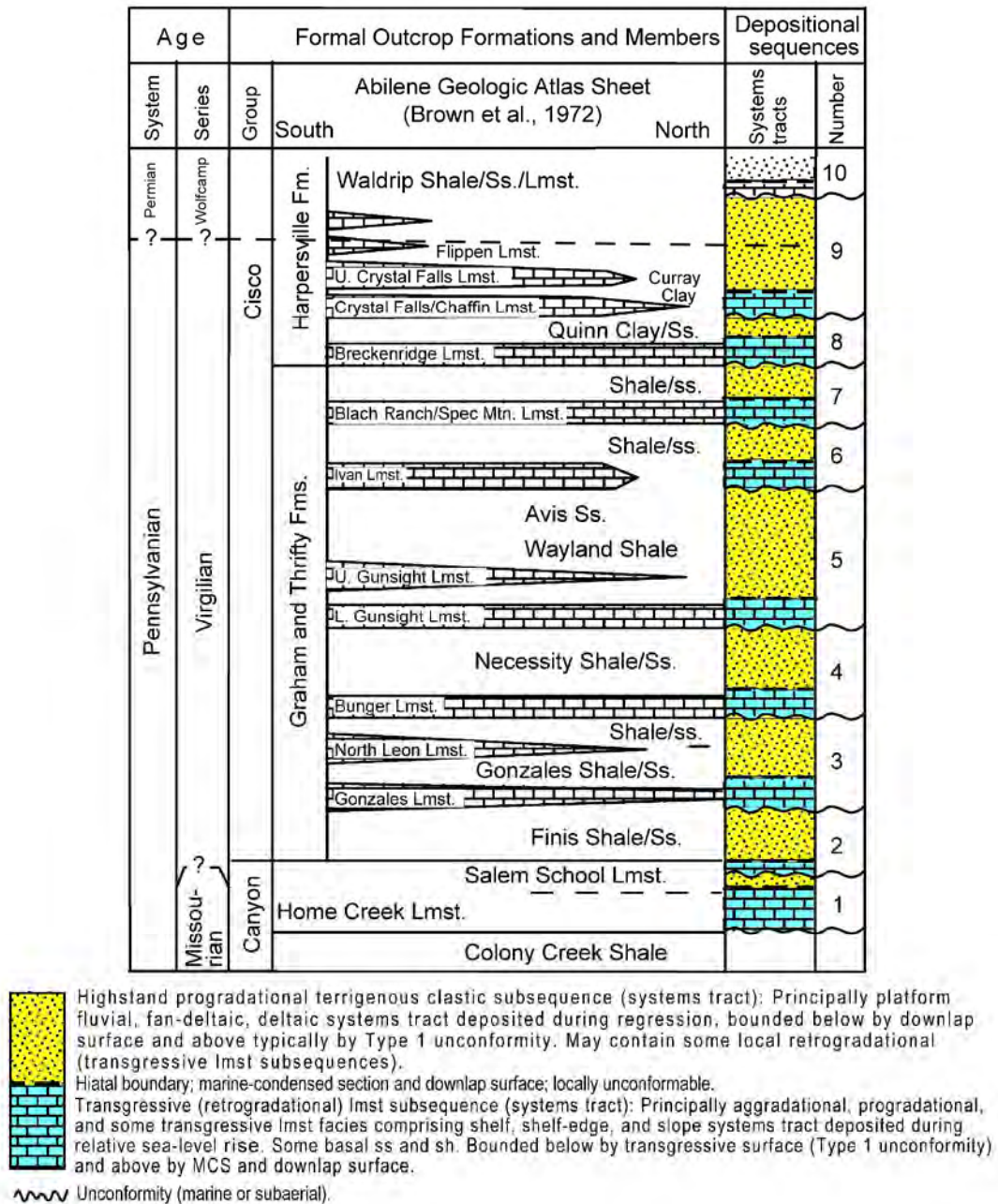


Figure 9. Chrono-, litho-, and sequence stratigraphy of the Cisco Group in a north-south orientation across the Eastern Shelf. Figure modified from Yang and Kominz (2003). Note dominance of highstand progradational siliciclastic systems tracts in the Virgilian when compared with the underlying Missourian succession. These tracts commonly contain facies from fluvial, fan-delta, and deltaic depositional environments.

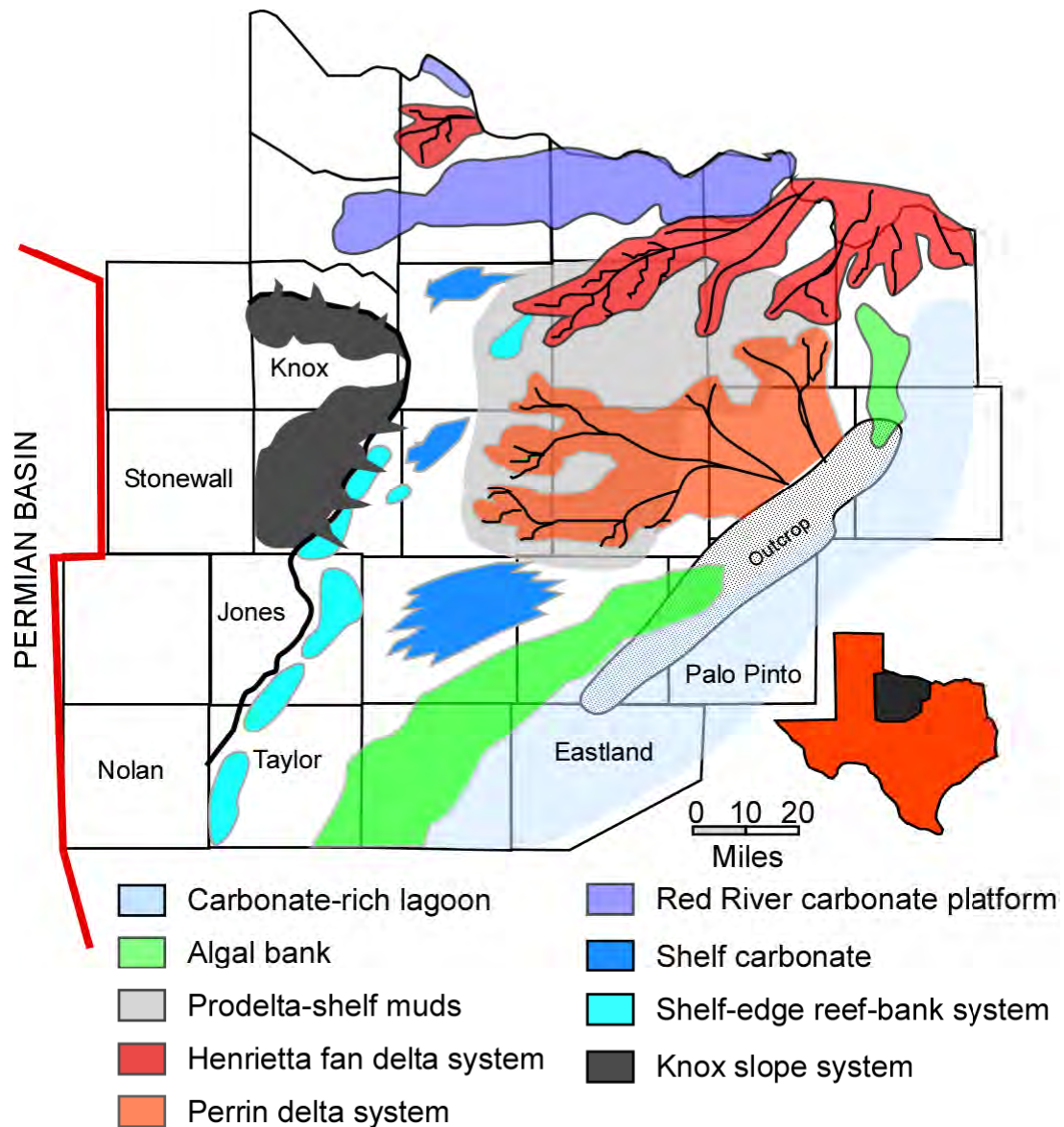


Figure 10. Mid-Canyon-age depiction of depositional environments and paleogeography of North-Central Texas (Eastern Shelf to Fort Worth Basin). Note that coarse or fine siliciclastic sediments are not reaching the Permian Basin (east margin—thick red line). The proposed Missourian-age Knox Slope System is generally confined to Knox and Baylor Counties. After Cleaves (2000).

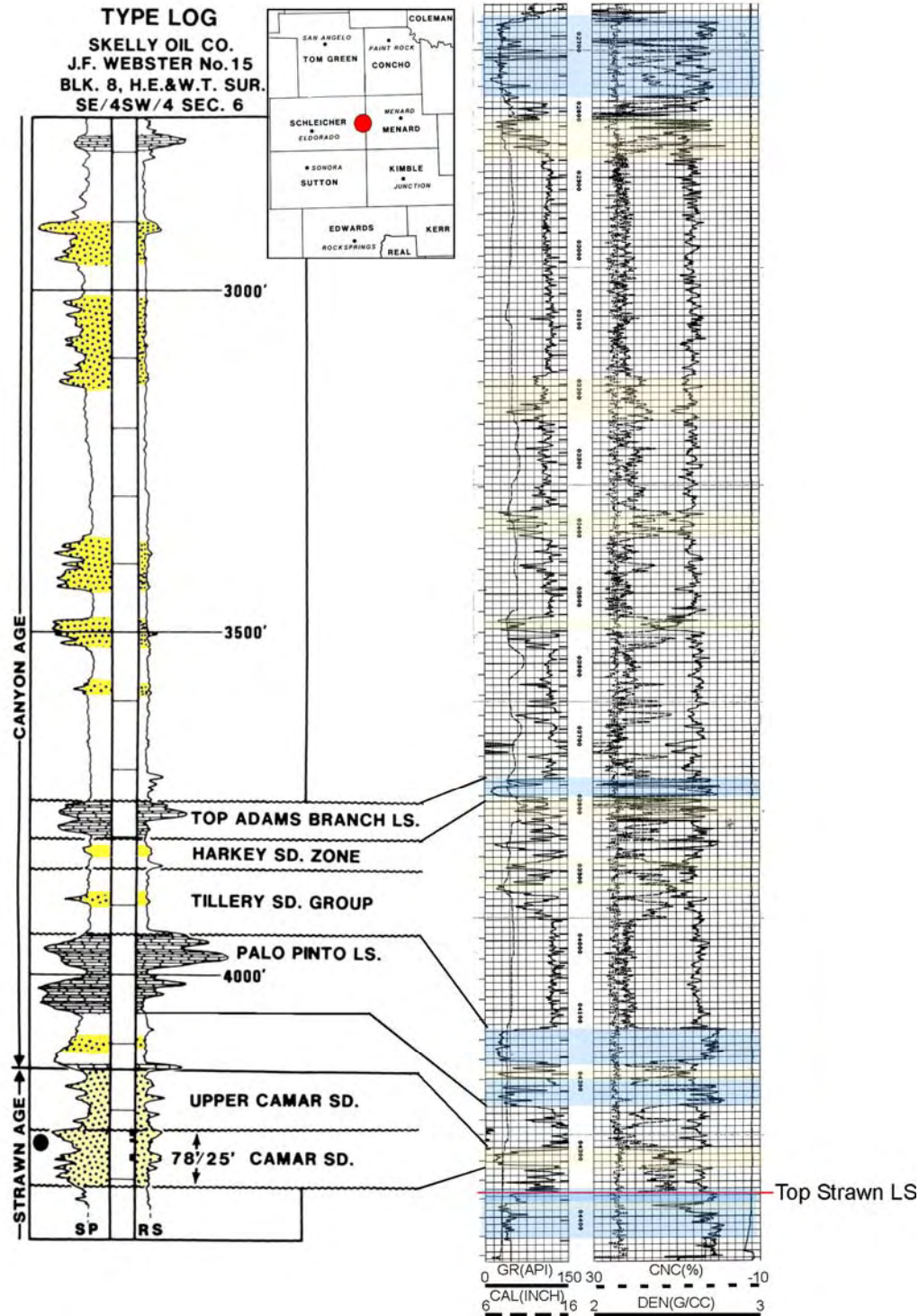


Figure 11. Regional location map of Camar field and type wireline log of Eastern Shelf Missourian sandstone succession on both SP- and GR-based well logs. After Hoffacker (1990). Note that the Adams Branch limestone is a local unit occurring between the Palo Pinto and Home Creek Formations and is not defined in figures 8 or 9.

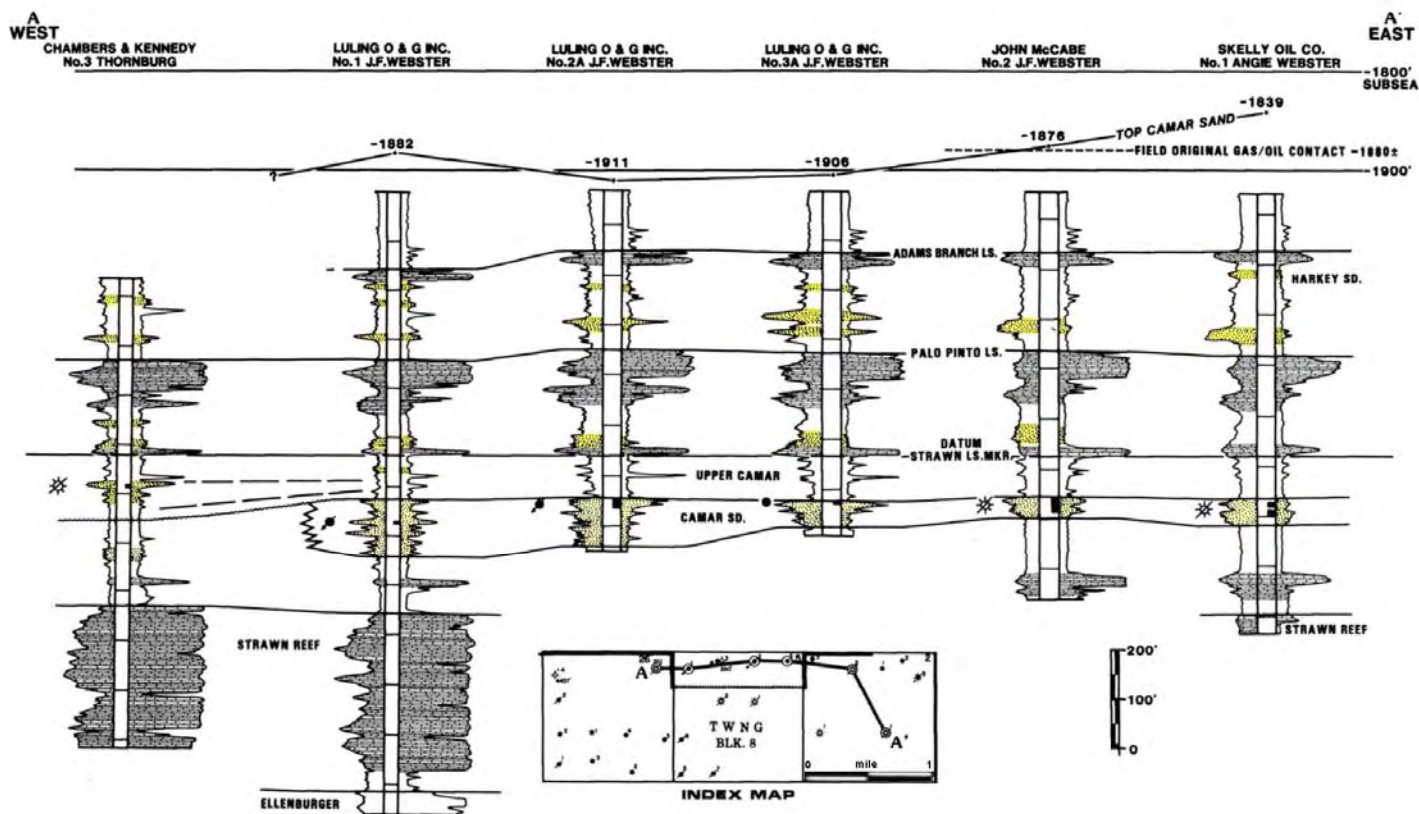


Figure 12. Regional cross section of the Missourian sandstone succession on the Eastern Shelf. Note apparent lateral continuity of sandstone bodies across several miles. Presence of underlying Desmoinesian “Strawn Reef” and overlying Palo Pinto Limestones indicates a true Missourian age for Camar sandstones.

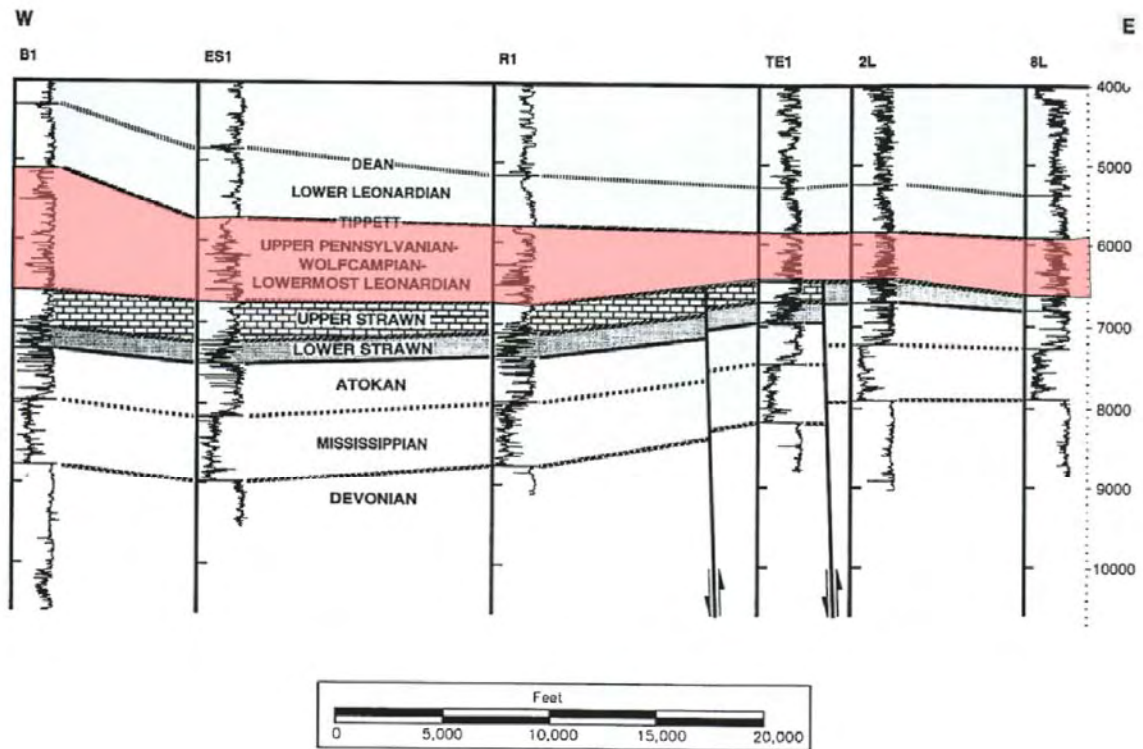


Figure 13. Regional well cross section of Wilshire field, Upton County (after Tai and Dorobek, 1999). Note dominantly shaly wireline-log signature and lack of differentiation in post-Strawn (Desmoinesian) to Leonardian succession.

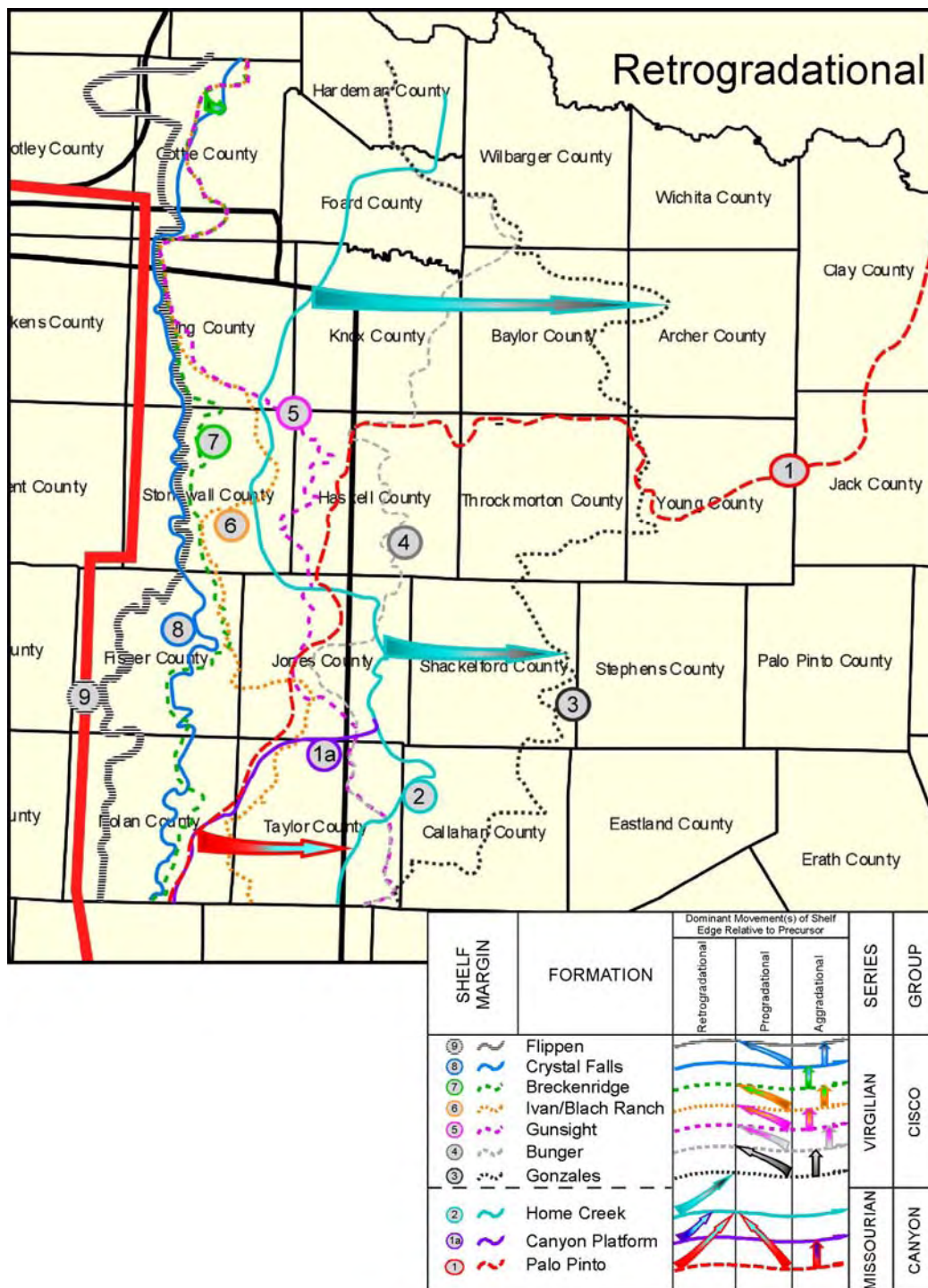
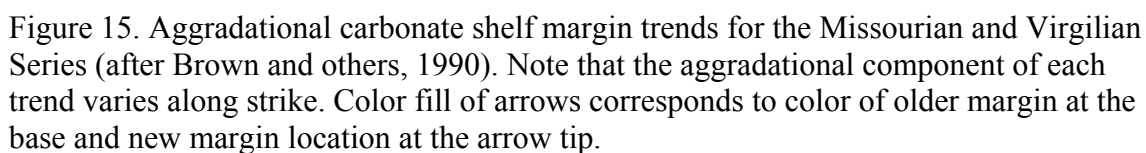


Figure 14. Retrogradational carbonate shelf margin trends for the Missourian and Virgilian Series (after Brown and others, 1990). Large-scale backstepping and retrogradation are largely restricted to the Missourian Series. Color fill of arrows corresponds to color of older margin at the base and new margin location at the arrow tip.



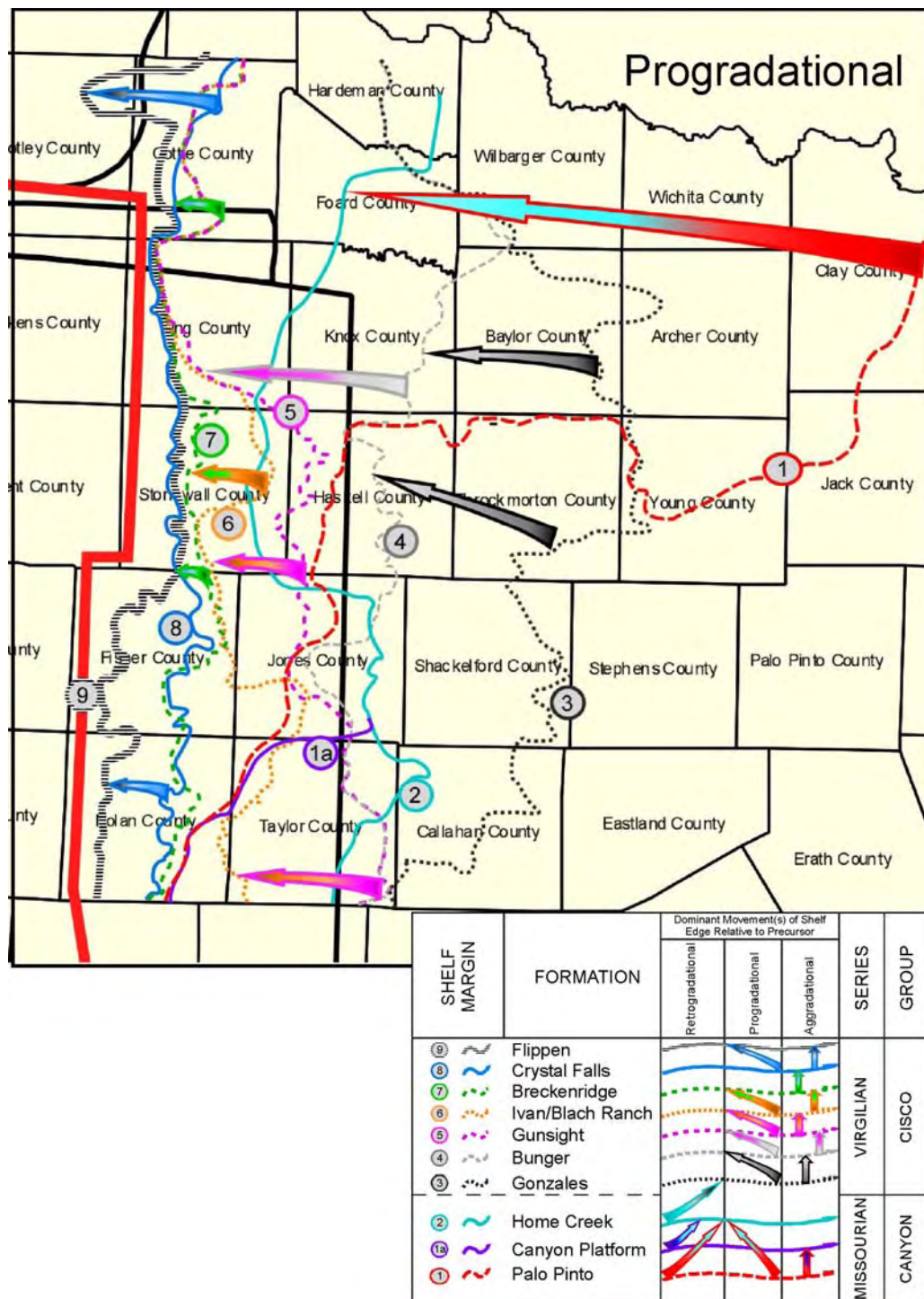


Figure 16. Progradational carbonate shelf margin trends for the Missourian and Virgilian Series (after Brown and others, 1990). Note that shelf margin 9 (Flippen Formation) does not pass into the Permian Basin (as defined by this study). Siliciclastic sediments are trapped largely behind this margin during the Virgilian.

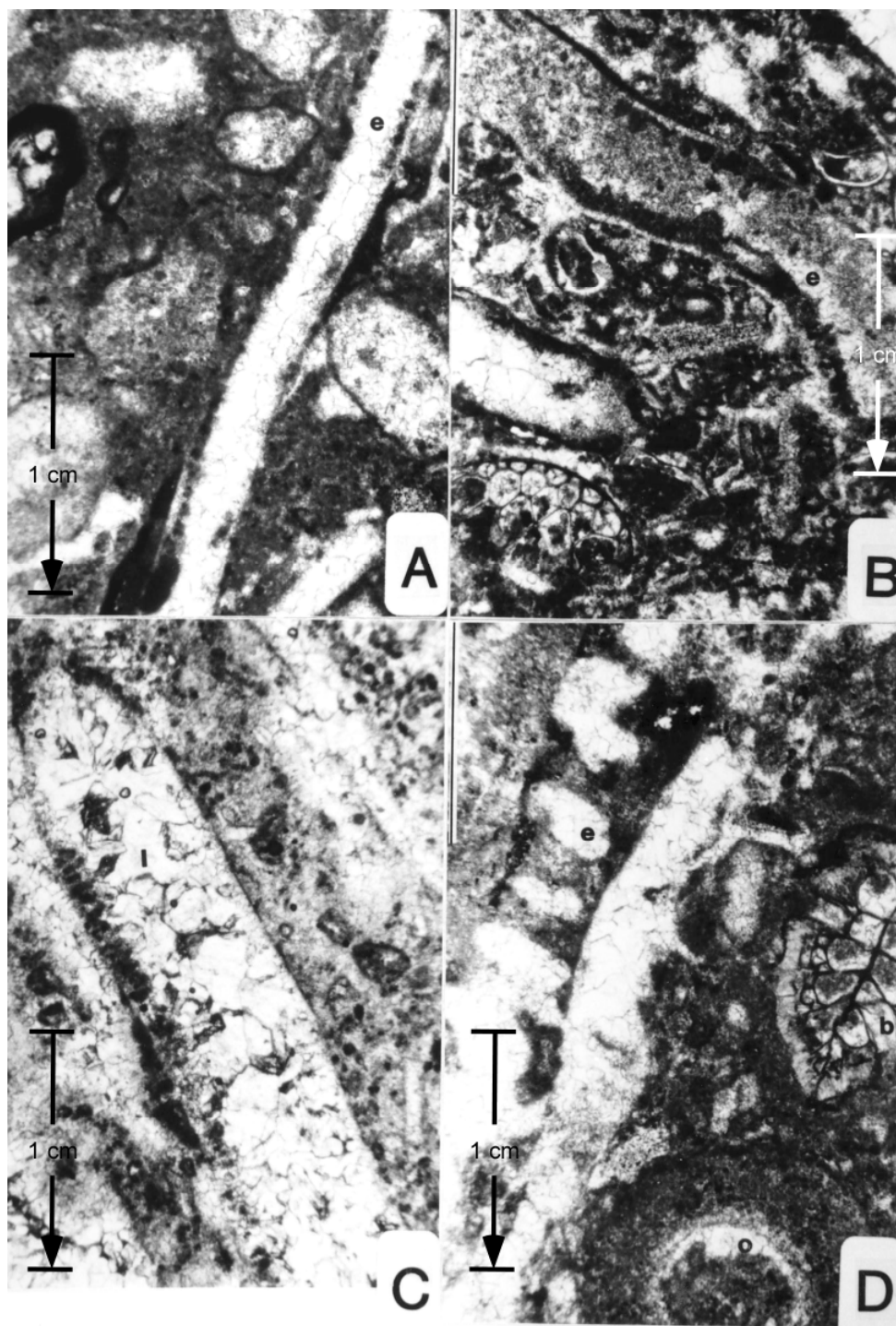


Figure 17. Photomicrographs of calcareous algae within phylloid-foram wackestones. A. and B. Phylloid algae *Eugonophyllum* (e). C. Phylloid; cf. *Ivanovia* (I) in pelletal microspar. D. Dasycladacean algae *Epimastopora* (e) with an oncolite (o) and a bryozoan (b); cf. *Rhombopora*. After Schatzinger (1987).

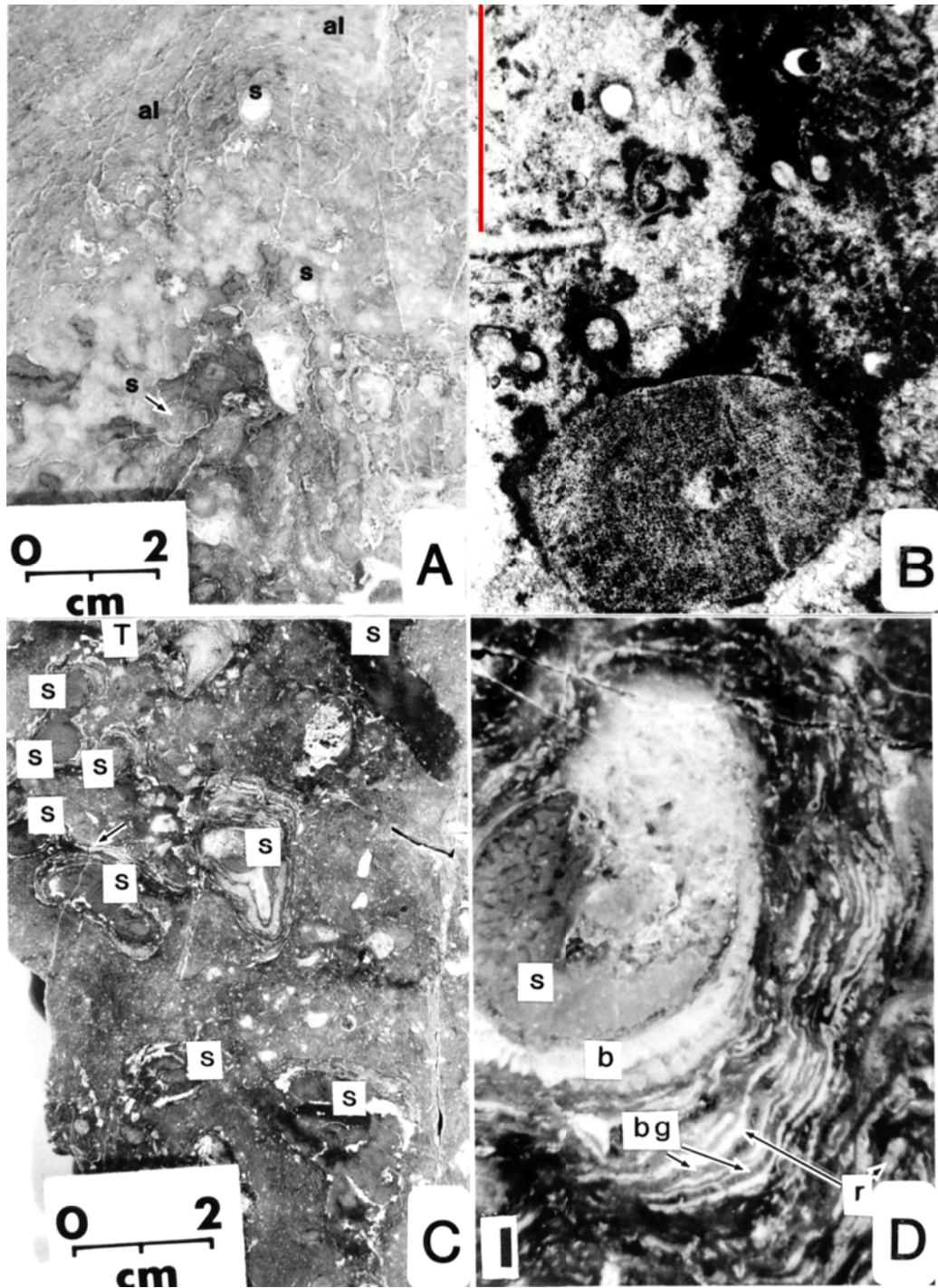


Figure 18. Core slab photos and photomicrographs of sponge-algal-bryozoan boundstone assemblage. A. Calcareous sponges (s) bound together by algal laminae (al). B. Crinoid ossicle and ostracods bound to pelletal micrite lumps. C. Core slab photograph of mound core illustrating numerous encrusted calcareous sponges and *Tubiphytes*. D. Composite rhodolith from C displaying sequential growth by calcareous sponge (s), bryozoa (b), blue-green alga (bg), and red alga (r). After Schatzinger (1987).

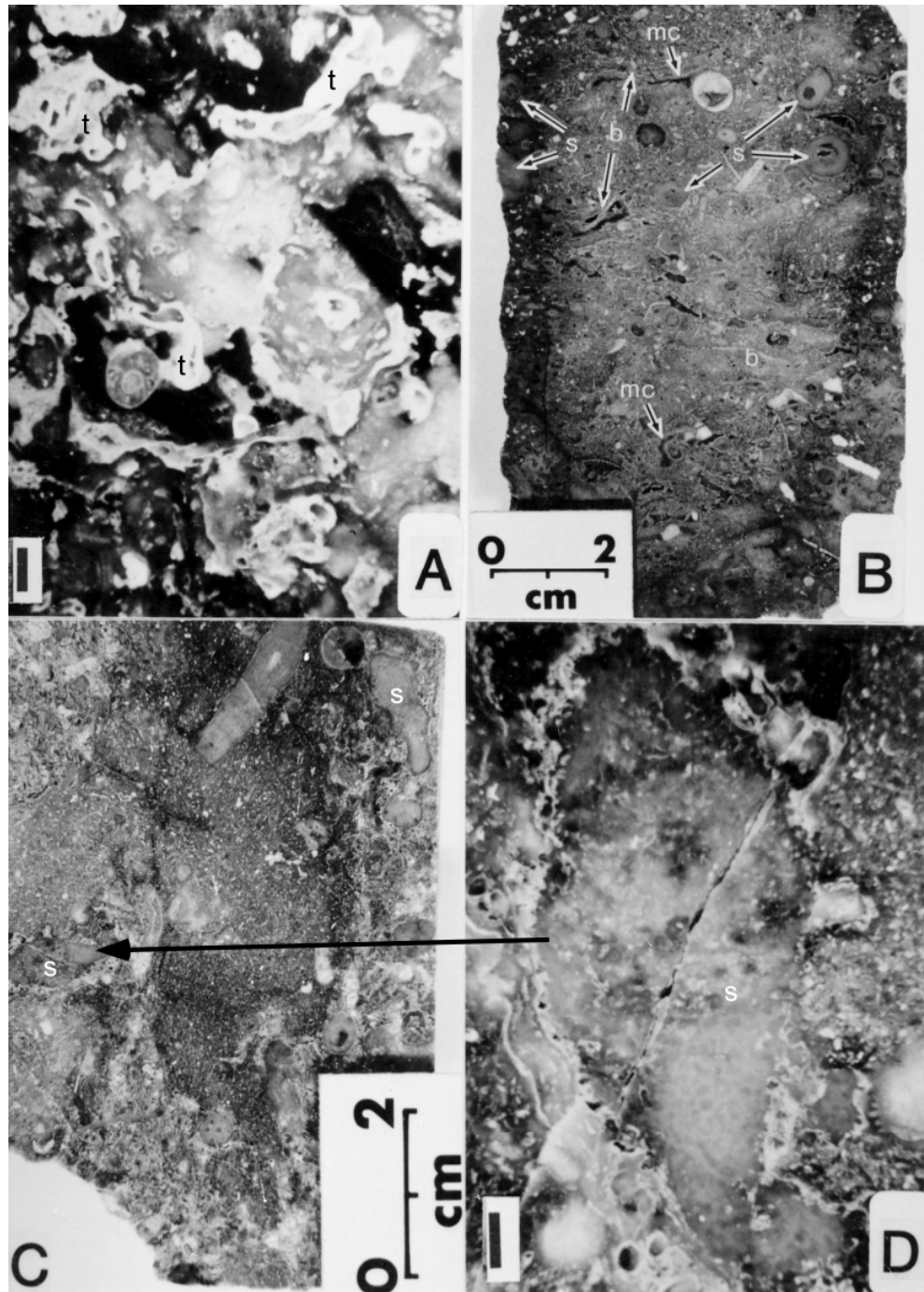


Figure 19. Core slab photos and photomicrographs of sponge-mound facies.
 A. *Tubiphytes* (t) boundstone (*Tubiphytes* binding and encrusting micritic lumps and large benthic forams). B. Porous sponge-bryozoan mound flank facies with abundant sponges (s) and bryozoan debris (b), algal coated and stabilized by marine cement (mc).
 D. Enlarged photo of C highlighting encrustation by algae and forams. After Schatzinger (1987).

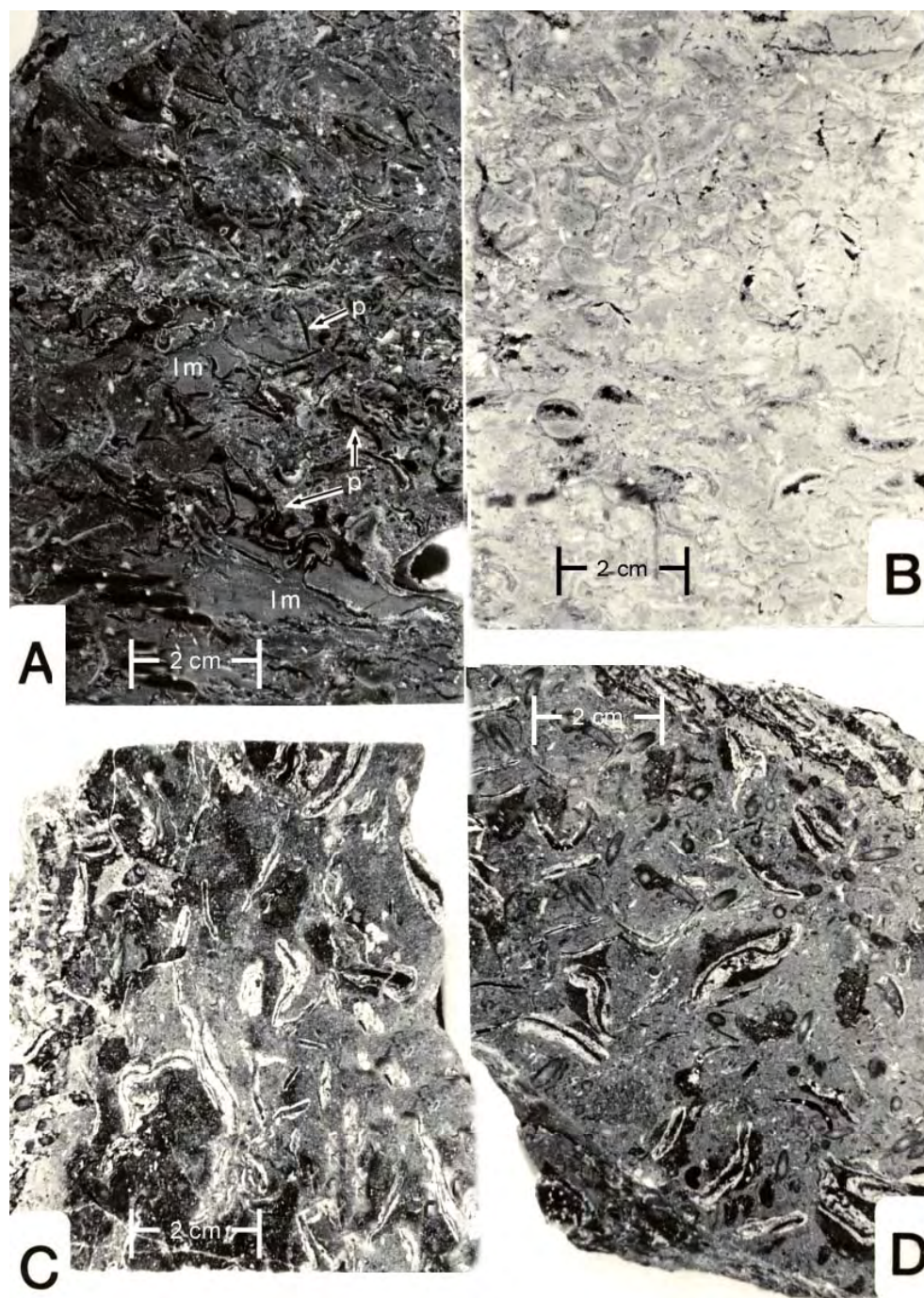
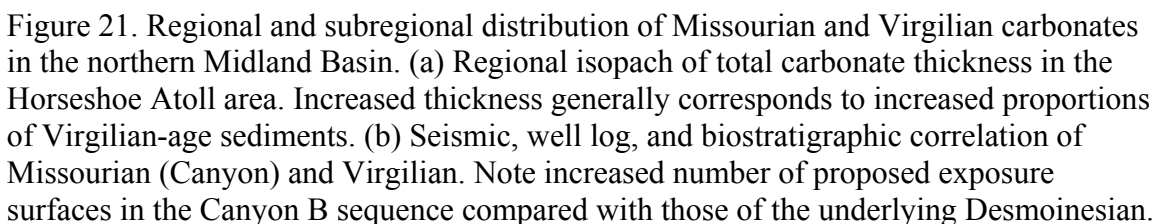


Figure 20. Core slab photographs of algal-mound facies. A. Laminated micrite (lm) deposited with and baffled by phylloid thalli (p), resulting in occlusion of shelter porosity. B. Porous phylloid-foram wackestone with porosity in partly filled brachiopods and leached phylloid thalli. C and D. Nonporous phylloid-foram wackestone with thick foram-algal encrustation (light) on phylloid thalli (dark). After Schatzinger (1987).



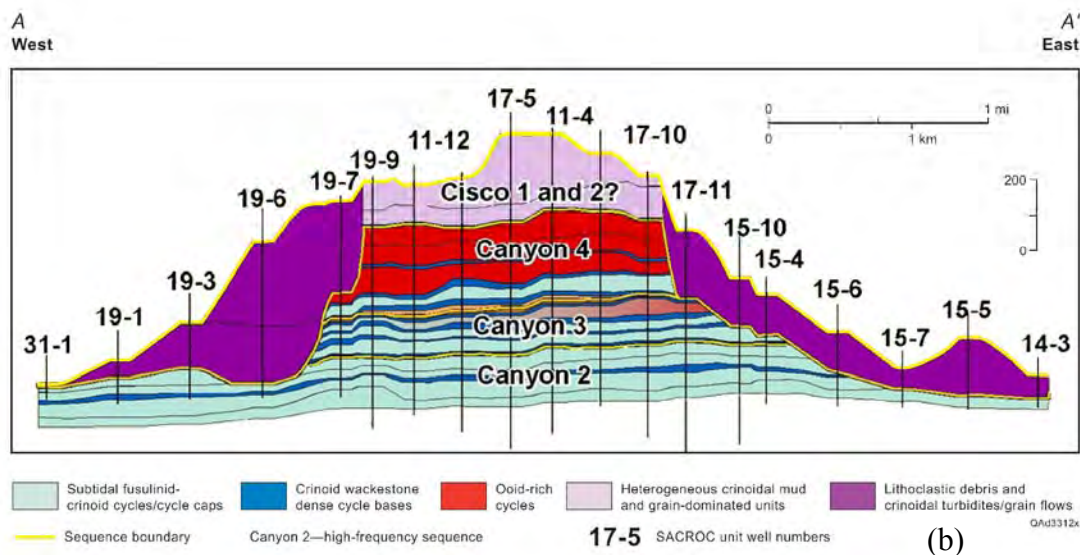
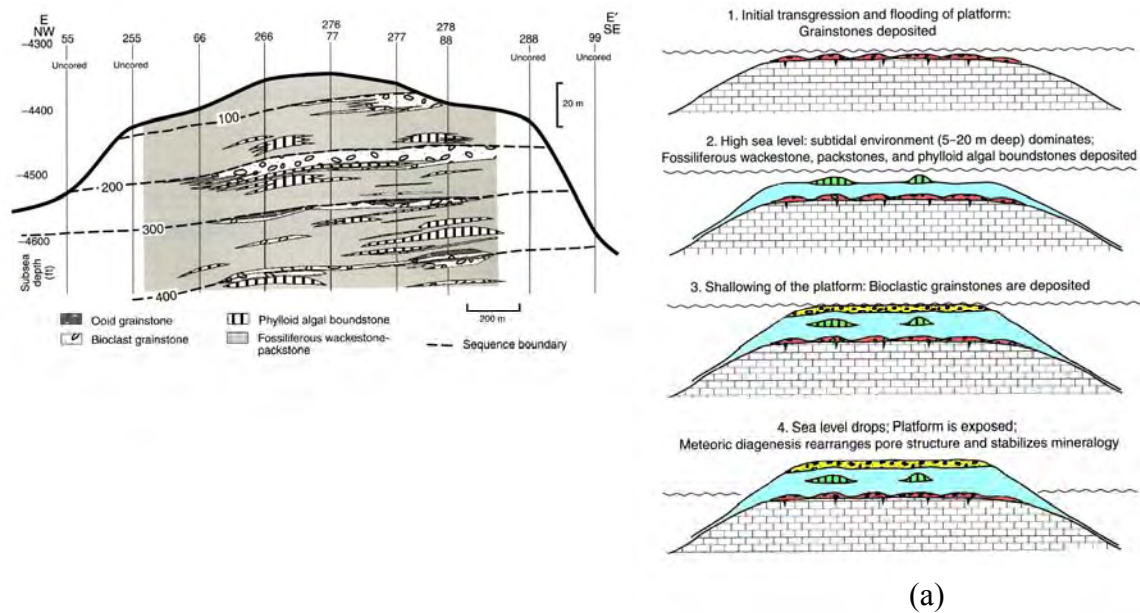


Figure 22. Facies architecture, distribution and evolution diagrams for Reinecke field (a) and SACROC (b) (after Saller and others, 2004, and Dutton and others, 2004). Upper two illustrations depict proposed stratiform depositional architecture and evolution of Virgilian-age carbonates at Reinecke field (after Saller and others, 2004). Note that although >300 ft of topography is expressed at the margins of the platform, the architecture is still proposed to be stratiform even at the margins. (b) Illustration of facies depositional architecture and evolution of Missourian- and Virgilian-age carbonates at SACROC (after Dutton and others, 2004). Note that at the margins of the platform, lithoclastic debris and crinoidal turbidites drape the structures. Also, Cisco 1 and 2 successions contain crinoidal mud mounds.

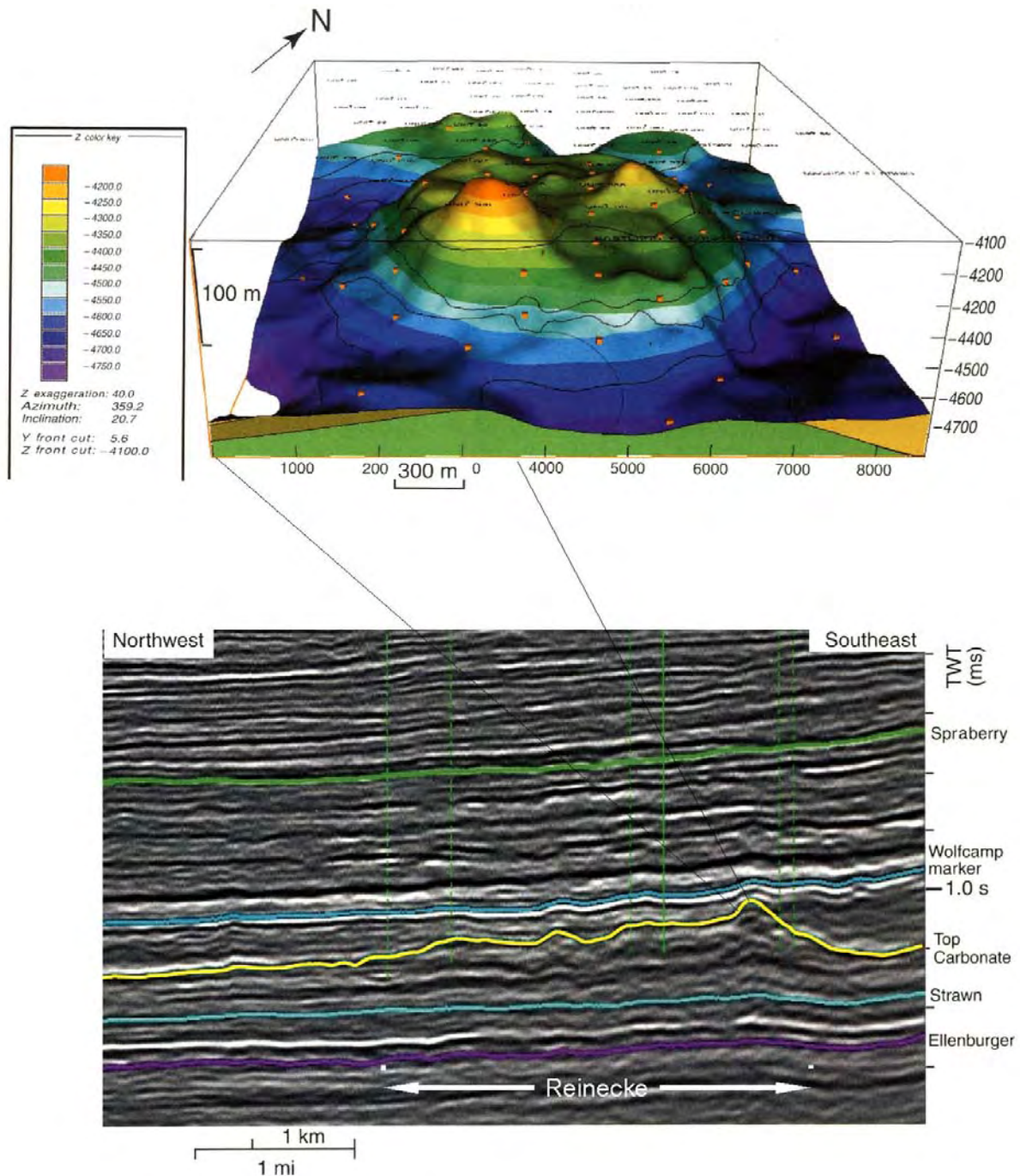


Figure 23. Regional seismic line through Reineke field (bottom) with inset of the South Dome area, top Virgilian carbonate structural map, based on seismic and well logs. Note that the inset is rotated relative to regional seismic (after Saller and others, 2004). This figure illustrates irregularity of the top Virgilian carbonate surface at both local (<300 m) and regional scale (<3 km).

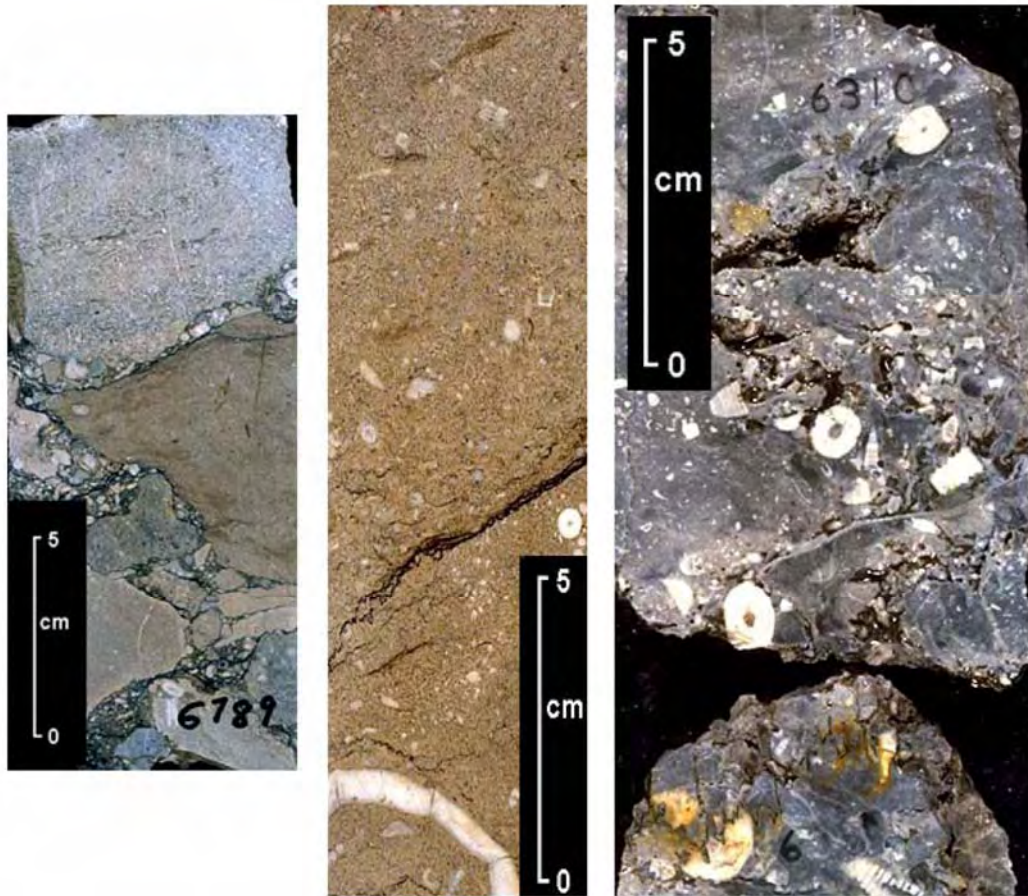


Figure 24. Core slab photos of typical Virgilian (Cisco) facies. Left photograph is a debris flow containing large lithoclasts and crinoidal debris. Middle image is crinoidal turbidite with steeply dipping beds to the left. Right photograph illustrates a stromatactid mud-mound facies with abundant, large, crinoid debris. After Janson and Kerans (2007).

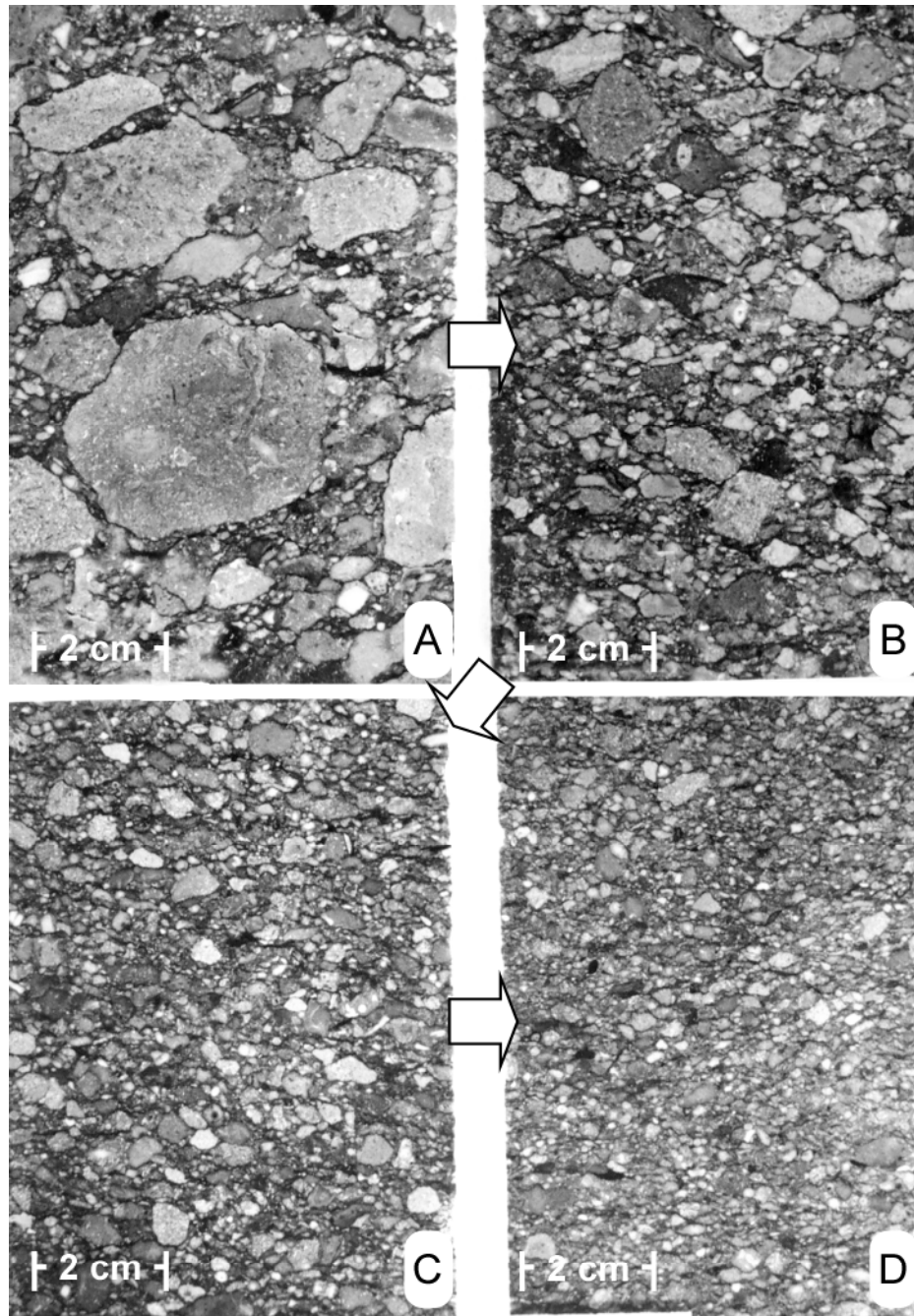


Figure 25. Core slab photographs of lithoclastic debris-flow breccias. A. Coarse base of flow at 2,061 m. B. Moderately coarse middle of flow at 2,059 m. C and D. Upper finer grained parts of the flow at 2,058 and 2,056 m. Note overall upward-fining nature of the sequence. After Schatzinger (1987).

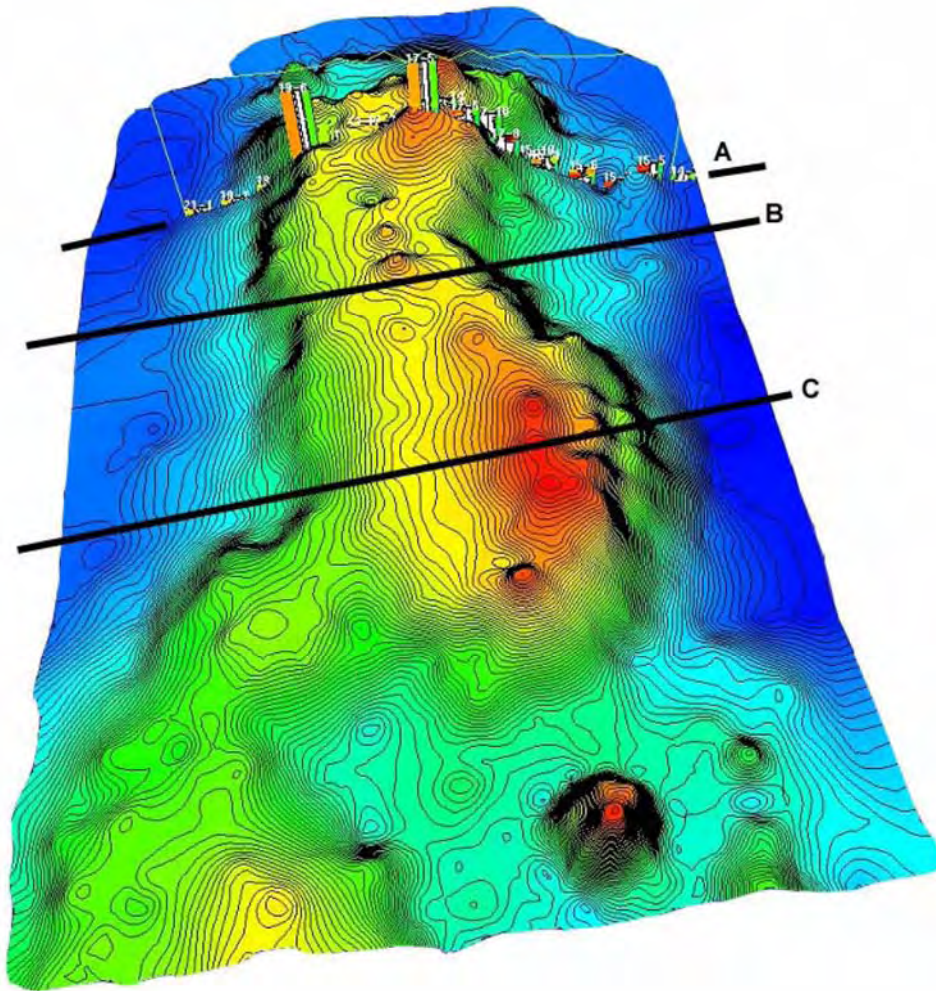


Figure 26. Structure-contour map of the top Virgilian (CISCO) carbonate at SACROC. Note change in architectural style from flat in the south (near C) to more rugose, narrow, and irregular to the north (near A). After Janson and Kerans (2007).

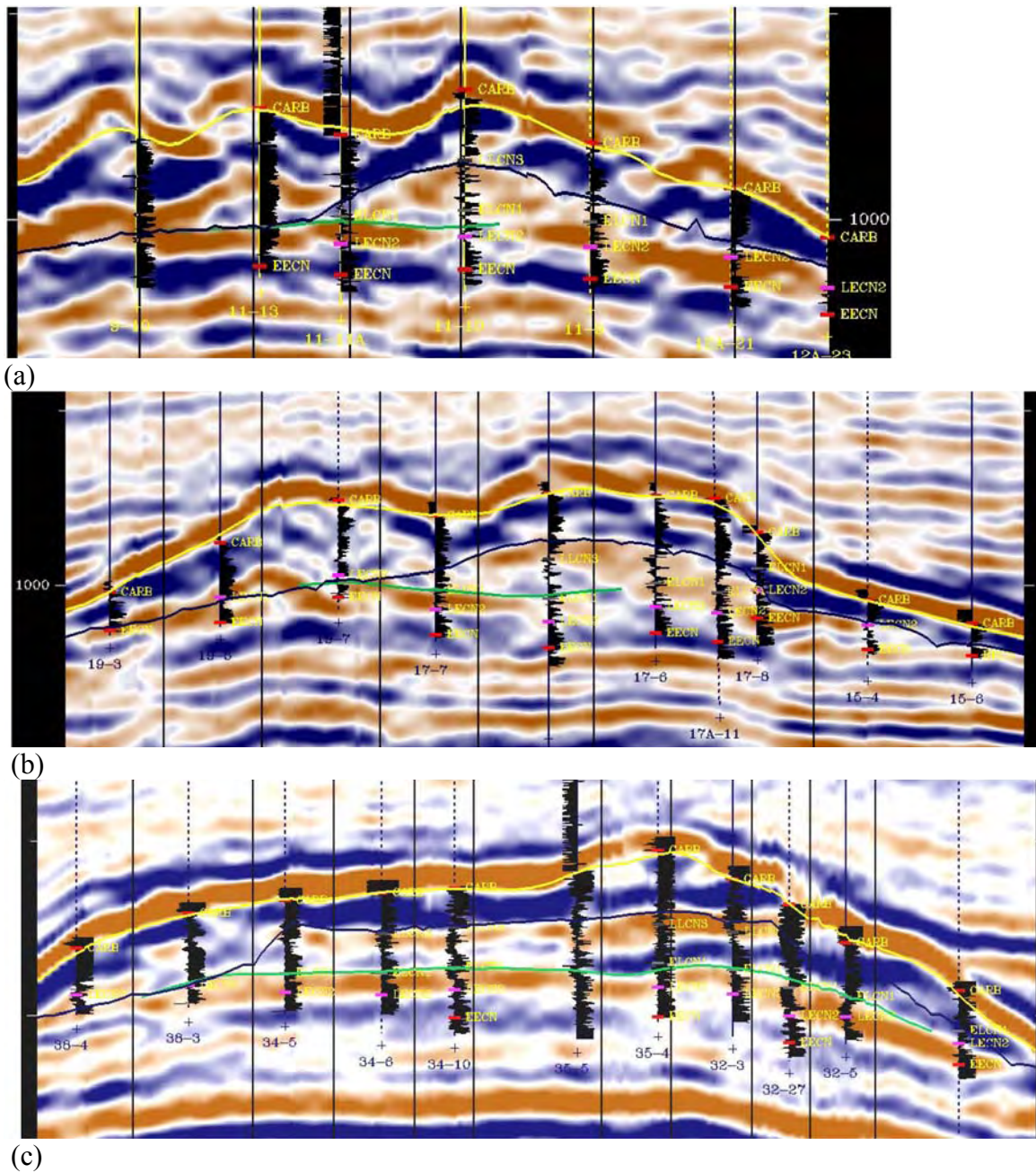
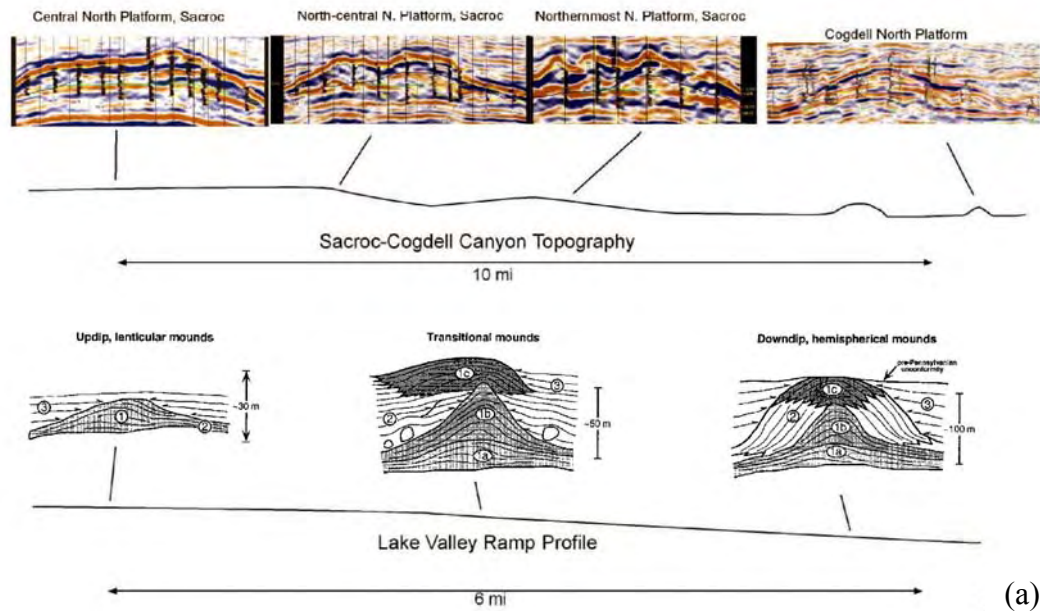
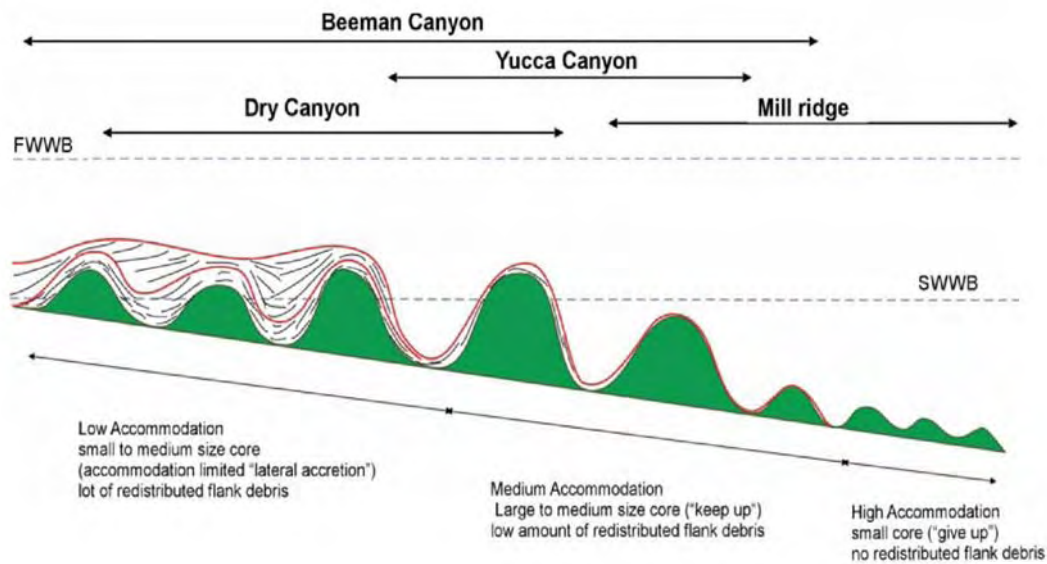


Figure 27. Seismic, cross-sectional profiles of the SACROC platform from south to north (c–a). Line placement indicated on figure 24. Note relatively stratiform architecture in line c, changing to a more mounded and shingled architecture in b, and ultimately to the isolated, high-relief mounds in a. After Janson and Kerans (2007).



(a)



(b)

Figure 28. Conceptual models for the development of architectural variations across the northern Midland Basin. (a) Comparison of updip-down dip architectural changes in Missourian and Virgilian carbonate succession of SACROC–Cogdell area with Mississippian-age Lake Valley sequence 2 of Dorobek and Bachtel (2001). (b) Conceptual model of accommodation and hydrodynamic energy control on phylloid mound and flank deposits in the Virgilian succession of the Orogrande Basin. After Janson (2007).

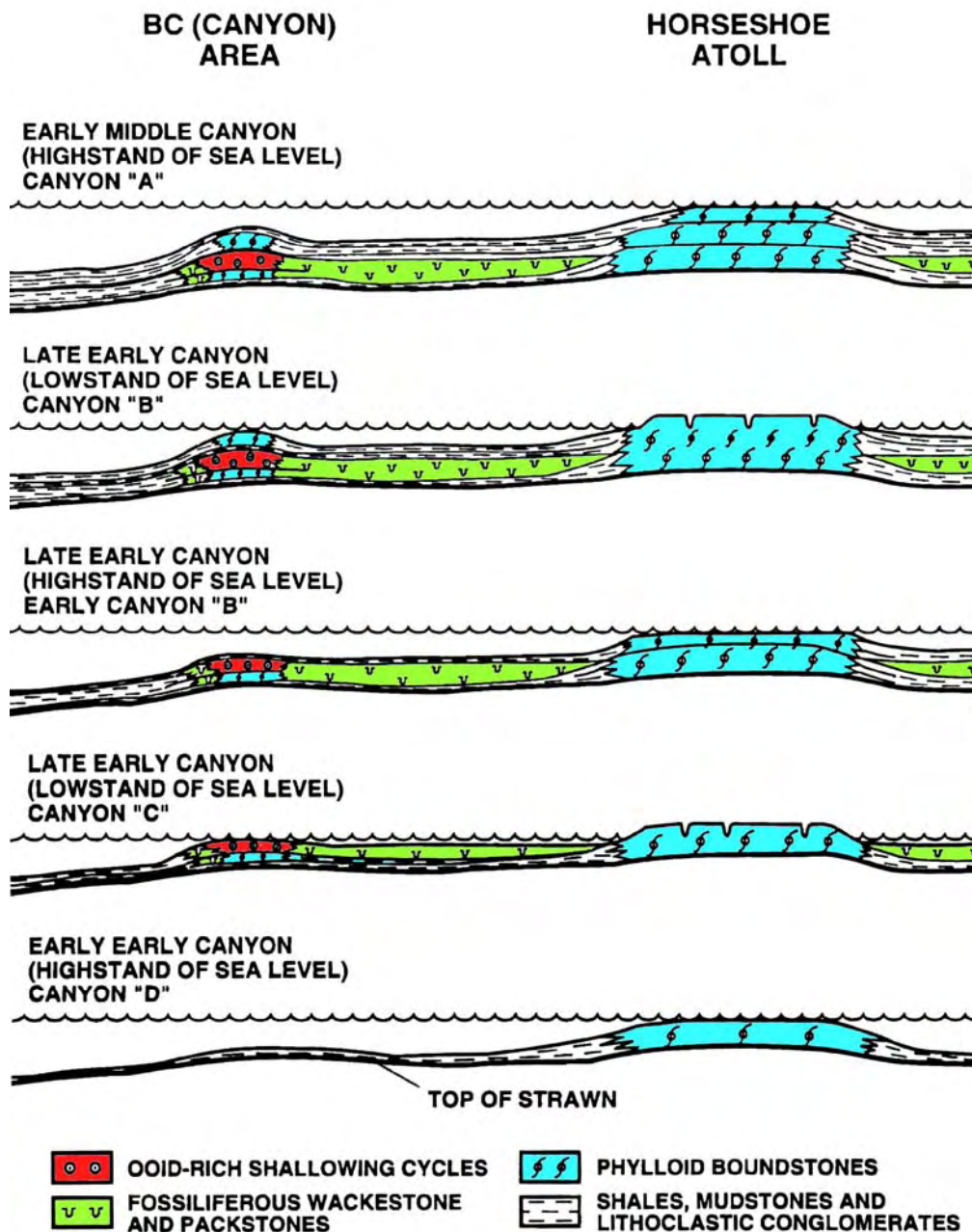


Figure 29. Conceptual model for lowstand carbonate deposition during the Missourian at BC field, Howard County (after Saller and others, 1993). BC is basinward (to the south) of the main carbonate platform. Also, labeling of Canyon sequences D–A is the reverse of the convention used on the main platform by Waite (1993) and others.

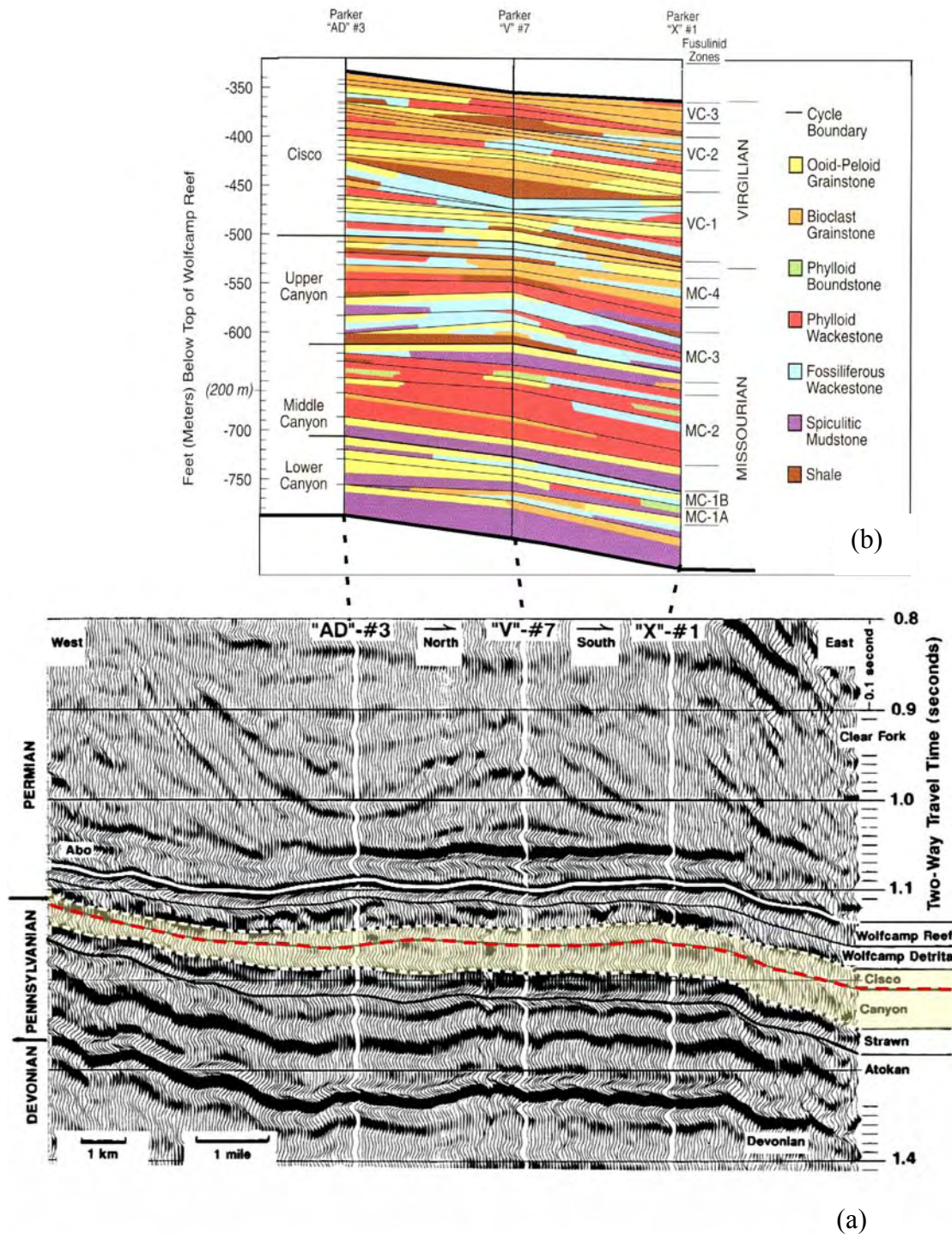


Figure 30. (a) Subregional seismic section of Southwest Andrews area. Yellow fill denotes Missourian and Virgilian succession, with red dashes demarking the transition. Note that the seismic section is chairlike in reality, with wells V#7 and X#1 being equally basinward of AD3 along strike. (b) Facies reconstruction of Missourian and Virgilian in the Southwest Andrews area. Refer also to comment above. After Saller and others (1999a, b).

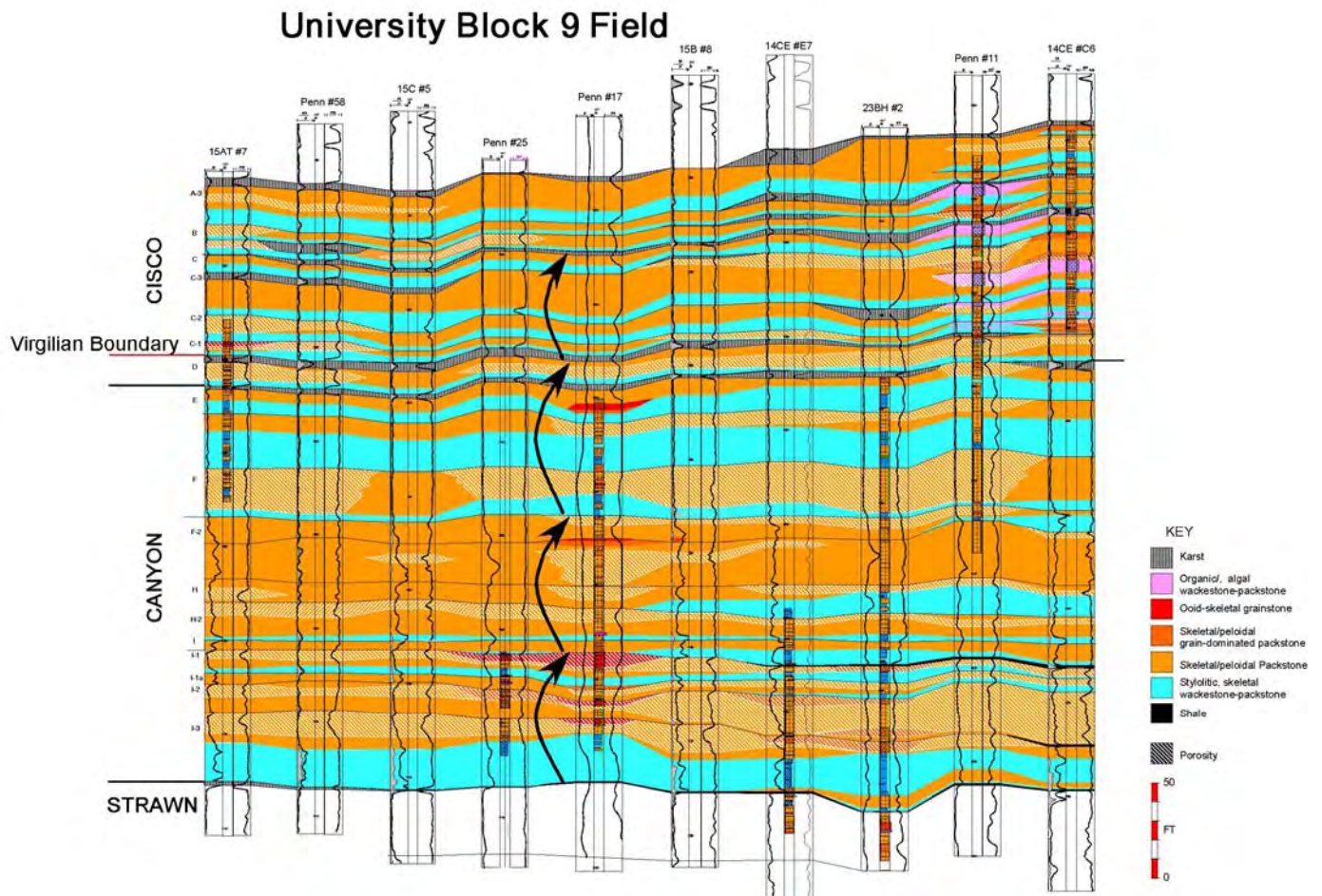


Figure 31. Regional fence diagram across University Block 9 field. Note predominance of skeletal peloidal packstones and wackestones throughout the succession. Three cycles are interpreted for the Missourian (Canyon) and two sequences for the Virgilian (Cisco). Note that porosity development is not always associated with sequence boundaries and exposure. Also note the lack of ooid grainstones, which are prominent in Southwest Andrews field. Modified from Barnaby (unpublished).

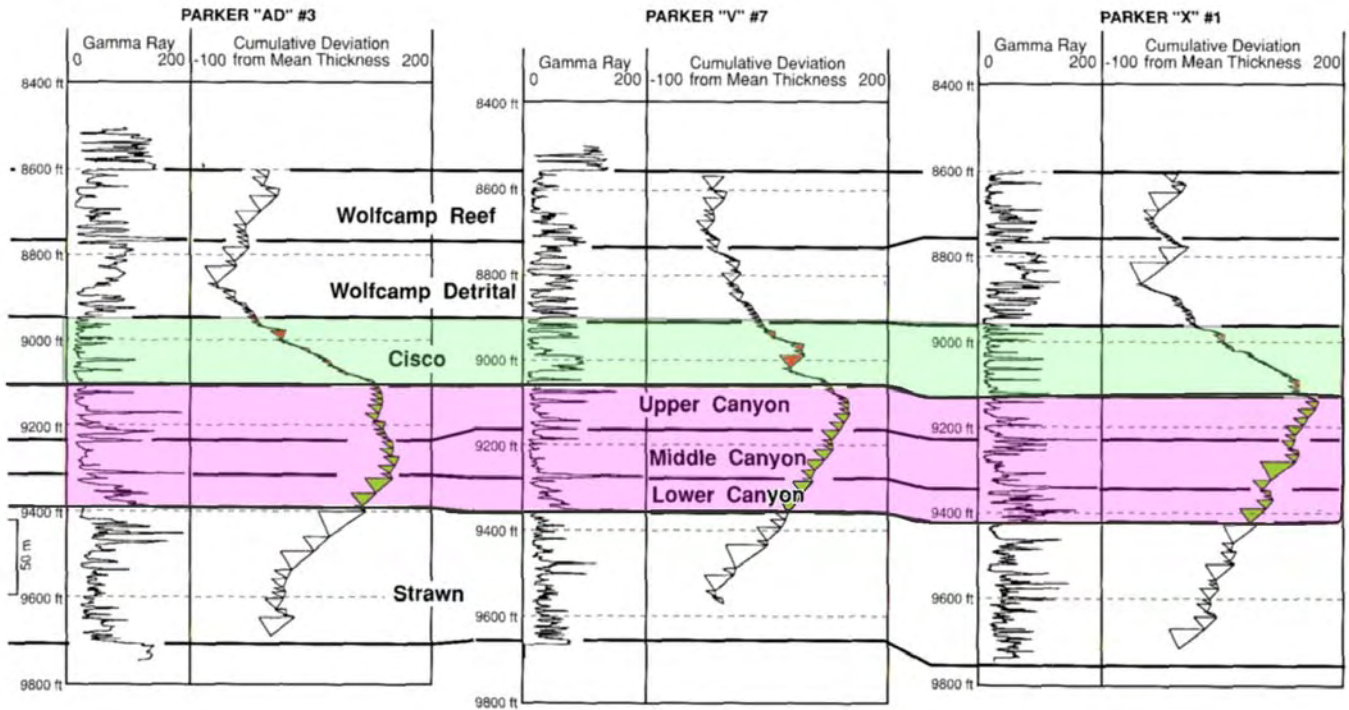


Figure 32. Fischer plot of cycle thickness and accommodation trends for Missourian and Virgilian succession in Southwest Andrews field area (after Saller and others, 1999b). Missourian (Canyon) interval highlighted in pink and Virgilian (Cisco) interval in light-blue. Note that thickness of the Missourian cycles is much greater than that in the Virgilian. Within the Missourian succession a dramatic decrease in cycle thickness from base (lower Canyon) to top (upper Canyon) is also present.

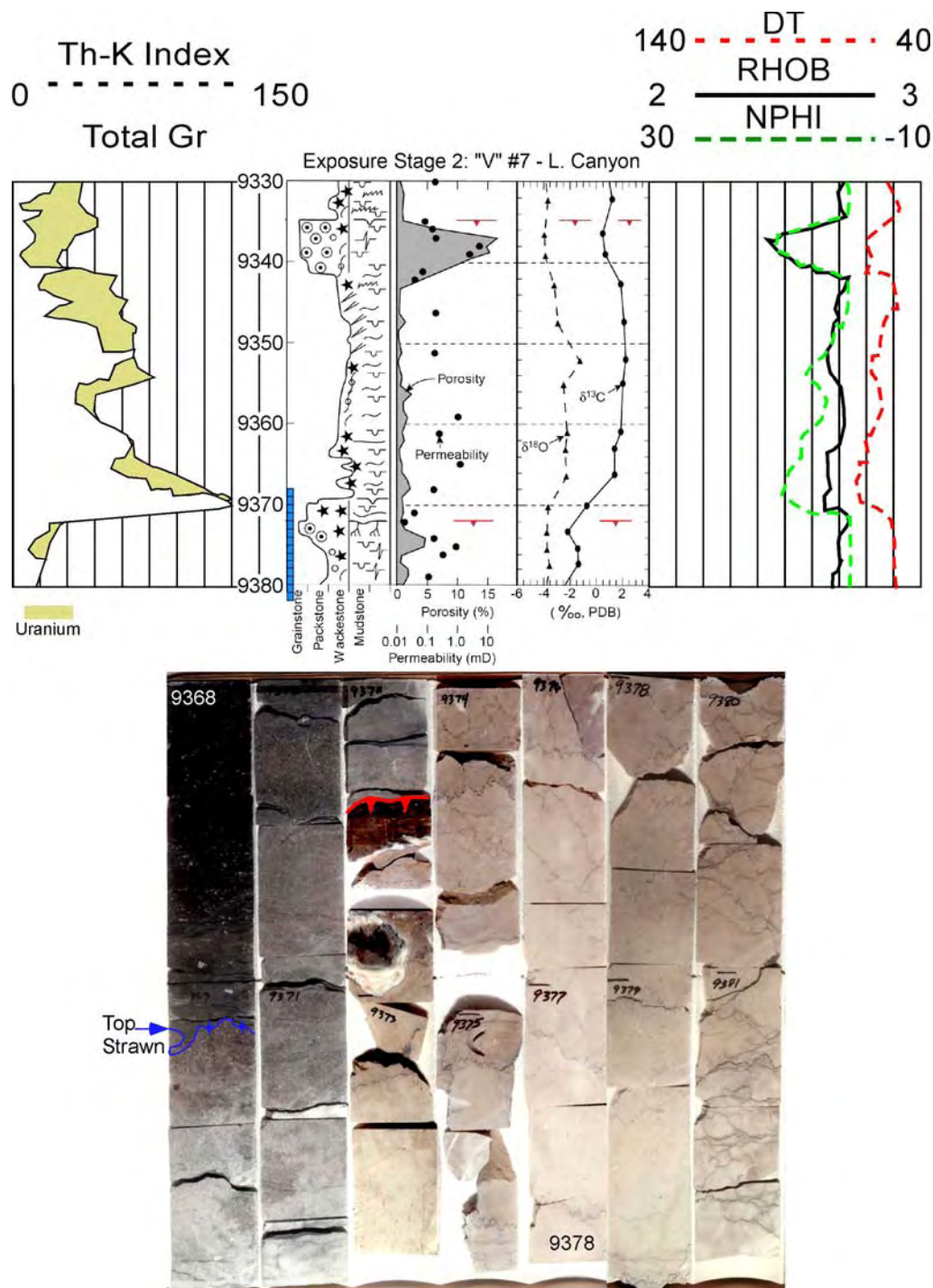


Figure 33. Core photograph, description, wireline-log signature, core analysis data, and stable isotope analysis of the lowermost Missourian (lower Canyon) interval. Proposed exposure surfaces indicated by red horizontal lines with downward-pointing triangles. Note that highest gamma-ray log readings occur above the exposure surface in the overlying crinoidal wackestones of the Missourian succession. Blue vertical bar indicates interval illustrated in core photograph.

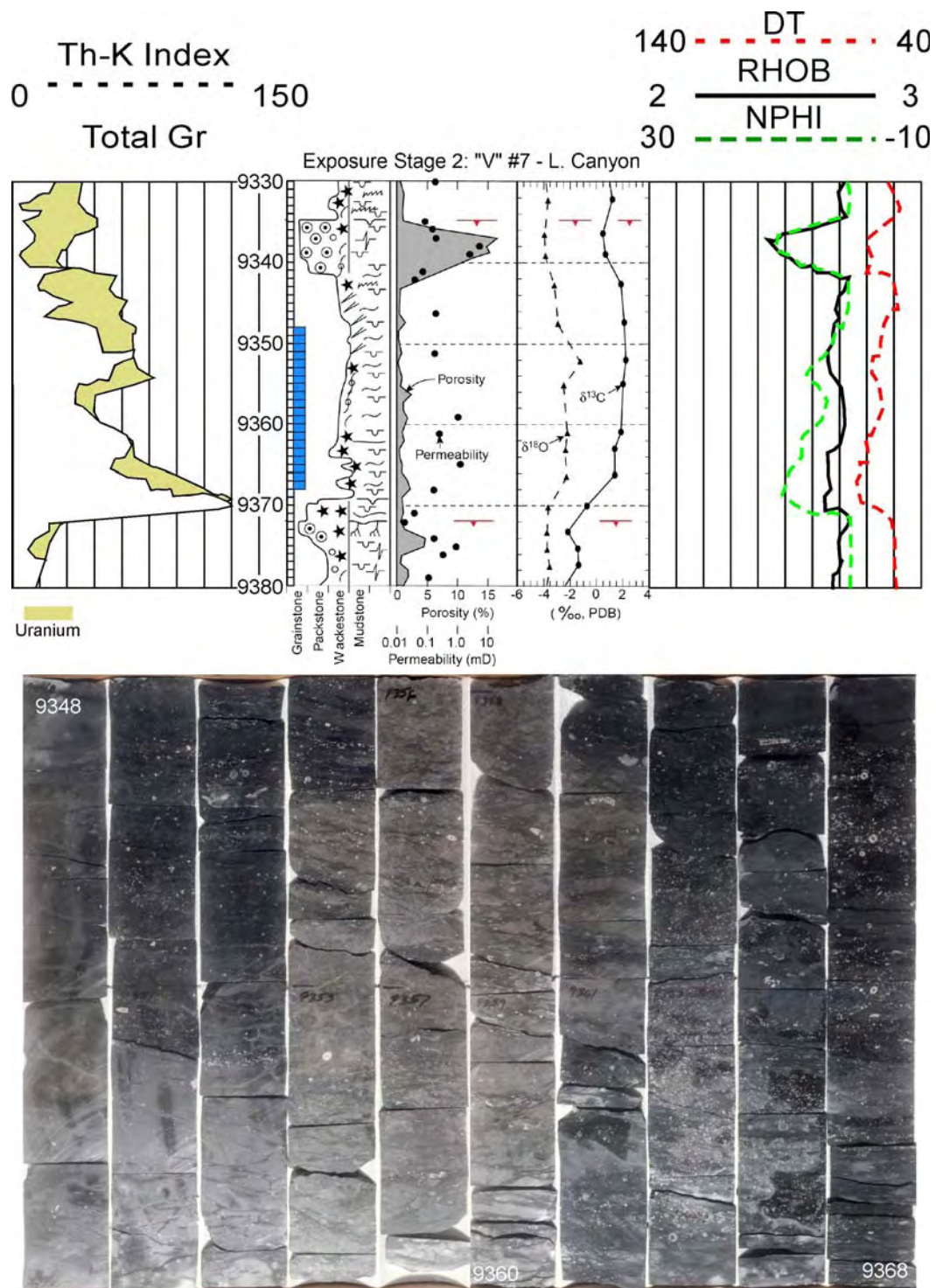


Figure 34. Core photograph, description, wireline-log signature, core analysis data, and stable isotope analysis of the Missourian (lower Canyon) interval. Proposed exposure surfaces indicated by red horizontal lines with downward-pointing triangles. Blue vertical bar indicates interval illustrated in core photograph.

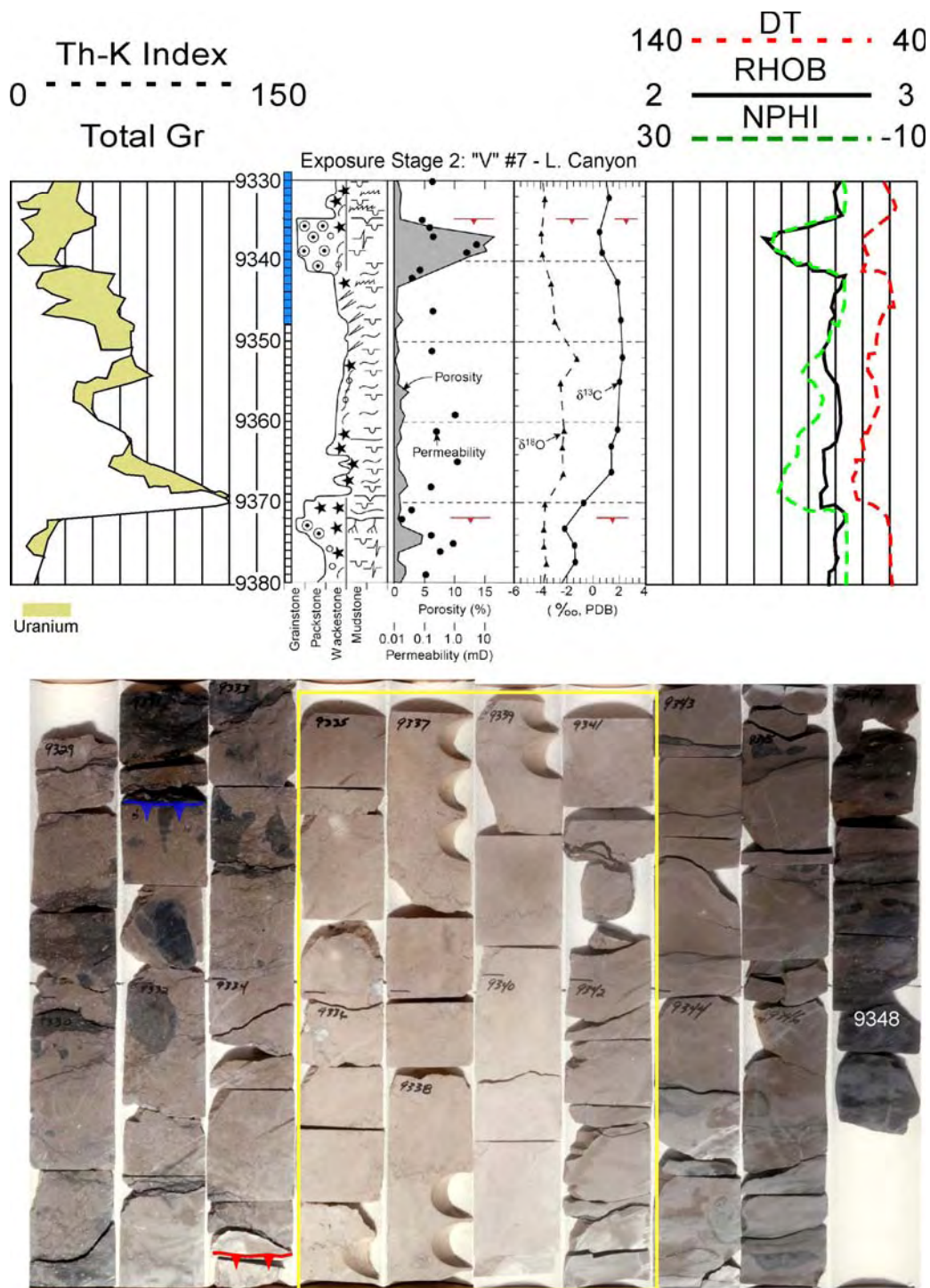


Figure 35. Core photograph, description, wireline-log signature, core analysis data, and stable isotope analysis of the Missourian (lower Canyon) interval. Proposed exposure surfaces indicated by red horizontal lines with downward-pointing triangles. Blue vertical bar indicates interval illustrated in core photograph. High-porosity and -permeability reservoir interval outlined in yellow.

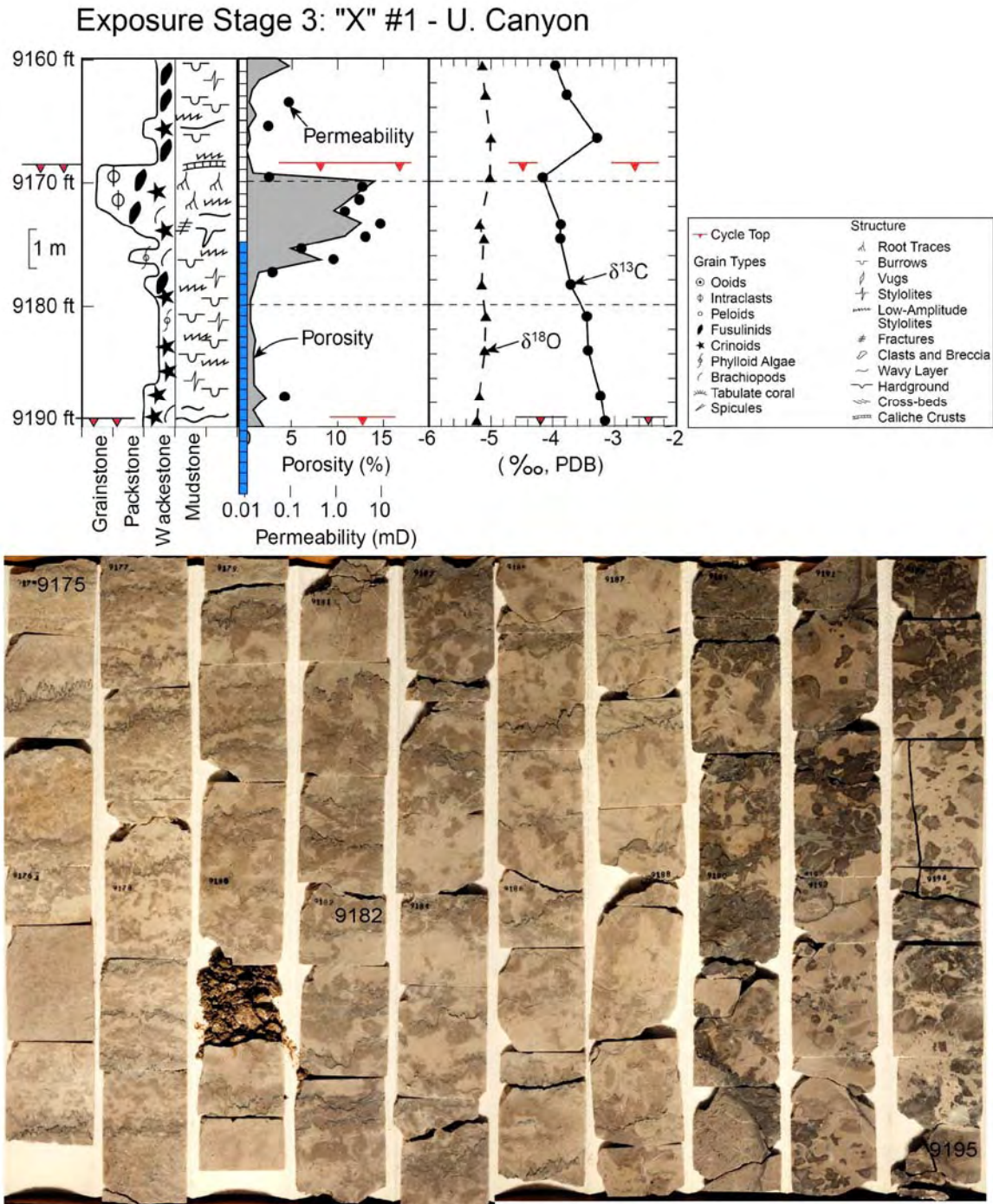


Figure 36. Upper Canyon core photographs, core description, and isotopic profiles (after Saller and others, 1999a, b). Note extensive textural alteration throughout the interval, which makes picking cycle boundaries difficult. Below 9,189 ft the interval seems to be highly brecciated, which may suggest some form of debris flow not indicated on the original interpretation.

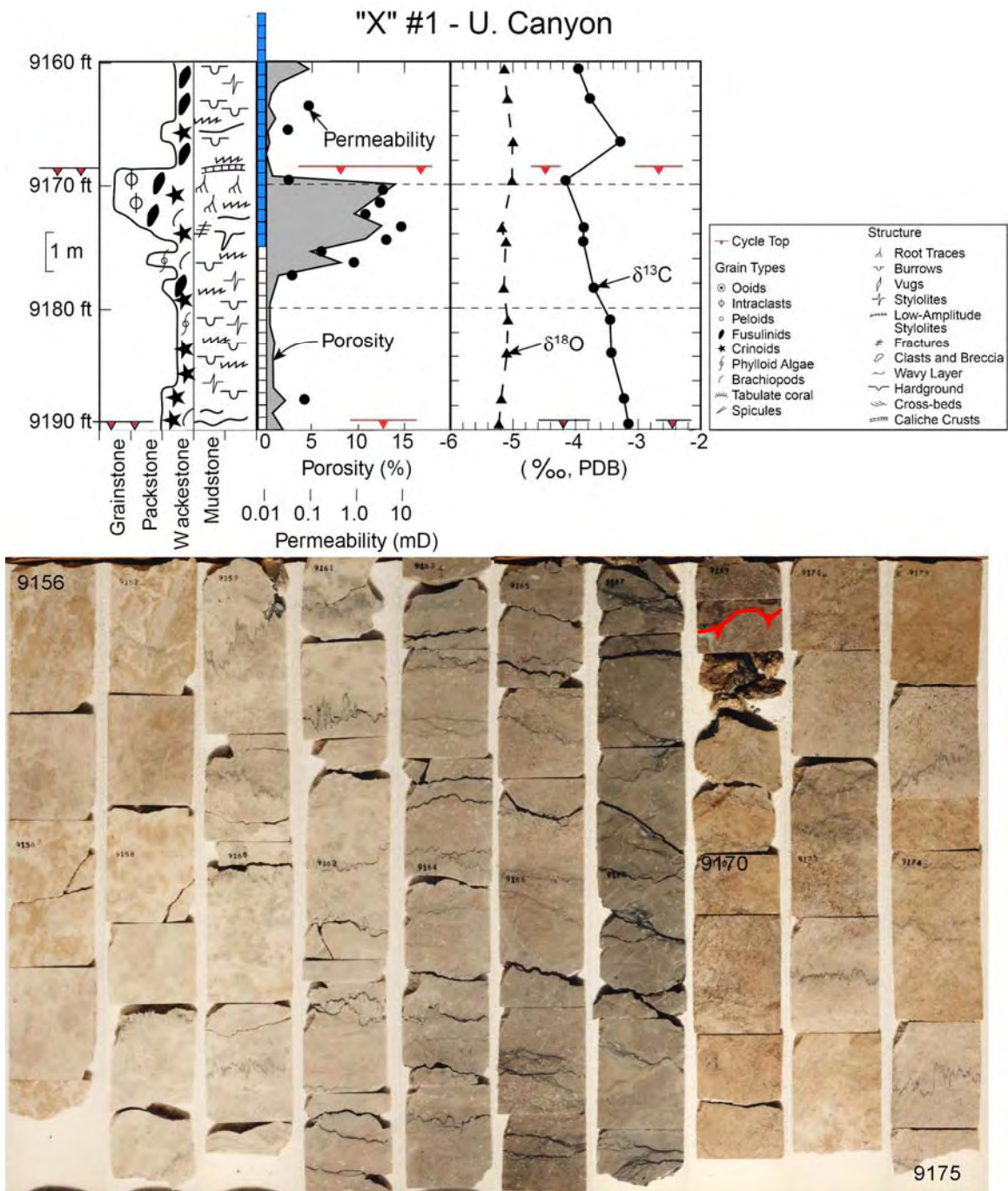


Figure 37. Upper Canyon exposure style 3 core photographs, core description, and isotopic profiles (after Saller and others, 1999a, b). Textural alteration is minimal compared with that of the underlying interval illustrated in figure 36. Cycle tops indicated in red on core photographs. Reservoir interval thickness approximately 8 ft.

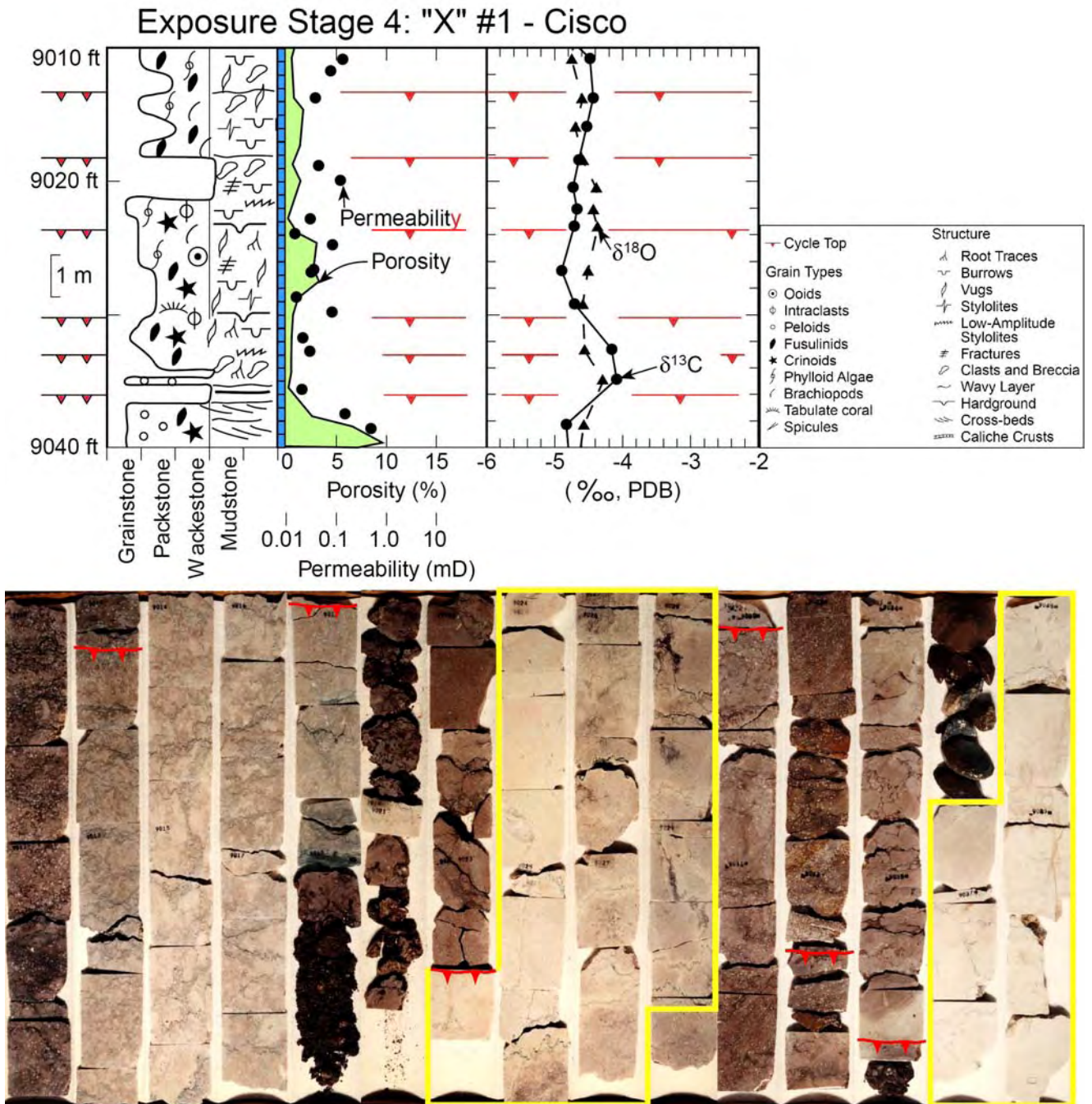


Figure 38. Middle Cisco exposure style 4 core photographs, core description, and isotopic profiles (after Saller and others, 1999a). Textural alteration is extensive compared with that of the underlying interval illustrated in figure 37. Cycle tops indicated in red on core photographs. Upper reservoir interval (yellow outline) thickness is approximately 6 ft, whereas lower is approximately 10 ft (not all depicted).

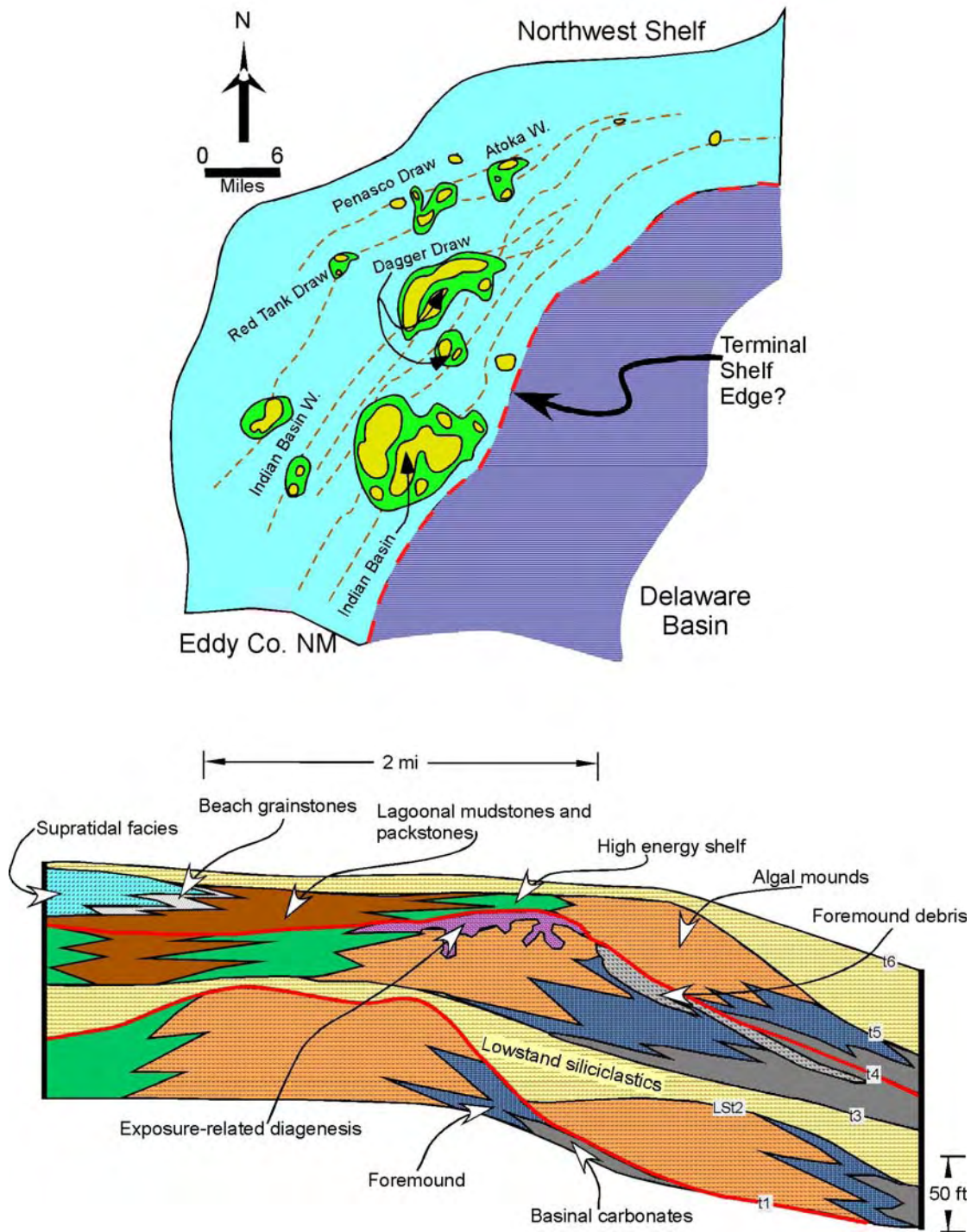


Figure 39. Generalized distribution and architecture of Missourian–Virgilian carbonate succession on the Northwest Shelf (New Mexico) (after Mazzullo, 1998). Red lines on lower schematic indicate sequence boundaries.

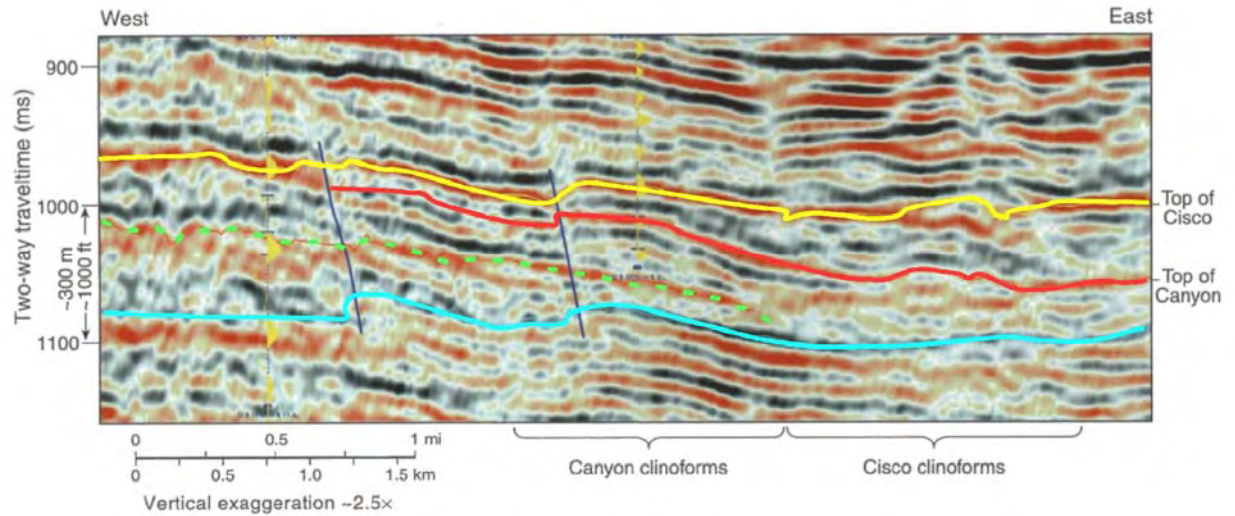


Figure 40. West-to-east (basinward) dip-section seismic line through South Dagger Draw field, Eddy County, New Mexico (after Tinker and others, 2004). Yellow line is interpreted top of Cisco (Virgilian), whereas red line is top of Canyon (Missourian) and blue line is possible base of Canyon. Note low-angle sigmoidal, clinoformal architecture of both successions.

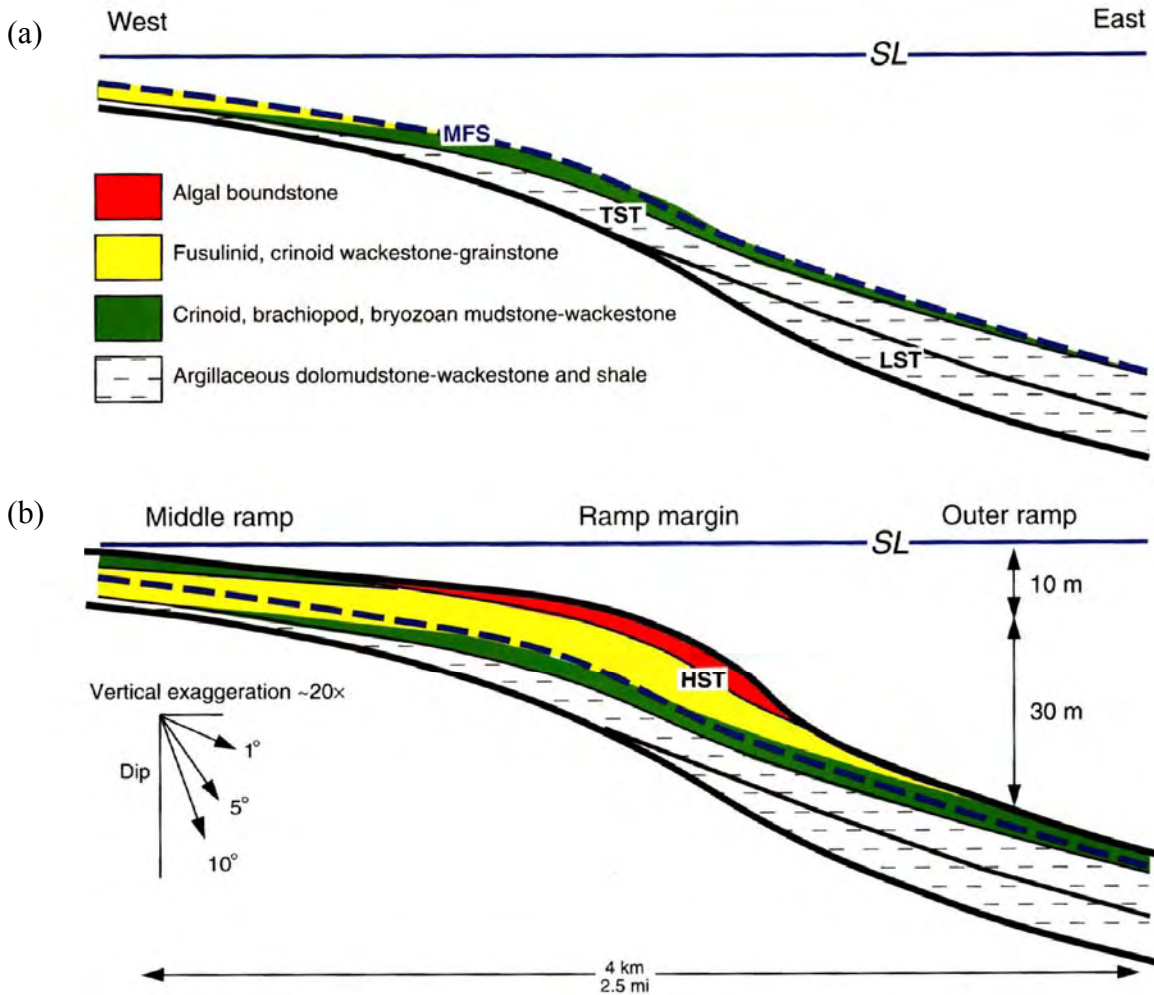


Figure 41. Depositional models for high-frequency stratigraphic architecture of South Dagger Draw field, New Mexico (after Tinker and others, 2004). (a) Facies distribution and depositional environments for lowstand and transgressive systems tracts (LST and TST). Note limited proportion of high-energy facies and their restrictions to the middle ramp area. (b) Facies distribution and depositional environments for highstand systems tract (LST and TST). Note basinward step of HST relative to LST and TST and dominance by higher-energy facies and algal boundstones. Note that water depths even at the ramp crest are thought to be in excess of 10 m.

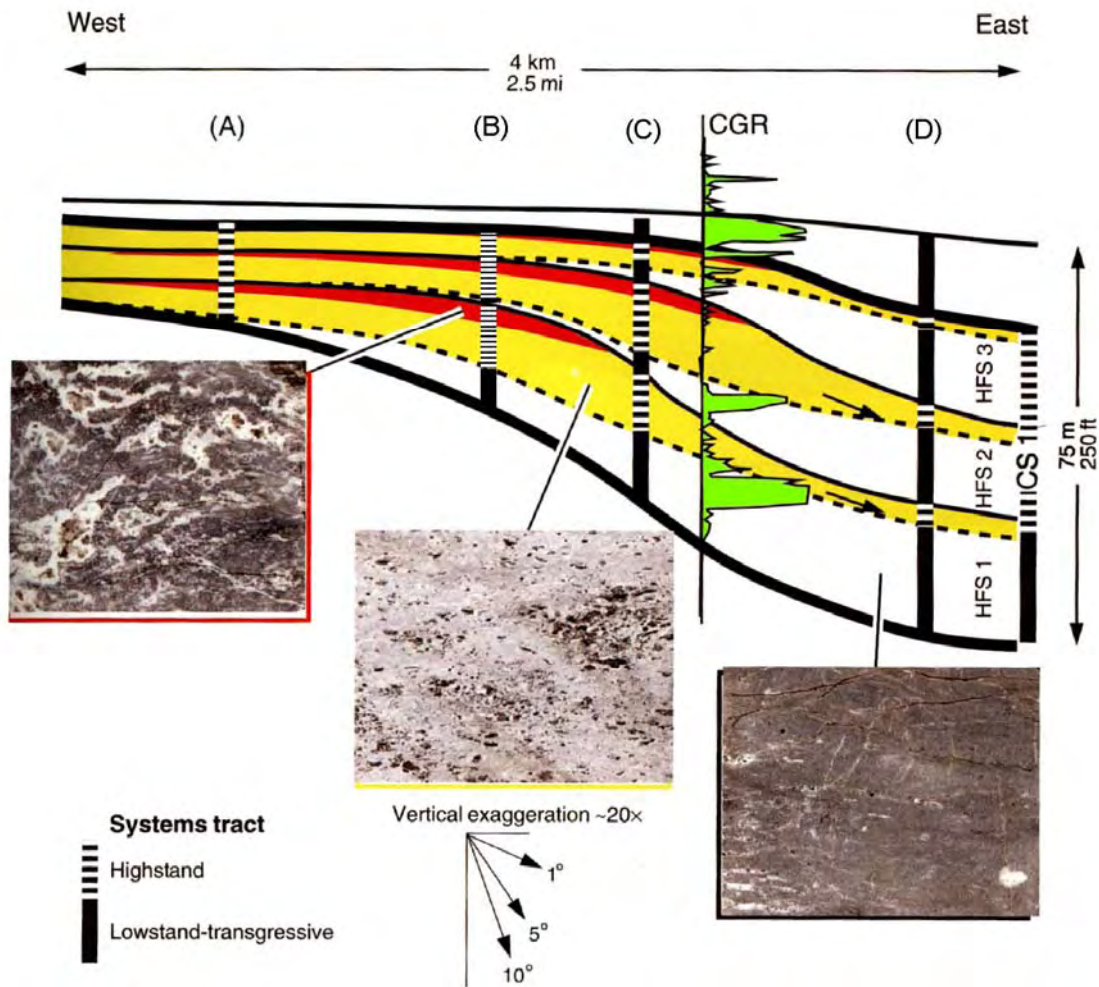


Figure 42. Schematic dip section illustrating stratigraphic hierarchy and lateral tract changes with a composite sequence (CS) (after Tinker and others, 2004). At position A, high-frequency sequences (HFS's) are asymmetrical and dominated by HST deposits. At B, cycles are still largely asymmetrical, with CS LST-TST overly represented. This location would also yield a facies association dominated by algal boundstones and give a false impression of an aggradational buildup. At location C, there is greater symmetry in HFS1, with increasing asymmetry in HFS2 to 3. At location D, HFS's are asymmetrical but dominated by LST-TST facies. Scale of photographs 8 cm horizontal. Left photograph—algal boundstone. Central photograph—fusulinid crinoidal packstone. Right photograph—argillaceous lime mudstone.

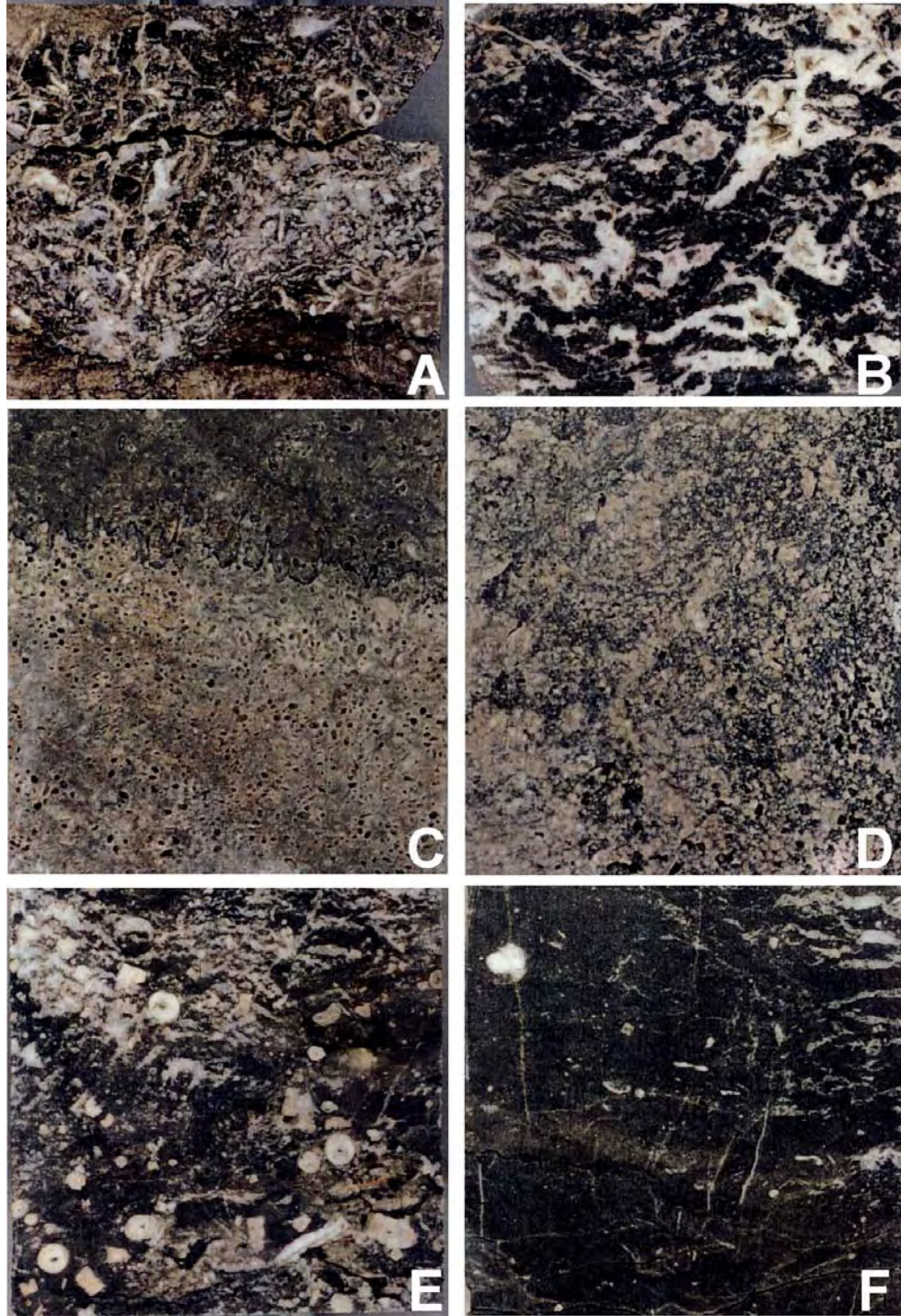


Figure 43. Core slab photographs of dominant Missourian and Virgilian facies at South Dagger Draw (Federal#5 8172C well) (after Brinton and others, 1998). Width of all photos approximately 3.5 inches. A. skeletal algal boundstone—Virgilian. B. Encrinitic algal foram boundstone—Missourian. C. Fusulinid packstone—Missourian. D. Fusulinid, crinoidal, algal, foraminiferal packstone—Virgilian. E and F. Crinoidal wackestone—Missourian.

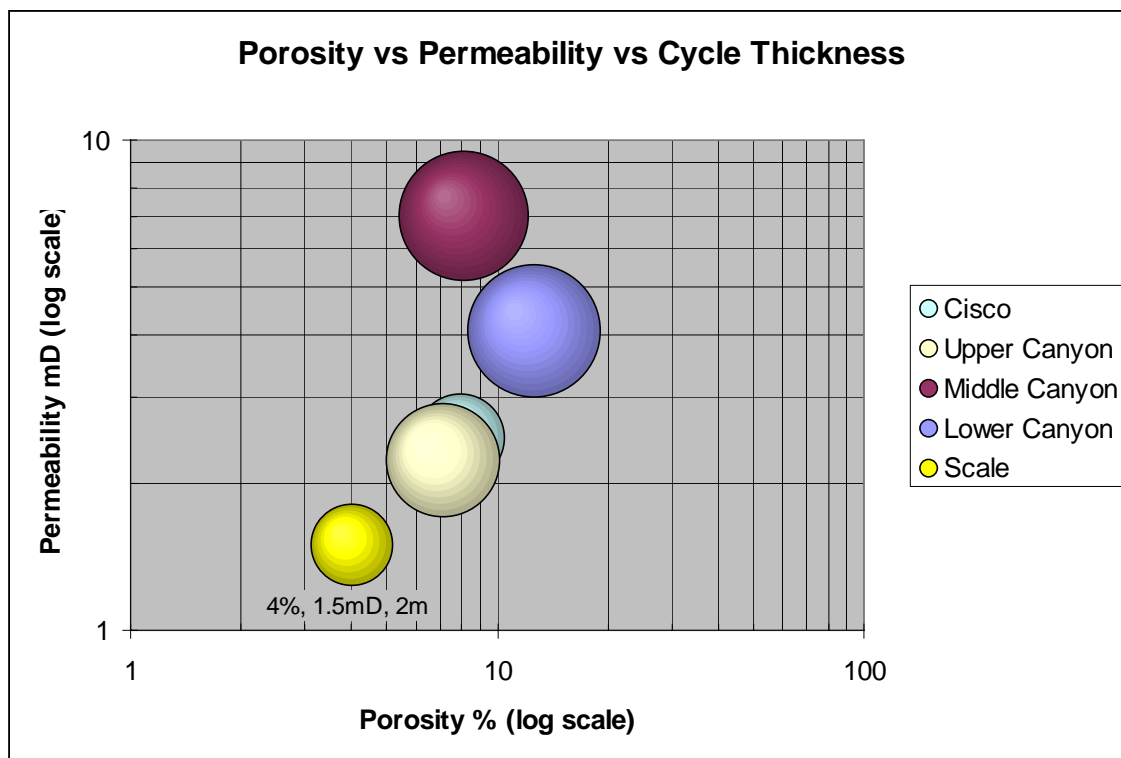


Figure 44. Summary bubble chart of porosity, permeability, and cycle thickness for Missourian and Virgilian carbonate succession in South Andrews field area (data from Saller and others, 1999a). Bubble area corresponds to cycle thickness. Overall, the lower Canyon interval (lower Missourian) has the best reservoir quality. Values used are averages of three wells' data. Note that original values did not include cycles in sequences with porosity less than 4 percent.

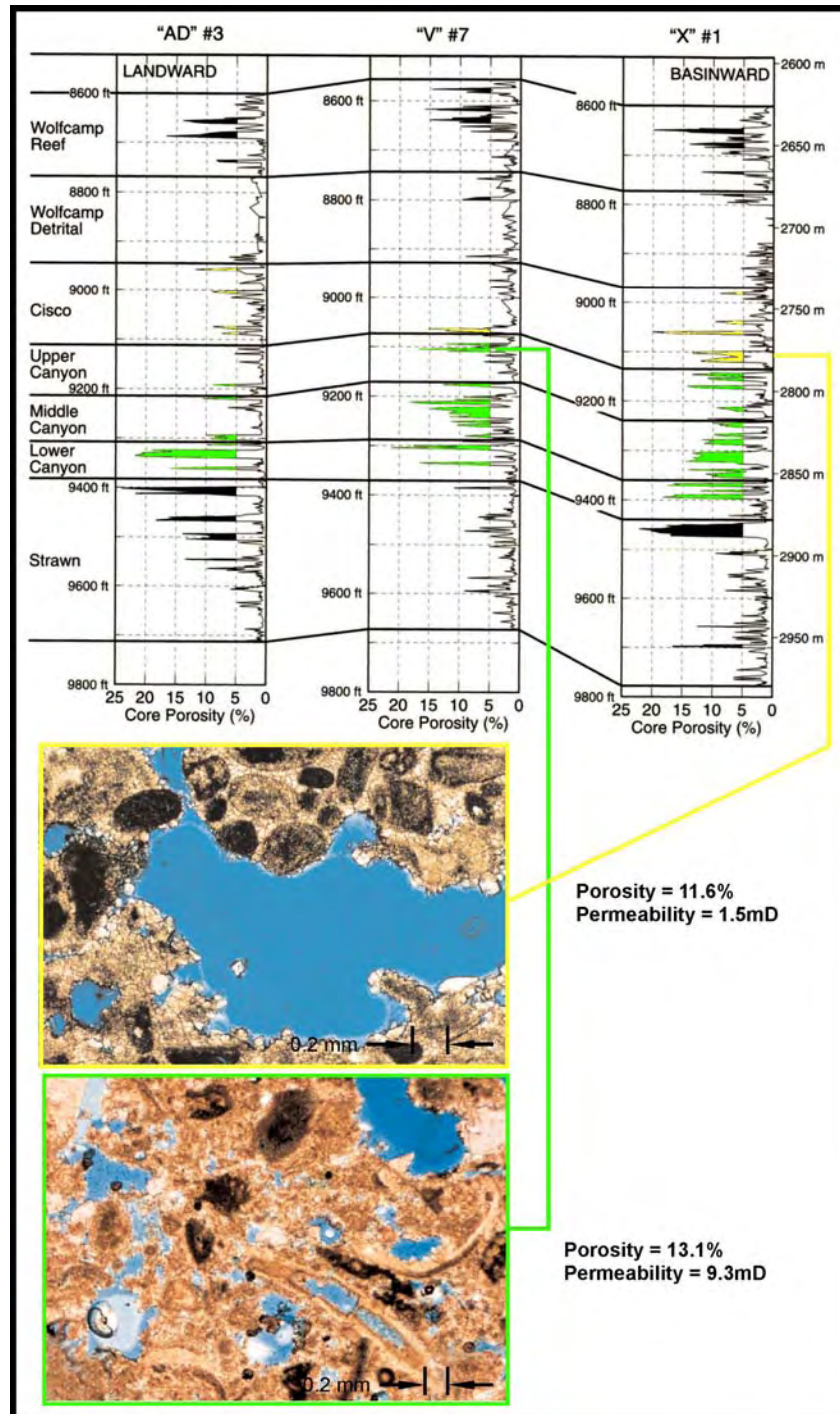


Figure 45. Dip line section through South Andrews field area illustrating distribution of porous intervals relative to sequence (after Saller and others, 1999a). Green infill is used for Missourian succession with greater than 4 percent porosity and yellow for the Virgilian. Photomicrographs correspond to each interval and illustrate moldic to slightly vuggy pore style in the Missourian and greater vug dominance in the Virgilian. Note that all porous zones appear to prograde basinward as they decrease in age.

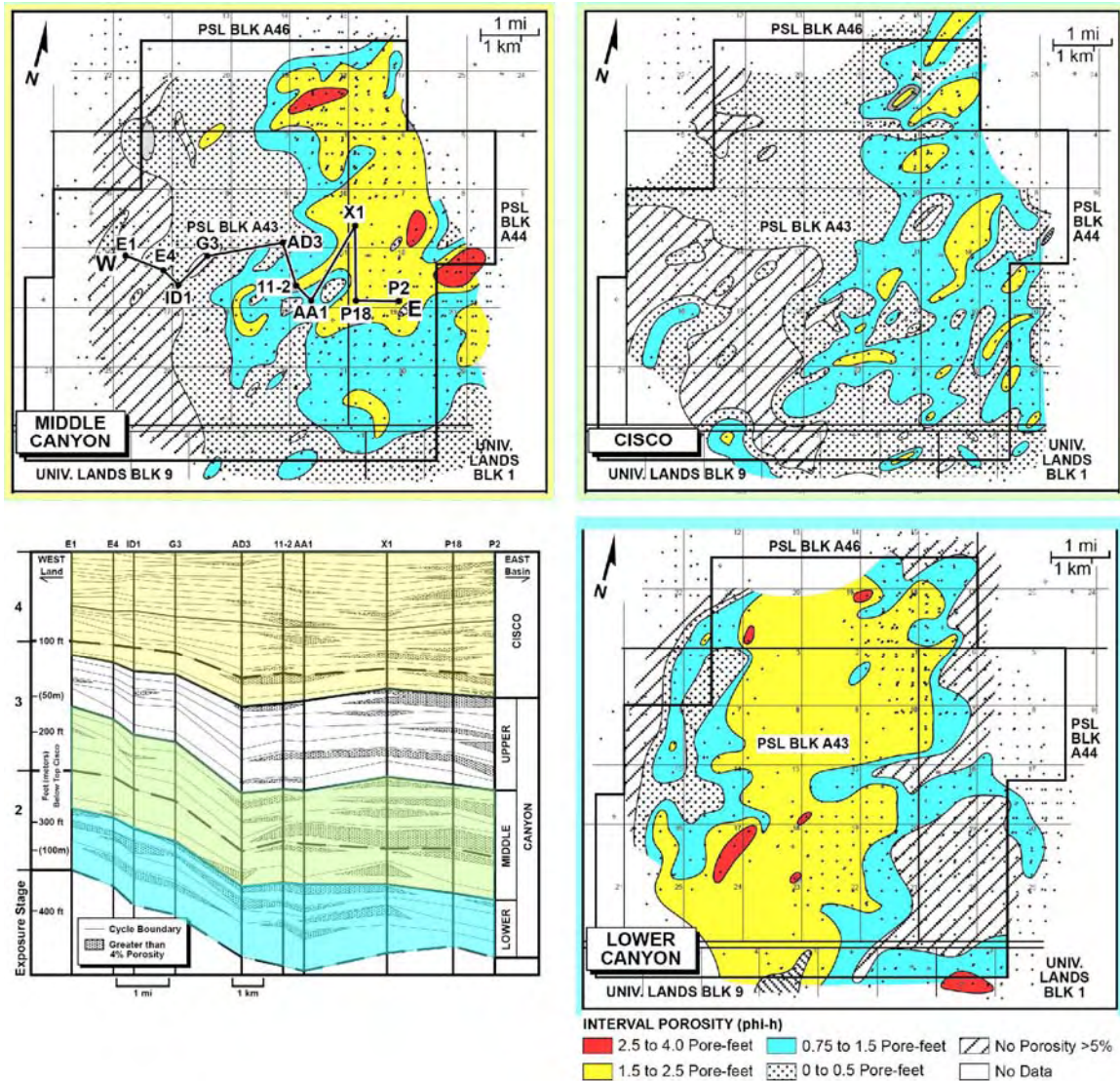


Figure 46. Cross section of porosity related to depositional episodes and exposure stage and corresponding regional maps of porosity versus thickness trends for the same intervals (modified from Saller and others, 1999a). Missourian succession represented by lower and middle Canyon intervals (blue and green, respectively). Virgilian succession represented by Cisco interval outlined in yellow.

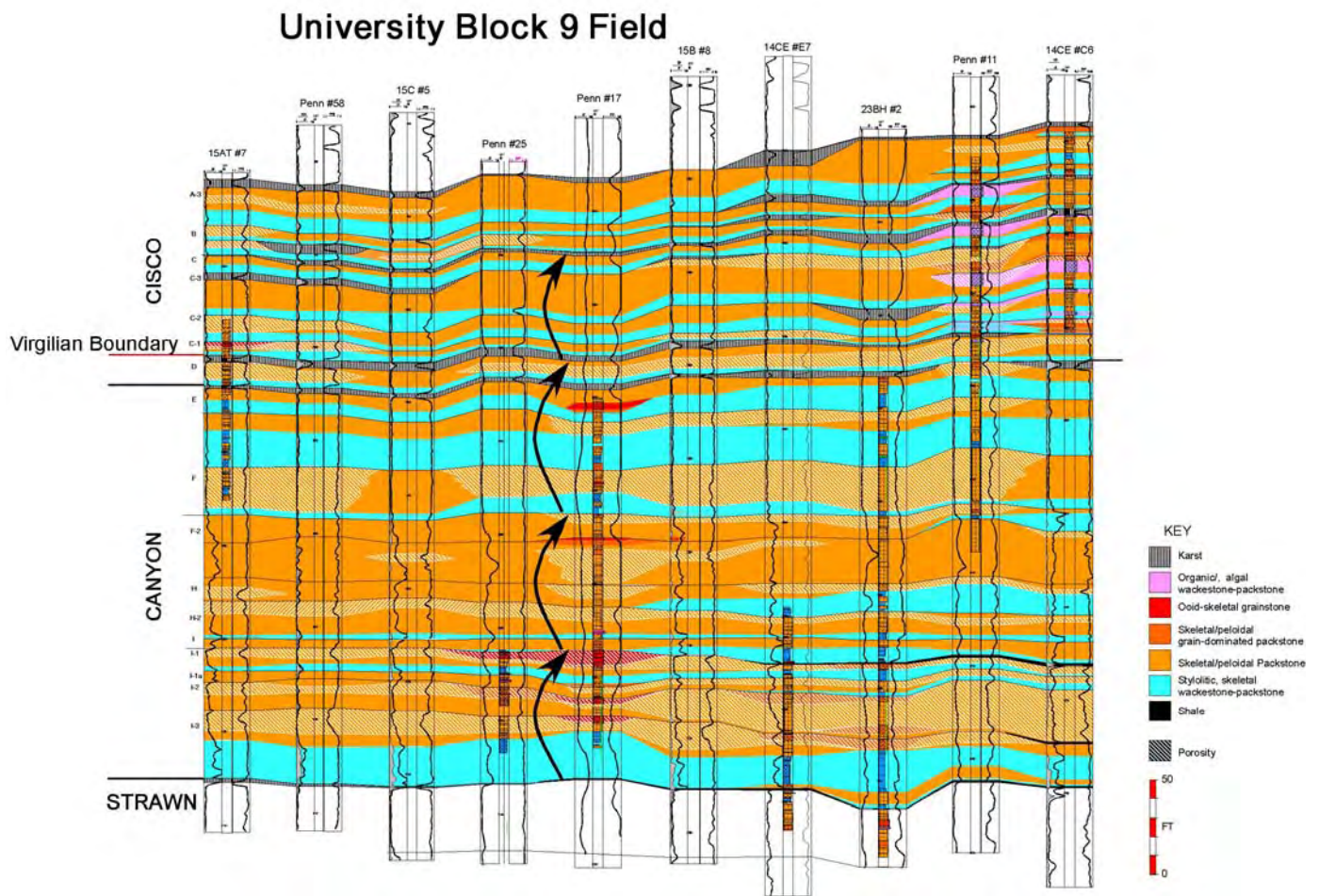


Figure 47. Regional core, FMI, and well-log-based correlation across University Block 9 area (modified from Barnaby, unpublished). Porous zones indicated by inclined hatch marks. The most regionally pervasive high-porosity zone is in cycle F, which is upper Canyon as defined by Saller and others (1999b). Note presence of algal wackestones and packstones in Penn #11 and 14CE #6 wells in the Virgilian succession.

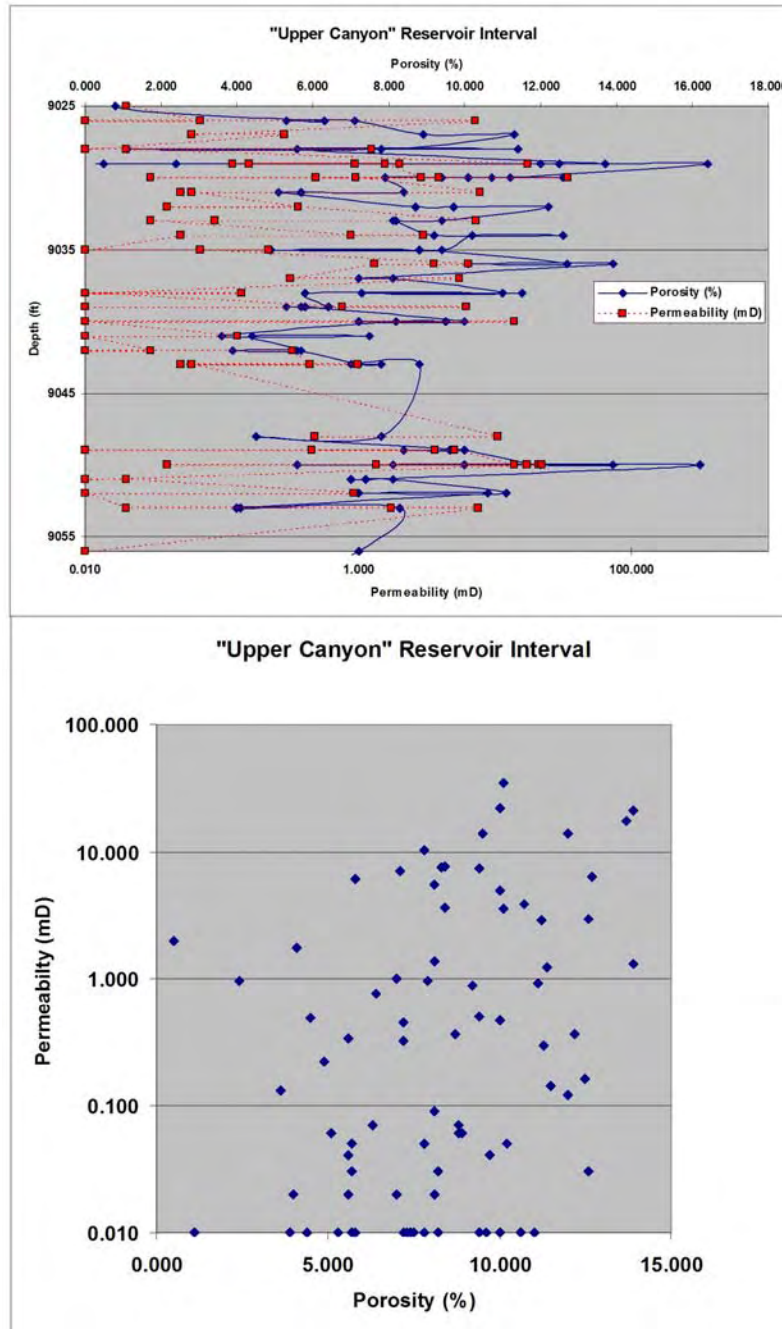


Figure 48. Upper diagram illustrates depth profile of porosity and permeability for the F sequence in University (Penn) #11 well. This interval corresponds roughly to the upper Canyon of Saller and others (1999a). Note that permeability does not increase with porosity throughout the interval, especially from depths 9,030 to 9,040 ft. Lower diagram is a crossplot of porosity and permeability for the same interval as in the upper diagram. Note high degree of scatter and lack of linear correlation between porosity and permeability. Linear correlation R^2 value for this data is 0.12.

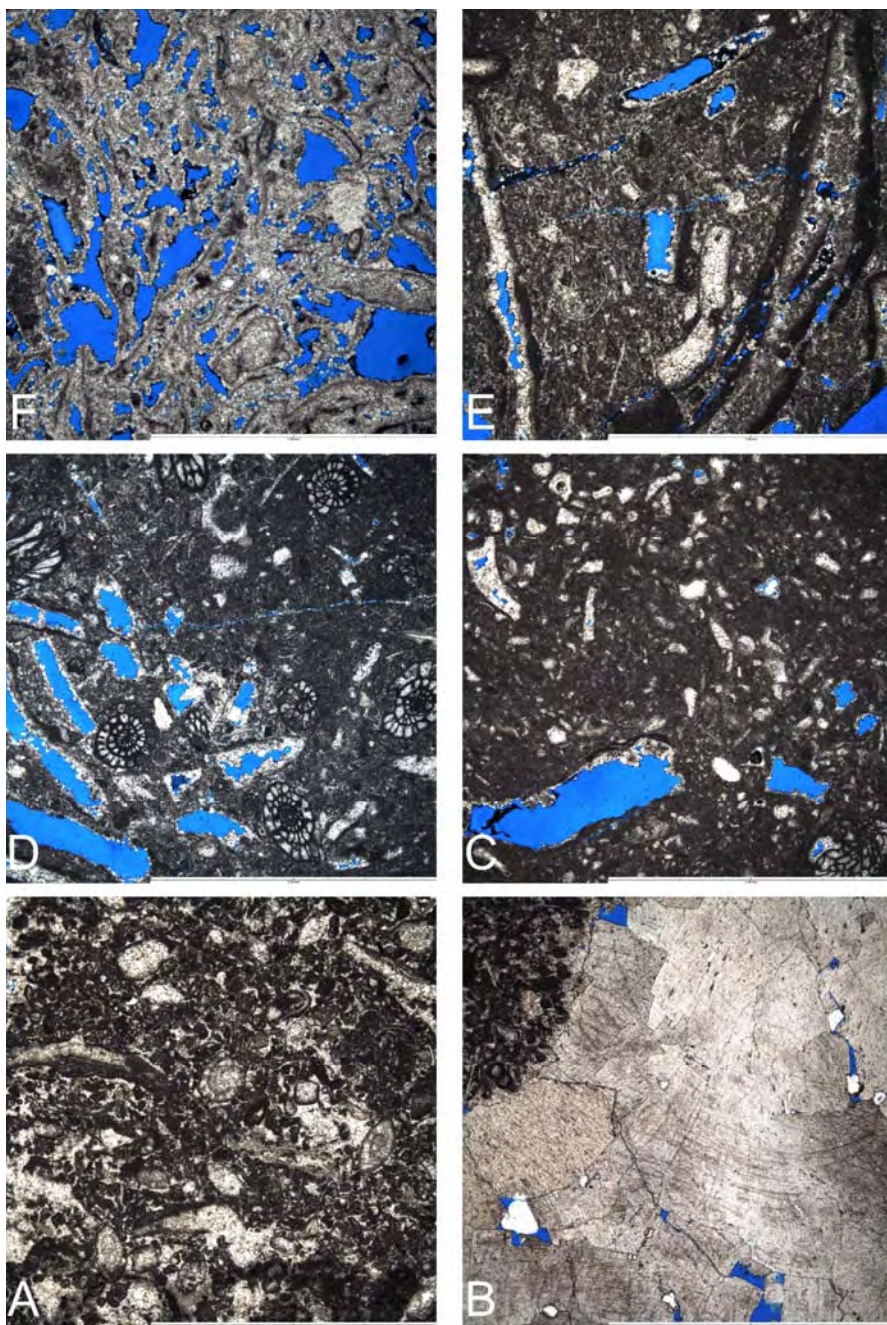


Figure 49. Thin-section photomicrographs of Missourian and Virgilian reservoir intervals (Penn #11 well, University Block 9). Scale bar is 5 mm in all photos. A–E. Upper Canyon reservoir interval. A and B. Calcite-cemented peloidal foraminiferal grainstone with B. Coarse saddle dolomite. Sample depth 9,060 ft. Core analysis measurements yielded a range of porosity (4.00, 2.90, and 5.70 percent) values and uniform permeability (0.010 md). C. Phylloid algal bioclastic wackestone to packstone with porosity values of 7.4 and 7.00 percent and permeability of 0.01 and 0.02 md. Sample depth 9,051 ft. Note that porosity is in molds after heterogeneously leached bioclasts (phylloid?). D. Phylloid algal foraminiferal packstone to mud-lean packstone with porosity values of 3.6, 7.50 and 4.4 percent and permeability of 0.13 and 0.01 md. Sample depth 9,041 ft. Porosity predominantly moldic within leached phylloid algal plates. E. Peloidal algal packstone with consistent porosity values of 6.4, 5.8, 5.3, and 5.7 percent and variable permeability values of 0.76, 6.190, and 0.01 md. Sample depth 9,039 ft. F. Virgilian reservoir interval depth 8,968 ft. Algal boundstone with porosity values of 4.6 and 12.6 percent and permeability of 0.370 and 1.55 md. Sample depth 8,968 ft.

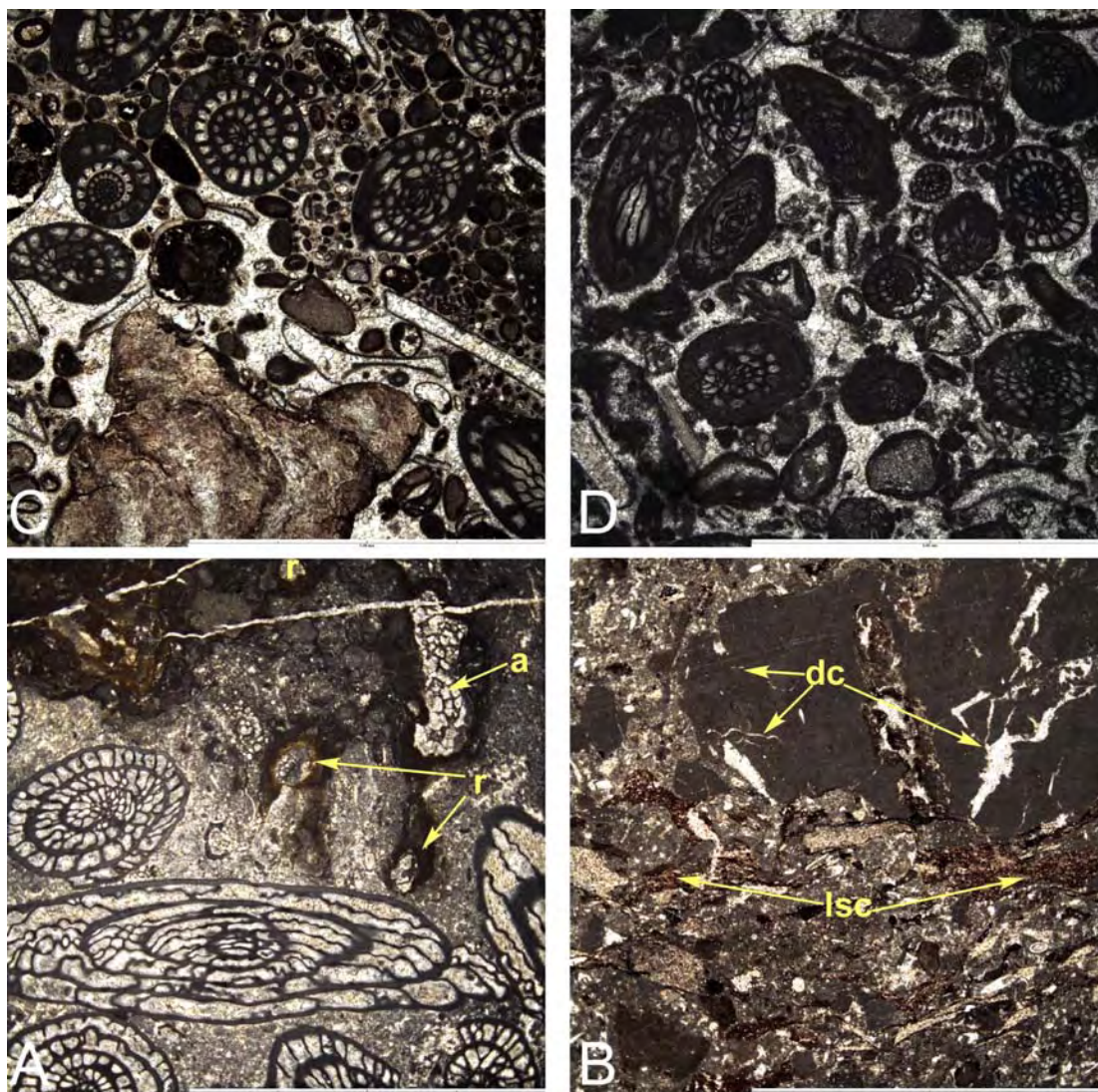


Figure 50. Examples of Virgilian-age (Cisco), exposure-related, diagenetic features and typical facies and corresponding poor reservoir quality. Scale bar is 5 mm in all photos. A. Example of icehouse-style exposure surface with a brecciated, rhizolith- (r) and alveo-septal-bearing (a) soil zone developing directly on a subtidal fusulinid-packstone (sample depth 8,947 ft: 2.9 percent porosity and 0.33 md permeability). B. This sample contains abundant evidence of exposure-related diagenesis, including laminated microcrystalline soil crusts (lsc), rhizoliths (r), and intraclasts with abundant radial desiccation cracks (dc). Many of the intraclasts appear to have incipient circumgranular fractures and may have been weakly developed glaeboles prior to erosion. At the thin-section scale, this exposure-related fabric irregularly overlies a spiculitic wackestone (sample depth 8,906 ft; 0.70 percent porosity and 0.010 md permeability). C. Example of calcite-cemented, fusulinid-bioclastic-intraclastic grainstone (sample depth 8,884 ft: 2.3 percent porosity and 0.010 md permeability). Note that leached moldic grains are also occluded by cement. D. Typically well cemented, tight, fusulinid grainstone characteristic of the Virgilian (sample depth 8,883 ft: 1.9 percent porosity and 0.010 md permeability).

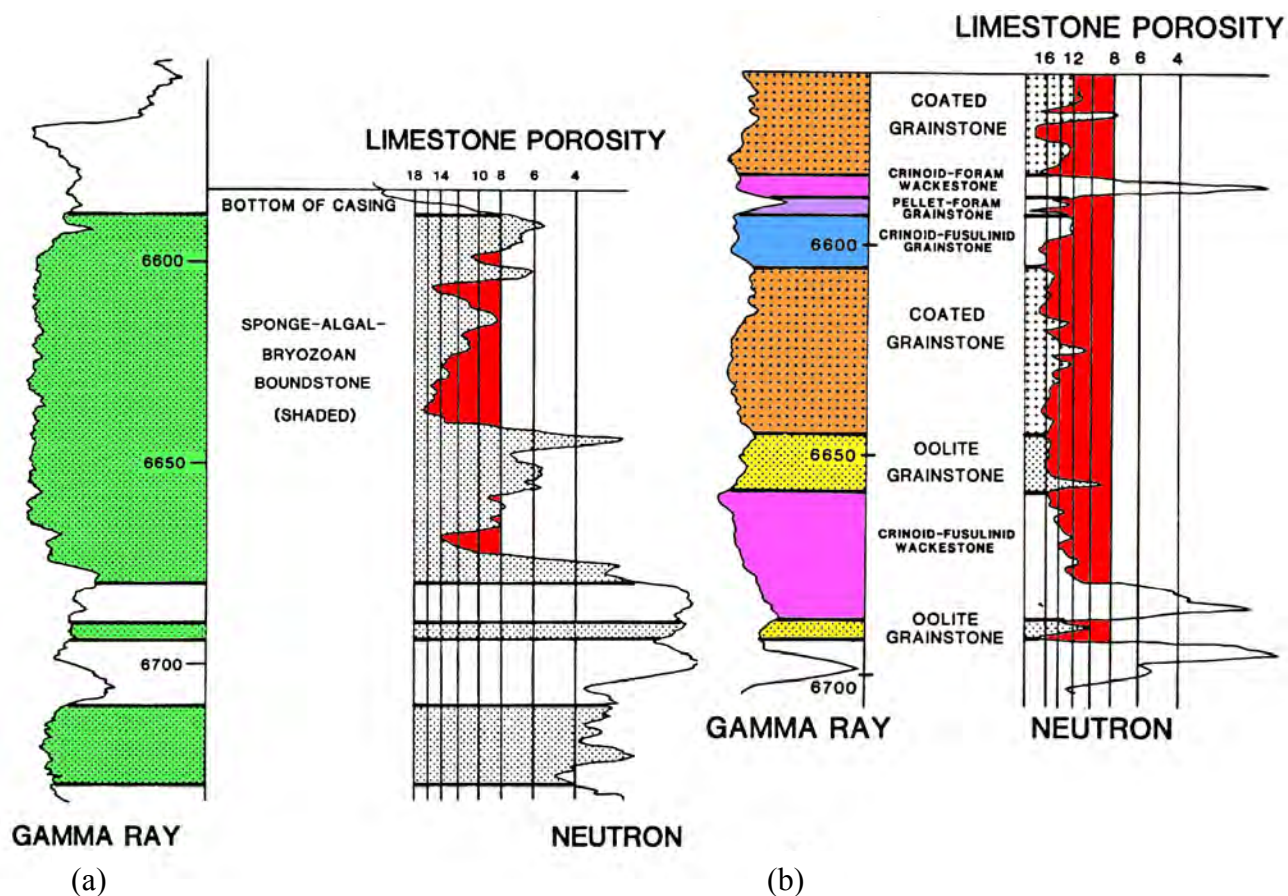


Figure 51. Facies versus wireline-log signature for (a) well 19-6 and (b) well 34-6 at SACROC field, Scurry County, Texas. Note that gamma-ray logs are similar for both wells; however, facies and associated porosity quality and extent are very different.

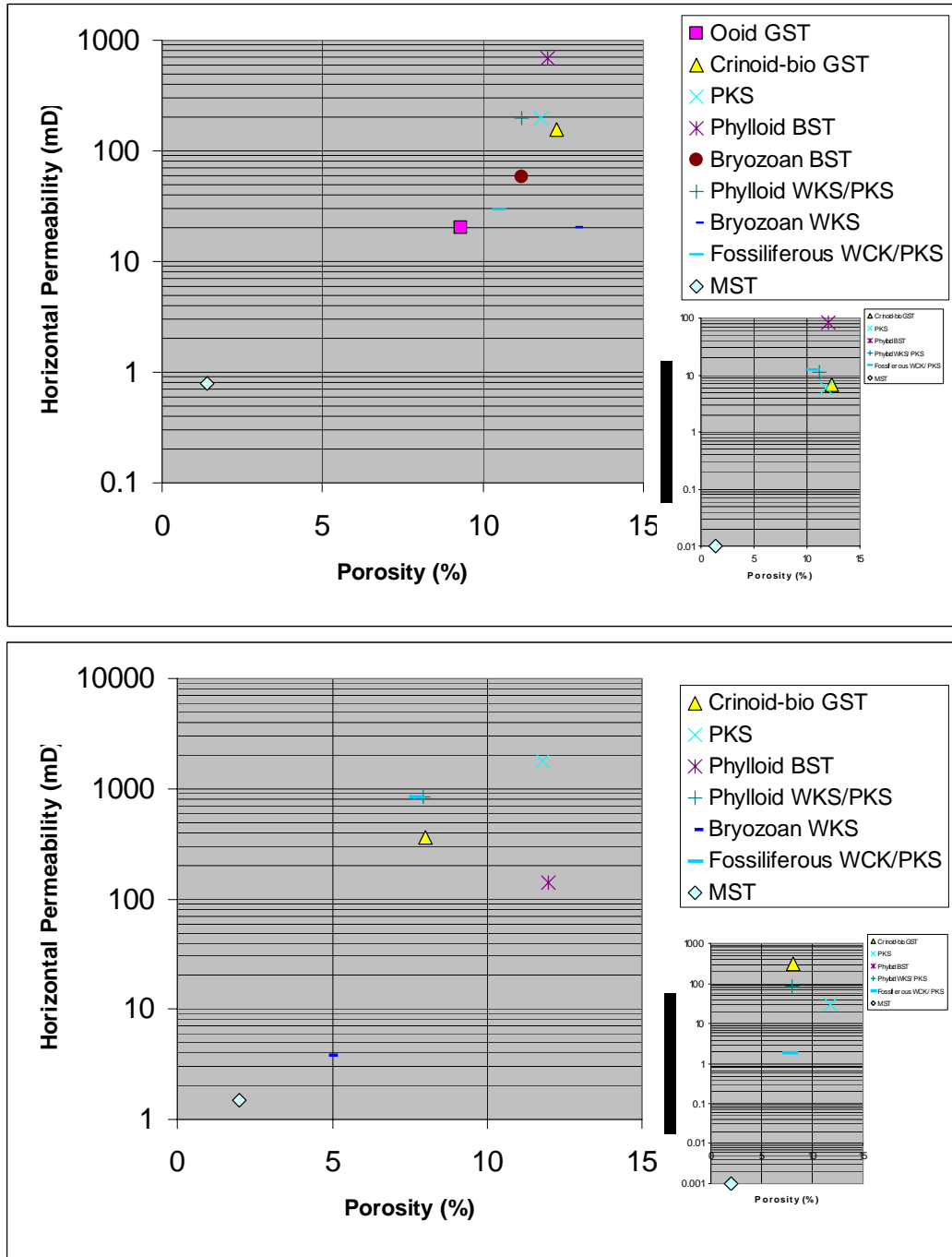


Figure 52. (Top) Porosity and permeability relationship to limestone facies at Reinecke field (data from Saller and others, 2004). Inset comprises a subset of the facies and is vertical permeability. Note that the best reservoir facies in both plots is phylloid algal boundstones. (Bottom) Porosity and permeability relationship to dolomitized facies at Reinecke field (data from Saller and others, 2004). Inset comprises a subset of the facies and is vertical permeability. Note that the best reservoir facies in using horizontal permeability is packstone, whereas crinoidal-bioclastic grainstone has the best vertical permeability.

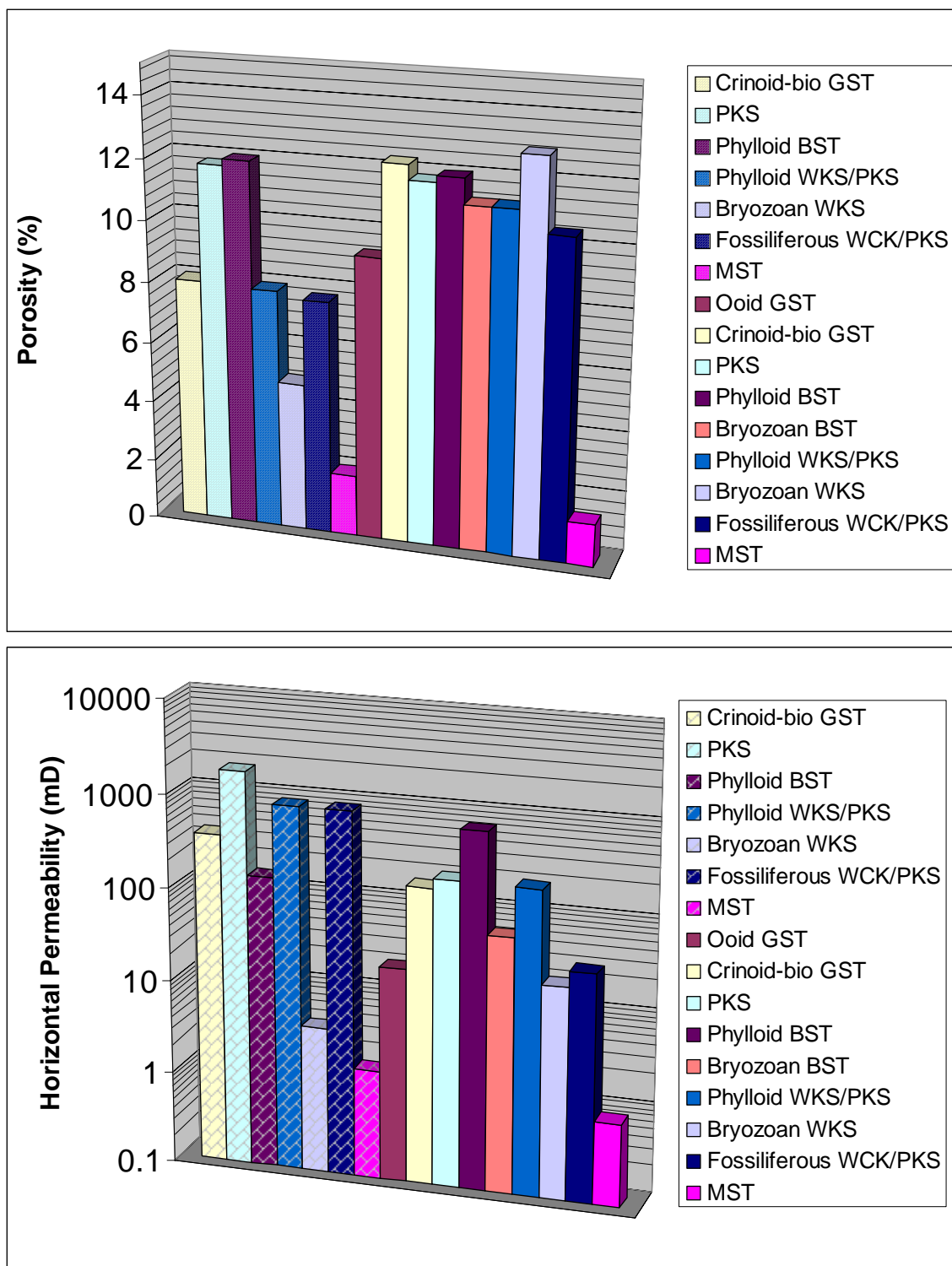


Figure 53. Bar charts comparing porosity and horizontal permeability between undolomitized (no fill pattern) and equivalent, dolomitized (fill pattern) facies at Reinecke field. Data from Saller and others (2004).

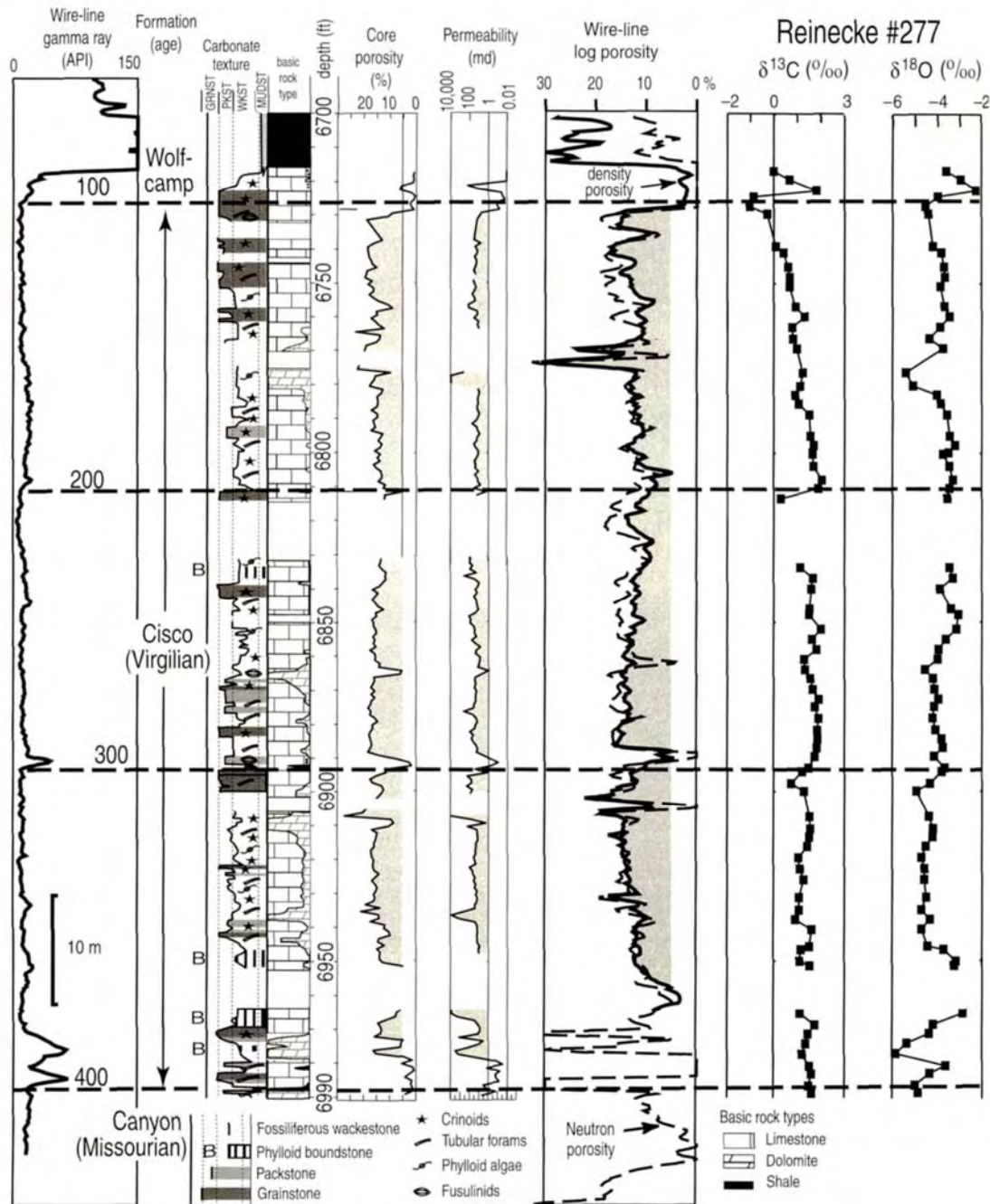
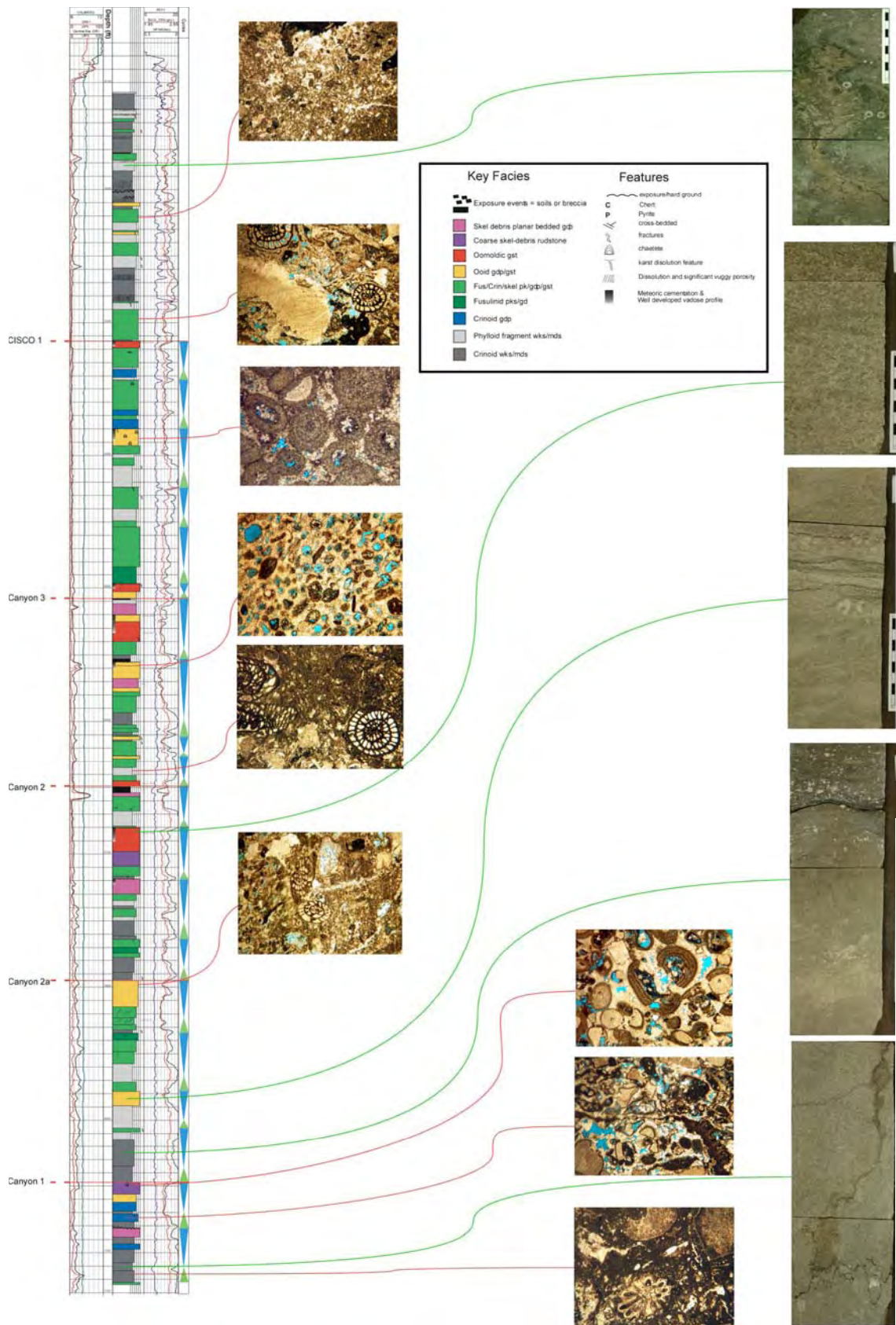


Figure 54. Single type well example from Reinecke field (after Saller and others, 2004). Note that wireline-log porosities are above 10 percent for the entire interval.



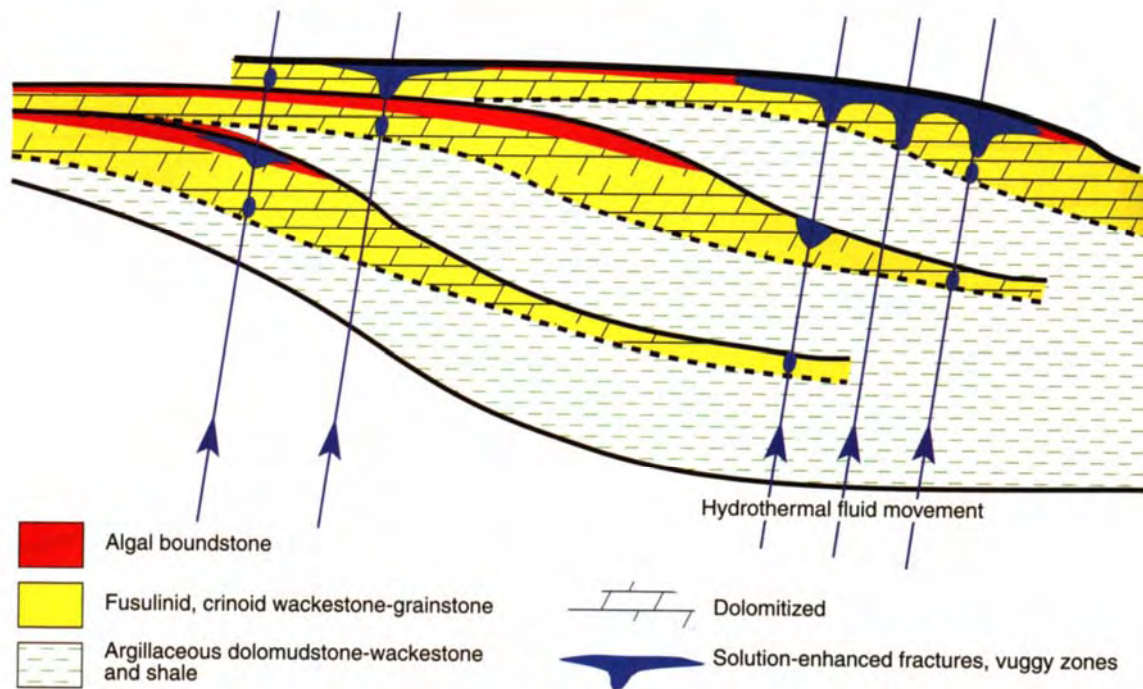


Figure 56. Conceptual dolomitization model for Missourian and Virgilian succession at Dagger Draw, Northwest Shelf. Dolomitization is thought to be diagenetically late, and fluids migrated into the succession from below via faults and fractures. After Tinker and others (2004).

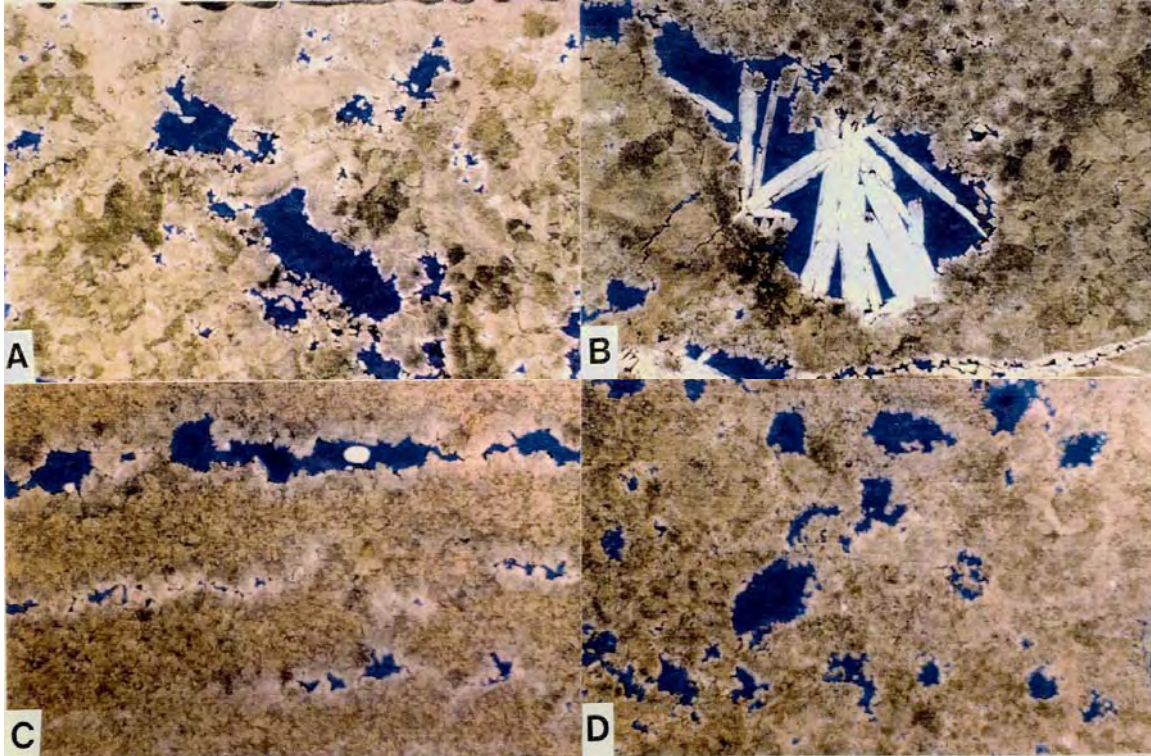


Figure 57. Thin-section photomicrographs of porosity (blue) and texture of the dolomitized facies (after Tinker and others, 2004). A. Fabric-destructive dolomitization of a possible packstone with irregular-shaped pores, possibly originally moldic and primary intergranular. All pores are technically intercrystalline now. B. Large, possibly solution enhanced pore in dolomitized wackestone packstone. Large pore partly occluded by barite cement. C. Dolomitized mudstone, which may have been originally algal laminated. Pores well connected horizontally but weak vertically. Texture commonly called zebra dolomite. D. Dolomitized packstone with moldic pores after leached bioclasts.

EARLY LEONARDIAN TO LATE WOLFCAMPIAN, DEEP-WATER CARBONATE
SYSTEMS IN THE PERMIAN BASIN: EVIDENCE FROM WEST TEXAS
OUTCROPS

Ted Playton and Charles Kerans

Bureau of Economic Geology
Jackson School of Geosciences
The University of Texas at Austin
Austin, Texas

ABSTRACT

Outcrops in the Victorio Flexure area of the Sierra Diablo Mountains, West Texas, provide evidence suggesting that (1) Ouachita-related tectonism remained active throughout Early Permian time in the Delaware Basin and (2) margin-to-slope topography generated from these tectonic events can focus sediment downslope, resulting in channelized carbonate debris accumulations. In the late Wolfcampian, a distally steepened carbonate ramp (Hueco 'C' Formation) developed near the Victorio Flexure monocline along the western margin of the Delaware Basin. In the latest Wolfcampian, significant rotation of the Victorio Flexure monocline increased slope height by more than 170 m and slope gradient by more than 6°. Preexisting ramp sediments were slump deformed, and significant reentrant topography formed along the upthrown hinge of the monocline. These reentrants and slump topography acted as downslope focusing mechanisms for early Leonardian (lower Abo Formation) carbonate debris. This debris bypassed the upper slope and was deposited at the lower slope/toe of slope in the form of amalgamated channel complexes that display proximal to distal relationships.

Knowledge of late Wolfcampian tectonic activity provides additional information to constrain the waning of Ouachita-related tectonism in the Delaware Basin and, perhaps, throughout the Permian Basin system. Shelf-margin and upper-slope topography as sediment-focusing controls are critical components of carbonate-slope channelization and basinward sediment transport. Basinal, grainy, carbonate accumulations can survive diagenetic deterioration of reservoir quality, and channelization linked to differential topography may help to predict their distribution.

INTRODUCTION

Outcrops near the Victorio Flexure (VF) monocline, Sierra Diablo Mountains, west Texas, provide a continuous dip exposure of an Early Permian, distally steepened carbonate ramp (Read, 1985) and slope deposits (late Wolfcampian lower and upper Hueco 'C' Formations and early Leonardian lower Abo Formation) along the western margin of the Delaware Basin (figs. 1, 2). These strata conformably overlie terrestrial to shoreline siliciclastics of the mid- to late Wolfcampian Powwow Formation (fig. 2). The Powwow through Abo Formations comprise the oldest Permian sediments near the VF and unconformably overlie uplifted Precambrian basement strata of the Hazel Formation (King, 1965). The VF, first identified by King (1965), is a deep structure that was active during Ouachita deformation and is expressed as a northward-plunging, WNW-trending monocline at the surface. Hueco 'C' ramp paleogeography and the distally steepened inflection are coincident with the upthrown, southern hinge point of the Victorio Flexure (SHVF). The mapped study area includes as much as 190 m of section and approximately 7 km of continuous, oblique dip exposure, outcropping along the VF (fig. 2).

Early Permian VF outcrops were comprehensively described by King (1965) and recently studied by Wilde (1995b), Kerans (2001), and Playton (2003a, b). This exposure especially highlights carbonate-slope deposits with a range of sediment gravity flows, including slump complexes and channelized to unchannelized debris-flow complexes. Because the exceptional dip continuity allows for correlation of ramp-crest to slope environments, slope facies and architectural element organization can be observed within a platform-constrained sequence stratigraphic context. Evidence suggests, however, significant northward rotation of the VF monocline and consequent deformation of the Hueco 'C' ramp in the latest Wolfcampian. This deformation implies that the latest Wolfcampian slope deposits were tectonically induced and not deposited as a result of typical ramp-slope depositional processes. Additionally, post-tectonic slope sediments of the early Leonardian Abo Formation show a clear response to antecedent differential topography generated from the latest Wolfcampian tectonic event. Therefore, tectonically induced slope deposits and the effects of tectonically generated topography on subsequent slope deposition are of interest and available for study. Field-data collection included measured sections with samples and thin sections, plan-view maps, and detailed interpreted photomosaics.

EARLY PERMIAN PALEOGEOGRAPHY OF THE WESTERN DELAWARE BASIN

The late Paleozoic Ouachita deformation reactivated deep-rooted structural features across North America (Yang and Dorobek, 1995). Flexural loading and structural reactivation associated with North American plate subduction formed a complex foreland basin system, the Permian Basin, in present-day Texas and New

Mexico (Yang and Dorobek, 1995). The Central Basin Platform was an intraforeland uplift that subdivided the Permian Basin into the Delaware Basin to the west and the Midland Basin to the east. The Diablo Platform was a structurally positive area that defined the western shelf of the Delaware Basin, along which were several north-dipping, WNW-trending, east-plunging monoclines, formed as a result of transtension (Yang and Dorobek, 1995). These structures were first mapped by King (1965) and called ‘flexures,’ which represent deep-rooted, half-graben structures that were surficially expressed as large-scale, rotated fault blocks along hinge points (monoclines).

Early Permian paleogeography strongly reflects the underlying flexure-controlled structure (fig. 3; King, 1965). The monoclinial flexures were expressed as large embayments along the primarily N-S striking, western Delaware Basin margin. These embayments acted as local depocenters and developed shelf-to-basin stratigraphy during their fill (fig. 4). The study area’s outcrop belt is an example of such and represents the northward advance of siliciclastic and carbonate systems into the VF embayment.

Early Permian strata unconformably overlie Precambrian basement in the study area (fig. 1). South of the VF monocline, Wolfcampian strata overlie an uplifted block of Proterozoic Hazel Formation sandstone. North of the SHVF, Hazel exposures plunge into the subsurface, reflecting the northward tilt of the VF monocline (King, 1965). Large-scale depositional geometries of the overlying Hueco ‘C’ and Abo sediments reflect this monoclinial structure, where flat-lying strata are observed south of the VF and north-dipping strata are observed along the VF monocline (fig. 1). This flexure-controlled, paleogeographical arrangement defines the southern edge of the VF-controlled embayment along the Delaware Basin shelf margin (figs. 3, 4).

MID- TO LATE WOLFCAMPIAN DEPOSITIONAL EVOLUTION

Mid- to late Wolfcampian strata in the VF area can be subdivided into three large-scale facies tracts that record uplift and subaerial erosion, transgression, and development of a low-angle, distally steepened carbonate ramp. These facies tracts are, in stratigraphic order, the mid- to late Wolfcampian Powwow Formation, the late Wolfcampian lower Hueco 'C' Formation, and the late Wolfcampian upper Hueco 'C' Formation (fig. 1).

The *mid- to late Wolfcampian Powwow Formation*, a nonmarine to shallow marine siliciclastic wedge, represents the oldest Permian strata in the area (fig. 5a). The Powwow directly overlies uplifted basement and marks a substantial angular unconformity. The wedgelike morphology reaches a maximum thickness at the SHVF of 60 to 65 m and thins in both directions along dip. Powwow sediments consist of siliciclastic conglomerates, sandstones, and siltstones that transition from basal alluvial fan/braided fluvial facies to capping shoreline facies. The Powwow succession displays an overall retrogradation of depositional systems and represents (1) subaerial erosion of uplifted basement blocks to the south of the VF, (2) development of alluvial-fan and braided fluvial terrestrial systems, (3) marine transgression, and (4) development of shallow marine shoreline systems (fig. 5a).

The *late Wolfcampian lower Hueco 'C' Formation* is an open marine limestone blanket that conformably overlies and drapes the Powwow across the exposure (fig. 5b). The lower Hueco 'C' maintains a relatively constant thickness of 25 to 30 m and displays a consistent upward facies succession throughout the study area, implying a relatively flat paleo-seascape during deposition. Lower Hueco 'C' limestones are thin bedded, nodular, and structureless, and they grade upward from basal silty skeletal wackestones/

packstones, into fusulinid wackestones/packstones, into capping crinoid wackestones. This succession records increasing paleo-water depth throughout lower Hueco 'C' time, where substorm wave-base (SWB), distal outer-ramp environments transitioned into basin-floor carbonate environments. Thus, the lower Hueco 'C' represents (1) initial submergence of a low-relief siliciclastic landscape, (2) waning of siliciclastic input during onset of carbonate production, and (3) continued transgression during distal outer-ramp carbonate accumulation (fig. 5b).

The *late Wolfcampian upper Hueco 'C' Formation* conformably overlies the lower Hueco 'C' and represents the youngest Wolfcampian strata in the area (fig. 5c). The upper Hueco 'C' tapers in thickness from more than 110 m south of the VF to less than 15 m north of the VF (fig. 1) and displays a northward transition from dolomite to limestone. The interval also shows a change from undeformed strata south of the VF to disrupted, slump-deformed, and resedimented strata along and north of the VF, respectively. These disrupted deposits are interpreted to be the result of a postlate Hueco 'C' deformation event (further explained in later sections); however, thickness distributions and facies constraints allow for reconstruction of the undeformed precursor accumulation (fig. 6). Reconstructed upper Hueco 'C' facies are arranged into a hierarchy of landward- and seaward-stepping packages and display Waltherian facies relationships. The most updip (southward) facies are dominated by dolomitic peloidal-fusulinid packstones/grainstones with high-energy SWB stratification. These facies transition northward across the VF monocline into skeletal lime packstones/wackestones with lower-energy SWB features. North of the VF, facies are assumed to have been similar to those of the lower Hueco 'C' distal outer ramp to basinal limestones but were disturbed

and resedimented after deposition. The reconstructed upper Hueco 'C' accumulation is interpreted as the sub-fair-weather wave base (FWWB) part of a larger-scale carbonate-ramp system (fig. 5) that prograded across the lower Hueco 'C' blanket. Facies record a northward transition from (1) high-energy, storm-dominated outer-ramp environments just below FWWB into (2) lower-energy, storm-dominated outer-ramp environments into (3) sub-SWB, distal outer-ramp to basin-floor environments (fig. 5c). A distally steepened break in slope marked by facies and thickness changes coincides with the SHVF monocline. A calculated slope gradient from reconstruction (Figure 6) of between 1° and 2° supports a ramp-profile interpretation. Thus, the upper Hueco 'C' represents (1) change from transgressive to regressive conditions; (2) development of a low-angle, distally steepened carbonate ramp; and (3) postdepositional deformation of partly lithified ramp sediments (further explained in later sections; fig. 5c).

Wolfcampian facies tracts in the VF area can be arranged into a sequence stratigraphic framework with systems tracts. Basal Powwow sediments represent lowstand (LST) conditions recording exposure, unconformity generation, and subaerial erosion. Upper Powwow and lower Hueco 'C' sediments represent transgressive (TST) conditions recording retreat of terrestrial systems, marine inundation of the landscape, and increasing paleo-water depth during sub-SWB carbonate deposition. Upper Hueco 'C' sediments represent highstand (HST) conditions where relative sea level stabilized, sedimentation filled in existing accommodation, and SWB carbonate depositional environments prograded. Early Leonardian lower Abo Formation slope deposits overlie Hueco 'C' shallow outer-ramp environments, suggesting a significant earliest Leonardian transgression and forcing a sequence boundary at the Wolfcampian/Leonardian contact.

Hueco 'C' deposition was approximately 7 Ma in duration (Wilde, 1995a); thus the Powwow/Hueco 'C' sequence is of 3rd-order composite sequence scale (Mitchum and others, 1977) and marks the basal sequence within the 2nd-order late Wolfcampian to late Leonardian supersequence (PW3 to L6 of Kerans, 2001, and Fitchen and others, 1995).

LATEST WOLFCAMPIAN TECTONIC ACTIVITY AND SEDIMENT DEFORMATION

Previous sections describe development of the late Wolfcampian, low-angle (1° to 2°) Hueco 'C' ramp, with a distally steepened break in slope at the SHVF (fig. 5). Assumptions of the low-angle nature of the ramp are based on uniform vertical facies succession and thickness of the lower Hueco 'C' (implying a flat, pre-Hueco 'C' landscape) and gradual thickness trends and facies changes of the upper Hueco 'C.' As exposed today, the outcrop displays the Hueco 'C' profile as a flat-topped shelf with flat-lying strata south of the VF, inclined strata dipping northward at 7° along the VF monocline, and gently dipping strata (1° or less) north of the VF (fig. 1). Depositional and stratal relationships of overlying Leonardian deposits reflect and conform to the present-day exhumed Hueco 'C' profile, suggesting that it represents latest Wolfcampian (post-Hueco 'C') paleogeography (fig. 1). Upper Hueco 'C' sediment deformation is stratigraphically constrained to the latest Wolfcampian because overlying Leonardian sediments are undeformed. Coherent failure features in deformed upper Hueco 'C' sediments suggest lithification of sediments and ramp development prior to failure. Therefore, a phase of structural rearrangement and slope adjustment occurred after Hueco 'C' deposition and prior to Leonardian deposition (constrained to latest Wolfcampian

time). This tectonic event transformed the low-angle (1° to 2°) upper Hueco 'C' ramp profile into a flat-topped shelf with a 7° -dipping slope along the VF monocline.

Tectonic movement along the VF monocline in the latest Wolfcampian is most likely responsible for the paleogeographic adjustment and resulting deformation of upper Hueco 'C' sediments. Reflecting late-phase Ouachita shearing (Yang and Dorobek, 1995), fault blocks to the north of the study area downdropped and caused significant northward rotation of the Victorio Flexure monocline, increasing shelf-to-basin relief by more than 170 m and slope gradient by more than 6° (figs. 5d, 6). This rotation relocated the preexisting upper Hueco 'C' outer ramp into an upper-slope position just basinward of a prominent break in slope at the SHVF. Former distal outer-ramp and basinal sediments of the upper Hueco 'C' were shifted into a gently dipping lower-slope position north of the VF. This change in paleogeography and slope gradient resulted in postdepositional failure of upper Hueco 'C' sediments.

Latest Wolfcampian tilting of the VF increased slope gradients enough to cause substantial instability and failure of preexisting upper Hueco 'C' sediments (fig. 7). At the SHVF, dramatic extension and coherent failure occurred in lithified outer-ramp sediments, resulting in high-relief, slump topography and reentrant formation. Along the tilted VF monocline, partly lithified outer-ramp sediments detached coherently on the less-coherent, underlying lower Hueco 'C' and display a spectrum of brittle to ductile deformation features, rotation, and translation. At the NHVF and northward, less-lithified distal outer-ramp and basinal sediments experienced less tilting but underwent noncoherent failure and resedimented into mud-supported breccias with skeletal WS clasts, interpreted as debris flows. The debris flows stacked into unconfined, mounded

complexes that display hierarchical organization and compensational stacking. These complexes coalesced to form a tabular debris-flow apron at the newly defined lower-slope position. This paleogeographical adjustment and resulting sediment deformation episode mark the terminal observable event in the Wolfcampian.

LEONARDIAN LOWER ABO FORMATION CHANNELIZATION

The *early Leonardian lower Abo Formation* (L1 TST of Kerans, 2001, and Fitchen and others, 1995) conformably overlies the upper Hueco 'C' and is concentrated primarily north of the VF, reaching thicknesses in excess of 40 m near the NHVF and thinning northward (fig. 5e). Along the VF monocline, the lower Abo pinches and swells along strike from 0 to more than 25 m and was not included in this study south of the VF. Lower Abo limestones are dominated by thick-bedded, polymict, matrix-supported carbonate breccias, with minor fractions of stratified packstones and laminated mudstones. Breccias are arranged into a hierarchy of compensational beds and contained within larger-scale erosional surfaces defining channel-form features. A discontinuous veneer of hemipelagic wackestone/mudstone locally appears at the base of the lower Abo along the VF monocline, suggesting a period of slope quiescence after the latest Wolfcampian VF rotation and supporting a Leonardian-age interpretation. The lower Abo possesses characteristics of a deep-water, channelized, slope or toe-of-slope carbonate environment composed of allochthonous debris in the form of various sediment gravity flows. Matrix-supported breccias are interpreted as submarine debris flows, and the packstone to mudstone facies represent varying concentrations of turbidites. The substantial increase in thickness coincident with a loss in slope gradient at the NHVF

indicates net-sediment bypass across the VF monocline and net-sediment deposition north of the VF. Occurrence of well-developed channelized complexes implies an updip sediment-focusing mechanism where allochthonous material is repeatedly exported through the same downslope pathway over time. The source of lower Abo debris is poorly constrained owing to lack of outcrop, but it is assumed to be shed from an early Leonardian platform that backstepped significantly relative to the terminal Wolfcampian margin, aggraded, and oversteepened (Kerans, 2001; Fitchen and others, 1995). Thus, the lower Abo represents (1) slope quiescence after the latest Wolfcampian tectonic event, (2) downslope focusing of allochthonous debris promoting channelization, (3) net-sediment bypass across the VF monocline, and (4) net-sediment deposition north of the VF in the form of amalgamated channel complexes (fig. 5e).

Perhaps the most striking features generated during the latest Wolfcampian VF rotation are high-relief reentrants and coherent slump topography present at the SHVF (fig. 7). This dramatic differential topography provided a sediment-funneling mechanism where early Leonardian debris (lower Abo) focused between and around positive areas at the SHVF, reoccupied the same downslope sediment pathways along the VF monocline, and were deposited as amalgamated channelized complexes north of the VF. This feedback between margin differential topography (that is, reentrants) and sediment focusing provides a mechanism for development of carbonate-slope channelization.

Lower Abo channel complexes display interesting downdip variations in plan-view architecture and thickness from the VF and northward (fig. 8). Near the SHVF along the VF monocline (proximal upper-slope position), lower Abo breccias primarily fill a thick (>25 m), single, strike-discontinuous debris axis with erosive margins, capped

by a laterally continuous, thinner (<10 m) breccia veneer. Farther north along the VF monocline (distal upper-slope position), breccias are thin (5–10 m) and strike-discontinuous and represent multiple smaller-scale sediment axes, as opposed to one primary axis observed updip. These architectural relationships along the VF monocline (upper slope) define a proximal primary feeder channel directly downdip of an active reentrant at the SHVF. This feeder channel bifurcated into multiple smaller scale channels toward the NHVF, partly in response to upper Hueco ‘C’ slump mass topography, but also as a function of increasing distance from the sediment focal point and decreasing slope gradient (fig. 8). North of the VF (lower-slope and toe-of-slope positions), lower Abo breccias thicken significantly to more than 40 m across the NHVF inflection and thin gradually northward. They form well-developed, amalgamated channel complexes that display slight sinuosity, offset relative to previous channel topography, and become less amalgamated (isolated) to the north (fig. 8). These plan-view architectural relationships and thickness changes of the lower Abo (figs. 5e, 8) represent a change from net-sediment bypass along the VF to net-sediment deposition north of the VF, reflecting increasing distance from the sediment focal point and a change in slope gradient from 7° to 1° across the NHVF.

Lower Abo internal channel architecture and channel shape also exhibit proximal to distal transitions (fig. 9), representing downdip increases in depositional versus erosional processes. Fill of the primary feeder channel at the SHVF (upper-slope position) is highly amalgamated, where bedding surfaces are difficult to recognize and track laterally. In contrast, channel complex internal architecture north of the VF (lower-slope and toe-of-slope positions) is beautifully preserved and displays hierarchical

organization of compensationally shingled, individual debris flows (fig. 9). Despite relatively small changes in gradient (1° dip) north of the VF, lower-slope, amalgamated channel complexes near the NHVF change northward from narrow (<150 m), flat topped, and highly incisional to broad (>200 m), mounded, weakly erosional, and isolated from other complexes at the toe of slope (fig. 9). These changes in channel-fill preservation and morphology reflect a basinward (upper slope to lower slope/toe of slope) increase in deposition:erosion ratio, as distance from the sediment source and focusing mechanism increases and slope gradient decreases.

SUMMARY AND DISCUSSION

The VF outcrop exposure records Early Permian carbonate-ramp development, tectonic deformation, and slope channelization. During the mid- to late Wolfcampian in the VF area, uplifted basement south of the VF was eroded and provided a source for siliciclastic alluvial and shoreline systems of the Powwow Formation. Transgression inundated the landscape, siliciclastic sources were choked, and the Hueco 'C' distally steepened carbonate ramp evolved in the late Wolfcampian. In the latest Wolfcampian, after Hueco 'C' ramp development, substantial northward rotation of the VF monocline increased slope height by more than 170 m and slope gradient by more than 6°, transforming gently dipping Hueco 'C' outer-ramp and basin-floor carbonate environments into upper- and lower-slope/toe-of-slope environments, respectively. This tectonic adjustment of the depositional profile triggered substantial failure of upper Hueco 'C' sediments and created reentrant topography at the SHVF that later acted as a sediment-focusing mechanism for early Leonardian (lower Abo Formation) carbonate

debris. Consequently, channelized lower Abo debris bypassed the VF monocline (upper slope) and ponded north of the VF (lower slope/toe of slope) in the form of amalgamated debris-flow channel complexes. Late Wolfcampian through early Leonardian exposures near the VF offer excellent examination of tectonically induced carbonate-slope deposits, as well as effects of tectonic-related differential topography on subsequent slope deposition.

VF outcrops provide stratigraphically constrained evidence suggesting local tectonic activity along the Delaware Basin margin in latest Wolfcampian time. This tectonism reflects the transtensional structural regime associated with waning stages of Ouachita deformation (Yang and Dorobek, 1995). Thus, Ouachita-related tectonic activity, at least locally, persisted throughout the Wolfcampian stage along the western Delaware Basin margin and perhaps elsewhere in the Permian Basin system. Latest Wolfcampian VF movement substantially postdates the Mid-Wolfcampian Unconformity (Ross, 1986; Candelaria and others, 1992; Fitchen and others, 1995; Yang and Dorobek, 1995).

VF outcrops represent a well-exposed outcrop analog for channelized carbonate-slope systems. They underscore the importance of updip sediment-focusing mechanisms (differential topography on the upper slope or margin) in the development of carbonate-slope channels, especially considering the strike-elongate nature of periplatform and margin sediment sources. In this case, local tectonic readjustment and slumping along the VF were responsible for reentrant formation that focused later Leonardian debris. In other reef-rimmed systems with steep, early-lithified margins, gravitational collapse of the margin and upper slope is a common process (Cook and others, 1972; McIlreath and

James, 1978; Playford, 1984; Coniglio and Dix, 1992) that results in differential margin topography and reentrant formation. Additionally, products of these collapse events are coarse, slope-megabreccia deposits that are often laterally discontinuous and mounded, creating differential topography on the slope itself. Thus, reentrants and slope-megabreccia topography generated from reef-margin collapse also provide mechanisms for sediment focusing and potential channel development.

Many of the productive deep-water carbonate reservoirs in the Permian Basin system are grain-rich, toe-of-slope to basinal accumulations associated with channelization. Carbonate deposits with primary porosity in these environments can survive diagenetic overprints that deteriorate reservoir quality in more proximal positions. Thus, these accumulations have significant reservoir potential, especially if associated with pelagic source rocks and stratigraphic seals. Powell Ranch field, eastern Midland Basin (Montgomery, 1996), is a late Wolfcampian/early Leonardian example of such a reservoir system. Mud-poor, grainy deposits on the basin floor are somewhat anomalous, considering that they should come to rest at higher angles of repose on the slope (Kenter, 1990). Channelization, as a more efficient sediment-transport process, could explain how these sediments bypass their preferred gradient range for deposition and are deposited in a substantially more distal, lower-gradient position. Therefore, as shown from VF outcrops, mapping reentrants and rugosity along shelf margins can delineate potential sediment-focusing mechanisms. Identification of these mechanisms provides another tool for predicting slope channelization and economic basinal accumulations. Additionally, occurrence of collapse-derived, slope-megabreccia deposits implies an associated updip collapse scar or reentrant in the margin, offering another

predictive tool for delineating sediment-focusing mechanisms. Considering the Permian Basin system, VF outcrops recorded tectonic activity and reentrant formation during latest Wolfcampian time. Similar local tectonism and margin topography development may have occurred elsewhere in the Permian Basin during this time and could help predict distribution of Wolfcampian/Leonardian-age basinal carbonate reservoirs.

ACKNOWLEDGMENTS

I thank the members of my Master's Thesis Committee at The University of Texas at Austin—Charles Kerans, Scott Tinker, and Bob Goldhammer—for their constructive input. Thanks also to the Bureau of Economic Geology and Jackson School of Geosciences at The University of Texas at Austin for providing support to this research. Critical funding was provided by the Reservoir Characterization Research Laboratory at the Bureau of Economic Geology, the Jackson School of Geosciences Geology Foundation, the Chevron Scholarship Program, and the AAPG Grants-In-Aid Program. I also wish to express my appreciation to former owners, managers, and caretakers of the Sierra Diablo and Corn Ranches in west Texas for land access. Finally, special thanks go to Jerome Bellian, Roger Wagerle, Chris Rhea, Jerry Lucia, Stephen Ruppel, and Bureau of Economic Geology scientists and staff for support both in the field and in the office.

REFERENCES

- Candelaria, M. P., Sarg, J. F., and Wilde, G. L., 1992, Wolfcampian sequence stratigraphy of the eastern Central Basin Platform, *in* Mruk, D. H., and Curran, B. C.,

- eds., Permian Basin Exploration and Production Strategies, West Texas Geological Society Publication No. 92-91, p. 27–44.
- Coniglio, M., and Dix, G. R., 1992, Carbonate slopes, *in* Walker, R. G. and James, N. P., eds., Facies models: response to sea-level change: Geological Association of Canada, p. 349–374.
- Cook, H. E., McDaniel, P. N., Mountjoy, E. W., and Pray, L. C., 1972, Allochthonous carbonate debris flows at Devonian bank ('reef') margins, Alberta, Canada: Bulletin of Canadian Petroleum Geology, v. 20, no. 3, p. 439–497.
- Fitchen, W. M., Starcher, M. A., Buffler, R. T., and Wilde, G. L., 1995, Sequence stratigraphic framework and facies models of early Permian carbonate platform margins, Sierra Diablo, West Texas, *in* Garber, R. A., and Lindsay, R. F., eds., Wolfcampian-Leonardian shelf margin facies of the Sierra Diablo—Seismic scale models for subsurface exploration: West Texas Geological Society Annual Field Trip Guidebook, No. 95-97, p. 23–66.
- Kenter, J. A. M., 1990, Carbonate platform flanks: slope angle and sediment fabric: Sedimentology, v. 37, p. 777–794.
- Kerans, C., 2001, Stratigraphy and reservoir facies development: slope-basin carbonate and mixed clastic-carbonate systems: The University of Texas at Austin, Bureau of Economic Geology, RCRL Annual Field Trip Guidebook, 22 p.
- King, P. B., 1965, Geology of the Sierra Diablo region, Texas: U.S. Geological Survey Professional Paper 480, 185 p.
- McIlreath, I. A. and James N. P., 1978, Facies models; 13, Carbonate slopes: Geoscience Canada, v. 5, 189–199.

- Mitchum, R. M., Jr., Vail, P. R., and Thompson, S., III, 1977, Seismic stratigraphy and global changes in sea level; Part 2, The depositional sequence as a basic unit for stratigraphic analysis, *in* Payton, C. E. ed., Seismic stratigraphy—applications to hydrocarbon exploration: American Association of Petroleum Geologists Memoir 26, p. 53–62.
- Montgomery, S. L., 1996, Permian ‘Wolfcamp’ limestone reservoirs; Powell Ranch Field, eastern Midland Basin: American Association of Petroleum Geologists Bulletin, v. 80, p. 1349–1365.
- Playford, P. E., 1984, Platform-margin and marginal-slope relationships in Devonian reef complexes of the Canning Basin, *in* Purcell, P. G., ed., Canning Basin Symposium, Proceedings: Perth, Geological Society of Australia and Petroleum Exploration Society of Australia, p. 189–214.
- Playton, T. E., 2003a, Tectonic deformation of a late Wolfcampian carbonate ramp, *in* Hunt, T. J., and Lufholm, P. H., eds., West Texas Geological Society, Publication No. 03-112, Fall Symposium, October 8–10, p. 143–164.
- Playton, T. E., 2003b, Tectonic deformation of a late Wolfcampian carbonate ramp and resulting channelization, Victorio Flexure, west Texas: The University of Texas at Austin, Master’s thesis, 199 p.
- Read, J. F., 1985, Carbonate platform facies models: American Association of Petroleum Geologists Bulletin, v. 69, p. 1–21.
- Ross, C. A., 1986, Paleozoic evolution of the southern margin of the Permian Basin: Geological Society of America Bulletin, v. 97, p. 536–544.

- Wilde, G. L., 1995a, Recent observations on the Hueco and Bone Springs Formations, Sierra Diablo, with subsurface analogies, *in* Garber, R. A. and Lindsay, R. F., eds., Wolfcampian-Leonardian shelf margin facies of the Sierra Diablo—seismic scale models for subsurface exploration: West Texas Geological Society Publication, No. 95-97, p. 105–122.
- Wilde, G. L., 1995b, Wolfcampian-Leonardian biostratigraphy, Sierra Diablo: its relationship to sequence stratigraphic markers on the surface and in the subsurface, *in* Garber, R. A. and Lindsay, R. F. eds., Wolfcampian-Leonardian shelf margin facies of the Sierra Diablo—Seismic scale models for subsurface exploration: West Texas Geological Society Publication, No. 95-97, p. 67–82.
- Yang, K. and Dorobek, S. L., 1995, The Permian Basin of west Texas and New Mexico: tectonic history of a “composite” foreland basin and its effects on stratigraphic development, *in* Dorobek, S. L. and Ross, G. M., eds., Stratigraphic evolution of foreland basins: SEPM (Society for Sedimentary Geology) Special Publication No. 52, p. 149–174.

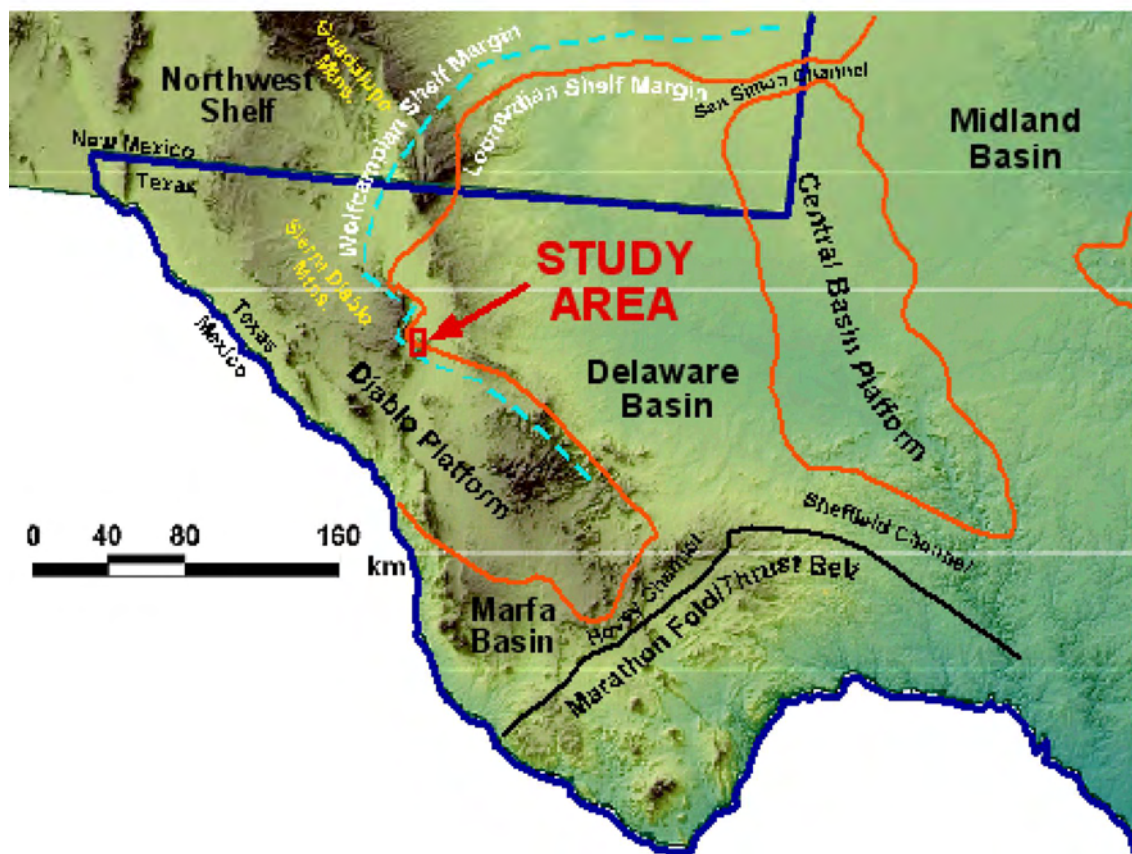


Figure 1. Digital elevation model of Permian Basin in west Texas and southeast New Mexico with outlines of major basins, platforms, structural features, and approximate Wolfcampian and late Guadalupian shelf margin trends.

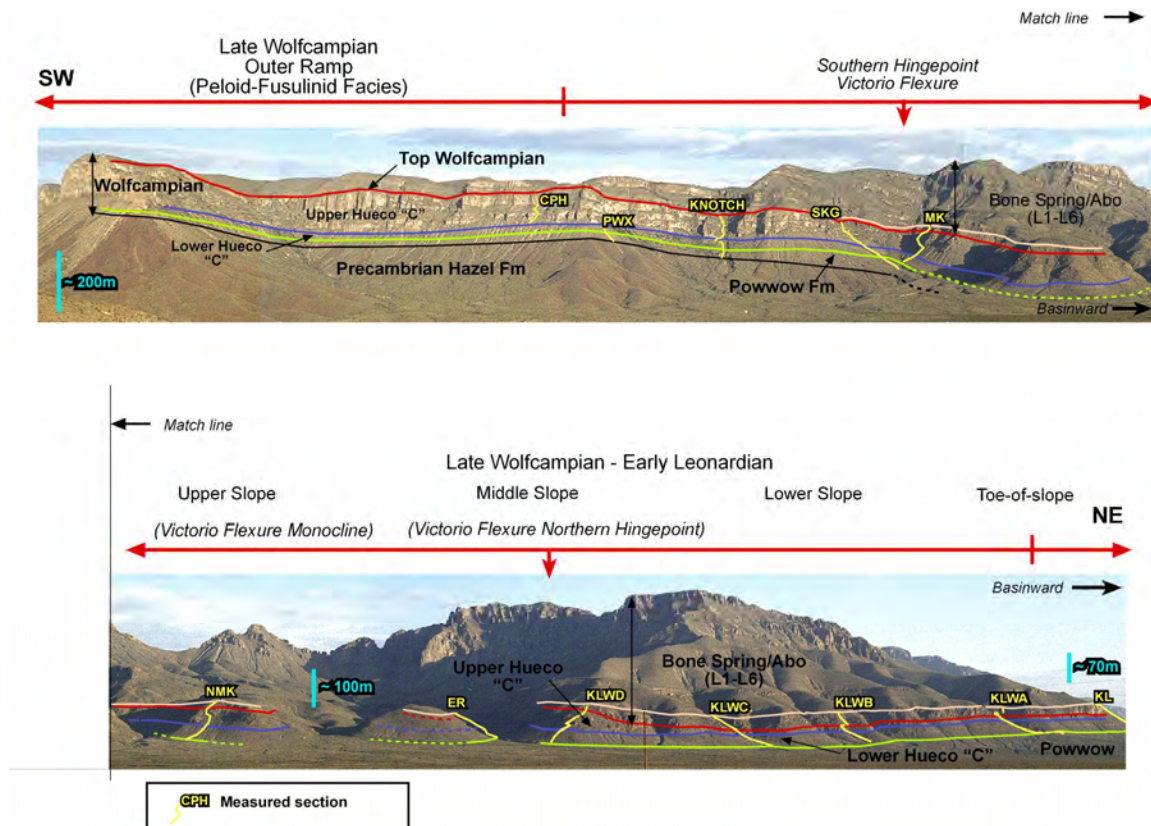


Figure 2. Regional photomosaic panel of study area looking westward along western Sierra Diablo escarpment, with interval break-out and measured section locations.

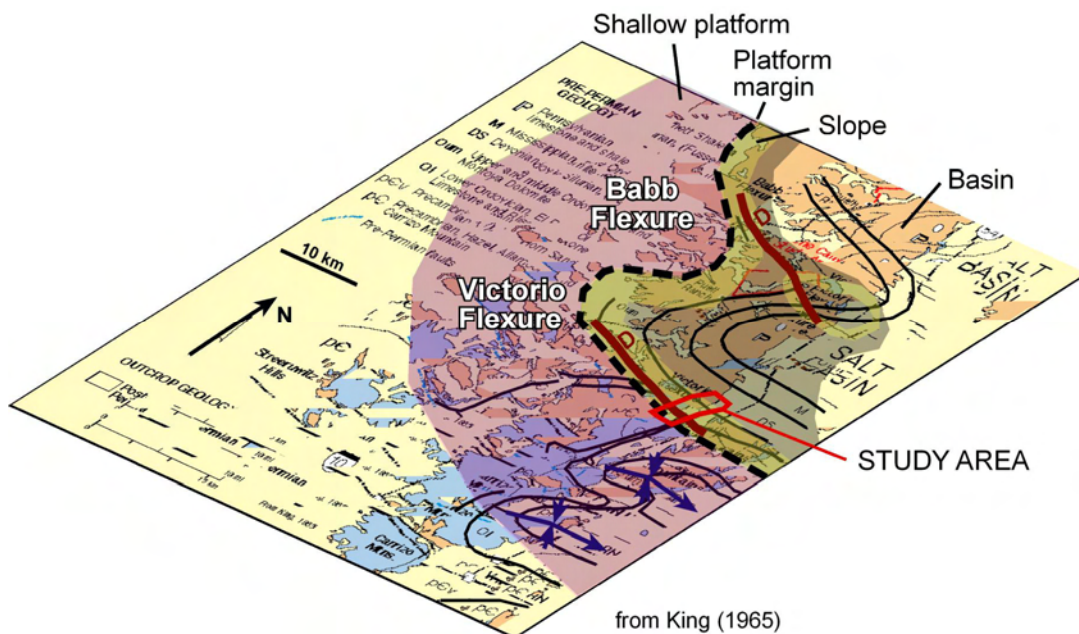


Figure 3. Late Wolfcampian paleogeography superimposed on King's (1965) geologic map of the Sierra Diablo Mountains, with flexures and study area highlighted. Large-scale subcrop synclines and shelf-margin embayments coincide with flexures.

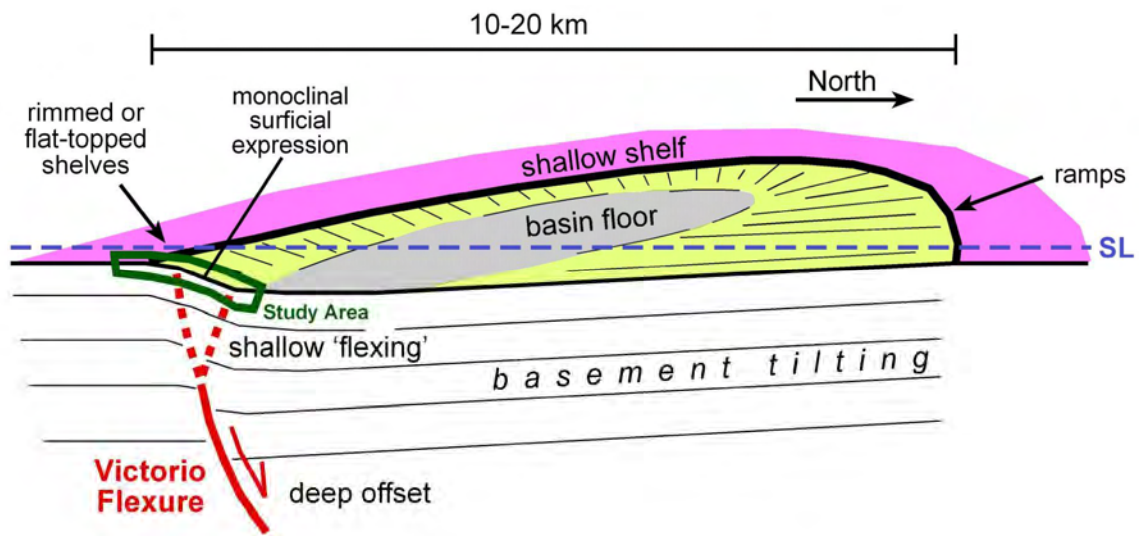


Figure 4. Hypothesized cross-sectional view of the Victorio Flexure showing the deep-rooted half-graben feature expressed as a monocline on the surface, with study area highlighted.

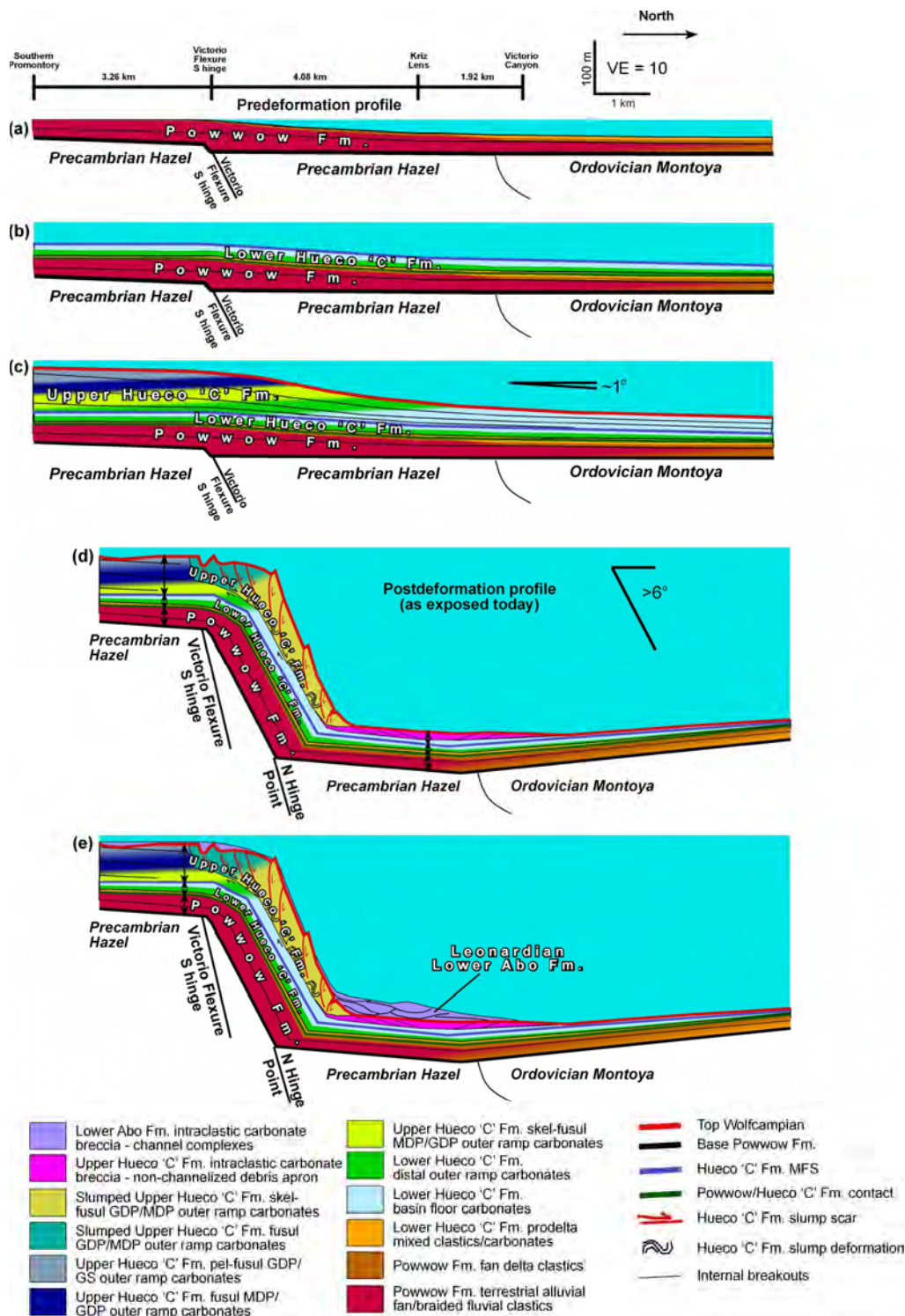


Figure 5. Sequential diagram of depositional and tectonic history of the study area, from mid-Wolfcampian to earliest Leonardian time, with relation to larger-scale ramp system. (a) Powwow terrestrial to shallow marine clastic deposition (mid- to late-Wolfcampian). (b) Lower Hueco 'C' distal outer-ramp to basin-floor carbonate blanket deposition (late Wolfcampian). (c) Upper Hueco 'C' prograding carbonate-ramp deposition (late Wolfcampian). (d) Tectonic rearrangement of slope profile along Victorio Flexure, causing failure of outer-ramp to basin-floor upper Hueco 'C' sediments (latest Wolfcampian). (e) Deposition of lower Abo carbonate debris-channel complexes, resulting from sediment focusing through reentrant topography at the southern hinge point of the Victorio Flexure (earliest Leonardian). Lower Abo debris bypassed the upper slope via a primary feeder channel and dispersed as channel complexes that ponded and amalgamated at the lower slope/toe of slope.

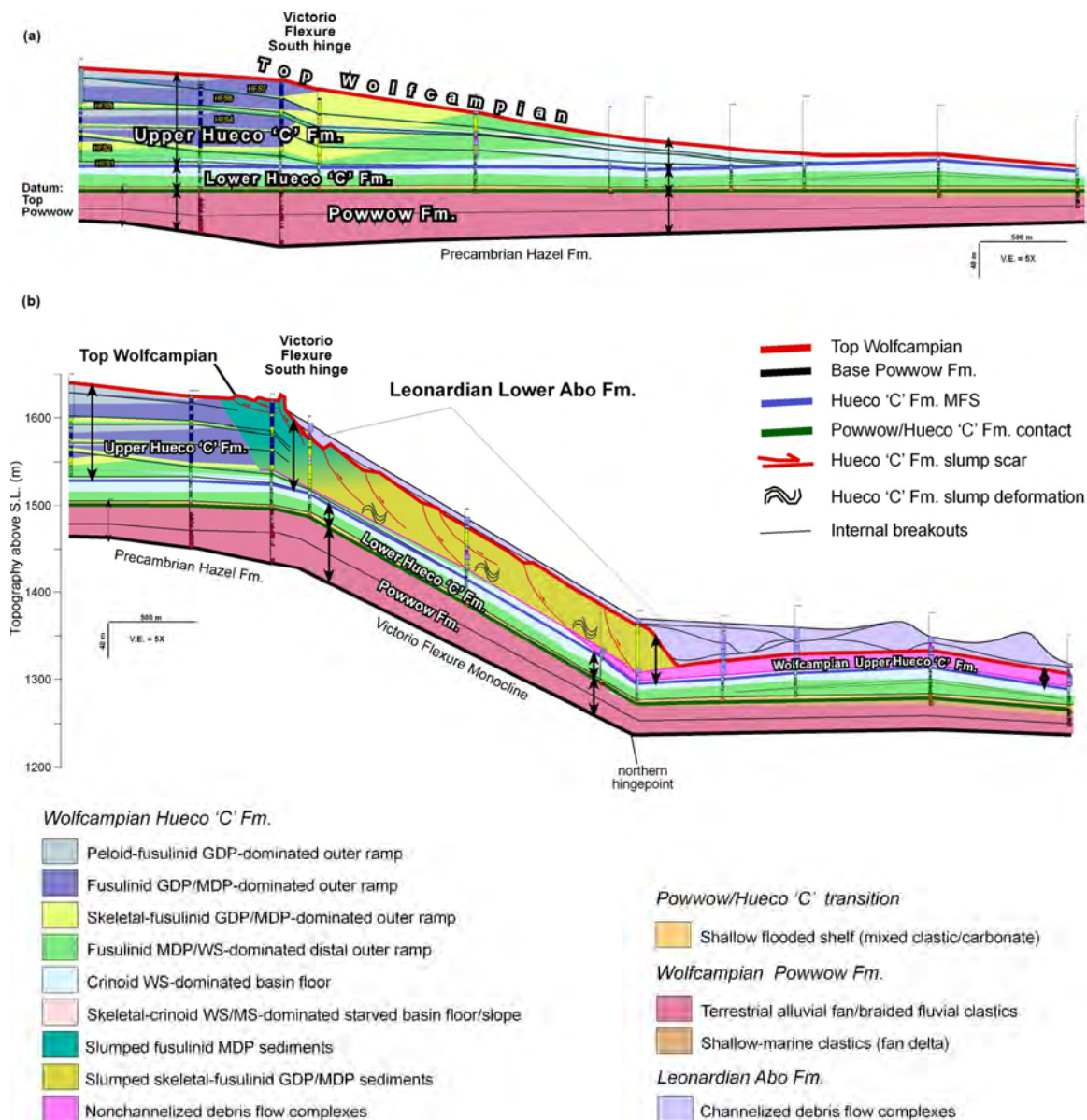


Figure 6. (a) Reconstructed regional cross section of distal part of a late Wolfcampian Hueco 'C' carbonate ramp based on measured section data. Cross section entails mid- to late-Wolfcampian deposition prior to tectonic deformation. Reconstruction was based on conformable facies and thickness relationships. (b) Postdeformation regional cross section as exposed today based on measured section data. Cross section is hung on present-day topography, assuming that exposed geometries are reflective of latest Wolfcampian/earliest Leonardian paleogeography that postdates Hueco 'C' development.

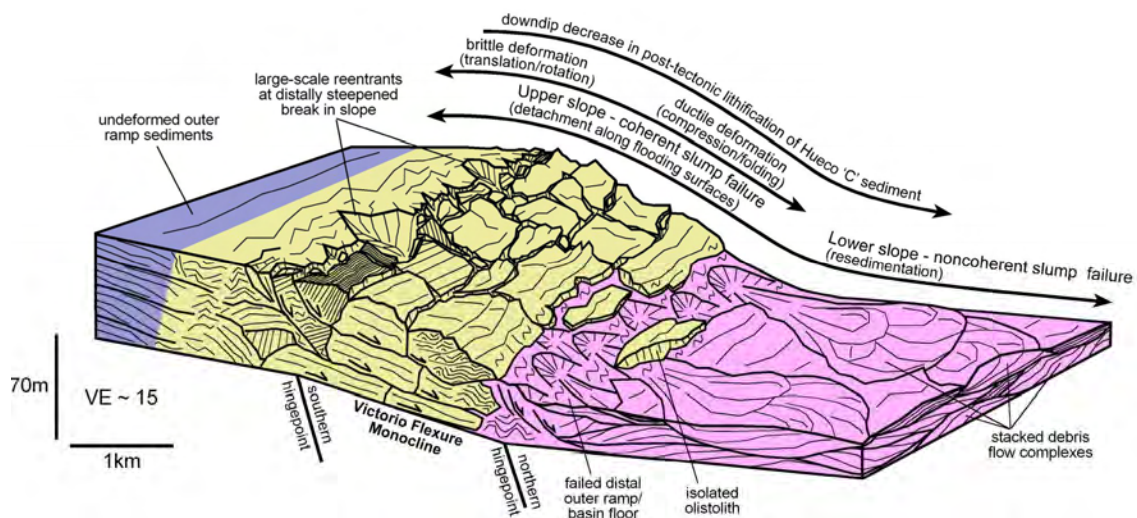


Figure 7. Sediment deformation diagram depicting response of Wolfcampian upper Hueco 'C' strata to latest Wolfcampian rotation along the Victorio Flexure. Coherent slump failure dominates the upper-slope setting, implying predeformation lithification of outer-ramp sediments. Noncoherent slump failure dominates the lower slope where relatively unlithified, muddier sediments completely disaggregated and resedimented as nonchannelized debris-flow lobe complexes that coalesced to form a lower-slope debris apron.

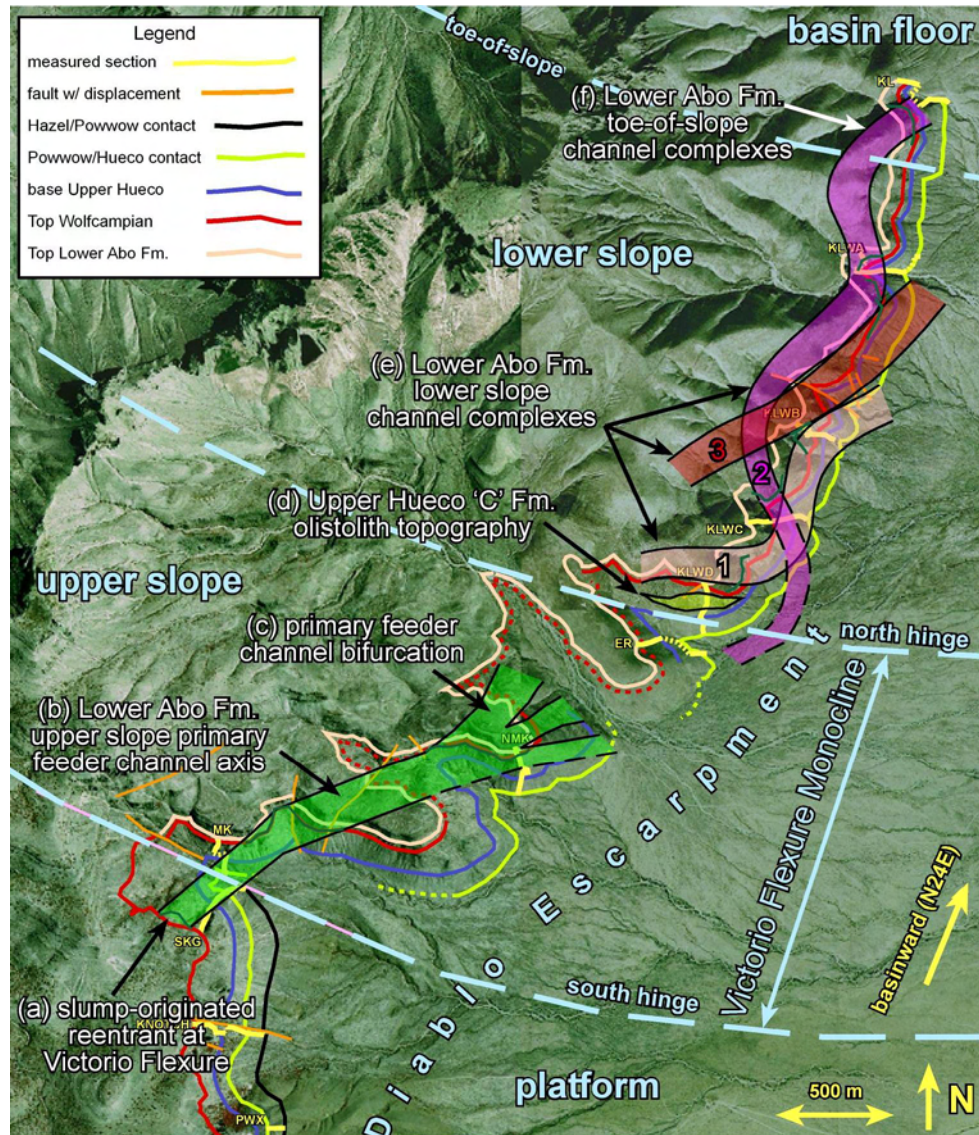


Figure 8. Plan view of lower Abo channel system, with latest Wolfcampian/early Leonardian paleogeography and depositional environments. From south to north, debris is concentrated in a primary feeder channel (b) resulting from sediment focusing through a large-scale reentrant at the southern hinge point of the Victorio Flexure (a). As distance from the updip focusing mechanism is increased and gradient is decreased, channel complexes begin to bifurcate from the primary feeder axis (c) and develop sinuosity. Channel complexes respond and offset relative to antecedent topography generated from the latest Wolfcampian slumping event, especially detached olistoliths at the northern hinge point of the Victorio Flexure (d). Channel complexes pond and erosionally amalgamate at the lower-slope position (e), coincident with the terminus of upper Hueco 'C' slump topography and the gradient decrease at the Victorio Flexure northern hinge-point inflection. As distance from the updip focusing mechanism becomes substantial and gradient continues to lessen, channel complexes become less incisive, more depositional, broader, mounded, and more isolated, marking the toe-of-slope position (f).

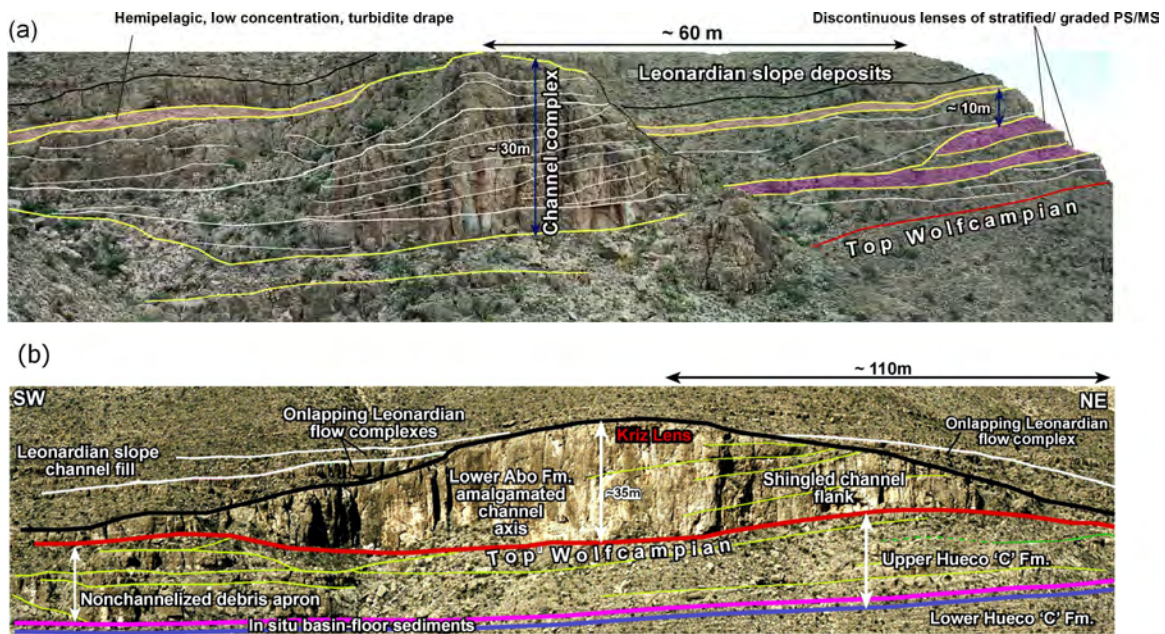


Figure 9. Outcrop photographs of Leonardian-Wolfcampian section. (a) Oblique strike view of lower Abo lower slope-channel complex. Lower slope-channel complexes exhibit higher degrees of incision narrower width and are flat topped relative to toe-of-slope channels. This geometry is due to higher erosion: deposition ratios at the lower-slope position. (b) Oblique strike view of the lower Abo, Kriz Lens, toe-of-slope channel complex. The Kriz Lens displays a mounded top (although erosionally enhanced), a relatively flat base, and it is broader, indicative of lesser erosion:deposition ratios common to the toe of slope.

MIDDLE PERMIAN BASINAL SILICICLASTIC DEPOSITION IN THE DELAWARE BASIN: THE DELAWARE MOUNTAIN GROUP (GUADALUPIAN)

H. S. Nance

Bureau of Economic Geology
Jackson School of Geosciences
The University of Texas at Austin
Austin, Texas

ABSTRACT

The Delaware Mountain Group (DMG) of the Delaware Basin of Texas and New Mexico comprises up to 4,500 ft (1,375 m) of Guadalupian-age arkosic to subarkosic sandstone, siltstone, and detrital limestone that was deposited in deep water, mainly during lowstand and early transgressive sea-level stages. Primary depositional processes include density-current flow and suspension settling. Regionally extensive organic-rich siltstones record largely highstand deposition and provided hydrocarbons to sandstone reservoirs. Authigenic illite and chlorite are present, but there is little detrital clay. The DMG is restricted to the slope and basin, was sourced from shelf-sediment source areas through poorly exposed incised valleys, and generally is not depositionally correlative with siliciclastics on the shelf. Interbedded carbonate units thicken shelfward and are typically correlative to “reef”-margin-complex carbonate sources along the shelf margin.

Gamma-ray and porosity logs are useful for differentiating primary sandstone, siltstone, and carbonate end-member rock types, although application of outcrop models is critical for differentiating channel, levee, and splay sandstone subfacies using well logs.

The basin succession is formally divided into the Brushy Canyon, Cherry Canyon, and Bell Canyon Formations. The Brushy Canyon, the coarsest grained, contains little detrital carbonate. The other formations contain prominent carbonate members that are used extensively for subsurface correlations and to subdivide the intervals into informally named productive units. The DMG has been interpreted to contain 28 high-frequency depositional sequences aggregated into 6 composite sequences.

The DMG contains more than 260 hydrocarbon reservoirs at 900 to 9,820 ft depth (274–2,993 m) that have produced more than 262.2 MMbbl of oil and 280,517,264 Mcf of gas from channel/lobe complexes and associated levee and splay facies deposited by turbidites.

Hydrocarbon source beds are intraformational, organic-rich siltstones that accumulated by suspension settling between episodes of turbidite activity. Hydrocarbon traps include both stratigraphic and structural components. Stratigraphic traps are formed where reservoir sandstone facies pinch out laterally into siltstone. Siltstone and calcite cements form stratigraphic seals. Hydrocarbon-bearing and water-bearing intervals alternate stratigraphically. Hydrocarbon migration is focused into stratigraphic traps that are located favorably on structural highs or in updip positions on structural ramps.

Structure is variably controlled by four processes, two of which are regional and two of which are reservoir-scale: (1) basin-slope rise toward shelf near shelf margins, (2) Laramide-generated regional eastward dip, (3) compaction over subjacent sandbodies, and (4) slumping in areas that are updip of reservoirs. Primary production is by solution-gas drive, and recovery efficiency is less than 15 percent in most reservoirs.

Development challenges include delineating productive sandbody geometries, controlling hydrofracture extension to avoid connecting water-bearing with hydrocarbon-productive intervals, preventing formation damage from interactions between acid treatments and Fe-bearing chlorite, and optimizing location of injection wells in continuous-permeability fields with production wells for EOR operations.

INTRODUCTION

The Guadalupian-age Delaware Mountain Group (DMG) of the Delaware Basin consists of as much as 4,500 ft (1,372 m) of stratigraphically cyclic, mixed siliciclastic/carbonate slope, and basin-floor strata (Dutton and others, 2005). The section hosts many economically important hydrocarbon reservoirs. Most of the hydrocarbon production has been from siliciclastic-dominated units in the Brushy Canyon, Cherry Canyon, and Bell Canyon Formations, with secondary production from associated detrital carbonate strata (fig. 1). More than 262.2 million barrels (MMbbl) of 39° gravity (production-weighted average) oil has been produced from approximately 267 reservoirs, within which 65 percent of the 2,103 total wells were producing in 2003. The section has also produced 280,517,264 thousand cubic feet (Mcf) of gas from approximately 95 reservoirs, within which 63 percent of the 183 total wells were producing in 2003. Production depths range from 900 to 9,820 ft (274–2,993 m) (Railroad Commission of Texas, 2003). Despite the economic significance of the DMG, most published technical information regarding its stratigraphy, lithology, and reservoir character is derived from geographically severely limited outcrop exposures and a few field locations.

The Ochoan Series is also present in the Delaware Basin and includes, from older to younger, the Castile, Salado, Rustler, and Dewey Lake Formations. However, only the Castile Formation is restricted to the basin; therefore, stratigraphy and sedimentology of the Salado, Rustler, and Dewey Lake Formations are discussed in the section of this report that deals with the Guadalupian and Ochoan shelf section. The Ochoan in the Delaware Basin hosts a few small reservoirs in the Castile and Rustler intervals. More than 186,403 bbl of 36.26° (production-weighted average) oil has been produced from approximately eight reservoirs, within which no wells were producing in 2003. The section has also produced 429,348 Mcf of gas from approximately six reservoirs. Only three wells were producing from one Rustler reservoir in 2003. Production depths that include all historical reservoirs range from 380 to 3,704 ft (Railroad Commission of Texas, 2003). The importance of the Ochoan to hydrocarbon issues in the Permian Basin is related to its generally low permeability and in its role as a regional top seal for the Delaware Mountain Group in the Delaware Basin. It has also been known to guide hydrocarbon migration from basinal source beds into reservoirs located on the Central Basin Platform and Northwest Shelf (Hills, 1972).

This report summarizes published information on the DMG, whose literature spans nearly 100 years—from initial reconnaissance expeditions early in the 20th century through definitive geologic formational characterizations in the 1940's, development of modern depositional and sequence stratigraphic models in the 1990's and early 2000's, and ongoing investigations of DMG petroleum systems. The DMG, a significant producer of hydrocarbons, still contains abundant resources, although its depositional and diagenetic characteristics are complex. The objective in this report is to provide a basis from which to advance our understanding of the geologic succession and to stimulate continued and more efficient exploitation of the resources of the DMG.

PREVIOUS WORK

The Delaware Mountain Group succession was first described by Richardson (1904), who described it as a formation that included the Bone Spring Limestone. He noted the lateral geometric variability in sandstone strata, which later were recognized as variations among depositional facies. Beede (1924) recognized a lithologic tripartite character in the Delaware Mountain sandstone interval, which formed the basis of its subsequent subdivision into three formations. King (1942) raised the classification of the section to group status and named the Brushy Canyon, Cherry Canyon, and Bell Canyon Formations. King (1942) raised the Bone Spring to formation rank, although its Leonardian age had been recognized previously (King and King, 1929), at which time it was also suggested that the Bone Spring be divided from the Delaware Mountain Formation because the two formations were obviously separated by a pronounced unconformity and were dissimilar lithologically. King (1948) produced several excellent cross sections in the Guadalupe Mountains that are accepted as largely accurate, even after 6 decades of additional investigation by many workers.

Hull (1957) discussed the petrogenesis of the Delaware Mountain sandstones, pointed out the generally finer grained character of the Delaware sands compared with mineralogically similar, coeval sandstones on the surrounding shelves (also recognized by King, 1942), interpreted the carbonate members as including reef detritus, and suggested a turbidite model for Delaware Basin deposition. Jacka and others (1968) summarized previous investigations of Delaware Mountain sedimentation that largely concluded that the section recorded deep-sea fan

deposition with submarine-canyon feeder systems, a conclusion reinforced by Meissner (1972). Payne (1976) described and interpreted siliciclastic subfacies from the Bell Canyon and proposed sand-transport directions from shelf areas and estimated relative importance of different source areas. Fischer and Sarnthein (1988) suggested an eolian source on the shelf for Delaware Mountain basinal siliciclastics. Harms and Brady (1996) summarized the several hypotheses historically suggested for deposition of the deep-water succession that, most importantly, contrast turbidite mechanisms with saline density-current mechanisms. Hills (1984) produced west-east cross sections for the Delaware Basin, suggested that the paleogeographically closed character of the Delaware Basin promoted accumulation of organic material that eventually generated hydrocarbons, and that the Castile evaporites overlying the Delaware Mountain effectively preserved hydrocarbons and guided hydrocarbon migration into reservoirs in the surrounding shelves. Facies models were developed from outcrop, core, and well log analyses by Gardner (1992, 1997a), Gardner and Sonnenfeld (1996), Barton (1997), Barton and Dutton (1999), Beaubouef and others (1999), Dutton and others (1999), Carr and Gardner (2000), and Gardner and Borer (2000). Sequence stratigraphic relationships in the Delaware Mountains were investigated and described by Gardner (1992, 1997b) and Kerans and Kempter (2002). Particularly useful discussions of hydrocarbon generation, source rocks, and reservoirs that were developed in Delaware Mountain strata include Payne (1976), Jacka (1979), Hayes and Tieh (1992a), Hamilton and Hunt (1996), May (1996), Gardner (1997b), Dutton and others (1999, 2000, 2003), Montgomery and others (1999, 2000), and Justman and Broadhead (2000). Impact of Delaware Mountain clay authigenesis on reservoir development was discussed by Walling and others (1992). Enhanced oil recovery (EOR) in certain Delaware Mountain Group fields was discussed by Kirkpatrick and others (1985), Pittaway and Rosato (1991), Dutton and others (1999, 2003).

REGIONAL SETTING

The Delaware Basin during deposition of the Delaware Mountain Group was a deep-water basin bounded by carbonate-ramp (San Andres and Grayburg) and carbonate-rim (Goat Seep and Capitan) margins that developed on the western edge of the Central Basin Platform, the Northwest Shelf, and the Diablo Platform. The primary connection between the Delaware Basin

intracratonic sea and the open ocean was through the Hovey Channel (fig. 2). Most deposition in the area during sea-level highstands was on the shelves and consisted of the mixed carbonate-siliciclastic San Andres Formation and Artesia Group (Grayburg, Queen, Seven Rivers, Yates, and Tansill Formations). The Delaware Mountain Group shelf-derived siliciclastics and shelf-margin-derived detrital carbonates were deposited during intermittent sea-level lowstands (for example, Silver and Todd, 1969; Meissner, 1972). Basin subsidence outpaced sediment supply such that deep-water conditions were maintained until the close of the Guadalupian, after which Ochoan evaporites filled the basin and eventually blanketed the entire greater Permian Basin area. Onset of basin evaporite accumulation corresponded with demise of the Capitan Reef system and is hypothesized to mark closing of the Hovey Channel, which promoted progressive restriction of the basin from marine influx (King, 1948).

FACIES AND SEDIMENTOLOGY OF THE DELAWARE MOUNTAIN GROUP

Distribution and Age

The Delaware Mountain Group (DMG) is Guadalupian in age, according to fauna described by Girty (1908). The DMG includes the uppermost occurrences of Guadalupian fauna in the Delaware Basin (Lang, 1937) and the three formations of the Delaware Mountain Group were defined to represent the early, middle, and late subdivisions, respectively, of Guadalupian time (King, 1948).

The DMG is formally divided into three formations. From base to top they are the Brushy Canyon, Cherry Canyon, and Bell Canyon Formations. These names, assigned by King (1942), reflect the names of canyons in the Delaware Mountains. The formations are lithologically similar except that the Brushy Canyon contains abundant medium-grained channelized sandstone beds. The other formations are significantly finer grained and dominated by laminated bedding in the outcrop area, although these differences may mark a shifting toward the east and southeast of shelf-edge siliciclastic storage areas that sourced Cherry Canyon and Bell Canyon deposition. The boundary in outcrop between the Brushy Canyon and the Cherry Canyon was placed at the top of the uppermost medium-grained sandstone bed in the Brushy (King, 1942). The contact with the overlying Cherry Canyon is unconformable (fig. 3), and the lower part of the Cherry Canyon composes the Cherry Canyon (sandstone) Tongue. Whereas the Brushy Canyon, most of

the Cherry Canyon, and the Bell Canyon are restricted to the Delaware Basin, the Cherry Canyon Tongue extends well onto the shelf and pinches out approximately 6 mi shelfward of the stratigraphically superjacent Goat Seep shelf margin (Kerans and Kempter, 2002). Goat Seep and Capitan shelf-margin carbonates form the updip limits of subsequently deposited Delaware Mountain successions.

The Brushy also lacks the prominent carbonate members that are characteristic of the Cherry Canyon and Bell Canyon intervals. Carbonate members were named by King (1942) for minor geographic features such as small canyons, hills, springs, or houses, where the correspondingly named strata were described. The Hegler (limestone) Member of the Bell Canyon is used to divide the Bell Canyon from the underlying Cherry Canyon. Other carbonate members are used to subdivide the Cherry Canyon (South Wells, Getaway, and Manzanita) and the Bell Canyon (Hegler, Pinery, Rader, McCombs, and Lamar) (fig. 1). South Wells and Getaway members of the Cherry Canyon are lenticular, whereas the Manzanita is more laterally persistent. Hegler, Pinery, Rader, McCombs, and Lamar carbonate members of the Bell Canyon are thinner overall and more laterally persistent than are Cherry Canyon carbonate members. All carbonate members thin basinward from their updip pinch-outs near the shelf margin. All three DMG formations are recognized throughout the Delaware Basin, although they may be more problematic to distinguish in parts of the basin where carbonate interbeds are thin or absent.

It was recognized early (for example, Cartwright, 1930) that the Delaware Mountain Group is a sea-level-lowstand wedge of sedimentary rock that is restricted to the Delaware Basin. Todd (1976) considered the Spraberry basinal sandstones (presumably the upper Spraberry of later usage; for example, Handford, 1981) of the Midland Basin to be Brushy Canyon equivalents and Guadalupian in age. Jeary (1978) and Handford (1981) concluded a Leonardian age for the Spraberry. If Jeary (1978) and Handford (1981) are correct, there may be no deep-water equivalents for the Delaware Mountain Group elsewhere in the Permian Basin. However, Ruppel and Park (2002) demonstrated the existence of Brushy-Canyon-equivalent lowstand-wedge deposits in the Midland Basin, as have other authors.

Facies

The Brushy Canyon was deposited upon an unconformity that developed on Leonardian-age (King, 1942, 1948) Bone Spring carbonates. The unconformity is locally marked on the

Western Escarpment of the Guadalupe, where the Cutoff and Victorio Peak Formations are truncated beneath the Brushy Canyon. On the flanks of the Bone Spring Flexure, an area between El Capitan and Shumard Peak in the Guadalupe Mountains where the top of the Bone Spring rises more than 1,000 ft, the outcropping basal 100 ft of the Brushy Canyon consists of conglomerates as much as 10 ft thick, with interbedded sandstone, limestone, and thinly to thickly bedded sandstone. Conglomerates are composed of gravel, cobbles, and boulders as much as 4 ft in diameter. Conglomerates include limestone material from the Bone Spring and Victorio Peak Formations. Conglomerate bodies are lenticular (channelized) and absent from higher areas of the flexure where Brushy Canyon sandstones onlap (King, 1948). Conglomerates are not reported from Brushy Canyon intervals in the hydrocarbon-productive areas, which are largely located a minimum of several miles from Delaware Basin shelf margins (figs. 2, 4).

Dominant facies in the Delaware Mountain Group are arkosic to subarkosic sandstones and siltstones (for example, Hull, 1957; Kane, 1992; Thomerson and Asquith, 1992) (fig. 5). Sediment texture ranges mainly between coarse silt and very fine grained sand, although fine-grained sand is found in the Brushy Canyon. Shales are rare. Finer grained intervals, even those that contain several percent organic carbon, are properly classified as siltstone (Thomerson and Asquith, 1992). Siltstones compose organic-rich (up to 46 percent total organic content [TOC]; average 2.36 percent TOC) and organic-poor subfacies (average 0.52 percent TOC) (Sageman and others, 1998; Wegner and others, 1998; Dutton and others, 1999) (fig. 6). Clay content is dominantly authigenic illite and chlorite (fig. 5) rather than detrital and is not abundant (for example, 11.6 percent average in the Brushy Canyon, Lea County) (Green and others, 1996).

Siliciclastic sources are updip of and on the surrounding shelves, given the lithologic similarities between the DMG and Guadalupian elastic strata on the shelves (King, 1948; Hull, 1957). Carbonates are volumetrically of secondary importance and increase in prominence shelfward. Limestone is most common; however, some diagenetic dolomite is present. Carbonates are dominantly detrital and derived from the lower San Andres/Victorio Peak ramp margin (Brushy Canyon), Grayburg ramp-margin (lower Cherry Canyon), and Goat Seep (upper Cherry Canyon) and Capitan (Bell Canyon) rimmed shelf-margin complexes (Beaubouef and others, 1999; Kerans and Kempter, 2002).

Depositional Setting and Facies Architecture

DMG facies successions are typical of those found in deep basins in areas relatively proximal to carbonate-shelf margins. Sandstones compose channel, levee, overbank-splay, and lobe subfacies (for example, Galloway and Hobday, 1996; Gardner and Sonnenfeld, 1996; Beaubouef and others, 1999; Dutton and others, 1999, 2003) (figs. 7–10) that were deposited as sea-level-lowstand submarine fans basinward of the shelf-margin break and as lowstand wedges shelfward of ramp margins (Beaubouef and others, 1999). Turbidity flow appears to be the primary transport mechanism for coarser sediment (sand and shelf-margin carbonate debris) (for example, Hull, 1957; Jacka and others, 1968; Silver and Todd, 1969; Meissner, 1972; Zeldt and Rosen, 1995), whereas suspension settling may be an important mechanism for silt-sized sediment, especially the organic content (Payne, 1976). Eolian transport of silt has been proposed as a mechanism for conveyance of silt to the basin margins (for example, Fischer and Sarnthein, 1988; Gardner, 1992). Margins of the Guadalupian platform are well defined by the change from Lower Guadalupian (San Andres Formation) ramp and Upper Guadalupian (Goat Seep/Capitan) reef facies to slope, carbonate-debris-rich facies of the carbonate members of the Delaware Mountain Group (figs. 1, 11). Because of the limited availability of cores through these slope and basin-floor complexes, understanding of their paleoenvironmental setting and facies geometries is greatly facilitated by analyses of the well-exposed Delaware Mountain Group outcrops in the Delaware Mountains (figs. 12, 13).

Facies architecture is controlled by relative sea level and position along the shelf-margin to basin-floor profile. During falling sea level the slope is incised by submarine erosion. Incised channels are (1) barren as long as all throughgoing sediment bypasses the location, (2) containers of laterally discontinuous conglomerates as lag, or (3) blanketed by thin accumulations of silt or sand that mark the waning stages of throughgoing turbidity-current deposition (Beaubouef and others, 1999). Potential for net deposition of sandstone soon following incision increases for basinward locations. Incised channels that are initially bypassed by sediment are eventually back filled.

Channel-levee-complex sandstone deposits are variably sinuous (figs. 14, 15) and asymmetrical in cross section normal to flow direction. Channel sinuosity generally increases downslope, marking decrease in flow velocity attendant upon decreasing topographic gradients.

Channel-facies geometries and stacking patterns systematically vary according to position along the slope-to-basin-floor profile. On the upper slope, which is constructed largely of laminated siltstone intervals that are deposited during sea-level rise, deep incised channels are less numerous than are shallower channels farther down slope. Upper-slope channel deposits are generally isolated and vertically stacked. Channel fills compose multiple, onlapping strata, thus recording backfilling of incised channels. At the toe of slope, avulsion (channel abandonment) promotes development of laterally offset complexes of amalgamated channel deposits (for example, fig. 16a). In progressively downslope locations on the basin floor, avulsion-prone channel systems bifurcate into channel-levee complexes, and overbank sediments (splays) increase in prominence (fig. 8). Along the basin-floor profile, proximal channelized-fan sedimentation transitions to sheet deposition on lobes. Although approximately sheetlike, sandstone packages in distal positions are still deposited in compensatory fashion (Beaubouef and others, 1999) (fig. 8). The overall thickness distribution of individual Delaware sandstone intervals (that is, bounded top and bottom by laterally extensive siltstone sheets) is marked by dominance of channel facies along the axes of maximum thickness (fig. 16b).

Thin, laterally discontinuous siltstones are interlaminated with sandstones in overbank-splay deposits. In many cases siltstones blanket the sandstone deposits that remain after channel abandonment. However, the more important siltstones, in terms of reservoir development, are laterally extensive sheetlike organic-rich and organ-poor accumulations that stratigraphically separate successions of channelized sandstone deposits on the lowstand fan complex. Brushy Canyon correlative siltstone units have been mapped over distances exceeding 50 mi in southern New Mexico (Broadhead and Justman, 2000). In some places, siltstones compose nearly 80 percent of the Delaware Mountain Group (Hayes and Tieh, 1992b). Particularly thick siltstone accumulations (lowstand wedge) occurred during the latest stages of lowstand deposition, when relative sea level rose onto the shelf edge and sand transport to the basin largely ceased (Beaubouef and others, 1999).

DMG carbonate units are constructed largely of allochthonous debris derived from the outer shelf and shelf margins (King, 1948). Rock types range from lutite to boulder conglomerates. Conglomerates from Brushy Canyon carbonate units occur mainly as lag on the bedrock floors of incised channels at the shelf margin and generally do not compose a significant fraction of the formation in more basinward areas (King, 1948; Beaubouef and others, 1999). No

carbonate members are formally recognized in the Brushy Canyon or Cherry Canyon sandstone tongue. In the basin-restricted Cherry Canyon and Bell Canyon Formations, however, widespread carbonate-bearing intervals are present and are formally recognized as members (King, 1948). The geometry of carbonate members ranges from lenticular in older units to more sheetlike forms in the younger units (King, 1948). Although conspicuous for their carbonate content, these units comprise cyclic interbeds of carbonate and siliciclastic sandstone and siltstone; carbonate-dominated beds may represent less than half of the thickness of the member (fig. 17).

Diagenesis

The most economically important diagenetic processes in the Delaware Mountain Group are (1) feldspar dissolution, (2) feldspar and quartz authigenesis, (3) clay authigenesis, and (4) calcite cementation. Similar to processes observed in Guadalupian shelf siliciclastics, DMG siliciclastics show evidence of K-feldspar dissolution, which imparts a component of secondary porosity to reservoir facies, although initial porosity enhancement may be destroyed by subsequent collapse of remaining crystal elements. Dissolution of feldspar and quartz (the latter evidenced by sutured contacts between detrital quartz grains) created fluids that resulted in feldspar and quartz overgrowths elsewhere in DMG sandstones, reducing already impoverished permeability (Behnken, 1996). Clay authigenesis (chlorite and illite) probably had the greatest single effect on reservoir quality in DMG sandstones (Green and others, 1996; Thomerson and Asquith, 1992). Whisker- and weblike clays dissect pore space, illite/smectite species may swell when contacted by drilling fluids, and chlorites may decompose in the presence of acidic solutions to form pore-clogging, insoluble, Fe-hydroxide gels if the acids are left in the formation long enough for the pH to rise above 2.2 (Spain, 1992; Behnken, 1996; Green and others, 1996). No stratigraphic or lateral systematic variations in clay mineralogy have been defined in the DMG, although Thompkins (1981, cited in Walling and others, 1992) noted changes in chlorite fabric with depth. Calcite cements occur in thin stratiform accumulations that impart a component vertical porosity and permeability heterogeneity to DMG facies (Dutton and others, 1999) (fig. 18). Calcite cement appears to be most abundant in finer grained siliciclastics that are outside of channel-sandstone subfacies (Spain, 1992; Dutton and others, 1999) (fig. 19).

Hayes and Tieh (1992a) recognized a four-phase sequence of diagenesis in Delaware Mountain sandstones from Reeves and Eddy Counties: (1) early cementation by carbonate, sulfate, and halite that preserved significant intergranular porosity during early burial; (2) dissolution of cements and detrital minerals to produce secondary porosity; (3) chlorite authigenesis that dissected porosity; and (4) authigenesis of dolomite, feldspar, Ti-oxides, and illite. Although Hayes and Tieh (1992a) did not recognize illite/smectite as being as prominent in their studies from Waha field and Big Eddy Unit (Reeves and Eddy Counties), Thomerson and Asquith (1992) in their study of Hat Mesa field (Lea County) and Behnken (1996) in his study of Nash Draw field (Eddy County) did. Walling and others (1992) proposed that chlorite evolved from smectitic precursors and that chlorite may revert to expansive and migratory forms in the presence of some fluids used in well development and completion.

SUBSURFACE RECOGNITION AND CORRELATION

Identification of DMG formation boundaries in the subsurface is based largely on relationships between the formations observed in Guadalupe Mountain outcrops that were described by King (1948). One of the most useful subsurface cross sections based on well log correlations is found in Meissner (1972). Boundary correlations are lithostratigraphic. The Delaware Mountain Group is overlain by the evaporite-dominated Castile Formation, which produces a relatively low gamma-ray response and high acoustic velocity compared with those of the feldspathic siliciclastics of the DMG (Payne, 1976; Dutton and others, 1997, 1999) (fig. 20). The Castile is characterized by bed thickness that is distinctively greater than that of any of the beds in the underlying Delaware Mountain Group (fig. 10).

The base of the Delaware Mountain Group (base of Brushy Canyon Formation) is defined at the base of the lowermost siliciclastic interval that overlies the thick carbonate interval assigned to the Bone Spring limestone. This relationship appears to be basinwide. The Bone Spring typically has a gamma-ray signature that is distinctively lower than that of the siliciclastic-dominated DMG and has comparatively greater resistivity, density, and acoustic velocity. The Bone Spring strata also exhibit greater carbonate-bed thickness than do DMG strata.

The boundary between Cherry and Bell Canyons is extrapolated into the subsurface from relationships observed in the Guadalupe and Delaware Mountain outcrops. The Cherry Canyon/Bell Canyon boundary is between the Manzanita and Hegler Limestone Members in outcrop. These strata have been interpreted into nearby wells (for example King, 1948; Tyrrell and others, 2004) (figs. 17, 21) and form the link between outcrop-defined formation boundaries and the subsurface. In particular, a volcanic ash mapped in the outcropping Manzanita succession by King (1948) has been interpreted as regionally widespread and correlated extensively into the subsurface (BCB marker of Tyrrell and others, 2004) (figs. 17, 21).

The boundary between Brushy and Cherry Canyons was defined by Gardner and Sonnenfeld (1996) to be an organic-rich siltstone (lutite) similar to that observed between the Brushy Canyon and the Bone Spring. Most workers place the boundary at the base of the organic siltstone interval (for example, May, 1996) (fig. 22), which is consistent with King's (1948) original pick at the top of the uppermost sandstone on the Brushy Canyon outcrop. Gamma-ray-log responses for this facies are typically high (fig. 22). These units record transgressive and highstand basin starvation where deposition of windblown silt and marine plankton dominated. The organic-rich siltstones and interbedded carbonate probably record the transgressive leg of late Brushy Canyon deposition and, in light of sequence stratigraphic analysis, might better be placed in the Brushy Canyon Formation.

Most DMG carbonates also have gamma-ray values that are lower than those of most DMG siliciclastics, the exceptions being thinly bedded examples that are interbedded with siliciclastics. A more reliable log for carbonate identification is the density log, however, which indicates much higher densities for the carbonate-dominated strata (figs. 17, 20) than for the more porous siliciclastics. Siltstones have significantly higher gamma-ray values than do sandstones, and organic-rich siltstones (which often include a fraction of volcanic ash) show the highest gamma-ray values of all (for example, fig. 10a).

Sandbodies can be discriminated by their overall lower radioactivity compared with that of the siltstones that envelop them. Widespread siltstones, especially those that are organic rich, are useful for correlation and allow confident mapping of correlative sandstones. Discrimination of DMG sandstone subfacies is more problematic and attempts to define log facies for channel, splay, levee, and lobe deposits that have been largely model driven (for example, Dutton and others, 1999). Interpreted channel subfacies tend to show little gamma-ray variation, such as

might be expected in less massive subfacies. Levee deposits have been interpreted where log responses suggest some interbedding of coarser and finer grained siliciclastics, the finer grained of which contain marginally more clay and feldspar and, thus, are slightly more radioactive. Outcrops indicate that levees are most common where sandbodies thin laterally, and this criterion is useful for interpreting the probability of levee development.

The Brushy Canyon/Cherry Canyon boundary in outcrop is picked at the top of the uppermost medium-grained sandstone interpreted to be in the Brushy Canyon (for example, fig. 6). However, the textural fineness of Cherry Canyon compared with that of Brushy Canyon is probably somewhat a function of evolving paleogeography. By Cherry Canyon deposition, sand depocenters had begun to shift toward the east from positions that were prominent during Brushy Canyon deposition (fig. 4). In the north part of the Delaware Basin the Brushy contains no significant carbonate except at the bases of incised channels on the Bone Spring shelf margin. Along the Central Basin Platform margin prominent Brushy Canyon carbonate intervals are evident within the lower part of the section, although they are subordinate in thickness to those in the Cherry Canyon and Bell Canyon.

The Cherry Canyon/Bell Canyon boundary is defined in outcrop at the base of the Hegler limestone member, a pick that King (1948) considered to be correlative to the lowermost part of the Capitan shelf margin. Acceptance of this boundary places the Getaway, South Wells, and Manzanita carbonate members entirely within the Cherry Canyon. Further, the Manzanita was correlated by King (1948) into the Shattuck sandstone member of the Queen. This correlation places the Manzanita stratigraphically between the Goat Seep and Capitan shelf-margin successions. Some subsequent writers agreed with King's correlation (for example, Newell and others, 1953), although some placed the Manzanita at the top of Cherry Canyon (for example, Kerans and Kempter, 2002; Tyrrell and others, 2004) (fig. 11). Others suggested that the Manzanita correlates at least partly into the Capitan (for example, McRae, 1995a; Beaubouef and others, 1999).

There is some uncertainty concerning the stratigraphic equivalence of the Manzanita to either the Goat Seep or Capitan margins. Tyrrell and others (2004) correctly pointed out the potential ambiguities inherent in using only well log criteria for correlations of the Manzanita, which can lead to its correlation into the Capitan in some areas in the north part of the basin, and into the Goat Seep in other areas (fig. 21). The root of the problem may well be that carbonate

members and the shelf-margin carbonates are significantly diachronous; thus, lithostratigraphic correlations are not always justified. Carbonate intervals identified as Manzanita may be equivalent to the Goat Seep in some locations and to the Capitan in others.

The top of the DMG (Bell Canyon Formation) is a relatively straightforward pick on the base of the Castile evaporites (anhydrite and calcite), the latter of which is expressed by a regionally extensive, thick interval of very low radioactivity on a gamma-ray log and generally high sonic velocity on an acoustic log (figs. 10, 20).

DEPOSITIONAL MODELS FOR THE DELAWARE MOUNTAIN GROUP

Water Depth

The presence in outcrops of texturally coarse, rippled and cross-laminated, channelized sandstone with current-oriented fossils prompted King (1942, 1948) to interpret the Brushy Canyon as having been deposited under “agitated” conditions and, thus, was an overall shallow-water deposit. King recognized alterations between high-energy and low-energy deposits; however, he did not think that this sedimentary cyclicity indicated significantly varying water depths. He drew similar conclusions for the lower half of the Cherry Canyon, including the carbonate-bearing intervals. However, he interpreted the largely unchannelized upper part of the Cherry Canyon as recording overall deepening of the depositional environment.

It is important to appreciate that King was describing data compiled near the shelf margin of the basin, where water depths were shallower than those anticipated toward the basin center. Even so, King (1948) calculated water depths to be more than 1,000 ft (>305 m) in the area on the basis of the difference in altitudes between updip and downdip extents of the outcropping Lamar limestone member at the top of the Bell Canyon.

Based on differences between updip and downdip altitudes of correlative stratigraphic horizons, King’s cross sections (1948) suggest an overall deepening of the Delaware Basin sea during DMG accumulation. One explanation is that development of shelf-margin barriers over time more efficiently attenuated continental sediment influx while the basin continued to subside at historically comparable rates, such that sediment influx was increasingly unable to match basin subsidence. Alternatively, or concurrently with barrier development, siliciclastic source areas may have become exhausted or buried (King, 1948). Siliciclastic influx into the basin

eventually ceased, as evidenced by post-DMG deposition of the virtually clastic-free Castile Formation that filled the basin to its rim.

Sediment Sources and Depositional Processes

Areas to the northwest, north, and northeast of the Delaware Basin were siliciclastic depocenters during sea-level lowstands throughout the Permian and probable sources to the basin for DMG siliciclastics. The Queen and Yates Formations of the Artesia Group (Tait and others, 1962) are especially notable for their abundant siliciclastic content. Broadhead and Justman (2000) interpreted the source of Brushy Canyon sand to be entirely from the Northwest Shelf. This interpretation is supported by the preferred location of Brushy oilfields in the north part of the basin (fig. 4). DMG depocenters shifted toward the east side of the basin during Cherry and Bell Canyon deposition (figs. 4, 23). The dominant original source of DMG siliciclastics was probably granitic rock in the ancestral Front Range in Colorado, given the high feldspar content of siliciclastic facies (Basham, 1996).

Carbonate sediments appear to have been mainly allochthonous and derived from erosion of carbonate shelf margins. Additional carbonate material was swept from outer-shelf back-reef environments, which bounded the Delaware Basin.

Adams (1936) was one of the first to suggest that the very fine siliciclastics found in the Delaware Mountain Group may have been wind borne (see also Fischer and Sarnthein, 1988; Gardner, 1992). Requirements for eolian sedimentation include (1) the presence of winds of adequate power to entrain significant quantities of sediment and (2) proximity to the basin margin of a large sediment reservoir having textural and pedogenic properties amenable to wind transport. Prevailing wind directions during Guadalupian time have been suggested to be northeasterly, northerly, or northwesterly (present azimuths) on the basis of crossbedding measurement across the southwestern U.S. (Peterson, 1988). These directions are mirrored in the orientations of Delaware Mountain submarine-channel systems.

Most depositional models for the Delaware Mountain Group, including and since the early work of Richardson (1904) and King (1934, 1942, 1948), have recognized that patterns of siliciclastic and carbonated sedimentation record the systematic effects of sea-level changes. However, details of this process are debated. For example, sandstones have been interpreted by many to have been transported into the basin during sea-level lowstand from eolian-dominated

ergs near the emergent shelf margin. In this mode, sand was transported to the upper slope by wind and then distributed by waves. Upper-slope sand stores grew until a critical mass was reached and sediment began to slump or avalanche into deeper water and eventually be carried farther into the basin by turbidity currents (for example, Gardner, 1992) or saline-density currents (for example, Harms, 1974). By contrast, Loftin (1996) thought that most of the sand that had accumulated during lowstand was “cannibalized” during transgressions and transported into the basin from shelf-margin ergs that had been stabilized by a rising coastal water table.

Similarly, there has been disagreement regarding the timing of carbonate transported to the basin. Some (for example, Gardner, 1992) concluded that carbonates were shed from platforms during highstand when primary carbonate production was optimal. Others (for example, Loftin, 1996) suggested that carbonate was mobilized by erosive wave energy that impinged on an exposed carbonate-shelf margin during the transgressive leg of sea-level change. Both propositions may be correct. During early stages of transgression, shore lines were probably near the shelf margin and wave base probably impinged on parts of the antecedent carbonate margin.

Most carbonate members of the DMG contain gravels, cobbles, and even boulders, with maximum grain size and interval thickness increasing toward the shelves. These deposits are lenticular and have been suggested to be turbidites. Regardless of the sea level, it appears likely that a steepened carbonate margin facilitated carbonate deposition. This conclusion follows from the observation that the carbonate-poor Brushy Canyon and Cherry Canyon tongues lap onto low-angle lower San Andres and Grayburg ramp margins, whereas the carbonate-“rich” Cherry Canyon and Bell Canyon lap onto higher angle forereef deposits of Goat Seep and Capitan rimmed margins.

DMG sandstones have been interpreted by most to compose channel, levee, overbank splay, and lobe subfacies (Galloway and Hobday, 1996; Beaubouef and others, 1999; Dutton and others, 1999, 2003) deposited by turbidity currents (Hull, 1957; Jacka and others, 1968; Silver and Todd, 1969; Meissner, 1972; Zeldt and Rosen, 1995). The alternate theory of hypersaline density current flow proposed by Harms (1974) has recently been challenged by Kerans and Fitchen (1996) and others. These workers contended that the evaporative hypersaline lagoons invoked by Harms (1974) and Harms and Brady (1996) to generate high-density transport fluids

could not have existed on the emergent lower San Andres shelf during mid-San Andres time Brushy Canyon sea-level lowstand.

Siltstones include organic-poor and organic-rich subfacies (Sageman and others, 1998) and have been interpreted to occur in three modes: (1) discontinuous drapes and lenses associated with channel sandstones during turbidity-current deposition, (2) laterally continuous intervals deposited by hemipelagic suspension during channel abandonment, and (3) laterally continuous sandstones interbedded with organic-rich siltstones deposited during basin starvation associated with transgressions (Wegner and others, 1998). Organic-rich siltstones are laterally continuous. Organic content varies generally between 0.5- and 4-percent TOC in Brushy Canyon (Sageman and others, 1998) but is as high as 46 percent in uppermost Bell Canyon (Dutton and others, 1999). Organic material, interpreted as being largely hemipelagic, probably accumulated during highstand periods of reduced sand transport to the basin (Gardner, 1992).

Most workers have generally agreed on the sequence of depositional phases that are recorded in DMG successions (fig. 24). During highstand, deposition in the basin consisted of hemipelagic silts that settled from suspension under conditions of basin-sediment starvation (Gardner, 1992; Beaubouef and others, 1999) (figs. 6, 10a, 25a). Organic matter, which is dominantly of algal (Sageman and others, 1998; Wegner and others, 1998) or bacterial (Sageman and others, 1998) origin, occurs in all DMG siltstone. Organic-rich siltstone records relatively high rates of organic production relative to silt deposition and may indicate either an absolute increase in organic productivity or a decrease in silt influx to the basin. High hydrogen-index values, an indicator of marine organic carbon, is correlated approximately with relative organic-carbon abundance in Brushy Canyon siltstones (Sageman and others, 1998). Assuming that organic carbon deposition over the long term occurred at an approximately continuous rate, higher organic-carbon content implies reduced rates of silt deposition. Reduced silt influxes probably occurred when silt sources were at greater distances from the location of deposition. Thus, more organic-rich siltstones were probably deposited during sea-level highstands.

During lowstand, siliciclastics prograde into the basin as channel, levee, splay, and lobe architectural elements of a basin-fan system. Several pulses of deposition are common and show laterally offset (compensatory) depositional axes (figs. 13, 16, 24). Silt deposition commences in areas of channel abandonment. Intermittent splay deposition may also occur in areas near active

channels. As sediment supply from the shelf slows, commonly during sea-level rise, sand depocenters backstep onto the slope until widespread silt deposition dominates.

CYCLICITY AND SEQUENCE STRATIGRAPHY OF THE DELAWARE MOUNTAIN GROUP

Cyclicity

Core and outcrop studies demonstrate that the Delaware Mountain Group in the Permian basin is cyclic at several scales. As discussed earlier, DMG successions include alternating sandstone, siltstone, and organic-rich siltstone on the slopes and on the basin floor and interbedding with basinward-thinning, carbonate-debris-bearing intervals along basin slopes. The largest-scale cycles are the three formations that each exhibit overall upward fining that records third-order sea-level rise. Highest frequency cycles consist of channel-levee-splay-lobe complex, sandstone-dominated intervals that alternate with generally widespread sheets of siltstone. These cycles record updip avulsion and channel abandonment (lobe shifting) or shorter term sea-level rises, during which sandstone-depositional environments migrate upslope. Within lobe deposits, sandstone intervals alternate with siltstone intervals, a characteristic that may record episodic deposition of sand and silt under waning current energy or episodes of density-driven sand deposition followed by relatively quiescent periods, when silt entered the basin either by wind or in hypopycnal plumes. Finally, within the siltstone-dominated intervals, organic-rich beds alternate with organic-poor beds—a pattern that records alternating periods of lower and higher siliciclastic sedimentation, respectively (for example, Sageman and others, 1998).

Sequence Stratigraphy

The sequence stratigraphic approach applied to the Guadalupe Mountain DMG succession by recent workers is based essentially on the “Exxon model” (Mitchem and others, 1977). This model was applied to the Guadalupian shelf carbonate succession in the Permian Basin outcrop by Kerans and Kempter (2002) and to the DMG outcrop slope/basin succession by Gardner (1992), Gardner and Sonnenfeld (1996), and Gardner (1997b). The outcrop-based sequence stratigraphic framework was extended into the subsurface of the Delaware Basin by Kerans and Kempter (2002) and Tyrrell and others (2004).

Delaware Mountain Group Sequences in Outcrop

Although the Delaware Mountain Group has historically been subdivided into three formations (Brushy Canyon, Cherry Canyon, and Bell Canyon), it has been interpreted to comprise the basinal components of at least 21 high-frequency depositional sequences recognized on the shelf. Three additional sequences are recognized in the basin that are not present on the shelf. Equivalences between shelf and basin strata are difficult or impossible to establish because shelf-equivalent strata are either not coupled with basinal strata or are so thin as to be below resolution. A possible exception is the Shattuck sandstone of the uppermost Queen Formation, which can be traced convincingly onto a surface that separates the Goat Seep from the Capitan shelf-margin complex, the latter of which can be correlated into the Manzanita Limestone Member of the uppermost Cherry Canyon Formation (King, 1948).

On the basis of studies in the Guadalupe Mountains Kerans and Kempster (2002) defined a sequence stratigraphic framework for the Guadalupian succession that comprised all or part of 6 composite sequences and a total of 28 high-frequency sequences (HFS's). The six composite sequences each record a third-order sea-level cycle. Twenty-five Guadalupian HFS's are recognized on the shelf and in the basin, whereas three HFS's are recognized only in the basin, all of which compose approximately the lower 95 percent of the Brushy Canyon. The Brushy Canyon is interpreted to onlap the upper surface that is developed on the lowermost of the six composite sequences; therefore, the DMG is contained in the younger five of six composite sequences. The DMG includes 24 of the 28 Guadalupian HFS's. Because a complete review of this framework is beyond the scope of this paper, the reader is directed to Kerans and Kempster (2002) for a complete treatment of terminology, concepts, and interpretations. Figure 11 delineates high-frequency and composite sequence boundaries mapped by Kerans, Gardner, and others. However, only composite sequences are labeled. A horizontally extended, more completely labeled version is found in Kerans and Kempster (2002).

RESERVOIR DEVELOPMENT

Delaware Mountain Group reservoirs were assigned to the Delaware Mountain Basinal Sandstone Play by Dutton and others (2003). All of these reservoirs are productive from mainly subarkosic sandstones of the Brushy Canyon, Cherry Canyon, and Bell Canyon Formations.

According to Dutton and others (2005), 78 reservoirs produced more than 1 MMbbl from this play through 2002. Total production from the play, as of 2003, stood at 262.2 MMbbl of oil from 267 reservoirs and 280.5 Mcf of gas from 95 reservoirs (Railroad Commission of Texas, 2003). As of 2003 2,103 oil wells and 183 gas wells were producing.

Controls on Reservoir Distribution

The primary control on reservoir distribution is the geometry of channel-lobe complexes in the context of local structure. A major component of reservoir geometry is the pinch-out of permeable sandstone facies into adjacent low-permeability siltstone. Levee, splay, and lobe subfacies have, to varying degrees, contact with sinuous, depositional-dip-trending channel-sandstone facies. All these stratigraphic elements pinch out laterally into siltstone baffles. However, the overall dip-aligned channel facies provides a potential pathway for fluid migration out of the reservoir system (fig. 26).

Structural elements that affect Delaware Mountain reservoir development are of four types. Regional-scale structures include (1) regional Laramide-induced tilting of the Delaware Basin to the east (figs. 26, 27) and (2) shelfward structural rise near shelf margins that is inherited from original depositional topography (figs. 11, 26). Reservoir-scale structures include (1) local compactional structures developed over subjacent sandstone bodies (fig. 28) and (2) slumps at the updip margin of channel-lobe complexes (fig. 25). Most reservoirs are developed where permeable facies are draped over or pinch out against local structural highs. Highs formed by differential compaction over reservoir-subjacent channel-lobe complexes. A common type of DMG reservoir occurs where a channel meander bend is in an updip position (figs. 26, 27) such that fluids cannot escape into the rest of the channel belt. More regional-scale hydrocarbon migration toward reservoir traps is controlled by the eastward dip imparted to the Delaware Basin by Laramide deformation. Many Bell Canyon reservoirs are located in the basinward extents of channel-lobe complexes rather than toward the Central Basin Platform shelf edge, from which the Bell Canyon feeder channels originate (figs. 4, 26), probably in response to structural tilting to the east. The paucity of basin-margin reservoirs probably reflects the structural rise toward the shelf edge that is inherited from original depositional topography and that may allow hydrocarbons to escape into reservoirs located on the shelf (fig. 26). Although basin and shelf reservoirs are not well connected in the sense that a basin reservoir interval can

be traced directly into a shelf reservoir, fluid migration into shelf strata could occur along surfaces where basin strata onlap the slope or through the dip-aligned incised valleys that directed shelf-derived sediment into the basin.

Development of reservoirs in the DMG depends on the location of development of favorable facies, which is a function of the shifting of deep-water sandstone depocenters through the Guadalupian. King (1948) suggested that development of a post-Brushy rimmed margin comprising Goat Seep and Capitan carbonates may have obstructed formerly active clastic-transport fairways across the Guadalupe Mountains region during later DMG deposition. Consequently, early Guadalupian Brushy Canyon reservoirs are most abundant in the northern part of the basin in southeastern New Mexico (Lea and Eddy Counties). Several middle Guadalupian Cherry Canyon reservoirs are also located in the north part of the basin, although some also occur along the margin of the Central Basin Platform in Texas (Loving, Reeves, and Ward Counties) (fig. 4). Late Guadalupian Bell Canyon reservoirs are developed mainly in the northeast and east parts of the basin.

DMG reservoirs are not developed extensively to the west of the basin midline axis (figs. 2, 4), even though channel-lobe complexes occur in the west part of the basin. Channel-lobe complexes are especially evident in the Brushy Canyon outcrops that provide data for the facies models that have been developed (for example, Gardner and Sonnenfeld, 1992; Barton and Dutton, 1999). Absence of reservoirs in the western Delaware Basin partly reflects the absence of a top seal for the Delaware Mountain Group in the west such as the Castile and Salado provide in the subsurface. Channel-lobe complexes on the west side of the basin are sourced from the west and, in the absence of a top seal, dip-aligned channel systems provide a ready conduit for escape to the west of fluids generated in the subsurface.

Porosity and Permeability Development

The present state of DMG reservoir sandstone porosity development reflects the complexities of primary depositional and secondary diagenetic processes. Typical reservoir porosity values range from 10 to 26 percent; permeability values range from 0.1 to 155 md (Spain, 1992; Dutton and others, 1999; Broadhead and Justman, 2000). In spite of overall textural differences between the overall coarser grained Brushy Canyon and very fine grained Bell Canyon intervals, however, productive reservoir intervals from both formations show

similar porosity/permeability relationships (fig. 29). Further, there appear to be no significant differences in the porosity/permeability relationships among various sandstone depositional facies (Dutton and others, 1999).

Two of the best single summaries of DMG porosity development and its effects on reservoir performance and well-log-based calculations of fluid saturation come from studies of the Brushy Canyon in Nash Draw field (Eddy County, NM) by Behnken (1996), who used XRD and SEM in his analyses of sidewall cores and cuttings, and by Thomerson and Asquith (1992), who used petrographic analyses coupled with well-log analyses on Brushy core from Mesa Hat field (Lea County, NM). Behnken (1996) recognized that very fine grained texture, grain angularity, and poor sorting caused vertically extended oil/water transition zones and high irreducible oil saturations in subarkosic clastics at Nash Draw. Thomerson and Asquith (1992) interpreted moderate to good sorting of subarkoses in Mesa Hat samples but recognized reduced permeability and enhanced irreducible fluid saturations accompanying very fine grained textures.

Diagenesis in DMG siliciclastics has produced secondary porosity due to feldspar dissolution. Pore throats have been further reduced by pressure solution of quartz grains, which produced a slitlike geometry. Authigenesis of feldspar, quartz, and clay minerals, which occurred in pores, was caused by the presence of organic fluids that were probably sourced from DMG organic-rich siltstones (Hayes and Tieh, 1992 a). However, the most common cements are carbonate (Thomerson and Asquith, 1992; Dutton and others, 1999). Predictably, total cements are the main control on porosity and permeability (Dutton and others, 1999).

Authigenic clay minerals present a particularly troublesome set of complications. Fibrous illite and chlorite, in particular, have developed bridges across pore throats and dissected porosity. Weblike growths of illite/smectite may swell 15 to 20 percent when contacted by drilling fluids, thus occluding even more pore space. Chlorite, as well as other iron-bearing authigenic minerals, can promote precipitation of pore-occluding, insoluble, Fe-hydroxide gels when contacted by acids.

Reservoir Quality Determination from Well Logs

Several critical issues must be dealt with when well log data are used to identify and evaluate DMG reservoirs. First, DMG siliciclastics are subarkosic to arkosic and produce elevated gamma-ray-log responses in shale-free sandstones. Shale is rare in the Delaware

Mountain Group, probably owing to sand storage in an eolian environment prior to basinal deposition.

Second, authigenesis of clays provided abundant microporosity, which is detected by neutron logging because of the presence of bound water. The effect is an overestimate of effective porosity and calculation of high water saturations (Thomerson and Asquith, 1992; Behnken, 1996). The pessimism generated from calculations of high water saturations may be mitigated by the insight that much of the water bound in the clay fraction is irreducible (Behnken, 1996).

Third, resistivity contrasts between oil- and water-productive intervals are low because of high residual oil saturations in the invaded zone, as well as high irreducible water saturations (Thomerson and Asquith, 1992).

Calculation of effective porosity requires corrections of total porosity for included microporosity. Thus, determination of clay content is required, which cannot be performed using gamma-ray data alone because of the abundance of K-feldspar. In Hat Mesa field (Brushy Canyon), Thomerson and Asquith (1992) used neutron-porosity (ϕ_N) and density-porosity (ϕ_D) data to calculate the clay volume (V_{clay}):

$$V_{\text{clay}} = (\phi_N \text{ shaly sand} - \phi_D \text{ shaly sand}) / (\phi_N \text{ shale} - \phi_D \text{ shale}),$$

where all porosities were corrected to a sandstone matrix. Complications arising from borehole rugosity (observed in caliper logs) and gas (observed in gas/oil data) were minimal in Hat Mesa field. Thereafter, Thomerson and Asquith (1992) generated a series of petrophysical crossplots that were interpreted to differentiate permeable water-productive from permeable oil-productive zones.

Integration of the results from crossplot analyses produced cutoff values for productive intervals in Hat Mesa (Brushy Canyon) reservoir: $\phi = 12$ percent at 0.1 md. Very similar cutoff values were determined by Dutton and others (1999) for hydrocarbon-productive Ramsey sandstone at Ford Geraldine (Bell Canyon) reservoir in Reeves and Culberson Counties, Texas.

Identification of widespread organic-rich siltstone intervals is important because they act both as local source beds for hydrocarbons and as part of the reservoir seal. Organic-rich beds correspond to some of the most radioactive units observed in gamma-ray logs. Only volcanic-ash deposits show similarly elevated gamma-ray responses.

Older resistivity logs often show an increase in resistivity beginning within the upper part of the Bell Canyon several feet below the contact with the Castile. This effect, called the “Delaware Effect,” is a function of electrode spacing of the resistivity tool (Laterolog). The result can be a misinterpretation that hydrocarbons are trapped below the Castile, when, in reality, the interval may be water bearing. Improvements were eventually made in electrode spacing and tool design (Asquith and others, 1997a).

Traps, Seals, and Sources

DMG reservoirs reflect both stratigraphic and structural controls on hydrocarbon migration and trapping. Stratigraphic controls include lateral pinch-outs of permeable, laterally discontinuous, channel-levee-complex, overbank-splay, and lobe sandstone- and coarse-siltstone facies into much lower permeability, laterally more extensive siltstone facies. Further, the laterally extensive siltstones provide reservoir-scale top seals (for example, Kane, 1992). Gardner (1992) recognized that deposition of regionally extensive fine-grained sediments during third-order sea-level rise recorded progressive basin starvation and produced top seals that genetically and hydraulically separate the three DMG formations. Carbonate strata in DMG carbonate members, which also contain siliciclastics reservoirs, may also form lateral and top seals on siliciclastic reservoirs contained within or below such members (for example, in Avalon reservoir, described by Kane, 1992) (fig. 17). Locally, stratiform calcite-cemented intervals provide additional controls over vertical flow (for example, Dutton and others, 1999) (figs. 18, 19).

Hydrocarbon sources are thought to be organic-carbon-bearing siltstone strata that are interbedded with, and laterally adjacent to, reservoir facies (fig. 6). DMG organic carbon in siltstones and in most of the oil accumulations has similar sulfur and carbon isotopic composition (Hayes and Tieh, 1992a). Evolution of organic fluids appears to have controlled much of DMG diagenesis, including development of dissolution-produced secondary porosity and subsequent mineral authigenesis (Hayes and Tieh, 1992a). Some siltstones are remarkably organic rich. Dutton and others (1999) reported a Bell Canyon coarse-grained siltstone (average grain size of 4.94 phi, with an organic-carbon content of 46 percent by weight. Most so-called organic-rich siltstones are not so carboniferous, however, averaging less than 4 percent by weight (Sageman and others, 1998).

Structural controls on reservoir development include a Laramide-induced, regional monoclinical dip down to the east (fig. 26); local compactional antiformal and synformal structures over subjacent sandstone bodies (for example, fig. 28); and syndepositional slumps that bound the up-depositional-dip ends of channel systems (for example, Gardner and Sonnenfeld, 1996) (fig. 25).

Production Characteristics and Completion Challenges

Primary oil production is typically only about 50,000 to 100,000 bbl per well (10 percent of OOIP) in DMG fields. (Montgomery and others, 1999). Production decline rates are initially high as solution gas, the predominant drive mechanism, is depleted. Production characteristics vary significantly over short distances (fig. 30), probably reflecting the laterally restricted extent of productive channel-levee-lobe complex sandbodies.

Porosity and permeability attributes in DMG reservoir facies are modest. Reservoir porosity ranges typically from 12 to 25 percent; permeability ranges from 1 to 5 md, with exceptional occurrences of 200 md in thin, laterally restricted units (Montgomery and others, 1999). Although detrital clay (kaolinite) composes less than 1 percent of the rock, the already impoverished permeability would be further diminished by clogging of pore throats by Fe-hydroxide gels precipitated through the contact of iron-bearing minerals (for example, chlorite) with acidic borehole fluids (Behnken, 1996). Walling and others (1992) warned that chlorites could de-evolve to water-expandable forms in the presence of some anthropogenic borehole fluids and become migratory. Behnken suggested that addition of as little as 2 percent KCl will mitigate potential clay deflocculation and clay-particle migration. Other additives are available to prevent precipitation of Fe-hydroxides, including acetic or citric acid (Green and others, 1996).

Because DMG permeability is marginal, fracture stimulation with sand propping is commonly used in the final stages of well completion. However, reservoirs characteristically comprise numerous thin hydrocarbon-productive intervals that are interbedded with thin water-productive intervals. Further, control of fracture propagation is problematic because of the microlaminated, lithologic variability of reservoir intervals and lack of shaly, stratal, fracture barriers. The danger of connecting water-bearing and hydrocarbon-bearing intervals with induced fractures (“treating out of zone”) is always present, and it can result in excessive water production or “watered-out” hydrocarbon reservoirs (Scott and Carrasco, 1996). Fracture-

stimulation jobs are customized for local geologic conditions by varying pump rates, pad-stage volumes (amount of fluid used to create fractures), fluid viscosities, sand concentrations, and fluid-loss additives (Scott and Carrasco, 1996). Success of fracture treatments has traditionally been tested by posttreatment injection of radio tracers (for example, iridium and scandium) and gamma-ray relogging of the well. Posttreatment assessment of the success of the treatment may potentially be performed after formation damage has occurred, a problem whose recognition has prompted the design of real-time fracture-treatment monitoring techniques that allow timely discontinuance of treatments (Scott and Carrasco, 1996). Increased productivity is an obvious indicator of success. Design criteria for fracture stimulation in relatively lower permeability units are different than those for higher permeability units. After successful fracture stimulation, ultimate recoveries in lower permeability units are increased over what might otherwise be expected, whereas they are not increased for higher permeability units (Scott and Carrasco, 1996).

The primary drive for DMG sandstone reservoirs is solution-gas and water drive (Spain, 1992). Per-well initial production may exceed 80 bbl/d ($13.25 \text{ m}^3/\text{d}$) but will decline to less than 12 bbl/d ($<2 \text{ m}^3/\text{d}$) after 4 years as solution gas is depleted (fig. 31). Injection of water for pressure maintenance has yielded significant improvement in some cases (for example, Dutton and others, 2005; after Broadhead and others, 1998) (fig. 32). Injection of CO_2 has also proven successful, for example, in Ford Geraldine field (Bell Canyon) (Dutton and others, 2003) (figs. 33, 34).

Limited lateral continuity of productive facies presents a challenge for economic development of DMG reservoirs. The geographic limitation of reservoir continuity is demonstrated by differences in production characteristics in closely spaced wells. Drainage areas for wells at Nash Draw (lower Brushy Canyon) range from 19 to 66 acres, with an average of 34 acres (Montgomery and others, 1999). The effects of limited reservoir are shown by comparing production characteristics in closely spaced wells. Figure 30 shows oil, gas, and water production in three wells that are 0.25 to 0.5 mi (0.4 to 0.8 km) apart. Dutton and others (1999) pointed out that pinch-outs of channel, levee, and lobe sandstone into siltstone are the primary control on lateral reservoir heterogeneity. Additional complications include the pinch-out of splay reservoir sandstone onto topographically elevated levee complexes. Vertical heterogeneities are produced by deposition of both laterally extensive and discontinuous

siltstones between stacked channel sandbodies (fig. 8). As discussed earlier, laterally discontinuous distribution of stratiform calcite cements also imparts interwell heterogeneity to reservoirs.

SUMMARY AND CONCLUSIONS

The Guadalupian-age Delaware Mountain Group contains the rock record from deep-water deposition in the Delaware Basin. Rock types include shelf-derived, fine-grained, feldspar-bearing siliciclastics and limestone-dominated carbonates derived from the outer-shelf and shelf margin. Sandstones were deposited mainly by density flow during lowstand and early transgressive sea-level stages, whereas regionally extensive siltstone intervals were deposited from suspension most abundantly during sea-level highstands. Carbonates were probably deposited during periods when the greatest amount of energy was imposed on shelf-margin source areas, which may have been during transgressions or when early highstand shorelines were near the shelf margin. Calcite cement is common and is most often associated with finer grained sandstone and coarse-grained siltstones in areas dominated by overbank deposits. Detrital clay is not abundant, and most clays comprise authigenic chlorite or illite. Clay content decreases sandstone permeability without significantly affecting porosity and increases irreducible water content.

The DMG succession has been formally divided into 3 formations (Brushy Canyon, Cherry Canyon, and Bell Canyon), 5 composite sequences, and 24 high-frequency sequences. The Brushy Canyon, the coarsest grained formation in the outcrop area, contains little carbonate compared with that of the others. Correlations between wells generally depend on recognition of the carbonate members and widespread siltstone intervals. Recognition of the prominence of organic-rich siltstone in the upper parts of the Brushy Canyon and Cherry Canyon facilitates correlations between wells of the Brushy Canyon/Cherry Canyon and Cherry Canyon/Bell Canyon boundaries, respectively. Interpretation of siliciclastic and carbonate end-member rock types from gamma-ray and porosity well logs is relatively straightforward, in most cases. High irreducible water content associated with the clay fraction produces lower-than-expected resistivities in hydrocarbon-productive strata.

Hydrocarbon reservoirs have both stratigraphic and structural elements. Lateral pinch-outs of sandstone porosity into low-permeability siltstones and superposition of siltstones over sandbodies compose the stratigraphic elements. The structural components may include (1) anticline formation caused by differential compaction over and around subjacent sandbodies and (2) regional dip arising either from Laramide deformation or (3) depositional topography on slopes approaching shelf margins. Reservoir traps are preferentially developed where porosity-pinch-out areas are in updip positions. Hydrocarbons may escape to shelf reservoirs where porous and permeable facies are positioned on slopes that rise toward shelf areas.

The DMG is an underexploited reservoir succession; estimated typical primary recovery efficiency is only 10 percent of OOIP. Most enhanced recovery efforts recover an addition of less than 20 percent of OOIP, with some notable exceptions. This modest performance arises largely from laterally restricted distribution of reservoir sandbodies, generally low permeability, and characteristic interbedding of thin hydrocarbon- and water-productive intervals. Economically acceptable production requires fracture stimulation that risks interconnecting water- and hydrocarbon-productive reservoirs and acid stimulation that risks production of formation-damaging Fe-hydroxide gels from decomposing Fe-bearing minerals such as chlorite. Successful application of enhanced recovery techniques depends on accurate knowledge of the interconnectedness of permeable facies between injection and production wells. For example, productive lobe and channel sandbodies may be well connected, whereas productive overbank-splay sandbodies may be isolated from the others. High-resolution 3-D seismic imaging may facilitate mapping of laterally and stratigraphically heterogeneous sandstone distribution. Horizontal drilling may intercept and facilitate production from laterally disconnected sandbodies, although maintaining stratigraphic separation of hydrocarbon- from water-productive intervals may be more complicated than with vertical completions.

REFERENCES AND RELATED READING

- Adams, J. E., 1936, Oil pool of open reservoir type [with discussion by W. B. Wilson]:
Bulletin of the American Association of Petroleum Geologists Bulletin, v. 20, no. 6.
- Ahr, W. M., and Berg, R. R., 1982, Deepwater evaporites in the Bell Canyon Formation,
Delaware Basin, West Texas, *in* Handford, C. R., Loucks, R. G., and Davies, G. R., eds.,

Depositional and diagenetic spectra of evaporites—a core workshop: Society of Economic Paleontologists and Mineralogists Core Workshop 3, p. 305–323.

- Asquith, G. B., Dutton, S. P., and Cole, A. G., 1997, “Delaware effect” and the Ramsey Sandstone, Ford Geraldine Unit, Reeves and Culberson Counties, Texas, *in* DeMis, W. D., ed., Permian Basin oil and gas fields: turning ideas into production: West Texas Geological Society Publication 97-102, p. 71–74.
- Asquith, G. B., Dutton, S. P., Cole, A. G., Razi, M., and Guzman, J. I., 1997, Petrophysics of the Ramsey Sandstone, Ford Geraldine Unit, Reeves and Culberson Counties, Texas, *in* DeMis, W. D., ed., Permian Basin oil and gas fields: turning ideas into production: West Texas Geological Society Publication 97-102, p. 61–69.
- Asquith, G. B., Thomerson, M. D., and Arnold, M. D., 1994, Variations in cementation exponent (m) and fracture porosity, Permian Delaware Mountain Group sandstones, Reeves and Culberson counties, Texas, *in* Ahlen, Jack, Peterson, John, and Bowsher, A. L., eds., Geologic activities in the 90s: New Mexico Bureau of Mines & Mineral Resources Bulletin, p. 97–100.
- Asquith, G. B., Thomerson, M. D., and Arnold, M. D., 1995, The recognition of possible oil and water wettability changes in the Permian Delaware Mountain Group sandstones from petrophysical logs, *in* Martin, R. L., ed., In search of new Permian oil and gas fields: West Texas Geological Society Fall Symposium, Publication 95-98, p. 39–50.
- Barton, M. D., 1997, Facies architecture of submarine channel-levee and lobe sandstones: Permian Bell Canyon Formation, Delaware Mountains, West Texas: The University of Texas at Austin, Bureau of Economic Geology Field Trip Guidebook, 40 p.
- Barton, M. D., and Dutton, S. P., 1999, Outcrop analysis of a sand-rich, basin-floor turbidite system, Permian Bell Canyon Formation, West Texas, *in* Transactions, Gulf Coast Section Society of Economic Paleontologists and Mineralogists 19th Annual Bob F. Perkins Research Conference, December 5–8, Houston, p. 53–64.
- Basham, W. L., 1996, Delaware Mountain Group sandstone channel orientations: implications for sediment source and deposition, *in* DeMis, W. D., and Cole, A. G., eds., The Brushy Canyon play in outcrop and subsurface: concepts and examples: Society of Economic Paleontologists and Mineralogists Permian Basin Section Publication 96-38, p. 91–102.
- Basu, D., and Bouma, A. H., 1996, New method to determine the depositional mechanism in a submarine fan channel-levee complex, Brushy Canyon Formation, West Texas, *in* DeMis, W. D., and Cole, A. G., eds., The Brushy Canyon play in outcrop and subsurface: concepts and examples: Society of Economic Paleontologists and Mineralogists Permian Basin Section Publication 96-38, p. 85–90.

- Batzle, M., and Gardner, M. H., 2000, Lithology and fluids: seismic models of the Brushy Canyon Formation, west Texas, *in* Bouma A. H., and Stone, C. G., eds., Fine-grained turbidite systems: American Association of Petroleum Geologists Memoir 72/ Society of Economic Paleontologists and Mineralogists Special Publication 68, p. 127–141.
- Beaubouef, R. T., Rossen, C., Zelt, F. B., Sullivan, M. D., Mohrig, D. C., and Jennette, D. C., 1999, Deep-water sandstones, Brushy Canyon Formation, West Texas: American Association of Petroleum Geologists, Continuing Education Course Note Series #40, 50 p.
- Beede, J. W., 1924, Geologic map of a part of West Texas: University of Texas Bulletin 2607.
- Behnken, F. H., 1996, Reservoir characterization of the Brushy Canyon Formation sandstone (Late Permian), strata production, Nash unit #15, Nash Draw Delaware field, Eddy County, New Mexico, *in* DeMis, W. D., and Cole, A. G., eds., The Brushy Canyon play in outcrop and subsurface: concepts and examples: Society of Economic Paleontologists and Mineralogists Permian Basin Section Publication 96-38, p. 173–182.
- Behnken, F. H., and Troschinetz, J., 1994, Impact of reservoir characterization on well completion and production economics, Permian Cherry Canyon sandstones, Loving County, Texas, *in* Gibbs, J. F., ed., Synergy equals energy—teams, tools, and techniques: West Texas Geological Society Publication 94-94, p. 3–13.
- Berg, R. R., 1979, Reservoir sandstones of the Delaware Mountain Group, southeast New Mexico, *in* Sullivan, N. M., ed., Guadalupian Delaware Mountain Group of West Texas and southeast New Mexico, Symposium and Field Trip Conference Guidebook: Society of Economic Paleontologists and Mineralogists Permian Basin Section Publication 79-18, p. 75–95.
- Bouma, A. H., 1996, Initial comparison between fine- and coarse-grained submarine fans and the Brushy Canyon Formation sandstones, *in* DeMis, W. D., and Cole, A. G., eds., The Brushy Canyon play in outcrop and subsurface: concepts and examples: guidebook: Society of Economic Paleontologists and Mineralogists Permian Basin Section Publication 96-38, p. 41–50.
- Bozanich, R. G., 1979, The Bell Canyon and Cherry Canyon formations, eastern Delaware Basin, Texas: lithology, environments and mechanisms of deposition, *in* Sullivan, N. M., ed., Guadalupian Delaware Mountain Group of West Texas and southeast New Mexico: Society of Economic Paleontologists and Mineralogists Permian Basin Section Publication 79-18, p. 121–141.
- Bradshaw, W., 1995, Lea Delaware, Northeast, *in* Worrall, J. general chairman, A symposium of the oil and gas fields of southeastern New Mexico: Roswell Geological Society, p. 32–49.

- Broadhead, R. F., and Justman, H. A., 2000, Regional controls on oil accumulations, lower Brushy Canyon Formation, southeast New Mexico, *in* DeMis, W. D., Nelis, M. K., and Trentham, R. C., eds., *The Permian Basin: proving ground for tomorrow's technologies*: West Texas Geological Society Publication 00-109, p. 9–18.
- Broadhead, R. F., and Luo, F., 1996, Oil and gas resources in the Delaware Mountain Group at the WIPP site, Eddy County, New Mexico, *in* DeMis, W. D., and Cole, A. G., eds., *The Brushy Canyon play in outcrop and subsurface: concepts and examples: guidebook*: Society of Economic Paleontologists and Mineralogists Permian Basin Section Publication 96-38, p. 41–50.
- Broadhead, R. F., Luo, F., and Speer, S. W., 1998, Oil and gas resources at the Waste Isolation Pilot Plant (WIPP) site, Eddy County, New Mexico, *in* New Mexico Bureau of Mine and Mineral Resources Circular 206, p. 3–72.
- Brown, A., 1996, Position of the Polydiexodina last-occurrence datum in Guadalupian strata: revised correlations at McKittrick Canyon, *in* DeMis, W. D., and Cole, A. G., eds., *The Brushy Canyon play in outcrop and subsurface: concepts and examples: guidebook*: Society of Economic Paleontologists and Mineralogists Permian Basin Section Publication 96-38, p. 75–83.
- Brown, A., and Loucks, R. G., 1993, Toe of slope, *in* Bebout, D., and Kerans, C., eds., *Guidebook to the Permian reef trail, McKittrick Canyon, Guadalupe Mountains National Park, West Texas*: The University of Texas at Austin, Bureau of Economic Geology, Guidebook 26, p. 5–13.
- Cantrell, D. L., and Kane, T. V., 1993, Production history and geology of Avalon (Delaware) field, *in* Love, D. W., Hawley, J. W., Kues, B. S., and Adams, J. W., Austin, G. S., and Barker, J. M., eds., *Carlsbad region, New Mexico and West Texas*: New Mexico Geological Society, 44th Field Conference Guidebook, p. 81–83.
- Cantrell, D. L., and Kane, T. V., 1995, Production history and geology, Avalon (Delaware field), *in* Worrall, J. general chairman, *A symposium of the oil and gas fields of southeastern New Mexico*: Roswell Geological Society, p. 50–54.
- Carr, M., and Gardner, M. H., 2000, Portrait of a basin-floor fan for sandy deepwater systems, Permian lower Brushy Canyon Formation, west Texas, *in* Bouma, A. H., and Stone, C. G., eds., *Fine-grained turbidite systems*: American Association of Petroleum Geologists Memoir 72/ Society of Economic Paleontologists and Mineralogists Special Publication 68, p. 215–231.
- Cartwright, L. D., Jr., 1930, Transverse section of Permian Basin, West Texas and southeast New Mexico: American Association of Petroleum Geologists Bulletin, v. 14, no. 8, p. 969–981.

- Clifton, R. L., 1944, Ammonoids from upper Cherry Canyon of Delaware Mountain Group in Texas: American Association of Petroleum Geologists Bulletin, v. 28, p. 1644–1646.
- Cole, A., 1996, Ford West (Cherry Canyon) field, Culberson County, Texas, *in* Oil and Gas Fields in West Texas, Symposium VII: West Texas Geological Society Publication 96-99, p. 49–52.
- Crawford, G. A., 1979, Sedimentology of the Goat Seep Dolomite (Guadalupian, Permian), Guadalupe Mountains, west Texas and New Mexico (abs.): American Association of Petroleum Geologists Bulletin, v. 63, no. 3, p. 437.
- Cromwell, D. W., 1979, Indian Draw Delaware field: a model for deeper Delaware sand exploration, *in* Sullivan, N. M., ed., Guadalupian Delaware Mountain Group: Society of Economic Paleontologists and Mineralogists Permian Basin Section Publication 79-18, p. 153–182.
- DeMis, W. D., and Cole, A. G., 1996, The Brushy Canyon play in outcrop and subsurface: concepts and examples: Society of Economic Paleontologists and Mineralogists Permian Basin Section Publication 96-38, 188 p.
- Dutton, S. P., and Barton, M. D., 1999, Application of outcrop analogs to reservoir characterization of Permian deep-water sandstones, Bell Canyon Formation, Ford Geraldine Unit, West Texas (Delaware Basin), *in* Transactions, Gulf Coast Section Society of Economic Paleontologists and Mineralogists 19th Annual Bob F. Perkins Research Conference, December 5–8, Houston, p. 65–76.
- Dutton, S. P., Barton, M. D., Asquith, G. B., Malik, M. A., Cole, A. G., Gogas, J., Guzman, J. I., and Clift, S. J., 1999, Geologic and engineering characterization of turbidite reservoirs, Ford Geraldine Unit, Bell Canyon Formation, West Texas: The University of Texas at Austin, Bureau of Economic Geology Report of Investigations No. 255, 88 p.
- Dutton, S. P., Barton, M. D., Clift, S. J., and Guzman, J. I., 1998, Ramsey sandstone deep-water channel-levee and lobe deposits, Bell Canyon Formation, Ford Geraldine unit, Reeves and Culberson Counties, Texas, *in* Stoudt, E. L., Dull, D. W., and Raines, M. R., eds., Permian Basin Core Workshop-DOE funded reservoir characterization projects: Society of Economic Paleontologists and Mineralogists Permian Basin Section Publication 98-40, 33 p.
- Dutton, S. P., Barton, M. D., Clift, S. J., Guzman, J. I., and Cole, A. G., 1997, Depositional history of Ramsey Sandstone channel-levee and lobe deposits, Bell Canyon Formation, Ford Geraldine Unit, West Texas (Delaware Basin), *in* DeMis, W. D., ed., Permian Basin oil and gas fields: turning ideas into production: West Texas Geological Society Publication 97-102, p. 53–60.
- Dutton, S. P., Barton, M. D., Zirczy, H. H., and Flanders, W. A., 2000, Characterization of reservoir heterogeneity in slope and basin clastic reservoirs, Bell Canyon Formation,

- Delaware Basin, Texas, *in* Reid, S. T., Southwest Section AAPG 2000 Convention transactions: West Texas Geological Society, Publication SWS 2000-107, p. 116–129.
- Dutton, S. P., and Flanders, W. A., 2001, Application of advanced reservoir characterization, simulation, and production optimization strategies to maximize recovery in slope and basin clastic reservoirs, West Texas (Delaware Basin): The University of Texas at Austin, Bureau of Economic Geology, final report prepared for U.S. Department of Energy, DOE/BC/14936-18, 170 p.
- Dutton, S. P., and Flanders, W. A., 2001, Deposition and diagenesis of turbidite sandstones in East Ford field, Bell Canyon Formation, Delaware Basin, Texas: American Association of Petroleum Geologists Southwest Section, Annual Meeting Papers and Abstracts, Dallas, Texas, March 10–13, 12 p.
- Dutton, S. P., Flanders, W. A., and Barton, M. D., 2003, Reservoir characterization of a Permian deep-water sandstone, East Ford field, Delaware basin, Texas: American Association of Petroleum Geologists Bulletin, v. 87, p. 609–627.
- Dutton, S. P., Kim, E. M., Broadhead, R. F., Breton, C. L., Raatz, W. D., Ruppel, S. C., and Kerans, Charles, 2004, Play analysis and digital portfolio of major oil reservoirs in the Permian Basin: application and transfer of advanced geological and engineering technologies for incremental production opportunities: The University of Texas at Austin, Bureau of Economic Geology, and New Mexico Bureau of Geology and Mineral Resources, New Mexico Institute of Mining and Technology, annual report prepared for U.S. Department of Energy, under contract no. DE-FC26-02NT15131, 104 p.
- Fischer, A. G., and Sarnthein, M., 1988, Airborne silts and dune-derived sands in the Permian of the Delaware Basin: Journal of Sedimentary Petrology, v. 58, p. 637–643.
- Fitchen, W. M., 1993, Sequence stratigraphic framework of the upper San Andres Formation and equivalent basinal strata in the Brokeoff Mountains, Otero County, New Mexico *in* Love, D. W., Hawley, J. W., Kues, B. S., Adams, J. W., Austin, G. S., and Barker, J. M., eds., Carlsbad region, New Mexico and West Texas: New Mexico Geological Society, 44th Field Conference Guidebook, p. 185–193.
- Flanders, W. A., and DePauw, R. M., 1993, Update case history: performance of the Twofreds Tertiary CO₂ project, *in* Proceedings, Society of Petroleum Engineers Annual Technical Conference: Society of Petroleum Engineers, Paper 26614, 10 p.
- Galley, J. E., 1958, Oil and geology in the Permian Basin of Texas and New Mexico, *in* Weeks, L. G., ed., Habitat of oil: Tulsa, American Association of Petroleum Geologists, p. 395–446.
- Galloway, W. E., Ewing, T. E., Garrett, C. M., Jr., Tyler, N., and Bebout, D. G., 1983, Atlas of major Texas oil reservoirs: The University of Texas at Austin, Bureau of Economic Geology Special Publication, 139 p.

- Galloway, W. E., and Hobday, D. K., 1996, Terrigenous clastic depositional systems: applications to fossil fuel and groundwater resources, 2nd edition: New York, Springer-Verlag, 489 p.
- Garber, R. A., Grover, G. A., and Harris, P. M., 1989, Geology of the Capitan shelf margin; subsurface data from the northern Delaware Basin, *in* Garber, R. A., Grover, G. A. and Harris, P. M., eds., Subsurface and outcrop examination of the Capitan shelf margin, northern Delaware Basin: Society of Economic Paleontologists and Mineralogists Core Workshop, v. 13, p. 3–269.
- Gardner, M. H., 1992, Sequence stratigraphy of eolian-derived turbidites; deep water sedimentation patterns along an arid carbonate platform and their impact on hydrocarbon recovery in Delaware Mountain Group reservoirs, West Texas, *in* Mruk, D. H., and Curran, B. C., eds., Permian Basin exploration and production strategies; applications of sequence stratigraphic and reservoir characterization concepts: West Texas Geological Society Publication, v. 92-91, p. 7–11.
- Gardner, M. H., 1997a, Characterization of deep-water siliciclastic reservoirs in the upper Bell Canyon and Cherry Canyon Formations of the northern Delaware Basin, Culberson and Reeves Counties, Texas, *in* Major, R. P., ed., Oil and gas on Texas State Lands: an assessment of the resource and characterization of type reservoirs: The University of Texas, Bureau of Economic Geology Report of Investigations No. 241, p. 137–146.
- Gardner, M. H., 1997b, Sequence stratigraphy and hydrocarbon habitat of the Permian (Guadalupian) Delaware Mountain Group, Delaware Basin, West Texas, *in* Major, R. P., ed., Oil and gas on Texas State Lands: an assessment of the resource and characterization of type reservoirs: The University of Texas, Bureau of Economic Geology Report of Investigations No. 241, p. 147–157.
- Gardner, M. H., and Borer, J. M., 2000, Submarine channel architecture along a slope to basin profile, Brushy Canyon Formation, west Texas, *in* Bouma, A. H., and Stone, C. G., eds., Fine-grained turbidite systems: American Association of Petroleum Geologists Memoir 72/ Society of Economic Paleontologists and Mineralogists Special Publication 68, p. 195–214.
- Gardner, M. H., and Sonnenfeld, M. D., 1996, Stratigraphic changes in facies architecture of the Permian Brushy Canyon Formation in Guadalupian Mountains National Park, west Texas, *in* DeMis, W. D., and Cole, A. G., eds., The Brushy Canyon play in outcrop and subsurface: concepts and examples: guidebook: Society of Economic Paleontologists and Mineralogists Permian Basin Section Publication 96-38, p. 51–59.
- Gawloski, T., 1995, Geronimo Delaware, in Oil and gas fields of southeastern New Mexico: supplement: Roswell Geological Society, p. 225–226.

- Girty, G. H., 1908, The Guadalupian fauna: U. S. Geological Survey Professional Paper 58, 651 p.
- Grauten, W. F., 1979, Fluid relations in Delaware Mountain sandstone, in Guadalupian Delaware Mountain Group of west Texas and southeast New Mexico: Society of Economic Paleontologists and Mineralogists Permian Basin Section Publication 79-18, p. 191–204.
- Green, K. M., Frailey, S. M., and Asquith, G. B., 1996, Laboratory analysis of the clays within the Brushy Canyon Formation and their reservoir and petrophysical implications: Red Tank field, Lea County, New Mexico, *in* DeMis, W. D., and Cole, A. G., eds., The Brushy Canyon Play in outcrops and subsurface: concepts and examples: Society of Economic Paleontologists and Mineralogists Permian Basin Section Publication 96-38, p. 165–171.
- Hamilton, D. C., 1984, Ken Regan (Delaware) field, Reeves County, Texas, *in* Moore, G., and Wilde, G., eds., Transactions, Southwest Section: West Texas Geological Society Publication SWS 84-78, p. 11–15.
- Hamilton, D. C., 1996, Mid-lower Cherry Canyon play in War-Wink area of the Delaware Basin, Ward and Winkler Counties, Texas, *in* DeMis, W. D., and Cole, A. B., eds., The Brushy Canyon play in outcrop and subsurface: concepts and examples: Society of Economic Paleontologists and Mineralogists Permian Basin Section Publication 96-38, p. 131–156.
- Hamilton, D., and Hunt, T., 1996, War-Wink Cherry Canyon trend, “serendipity in spades,” *in* Martin, R. L., ed., Permian Basin oil and gas fields: keys to success that unlock future reserves: West Texas Geological Society Publication 96-101, p. 107–115.
- Hampton, B. D., 1989, Carbonate sedimentology of the Manzanita Member of the Cherry Canyon Formation, *in* Harris, P. M., and Grover, G. S., eds., Subsurface and outcrop examination of the Capitan shelf margin, Northern Delaware Basin: Society of Economic Paleontologists and Mineralogists Core Workshop 13, p. 431–439.
- Handford, C. R., 1981, Sedimentology and genetic stratigraphy of Dean and Spraberry formations (Permian), Midland Basin, Texas: American Association of Petroleum Geologists Bulletin, v. 65, no. 9, p. 1602–1616.
- Hardage, B. A., Simmons, J. L., Jr., Pendleton, V. M., Stubbs, B. A., and Uszynski, B. J., 1998, 3-D seismic imaging and interpretation of Brushy Canyon slope and basin thin-bed reservoirs, northwest Delaware Basin: Geophysics, v. 63, p. 1507–1519.
- Harms, J. C., 1968, Permian deep-water sedimentation by non-turbid currents, Guadalupe Mountains, Texas: Geological Society of America Special Paper 121, 127 p.
- Harms, J. C., 1974, Brushy Canyon Formation, Texas: a deep-water density current deposit: Geological Society of American Bulletin, v. 85, p. 1763–1784.

- Harms, J. C., and Williamson, C. R., 1988, Deep-water density current deposits of Delaware Mountain Group (Permian), Delaware Basin, Texas and New Mexico: American Association of Petroleum Geologists Bulletin, v. 72, no. 3, p. 299–317.
- Harms, J. C., and Brady, M. J., 1996, Deposition of the Brushy Canyon Formation: 30 years of conflicting hypotheses *in* DeMis, W. D., and Cole, A. G., eds., The Brushy Canyon play in outcrop and subsurface: concepts and examples: Guidebook, Society of Economic Paleontologists and Mineralogists Permian Basin Section Publication 96-38, p. 51–59.
- Hayes, P. D., and Tieh, T. T., 1992a, Organic geochemistry and diagenesis of the Delaware Mountain Group, west Texas and southeast New Mexico, *in* Cromwell, D. W., Moussa, M. T., and Mazzullo, L. J., eds., Southwest Section American Association of Petroleum Geologists Transactions, SWS 92-90, p. 155–175.
- Hayes, P. D., and Tieh, T. T., 1992b, Organic matter in Delaware Mountain Group sediments; geochemistry, source, and role in diagenetic alteration of reservoir sandstones: American Association of Petroleum Geologists Bulletin, v. 76, no. 4, pp. 576.
- Hayes, P. T., 1964, Geology of the Guadalupe Mountains, New Mexico: U.S. Geological Survey Professional Paper 446, 69 p.
- Hills, J. M., 1972, Late Paleozoic sedimentation in west Texas Permian Basin: American Association of Petroleum Geologists Bulletin, v. 56, no. 12, p. 2303–2322.
- Hills, J. M., 1984, Sedimentation, tectonism, and hydrocarbon generation in Delaware Basin, west Texas, and southeastern New Mexico: American Association of Petroleum Geologists Bulletin, v. 68, no. 3, p. 250–267.
- Hoose, G., and Dillman, G., 1995, Sand Dunes Delaware, W.; Sand Dunes Delaware, S., *in* Worrall, general chairman, Symposium of the oil and gas fields of southeastern New Mexico, 1995 supplement: Roswell Geological Society, p. 325–328.
- Hull, J. P. D., 1957, Petrogenesis of Delaware Mountain sandstone Texas and New Mexico: American Association of Petroleum Geologists Bulletin, v. 41, no. 2, p. 278–307.
- Hull, J. P. D., 1979, Petrogenesis of Delaware Mountain sandstone Texas and New Mexico, *in* Sullivan, N. M., ed., Guadalupian Delaware Mountain Group: Society of Economic Paleontologists and Mineralogists Permian Basin Section Publication 79-18, p. 153–182.
- Hutchings, W. D., 2000, Sequence stratigraphy of the Permian Delaware Mountain Group, Delaware Basin, West Texas: American Association of Petroleum Geologists Bulletin, v. 84, no. 11, p. 1865.
- Jacka, A. D., 1979, Deposition and entrapment of hydrocarbons in Bell Canyon and Cherry Canyon deep-sea fans of the Delaware Basin, *in* Sullivan, N. M., ed., Guadalupian Delaware Mountain Group of West Texas and Southeast New Mexico: Society of

- Economic Paleontologists and Mineralogists Permian Basin Section Publication 79-18, p. 104–120.
- Jacka, A. D., Beck, R. H., St. Germain, L. C., and Harrison, S. C., 1968, Permian deep-sea fans of the Delaware Mountain Group (Guadalupian), Delaware Basin, *in* Guadalupian facies, Apache Mountains area, West Texas: Society of Economic Paleontologists and Mineralogists Permian Basin Section Publication 68-11, p. 49–90.
- Jacka, A. D., Thomas, R. H., Beck, R. H., Williams, K. W., and Harrison, S. C., 1972, Guadalupian depositional cycles of the Delaware Basin and Northwest Shelf, *in* Elam, J. G., and Chuber, S., eds., *Cyclic sedimentation in the Permian Basin: West Texas Geological Society Publication 72-60*, p. 151–195.
- James, W. C., 1987, Channel and channel-adjacent deposits, Delaware Mountain Group (Permian), West Texas, *in* Powers, D. W., and James, W. C., eds., *Geology of the western Delaware Basin, West Texas and southeastern New Mexico*, El Paso Geological Society, Annual Field Trip Guidebook, v. 18, p. 49–62.
- Jeary, G. L. 1978, Leonardian strata in the northern Midland Basin of West Texas, *in* Gilbertson, R. L., ed., *Energy quest for the Southwest: West Texas Geological Society Publication 78-69*, p. 30–47.
- Jones, T. S., and Smith, H. M., 1965, Relationships of oil composition and stratigraphy in the Permian Basin of West Texas and New Mexico, *in* Young, A., and Galley, A. E., eds., *Fluids in subsurface environments: American Association of Petroleum Geologists Memoir 4*, p. 101–224.
- Justman, H. A., and Broadhead, R. F., 2000, Source rock analysis for the Brushy Canyon Formation, Delaware Basin, southeastern New Mexico, *in* DeMis, W. D., Nelis, M. K., and Trentham, R. C., eds., *The Permian Basin: proving ground for tomorrow's technologies: West Texas Geological Society Publication 00-109*, p. 211–220.
- Kane, T. V., 1992, Sequence stratigraphy improves definition of reservoir architecture at Avalon (Delaware) field, Eddy County, New Mexico, *in* Mruk, D. H., and Curran, B. C., eds., *Permian Basin exploration and production strategies: applications of sequence stratigraphic and reservoir characterization concepts: West Texas Geological Society Publication 92-91*, p. 12–18.
- Kashatus, G. P., 1986, Depositional environment and reservoir morphology of Guadalupian Bell Canyon sandstones, Scott field, Ward and Reeves Counties, Texas: Texas A & M University, Master's thesis, 85 p.
- Kerans, C., and Fitchen, W. M., 1996, Stratigraphic constraints on the origin of Brushy Canyon sandstones, *in* DeMis, W. D., and Cole, A. G., eds., *The Brushy Canyon Play in outcrops and subsurface: concepts and examples: Permian Basin Section, Society of Economic Paleontologists and Mineralogists Publication 96-38*, p. 61–68.

- Kerans, C., Fitchen, W. M., Gardner, M. H., Sonnenfeld, M. D., Tinker, S. W., and Wardlaw, B. R., 1992, Styles of sequence development within uppermost Leonardian through Guadalupian strata of the Guadalupe Mountains, Texas and New Mexico, *in* Mruk, D. H., and Curran, B. C., eds., *Permian Basin exploration and production strategies: applications of sequence stratigraphic and reservoir characterization concepts*: West Texas Geological Society Publication 92-91, p. 1–6.
- Kerans, C., Fitchen, W. M., Gardner, M. H., and Wardlaw, B. R., 1993, A contribution to the evolving stratigraphic framework of latest Leonardian-Guadalupian strata of the Delaware Basin, *in* Adams, J. W., Austin, G., Barker, J., Hawley, J. W., and Love, D. W., eds., *Carlsbad region, Permian Basin, New Mexico and Texas*: New Mexico Geological Society/West Texas Geological Society Annual Field Conference Guidebook, p. 175–184.
- Kerans, Charles, and Kempter, Kirt, 2002, Hierarchical stratigraphic analysis of a carbonate platform, Permian of the Guadalupe Mountains: American Association of Petroleum Geologists, Datapages Discovery Series No. 5, Compact disk.
- Kerans, C., Lucia, F. J., and Senger, R. K., 1994, Integrated characterization of carbonate ramp reservoirs using Permian San Andres Formation outcrop analogs: American Association of Petroleum Geologist Bulletin, v. 78, p. 181–216.
- King, P. B., 1934, Permian stratigraphy of trans-Pecos Texas: Geological Society of America Bulletin, v. 45, no. 4, p. 697–798.
- King, P. B., 1942, Permian of west Texas and southeastern New Mexico: American Association of Petroleum Geologist Bulletin, v. 26, no. 4, p. 535–763.
- King, P. B., 1948, Geology of the southern Guadalupe Mountains, Texas: U.S. Geological Survey Professional Paper, 183 p.
- King, P. B., and King, R. E., 1929, Stratigraphy of outcropping carboniferous and Permian rocks of Trans-Pecos Texas: American Association of Petroleum Geologists Bulletin, v. 13, no. 8, p. 907–926.
- King, P. B., and Newell, N., 1956, McCombs Limestone Member of Bell Canyon Formation, Guadalupe Mountains, Texas: American Association of Petroleum Geologists Bulletin, v. 40, p. 386–387.
- Kirkpatrick, R. K., Flanders, W. A., and DePauw, R. M., 1985, Performance of the Twofreds CO₂ injection project: Society of Petroleum Engineers Annual Technical Conference and Exhibition, Society of Petroleum Engineers Paper 14439, 12 p.

- Kosters, E. C., Bebout, D. G., Seni, S. J., Garrett, C. M., Brown, L. F., Hamlin, H. S., Dutton, S. P., Ruppel, S. C., Finley, R. J., and Tyler, N., 1989, Atlas of major Texas gas reservoirs: The University of Texas at Austin, Bureau of Economic Geology, 161 p.
- Lang, W. T., 1937, The Permian formations of the Pecos Valley of New Mexico and Texas: American Association of Petroleum Geologists Bulletin, v. 21, no. 7, p. 833–898.
- Lawson, E. C., 1989, Subaqueous gravity flows and associated deposits in the Rader Member, Capitan reef complex (Permian), Delaware Mountains, West Texas: University of Wisconsin, Madison, Master's thesis, 160 p.
- Leiphart, D. J., and Hart, B. S., 2000, Probabilistic neural network used to predict porosity from 3-D seismic attributes in lower Brushy Canyon Formation, southeast New Mexico, *in* DeMis, W. D., Nelis, M. K., and Trentham, R. C., eds., The Permian Basin: proving ground for tomorrow's technologies: West Texas Geological Society Publication 00-109, p. 187–191.
- Lewis, P., Cross, S., and Hoose, G., 1996, Delaware Mountain Group production map, *in* DeMis, W. D., and Cole, A. G., eds., The Brushy Canyon play in outcrop and subsurface: concepts and examples: Society of Economic Paleontologists and Mineralogists Permian Basin Section Publication 96-38, separate map in back pocket.
- Linn, A. M., 1985, Depositional environment and hydrodynamic flow in Guadalupian Cherry Canyon sandstone, West Ford and West Geraldine fields, Delaware Basin, Texas: Texas A&M M. S. thesis, 152 p.
- Loftin, T. R., Jr., 1996, Depositional stacking patterns within the Cherry Canyon Formation, Delaware Basin, west Texas, *in* DeMis, W.D., and Cole, A.G., eds., The Brushy Canyon play in outcrop and subsurface: concepts and examples: Society of Economic Paleontologists and Mineralogists Permian Basin Section Publication 96-38, p. 113–118.
- Logan, D., Morriss, C., and Williams, R., 1995, Comparison of nuclear magnetic resonance techniques in the Delaware, *in* Worrall, J., general chairman, a symposium of the oil and gas fields of southeastern New Mexico: Roswell Geological Society, p. 112–136.
- Malik, M. A., 1998, Compositional simulations of a CO₂ flood in Ford Geraldine unit, Texas, *in* Proceedings, Society of Petroleum Engineers Permian Basin Oil and Gas Recovery Conference, Paper 39794, p. 375–383.
- Martin, D. F., Hardage, B. A., Murphy, M. B., Kendall, R. P., Stubbs, B. A., Uszynski, B. J., Weiss, W. W., and Whitney, E. M., 1997, Reservoir characterization as a risk reduction tool at the Nash Draw pool: Society of Petroleum Engineers Paper 38916, 14 p.
- May, B. A., 1996, Geology and development history of the Livingston Ridge and Lost Tank Delaware pools, southeastern New Mexico, *in* DeMis, W. D., and Cole, A. G., eds., The Brushy Canyon play in outcrop and subsurface: concepts and examples: Society of

Economic Paleontologists and Mineralogists Permian Basin Section Publication 96-38, p. 113–118.

McDermott, R. W., 1983, Depositional processes and environments of the Permian sandstone tongue of the Cherry Canyon Formation and the upper San Andres Formation, Last Chance Canyon, southeastern New Mexico: The University of Texas at Austin, Master's thesis, 179 p.

McNeal, R. P., and Mooney, T. D., 1979, Relations of oil composition and stratigraphy of Delaware reservoirs: Guadalupian Delaware Mountain Group of West Texas and Southeast New Mexico: Society of Economic Paleontologists and Mineralogists Permian Basin Section Publication 79-18, p. 183–190.

McRae, J. R., 1995a, Lusk Delaware East, *in* Worrall, J., general chairman, a symposium of the oil and gas fields of southeastern New Mexico: Roswell Geological Society, p. 291–295.

McRae, J. R., 1995b, Salt Lake Delaware: *in* Worrall, J. (general chairman), a symposium of the oil and gas fields of southeastern New Mexico: Roswell Geological Society, p. 321–323.

Meissner, F. G., 1972, Cyclic sedimentation in middle Permian strata of the Permian Basin, *in* Elam, J. G., and Chuber, S., eds., Cyclic sedimentation in the Permian Basin: West Texas Geological Society, p. 203–232.

Mitchell, S. T., 1995, Nash Draw Brushy Canyon, *in* Worrall, J. general chairman, A symposium of the oil and gas fields of southeastern New Mexico: Roswell Geological Society, p. 321–323.

Mitchum, R. M., Jr., Vail, P. R., Thompson, S., III, and Payton, C. E., eds., 1977, Seismic stratigraphy; applications to hydrocarbon exploration: American Association of Petroleum Geologists Memoir, no. 26, 212 p.

Montgomery, S. L., 1997a, Permian Bone Spring Formation Sandstone Play in the Delaware Basin, Part I-slope: American Association of Petroleum Geologists Bulletin, v. 81, no. 8, p. 1239–1258.

Montgomery, S. L., 1997b, Permian Bone Spring Formation Sandstone Play in the Delaware Basin, Part II-basin: American Association of Petroleum Geologists Bulletin, v. 81, no. 9, p. 1423–1434.

Montgomery, S. L., Hamilton, Dean, Hunt, Tim, and Worrall, John, and Hamilton, Dean, 2000, Delaware Mountain Group, West Texas and southeastern New Mexico, a case of refound opportunity; Part 2; Cherry Canyon Formation: American Association of Petroleum Geologists Bulletin, v. 84, no. 1, p. 1–11.

Montgomery, S. L., Worrall, John, and Hamilton, Dean, 1999, Delaware Mountain Group, West Texas and southeastern New Mexico, a case of refound opportunity; Part 1; Brushy

- Canyon: American Association of Petroleum Geologists Bulletin, v. 83, no. 12, p. 1901–1926.
- Nance, H. S., 2006, Upper Guadalupian and Ochoan of the Permian Basin shelves: effects of deposition, diagenesis, and structure on reservoir development (http://www.beg.utexas.edu/resprog/permianbasin/geolog_synth/index.htm).
- New, M. E., 1988, Sedimentology of the Cherry Canyon Tongue (Cherry Canyon Formation, Permian), western Guadalupe Mountains, Texas and New Mexico: University of Wisconsin, Madison, Master's thesis, 287 p.
- Newell, N. D., Rigby, J. K., Fischer, A. G., Whiteman, A. J., Hickox, J. E., and Bradley, J. S., 1953, The Permian Reef Complex of the Guadalupe Mountains region, Texas and New Mexico: San Francisco, W. H. Freeman Co., 236 p.
- Nicklen, B. L., 2003, Middle Guadalupian (Permian) bentonite beds, Manzanita Member, Cherry Canyon Formation, West Texas: stratigraphic and tectonomagmatic applications: University of Cincinnati, Master's thesis, 66 p.
- Oriel, S. S., Meyers, D. A., and Crosby, E. J., 1967, West Texas Permian basin region, *in* McKee, E. D., and Oriel, S. S., eds., Paleotectonic investigation of the Permian System in the United States: U.S. Geological Survey Professional Paper 515C, p. 17–60.
- Payne, M. W., 1973, Basinal sandstone facies of the Delaware Mountain Group, West Texas and southeast New Mexico: Texas A&M University, Ph.D. dissertation, 150 p.
- Payne, M. W., 1976, Basinal sandstone facies, Delaware Basin, West Texas and southeast New Mexico: American Association of Petroleum Geologists Bulletin, v. 60, p. 517–527.
- Payne, M. W., 1979, Submarine fan channel depositional processes in the Permian Bell Canyon Formation, West Texas and southeast New Mexico, *in* Sullivan, N. M., ed., Guadalupian Delaware Mountain Group of West Texas and southeast New Mexico, Symposium and Field Trip Conference Guidebook: Society of Economic Paleontologists and Mineralogists Permian Basin Section Publication 79-18, p. 75–95.
- Peterson, Fred, 1988, Pennsylvanian to Jurassic eolian transportation systems in the Western United States, *in* Kocurek, Gary, ed., Late Paleozoic and Mesozoic eolian deposits of the Western Interior of the United States: Sedimentary Geology, v. 56, no. 1-4, p. 207–260.
- Phillips, S., 1981, Depositional patterns and reservoir morphology of Guadalupian Cherry Canyon sandstones, Indian Draw field, Eddy County, New Mexico: Texas A&M University, Master's thesis, 173 p.
- Pittaway, K. R., and Rosato, R. J., 1991, The Ford Geraldine unit CO₂ flood—update 1990: Society of Petroleum Engineers Reservoir Engineering, v. 6, no. 4, p. 410–414.

- Railroad Commission of Texas, 2003, Annual Report, electronic spreadsheet.
- Richardson, G. B., 1904, Report of a reconnaissance in trans-Pecos Texas, north of the Texas and Pacific Railway: University of Texas, Austin, Bulletin 23, 119 p.
- Ring, 1995, An overview of the North Ward Estes CO₂ flood: Society of Petroleum Engineers Annual Technical Conference and Exhibition, 22–25 October, Dallas.
- Rosen, C., 1985, Sedimentology of the Brushy Canyon Formation (Permian, Early Guadalupian) in the onlap area, Guadalupe Mountains, West Texas: University of Wisconsin, Madison, Master's thesis, 314 p.
- Rosen, C., and Sarg, J. F., 1988, Sedimentology and regional correlation of a basinally restricted deep-water siliciclastic wedge: Brushy Canyon Formation-Cherry Canyon tongue (Lower Guadalupian), Delaware Basin, *in* Reid, S. T., Bass, R. O., and Welch, P., eds., Guadalupe Mountains revisited, Texas and New Mexico: West Texas Geological Society Publication 88-84, p. 127–132.
- Ruggiero, R. W., 1985, Depositional history and performance of a Permian Bell Canyon sandstone reservoir, Ford-Geraldine field, West Texas: The University of Texas at Austin, Master's thesis, 242 p.
- Ruggiero, R. W., 1993, Depositional history and performance of a Permian Bell Canyon sandstone reservoir, Ford-Geraldine field, West Texas, *in* Rhodes, E. G., and Moslow, T. F., eds., Marine clastic reservoirs: New York, Springer-Verlag, p. 201–229.
- Ruppel, S. C., Park, Y. J., and Lucia, F. J., 2002, Applications of 3-D seismic to exploration and development of carbonate reservoirs: South Cowden Grayburg field, West Texas, *in* Hunt, T. J., and Lufholm, P. H., eds., The Permian Basin: Preserving our past—securing our future: West Texas Geological Society, Publication 02-111, p. 71–87.
- Sageman, B. B., Gardner, M. H., Armentrout, J. M., and Murphy, A. E., 1998, Stratigraphic hierarchy of organic-rich siltstones in deep-water facies, Brushy Canyon Formation (Guadalupian), Delaware Basin, West Texas: *Geology*, v. 26, no. 5, p. 451–454.
- Sarg, J. F., Rossen, C., Lehmann, P. J., and Pray, L. C., eds., 1988, Geologic guide to the Western Escarpment, Guadalupe Mountains, Texas: Society of Economic Paleontologists and Mineralogists Permian Basin Section Publication 88-30, 60 p.
- Scholle, P. A., 1999, <http://geoinfo.nmt.edu/staff/scholle/graphics/permphotos/220.html>.
- Scott, G. L., and Carrasco, A., 1996, Delaware sandstone reservoir completions and real-time monitoring of hydraulic fractures, *in* DeMis, W. D., and Cole, A. G., eds., The Brushy Canyon play in outcrop and subsurface: concepts and examples: Society of Economic Paleontologists and Mineralogists Permian Basin Section Publication 96-38, p. 183–188.

- Segrest, C. C., 1993, Identification of productive intervals and definition of original oil in place, Brushy Canyon Delaware Formation, Delaware Basin, *in* Gibbs, J., and Cromwell, D., eds., *New dimensions in the Permian Basin: West Texas Geological Society Publication 93-93*, p. 47–54.
- Silver, B. A., and Todd, R. G., 1969, Permian cyclic strata, northern Midland and Delaware Basins, West Texas and southeastern New Mexico: *American Association of Petroleum Geologists Bulletin*, v. 53, p. 2223–2251.
- Spain, D. R., 1992, Petrophysical evaluation of a slope fan/basin-floor fan complex: Cherry Canyon Formation, Ward County, Texas: *American Association of Petroleum Geologists Bulletin*, v. 76, p. 805–827.
- SPWLA, 1982, a survey of resistivities of water from subsurface formations in west Texas and southeastern New Mexico: *Society of Petroleum Engineers Permian Basin Section and Permian Basin Well Logging Society of Professional Well Log Analysts*, 17 p.
- St. Germain, L. C., 1966, Depositional dynamics of the Brushy Canyon Formation, Delaware Basin, Texas: Texas Tech University, Master's thesis, 119 p.
- Szantay, A., and Babin, C., 1995, Cortin Delaware, West, *in* Worrall, J., general chairman, *A symposium of the oil and gas fields of southeastern New Mexico: Roswell Geological Society*, p. 203–206.
- Tait, D. R., Ahlen, J. L., Gordon, A., Scott, G. L., Motts, W. S., and Spider, M. E., 1962, Artesia Group of New Mexico and West Texas: *American Association of Petroleum Geologists Bulletin*, v. 26, p. 504–517.
- Thomerson, M. D., 1992, Petrophysical analysis of the Brushy Canyon Formation, Hat Mesa Delaware field, Lea County, New Mexico: Texas Tech University, Master's thesis, 124 p.
- Thomerson, M. D., and Asquith, G. B., 1992, Petrophysical analysis of the Brushy Canyon Formation, Hat Mesa field, Lea County, New Mexico, *in* Mruk, D. H., and Curran, C., eds., *Permian Basin Exploration and production strategies: application of sequence stratigraphic and reservoir characterization concepts: West Texas Geological Society Publication 92-91*, p. 80–90.
- Thomerson, M. D., and Catalano, L. E., 1996, Depositional regimes and reservoir characteristics of the Brushy Canyon sandstones, East Livingston Ridge Delaware field, Lea County, New Mexico, *in* DeMis, W. D., and Cole, A. G., eds., *The Brushy Canyon play in outcrop and subsurface: concepts and examples: Society of Economic Paleontologists and Mineralogists Permian Basin Section Publication 96-38*, p. 103–111.
- Tittle, J. S., 1995, Herradura Bend Delaware East: *in* Worrall, J., general chairman, *a symposium of the oil and gas fields of southeastern New Mexico: Roswell Geological Society*, p. 235–238.

- Todd, R. G., 1976, Oolite-bar progradation, San Andres Formation, Midland Basin, Texas: American Association of Petroleum Geologists Bulletin, v. 60, no. 6, p. 907–925.
- Tyrrell, W. W., and Diemer, J. A., 2003, Relationship of two widespread Guadalupian subsurface marker units (Bowers Sand and Two Finger Limestone) to outcrop-defined sequences in the Guadalupe Mountains, New Mexico and west Texas, *in* Hunt, T. J., and Lufholm, P. H., eds., The Permian Basin: back to basics: West Texas Geological Society, Publication 03-112, p. 97–118.
- Tyrrell, W. W., and Diemer, J. A., 2004, Subsurface sequence stratigraphy of the Middle Permian (Guadalupian) Bell Canyon and upper Cherry Canyon Formations, northern Delaware Basin, New Mexico and west Texas, *in* Trentham, R., ed., Proceedings, WTGS Fall Symposium.
- Tyrrell, W. W., Diemer, J. A., Bell, G. L., and Griffing, D. H., 2004, Subsurface sequence stratigraphy of the Manzanita limestone member, Cherry Canyon Formation, northern Delaware Basin, New Mexico and West Texas, *in* Trentham, R. C., ed., Banking on the Permian Basin: plays, field studies, and techniques: West Texas Geological Society Publication 04-112.
- Walling, S. D., 1992, Authigenic clay minerals in sandstones of the Delaware Mountain Group: Bell Canyon and Cherry Canyon Formations, Waha field, West Texas: Texas A&M University, Master's thesis, 63 p.
- Walling, S. D., Hays, P. D., and Tieh, T. T., 1992, Chlorites in reservoir sandstones of the Guadalupian Delaware Mountain Group, *in* Cromwell, D. W., Moussa, M. T., and Mazzullo, L. J., eds., Southwest Section American Association of Petroleum Geologists Transactions, SWS 92-90, p. 149–154.
- Ward, R., Kendall, C. G. St. C., and Harris P. M., 1986, Upper Permian (Guadalupian) facies and their association with hydrocarbons Permian Basin, West Texas and New Mexico: American Association of Petroleum Geologists Bulletin, v. 70, p. 239–262.
- Wegner, MaryBeth, Bohacs, K. M., Simo, J. A., Carroll, A. R., and Pevear, D., 1998, Siltstone facies of the Upper Brushy Canyon and lower Cherry Canyon Formations (Guadalupian), Delaware Basin, West Texas: depositional processes and stratigraphic distribution, *in* DeMis, W. D., and Nelis, M. K., eds., The search continues into the 21st Century: West Texas Geological Society Publication 98-105, p. 59–65.
- Weiss, W. W., Stubbs, B. A., and Balch, R. S., 2001, A new tool for lower Brushy Canyon completion decisions, *in* Viveiros, J. J., and Ingram, S. M., eds., The Permian Basin: microns to satellites—looking for oil and gas at all scales: West Texas Geological Society Publication 01-110, p. 99–104.

- White, D., 1995, Los Mendanos, in Worrall, J., general chairman, A symposium of the oil and gas fields of southeastern New Mexico: Roswell Geological Society, p. 275–278.
- Williamson, C. R., 1977, Deep-sea channels of the Bell Canyon Formation (Guadalupian), Delaware Basin, Texas-New Mexico, *in* Hileman, M. E., and Mazzullo, S. J., eds., Upper Guadalupian facies, Permian reef complex, Guadalupe Mountains, New Mexico and Texas: Society of Economic Paleontologists and Mineralogists Permian Basin Section Publication 77-16, p. 409–431.
- Williamson, C. R., 1978, Depositional processes, diagenesis and reservoir properties of Permian deep-sea sandstones, Bell Canyon Formation, Texas-New Mexico: The University of Texas at Austin, Ph.D. dissertation, 262 p.
- Williamson, C. R., 1979, Deep sea sedimentation and stratigraphic traps, Bell Canyon Formation (Permian), Delaware basin, *in* Sullivan, N. M., ed., Guadalupian Delaware Mountain Group of West Texas and southeast New Mexico, Symposium and Field Trip Conference Guidebook: Society of Economic Paleontologists and Mineralogists Permian Basin Section Publication 79-18, p. 39–74.
- Williamson, C. R., 1980, Sedimentology of Guadalupian deep-water clastic facies, Delaware Basin, New Mexico and West Texas: New Mexico Geological Society Guidebook, 31st Field Conference, Trans-Pecos region, p. 195–204.
- Worrall, J., 1995, Hat Mesa Delaware, *in* Oil and gas fields of southeastern New Mexico: supplement: Roswell Geological Society, p. 275–278.
- Worthington, R., 1995, Shugart Delaware, East, *in* Worrall, J., general chairman, a symposium of the oil and gas fields of southeastern New Mexico: Roswell Geological Society, p. 329–333.
- Worthington, R., and Uszynski, B., 1995, Willow Lake Delaware, *in* Worrall, J., general chairman, A symposium of the oil and gas fields of southeastern New Mexico: Roswell Geological Society, p. 347–350.
- Yahney, G. K., 1995, Young Delaware, North, *in* Worrall, J., general chairman, a symposium of the oil and gas fields of southeastern New Mexico: Roswell Geological Society, p. 352–356.
- Yang, K. M., and Dorobek, S. L., 1995, The Permian Basin of west Texas and New Mexico: tectonic history of a “composite” foreland basin and its effects on stratigraphic development, *in* Dorobek, S. L., and Ross, G. M., eds., Stratigraphic evolution of foreland basins: Society of Economic Paleontologists and Mineralogists, Special Publication 52, p. 149–174.
- Ye, Q., and Kerans, C., 1996, Reconstructing Permian eustacy from 2-D backstripping and its use in forward models, *in* DeMis, W. D., and Cole, A. G., eds., The Brushy Canyon Play

in outcrops and subsurface: concepts and examples: Society of Economic Paleontologists and Mineralogists Permian Basin Section Publication 96-38, p. 69–74.

Zelt, F. B., and Rosen, C., 1995, Geometry and continuity of deep-water sandstones and siltstones, Brushy Canyon Formation (Permian) Delaware Mountains, Texas, in Pickering, K. T., Hiscott, R. N., Keyton, N. H., Lucchi, F. R., and Smith, R. D. A., Atlas of deep water environments: architectural style in turbidite systems: London, Chapman and Hall, p. 167–181.

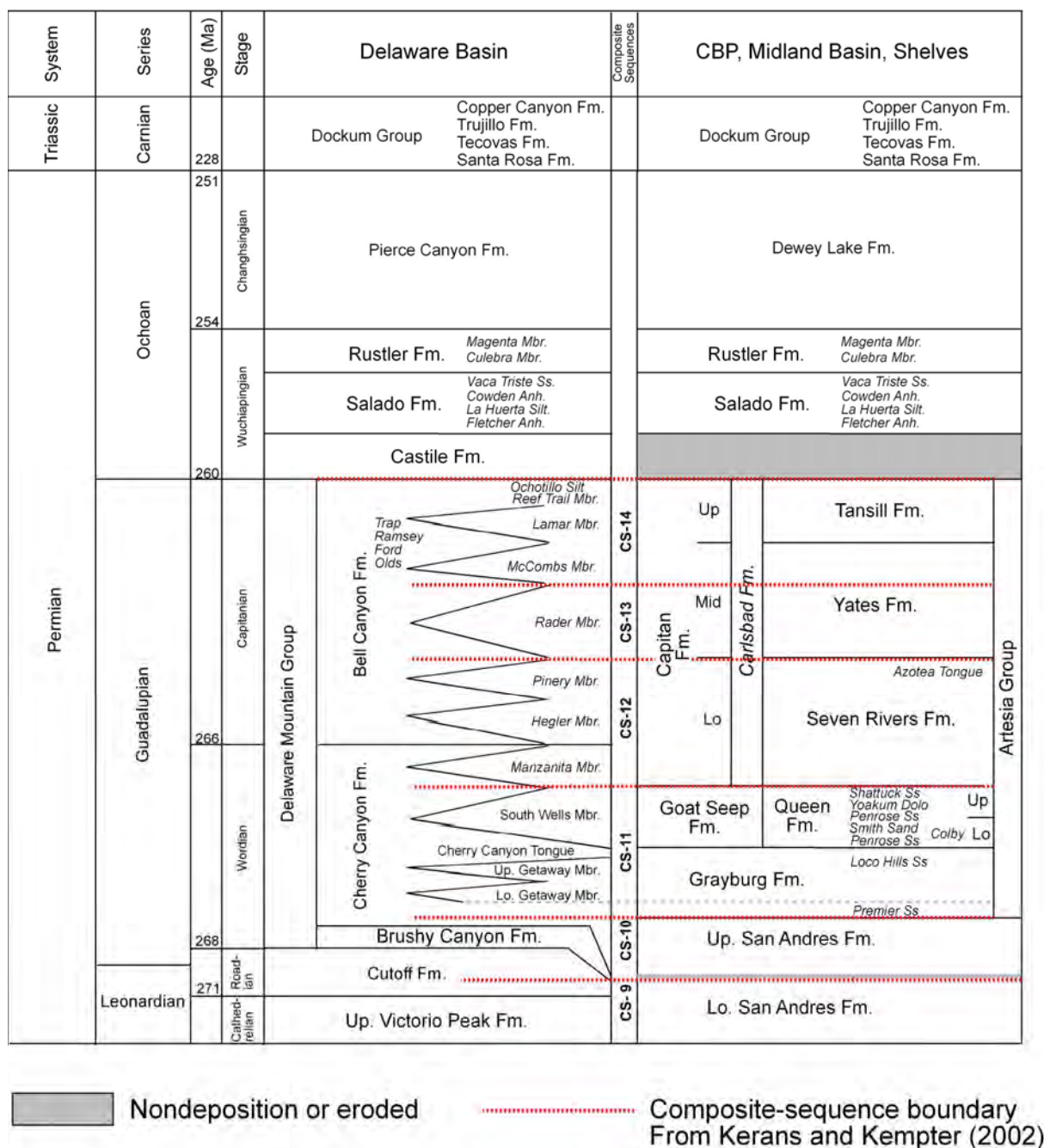


Figure 1. Correlation chart for uppermost Leonardian and Guadalupian strata in the Permian Basin.

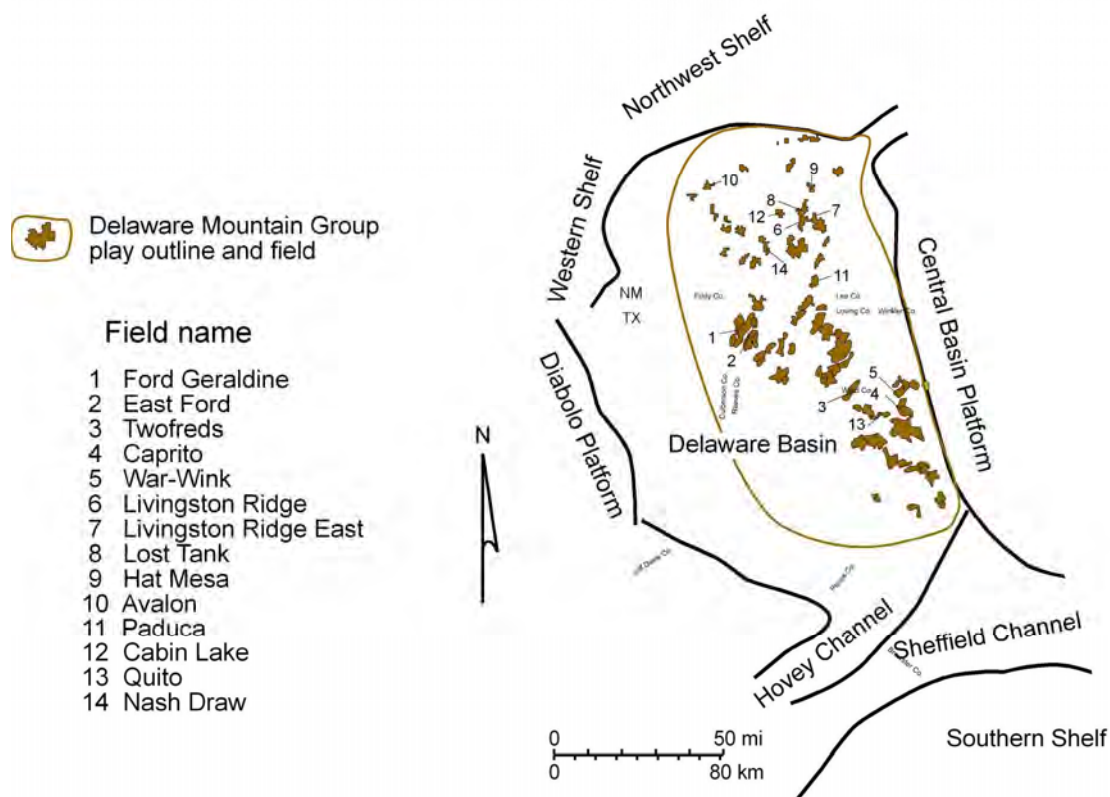
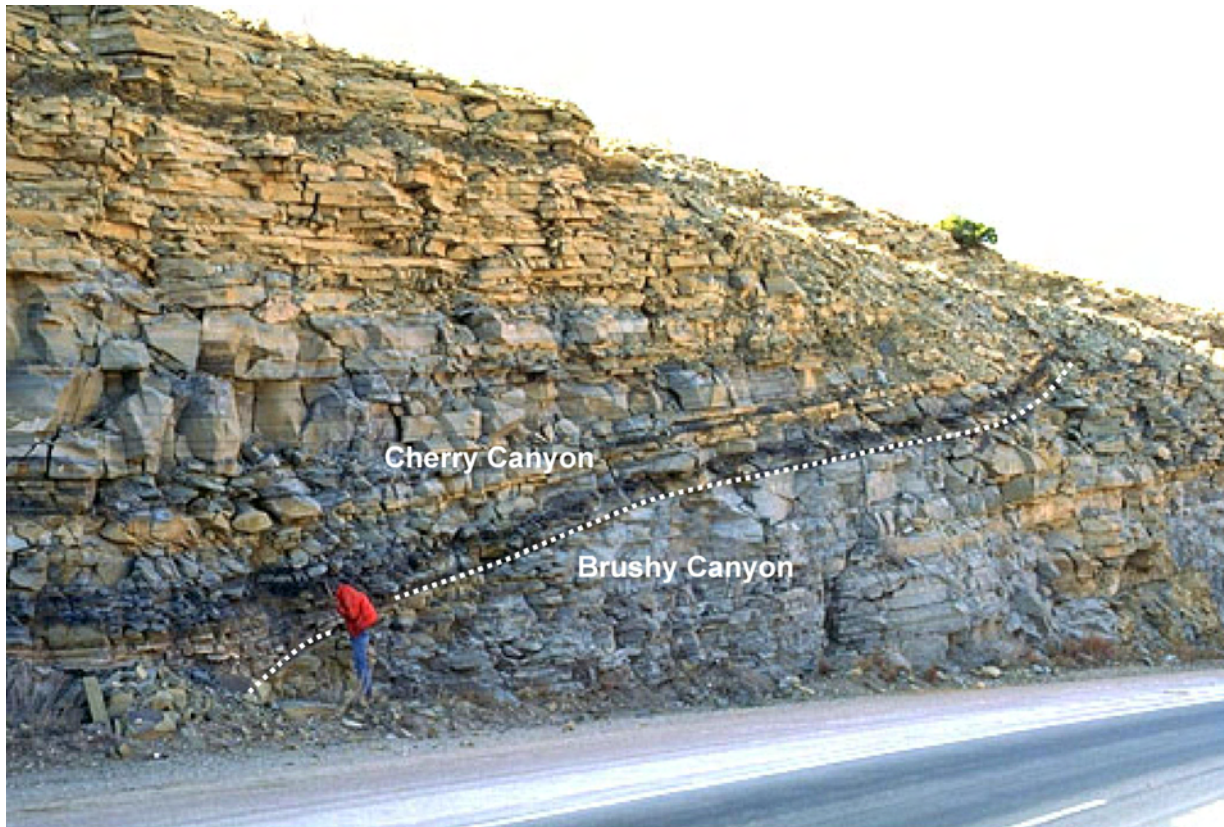


Figure 2. Map showing locations of reservoirs (cumulative production > 1MMbbl) within the Delaware Mountain Group play. Also shown are approximate positions of major tectonic elements and suggested boundaries of plays. Reservoirs specifically discussed in this report are indicated.



Modified from Scholle (1999)

Figure 3. Unconformable contact between the Cherry Canyon and underlying Brushy Canyon Formations. Outcrop is on Hwy 62-180, south of Guadalupe Pass and north of El Capitan scenic turnout, Guadalupe Mountains. Strata are composed of subarkosic sandstone and siltstone.

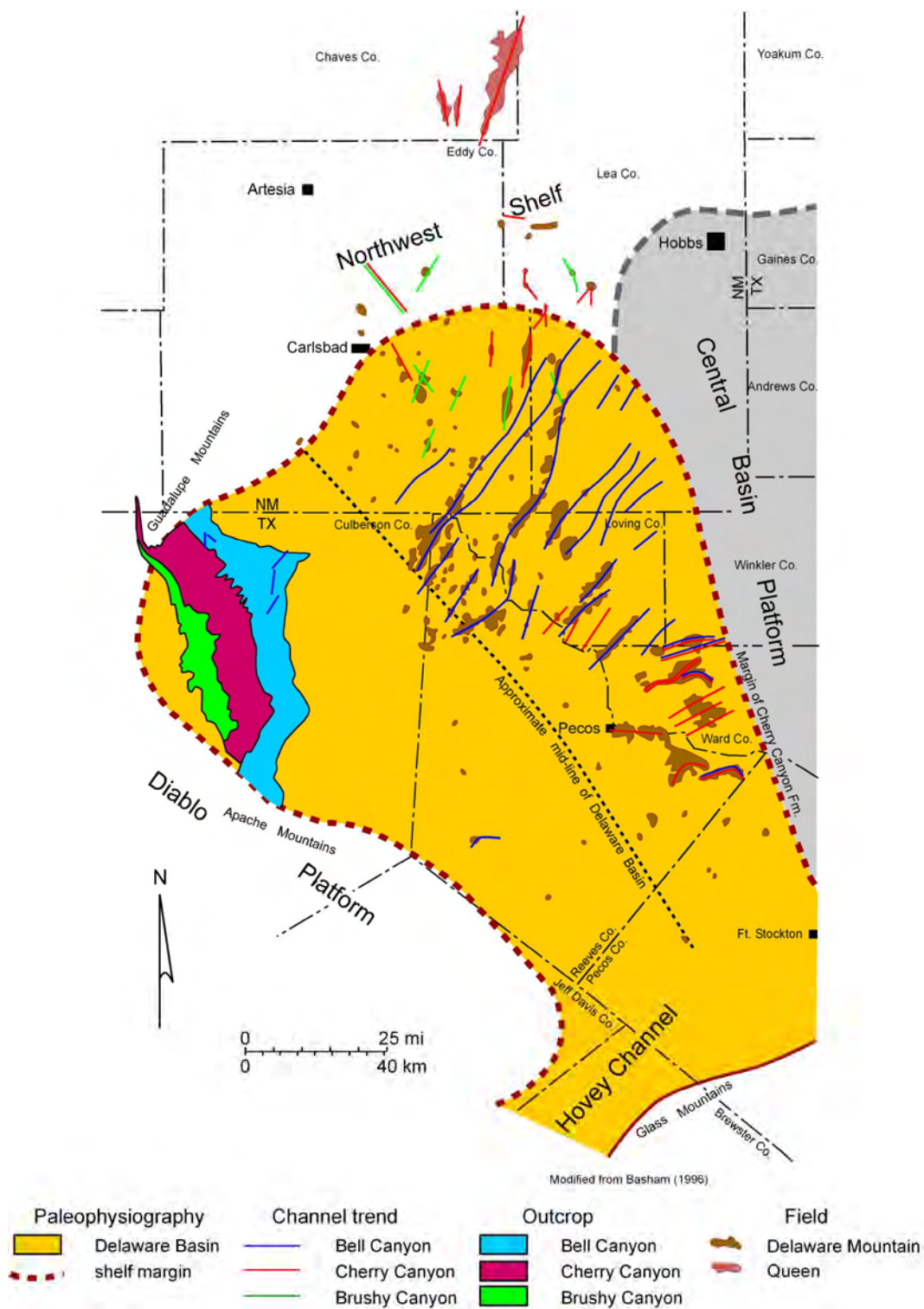


Figure 4. Map of Delaware Mountain Group reservoirs. Also shown are inferred submarine channel trends that are color coded to indicate primary reservoir intervals. Note that Brushy sandstone fairways trend preferentially north to south, Bell Canyon fairways trend northeast to southwest, and Cherry Canyon fairways trend from the north and from the east.

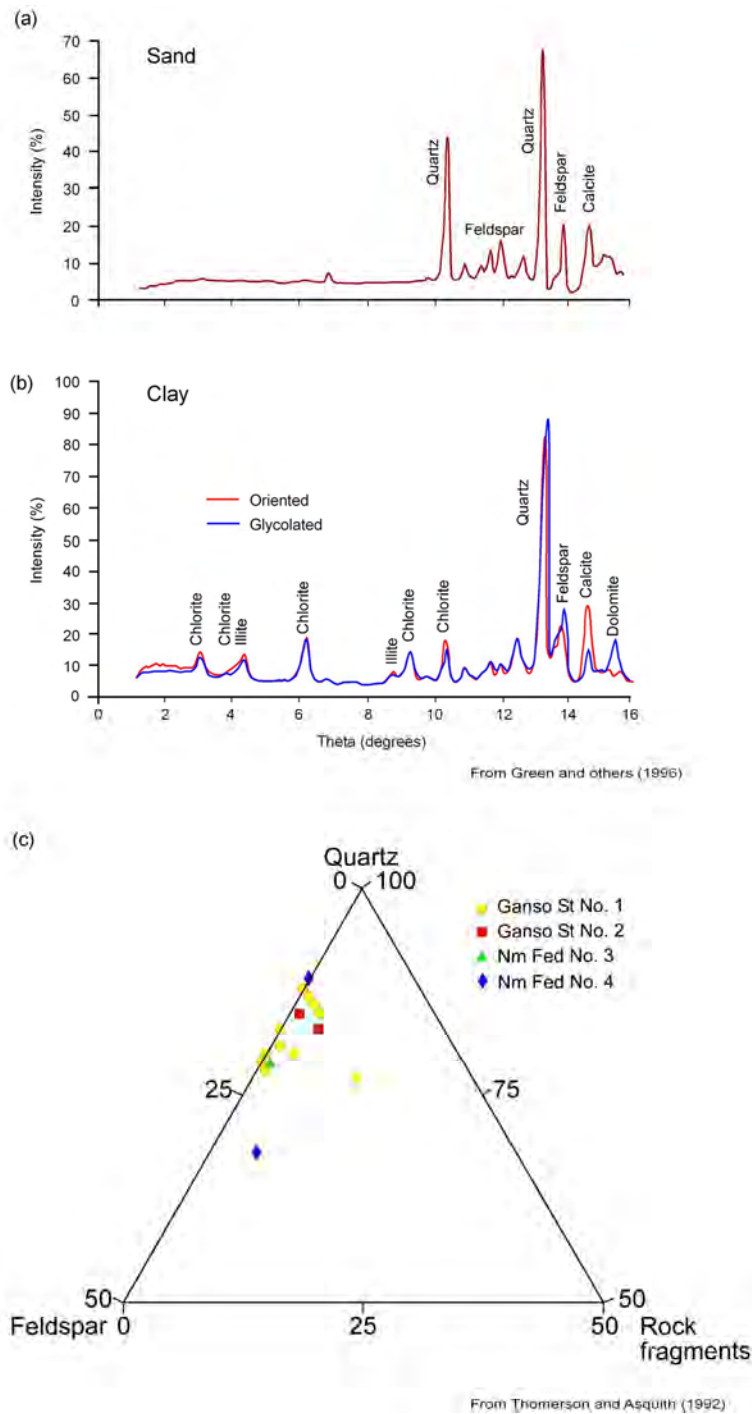
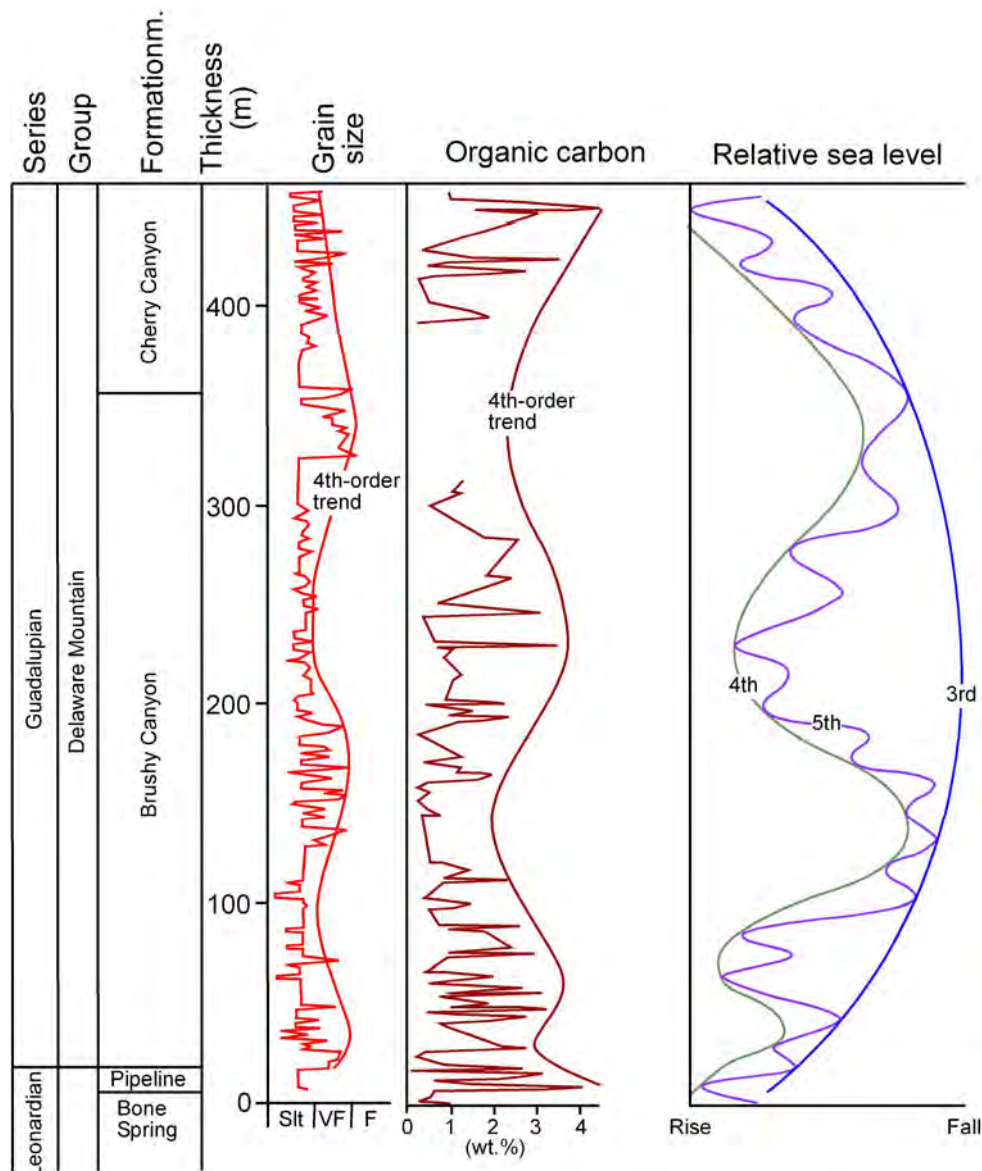


Figure 5. Mineralogy of Delaware Mountain Group siliciclastics: (a) x-radiogram of typical fine- to very fine grained Brushy Canyon sandstone showing prominence of quartz, feldspar, and calcite (cement); (b) x-radiogram of typical, mainly authigenic clay fraction composed of illite, chlorite, feldspar, calcite, and dolomite; (c) ternary compositional diagram of sand fraction from four Brushy Canyon wells showing subarkosic to arkosic character of DMG reservoir facies.



Modified from Sageman and others (1998)

Figure 6. Graphs showing correspondences of grain size, organic carbon content, and interpreted relative sea-level stages for the Brushy Canyon and lowermost Cherry Canyon Formations. Samples are from outcrops in the Guadalupe and Delaware Mountains. Peaks in deposition of silt and organic matter tend to be associated with interpreted rises and highstands of sea level. Modified from Sageman and others (1998).

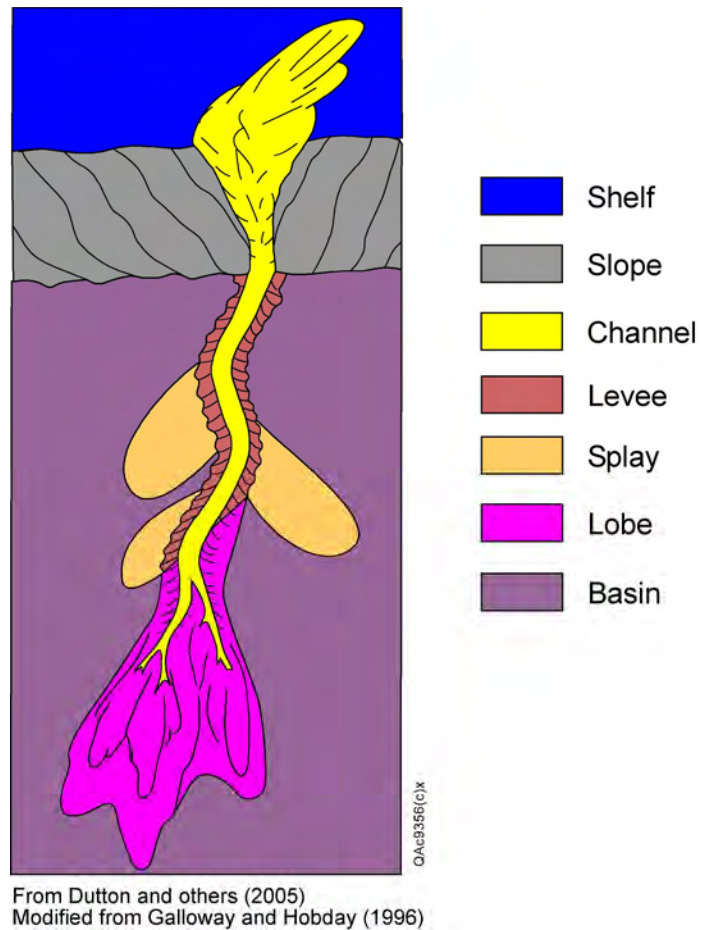


Figure 7. Simplified model of generalized shelf-margin paleogeographic and depositional elements of Delaware Mountain Group deep-water sandstone facies. From Dutton and others (2005); modified from Galloway and Hobday (1996).

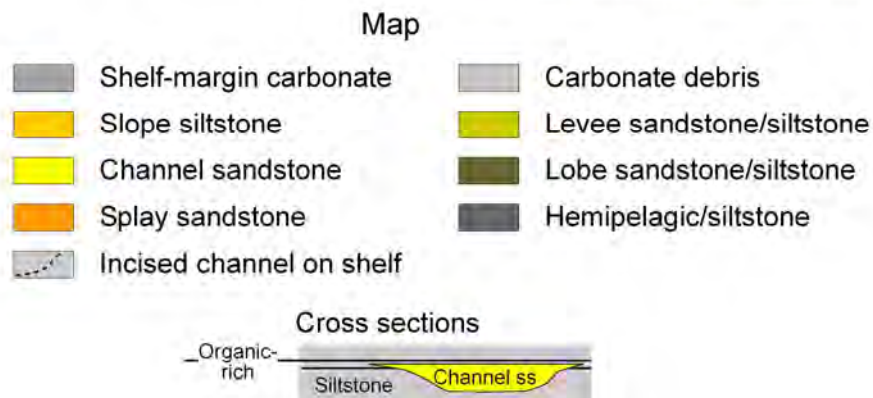
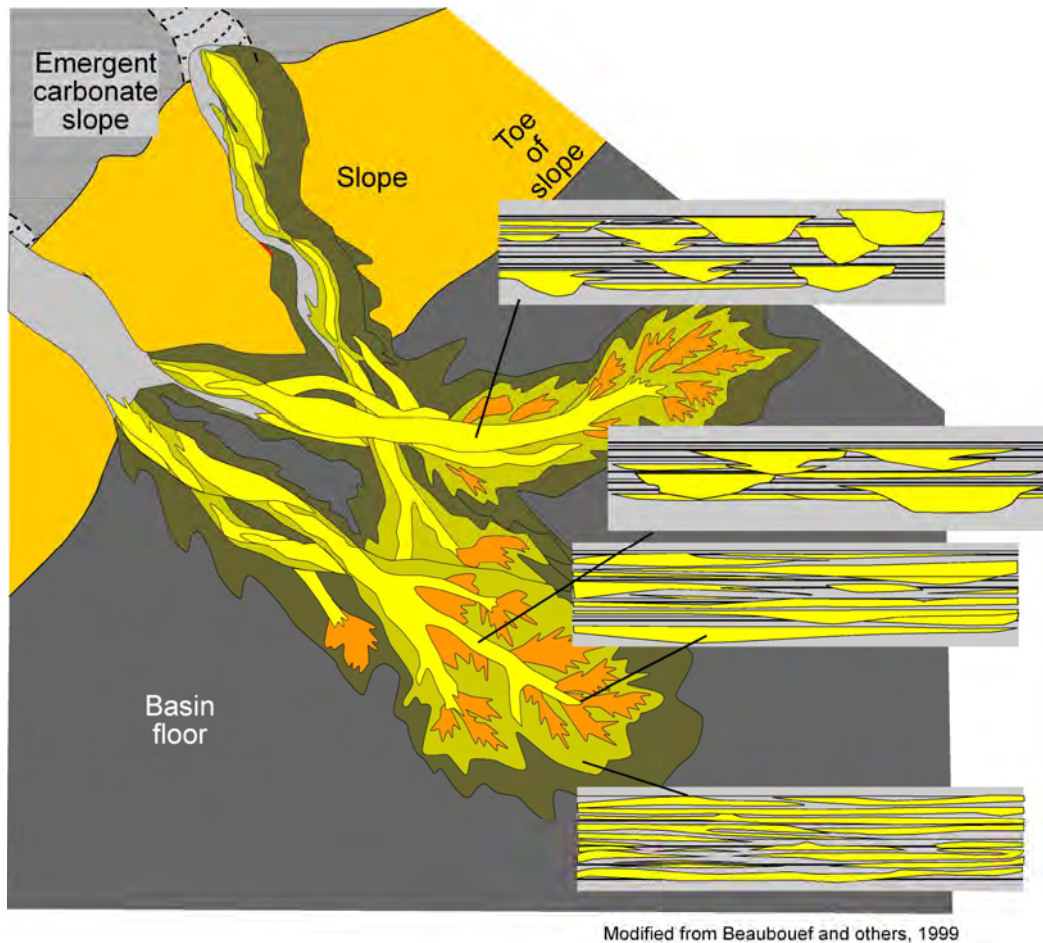


Figure 8. Schematic model of principal reservoir facies of the Delaware Mountain Group showing idealized cross sections of sandbody development along depositional dip. Sandbodies tend to become laterally more extensive with less vertical incision downdip, although compensatory stacking of sandstone units is a characteristic process along the slope profile. Modified from Beaubouef and others (1999).

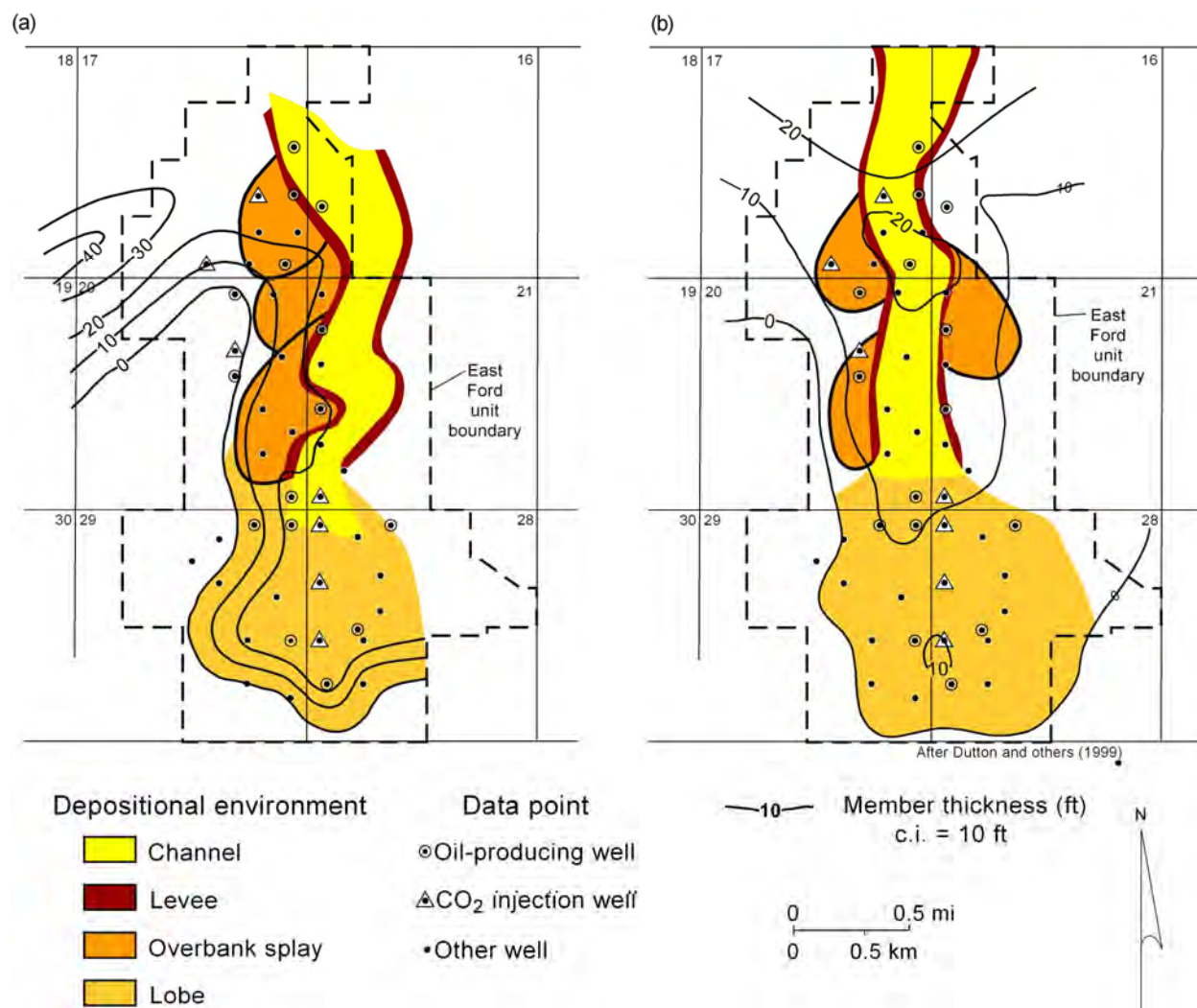
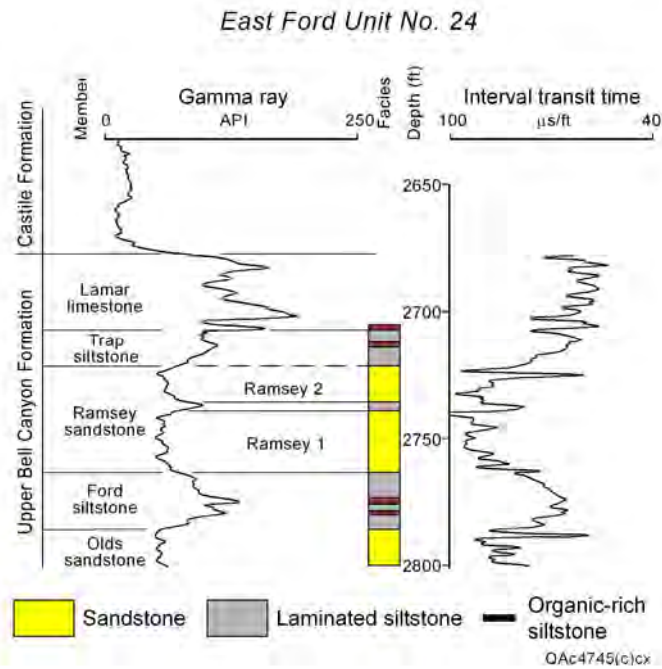
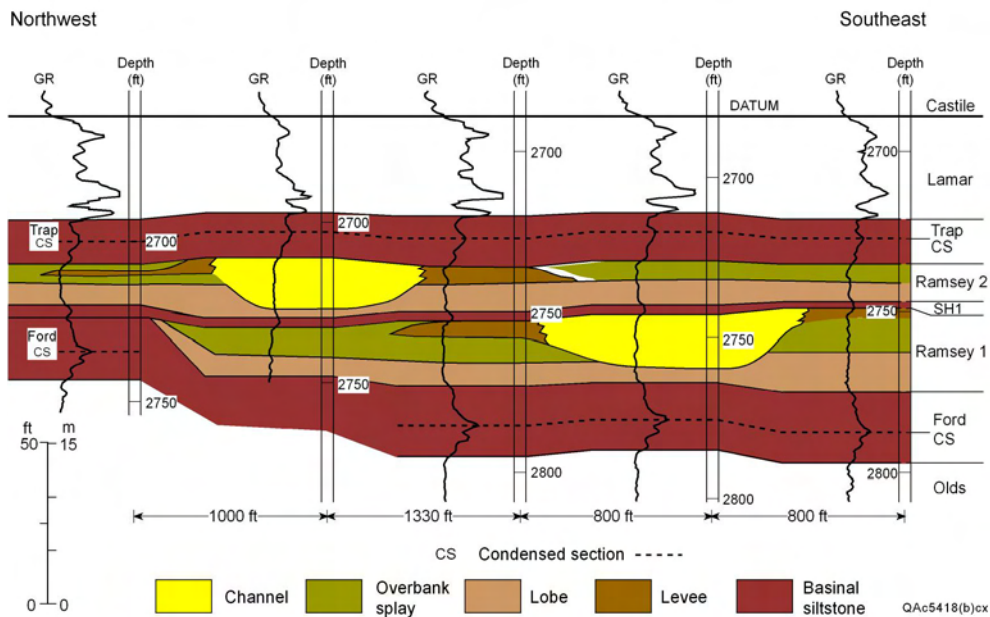


Figure 9. Isopach and interpreted facies maps of (a) Ramsey 1 and (b) Ramsey 2 sandstone, East Ford Unit (Bell Canyon). Facies are based on classification scheme illustrated in figure 7. Field location shown in figure 2.

(a)



(b)



From Dutton and others (2003)

Figure 10.
Stratigraphy of Bell Canyon Formation at East Ford unit.
(a) Type log showing representative gamma-ray and acoustic logs for the upper part of the formation; Ramsey primary sandstone reservoir intervals are highlighted;
(b) Northwest-to-southeast stratigraphic cross section showing compensatory stacking of sandbodies and laterally extensive siltstone seals. Field location shown in figure 2.

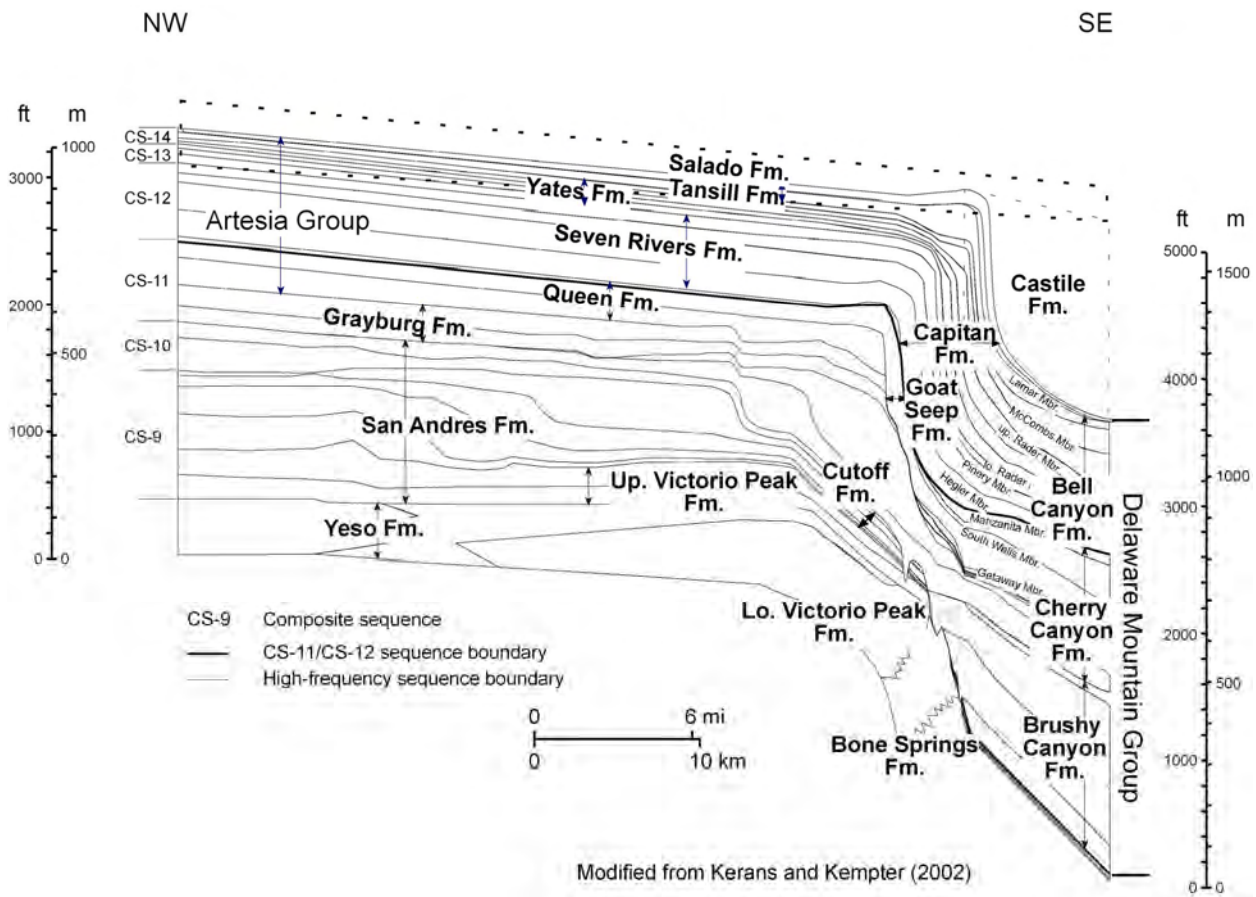
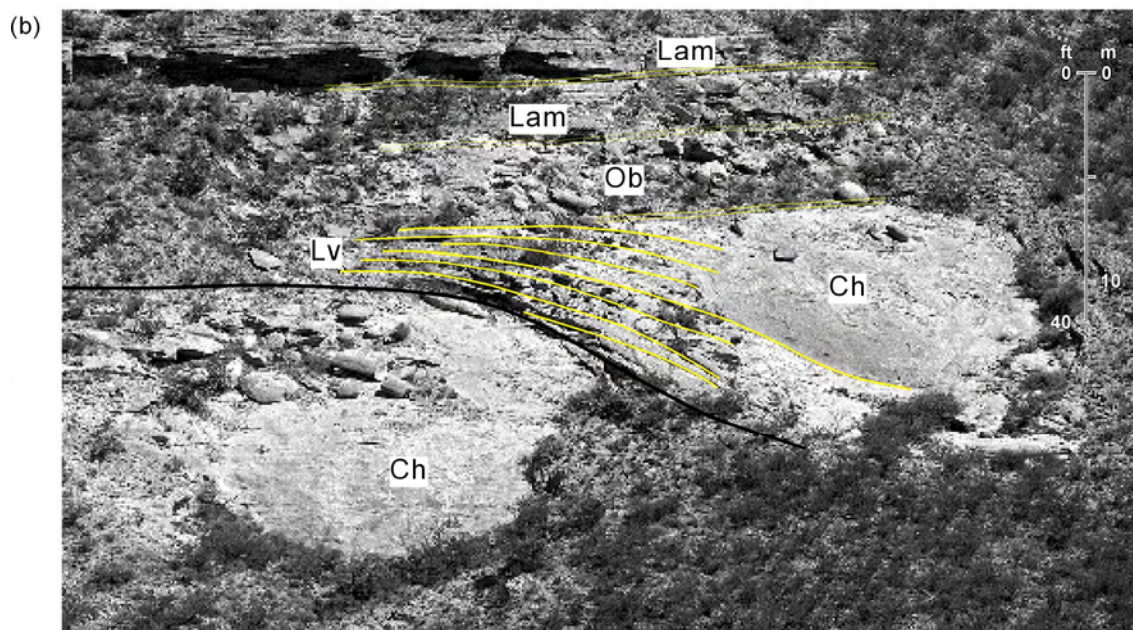


Figure 11. Composite structure dip section of the uppermost Leonardian, Guadalupian, and lower part of the Ochoan in the Guadalupe and Delaware Mountains area showing formation and member names. Also shown are sequence stratigraphic subdivisions, including composite sequences (CS), and high-frequency sequences (not labeled). Sequence boundary that separates the sequences associated with the Capitan shelf margin (Bell Canyon in the basin) from the underlying sequences (Brushy Canyon and Cherry Canyon in the basin) is indicated by the bold line. Modified from Kerans and Kempter (2002).



From Scholle (1999)

Figure 12. Channel and overbank facies, Brushy Canyon Formation, Guadalupe Mountains. (a) Incised valley in overbank deposits with channelized sandstone fill and (b) overbank sandstones and siltstones overlain by channel sandstone. Dark strata are organic-rich siltstones similar to those that act as hydrocarbon source beds for reservoir sandstones. Outcrops are on Hwy 62-180, south of Guadalupe Pass and north of El Capitan scenic turnout, Guadalupe Mountains.



From Dutton and others (1999)

— Channel bounding surface	Lam Laminated siltstone
- - - Bedset bounding surface	Ch Channel
— Top of sandstone lamina	Lv Levee
	Ob Overbank

Figure 13. Outcropping channel-levee complexes, overbank deposits, and laminated siltstone deposits at Willow Mountain outcrop area, Delaware Mountains, Bell Canyon Formation: (a) outcrop photo and (b) annotated outcrop photo. Note compensatory stacking of channel sandbodies. From Dutton and others (1999).

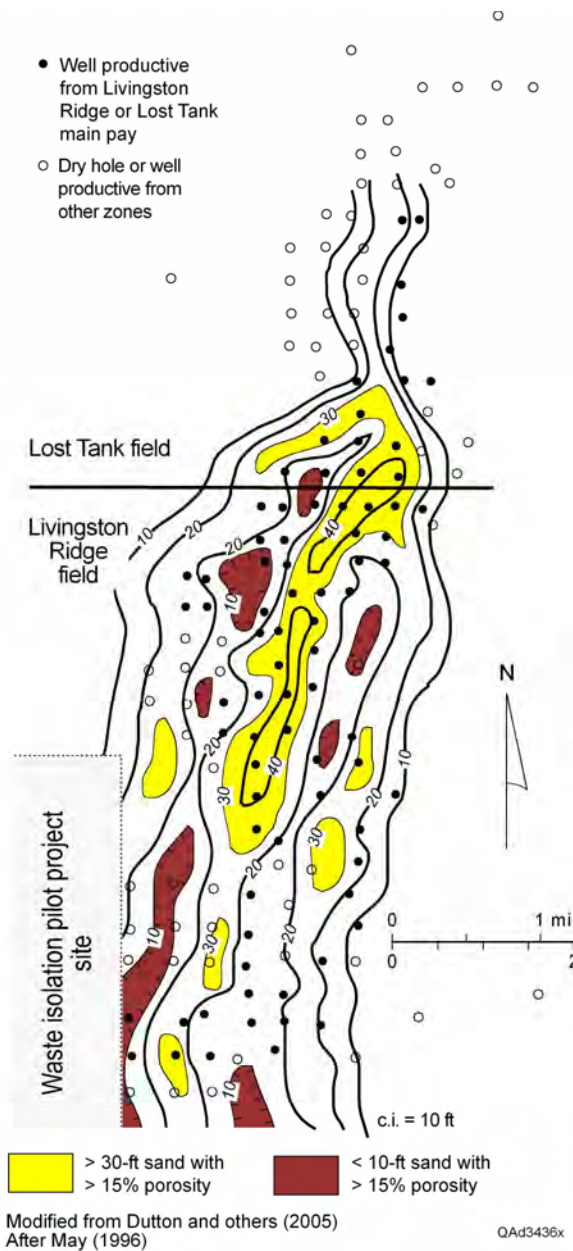


Figure 15. Thickness map of the main pay (porosity >15%) in the Brushy Canyon Formation, Livingston Ridge and Lost Tank fields. Thicknesses greater than 20 ft correspond to main channel complexes. Note that production is not limited to thicker intervals. Field location shown in figure 2.

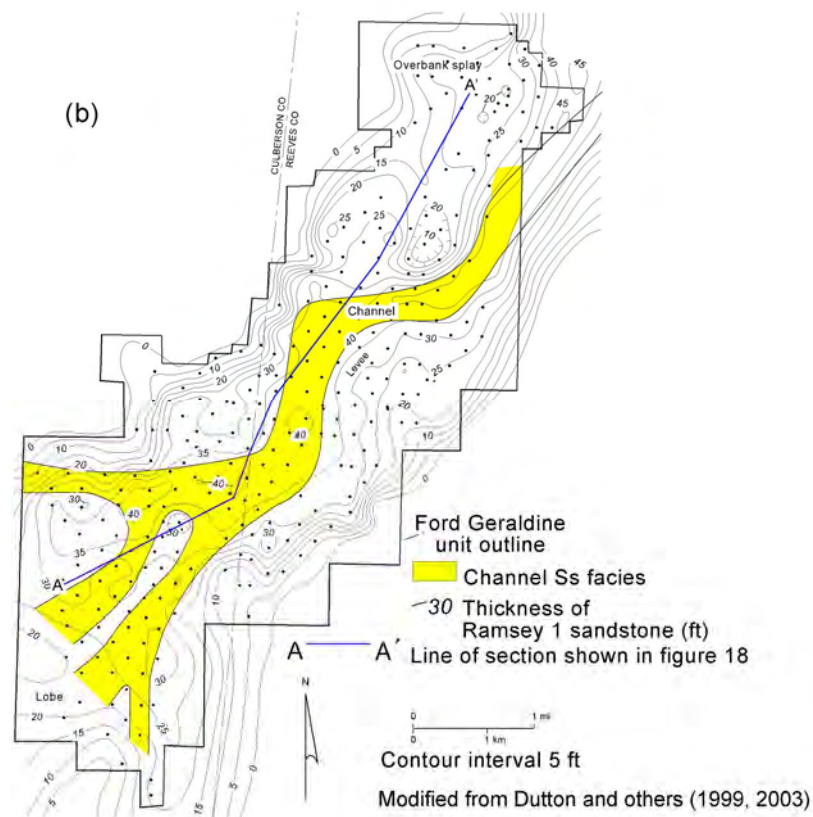
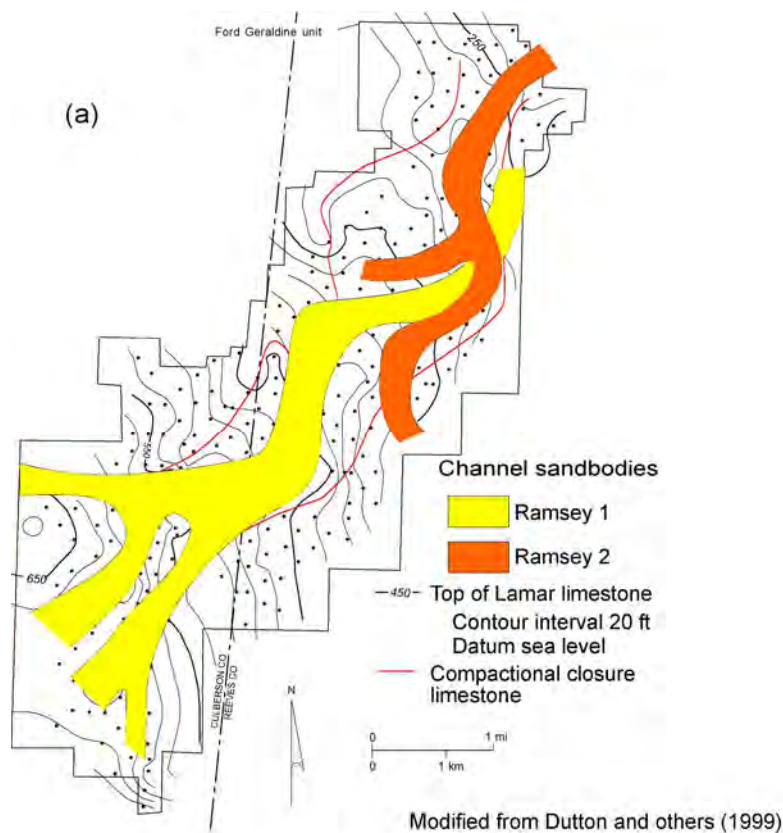


Figure 16. Ramsey Sandstone and Lamar Limestone (Bell Canyon) maps, Ford Geraldine field. (a) Thickness of Ramsey 1 sandstone interval. Thickest accumulations correspond to locations of channel and splay facies development. Note compensatory stacking of channel sandstone facies. (b) Structure on the top of the Lamar Limestone Member of the Bell Canyon Formation showing compactional anticline development over trend of dominant Ramsey Sandstone channel system. Note correspondence with isopach thickness trend shown in a. Field location shown in figure 2.

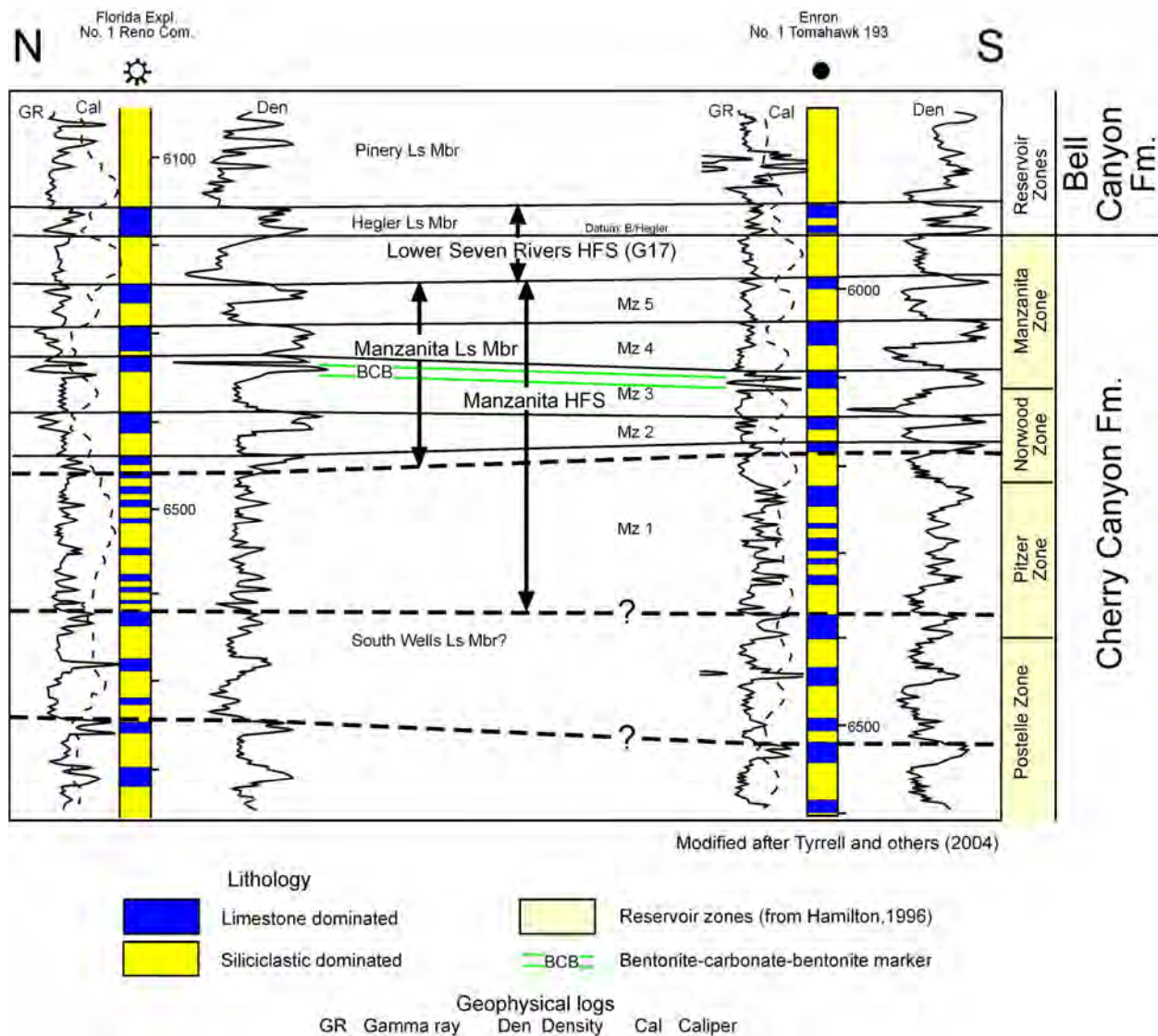


Figure 17. North-south correlation section in Quito field area showing upper Cherry Canyon and lowermost Bell Canyon limestone and siliciclastic intervals and sequence stratigraphy. Reservoir zones designated by Hamilton (1986). Quito field area shown in figure 2.

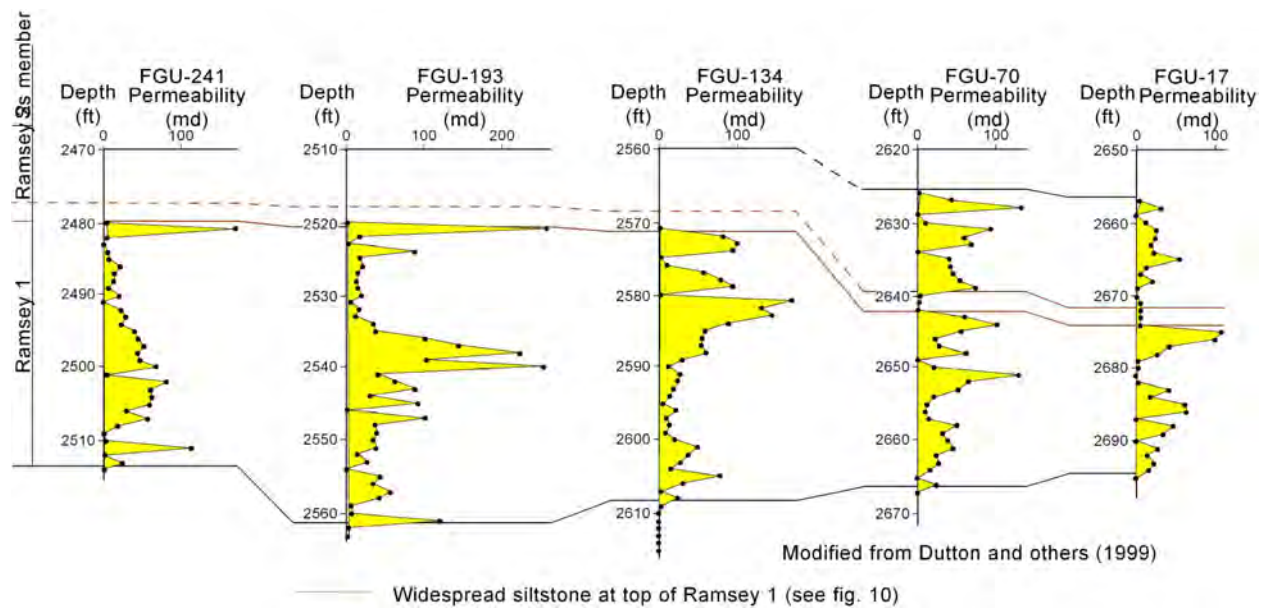


Figure 18. Vertical profiles of permeability distribution for five wells from core analyses. Significant permeability variations are tied more to presence of cement than to grain-size variation. High-permeability zones underlain by calcite-cemented low-permeability zones are common at the top of Ramsey 1 and Ramsey 2 intervals. High permeability at the tops may record calcite dissolution. Location of wells shown in figure 20. Map of calcite cement distribution shown in figure 20. Field location shown in figure 2.

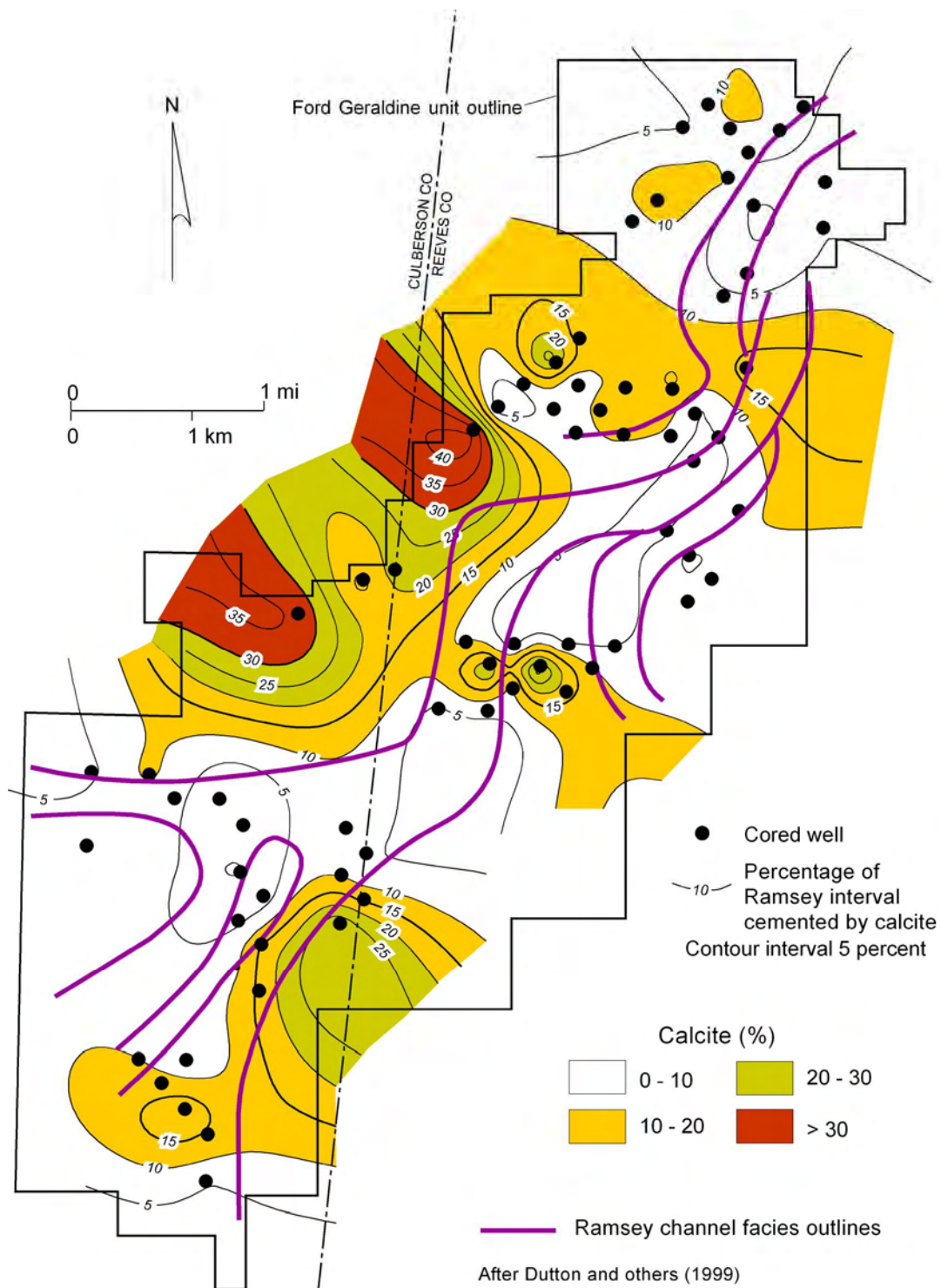


Figure 19. Map of interpreted calcite cement distribution in Ramsey sandstone based on core analyses. Also shown is the outline of combined Ramsey 1 and Ramsey 2 channel sandstone facies. It is possible to recontour the cement map to show a correlation between cement distribution and facies outside the channel complexes. Field location shown in figure 2.

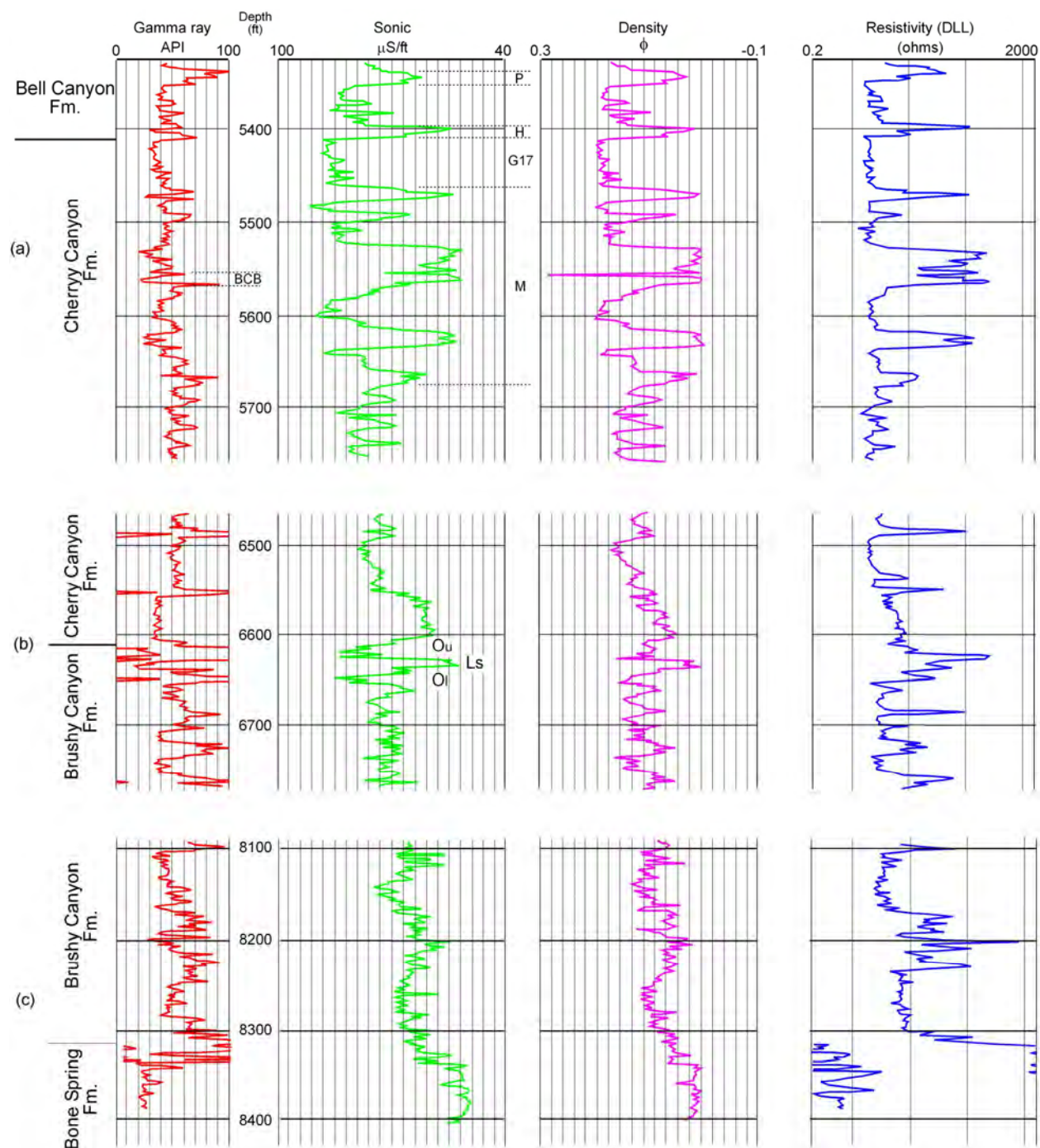


Figure 20. Well log responses in Eddy County Yates Petroleum No. 5 Martha "AK" Federal well (Livingston Ridge field) showing typical stratigraphic boundaries of formations in the Delaware Mountain Group, including (a) top of the Bell Canyon Formation, (c) Cherry Canyon and Brushy Canyon Formations, and (c) base of the Brushy Canyon Formation. Castile and Bone Spring strata at the top and base of the DMG, respectively, are distinguished by distinctively lower gamma-ray values, higher acoustic velocities, lower density porosities, and higher resistivities than those that characterize Delaware Mountain strata. Field location shown in figure 2.

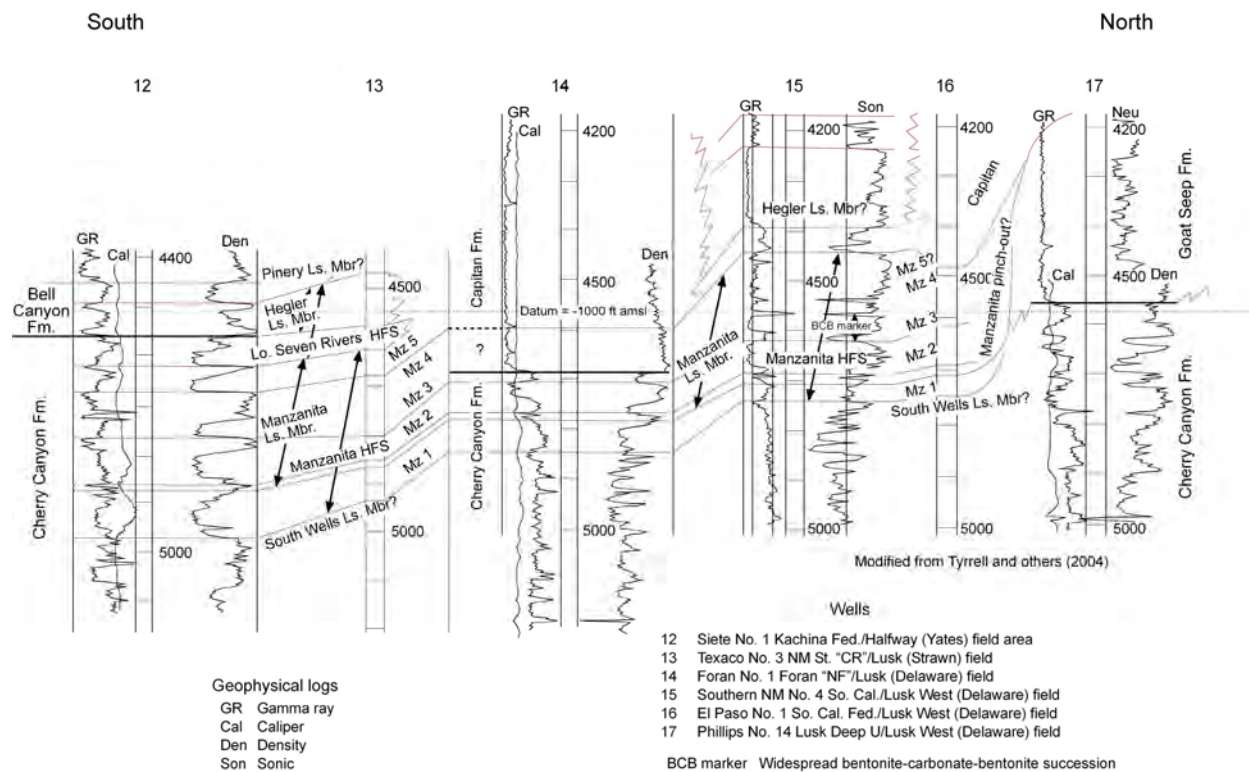


Figure 21. South-north stratigraphic cross section from Halfway field to Lusk West field, northern Delaware Basin, showing correlations within the uppermost Cherry Canyon interval to the Guadalupe shelf margin.

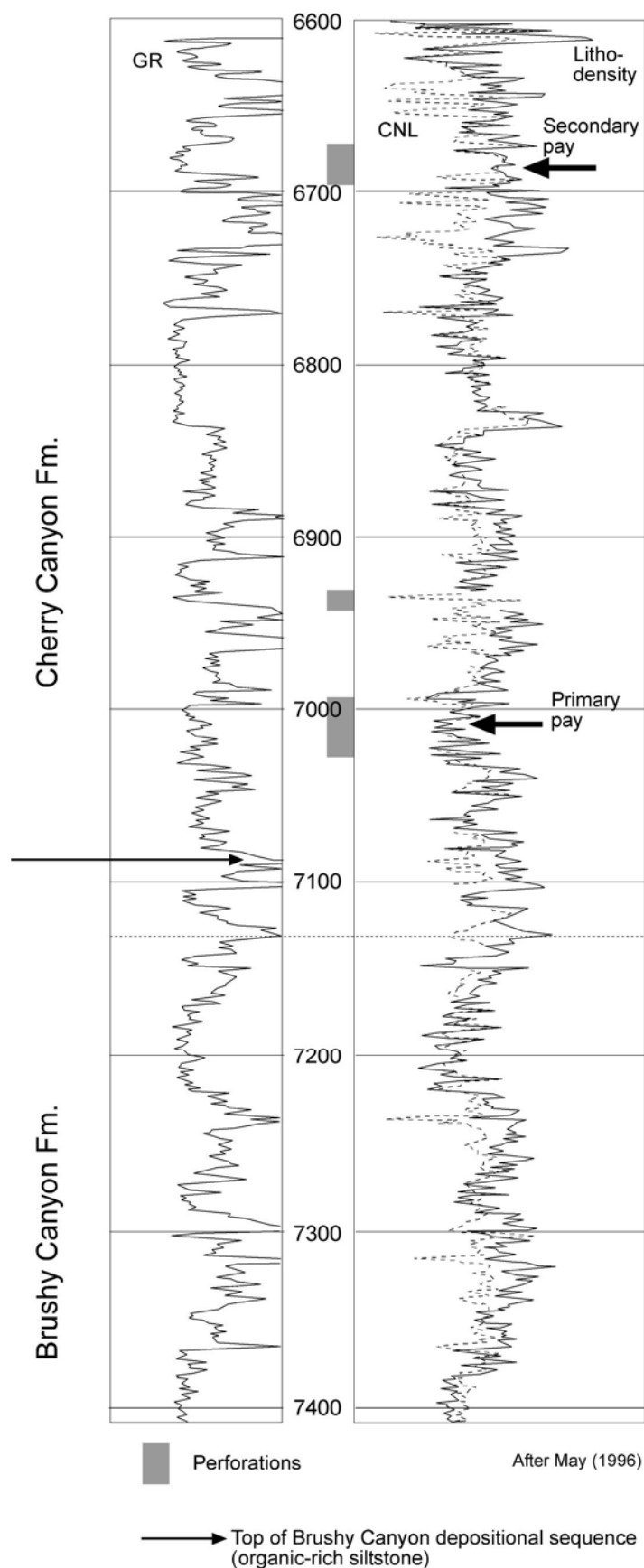


Figure 22. Type log from Livingston Ridge field. Shown are responses for organic-rich siltstone at the Brushy Canyon/Cherry Canyon boundary. The top of the Brushy Canyon depositional sequence is designated to be at the top of the organic-rich siltstone at approximately 7,090 ft, interpreted to record maximum flooding of the shelf. Field location shown in figure 2.

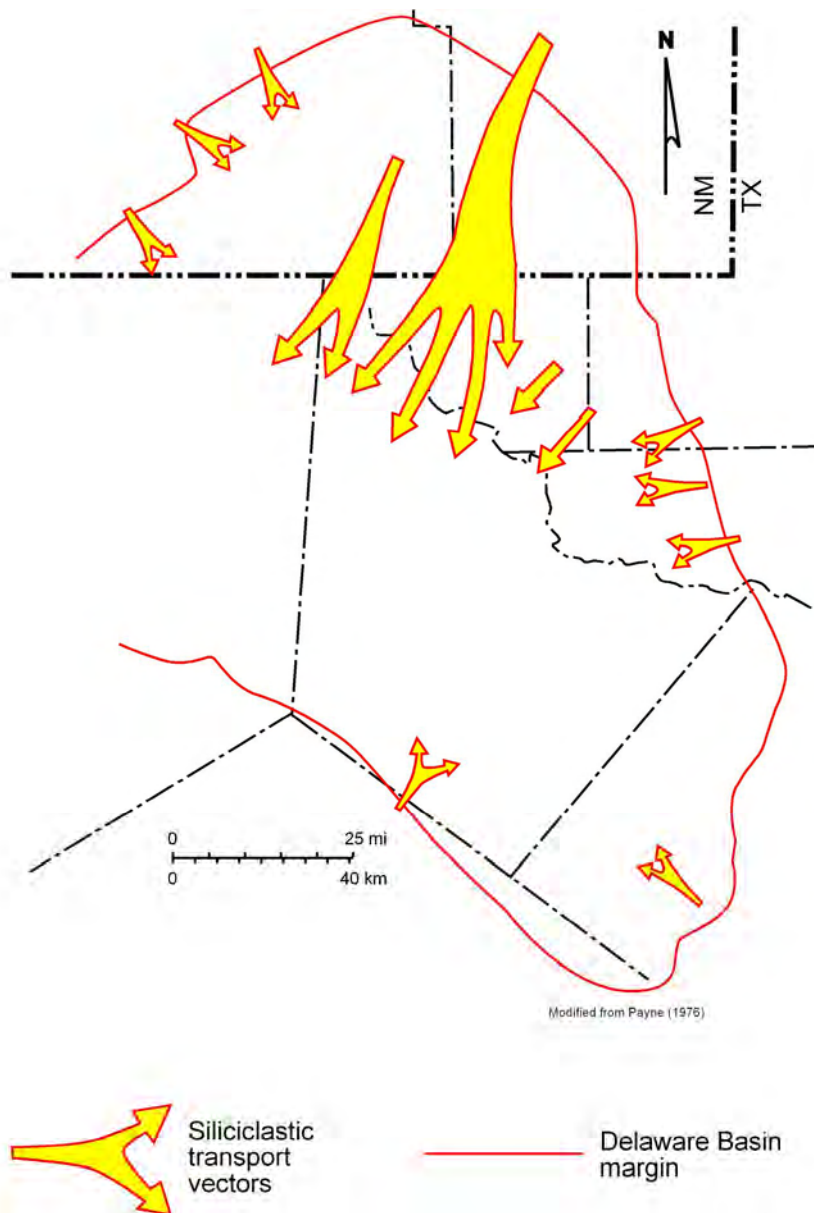


Figure 23. Interpreted Bell Canyon sand depositional fairways based on relative incidence of channel-complex facies. Size of arrows indicates relative importance of fairway.

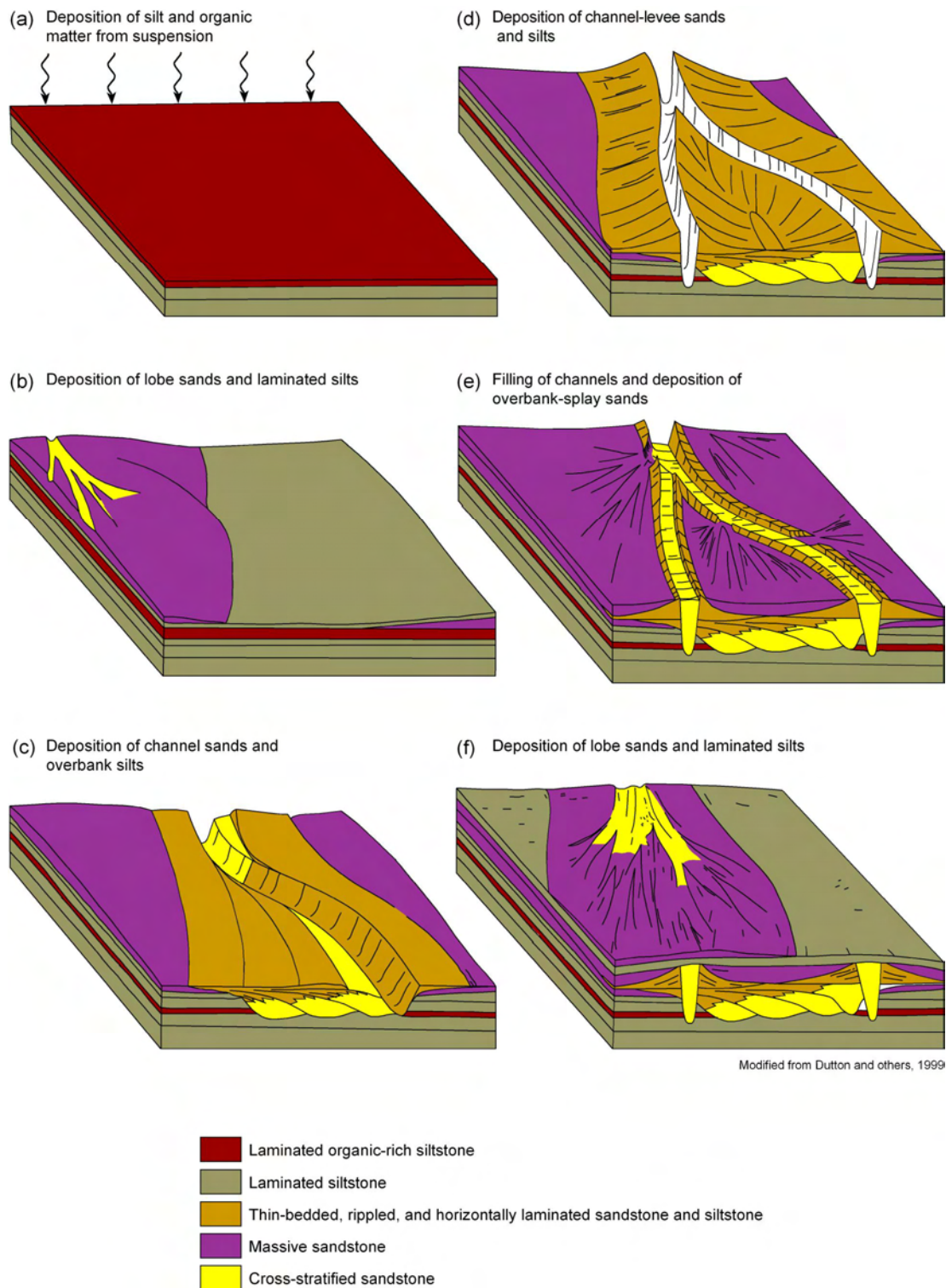


Figure 24. Models of facies development for Delaware Mountain Group depositional units. Organic rich siltstones depicted in a are probable hydrocarbon sources for adjacent sandstone reservoir intervals (see fig. 30). Silt-rich units form top seals. Lateral boundaries for reservoirs are pinch-outs of permeable sandstone facies.

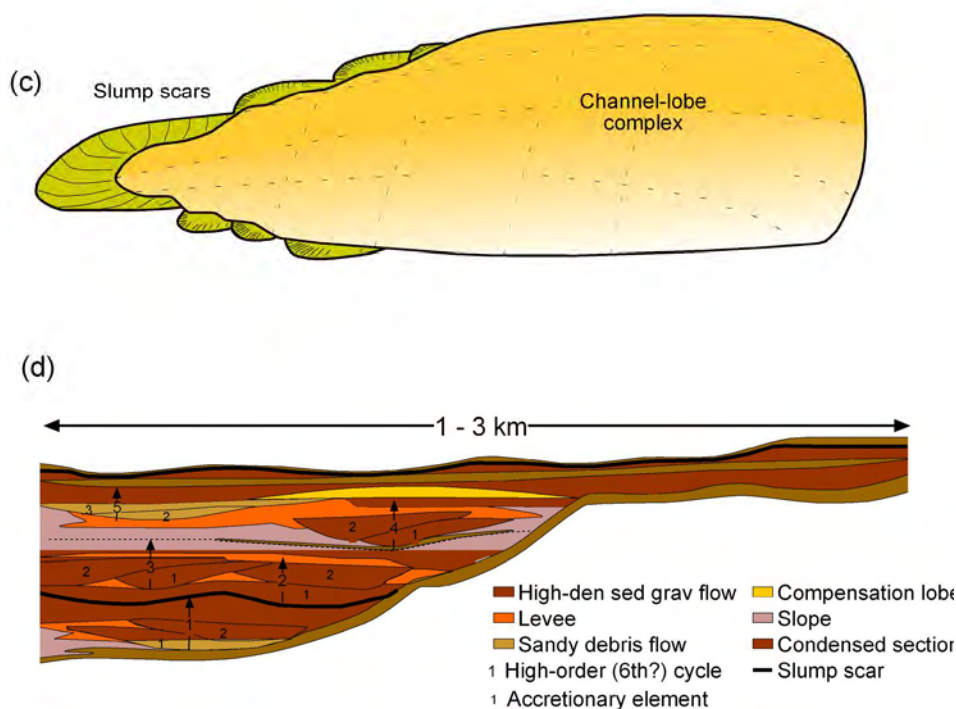
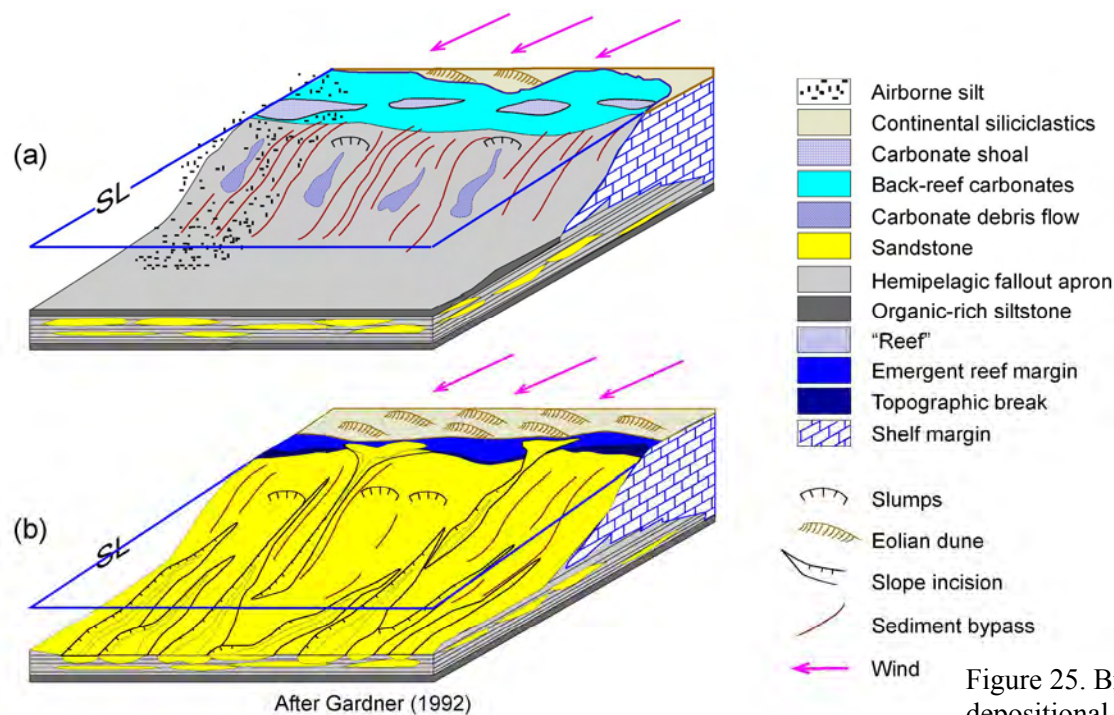
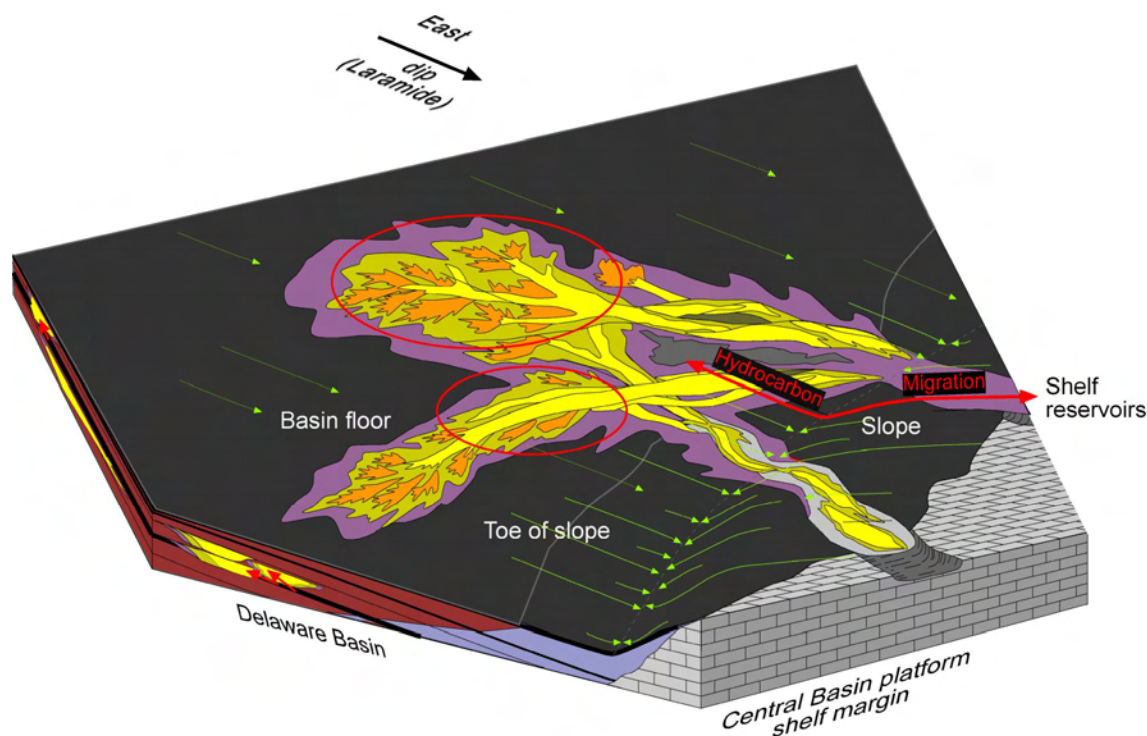


Figure 25. Brushy Canyon depositional cycle models of Gardner (1992): (a) processes during sea-level highstand include restriction of continental siliciclastic depositional environments well shelfward of shelf margin, deposition in basin of windblown silt, and gravity transport of shelf-margin carbonate debris; (b) processes during sea-level lowstand include encroachment of prominently eolian depositional environments on shelf margin, accumulation of siliciclastics on upper slope, slumping of accumulated siliciclastics, and downslope transport of siliciclastics by turbidity flow; (c) idealized model of relationship of channel-lobe complex to slump scar; and (d) idealized strike section showing depositional environments, slump scars, and depositional elements of high-order cycles. Slumping may place updip margins of reservoir facies in contact with low-permeability slope siltstones, thus providing updip lateral seal to some reservoirs.



Modified from Beauboef and others (1999)

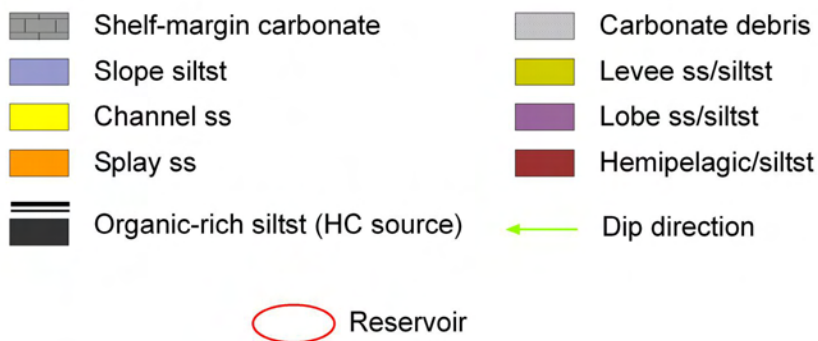


Figure 26. Model of Delaware Mountain Group reservoirs showing paleogeographic elements, principal reservoir and hydrocarbon source facies, regional structural components, and generalized hydrocarbon migration directions. Hydrocarbon reservoirs are preferentially developed in favorable facies, where porous sandstone facies laterally pinch out into low-permeability siltstones. Depending on location, hydrocarbon migration is directed toward the west by easterly dip imparted by Laramide epeirogeny or toward the east into shelf reservoirs by residual, depositionally controlled structural rise on the slope toward the shelf margin.

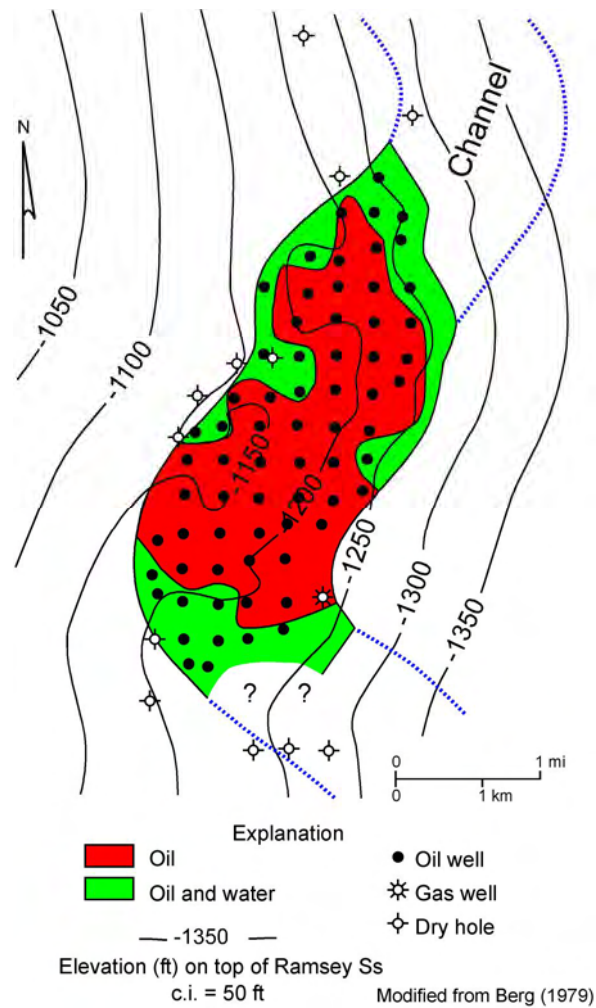
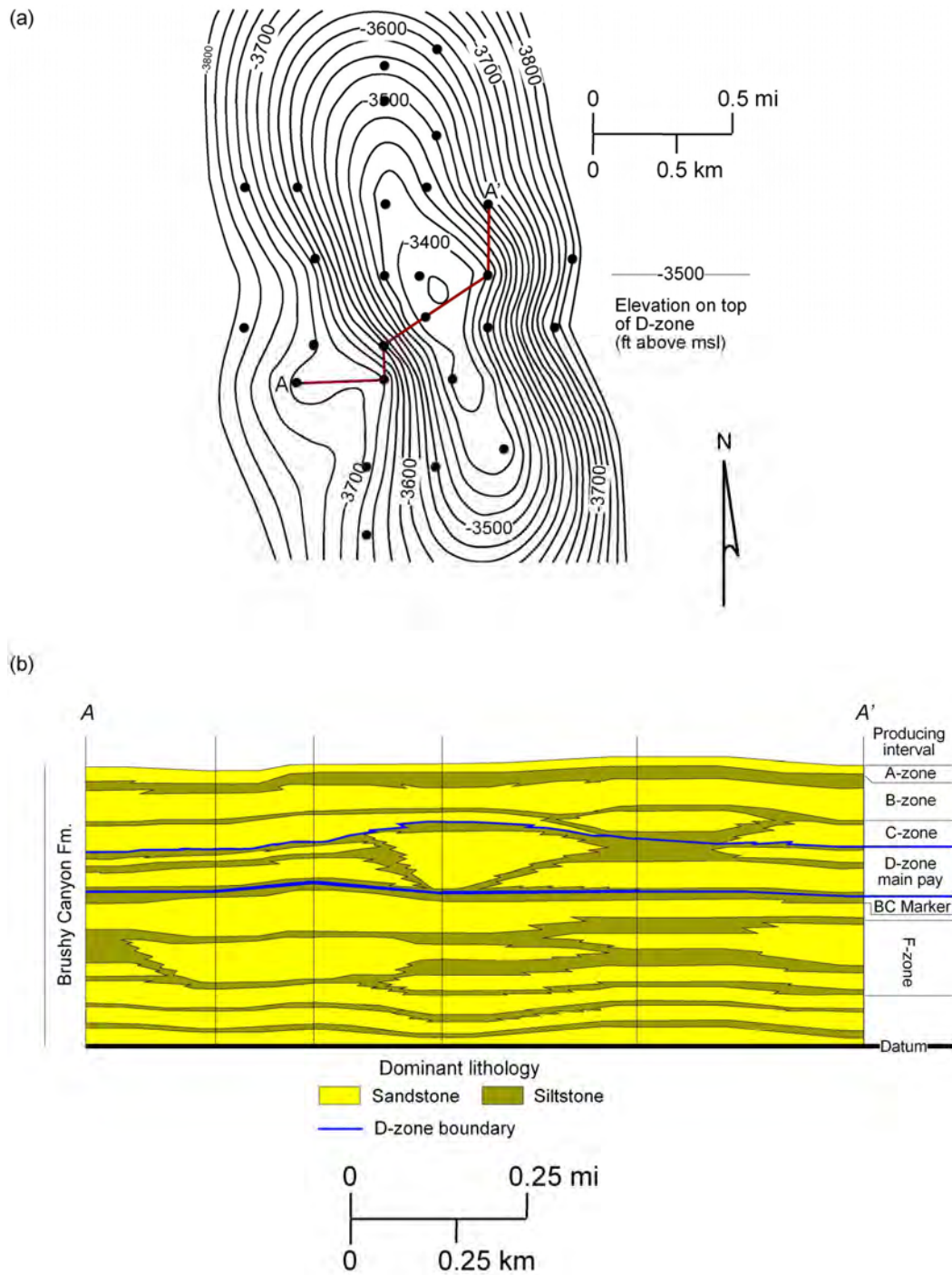
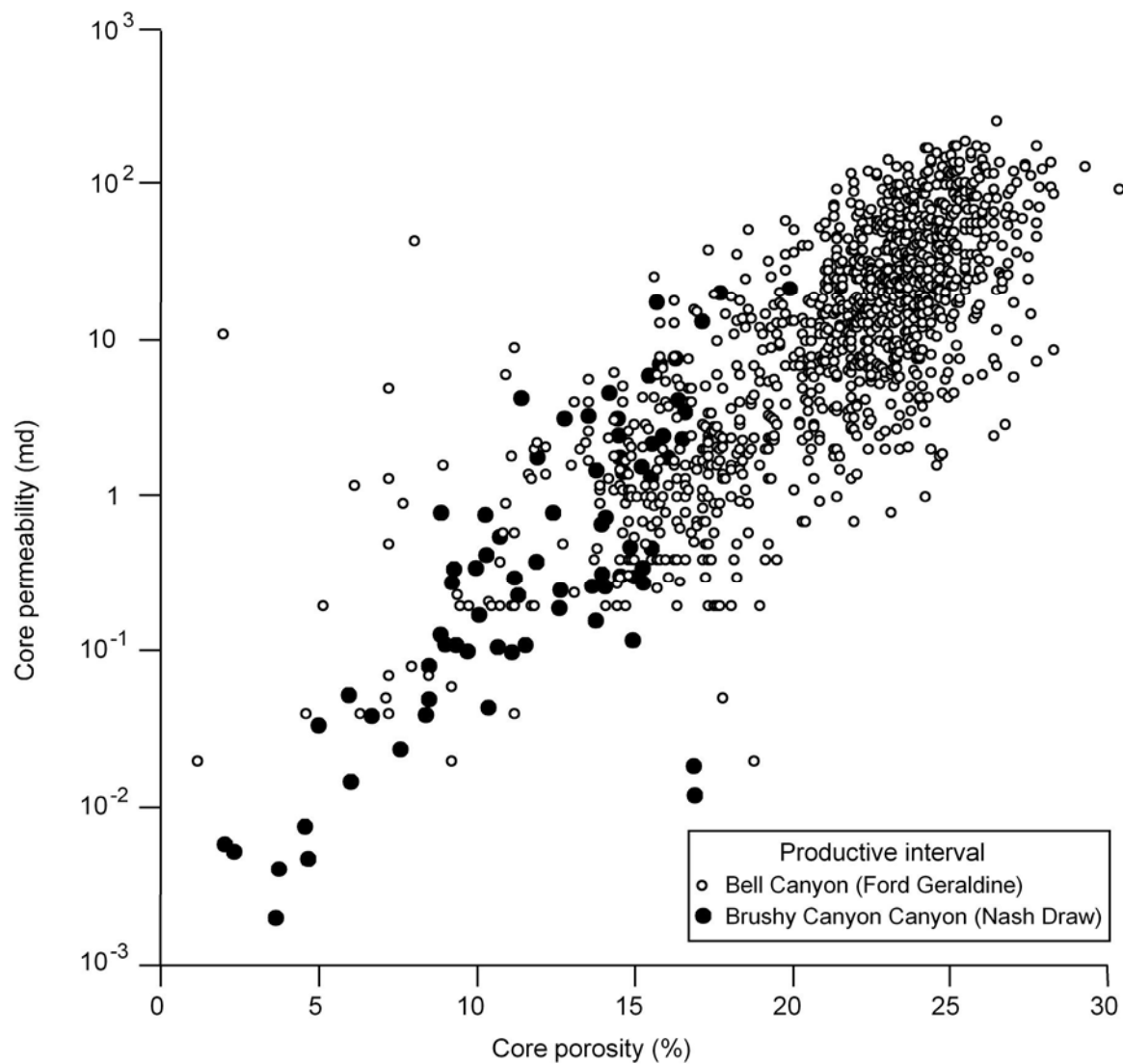


Figure 27. Simplified model of Ramsey sandstone reservoir (Bell Canyon) configuration in Paduca field. Hydrocarbons accumulated in channel-complex meander bend in updip location on regional eastward-dipping structure produced by Laramide epeirogeny. Field location shown in figure 2.



Modified from Thomerson and Catalano (1996)

Figure 28. Sandbody architecture, East Livingston Ridge field, Upper Brushy Canyon Formation. (a) Structure map on top of D-zone (primary reservoir) and (b) southwest-northeast stratigraphic cross section of productive intervals. Cross section shows compactional anticlinal structures over thicker parts of sandbodies, especially over D-zone channel sandbody and compensatory offsets of stratigraphically sequential sandbodies. Field location shown in figure 2.



Modified from Thomerson and Asquith (1992)
and Dutton and others (1999)

Figure 29. Plot of core-derived porosity and permeability measurements of productive sandstones from Ford Geraldine (Bell Canyon) and Nash Draw (Brushy Canyon) fields. Although Brushy Canyon porosity and permeability values are overall less than Bell Canyon values, the linear relationship between the parameters is similar in both reservoirs.

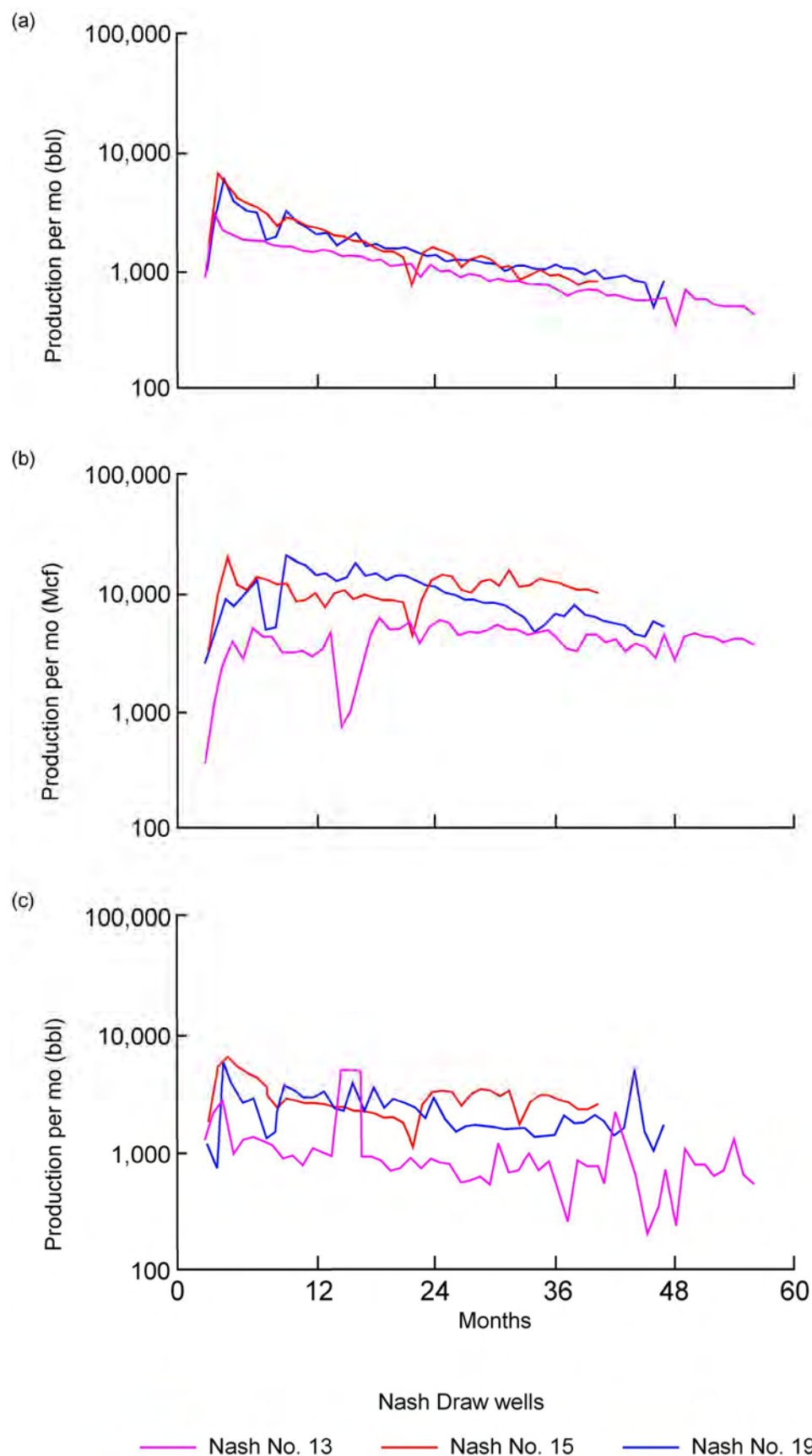


Figure 30. Graphs showing monthly production rates for (a) oil, (b) gas, and (c) water from three closely spaced wells in Nash Draw field. Dissimilarity of production responses in closely spaced (0.25–0.5 mi) may reflect lateral petrophysical variability in channel-levee-lobe complex facies. Note rates of oil-production decline similar to those seen at Livingston Ridge/Lost Tank fields (fig. 31). Field location shown in figure 2. Modified from Montgomery and others (1999).

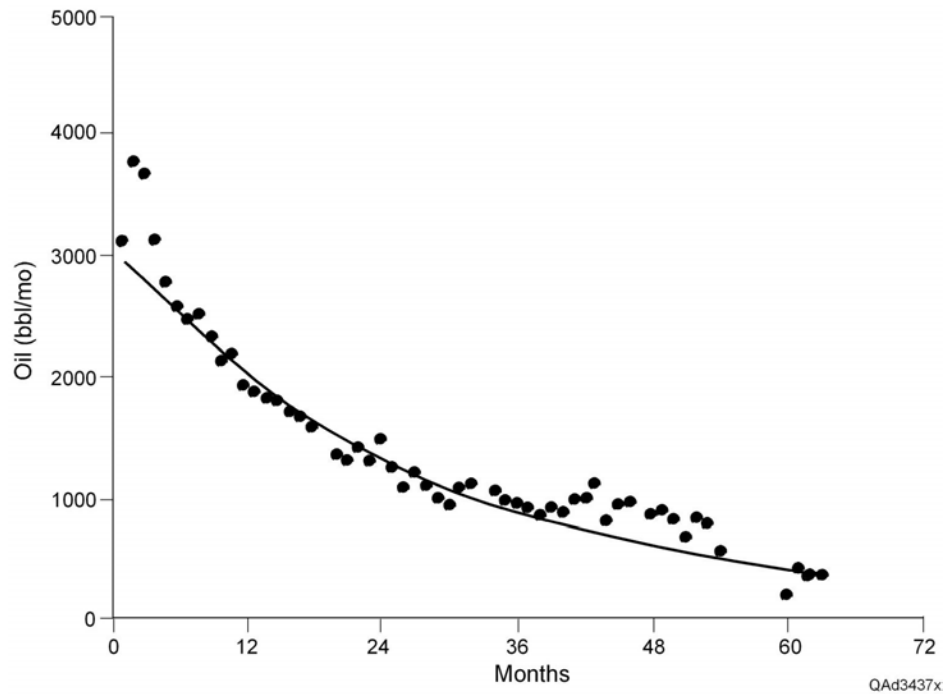


Figure 31. Average production-decline curve for wells in Livingston Ridge/Lost Tank field. Average production is reduced to approximately 10 percent of initial rates after 5 years. Modified from Broadhead and others (1998). Field location shown in figure 2.

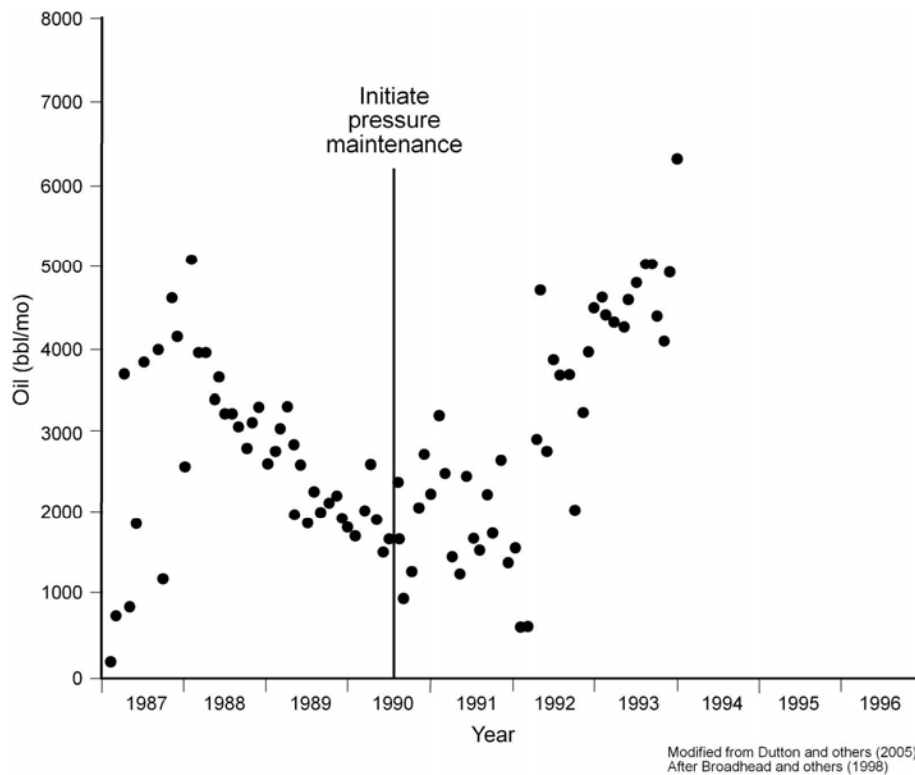


Figure 32. Monthly oil production from Phillips No. 2 James A well, Cabin Lake field, showing production increase after water injection for pressure maintenance. Field location shown in figure 2.

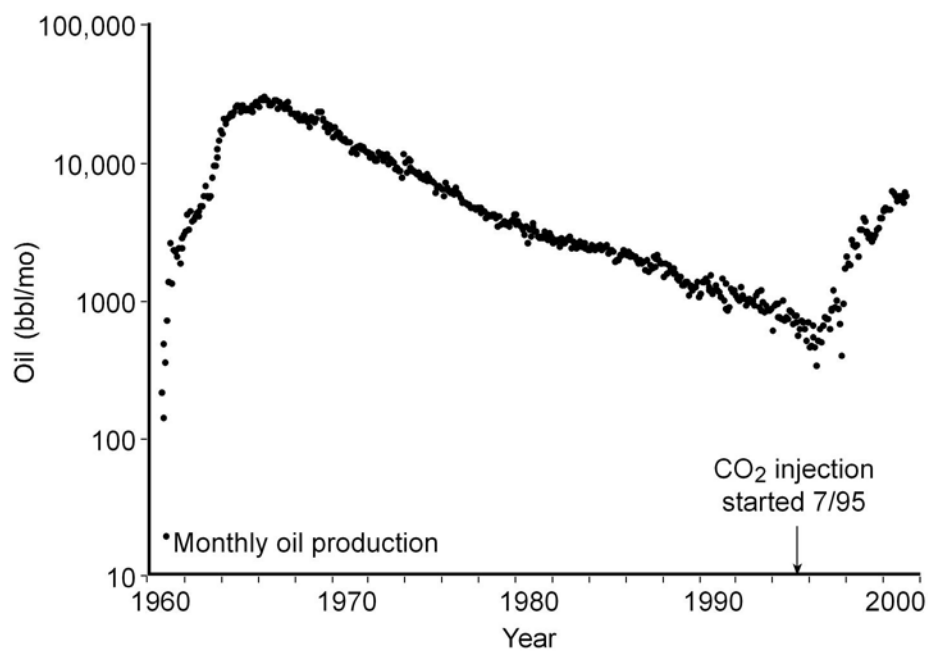


Figure 33. Monthly oil production from East Ford Unit (Bell Canyon), showing production improvement after change from primary to secondary production with initiation of CO₂ injection in 1995. Field location shown in figure 2. From Dutton and others (2003).

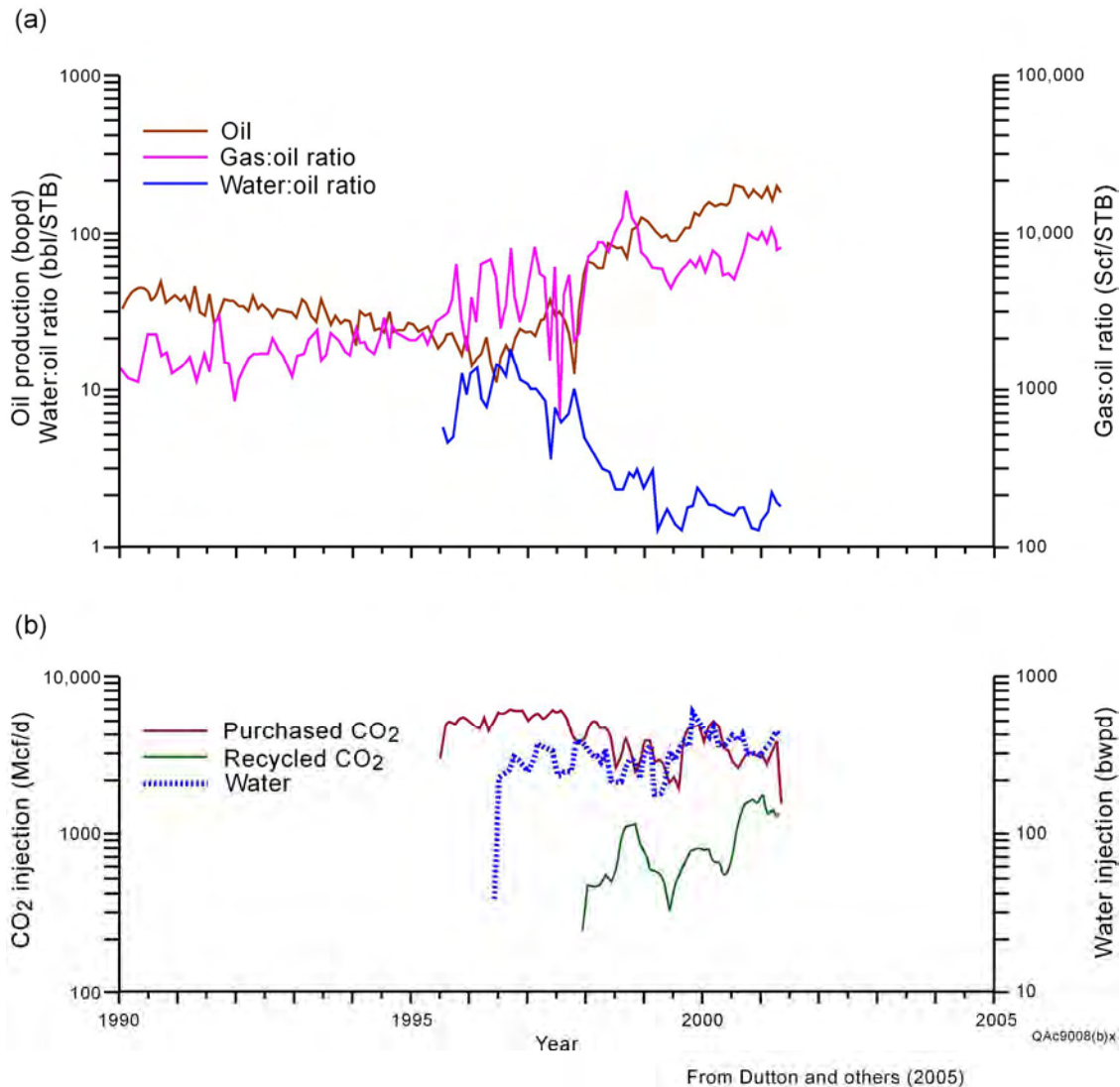


Figure 34. Graphs showing (a) values of oil production, gas/oil, and water/oil for a typical well in the East Ford unit, Reeves County, for 1990 through first half of 2002 and (b) injected volumes of CO₂ and water. Gas injection began in 1995, and water injection began in 1998. Note that production shows an overall increase soon after initiation of water injection. However, water:oil values decrease while gas:oil values increase, suggesting that overall production increases more probably reflect success of CO₂ injection. Field location shown in figure 2.

GUADALUPIAN (ARTESIA GROUP) AND OCHOAN SHELF SUCCESSION OF
THE PERMIAN BASIN: EFFECTS OF DEPOSITION, DIAGENESIS,
AND STRUCTURE ON RESERVOIR DEVELOPMENT

H. S. Nance

Bureau of Economic Geology
Jackson School of Geosciences
The University of Texas at Austin
Austin, Texas

ABSTRACT

The middle and upper Artesia Group (Upper Guadalupian Series) in the Permian Basin composes a section of as much as 2,650 ft (808 m) of stratigraphically cyclic, mixed siliciclastic/carbonate/evaporite platform strata that were deposited shelfward of the Guadalupian reef complex that rims the Delaware Basin. The section includes the Queen, Seven Rivers, Yates, and Tansill Formations and hosts many hydrocarbon reservoirs that are located along the margins of the Central Basin Platform in Texas and on the Northwest Shelf in southern New Mexico. As of 2003, cumulative oil production from middle and upper Artesia Group intervals exceeded 254.5 MMbbl ($4.05 \times 10^7 \text{ m}^3$) from more than 236 reservoirs; cumulative gas production exceeded 356,700,000 Mcf from more than 157 reservoirs. Most of the hydrocarbon production has been from siliciclastic-dominated sections in the Queen and Yates Formations, with secondary production from siliciclastics in the Seven Rivers and Tansill Formations, and from grain-dominated carbonate facies in the near back-reef area. Trapping mechanisms include basinward-dipping stratal dip, updip porosity occlusion by evaporite minerals, top seals composed of impermeable carbonate or evaporite, and local, deep-seated anticlinal structures.

Artesia facies tracts include, from basin to shelf, immediate-back-reef carbonate grainstone to packstone; shelf-crest pisolite-bearing carbonate shoals; lagoonal wackestone to mudstone and siliciclastic siltstone; algal-laminated, tidal-flat carbonate packstone to wackestone and fine- to very fine grained sandstone; beach-ridge fine sandstone; siliciclastic-sabkha anhydrite and halite; brine-pool and evaporitic-lagoon anhydritic dolomite, dolomitic anhydrite, anhydrite, and halite; and eolian to fluvial siliciclastics. During sea-level highstand, siliciclastics

are limited to updip areas, whereas eolian-siliciclastic depositional environments migrate downdip during sea-level lowstands. During transgressions, siliciclastics in more basin-proximal positions were reworked by marine and marginal processes. Reservoir quality was impacted mostly by dissolution of feldspar and carbonate allochems and precipitation of authigenic feldspar, clay, and evaporite. Overall progradation during Artesia Group deposition resulted in progressively more downdip development of reservoir facies through time.

Additional resource will be produced by infield drilling, field extension, exploitation of previously less productive or bypassed intervals, and by application of enhanced recovery techniques.

INTRODUCTION

The middle and upper parts of the Artesia Group of the Permian Basin compose a section of as much as 2,650 ft (808 m) of stratigraphically cyclic, mixed siliciclastic/carbonate/evaporite platform strata. The section hosts many economically important hydrocarbon reservoirs. Most of the hydrocarbon production has been from siliciclastic-dominated units in the Queen and Yates Formations (figs. 1, 2). More than 254.5 MMbbl of 32.12° (average) oil has been produced from approximately 236 reservoirs, within which 49 percent of the 19,536 total wells were producing in 2003. The section has also produced 356,700,000 Mcf of gas from approximately 157 reservoirs, within which 63 percent of the 817 total wells were producing in 2003. Production depths range from 42 to 4,875 ft (12.8–1,485.9 m) (Railroad Commission of Texas, 2003). The Seven Rivers and Tansill Formations are also productive in some fields, often where either or both Yates and Queen are the primary producing intervals. Despite the economic significance and broad geographic distribution of several reservoir plays that contain these formations, most published technical information regarding their stratigraphy, lithology, and reservoir character is derived from only a few outcrop and field locations.

Also briefly addressed in this report are the Ochoan Series shelf intervals, which attain a maximum cumulative thickness of 3,200 ft (975m) in the Permian Basin. Ochoan strata are not prolifically hydrocarbon productive on the shelf; however, there are a few noteworthy reservoirs (Castile, Rustler) in the Delaware Basin. Ochoan strata are important to Permian Basin shelf hydrocarbon province mainly because evaporite-prone strata of the Salado Formation provide a regional top seal for Guadalupian plays. This chapter documents the depositional and diagenetic

history of the Guadalupian and Ochoan shelf intervals on the basis of available data and describes the geologic controls on reservoir development, distribution, and heterogeneity.

PREVIOUS WORK

Tait and others (1962) summarized the historical development of Upper Guadalupian nomenclature in the Permian Basin. The Grayburg Formation was originally described as a subsurface unit in Eddy County, New Mexico, by Dickey (1940), extended to a surface exposure by Moran (1954), and modified somewhat by Hayes and Koogler (1958). The Queen Formation designation evolved through several iterations, including DeFord and others (1940), Woods (1940), Dickey (1940), and Moran (1954). The Seven Rivers section was defined partly by Meinzer and others (1926), described in the subsurface by Dickey (1940), and defined in the Guadalupe Mountains by Hayes and Koogler (1958). Tait and others (1962) recognized that post-San Andres Guadalupian formations in the Permian Basin (including the Palo Duro Basin) were essentially a series of genetically related intervals that possessed similar depositional components and whose similar facies tracts cyclically migrated up and down depositional slope in response to relative sea-level changes. Further, they renamed this series the *Artesia Group* because previous nomenclature (for example, Chalk Bluff Formation: Lang, 1937; Whitehorse Group: Lewis, 1938; Fritz and Fitzgerald, 1940; Davis, 1955; Bernal: Bachman, 1953) was based on imprecise or uncertain correlations, some of which were from basins outside the Permian Basin. Silver and Todd (1969) discussed the interfingering relationships between Artesia strata and the Guadalupian reef complex. However, their understanding that the Artesia Group were shelf equivalents of the Capitan-Goat Seep reef margin was shown to be technically incorrect when Fekete and others (1986) and Franseen and others (1989) demonstrated that a top-of-Grayburg unconformably underlies the Goat Seep and, therefore, the Grayburg does not interfinger with the reef complex. The controversial nature and paleobathymetry of the Capitan reef system and its position in the shelf topographic profile have been discussed by many, most notably by Lloyd (1929), Johnson (1942), Achauer (1969), Estaban and Pray (1976, 1977), Cys and others (1977), and Garber and others (1989). Other discussions of Capitan reef facies include Tyrrell (1969), Estaban and Pray (1976, 1977), Biggers (1984, 1985), and Senowbari-Daryan and Rigby (1996).

A considerable body of literature discusses the geology of the Upper Guadalupian shelf section. Particular references are provided in the following discussions of geologic aspects of the

Artesia Group. A comprehensive listing of most of the literature that discusses the geology of Artesia Group formations is provided in the references section of this chapter.

Kerans and Kempter (2002) provided the most recent and comprehensive summary of the sequence stratigraphic relationships among Artesia Group formations and between Artesia Group formations and equivalent lowstand intervals (Cherry Canyon and Bell Canyon Formations) in the Delaware Basin. Borer and Harris (1991) provided a comprehensive analysis of relative sea-level control on Yates deposition that can be applied to other Artesia Group Formations.

Comprehensive summaries of Upper Permian shelf reservoir geology and hydrocarbon plays include Galloway and others (1983), Ward and others (1986), and Dutton and others (2005). Field-scale studies of reservoir-related characteristics were discussed for the Queen by Harris and others (1984), George and Stiles (1986), Holley and Mazzullo (1988), Malicse and Mazzullo (1990), Vanderhill (1991), Holtz (1994), Harris and others (1995), Price and others (2000), and Changsu (2002); for the Seven Rivers by Bain (1994) and Kosa and others (2001); for the Yates by Casavant (1988), Borer and Harris (1991), Bain (1994), and Kosa and others (2001); and for the Tansill by Kosa and others (2001).

REGIONAL SETTING

Upper Guadalupian platform-margin units include the Goat Seep and overlying Capitan Reef trends that were located around most of the periphery of the Delaware Basin. Paleo-biota in reef facies indicates a Late Permian age (Silver and Todd, 1969; Bigger, 1984). Reef development during middle and late Guadalupian time marked a profound change in paleogeographical architecture in the Permian Basin. Previous basin margins were low-relief carbonate ramps. The Goat Seep was constructed on the eroded crest of the Grayburg carbonate ramp (Fekete and others, 1986; Franseen and others, 1989), and the Capitan Reef built up on the Goat Seep and prograded into the Delaware Basin over underpinnings of previously deposited reef talus and Delaware Mountain Group siliciclastic basinal deposits.

Much conjecture and argument have been focused on the nature of the reef system. Some writers have maintained that it resided at or near sea level (for example, Lloyd, 1929; Johnson, 1942); and even produced barrier islands (Kirkland-George, 1992), whereas others have maintained that the living reef was composed largely of algally bound silt- and sand-sized skeletal debris derived from the Northwest Shelf, contained indigenous nonframework biota (for

example, sponges), and was submerged below wave base (for example, Achauer, 1969), and that the shelf crest was in a more landward position and marked by tepee structures and intertepee pisolite (for example, Esteban and Pray, 1976). Summaries of the basic models (fig. 3) for Capitan Reef development can be found in Cys and others (1977), Garber and others (1989), and Kirkland and others (1993).

The Goat Seep/Capitan reef system, a profoundly critical component of Permian Basin Guadalupian paleogeography, prominently divides the shelves of the Central Basin Platform, Northwest Shelf, and Western Shelf from the Delaware Basin. Equivalence between basin and shelf strata has long been the subject of investigation and controversy. The reef is largely massive in appearance and, although shelf strata and basin strata can be traced into their respective sides of the reef mass, none of the shelf and basin intervals can be correlated directly through the reef in outcrop or in the subsurface by using well logs. The Upper Queen Shattuck sandstone is correlated into the reef complex and is used to divide the Capitan from the older Goat Seep. However, the reef system will not be discussed in greater detail here because, although it is quite porous in many areas, it is mainly an aquifer. Only very locally (for example, Cheyenne field in Winkler County and MPF, Cutthroat, and Ft. Stockton fields in Pecos County) is the Capitan recognized as a hydrocarbon reservoir and it had cumulatively produced only 0.72 MMbbl of oil and 63,386 Mcf of gas as of 2003 (Railroad Commission of Texas, 2003).

Delaware Basin equivalents of the reef trend include the upper part of the Cherry Canyon Formation and the overlying Bell Canyon Formation (figs. 2, 4), both included in the sandstone-prone Delaware Mountain Group. The oldest Guadalupian basin unit is the Brushy Canyon Formation, which was deposited during early Guadalupian sea-level fall. The regionally widespread “pi-marker” well log interval (cored in Palo Duro Basin; Fracasso and Hovorka, 1986) may correspond to the sequence boundary (CS9/CS10 in fig. 2) between the upper and Lower San Andres Formations that marks this sea-level fall.

Shelfward of the Delaware Basin, similar cyclic facies tracts characterized each of the Goat Seep/Capitan-equivalent intervals. Nearest the shelf margin, normal-marine grain-rich carbonate facies dominated. In progressively updip positions, carbonate-depositional environments became more prone to fine-grained, biologically and circulation-restricted intertidal, supratidal, and lagoon carbonate production. Farther updip, evaporite-depositional environments and, most upslope, siliciclastic-depositional environments prevailed. Siliciclastic

abundance and texture depended somewhat on proximity of source areas; however, some intervals (Yates and Queen) contain much more siliciclastic sediment than others, and other potential controls on siliciclastic influx must be addressed. Upper Guadalupian shelf equivalents include, from oldest to youngest, the Queen, Seven Rivers, Yates, and Tansill Formations of the Artesia Group (fig. 2). Ochoan units postdate demise of the Guadalupian reef system and include, from oldest to youngest, the Castile (restricted to the Delaware Basin), Salado, Rustler, and Pierce Canyon/Dewey Lake Formations (fig. 2).

The Guadalupian was a period when many of Earth's cratonic masses were in close proximity following continental collisions that commenced during the Pennsylvanian. The South American craton was adjacent to the southern region of the North American craton (figs. 5, 6). Early Pennsylvanian collision of these continental masses created numerous uplifts and basins and set the stage for the depositional patterns that characterized the later Pennsylvanian and Permian systems. During the Guadalupian, the Permian Basin region became increasingly tectonically quiescent, and the climate was dominantly arid. In contrast to earlier Permian depositional patterns, carbonate sedimentation was limited, whereas evaporite and redbed deposition was widespread. Desert eolian and associated aqueous sedimentary environments prevailed on land, whereas restricted-marine conditions that included low biotic diversity and abundance and widespread precipitation of evaporites characterized shallow subtidal, peritidal, and nearshore areas. The Midland Basin subsided slowly and remained relatively shallow (evaporitic), even during sea-level highstands. The Delaware Basin, however, continued to subside at considerably greater rates, and water depths ranged from 1,000 ft (305 m) to 1,800 ft (549 m) (Garber and others, 1989, citing King, 1948; Newell and others, 1953; and Silver and Todd, 1969). By late Guadalupian time the Midland Basin was filled and hosted mainly evaporite and terrestrial siliciclastic deposition. A persistent gap in the Guadalupian reef trends was maintained in Brewster/Pecos County, to the west of the Glass Mountains. Here the intracratonic basin was open to the extracratonic ocean system through the Hovey Channel (fig. 1).

Shallow basinal areas were in the process of infilling with mainly siliciclastics and evaporites while shelves were dominated by carbonate and evaporite deposition during sea-level highstands and by siliciclastic deposition during lowstands. Carbonate buildups were subjected to subaerial weathering during lowstands, and shelf-interior siliciclastics and shelf-margin

carbonate debris were shed onto submarine slopes and deep-basin floors in the Delaware Basin (Delaware Mountain Group).

During the Ochoan both the Midland and Delaware Basins became filled, initially with evaporites and, finally, by siliciclastics (fig. 7). Appearance of widespread intracratonic fluvial and lacustrine deposition during the Late Triassic signaled onset of net deposition during overall wetter conditions after a protracted period of net nondeposition that accompanied the continental emergence that prevailed earlier in the Triassic (McGowen and others, 1979).

DEPOSITIONAL FACIES, DIAGENESIS, AND CONTROLS ON POROSITY DEVELOPMENT

Although formations of the Artesia Group are discussed as geologically distinctive units in the literature, they comprise generally similar facies, with similar lateral and vertical associations. All the Artesia Group units on the Northwest Shelf and western Central Basin Platform were deposited shelfward of the Guadalupian (Goat Seep/Capitan) reef complex in depositional settings dominated by carbonates in outer shelf positions, by evaporites and siliciclastics in middle shelf positions, and by siliciclastics in the most shelfward positions. More basinward positions on the evaporitic shelf are dominated by anhydrite, and more shelfward positions by halite. The characteristics of depositional cycles and diagenetic facies are also similar. The paleogeography was somewhat different on the east margin of the Central Basin Platform and the Northern Shelf of the Midland Basin, where carbonate strata thinned and equivalent units became evaporitic and siliciclastic. Nonetheless, primary facies and facies tracts associated with the Guadalupian hydrocarbon province on the shelves are similar. The differences between formations at any given location reflect differences in overall relative sea-level setting, within which depositional facies developed and the distance to siliciclastic source areas varied. Location-specific differences in vertical facies associations have compelled geologists to group intervals into formations. It is important to recognize, however, that a given set of facies associations that distinguishes the Queen Formation in one area may be similar to that of a section located farther shelfward in the Seven Rivers Formation. For these reasons it is most instructive to discuss Artesia Group facies rather than formation-specific facies.

Artesia Group facies are highly cyclic; facies components vary systematically vertically and geographically. In the most basinward areas of the platform, carbonate and sandstone

typically compose a depositional cycle. In most of the cycles observed in cores during this study, sandstones are interpreted to represent transgressive-leg depositional cycles, and carbonates represent highstand, or the upper part of cycles. In progressively updip positions, carbonates diminish in abundance and anhydrite increases. In the still more updip areas, halite becomes common. In the most proximal areas, siliciclastics are dominant. Artesia Group carbonate and evaporite facies examined in core during this study commonly contained varying abundances of admixed siliciclastics and were compositionally transitional to overlying siliciclastic strata.

Siliciclastics are the primary reservoir facies in the Artesia Group, whereas relatively impermeable carbonates and evaporites provide updip occlusion of interparticle porosity and form top seals. Porous, grain-rich carbonates locally may provide minor secondary production in downdip positions.

Artesia Group Stratigraphy

The Artesia Group includes, from oldest to youngest, the Grayburg, Queen, Seven Rivers, Yates, and Tansill Formations. This report focuses on the middle and upper formations of the Artesia Group, which all contain similar facies and facies tracts. All were deposited shelfward of the Guadalupian Goat Seep and Capitan “reef” trends. The Goat Seep developed on an unconformity located on the Grayburg shelf margin (Fekete and others, 1986; Franseen and others, 1989). Previous workers considered the Goat Seep to be equivalent to the Grayburg (for example, Silver and Todd, 1969). The Goat Seep and Capitan are vertically separated by the Shattuck sandstone member of the Queen Formation (Newell and others, 1953). Designation of the Goat Seep and Capitan Formations as reefs is historical. Early geologic researchers envisioned these facies as shelf-margin barriers that resided near and slightly above sea level (for example, Newell and others, 1953), that is, at the shelf crest. More recently it has been advanced that the Goat Seep and Capitan are composed largely of algally bound shelf detritus and, considering their correlation to exposure surfaces in more updip positions, are more properly interpreted as shelf-margin-aligned submarine mounds (for example, Garber and others, 1989; Kerans and Harris, 1993). The facies located at the shelf crest are now recognized as pisolite-bearing shoals and closely associated peritidal facies (for example, tepee structures) that occur shelfward of the Capitan and Goat Seep (Newell and others, 1953; Thomas, 1968; Dunham;

Smith, 1974; Esteban and Pray, 1977, 1983; Borer and Harris, 1989, 1991; Garber and others, 1989; Neese, 1989; Parsley and Warren, 1989; Kerans and Harris, 1993).

Division of Artesia Group intervals into formations is originally based on lithostratigraphic distinctions at type sections. On the basis of lithology defined in type sections, Artesia Group formations are readily correlated for great distances (even hundreds of miles) across the Permian Basin region. This correlation is facilitated by the stratigraphic alternation between siliciclastic-dominated sections (Queen and Yates Formations) and carbonate- or evaporite-dominated sections (Grayburg, Seven Rivers, and Tansill Formations). From a regional point of view, the Artesia Group records migrations of similar carbonate-siliciclastic-evaporite facies tracts in response to 3rd-order (approximately formation scale) relative sea-level variations (Meissner, 1972; Borer and Harris, 1991). The Queen and Yates Formations are characterized by thick accumulations of siliciclastics in areas that are relatively close to the Northwest Shelf and Central Basin Platform shelf margins. In contrast, Seven Rivers and Tansill Formation siliciclastic-rich facies depocenters are displaced to more shelfward positions.

Each formation is characterized by cyclic vertical facies successions that reflect higher-order relative sea-level variations. Ideal vertical successions of facies vary along the shelf profile. In more seaward positions, cycle bases include transgressively reworked terrigenous siliciclastic facies overlain by upward-shoaling carbonates (figs. 8, 9). In more shelfward positions, carbonates are less abundant, include displacive and replacive anhydrite, and are overlain by bedded anhydrite, siliciclastic-bearing anhydrite, and anhydrite-bearing siliciclastics (sabkha or evaporative lagoon environments) (fig. 9). Still farther shelfward, carbonates are absent, and massive halite and halite-bearing siliciclastics overlie anhydrite facies (figs. 9, 10). In positions even farther upslope, eolian siliciclastics may locally overlie evaporite facies. During 3rd-order relative sea-level fall, higher-order cyclic vertical facies successions in basinward positions are replaced by those typical of more shelfward positions.

Permian shelf strata crop out mainly in the Guadalupe Mountains of Texas and New Mexico and nearby areas. These areas include part of the Northwest Shelf and northwestern Delaware Basin. Exposures of the Queen and Yates Formations are dominantly near-reef, carbonate equivalents of intervals elsewhere dominated by siliciclastics and evaporites. Other exposures occur in the Glass and Apache Mountains of West Texas, which include along-strike equivalents of Guadalupe Mountain exposures. Other limited exposures occur in small areas in

the drainages of the Pecos, Upper Colorado, and Brazos Rivers. These latter two areas are part of the Eastern Shelf of the Midland Basin, where siliciclastics and evaporites dominate the Upper Permian section. Most of the Permian Basin region is covered by younger deposits that include the Upper Triassic Dockum Group, Lower Cretaceous Fredericksburg Division, Neogene Ogallala Formation, and Quaternary cover sand.

Yates Formation

Yates facies have been described in more detail than the other middle and upper Artesia Group intervals, probably reflecting their significance as a hydrocarbon play. The similarity of facies among the formations of the Artesia Group makes the very detailed descriptions of the Yates invaluable for providing insights into the Queen, Seven Rivers, and Tansill Formations. Cores from the Queen, Seven Rivers, and Yates Formations examined for this chapter show strong similarities to those of published studies. The Yates Formation will therefore be discussed before the other formations of the Artesia Group.

Stratigraphy, Type Section, and Regional Correlation

The siliciclastic-rich Yates Formation is in the Artesia Group (Tait and others, 1962) and is bounded bottom and top by the Seven Rivers and Tansill Formations, respectively. Except for the Delaware Basin, the Yates has been correlated everywhere in the rest of the greater Permian Basin, including the Palo Duro Basin. Thickness of the unit is more than 300 ft (91.4 m) in the back-reef area (Andreason, 1992). In the east (Scurry County) the Yates Formation thins to about 150 ft (45.7 m) (Dickey, 1940). Mear and Yarbrough (1961) suggested that the Sumrall Douglas Well No. 5 in Yates field, Pecos County, be designated as the type section and redefined the Yates Formation as including all strata between the Seven Rivers and Tansill Formations. Previously the Yates Sand was described from Yates field (Gester and Hawley, 1929), but the description included only 50 ft (15.2 m) of anhydritic sandstone and did not include any of the carbonates or evaporites that underlie or overlie the sandstone-dominated interval. Abundant large, frosted sand grains were a diagnostic indicator of Yates facies, although they also occur in some Queen and Seven Rivers sandstone intervals.

Stratigraphic equivalents elsewhere in the Permian Basin include the middle part of the Altuda Formation in the Glass Mountains and the uppermost part of the Whitehorse Group in

west-central Texas. In sequence stratigraphic terms, the lower Yates composes the shelf component of a composite sequence (CS-13 of Kerans and Kempter, 2002) (figs. 2, 4). According to field correlations that led to these sequence divisions, the approximate Delaware Basin equivalent (Delaware Mountain Group) of the Yates is the Rader member of the Bell Canyon Formation. The upper part of the Yates, along with the overlying Tansill Formation, composes the shelf component of another composite sequence (CS-14). Delaware Basin equivalents of CS-14 include, from older to younger, the McCombs and Lamar carbonate members, as well as several siliciclastic members that interfinger with the carbonates (figs. 2, 4). Yates-equivalent Delaware Basin strata are discussed elsewhere in this volume.

The Yates is one of the two overall siliciclastic-dominated, Guadalupian-age formations of the Permian Basin shelf. It is similar to the Queen Formation in many ways. Both are located landward of the Permian reef complexes that rim the Delaware Basin, and both comprise similar facies types, cyclic relationships between facies, and geographic distribution of facies. In both formations, sandstone is arkosic (fig. 11).

Subsurface Recognition and Correlation

The Yates Formation is recognized as an interval composed of thick sandstone beds and subordinate carbonate and evaporite that are overlain by thick carbonate or evaporite of the Tansill Formation and underlain by thick carbonate or evaporite of the Seven Rivers Formation. Occurrence of carbonate or evaporite in stratigraphically bounding units depends on position along the basin-to-shelf profile. Historically the top of Yates has been recognized by presence of well-rounded, frosted, medium-grained sand (for example, Gester and Hawley, 1929). Such material is not everywhere present in the Yates, however, and also occurs locally in the Queen and Seven Rivers. Their occurrence probably depends on the presence or former presence (in the case of marine reworking) of eolian facies, coarser grains of which may represent interdune lag deposits (Nance, 1988a, b).

In the absence of core, readily available gamma-ray logs are generally adequate for recognition and correlation of the Artesia Group. Yates carbonates and evaporites (anhydrite and halite) have significantly lower gamma-ray values than do siliciclastics (figs. 8, 10). The higher values for siliciclastics are controlled by the high content of K-feldspar in the subarkosic to

arkosic sandstone that is typical in the Permian Basin. A problem arises locally when only a gamma-ray log is used to pick the top of the Yates. In some areas the Tansill contains uranium-bearing dolomite and magnesite intervals that can be misinterpreted as siltstone beds (Garber and others, 1989). Elevated gamma-ray responses in the Tansill may compel the log analyst to pick the top of Yates within, or even at the top of, the Tansill. Availability of acoustic or density logs provides an independent basis from which to make a more appropriate interpretation, however, because siltstone density is generally much lower than that of carbonate.

Correlations are further facilitated by the laterally extensive tabular geometry of facies and by the basin-to-shelf facies tract structure whereby carbonate transitionally merges with stratigraphically equivalent evaporite. Yates rock-type recognition is facilitated in wells for which density, acoustic, or caliper logs are available. Carbonate- and anhydrite-dominated facies have higher bulk densities, lower density porosities (fig. 12), and lower acoustic-interval transit times than do siliciclastic-dominated facies. Halite-dominated strata have low gamma-ray values coupled with very low densities and interval transit times. Caliper logs show borehole enlargement in intervals of poorly cemented siliciclastics (fig. 12), as well as in intervals of halite-bearing strata if halite-undersaturated, water-based fluid was used to drill the well. Values of various geophysical well log responses from representative Upper Permian rock types are presented in the facies section of this chapter.

Regionally the Yates Formation is distinguished by a greater abundance of siliciclastics relative to other facies compared with most of the remaining Upper Permian section. However, textural, compositional, and diagenetic characteristics observed in Yates siliciclastics are present in the siliciclastic facies of the other Artesia formations. Sandstones are typically well- to very well sorted, and grains finer than coarse silt sized are not abundant. Feldspar is a common accessory mineral in Artesia sand and siltstone facies (fig. 11), and secondary porosity developed from its dissolution is common. One of the most notable features of some Yates sandstones is the presence of well-rounded pitted or frosted quartz grains within the coarser sand fraction (Page and Adams, 1940; Mear and Yarbrough, 1961). Frosted grains have also been described in the Queen (Nance, 1988a, b).

Yates siliciclastics and associated carbonate and evaporite were deposited landward of the Capitan reef system. Consequently, carbonate (mainly dolomitic mudstone and pisolitic dolopackstone and dolograinstone) is more relatively abundant in seaward positions on the Yates

shelf. Evaporites (halite and anhydrite) are increasingly important in inner-shelf positions, whereas major sandstone reservoir facies occur in middle-shelf positions.

The most comprehensive published summaries of Yates siliciclastic facies are those of Borer and Harris (1991) and Andreason (1992). Borer and Harris (1991) recognized six paleogeographically related, siliciclastic-dominated subfacies on the basis of cores from the Northwest Shelf and the western Central Basin Platform. They also discussed associated dolostone and evaporitic facies, although in less detail. Borer and Harris (1991) also provided useful graphic depictions of well log responses to various facies.

Andreason (1992) studied Yates cores and well logs from North Ward-Estes field, located on the west margin of the Central Basin Platform in Ward County, the largest and most productive Yates field. Andreason (1992) classified siliciclastic facies according to their general sedimentary structure and interpretations of depositional environments that were bolstered by mapping of well log facies. Andreason (1992) discussed Yates carbonate and evaporite facies in more detail than Borer and Harris (1991), although sandstone is the primary Yates reservoir facies. Andreason (1992) also provided core-plug porosity and permeability data. Both studies focused on facies from the outer shelf and outer-inner evaporitic shelf. None of the investigators discussed halite facies or evidence of their former presence.

Borer and Harris (1991) suggested that three main shelf settings could be distinguished on the basis of resident facies and facies associations (fig. 9). The outer shelf began where formation thickening accelerated abruptly to the Capitan reef shelf break, a distance of 3 to 4 mi (5 to 6 km). Lowstand deposits are composed mainly of siliciclastic facies. Highstand deposits are composed mainly of carbonate in downslope areas and evaporite-bearing carbonate or evaporite (anhydrite and halite) in upslope areas. Pisolite shoal carbonate facies are abundant and mark the topographically most elevated position on the outer shelf.

Artesia Group Core

Yates siliciclastics, as well as siliciclastics in other Artesia intervals, are represented by siltstone and very fine to fine-grained sandstone. A very minor fraction of prominent spherical medium-grained sand occurs locally in all Artesia Group formations. Coarser grained sand and gravel-sized particles are limited mainly to intraclastic facies or collapse breccias. Rock colors are generally red, gray, or brown. Feldspar, often partly dissolved, composes a prominent

fraction, and most of the siliciclastics can be classified as subarkose to arkose. Kaolinite, a product of feldspar weathering, is commonly present (Borer and Harris, 1991). Porosity and reservoir potential are best developed in fine-grained sandstone where feldspar has been significantly dissolved. In more basinward positions, dolomite matrix is a significant component, and siliciclastics grade laterally into siliciclastic-bearing dolostone. Where siltstone or sandstone overlies or underlies dolomite, a compositionally transitional interval between the two end members is commonly present. In more shelfward positions, interstitial anhydrite is a prominent component, and anhydrite nodules are commonly present. The plugging of sandstone porosity by dolomite and evaporites in upslope positions and in units vertically adjacent to porous fine sandstone forms the primary reservoir architecture (stratigraphic traps) in the Artesia Group.

Borer and Harris (1991) performed extensive petrographic analyses on cores from the Yates Formation on the Central Basin Platform and the Northwest Shelf and provided a petrographically based classification scheme of facies types. Andreason (1992) described cores from North Ward Estes field on the west edge of the Central Basin Platform and provided a classification scheme based on texture and sedimentary structures. There is considerable overlap of the two classification systems. However, there generally is not a one-to-one correspondence between the descriptive categories from each. The classification system of Borer and Harris may be more helpful when comprehensive petrographic analyses are, whereas the macro-scale descriptions provided by Andreason (1992) (based largely on texture, readily observed compositional features, and sedimentary structures) may be more helpful to one who is describing core without the advantage of thin sections.

Facies Classification Based on Petrographic Criteria

Outer-shelf facies

The idealized outer-shelf siliciclastic facies tract include, in downslope order, (1) dolomitic subarkosic siltstone and sandstone, (2) anhydritic siltstone and sandstone, and (3) bioturbated kaolinitic dolomitic quartz sandstone (fig. 9).

The dolomitic subarkosic siltstone and sandstone facies ranges from mudstone to sandstone. Compositionally this facies can be classified as a micaceous lithic subarkose. Potassium feldspar and plagioclase are subequally represented and compose 5 to 15 percent of typical samples. Dissolution of some feldspar grains is apparent. Volcanic, metamorphic, and

chert constituents compose most of the lithic fragments. The facies is typically green-gray and generously interbedded with algal dolomudstones and minor pisolite packstones. Thin interlaminae of dolomudstone occur and may record short-term rises in relative sea level or shifts of siliciclastic depositional axes. Vertical transitions of this facies from and to dolomudstone strata are typically mud rich, with lower contacts tending to be sharp and upper contacts typically transitional. The character of the dolostone-siliciclastic contacts may signify rapid fall and slow rises of sea level, respectively. Intercalation with carbonates suggests a distal tidal-flat to shallow subtidal depositional setting for dolomitic siliciclastic facies.

The anhydritic siltstone and sandstone facies ranges from very fine grained, sandy, argillaceous siltstone to silty, very fine grained sandstone. Compositionally this facies can be classified as anhydrite- and dolomite/magnesite-bearing subarkose to arkose. Detrital grains compose 50 to 60 percent of the facies. Anhydrite, dolomite, and magnesite interstitial cements compose the remaining 40 to 50 percent of the rock, although some matrix dolomite appears to be diagenetic. Monocrystalline quartz dominates the framework, with feldspars composing 20 to 30 percent. Largely Na-rich plagioclase is altered or dissolved to varying degrees. Rock fragments, heavy minerals (primarily ilmenite), and mica each compose approximately 1 to 5 percent of the remaining framework. Volcanic, metamorphic, and chert constituents compose most of the lithic fragments. Larger, well-rounded, and pitted or frosted quartz grains also occur in minor proportion. Sorting varies from moderately good to poor and is generally better in coarser grained examples. Siliciclastic laminae may be graded, and very fine grained sand lenses are common. Red, detrital, illitic clay composes up to 20 percent of the matrix in the siltstone and occurs as laminae or grain coats. The facies typically is red and alternates with thicker bedded pisolite-shoal-complex dolomite. Dolomites record shoaling cycles characterized by basal dolomudstone that grades up through fenestral dolowackestone to packstone and, ultimately, to intraclastic and pisolitic dolopackstones and grainstones. Tepee and fenestral voids are typically filled with anhydrite, and desiccation features are evident. Intercalation with shelf-crest peritidal carbonates, presence of evaporite cements, red color, and presence of frosted grains suggest an evaporitic tidal-flat depositional setting in which precursor siliciclastics were transported to the area by eolian processes.

Bioturbated kaolinitic dolomitic quartz sandstone ranges in size from clay to medium-grained sand. Detrital clay composes less than 5 percent and is not red. Quartz composes up to

70 percent of the facies, with dolomite cement or recrystallized matrix and authigenic kaolinite composing most of the remainder. Borer and Harris (1991) indicated that kaolinite fills secondary porosity following feldspar solution. Well-rounded pitted or frosted quartz grains occur within the coarser fraction as thin laminae or are dispersed. The facies is typically gray and associated with carbonates similar to those interbedded with the red anhydritic siltstones and sandstones, except that carbonate mudstone is more prominent and allochems are finer grained. Desiccation features are absent, and pore-filling anhydrite is absent. Pores are filled with fine-siliciclastic-bearing dolomicritic cement. Thinly bedded fusulinid packstone also occurs. Intercalation of this siliciclastic facies with subtidal carbonates, bioturbated fabric, and presence of frosted grains suggests deposition in a shallow subtidal setting where the clastics were transported to the nearshore terrestrial area by eolian processes and were ultimately transported into the subtidal zone by storm surge or fluvial-deltaic processes.

Middle-shelf facies

Middle shelf siliciclastic facies tract include, updip to downdip, (1) arkosic sandstone and (2) argillaceous siltstone (fig. 9).

Arkosic sandstone (fig. 13A) is the dominant reservoir facies in the Yates and ranges in grain size from silty, very fine grained to fine-grained sandstone and is typically well to very well sorted. Similar reservoir facies occur in the Queen in North Ward-Estes field (fig. 13B). It is generally poorly consolidated. Detrital clay occurs in association with wispy, plane, or ripple laminae. Feldspar solution has produced secondary porosity locally. Authigenic feldspar, dolomite, anhydrite, and corrensite (Mg-Fe smectite) cements partly fill pores. The facies, generally light-brown in color, is associated with relatively thinner intervals of dolomudstones; however, a transitional interval of argillaceous siltstone usually occurs between the sandstone and dolomite. Intercalation of these sandstones with thinly bedded dolomudstone and argillaceous siltstone, very good sorting, and vague, disrupted, ripple lamination with fine-grained drapes suggests deposition along the shelfward margins of shallow lagoons located shelfward of the pisolitic shelf crest. Finer grained clastics were probably winnowed by wind action. The brown color may be oil staining, judging from core examinations for this chapter.

Argillaceous siltstone ranges from mudstone to argillaceous silty sandstone. Clay occurring in abundances of 5 to 25 percent is present as wispy laminae, intraclasts, and

disseminated matrix. Argillaceous siltstone is typically dark-gray and occurs at the base and top of arkosic sandstone intervals. Intercalation of this facies with arkosic sandstone that is interpreted to be deposited on the shelfward margins of lagoons suggests a nearby environment for argillaceous siltstone, probably the lagoons. Deposition of the finer grained siliciclastics over sandstones probably occurred during a time of lagoonal expansion onto the margins where sandstone was previously deposited. Silt-sized particles would have been winnowed from updip deposits and trapped in lagoons.

Inner-shelf facies

The inner shelf is characterized by (1) evaporites and (2) red siliciclastics (fig. 9). According to descriptions provided by Borer and Harris (1991) and core described for this report, evaporite intervals may be dominated by anhydrite (fig. 14A,B) or halite (figs. 14C), with halite occupying more shelfward areas. In intervals with no halite, the former presence of halite is suggested by compacted anhydritic or siliciclastic components that are interpreted as representing the insoluble fractions of halite-bearing strata (fig. 14C). Abundance or absence of primary dolomite strata probably reflects paleogeographic proximity to or removal from normal marine conditions, with more abundant carbonate anticipated to have been deposited in more basinward areas at any given time. However, some of the dolomite fabrics (ghosts of gypsumlike swallowtails) probably record carbonate replacement of formerly occurring sulfate. And darker red colors (iron sulfide) in some of the siliciclastic siltstone and mudstone that, in places, underlie dolostone may record percolation of sulfide-rich solutions generated during the replacement process. Halite-solution features are more abundant in core, with greater relative amounts of dolomite in close stratigraphic proximity. It is reasonable to expect that halite dissolution in any depositional cycle occurred preferentially in paleo-basinward areas during the next marine transgression.

The primary siliciclastic facies in the inner shelf setting are argillaceous siltstone and sandstone, which are compositionally micaceous subarkose to arkose. Detrital illitic clay is abundant, and authigenic anhydrite and dolomite occur. However, dolomite abundance decreases toward eventual absence in more updip paleogeographic areas. Argillaceous siltstone from the inner shelf is typically red from hematite stain.

Facies Classification Based on Texture and Sedimentary Structure Criteria

Andreason (1992) used a depositional-fabric approach to classification of siliciclastic facies that he interpreted from core in North Ward-Estes field. Facies-specific porosity and permeability data reported from North Ward-Estes field are presented in table 1.

Table 1. Log responses and core test results for Yates facies, North Ward-Estes field, Ward County (Andreason, 1992). Halite values are from the author, and they are based on responses from University 3210-2 well, Andrews County.

Facies	Log response		Core test			
	Gamma ray (API)	Bulk den. (g/cm ³)	Por. range (%)	Avg. por. (%)	Perm. range (md)	Avg. perm. (md)
Disturbed silic.	70-100	2.38-2.56	5-29	14	0.1-68	7
Homog. silic.	50-70	2.25-2.45	7-26	16	0.5-4.90	42
Bioturb. silic.			9-14	11	0.4-10	2
Lamin. silic.			8-19	12	0.2-15	
Carbonate	12-63*	2.69-2.88	Negligible	Negligible	Negligible	Negligible
Anhydrite	5-36*	2.85-2.99	Negligible	Negligible	Negligible	Negligible
Halite	5-36*	2.17-2.36**	Negligible	Negligible	Negligible	Negligible

*Estimated higher value is admixture with siliciclastics

**Estimated higher value is 50% admixture with sandstone

Andreason (1992) recognized four basic siliciclastic facies on the basis of their general depositional fabric: (1) disturbed (with bedded and intraclastic subfacies), (2) homogenized, (3) laminated, and (4) bioturbated.

Disturbed facies

Disturbed facies range in degree of disturbance of original even lamination (fig. 13D). Presence of cubic ghosts after formerly present halite in some examples suggests that haloturbation was the primary cause of sediment disturbance. Some examples still include halite crystals (fig. 14D) and may have been produced in a sabkha setting that was sufficiently updip to be unaffected by subsequent inundation by marine-derived, halite-undersaturated water. The facies is argillaceous in places. Andreason (1992) interpreted cubic ghosts and salt-ridge structures to indicate development in coastal and continental sabkha settings on the basis of comparisons with examples from Saudi Arabia (Fryberger and others, 1983), Mexico (Fryberger and others, 1988; Thompson, 1968), Abu Dhabi (Kendall and Shipwith, 1968), India (Glennie and Evans, 1976), and New Mexico (Fryberger and others, 1988).

Homogenized facies

Homogenized facies include sandstone and silty sandstone that generally lack well-developed sedimentary structures, although some vague lamination may be evident (fig. 13A, B). They are the primary reservoir facies in the Yates and Queen middle-shelf trend and correspond to the light-brown arkosic sandstone of Borer and Harris (1991). This facies contains as much as 4 percent of the frosted or pitted medium sand grains for which the Yates is noted (Page and Adams, 1940; Mear and Yarbrough, 1961). Beds range from 6 inches (15.2 cm) to 12 ft (3.7 m) in thickness, which Andreason (1992) interpreted as representing beach-ridge deposition as eolian dunes and sand sheets, sand-rich sabkhas, and shorefaces. Homogenization of original dune crossbedding presumably reflects coastal marine reworking and tidally driven liquefaction. Proximity to evaporite-undersaturated marine water is interpreted as promoting preservation of interparticle porosity by maintaining conditions unfavorable to evaporite precipitation or preservation. Homogenized facies geometries are lenticular and are not everywhere the dominant facies of specific sand intervals on the middle shelf.

Laminated facies

Laminated facies have preserved original sedimentary structures. Subfacies include ripple- and plane-bedded varieties. Ripple-laminated facies (lower and middle areas in figs. 13C, 15A) typically occur as beds less than 1 ft (0.3 m) thick, sometimes within otherwise disturbed facies, and are interpreted as recording seasonal flooding of sabkha flats. Planar-laminated facies (most of fig. 13C), typically occurring as intervals less than 1 cm thick, are characterized by graded bedding that is interpreted as recording sedimentation from suspension in ponds following storms or subtidally during eustatic sea-level rises. The latter explains the facies occurrence at the base of many shoaling cycles.

An example of ripple cross-laminated, very well sorted, fine sandstone is shown in figure 15A. The fine laminae are similar to those interpreted to be eolian by Nance (1988a, b) from the Queen in Palo Duro Basin. These features are not common in cores described from the west margin of the Central Basin Platform, where plane-laminated and disturbed-ripple-laminated fabrics in siliciclastics are more common. Rarity of eolian-produced sedimentary structures may reflect marine reworking of lowstand terrestrial siliciclastics that is expected on shelf areas

proximal to the shelf margin. Inclined cross-laminated sandstone facies are more commonly reported from Artesia Group rocks on the east margin of the platform (for example, Mazzullo and others, 1992).

Bioturbated facies

Bioturbated facies include a range of biologically modified sediments, including burrows, mottling not related to evaporites, and anhydritic root-cast nodules. Burrowed and mottled varieties are reported to be located preferentially on the paleo-seaward side of the middle shelf, where they occur in cycle bases beneath carbonates. Bioturbated facies are the most uncommon of the facies in Andreason's (1992) classification, which testifies to the rarity of infauna and vegetation in Artesia Group terrestrial depositional environments.

Redbeds

Andreason (1992) noted that all four main facies locally could be red in color (for example, figs. 13C, 14C, D, 15, 16) but observed that most redbeds comprised disturbed facies. Redbeds signify pervasively oxidizing environments of the inner shelf and generally incorporated more interstitial anhydrite than reduced equivalents of similar coeval facies that occur downdip. Redbeds are less common in paleo-seaward positions presumably because sedimentation rates were higher and reducing conditions could thus be maintained more easily. Anhydrite is more common on the inner shelf than in more paleo-seaward positions. Andreason (1992) proposed that the scarcity of downslope anhydrite reflects the presence of porous and permeable beach-ridge complexes, which provided avenues for circulating evaporite-undersaturated water to adjacent sabkha settings. This development provides the porous middle-shelf reservoirs and updip evaporite plugging of porosity that characterizes stratigraphic traps in the Yates play, as well as in other Permian shelf plays.

Carbonates

Largely because the world-class exposures of Upper Guadalupian strata in the Guadalupe Mountains compose reef and proximal back-reef facies, many of the descriptions of carbonate facies originate from investigations in that region. An excellent succession of those facies was cored on the north margin of the Delaware Basin (Gulf PDB-04: Garber and others, 1989). Other

cores include those of Andreason (1992) from North Ward-Estes, where dolomud/wackestone dominates Yates carbonate facies, and those of Spencer (1987) from Yates field, where algal-laminated pellets and calcisphere-rich dolopackstone dominate Queen carbonate facies.

Carbonates are the most prominent shelf facies in proximal back-reef positions and grade shelfward from cross-laminated (fig. 17A) to vaguely laminated grainstone and packstone (fig. 17B) deposited on or around shoals to pisolitic shoals that formed the topographically highest area on the outer shelf (fig. 17C) to massive, bioturbated dolomudstone deposited in quiet lagoons (fig. 17D) to finely laminated dolowacke/mudstone deposited on tidal flats (fig. 18A, and lower half of fig. 18B). Carbonates also occur in fine interlamination, with anhydrite (originally gypsum; fig. 16 and upper half of fig. 18) deposited in brine pools that developed in depressions shelfward of lagoons.

Yates carbonate strata in North Ward-Estes field are dominantly dolostone. Although dolomicrite is dominant, organic and inorganic allochems are present in some intervals, and admixed siliciclastics are ubiquitous. Moldic and vuggy porosity is most common, is usually anhydrite- or dolomite-cement filled, and usually not in significant reservoirs. Andreason (1992) suggested an ideal shoaling sequence in carbonate intervals that included, from base to top, (1) fossiliferous peloidal dolowackestones to grainstones, (2) peloid/oncoid dolowackestones to grainstones, (3) fenestral-cryptalgalaminite dolomicrite, and (4) intraclastic breccias with admixed siliciclastics. Siliciclastic facies located immediately beneath carbonate strata probably record transgressive reworking of lowstand siliciclastic accumulations. If so, then these rocks represent the transgressive record at the base of a shoaling cycle rather than at the top.

From the lower Tansill Formation in the Guadalupe Mountains Neese (1979) described back-reef fossiliferous dolowackestone and packstone (including ostracodes, gastropods, forams), shelf-crest (pisolite and tepee structures with erosion surfaces), and intertidal peloid grainstone with admixed siliciclastics facies. Parsley and Warren (1989) described Tansill back-reef facies from Dark Canyon that included, from oldest to youngest, (1) subtidally deposited wackestone and poorly sorted packstone; (2) subtidally and intertidally deposited laminated and crossbedded, well-sorted, skeletal-peloid grainstone; and (3) peritidally deposited laminated mudstone and fenestral peloid packstone/wackestone. A barrier-island facies assemblage included tepees and coarse-grained pisolite that were interbedded with fenestral mudstone, fenestral wackestone/packstone, and local calcisphere-bearing mudstone/wackestone. A lagoonal

assemblage included dolomitized, extensive, calcisphere-rich mudstone and wackestone, algal-laminated packstone, and peloid-intraclast packstone.

Mazzullo (1999) recognized shoaling facies in the Tansill (also from Dark Canyon) on the basis of observation of (1) subtidally developed bioclastic wackestones, packstones, and graded and locally cross-stratified grainstones, as well as biostromes; (2) fenestral and locally desiccated mudstone interpreted to have developed on peritidal flats; and (3) admixed subtidal and peritidal deposits interpreted to have been developed on shorefaces.

Evaporite facies

The prominence of bedded evaporite over carbonate marks the transition from middle- to inner-shelf environments. Similar to Permian carbonate-evaporite facies tracts from the evaporite-rich Palo Duro Basin in the Texas Panhandle, the updip increase in abundance of Yates evaporites signifies progressive evaporative evolution of marine-derived water, with updip distance from normal marine environments that existed seaward of the pisolite shoal zone.

Andreason (1992) recognized two main evaporite facies in Ward-Estes field, both of which are dominated by sulfate: (1) nodular anhydrite (figs. 14A, 18D) and (2) massive (essentially homogeneous) anhydrite (no photo). Nodular facies overlies massive facies in the east part of the field and probably records infilling of playas or evaporitic lagoons. Apart from cubic ghosts after halite and deformation in disturbed siliciclastic facies, halite-bearing rocks were not indicated.

Nodular anhydrite facies were constructed of nodules with no less than 40 percent supporting dolomite or siliciclastic matrix. Andreason (1992) noted the similarities between Yates nodular anhydrite and that from Trucial Coast sabkhas, where anhydrite is precipitated in the capillary zone. The thickness of nodular anhydrite accumulations is controlled by limits on capillary-zone thickness, which is as much as 6.6 ft (2 m) in siliciclastics and less than 3.3 ft (1 m) in carbonate-dominated terrain. However, slowly rising sea level is thought to produce thicker nodular intervals by raising the capillary zone into accumulating host sediments (Warren and Kendall, 1985).

Massive anhydrite from North Ward-Estes contains less than 20 percent dolomite or siliciclastic matrix that is typically vertically oriented as stringers between nodules. The facies, sharply bounded at its base and top, is most prominent in the east part of Ward-Estes field.

Where overlain by dolostone, the boundary is corrosive and indicates the presence of gypsum-undersaturated water in the depositional environment. Where overlain by nodular facies, the section probably records infilling of brine pools.

A laminated variety of anhydrite is observed in some cores (fig. 14B). These probably record gypsum precipitation shallow pools, where tall crystals cannot develop or where agitation of the pool surface abrades crystals and distributes the debris in even layers.

Finely interlaminated anhydrite and dolomite (fig. 18C) occur in the evaporative inner shelf and were probably precipitated in brine pools free of siliciclastic influx. Anhydrite pseudomorphs after gypsum swallowtail twins are locally common and appear to be draped by fine laminae of dolomite. The alternations between anhydrite and dolomite reflect cyclic variations of salinity in the brine pool, whereby hydrochemical conditions oscillated between gypsum saturation and undersaturation. Fine laminations within the dolomite intervals may record algal growth (fig. 18A, B). In an ideal, complete depositional sequence, the vertical facies progression is anhydrite, halite, halite-mudstone (mud salt), and sandstone. Where sandstone overlies anhydrite, the original halite-bearing strata may have been disaggregated by dissolution of halite, and included siliciclastics reworked by erosive processes. These conditions develop in an evaporative lagoon or wind-deflated depression, where ponded water (groundwater source, perhaps) is already close to calcium sulfate supersaturation, and substrate moisture within the pond-margin sediment precludes eolian siliciclastic transport to the brine pool. Eventually the pool filled with gypsum, then halite. Siliciclastics along pool margins were occluded with evaporites, and eolian-transported siliciclastics covered the area. Cover sands were inundated with saline, near-surface groundwater through capillary action, and halite precipitated within the cover sands (fig. 14D). Eventual dissolution of the halite fraction produced the disturbed sedimentary fabrics described by Borer and Harris (1991) and Andreason (1992) (fig. 13D).

Solution-collapse breccia

Solution-collapse breccias comprise angular dolostone clasts either supported by a fine-grained siliciclastic (fig. 15B) matrix or supported as a clast-supported facies with dolomite-dominated matrix (fig. 18B). Clasts are typically cryptogally laminated. Clasts are generally rotated chaotically and contrast with intraclastic breccias from more seaward positions that have more rounded clasts, which have imbricate orientations that suggest storm depositional

processes. Judging from correlations of solution-collapse breccias with locations where massive anhydrite beds are preserved, it appears that dissolution of sulfide beds provided the loss of support for brecciated precursor strata (Andreasson, 1992).

Andreasson's (1992) data indicate that either normal sulfate-undersaturated marine or meteoric water could dissolve the evaporite facies. However, concentration of the zone of collapse on the seaward margin of massive anhydrite accumulations compelled Andreasson (1992) to conclude that sulfate dissolution most probably occurred during marine transgression.

Halite facies

During the present study, several cores have been described that recorded evaporite precipitation and the former presence of evaporites. Evaporite facies include anhydrite, halite, and halite-mudstone that were deposited in and at the landward margins of broad, shallow brine pans (salinas and sabkhas). Extensive discussions of similar facies and conditions of deposition from the Queen/Grayburg interval in Palo Duro Basin (essentially the northern extension of the northern shelf of Midland Basin) can be found in Nance (1988a, b).

Halite facies and halite-dissolution facies include (1) massive, polycrystalline varieties; (2) admixtures with siliciclastics; and (3) compacted siliciclastic and sulfate residues after halite dissolution. Massive, polycrystalline halite (fig. 14C) occurs as mosaics of halite crystals. Intercrystalline stringers of anhydrite are often present and testify to the occasional reduction of salinity to below that of halite saturation. Occasionally it is possible to observe chevron-shaped ghosts in halite crystals that reflect incremental precipitation in the brine pool and entrapment of fluid inclusions (Fracasso and Hovorka, 1986; Nance, 1988a, b). In most instances, however, the halite deposits have been cyclically dissolved and reprecipitated so that relict zonation is lost. In cases where postdepositional halite dissolution has not occurred, siliciclastic admixtures with halite (uppermost part of fig. 19) often occur in intervals that directly overlie massive varieties. Siliciclastic fractions range from trace to dominant. Where halite has been completely dissolved, compacted mixtures of siliciclastics and anhydrite stringers are preserved (fig. 14C). Most, but not all, admixed siliciclastics are very fine grained (mud) and exhibit very little permeability so that they may provide a potential reservoir seal even in the absence of halite.

It has been hypothesized that dissolution of small halite crystals from laminated siliciclastics may have produced the disturbed aspect of laminations widely observed in Artesia

siliciclastics (haloturbation), although bioturbation is also recognized as a potential influence. As relative-sea-level-controlled accommodation volumes were filled with sediment and rates of evaporation relative to influx of marine-derived water increased, developing higher-density, halite-supersaturated brines would be expected to percolate into tidal-flat sediment, displace less-dense marine water, and eventually precipitate interstitially varying amounts of halite in what might be considered a sabkha environment. Evaporite precipitation in tidal-flat sediments is anticipated to occur in positions basinward of the primary, halite-precipitating brine pools and, thus, be exposed to subsequent influxes of halite-undersaturated marine-derived water. What remains is an originally planar laminated fabric that has been displaced by crystal growth and eventual collapse during halite dissolution.

Queen Formation

Stratigraphy, Type Section, and Regional Correlation

Thickness of the Queen Formation, possibly exceeding 1,000 ft (304.8 m) in the Midland Basin, thins to about 130 ft (39.6 m) in Coke County on the Eastern Shelf (Mear, 1963). The Queen is the back-reef equivalent to the Goat Seep reef complex. The uppermost beds of the Shattuck sandstone member of the Queen overlap the Goat Seep and stratigraphically divide the Goat Seep from the Capitan complex (Silver and Todd, 1969; Ball and others, 1971).

The Queen is one of the two overall siliciclastic-dominated, Guadalupian-age formations of the Permian Basin shelf. It is similar to the Yates Formation in many ways. Both are located landward of the Permian reef complexes that rim the Delaware Basin. Both probably record periods of relative sea-level lowstand compared with those of the other Guadalupian formations (on the basis of relative siliciclastic abundance), and both comprise similar facies types with similar cyclic vertical facies progressions.

At the type section on the Northwest Shelf 2 miles south of the old Queen Post Office (40 mi (64.4 km) SW of Carlsbad, New Mexico) Moran (1962) characterized the Queen as 421 ft (128.3 m) of sandstone, sandy dolomite, and dolomite. The lower 41 ft (12.5 m) consists of crossbedded sandstone. At this location the Queen is overlain by Seven Rivers dolomite. A type well was defined by Tait and others (1962) in Artesia field (Eddy County, New Mexico), wherein the Queen was described as comprising 420 ft (128 m) of sandstone and anhydrite, with the uppermost 30 ft (9.1 m) composed of bimodal sandstone. The upper sandstone unit is part of

the Shattuck Member (Newell and others, 1953), which is generally about 100 ft (30.5 m) thick over much of the shelf in the Guadalupe Mountains, except near the reef where it thins.

At Keystone field, a few miles shelfward of the Goat Seep reef, the 220-ft (67.1-m) Colby productive sandstone interval is equivalent to the lower half of the Queen Formation. Sandstone represents approximately 55 percent of the interval that also includes dolomite and anhydrite (Vanderhill, 1991).

At Yates field on the southeast tip of the Central Basin Platform, Queen facies include coarse-grained siltstone, very fine grained sandstone, and dolomite (Spencer and Warren, 1986). Within the siliciclastics are wispy clay streaks and dolomitic crusts. Intraclasts of dolomitic crusts are locally common. Dolomites include massive (bioturbated?) and laminated pellet packstone to wackestone.

Core representing the complete Queen interval from North Ward-Estes field in Ward County, Texas, was described for this chapter (fig. 20). Similar to Yates intervals described from other Guadalupian outer- to middle-shelf positions in the Permian Basin, the Queen in this area is composed of cycles of shallow water carbonates and siliciclastics. Carbonate is dominantly dolomudstone and wackestone, although thin packstone is locally common. These rocks contain pel-moldic porosity and oil staining. Megafossils are rare. Siliciclastics are mainly gray, well-sorted, very fine sandstone with varying portions of coarse silt. It has a red color in the lowermost 50 ft (15.2 m) of the interval. Very well sorted, fine-grained sandstone is subordinate but is very porous and permeable and comprises the primary hydrocarbon reservoir facies, as indicated by its brown color and petroleum odor (fig. 13A).

Subsurface Recognition and Correlation

The Queen Formation is recognized as an interval composed of thick sandstone beds and subordinate carbonate and evaporite that are overlain by thick carbonate or evaporite of the Seven Rivers Formation and underlain by thick carbonate or evaporite of the Grayburg Formation (fig. 20). The occurrence of carbonate or evaporite in stratigraphically bounding units depends on position along the basin-to-shelf profile.

In the absence of core, readily available gamma-ray logs are generally adequate for recognition and correlation of Queen end-member (pure anhydrite, carbonate, and siliciclastic)

facies. Carbonates and evaporites (anhydrite and halite) have significantly lower gamma-ray values than do the siliciclastics (figs. 8, 10, 20). Higher values of siliciclastics are controlled by the high content of K-feldspar in the subarkosic to arkosic sandstone that is typical in the Permian Basin. Correlations are further facilitated by the laterally extensive tabular geometry of facies and by the basin-to-shelf facies tract structure, whereby carbonate transitionally merges with stratigraphically equivalent evaporite. Rock-type recognition is facilitated in wells for which density, acoustic, or caliper logs are available. Carbonate- and anhydrite-dominated facies have higher bulk densities, lower neutron porosities, and acoustic-interval transit times than do siliciclastic-dominated facies (figs. 12, 20). Halite-dominated strata have low gamma-ray values coupled with very low densities, interval transit times, and porosity (fig. 10). Caliper logs show borehole enlargement in intervals of poorly cemented siliciclastics, as well as in intervals of halite-bearing strata if halite-undersaturated, water-based fluid was used to drill the well. Values of various geophysical well log responses from representative Upper Permian rock types are presented in the facies section of this chapter.

Seven Rivers Formation

Stratigraphy, Type Section, and Regional Correlation

The Seven Rivers Formation in the Artesia Group (Tait and others, 1962) is bounded at its base by the Shattuck sandstone member of the Queen and at its top by the siliciclastic-dominated Yates Formation. The interfingering relationship with lower Capitan Reef carbonates (Silver and Todd, 1969) indicates a late Guadalupian age. On the Eastern Shelf the Seven Rivers is about 200 ft (61 m) thick and composed mainly of sandstone. Dominated by anhydrite on the Central Basin Platform, it is approximately 500 ft (152.4 m) thick. On the Northwest Shelf it is dominated by dolomite and anhydrite and is 650 to 1,000 ft (198.1–304.8 m) thick (West Texas Geological Society, 1976).

The Seven Rivers was described originally from exposures of limy shale and limestone and limestone breccia northwest of Carlsbad (Meinzer and others, 1926) but was redefined by Lang (1937) to exclude some of the uppermost part of the section. Mear and Yarbrough (1961) fixed the upper boundary at the base of the Yates Formation. It was recognized generally in the oil fields as the evaporite- and carbonate-dominated interval between the siliciclastic-rich Queen and Yates Formations.

Stratigraphic equivalents elsewhere in the Permian Basin include the lower part of the Altuda Formation in the Glass Mountains and the middle part of the Whitehorse Group in west-central Texas. It is capped by the Azotea Tongue, a bedded dolostone interval that is several hundred feet thick (West Texas Geological Society, 1976). In sequence stratigraphic terms, the Seven Rivers composes the shelf component of composite sequence CS-12 (Kerans and Kempter, 2002). According to field correlations that led to these sequence divisions, the Delaware Basin equivalent (Delaware Mountain Group) is the Pinery and Hegler members of the Bell Canyon Formation and the Manzanita member of the Cherry Canyon Formation. (fig. 2). Delaware Basin strata are discussed in greater detail elsewhere in this volume.

Subsurface Recognition and Correlation

The Seven Rivers Formation is recognized as an interval composed of thick carbonate and evaporite beds and subordinate siliciclastics that are overlain by thick sandstone beds of the Yates Formation and underlain by thick sandstone beds of the Queen Formation. In the absence of core, readily available gamma-ray logs are generally adequate for recognition and correlation of Artesia Group Formations. Seven Rivers carbonates and evaporites (anhydrite and halite) have significantly lower gamma-ray values than do the Queen and Yates subarkosic and arkosic siliciclastics. Correlations are facilitated by the laterally extensive tabular geometry of facies and by the basin-to-shelf facies tract structure whereby carbonate transitionally merges with stratigraphically equivalent evaporite. Rock-type recognition is facilitated in wells for which density, acoustic, or caliper logs are available. Carbonate- and anhydrite-dominated facies have higher bulk densities and acoustic interval transit times than do siliciclastic-dominated facies. Halite-dominated strata have low gamma-ray values coupled with very low densities and interval transit times. Caliper logs show that borehole enlargement in intervals of halite-bearing strata is present if halite-undersaturated, water-based fluid was used to drill the well and, in the absence of density or acoustic logs, provides a reliable basis from which to differentiate halite from carbonate and anhydrite in low-gamma-ray strata. Values of various geophysical well log responses from representative Upper Permian rock types are presented in the facies section of this chapter.

Tansill Formation

Stratigraphy, Type Section, and Regional Correlation

The Tansill Formation is in the Artesia Group (Tait and others, 1962) and is bounded at its base by the Yates Formation and at its top by the Salado Formation. The upper surface of the Tansill is considered to be the boundary between Guadalupian and Ochoan Series strata (for example, DeFord and Riggs, 1941). Thickness of the unit is approximately 125 ft (38.1 m) throughout its extent over much of the Permian Basin. It is as much as 350 ft (106.7 m) thick where it merges with the Capitan (West Texas Geological Society, 1976). DeFord and Riggs (1941) defined the formation and suggested that an outcrop 3.7 mi (6 km) along the Artesia-Carlsbad Highway from the Eddy County courthouse in Carlsbad be designated as the type section. At this location the Tansill is 123.5 ft (37.6 m) thick and composed of interbedded magnesium limestone and siliceous siltstone and sandstone. DeFord and Riggs (1941) also proposed recognition of the Ocotillo Member, a widespread 13.5-ft-thick (4.1-m) siliciclastic-dominated interval in the upper part of the formation that the authors claimed could be traced for more than 100 mi (160.9 km), although their cross section depicted only about 33 mi (53.1 km) of correlation distance across the Northwest Shelf between the type section and Halfway field in Lea County, New Mexico.

Stratigraphic equivalents of the Tansill elsewhere in the Permian Basin may include parts of the Tessey, Altuda, or Capitan Formations in the Glass Mountains. The upper part of the Yates, along with the overlying Tansill Formation, composes the upper part of the shelf component of a composite sequence (CS-14). Delaware Basin approximate equivalents of the Tansill include the Lamar carbonate member of the Bell Canyon Formation (Tyrrell, 1962; Kerans and Kempter, 2002), as well as several siliciclastic members (probably the Trap and Ramsey) that interfinger with the carbonates (fig. 2). However, Achauer (1971) argued (on the basis of his own fieldwork) that the Lamar merged with the upper part of the Capitan, not the Tansill. Kerans and Kempter (2002) correlated the Lamar in the Bell Canyon Formation with the lower half of the Tansill; however, the two intervals appear to be uncoupled by the intervening Capitan reef complex. Delaware Basin strata are discussed in greater detail elsewhere in this volume.

Subsurface Recognition and Correlation

The Tansill Formation is recognized as an interval composed largely of carbonate and evaporite that are overlain by thick evaporite of the Salado Formation and underlain by thick sandstone beds of the Yates Formation. The occurrence of anhydrite or halite in the basal interval of the Salado depends on position along the basin-to-shelf profile, with halite becoming more prevalent at greater distances from the reef zone. The top of the Yates has been recognized traditionally by presence of well-rounded, frosted, medium-grained sand (for example, Gester and Hawley, 1929). Such material, however, also occurs in the Queen and Seven Rivers and is probably more facies dependent than formation dependent.

The Tansill is recognized everywhere on the Permian Basin shelves and in the Midland Basin (DeFord and Riggs, 1941) and appears to be the uppermost unit that was deposited in the lee of the Capitan Reef. The laterally extensive Fletcher anhydrite unit overlies the Tansill and is considered to be the base of the Salado Formation. The extension of the Fletcher into the Delaware also marks the boundary between the Salado and the underlying, basin-limited Castile Formation. Tansill carbonate is primarily dolostone and is limited to a 10- to 25-mi-wide (16.1- to 40.2-km) zone in the immediate back-reef area on the Central Basin Platform and Northwest Shelf. Farther shelfward the Tansill is dominated by anhydrite and eventually subequal amounts of anhydrite and halite. The author has not identified a map that describes the mappable extent of the Fletcher unit; however, Page and Adams (1940) mapped the Tansill into Mitchell County on the Eastern Shelf, where it unconformably abuts Dockum Group strata. On their published cross section, Page and Adams (1940) considered the sulfate-dominated unit below halite (so-called "Upper Castile") and above the siliciclastic-dominated Yates to be the Tansill. In the Texas Panhandle the Tansill is thought to be indistinguishable from the Salado, where the composite section is dominated by halite and contains subordinate sulfate and siliciclastics. The upper part of the unit is variably truncated by halite dissolution (McGillis and Presley, 1981). Distribution of siliciclastics suggests east and northeast sources (McGillis and Presley, 1981).

In the absence of core, readily available gamma-ray logs are generally adequate for recognition and correlation of the Artesia Group. Tansill carbonates and evaporites (anhydrite and halite) have significantly lower gamma-ray values than do the underlying Yates K-feldspar-bearing siliciclastics (fig. 12). As briefly noted earlier in the Yates section, however, a correlation problem arises locally when only a gamma-ray log is available for picking the

boundary between the Yates and Tansill Formations. Locally the Tansill contains numerous uranium-bearing dolomite and magnesite intervals that can be misinterpreted as siltstone beds (Garber and others, 1989). Acoustic or density logs facilitate an appropriate rock-type-based interpretation, however, because siltstone density is diagnostically lower than that of the relatively dense dolomite that composes most Tansill carbonate.

Correlations are further facilitated by the laterally extensive, tabular geometry of facies and by the shelf-to-basin facies tract whereby carbonate laterally transitions to evaporite. Tansill rock-type recognition is facilitated in wells for which density, acoustic, or caliper logs are available. Carbonate- and anhydrite-dominated facies have higher bulk densities, lower density porosities (fig. 12), and lower acoustic-interval transit times than do siliciclastic-dominated facies. Halite-dominated strata have low gamma-ray values coupled with very low densities and interval transit times. Caliper logs show borehole enlargement in intervals of poorly cemented siliciclastics, as well as in intervals of halite-bearing strata if halite-undersaturated, water-based fluid was used to drill the well.

Artesia Group Diagenesis

Diagenetic processes that have affected the Artesia Group include marine and meteoric phreatic cementation, meteoric vadose, dolomitization, dolomite cementation, dehydration of gypsum to anhydrite, replacement of carbonates by sulfates, replacement of sulfates by carbonates, evaporite dissolution, dissolution of feldspar and carbonate grains (creating secondary porosity), and clay and feldspar authigenesis (dissecting and obliterating porosity). The importance at any location of any specific control or combination of controls is determined by the presence of specific depositional facies. Examples include replacement of carbonate by sulfate that was facilitated in rocks where sulfate-oversaturated brine (indicated currently by abundant anhydrite) overlay carbonate (fig. 21); secondary-porosity development after feldspar dissolution and clay authigenesis is pronounced in arkoses and subarkoses; and pel- or fossil-moldic secondary porosity is most pronounced in grain-rich carbonate.

Lucia (1961) performed some of the early investigations of Tansill diagenesis. He noted occurrences of lacy calcite crystals with included dolomite. The crystal form of anhydrite is outlined by the distribution of inclusions, suggesting that calcite has replaced anhydrite.

Replacement of dolomite by calcite is suggested by the decrease in number of dolomite inclusions toward the edge of the calcite crystals.

Parsley and Warren (1989) described diagenetic characteristics in the Tansill from Dark Canyon that might be similar to those of Tansill intervals that are situated in similar paleogeographical settings elsewhere on shelves surrounding the Delaware Basin. They observed isopachous bladed and subsequent high-Mg calcite and aragonitic cements in samples from the outer shelf, whereas in the barrier samples, they observed parallel-fibrous and botryoidal-fibrous aragonite in sheet cracks. Geopetal cements in crossbedded and pisolite grainstones indicated vadose diagenetic conditions. Local terra rosa fills in tepee sheet cracks indicated some dissolution and accumulations of insoluble residue. Dolomitization was pervasive. Stable isotope ($\delta^{13}\text{C}$ and $\delta^{18}\text{O}$) data indicated that dolomitizing fluids were evaporated almost to calcium sulfate saturation and thus suggested their formation in penecontemporaneous evaporative lagoons. Occurrences of pseudomorphs after evaporites suggested previous pore filling by evaporites. Zoned luminescence in calcite spar indicated at least two episodes of meteoric diagenesis, which promoted replacement and removal of evaporite cement, as well as neomorphism of aragonite and high-Mg calcite. Meteoric dissolution of skeletal material also promoted secondary porosity development.

Mazzullo (1999) noted that marine cements in the Tansill are dominated by prismatic calcites with microdolomite inclusions and some radiaxial-fibrous form that he interpreted as former high-Mg calcite. The $\delta^{18}\text{O}$ and $\delta^{13}\text{C}$ compositions of the least-altered cements (-1.6‰ and 5.8‰ PDB, respectively) suggest that precipitation was from marine pore fluid. Original aragonitic cement with similar isotopic composition is volumetrically minor. In contrast, former aragonite marine cement dominates in coeval platform-margin patch reefs, the Capitan reef, and in shelf-crest pisolites. Mean $\delta^{18}\text{O}$ composition of the dolomite that replaced peritidal deposits (0.1‰ PDB) suggests that it precipitated from marine fluids of elevated salinity. Stabilization of earlier diagenetic phases most likely attended precipitation of equant calcites in the rocks, which is interpreted to have occurred in a subsequent meteoric phreatic system. A second generation of equant cements precipitated still later in a deeper, meteoric-dominated system. Replacement by poikilotopic calcite of syndepositional evaporites is the most recent diagenetic phase and appears to have accompanied meteoric dolomite calcification during the Tertiary, according to stable, oxygen-carbon isotope data.

Mazzullo (1999) suggested that abundant marine cementation in Tansill rocks may have been promoted by seawater pumping through the sediments on a wide, shallow shelf. Microbial activity in the grainstones may have been promoted by restricted circulation around associated peritidal islands. In contrast, dominantly micritic cements in the late highstand facies of Tansill sequences were suggested to mark more restricted environments in terms of shelf width and energy.

Examples of feldspar dissolution, along with feldspar and clay authigenesis, were documented by Spencer (1987) in Queen sandstone from Yates field, southeastern Central Basin Platform. Here the three processes occur in the same 1-ft (0.3-m) cored interval, suggesting that deposition of feldspar and kaolin cement in some pores was accompanied by production of secondary porosity elsewhere. Spencer (1987) cited Dunham (1972) to suggest that these processes probably record vadose meteoric diagenesis.

Controls on Porosity and Permeability

Interparticle porosity and moldic porosity that formed by feldspar dissolution provide the primary reservoirs for hydrocarbon accumulations in Upper Guadalupian siliciclastic strata. Siliciclastic interparticle porosity is optimized by the well-sorted textures where fine-grained material is generally absent to plug pore throats formed between fine- to very fine grained sand particles. In some cases dissolution of cements enhanced interparticle porosity (for example, in the Queen at Concho Bluff; Mazzullo and others, 1992). Plugging of porosity by evaporites (for example, in the Yates at North Ward-Estes; Borer and Harris, 1991) and changes to finer grained facies (for example, in the Queen at Concho Bluff; Mazzullo and others, 1992) provide the updip seals for most Guadalupian siliciclastic reservoirs. Tansill reservoirs produce mainly from shelf carbonate strata; therefore, the appropriate outcrop analogs are located in the back-reef shelf, downslope of evaporite settings. Parsley and Warren (1989) observed that interparticle and intraskeletal porosity are the dominant porosity modes in Tansill carbonates from Dark Canyon. Original porosity as high as 45 percent has been reduced by cement to an average of 7 percent, with local occurrences as high as 17 percent. Well-sorted skeletal-peloid grainstones show the most consistency in porosity values that the writers described as comprising strike-aligned lenses that fringe barrier islands. Brister and Ulmer-Scholle (2000) described interparticle porosity in Seven Rivers dolomite reservoir facies from the Grayburg Jackson Pool (Northwest Shelf, Eddy

County, New Mexico). They interpreted productive interparticle porosity as resulting from deposition in tidal channels, judging from the geographic pattern of their pore-volume (neutron- $\phi \times$ thickness) map (fig. 22).

DEPOSITIONAL SETTING AND GEOGRAPHIC VARIATIONS IN FACIES DISTRIBUTIONS

Artesia Group facies are, by definition, endemic to the back-reef shelf of the Guadalupian reef complex. Biota is relatively scarce in areas shelfward of the immediate back-reef zone, and carbonate sediment texture becomes progressively more fine grained, suggesting that marine circulation in more shelfward positions was restricted and was prone to above-normal marine salinity (Garber and others, 1989). Evaporite precipitation occurred within a few hundred meters of marine- to near-marine carbonate depositional environments (Sarg, 1981) and occurred in the lee of shoals, suggesting evaporative lagoon conditions. Farther shelfward (6–8 mi of the pisolitic shelf crest; Garber and others, 1989), evaporites were deposited in salinas and sabkhas. In many sandstone intervals, textures were well to very well sorted, and sediment color is red. Silt- and clay-sized sediment is observed in some intervals; therefore, its absence in well-sorted sandstone intervals suggests sorting processes that finely discriminate among available particle sizes. These are characteristics that suggest arid conditions where sand grains were sorted by eolian processes. Finer grained, more poorly sorted sediments are often contained in halite-bearing intervals or halite-dissolution residue or are in stratigraphic contact with carbonate mudstone. Thus, finer grained siliciclastics were probably trapped in ephemeral ponds, on sabkhas, and in lagoons.

The abundance of siliciclastics in the Queen and Yates Formations probably indicates deposition during periods of relative sea-level lowstand, compared with the other Guadalupian formations (for example, Borer and Harris, 1991). Additionally, uplift in siliciclastic source areas and climatic changes could have influenced siliciclastic depositional patterns.

It is well documented that Upper Guadalupian depositional facies are systematically distributed along depositional slope. The distribution of depositional facies is also controlled by phase of sea-level change; that is, facies distributions vary between highstand, lowstand, and transgressive stages. A good summary of ideal depositional patterns in the context of sea-level phase was given by Andreason (1992) (fig. 23). During sea-level highstand, carbonate facies

dominate basinward of the shoreface area. The most grain-rich depositional facies are in the immediate back-reef area basinward of and including the pisolite-shoal zone. Lagoonal areas are characterized by wackestone and mudstone, and algal-laminated carbonates are typical of tidal flats. Farther shelfward, shoreface then sabkha and associated brine pools occur. In formation or subformation-scale intervals (for example, Queen, lower Seven Rivers, and Yates) that contain prominent siliciclastic-dominated strata, siliciclastics may also compose a significant fraction of otherwise carbonate- or evaporite-dominated facies.

Facies tract profile depends on the phase of the relative sea-level transition (Andreasson, 1992). During fall of sea level, evaporitic-inner-shelf and siliciclastic-dominated depositional environments migrate basinward, siliciclastics may be deposited in previously carbonate or evaporite dominated lagoons, and eolian environments may extend to the shelf margin. Eolian siliciclastics deposited during lowstand were reworked during transgressions into broad sand sheets that occur over large areas of the shelf prior to establishment of carbonate depositional environments during subsequent sea-level highstand.

SEQUENCE STRATIGRAPHY OF THE ARTESIA GROUP

Sequence stratigraphy is a method of interpreting stratigraphic development within the context of relative sea-level change. A stratigraphic sequence is an unconformity-bounded package of genetically related strata deposited during a single cycle of sea-level rise and fall, where unconformities record periods of sea-level lowstand. No cycle order (length or time scale) is implicit in the definition of a sequence; however, the most readily recognized unconformities (sequence boundaries) are regionally extensive and record prolonged erosion on the shelf and coastal plain during sea-level falls of relatively high magnitudes. Cyclic strata (parasequences or high-frequency cycles) within sequences record deposition during higher frequency, relative sea-level rises and falls of lower magnitude than those that promote unconformity development. High-frequency cycles are organized into coeval sedimentary facies, or system tracts, that record lateral distribution of depositional environments. System tracts include those deposited during sea-level lowstands (LST), transgressions (TST), and highstands (HST). Sequence boundaries, submarine fans, and lowstand wedges develop within the LST. Marine flooding surfaces (transgressive and maximum flooding surfaces) and overlapping high-frequency cycles on the

shelf are indicative of the TST. Sedimentary aggradation on the shelf and progradation of shelf facies tracts are indicative of the HST.

Variations in stratal thickness are limited by accommodation space or the volume available for accumulation of sediment. Accommodation is greatest during sea-level highstands and lowest or absent during lowstands. Changes in local sea level result from combinations of eustatic and local to regional tectonic (uplift and subsidence) processes. Glacio-eustatic cycles are fairly well documented for more recent Earth history and for certain periods during late Precambrian, Late Ordovician, Pennsylvanian, and mid-Permian time. Similarly, most agree that worldwide cyclic depositional signals were controlled by late Cenozoic glacial cycles. However, little evidence of glaciations has been recognized for many other periods for which sea-level related cyclic geologic sections are abundant. The Late Permian is a time of abounding cyclic deposition for which significant glacial features have not been recognized. Nonetheless, orbitally forced climatic models are often evoked to tentatively date depositional-cycle periodicity throughout the Permian record (for example, for the Yates in the Permian Basin; Borer and Harris, 1991). Increases in seafloor spreading rates and ridge lengths are also hypothesized to potentially produce the magnitudes of sea-level variation interpreted from the geologic record. Different processes are conjectured to produce cycles of different periodicities. Hallam (1992) provided a good summary of issues and theories concerning sea-level change and the geologic record.

Two general sequence stratigraphic models are popular today: one developed at Exxon that systematically groups strata between unconformities or hiatal surfaces developed during sea-level lowstands (Vail and others, 1977) and another that groups strata between widespread maximum flooding surfaces (Galloway, 1989). The Exxon approach has been most commonly used in the Permian Basin. It is particularly viable there because a large part of the stratigraphic section includes carbonates upon which erosional unconformities (type 1 sequence boundaries) are frequently recognized. The Galloway model has been used extensively on the Gulf Coast, where siliciclastics are the most abundant sediment type and unconformities are generally difficult to recognize.

So-called third-order (Vail and others, 1977) or composite (Kerans and Kempter, 2002) sequence boundaries are at the approximate vertical scale of formations. However, sequence boundaries are not necessarily reflected in historically recognized formation boundaries. For

example, in the outcrop-based (Guadalupe Mountains) analysis of Kerans and Kempter (2002), boundaries between the Queen and Seven Rivers Formations, between the Seven Rivers and Yates Formations, and between the Tansill and Salado Formations are also boundaries between composite sequences. However, another sequence boundary divides the Yates into lower and upper parts. The lower Yates composes a single composite sequence (CS-13), whereas the upper Yates and the Tansill Formations compose CS-14 (fig. 2).

Higher order (presumably fourth- and fifth-order) cycles compose composite sequences. At this level of resolution, Kerans and Kempter (2002) divided the Queen into two sequences (Q1, Q2), the Seven Rivers into four sequences (Sr1-4), the Yates into five sequences (Y1-6), and the Tansill into two sequences (T1, T2). Mazzullo's analysis (1999) of the Tansill exposure in Dark Canyon (Guadalupe Mountains) demonstrates how sequences are identified. Two sequences were recognized by Mazzullo (1999) in the Tansill section on the basis of biotic diversity, parasequence thickness, and facies-stacking patterns. The boundary between them was suggested to be at or near the base of the Ocotillo Member (fig. 2). Maximum flooding of the platform occurred during deposition of sequence 1 in the lower part of the middle Tansill. Environments were biostromes, mainly high-energy, shallow subtidal packstones and grainstones and associated peritidal islands in the early highstand system tract in this sequence.

Borer and Harris (1991) suggested that the Yates Formation on the Northwest Shelf and Central Basin Platform composed one third-order sequence that encompassed as many as 22 high-frequency (fifth-order) cycles bundled into five lower (fourth-) order cycles. They suggested that the Yates was deposited over 1.5 to 2 m.y. and that depositional cyclicity reflected orbitally forced sea-level or climatic variations of 100- and 400-ky periodicity (orbital eccentricity cycles in Milankovitch climate theory). In the view of Borer and Harris (1991), the lower part of the Yates records a third-order sea-level rise and the upper part records a third-order sea-level fall. The magnitude of fourth- and fifth-order sea-level oscillation affected the relative prominence of carbonate, evaporite, and siliciclastic facies; third-order sea-level rise produced a greater abundance of carbonate in the lower part of the Yates, whereas third-order sea-level fall produced proportionally more siliciclastic facies in the upper part (Borer and Harris, 1991). Vertical trends of cycle thickness are also affected. Thicknesses might be expected to decrease in sequential sedimentary cycles (fig. 20) because higher-order cyclic accommodation volumes at any given location are progressively reduced overall during the third-

order sea-level fall. Cycle boundaries may be difficult to recognize in units where sequence boundaries occur within siliciclastic intervals, however, and the result may be apparent deviations from the upward pattern of cycle thinning. Occurrences of intraclasts in siliciclastic intervals may be at sequence boundaries, on maximum flooding (ravinement) surfaces (as interpreted for fig. 24), or they may simply be channel deposits within a cycle. The example in figure 24 is interpreted as a ravinement surface because it is near the top of a siliciclastic interval (TST) that underlies a carbonate interpreted as part of the HST.

It is noteworthy that Kerans and Kempter (2002) interpreted the Yates in the Guadalupe Mountains to contain a third-order (composite) sequence boundary within the formation (fig. 2).

STRUCTURE OF THE ARTESIA GROUP AND CONTROLS OF INTERVAL THICKNESS

Formation isopach maps show similar regional thickness distributions for all Artesia Formations and reflect the regional structural configuration of the Permian Basin. Units thin from the Midland Basin onto its northern and eastern shelves and onto the Central Basin Platform. On the Northwest Shelf, units are thickest in the near-back-reef zone and thin onto the platform. Rates of shelfward unit thinning are greater along the west edge of the Central Basin Platform than on the Northwest Shelf, probably because of a steeper shelf-to-basin profile that was maintained along the margin of the Central Basin Platform (Borer and Harris, 1991). Ranges of formation thickness are noted in the sections for each formation.

Structural patterns are similar for all Artesia Group formations. The primary structural element is the down-to-the-basin dip of strata that is the primary control on migration of hydrocarbons from basinal source beds into reservoirs that are developed on the surrounding shelves. Field-scale structures are common to most fields and reflect deep-seated structural elements that are reflected on pre-Permian surfaces. Documented examples of stratigraphically persistent field-scale structures include Keystone field in Winkler County, where Guadalupian-productive anticlinal structure can be mapped on horizons as deep as the top of the Ellenburger, where it is interpreted as a faulted anticline (fig. 25) (Galloway and others, 1983). North Ward-Estes (Ward County) resides on a north-northwest-trending anticline located along the west margin of the Central Basin Platform in Ward County, which can be mapped for more than 13 mi (21 km) (fig. 26). Means field on the northeast edge of the Central Basin Platform in Andrews

County contains two domal anticlines (fig. 27) (Price and others, 2000). At Yates field in Pecos County the geometry of the southeast corner of the Central Basin Platform is reflected in Guadalupian stratal structure (fig. 28) (Craig, 1988). Concho Bluff and North Concho Bluff fields are located on two anticlinal noses on the east-central edge of the Central Basin Platform in Crane, Ector, and Upton Counties (Mazzullo and others, 1992) (fig. 29). The McFarland-Magutex field area is developed on an anticlinal nose on the northeast edge of the Central Basin Platform (fig. 30) (Holtz, 1993). The stratigraphic persistence of structures and apparent syntectonic deposition in Upper Guadalupian units suggest that tectonic movement of structural elements continued throughout the Late Permian.

Smaller-scale structures are present in some fields that are limited to various Permian horizons. These are most likely to reflect local carbonate or evaporite dissolution episodes. Two notable examples occur in Yates field and North Ward-Estes field. At Yates field the top of the San Andres was heavily karsted during emergence of the San Andres platform, thus creating topography that is reflected in overlying Grayburg, Queen, and Seven Rivers horizons (fig. 28B) (Craig, 1988). In places more stratigraphically limited, effects may be observed. In North Ward-Estes, Andreason (1992) mapped locally thinned areas (fig. 31) that he interpreted on the basis of observations of brecciated intervals in core, as resulting from sulfate dissolution. An isopach map of the overlying sandstone interval (discussed briefly later) indicates local structural depressions in the karst-affected area.

Control of interval thickness by field-scale structure has been documented. Productive Queen Colby sandstone units in Keystone field pinch out onto an anticline within the field, thus suggesting structure-controlled sand accumulation (fig. 25D) (Major and Ye, 1992, 1997). Concho Bluff and North Concho Bluff fields (discussed briefly earlier) are marked by thinning of evaporites onto anticlinal noses (fig. 29D). A stronger case can be made for thinning of siliciclastic units onto the main structure in the center of the field (fig. 29C). At Means field, west of and adjacent to McFarland field, cross sections of Queen sandstone show thinning of sandstone intervals onto the structural domes (Galloway and others, 1983). At North Ward-Estes field Andreason (1992) observed that locations of sulfate-dissolution thinning of one dolomite-bearing interval coincide with thickening in the overlying siliciclastic-dominated interval (fig. 31), thus establishing relative timing of the dissolution event and deposition of the Strays unit. Karsting of the emergent San Andres surface at Yates field modified structure-influenced

topography that affected thickness distributions in several overlying units (fig. 28B, C, D) (Spencer, 1987; Craig, 1988). The effect can be observed in individual facies as well. For example, thickness trends of the basal Seven Rivers anhydrite interval (fig. 28D) (Spencer, 1987) mimic those of the Grayburg and Queen Formations, which themselves show thickness relationships to the topography developed by dissolution on the top of the San Andres (fig. 28B) (Craig, 1988).

RESERVOIR DEVELOPMENT

Most middle and upper Artesia Group platform oil reservoirs are assigned to either the Queen Tidal-Flat Sandstone (eastern side of the Central Basin Platform) or Artesia Platform Sandstone Play (west side of the Central Basin Platform) (Dutton and others, 2005). These reservoirs are mainly productive from siliciclastics of the Queen and Yates Formations, although Seven Rivers sandstone also contributes in many fields. Dolostones of the Queen, Seven Rivers, Yates, and Tansill Formations form secondary reservoirs. Production from the dolostones is generally commingled with production from sandstone reservoirs.

Not all reservoirs for which plays are named (for example, Grayburg High-Energy Platform Carbonate—Ozona Arch Play) produce only in those plays. For example, Farmer field (Grayburg High-Energy Platform Carbonate—Ozona Arch Play) also produces from the lower Queen (Bebout, 1994). Similarly, the main reservoir at Shafter Lake (Queen Tidal-Flat Sandstone Play) is the Yates (Dutton and others, 2005). According to Dutton and others (2005), 94 reservoirs had produced more than 2,035 MMbbl of oil from the two Upper Permian sandstone plays through 2002. Many of these fields produce from multiple Artesia Group formations (including Grayburg carbonate), and a few include San Andres carbonate. Production from these other reservoirs is included in cumulative production figures.

Yates reservoirs are especially noted for gas production and are classified in the Upper Guadalupian Platform Sandstone Play (Kosters and others, 1989). In a survey of Texas fields whose reservoir name specified Yates as the primary productive interval, 1,295 wells were listed as producing from 88 reservoirs. Of these wells, 69 percent are classified as gas producers (Railroad Commission of Texas, 2003).

Reservoir Distribution

Hydrocarbon production from upper Guadalupian shelf strata largely occurs from Northwest Shelf and Central Basin Platform carbonate and siltstone that lie between the Goat

Seep/Capitan reefs and evaporitic lagoons (Ward and others, 1986; Dutton and others, 2005). A few more occur on the Northern Shelf, Ozona Arch, and Eastern Shelf. They are positioned in shelf-margin-aligned belts generally upslope of the carbonate depositional environments that mark the shelf margins during sea-level highstands.

More than one Artesia Group formation may be productive in some fields. It is common for either or both the Seven Rivers and Tansill to provide secondary production in a field where the Yates is the primary reservoir. North Ward-Estes field on the west margin of the Central Basin Platform, for example, produces from both the Yates and Seven Rivers Formations (Ward and others, 1986). Generally, productive reservoirs are at progressively higher stratigraphic positions as the platform is traversed from east to west toward the Delaware Basin or north to south on the Northwest Shelf, reflecting the progradational character of the Artesia Group (Ward and others, 1986).

Trapping Mechanisms

Most Upper Permian hydrocarbon shelf reservoirs are developed in porous sandstone and siltstone (mainly in the Queen and Yates Formations, but also in the Seven Rivers sandstone locally) that were deposited on the back-reef middle shelf. Porous carbonate, especially the Tansill (Ward and others, 1986) forms secondary reservoirs locally, although more often carbonate is relatively impermeable and forms sandstone-reservoir top seals. Reservoirs are plugged along their updip extents by impermeable evaporites, mainly anhydrite. Evaporite and impermeable carbonate form reservoir-specific top seals over large areas. Regionally extensive Salado evaporites, where still present following regionwide dissolution of upper parts of the interval, provide a basinwide top seal (Hills, 1984). Source beds are most probably organic-rich deposits in the adjacent basinal areas, especially the Delaware Basin (Hills, 1984).

The basinward dip of reservoir strata provides the primary structural control on hydrocarbon migration and accumulation. Field-specific focusing of hydrocarbon migration and entrapment for shelf units is provided by anticlines. Prominent examples include the Keystone Colby reservoir that formed over a deep-seated faulted anticline on the west margin of the Central Basin Platform in Winkler County (fig. 25) (Galloway and others, 1983; Ward and others, 1986; Major and Ye, 1992, 1997); North Ward-Estes field that formed over a strike-elongate anticline on the west flank of the Central Basin Platform in Ward County (fig. 26) (Ring and Smith, 1995); Means field that formed over two north-south-aligned domes on the northeast

margin of the Central Basin Platform in Andrews County (fig. 27) (Price and others, 2000); Yates field that formed over an apparently folded, U-shaped anticline in Pecos County (fig. 28); and Concho Bluff and Concho Bluff North, located over structural noses (fig. 29) in Upton, Crane, and Ector Counties, and McFarland Queen reservoir, which formed over an east-dipping structural nose on the northeast margin of the Central Basin Platform in Andrews County (fig. 30) (Holtz, 1993).

The following summary of Artesia reservoirs in Texas is based on a Railroad Commission of Texas Annual Report (2003) list of reservoirs for which entries designate a specific reservoir in the field name (table 2). There are at least 41 Queen reservoirs, all located on the Central Basin Platform; at least 7 Seven Rivers reservoirs located on the Central Basin Platform and 1 on the Eastern Shelf; at least 72 Yates reservoirs located on the Central Basin Platform, 11 on the Northern Shelf (east and northeast of Seminole), 2 on the Eastern Shelf, and 3 on the Ozona Arch in the south part of the Midland Basin; and at least 9 Tansill reservoirs, all on the Central Basin Platform in Pecos County, Texas. Comprehensive data on all Artesia Group reservoirs on the Northwest Shelf in New Mexico were unavailable for this report. Of the larger reservoirs (cumulative production >1 MMbbl), however, 24 are in the Queen, 18 are in the Seven Rivers, 15 are in the Yates, and 1 is in the Tansill (Dutton and others, 2005).

Table 2. Numbers of Upper Guadalupian reservoirs in Texas and New Mexico, sorted by reservoir. Texas values were summarized by the author from the annual report of the Railroad Commission of Texas (2003); New Mexico values are from Dutton and others (2005).

Texas reservoir	CBP	E Shelf	N Shelf	Ozona Arch	Reservoir total
Queen	41	0	0	0	41
Seven Rivers	7	1	0	0	8
Yates	72	2	11	3	88
Tansill	9	0	0	0	9
Total					146
NM reservoir	NW Shelf				
Queen	24*				
Seven Rivers	18*				
Yates	15*				
Tansill	1*				
Total					16*

*Cumprod >1 MMbbl

Reservoir Examples

The McFarland Queen reservoir (fig. 30) in Andrews County, the most productive field in the Queen Tidal-Flat Sandstone Play, produces from two sandstones in the lower Queen Formation (fig. 30B) (Tyler and others, 1991; Holtz, 1994). The sandstones, which form the bases of progradational, upward-shoaling cycles, were deposited in intertidal-flat tidal-channel, and shoreface environments. They are overlain by supratidal dolomudstones and massive anhydrite at the top (Holtz, 1994). Production is highest where the sandstones are thickest, in areas interpreted to be tidal-channel deposits. Porosity ranges from 11 to 24 percent and averages 12 percent; permeability ranges from 3 to 24 md ($3 \text{ to } 24 \times 10^{-3} \mu\text{m}^2$) and averages 12 md ($12 \times 10^{-3} \mu\text{m}^2$) (Holtz, 1994). A structural nose focused hydrocarbon migration into the field (fig. 30A).

The North Ward-Estes reservoir (fig. 32) in Ward County, the most productive field in the Artesia Platform Sandstone Play, produces from the Yates, Queen, and Seven Rivers Formations (Andreason, 1992; Eide and Mazzullo, 1993; Bain, 1994; Mazzullo and others, 1996). Most of the production is from nine very fine grained sandstone and siltstone reservoirs in the Yates Formation that are interbedded with low-permeability dolomite seals (Ring and Smith, 1995; 13B; table 1). The sandstone reservoirs comprise marine-reworked-eolian or late-highstand-lagoonal siliciclastic components of fifth-order depositional sequences. Hydrocarbon migration was focused into a strike-elongate anticline that lies at the crest of a basinward-dipping structural monocline.

The reservoir interval at Concho Bluff and North Concho Bluff fields is on the east edge of the Central Basin Platform in Crane and Upton Counties and consists of several sandstone beds that are interbedded with thin anhydrite and salt in the upper Queen Formation (Mazzullo and others, 1992; Lufholm and others, 1996) (fig. 29). The depositional setting was a broad, low-relief shelf where lowstand fluvial and associated clastics interfingered with highstand evaporite deposits. Mazzullo and others (1992) argued that the siliciclastics are marked by little, if any, marine reworking. Permeability in the reservoir sandstones ranges from 1 to 1,200 md ($1 \text{ to } 1,200 \times 10^{-3} \mu\text{m}^2$) and averages 70 md ($70 \times 10^{-3} \mu\text{m}^2$); porosity ranges from 9 to 26 percent and averages 16 percent (Mazzullo and others, 1992). Structural position and porosity distribution, rather than net sandstone thickness, are the primary controls on production at Concho Bluff and North Concho Bluff fields (fig. 29).

The Keystone Colby reservoir, located on the northwest edge of the Central Basin Platform (Winkler County), encompasses 16 mi² and comprises five productive, massive, arkosic sandstone intervals (fig. 25) that are interbedded with nonproductive, low-porosity dolomite and anhydritic dolomite (Major and Ye, 1992, 1997). Colby reservoir rocks are interpreted as having been deposited in a lagoonal setting behind a carbonate-rimmed bank margin in a series of upward-shoaling cycles composed of sandstone and dolomite. During sea-level highstands, the lagoon was flooded, and carbonate sediments were deposited. During sea-level lowstands, the lagoonal carbonate sediments probably were exposed and subjected to karst processes (Major and Ye, 1992, 1997). As sea level rose again, windblown sand was deposited in marine and peritidal environments in the lagoon. The most porous sandstones are interpreted as having been deposited in relatively shallow marine water (Major and Ye, 1992, 1997).

Opportunities for Additional Resource Recovery

For the Queen Tidal-Flat and Artesia Platform sandstone plays, remaining reserves are estimated to be 69 MMbbl (Dutton and others, 2005). The Upper Guadalupian Plays in the Permian Basin are in a mature stage of development, and few new fields have been discovered recently (Dutton and others, 2005). For example, Yates reservoir discovery peaked in the 1970's (fig. 33A), annual gas and oil production rates are in steep decline (fig. 33B), and many fields have been in EOR for some time. Even the most optimistic forecasts suggest that Yates gas production will decline to 50 percent of present rates by 2025 (fig. 33C) (Combs and others, 2003). Recovery efficiencies range from 29 to 47 percent, with the high value coming from North Ward-Estes; however, most fields average about 30 percent (Galloway and others, 1983).

Some fields have been in waterflood since the 1960's. For example, Means field initiated waterflooding in late 1961; daily oil production increased sixfold over the next year and ninefold over 4 years. Two Upper Guadalupian reservoirs (at Yates and North Ward-Estes fields) have been flooded with CO₂ (Mark Holtz, personal communication), and CO₂ injection may become more economically viable in the future. Traditional application of field extension and infill drilling methods will also play a role in continued production from Upper Guadalupian reservoirs, as well as development of secondary or tertiary reservoirs that were not economically viable in the past. In some cases productive intervals may have been bypassed in wells drilled to deeper targets. Sandstone porosity ranges from 6 to 19 percent. Major and Ye (1992, 1997) noted

that several thick, potentially productive sandstone units in Keystone Colby field are not open to many well bores.

OCHOAN SERIES ON THE PERMIAN BASIN SHELF

The Ochoan in the Permian Basin contains no hydrocarbon reservoirs on the shelf, although basal Ochoan evaporites form the ultimate top seal for underlying Guadalupian reservoirs. Therefore, the following discussion will be introductory and brief. Superposition of the Salado Formation evaporites on the top of the Guadalupian Series (fig. 2) effectively inhibits hydrocarbon migration into Ochoan units, and lack of a seal above the Ochoan precludes widespread entrapment within the interval of hydrocarbons that may have been generated within the series. Drilling through the Ochoan to deeper reservoirs in the immediate vicinity of the WIPP salt-hosted nuclear-waste repository in Eddy County (near Carlsbad, New Mexico) is prohibited because of potential compromise of seal integrity at the site.

Units that compose the Ochoan Series on the shelf and Midland Basin include, from oldest to youngest, the Salado, Rustler, and Dewey Lake Formations. The Salado is locally more than 2,800 ft (853 m) thick and was named by Lang (1935) for a halite-rich interval that he originally designated in 1923 as the upper part of the Castile Formation. The upper Castile unit was differentiated from the lower part (still called Castile) by overall color, shale content, and K₂O concentration. The older terminology continued to be used for a while thereafter (for example, Page and Adams, 1940). The Castile of present usage is restricted to the Delaware Basin (Adams, 1944) and will not be discussed further here except to indicate that it is considered to be the top seal for Delaware Basin hydrocarbon reservoirs and ultimately responsible for controlling migration of hydrocarbons from basinal source beds into reservoirs on the surrounding shelves (Hills, 1984). The Rustler is locally more than 500 ft (152 m) thick and was named by Richardson (1904) for an incomplete section of magnesian limestone and siliciclastics that overlies the Castile Gypsum (currently called Salado) in Culberson County. A description of a complete subsurface section was provided by Adams (1944) that included stratigraphically and geographically varying intervals of dolomite, evaporites, and clastics. The Dewey Lake Formation, locally more than 350 ft (107 m) thick, was named by Page and Adams (1940) and further described by Giesey and Fulk (1941) for redbeds and minor gypsum that overlie the Rustler and underlie Triassic redbeds in the Midland Basin. Miller (1966) recognized

the Pierce Canyon Formation in the Delaware Basin as equivalent to the Dewey Lake. The Dewey Lake/Pierce Canyon and stratigraphically younger but superficially similar Triassic redbeds are distinguished locally by mineralogic similarity of the Dewey Lake/Pierce Canyon to underlying Upper Permian siliciclastics; occurrence of anhydrite cement in the Permian interval; deeper red color, higher gypsum content, and wider textural range in the basal Triassic beds; and a zone of bleaching at the interpreted Permian-Triassic unconformity.

Most interest concerning the Ochoan has been related to the role of the Salado (1) as a potash resource (for example, Udden, 1915; Schaller and Henderson, 1932; Lang, 1942; Jones, 1954, 1972; Adams, 1969; Hiss, 1976; Cheeseman, 1978; Lowenstein, 1982, 1988; Bachman, 1984; Harville and Fritz, 1986; Holt and Powers, 1987; Stein and Krumhansl, 1988; and Barker, 1993, 1999); (2) as a nuclear-waster repository (for example, the more recent include Brookins, 1990; Stormont, 1990; Milligan, 1991; Chaturvedi, 1996; Borns, 1997; Hurtado, 1997; Weart, 1997; Holt, 1999; Beauheim, 2002; Snow, 2002; Powers and others 2003; and Brush, 2004), and (3) because Salado halite dissolution may underpin topographic development and surface-water salinization in the region, especially in the High Plains (for example, Johnson, 1901; Baker, 1915; Gustavson and others, 1985; Baumgardner and others, 1982; Goldstein and Collins, 1984; Gustavson and Finley, 1985; and Dutton, 1987, among others).

Steiner (2001) used the Dewey Lake and Rustler Formations for magnetostratigraphic analyses, and Fracasso and Kolker (1985) and Kolker and Fracasso (1985) dated Dewey Lake (Midland Basin and Texas Panhandle) volcanic ash to determine absolute ages for part of the Upper Permian section. Miller performed the most comprehensive analysis of the Pierce Canyon (apparent Dewey Lake equivalent in the Delaware Basin), where he described petrographic affinities to other Upper Permian siliciclastic intervals in the region and developed criteria for distinguishing the Pierce Canyon from overlying Triassic strata of similar appearance. Several theses and dissertations have dealt with the Ochoan evaporites, including Snider (1966) and Hovorka (1990).

SUMMARY AND CONCLUSIONS

The Artesia Group of the Permian Basin comprises a diverse assemblage of carbonate, evaporite, and siliciclastic facies that occur in stratigraphically cyclic packages and record deposition in marginal marine and terrestrial environments in a region characterized by climatic

aridity. Gamma-ray logs can be used readily to differentiate pure carbonate, anhydrite, and halite facies from sandstone facies, wherein siliciclastics are notably more radioactive because they contain abundant potassium in the form of K-feldspar and K-bearing clay. Differentiation of halite from anhydrite and dense carbonate is significantly facilitated by availability of density, acoustic, and caliper logs. The Artesia Group consists of two broad paleo-geographic realms: (1) back-reef, shallow subtidal, intertidal, and peritidal environments and (2) terrestrial evaporitic, fluvial, and eolian environments. In near-reef areas on the shelf, sea-level lowstand terrestrial deposits are largely reworked by transgressive marine processes, whereas original terrestrial character may be preserved in areas farther shelfward. Interval thicknesses are controlled mainly by accommodation volumes that reflect relative sea-level changes; however, preexisting topography that reflects either or both deep-rooted structural movements and erosional processes locally affects unit thickness and facies distributions. Patterns of stratigraphic cyclicity record systematic variations in sediment accommodation volumes, salinity, and siliciclastic sediment supply; however, the relative importance of controls by eustatic sea level, tectonism, or climatic variation remains difficult to assess. Primary hydrocarbon reservoirs are developed in well-sorted fine to very fine sandstone units with interparticle porosity that were deposited in middle-shelf positions; secondary reservoirs occur locally in grain-rich carbonate units that are characterized by interparticle or moldic porosity. The Yates and Queen Formations contain the most prolific reservoirs. Younger reservoirs tend to be located basinward of older ones, thus reflecting overall progradation of the Guadalupian reef complex and Guadalupian shelf. Traps are mainly stratigraphic: updip porosity pinch-outs arise from porosity occlusion by anhydrite and top seals are composed of impermeable carbonate and evaporite. Most reservoirs also have structural components, including (1) regional basinward stratal tilt and (2) draping of productive units on deep-rooted anticlines. Systematic thickness variations in many instances reflect structural configurations and indicate that syndepositional tectonic movements persisted through the Late Permian.

Although many common elements of Artesia facies and diagenesis can be abstracted from existing core investigations, additional rock- and well-log-based studies are needed to adequately characterize regional and field-scale facies distributions and controls on reservoir-related porosity and permeability distribution if more effective methods for targeting remaining oil in these reservoirs are to be developed.

The Castile Formation of the Delaware Basin and regionally extensive Salado Formation of the Ochoan Series include thick evaporite deposits and record a long-term salinity crisis in the region. Positioned above the Salado, the Rustler carbonates, evaporites, and siliciclastics mark a relatively abbreviated return of marginal-marine conditions to the region. The Dewey Lake (Midland Basin) and Pierce Canyon Formations (Delaware Basin) mark the youngest episode of preserved Permian deposition in the region, after which a significant net-depositional hiatus prevailed until onset of Late Triassic Lower Dockum Group accumulation. A few sparsely productive, shallow Ochoan reservoirs have been discovered, mainly in the Castile and Rustler. The most important capacity of the Ochoan Series, however, is the dual function of its laterally extensive evaporites as a regional top seal for the underlying Guadalupian reservoir complex and as a guide for hydrocarbon migration from basinal sources into reservoirs situated on the shelves. At present, there appears to be little incentive for exploring potential Ochoan hydrocarbon targets.

ACKNOWLEDGMENTS

This report was funded by the U.S. Department of Energy. Discussions with Bureau researchers Susan Hovorka regarding core interpretations, Steve Ruppel regarding concepts of depositional cyclicity, and Mark Holtz regarding reservoir geology and EOR in the Permian Basin significantly contributed to the content of this report.

REFERENCES AND RELATED READING

- Achauer, C. W., 1969, Origin of Capitan Formation, Guadalupe Mountains, New Mexico and Texas: American Association of Petroleum Geologists Bulletin, v. 53, no. 11, p. 2314–2323.
- Achauer, C. W., 1971, Origin of Capitan Formation, Guadalupe Mountains, New Mexico and Texas; reply: American Association of Petroleum Geologists Bulletin, v. 55, no. 2, p. 313–315.
- Adams, J. E., 1944, Upper Permian Ochoa series of Delaware Basin, West Texas and southeastern New Mexico: American Association of Petroleum Geologists Bulletin, v. 28, no. 11, p. 1596–1625.
- Adams, S. S., 1969, Bromine in the Salado Formation, Carlsbad potash district, New Mexico: New Mexico Bureau of Mines & Mineral Resources Bulletin.
- Ali, Eram, 1996, Magnolia Sealy (Yates) field, *in* Dull, Dennis, and Garber, Ray, eds., Oil and gas fields in West Texas; volume VII: West Texas Geological Society Publication, v. 96-99, p. 107–111.
- Ali, Eram, 1996, Spencer (Yates) field, *in* Dull, Dennis, and Garber, Ray, eds., Oil and gas fields in West Texas; volume VII: West Texas Geological Society Publication, v. 96-99, p. 183–188.
- Andreason, M. W., 1992, Coastal siliciclastic sabkhas and related evaporative environments of the Permian Yates Formation, North Ward-Estes Field, Ward County, Texas: American Association of Petroleum Geologists Bulletin, v. 76, no. 11, p. 1735–1759.
- Bachman, G. O., 1953, Geology of a part of Mora County, New Mexico: United States Geological Survey, Oil and Gas Investigations OM 137.
- Bachman, G. O., 1984, Regional geology of Ochoan evaporites, northern part of Delaware Basin: New Mexico Bureau of Mines and Mineral Resources Circular, v. 184.
- Bain, R. C., 1994, North Ward-Estes (Yates, Seven Rivers, Queen), *in* Oil and gas fields in West Texas: West Texas Geological Society Publication, v. 6, p. 275-279.
- Baker, C. L., 1915, Geology and underground waters of the northern Llano Estacado: University of Texas, Austin, Bulletin 57, 93 p.
- Baker, S. G., 1990, Depositional environment of the Yates Formation in Kermit Field, Winkler County, Texas: American Association of Petroleum Geologists Bulletin, v. 74, no. 5, p. 604.

- Ball, S. M., Roberts, J. W., Norton, J. A., and Pollard, W. D., 1971, Queen Formation (Guadalupian, Permian) outcrops of Eddy County, New Mexico, and their bearing on recently proposed depositional models: *American Association of Petroleum Geologists Bulletin*, v. 55, no. 8, p. 1348–1355.
- Barker, J. M., 1993, Economic geology of the Carlsbad potash district, New Mexico: *New Mexico Geological Society Guidebook*, v. 44, p. 283–291.
- Barker, J. M., 1999, Overview of the Carlsbad potash district, New Mexico: *New Mexico Bureau of Mines and Mineral Resources Circular*, p. 7–16.
- Baumgardner, R. W., Jr., Hoadley, A. D., and Goldstein, A. G., 1982, Formation of the Wink Sink, a salt dissolution and collapse feature, Winkler County, Texas: *The University of Texas at Austin, Bureau of Economic Geology Report of Investigations No. 114*, 38 p.
- Beauheim, R. L., 2002, Hydrology and hydraulic properties of a bedded evaporite formation: *Journal of Hydrology*, v. 259, no. 1–4, p. 66–88.
- Bebout, D. G., 1994, Farmer (Grayburg) field, *in* Pausé, P., and Entzminger, D., eds., *Oil and gas fields in West Texas*, symposium volume VI: *West Texas Geological Society Publication No. 94-96*, p. 61–69.
- Bebout, D. G., Kerans, C., and Harris, P. M., 1993, Introduction, *in* Bebout, D. G., and Kerans, C., eds., *Guide to the Permian Reef geology Trail, McKittrick Canyon, Guadalupe Mountains National Park, West Texas*: *The University of Texas at Austin, Bureau of Economic Geology, Guidebook 26*, p. 1–4.
- Bebout, D. G., and Meador, K. J., 1985, Regional cross sections—Central Basin Platform, West Texas: *The University of Texas at Austin, Bureau of Economic Geology*, 11 plates.
- Biggers, Barbara, 1984, Reef to back-reef microfacies and diagenesis of Permian (Guadalupian) Tansill-Capitan transition, Dark Canyon, Guadalupe Mountains, New Mexico: *American Association of Petroleum Geologists Bulletin*, v. 68, no. 4, p. 454–455.
- Biggers, Barbara, 1985, Reef to back-reef facies and diagenesis of the (Guadalupian) Tansill-Capitan formations in Dark Canyon, Guadalupe Mountains, New Mexico, *in* Pausé, P. H., ed., *Permian carbonate/clastic sedimentology, Guadalupe Mountains; analogs for shelf and basin reservoirs*: *Society of Economic Paleontologists and Mineralogists, Permian Basin Section*, p. 15.
- Blakey, Ron, 2004, Paleogeographic reconstructions, University of Arizona, <http://jan.ucc.nau.edu/~rcb7/270NAt.jpg>
- Borer, J. M., and Harris, P. M., 1989, Depositional facies and cycles in Yates Formation outcrops, Guadalupe Mountains, New Mexico, *in* Harris, P. M., and Grover, G. A., eds., *Subsurface and outcrop examination of the Capitan shelf margin, northern Delaware*

- Basin: Society of Economic Paleontologists and Mineralogists Core Workshop, v. 13, p. 305–317.
- Borer, J. M., and Harris, P. M., 1990, Cyclostratigraphy and duration of the Yates Formation (Permian, late Guadalupian) of the Permian Basin: American Association of Petroleum Geologists Bulletin, v. 74, no. 5, p. 614–615.
- Borer, J. M., and Harris, P. M., 1991, Lithofacies and cyclicity of the Yates Formation, Permian Basin; implications for reservoir heterogeneity: American Association of Petroleum Geologists Bulletin, v. 75, no. 4, p. 726–779.
- Borer, J. M., and Harris, P. M., 1993, Depositional facies, cyclicity, and stratigraphic computer modeling of the upper Guadalupian Yates Formation, U.S. Permian Basin, *in* Glass, Don ed., Carboniferous to Jurassic Pangea, First International Symposium; program and abstracts: Canadian Society of Petroleum Geologists, p. 30.
- Borns, D. J., 1997, History of geophysical studies at the Waste Isolation Pilot Plant (WIPP), southeastern New Mexico, *in* Proceedings of the Symposium on the Application of Geophysics to Environmental and Engineering Problems, v. 1997, p. 1–10.
- Brister, B. S., and Ulmer-Scholle, Dana, 2000, Interpretation of depositional environments of upper Seven Rivers Formation from core and well logs, Grayburg Jackson Pool, Eddy County, New Mexico, *in* DeMis, W. D., Nelis, M. K., and Trentham, R. C., eds., The Permian Basin: proving ground for tomorrow's technologies: West Texas Geological Society Publication, v. 00-109, p. 65–72.
- Brookins, D. G., Authigenic clay minerals in the Rustler Formation, WIPP site area, New Mexico: Materials Research Society Symposia Proceedings, v. 176, p. 665–672.
- Brush, L. H., 2004, Overview of near-field geochemical processes and conditions expected in the WIPP: Geological Society of America Abstracts with Programs, v. 36, no. 5, p. 108.
- Candelaria, M. P., 1989, Shallow marine sheet sandstones, upper Yates Formation, northwest shelf, Delaware Basin, New Mexico, *in* Harris, P. M., and Grover, G. A., eds., Subsurface and outcrop examination of the Capitan shelf margin, northern Delaware Basin: Society of Economic Paleontologists and Mineralogists Core Workshop, v. 13, p. 319–324.
- Casavant, R. R., 1988, Reservoir geology and paleoenvironmental reconstruction of Yates Formation, Central Basin platform, West Texas: American Association of Petroleum Geologists Bulletin, v. 72, no. 2, p. 169.
- Changsu, Ryu, 2002, Sequence stratigraphic controls of hydrocarbon reservoir architecture; case study of Late Permian (Guadalupian) Queen Formation, Means Field, Andrews County, Texas: Texas A&M University, Ph.D. dissertation.

- Chaturvedi, Lokesh, 1993, WIPP-related geological issues: New Mexico Geological Society Guidebook, v. 44, p. 331–338.
- Chaturvedi, Lokesh, 1996, Issues in predicting the long-term integrity of the WIPP site: Eos, Transactions, American Geophysical Union, v. 77, no. 46, Supplement, p. F19–F20.
- Cheeseman, R. J., 1978, Geology and oil/potash resources of Delaware Basin, Eddy and Lea counties, New Mexico, *in* Austin, G. S., ed., Geology and mineral deposits of Ochoan rocks in Delaware Basin and adjacent areas: New Mexico Bureau of Mines and Mineral Resources Circular, No. 159, p. 7–14.
- Combs, D. M., Kim, E. M., and Hovorka, S. D., 2003, Stratigraphic characterization of the Yates Formation, Permian Basin, Texas, *in* Hunt, T. J., and Luftholm, P. H., eds., The Permian Basin: back to basics: West Texas Geological Society Publication No. 03-112.
- Craig, D. H., 1985, Paleokarst in the San Andres dolomite, Yates field, West Texas: Society of Economic Paleontologists and Mineralogists Midyear Meeting, v. 2, p. 21.
- Craig, D. H., 1988, Caves and other features of Permian karst in San Andres Dolomite, Yates Field Reservoir, West Texas, *in* Choquette, P. W. ed., Paleokarst: New York, Springer-Verlag, p. 342–363.
- Crawford, G. A., and Dunham, J. B., 1982, Evaporite sedimentation in the Permian Yates Formation, Central Basin Platform, Andrews County, West Texas, *in* Handford, C. R., Loucks, R. G., and Dunham, J. B., eds., Depositional and diagenetic spectra of evaporites; a core workshop: Society of Economic Paleontologists and Mineralogists Core Workshop, June, v. 3, p. 238–275.
- Cys, J. M., Brezina, J. L., and Greenwood, E., 1977, Capitan ‘reef’: evolution of a concept American Association of Petroleum Geologists Bulletin, v. 61, no. 2, p. 294.
- Davis, L. V., 1955, Geology and ground-water resources of Grady and southern Stephens Counties, Oklahoma: Oklahoma Geological Survey Bulletin, 73, p. 184.
- DeFord, R. K., and Lloyd, E. R., 1940, West Texas-New Mexico symposium, Part 1: American Association of Petroleum Geologists Bulletin, v. 24, no. 1, Part 2, p. 1–188.
- DeFord, R. K., and Riggs, G. D., 1941, Tansill formation, west Texas and southeastern New Mexico: American Association of Petroleum Geologists Bulletin, v. 25, no. 9, p. 1713–1728.
- Dickey, R. I., 1940, Geologic section from Fisher County through Andrews County, Texas, to Eddy County, New Mexico, *in* DeFord, R. K., and Lloyd, Kinnison, eds., West Texas–New Mexico symposium: American Association of Petroleum Geologists Bulletin, v. 24, no. 1, p. 37–51

- Donnelly, A. S., 1941, High-pressure Yates sand gas problem, east Wasson field, Yoakum County, west Texas: American Association of Petroleum Geologists Bulletin, v. 25, no. 10, p. 1880–1897.
- Dunham, R. J., 1972, Capitan Reef, New Mexico and Texas: facts and questions to aid interpretation and group discussion: Society of Economic Paleontologists and Mineralogists, Permian Basin Section, Publication No. 72-14.
- Dutton, A. R., 1987, Hydrogeologic and hydrochemical properties of salt-dissolution zones, Palo Duro Basin, Texas Panhandle-preliminary assessment: The University of Texas at Austin, Bureau of Economic Geology Geological Circular 87-2, 32 p.
- Dutton, S. P., Kim, E. M., Broadhead, R. F., Breton, C. L., Raatz, W. D., Ruppel, S. C., and Kerans, Charles, 2005, Play analysis and digital portfolio of major oil reservoirs in the Permian Basin: application and transfer of advanced geological and engineering technologies for incremental production opportunities: The University of Texas at Austin Bureau of Economic Geology and New Mexico Bureau of Geology and Mineral Resources, Report of Investigations 271, compact disk.
- Eide, M., and Mazzullo, J., 1993, Facies, depositional environments and stratigraphy of the Queen Formation in North Ward-Estes field, Ward County, Texas, *in* Gibbs, J., and Cromwell, D., eds., New dimensions in the Permian Basin: West Texas Geological Society Publication 93-93, p. 28–42.
- Esteban, M., and Pray, L. C., 1976, Nonvadose origin of pisolitic facies, Capitan reef complex (Permian), Guadalupe Mountains, New Mexico and West Texas: American Association of Petroleum Geologists Bulletin, v. 60, no. 4, p. 670.
- Esteban, M., and Pray, L. C., 1977, Origin of the pisolite facies of the shelf crest, *in* Hileman, M. E., and Mazzullo, S. J., eds., Upper Guadalupian facies, Permian Reef Complex, Guadalupe Mountains, New Mexico and West Texas: Society of Economic Paleontologists and Mineralogists, Permian Basin Section, Field Conference Guidebook, v. 1, Publication 77-16, p. 479–486.
- Esteban, M., and Pray, L. C., 1983, Pisoids and pisolite facies (Permian), Guadalupe Mountains, New Mexico and West Texas, *in* Peryt, T. M., ed., Coated grains: New York, Springer-Verlag, p. 503–537.
- Fekete, T. E., Franseen, E. K., and Pray, L. C., 1986, Deposition and erosion of the Grayburg Formation (Guadalupian, Permian) at the shelf-to-basin margin, Western Escarpment, Guadalupe Mountains, Texas, *in* Moore, G. E., and Wilde, G. L., eds., Lower and middle Guadalupian facies, stratigraphy, and reservoir geometries, San Andres and Grayburg Formations, Guadalupe Mountains, New Mexico and Texas: Society of Economic Paleontologists and Mineralogists, Permian Basin Section, Publication 86-25, p. 69–81.

- Folk, R. L., 1968, Petrology of sedimentary rocks: University of Texas, Austin, Geology 370K, 383L, 383M.
- Fracasso, M. A., and Hovorka, S. D., 1986, Cyclicity in the San Andres Formation, Palo Duro Basin, Texas: The University of Texas at Austin, Bureau of Economic Geology Report of Investigations No. 156, 48 p.
- Fracasso, M. A., and Kolker, Allan, 1985, Late Permian volcanic ash beds in the Quartermaster–Dewey Lake formations, Texas Panhandle: West Texas Geological Society Bulletin, February 1985, v. 24, no. 6, p. 5–10.
- Franseen, E. K., Fekete, T. E., and Pray, L. C., 1989, Evolution and destruction of a carbonate bank at the shelf margin: Grayburg Formation (Permian), western escarpment, Guadalupe Mountains, Texas, *in* Crevello, P. D., and Wilson, J. J., eds., Controls on carbonate platform and basin development: Society of Economic Paleontologists and Mineralogists Special Publication, v. 44, p. 289–304.
- Fritz, W. C., and FitzGerald, James, Jr., 1940, South-north cross section from Pecos County through Ector County, Texas, to Roosevelt County, New Mexico: West Texas-New Mexico Symposium: American Association of Petroleum Geologists Bulletin, v. 24, no. 1, p. 15–28.
- Fryberger, S. G., Al-Sari, A. M., and Clisham, T. J., 1983, Eolian dune, interdune, sand sheet, and siliciclastic sabkha sediments of an offshore prograding sand sea, Dhahran area, Saudi Arabia: American Association of Petroleum Geologists Bulletin, v. 67, p. 280–312.
- Fryberger, S. G., Schenk, C. J., and Krystinik, L. F., 1988, Stokes surfaces and the effects of near-surface groundwater-table on Aeolian deposition: Sedimentology, v. 35, p. 21–41.
- Galloway, W. E., 1989, Genetic stratigraphic sequences in basin analysis I: architecture and genesis of flooding-surface bounded depositional units: American Association of Petroleum Geologists Bulletin, v. 73, no. 10, p. 125–142.
- Galloway, W. E., Ewing, T. E., Garrett, C. M., Jr., Tyler, N., and Bebout, D. G., 1983, Atlas of major Texas oil reservoirs: The University of Texas at Austin, Bureau of Economic Geology Special Publication, 139 p.
- Garber, R. A., Grover, G. A., and Harris, P. M., 1989, Geology of the Capitan shelf margin-subsurface data from the northern Delaware Basin, *in* Harris, P. M., and Grover, G. A., eds., Subsurface and outcrop examination of the Capitan shelf margin, northern Delaware Basin: Society of Economic Paleontologists and Mineralogists Core Workshop no. 13, 481 p.
- Garber, R. A., Harris, P. M., and Borer, J. M., 1990, Occurrence and significance of magnesite in Upper Permian (Guadalupian) Tansill, and Yates formations, Delaware Basin, New

- Mexico: American Association of Petroleum Geologists Bulletin, v. 74, no. 2, p. 119–134.
- George, C. J., and Stiles, L. H., 1987, Planning a CO₂ tertiary recovery project, Means San Andres unit: American Association of Petroleum Geologists Bulletin, v. 71, no. 2, p. 238.
- Gester, G. C., and Hawley, H. J., 1929, Yates field, Pecos County, Texas, *in* Structure of typical American oil fields, v. 2: American Association of Petroleum Geologists, p. 488.
- Gieseey, S. C., and Fulk, F. F., 1941, North Cowden field, Ector County, Texas: American Association of Petroleum Geologists Bulletin, v. 25, no. 4, p. 593–629.
- Given, R. K., and Lohmann, K. C., 1986, Isotopic evidence for the early meteoric diagenesis of the reef facies, Permian Reef complex of West Texas and New Mexico: Journal of Sedimentary Petrology, v. 56, p. 183–193.
- Glennie, K. W., and Evans, G., 1976, A reconnaissance of the recent sediments of the Ranns of Kutch, India: Sedimentology, v. 23, p. 625–647.
- Goldstein, A. G., and Collins, E. W., 1984, Deformation of Permian strata overlying a zone of salt dissolution and collapse in the Texas Panhandle: Geology, v. 12, no. 5, p. 314–317.
- Gustavson, T. C., and Finley, R. J., 1985, Late Cenozoic geomorphic evolution of the Texas Panhandle and northeastern New Mexico: case studies of structural controls on regional drainage development: The University of Texas at Austin, Bureau of Economic Geology Report of Investigations No. 148, 42 p.
- Gustavson, T. C., Finley, R. J., and McGillis, K. A., 1980, Regional dissolution of Permian salt in the Anadarko, Dalhart, and Palo Duro basins of the Texas Panhandle: The University of Texas at Austin, Bureau of Economic Geology Report of Investigations No. 106, 40 p.
- Gustavson, T. C., Holliday, V. T., and Hovorka, S. D., 1995, Origins and development of playa basins, sources of recharge to the Ogallala aquifer, Southern High Plains, Texas and New Mexico: The University of Texas at Austin, Bureau of Economic Geology Report of Investigations No. 229, 44 p.
- Hallam, Anthony, 1992, Phanerozoic sea-level changes, *in* Bottjer, D. J., and Bambach, R. K., eds., The perspectives in paleobiology and Earth history series: New York: Columbia University Press.
- Harms, J. C. and Pray, L. C., 1974, Erosion and deposition along the Mid-Permian intracratonic basin margin, Guadalupe Mountains, Texas (abs.), *in* Dickinson, W. R., ed., Tectonics and sedimentation: Society of Economic Paleontologists and Mineralogists, Special Publication No. 19, p. 37.

- Harris, P. M., Dodman, C. A., and Bliefnick, D. M., 1984, Permian (Guadalupian) reservoir facies, McElroy Field, West Texas, *in* Harris, P. M., ed., Carbonate sands: a core workshop: Society of Economic Paleontologists and Mineralogists Core Workshop, v. 5, p. 136–174.
- Harris, J. M., Langan, R. T., Van Schaack, Mark, Lazaratos, S. K., and Rector, J. W., 1995, High-resolution crosswell imaging of a west Texas carbonate reservoir: part I—project summary and interpretation: *EOPHYSICS*, v. 60, no. 3 (May–June), p. 667–681.
- Harville, D. G., and Fritz, S. J., 1986, Modes of diagenesis responsible for observed succession of potash evaporites in the Salado Formation, Delaware Basin, New Mexico: *Journal of Sedimentary Petrology*, v. 56, no. 5, p. 648–656.
- Harwood, Gill, 1990, Sandstone stromatolites from the Yates Formation, New Mexico, United States: *American Association of Petroleum Geologists Bulletin*, v. 74, no. 5, p. 671.
- Hayes, P. T., and Koogler, R. L., 1958, Geology of the Carlsbad Caverns West Quadrangle, New Mexico–Texas: U.S. Geological Survey Geologic Quadrangle Map.
- Hills, J. M., 1972, Late Paleozoic sedimentation in West Texas Permian Basin: *American Association of Petroleum Geologists Bulletin*, v. 56, no. 12, p. 2303–2322.
- Hills, J. M., 1984, Sedimentation, tectonism, and hydrocarbon generation in Delaware Basin, West Texas and southeastern New Mexico: *American Association of Petroleum Geologists Bulletin*, v. 68, no. 3, p. 250–267.
- Hiss, W. L., 1976, Structure of the Permian Ochoan Rustler Formation, Southeast New Mexico and West Texas: resource map: New Mexico Bureau of Mines & Mineral Resources Resource Map, Issue 7.
- Holley, Carolayne, and Mazzullo, Jim, 1988, The lithology, depositional environments, and reservoir properties of sandstones in the Queen Formation, Magutex North, McFarland North, and McFarland fields, Andrews County, Texas, *in* Cunningham, B. K., ed., Permian and Pennsylvanian stratigraphy, Midland Basin, West Texas; studies to aid hydrocarbon exploration: Society of Economic Paleontologists and Mineralogists, Permian Basin Chapter, v. 88-28, p. 55–63.
- Holt, R. M., 1999, The Los Medanos Member of the Permian (Ochoan) Rustler Formation: *New Mexico Geology*, v. 21, no. 4, p. 97–103.
- Holt, R. M., and Powers, D. W., 1987, The Permian Rustler Formation at the WIPP site, southeastern New Mexico, *in* Powers, D. W., and James, W. C., eds., Geology of the western Delaware Basin, West Texas and southeastern New Mexico: El Paso Geological Society Guidebook, Annual Field Trip, v. 18, p. 140–148.

- Holtz, M. H., 1991, Porosity and permeability characteristics in a mixed carbonate-siliciclastic sequence: an example from the upper Guadalupian (Permian), West Texas and New Mexico, *in* Candelaria, M. P., ed., *Permian Basin plays: tomorrow's technology today*: West Texas Geological Society Publication No. 91-89, p. 123–124.
- Holtz, M. H., 1993, Reservoir characteristics of the McFarland and Magutex (Queen) reservoirs, Permian Basin, Texas, *in* Johnson, K. S., and Campbell, J. A., eds., *Petroleum-reservoir geology in the southern Midcontinent, 1991 symposium*: Oklahoma Geological Survey Circular, p. 60–65.
- Holtz, M. H., 1994, McFarland (Queen) reservoir, *in* *Selected oil and gas fields in West Texas*, v. 6: West Texas Geological Society, Publication No. 94-96, p. 169–177.
- Hovorka, S. D., 1990, Sedimentary processes controlling halite deposition, Permian Basin, Texas: The University of Texas at Austin, Ph.D. dissertation, 427 p.
- Hurley, N. F., 1978, Facies mosaic of the lower Seven Rivers Formation (Permian), North McKittrick Canyon, Guadalupe Mountains, New Mexico: University of Wisconsin, M.S. thesis, 198 p.
- Hurley, N. F., 1989, Facies mosaic of the lower Seven Rivers Formation, McKittrick Canyon, New Mexico, *in* Harris, P. M., and Grover, G. A., eds., *Subsurface and outcrop examination of the Capitan Shelf Margin, northern Delaware Basin*: Society of Economic Paleontologists and Mineralogists Core Workshop No. 13, p. 325–346.
- Hurtado, L. D., Knowles, M. K., Kelley, V. A., Jones, T. L., and Ogintz, J. B., 1997, WIPP shaft seal system parameters recommended to support compliance calculations: SAND, Sandia National Laboratories, Albuquerque, 100 p.
- Janks, J. S., Yusas, M. R., and Hall, C. M., 1992, Clay mineralogy of an interbedded sandstone, dolomite, and anhydrite; the Permian Yates Formation, Winkler County, Texas, *in* Houseknecht, D. W., and Pittman, E. D., eds., *Origin, diagenesis, and petrophysics of clay minerals in sandstones*: Society of Economic Paleontologists and Mineralogists Special Publication, v. 47, p. 145–157.
- Johnson, D. B., 1984, Inverse grading in pisolites; a model with application to the Yates Formation (Permian), New Mexico and Texas: Geological Society of America, 97th Meeting Abstracts with Programs, v. 16, no. 6, p. 552.
- Johnson, J. H., 1942, Permian lime-secreting algae from the Guadalupe Mountains, New Mexico: Geological Society of America Bulletin, v. 53, no. 2, p. 195–226
- Johnson, Ron, and Mazzullo, J. M., 1996, Stratigraphy, facies, and environment of deposition of the Yates Formation, North Ward Estes Field, Ward County, Texas: American Association of Petroleum Geologists Bulletin, v. 80, no. 9, p. 1505.

- Johnson, Ron, and Mazzullo, Jim, 2001, Facies and sequence stratigraphy of the Upper Permian Yates Formation on the western margin of the Central Basin Platform of the Permian Basin: Oklahoma Geological Survey Circular, p. 229.
- Johnson, W. D., 1901, The High Plains and their utilization: U.S. Geological Survey, 21st Annual Report, pt. 4, p. 601–732.
- Jones, C. L., 1954, The occurrence and distribution of potassium minerals in southeastern New Mexico: New Mexico Geological Society Guidebook, 5th Field Conference, p. 107–112.
- Jones, C. L., 1972, Permian basin potash deposits, south-western United States, *in* Geology of saline deposits—Geologie des depots salins, Earth Science Paris: Sciences de la Terre Paris, v. 7, p. 191–201.
- Kendall, C. G. St.C., and Shipwith, P. A. d'E., 1968, Recent algal mats of the Persian Gulf lagoon: Journal of Sedimentary Petrology, v. 38, p. 1040–1058.
- Kerans, Charles, and Harris, P. M., 1993, Outer shelf and shelf crest, *in* Bebout, D. G., and Kerans, C., eds., Guide to the Permian Reef Geology Trail, McKittrick Canyon, Guadalupe Mountains National Park, West Texas: The University of Texas at Austin, Bureau of Economic Geology, Guidebook 26, p. 32–43.
- Kerans, Charles, and Kempter, Kirt, 2002, Hierarchical stratigraphic analysis of a carbonate platform, Permian of the Guadalupe Mountains: American Association of Petroleum Geologists, Datapages Discovery Series No. 5.
- King, P. B., 1948, Geology of the southern Guadalupe Mountains, Texas: U.S. Geological Survey Professional Paper, 183 p.
- Kirkland-George, Brenda, 1992, Distinctions between reefs and bioherms based on studies of fossil algae—Mizzia, Permian Capitan reef complex (Guadalupe Mountains, Texas and New Mexico) and Eugonophyllum, Pennsylvanian Holder Formation (Sacramento Mountains, New Mexico): Louisiana State University, Ph.D. dissertation, 156 p.
- Kirkland, B. L., Longacre, S. A., and Stoudt, E. L., 1993, Reef, *in* Bebout, D. G., and Kerans, C., eds., Guide to the Permian Reef Geology Trail, McKittrick Canyon, Guadalupe Mountains National Park, West Texas: The University of Texas at Austin, Bureau of Economic Geology, Guidebook 26, p. 23–31.
- Kirkland, B. L., and Moore, C. H., 1996, Microfacies analysis of the Tansill outer shelf, Permian Capitan reef complex, *in* Martin, R. L., ed., Permian Basin oil and gas fields: keys to success that unlock future reserves: West Texas Geological Society Publication, v. 96-101, p. 99–106.

- Kolker, Allan, and Fracasso, M. A., 1985, K-Ar age of a volcanic ash bed in the Quartermaster and Dewey Lake formations (Late Permian), Texas Panhandle: *Isochron/West*, April, v. 42, p. 17–19
- Kosa, E., Hunt, D., Robinson, A., Fitchen, W. M., Roberts, G. P., and Bockel-Rebelle, M. O., 2001, Spatial and temporal heterogeneity in the architecture, fill and diagenesis of syndepositional faults and fractures, Permian Seven Rivers, Yates and Tansill formations, Guadalupe Mountains, New Mexico; implications for faulted carbonate reservoir: *American Association of Petroleum Geologists*, v. 2001, p. 108.
- Kosters, E. C., Bebout, D. G., Seni, S. J., Garrett, C. M., Brown, L. F., Hamlin, H. S., Dutton, S. P., Ruppel, S. C., Finley, R. J., and Tyler, N., 1989, Atlas of major Texas gas reservoirs: The University of Texas at Austin, Bureau of Economic Geology, 161 p.
- Lampert, L. M., 1977, Queen Sand in the Double L and Sulimar fields, Chaves County, New Mexico, *in* Havenor, K. C., ed., The oil and gas fields of southeastern New Mexico; supplement: Roswell Geological Society, p. 29–37.
- Lang, W. B., 1935, Upper Permian Formation of Delaware Basin of Texas and New Mexico: *American Association of Petroleum Geologists Bulletin*, v. 19, no. 2, p. 262–270.
- Lang, W. B., 1937, The Permian Formations of the Pecos Valley of New Mexico and Texas: *American Association of Petroleum Geologists Bulletin*, v. 21, no. 7 p. 833–898.
- Lang, W. B., 1942, Basal beds of Salado Formation in Fletcher potash core test, near Carlsbad, New Mexico: *American Association of Petroleum Geologists Bulletin*, v. 26, no. 1, p. 63–79.
- Lanphere, Starr, 1972, Proposed surface reference section for Yates Formation, Eddy County, New Mexico: *American Association of Petroleum Geologists Bulletin*, v. 56, no. 8, p. 1534–1540.
- Lewis, F. E., 1938, Stratigraphy of the Upper and Middle Permian of West Texas and southeastern New Mexico: *American Association of Petroleum Geologists Bulletin*, v. 22, no. 12, p. 1710–1711.
- Lindsay, R. F., Trentham, R. C., Ward, R. F., and Smith, A. H., 2000, Munn Formation (Permian, Guadalupian) depositional setting, facies and sequence stratigraphy, Apache Platform, West Texas, *in* DeMis, W. D., Nelis, M. K., and Trentham, R. C., eds., The Permian Basin; proving ground for tomorrow's technologies, v. 00-109, p. 19–35.
- Lloyd, E. R., 1929, Capitan limestone and associated formations of New Mexico and Texas: *American Association of Petroleum Geologists Bulletin*, v. 13, no. 6, p. 645–658.
- Longley, Andrew, and Harwood, G. M., 1993, Yates Formation small-scale cyclicity (Permian, Guadalupe Mountains); an alternative hypothesis: *American Association of Petroleum*

Geologists and Society of Economic Paleontologists and Mineralogists Annual Meeting Abstracts, v. 1993, p. 140.

- Lowenstein, Tim, 1982, Primary features in a potash evaporite deposit, the Permian Salado Formation of West Texas and New Mexico, *in* Handford, C. R., Loucks, R. G., and Davies, G. R., eds., Depositional and diagenetic spectra of evaporites; a core workshop: Society of Economic Paleontologists and Mineralogists Core Workshop, v. 3, p. 276–304.
- Lowenstein, Tim, 1988, Origin of depositional cycles in a Permian ‘saline giant’; the Salado (McNutt Zone) evaporites of New Mexico and Texas: Geological Society of America Bulletin, v. 100, no. 4, p. 592–608.
- Lucia, F. J., 1961, Dedolomitization in the Tansill (Permian) formation: Geological Society of America Bulletin, v. 72, no. 7, p. 1107–1109.
- Lufholm, P. W. G., and Lofton, L., 1996, Improved reservoir modeling using gridded seismic attributes: North Concho Bluff field, west Texas, *in* Martin, R. L., ed., Permian Basin oil and gas fields: keys to success that unlock future reserves: West Texas Geological Society Publication 96 -101, p. 145–159.
- Major, R. P., and Ye, Q., 1992, Lateral and vertical reservoir heterogeneity in siliciclastic peritidal facies, Keystone (Colby) reservoir, west Texas, *in* Mruk, D. H., and Curran, C., eds., Permian Basin exploration and production strategies: application of sequence stratigraphic and reservoir characterization concepts: West Texas Geological Society Publication 92-91, p. 91–99.
- Major, R. P., and Ye, Q., 1997, Characterization of siliciclastic tidal-flat reservoir: Keystone (Colby) field, Winkler County, Texas, *in* Major, R. P., ed., Oil and gas on Texas State Lands: an assessment of the resource and characterization of type reservoirs: The University of Texas at Austin, Bureau of Economic Geology Report of Investigations No. 241, p. 127–135.
- Malicse, A., and Mazzullo, J., 1990, Reservoir properties of the desert Shattuck member, Caprock field, New Mexico, *in* Barwis, J., McPherson, J., and Studlick, J. eds., Sandstone petroleum reservoirs: New York, Springer-Verlag, p. 133–152.
- Mazzullo, Jim, 2001, Depositional and diagenetic origins of sandstone reservoirs in the Queen Formation, Permian Basin of Texas, *in* Johnson, K. S., ed., Pennsylvanian and Permian geology and petroleum in the southern Midcontinent, 1998 symposium: Oklahoma Geological Survey Circular, p. 232.
- Mazzullo, Jim, Dronamraju, Sharma, Johnson, Ron, and Ahr, Wayne M., 1996, Facies and sequence stratigraphy of the Late Permian Yates Formation on the western margin of the Central Basin Platform of the Permian Basin, North Ward-Estes and South Ward fields, Ward County, Texas, *in* Martin, R. L., ed., Permian Basin oil and gas fields; keys to

- success that unlock future reserves: West Texas Geological Society, v. 96-101, p. 117–120.
- Mazzullo, J., Malicse, A., Newsom, D., Harper, J., McKone, C. and Price, B., 1992, Facies, depositional environments, and reservoir properties of the upper Queen Formation, Concho Bluff and Concho Bluff North fields, Texas, *in* Mruk, D. H., and Curran, B. C., eds., Permian Basin exploration and production strategies: applications of sequence stratigraphic and reservoir characterization concepts: West Texas Geological Society, Publication 92-91, p. 67–78.
- Mazzullo, J., Malicse, A., and Siegel, J., 1991, Facies and depositional environments of the Shattuck Sandstone of the Northwest Shelf of the Permian Basin: *Journal of Sedimentary Petrology*, v. 61, p. 940–958.
- Mazzullo, Jim, Price, Catherine, and Ryu, Changsu, 2000, Depositional lithofacies, cycle stacking patterns, and reservoir heterogeneity of Grayburg and Queen reservoirs, Means Field, Andrews County, Texas, *in* Tomlinson Reid, Sue, ed., Transactions, American Association of Petroleum Geologists Southwest Section, GEO-2000, into the future, West Texas Geological Society Publication, v. 2000-107, p. 253.
- Mazzullo, Jim, Williams, Matt, and Mazzullo, S. J., 1984, The Queen Formation of Millard field, Pecos County, Texas: its lithologic characteristics, environment of deposition, and reservoir petrophysics, *in* Transactions, American Association of Petroleum Geologists, Southwest Section, p. 103–109.
- Mazzullo, S. J., 1999, Paleoenvironments, cyclicity, and diagenesis in the outer shelf Tansill Formation in the Carlsbad Embayment (Dark Canyon), northern Guadalupe Mountains, New Mexico, *in* Saller, A. H., Harris, P. M., Kirkland, B. L., and Mazzullo, S. J., eds., Geologic framework of the Capitan Reef: Special Publication, v. 65, p. 107–128.
- Mazzullo, S. J., Bischoff, W. D., and Hedrick, C. L., 1989, Stacked island facies in Tansill outer-shelf platform, Dark Canyon, Guadalupe Mountains, New Mexico, *in* Harris, P. M., and Grover, G. A., eds., Subsurface and outcrop examination of the Capitan shelf margin, northern Delaware Basin: Society of Economic Paleontologists and Mineralogists Core Workshop, v. 13, p. 287–293.
- Mazzullo, S. J., and Cys, J. M., 1982, Extensive coniatolite-pelagosite diagenetic sedimentation in marine limestones, Tansill Formation (Permian), New Mexico: *American Association of Petroleum Geologists Bulletin*, v. 66, no. 5, p. 602.
- McGillis, K. A., and Presley, M. W., 1981, Tansill, Salado, and Alibates formations; Upper Permian evaporite/carbonate strata of the Texas Panhandle: The University of Texas at Austin, Bureau of Economic Geology Geological Circular 81-8, 31 p.

- McGowen, J. H., Granata, G. E., and Seni, S. J., 1979, Depositional framework of the Lower Dockum Group (Triassic) Texas Panhandle: The University of Texas at Austin, Bureau of Economic Geology Report of Investigations No. 97, 60 p.
- Mear, C. E., 1963, Stratigraphy of Permian outcrops, Coke County, Texas: Bulletin of the American Association of Petroleum Geologists, v. 47, no. 11, p. 1952–1962.
- Mear, C. E., and Yarbrough, D. V., 1961, Yates Formation in southern Permian basin of West Texas: American Association of Petroleum Geologists Bulletin, v. 45, no. 9, p. 1545–1556.
- Meinzer, Oscar, Renick, Edward, Coleman, B., and Bryan, Kirk, 1926, Geology of No. 3 reservoir site of the Carlsbad irrigation project, New Mexico, with reference to water-tightness: U.S. Geological Survey Water-Supply Paper, p. 1–39.
- Meissner, F. G., 1972, Cyclic sedimentation in middle Permian strata of the Permian Basin, *in* Elam, J. G., and Chuber, S., eds., Cyclic sedimentation in the Permian Basin: West Texas Geological Society, p. 203–232.
- Miller, D. N., Jr., 1957, Authigenic biotite in spheroidal reduction spots, Pierce Canyon redbeds, Texas and New Mexico: Journal of Sedimentary Petrology, v. 27, no. 2, p. 127–180.
- Miller, D. N., Jr., 1966, Petrology of Pierce Canyon redbeds, Delaware Basin, Texas and New Mexico: American Association of Petroleum Geologists Bulletin, v. 50, no. 2, p. 283–307.
- Milligan, D. J., 1991, Geochronologic study of clay minerals from the Salado Formation, WIPP Site area, New Mexico: Geological Society of America Abstracts with Programs, v. 23, no. 4, p. 49.
- Moran, W. R., 1954, New Mexico Geological Society guidebook, 5th Field Conference., October: Geological Society of America Bulletin, v. 65, no. 12, Part 2, p. 147–150.
- Moran, W. R., 1962, Permian of the central Guadalupe Mountains, Eddy County, New Mexico—Field trip guidebook and geological discussions: West Texas Geological Society Publication, p. 76–86.
- Mutti, Maria, and Simo, J. A., 1993, Stratigraphic patterns and cycle-related diagenesis of upper Yates Formation, Permian, Guadalupe Mountains, *in* Loucks, R. G., and Sarg, J. F., eds., Carbonate sequence stratigraphy; recent developments and applications: American Association of Petroleum Geologists Memoir, v. 57, p. 515–534.
- Mutti, M., and Simo, J. A., 1994, Distribution, petrography and geochemistry of early dolomite in cyclic shelf facies, Yates Formation (Guadalupian), Capitan Reef Complex, USA, *in* Purser, Bruce, Tucker, Maurice, and Tucker, Maurice, eds., Dolomites; a volume in

- honour of Dolomieu: Special Publication of the International Association of Sedimentologists, v. 21, p. 91–107.
- Nance, H. S., 1988a, Facies relations and controls on Artesia Group deposition in the Matador Arch Area, Texas: The University of Texas at Austin, M.A. thesis, 142 p.
- Nance, H. S., 1988b, Interfingering of evaporites and red beds: an example from the Queen/Grayburg Formation, Texas: *Sedimentary Geology*, v. 56, p. 357–381.
- Neese, D. G., 1979, Carbonate facies variation on Guadalupian shelf crest (upper Yates and lower Tansill formations), Guadalupe Mountains, New Mexico: *American Association of Petroleum Geologists Bulletin*, v. 63, no. 3, p. 501–502.
- Neese, D. G., 1989, Peritidal facies of the Guadalupian shelf crest, Walnut Canyon, New Mexico, *in* Harris, P. M., and Grover, G. A., eds., *Subsurface and outcrop examination of the Capitan shelf margin, northern Delaware Basin*: Society of Economic Paleontologists and Mineralogists Core Workshop, v. 13, p. 295–303.
- Newell, N. D., Rigby, J. K., Fischer, A. G., Whiteman, A. J., Hickox, J. E., and Bradley, J. S., 1953, *The Permian Reef Complex of the Guadalupe Mountains region, Texas and New Mexico*: San Francisco, W. H. Freeman Co., 236 p.
- Noe, S. U., 1996, Late-stage reef evolution of the Permian Reef Complex; shelf margin and outer-shelf development of the Tansill Formation (Late Permian), northern Guadalupe Mountains, New Mexico, USA, *in* Reitner, Joachim, Neuweiler, Fritz, and Gunkel, Felix, eds., *Global and regional controls on biogenic sedimentation 1: Goettinger Arbeiten zur Geologie und Palaeontologie. Sonderband*, v. SB2, p. 317–324.
- Noe, S. U., and Mazzullo, S. J., 1992, Upper Tansill patch reef facies, Sheep Draw Canyon, Guadalupe Mountains, Eddy County, New Mexico: *West Texas Geological Society Bulletin*, v. 32, no. 1, p. 5–11.
- Noe, S. U., and Mazzullo, S. J., 1994, Patch reef dominated outer-shelf facies along a non-rimmed platform, middle to upper Tansill Formation, northern Guadalupe Mountains, New Mexico: *West Texas Geological Society Bulletin*, v. 33, no. 5, p. 5–11.
- Ordonez, S. R., 1984, Permian (Guadalupian) Shelf deposition and diagenesis; Tansill Formation of Cheyenne Field, Winkler County, Texas: *American Association of Petroleum Geologists Bulletin*, v. 68, no. 1, p. 118.
- Osleger, D. A., and Tinker, S. W., 1999, Three-dimensional architecture of Upper Permian high-frequency sequences, Yates-Capitan shelf margin, Permian Basin, U.S.A., *in* Harris, P. M., Saller, A. H., and Simo, J. A., eds., *Advances in carbonate sequence stratigraphy; application to reservoirs, outcrops and models*: Society for Sedimentary Geology Special Publication, v. 63, p. 169–185.

- Page, L. R., and Adams, J. E., 1940, Stratigraphy, eastern Midland Basin, Texas, *in* DeFord, R. K., and Lloyd, E. R., eds., West Texas-New Mexico symposium: American Association of Petroleum Geologists Bulletin, v. 24, no. 1, p. 52–64.
- Parsley, M. J., and Warren, J. K., 1989, Characterization of an upper Guadalupian barrier-island complex from the middle and upper Tansill Formation (Permian), East Dark Canyon, Guadalupe Mountains, New Mexico, *in* Harris, P. M., and Grover, G. A., eds., Subsurface and outcrop examination of the Capitan shelf margin, northern Delaware Basin: Society of Economic Paleontologists and Mineralogists Core Workshop, v. 13, p. 279–285.
- Powers, D. W., Holt, R. M., Beauheim, R. L. and McKenna, S. A., 2003, Geological factors related to the transmissivity of the Culebra Dolomite Member, Permian Rustler Formation, Delaware Basin, southeastern New Mexico, *in* Johnson, K. S., and Neal, J. T., eds., Evaporite karst and engineering/environmental problems in the United States: Oklahoma Geological Survey Circular, p. 211–218.
- Pray, L. C., and Esteban, M., eds., 1977, Upper Guadalupian facies, Permian reef complex Guadalupe Mountains, New Mexico and West Texas: Society of Economic Paleontologists and Mineralogists, Permian Basin Chapter, no. 77-16, v. 2, West Texas Geological Society.
- Price, Catherine, Ryu, Changsu, and Mazzullo, Jim, 2000, Lithofacies, depositional environments and reservoir properties of the Permian (Guadalupian) Grayburg and Queen formations, Means Field, Andrews County, Texas, *in* Tomlinson Reid, Sue, ed., Transactions, American Association of Petroleum Geologists Southwest Section, GEO-2000, into the future: West Texas Geological Society Publication, v. 2000-107, p. 80–97.
- Railroad Commission of Texas, 2003, RRC Oil and Gas Annual Report.
- Rankey, E. C., and Lehrmann, D. J., 1996, Anatomy and origin of toplap in a mixed carbonate-clastic system, Seven Rivers Formation (Permian, Guadalupian), Guadalupe Mountains, New Mexico, USA: Sedimentology, v. 43 no. 5, p. 807–827.
- Ring, J. N., and Smith, D. J., 1995, An overview of the North Ward-Estes CO₂ flood, *in* SPE Annual Technical Conference: Society of Petroleum Engineers, Paper 30729, p. 293–300.
- Rosenblum, Mark, 1985, Early-diagenetic sheet-crack cements of Guadalupian shelf, Yates and Tansill formations, New Mexico; a field and chemical study: American Association of Petroleum Geologists Bulletin, v. 69, no. 2, p. 302.
- Saeb, S., 1995, Effect of clay seams on the performance of WIPP excavations, *in* Proceedings of the International Conference on the Mechanics of Jointed and Faulted Rock, v. 2, p.835–840.

- Sarg, J. F., 1981, Petrology of the carbonate-evaporite facies transition of the Seven Rivers Formation (Guadalupian, Permian), southeast New Mexico: *Journal of Sedimentary Petrology*, v. 51, no. 1, p. 73–96.
- Schaller, W. T., and Henderson, E. P., 1932, Mineralogy of drill cores from the potash field of New Mexico and Texas: *U.S. Geological Survey Bulletin*.
- Senowbari-Daryan, Baba, and Rigby, J. K., 1996, Brachiopod mounds not sponge reefs, Permian Capitan-Tansill formations, Guadalupe Mountains, New Mexico: *Journal of Paleontology*, v. 70, no. 4, p. 697–701.
- Silver, B. A., and Todd, R. G., 1969, Permian cyclic strata, northern Midland and Delaware Basins, West Texas and southeastern New Mexico: *American Association of Petroleum Geologists Bulletin*, v. 53, p. 2223–2251.
- Slone, J. C., and Mazzullo, J., 2000, Lithofacies, stacking patterns, and depositional environments of the Permian Queen Formation, Sterling and Glasscock Counties, Texas, *in* DeMis, W. D., Nelis, M. K., and Trentham, R. C., eds., *The Permian Basin: proving ground for tomorrow's technologies*: West Texas Geological Society Publication No. 00-109, p. 63–64.
- Smith, D. B., 1974, Sedimentation of Upper Artesia (Guadalupian) cyclic shelf deposits of northern Guadalupe Mountains, New Mexico: *American Association of Petroleum Geologists Bulletin*, v. 58, no. 9, p. 1699–1730.
- Snider, H. I., 1966, Stratigraphy and associated tectonics of the upper Permian Castile-Salado-Rustler evaporite complex, Delaware Basin, West Texas: University of New Mexico, Ph.D. dissertation, 196 p.
- Snow, D. T., 2002, Unsafe radwaste disposal at WIPP: *New Mexico Geology*, v. 24, no. 2, p. 57.
- Spencer, A. W., 1987, Evaporite facies related to reservoir geology, Seven Rivers Formation (Permian), Yates field, Texas: The University of Texas at Austin, M.S. thesis, 125 p.
- Spencer, A., and Warren, J. K., 1986, Depositional styles in the Queen and Seven Rivers formations; Yates Field, Pecos County, Texas, *in* Bebout, D. G., and Harris, P. M., eds., *Hydrocarbon reservoir studies; San Andres/Grayburg formations, Permian Basin*: Society of Economic Paleontologists and Mineralogists, Permian Basin Section, v. 86-26, p. 135–137.
- Stein, C. L., and Krumhansl, J. L., 1988, A model for the evolution of brines in salt from the lower Salado Formation, southeastern New Mexico: *Geochimica et Cosmochimica Acta*, v. 52, p. 1037–1046.
- Steiner, Maureen, 2001, Magnetostratigraphic correlation and dating of West Texas and New Mexico Late Permian strata: *Association of Petroleum Geologists*, v. 85, no. 9, p. 1695.

- Stormont, J. C., 1990, Discontinuous behaviour near excavations in a bedded salt formation: *International Journal of Mining and Geological Engineering*, v. 8, no.1, p. 35–56
- Tait, D. R., Ahlen, J. L., Gordon, A., Scott, G. L., Motts, W. S., and Spider, M. E., 1962, Artesia Group of New Mexico and West Texas: *American Association of Petroleum Geologists Bulletin*, v. 26, p. 504–517.
- Thomas, Carroll, 1968, Vadose pisolites in the Guadalupe and Apache Mountains, west Texas, *in* Silver, B. A., ed., *Guadalupean facies, Apache Mountains area, west Texas: Society of Economic Paleontologists and Mineralogists Permian Basin Section Field Trip Symposium*, p. 32–35.
- Thompson, R. W., 1968, Tidal flat sedimentation on the Colorado River delta, northwestern Gulf of California: *Geological Society of America Memoir* 107, 133 p.
- Trentham, R. C., 2003, Impact of paleostructure on Guadalupian age clastic sediment distribution in the Midland Basin, Central Basin Platform, and eastern Delaware Basin, *in* Hunt, T. J., and Lufholm, P. H., eds., *The Permian Basin: back to basics: West Texas Geological Society Publication No. 03-112*, p. 79–95.
- Tyler, N., Bebout, D. G., Garrett, C. M., Jr., Guevara, E. H., Hocott, C. R., Holtz, M. H., Hovorka, S. D., Kerans, C., Lucia, F. J., Major, R. P., Ruppel, S. C., and Vander Stoep, G. W., 1991, Integrated characterization of Permian Basin reservoirs, University Lands, West Texas: targeting the remaining resource for advanced oil recovery: *The University of Texas at Austin, Bureau of Economic Geology Report of Investigations No. 203*, 136 p.
- Tyrrell, W. W., Jr., 1961, Petrology and stratigraphy of near-reef Tansill-Lamar strata, Guadalupe Mountains, Texas and New Mexico, *in* *Permian of the central Guadalupe Mountains, Eddy County, New Mexico—Field trip guidebook and geological discussions: West Texas Geological Society Publication*, p. 59–69.
- Tyrrell, W. W., Jr., 1962, Petrology and stratigraphy of near-reef Tansill-Lamar strata, Guadalupe Mountains, Texas and New Mexico: *Permian of the central Guadalupe Mountains, Eddy County, New Mexico: West Texas Geological Society Publication, Field trip guidebook and geological discussions*, p. 59–69.
- Tyrrell, W. W., Jr., 1964, Petrology and stratigraphy of near-reef Tansill-Lamar strata, Guadalupe Mountains, Texas and New Mexico, *in* *Guidebook to the geology of the Capitan Reef complex of the Guadalupe Mountains: Roswell Geological Society Field Trip Guidebook*, p. 66–82.
- Tyrrell, W. W., Jr., 1969, Criteria useful in interpreting environments of unlike but time-equivalent carbonate units (Tansill-Capitan-Lamar), Capitan reef complex, west Texas and New Mexico, *in* *Depositional environments in carbonate rocks; a symposium*:

Society of Economic Paleontologists and Mineralogists Special Publication, v. 14, p. 80–97.

Udden, J. A., 1915, Potash in the Texas Permian: University of Texas, Austin, Bulletin, 59 p.

Vail, P. R., Mitchum, R. M., Todd, R. G., Widmier, J. M., Thompson, S., Songree, J. B., Bubbs, J. N., and Hatlelid, W. G., 1977, Seismic stratigraphy and global changes of sea level, *in* American Association of Petroleum Geologists Memoir 26, p. 49–212.

Vanderhill, J. B., 1991, Depositional setting and reservoir characteristics of Hower Queen (Permian, Guadalupian) sandstones, Keystone (Colby) field, Winkler County, Texas, *in* Meader-Roberts, Sally, Candelaria, M. P., and Moore, G. E., eds., Sequence stratigraphy, facies, and reservoir geometries of the San Andres, Grayburg, and Queen Formations, Guadalupe Mountains, New Mexico and Texas: Society of Economic Paleontologists and Mineralogists, Permian Basin Section, Publication 91-32, p. 119–129.

Ward, R., Kendall, C. G. St.C., and Harris P. M., 1986, Upper Permian (Guadalupian) facies and their association with hydrocarbons Permian Basin, West Texas and New Mexico: American Association of Petroleum Geologists Bulletin, v. 70, p. 239–262.

Warren, J. K., and Kendall, C. G. St. C., Christopher, G., 1985, Comparison of sequences formed in marine sabkha (subaerial) and salina (subaqueous) settings: modern and ancient: American Association of Petroleum Geologists Bulletin, v. 69, no. 6, p. 1013–1023.

Weart, W. D., 1997, Critical scientific issues in the demonstration of WIPP compliance with EPA repository standards: SAND, Sandia National Laboratory, 100 p.

West Texas Geological Society, 1976, Lexicon of Permian stratigraphic names of the Permian Basin of West Texas and southeastern New Mexico: West Texas Geological Society Publication, 341 p.

West Texas Geological Society, 1994, Oil and gas fields in West Texas, v. VI: West Texas Geological Society Publication 94-96, p. 275–279.

Woods, E. H., 1940, South-north cross section from Pecos County through Winkler County, Texas to Roosevelt County, New Mexico, *in* DeFord, R. K., and Lloyd, eds., West Texas-New Mexico symposium: American Association of Petroleum Geologists Bulletin, v. 24, no. 1, p. 29–36.

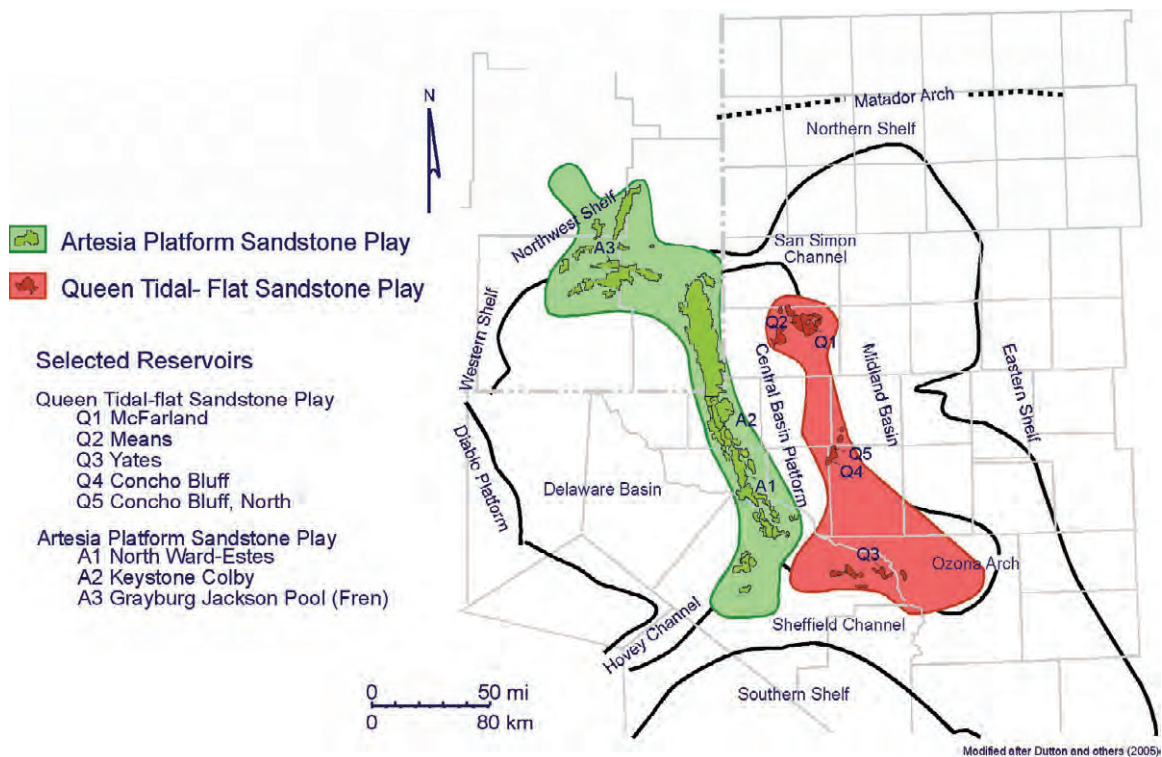


Figure 1. Map showing play boundaries and included oil fields for the Artesia Platform Sandstone Play and the Queen Tidal-Flat Sandstone Play in the Permian Basin. From Dutton and others (2005).

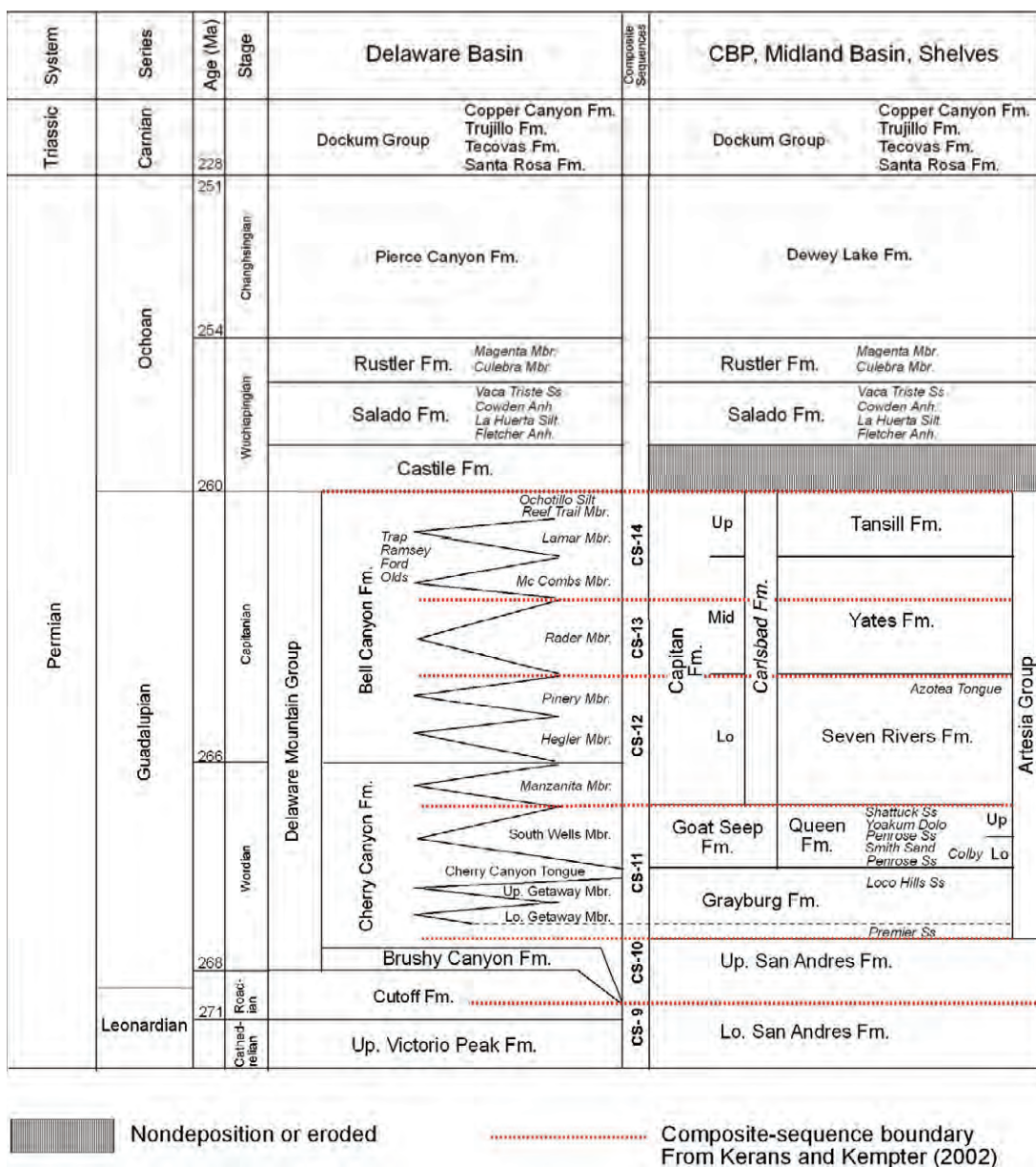


Figure 2. Stratigraphic correlation chart for the Permian Basin. Also shown are composite sequences of Kerans and Kempter (2002). Data from Kerans and Kempter (2002).

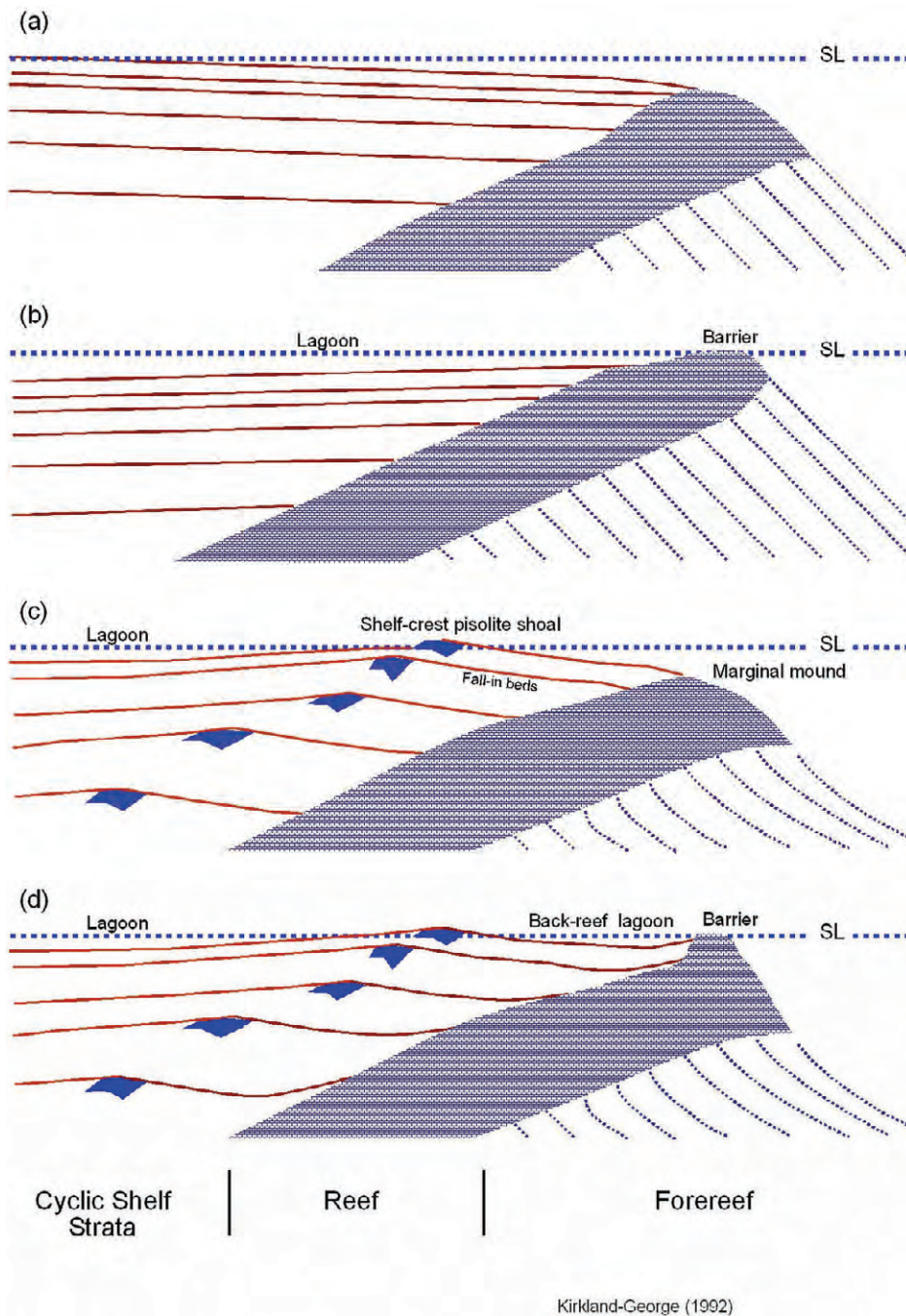


Figure 3. Proposed models for the Guadalupian shelf margin: (a) uninterrupted shelf, (b) barrier reef, (c) marginal mound with pisolite-shoal shelf crest, and (d) barrier island with back-reef lagoon and pisolite shoal. Modified from Kirkland-George (1992).

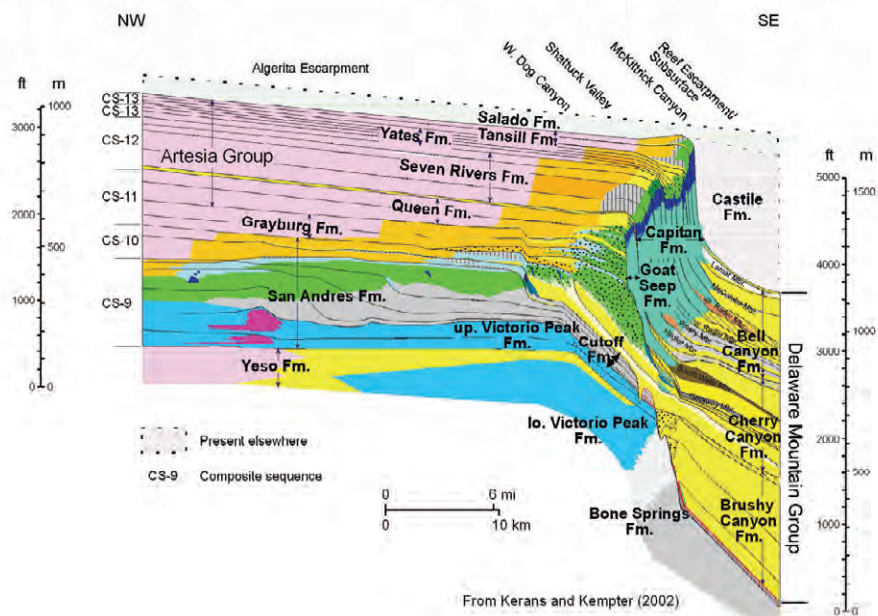
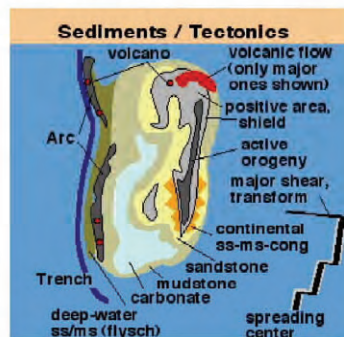
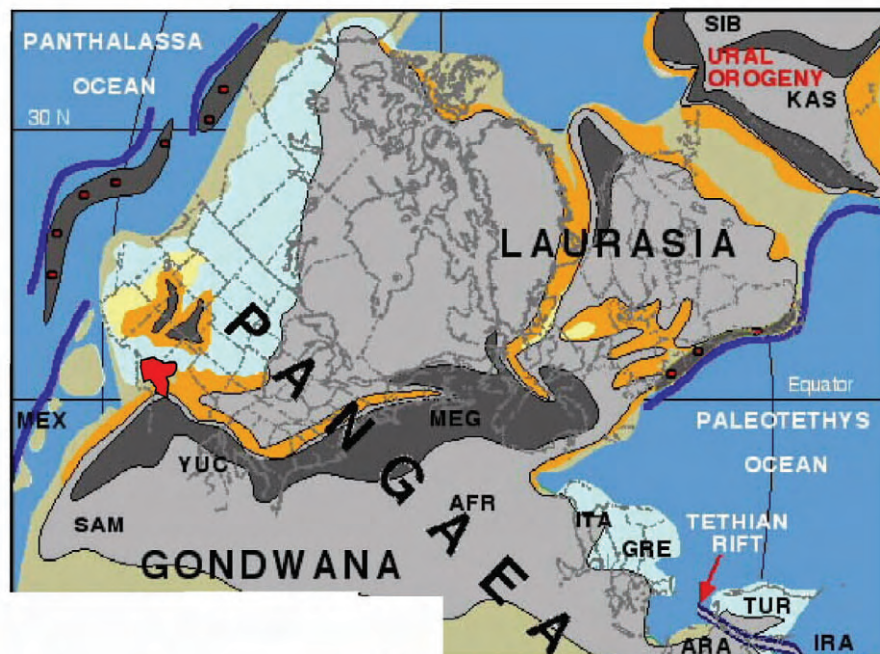



Figure 4. Northwest-southeast schematic cross section of uppermost Leonardian to Ochoan strata, Guadalupe Mountains area, showing formations, carbonate-bearing members of the Delaware Mountain Group, and boundaries of high-frequency sequences and composite sequences. Modified from Kerans and Kempter (2002).



Figure 5. Early Permian paleogeographic global reconstruction of the western hemisphere. Modified from Blakey (2004).



Explanation

AFR	Africa	MEX	Mexico
ARA	Arabia	MEG	Meguma (East U.S.)
GRE	Greece	SAM	South America
IRA	Iran	SIB	Siberia
ITA	Italy	TUR	Turkey
KAS	Kasakhstan (C. Asia)	YUC	Yucatan
 Permian Basin			

From Blakey (2004)

Figure 6. Late Permian paleogeographic reconstruction. Also shown are approximate positions of the Permian Basin. From Blakey (2004).

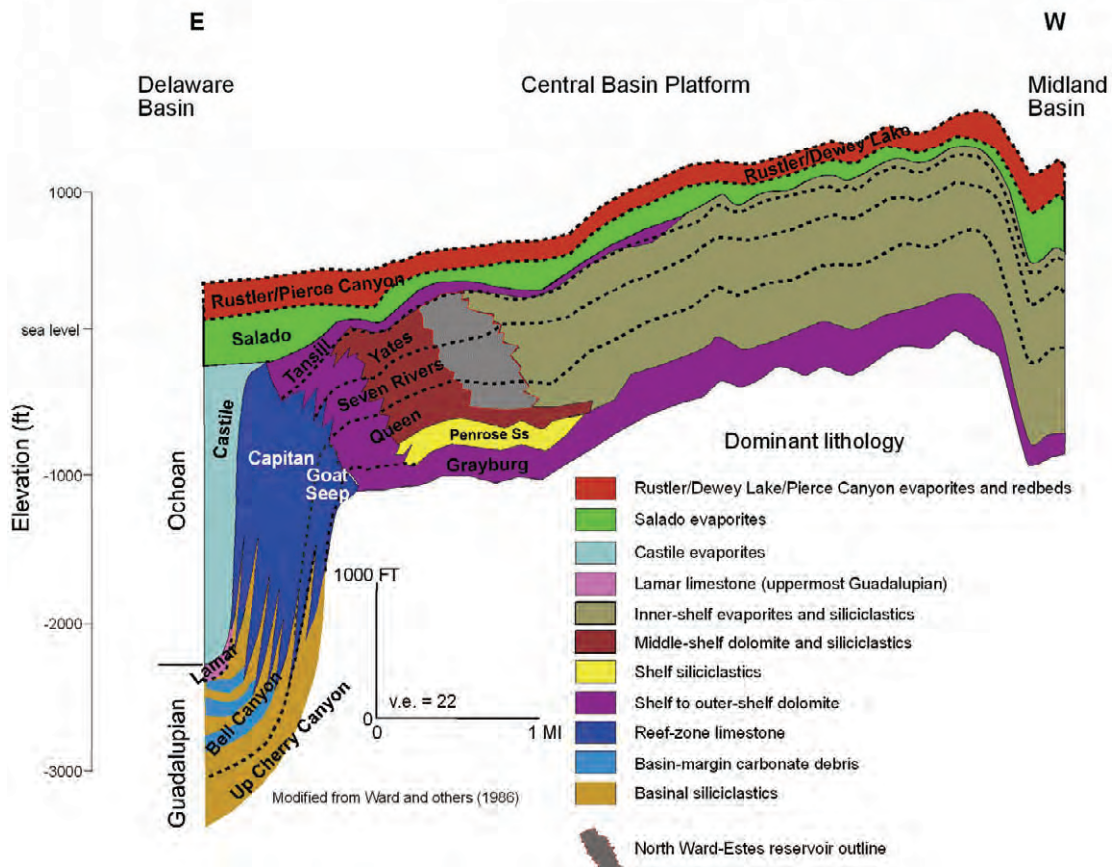


Figure 7. East-west cross section of the Upper Guadalupian shelf intervals and equivalent intervals in the Delaware Mountain Group. Also shown is the North Ward-Estes reservoir. Overall progradational aspect of stratigraphic development is reflected in basinward offsets of stratigraphically younger reservoir units in North Ward-Estes field. Modified from Ward and others (1986).

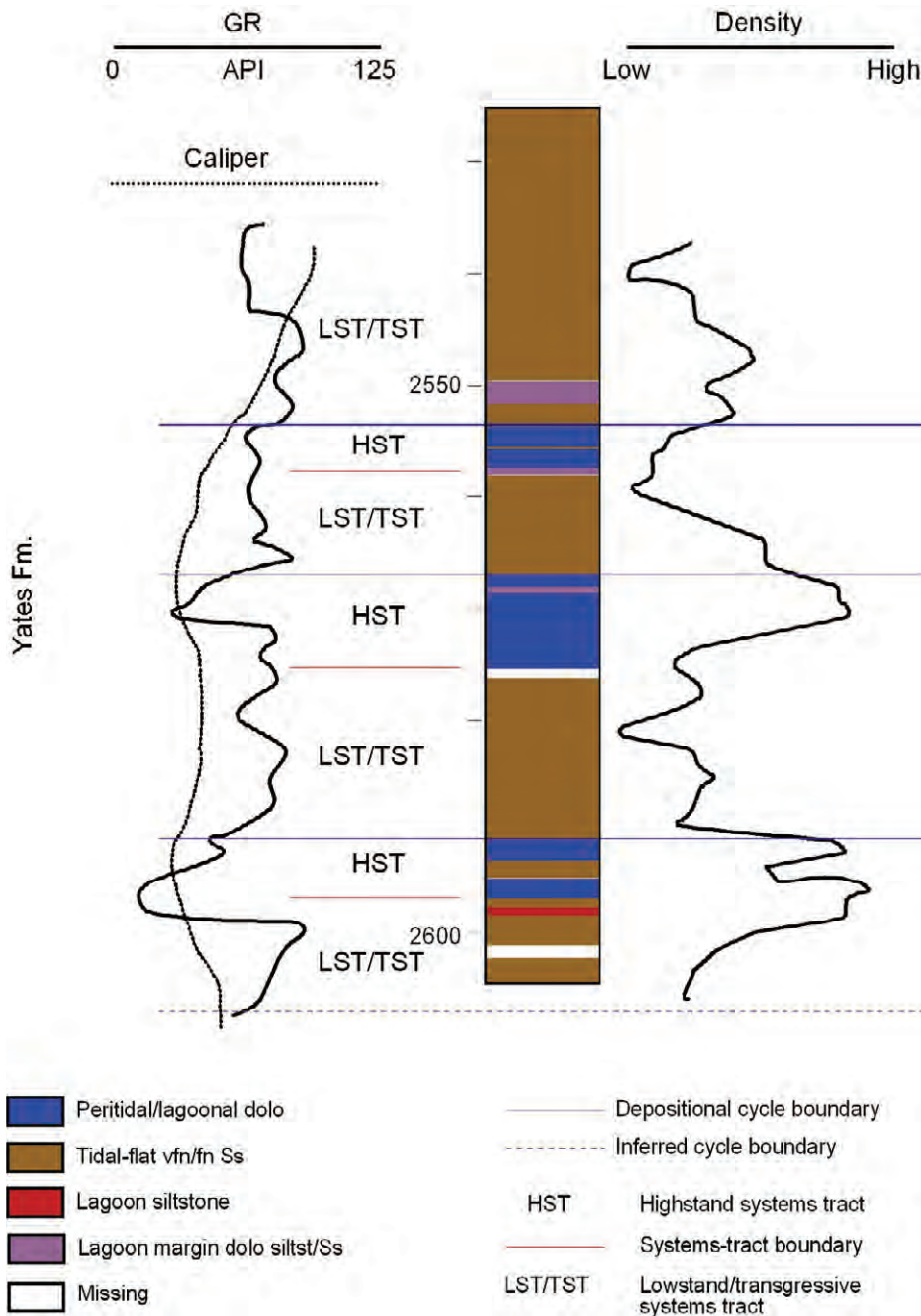


Figure 8. Core description and corresponding well logs for part of the Yates interval from HSA No. 1281, North Ward-Estes reservoir, Ward County. Also shown are boundaries between depositional cycles and systems tracts. Thin siliciclastic breaks in carbonate-dominated intervals may record higher frequency depositional cycles or nearness of carbonate depositional environments to siliciclastic source areas.

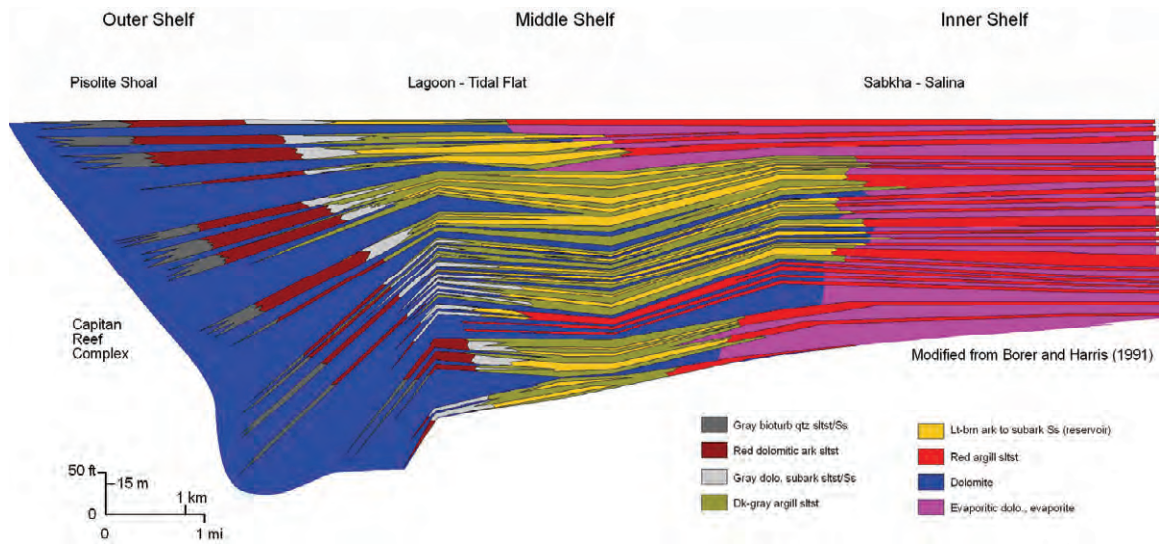


Figure 9. Composite stratigraphic cross section showing shelf-to-basin facies relations in the Yates Formation along the margin of the Delaware Basin. Section was constructed from descriptions of cores from the Northwest Shelf and west edge of the Central Basin Platform. Primary reservoirs are in sandstones of the middle-shelf area. Updip pinch-outs of reservoir sandstones into evaporate-bearing siliciclastics and stratigraphically adjacent evaporate-bearing and evaporate strata (top and bottom seals) compose the stratigraphic components of hydrocarbon trapping. Modified from Borer and Harris (1991).

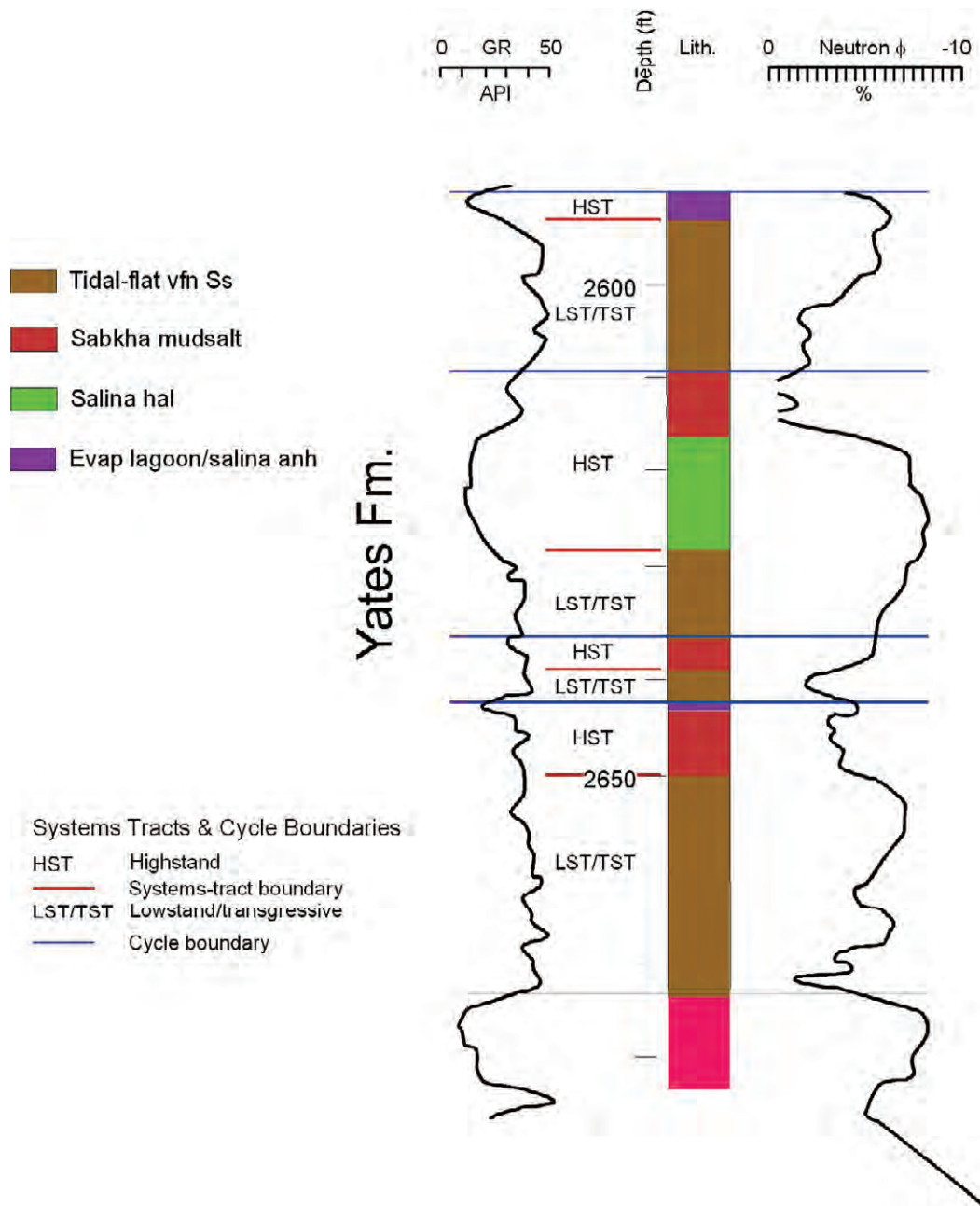


Figure 10. Core description and corresponding well logs for a part of the Yates interval from University No. 3210-2, Embar reservoir, Andrews County. Also shown are boundaries between depositional cycles and systems tracts. The evaporite facies in this well are representative of areas that are up depositional dip of those represented by carbonate facies, such as are shown in HSA No. 1281 well (fig. 8).

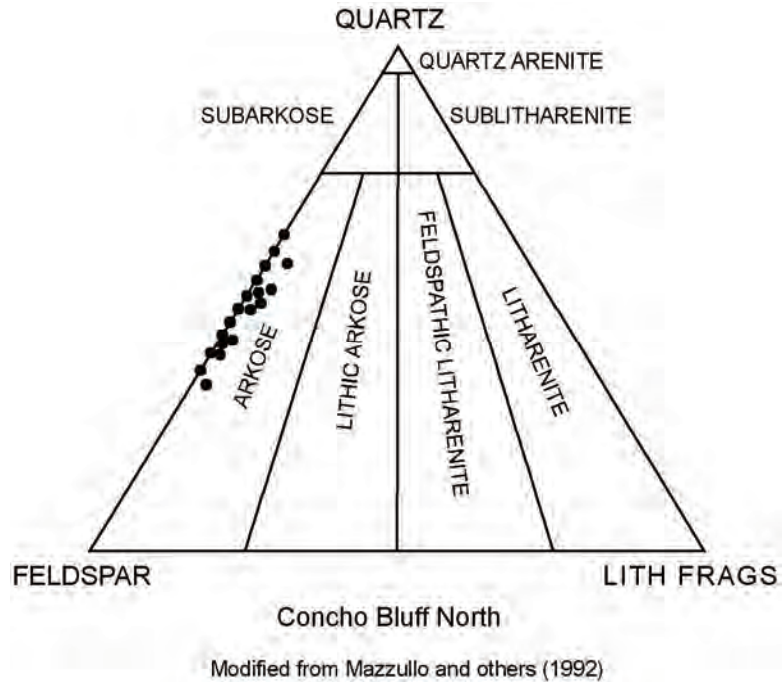
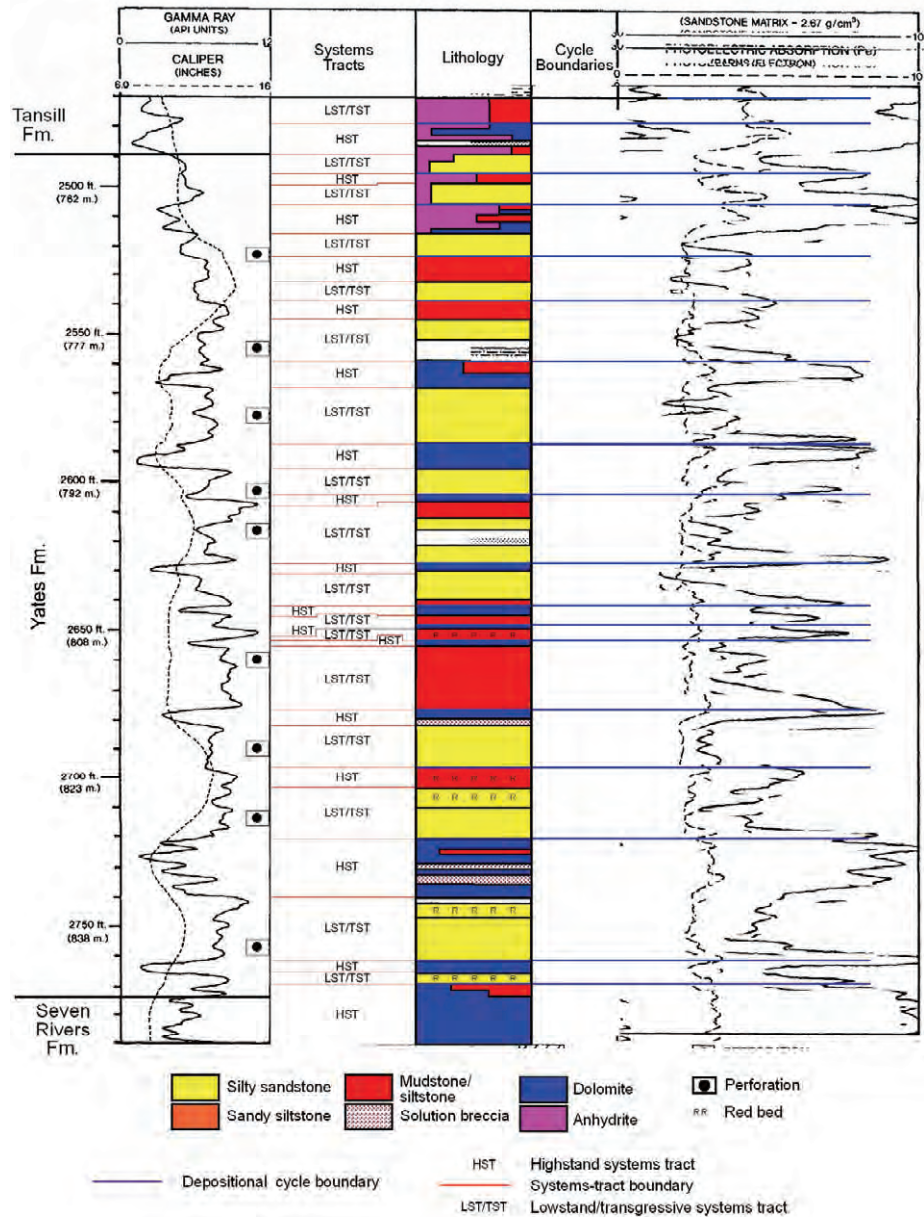


Figure 11. Ternary composition diagram for North Concho Bluff sandstone (classification of Folk, 1968). Diagram is generally representative of Guadalupian sandstone and siltstone compositions in the Permian Basin. The significant fraction of K-feldspar produces relatively high gamma-ray values even in clay-free sandstone. Modified from Mazzullo and others (1992).



Modified from Andreason (1992)

Figure 12. Core description and corresponding well logs of the Yates interval from HSA No. 1281, North Ward-Estes reservoir, Ward County. Also shown are boundaries between depositional cycles and systems tracts. Note that evaporites (anhydrite) are more common in the uppermost parts of the Yates, reflecting the overall reduction of accommodation during deposition of marine-derived chemical portions of the formation. Note also the thinning of carbonate units at higher stratigraphic intervals in the lower half of the Yates. The return of thicker carbonate beds above the 2,600-ft level may mark the mid-Yates sea-level turnaround interpreted by Kerans and Kempton (2002) in the Guadalupe Mountains (CS13/CS14 boundary in figure 2). Modified from Andreason (1992).

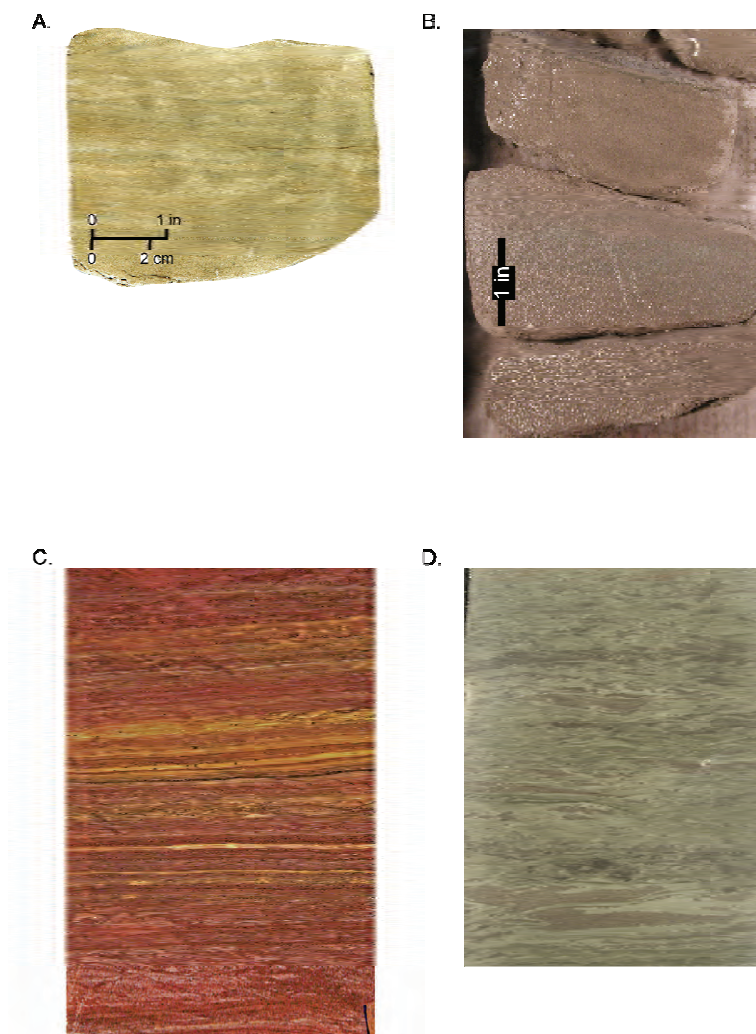


Figure 13. Artesia Group beach-ridge and tidal-flat sandstone facies: (A) Queen reservoir (oil-stained) beach-ridge, coarsely laminated, fine-grained feldspathic sandstone (HSA No. 475 well, North Ward-Estes, Ward County); (B) Yates reservoir (oil-stained) beach-ridge, coarsely laminated, fine-grained feldspathic sandstone (HSA No. 1257 well, North Ward-Estes, Ward County); (C) Queen nonreservoir, mm-scale, planar- and ripple-laminated, fine/very fine grained sandstone (HSA No. 475 well, North Ward-Estes, Ward County); and (D) Yates haloturbated, mm-scale, planar- and ripple-laminated, fine/very fine grained sandstone (HSA No. 1281 well, North Ward-Estes, Ward County).

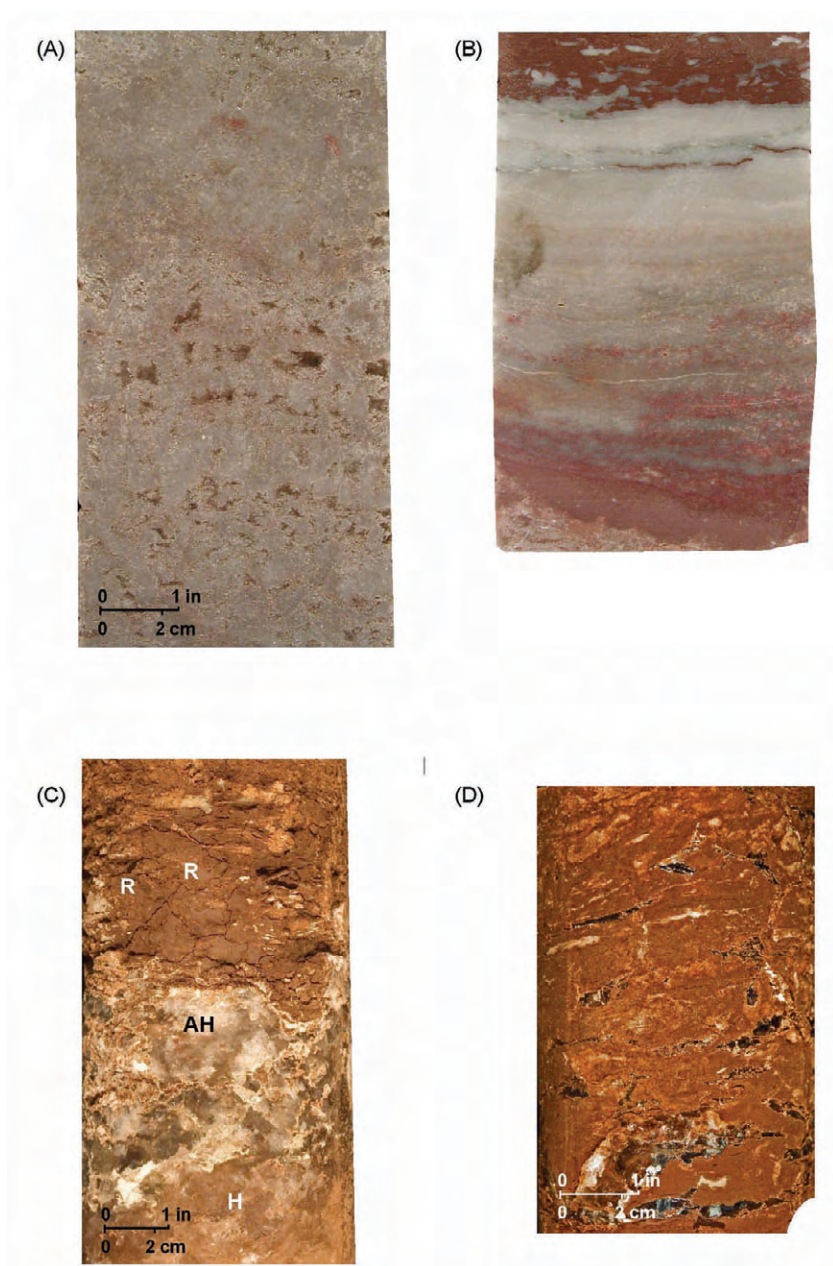


Figure 14. Artesia Group evaporite facies (University No. 3210-2 well, Embar field, Andrews County): (A) Yates Formation brine-pool, vuggy to massive, nodular anhydrite; vugs are filled with halite and may be molds after gypsum crystals; alternatively, vuggy interval may be fenestral tidal-flat carbonate that has been replaced by sulfate; (B) Yates brine-pool, plane-laminated anhydrite may record cycles of gypsum growth and abrasion in a shallow pool; (C) brine-pool and brine-pool-margin (sabkha) succession of mosaic halite, anhydritic halite, and mudrock residue after dissolution of halite from mixed halite-mudrock facies; and (D) sabkha, silty, very fine grained sandstone containing cm-scale halite crystals. Dissolution of halite would produce haloturbated sandstone such as is shown in figure 13D.

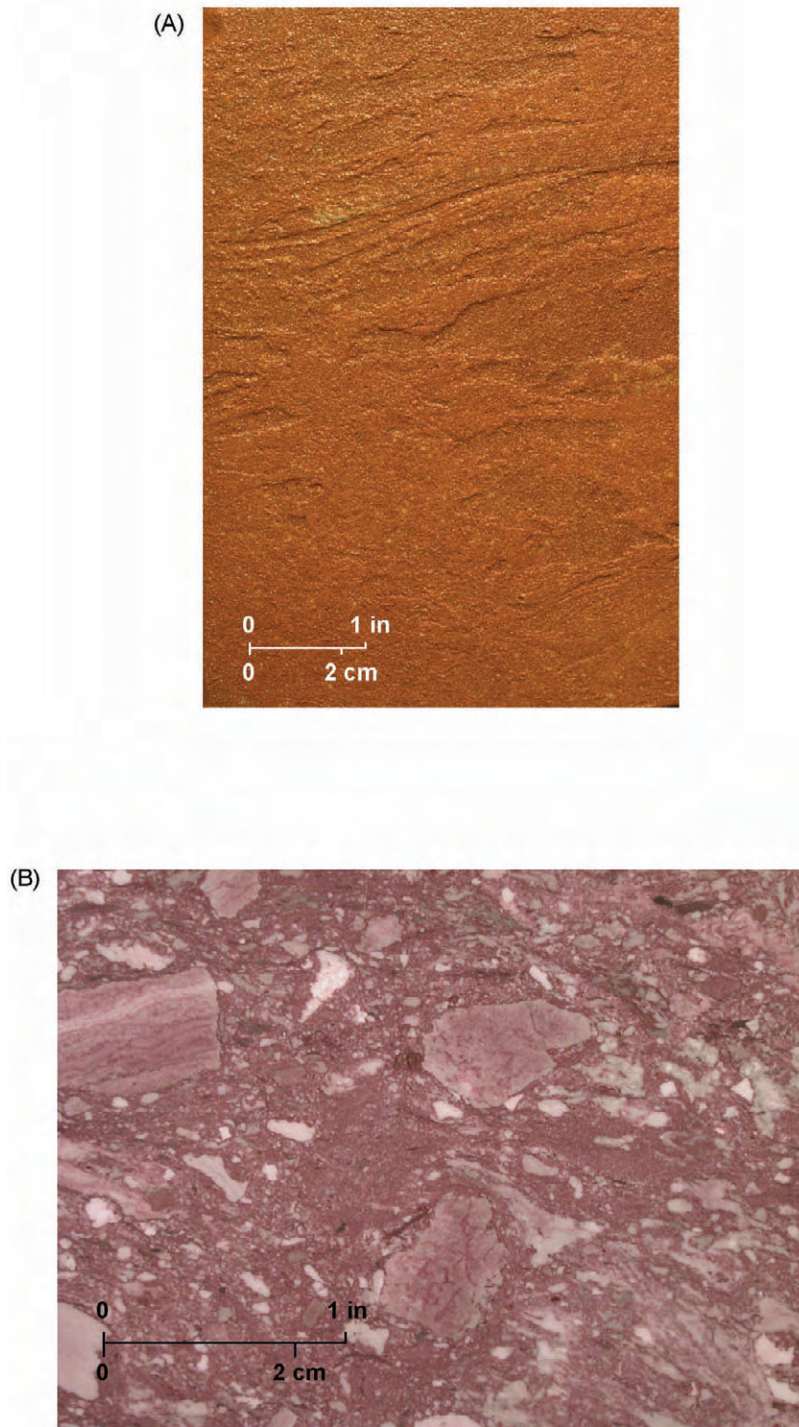


Figure 15. Artesia Group eolian sandstone and mixed sandstone/carbonate facies: (A) Yates uncommon, ripple-laminated, fine-grained sandstone from probable eolian setting (University No. 3210-2 well, Embar field, Andrews County) and (B) Yates dissolution-collapse-brecciated dolomite in siliciclastic matrix. Facies is similar to that found in dissolution zone depicted in figure 31 (HSA No. 1281 well, North Ward-Estes, Ward County).

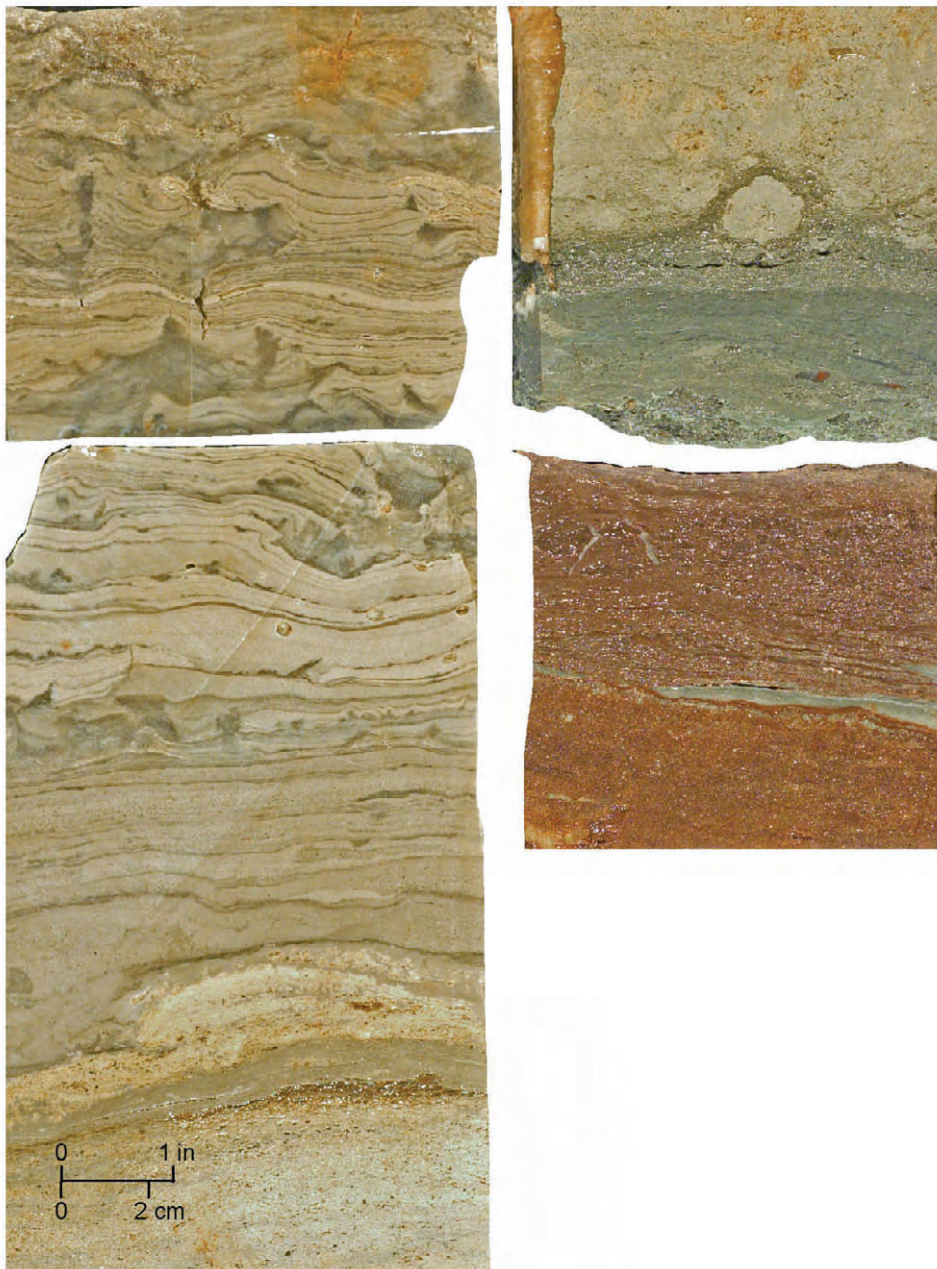


Figure 16. Yates succession of tidal-flat, haloturbated, fine- to very fine grained sandstone and anhydritic dolomite; it may record transgressive reworking of terrestrial sandstone into tidal flats and establishment of evaporative lagoon wherein algal-laminated carbonate deposition alternates with gypsum precipitation. Upper half of carbonate-anhydrite interval shows carbonate draping over pseudomorphs after standing gypsum crystals (University No. 3210-2 well, Embar field, Andrews County).

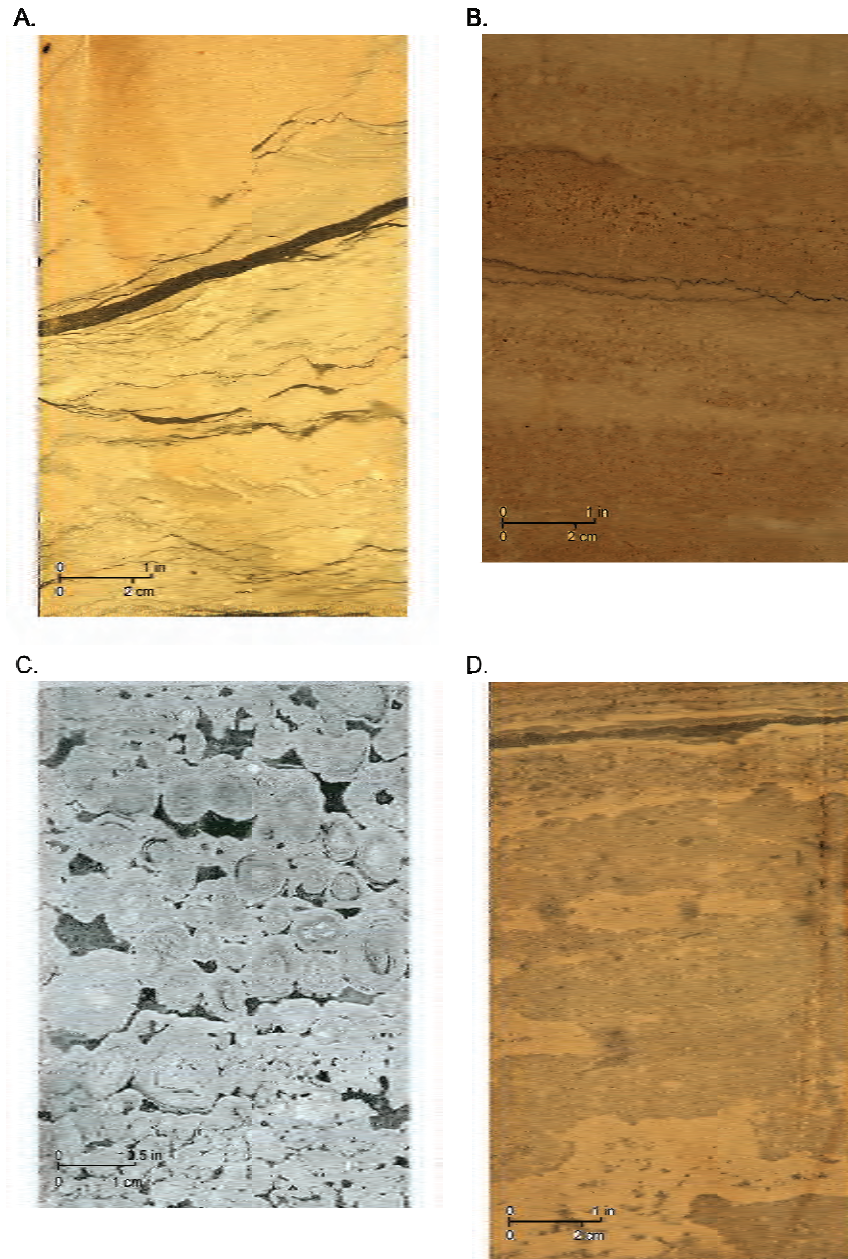


Figure 17. Artesia Group dolostone facies: (A) Queen shoal cross-laminated grainstone; (B) Queen tidal-flat packstone; (C) Yates shelf-crest shoal, pisolite grainstone; and (D) Queen lagoon bioturbated wackestone to packstone. Cores A, B, and D are from HSA No. 475 well, Ward-Estes, Ward County; C is from Gulf PDB-04 well, Eddy County, New Mexico.

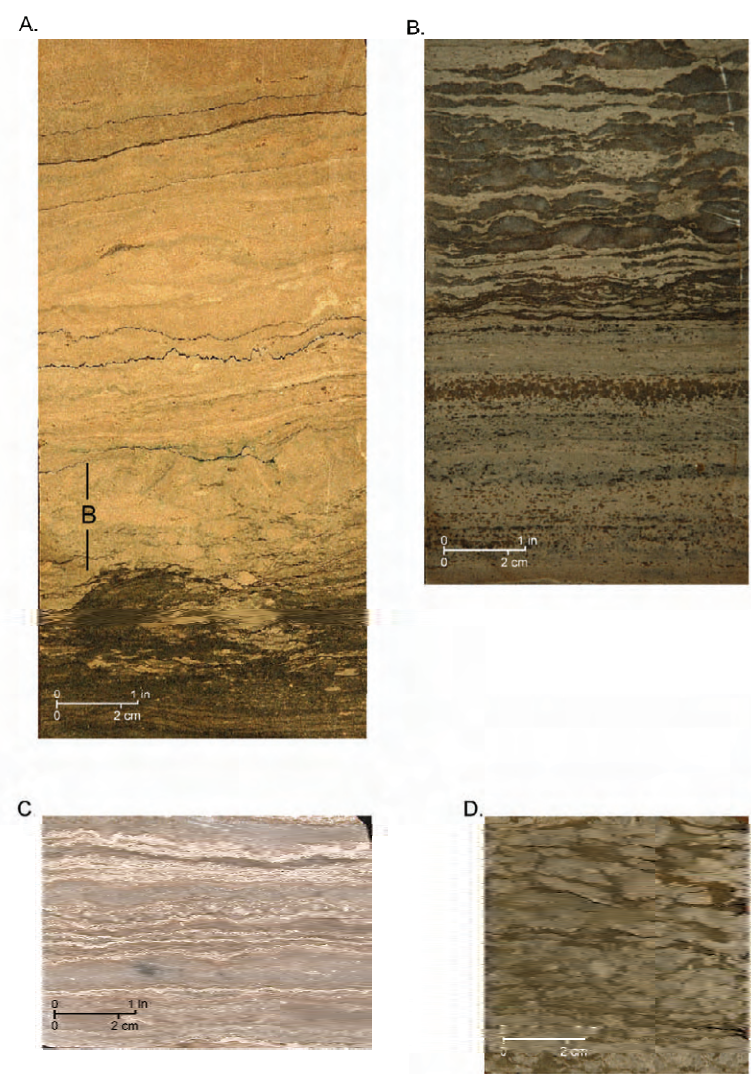


Figure 18. Artesia dolostone and evaporite facies: (A) succession of Queen tidal-flat, laminated siliciclastic siltstone; collapse-breccia dolostone; and tidal-flat, algal-laminated wackestone/packstone (HSA No. 475 well, Ward-Estes, Ward County); (B) succession of tidal-flat dolostone with mm-scale anhydrite (sabkha) and interlaminated brine-pool dolomudstone and anhydrite (HSA No. 475 well, Ward-Estes, Ward County); succession records establishment of a sabkha in a previously deposited tidal-flat interval and subsequent development of a brine pool wherein conditions alternated between sulfate undersaturation (carbonate laminae) and supersaturation (anhydrite intervals); (C) Yates brine-pool, mm-scale, interlaminated dolomite (thin laminae) and anhydrite (University No. 3210-2 well, Embar field, Andrews County); and (D) Seven Rivers sabkha anhydrite in siliciclastic matrix (HSA No. 475 well, Ward-Estes, Ward County).

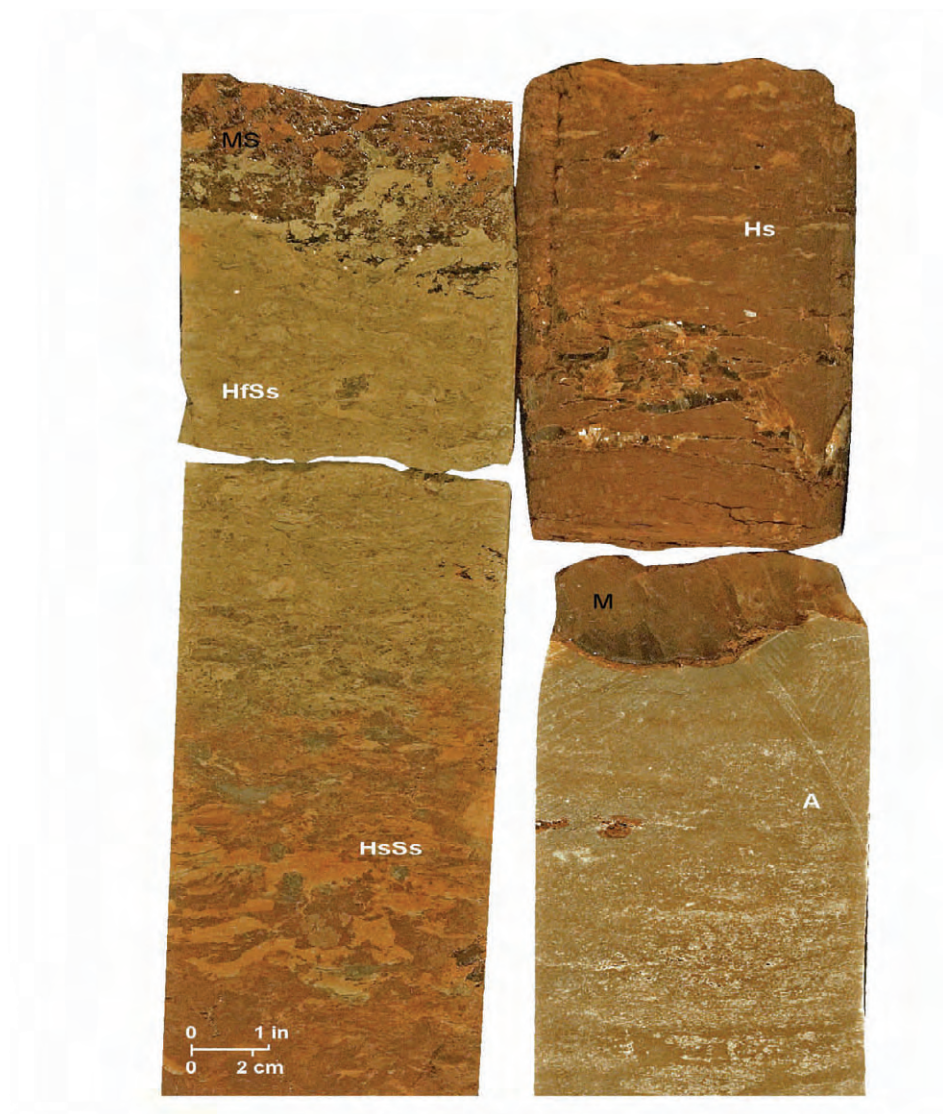
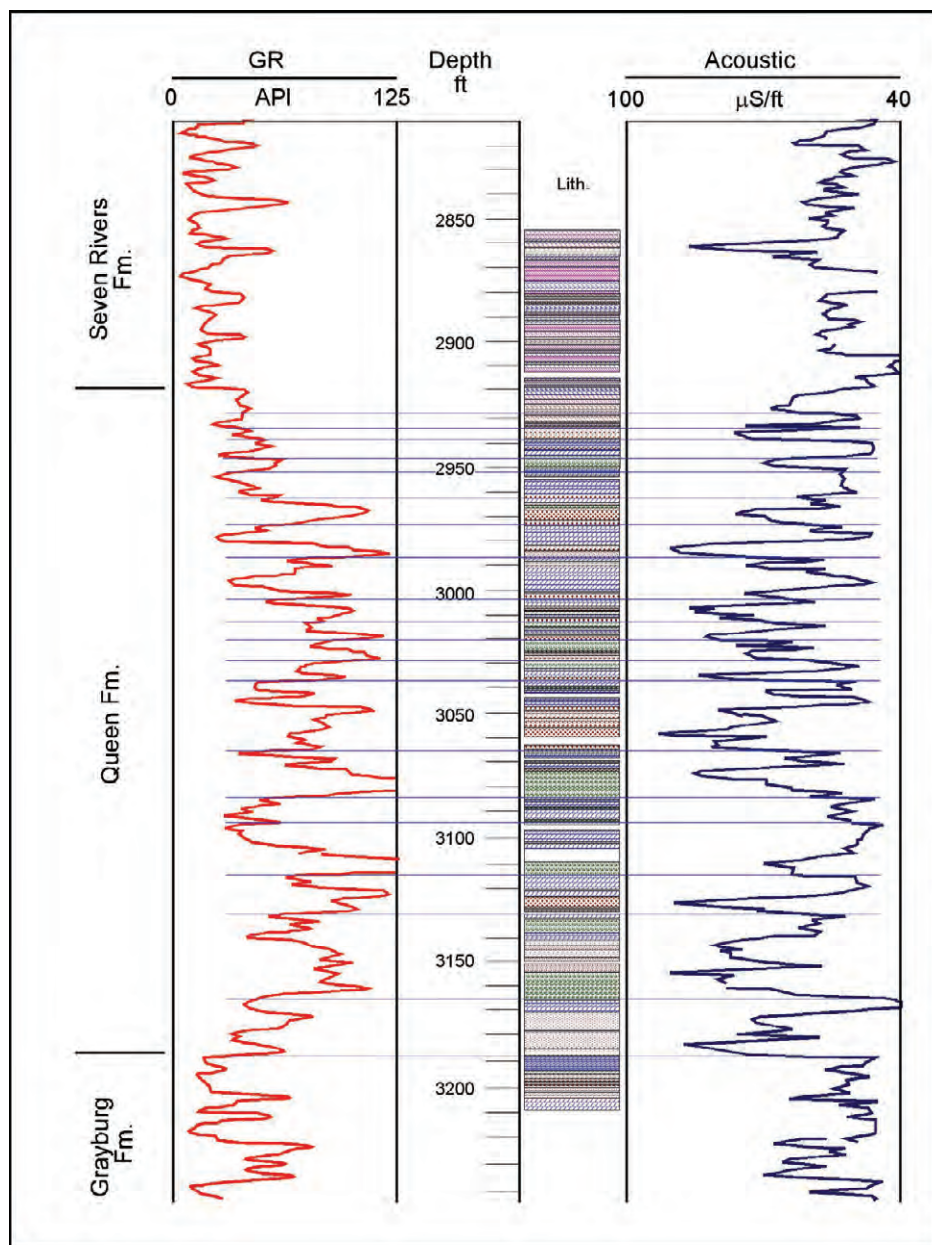


Figure 19. Succession of Yates brine-pool anhydrite, brine-pool fill of mudrock and haloturbated siltstone to fine-grained sandstone, and sabkha halite-mudrock (University No. 3210-2 well, Embar field, Andrews County). A = brine-pool anhydrite; M = brine-pool-margin mudstone residue after halite dissolution in halite-mudrock; Hs = sabkha haloturbated, sandy siltstone; HsSs = sabkha haloturbated, silty, very fine grained sandstone; HfSs = sabkha haloturbated, fine-grained sandstone; and MS = sabkha admix of halite and fine-grained sandstone. MS is representative of HfSs prior to halite dissolution. Prior to halite dissolution mosaic halite may have occurred immediately above the anhydrite.



— Queen depositional cycle boundary

- | | |
|------------------------------|--------------------------------------|
| Peritidal/lagoonal dolo | Tidal-flat vfn Ss |
| Evap lagoon anh dolo | Lagoon siltst |
| Lagoon slty dolo | Sabkha anh Ss |
| Lagoon margin dolo siltst/Ss | Evap lagoon/salina margin v slty anh |
| Beach-ridge fn Ss | Evap lagoon dolo anh |
| Tidal-flat vfn/fn Ss | Evap lagoon/salina anh |
| Tidal-flat slty vfn Ss | Evap lagoon/salina slty anh |

Figure 20. Core description and well logs for Queen Formation and stratigraphically adjacent units from HSA No. 475, N. Ward-Estes reservoir, Ward County. Also shown are depositional cycle boundaries within the Queen.



Figure 21. Queen peritidal dolopackstone with tepee structure and probable replacive anhydrite. Swirl in lower part of upper anhydrite interval is composed of dolomite inclusions.

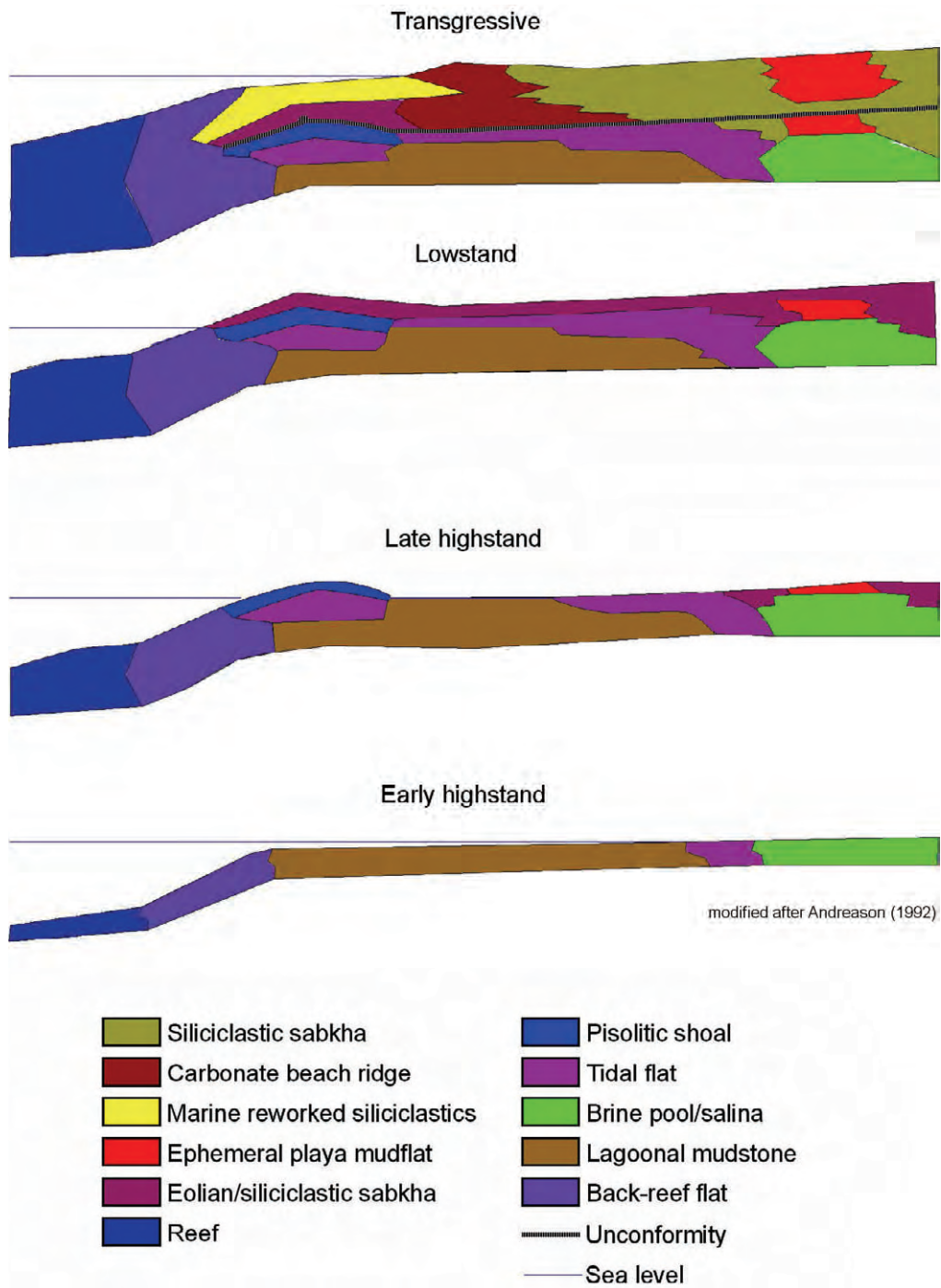


Figure 23. Shelf-margin to inner-shelf cross sections schematically illustrating sea-level-related stages of Yates deposition at Ward-Estes field. Model is generally representative of Upper Permian depositional styles. Modified from Andreason (1992).

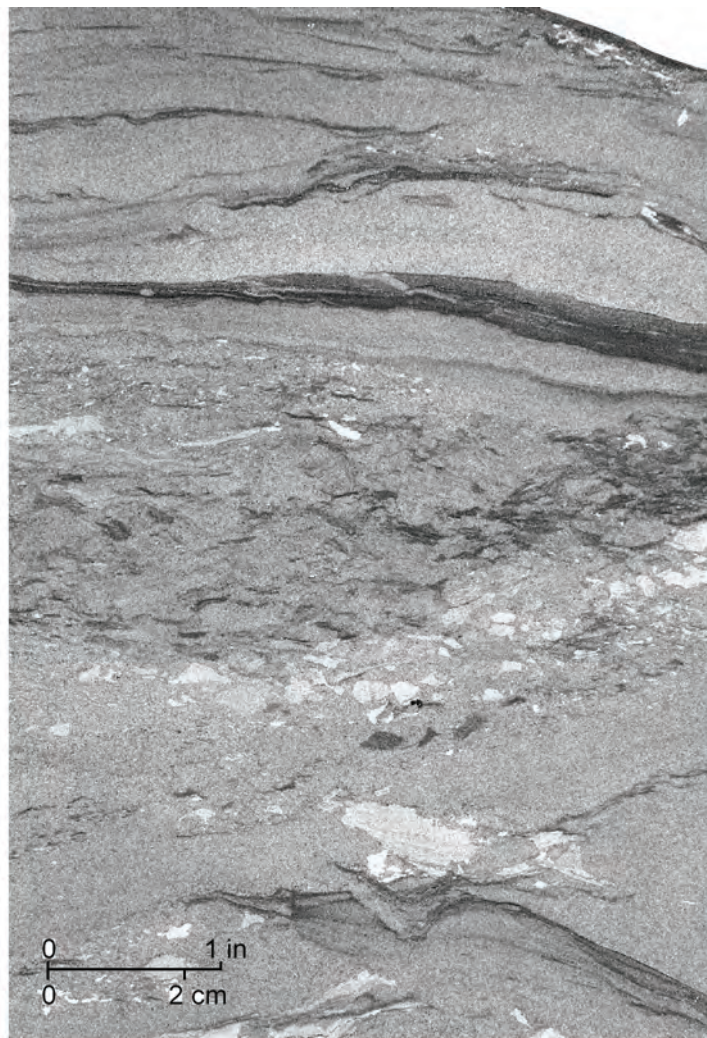


Figure 24. Queen intraclastic, fine-grained sandstone of possible tidal-channel origin. This sample lies below a marine-derived cycle-top dolostone bed and may record a transgressive ravinement surface. Similar samples elsewhere may mark high-frequency sequence boundaries within siliciclastic intervals where no marine-derived sediment was deposited during the highstand depositional phase (HSA No. 475 well, 2945.5 ft, North Ward-Estes reservoir, Ward County).

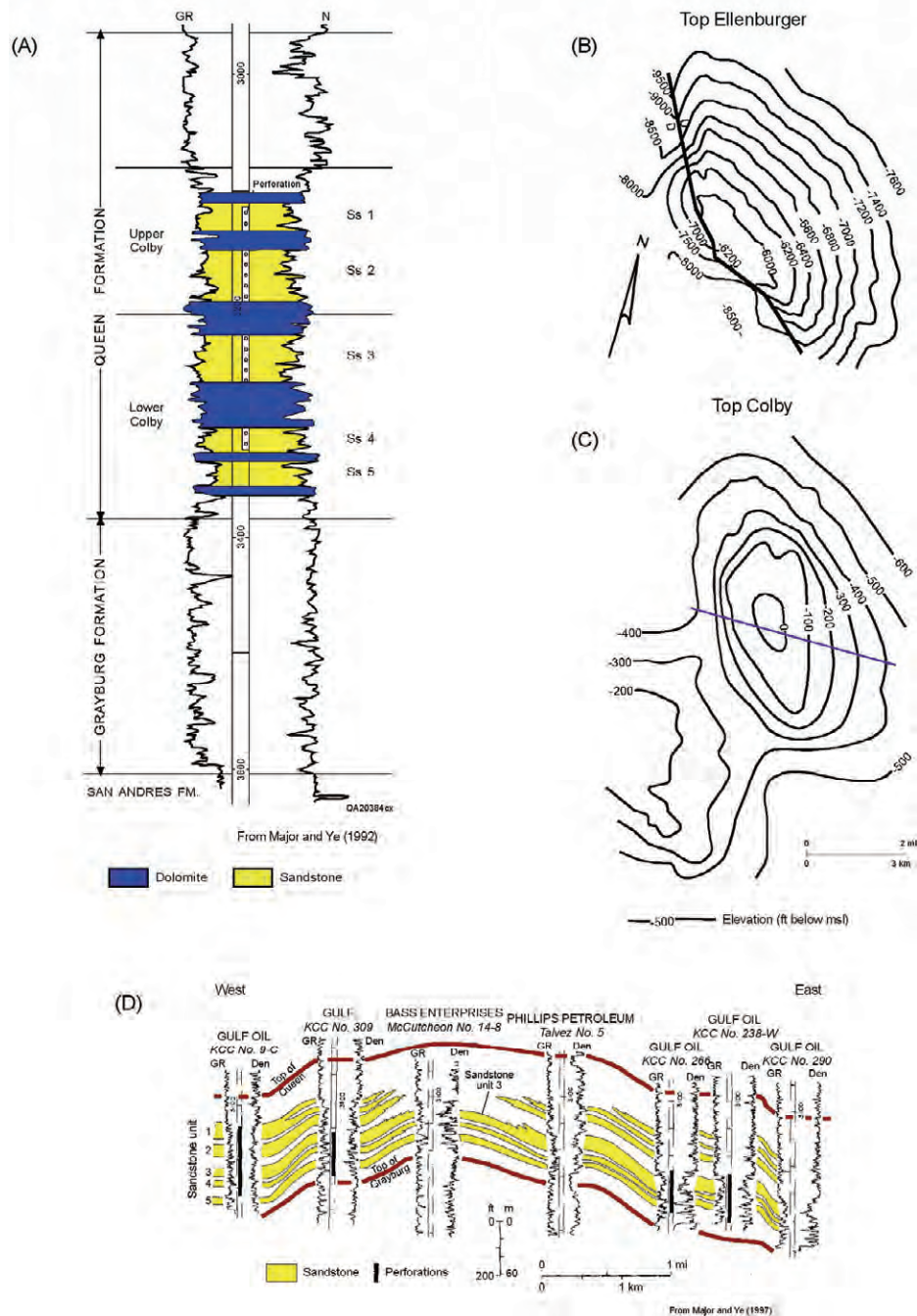


Figure 25. Keystone Colby reservoir: (A) representative well log showing reservoir sandstone intervals and stratigraphically adjacent dolostone intervals; structure maps on the tops of the (B) Ellenberger Formation and (C) Colby (Queen) sandstone interval, demonstrating the deeply rooted origins of structures in the Upper Permian section; and (D) west-east cross section of the Colby sandstone interval showing off-structure thickening of the Queen and reservoir-sandstone pinch-outs onto the Keystone structure. Approximate line of section shown in C. Modified from Galloway and others (1983) and Major and Ye (1997).

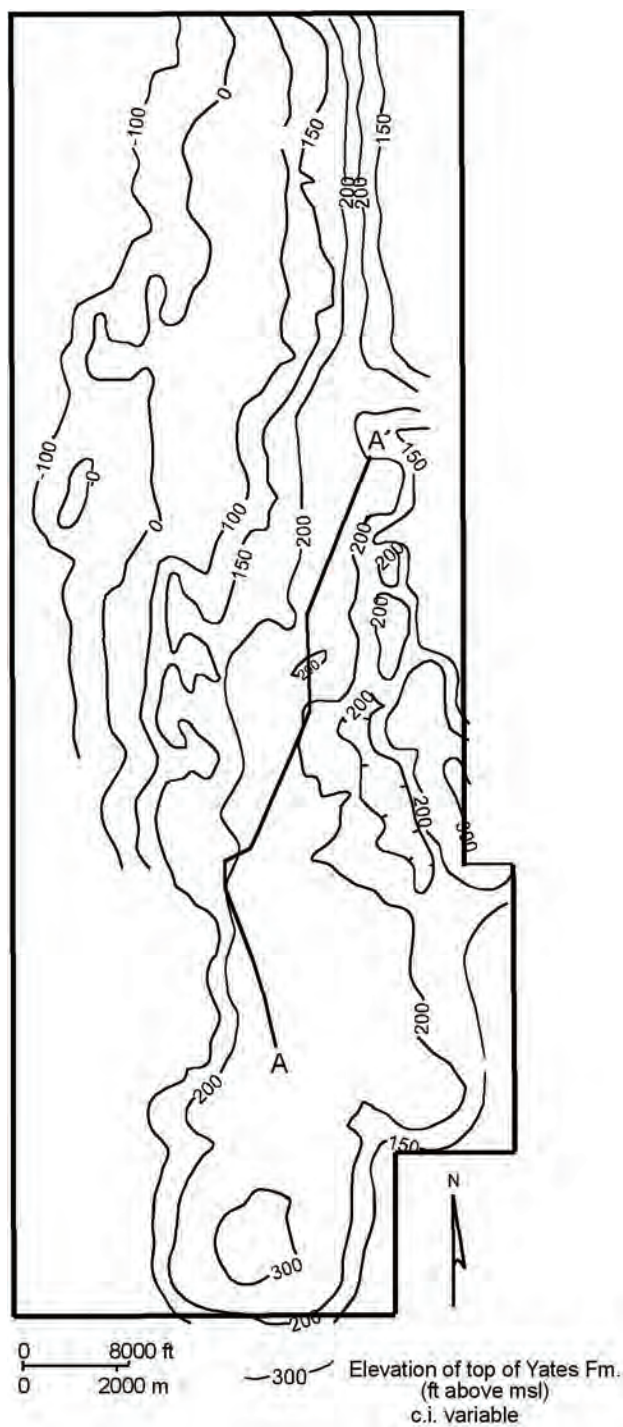


Figure 26. Structure map on top of the Yates Formation, North Ward-Estes reservoir, Ward County. Location of section A-A' (figure 32) is shown. Primary structure is a narrow strike-elongate anticline. Modified from West Texas Geological Society (1994).

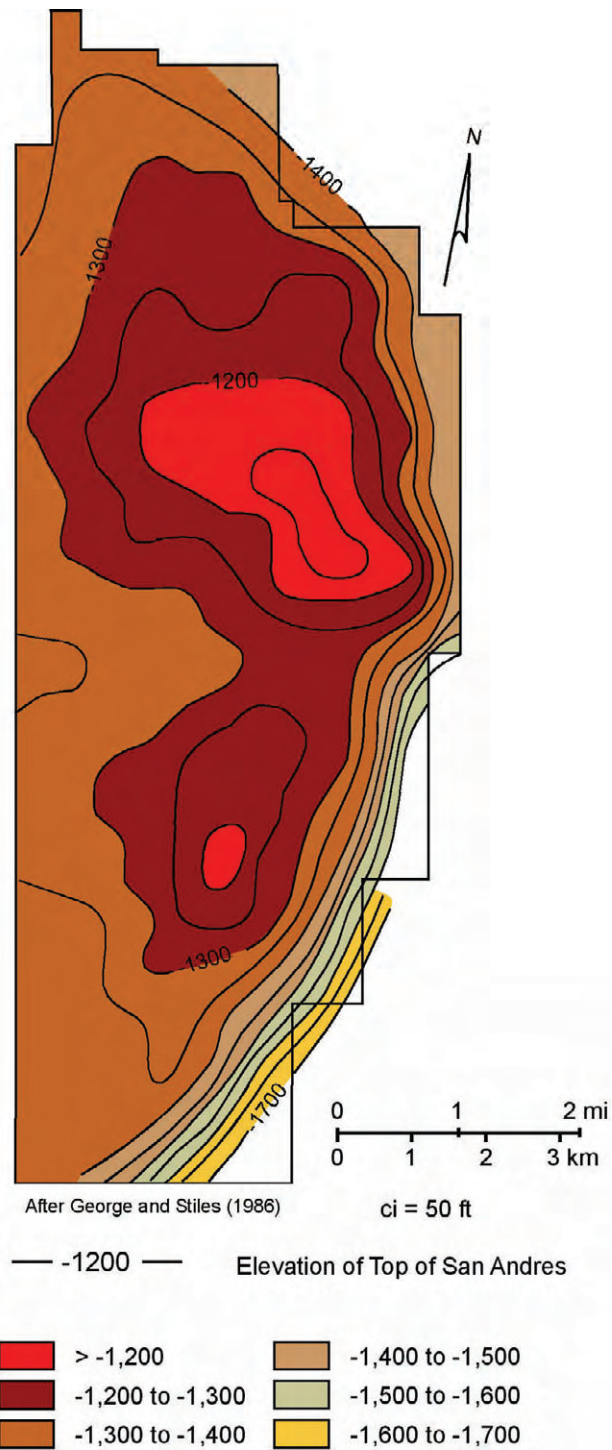


Figure 27. Structure map on top of the Queen Formation, Means reservoir, Andrews County, showing twin-domal configuration reservoir structure. After George and Stiles (1986).

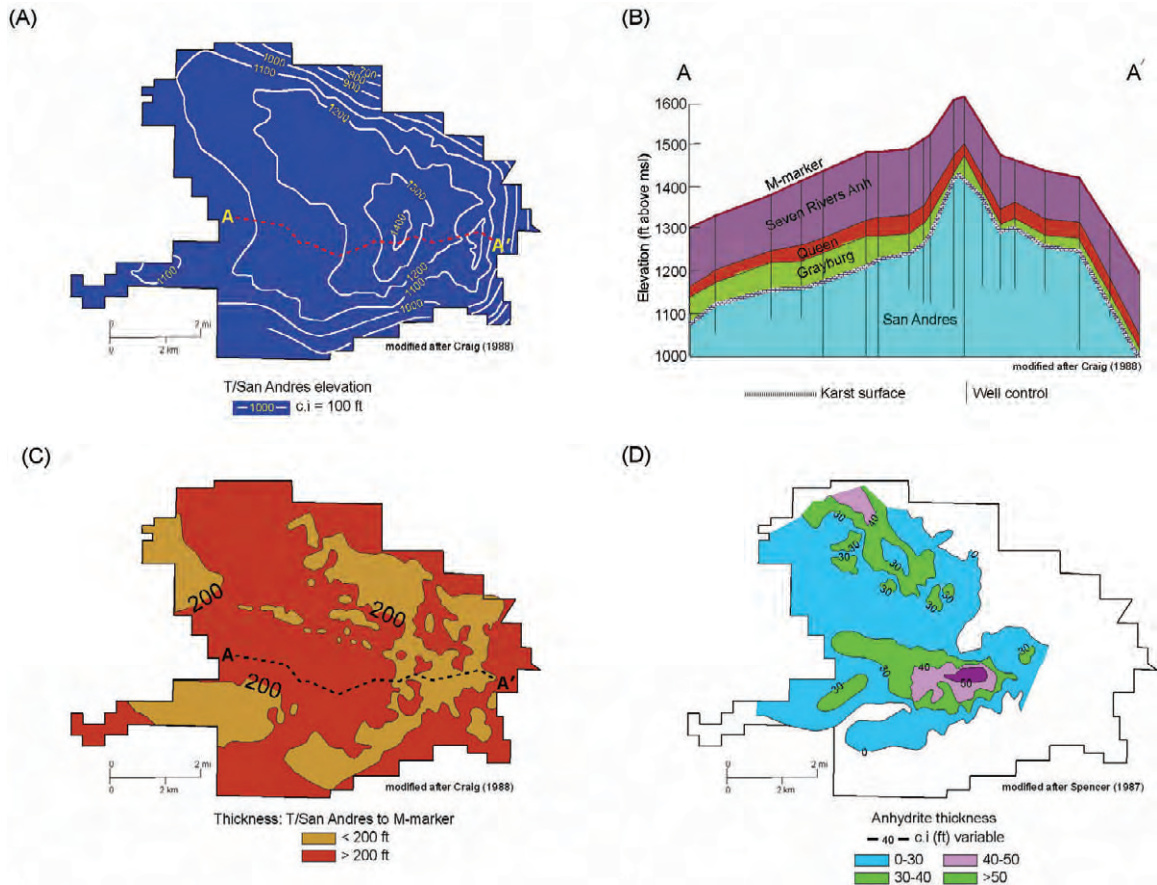
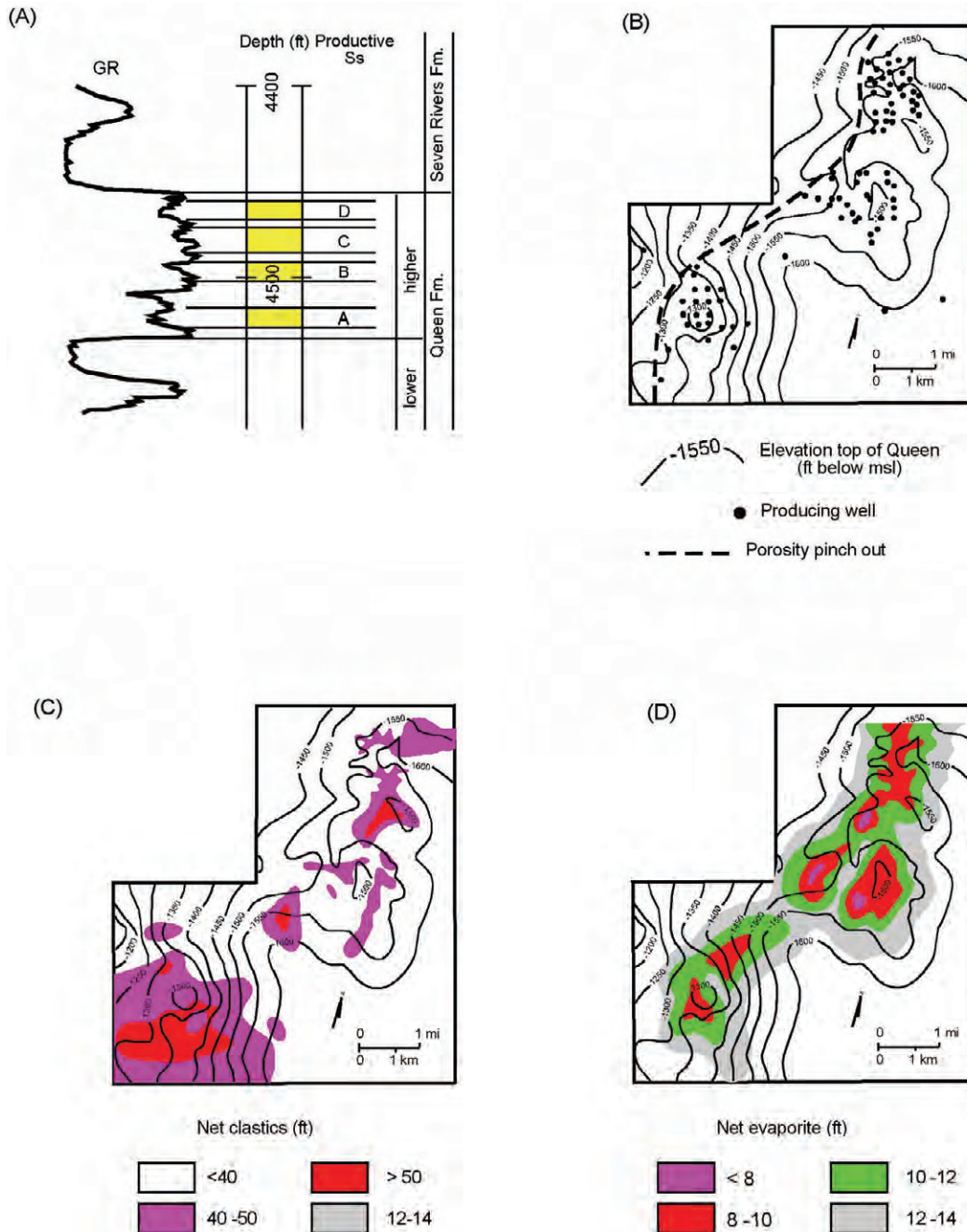


Figure 28. Yates reservoir, Pecos County: (A) U-shaped structure on top of the San Andres Formation; (B) west-east cross section A-A' of Yates field, showing karst surface on the San Andres surface and thinning of overlying intervals onto structure (line of section shown in A and C); (C) isopach map of the interval between the San Andres top and the M-marker within the Seven Rivers Formation, showing thinning of interval onto structure; and (D) isopach map of the Seven Rivers anhydrite, showing thinning of evaporate facies onto structure, thus demonstrating control of brine-pool depth by underlying structure.



Modified from Mazzullo and others (1992)

Figure 29. Concho Bluff and North Concho Bluff reservoirs: (A) representative well log of upper Queen reservoir-sandstone interval; (B) structure map on top of the Queen showing preferential locations of producing wells on structural highs or ramps downdip of porosity-pinch-out margin (shown in C); (C) net clastics map of the reservoir interval and position of the downdip margin of porosity plugging by evaporites; and (D) net evaporate map of the Queen showing thinning of evaporate facies onto structure. Modified from Mazzullo and others (1992).

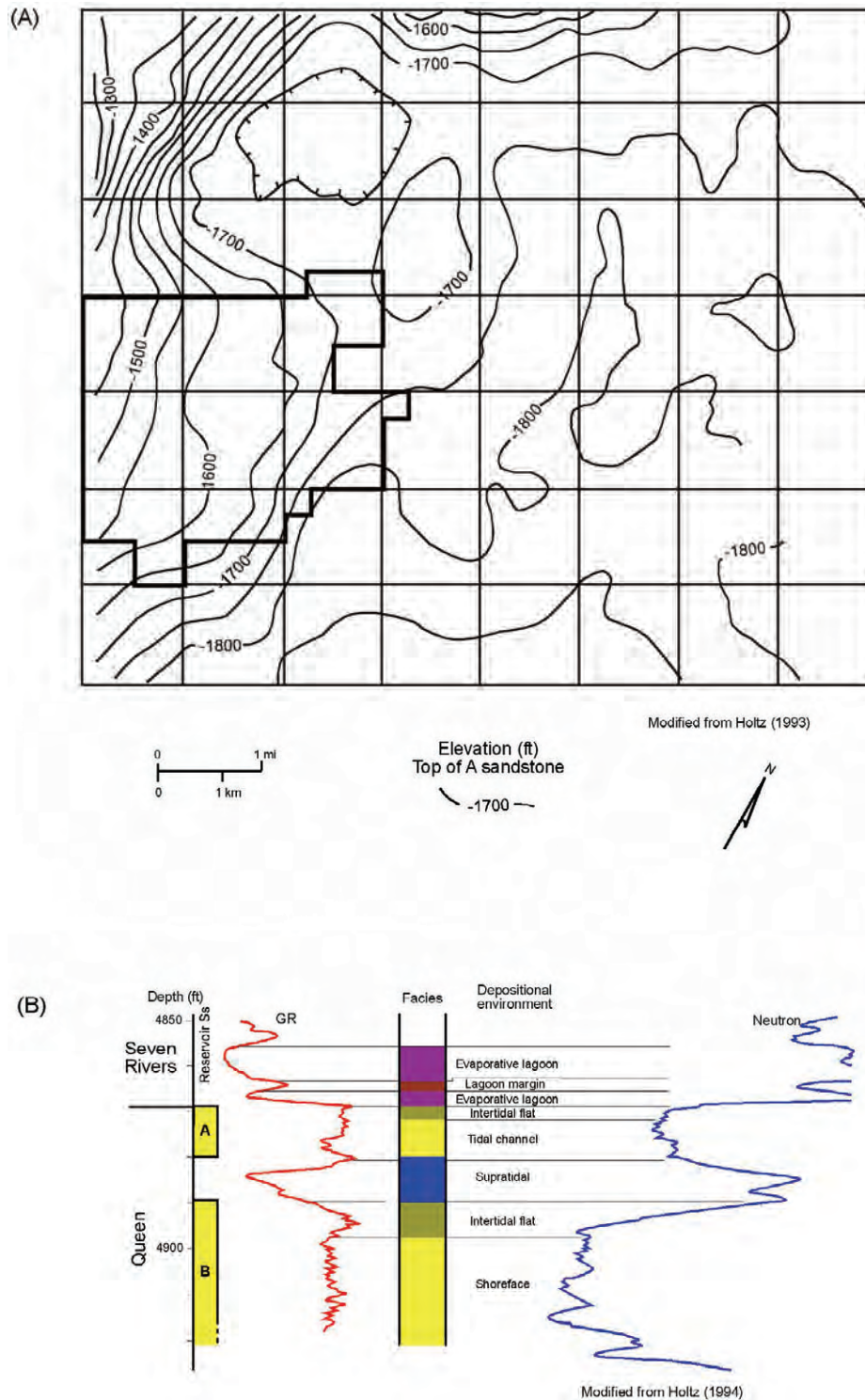


Figure 30. McFarland reservoir: (A) structure map on top of the Queen Formation; State University Units No. 1 and 2 are outlined; and (B) representative well log of the upper Queen productive-sandstone interval. Production is from interpreted tidal-channel and shoreface (probable beach ridge) sandstone. Supratidal carbonate provides baffle between productive sandstones. Modified from Holtz (1994).

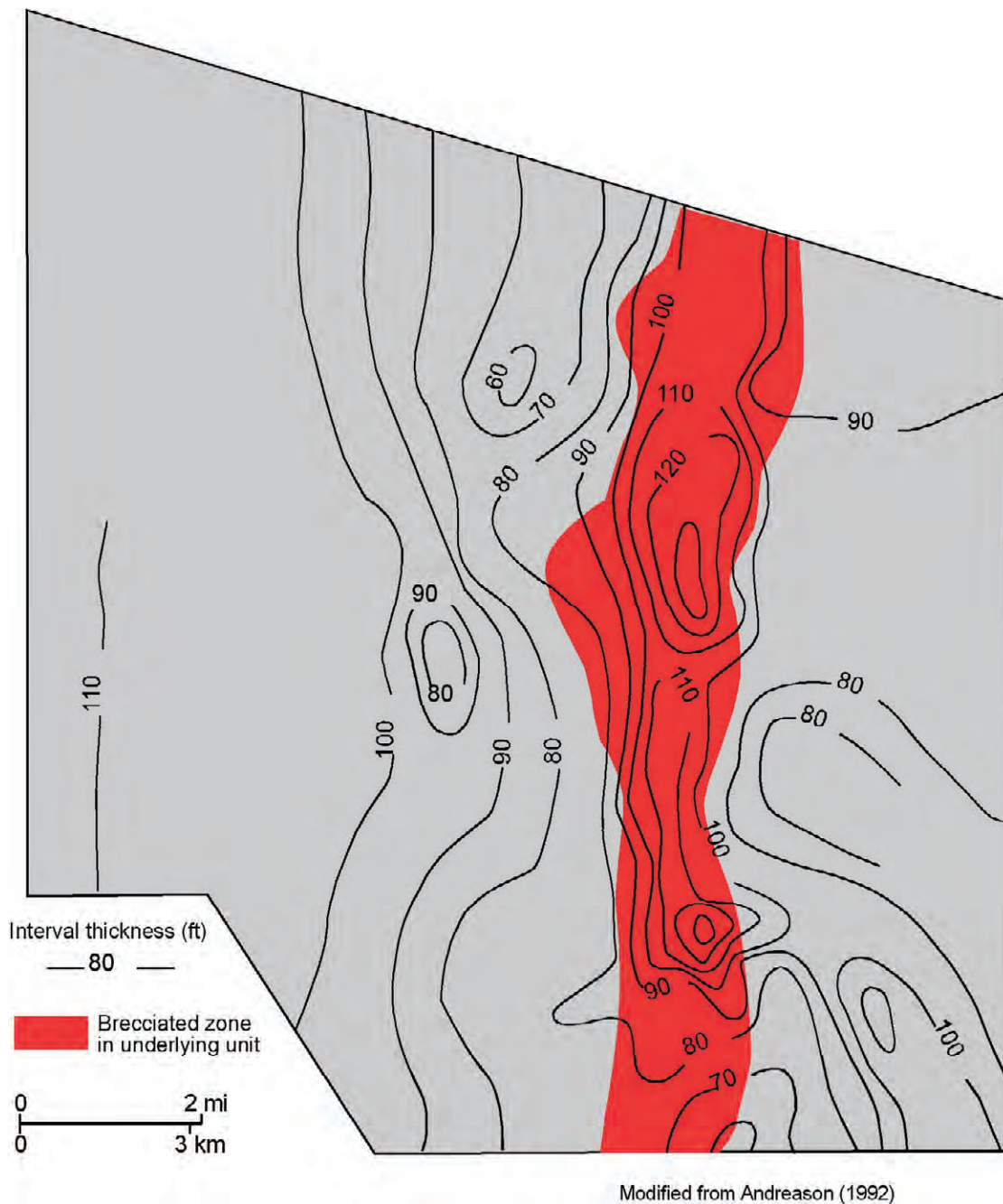


Figure 31. North Ward-Estes reservoir: isopach map of siliciclastic-dominated productive interval (fig. 12, 2,645–2,720 ft). Also shown is zone characterized by occurrences of dolostone solution breccia in underlying interval (fig. 12, 2,720–2,738 ft). Sandstone reservoir interval shows conspicuous thickening over area of solution collapse. Modified from Andreason (1992).

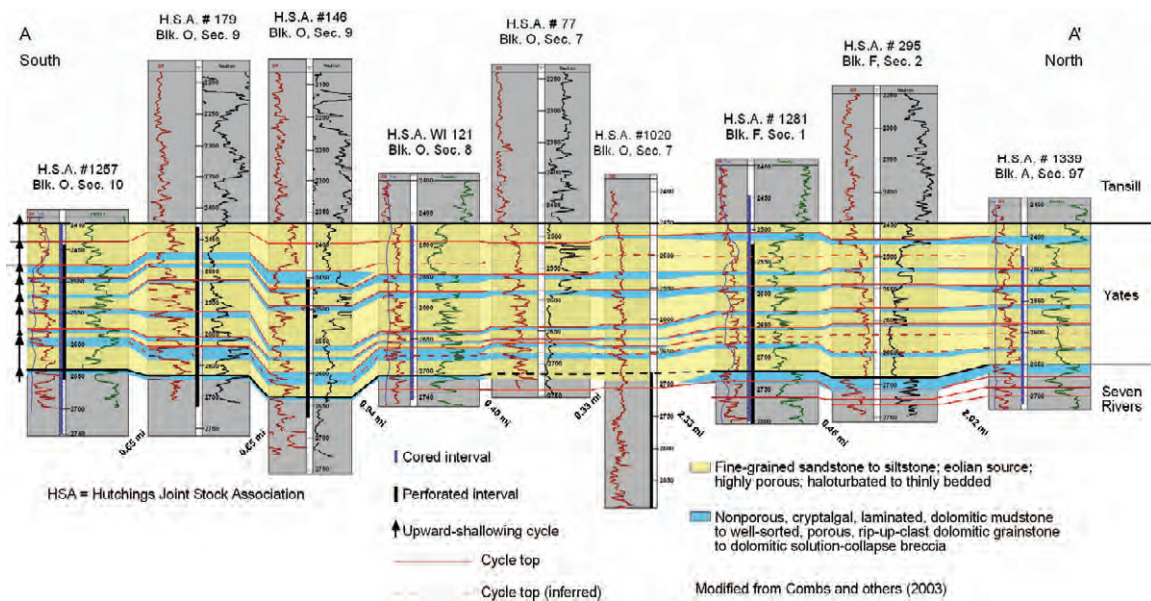


Figure 32. Strike cross section A-A' of Yates reservoir at North Ward-Estes field, Ward County. Shown are depositional cycle boundaries and generalized rock types. Location of section shown in figure 26. Although siliciclastics had late-highstand-lowstand-phase eolian sources, their present character indicates reworking by marine processes during the transgressive phase. Modified from Combs and others (2003).

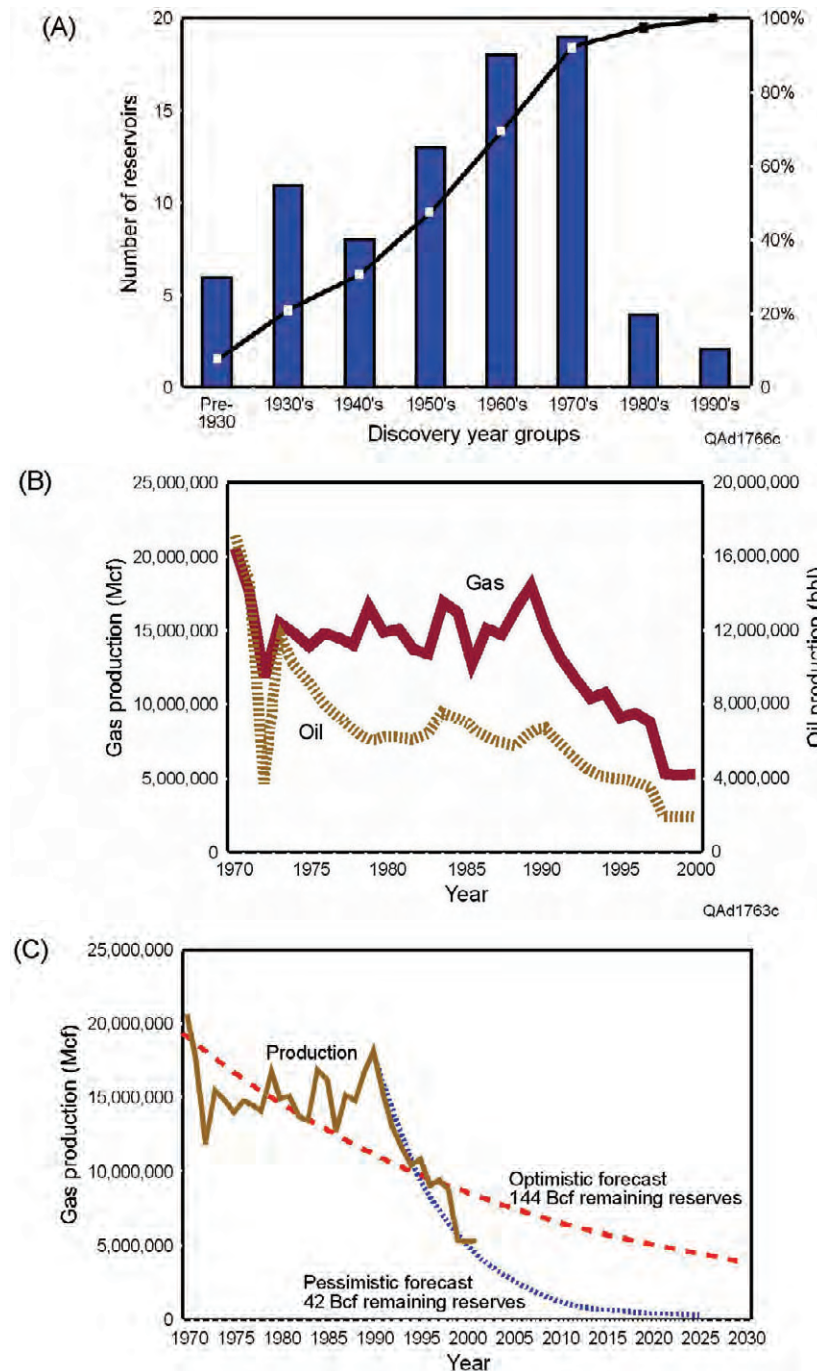


Figure 33. Histograms for Yates Formation productivity (A) new field discoveries summarized by decade showing abrupt decline since the 1970's; (B) hydrocarbon production where oil production has shown decline since the early 1970's, and gas production has shown decline since 1990; and (C) optimistic and pessimistic forecasts of gas productivity, based on reservoir performance since 1970. Optimistic forecast is based on average performance since 1979, whereas pessimistic forecast is based on declining performance since 1990. From Combs and others, 2003.

APPENDIX. TECHNOLOGY TRANSFER ACTIVITIES

Published Papers

- Ali, W., 2009, Lithofacies, depositional environment, burial history and calculation of organic richness from wireline logs: a study of the Barnett Shale in the Delaware Basin, Pecos Co., West Texas, and comparison with the Barnett Shale in the Fort Worth Basin: The University of Texas at Austin, Master's thesis, 210 p.
- Ali, W., and Gale, J., 2009, Characterization of the Barnett Shale, Permian basin, *in* Ruppel, S. C., Loucks, R. G., Hamlin, H. S., Nance, H. S., Gale, J., Fu, Q., Ali, W., Helbert, D., Applications of Cores to Permian Basin Reservoir Characterization A Core Workshop: Permian Basin SEPM, p. 20–21.
- Day-Stirrat, R. J., Loucks, R. G., Milliken, K. L., Hiller, S., and van der Pluijm, B. E., 2008, Phyllosilicate orientation as evidence for early timing of calcite cemented concretions in the Barnett Shale (Late Mississippian), Fort Worth Basin, Texas (U.S.A): *Sedimentary Geology*, v. 208, p. 27–35.
- Gale, J., 2009, Fracture characteristics of the Barnett Shale in the Permian basin, *in* Ruppel, S. C., Loucks, R. G., Hamlin, H. S., Nance, H. S., Gale, J., Fu, Q., Ali, W., Helbert, D., Applications of Cores to Permian Basin Reservoir Characterization A Core Workshop: Permian Basin SEPM, p. 22–23.
- Gale, J. F. W., Reed, R. M., and Holder, J., 2007, Natural fractures in the Barnett Shale and their importance for hydraulic fracture treatments: *AAPG Bulletin*, v. 91, p. 603–622.
- Fu, Q., 2009, Wolfcamp platform carbonates: facies and cyclicity, *in* Ruppel, S. C., Loucks, R. G., Hamlin, H. S., Nance, H. S., Gale, J., Fu, Q., Ali, W., Helbert, D., Applications of Cores to Permian Basin Reservoir Characterization A Core Workshop: Permian Basin SEPM, p. 28–29.
- Hamlin, H. S., 2009, Dean sandstone basin-floor facies, *in* Ruppel, S. C., Loucks, R. G., Hamlin, H. S., Nance, H. S., Gale, J., Fu, Q., Ali, W., Helbert, D., Applications of Cores to Permian Basin Reservoir Characterization A Core Workshop: Permian Basin SEPM, p. 16–17.
- Hamlin, H. S., 2009, Ozona sandstone, Val Verde Basin, Texas: synorogenic stratigraphy and depositional history in a Permian foredeep basin: *AAPG Bulletin*, v. 93, no. 5, p. 573–594.
- Hamlin, H. S., 2009, Spraberry sandstone basin-floor facies, *in* Ruppel, S. C., Loucks, R. G., Hamlin, H. S., Nance, H. S., Gale, J., Fu, Q., Ali, W., Helbert, D., Applications of Cores to Permian Basin Reservoir Characterization A Core Workshop: Permian Basin SEPM, p. 14–15.
- Helbert, D. 2009, San Andres Facies and Cyclicity: Fullerton field, *in* Ruppel, S. C., Loucks, R. G., Hamlin, H. S., Nance, H. S., Gale, J., Fu, Q., Ali, W., Helbert, D., Applications of Cores to Permian Basin Reservoir Characterization A Core Workshop: Permian Basin SEPM, p. 26–27.
- Loucks, R. G., 2009, Lower Ordovician (Ellenburger) karst facies, *in* Ruppel, S. C., Loucks, R. G., Hamlin, H. S., Nance, H. S., Gale, J., Fu, Q., Ali, W., Helbert, D., Applications of Cores to Permian Basin Reservoir Characterization A Core Workshop: Permian Basin SEPM, p. 2–7.
- Loucks, R. G., 2009, Middle and Upper Paleozoic (Silurian, Permian) karst facies, *in* Ruppel, S. C., Loucks, R. G., Hamlin, H. S., Nance, H. S., Gale, J., Fu, Q., Ali, W., Helbert, D.,

- Applications of Cores to Permian Basin Reservoir Characterization A Core Workshop: Permian Basin SEPM, p. 8–13.
- Loucks, R. G., Reed, R. M., Ruppel, S. C., and Jarvie, D. M., 2009 (in press), Morphology, genesis, and distribution of nanometer-scale pores in siliceous mudstones of the Mississippian Barnett Shale: *Journal of Sedimentary Research*.
- Loucks, R. G., and Ruppel, S. C., 2007, Mississippian Barnett Shale: lithofacies and depositional setting of a deepwater shale-gas succession in the Fort Worth Basin, Texas: *AAPG Bulletin*, v. 91, p. 579–601.
- Loucks, R. G., and Ruppel, S. C., 2008, Lower Ordovician Ellenburger Group collapsed-paleocave facies and associated pore network in the Goldrus Unit #3 core, Barnhart field, Texas (ext. abs.), *in* Sasowsky, I. D., Feazel, C. T., Mylroie, J. E., Palmer, A. N., and Palmer, M. V., *Karst from recent to reservoirs: Karst Waters Institute, Special Publication 14*, p. 127–129.
- McDonnell, A., Loucks, R. G., and Dooley, T., 2007, Quantifying the origin and geometry of circular sag structures in northern Fort Worth Basin, Texas: paleocave collapse, pull-apart fault systems, or hydrothermal alteration? *AAPG Bulletin* v. 4, p. 603–622.
- Milliken, K. L., Choh, S.-J., Papazis, P., and Jürgen Schieber, J., 2007, “Cherty” stringers in the Barnett Shale are agglutinated foraminifera: *Sedimentary Geology*, v. 1, p. 221–232.
- Nance, H. S., 2009, Bone Spring Fm slope and basin carbonates and siliciclastics, *in* Ruppel, S. C., Loucks, R. G., Hamlin, H. S., Nance, H. S., Gale, J., Fu, Q., Ali, W., Helbert, D., *Applications of Cores to Permian Basin Reservoir Characterization A Core Workshop: Permian Basin SEPM*, p. 18–19.
- Nance, H. S., 2009, Yates middle to inner shelf carbonates, evaporites, and siliciclastics, *in* Ruppel, S. C., Loucks, R. G., Hamlin, H. S., Nance, H. S., Gale, J., Fu, Q., Ali, W., Helbert, D., *Applications of Cores to Permian Basin Reservoir Characterization A Core Workshop: Permian Basin SEPM*, p. 24–25.
- Rowe, H. D., Loucks, R. G., Ruppel, S. C. and Rimmer, S. M., 2008, Mississippian Barnett Formation, Fort Worth Basin, Texas: bulk geochemical constraints on the severity of hydrographic restriction and the biogeochemical cycling and fate of iron: *Chemical Geology*, v. 257, p. 16–25.
- Ruppel, S. C., 2009, Abo/Wichita/Lower Clear Fork Reservoir Successions, *in* Ruppel, S. C., Loucks, R. G., Hamlin, H. S., Nance, H. S., Gale, J., Fu, Q., Ali, W., Helbert, D., *Applications of Cores to Permian Basin Reservoir Characterization A Core Workshop: Permian Basin SEPM*, p. 32–33.
- Ruppel, S. C., 2009, Middle-Upper Clear Fork/Glorieta Reservoir Successions, *in* Ruppel, S. C., Loucks, R. G., Hamlin, H. S., Nance, H. S., Gale, J., Fu, Q., Ali, W., Helbert, D., *Applications of Cores to Permian Basin Reservoir Characterization A Core Workshop: Permian Basin SEPM*, p. 30–31.
- Ruppel, S. C., Gale, J., Loucks, R. G., and Wright, W. R., 2007, Stop 2: Chappel type section and quarry, San Saba, Texas: Mississippian Barnett Formation mudrocks: stratigraphy, facies, mineralogy, and chemistry, *in* Wright, Wayne, Loucks, Bob, Gale, Julia, Kane, Jeff, and McDonnell, Angela, *field-trip leaders, Paleozoic reservoir systems: Texas Hill Country—stratigraphy to petrophysics: a field trip for the Annual Meeting of the Petrophysicists and Well Log Analysts*, p. 37–58.
- Ruppel, S. C., and Loucks, R. G., 2008, Black mudrocks: Lessons and questions from the Barnett shale in the Southern midcontinent: *Sedimentary Record*, v. 6, no. 2, p. 4–8.

- Ruppel, S. C., Loucks, R. G., and Gale, J. F. W., 2008, Barnett, Woodford, and related mudrock successions in Texas cores and outcrops: a field trip prepared for the 2008 AAPG/SEPM Annual Convention: The University of Texas at Austin, Bureau of Economic Geology, 82 p.
- Ruppel, S. C., Loucks, R. G., Hamlin, H. S., Nance, H., S., Gale, J., Fu, Q., Ali, W., Helbert, D., Applications of Cores to Permian Basin Reservoir Characterization A Core Workshop: Permian Basin SEPM, Southwest Section AAPG, Annual Meeting, 33 p.
- Wright, W. R., 2007, Stop 3: Hoover Point, Kingsland, Texas: Upper Cambrian Moore Hollow Group (Riley and Wilberns Formations): lithologic, lateral, and vertical variability, *in* Wright, Wayne, Loucks, Bob, Gale, Julia, Kane, Jeff, and McDonnell, Angela, field-trip leaders, Paleozoic reservoir systems: Texas Hill Country—stratigraphy to petrophysics: a field trip for the Annual Meeting of the Petrophysicists and Well Log Analysts, p. 59–68.
- Wright, W. R., Gale, J., Ruppel, S. C., and Loucks, R. G., 2007, Stop 1: Bend section, Colorado River, San Saba, Texas: Lower Pennsylvanian (Atokan) Upper Marble Falls Formation carbonates and Smithwick Formation mudrocks: stratigraphy, ecology, facies, structure, and mineralogy: their influence on lateral and vertical variations in reservoir quality, *in* Wright, Wayne, Loucks, Bob, Gale, Julia, Kane, Jeff, and McDonnell, Angela, field-trip leaders, Paleozoic reservoir systems: Texas Hill Country—stratigraphy to petrophysics: a field trip for the Annual Meeting of the Petrophysicists and Well Log Analysts, p. 5–36.
- Wright, Wayne, Loucks, Bob, Gale, Julia, Kane, Jeff, and McDonnell, Angela, 2007, Paleozoic reservoir systems: Texas Hill Country—stratigraphy to petrophysics: a field trip for the Annual Meeting of the Petrophysicists and Well Log Analysts: The University of Texas at Austin, Bureau of Economic Geology Field-Trip Guidebook, 77 p.

Oral Presentations

Professional Conferences

2005

- Brown, L., F., Upper Pennsylvanian and Lower Permian Sequence Stratigraphy and Depositional Systems Tracts, Intracratonic Eastern Shelf and Adjacent West Texas Basin, North- and West-Central Texas: American Association of Petroleum Geologists, Annual Meeting, Calgary, June.
- Ruppel, S. C., Multidisciplinary Reservoir Characterization of a Giant Permian Carbonate Platform Reservoir: Insights for Recovering Remaining Oil in a Mature U.S. Basin: American Association of Petroleum Geologists, Annual Meeting, Calgary, June.
- Ruppel, S. C., Surprising Lessons from Multidisciplinary Characterization of a Permian Carbonate Platform Reservoir: American Association of Petroleum Geologists, Annual Meeting, Calgary, June.

2006

- Dutton, S. P., Oil-Play Analysis of the Permian Basin: A Tool for Increasing Recovery from a Mature Oil-Producing Province: American Association of Petroleum Geologists, Annual Meeting, Houston, Texas.

- Loucks, R. G., Sedimentology and Depositional Setting of the Mississippian Barnett Shale, Wise County, Texas: South Central Meeting, Geological Society of America, March.
- Reed, R. M., Preliminary Fracture Analysis of Mississippian Barnett Shale Samples, Fort Worth Basin, Texas: South Central Meeting, Geological Society of America, March.
- Ruppel, S. C., Stratigraphy and Depositional History of the Barnett Formation and Equivalent Mississippian Rocks in the Ft. Worth Basin: South Central Meeting, Geological Society of America, March.
- Ruppel, S. C., Fundamentals of Rock-Based Reservoir Modeling: A Case History from the Lower Permian Fullerton Field, Permian Basin: American Association of Petroleum Geologists, Annual Meeting, Houston, Texas.
- Ruppel, S. C., Key role of Outcrops and Cores in Carbonate Reservoir Characterization and Modeling, Lower Permian Fullerton Field, Permian Basin, USA: American Association of Petroleum Geologists, Annual Meeting, Houston, Texas.

2007

- Gale, J., Natural Fractures in the Barnett Shale: Society of Petrophysicists and Well Log Analysts Annual Meeting Short Course, Barnett Shale-Gas Play of the Fort Worth Basin: Overview of Geology, Wireline-Log Analysis, and Engineering, Austin, Texas.
- Gale, J. F. W., Holder, J., and Reed, R. M., 2007, Natural Fractures in the Barnett Shale: Why They Are Important: American Association of Petroleum Geologists, Annual Meeting.
- Jarvie, J., Geochemical Characteristics of Productive Unconventional Shales: Society of Petrophysicists and Well Log Analysts Annual Meeting Short Course, Barnett Shale-Gas Play of the Fort Worth Basin: Overview of Geology, Wireline-Log Analysis, and Engineering, Austin, Texas.
- Kane, J., Petrophysical Considerations with Regard to the Barnett Shale: Society of Petrophysicists and Well Log Analysts Annual Meeting Short Course, Barnett Shale-Gas Play of the Fort Worth Basin: Overview of Geology, Wireline-Log Analysis, and Engineering, Austin, Texas.
- Loucks, R., Lithofacies, Depositional Setting and Pore Network of the Barnett Formation: Society of Petrophysicists and Well Log Analysts Annual Meeting Short Course, Barnett Shale-Gas Play of the Fort Worth Basin: Overview of Geology, Wireline-Log Analysis, and Engineering, Austin, Texas.
- Loucks, R. G., and Ruppel, S. C., Mississippian Barnett Shale: Lithofacies and Depositional Setting of a Deepwater Mudstone Succession: American Association of Petroleum Geologists, Annual Meeting.
- McDonnell, A., Quantifying Paleocave Collapse from 3D-Seismic; Examples from the Texas Paleozoic: Society of Petrophysicists and Well Log Analysts Annual Meeting Short Course, Barnett Shale-Gas Play of the Fort Worth Basin: Overview of Geology, Wireline-Log Analysis, and Engineering, Austin, Texas.
- Reed, R. M., and Loucks, R. G., Imaging Nanoscale Pores in the Mississippian Barnett Shale of the Northern Ft. Worth Basin: American Association of Petroleum Geologists, Annual Meeting.
- Ruppel, S. C., Loucks, R. G., Wright, W. R., Kane, J. A., and Wang, F., 2007, Similarities and Contrasts among Major Paleozoic Shale Gas Reservoir Plays in Texas and New Mexico: American Association of Petroleum Geologists, Annual Meeting.

Wright, W., Regional Distribution and Stratigraphic Architecture of the Barnett Formation, Greater Fort Worth Basin: Society of Petrophysicists and Well Log Analysts Annual Meeting Short Course, Barnett Shale-Gas Play of the Fort Worth Basin: Overview of Geology, Wireline-Log Analysis, and Engineering, Austin, Texas.

2008

Ali, W., Gale, J. F. W., Ruppel, S. C. , and Loucks, R. G., Lithofacies, Depositional Environment and Burial History of the Barnett Shale in the Delaware Basin, Pecos Co. West Texas, and comparison with the Barnett Shale in the Fort Worth Basin: West Texas Geological Society Symposium, Midland, Texas, September.

Breton, C. L., and Ruppel, S.C., Information Database of Permian Basin Geology: Content, Structure, and Access: West Texas Geological Society Symposium, Midland, Texas, September.

Day-Stirrat, R. J. , Loucks, R. G., Milliken, K. L., and van der Pluijm, B. A., Mississippian Barnett Shale: Characterization and Concretions: American Association of Petroleum Geologists, Annual Meeting.

Gale, J. F., and Holder, J., Natural Fractures in Shales: Origins, Characteristics and Relevance for Hydraulic Fracture Treatments: American Association of Petroleum Geologists, Annual Meeting.

Gale, J. F. W., Natural Fractures in the Barnett Shale in the Delaware Basin, Pecos Co., West Texas: comparison with the Barnett Shale in the Fort Worth Basin: West Texas Geological Society Symposium, Midland, Texas, September.

Jones, R. H., and Ruppel, S. C., Simpson Group Facies: Interpretations from the McKee Member Formation, Pecos County, Texas: West Texas Geological Society Symposium, Midland, Texas, September.

Loucks, R. G., and Ruppel, S. C., Shell and Grain Layers in the Barnett Shale; Event Deposition or In Situ Accumulations? American Association of Petroleum Geologists, Annual Meeting.

Nance, H. S., and Ruppel, S.C., Yates Formation gas-reservoir and seal facies, depositional and diagenetic models, northeast Central Basin Platform, Texas: West Texas Geological Society Symposium, Midland, Texas, September.

Reed, R. M. Loucks, R. G., Jarvie, D. M. and Ruppel, S. C., Differences in Nanopore Development Related to Thermal Maturity in the Mississippian Barnett Shale: Preliminary Results: Geological Society of America Annual Meeting, Houston, Texas, October.

Reed; R. M., Loucks, R. G., Jarvie, D. M., and Ruppel, S. C., Morphology, Distribution, and Genesis of Nanometer-Scale Pores in the Mississippian Barnett Shale: American Association of Petroleum Geologists, Annual Meeting.

Rowe, H., Loucks, R., Ruppel, S., and Rimmer, S., Mississippian Barnett Formation: Bulk Geochemical Constraints on the Severity of Hydrographic Restriction and the Biogeochemical Cycling and Fate of Iron: American Association of Petroleum Geologists, Annual Meeting.

Ruppel, S. C., Geological Complexities in Shale Gas Systems: Coalbed Methane and Shale Gas Exploration Strategies: Workshop for Sorbed Gas Reservoir Systems: American Association of Petroleum Geologists, Annual Meeting.

- Ruppel, S. C., and Loucks, R. G., The Barnett Shale of the Southern Fort Worth Basin; Comparison of Depositional Setting, Lithofacies, and Mineralogy with Equivalent Deposits in the Northern Basin: American Association of Petroleum Geologists, Annual Meeting.
- Ruppel, S. C., and Loucks, R. G., Devonian and Mississippian mudrock systems in Texas: similarities and differences: West Texas Geological Society Symposium, Midland, Texas, September.
- Ruppel, S. C., and Loucks, R. G., The Devonian Woodford Fm of the Permian Basin: Complex Depositional and Temporal Variations across an Anaerobic Marine Basin: American Association of Petroleum Geologists, Annual Meeting.
- Stucker, J. D., Rowe, H. D., Rimmer, S., Ruppel, S. C., and Loucks, R. G., Use of Modern Depositional Settings as Analogs for the Interpretation of Ancient Mudrocks: Geological Society of America Annual Meeting, Houston, Texas, October.

2009

- Gale, J. F., Reed, R. M., Becker, S., and Ali, A., Natural Fractures in the Barnett Shale in the Delaware Basin, Pecos Co. West Texas: comparison with the Barnett Shale in the Fort Worth Basin: American Association of Petroleum Geologists, Annual Meeting.

Workshop/Short Course Presentations

2004

- Kerans, C., 2004, Deep Water Carbonates in the Permian: Models and Directions: Stratigraphic Synthesis of Paleozoic Oil-bearing Depositional Systems: Data and Models for Recovering Existing and Undiscovered Oil Resources from the Permian Basin: Startup Workshop, November 30 (Midland, TX) and December 7 (Houston, TX).
- Loucks, R. G., Challenges in Ellenburger Hydrocarbon Exploitation: Stratigraphic Synthesis of Paleozoic Oil-bearing Depositional Systems: Data and Models for Recovering Existing and Undiscovered Oil Resources from the Permian Basin: Startup Workshop, November 30 (Midland, TX) and December 7 (Houston, TX).
- Ruppel, S. C., 2004, Key Questions and Issues in Permian Basin Reservoir Plays: Stratigraphic Synthesis of Paleozoic Oil-bearing Depositional Systems: Data and Models for Recovering Existing and Undiscovered Oil Resources from the Permian Basin: Startup Workshop, November 30 (Midland, TX) and December 7 (Houston, TX).

2006

- Breton, C., Wright, W., and Ruppel, S., Tour of Webpage and GIS Project: Annual Project Meeting and Workshop for 2005, Austin, Texas, February.
- Gale, J., Barnett Shale Fracture Overview: Annual project Meeting and Workshop for 2005, Austin, Texas, February.
- Gale, J., Natural Fractures in the Barnett Shale: Barnett Shale-Gas Play of the Fort Worth Basin: Texas Region Petroleum Technology Transfer Council Workshop, November 8 (Midland, TX) and November 14 (Houston, TX).
- Guevara, E., Spraberry/Dean Basinal Clastic Systems: Annual Project Meeting and Workshop for 2005, Austin, Texas, February.

- Guevara, E., Spraberry/Dean Cores, Permian Basin: Annual Project Meeting and Core Workshop for 2005, Austin, Texas, February.
- Jarvie, D., Geochemical Characteristics of Productive Unconventional Shales: Barnett Shale-Gas Play of the Fort Worth Basin: Texas Region Petroleum Technology Transfer Council Workshop, November 8 (Midland, TX) and November 14 (Houston, TX).
- Kane, J., Petrophysical Characterization of the Barnett: Annual Project Meeting and Workshop for 2005, Austin, Texas, February.
- Kane, J., Petrophysical Considerations with Regard to the Barnett Shale: Barnett Shale-Gas Play of the Fort Worth Basin: Texas Region Petroleum Technology Transfer Council Workshop, November 8 (Midland, TX) and November 14 (Houston, TX).
- Kerans, C., Sequence Stratigraphy of the San Andres: Annual Project Meeting and Workshop for 2005, Austin, Texas, February.
- Loucks, R. G., Barnett Shale-Gas Play of the Fort Worth Basin: Barnett Shale-Gas Play of the Fort Worth Basin: Texas Region Petroleum Technology Transfer Council Workshop, November 8 (Midland, TX) and November 14 (Houston, TX).
- Loucks, R. G., Ellenburger: Annual Project Meeting and Workshop for 2005, Austin, Texas, February.
- Loucks, R. G., Mississippian Barnett Shale in the Fort Worth Basin: Lithofacies and Depositional Setting of a Deep-Water Gas-Shale Succession: Barnett Shale-Gas Play of the Fort Worth Basin: Texas Region Petroleum Technology Transfer Council Workshop, November 8 (Midland, TX) and November 14 (Houston, TX).
- Loucks, R. G., Review of the Lower Ordovician Ellenburger Group: Annual Project Meeting and Workshop for 2005, Austin, Texas, February.
- McDonnell, A., Sag Structures in the Northern Fort Worth Basin: Origin and Influence on the Barnett Formation: Barnett Shale-Gas Play of the Fort Worth Basin: Texas Region Petroleum Technology Transfer Council Workshop, November 8 (Midland, TX) and November 14 (Houston, TX).
- Nance, H. S., Delaware Mountain Group: Annual Project Meeting and Workshop for 2005, Austin, Texas, February.
- Nance, H. S., Delaware Mtn, Group cores, Permian Basin: Annual Project Meeting and Workshop 2005, Austin, Texas, February.
- Nance, H. S., Depositional Styles in the Yates, Seven Rivers, and Queen: Annual Project Meeting and Workshop for 2005, Austin, Texas, February.
- Nance, H. S., Yates/Queen cores, Permian Basin: Annual Project Meeting and Workshop for 2005, Austin, Texas, February.
- Potter, E., Overview of Barnett Play: Barnett Shale-Gas Play of the Fort Worth Basin: Texas Region Petroleum Technology Transfer Council Workshop, November 8 (Midland, TX) and November 14 (Houston, TX).
- Playton, T., Wolfcamp Deep-water Systems: Annual Project Meeting and Workshop for 2005, Austin, Texas, February.
- Reed, R. M., Barnett Matrix Pore-Network Analysis: Barnett Shale-Gas Play of the Fort Worth Basin: Texas Region Petroleum Technology Transfer Council Workshop, November 8 (Midland, TX) and November 14 (Houston, TX).
- Ruppel, S. C., Clear Fork/Abo/Wichita cores, Permian Basin: Annual Project Meeting and Workshop for 2005, Austin, Texas, February.

- Ruppel, S. C., Depositional History and Sedimentology of the Barnett Shale in the Fort Worth Basin: Barnett Shale-Gas Play of the Fort Worth Basin: Texas Region Petroleum Technology Transfer Council Workshop, November 8 (Midland, TX) and November 14 (Houston, TX).
- Ruppel, S. C., Depositional Styles in Lower Devonian Chert and Carbonate Systems: Annual Project Meeting and Workshop for 2005, Austin, Texas, February.
- Ruppel, S. C., Keys to Interpreting the Clear Fork/Abo/Wichita Succession: Annual Project Meeting and Workshop for 2005, Austin, Texas, February.
- Ruppel, S. C., A Regional Look at the Barnett "Shale": Annual Project Meeting and Workshop for 2005, Austin, Texas, February.
- Ruppel, S. C., San Andres cores, Permian Basin: Annual Project Meeting and Workshop for 2005, Austin, Texas, February.
- Ruppel, S. C., Thirtyone cores, Permian Basin: Annual Project Meeting and Workshop for 2005, Austin, Texas, February.
- Ruppel, S. C., Woodford cores, Permian Basin: Annual Project Meeting and Workshop for 2005, Austin, Texas, February.
- Ruppel, S. C., The Woodford Shale: a developing resource? Annual Project Meeting and Workshop for 2005, Austin, Texas, February.
- Ruppel, S. C., Wristen cores, Permian Basin: Annual Project Meeting and Workshop for 2005, Austin, Texas, February.
- Ruppel, S. C., Loucks, R. G., and Wright, W., Mississippian/Barnett cores, Ft. Worth Basin: Annual Project Meeting and Workshop for 2005, Austin, Texas, February.
- Wang, F., A Review of Production Technology of Barnett Shale: Barnett Shale-Gas Play of the Fort Worth Basin: Texas Region Petroleum Technology Transfer Council Workshop, November 8 (Midland, TX) and November 14 (Houston, TX).
- Wright, W., Pennsylvanian cores, Permian Basin: Annual Project Meeting and Workshop for 2005, Austin, Texas, February.
- Wright, W., Stratigraphic Architecture of the Barnett Formation in the Greater Fort Worth Basin: Barnett Shale-Gas Play of the Fort Worth Basin: Texas Region Petroleum Technology Transfer Council Workshop, November 8 (Midland, TX) and November 14 (Houston, TX).
- Wright, W., Unraveling the Pennsylvanian: Annual Project Meeting and Workshop for 2005, Austin, Texas, February.
- Zeng, H., Clinoforms in the Barnett Shale, Wise County, Fort Worth Basin, Texas: Barnett Shale-Gas Play of the Fort Worth Basin: Texas Region Petroleum Technology Transfer Council Workshop, November 8 (Midland, TX) and November 14 (Houston, TX).

2007

- Gale, J., Fracture Development in the Woodford and Barnett: 2006 Annual Meeting and Workshop, Austin, Texas, February.
- Jarvie, D., Organic Geochemistry of the Woodford: 2006 Annual Meeting and Workshop, Austin, Texas, February.
- Kane, J., Petrophysical Comparison of Barnett and Woodford: 2006 Annual Meeting and Workshop, Austin, Texas, February.
- Kerans, C., Early Permian Carbonate Reservoir Systems: 2006 Annual Meeting and Workshop, Austin, Texas, February.

- Loucks, R. G., Lower Ordovician Ellenburger Karst System Research: 2006 Annual Meeting and Workshop, Austin, Texas, February.
- Loucks, R. G., Lower Ordovician Outcrops, Marble Falls, Texas: 2006 Annual Meeting and Workshop, Austin, Texas, February.
- Loucks, R. G., and Ruppel, S.C., Sedimentology of the Woodford Shale: 2006 Annual Meeting and Workshop, Austin, Texas, February.
- McDonnell, A., Seismic Analysis of Ellenburger Karst: 2006 Annual Meeting and Workshop, Austin, Texas, February.
- Nance, H. S., Bone Spring Sandstones in the Delaware Basin: 2006 Annual Meeting and Workshop, Austin, Texas, February.
- Ruppel, S. C., Regional Trends in the Clear Fork/Abo/Wichita Succession: 2006 Annual Meeting and Workshop, Austin, Texas, February.
- Ruppel, S. C., Gale, J., Loucks, R. G., and Wright, W., Mississippian Barnett Fm. Mudrocks: Stratigraphy, Facies, Mineralogy, and Chemistry: 2006 Annual Meeting and Workshop, Austin, Texas, February.
- Ruppel, S.C., and Loucks, R. G., New Insights on the Barnett System: 2006 Annual Meeting and Workshop, Austin, Texas, February.
- Ruppel, S.C., Wright, W., and Loucks, R. G., Nature and Significance of Barnett (Mississippian)—Marble Falls (Pennsylvanian) Contact: 2006 Annual Meeting and Workshop, Austin, Texas, February.
- Wright, W., The Pennsylvanian Canyon and Cisco Series: 2006 Annual Meeting and Workshop, Austin, Texas, February.
- Wright, W., and Gale, J., Regional Structure and Tectonics of the Permian Basin: 2006 Annual Meeting and Workshop, Austin, Texas, February.
- Wright, W., Gale, J., Ruppel, S. C., and Loucks, R. G., Lower Pennsylvanian (Atokan) Upper Marble Falls Fm Carbonates and Smithwick Fm Mudrocks: Stratigraphy, Ecology, Facies, Structure, and Mineralogy; Their Influence on Lateral and Vertical Variations in Reservoir Quality: 2006 Annual Meeting Field Trip, Austin, Texas, February.
- Wright, W., and Ruppel, S. C., Lower Pennsylvanian (Atokan) Upper Marble Falls Fm; lateral and vertical variations in carbonate facies and reservoir quality: 2006 Annual Meeting and Workshop, Austin, Texas, February.

2008

- Gale, J., Natural Fractures in the Barnett Shale and their Importance for Hydraulic Fracture Treatments, in Barnett, Woodford, and Related Mudrock Successions in Texas Cores and Outcrops: A Core Workshop Prepared for the 2008 AAPG/SEPM Annual Convention, San Antonio, Texas, April.
- Gale, J., and Day-Stirrat, Fracture Development over the Life of a Shale Basin: 2007 Annual Meeting and Workshop, Austin, Texas, February.
- Hamlin, H. S., Spraberry, Dean, and “Wolfberry” Mixed Clastic/Carbonate Basin-Floor Reservoirs, Midland Basin: 2007 Annual Meeting and Workshop, Austin, Texas, February.
- Jones, R. H., Facies and Reservoir Development in the Middle Ordovician Simpson Group: 2007 Annual Meeting and Workshop, Austin, Texas, February.
- Jones, R. H., Upper Ordovician Montoya Group Facies and Stratigraphy: 2007 Annual Meeting and Workshop, Austin, Texas, February.

- Kerans, C., Permian San Andres Platform Carbonates: 2007 Annual Meeting and Workshop, Austin, Texas, February.
- Loucks, R.G., Introduction to Research on the Barnett Shale in the Fort Worth Basin: 2007 Annual Meeting and Workshop, Austin, Texas, February.
- Loucks, R., Overview of Barnett Shale and Associated Strata in the Fort Worth Basin, in Barnett, Woodford, and Related Mudrock Successions in Texas Cores and Outcrops: A Core Workshop Prepared for the 2008 AAPG/SEPM Annual Convention, San Antonio, Texas, April.
- Nance, H. S., Leonardian Slope/Basinal Facies, Rock-Body Geometries, and Depositional Model, Delaware Basin: 2007 Annual meeting and workshop, Austin, Texas, February 2008
- Reed, R. M., Nanopore Architecture in Paleozoic Black Shales of Texas: Barnett and Beyond: 2007 Annual Meeting and Workshop, Austin, Texas, February.
- Ruppel, S. C., Competing Effects of Deposition and Diagenesis on Reservoir Development: Permian Grayburg Platform Carbonates: 2007 Annual Meeting and Workshop, Austin, Texas, February.
- Ruppel, S. C., Controls on Facies and Diagenesis in Wolfcamp Platform Carbonates: 2007 Annual Meeting and Workshop, Austin, Texas, February.
- Ruppel, S. C., Introduction to the Geology of Middle Paleozoic Mudrock Systems in Texas, in Barnett, Woodford, and Related Mudrock Successions in Texas Cores and Outcrops: A Core Workshop Prepared for the 2008 AAPG/SEPM Annual Convention, San Antonio, Texas, April.
- Ruppel, S. C., The Woodford Mudrock System in Texas, in Barnett, Woodford, and Related Mudrock Successions in Texas Cores and Outcrops: A Core Workshop Prepared for the 2008 AAPG/SEPM Annual Convention, San Antonio, Texas, April.
- Ruppel, S. C., Woodford (Devonian) and Barnett (Mississippian) Depositional Systems a Brief Overview: 2007 Annual Meeting and Workshop, Austin, Texas, February.

2009

- Ali, W., Characterization of the Barnett Shale, Permian Basin: 2008 Annual Meeting and Workshop, Austin, Texas, February.
- Ali, W., and Gale, J., Barnett Shale, Permian Basin: Facies, Mineralogy, and Wireline Analysis: 2008 Annual Meeting and Workshop, Austin, Texas, February.
- Ali, W., and Gale, J., 2009, Characterization of the Barnett Shale, Permian Basin: Permian Basin SEPM Core Workshop, Midland, Texas.
- Fu, Q., Wolfcamp Platform Carbonates: Facies and Cyclicity: 2008 Annual Meeting and Workshop, Austin, Texas, February.
- Fu, Q., Wolfcamp Platform Carbonates: Facies and Cyclicity: Permian Basin SEPM Core Workshop, Midland, Texas.
- Gale, J., Barnett Shale Fractures: Permian Basin: 2008 Annual Meeting and Workshop, Austin, Texas, February.
- Gale, J., Fracture Characteristics of the Barnett Shale in the Permian Basin: 2008 Annual Meeting and Workshop, Austin, Texas, February.
- Gale, J., Fracture Characteristics of the Barnett Shale in the Permian Basin: Permian Basin SEPM Core Workshop, Midland, Texas.

Hamlin, H. S., Clear Fork/Spraberry Slope/Basin Systems in the Northern Midland Basin: 2008 Annual Meeting and Workshop, Austin, Texas, February.

Hamlin, H. S., Clear Fork/Spraberry Proximal Slope/Basin System: 2008 Annual Meeting and Workshop, Austin, Texas, February.

Hamlin, H. S., 2009, Dean Sandstone Basin-Floor Facies: Permian Basin SEPM Core Workshop, Midland, Texas.

Hamlin, H. S., Spraberry Distal Basin-Floor System Facies: 2008 Annual Meeting and Workshop, Austin, Texas, February.

Hamlin, H. S., Spraberry Sandstone Basin-Floor Facies: Permian Basin SEPM Core Workshop, Midland, Texas.

Helbert, D. San Andres Facies and Cyclicity: Fullerton Field: Permian Basin SEPM Core Workshop, Midland, Texas.

Helbert, D., San Andres Facies and Cyclicity: Fullerton Field: 2008 Annual Meeting and Workshop, Austin, Texas, February.

Jarvie, D., Update on the Organic Geochemistry of Shale Gas Systems: 2008 Annual Meeting and Workshop, Austin, Texas, February.

Kerans, C., Wolfcamp Slope/Basin Systems, Midland Basin: 2008 Annual Meeting and Workshop, Austin, Texas, February.

Loucks, R. G., Lower Ordovician (Ellenburger) Karst Facies: 2008 Annual Meeting and Workshop, Austin, Texas, February.

Loucks, R. G., Lower Ordovician (Ellenburger) Karst Facies: Permian Basin SEPM Core Workshop, Midland, Texas.

Loucks, R. G., Middle and Upper Paleozoic (Silurian, Permian) Karst Facies: Permian Basin SEPM Core Workshop, Midland, Texas.

Loucks, R. G., Middle and Upper Paleozoic (Silurian, Permian) Karst Facies: 2008 Annual Meeting and Workshop, Austin, Texas, February.

Loucks, R. G., Paleozoic Karst Systems in the Permian Basin: 2008 Annual Meeting and Workshop, Austin, Texas, February.

Nance, H. S., Bone Spring Fm Slope and Basin Carbonates and Siliciclastics: Permian Basin SEPM Core Workshop, Midland, Texas, 2009.

Nance, H. S., Middle Permian Slope/Basin Systems in the Delaware Basin: Bone Spring: 2008 Annual Meeting and Workshop, Austin, Texas, February.

Nance, H. S., Proximal and Distal Bone Spring Facies and Architecture: 2008 Annual Meeting and Workshop, Austin, Texas, February.

Nance, H. S., Upper Permian Inner Shelf Evaporite-Bearing Clay-Rich Sandstones: Yates Fm: 2008 Annual Meeting and Workshop, Austin, Texas, February.

Nance, H. S., Yates Fm: Proximal to Distal Trends in Facies and Mineralogy: 2008 Annual Meeting and Workshop, Austin, Texas, February.

Nance, H. S., Yates Middle to Inner Shelf Carbonates, Evaporites, and Siliciclastics: Permian Basin SEPM Core Workshop, Midland, Texas.

Reed, R., M., and Loucks, R. G., Nanoscale Imaging of Shales in the Permian and Ft. Worth Basins: 2008 Annual Meeting and Workshop, Austin, Texas, February.

Rowe, H., Geochemistry of the Barnett Shale: Implications for Depositional Environment: 2008 Annual Meeting and Workshop, Austin, Texas, February.

Ruppel, S. C., Abo/Wichita/Lower Clear Fork Reservoir Successions: 2008 Annual Meeting and Workshop, Austin, Texas, February.

Ruppel, S. C., Abo/Wichita/Lower Clear Fork Reservoir Successions: Permian Basin SEPM Core Workshop, Midland, Texas.

Ruppel, S. C., Black Shale Resource Systems; Evaluation Based on Cores, Logs, Geochemistry, and Geomechanical Properties: Platts 4th Annual Oil and Shale Gas Developer Conference, Houston, Texas, May.

Ruppel, S. C., Middle-Upper Clear Fork/Glorieta Reservoir Successions: Permian Basin SEPM Core Workshop, Midland, Texas.

Ruppel, S. C., Middle-Upper Clear Fork/Glorieta reservoir successions: 2008 Annual Meeting and Workshop, Austin, Texas, February.

Ruppel, S. C., Regional Patterns of Leonard Facies Development: Definition and importance: 2008 Annual Meeting and Workshop, Austin, Texas, February.

Wang, F., Key Controls on Shale-Gas Production: 2008 Annual Meeting and Workshop, Austin, Texas, February.

Workshops, Short Courses, and Special Sessions

Stratigraphic Synthesis of Paleozoic Oil-bearing Depositional Systems: Data and Models for Recovering Existing and Undiscovered Oil Resources from the Permian Basin: Startup Workshop, November 30 (Midland, TX) and December 7 (Houston, TX), 2004.

Annual Project Meeting and Workshop for 2005, Austin, Texas, February 2006.

Barnett Shale-Gas Play of the Fort Worth Basin: Texas Region Petroleum Technology Transfer Council Workshop, November 8 (Midland, TX) and November 14 (Houston, TX), 2006.

Annual Project Meeting and Workshop for 2006, Austin, Texas, February 2007.

Barnett Shale-Gas Play of the Fort Worth Basin: Overview of Geology, Wireline-Log Analysis, and Engineering, Short course and field trip: Society of Petrophysicists and Well Log Analysts Annual Meeting Short Course, June 2007, Austin, TX.

Annual Project Meeting and Workshop for 2007, Austin, Texas, February 2008.

Geology of Shale/Mudrock Reservoir Systems, Special Oral and Poster Sessions for the 2008 AAPG/SEPM Annual Convention, San Antonio, Texas, April 2008.

Barnett, Woodford, and Related Mudrock Successions in Texas Cores and Outcrops: A Core Workshop Prepared for the 2008 AAPG/SEPM Annual Convention, San Antonio, Texas, April 2008.

Annual Project Meeting and Workshop for 2008, Austin, Texas, February 2009.

Applications of Cores to Permian Basin Reservoir Characterization: A Core Workshop: Permian Basin SEPM, Southwest Section AAPG, Annual Meeting, Midland, Texas, April 2009.

Direct Company Training

Short Course on Clear Fork Reservoir Systems in the Permian Basin: presented to
ConocoPhillips, Houston, Texas, November 2008.

Field Trip on Barnett and Associated Reservoir Systems, Central Texas for Shell, Hill Country,
Texas, November, 2005.

National Energy Technology Laboratory

626 Cochrans Mill Road
P.O. Box 10940
Pittsburgh, PA 15236-0940

3610 Collins Ferry Road
P.O. Box 880
Morgantown, WV 26507-0880

One West Third Street, Suite 1400
Tulsa, OK 74103-3519

1450 Queen Avenue SW
Albany, OR 97321-2198

2175 University Ave. South
Suite 201
Fairbanks, AK 99709

Visit the NETL website at:
www.netl.doe.gov

Customer Service:
1-800-553-7681

